VOLTAMMETRIC PROPERTIES OF BORON CARBIDE ELECTRODES

by

Chee On Too, B.Sc., M.Sc., A.K.C.

June 1983

A thesis submitted for the degree of Doctor of Philosophy of the University of London, and for the Diploma of Membership of the Imperial College.

Department of Metallurgy and Materials Science,
Imperial College of Science and Technology,
Prince Consort Road,
London SW7 2BP.

ABSTRACT

The voltammetric behaviour (d.c., linear sweep and/or cyclic) of boron carbide solid working electrodes has been examined in the following inorganic aqueous systems:-

(1) $(NH_4)_2IrCl_6$ in $HClO_4$, HCl, or $NaClO_4$ supporting electrolyte.
(2) Ir(IV) perchlorate in $HClO_4$ supporting electrolyte.
(3) Ir(IV) sulphate in H_2SO_4 supporting electrolyte.
(4) Ir(IV) phosphate in H_3PO_4-$HClO_4$ supporting electrolyte.
(5) Fe(III) perchlorate in $HClO_4$ supporting electrolyte.
(6) Fe(III) chloride in HCl supporting electrolyte.
(7) $K_3Fe(CN)_6$ in KCl supporting electrolyte.
(8) Ag(I) perchlorate in $NaClO_4$ supporting electrolyte.
(9) Cu(II) sulphate in $NaClO_4$ supporting electrolyte.
(10) Pd(II) perchlorate in $HClO_4$ supporting electrolyte.

For some of these systems, comparative studies have been conducted with boron carbide/carbon composite solid electrodes (composition range of $B_{3.86}C$ to $B_{2.56}C$) as well as with the graphite electrode. The electrode reaction mechanisms have been elucidated. In several systems, notably system 2 above, the electron charge transfer has been shown to be complicated by adsorption and/or a chemical reaction.

One of the consequences of these investigations is the development of the chemical analysis of boron carbide, where: (1) The boron content is determined by pyrohydrolysis followed by the potentiometric titration of the boric acid product, with a reproducibility of ±0.3 %B. (2) The carbon content is determined by a variant of the Direct-Combustion Method, with a reproducibility of ±0.1 %C.

ACKNOWLEDGEMENTS

I wish to gratefully thank Dr. D. Inman (supervisor) and Dr. D. A. Pantony (retired supervisor) for their much appreciated advice and assistance in the work of this thesis.

I also wish to thank the staff (especially Messrs R. J. Chater, M. J. L. Haddon, and P. R. Monk) of the Analytical Services Laboratory, Department of Metallurgy and Materials Science, for their practical help at sundry times.

Fig. 4-4 was drawn by Mr. A. J. Tipple, Department of Metallurgy and Materials Science.

I thank the Science Research Council for funding the first 2 years of this research, and I also thank Imperial College for the financial assistance in the payment of sessional fees.

Last but not least, I wish to acknowledge my debt of gratitude to my parents who have patiently been extending to me their moral and financial support despite the sacrifices involved.

CONTENTS

	Page
Title	1
Abstract	2
Acknowledgements	3
Contents	4
List of Tables and selected Figures	11
List of Symbols and Abbreviations	20
Potentials and Sign Convention	22
1. INTRODUCTION	23
1-1 General Introduction	23
1-2 Boron Carbide Solid Electrodes	24
1-3 Summary	30
1-4 References	30
2. CHEMISTRY AND ELECTROCHEMISTRY OF SELECTED INORGANIC AQUEOUS SYSTEMS	32
2-1 Iridium	32
2-1.1 Chloroiridate-chloroiridite system	32
2-1.2 Ir(IV)-Ir(III) perchlorate system	33
2-1.3 Ir(IV) sulphate system	35
2-1.4 Ir(IV) phosphate system	36
2-1.5 Electrochemistry of selected iridium species	36
2-2 Palladium	39
2-3 Iron	40
2-3.1 Fe(III)-Fe(II) perchlorate system	40
2-3.2 Fe(III)-Fe(II) chloride system	41
2-3.3 Fe(III)-Fe(II) cyanide system	41
2-4 Silver	42
2-5 Copper	42
2-6 References	43

Page

3. SOLID ELECTRODE VOLTAMMETRY 47

3-1 Instrumentation 47

3-2 D.C. Voltammetry in Stirred Solutions 48

3-2.1 Reversible and irreversible electrode processes involving a soluble reductant 48

3-2.2 Reversible and irreversible electrode processes involving the deposition of a metal on an inert electrode 51

3-3 Linear Sweep Voltammetry 53

3-3.1 Reversible electrode processes involving a soluble reductant 53

3-3.2 Reversible electrode process involving the deposition of a metal on an inert electrode 54

3-3.3 Irreversible electrode process involving a soluble reductant 55

3-3.4 Consecutive peak currents 57

3-4 Cyclic Voltammetry 58

3-4.1 Uncomplicated charge transfers 58

3-4.2 Multiple charge transfers 60

3-5 Application to Kinetic Systems 63

3-5.1 D.c. voltammetry 63

3-5.2 Linear sweep and cyclic voltammetry 65

3-6 Application to Adsorption Systems 73

3-6.1 D.c. voltammetry 73

3-6.2 Linear sweep and cyclic voltammetry 75

3-7 References 83

4. EXPERIMENTAL 86

4-1 Electrodes and Voltammetric Procedure 86

4-1.1 Construction of the working electrode 86

4-1.2 Construction of the saturated calomel electrode 86

4-1.3 Apparatus 88

4-1.4 D.c. voltammetric procedure 88

4-1.5 Linear sweep and cyclic voltammetric procedure 89

4-2 Specific Treatment Procedures for Boron Carbide Electrodes in Application to the Chloroiridate-Chloroiridite System 89

Page

4-2.1 Carbon enrichment of electrode working surfaces 90
4-2.2 Chemical treatments 90
4-2.3 Electrochemical treatment 90
4-3 Treatment with Ir(IV) Perchlorate 90
4-4 Iridium 91
4-4.1 Chloroiridate-chloroiridite system 91
4-4.2 Ir(IV) perchlorate system 91
4-4.3 Ir(IV) sulphate system 91
4-4.4 Ir(IV) phosphate system 92
4-5 Iron 92
4-5.1 Fe(III)-Fe(II) perchlorate system 92
4-5.2 Fe(III)-Fe(II) chloride system 92
4-5.3 Fe(III)-Fe(II) cyanide system 92
4-6 Palladium 93
4-7 Silver 93
4-8 Copper 93
4-9 Mixed Ion Solution 93
4-10 Chemical Analysis of Boron Carbide 94
4-10.1 Boron analysis 94
4-10.2 Carbon analysis 94
4-10.3 Impurities 97
4-11 Chemical Analysis of Lamp Black and Graphite 97
4-12 Miscellaneous Methods 97
4-12.1 Fabrication of boron carbide and boron carbide/ carbon composite rods 97
4-12.2 Tyndall effect 98
4-12.3 Paper electrophoresis 98
4-12.4 Spectrophotometry 98
4-13 References 98

5. ANALYSIS OF RESULTS 100
5-1 Iridium 100
5-1.1 Chloroiridate-chloroiridite in perchloric acid supporting electrolyte system 100

Page

5-1.1.(i) Effect of electrode composition on voltammetric properties 100

5-1.1.(ii) Chemical treatments on electrodes 115

5-1.1.(iii) Effect of Ir(IV) perchlorate treatment on electrodes 115

5-1.1.(iv) Effect of electrochemical treatment on electrodes 144

5-1.1.(v) Graphite solid electrode 151

5-1.1.(vi) Summary 151

5-1.2 Chloroiridate-chloroiridite in hydrochloric acid supporting electrolyte system 157

5-1.2.(i) Effect of electrode composition on voltammetric properties 157

5-1.2.(ii) Effects of Ir(IV) perchlorate treatment and electrochemical treatment on the boron carbide solid electrode 157

5-1.2.(iii) Summary 180

5-1.3 Chloroiridate-chloroiridite in sodium perchlorate supporting electrolyte system 183

5-1.3.(i) Effect of electrochemical treatment on the boron carbide solid electrode 183

5-1.3.(ii) Summary 193

5-1.4 Spectrophotometry of chloroiridate 193

5-1.5 Ir(IV) perchlorate system 198

5-1.5.(i) D.c. voltammetry 198

5-1.5.(i).a Boron carbide solid electrode $B_{4.05}C$ 198

5-1.5.(i).b Boron carbide solid electrode $B_{3.86}C$ 212

5-1.5.(i).c Boron carbide/carbon composite solid electrode $B_{3.11}C$ 218

5-1.5.(i).d Boron carbide/carbon composite solid electrode $B_{2.56}C$ 218

5-1.5.(i).e Graphite solid electrode 224

5-1.5.(i).f Summary 234

5-1.5.(ii) Linear sweep and cyclic voltammetry 237

5-1.5.(ii).a Boron carbide solid electrode $B_{4.05}C$ 237

5-1.5.(ii).b Boron carbide solid electrode $B_{3.86}C$ 255

5-1.5.(ii).c Boron carbide/carbon composite solid electrode $B_{3.77}C$ 266

Page

5-1.5.(ii).d Boron carbide/carbon composite solid electrode $B_{3.69}C$ 276
5-1.5.(ii).e Boron carbide/carbon composite solid electrode $B_{3.53}C$ 276
5-1.5.(ii).f Boron carbide/carbon composite solid electrode $B_{3.38}C$ 282
5-1.5.(ii).g Boron carbide/carbon composite solid electrode $B_{3.24}C$ 289
5-1.5.(ii).h Boron carbide/carbon composite solid electrode $B_{3.11}C$ 289
5-1.5.(ii).i Boron carbide/carbon composite solid electrode $B_{2.98}C$ 304
5-1.5.(ii).j Boron carbide/carbon composite solid electrode $B_{2.76}C$ 304
5-1.5.(ii).k Boron carbide/carbon composite solid electrode $B_{2.56}C$ 310
5-1.5.(ii).l Graphite solid electrode 320
5-1.5.(ii).m Effect of Ir(IV) perchlorate adsorption on the residual current at the working electrode 335
5-1.5.(ii).n Summary 341

5-1.5.(iii) The influence of nitrogen aeration on the Ir(IV) perchlorate system 348
5-1.5.(iii).a Boron carbide solid electrode $B_{4.05}C$ 348
5-1.5.(iii).b Boron carbide solid electrode $B_{3.86}C$ 357
5-1.5.(iii).c Boron carbide/carbon composite solid electrode $B_{3.11}C$ 357
5-1.5.(iii).d Boron carbide/carbon composite solid electrode $B_{2.56}C$ 369
5-1.5.(iii).e Graphite solid electrode 380
5-1.5.(iii).f Summary 380

5-1.5.(iv) The influence of boron carbide treatment on the Ir(IV) perchlorate system 387
5-1.5.(iv).a Without nitrogen aeration 387
5-1.5.(iv).b With nitrogen aeration 387
5-1.5.(iv).c Summary 395

5-1.5.(v) Spectrophotometry of Ir(IV) perchlorate 416

Page

5-1.6 Ir(IV) sulphate system 416

5-1.7 Ir(IV) phosphate system 429

5-2 Iron 429

5-2.1 Fe(III)-Fe(II) perchlorate system 429

5-2.1.(i) Effect of electrode composition on voltammetric properties 429

5-2.1.(ii) Effect of Ir(IV) perchlorate treatment on the working electrode 443

5-2.1.(iii) Summary 448

5-2.2 Fe(III)-Fe(II) chloride system 448

5-2.2.(i) D.c. voltammetry 450

5-2.2.(ii) Linear sweep and cyclic voltammetry 450

5-2.2.(iii) Summary 463

5-2.3 Fe(III)-Fe(II) cyanide system 472

5-2.3.(i) D.c. voltammetry 474

5-2.3.(ii) Cyclic voltammetry 480

5-2.3.(iii) Summary 500

5-3 Silver 521

5-3.1 D.c. voltammetry 521

5-3.2 Cyclic voltammetry 521

5-3.3 Summary 530

5-4 Copper 537

5-5 Palladium 542

5-6 Mixed Ion Solution 545

5-7 References 556

6. CONCLUSIONS 557

6-1 Chloroiridate-Chloroiridite System 557

6-2 Ir(IV) Perchlorate System 587

6-3 Ir(IV) Sulphate System 591

Page

6-4 Ir(IV) Phosphate System 592
6-5 Fe(III)-Fe(II) Perchlorate System 592
6-6 Fe(III)-Fe(II) Chloride System 594
6-7 Fe(III)-Fe(II) Cyanide System 594
6-8 Ag(I) Perchlorate System 596
6-9 Cu(II) Perchlorate System 597
6-10 Pd(II) Perchlorate System 597
6-11 Mixed Ion System 598
6-12 Summary 599

7. CUMULATIVE REFERENCES 600

8. APPENDIX 606
8-1 Derivation of the Current-Potential Curve for Processes Controlled both by the Rate of Charge Transfer and by the Mass-Transport Process involving a Solid Reductant 606

LIST OF TABLES AND SELECTED FIGURES

Table		Page
1-1	Potential limits of B_4C electrodes	24
1-2	Survey of voltammetry at boron carbide solid electrodes in inorganic aqueous systems	25
2-1	Electrode potentials of selected iridium species at 25°C	37
3-1	Variations of ΔE_p with charge-transfer parameters for cyclic voltammetry	60
5-1	Ir(IV)-Ir(III) chloroiridate/Perchloric acid supporting electrolyte system: Initial investigation of d.c. voltammetric performance of boron carbide solid electrodes	101
5-2	Initial investigation on the composition of boron carbide solid electrodes	102
5-3	Impurities in boron carbide	106
5-4	Ir(IV)-Ir(III) chloroiridate system: D.c. voltammetric performance of boron carbide solid electrodes with graphite enriched surfaces	111
5-5	Composition of boron carbide/carbon composite solid electrodes	112
5-6	Ir(IV)-Ir(III) chloroiridate system: Values of limiting current per unit area as a function of concentration of ammonium hexachloroiridate obtained at boron carbide/carbon composite solid electrodes	114
5-7	Ir(IV)-Ir(III) chloroiridate/Perchloric acid supporting electrolyte system: D.c. voltammetric performance of the graphite solid electrode	153
5-8	Ir(IV)-Ir(III) chloroiridate/Hydrochloric acid supporting electrolyte system: Values of limiting current per unit area as a function of concentration of ammonium hexachloroiridate obtained at boron carbide/carbon composite solid electrodes	160
5-9	Ir(IV) phosphate/Phosphoric acid-Perchloric acid supporting electrolyte system: D.c. voltammetry at the boron carbide solid electrode	431
5-10	Ir(IV) chloroiridate-Fe(III) chloride/Hydrochloric acid supporting electrolyte system: D.c. voltammetry of the mixture	551

		Page
6-1	Summary of d.c. voltammetric data	558
6-2	Summary of linear and cyclic sweep voltammetric data	572
6-3	Variation of standard electrode potentials with concentration of Ir(IV) perchlorate at 25 ^{o}C	588
6-4	Variation of standard electrode potentials for Ir(IV) perchlorate with concentration of perchloric acid at 25°C	589
6-5	Variation of the standard electrode potential for Fe(III) perchlorate with concentration of perchloric acid supporting electrolyte at 25 ^{o}C	593

Figure

3-2	Plots of current function, $i_p/v^{\frac{1}{2}}$ or $i/v^{\frac{1}{2}}$, versus $v^{\frac{1}{2}}$ for reversible and irreversible systems	57
3-6	Variation of peak current functions with rate of potential sweep	66
3-7	Rate of shift of potential as a function of scan rate	68
3-8	Ratio of anodic to cathodic peak current as a function of rate of potential sweep	68
3-14	Illustration of polarographic waves due to a reversible two-electron reduction complicated by adsorption	74
3-15	Theoretical cyclic voltammograms of reversible charge transfers involving adsorption	76
4-1	The solid working electrode	87
4-2	Saturated calomel electrode	87
4-4	Apparatus for the pyrohydrolysis of boron carbide	95
4-5	Apparatus for the determination of carbon	96
5-6	Absorption spectrum of 93.1% ± 0.2% pure boron carbide	108
5-7	Absorption spectrum of 96.7% ± 0.2% pure boron carbide	109
5-8	Absorption spectrum of 100% ± 0.2% pure boron carbide	110
5-14	(a) Residual current obtained at the anodically stripped boron carbide solid electrode. (b) Voltammogram of the reduction of chloroiridate at the anodically stripped boron carbide solid electrode. (c) Residual current obtained after Ir(IV) perchlorate (1.0×10^{-3} M) treatment of the boron carbide solid electrode. (d) Voltammogram of the reduction of chloroiridate after Ir(IV) perchlorate treatment of the boron carbide solid electrode	118
5-18	Perchloric acid (0.1 M) supporting electrolyte: Linear	

Page

sweep voltammograms at different scan rates, v, showing the presence of adsorbed species on the boron carbide solid electrode after treatment with Ir(IV) perchlorate (2.3×10^{-3} M) solution 120

5-23 Perchloric acid (0.1 M) supporting electrolyte: Cyclic voltammogram of adsorbed species on the boron carbide solid electrode which had been treated with Ir(IV) perchlorate (2.3×10^{-3} M) solution 126

5-30 Ir(IV)-Ir(III) chloroiridate (1.0×10^{-4} mol dm^{-3})/ Perchloric acid (0.1 M) supporting electrolyte system: Linear sweep voltammograms at the boron carbide solid electrode which had been treated with Ir(IV) perchlorate (2.3×10^{-3} M) solution 133

5-31 Ir(IV)-Ir(III) chloroiridate (1.0×10^{-4} mol dm^{-3})/ Perchloric acid (0.1 M) supporting electrolyte system: Cyclic voltammogram at the boron carbide solid electrode which had been treated with Ir(IV) perchlorate (2.3×10^{-3} M) solution 134

5-42 (a) Residual current after cathodic polarisation (at -1 V) in the supporting electrolyte. (b) D.c. voltammogram of the reduction of chloroiridate. (c) Reduction of chloroiridate after the boron carbide solid electrode had been cathodically polarised (at -1 V) in the sample solution. (d) Reduction of chloroiridate after the electrode had been cathodically polarised (at -1 V) in chloroiridate (2.0×10^{-3} M) solution 145

5-46 Ir(IV)-Ir(III) chloroiridate (8.0×10^{-5} mol dm^{-3})/ Perchloric acid (0.1 M) supporting electrolyte system: Linear sweep voltammograms at the boron carbide solid electrode which had been treated by cathodic polarisation (at -1 V) in chloroiridate (8.0×10^{-4} M) solution 148

5-49 Graphite solid electrode. (a) Residual current. (b) D.c. voltammogram of the reduction of chloroiridate 152

5-50 Ir(IV)-Ir(III) chloroiridate (1.0×10^{-4} mol dm^{-3})/ Perchloric acid (0.1 M) supporting electrolyte system: Linear sweep voltammetry at the graphite solid electrode 154

5-55 Boron carbide solid electrode treated with Ir(IV) perchlorate (1.0×10^{-3} M) solution. (a) Residual current. (b) D.c. voltammogram of the reduction of chloroiridate in HCl (0.1 M) supporting electrolyte 161

Page

5-56 Boron carbide solid electrode treated by cathodic polarisation (at -4 V vs SCE). (a) Residual current. (b) D.c. voltammogram of the reduction of chloroiridate, in HCl (0.1 M) supporting electrolyte, after cathodic polarisation in chloroiridate (8.0×10^{-4} M) 161

5-63 Boron carbide solid electrode treated with Ir(IV) perchlorate (1.0×10^{-3} M) solution. Linear sweep voltammetry: (a) Residual current and (b) electroreduction of chloroiridate in HCl (0.1 M) supporting electrolyte 168

5-78 Ir(IV)-Ir(III) chloroiridate (1.0×10^{-4} mol dm^{-3})/ Sodium perchlorate (0.1 M) supporting electrolyte system: (a) Residual current. (b) D.c. voltammogram of chloroiridate. (c) D.c. voltammogram of chloroiridate after the boron carbide solid electrode had been treated by cathodic polarisation (at -1 V vs SCE) in chloroiridate solution 184

5-82 Ir(IV)-Ir(III) chloroiridate (4.0×10^{-4} mol dm^{-3})/ Sodium perchlorate (0.1 M) supporting electrolyte system: Linear sweep voltammograms at the boron carbide solid electrode which had been treated by cathodic polarisation (at -1 V vs SCE) in chloroiridate 186

5-83 Ir(IV)-Ir(III) chloroiridate (2.0×10^{-3} mol dm^{-3})/ Sodium perchlorate (0.1 M) supporting electrolyte system: Cyclic voltammetry at the boron carbide solid electrode which had been treated by cathodic polarisation (at -1 V vs SCE) in chloroiridate 187

5-98 Absorption spectra of hexachloro-iridium(IV) ions 197

5-99 Ir(IV) perchlorate (1.0×10^{-4} mol dm^{-3})/Perchloric acid (0.1 M) supporting electrolyte system: D.c. voltammograms obtained at boron carbide solid electrodes, (a) $B_{4.05}C$ and (b) $B_{3.86}C$; and boron carbide/carbon composite solid electrodes, (c) $B_{3.77}C$, (d) $B_{3.69}C$, (e) $B_{3.53}C$, and (f) $B_{3.38}C$ 199

5-100 Ir(IV) perchlorate (1.0×10^{-4} mol dm^{-3})/Perchloric acid (0.1 M) supporting electrolyte system: D.c. voltammograms obtained at boron carbide/carbon composite solid electrodes, (g) $B_{3.24}C$, (h) $B_{3.11}C$, (i) $B_{2.98}C$, (j) $B_{2.76}C$, and (k) $B_{2.56}C$; and the graphite

		Page
	solid electrode, (1)	200
5-104	D.c. voltammograms obtained at the boron carbide solid electrode $B_{4.05}C$ for a concentration range of Ir(IV) perchlorate	205
5-108	D.c. voltammograms of Ir(IV) perchlorate (1.0×10^{-4} mol dm^{-3}) at the boron carbide solid electrode $B_{4.05}C$ in a concentration range of perchloric acid supporting electrolyte	208
5-112	D.c. voltammograms of Ir(IV) perchlorate (1.0×10^{-4} mol dm^{-3}) at the boron carbide solid electrode $B_{3.86}C$ in a concentration range of perchloric acid supporting electrolyte	214
5-116	Ir(IV) perchlorate (1.0×10^{-4} mol dm^{-3})/Perchloric acid (0.1 to 2.0 M) supporting electrolyte system: D.c. voltammograms at the boron carbide/carbon composite solid electrode $B_{3.11}C$	219
5-120	Ir(IV) perchlorate (1.0×10^{-4} mol dm^{-3})/Perchloric acid (0.1 to 2.0 M) supporting electrolyte system: D.c. voltammograms at the boron carbide/carbon composite solid electrode $B_{2.56}C$	223
5-124	Ir(IV) perchlorate (1.0×10^{-4} mol dm^{-3})/Perchloric acid (0.1 to 2.0 M) supporting electrolyte system: D.c. voltammograms at the graphite solid electrode	229
5-129	Ir(IV) perchlorate (1.0×10^{-4} mol dm^{-3})/Perchloric acid (0.1 M) supporting electrolyte system: Cyclic voltammograms obtained at the boron carbide solid electrode $B_{4.05}C$ over a range of potential sweep rates	238
5-135	Ir(IV) perchlorate (1.0×10^{-4} mol dm^{-3})/Perchloric acid (0.1 M) supporting electrolyte system: Linear sweep voltammograms obtained at the boron carbide solid electrode $B_{4.05}C$ - variation with sweep rate	245
5-154	Ir(IV) perchlorate (1.0×10^{-4} mol dm^{-3})/Perchloric acid (0.1 M) supporting electrolyte system: Linear sweep voltammograms obtained at the boron carbide solid electrode $B_{3.86}C$ over a range of sweep rates	263
5-164	Ir(IV) perchlorate (1.0×10^{-4} mol dm^{-3})/Perchloric acid (0.1 M) supporting electrolyte system: Linear sweep voltammograms obtained at the boron carbide/carbon composite solid electrode $B_{3.77}C$ over a	

		Page
	range of sweep rates	273
5-168	Ir(IV) perchlorate (1.0×10^{-4} mol dm^{-3})/Perchloric acid (0.1 M) supporting electrolyte system: Cyclic and linear sweep voltammograms obtained at the boron carbide/carbon composite solid electrode $B_{3.69}C$	277
5-172	Ir(IV) perchlorate (1.0×10^{-4} mol dm^{-3})/Perchloric acid (0.1 M) supporting electrolyte system: Cyclic and linear sweep voltammograms obtained at the boron carbide/carbon composite solid electrode $B_{3.53}C$	280
5-177	Ir(IV) perchlorate (1.0×10^{-4} mol dm^{-3})/Perchloric acid (0.1 M) supporting electrolyte system: Cyclic and linear sweep voltammograms obtained at the boron carbide/carbon composite solid electrode $B_{3.38}C$	285
5-181	Ir(IV) perchlorate (1.0×10^{-4} mol dm^{-3})/Perchloric acid (0.1 M) supporting electrolyte system: Cyclic and linear sweep voltammograms obtained at the boron carbide/carbon composite solid electrode $B_{3.24}C$	290
5-186	Ir(IV) perchlorate (1.0×10^{-4} mol dm^{-3})/Perchloric acid (0.1 to 2.0 M) supporting electrolyte system: Linear sweep voltammograms obtained at the boron carbide/carbon composite solid electrode $B_{3.11}C$	294
5-196	Ir(IV) perchlorate (1.0×10^{-4} mol dm^{-3})/Perchloric acid (0.1 M) supporting electrolyte system: Cyclic and linear sweep voltammograms obtained at the boron carbide/carbon composite solid electrode $B_{2.98}C$	305
5-200	Ir(IV) perchlorate (1.0×10^{-4} mol dm^{-3})/Perchloric acid (0.1 M) supporting electrolyte system: Cyclic and linear sweep voltammograms obtained at the boron carbide/carbon composite solid electrode $B_{2.76}C$	309
5-204	Ir(IV) perchlorate (1.0×10^{-4} mol dm^{-3})/Perchloric acid (0.1 to 2.0 M) supporting electrolyte system: Linear sweep voltammograms obtained at the boron carbide/carbon composite solid electrode $B_{2.56}C$	314
5-214	Ir(IV) perchlorate (1.0×10^{-4} mol dm^{-3})/Perchloric acid (0.1 M) supporting electrolyte system: Cyclic and linear sweep voltammograms obtained at the graphite solid electrode	324
5-220	Ir(IV) perchlorate (1.0×10^{-4} mol dm^{-3}): Linear sweep voltammograms obtained at the graphite solid electrode - variation with concentration of perchloric	

		Page
	acid supporting electrolyte	331
5-225	Linear sweep voltammograms for the residual current obtained at the boron carbide solid electrode $B_{4.05}C$	336
5-226	Perchloric acid (0.1 M) supporting electrolyte: Cyclic and linear sweep voltammograms obtained at the boron carbide solid electrode $B_{4.05}C$ which had been treated with Ir(IV) perchlorate	337
5-230	Perchloric acid (0.1 M): Linear sweep voltammograms for the residual current (A to C) and cyclic voltammograms for the adsorbed Ir(IV) perchlorate species (D to F) obtained at the graphite solid electrode	342
5-234	Nitrogen aerated (16 hours) Ir(IV) perchlorate (8.0×10^{-4} mol dm^{-3})/Perchloric acid (0.1 M) supporting electrolyte system: D.c. voltammograms obtained at boron carbide, boron carbide/carbon composite, and graphite solid electrodes	349
5-238	Nitrogen aerated (16 hours) Ir(IV) perchlorate (8.0×10^{-4} mol dm^{-3})/Perchloric acid (0.1 M) supporting electrolyte system: Linear sweep voltammograms obtained at the boron carbide solid electrode $B_{4.05}C$	355
5-242	Ir(IV) perchlorate (8.0×10^{-4} mol dm^{-3})/Perchloric acid (0.1 M) supporting electrolyte system: Linear sweep voltammograms obtained at the boron carbide solid electrode $B_{3.86}C$ - variation with sweep rate. A, B, and C: sample as prepared. D, E, and F: sample aerated with nitrogen for 16 hours	361
5-246	Ir(IV) perchlorate (8.0×10^{-4} mol dm^{-3})/Perchloric acid (0.1 M) supporting electrolyte system: Linear sweep voltammograms obtained at the boron carbide/carbon composite solid electrode $B_{3.11}C$ - variation with sweep rate. A to D inclusive: sample as prepared. E to H inclusive: sample aerated with nitrogen for 16 hours	368
5-250	Ir(IV) perchlorate (8.0×10^{-4} mol dm^{-3})/Perchloric acid (0.1 M) supporting electrolyte system: Linear sweep voltammograms obtained at the boron carbide/carbon composite solid electrode $B_{2.56}C$ - variation with sweep rate. A to C inclusive: sample as prepared. D to F inclusive: sample aerated with nitrogen for 16 hours	376

		Page
5-254	Nitrogen aerated (16 hours) Ir(IV) perchlorate (8.0×10^{-4} mol dm^{-3})/Perchloric acid (0.1 M) supporting electrolyte system: Linear sweep voltammograms obtained at the graphite solid electrode	383
5-258	Ir(IV) perchlorate (2.3×10^{-3} mol dm^{-3})/Perchloric acid (0.1 M) supporting electrolyte system: Linear sweep voltammograms obtained at the boron carbide solid electrode $B_{3.86}C$ - variation with sweep rate. A to C inclusive: sample as prepared. D to F inclusive: sample treated by prolonged contact with boron carbide	388
5-262	Ir(IV) perchlorate (2.0×10^{-4} mol dm^{-3})/Perchloric acid (0.1 M) supporting electrolyte system: Linear sweep and cyclic voltammograms obtained at the boron carbide solid electrode $B_{3.86}C$. A & D: sample solution as prepared. B & E: sample solution aerated with nitrogen for 16 hours. C & F: nitrogen aerated sample was treated with boron carbide for 2 minutes	396
5-270	Absorption spectra of Ir(IV) perchlorate	417
5-271	Ir(IV) sulphate (1.0×10^{-4} mol dm^{-3})/Sulphuric acid (0.05 M) supporting electrolyte system: Cyclic voltammograms obtained at the boron carbide solid electrode	418
5-272	Ir(IV) sulphate (1.0×10^{-4} mol dm^{-3})/Sulphuric acid (0.05 to 0.4 M) supporting electrolyte system: Cyclic voltammograms obtained at the boron carbide solid electrode	419
5-285	Ir(IV) phosphate (5.2×10^{-4} mol dm^{-3})/Phosphoric acid (0.32 M)-Perchloric acid (0.1 M) supporting electrolyte system: A. D.c. voltammogram; B-G. Linear sweep voltammograms obtained at the boron carbide solid electrode	430
5-289	Fe(III) perchlorate (1.0×10^{-3} mol dm^{-3})/Perchloric acid (0.1 M) supporting electrolyte system: (A) d.c. voltammogram, and (B) cyclic voltammogram obtained at the boron carbide solid electrode $B_{3.86}C$	434
5-308	Fe(III) chloride (2×10^{-3} M)/Hydrochloric acid (0.1 M) supporting electrolyte system: A) d.c. voltammogram, and B) cyclic voltammogram obtained at the boron carbide solid electrode $B_{4.04}C$	449

Page

5-330 Fe(III) cyanide (2.0×10^{-4} mol dm^{-3})/Potassium chloride (0.5 M) supporting electrolyte system: D.c. voltammograms (A & B) and cyclic voltammograms (C & D) obtained at the boron carbide solid electrode 473

5-374 Ag(I) perchlorate (2.0×10^{-5} mol dm^{-3})/Sodium perchlorate (0.1 M) supporting electrolyte system: D.c. voltammograms (A & B) and cyclic voltammogram (C) obtained at the boron carbide solid electrode 522

5-393 Cu(II) sulphate (2.0×10^{-4} mol dm^{-3})/Sodium perchlorate (0.1 M) supporting electrolyte system: D.c. voltammograms obtained at the boron carbide solid working electrode 538

5-394 Cu(II) sulphate (2.0×10^{-4} mol dm^{-3})/Sodium perchlorate (0.1 M) supporting electrolyte system: Cyclic voltammograms obtained at the boron carbide solid working electrode 539

5-401 Pd(II) perchlorate (4.0×10^{-4} mol dm^{-3})/Perchloric acid (2.0 M) supporting electrolyte system: D.c. voltammograms obtained at the boron carbide solid working electrode 544

5-402 Pd(II) perchlorate (4.0×10^{-4} mol dm^{-3})/Perchloric acid (2.0 M) supporting electrolyte system: Cyclic voltammograms, at different sweep rates, obtained at the boron carbide solid working electrode 546

5-407 Pd(II) perchlorate (4.0×10^{-4} mol dm^{-3})/Perchloric acid (2.0 M) supporting electrolyte system: (a) Cyclic voltammogram for the residual current, and (b) multiple cyclic sweep voltammogram obtained at the boron carbide solid working electrode which had been treated with aqua regia 549

5-408 Ir(IV) chloroiridate (1.0×10^{-4} mol dm^{-3})-Fe(III) chloride (1.0×10^{-4} mol dm^{-3})/Hydrochloric acid (0.1 M) supporting electrolyte system: A) d.c. voltammogram obtained at the boron carbide solid working electrode, B) d.c. voltammogram obtained after treatment of boron carbide electrode by cathodic polarisation (at -3.9 V vs SCE) in the sample, and C) & D) cyclic voltammograms 550

LIST OF SYMBOLS AND ABBREVIATIONS

α	charge-transfer coefficient
β	Henry's law adsorption coefficient, unless stated otherwise
β'	Langmuir adsorption coefficient
δ	Nernst diffusion-layer thickness
Γ	surface concentration
Γ^s	saturation value of the surface concentration at maximum surface coverage
μ	reaction-layer thickness
ϕ_2	potential of the outer Helmholtz plane
A	area of the working electrode, unless stated otherwise
a	mean distance of approach of ions
ads	adsorbed; where (s) = strongly, (m) = moderately strongly, and (w) = weakly
ANOVA	analysis of variance
AUX	auxiliary (or counter) electrode
C	concentration; where superscripts b and e refer to conditions in the bulk solution and at the electrode surface respectively
C_d	differential capacity of the electric double-layer
D	diffusion coefficient
DME	dropping mercury electrode
E	electrode potential
e	electron
E^o	standard electrode potential
$E^{o'}$	formal electrode potential
$E_{\frac{1}{2}}$	half-wave potential
E_i	initial potential
E_λ	switching potential in cyclic voltammetry
E_p	peak potential
$E_{p/2}$	half-peak potential
e.a.s.	electroactive species
F	Faraday constant (9.64867×10^4 C mol^{-1})
f	activity coefficient
FET	field effect transistor
HMDE	hanging mercury drop electrode
I	ionic strength, unless stated otherwise
i	current, unless stated otherwise
i_c	capacity current, or catalytic current, unless stated otherwise

i_L	limiting current
i_{max}	maximum current (i_L or i_p)
i_p	peak current
k	formal rate constant of a chemical reaction
k_f, k_b	chemical reaction rate constants
k'_f	pseudo first-order chemical reaction rate constant
k^o	standard electrode reaction rate constant
k_s, k'_s	standard heterogeneous rate constant for the charge transfer at $E = E^o$
k'	charge-transfer rate constant at $E = E^{o'}$
k_{Red}	electrode reaction rate constant
MFE	mercury film electrode
n	number of electrons
O	oxidant
OA	operational amplifier
p	statistical level of significance
R	reductant, or gas constant (8.31434 J K^{-1} mol^{-1}), unless stated otherwise
RDE	rotating disk electrode
RDGE	rotating disk graphite electrode
REF	reference electrode
SCE	saturated calomel electrode
SHE	standard hydrogen electrode
SMDE	sitting mercury drop electrode
soln	solution
T	absolute temperature
t	time elapsed since the commencement of the linear potential sweep
TTE	turbulent tubular electrode
v	rate of potential change, sweep rate
WE	working electrode
w%	weight per cent
Z	electroinactive species
z	ionic charge

POTENTIALS AND SIGN CONVENTION

The electrode reactions are reported in the sense of reductions, according to the general scheme

$$Ox + ne^- \rightleftharpoons Red$$

where Ox symbolizes the whole system in the oxidised state, while Red represents the same system in the reduced state. This is in conformity with the 'European Convention', and the IUPAC 'Stockholm Convention' of 1953.

All E° and $E^{\circ\prime}$ values are quoted with reference to the SHE, whereas the experimental $E_{\frac{1}{2}}$, E_p, and $E_{p/2}$ values have been reported with reference to the SCE unless stated otherwise.

1. INTRODUCTION

1-1 General Introduction

Voltammetry within the negative potential range is dominated by the use of mercury working electrodes, DME in polarography, HMDE, SMDE, and MFE (where a film of mercury is electrolytically deposited on a noble metal or graphite support), because of the distinct advantages of mercury over other materials. These advantages include: (i) the high overpotential of hydrogen on mercury, (ii) mercury amalgamates with many metals thereby lowering their reduction potential, (iii) the diffusion current assumes a steady state value immediately and is reproducible, and (iv) in the case of the DME, the surface is constantly and reproducibly renewed thus eliminating passivity or poisoning effects; although a self-cleaning RDGE has recently been employed[1.1, 1.2]. In neutral solutions, the useful potential range of mercury is approximately from -2.5 to +0.2 V (vs SCE); the anodic limiting background potential being caused by the dissolution of mercury.

Alternative working electrode materials, which can be applied within the positive potential range, include Pt, Au, Ag, C, and B_4C. The potential ranges of several electrode materials in aqueous solutions are presented in Fig. 1-1[1.3].

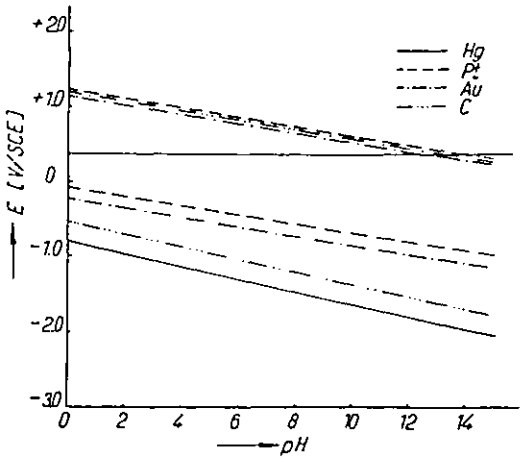

Fig. 1-1 Schematic representation of potential ranges of several electrode materials in aqueous solutions, assuming that the potential limits are determined only by the electrode reactions of H_2 and O_2 or Hg dissolution (without complex or precipitate formation).

Noble metal electrodes and, to a lesser degree, the graphite solid electrode suffer from the relative ease of oxidation of their surfaces at high positive potentials; and Pt also adsorbs the H_2 produced from the reduction of hydrogen ions at sufficiently cathodic potentials[1.3, 1.4]. Chemical treatment of these electrodes is also known to affect their subsequent voltammetric behaviour[1.5]. The boron carbide (B_4C) solid electrode, introduced by Mueller et al[1.6, 1.7], is reported to be characterised by extreme inertness, low residual currents, and a wide potential range (Table 1-1)[1.6].

Table 1-1 Potential limits of B_4C electrodes

Medium	Anodic (V vs SCE)	Cathodic (V vs SCE)
H_2SO_4 (1 M)	+1.13	-0.9
HCl (1 M)	+1.0	-0.9
KCl (0.4 M)	+1.0	-1.6
NaOH (0.2 M)	+0.4	-1.67
Na_2CO_3 (0.1 M)	+0.6	-1.6

1-2 Boron Carbide Solid Electrodes

The history of the voltammetric application of boron carbide solid electrodes has been one of controversy over its effectiveness as a working electrode. A survey of the inorganic aqueous systems which have been investigated at the boron carbide solid working electrode by previous researchers is presented in Table 1-2.

Mueller et al[1.6, 1.7] successfully applied the B_4C ("Norbide", a pressure-sintered 99+% B+C product from the Norton Company[1.8]) as a solid working electrode in the voltammetry of several organic and inorganic aqueous systems; at a linear sweep rate of $3\frac{1}{3}$ mV s^{-1}. Subsequently, Sawyer and Seo[1.9] were also successful in applying linear sweep voltammetry (at a sweep rate of 5 mV s^{-1}) at the "Norbide" solid electrode in their study of the reduction of dissolved oxygen. They concluded that, with respect to the reduction of dissolved oxygen, the boron carbide electrode behaved similarly to a pre-reduced Pt electrode. Furthermore, they also reported that dissolved hydrogen was not oxidised

Table 1-2 Survey of voltammetry at boron carbide solid electrodes in inorganic aqueous systems.

Electroactive species	Supporting electrolyte	Researchers (chronologically from left to right): Mueller et al[1.6, 1.7]	Sawyer & Seo[1.9]	Mountcastle[1.10]	Hartley & Axelrod[1.11]	Jackson & Pantony[4.5, 1.12]	Alder et al[1.13]	Blaedel & Schieffer[1.14]
Cu(II)	KCl (1 M, pH 3-4)	•	-	-	-	-	-	-
	KCl (1 M)	-	-	-	•	-	-	-
	KCl (0.5 M, pH 4.4 -5.4)	•	-	-	-	-	-	-
	$NaClO_4$ (0.1 M)	-	-	-	-	•	-	-
	Na_2SO_4 (0.1 M)	-	-	-	-	•	-	-
	Na_3Cit (0.5 M, pH 4.6)	•	-	-	-	-	-	-
	$Na_4P_2O_7$ (0.1 M, pH 4.7)	•	-	-	-	-	-	-
	H_2SO_4 (1 M)	•	-	-	-	-	-	-
	H_2SO_4 (0.5 M)	-	-	•	-	-	-	-
	HNO_3 (1 M)	-	-	•	-	-	-	-
	HCl (1 M)	-	-	•	-	-	-	-
Ag(I)	KNO_3 (0.1 M)	•	-	-	-	-	-	-
	$NaClO_4$ (0.1-1 M)	-	-	-	-	•	-	-
	Na_2SO_4 (0.1 M)	-	-	-	-	•	-	-
$Zn(OH)_4^{--}$	NaOH (0.1 M)	•	-	-	-	-	-	-
Cd(II)	NH_4OH (8 M)	-	-	•	-	-	-	-
	KCl (1 M)	-	-	-	•	-	-	-
Tl(I)	KCl (0.1 M)	•	-	-	-	-	-	-
	NaOH (1 M)	•	-	-	-	-	-	-

Table 1-2 (continued)

Electroactive species	Supporting electrolyte	Researchers (chronologically from left to right): Mueller et al[1.6, 1.7]	Sawyer & Seo[1.9]	Mountcastle[1.10]	Hartley & Axelrod[1.11]	Jackson & Pantony[4.5, 1.12]	Alder et al[1.13]	Blaedel & Schieffer[1.14]
Tl_2O_3	NaOH (1 M)	*	-	-	-	-	-	-
Sn(II)	NH_4Cl (4 M)/							
	HCl (1 M)	*	-	-	-	-	-	-
	KCl (1 M)	*	-	-	-	-	-	-
	HCl (1 M)	*	-	-	-	-	-	-
Pb(II)	KNO_3 (0.1 M)	*	-	-	-	-	-	-
	HNO_3 (1 M)	-	-	*	-	-	-	-
Sb(V)	HCl (20 v/v %)	-	-	*	-	-	-	-
O_2	Britton-Robinson							
(dissolved)	buffers.	-	*	-	-	-	-	-
	NaOH (1 M)	-	*	-	-	-	-	-
	K_2SO_4 (0.1 M)	-	*	-	-	-	-	-
	KCN (0.1 M)	-	*	-	-	-	-	-
	KI (0.1 M)	-	*	-	-	-	-	-
O_2	H_2SO_4 (1 M)	-	-	-	*	-	-	-
(adsorbed &	KCl (1 M)	-	-	-	*	-	-	-
chemisorbed)	NaOH (1 M)	-	-	-	*	-	-	-
H^+	HNO_3 (1 M)	-	-	*	-	-	-	-
	HCl (1 M)	-	-	*	-	-	-	-
	H_2SO_4 (0.5 M)	-	-	*	-	-	-	-
$Cr_2O_7^{--}$	KCl (1 M)	-	-	-	*	-	-	-

Table 1-2 (continued)

Electroactive species	Supporting electrolyte	Researchers (chronologically from left to right): Mueller et al[1.6, 1.7]	Sawyer & Seo[1.9]	Mountcastle[1.10]	Hartley & Axelrod[1.11]	Jackson & Pantony[4.5, 1.12]	Alder et al[1.13]	Blaedel & Schieffer[1.14]
BrO_3^-	H_2SO_4 (1 M)	-	-	-	*	-	-	-
I^-	H_2SO_4 (1 M)	*	-	-	-	-	-	-
IO_3^-	H_2SO_4 (1 M)	*	-	-	*	-	-	-
	KCl (1 M)	-	-	-	*	-	-	-
Mn(II)	HAc (0.1 M)	*	-	-	-	-	-	-
Fe(III)	H_2SO_4 (0.5 M)	-	-	*	-	-	-	-
	HNO_3 (1 M)	-	-	*	-	-	-	-
	$HClO_4$ (0.1-1 M)	-	-	-	-	*	-	-
	HCl (0.05-1 M)	-	-	-	-	*	-	-
Fe(II)	HCl (1 M)	*	-	-	-	-	-	-
$[Fe(CN)_6]^{3-}$	KCl (1 M)	-	-	-	*	-	-	-
	KCl (0.5 M)	*	-	-	-	-	-	-
	Phosphate (0.005 M, pH 6.6)/KCl (0.1 M)	-	-	-	-	-	-	*
	Phosphate (0.1 M) buffer (pH 7.5).	-	-	-	-	-	-	*
$[Fe(CN)_6]^{4-}$	KCl (0.5 M)	*	-	-	-	-	-	-
	KCl (1 M)	-	-	-	*	-	-	-
	Phosphate (0.1 M) buffer.	-	-	-	-	-	-	*
	Not stated.	-	-	-	-	-	*	-
Co(III)	NH_4OH (8 M)	-	-	*	-	-	-	-

Table 1-2 (continued)

Electroactive species	Supporting electrolyte	Researchers (chronologically from left to right): Mueller et al[1.6, 1.7]	Sawyer & Seo[1.9]	Mountcastle[1.10]	Hartley & Axelrod[1.11]	Jackson & Pantony[4.5, 1.12]	Alder et al[1.13]	Blaedel & Schieffer[1.14]
Ni(II)	NH_4OH (8 M)	-	-	*	-	-	-	-
Ru(IV)	H_2SO_4 (0.5 M)	-	-	*	-	-	-	-
Pd(II)	$HClO_4$ (0.1-1 M)	-	-	-	-	*	-	-
	NaCl (0.01-0.1 M)	-	-	-	-	*	-	-
	Li_2SO_4 (0.1-1 M)	-	-	-	-	*	-	-
$(NH_4)_2IrCl_6$	$HClO_4$ (0.1-1 M)	-	-	-	-	*	-	-
	$NaClO_4$ (0.1-1 M)	-	-	-	-	*	-	-
	$NaNO_3$ (0.1 M)	-	-	-	-	*	-	-
K_2IrBr_6	$HClO_4$ (0.1-1 M)	-	-	-	-	*	-	-
	$NaClO_4$ (0.1-1 M)	-	-	-	-	*	-	-
	NaBr (0.1-0.7 M)	-	-	-	-	*	-	-
Ir(IV) perchlorate.	$HClO_4$ (0.1-1 M)	-	-	-	-	*	-	-
Ir(IV) sulphate.	H_2SO_4 (0.36 M)	-	-	-	-	*	-	-
U(VI)	H_2SO_4 (0.5 M)	-	-	*	-	-	-	-

NOTE: * denotes the researcher(s).

at boron carbide.

Further evaluation of the effectiveness of "Norbide", including "Norbide" material obtained via Mueller and Adams[1.6-1.8], as a working electrode material was conducted by Mountcastle[1.10]. These linear sweep voltammetric studies, at a sweep rate of $1\frac{2}{3}$ mV s^{-1}, of several inorganic aqueous systems proved to be of limited success; broad maxima being obtained, and only the peak currents of the Fe(III) and U(VI) systems exhibited a linear concentration dependence.

By employing boron carbide material from the Carborundum Company, Hartley and Axelrod[1.11] also tried to confirm the work of Mueller et al but came to the conclusion that the boron carbide solid electrode had little utility in electrochemical analysis; the general electrode response and reproducibility being very poor. Voltammetry, at sweep rates ranging from slow to fast (100 mV s^{-1}, and even 1.0 V s^{-1}), showed that the electron charge transfers were poorly reversible, peak potentials were influenced by sweep rate, and peak currents were low and irreproducible. Furthermore, pre-treatment of the boron carbide working electrode influenced its subsequent voltammetric performance.

In contrast, Jackson and Pantony[4.5, 1.12] successfully investigated the electrochemistry of some platinum group metals, mainly iridium and palladium, at the "Norbide" solid working electrode. The technique of d.c. voltammetry, at a scan rate of 2.5 mV s^{-1}, in stirred solutions was employed in the examination of several iridium and palladium aqueous systems as well as a few aqueous systems of non-platinum group metals for comparison. Later investigations, however, revealed a deterioration in the applicability and reproducibility of boron carbide as solid working electrodes[4.2].

Alder et al[1.13] included boron carbide in their evaluation of electrode materials for solid electrode voltammetry. The anodic cyclic voltammograms, obtained at a sweep rate of 5 mV s^{-1}, for ferrocyanide were not very reproducible. Blaedel and Schieffer[1.14] also included boron carbide in their investigation of the ferricyanide/ferrocyanide system with the RDE (at 50-3000 rpm) and the TTE (at 2.69 cm^3 min^{-1}). The electron charge transfer was found to be poorly reversible and a hysteresis effect was observed. They concluded, however, that because of the low residual current obtained the B_4C TTE would be useful in trace analysis.

1-3 Summary

The survey of previous research, concerning the application of boron carbide solid working electrodes in voltammetry, reveals that only eight (Cu(II), Ag(I), Cd(II), Pb(II), O_2-dissolved, -adsorbed, or -chemisorbed, IO_3^-, Fe(III)/Fe(II), and ~~$[Fe(CN)_6]^{3-}/[Fe(CN)_6]^{4-}$~~) out of all the e.a.s. listed in Table 1-2 have been investigated by two or more research groups; and even then not necessarily in comparable supporting electrolyte systems. Most of the researchers employed linear sweep voltammetry or cyclic voltammetry; the exceptions being Jackson and Pantony[4.5, 1.12] who employed d.c. voltammetry in stirred solutions, and Blaedel and Schieffer[1.14] who employed the RDE. Moreover, most investigators reported results obtained with only a single scan rate (within the range $1\frac{2}{3}$-5 mV s^{-1}); although Hartley and Axelrod[1.11] did employ sweep rates as fast as 1 V s^{-1}. Therefore, in terms of the type of e.a.s./supporting electrolyte system, scan rate, and voltammetric method, the results obtained by different research groups are not strictly comparable. It is also apparent that the boron carbide used by different research groups was not necessarily obtained from the same source; although the "Norbide" material has been shown to be more effective in voltammetry[1.6-1.10, 1.12, 4.5].

In view of the criticisms above, it was decided: (i) to investigate the voltammetric performance of boron carbide solid working electrodes with respect to electrode B:C composition; (ii) to employ d.c. voltammetry in stirred solutions, complementing with linear sweep and cyclic voltammetry; (iii) whenever appropriate, to employ a wide range of scan rates; (iv) where appropriate, to employ a spectrographic grade graphite solid working electrode for comparison; and (v) to concentrate the investigations on inorganic aqueous systems which have been successfully studied, but widen the concentration range of both the e.a.s. and the supporting electrolyte.

1-4 References

1.1 Kulev I. and Stanev D.; God. Vissh. Khim. - Tekhnol. Inst., Burgas, Bulg. 1980 (Pub. 1981). 15, Pt 1, 27-36.

1.2 Kulev I. and Stanev D.; Collection Czech. Chem. Commun. 1981, 46 (12), 3183-5.

1.3 Vydra F., et al; Electrochemical Stripping Analysis, Chapter 2, 2.4. Ellis Horwood Ltd., 1976.

1.4 Adams R. N.; Electrochemistry at Solid Electrodes, Chapter 2. Dekker, New York, 1969.

1.5 Ibid, Chapter 7.

1.6 Mueller T. R., et al; Advances in Polarography, Vol I, Proc. 2nd International Congr. of Polarography, Cambridge, 1959.

1.7 Mueller T. R. and Adams R. N.; Anal. Chim. Acta, 1960, 23, 467.

1.8 Norton Co.; Moulding of Boron Carbide, British Patent 439,529 (9th Dec., 1935).

1.9 Sawyer D. T. and Seo E. T.; J. Electroanal. Chem., 1962, 3, 410.

1.10 Mountcastle W. R., Jr.; Anal. Chim. Acta, 1965, 32, 332-338.

1.11 Hartley A. M. and Axelrod H. D.; J. Electroanal. Chem., 1968, 18, 115-121.

1.12 Jackson E. and Pantony D. A.; J. Appl. Electrochem., 1971, 1, 283-291.

1.13 Alder J. F., et al; J. Electroanal. Chem., 1971, 30, 427.

1.14 Blaedel W. J. and Schieffer G. W.; J. Electroanal. Chem. Interfacial Electrochem., 1977, 80(2), 259-71.

4.2 Jackson E. and Pantony D. A.; J. Appl. Electrochem., 1972, 2, 353.

4.5 Ibid, 1971, 1, 113.

2. CHEMISTRY AND ELECTROCHEMISTRY OF SELECTED INORGANIC AQUEOUS SYSTEMS

2-1 Iridium

Iridium species that contain iridium in oxidation states ranging from 0 to +6 have been characterised, but nitrosyls formally containing Ir(-I) and Ir(-II) are also known[2.1]. The aqueous chemistry of iridium, however, centres mainly around the oxidation states of I, III, and IV[2.2]; with Ir(III) and Ir(IV) being more common[2.1]. Ir(I) involves square and 5-coordinate species which are invariably prepared by some form of reduction, either of similar Ir(III) complexes or of halide complexes such as K_2IrCl_6 in the presence of the complexing ligand. An important feature of the chemistry of Ir(I) is that it undergoes oxidative-addition reactions to form octahedral Ir(III) species which are stable. Ir(III) forms a large number of cationic, neutral, and anionic octahedral complexes. The reduction of Ir(III) leads to the metal, or to Ir(I) hydridic species when π-bonding ligands are involved. The conversion of Ir(III) complexes to Ir(IV) complexes, or vice versa, could very easily occur.

2-1.1 Chloroiridate-chloroiridite system

In basic solution the reaction:

$$2[IrCl_6]^{2-} + 2OH^- \rightleftharpoons 2[IrCl_6]^{3-} + \tfrac{1}{2}O_2 + H_2O \qquad (2\text{-}1)$$

occurs spontaneously within minutes[2.3, 2.4]. When maintained (15-30 minutes) at 100 °C in NaCl (0.5 M)/NaOH (pH 12), $[IrCl_6]^{2-}$ is reported to be hydrolysed to $[Ir(OH)_6]^{2-}$ (spectrophotometric absorption peak at 313 nm)[2.5]. From known potentials the acid reaction can be expressed as[2.2]:

$$2[IrCl_6]^{2-} + H_2O = 2[IrCl_6]^{3-} + \tfrac{1}{2}O_2 + 2H^+ \qquad (2\text{-}2)$$

and $K = 7 \times 10^{-8}$ $atm^{\frac{1}{2}}$ mol^2 l^{-2} (25 °C). Thus in strong acid, such as HCl (12 M), $[IrCl_6]^{3-}$ is partially oxidised to $[IrCl_6]^{2-}$ in the cold and completely on heating. In contrast, $[IrCl_6]^{2-}$ is rapidly and quantitatively reduced to $[IrCl_6]^{3-}$ in strong base (pH > 11); but the reduction is slow, although spontaneous, in neutral solutions. The $[IrCl_6]^{2-}$

ion seems to be rather stable in dilute HCl at room temperature[2.6, 2.7]. At the higher temperature of 50 °C, the $[IrCl_6]^{2-}$ ion is reported to undergo the aquation reaction[2.8]:

$$[IrCl_6]^{2-} + H_2O \rightleftharpoons [Ir(OH_2)Cl_5]^{-} + Cl^{-} \qquad (2\text{-}3)$$

in 1.0-2.5 M $HClO_4$ or HCl. Spectral evidence for the presence of the chlorohydroxy species $[IrCl_4(OH)_2]^{2-}$ and $[IrCl_2(OH)_4]^{2-}$ in solutions of $[IrCl_6]^{2-}$/HCl (< 1 M) has been obtained[2.9].

The $[IrCl_6]^{3-}$ ion, however, is reported to undergo aquation even at room temperature or below[2.7, 2.10, 2.28]:

$$[IrCl_6]^{3-} + H_2O \rightleftharpoons [Ir(OH_2)Cl_5]^{2-} + Cl^{-} \qquad (2\text{-}4)$$

in $HClO_4$ (≤ 1 M), HCl (1 M), or NaCl (1 M). Studies at higher temperatures (≥ 40 °C) have revealed that the aquation reaction proceeds further[2.8, 2.11]:

$$[Ir(OH_2)Cl_5]^{2-} + H_2O \rightleftharpoons [Ir(OH_2)_2Cl_4]^{-} + Cl^{-} \qquad (2\text{-}5)$$

in 1.0-2.5 M $HClO_4$ or HCl. The species $[Ir(OH_2)_2Cl_4]$, $[Ir(OH_2)_3Cl_3]$, and $[Ir(OH_2)_3Cl_3]^{+}$ have also been characterised. The spectrum of $[Ir(OH_2)_3Cl_3]^{+}$ has absorption maxima at 373 and 510 nm. Aquation studies of $[IrCl_6]^{3-}$ in concentrated $HClO_4$ (4 and 6 M) solutions at 42-70 °C have shown that the $[Ir(OH_2)Cl_5]^{2-}$ species can also react as follows (2.12):

$$[IrCl_6]^{2-} + [Ir(OH_2)Cl_5]^{2-} \rightleftharpoons [IrCl_6]^{3-} + [Ir(OH_2)Cl_5]^{-} \qquad (2\text{-}6)$$

Single-, double-, and triple-charged cations have been shown to inhibit the aquation of $[IrCl_6]^{3-}$ by forming ion-pairs, such as $[M^{3+}.IrCl_6^{3-}]$ (2.13-2.16). The aquation and hydrolysis of $[IrCl_6]^{2-}$ and $[IrCl_6]^{3-}$ have also been studied by the use of radioactive labelled ^{36}Cl and ^{192}Ir (2.17, 2.18).

2-1.2 Ir(IV)-Ir(III) perchlorate system

Ir(IV) perchlorate solution has been prepared by the evaporation of $[IrCl_6]^{2-}$ or $[IrCl_6]^{3-}$ with $HClO_4$ (50%, 60%, or 72%) to strong fumes resulting in a red-violet product[2.6, 2.19, 2.20, 4.3-4.5]. The spectrum of Ir(IV) perchlorate has an absorption maximum at 500 nm[2.20, 4.4]. The potentiometric titration of Ir(IV) perchlorate against $C_6H_6O_2$

or $(NH_4)_2SO_4.FeSO_4.6H_2O$ (Mohr's salt), at a platinum indicator electrode (vs SCE), produced non-stoichiometric titres[2.19, 2.20, 4.3]; which were attributed to the presence of soluble reduction products (Cl_2O and Cl_2) of $HClO_4$. Two end-points were obtained: (i) the first end-point corresponded to the titration of one of the reduction products of $HClO_4$ and required less than one equivalent of titrant; (ii) the second end-point corresponded to the simultaneous titration of the other reduction product of $HClO_4$ and Ir(IV) perchlorate, requiring between one and two equivalents of titrant relative to the first end-point[2.20, 4.3]. Attempts to remove the Cl_2O and Cl_2 soluble species by heating the solution at 82 °C to boiling point failed[2.20, 4.3]; neither was the treatment by nitrogen aeration successful[4.3]. Nitrogen aeration of the nearly boiling iridium solution, however, was successful after 8 hours; thus removing the first end-point and achieving a stoichiometric one-electron reduction at the second end-point[4.3]. Ion-exchange tests revealed that the Ir(IV) species was cationic[4.3] but the formal potential for Ir(IV) perchlorate shifted anodically with increasing ionic strength. This anomalous behaviour was also apparent in d.c. voltammetric studies of Ir(IV) perchlorate at the RPE and "Norbide" electrode (in stirred solutions)[4.5]. The difficulty in removing the Cl_2O and Cl_2 soluble species coupled with the observation that the first titre and the excess of the second titre (relative to a one-electron reduction) were proportional to the iridium concentration[2.20] suggest that these interfering species were closely associated with the Ir(IV) species. Ir(IV) (10^{-7}-10^{-6} mol dm^{-3}) is reported to be hydrolysed even in $HClO_4$ (2 M) and at the ionic strength 2, and at 20 °C; the product being $[Ir(OH_2)_5(OH)]^{3+}$ [2.21].

The Ir(III) cation, $[Ir(OH_2)_6]^{3+}$, has been prepared in aqueous perchloric media and characterised by spectrophotometry, ion-exchange, ^{18}O-tracer technique, and x-ray diffraction[2.4, 2.22]. The u.v.-visible spectrum of $[Ir(OH_2)_6]^{3+}$ in $HClO_4$ (0.1 M) has absorption maxima at 265 and 310 nm[2.4] whilst the x-ray diffraction patterns of Ir(III) perchlorate hydrate[2.22] were almost identical with those of $Rh(ClO_4)_3.6H_2O$[2.23]. The hydrolysis of $[Ir(OH_2)_6]^{3+}$ has been investigated in aqueous solutions of constant perchlorate molality (1.05 mol kg^{-1}) at temperatures of 5, 15, 25, and 35 °C[2.22]:

$$[Ir(OH_2)_6]^{3+} \rightleftharpoons [Ir(OH_2)_5(OH)]^{2+} + H^+ \qquad (2\text{-}7)$$

with $K_1 = [\ Ir(OH_2)_5(OH)^{2+}\ ].[\ H^+\ ]/[\ Ir(OH_2)_6^{3+}\ ]$;

$$[Ir(OH_2)_5(OH)]^{2+} \rightleftharpoons [Ir(OH_2)_4(OH)_2]^{+} + H^{+} \qquad (2\text{-}8)$$

with $K_2 = [\ Ir(OH_2)_4(OH)_2^{+}\ ].[\ H^{+}\ ]/[\ Ir(OH_2)_5(OH)^{2+}\ ]$; and

$$[Ir(OH_2)_3(OH)_3]_{(s)} + 3H^{+} \rightleftharpoons [Ir(OH_2)_6]^{3+} \qquad (2\text{-}9)$$

with $K_{so} = [\ Ir(OH_2)_6^{3+}\ ]/[\ H^{+}\ ]^3$. At 25 °C: $\log K_1 = -4.37 \pm 0.02$, $\log K_2 = -5.20 \pm 0.15$, and $\log K_{so} = 10.22 \pm 0.05$.

2-1.3 Ir(IV) sulphate system

Generally, the Ir(IV) sulphate system has been prepared by two routes: (1) oxidation of Ir(III) solution in dilute H_2SO_4 with oxidants ($Ce(SO_4)_2$, $KMnO_4$, or $NaBiO_3$) at room temperature[2.19, 2.20, 2.24]; and (2) evaporation of Ir(IV) or Ir(III) solution (e.g. $[IrCl_6]^{2-}$ or $[IrCl_6]^{3-}$) with c.H_2SO_4 in the presence of an oxidant ($HClO_4$, HNO_3/$HClO_4$, $K_2Cr_2O_7$, $Ce(SO_4)_2$, or $NaBiO_3$)[2.20, 2.25, 2.53, 4.5].

Route 1 is reported by Dwyer and Gyarfas[2.24] to produce blue-violet solutions whereas Pshenitsyn et al[2.20] obtained red-violet solutions (spectrophotometric absorption maximum at 500 nm) which had similar characteristics to the Ir(IV) perchlorate system (section 2-1.2). Pshenitsyn et al, therefore, concluded that Ir(IV) was probably present as a complex hydrated cation which did not involve SO_4^{2-}.

Route 2 is reported by Pshenitsyn et al[2.20] to produce blue solutions (absorption maximum at 570 nm) which indicated a stoichiometric one—electron reduction when titrated potentiometrically; although interference from residual oxidant or decomposition products of $HClO_4$ sometimes occurred. Analysis of solid products[2.20] showed that Ir(IV) was present in the form of a complex anion which also involved SO_4^{2-}. Jackson and Pantony[4.5] reported that on evaporating $[IrCl_6]^{3-}$ with c.H_2SO_4/$HClO_4$ to fumes a blue-purple solution was obtained which had an absorption maximum at 580 nm (for unboiled solution) or 555 nm (for boiled solution). Only the boiled solutions produced stoichiometric one-electron reductions for the potentiometric titrations. If the evaporation was allowed to proceed further to strong fumes, however, pink-purple solutions were obtained[4.5] which required excessive titres irrespective of whether the solutions were boiled or unboiled; a behaviour similar to the Ir(IV) perchlorate system (section 2-1.2). Ion-exchange tests[4.5] on both types of solution (blue- or pink-purple) indicate that: (i) when unboiled, the Ir(IV) species was

anionic; (ii) when boiled, Ir(IV) was present as a mixture of cationic and anionic species.

2-1.4 Ir(IV) phosphate system

Ir(IV) phosphate has been prepared by the evaporation of Ir(IV) or Ir(III) solutions (e.g. $[IrCl_6]^{2-}$ or $[IrCl_6]^{3-}$), in the presence of an oxidant (e.g. $HClO_4$), with: (1) dilute H_3PO_4 to obtain the red-violet Ir(IV) complex hydrated cation (absorption maximum at 500 nm) not involving PO_4^{3-} [2.20]; or (2) with c.H_3PO_4 [2.20, 2.25, 2.26, 4.5] to fumes and so obtain a variety of coloured Ir(IV) species depending on the temperature of the solution. Thus Ayres and Bolleter[2.25] reported on a wine red Ir(IV) species which had an absorption maximum at 495 nm (for the unboiled solution; irreproducible) or 510 nm (for the boiled solution; reproducible). Pshenitsyn et al[2.20, 2.26], however, obtained a blue-violet product (absorption maximum at 570 nm) which was shown to be an Ir(IV) complex anion which involved PO_4^{3-}. The proposed reaction scheme is[2.26]:

$$[IrCl_6]^{2-} \longrightarrow [Ir(OH_2)_6]^{4+} \longrightarrow \left[{}^{(OH_2)_{6-x}}_{Ir_{(OH)_x}} \right]^{4-x} \longrightarrow$$

$$\longrightarrow [(H_2O)_2Ir(OH)_2Ir(OH_2)_2]^{3+} \longrightarrow [(H_2PO_4)_3Ir(O)_2Ir(H_2PO_4)_3]^{4-} \quad (2\text{-}10)$$

Jackson and Pantony[4.5] reported obtaining orange Ir(IV) species (absorption maximum at 333 nm), at the stage of light fumes, which was converted to the blue-purple species on continued fuming to higher temperatures. Ion-exchange tests indicated that both Ir(IV) species were anionic.

2-1.5 Electrochemistry of selected iridium species

The electrode potentials of selected iridium species at 25 °C are surveyed in Table 2-1. For the $[IrCl_6]^{2-}/[IrCl_6]^{3-}$ couple, the standard electrode potential of 0.8665 V reported by George et al[2.27] appears to be the most reliable[2.32, 2.33]. The other more anodic E^o or $E^{o'}$ values reported by several researchers are probably due to the higher ionic strengths of the respective solutions. Aquation of the iridium species can also lead to more anodic electrode potentials: (a)[2.7, 2.28]

Table 2-1 Electrode potentials of selected iridium species at 25 °C

Working electrode	Electroactive species	Supporting electrolyte	Electrochemical method	Electrode reaction	Reversibility	E° or $E^{\circ\prime}$ (denoted by *) in V.	Uncertainty in mV.	Reference
Rh	K_3IrCl_6 (2×10^{-3} mol dm^{-3})	HCl (0.31 M)	potentiometric	$[IrCl_6]^{2-} + e^- \rightleftharpoons [IrCl_6]^{3-}$		0.8665		2.27
Pt, Rh, or Ir	$[IrCl_6]^{2-}$ (10^{-4}, 10^{-3}, and 10^{-2} mol dm^{-3})	HCl (1 M) or NaCl (1 M)	potentiometric	$[IrCl_6]^{2-} + e^- \rightleftharpoons [IrCl_6]^{3-}$		0.932*	±3	2.7
						0.933*	±4	
Rh or "Norbide"	$(NH_4)_2IrCl_6$	$NaClO_4$ (0.1 M)	potentiometric	$[IrCl_6]^{2-} + e^- \rightleftharpoons [IrCl_6]^{3-}$		0.899*	±1	4.5
Pt	$[IrCl_6]^{2-}$	HCl (1 M)	galvanostatic	$[IrCl_6]^{2-} + e^- \rightleftharpoons [IrCl_6]^{3-}$		1.172*		2.29
Pt or RPE (800 rpm)	H_2IrCl_6 (5.2×10^{-6} to 2.4×10^{-3} mol dm^{-3})	NaCl (0.1 M, pH ≈ 2) or $NaNO_3$ (0.1 M)	voltammetric	$[IrCl_6]^{2-} + e^- \rightleftharpoons [IrCl_6]^{3-}$	poor	0.972*		2.28
					poor	0.992*		
"Norbide"	$(NH_4)_2IrCl_6$	$NaClO_4$ (0.1 M)	voltammetric	$[IrCl_6]^{2-} + e^- \rightleftharpoons [IrCl_6]^{3-}$	$\alpha n = 1$	0.89*	±10	4.5
Pt	Na_2IrCl_6	HCl (0.2 M)	voltammetric	$[IrCl_6]^{2-} + e^- \rightleftharpoons [IrCl_6]^{3-}$		1.05		2.6
Pt	Na_2IrCl_6 (2×10^{-3} mol dm^{-3})	HCl (1 M)	voltammetric	$[IrCl_6]^{2-} + e^- \rightleftharpoons [IrCl_6]^{3-}$	$\alpha n = 0.5$	0.927*		2.30
Rh	$(NH_4)_2[Ir(OH_2)Cl_5]$ ((4.86 to 10.8) $\times 10^{-3}$ mol dm^{-3})	HNO_3 (0.2 M)	potentiometric	$[Ir(OH_2)Cl_5]^- + e^- \rightleftharpoons [Ir(OH_2)Cl_5]^{2-}$		1.0		2.11

Table 2-1 (continued)

Working electrode	Electroactive species	Supporting electrolyte	Electrochemical method	Electrode reaction	Reversibility	E^{o} or $E^{o'}$ (denoted by *) in V.	Uncertainty in mV.	Reference
DME	$[Ir(OH)_6]^{2-}$	NaCl (0.5 M)/NaOH (pH 12)	polarographic	$[Ir(OH)_6]^{2-} + H_2O + e^- \rightleftharpoons [Ir(OH_2)(OH)_5]^{2-} + OH^-$	$\alpha n = 1$	-0.358*		2.5
Pt	Ir(IV) perchlorate	$HClO_4$ (1 M)	potentiometric	$Ir(IV)_c + e^- \rightleftharpoons Ir(III)_c$		0.82*		4.3, 4.5
"Norbide"	Ir(IV) perchlorate	$HClO_4$ (1 M)	voltammetric	$Ir(IV)_c + e^- \rightleftharpoons Ir(III)_c$	$\alpha n = 1$	1.27*	±20	4.5
unstated	Ir(IV) sulphate	H_2SO_4 (0.18 M)	potentiometric	$Ir(IV)_a + e^- \rightleftharpoons Ir(III)_a$		1.08*	±30	4.5
"Norbide" and RPE	Ir(IV) sulphate	H_2SO_4 (0.36 M)	voltammetric	$Ir(IV)_a + e^- \rightleftharpoons Ir(III)_a$	$\alpha n = 0.6$-1.0	1.01*		4.5
RPE	Ir(IV) phosphate	H_3PO_4 (0.3 M)	voltammetric	$Ir(IV)_a + e^- \rightleftharpoons Ir(III)_a$	$\alpha n = 0.85$ (orange form) $\alpha n = 0.75$ (blue form)	0.94* (orange form) 0.99* (blue form)	±4 ±4	4.5

Note: literature $E_{\frac{1}{2}}$ values (vs SCE) were converted to $E^{o'}$ values, when not reported, by the addition of +0.242 V[2.31].
If the electron charge transfer is poorly reversible, such $E^{o'}$ values can only serve as an indication.
Subscripts; a = anionic and c = cationic.

$$[IrCl_6]^{2-} + e^- \rightleftharpoons [IrCl_6]^{3-} \qquad (2\text{-}11)$$

$$[IrCl_6]^{3-} + H_2O \rightleftharpoons [Ir(OH_2)Cl_5]^{2-} + Cl^- \qquad (2\text{-}4)$$

or (b)[2.11]

$$[Ir(OH_2)Cl_5]^- + e^- \rightleftharpoons [Ir(OH_2)Cl_5]^{2-} \qquad (2\text{-}12)$$

The diffusion coefficients of $[IrCl_6]^{2-}$ and $[IrCl_6]^{3-}$ have been determined[2.29] as $(8.2 \pm 0.4) \times 10^{-6}$ cm^2 s^{-1} and $(7.8 \pm 0.3) \times 10^{-6}$ cm^2 s^{-1} respectively.

2-2 Palladium

The principal oxidation states of palladium are II and IV[2.2]; with Pd(II) being the more stable. Pd(II) complexes are, in general, square or 5-coordinate. The square d^8 complexes undergo oxidative-addition reactions which tend to be reversible except when strong oxidants are involved. Pd(IV) has a coordination number of 6, and exist mainly as the octahedral halide anions in the compounds $M_2[PdX_6]$; where X = F, Cl, Br, or I.

Both the Pd(0)/Pd(II) and Pd(II)/Pd(IV) oxidation potentials[2.34] show that oxidation becomes more favourable as the halogen increases in atomic weight. Thus palladium is described as a class 'b' or 'soft' metal[2.35, 2.36]; the stabilities of the halide complexes decreasing in the order $I^- > Br^- > Cl^- >> F^-$.

Pd(II) perchlorate has been prepared by the evaporation of Pd(II) nitrate with $HClO_4$ to fumes[1.12, 2.37, 2.38], and the $[Pd(OH_2)_4]^{2+}$ ion is stable in $HClO_4$ ($\geqslant 0.1$ M). In aqueous solution, the $[Pd(OH_2)_4]^{2+}$ ion is diamagnetic and is, therefore, presumably square planar. $[Pd(OH_2)_4](ClO_4)_2$ can be crystallised from solutions of PdO in dilute $HClO_4$. The electrode potentials, at 25 °C, for the reduction:

$$Pd^{2+} + 2e^- \rightleftharpoons Pd \qquad (2\text{-}13)$$

have been determined in perchloric acid media. Templeton et al[2.39] reported that $E^{o\prime} = 0.987$ V in $HClO_4$ (4 M); Izatt et al [2.40, 2.41] quoted $E^{o\prime} = 0.979$ V in $HClO_4$ (3.94 M) or $E^o = 0.915 \pm 0.005$ V; Jackson and Pantony[1.12], from voltammetry at the "Norbide" electrode, reported $E^o = 0.91 \pm 0.06$ V but the electron charge transfer was quasi-reversible

($\alpha n = 1.50 \pm 0.29$). Recently, for $Pd(ClO_4)_2$ in $HClO_4$ at 25 °C, the standard electrode potential has been quoted as $E^\circ = 0.951$ V; determined potentiometrically at a Pd electrode[2.33].

2-3 Iron

Most of the chemistry of iron concerns Fe(II) and Fe(III); both form salts with most anions (except those which behave as reducing agents with respect to Fe(III), e.g. I^-, will be unable to form Fe(III) salts). Thus compounds such as $[Fe(OH_2)_6]Cl_2$, $[Fe(OH_2)_6](ClO_4)_2$, $Fe(ClO_4)_3.10H_2O$, $Fe(NO_3)_3.9$(or 6)H_2O, and $Fe_2(SO_4)_3.10H_2O$ are known. The most conspicuous feature of Fe(III) in aqueous solution is its tendency to hydrolyse and/or to form complexes.

2-3.1 Fe(III)-Fe(II) perchlorate system

Aqueous solutions of Fe(II) contain the pale blue-green hexaaquo-iron(II) ion, $[Fe(OH_2)_6]^{2+}$. The standard electrode potential for:

$$Fe^{3+} + e^- \rightleftharpoons Fe^{2+} \qquad (2\text{-}14)$$

is reported as $E^\circ = 0.771$ V[2.33, 2.42]. Therefore, Fe(II) compounds should, thermodynamically, be oxidised in air at $[H^+] = 1$. The reaction may be expressed as[2.2]:

$$2Fe^{2+} + \tfrac{1}{2}O_2 + 2H^+ = 2Fe^{3+} + H_2O \qquad (2\text{-}15)$$

with $E^\circ = 0.46$ V; but oxidation becomes less rapid with increasing acidity.

The hydrolysis of $[Fe(OH_2)_6]^{3+}$, in its initial stages, is governed by the following equilibrium constants[2.2]:

$$[Fe(OH_2)_6]^{3+} = [Fe(OH_2)_5(OH)]^{2+} + H^+ \qquad K = 10^{-3.05} \qquad (2\text{-}16)$$

$$[Fe(OH_2)_5(OH)]^{2+} = [Fe(OH_2)_4(OH)_2]^{+} + H^+ \qquad K = 10^{-3.26} \qquad (2\text{-}17)$$

$$2[Fe(OH_2)_6]^{3+} = [(H_2O)_4Fe\langle^{H}_{O}\rangle Fe(OH_2)_4]^{4+} + 2H^+ \qquad K = 10^{-2.91} \qquad (2\text{-}18)$$

Therefore even at pH 2-3, the extent of hydrolysis is very great, and

a pH of around zero would be required to ensure that the Fe(III) exists mainly (≈99%) as the pale purple $[Fe(OH_2)_6]^{3+}$ ion.

The Fe^{3+}/Fe^{2+} couple has been studied by voltammetry at the "Norbide" electrode: (1) Mueller et al[1.6, 1.7] obtained $E_{p/2}$ = 0.456 ± 0.005 V (vs SCE) in HCl (1 M), (2) Mountcastle[1.10] obtained $E_{p/2}$ = 0.35 V or 0.30 V (vs SCE) in H_2SO_4 (0.5 M) or HNO_3 (1 M) respectively, (3) Jackson and Pantony[4.5] reported $E_{\frac{1}{2}}$ (V vs SCE) values for Fe(III) (2×10^{-4} mol dm^{-3}) of 0.411 ± 0.003 and 0.277 ± 0.009 in $HClO_4$ (0.1 and 1.0 M respectively), 0.394 ± 0.003 and 0.200 ± 0.004 in HCl (0.1 and 1.0 M respectively); the charge transfer being reversible only in $HClO_4$ (0.1 M) with αn = 0.96 ± 0.03.

2-3.2 Fe(III)-Fe(II) chloride system

Fe(III) behaves as a class 'a' metal[2.35, 2.43] with respect to its halide complexes; the stabilities in descending order being $F^- >> Cl^- > Br^-$. Fe(III) chloride, usually in the form of the yellow-brown hydrate ($FeCl_3.6H_2O$), is really trans $[Fe(OH_2)_4Cl_2]Cl.2H_2O$[2.44]. The nature of more concentrated aqueous solutions of $FeCl_3$ is complex. Solutions dilute in Fe^{3+} and concentrated in HCl (or Cl^-) contain mainly the yellow tetrahedral $[FeCl_4]^-$ anion. At higher concentrations of Fe^{3+} and/or lower H^+ concentrations, octahedral species such as $[FeCl_4(OH_2)_2]^-$ and polymers of uncertain nature exist[2.45].

2-3.3 Fe(III)-Fe(II) cyanide system

The standard electrode potential at 25 °C, determined potentiometrically at a Pt or Au electrode, for the reaction:

$$[Fe(CN)_6]^{3-} + e^- \rightleftharpoons [Fe(CN)_6]^{4-} \qquad (2\text{-}19)$$

is reported as E° = 0.358 ± 0.003 V[2.33, 2.46, 2.47]. Therefore, $[Fe(CN)_6]^{4-}$ is easier to oxidise than $[Fe(OH_2)_6]^{2+}$ in aqueous solution, and $[Fe(CN)_6]^{3-}$ is more stable than $[Fe(CN)_6]^{4-}$.

The $[Fe(CN)_6]^{3-}/[Fe(CN)_6]^{4-}$ couple has been voltammetrically studied at boron carbide solid working electrodes: (1) Mueller et al[1.6, 1.7] obtained $E_{p/2}$ = 0.226 ± 0.002 V and 0.198 ± 0.005 V (vs SCE) in KCl (0.5 M) for the reduction and oxidation reactions respectively; (2) Alder et al[1.13] reported E_p (V vs SCE) values for the oxidation of $[Fe(CN)_6]^{4-}$ (1×10^{-3} mol/dm^3) as 0.35 (pH 1.0) and 0.27 (pH 4.2), but the reproducibility was poor; (3) Hartley and Axelrod[1.11], and

Blaedel and Schieffer[1.14] found the electron charge transfer to be poorly reversible.

2-4 Silver

Ag(I) is the normal and dominant oxidation state; and the only stable cationic species, apart from complex ions, is Ag^+. Ag^+ is a class 'b' metal[2.35, 2.43]; the stabilities of its halide complexes being in the descending order $I^- > Br^- > Cl^- > F^-$.

Ag^{2+} is obtained in $HClO_4$ or HNO_3 solution by the oxidation of Ag^+ with ozone, or by dissolution of AgO in acid. Ag^{2+} is a powerful oxidant:

$$Ag^{2+} + e^- \rightleftharpoons Ag^+ \qquad (2\text{-}20)$$

with $E^{o'} = 2.00$ V in $HClO_4$ (4 M)[2.2] or $E^o = 1.98$ V[2.33, 2.48]. Thus Ag^{2+} is reduced by water, even in strongly acid solution[2.49].

The standard electrode potential, at 25 °C, for the reaction:

$$Ag^+ + e^- \rightleftharpoons Ag \qquad (2\text{-}21)$$

is quoted as $E^o = 0.800$ V[2.33, 2.48, 2.50]; obtained potentiometrically at the Ag electrode for $AgClO_4$ in $NaClO_4$ solution. The Ag^+/Ag couple has been studied by voltammetry at the "Norbide" electrode: (1) Mueller and Adams[1.7] obtained $E_{p/2} = 0.19$ V (vs SCE) for Ag^+ (2×10^{-4} mol dm^{-3}) in KNO_3 (0.1 M) supporting electrolyte; (2) Jackson and Pantony[1.12] reported obtaining $E^o = 0.805 \pm 0.009$ V for $AgClO_4$ in $NaClO_4$ supporting electrolyte, $E_{\frac{1}{2}}$ (V vs SCE) = 0.22 and 0.23 in $NaClO_4$ (0.1 and 1.0 M respectively) for Ag^+ (1×10^{-4} mol dm^{-3}), and reversible electron charge transfers ($n = 0.92 \pm 0.30$).

2-5 Copper

From the following standard electrode potentials[2.33, 2.48, 2.51]:

$$Cu^+ + e^- \rightleftharpoons Cu \qquad E^o = 0.521 \text{ V} \qquad (2\text{-}22)$$

$$Cu^{2+} + e^- \rightleftharpoons Cu^+ \qquad E^o = 0.153 \text{ V} \qquad (2\text{-}23)$$

the standard potential for the reaction

$$Cu^{2+} + Cu = 2Cu^{+} \qquad K = 1 \times 10^{-6} \ ^{(2.52)} \qquad (2\text{-}24)$$

is calculated as $E^{o} = -0.368$ V. Therefore, Cu^{+} is unstable with respect to Cu^{2+} and Cu. In aqueous solution only low equilibrium concentrations ($< 10^{-2}$ M) of Cu^{+} can exist.

The most important oxidation state of copper is Cu(II); the favoured oxidation state in aqueous ClO_4^- or SO_4^{2-} solution. Most cupric salts, such as $CuSO_4.5H_2O$, dissolve in water to give the aquo cation $[Cu(OH_2)_6]^{2+}$ which has a distorted octahedral structure. The standard electrode potential for the reaction:

$$Cu^{2+} + 2e^{-} \rightleftharpoons Cu \qquad (2\text{-}25)$$

is quoted as $E^{o} = 0.3419$ V $^{(2.33,\ 2.48)}$.

The voltammetry of Cu(II) at the "Norbide" electrode has been investigated: (1) Mueller et al$^{(1.7)}$ reported obtaining, in nitrogen aerated solutions, $E_{p/2} = 0.218 \pm 0.001$ V (vs SCE) in KCl (1 M, pH 3-4) for the Cu^{2+}/Cu^{+} couple, $E_{p(1)/2} = 0.16$ V and $E_{p(2)/2} = -0.48$ V (vs SCE) in KCl (0.5 M, pH 4.4-5.4) for the stepwise reduction $Cu^{2+} \longrightarrow Cu^{+} \longrightarrow Cu$, $E_{p/2} = -0.09 \pm 0.002$ V (vs SCE) in H_2SO_4 (1 M) for the Cu^{2+}/Cu couple. (2) Mountcastle$^{(1.10)}$ reported obtaining $E_{p/2} = -0.10$ V and -0.11 V (vs SCE) in H_2SO_4 (0.5 M) and HNO_3 (1.0 M) respectively (although there was evidence of the stepwise reduction $Cu^{2+}/Cu^{+}/Cu$), $E_{p(1)/2} = 0.03$ V and $E_{p(2)/2} = -0.40$ V (vs SCE) in HCl (1 M) for the stepwise reduction $Cu^{2+} \longrightarrow Cu^{+} \longrightarrow Cu$. (3) Hartley and Axelrod$^{(1.11)}$ obtained irreversible electron charge transfers with E_p values dependent on scan rate, as well as low and irreproducible peak currents, for the Cu(II)/KCl (1 M) system. (4) Jackson and Pantony$^{(1.12)}$ obtained $E_{\frac{1}{2}}$ (V vs SCE) = -0.13 and -0.15 in $NaClO_4$ (0.1 M) and Na_2SO_4 (0.1 M) respectively for $CuSO_4$ (1×10^{-4} mol dm^{-3}), and the charge transfer for the Cu^{2+}/Cu couple was reversible ($n = 1.95 \pm 0.50$).

2-6 References

1.6 Mueller T. R., et al; Advances in Polarography, Vol I, Proc. 2nd International Congr. of Polarography, Cambridge, 1959.

1.7 Mueller T. R. and Adams R. N.; Anal. Chim. Acta, 1960, 23, 467.

1.10 Mountcastle W. R., Jr.; Anal. Chim. Acta, 1965, 32, 332-338.

1.11 Hartley A. M. and Axelrod H. D.; J. Electroanal. Chem., 1968, 18, 115-121.

1.12 Jackson E. and Pantony D. A.; J. Appl. Electrochem., 1971, 1, 283-291.

1.13 Alder J. F., et al; J. Electroanal. Chem., 1971, 30, 427.

1.14 Blaedel W. J. and Schieffer G. W.; J. Electroanal. Chem. Interfacial Electrochem., 1977, 80(2), 259-71.

2.1 Griffith W. P.; The Chemistry of the Rarer Platinum Metals (Os, Ru, Ir and Rh). Interscience Publishers, 1967.

2.2 Cotton F. A. and Wilkinson G.; Advanced Inorganic Chemistry (A Comprehensive Text), 3rd edition. Interscience Publishers, 1972.

2.3 Fine D. W.; Inorg. Chem., 1969, 8, 1014.

2.4 Beutler P., et al; J. C. S. Chem. Comm., 1976, 554; and Chimia, 1978, 32(5), 163-4.

2.5 Van Loon G. and Page J. A.; Can. J. Chem., 1966, 44, 515.

2.6 Page J. A.; Talanta, 1962, 9, 365.

2.7 Kravtsov V. I. and Petrova G. M.; Russ. J. Inorg. Chem., 1964, 9(4), 552.

2.8 Poulsen I. A. and Garner C. S.; J. Am. Chem. Soc., 1962, 84, 2032.

2.9 Blasius E., et al; J. Inorg. Nucl. Chem., 1961, 19, 115.

2.10 Domingos A. J. P., et al; J. Inorg. Nucl. Chem., 1969, 31, 2563.

2.11 Chang J. C. and Garner C. S.; Inorg. Chem., 1965, 4, 209.

2.12 Zimina S. M., et al; Soviet Electrochem., 1979, 15(4), 488.

2.13 Kravtsov E. G., et al; Zh. Neorg. Khim., 1970, 15, 81; Ibid, 1971, 16, 2498; Ibid, 1973, 18, 1998.

2.14 Lakatos-Varsanyi M., et al; Zh. Neorg. Khim., 1973, 18, 3014.

2.15 Smirnova L. Ya., et al; Elektrokhimiya, 1978, 14, 290.

2.16 Kravtsov V. I., et al; Soviet Electrochem., 1979, 15(11), 1490.

2.17 Bell R. and Herr W.; Chem. Effects Nucl. Transformations, Proc. Symp., Vienna, 1964, 2, 315 (pub. 1965).

2.18 Cabral J. M. P.; J. Inorg. Nucl. Chem., 1964, 26, 1657.

2.19 McBryde W. A. E. and Cluett M. L.; Can. J. Research, 1950, 28B, 788-98.

2.20 Pshenitsyn N. K., et al; Russ. J. Inorg. Chem., 1959, 4, 130-137.

2.21 Yatsimirskii K. B., et al; Tezisy Dokl. - Vses. Soveshch. Khim. Anal. Tekhnol. Blagorodn. Met., 10th, 1976, 1, 23.

2.22 Gamsjaeger H. and Beutler P.; J. Chem. Soc., Dalton Trans., 1979, 9, 1415-18.

2.23 Ayres G. H. and Forrester J. S.; J. Inorg. Nucl. Chem., 1957, 3, 365.

2.24 Dwyer F. P. and Gyarfas E. C.; J. Proc. Roy. Soc. N. S. Wales, 1950, 84, 123.

2.25 Ayres G. H. and Bolleter W. T.; Anal. Chem., 1957, 29, 72.

2.26 Pshenitsyn N. K., et al; Russ. J. Inorg. Chem., 1960, 5, 399-404.

2.27 George P., et al; J. Chem. Soc., 1957, 3048-3052.

2.28 Pshenitsyn N. K., et al; Russ. J. Inorg. Chem., 1958, 3(8), 99.

2.29 Kravtsov V. I. and Petrova G. M.; Proc. Academy of Sciences USSR, Phys. Chem., 1964, 154, 64.

2.30 Saji T., et al; J. Electroanal. Chem. Interfacial Electrochem., 1978, 86(1), 219-22.

2.31 Weast R. C. (editor); CRC Handbook of Chemistry and Physics, 60th edition, 1979-80.

2.32 Goldberg R. N. and Hepler L. G.; Chem. Rev., 1968, 68, 229.

2.33 Milazzo G. and Caroli S.; Tables of Standard Electrode Potentials. John Wiley & Sons Ltd., 1978.

2.34 Hartley F. R.; The Chemistry of Platinum and Palladium. Applied Science Publishers Ltd., 1973.

2.35 Ahrland St., et al; Quart. Rev., 1958, 12, 265.

2.36 Pearson R. G.; J. Am. Chem. Soc., 1963, 85, 3533.

2.37 Sundaram A. K. and Sandell E. B.; J. Am. Chem. Soc., 1955, 77, 855.

2.38 Livingstone S. E.; J. Chem. Soc., 1957, 5091.

2.39 Templeton D. H., et al; J. Am. Chem. Soc., 1943, 65, 1608.

2.40 Izatt R. M., et al; J. Chem. Soc., A, 1970, 2514.

2.41 Ibid., 1967, 1301.

2.42 Mattoo B. N.; Zh. Priklad. Khim., 1960, 33, 2015-2020.

2.43 Harvey K. B. and Porter G. B.; Introduction to Physical Inorganic Chemistry, Chapter 9. Addison-Wesley Publishing Co., Inc., 1963.

2.44 Sharpe A. G.; Inorganic Chemistry. Longman Group Ltd., 1981.

2.45 Brady G. W., et al; Inorg. Chem., 1964, 3, 1168.

2.46 Hanania G. I. H., et al; J. Phys. Chem., 1967, 71, 2022-2030.

2.47 Murray R. C., Jr., and Rock P. A.; Electrochim. Acta, 1968, 13, 969-975.

2.48 De Bethune A. J. and Swendeman-Loud N. A.; Standard Aqueous Electrode Potentials and Temperature Coefficients at 25 ^{o}C. Clifford A. Hampel, Ill.

2.49 Viste A., et al; Inorg. Chem., 1971, 10, 631.

2.50 Papon C. and Jacq J.; Bull. Soc. Chim. France, 1965, 13-17.

2.51 Latimer W. M.; Oxidation Potentials, 2nd edition. Prentice-Hall, Inc., 1952.

2.52 Fenwick F.; J. Am. Chem. Soc., 1926, 48, 860.

2.53 Pollard W. B.; Trans. Inst. Min. Met., 1948, 57, 377.

4.3 Jackson E. and Pantony D. A.; Talanta, 1967, 14, 973.

4.4 Jackson E.; Ph. D. thesis, "An Electrochemical Study of Platinum Metals as a Basis for their Separation with Organic Reagents", University of London, 1969.

4.5 Jackson E. and Pantony D. A.; J. Appl. Electrochem., 1971, 1, 113.

3. SOLID ELECTRODE VOLTAMMETRY

3-1 Instrumentation

The main functions of a modern polarograph are performed by electronic circuits involving Operational Amplifiers (OA). The OA may be regarded as a differential d.c. amplifier with two input terminals, a high open loop gain (of the order of 10^4 to 10^6), and a small drift. A scheme of a circuit[3.1] for a three-electrode polarograph is presented in Fig. 3-1.

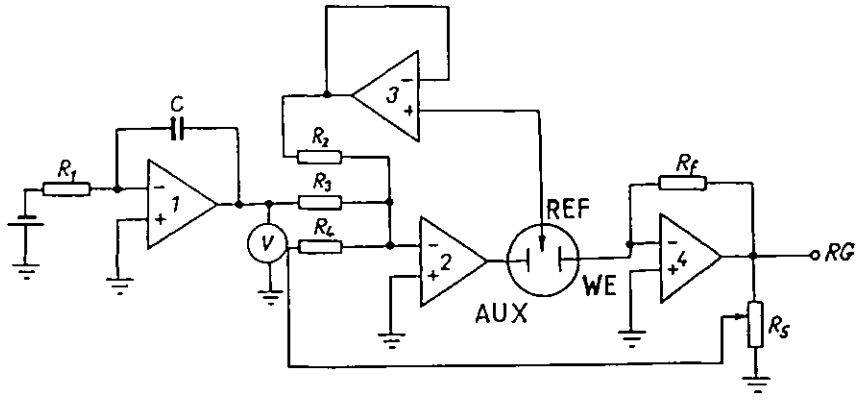

Fig. 3-1 Three-electrode polarograph. 1 and 4 - FET amplifiers; 2 and 3 - bipolar transistor amplifiers.

Amplifier 1 functions as a ramp generator of voltage increasing linearly with time; monitored on voltmeter V. After a preset value has been reached, the charging supply voltage can be reversed to provide a linearly decreasing voltage for cyclic voltammetry. Amplifier 2 functions as an adder as well as a potentiostat. To its inverting input are connected: (i) the ramp generator output; (ii) the output of voltage-follower 3, which protects the reference electrode (REF e.g. the SCE) from over-loading; and (iii) the feedback link at the output of of current-follower 4, which results in the automatic compensation for iR drop.

The auxiliary electrode (AUX e.g. any inert electrode or the SCE) is connected to the output of potentiostat 2 whereas the working electrode (WE e.g. boron carbide or graphite) is connected to the inverting input of current-follower 4. The output of current-follower 4 can be monitored by an X-Y recorder or a cathode ray oscilloscope.

3-2 D.C. Voltammetry in Stirred Solutions

3-2.1 Reversible and irreversible electrode processes involving a soluble reductant

In stirred solutions, where a steady state in the system is achieved, application of the Nernst-diffusion-layer[3.2] concept of a linear concentration gradient results in the following relationships[3.3, 3.4]:

$$\left(\frac{\partial C_O}{\partial x} \right)_{x = 0} = \frac{C_O^b - C_O^e}{\delta_O} \; ; \; \left(\frac{\partial C_R}{\partial x} \right)_{x = 0} = - \frac{C_R^e}{\delta_R} \qquad (3\text{-}1)$$

where the C's are the concentrations, the δ's are the Nernst diffusion-layer thicknesses, x is the distance from the electrode surface, the subscripts O and R refer to the oxidant and reductant respectively, and the superscripts b and e refer to conditions in the bulk solution and at the electrode surface respectively.

The current is then given by

$$i = nFAD \left(\frac{\partial C}{\partial x} \right)_{x = 0} \qquad (3\text{-}2)$$

which can be expressed by the equation

$$i = nFAD_O \frac{C_O^b - C_O^e}{\delta_O} = - nFAD_R \frac{C_R^e}{\delta_R} \qquad (3\text{-}3)$$

where i is the current, n is the number of electrons involved in the reduction, F is the faraday, A is the area of the working electrode, and the D's are the diffusion coefficients.

The limiting current, when $C_O^e = 0$, is

$$i_L = \frac{nFAD_O C_O^b}{\delta_O} \qquad (3\text{-}4)$$

Equation 3-4 presents a quantitative measure of the bulk concentration of electroactive species (e.a.s.) by the limiting current. Since the limiting current is inversely proportional to the Nernst diffusion-layer thickness, the stirring rate which affects δ_O should be held constant during quantitative analyses.

The current-potential curve for processes controlled both by the rate of charge transfer and by the mass-transport process under steady-

state conditions may be expressed as[3.3, 3.4]

$$\frac{i_L - i}{i} \frac{D_R \delta_O}{D_O \delta_R} = \exp\left[\frac{nF}{RT}(E - E^{o'})\right] + \frac{D_R}{\delta_R k'} \exp\left[\frac{\alpha nF}{RT}(E - E^{o'})\right] \quad (3\text{-}5)$$

where R is the gas constant, T is the absolute temperature, E is the electrode potential, $E^{o'}$ is the formal standard electrode potential, k' is the charge-transfer rate constant at $E = E^{o'}$, and α is the transfer coefficient.

For Reversible Systems, where k' is large, the second term on the right-hand side of equation 3-5 may be neglected and, after rearrangement, the current-potential curve is reduced to

$$E = E^{o'} + \frac{RT}{nF} \ln \frac{D_R \delta_O}{D_O \delta_R} + \frac{RT}{nF} \ln \frac{i_L - i}{i} \quad (3\text{-}6)$$

The half-wave potential, when $i = 0.5\, i_L$, is obtained from equation 3-6:

$$E_{\frac{1}{2}} = E^{o'} + \frac{RT}{nF} \ln \frac{D_R \delta_O}{D_O \delta_R} \quad (3\text{-}7)$$

Therefore equation 3-6 may be re-expressed as

$$E = E_{\frac{1}{2}} + \frac{RT}{nF} \ln \frac{i_L - i}{i} \quad (3\text{-}8)$$

From equation 3-8, a plot of E versus $\log \frac{i_L - i}{i}$ is linear with a slope of 2.303 RT/nF (from which n can be calculated) and yields $E_{\frac{1}{2}}$ where $\log \frac{i_L - i}{i} = 0$.

If activity coefficients are also considered, equation 3-7 may be re-expressed as[3.5]

$$E_{\frac{1}{2}} = E^{o} + \frac{RT}{nF} \ln \frac{f_O}{f_R} + \frac{RT}{nF} \ln \frac{D_R \delta_O}{D_O \delta_R} \quad (3\text{-}9)$$

where E^o is the standard electrode potential and the f's are activity coefficients. For dilute solutions, application of the Debye-Hückel Theory to equation 3-9 results in:

$$E_{\frac{1}{2}} = E^{o} + \frac{RT}{nF} \ln \frac{D_R \delta_O}{D_O \delta_R} + 2.303 \frac{RT}{nF} \frac{A\sqrt{I}}{1 + aB\sqrt{I}} (z_R^2 - z_O^2) \quad (3\text{-}10)$$

where A and B are constants (for dilute aqueous solutions at 25 °C, A = 0.5115 $mol^{-\frac{1}{2}}\ l^{\frac{1}{2}}$ and B = 0.3291 x 10^8 $cm^{-1}\ mol^{-\frac{1}{2}}\ l^{\frac{1}{2}}$); a is the mean distance of approach of the ions, positive or negative; and z's are the ionic charges.

Therefore, (i) $E_{\frac{1}{2}}$ of a cationic e.a.s. is shifted to less positive or more negative potentials with increasing ionic strength. (ii) $E_{\frac{1}{2}}$ of an anionic e.a.s. is shifted to more positive or less negative potentials with increasing ionic strength.

In general, diffusion coefficient values decrease with increasing ionic charge and hence the D_R/D_O ratio in equation 3-10 is affected. (i) For cationic e.a.s., $D_R/D_O > 1$ and assuming $\delta_O/\delta_R = 1$, the term $\frac{RT}{nF} \ln \frac{D_R \delta_O}{D_O \delta_R}$ is positive. (ii) For anionic e.a.s., $D_R/D_O < 1$ and the term is negative.

Diffusion coefficients are also likely to decrease with increasing ionic strength but the D_R/D_O ratio should remain relatively unchanged.

In practice, a constant large excess (e.g. 100 : 1) of supporting electrolyte is added to the e.a.s. so that small variations in ionic strength over the concentration range of e.a.s. leave $E_{\frac{1}{2}}$ relatively unchanged.

If the electrode reaction involves m moles of hydrogen ion, the current - potential curve is given by

$$E = E^{\circ} + \frac{RT}{nF} \ln \frac{D_R \delta_O f_O}{D_O \delta_R f_R} + m \frac{RT}{nF} \ln f_{H^+} C_{H^+} + \frac{RT}{nF} \ln \frac{i_L - i}{i} \qquad (3\text{-}11)$$

and the $E_{\frac{1}{2}}$ varies as

$$E_{\frac{1}{2}} = E^{\circ} + \frac{RT}{nF} \ln \frac{D_R \delta_O f_O}{D_O \delta_R f_R} + m \frac{RT}{nF} \ln f_{H^+} C_{H^+} \qquad (3\text{-}12)$$

Equation 3-12 may be re-expressed as

$$E_{\frac{1}{2}} = E^{\circ} + \frac{RT}{nF} \ln \frac{D_R \delta_O}{D_O \delta_R} + \frac{RT}{nF} \ln \frac{f_O}{f_R} + m \frac{RT}{nF} \ln f_{H^+} - 2.303\ m \frac{RT}{nF}\ pH \qquad (3\text{-}13)$$

Therefore $E_{\frac{1}{2}}$ is shifted to less positive or more negative potentials with increasing pH.

For Irreversible Systems, when k' is very small, the first term on the right-hand side of equation 3-5 may be neglected, yielding

$$E = E^{\circ\prime} + \frac{RT}{\alpha nF} \ln \frac{\delta_O k'}{D_O} + \frac{RT}{\alpha nF} \ln \frac{i_L - i}{i} \qquad (3\text{-}14)$$

$$= E_{\frac{1}{2}} + \frac{RT}{\alpha nF} \ln \frac{i_L - i}{i} \qquad (3\text{-}15)$$

$$\text{where} \quad E_{\frac{1}{2}} = E^{o\prime} + \frac{RT}{\alpha nF} \ln \frac{\delta_o k'}{D_o} \qquad (3\text{-}16)$$

It is seen from equation 3-15 that the shape of current-potential curves for totally irreversible processes is determined by the value of αn and not by the value of k'. The position of the current-potential curve in the scale of potentials is influenced by k' and the rate of stirring (which affects δ_o), as can be seen from equation 3-16.

If the rate determining step involves a number of electrons smaller than the total number of electrons consumed in the over-all electrode reaction, n_a should be substituted for n in equations 3-14 to 3-16 .

Equation 3-15 indicates that a plot of E versus $\log \frac{i_L - i}{i}$ is linear with a slope of $2.303 \frac{RT}{\alpha nF}$ (hence αn and α) and yields $E_{\frac{1}{2}}$ where $\log \frac{i_L - i}{i} = 0$. The value of k' may then be evaluated from equation 3-16 if $E^{o\prime}$ is known.

Since k' can be expressed as (3.6)

$$k' = k^o \exp \left[- (z_o - \alpha n) \frac{F\phi_2}{RT} \right] \qquad (3\text{-}17)$$

where k^o is the standard electrode reaction rate constant and ϕ_2 is the potential of the outer Helmholtz plane, the value of k^o may be evaluated if ϕ_2 is known.

3-2.2 Reversible and irreversible electrode processes involving the deposition of a metal on an inert electrode

Generally the variations of activity of the deposit on an inert electrode during the course of the electrode process are unknown. The alternative is to assume that the activity of the deposit is equal to unity shortly after the commencement of electrolysis. On this basis, modifications (section 8-1) to the theoretical considerations for a soluble reductant in section 3-2.1 results in the current-potential curve for processes controlled both by the rate of charge transfer and by the mass-transport process involving a solid reductant:

$$(i_L - i) \cdot \frac{\delta_o}{nFD_o} = \exp \left[\frac{nF}{RT} (E - E^{o\prime}) \right] + \frac{i}{nFk'} \exp \left[\frac{\alpha nF}{RT} (E - E^{o\prime}) \right] \qquad (3\text{-}18)$$

For a Reversible Deposition, where k' is large, equation 3-18 when rearranged is reduced to

$$E = E^{o'} + \frac{RT}{nF} \ln \frac{\delta_O}{nFD_O} + \frac{RT}{nF} \ln (i_L - i) \qquad (3\text{-}19)$$

$$= E^{o'} + \frac{RT}{nF} \ln \frac{C_O^b}{i_L} + \frac{RT}{nF} \ln (i_L - i) \qquad (3\text{-}20)$$

When $i = 0.5\ i_L$,

$$E_{\frac{1}{2}} = E^{o'} + \frac{RT}{nF} \ln C_O^b + \frac{RT}{nF} \ln 0.5 \qquad (3\text{-}21)$$

Therefore, equation 3-20 may be re-expressed as

$$E = E_{\frac{1}{2}} + \frac{RT}{nF} \ln 2 \frac{(i_L - i)}{i_L} \qquad (3\text{-}22)$$

and a plot of E versus $\log 2 \frac{(i_L - i)}{i_L}$ will be linear with a slope of $2.303 \frac{RT}{nF}$ (hence n) and yields $E_{\frac{1}{2}}$ at $\log 2 \frac{(i_L - i)}{i_L} = 0$. The limiting current is given by equation 3-4.

When activity coefficients are considered, application of the Debye-Hückel Theory for dilute solutions to equation 3-21 results in

$$E_{\frac{1}{2}} = E^{o} + \frac{RT}{nF} \ln C_O^b + \frac{RT}{nF} \ln 0.5 - 2.303 \frac{RT}{nF} \frac{Az_O^2 \sqrt{I}}{1 + aB\sqrt{I}} \qquad (3\text{-}23)$$

where A and B are constants; a is the mean distance of approach of the ions, positive or negative; and z_O is the ionic charge of the oxidant. Equation 3-23 shows that $E_{\frac{1}{2}}$ is shifted: (i) to more positive or less negative potentials with increasing bulk concentration of e.a.s., and (ii) to less positive or more negative potentials with increasing ionic charge of oxidant and increasing ionic strength.

For an Irreversible Deposition, where k' is very small, equation 3-18 rearranged is reduced to

$$E = E^{o'} + \frac{RT}{\alpha nF} \ln \frac{\delta_O k'}{D_O} + \frac{RT}{\alpha nF} \ln \frac{i_L - i}{i} \qquad (3\text{-}24)$$

Equation 3-24 is similar to the current-potential curve for an irreversible process involving a soluble reductant (equation 3-14), but $E^{o'}$ involves only f_O because f_R is equal to unity in the case of deposition.

3-3 Linear Sweep Voltammetry

The linear potential sweep may be expressed as

$$E = E_i \pm vt \tag{3-25}$$

where E is the electrode potential, E_i is the initial potential, v is the potential sweep rate (in V s^{-1}), and t is the time (in s) elapsed since the commencement of the linear potential sweep.

3-3.1 Reversible electrode process involving a soluble reductant

The theory of linear sweep voltammetry was originally developed independently by Randles[3.7] and Sevcik[3.8] resulting in the following current-potential curve:

$$i = \frac{n^{3/2} F^{3/2}}{R^{\frac{1}{2}} T^{\frac{1}{2}}} A D_O^{\frac{1}{2}} C_O^b v^{\frac{1}{2}} P\left(\frac{nF}{2RT} vt\right) \tag{3-26}$$

The function P has a maximum value[3.9] of 0.4463 and thus the peak current may be expressed as[3.10]:

$$i_p = 0.4463 \frac{n^{3/2} F^{3/2}}{R^{\frac{1}{2}} T^{\frac{1}{2}}} A D_O^{\frac{1}{2}} C_O^b v^{\frac{1}{2}} \tag{3-27}$$

where i_p is the peak current (in A), n is the number of electrons involved in the charge transfer, F is the faraday, R is the gas constant, T is the absolute temperature, A is the electrode area (in cm^2), D_O is the diffusion coefficient (in cm^2 s^{-1}) of the oxidant, C_O^b is the bulk concentration (in mole cm^{-3}) of oxidant, and v is the rate of potential change (in V s^{-1}).

The maximum occurs at the peak potential[3.9]

$$E_p = E_{\frac{1}{2}} - 1.109 \frac{RT}{nF} \tag{3-28}$$

and the half-peak potential[3.9] (where $i = 0.5\ i_p$) is given by

$$E_{p/2} = E_{\frac{1}{2}} + 1.09 \frac{RT}{nF} \tag{3-29}$$

$$\text{where } E_{\frac{1}{2}} = E^{O'} + \frac{RT}{nF} \ln\left(\frac{D_R}{D_O}\right)^{\frac{1}{2}} \tag{3-30}$$

Equation 3-27 indicates that i_p is proportional to the bulk concentration of e.a.s. and the sensitivity increases with increasing sweep rate ($i_p \propto v^{\frac{1}{2}}$) and increasing number of electrons involved in the charge transfer ($i_p \propto n^{3/2}$). Equations 3-28 and 3-29 show that the peak

and half-peak potentials are independent of the concentration of e.a.s. and thus characterize the nature of the e.a.s. It can also be seen that for a reversible electrode process

$$|E_p - E_{p/2}| = 2.199 \frac{RT}{nF} \tag{3-31}$$

which at 25°C becomes

$$|E_p - E_{p/2}| = \frac{0.056}{n} \text{ volts;} \tag{3-32}$$

where $R = 8.31434\ J\ K^{-1}\ mol^{-1}$, $T = 298.15^{\circ}\ K$, and $F = 9.648670 \times 10^4\ C\ mol^{-1}$.

In practice the shape of the peak may be distorted by the capacity current and the ohmic drop between the electrodes. The capacity current is given by[3.11]

$$i_c = A\ C_d\ v \tag{3-33}$$

where A is the surface area of the electrode, C_d is the differential capacity of the electric double-layer at the given potential in $F\ cm^{-2}$, and v is the potential sweep rate. For a reversible electrode reaction, comparison of the faradaic with the capacity current results in[3.11]

$$\frac{i_c}{i_p} \approx 2.3 \times 10^{-8} \frac{v^{\frac{1}{2}}}{n^{3/2}\ C_O^b} \tag{3-34}$$

where C_O^b is in mole cm^{-3}. Thus the effect of the capacity current increases with increasing sweep rate and decreasing bulk concentration of e.a.s. Unfortunately, C_d is not independent of v and so its effect on i_c is not constant.

The ohmic drop causes a decrease in the peak current, a shift in E_p, and a substantial peak broadening. However, iR drop can be compensated for (up to values[3.10] of about 20/n mV) by the use of a three-electrode circuit (see section 3 - 1).

3-3.2 Reversible electrode process involving the deposition of a metal on an inert electrode

Berzins and Delahay[3.11, 3.12], by assuming unit activity of the deposit, derived the following current-potential curve:

$$i = \frac{2}{\pi^{\frac{1}{2}}} \frac{n^{3/2}\ F^{3/2}}{R^{\frac{1}{2}}\ T^{\frac{1}{2}}} A\ C_O^b\ D_O^{\frac{1}{2}}\ v^{\frac{1}{2}}\ \Phi\left[\left(\frac{nF}{RT} vt\right)^{\frac{1}{2}}\right] \tag{3-35}$$

The function Φ has a maximum value of 0.541 and thus the peak current may be expressed as

$$i_p = 0.610 \frac{n^{3/2} F^{3/2}}{R^{\frac{1}{2}} T^{\frac{1}{2}}} A D_O^{\frac{1}{2}} C_O^b v^{\frac{1}{2}} \qquad (3\text{-}36)$$

where the units are the same as in equation 3-27. Comparison of equation 3-36 with 3-27 shows that the peak current of deposition is greater than the peak current involving a soluble reductant by a factor of 1.37.

The peak potential is given by[3.12]

$$E_p = E^o + \frac{RT}{nF} \ln f_O C_O^b - \frac{RT}{nF} (0.9241)^2 \qquad (3\text{-}37)$$

which indicates that E_p is shifted to more positive or less negative potentials with increasing bulk concentration of e.a.s. At 25°C, equation 3-37 may be re-expressed as

$$E_p = E^o + \frac{0.0591}{n} \log f_O C_O^b - \frac{0.0218}{n} \qquad (3\text{-}38)$$

3-3.3 Irreversible electrode process involving a soluble reductant

The current-potential curve for totally irreversible systems may be expressed as[3.13, 3.19]

$$i_{(ir)} = \frac{n(\alpha n_a)^{\frac{1}{2}} F^{3/2}}{R^{\frac{1}{2}} T^{\frac{1}{2}}} A D_O^{\frac{1}{2}} C_O^b v^{\frac{1}{2}} \pi^{\frac{1}{2}} P' \left(\frac{\alpha n_a F}{RT} vt \right) \qquad (3\text{-}39)$$

where α is the charge-transfer coefficient and n_a is the number of electrons exchanged in the rate-determining step. The function $\pi^{\frac{1}{2}} P'$ has a maximum value[3.9] of 0.4958 and thus the peak current may be expressed as[3.10]

$$i_{p(ir)} = 0.4958 \frac{n(\alpha n_a)^{\frac{1}{2}} F^{3/2}}{R^{\frac{1}{2}} T^{\frac{1}{2}}} A D_O^{\frac{1}{2}} C_O^b v^{\frac{1}{2}} \qquad (3\text{-}40)$$

where the units are the same as in equation 3-27

Delahay[3.11, 3.13] originally derived the equation for the peak potential of a totally irreversible system but it may be expressed as[3.9]

$$E_p = E^o - \frac{RT}{\alpha n_a F} \left(0.780 + \ln \left(\frac{D_O \alpha n_a F v}{RT} \right)^{\frac{1}{2}} - \ln k_s \right) \qquad (3.41)$$

where k_s is the heterogeneous rate constant for the charge transfer. It can also be shown[3.9] that

$$|E_p - E_{p/2}| = 1.857 \frac{RT}{\alpha n_a F} \qquad (3\text{-}42)$$

which at 25°C becomes

$$|E_p - E_{p/2}| = \frac{0.048}{\alpha n_a} \qquad (3.43)$$

Equation 3-40 indicates that the irreversible peak current is proportional to the bulk concentration of e.a.s. and that the sensitivity increases not only with increasing n and $v^{\frac{1}{2}}$ but also increasing $(\alpha n_a)^{\frac{1}{2}}$. Therefore, in analytical applications, the strong dependence of α on the presence of surface-active substances may cause difficulties[3.11].

It can be seen from equation 3-41 that, although E_p is independent of C_O^b, E_p is a complex function of k_s, α, n_a, and v. At 25°C, the variation of E_p with v is about $0.03/\alpha n_a$ volts per tenfold change in sweep rate. The value of αn_a, and hence the value of α, can be evaluated by the application of equation 3-41. Alternatively, αn_a could be evaluated by measuring the shift in $E_{p/2}$ at two sweep rates and applying the expression[3.9]

$$(E_{p/2})_2 - (E_{p/2})_1 = (E_p)_2 - (E_p)_1 = \frac{RT}{\alpha n_a F} \ln \left(\frac{v_1}{v_2} \right)^{\frac{1}{2}} \qquad (3\text{-}44)$$

$E_{p/2}$'s are measured instead of E_p's because the position of E_p's on broad peaks are difficult to locate with certainty.

Another means of evaluating αn_a is to compare $i_{p(ir)}$ with i_p of of a reversible one-electron process[3.14]:

$$\frac{i_{p(ir)}}{i_p} = \frac{n(\alpha n_a)^{\frac{1}{2}} (1.111)}{n^{3/2}} \qquad (3\text{-}45)$$

If the total n corresponding to the irreversible case is available, then αn_a is obtainable.

If equation 3-41 is expressed in an alternate form[3.9, 3.15]:

$$i_{p(ir)} = 0.227\, nFAC_O^b k_s \exp\left[- \alpha n_a F(E_p - E^o)/RT \right] \qquad (3\text{-}46)$$

then a plot of ln i_p versus $E_p - E^o$ (or $E_{p/2} - E^o$) for different sweep rates would be linear with a slope proportional to αn_a, and an intercept proportional to k_s.

A convenient method of differentiating between uncomplicated

reversible (rapid electron transfer) and irreversible (slow electron transfer) reactions is to plot values of $i_p/v^{\frac{1}{2}}$ and $i/v^{\frac{1}{2}}$ versus v or $v^{\frac{1}{2}}$; where i's are measured at potentials preceding E_p along the wave. Examples of such plots are presented in Fig. 3-2 (3.15).

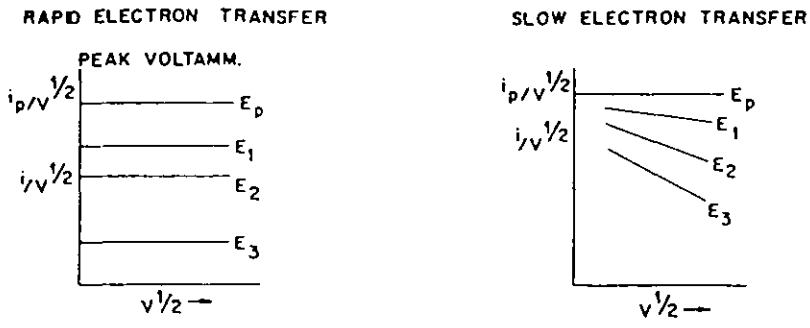

Fig. 3-2 Plots of current function, $i_p/v^{\frac{1}{2}}$ or $i/v^{\frac{1}{2}}$, versus $v^{\frac{1}{2}}$ for reversible and irreversible systems.

As can be seen, plots of $i_p/v^{\frac{1}{2}}$ and $i/v^{\frac{1}{2}}$ for a reversible electrode reaction are independent of $v^{\frac{1}{2}}$. For an irreversible electrode reaction, $i_p/v^{\frac{1}{2}}$ is independent of $v^{\frac{1}{2}}$ but $i/v^{\frac{1}{2}}$ decreases with increasing $v^{\frac{1}{2}}$.

3-3.4 Consecutive peak currents

The current-potential curve for a solution containing several e.a.s. is the sum of the corresponding individual current-potential curves of each of the e.a.s. If the peaks are too close to each other then there will be distortion; resulting in an error, possibly exceeding 10 per cent (3.11), in peak height measurements.

The situation is somewhat different for a multistep charge transfer reaction; which can be represented by $O + n_1e \longrightarrow R_1 + n_2e \longrightarrow R_2$ where O and R_1 are electroactive, and n_1 and n_2 are the number of electrons involved in the successive steps. Gokhshtein and Gokhshtein (3.16, 3.17) have given the theoretical treatment for the case where O and R_1 react at sufficiently separated potentials with O more easily reducible than R_1. The voltammogram consists of two separate waves. The first wave represents the reduction of O to R_1 involving n_1 electrons, whereas the second wave represents the sum of the reductions of R_1 to R_2 by n_2 electrons and O to R_2 by $(n_1 + n_2)$ electrons.

Polcyn and Shain (3.29), however, have developed a more straightforward treatment which is more readily applied to experimental situations. Their theory also includes cases where the peaks overlap

and the study is extended to cyclic voltammetry (see section 3-4).

3-4 Cyclic Voltammetry

Cyclic voltammetry employs a potential scan which varies along the equal arms of an isosceles triangle (Fig. 3-3). The technique was apparently first practised by Sevcik[3.8]. Subsequently other investigators, including Koutecky[3.18], Matsuda[3.19], Kemula and co-workers [3.20 - 3.24], Gokhshtein[3.25], Weber[3.26], Nicholson and Shain[3.9, 3.27, 3.28], Polcyn and Shain[3.29, 3.30], and Wopschall and Shain[3.31, 3.32], applied the method to studies of electrode mechanisms.

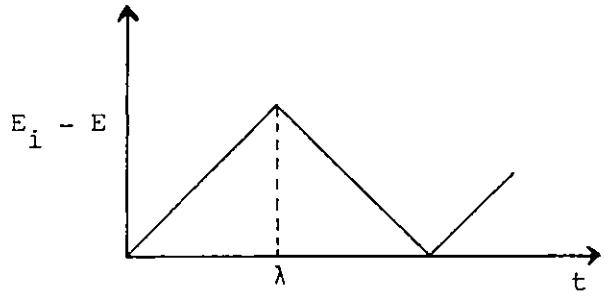

Fig. 3-3 Wave form of the potential scan for cyclic voltammetry.

3-4.1 Uncomplicated charge transfers

The cyclic voltammogram of a reversible charge-transfer reaction exhibits both cathodic and anodic segments of the current-potential curve. The segment corresponding to the linearly increasing part of the potential scan up to the switching potential, E_λ, is identical to the current-potential curve for linear sweep voltammetry. However, the height and position of the segment of the current-potential curve corresponding to the linearly decreasing part of the potential scan depends on E_λ. The sweep rates employed are similar to those in linear sweep voltammetry.

Nicholson and Shain[3.9] have investigated the effect of E_λ on the peak potential of the anodic reverse wave. They calculated that, for a reversible charge transfer at 25°C, E_p of the anodic reverse wave will remain relatively unaffected provided that E_λ is not less than about $35/n$ mV past the cathodic peak for sweep rates as slow as 3 V min^{-1}. This means that $(E_{\frac{1}{2}} - E_\lambda)n$ must be about 2-300 mV and represents a time interval of only 4-6 seconds past the peak.

According to Sevcik[3.8], when referring to a reversible charge transfer at 25°C,

$$E_{p(c)} = E_{\frac{1}{2}} - \frac{0.029}{n} \text{ volts} \tag{3-47}$$

$$E_{p(a)} = E_{\frac{1}{2}} + \frac{0.029}{n} \text{ volts} \tag{3-48}$$

Therefore

$$E_{p(a)} - E_{p(c)} = \frac{0.058}{n} \text{ volts} \tag{3-49}$$

where $E_{p(c)}$ is the cathodic and $E_{p(a)}$ the anodic peak potential. However, equation 3-49 only holds for single-sweep voltammograms of individual solutions of oxidant and reductant, or when E_λ of the cyclic voltammogram is far enough past $E_{p(c)}$ for the condition $C_R^e = C_O^b$ to be attained prior to the anodic reverse scan. Under these conditions, the ratio of anodic to cathodic peak current is unity.

Quasi-reversible systems show a greater separation in E_p's. The voltammograms are more drawn out and the peaks more rounded.

For very slow charge-transfer processes, the anodic and cathodic processes are completely separated. When the charge transfer is totally irreversible, no reverse wave will be exhibited.

R. S. Nicholson[3.33] has applied values of $E_{p(a)} - E_{p(c)}$ to the measurement of rate constants for electron transfer. The separation in peak potentials was correlated to a function ψ given by

$$\psi = \gamma^{\alpha} \frac{k_s}{\pi^{\frac{1}{2}} D_O (nF/RT)^{\frac{1}{2}} v^{\frac{1}{2}}} \tag{3-50}$$

where $\gamma = (D_O/D_R)^{\frac{1}{2}}$, α is the transfer coefficient, and k_s is the standard rate constant at $E = E^o$. A working curve may be constructed from the theoretical values in Table 3-1[3.33], where the conditions $(E_\lambda - E_{\frac{1}{2}}) = 141/n$ mV and $\alpha = 0.5$ are assumed to obtain.

Table 3-1 Variations of ΔE_p with charge-transfer parameters for cyclic voltammetry

ψ	$\Delta E_p \times n$ (mV)
20	61
7	63
6	64
5	65
4	66
3	68
2	72
1	84
0.75	92
0.5	105
0.35	121
0.25	141
0.1	212

For a majority of cases, γ^{α} in Equation 3-50 is very nearly equal to unity regardless of α because $D_O \approx D_R$.

If cyclic voltammetry is applied under multiple sweep conditions then, in the absence of kinetic complications, the continuing cycles merely gradually alter the concentration profiles near the electrode surface. The anodic and cathodic peaks slightly change shape and decrease until a steady state is achieved. For a reversible system Matsuda[3.19] showed that the difference between initial and steady-state E_p's is only a few millivolts and relatively insignificant.

3-4.2 Multiple charge transfers

Polcyn and Shain[3.29] have quantitatively characterised systems involving multiple charge transfers limited to only two species. The reaction may be represented by

$$O + n_1 e \rightarrow R_1 + n_2 e \rightarrow R_2$$

If quasireversible systems are not considered, the four possible sets of charge transfer conditions are: (i) Reversible - Reversible, (ii) Reversible - Irreversible, (iii) Irreversible - Reversible, and (iv) Irreversible - Irreversible. The characteristics of the theoretical voltammograms depend on several factors including the nature of the

charge-transfer steps, the potential separation between the individual charge transfers, the number of electrons in the specific steps, and the switching potential, E_λ .

For reversible charge transfers, four possible theoretical voltammograms are presented in Fig. 3-4[3.29].

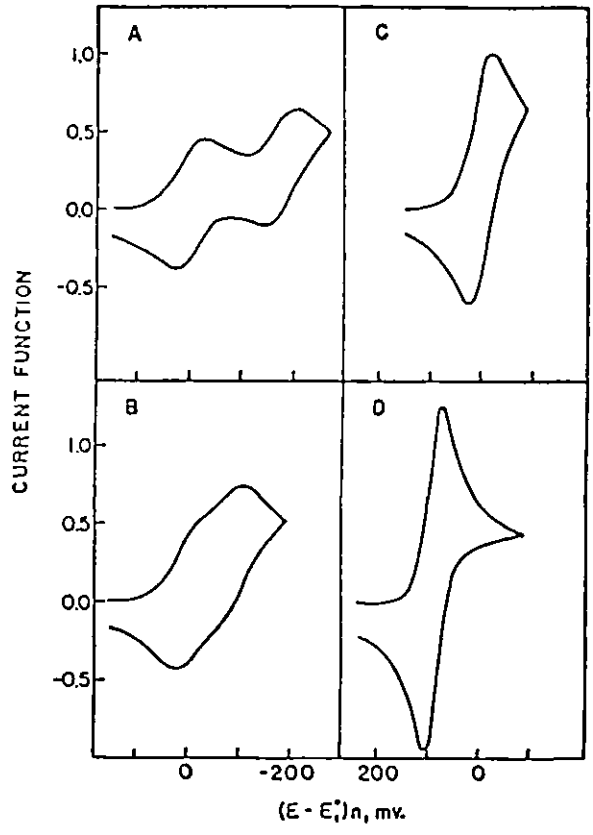

Fig. 3-4 Cyclic voltammograms for the case Reversible-Reversible, and $n_2/n_1 = 1$. A) $\Delta E^{o'} = -180$ mV, B) $\Delta E^{o'} = -90$ mV, C) $\Delta E^{o'} = 0$ mV, and D) $\Delta E^{o'} = 180$ mV.

Curve A represents the current-potential curve for the reversible charge transfers of the e.a.s. O and R_1 where the formal potential separation $\Delta E^{o'}$ is -180 mV. According to Gokhshtein and Gokhshtein[3.16], a minimum separation of about 118/n mV between the formal reduction potentials is required in order that the individual waves behave as independent reversible waves. Furthermore, Polcyn and Shain[3.29] calculated that the switching potential E_λ should be a minimum of about 65/n mV past the most cathodic $E^{o'}$ if the anodic reverse waves are to have the same shape and height as the cathodic waves.

As $\Delta E^{o'}$ decreases below about 100/n mV the individual waves merge into one broad and distorted wave which might be mistaken for an irreversible voltammogram. However, unlike irreversible charge transfers, the potential of the distorted wave does not shift with varying scan rate and an anodic reverse wave is exhibited; as can be seen in Curve B where $\Delta E^{o'}$ is -90 mV.

Curve C is for the particular case when both O and R_1 are reduced at the same potential ($\Delta E^{o'} = 0$). Assuming that $n_1 = n_2 = 1$, the peak height is intermediate between a one-electron and a two-electron reversible wave. $E_p - E_{\frac{1}{2}}$ is about 21 mV. As R_1 becomes easier to reduce than O, the wave height increases and the peak narrows until the wave assumes the characteristics of a two-electron reversible charge transfer (Curve D, $\Delta E^{o'} = 180$ mV). The effective $E^{o'}$ for the composite two-electron wave is given by $(E_O^{o'} + E_R^{o'})/2$.

The number of electrons involved in the charge-transfer steps affects both the shape and position of the waves because the current function increases with increasing values of n_1 and n_2, and the potential scale is defined as $(E - E^{o'})n$.

Irreversible charge-transfer voltammograms are presented in Fig 3-5[3.29].

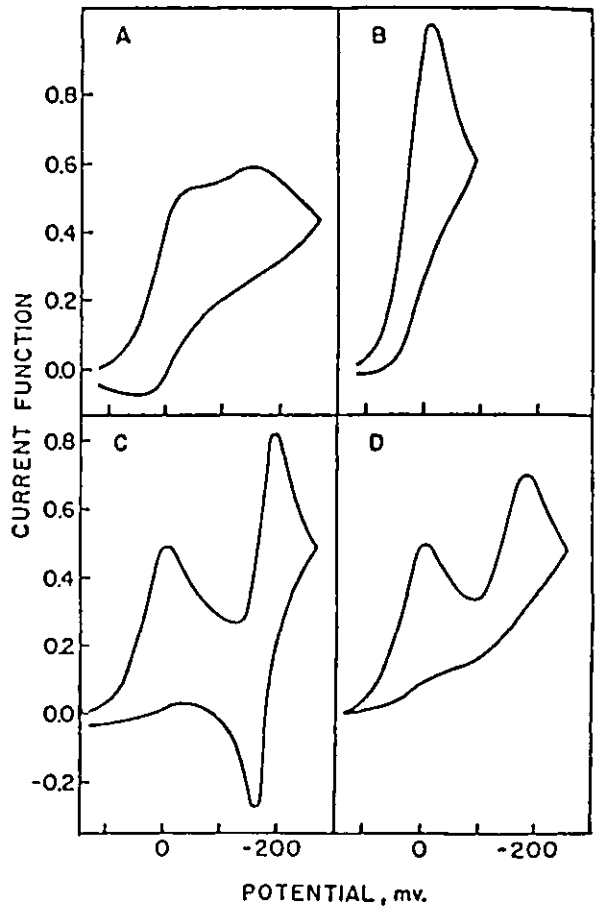

Fig. 3-5 Cyclic voltammograms with irreversible charge transfers,

and $n_1 = n_2$, $\alpha = 0.5$. A) Case R-I, $\Delta E^{o'} = -180$ mV; B) Case R-I, $\Delta E^{o'} = 0$ mV; C) Case I-R, $\Delta E^{o'} = -180$ mV; D) Case I-I, $\Delta E^{o'} = -180$ mV; where R = reversible and I = irreversible.

When the two e.a.s. O and R_1 are reduced at sufficiently different potentials, the waves can be considered as resulting from separate reactions even if one (or both) of the charge transfers is irreversible. Under these circumstances, the irreversible wave will be characteristic of an isolated irreversible charge transfer (section 3-3.3). No anodic counterpart is observed for the wave of an irreversible reduction.

As the potential separation between successive reductions decreases below about $100/\alpha n_a$ mV, the individual waves merge and are distorted. When O and R_1 are reduced at the same potential, a single wave is observed with the combined characteristics of the two charge transfers involved. When R_1 becomes easier to reduce than O the wave increases in height and sharpness, but the characteristics of the combined wave depend primarily on the first charge transfer in the sequence.

3-5 Application to Kinetic Systems

The voltammetry of kinetic systems involve situations where homogeneous reversible or irreversible chemical reactions are coupled in various combinations to the reversible or irreversible electron transfers. These chemical reactions might precede or follow the charge transfer, or might be catalytic (where the follow-up reaction regenerates the original e.a.s.). The catalytic reaction is also known as a parallel chemical reaction.

3-5.1 *D. c.* voltammetry

According to Brdicka and Wiesner[3.34], and Koutecky and Brdicka [3.35 - 3.37], an electrochemical process governed by a preceding chemical reaction can be described by a combination of Fick's second law and the rate equation for the chemical reaction. For the system

$$Z \underset{k_b}{\overset{k_f}{\rightleftharpoons}} O \xrightarrow{k_{Red}} R,$$ where the e.a.s. O (formed, within the reaction layer, by a chemical reaction from the inactive species Z) is irreversibly reduced to the species R, and $K = k_f/k_b \ll 1$, the concentration of O, C_O, is given by

$$C_O = KC_Z \left\{ 1 - \frac{1}{1 + (k_f D/K)^{\frac{1}{2}}/k_{Red}} \exp \left[- x \left(\frac{k_f}{KD} \right)^{\frac{1}{2}} \right] \right\} \qquad (3\text{-}51)$$

The electrode reaction rate constant is

$$k_{Red} = k' \exp \left[- \frac{\alpha nF}{RT} (E - E^{O'}) \right] \qquad (3\text{-}52)$$

and the thickness of the reaction layer is

$$\mu = \left(\frac{KD}{k_f} \right)^{\frac{1}{2}} \qquad (3\text{-}53)$$

where $D = D_Z = D_O$.

The current density is then given by[3.3, 3.38]

$$i = nFC_Z K \frac{(k_f D/K)^{\frac{1}{2}}}{1 + (k_f D/K)^{\frac{1}{2}}/k_{Red}} \qquad (3\text{-}54)$$

and the limiting current density (when $k_{Red} \gg (k_f D/K)^{\frac{1}{2}}$) is

$$i_L = nFC_Z (k_f KD)^{\frac{1}{2}} \qquad (3\text{-}55)$$

In the case of the catalytic reaction

$$\begin{array}{l} O + ne \longrightarrow R \\ \uparrow \quad\quad\quad\quad \downarrow \\ R + Z \underset{k_b}{\overset{k_f}{\rightleftharpoons}} O \end{array}$$

Brdicka and Wiesner[3.39] applied the concept of reaction layer to this system. They assumed that: (i) substance Z is electroinactive within the applied potential range and is present in large excess, (ii) the regenerating process occurs in a reaction layer thickness μ, (iii) $D = D_O = D_R$, (iv) $k_f \gg k_b$, and (v) all the regenerated molecules of O reach the electrode. Hence the number of moles of O regenerated is $\mu k_f C_Z^b C_R$ and the catalytic current is given by[3.40]

$$i_c = nFA\mu k_f C_Z^b C_O^b \qquad (3\text{-}56)$$

where $\mu = (D/k_f C_Z^b)^{\frac{1}{2}}$. Therefore the total current is easily obtained by adding the mass-transport controlled current (equation 3-3) to the catalytic current (equation 3-56):

$$i = nFAD_O \frac{C_O^b - C_O^e}{\delta_O} + nFA\mu k_f C_Z^b C_O^b \qquad (3\text{-}57)$$

The limiting current will then be given by

$$i_L = nFAC_O^b \left(\frac{D_O}{\delta_O} + \mu k_f C_Z^b \right) \qquad (3\text{-}58)$$

Thus the mass-transport controlled current is enhanced by the catalytic current.

The application of d.c. voltammetry to the study of kinetic systems is limited by: (i) the conditions under which kinetic currents can be observed, (ii) the kinetic effect cannot be detected if the rate of chemical reaction preceding the charge transfer is too high, and (iii) only first order processes can be treated rigorously. Therefore, kinetic systems are better studied by the techniques of linear sweep voltammetry and cyclic voltammetry (section 3-5.2).

3-5.2 Linear sweep and cyclic voltammetry

Several quantitative treatments for kinetic systems have been postulated[3.9, 3.27, 3.30, 3.41-3.51]. Of these, the more complex systems are the ECE mechanism[3.27, 3.49], and the catalytic reaction coupled to the first charge transfer of a multistep charge transfer process[3.30].

For kinetic systems involving a single charge transfer reaction, Nicholson and Shain[3.9] have developed diagnostic criteria which can be applied to trace the mechanism of unknown systems. The boundary value problem for each case is formulated in a manner similar to the uncomplicated reversible or irreversible system as appropriate, but modified to reflect the kinetic complications. The variation of peak current function, $i_p/nFAC_O^b(\pi D_O nFv/RT)^{\frac{1}{2}}$ for reversible systems or $i_{p(ir)}/nFAC_O^b(\pi D_O \alpha n_a Fv/RT)^{\frac{1}{2}}$ for irreversible systems, with the rate of potential sweep is followed. Such variations for different kinetic systems are graphically presented in Fig. 3-6[3.9].

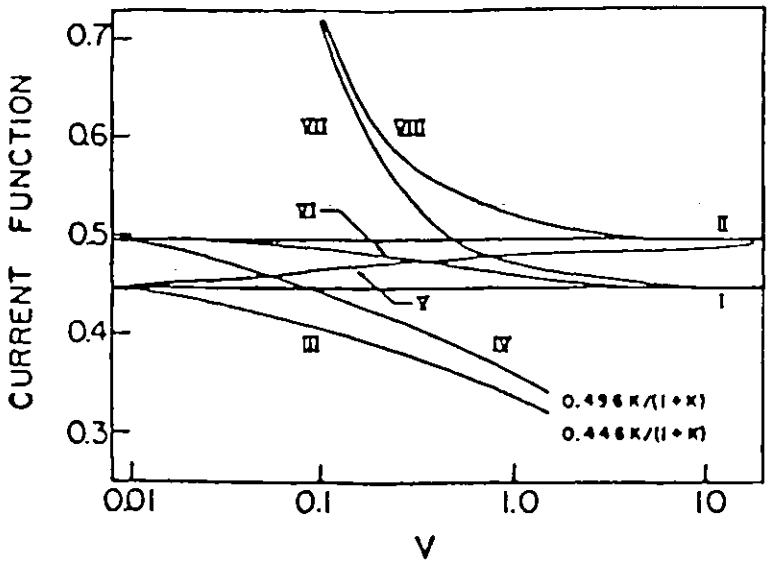

Fig. 3-6 Variation of peak current functions with rate of potential sweep.

I. Reversible charge transfer

$$O + ne \rightleftharpoons R$$

II. Irreversible charge transfer

$$O + ne \xrightarrow{k_s} R$$

III. Chemical reaction preceding a reversible charge transfer

$$Z \underset{k_b}{\overset{k_f}{\rightleftharpoons}} O$$

$$O + ne \rightleftharpoons R$$

IV. Chemical reaction preceding an irreversible charge transfer

$$Z \underset{k_b}{\overset{k_f}{\rightleftharpoons}} O$$

$$O + ne \xrightarrow{k_s} R$$

V. Charge transfer followed by a reversible chemical reaction

$$O + ne \rightleftharpoons R$$

$$R \underset{k_b}{\overset{k_f}{\rightleftharpoons}} Z$$

VI. Charge transfer followed by an irreversible chemical reaction

$$O + ne \rightleftharpoons R$$

$$R \xrightarrow{k_f} Z$$

VII. Catalytic reaction with reversible charge transfer

$$O + ne \rightleftharpoons R$$

$$R + Z \xrightarrow{k'_f} O$$

VIII. Catalytic reaction with irreversible charge transfer

$$O + ne \xrightarrow{k_s} R$$

$$R + Z \xrightarrow{k'_f} O$$

It can be observed from Fig. 3-6 that only the current functions for the uncomplicated reversible or irreversible charge transfer systems (I and II) remain constant with varying sweep rates. The current function for each kinetic system does vary with varying sweep rates, but approaches one of the horizontal straight lines for uncomplicated cases whenever the rate of potential sweep does not allow enough time for the chemical reaction to proceed significantly before the experiment is over. Experimentally, it is only necessary to plot $i_p/v^{\frac{1}{2}}$ versus v or $v^{\frac{1}{2}}$ to obtain this correlation.

Another useful correlation for investigating unknown systems is to study the rate at which the wave shifts along the potential axis as the potential sweep rate is varied (Fig. 3-7[3.9]). Experimentally, the function $E_{p/2}/\log v$ or $E_p/\log v$ versus v is to be plotted. However, $E_{p/2}/\log v$ is still applicable even if no peaks are definable.

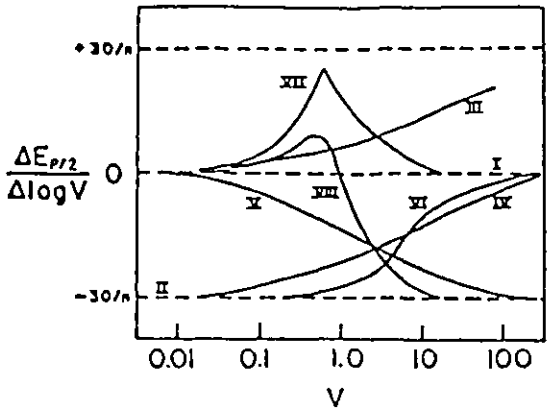

Fig. 3-7 Rate of shift of potential as a function of scan rate.

If cyclic voltammetry is applied to an unknown system, then for cases where the charge transfer is reversible, the correlation of the ratio of anodic to cathodic peak current with the variation in potential sweep rate serves as a quick test for the presence of kinetic complications. This correlation is graphically presented in Fig. 3-8[3.9]. It can be seen that $i_{p(a)}/i_{p(c)}$ is unity and invariable only for the reversible (Case I) and catalytic (Case VII) systems.

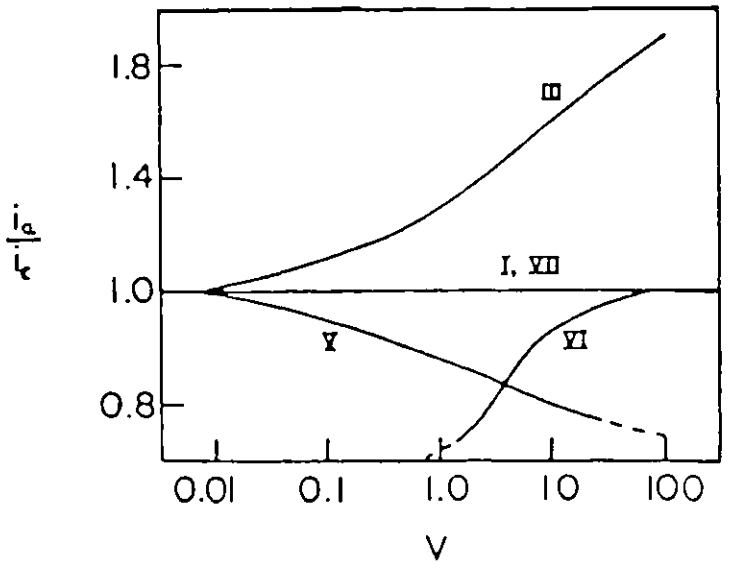

Fig. 3-8 Ratio of anodic to cathodic peak current as a function of rate of potential sweep.

Kinetic complications can also be detected if cyclic voltammetry is applied under multiple sweep conditions. For instance, a chemical follow-up reaction might produce an e.a.s. which will exhibit a peak only after the initial cycle. An example of this case is the oxidation of crystal violet in 1M sulphuric acid at a carbon paste electrode[3.14].

Nicholson and Shain extended their theory of cyclic voltammetry [3.9] to the characterisation of the ECE mechanism[3.27]; where a chemical reaction is coupled between two charge transfers. To reduce the complications, they confined their numerical treatment to cases involving irreversible chemical reactions. Thus the total reaction may be represented by

$$A \xrightarrow{n_1 e} B \xrightarrow{k_f} C \xrightarrow{n_2 e} D$$

Other factors to be considered are those connected with the character of multiple charge transfers (as discussed in section 3-4.2).

For multiple reversible charge transfers, the current-potential curve may be expressed as[3.27]

$$i = n_1 FAD^{\frac{1}{2}} C_A^b (nFv/RT)^{\frac{1}{2}} \pi^{\frac{1}{2}} \chi(nFvt/RT) + n_2 FAD^{\frac{1}{2}} C_A^b (nFv/RT)^{\frac{1}{2}} \pi^{\frac{1}{2}} \Phi(nFvt/RT) \qquad (3\text{-}59)$$

where the functions $\chi(nFvt/RT)$ and $\Phi(nFvt/RT)$ are related to the fluxes of substances A and C respectively, the diffusion coefficient $D = D_A = D_B = D_C = D_D$, n_1 and n_2 are the numbers of electrons involved in the reduction of A to B and C to D respectively. When the multiple charge transfers are irreversible the current functions $\chi(nFvt/RT)$ and $\Phi(nFvt/RT)$ in equation 3-59 are replaced by $\chi(\alpha n_a Fvt/RT)$ and $\Phi(\alpha n_a Fvt/RT)$ respectively and the factor $(nFv/RT)^{\frac{1}{2}}$ is replaced by $(\alpha n_a Fv/RT)^{\frac{1}{2}}$. Analogous equations for the cases Reversible-Irreversible and Irreversible-Reversible multiple charge transfers are obtained by the appropriate permutation of the current functions and factors for the reversible and irreversible terms.

The shape and height of the voltammogram are not only dependent on the parameters n's, αn_a's, $\Delta E^{o'}$'s and E_λ, but also on the kinetic parameter $k_f/(nFv/RT)$.

Nicholson and Shain[3.27] have graphically presented diagnostic criteria for the study of unknown ECE systems. For the condition $n_1 = n_2 = 1.0$, three possible sets of diagnostic plots[3.27] are presented which correspond to the further condition that $\Delta E^{o'} = -180$ mV (Fig. 3-9), $\Delta E^{o'} = 0$ (Fig. 3-10), and $\Delta E^{o'} = +180$ mV (Fig. 3-11). The four ECE mechanisms considered are:

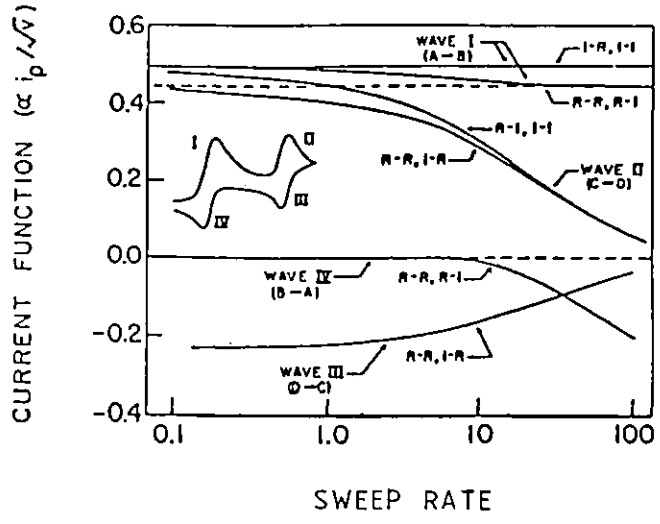

Fig. 3-9 Diagnostic criteria showing variation in peak current function with changes in sweep rate. $\Delta E^{o\prime} = -180$ mV; $n_2/n_1 = 1.0$.

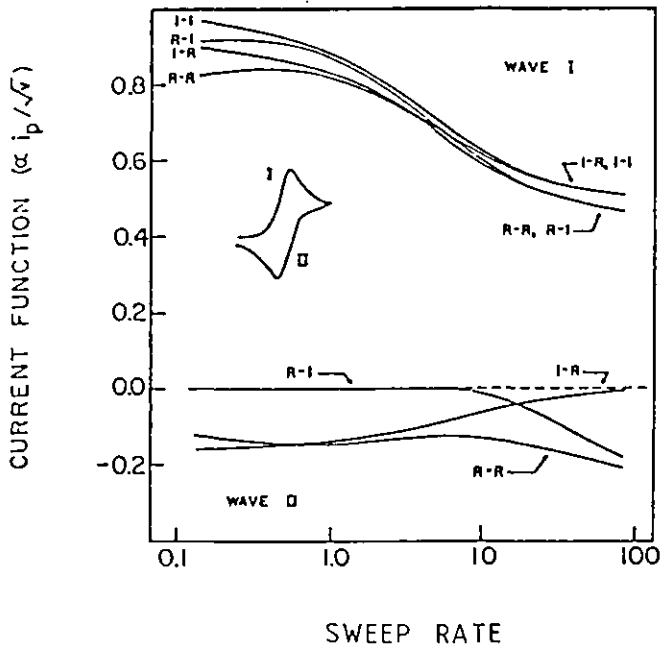

Fig. 3-10 Diagnostic criteria showing variation in peak current function with changes in sweep rate. $\Delta E^{o\prime} = 0$; $n_2/n_1 = 1.0$; Wave II is absent for Case I-I.

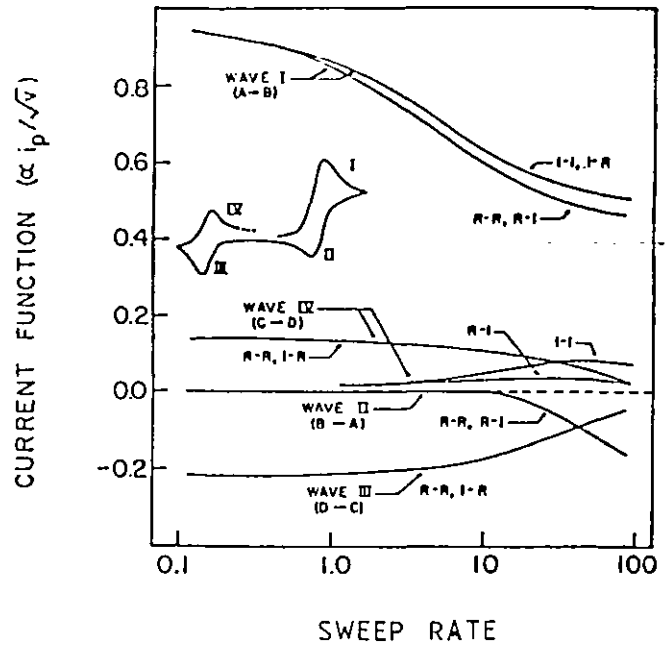

Fig. 3-11 Diagnostic criteria showing variation in peak current function with changes in sweep rate. $\Delta E^{o'}$ = +180 mV; $n_2 = n_1$; Wave II is absent for Cases I-R and I-I; Wave III is absent for Cases R-I and I-I.

1) Reversible-Reversible (R-R)

$$A \underset{}{\overset{n_1 e}{\rightleftharpoons}} B \xrightarrow{k_f} C \overset{n_2 e}{\rightleftharpoons} D$$

2) Reversible- Irreversible (R-I)

$$A \overset{n_1 e}{\rightleftharpoons} B \xrightarrow{k_f} C \xrightarrow[n_2 e]{k'_s} D$$

3) Irreversible-Reversible (I-R)

$$A \xrightarrow[n_1 e]{k_s} B \xrightarrow{k_f} C \overset{n_2 e}{\rightleftharpoons} D$$

4) Irreversible-Irreversible (I-I)

$$A \xrightarrow[n_1 e]{k_s} B \xrightarrow{k_f} C \xrightarrow[n_2 e]{k'_s} D$$

Experimentally, the current functions can be plotted as $i_p/v^{\frac{1}{2}}$ versus v or $v^{\frac{1}{2}}$ and the combination of trends can be compared with those of Figures 3-9 to 3-11 in order to obtain the ECE mechanism for the unknown system.

Polcyn and Shain[3.30] extended the theory of cyclic voltammetry[3.9, 3.27] to the characterisation of the kinetic system where a

catalytic chemical reaction is coupled between two charge transfers. Their investigations were confined to the case in which an irreversible catalytic reaction is coupled with the first charge transfer:

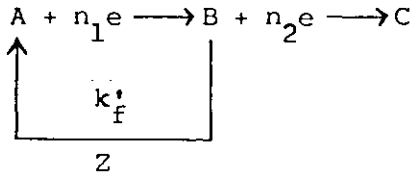

Substance Z is assumed to be electroinactive in the potential range of interest and is present in large excess. Thus the catalytic chemical reaction can be considered as pseudo first-order with the pseudo first-order rate constant $k'_f = kC_Z$; where k is the formal rate constant and C_Z is the concentration of substance Z.

Ignoring quasi-reversible systems, four sets of conditions are possible depending on the reversibility of the charge transfers: (i) Reversible-Catalytic-Reversible (R-C-R), (ii) Reversible-Catalytic-Irreversible (R-C-I), (iii) Irreversible-Catalytic-Reversible (I-C-R), and (iv) Irreversible-Catalytic-Irreversible (I-C-I).

The shape and height of the voltammogram are not only dependent on the parameters pertaining to multiple charge transfers (section 3-4.2), but also on the kinetic parameter $k'_f/(nFv/RT)$.

By employing a procedure analogous to that of Nicholson and Shain [3.9, 3.27], Polcyn and Shain formulated diagnostic criteria which are presented graphically[3.30] in Figures 3-12 and 3-13.

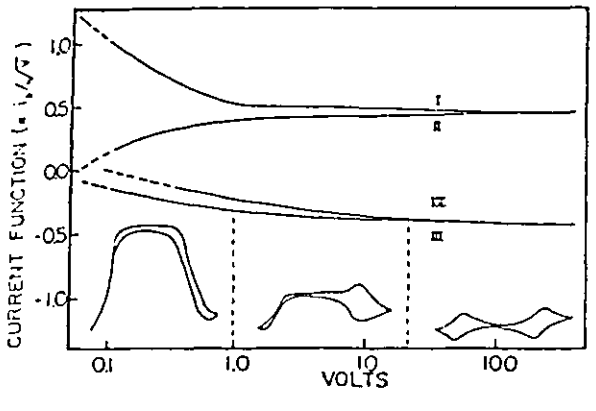

Fig. 3-12 Diagnostic criteria showing the variation in peak current function with changes in sweep rate for Case R-C-R. $\Delta E^{o'} = -500$ mV; $n_2/n_1 = 1.0$.

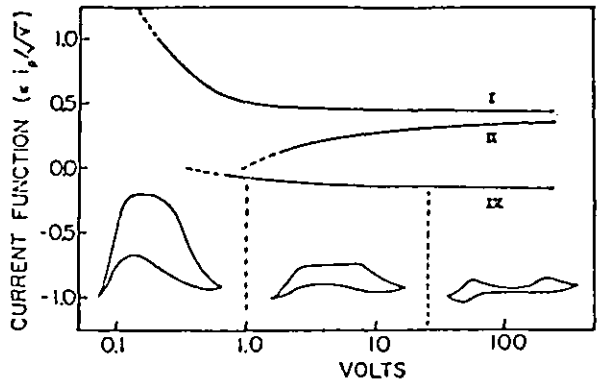

Fig. 3-13 Diagnostic criteria showing the variation in peak current function with changes in sweep rate for Case R-C-I. $\Delta E^{o'} = -500$ mV; $n_2/n_1 = 1.0$; $\alpha = 0.5$; and Wave III is absent.

The data in Figures 3-12 and 3-13 are based on the conditions of $\Delta E^{o'} = -500$ mV, $n_1 = n_2 = 1.0$, and $\alpha n_a = 0.5$. However, the general trends would still be valid for other values of these parameters. Experimentally, the trend of $i_p/v^{\frac{1}{2}}$ with v or $v^{\frac{1}{2}}$ is to be followed.

3-6 Application to Adsorption Systems

3-6.1 D.c. voltammetry

Brdicka[3.52] discussed the effects of adsorption on polarographic waves at the dropping mercury electrode (DME) in terms of the Langmuir adsorption isotherm. The Langmuir adsorption isotherm may be expressed as

$$\Gamma_i = \beta' C_i \Gamma_i^s/(1 + \beta' C_i) \qquad (3\text{-}60)$$

where Γ_i is the surface concentration of species i (in moles per unit area), β' is the adsorption coeffecient, C_i is the interfacial solution concentration of species i, and Γ_i^s is the saturation value at maximum surface coverage of species i.

Although the findings of Brdicka[3.52] are based on polarography at the DME, the conclusions may be applied to d.c. voltammetry in stirred solutions where steady-state conditions obtain. The conclusions are illustrated in Fig 3-14[3.52] for a reduction process, where π is the potential.

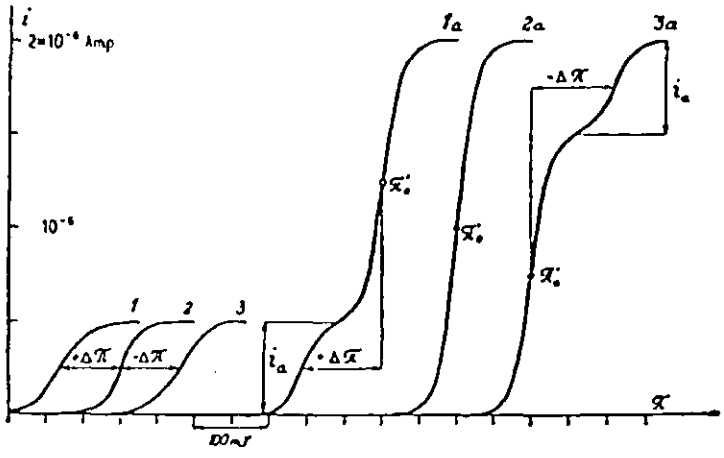

Fig. 3-14 Illustration of polarographic waves due to a reversible two-electron reduction complicated by adsorption. Waves 1 and 1a refer to the reductant; 2 and 2a refer to both the reductant and oxidant possessing either the same adsorption quantities or both being adsorption-inactive; 3 and 3a refer to the oxidant. Waves 1, 2, and 3 correspond to small concentrations of e.a.s. at which the electrode surface is not yet saturated by the adsorbed species, whereas waves 1a, 2a, and 3a correspond to larger concentrations.

If the oxidant is adsorbed and the reductant is surface inactive, the reduction of the adsorbed oxidant will require more energy than the reduction of the free form of oxidant because the energy of the adsorption bond has to be overcome. Thus in the case of strong adsorption of oxidant, the adsorption wave occurs at less positive or more negative potentials (Curve 3) with respect to the wave for the free form (Curve 2). When the bulk concentration of oxidant is high enough so that the adsorbed oxidant saturates the electrode surface, then the adsorption wave is preceded by the diffusion wave of the free form (Curve 3a).

Conversely, when the oxidant is surface inactive and the reductant is adsorbed, less energy is required to produce an adsorbed reductant than a free form of the reductant. Thus the adsorption wave for a strongly adsorbed reductant occurs at more positive or less negative potentials with respect to the wave for the free form (Curves 1 and 1a).

If both oxidant and reductant are adsorbed with the same free energy of adsorption, then the two different adsorption effects neutralise each other and the resultant wave is similar to a diffusion wave (Curves 2 and 2a).

For weak adsorption, the adsorption wave may occur at similar potentials to that of the diffusion wave and so might be concealed within a resultant composite wave. However, if the adsorption wave constitutes a reasonable part of the total composite wave, the non-linear concentration behaviour of the composite wave height signifies the presence of adsorption. Adsorption wave heights become independent of bulk concentration of e.a.s. when the bulk concentration is in excess of the concentration required to saturate the electrode surface with the adsorbed form of e.a.s.

3-6.2 Linear sweep and cyclic voltammetry

Wopschall and Shain[3.31] extended the theory of linear sweep and cyclic voltammetry[3.9] to systems involving the adsorption of electroactive species. The Langmuir adsorption isotherm was employed to describe the adsorption in the reaction scheme:

$$O_{soln} \rightleftharpoons O_{ads}$$

$$O + ne \rightleftharpoons R$$

$$R_{soln} \rightleftharpoons R_{ads}$$

where the charge transfer is reversible, and both product and reactant are adsorbed and in equilibrium with the dissolved species.

Examples of theoretical cyclic voltammograms of reversible charge transfers involving adsorption are presented in Fig. 3-15[3.31]. Curves A and B refer to the case where the e.a.s. are weakly adsorbed. The peak currents are enhanced[3.53, 3.54] because of electron transfer involving the adsorbed e.a.s. at nearly the same potential as the uncomplicated electron transfer. Curves C and D illustrate the presence of a separate adsorption post-peak and pre-peak, relative to the uncomplicated peak, for the case of strong adsorption of reactant and product respectively. This behaviour is analogous to the polarographic adsorption waves[3.52, 3.55] (section 3-6.1).

The boundary value problem is essentially the same as the case of uncomplicated electron transfer[3.9] except that the relation between the fluxes of O and R includes terms related to the rate of change of the surface concentrations of adsorbed species[3.31]:

$$D_O(\partial C_O/\partial x) - \partial \Gamma_O/\partial t = -D_R(\partial C_R/\partial x) + \partial \Gamma_R/\partial t \qquad (3\text{-}61)$$

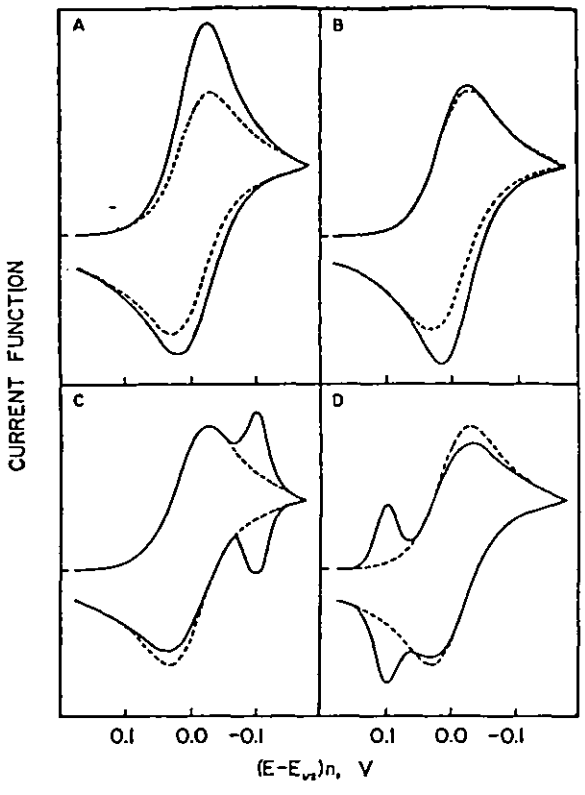

Fig. 3-15 Theoretical cyclic voltammograms of reversible charge transfers involving adsorption. A) reactant adsorbed weakly; B) product adsorbed weakly; C) reactant adsorbed strongly; D) product adsorbed strongly. Dashed lines indicate behaviour for the uncomplicated Nernstian charge transfer.

$$\Gamma_O = \Gamma_O^s \, C_O/(K_O + C_O) \qquad (3\text{-}62)$$

$$\Gamma_R = \Gamma_R^s \, C_R/(K_R + C_R) \qquad (3\text{-}63)$$

where t is the time, x is the distance from the electrode-solution interface, C_O and C_R are the solution concentrations of O and R, D_O and D_R are the diffusion coefficients, Γ_O and Γ_R are the surface concentrations (in moles per unit area), and Γ_O^s and Γ_R^s are the saturation values at maximum surface coverage. The potential dependent terms K_O and K_R in the Langmuir adsorption isotherms (equations 3-62 and 3-63) for species O and R are related to the free energies of adsorption, ΔG,

by $\quad -\ln K = \Delta G/RT \qquad (3\text{-}64)$

The total current is given by

$$i = nFA\left(C_O^b \pi^{\frac{1}{2}} D_O^{\frac{1}{2}} \left(\frac{nFv}{RT}\right)^{\frac{1}{2}} \chi_O\left(\frac{nFvt}{RT}\right) - \partial\Gamma_O/\partial t\right)$$

$$= -nFA\left(C_O^b \pi^{\frac{1}{2}} D_O^{\frac{1}{2}} \left(\frac{nFv}{RT}\right)^{\frac{1}{2}} \chi_R\left(\frac{nFvt}{RT}\right) - \partial\Gamma_R/\partial t\right) \qquad (3\text{-}65)$$

Wopschall and Shain[3.31] calculated a current function, $\psi\left(\frac{nFvt}{RT}\right)$, analogous to that for the uncomplicated reversible case[3.9] and so the current is defined by

$$i(t) = \frac{n^{3/2}F^{3/2}}{R^{\frac{1}{2}}T^{\frac{1}{2}}} A D_O^{\frac{1}{2}} C_O^b v^{\frac{1}{2}} \psi\left(\frac{nFv}{RT} t\right) \qquad (3\text{-}66)$$

On this basis, they developed diagnostic criteria for the characterisation of unknown systems.

The presence of strong adsorption is usually exhibited in the form of a pre-peak or post-peak; which predominates at high sweep rates or low concentrations. When however, the free energy of adsorption is high (weak adsorption) the adsorption and diffusion processes occur simultaneously resulting in charge transfer at the same potential; and so confirmation of the presence of adsorption is required. Three quick tests are recommended[3.31]. The first is to qualitatively observe for increased symmetry, relative to the case of uncomplicated Nernstian charge transfer, in the general shape of the current-potential curves as the sweep rate is increased or the concentration is decreased (Figures 3-16 and 3-17)[3.31].

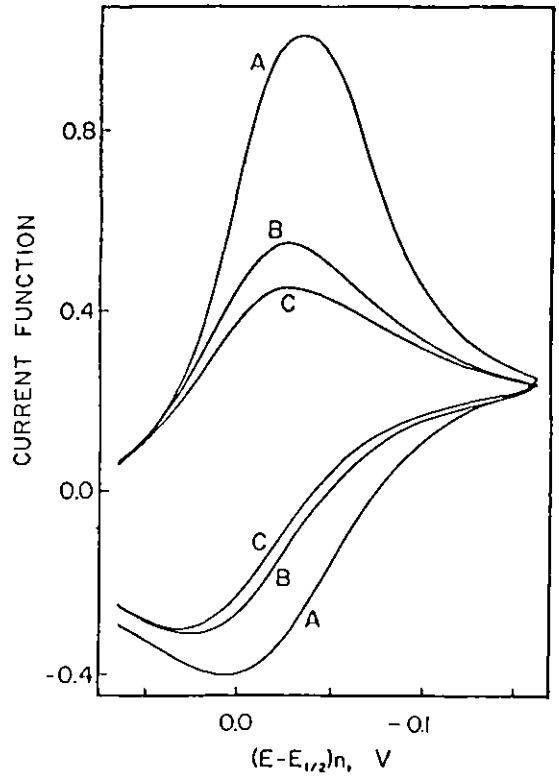

Fig. 3-16 Cyclic voltammograms with reactant weakly adsorbed -

Corresponding to relative sweep rates, v, of: A) 2500, B) 100, and C) 1.

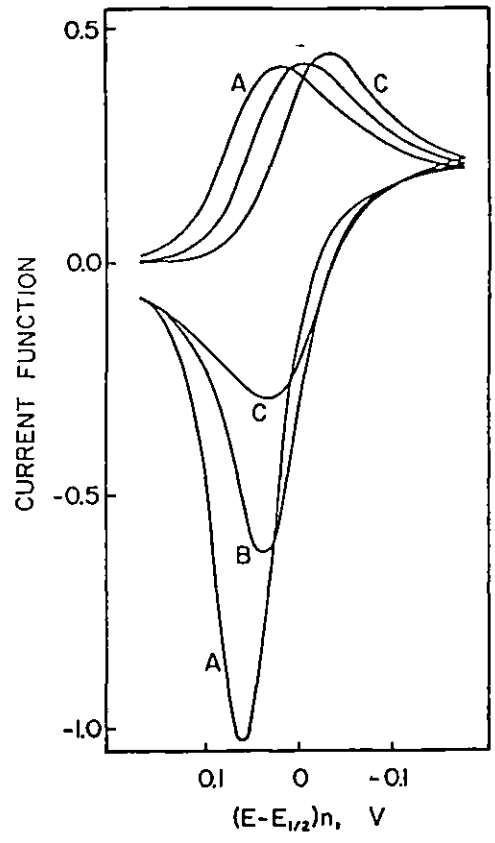

Fig. 3-17 Cyclic voltammograms with product weakly adsorbed - Corresponding to relative sweep rates, v, of: A) 4×10^4, B) 2.5×10^3, and C) 1.

The other two methods involve quantitative measurements but cannot be applied with certainty if the other processes, such as kinetic effects , are present. One of these methods is to plot the experimental equivalent of the current function, $i_p/C_O^b v^{\frac{1}{2}}$, against increasing v or $v^{\frac{1}{2}}$. If adsorption is present, $i_p/C_O^b v^{\frac{1}{2}}$ increases rapidly with increasing sweep rate while i_p/vC_O^b may remain nearly constant. Very few other processes are likely to exhibit similar behaviour[3.9].

The final method involves the monitoring of the concentration dependence of the peak current. Although i_p/C_O^b is constant for many processes, when adsorption is present i_p/C_O^{bp} usually increases with decreasing concentration and possibly levels off at some constant value for low concentrations, analogous to Figure 3-18[3.31]. However, results of such plots should be carefully considered because concentration

dependence may not be an important factor within the concentration range studied.

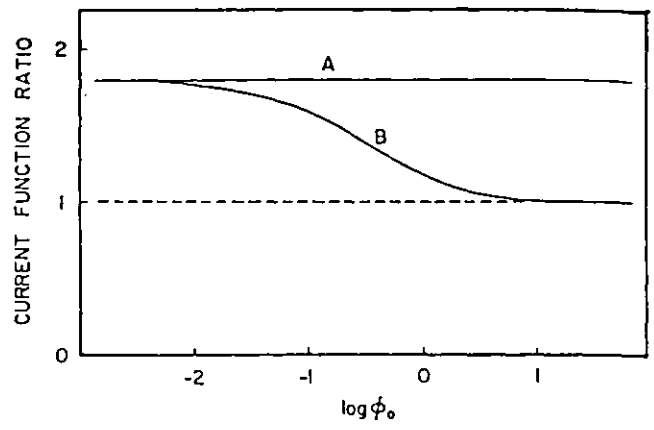

Fig. 3-18 Ratio of cathodic peak current function with adsorption, to that for uncomplicated Nernstian charge transfer - as a function of bulk concentration (i.e. $\phi_o \propto C_o^b$). A) Low concentration limiting behaviour (Henry's law); B) Langmuir behaviour. Dashed line indicates behaviour for uncomplicated Nernstian charge transfer.

At sufficiently low concentrations almost all adsorbates, regardless of the adsorption isotherms which they normally obey, will obey Henry's law. Thus when $C \ll K$, equations 3-62 and 3-63 reduce to[3.31]

$$\Gamma \approx (\Gamma^S/K)C \qquad (3\text{-}67)$$

where $(\Gamma^S/K) = \beta$ (the Henry's law adsorption coefficient). Therefore the current of the electrode reaction is a linear function of the bulk concentration, because the amount of adsorption is proportional to concentration. Furthermore, a separate adsorption peak for strong adsorption will not be exhibited. Instead, the adsorption peak will be superimposed onto the diffusion peak; similar to the case of weak Langmuir adsorption (Fig. 3-16 to 3-18).

Wopschall and Shain[3.32] have attempted to extend their theory of cyclic voltammetry involving adsorption to cover instances where both adsorption and kinetic effects are present. Direct correlation of their theory with experimental results was not completely successful, but a semi-empirical method was developed which appears to be generally applicable. They confined their study to the case of a reversible charge transfer followed by an irreversible chemical reaction with weak

Langmuir adsorption of the reactant:

$$O_{soln} \rightleftharpoons O_{ads}$$

$$O + ne \rightleftharpoons R \xrightarrow{k_f} Z$$

The boundary value problem is identical to that for charge transfer with adsorption alone[3.31] except that the Fick's Law diffusion equation for species R must be modified to include the kinetic term, and species R is assumed not adsorbed. Species Z is electroinactive within the potential range of interest. The current function $\psi(nFvt/RT)$ is defined as in equation 3-66 but in the numerical treatment it includes the kinetic parameter $k_f/(nFv/RT)$. Therefore, although weak adsorption enhances both the cathodic and anodic peak currents, the chemical rate constant k_f has a more profound effect on the anodic peak current than the cathodic peak current. These characteristics are illustrated in Fig. 3-19[3.32].

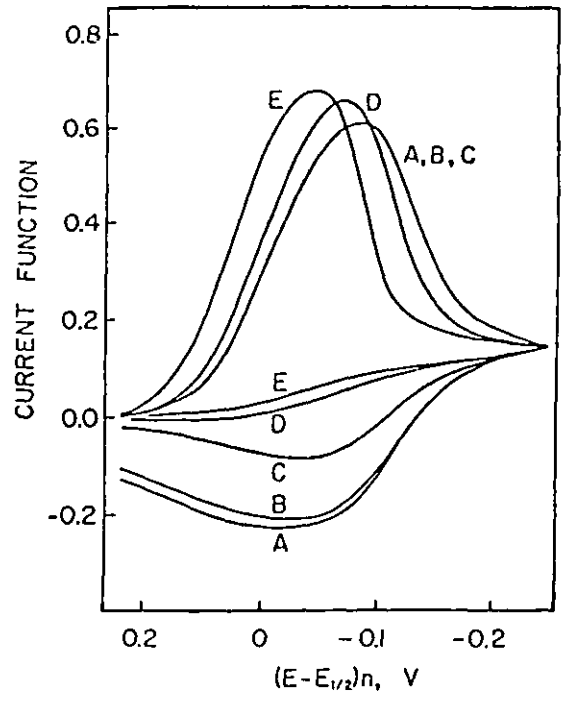

Fig. 3-19 Cyclic voltammograms for a reversible charge transfer coupled to an irreversible succeeding chemical reaction, with the reactant weakly adsorbed - variation with chemical rate constant, k_f. $k_f/(nFv/RT)$ equals: A) 0.001, B) 0.01, C) 0.1, D) 1.0, and E) 10.0.

The potential sweep rate affects the adsorption and kinetic parameters in two directly opposing manners (Fig. 3-20 and 3-21)[3.32]. An increase in sweep rate enhances the adsorption effect but reduces the kinetic effect. The converse occurs with decreasing sweep rate.

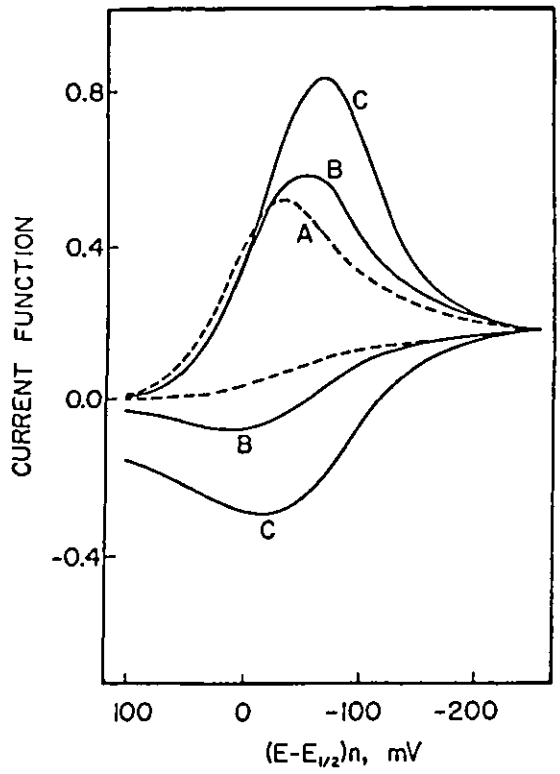

Fig. 3-20 Cyclic voltammograms for a reversible charge transfer coupled to an irreversible succeeding chemical reaction, with the reactant weakly adsorbed - variation with sweep rate, v. k_f = 1.0 s^{-1}. nFv/RT equals: A) 1 s^{-1}, B) 10 s^{-1}, and C) 100 s^{-1}.

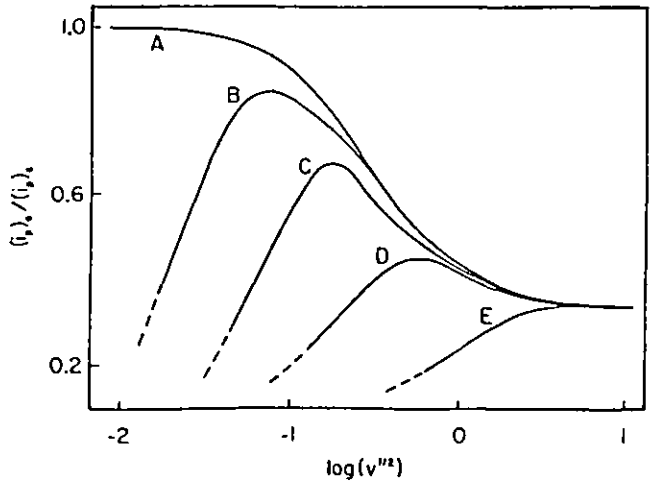

Fig. 3-21 Variation of the ratio of anodic to cathodic peak

current, $(i_p)_a/(i_p)_c$, with sweep rate for the cyclic voltammogram of a succeeding chemical reaction with reactant weakly adsorbed. E_λ = 240 mV. A) Chemical reaction negligible, $k_f = 0$; B) k_f = 0.13 s^{-1}, C) k_f = 1.3 s^{-1}, D) k_f = 13 s^{-1}, and E) k_f = 130 s^{-1}.

The effect of concentration is presented in Fig. 3-22(3.32). In general, an increase in bulk concentration causes the adsorption of reactant to have relatively less influence on the cyclic voltammograms. Furthermore, varying concentrations affect the anodic current function less than the cathodic current function.

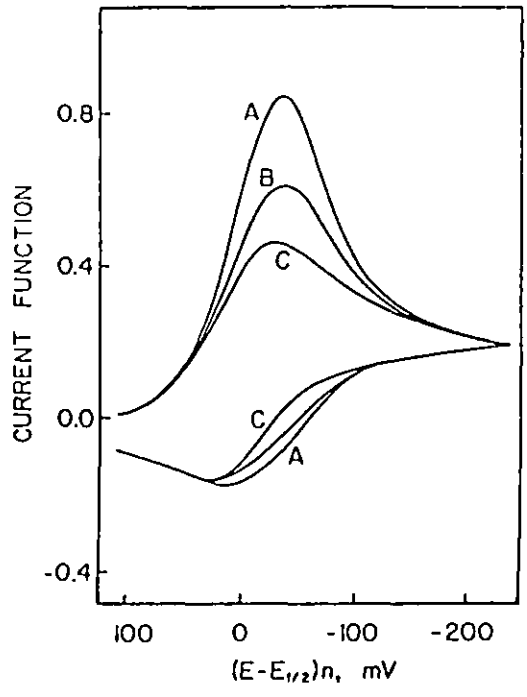

Fig. 3-22 Effect of variation of bulk concentration on cyclic voltammograms for the succeeding chemical reaction with reactant weakly adsorbed. $k_f/(nFv/RT)$ = 0.05. ϕ_O (which is proportional to C_O^b) equals: A) 0.1, B) 0.5, and C) 5.0 and greater.

3-7 References

3.1 Kalvoda R.; Operational Amplifiers in Chemical Instrumentation, p. 134. Ellis Horwood Ltd., 1975.

3.2 Nernst W.; Z. Physik. Chem., 1904, 47, 52.

3.3 Vydra F., et al; Electrochemical Stripping Analysis, Chapter 2, 2.1. Ellis Horwood Ltd., 1976.

3.4 Koryta J., et al; Electrochemistry, Chapter IV.C. Methuen & Co. Ltd., 1970.

3.5 Delahay P.; New Instrumental Methods in Electrochemistry, Chapter 9. Interscience Publishers, Inc., 1954.

3.6 Koryta J., et al; Electrochemistry, Chapter IV.B. Methuen & Co. Ltd., 1970.

3.7 Randles J. E. B.; Trans. Faraday Soc., 1948, 44, 327.

3.8 Sevcik A.; Collection Czech. Chem. Commun., 1948, 13, 349.

3.9 Nicholson R. S. and Shain I.; Anal. Chem., 1964, 36, 706.

3.10 Vydra F., et al; Electrochemical Stripping Analysis, Chapter 3. Ellis Horwood Ltd., 1976.

3.11 Delahay P.; New Instrumental Methods in Electrochemistry, Chapter 6. Interscience Publishers, Inc., 1954.

3.12 Berzins T. and Delahay P.; J. Am. Chem. Soc., 1953, 75, 555.

3.13 Delahay P.; J. Am. Chem. Soc., 1953, 75, 1190.

3.14 Adams R. N.; Electrochemistry at Solid Electrodes, Chapter 5. Dekker, 1969.

3.15 Ibid, Chapter 8.

3.16 Gokhshtein Y. P. and Gokhshtein A. Y.; Advances in Polarography, Longmuir I. S. (editor), Vol. II, p. 465. Pergamon Press, 1960.

3.17 Gokhshtein Y. P. and Gokhshtein A. Y.; Dokl. Akad. Nauk. SSSR, 1959, 128, 985.

3.18 Koutecky J.; Collection Czech. Chem. Commun., 1956, 21, 433.

3.19 Matsuda H.; Z. Elektrochem., 1957, 61, 489.

3.20 Kemula W. and Kublik Z.; Nature, 1958, 182, 793.

3.21 Kemula W. and Kublik Z.; Roczniki Chem., 1958, 32, 941.

3.22 Kemula W.; Advan. Polarog. Proc. Intern. Polarog. Congr., 2nd, Cambridge, 1959 (pub. 1960), 1, 105.

3.23 Kemula W., et al; Naturwiss., 1960, 22, 1.

3.24 Kemula W., et al; Roczniki Chem., 1962, 36, 1349.

3.25 Gokhshtein Y. P.; Doklady Akad. Nauk SSSR, 1959, 126, 598.

3.26 Weber J.; Collection Czech. Chem. Commun., 1959, 24, 1770.

3.27 Nicholson R. S. and Shain I.; Anal. Chem., 1965, 37, 178.

3.28 Ibid., p. 190.

3.29 Polcyn D. S. and Shain I.; Anal. Chem., 1966, 38, 370.

3.30 Ibid., p. 376.

3.31 Wopschall R. H. and Shain I.; Anal. Chem., 1967, 39, 1514.

3.32 Ibid., p. 1535.

3.33 Nicholson R. S.; Anal. Chem., 1965, 37, 1351.

3.34 Brdicka R. and Wiesner K.; Chem. Listy, 1946, 40, 66; and Collection Czech. Chem. Commun., 1947, 12, 138.

3.35 Koutecky J. and Brdicka R.; Collection Czech. Chem. Commun., 1947, 12, 337.

3.36 Koutecky J.; Chem. Listy, 1951, 45, 245; and Collection Czech. Chem. Commun., 1953, 18, 11.

3.37 Koutecky J.; Chem. Listy, 1952, 46, 193; and Collection Czech. Chem. Commun., 1953, 18, 183.

3.38 Koryta J., et al; Electrochemistry, Chapter IV.E. Methuen & Co. Ltd., 1970.

3.39 Brdicka R. and Wiesner K.; Collection Czech. Chem. Commun., 1947, 12, 39.

3.40 Delahay P.; New Instrumental Methods in Electrochemistry, Chapter 5. Interscience Publishers, Inc., 1954.

3.41 Reinmuth W. H.; Anal. Chem., 1960, 32, 1891.

3.42 Schwarz W. M.; Ph. D. thesis, Univ. Wisconsin, Madison, 1960.

3.43 Smith D. E.; Ph. D. thesis, Columbia Univ., New York, 1960.

3.44 Saveant J. M. and Vianello E.; Advan. Polarog. Proc. Intern. Polarog. Congr., 2nd, Cambridge, 1959 (pub. 1960), 1, 367.

3.45 Saveant J. M. and Vianello E.; Compt. Rend., 1963, 256, 2597.

3.46 Saveant J. M. and Vianello E.; Anal. Chim. Acta, 1963, 8, 905.

3.47 Nicholson R. S.; Anal. Chem., 1965, 37, 667.

3.48 Saveant J. M. and Vianello E.; Electrochim. Acta, 1967, 12, 629.

3.49 Saveant J. M.; Electrochim. Acta, 1967, 12, 753.

3.50 Lundquist J. T., Jr., and Nicholson R. S.; J. Electroanal. Chem., 1968, 16, 445.

3.51 Nelson R.; J. Electroanal. Chem., 1968, 18, 329.

3.52 Brdicka R.; Collection Czech. Chem. Commun., 1947, 12, 522.

3.53 Osteryoung R. A., et al; J. Electrochem. Soc., 1963, 110, 926.

3.54 Streuli C. A. and Cooke W. D.; Anal. Chem., 1954, 26, 963.

3.55 Kolthoff I. M. and Lingane J. J.; Polarography, 2nd ed., Vol. I, p 256. Interscience Publishers, Inc., 1952.

4. EXPERIMENTAL

4-1 Electrodes and Voltammetric Procedure

4-1.1 Construction of the working electrode

Disks (between 5 and 10 mm thicknesses) were cut from the rods of working-electrode materials (boron carbide, boron carbide/carbon composites, and spectrographic grade graphite). The disks were then polished, on diamond paste compound for boron carbide and boron carbide/carbon composites but on hard filter paper for spectrographic grade graphite, to a mirror finish for the electrode working surface. When required, further treatments on the disks were performed before mounting them. PTFE tape was wrapped around the edge of the disks, when mounting, to provide an effective waterproofing barrier. The rest of the electrode was assembled as illustrated (Fig. 4-1).

4-1.2 Construction of the saturated calomel electrode

The materials required for the construction of a SCE are illustrated in Fig. 4-2.

The lithium acetate/agar was prepared by dissolving agar (0.34 g) in gently boiling distilled water (10 cm^3). When the agar had dissolved, lithium acetate (4 g) was dissolved in the hot solution; which was then allowed to cool further. Whilst the lithium acetate/agar was still fluid, some of it was sucked into the polypropene tube with the aid of a rubber teat and left to set. When set, the lithium acetate/agar salt bridge was attached to the glass vessel (Fig. 4-2).

The calomel paste was prepared[4.1] by grinding, with a glass mortar and pestle, mercury(I) chloride and pure mercury together under a saturated solution of potassium chloride; the supernatant liquid was poured off and the grinding process repeated twice with fresh quantities of saturated potassium chloride solution.

Pure mercury (1 cm depth) was introduced into the glass vessel and the tungsten wire was inserted to make contact. The glass vessel was then filled with the other components in ascending order (as illustrated in Fig. 4-2) whilst ensuring that the tungsten wire contact remained within the mercury pool and thus remained dry.

When not in use, the SCE was stored with the lithium acetate/agar salt bridge dipping in distilled water.

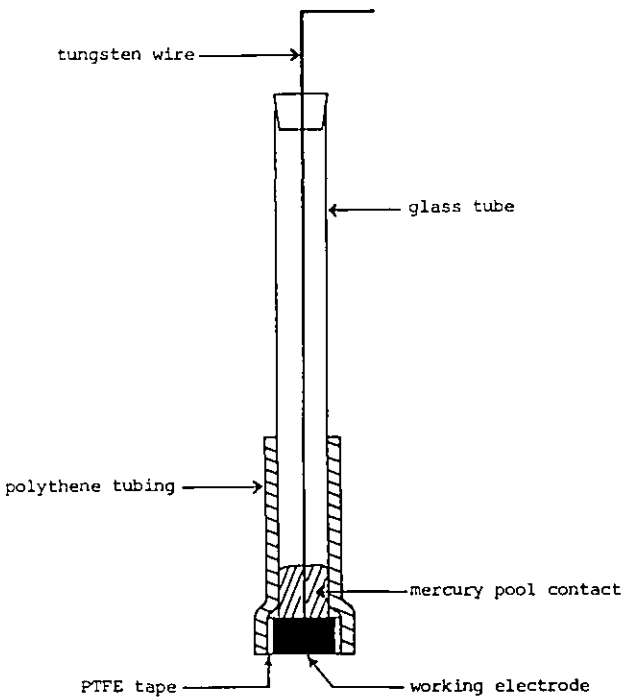

Fig. 4-1 The solid working electrode.

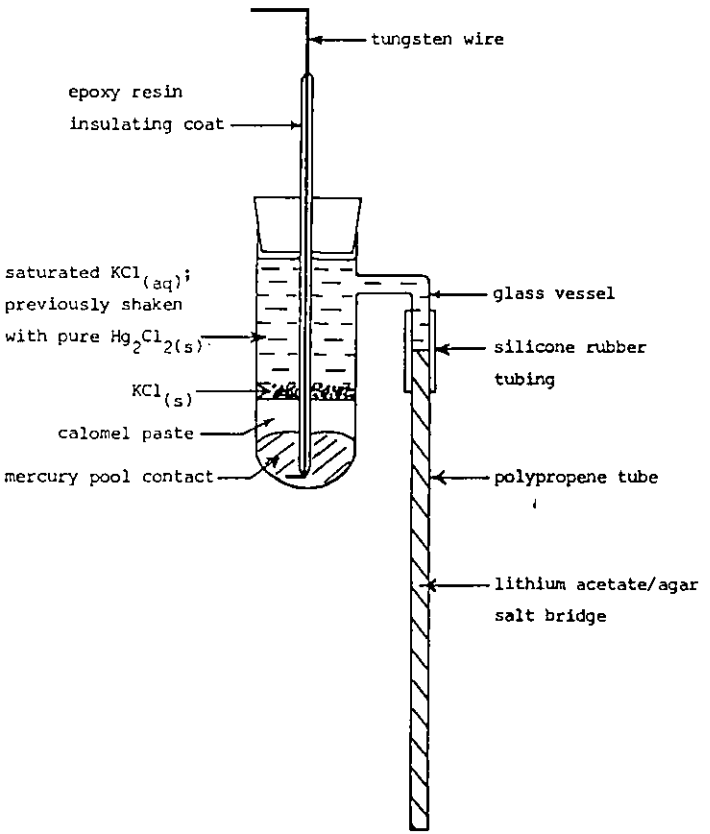

Fig. 4-2 Saturated calomel electrode.

4-1.3 Apparatus

Princeton Applied Research Corporation Model 174A Polarographic Analyzer: Initial potential is adjustable to ±1 mV; accuracy is ±1 mV plus 0.25% of full scale.

Sweep rate is selectable from 0.1 mV s^{-1} to 500 mV s^{-1} in 1-2-5 sequence. Internal switch allows factor of ten increase in the sweep rate.

Scan range of 0.75 V, 1.5 V, or 3.0 V, either polarity, starting at the initial potential which is selectable.

Keyboard functions: INITIAL, HOLD, SCAN, and SCAN REVERSE push-button switches control the operational cycle of the instrument.

Current range is selectable from 0.02 μA to 10 mA full scale in 1-2-5 sequence. Accuracy is ±0.25% from 0.05 μA to 10 mA full scale, and ±1.5% at 0.02 μA full scale.

Rikadenki X-Y chart recorder (for sweep rates ≤ 500 mV s^{-1}):
Accuracy is better than ±0.25% full scale.
Reproducibility is better than ±0.1% full scale.

Cathode-ray oscilloscope (for sweep rates > 500 mV s^{-1}).

Working electrodes and 2 SCE's (to function as reference and auxiliary electrodes).

Magnetic stirrer and follower.

Beaker (100 cm^3), measuring cylinder (50 cm^3), and thermometer (0 - 50 ^{o}C).

Oxygen-free nitrogen, and a glass tube with a sinter-glass enclosed end (for nitrogen aeration).

4-1.4 D.c. voltammetric procedure

The WE and two SCE's were mounted together in such a manner that their electrolytic ends were linearly adjacent (with the WE in the middle) and horizontally level. Precautions were taken to ensure that: (i) the position of the electrode assembly, at the centre of the beaker (100 cm^3) and 5 mm above the magnetic follower, was reproducible, (ii)

the volume (50 cm^3) of test solution in the voltammetric cell was kept constant, and (iii) the stirring rate was kept constant; so that δ_O in equation 3-4 was maintained constant ($i_L \propto \delta_O^{-1}$).

The electrodes were electrically connected to the PAR 174A Polarographic Analyzer in a three-electrode circuit (section 3-1) after the PAR 174A and the Rikadenki X-Y chart recorder had been checked and calibrated. When required, the stirred test solution was nitrogen aerated and a blanket of nitrogen was maintained over its surface. The WE was poised (for two minutes) at the initial potential, to allow the initial current to reach a steady state, before scanning (usually at a rate of 2 mV s^{-1}) over the selected potential range (usually 1.5 V). The supporting electrolyte was always voltammetrically studied, for the residual current, before the sample solutions. All the voltammetric investigations were performed at room temperature and every set of results was obtained on the same day.

4-1.5 Linear sweep and cyclic voltammetric procedure

The voltammetric cell for linear sweep and cyclic voltammetry was as for d.c. voltammetry. However, linear sweep voltammetry involved stirring (for 15 s) the test solution, poising (for two minutes) the WE at the initial potential in unstirred solution, and then potential scanning the unstirred solution over the selected potential range (usually 1.5 V). The sweep rates employed were usually from 5 mV s^{-1} to 500 mV s^{-1} (selectable in 1-2-5 sequence); although rates upto 5 V s^{-1} were occasionally used.

The procedure for cyclic voltammetry was similar to that for the linear sweep technique except that the potential scan was reversed, by pressing SCAN REVERSE, at a selected switching potential E_λ. It was assumed that, since the selected E_λ was not less than 35 mV past the most cathodic peak potential (section 3-4.1), any small error incurred in the pressing of SCAN REVERSE at the exact value of E_λ would not affect the anodic curves. When required, multiple cyclic sweeps were achieved by repeated use of the SCAN and SCAN REVERSE push-button switches.

4-2 Specific Treatment Procedures for Boron Carbide Electrodes in Application to the Chloroiridate-Chloroiridite System

4-2.1 Carbon enrichment of electrode working surfaces

Two polished boron carbide disks (electrodes 12 and 13) were treated by employing them as drill bits and drilling their electrode working surfaces into pure graphite at high speed until appreciable frictional heat developed[4.2]. Each disk was then sandwiched between two pure graphite moulds, secured with tungsten wire (Fig. 4-3), and heated at 1300 ^{o}C (for 50 hours) in an atmosphere of argon.

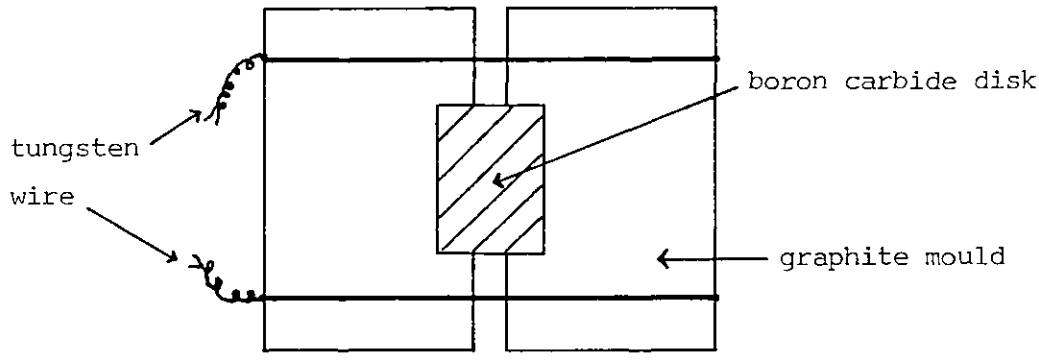

Fig. 4-3 Boron carbide disk/graphite mould assembly.

4-2.2 Chemical treatments

Boron carbide disks were treated with one of the following solutions : (i) nitric acid (23%)/hydrofluoric acid (2%)/teepol (2%), (ii) hot Sn(II) chloride (25%)/HCl (1 + 3), (iii) hot hydrogen peroxide, (iv) hot concentrated nitric acid, and (v) hot aqua regia. After treatment the disks were boiled twice in distilled water, and dried in the oven before mounting them as working electrodes.

4-2.3 Electrochemical treatment

The working electrode was cathodically polarised in the stirred chloroiridate (4.0×10^{-5} to 2.0×10^{-3} mol dm^{-3})/supporting electrolyte (0.1 M) sample solution for ten minutes prior to the voltammetric scans.

4-3 Treatment with Ir(IV) Perchlorate

The working electrode was subjected to anodic stripping at +4.8 V (vs. SCE) in a stirred solution of perchloric acid (0.1 M) for sixty seconds, dried with hard filter paper, dipped in a stirred solution of Ir(IV) perchlorate (1.0×10^{-5} to 2.3×10^{-3} M) in perchloric acid (0.1 M) for sixty seconds, rinsed thrice with perchloric acid (0.1 M),

dipped in a stirred solution of perchloric acid (0.1 M) for sixty seconds, and then finally dried with hard filter paper.

4-4 Iridium

4-4.1 Chloroiridate-chloroiridite system

A concentration range of ammonium hexachloroiridate (1.0×10^{-5} to 2.0×10^{-3} mol dm^{-3}) in perchloric acid (0.1 M) supporting electrolyte was prepared by direct dissolution of the salt followed by serial dilution. This was repeated for the other supporting electrolytes of hydrochloric acid (0.1 M) and sodium perchlorate (0.1 M). In the cases of perchloric acid and hydrochloric acid, solutions of ammonium hexachloroiridate (1.0×10^{-4} mol dm^{-3}) in a concentration range of supporting electrolyte (0.1 to 2.0 M) were also prepared. All these solutions were investigated voltammetrically over the potential range +1.1 V to -0.4 V (vs. SCE).

4-4.2 Ir(IV) perchlorate system

Ammonium hexachloroiridate, dissolved in the minimum of distilled water, was reduced with hydrazine hydrochloride (1.4 mg per 10 mg Ir) to the chloroiridite. Perchloric acid (60%) was then added (in the ratio of 1 ml to 5mg Ir) and the solution was evaporated to strong fumes[4.3]. After the solution was allowed to cool, a little distilled water was added and the solution was again evaporated to strong fumes; repeating twice more. It was ensured that the solution always remained a solution at the fuming stage, by the addition of extra minimal amount of perchloric acid (60%) if necessary.

Concentration ranges of Ir(IV) perchlorate (4.0×10^{-6} to 2.3×10^{-3} mol dm^{-3}) in perchloric acid (0.1 M) supporting electrolyte, and Ir(IV) perchlorate (1.0×10^{-4} mol dm^{-3}) in perchloric acid (0.1 to 2.0 M) were prepared by serial dilution and were voltammetrically scanned from +1.1 V to -0.4 V (vs. SCE). In some cases, nitrogen aeration of the sample solution was employed prior to voltammetry.

4-4.3 Ir(IV) sulphate system

Ir(IV) sulphate was prepared in a procedure similar to that for the preparation of Ir(IV) perchlorate (section 4-4.2) but the fuming agent employed[4.4, 4.5] was 1 ml concentrated sulphuric acid with 0.1 ml perchloric acid (60%) per 5 mg Ir. Solutions of Ir(IV) sulphate (1.0×10^{-4} mol dm^{-3}) in a concentration range of sulphuric acid (0.05

to 0.4 M) supporting electrolyte were prepared and scanned voltammetrically from +1.1 V to -0.4 V (vs. SCE).

4-4.4 Ir(IV) phosphate system

Ir(IV) phosphate was prepared by a procedure similar to that for the preparation of Ir(IV) perchlorate (section 4-4.2) but the fuming agent employed[4.4, 4.5] was 1 ml orthophosphoric acid with 0.1 ml perchloric acid (60%) per 5 mg Ir. Ir(IV) phosphate (5.2×10^{-4} mol dm^{-3}) in phosphoric acid (0.32 M) supporting electrolyte was scanned voltammetrically from +1.0 V to -0.5 V (vs. SCE).

4-5 Iron

4-5.1 Fe(III)-Fe(II) perchlorate system

Ferric perchlorate was prepared by evaporating ferric nitrate with perchloric acid to strong fumes[4.5]. Concentration ranges of ferric perchlorate (1.0×10^{-5} to 1.0×10^{-3} mol dm^{-3}) in perchloric acid (0.1 M) supporting electrolyte, and ferric perchlorate (1.0×10^{-4} mol dm^{-3}) in perchloric acid (0.1 to 1.0 M) were prepared by serial dilution and were scanned voltammetrically from +1.0 V to -0.5 V (vs. SCE).

4-5.2 Fe(III)-Fe(II) chloride system

A stock solution of ferric chloride (0.1 M) in hydrochloric acid (0.1 M) supporting electrolyte was prepared by the direct dissolution of $FeCl_3.6H_2O$. Despite the hygroscopic nature of $FeCl_3.6H_2O$, it was not considered necessary to standardise the stock solution because trends were looked for rather than absolute values.

Concentration ranges of ferric chloride (4×10^{-5} to 2×10^{-3} M) in hydrochloric acid (0.1 M), and ferric chloride (2×10^{-4} M) in hydrochloric acid (0.1 to 2.0 M) were prepared by serial dilution and were scanned voltammetrically from +1.0 V to -0.5 V (vs. SCE).

If required, the ferric chloride stock solution may be standardised[4.6] against EDTA at pH 2-3 using Tiron as indicator.

4-5.3 Fe(III)-Fe(II) cyanide system

Concentration ranges of potassium ferricyanide (8.0×10^{-5} to 2.0×10^{-3} mol dm^{-3}) in potassium chloride (0.5 M) supporting electrolyte, and potassium ferricyanide (2.0×10^{-4} mol dm^{-3}) in potassium chloride (0.1 to 2.0 M) were prepared by direct dissolution of the salt followed

by serial dilution. The prepared solutions were scanned voltammetrically from +0.6 V to -0.4 V (vs. SCE).

4-6 Palladium

Pd(II)-Pd(0) system

Palladium chloride was dissolved in dilute nitric acid and repeatedly evaporated to strong fumes with perchloric acid (60%). Palladium perchlorate (4.0×10^{-4} mol dm^{-3}) in perchloric acid (2.0 M) supporting electrolyte was scanned voltammetrically from +1.0 V to -0.5 V (vs. SCE).

4-7 Silver

Ag(I)-Ag(0) system

A concentration range of silver perchlorate (2.0×10^{-5} to 2.0×10^{-3} mol dm^{-3}) in sodium perchlorate (0.1 M) supporting electrolyte was prepared by direct dissolution of the salt followed by serial dilution. The solutions were then scanned voltammetrically from +0.5 V to -0.2 V (vs. SCE).

4-8 Copper

Cu(II)-Cu(0) system

Copper(II) sulphate (2.0×10^{-4} mol dm^{-3}) in sodium perchlorate (0.1 M) supporting electrolyte was prepared by direct dissolution of the salt and was scanned voltammetrically from +0.5 V to -0.5 V (vs. SCE).

4-9 Mixed Ion Solution

Chloroiridate/Fe(III) chloride system

A mixed ion solution of chloroiridate (1.0×10^{-4} mol dm^{-3}) and ferric chloride (1×10^{-4} M) in hydrochloric acid (0.1 M) supporting electrolyte was scanned voltammetrically from +1.1 V to -0.4 V (vs. SCE).

4-10 Chemical Analysis of Boron Carbide

Boron carbide, when not in powder form, was relatively easy to reduce to particles no larger than 50 mesh by use of a steel percussion mortar. Due to the hardness of boron carbide, grinding was not employed ; in order to ensure the minimum possibility of sample contamination by the sample processing container.

4-10.1 Boron analysis

The boron carbide particles were carefully sampled and weighed (0.1 g) into a clean pre-weighed platinum boat, and pyrohydrolysed[4.7] (at 1150 ^{o}C) in the apparatus illustrated in Fig. 4-4. The distillate was collected at the rate of 3-5 cm^3 per minute. On average, the boron carbide samples required 2-3 hours for complete pyrohydrolysis; depending on the nature of the sample. Although the time required for complete pyrohydrolysis was shortened at higher temperatures (e.g. 1-2 hours at > 1200 ^{o}C), the working life of the silica reaction tube was also significantly reduced. After each pyrohydrolysis the cooled platinum boat was re-weighed before cleaning.

The resultant boric acid distillate collected was nitrogen aerated, complexed with sorbitol[4.8] (3g per 100 cm^3 of distillate), and titrated potentiometrically under an atmosphere of nitrogen against standardised sodium hydroxide (0.3 N) with a Radiometer automatic titrator. Solutions of sorbitol (3g per 100 cm^3 of nitrogen aerated distilled water) were also titrated to obtain "blank" titres. Hence the boron composition of boron carbide was calculated from the concentration of boric acid product.

4-10.2 Carbon analysis

The total carbon content was determined by the Direct-Combustion Method, using a twin-tube furnace version of the apparatus illustrated in Fig. 4-5, at 1150 ^{o}C with an oxygen flow-rate of 100 cm^3 per minute.

The prefired (at 1100 ^{o}C for 1 hour) fireclay combustion boats were prepared by weighing into each boat lead(II) oxide (3 g) and fused alumina (1 g), igniting (for 15 minutes) in the combustion apparatus, and allowing them to cool in a desiccator. Boron carbide particles were then sampled and weighed (0.13 g), quantitatively transferred into a prepared combustion boat, and combusted (90 minutes) in the apparatus (Fig. 4-5). The resultant carbon dioxide was absorbed in a Nesbitt CO_2 absorption weighing bottle and weighed. "Blanks", being the weights of

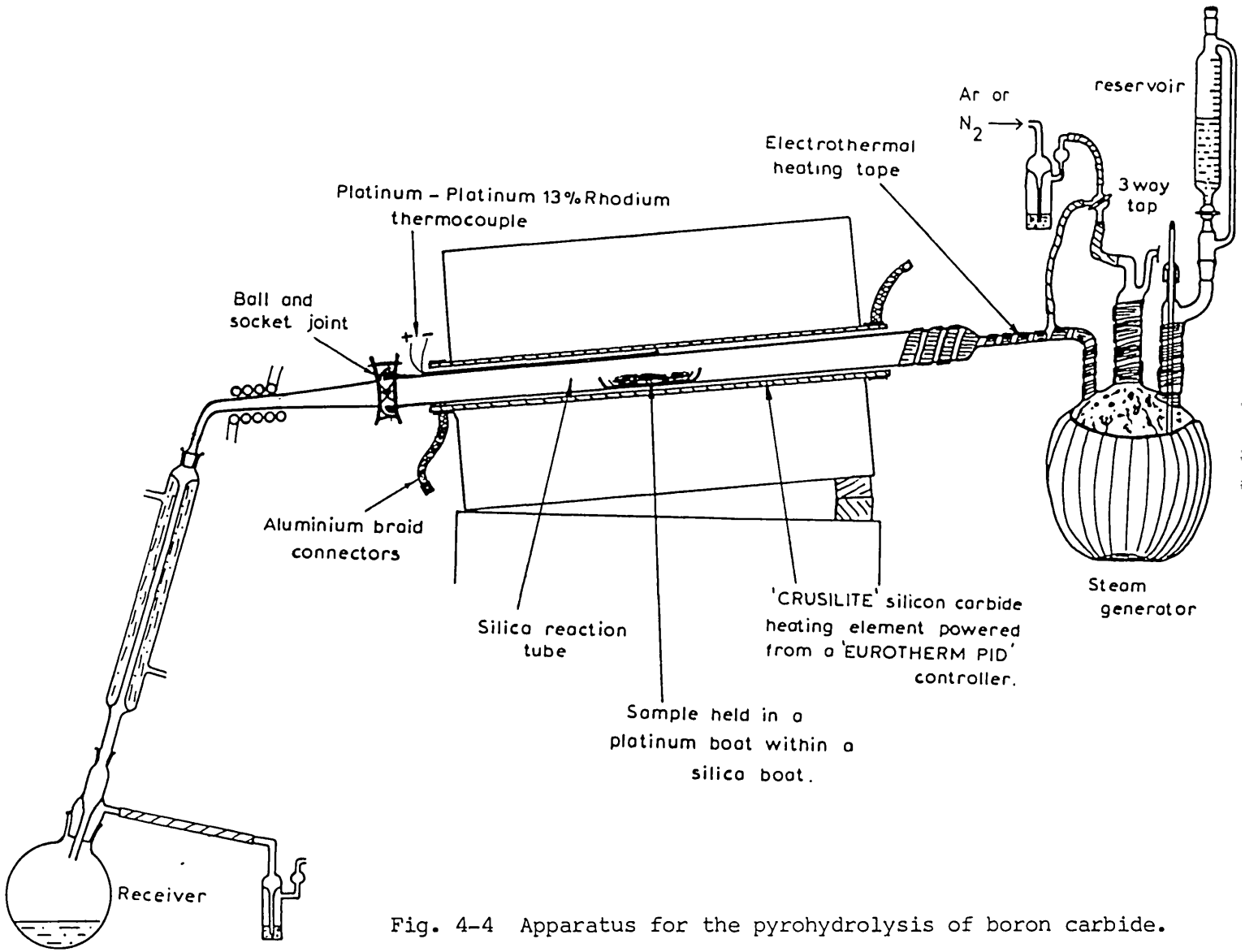

Fig. 4-4 Apparatus for the pyrohydrolysis of boron carbide.

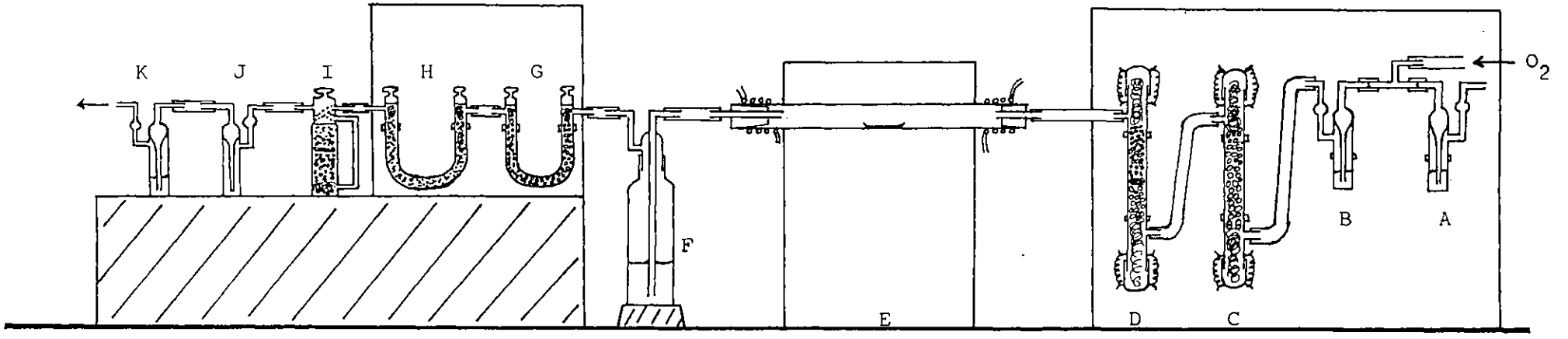

Fig. 4-5 Apparatus for the determination of carbon: A, mercury valve; B, bottle containing concentrated H_2SO_4; C, tower containing soda asbestos (12-20 mesh); D, tower containing silica gel topped up with anhydrone; E, electric furnace with combustion tube and boat; F, bottle containing chromic(VI) acid, inserted only for graphite and lamp black samples; G, U-tube containing zinc shot; H, U-tube containing anhydrone; I, Nesbitt CO_2 absorption weighing bottle containing soda asbestos (14-22 mesh) topped up with anhydrone (14-22 mesh); J, empty bottle; K, bottle containing concentrated H_2SO_4.

carbon dioxide derived from the prepared boats alone, were also determined. Hence the carbon composition of boron carbide was calculated from the weight of carbon dioxide product.

4-10.3 Impurities

When required, quantitative analyses of the impurities in boron carbide samples were obtained by mass spectrometry (Jeol JMS-01BM-2 Mass Spectrometer) or X-ray fluorescent spectrometry (Philips mass spectrometer) in the Analytical Services Laboratory, Department of Metallurgy and Materials Science, Imperial College of Science and Technology. Semi-quantitative analyses were also obtained by X-ray fluorescence.

4-11 Chemical Analysis of Lamp Black and Graphite

The lamp black (supplied by Borax Consolidated Ltd) was treated with dilute hydrochloric acid (1 : 1), and also with toluene.

The graphite powder ($\leq$ 1000 mesh) was obtained by the milling of a block of pure graphite.

The lamp black or graphite was sampled and weighed (0.04 g), quantitatively transferred into a prefired combustion boat, diluted with fused alumina (1 g), and combusted (at 900 ^{o}C for 30 minutes) in the twin-tube furnace version of the apparatus illustrated in Fig. 4-5. The resultant carbon dioxide was absorbed and weighed. "Blanks" were also obtained and hence the carbon composition of lamp black or graphite was calculated.

4-12 Miscellaneous Methods

4-12.1 Fabrication of boron carbide and boron carbide/carbon composite rods

Boron carbide pressure-sintered rods were supplied by Borax Consolidated Ltd.

Boron carbide powder and lamp black (both supplied by Borax Consolidated Ltd), and pure graphite powder ($\leq$ 1000 mesh) were chemically analysed (sections 4-10 and 4-11). Boron carbide/lamp black mixtures were then prepared to give boron:carbon ratios of 3.86, 3.77, 3.69, 3.53, 3.38, 3.24, 3.11, 2.98, 2.76, and 2.56. The boron:carbon ratios of 3.69 and 3.24 were duplicated with boron carbide/pure graphite mixtures.

The mixtures were tightly packed, with the aid of dampening with alcohol, into graphite dies; ensuring that the protrusion of the graphite plungers at both ends of the packed dies were of equal length. The packed dies were then sent to Borax Consolidated Ltd for pressure-sintering into rods.

4-12.2 Tyndall effect

A narrow beam of light, obtained by placing a slit in front of a microscope lamp, was employed to test (by the Tyndall effect) the prepared solutions of Ir(IV) perchlorate, Ir(IV) sulphate, and Ir(IV) phosphate for the presence of suspended particles.

4-12.3 Paper electrophoresis

Ir(IV) perchlorate (2.3×10^{-3} mol dm^{-3}) in perchloric acid (0.1 M) was subjected to paper electrophoresis, at a voltage gradient of 5 V cm^{-1}, to examine whether the Ir(IV) species was cationic or anionic. The purple colour of Ir(IV) perchlorate facilitated the identification of its position on the filter paper. Perchloric acid (0.1 M) was used to moisten the paper and to fill the electrode compartments.

4-12.4 Spectrophotometry

A Perkin-Elmer 124 u.v./visible double-beam ratio-recording spectrophotometer was employed to obtain spectra within the wavelength region 800-200 nm.

Infrared absorption spectra were obtained from boron carbide, (600 mesh) samples pressed into CsI disks, on a Perkin-Elmer 621 i.r. spectrophotometer in the Analytical Services Laboratory, Department of Metallurgy and Materials Science, Imperial College of Science and Technology.

4-13 References

4.1 Vogel A. I.; Quantitative Inorganic Analysis, p. 914, 3rd ed.. Longmans, 1961.

4.2 Jackson E. and Pantony D. A.; J. Appl. Electrochem., 1972, 2, 353.

4.3 Jackson E. and Pantony D. A.; Talanta, 1967, 14, 973.

4.4 Jackson E.; Ph. D. thesis, "An Electrochemical Study of Platinum Metals as a Basis for their Separation with Organic Reagents", University of London, 1969.

4.5 Jackson E. and Pantony D. A.; J. Appl. Electrochem., 1971, 1, 113.

4.6 Schwarzenbach G. and Flaschka H.; Complexometric Titrations. Methuen & Co. Ltd., 1969.

4.7 Morgan L.; Analyst, 1964, 89, 621-623.

4.8 Kolthoff I. M. and Sandell E. B.; Textbook of Quantitative Inorganic Analysis. Macmillan Co., 1936.

5. ANALYSIS OF RESULTS

5-1 Iridium

5-1.1 Chloroiridate-chloroiridite in perchloric acid supporting electrolyte system

5-1.1.(i) Effect of electrode composition on voltammetric properties.

Initial investigation of d.c. voltammetric behaviour at twenty-two different boron carbide solid electrodes (Table 5-1) indicated that the reversibility of the electrode reaction was invariably poor; characterised by αn values (0.25 to 0.79) well below the theoretical unity value for the electro-reduction

$$IrCl_6^{2-} + e^- \rightleftharpoons IrCl_6^{3-}$$

in perchloric acid (0.1 M) supporting electrolyte. The mean values of the half-wave potential ranged from 0.412 V to 0.658 V (vs. SCE). However, the linear concentration dependences of the limiting current were all statistically significant to at least the 0.05 level; the majority of electrodes attaining correlation coefficients better than that at the 0.01 level of significance.

Chemical analysis of eight of the above electrodes, covering the spread of αn values, indicated boron:carbon ratios ranging from 3.76 to 4.05 (Table 5-2). Correlations showing increasing αn values with: (i) increasing weight per cent carbon composition (Fig. 5-1), and (ii) decreasing B:C ratio (Fig. 5-2) were found. But, no correlation was found between αn values and weight per cent boron composition or weight per cent boron plus carbon composition (Fig. 5-3). Neither was there any correlation between half-wave potential and composition of boron carbide solid electrodes (Figures 5-4 and 5-5).

All the chemically analysed electrodes consisted of boron plus carbon combined contents which were below the 100% theoretical weight; indicating the presence of impurities. Analysis of some of the samples for impurities (Table 5-3), either by mass spectrometry or X-ray fluorescent spectrometry, showed that the common major impurity was iron; which could constitute between 13% and over 99% of the total detectable impurities per sample. Silicon was frequently encountered as an impurity and, when present, accounted for between less than 1% and over 40% of the total impurities. Iron, silicon, aluminium, and calcium, when

Table 5-1 Ir(IV)-Ir(III) Chloroiridate/Perchloric acid supporting electrolyte System: Initial investigation of D. C. Voltammetric Performance of Boron Carbide Solid Electrodes.

Electroactive species = $(NH_4)_2IrCl_6$ (4.0×10^{-5} to 1.0×10^{-3} mol dm^{-3}) Supporting electrolyte = $HClO_4$ (0.1 M)

Electrode number	αn mean	$E_{\frac{1}{2}}$ mean (V) vs SCE.	i_L / AC (10^4 μA cm^{-2} dm^3 mol^{-1}), linearly regressed slope. Correlation coefficient	Level of significance, p
1	0.69	0.619	13.2	0.9880	$0.01 < p < 0.02$
2	0.50	0.416	23.6	0.9968	$0.001 < p < 0.01$
3	0.65	0.451	11.4	0.9979	$p < 0.001$
4	0.56	0.445	12.4	0.9937	$0.001 < p < 0.01$
5	0.64	0.562	24.8	1.000	$p < 0.001$
6	0.71	0.655	13.9	0.9964	$0.001 < p < 0.01$
7	0.37	0.546	10.6	0.9728	$0.02 < p < 0.05$
8	0.34	0.518	12.8	0.9914	$0.001 < p < 0.01$
9	0.25	0.470	14.7	0.9948	$p < 0.001$
10	0.34	0.578	14.2	0.9966	$p < 0.001$
11	0.42	0.534	12.4	0.9828	$0.01 < p < 0.02$
12	0.26	0.412	12.5	0.9810	$0.001 < p < 0.01$
13	0.64	0.623	18.0	0.9883	$0.01 < p < 0.02$
14	0.47	0.528	10.3	0.9628	$0.001 < p < 0.01$
15	0.33	0.525	11.7	0.9970	$p < 0.001$
16	0.30	0.511	13.3	0.9964	$p < 0.001$
17	0.60	0.630	9.85	0.9833	$0.01 < p < 0.02$
18	0.73	0.640	13.4	0.9917	$0.001 < p < 0.01$
19	0.79	0.658	12.5	0.9800	$0.01 < p < 0.02$
20	0.35	0.599	8.59	0.9979	$0.001 < p < 0.01$
21	0.65	0.648	11.4	0.9862	$0.01 < p < 0.02$
22	0.46	0.629	14.0	0.9900	$0.001 < p < 0.01$
Combined standard deviation	0.05	0.013			
Degrees of freedom	71	73			

Table 5-2 Initial Investigation on Composition of Boron Carbide Solid Electrodes.

Theoretical composition of boron carbide, B_4C : Weight per cent boron = 78.28, weight per cent carbon = 21.72

Electrode number	Weight per cent boron, mean value	Weight per cent carbon, mean value	Weight per cent (boron+ carbon)	Boron:Carbon ratio
1	76.4	22.6	99.0	3.76
2	75.9	22.2	98.1	3.80
3	76.4	22.3	98.7	3.81
4	77.1	22.3	99.4	3.84
5	76.4	22.1	98.5	3.84
7	77.0	21.4	98.4	4.00
8	76.0	20.9	96.9	4.04
9	78.0	21.4	99.4	4.05
Combined standard deviation	0.23	0.11	0.25	0.023
Degrees of freedom	22	36	58	58

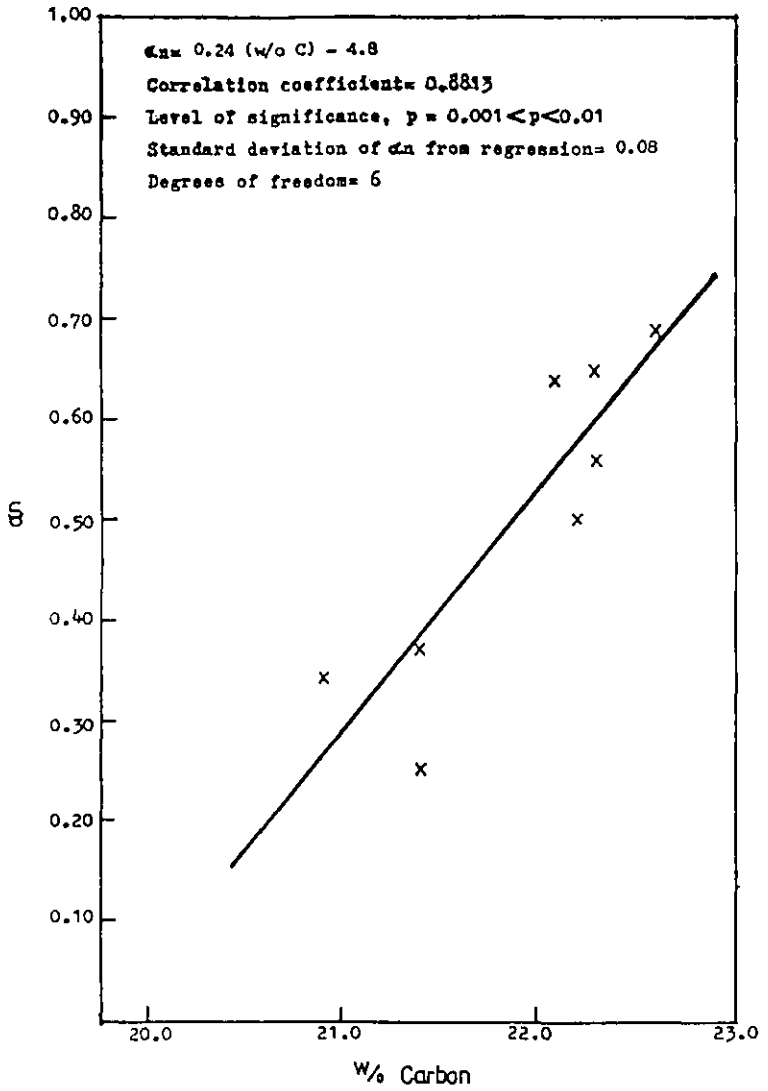

Fig. 5-1 Ir(IV)-Ir(III) Chloroiridate/Perchloric acid supporting electrolyte System: Values of αn for electrochemical reduction as a function of weight per cent carbon composition of boron carbide solid electrodes.

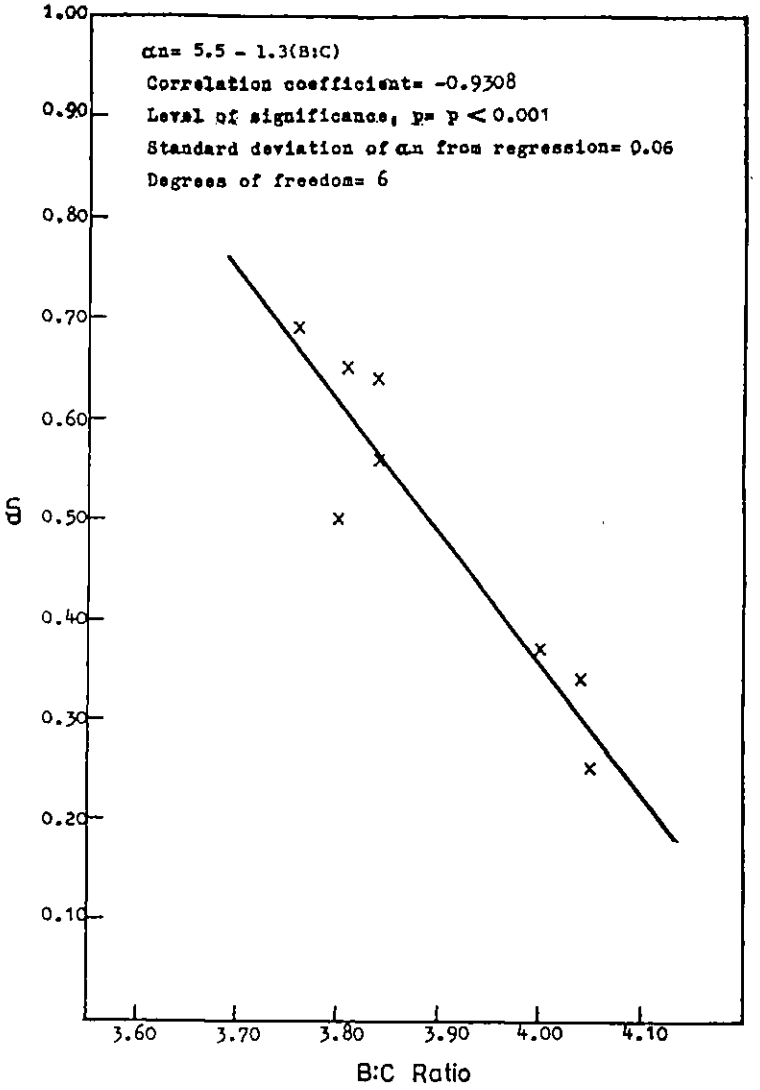

Fig. 5-2 Ir(IV)-Ir(III) Chloroiridate/Perchloric acid supporting electrolyte System: Values of αn for electrochemical reduction as a function of boron to carbon ratio of boron carbide solid electrodes.

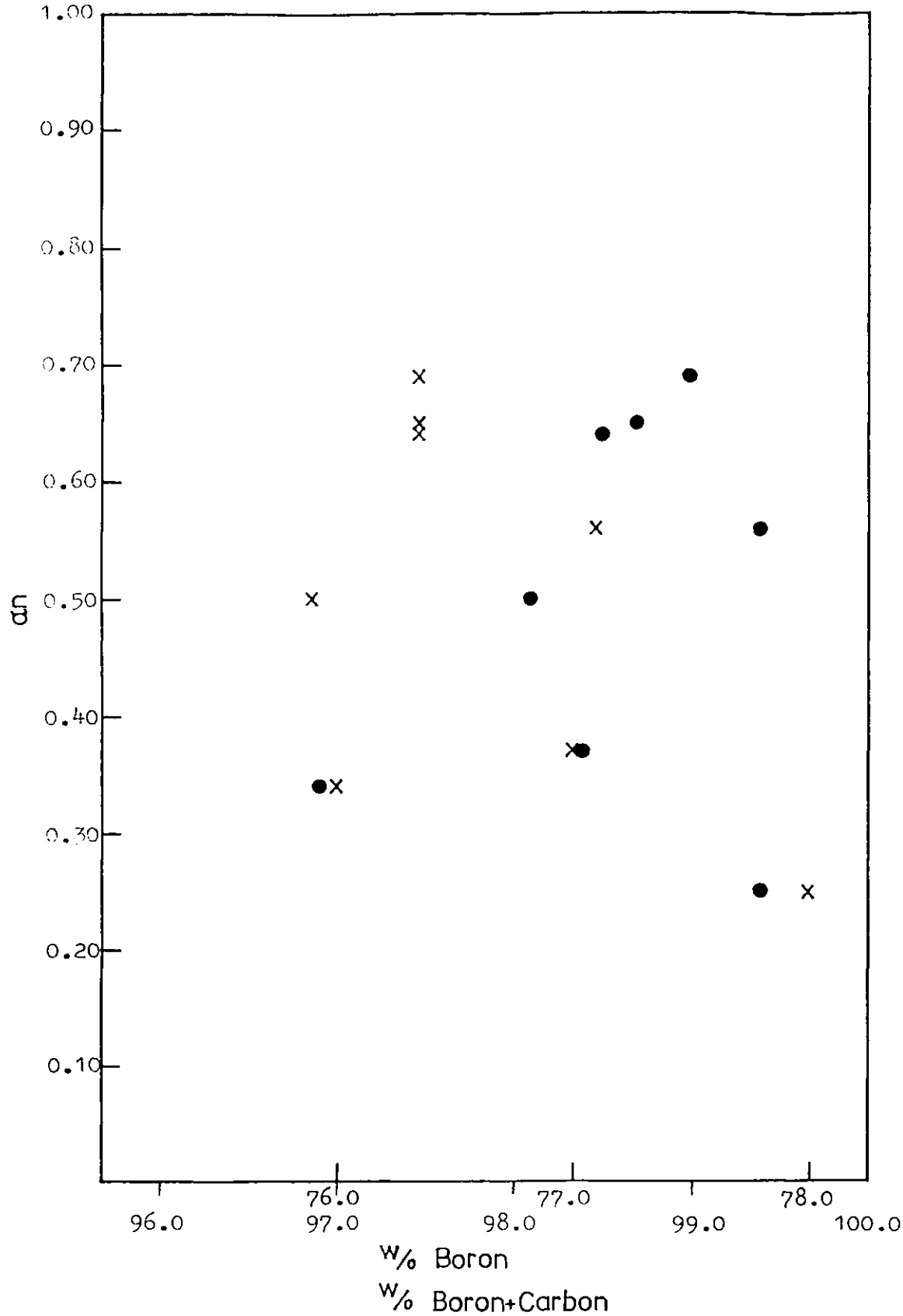

Fig. 5-3 Ir(IV)-Ir(III) Chloroiridate/Perchloric acid supporting electrolyte System: Scatter diagram of values of αn for electrochemical reduction as a function of weight per cent boron (X) and weight per cent boron+carbon(●) composition of boron carbide solid electrodes.

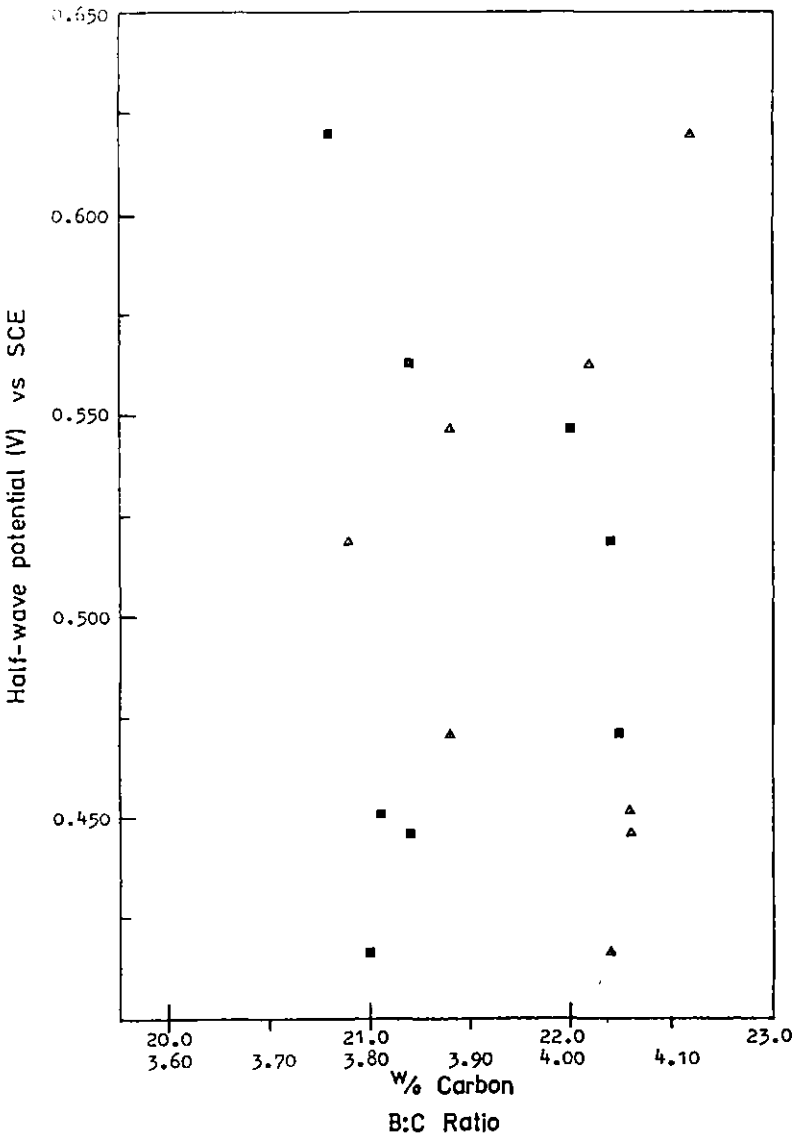

Fig. 5-4 Ir(IV)-Ir(III) Chloroiridate/Perchloric acid supporting electrolyte System: Scatter diagram of values of half-wave potential as a function of weight per cent carbon(△) and boron to carbon ratio(■) of boron carbide solid electrodes.

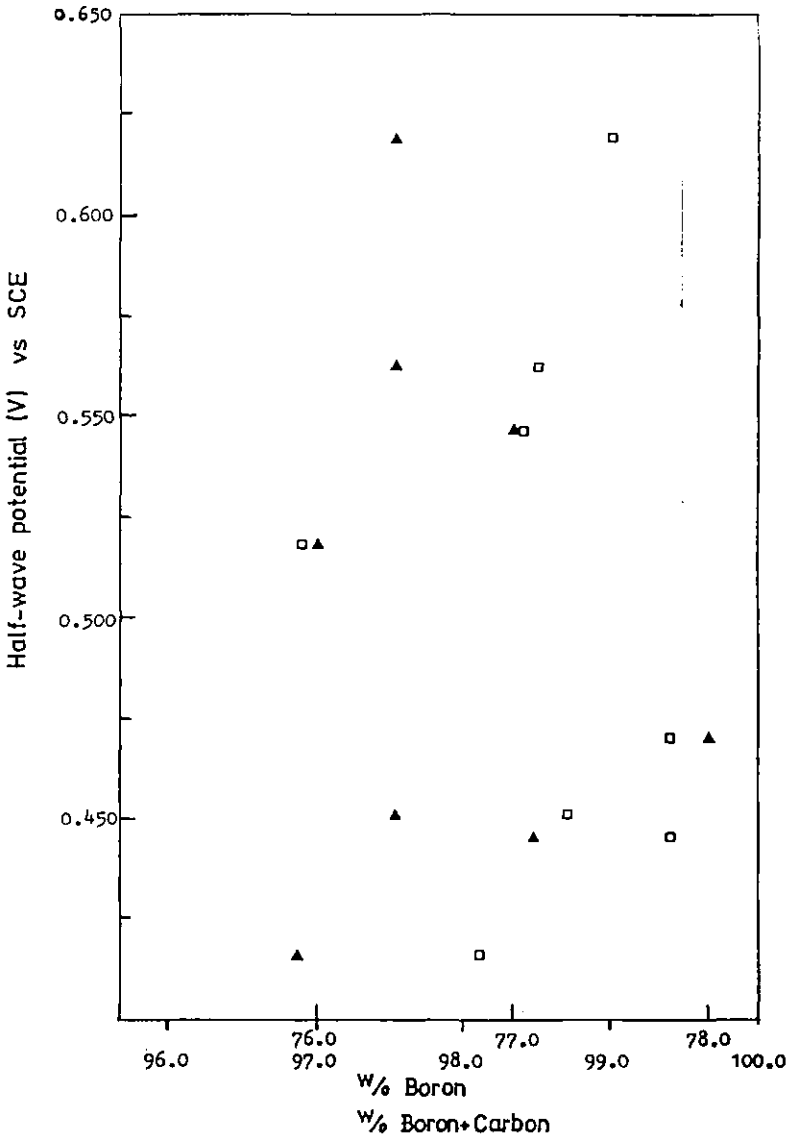

Fig. 5-5 Ir(IV)-Ir(III) Chloroiridate/Perchloric acid supporting electrolyte System: Scatter diagram of values of half-wave potential as a function of weight per cent boron(▲) and weight per cent boron+carbon(□) composition of boron carbide solid electrodes.

Table 5-3 Impurities in Boron Carbide.

Impurity detected	Analysis by Mass Spectrometry (10^{-4} w%).			Analysis by X-Ray Fluorescence (w%). Semi-quantitative analysis						Quantitative analysis	
	Sample number			Sample number						Sample number	
	1	4	7	14	15	21	22	23	24	17	19
Na	800	240	30								
Al	860	260	260					0.05 to 0.5			
Si	950	950	300	0.05 to o.5			< 0.05	0.5 to 5	< 0.05		0.4
P	95	15	30								
S	100	15	30								
Cl	4	4	0.4								
K	330	110	10	< 0.05				< 0.05	< 0.05		
Ca	1100	110	30	< 0.05	< 0.05	< 0.05	< 0.05	0.5 to 5	< 0.05		
Ti	15	5	50	< 0.05	< 0.05	< 0.05	0.05 to 0.5	0.05 to 0.5	< 0.05		
V	35	4	2					< 0.05			
Cr	140	45	55					< 0.05			
Mn	40	4	4					< 0.05	< 0.05		
Fe	1325	400	130	0.05 to 0.5	0.05 to 0.5	0.05 to 0.5	0.05 to 0.5	0.5 to 5	0.5 to 5	1.9	0.7
Co	375	4	4								
Ni	190	6	6	< 0.05	< 0.05	< 0.05		< 0.05	< 0.05		
Zn	8	3	1								
Cu	190	1.5	3								
Nb	25	< 1.5	1.5								
Zr	95	3	3					0.05 to 0.5			
Mo	180	55	6								
Total impurities (w%)	0.7	0.2	0.1	≯ 1.2	≯ 0.65	≯ 0.65	≯ 1.1	≯ 16.8	≯ 5.3	1.9	1.1

occurring together, accounted for 60% to over 99% of total impurities.

In some cases, the sum of the weights per cent of total impurities detected and the boron and carbon contents was still below the 100% theoretical weight of the sample. This anomaly is thought to be attributable to the presence of combined oxygen; as results of the following infrared transmission studies have suggested. The spectrum of 93.1% ± 0.2% pure boron carbide (Fig. 5-6) when compared with the spectrum of 100% ± 0.2% pure boron carbide (Fig. 5-8) showed enhancement of boron carbide peaks at 1565, 1375, 1085, 705, and 400 cm^{-1} and the presence of impurity peaks at 800 and 820 cm^{-1}. Another comparison of the spectrum for 96.7% ± 0.2% pure boron carbide (Fig. 5-7) with that for 100% ± 0.2% pure boron carbide (Fig. 5-8) indicated enhancement of the boron carbide peak at 1085 cm^{-1} and the presence of impurity peaks at 900, 800, and 370 cm^{-1}. These enhancement and impurity peaks occurred in the range of frequencies coinciding with those for oxides of boron, silicon, and iron.

The hypothesis that a high carbon content would be beneficial to electrode voltammetric performance was tested by the carbon enrichment, with pure graphite, of the boron carbide working electrode surfaces (section 4-2.1). Thus two boron carbide electrodes, numbers 12 (αn = 0.26) and 13 (αn = 0.64) from Table 2, generally showed improved mean values of αn after treatment (Table 5-4). However, the improvement appeared to have a ceiling within the range of 0.61 to 0.75 for αn values; which is consistent with the αn values in Table 5-1 where the best αn value is 0.79.

A further test to check the beneficial effects of increasing carbon content on the voltammetric behaviour of boron carbide was to fabricate boron carbide/carbon composite solid electrodes (section 4-12.1 and Table 5-5). The results (Figures 5-9 and 5-10) show that αn and $E_{\frac{1}{2}}$ values: (i) increase non-linearly, tending to reach a plateau, with increasing weight per cent carbon composition, and (ii) decrease non-linearly with increasing B:C ratio. None of the electrodes, however, achieved a reversible electrode reduction for chloroiridate at their surfaces. Furthermore, the linear concentration dependence of limiting current at these electrodes was poor; only three of the seven electrodes having correlation coefficients that were statistically significant at the 0.05 level of significance or better (Table 5-6).

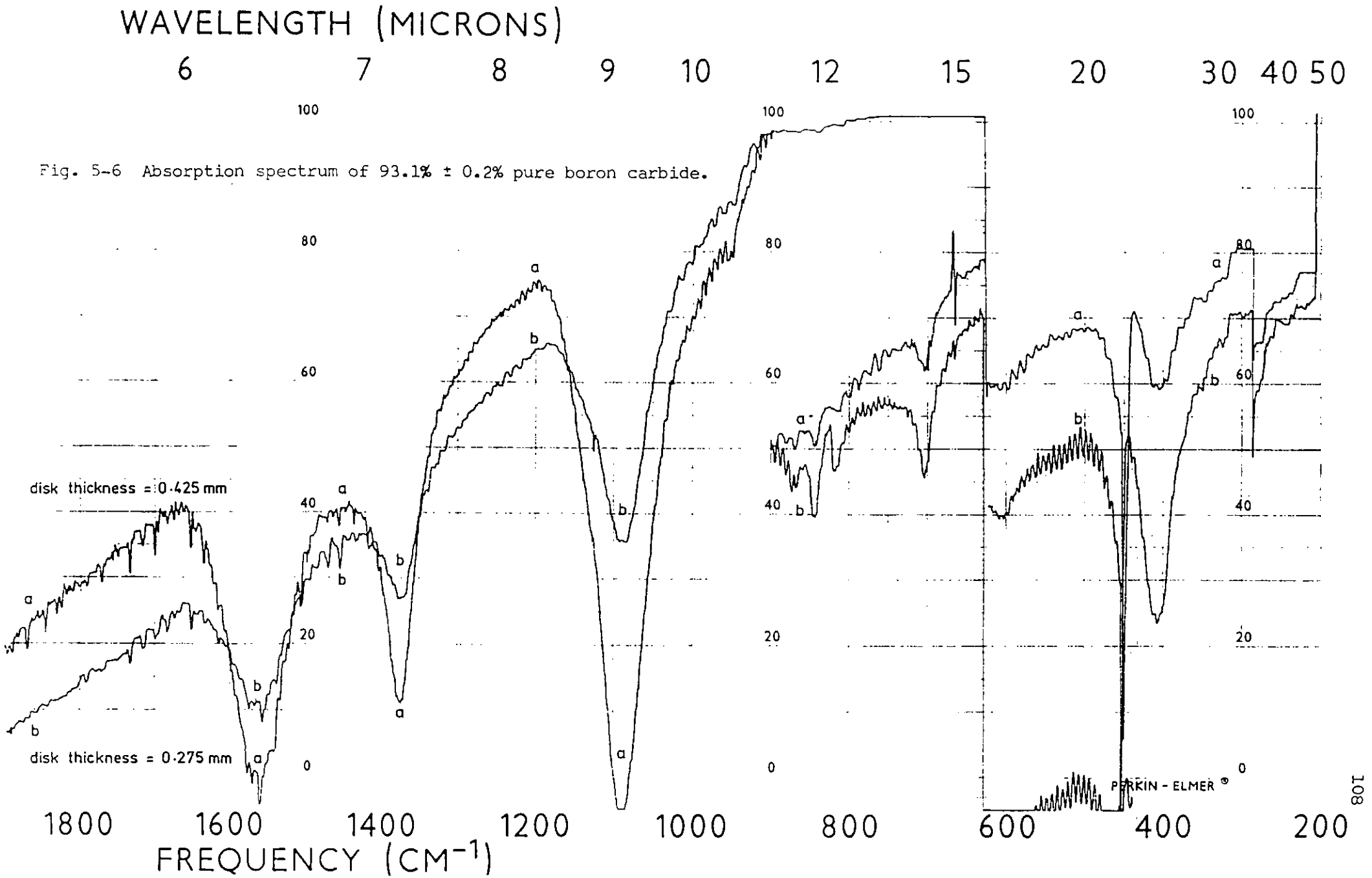

Fig. 5-6 Absorption spectrum of 93.1% ± 0.2% pure boron carbide.

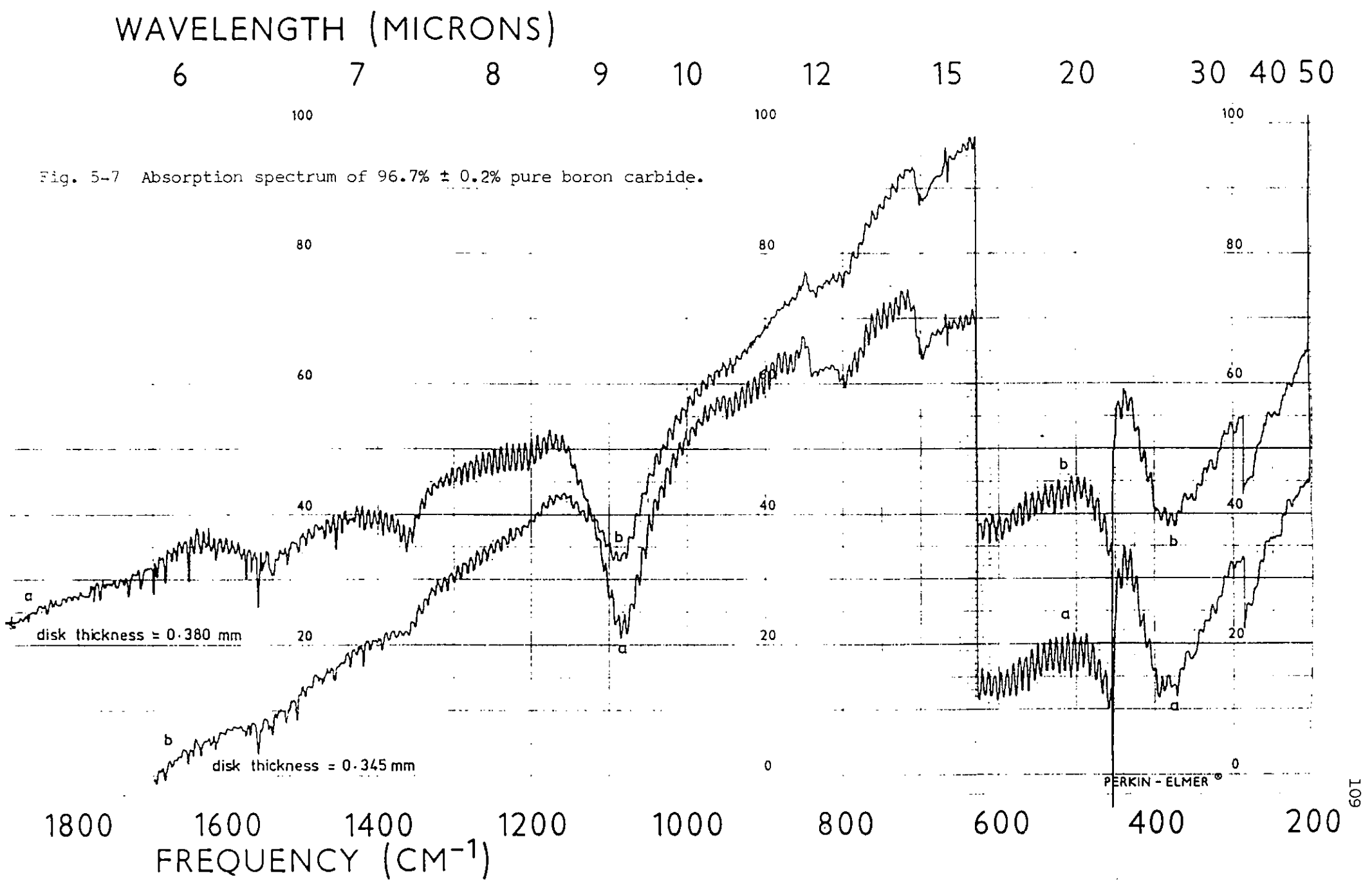

Fig. 5-7 Absorption spectrum of 96.7% ± 0.2% pure boron carbide.

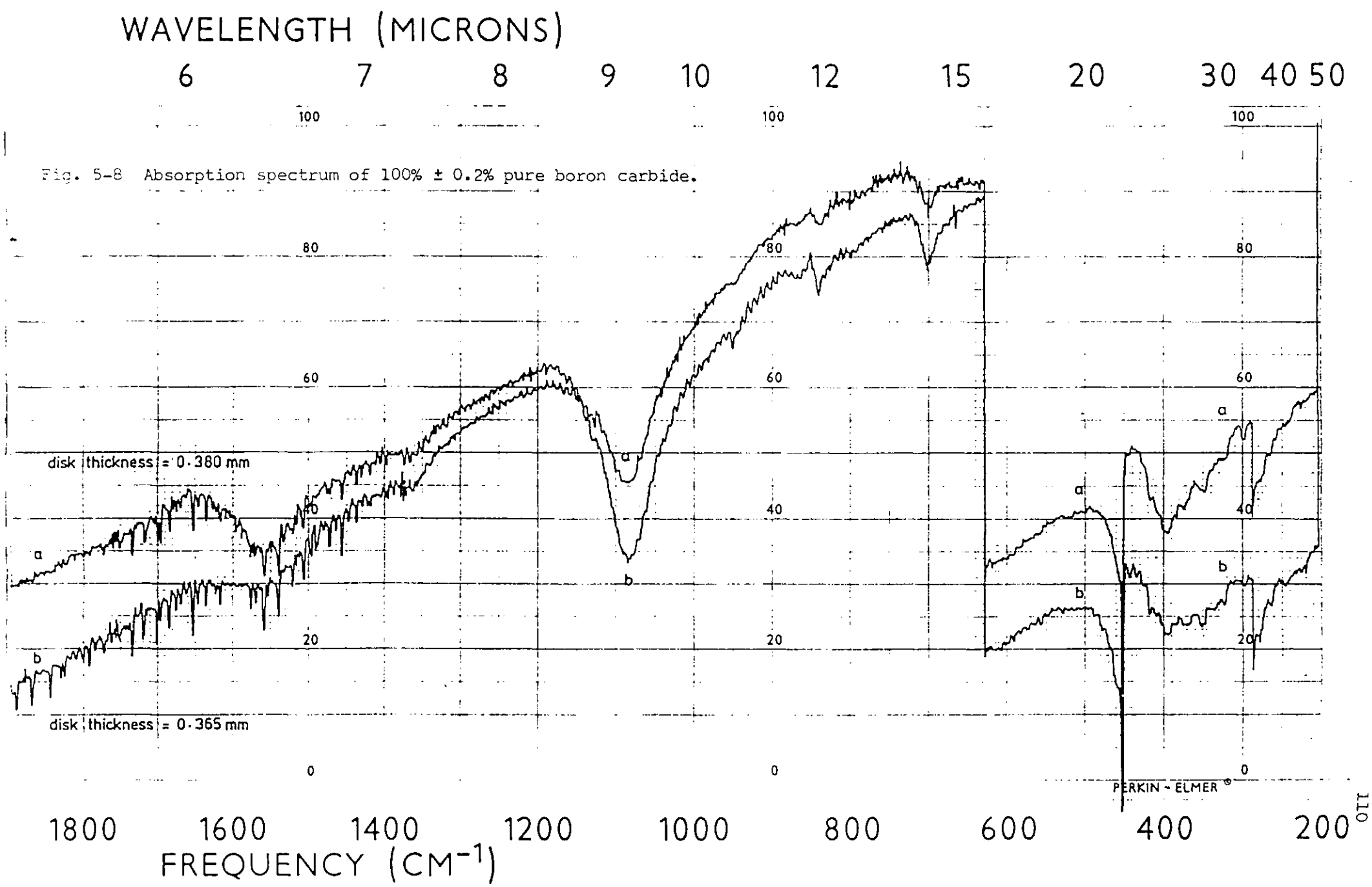

Fig. 5-8 Absorption spectrum of 100% ± 0.2% pure boron carbide.

Table 5-4 Ir(IV)-Ir(III) Chloroiridate System: D. C. Voltammetric Performance of Boron Carbide Solid Electrodes with Graphite enriched surfaces.

Electroactive species = $(NH_4)_2IrCl_6$ (4.0×10^{-5} to 1.0×10^{-3} mol dm^{-3})
Supporting electrolyte = $HClO_4$ (0.1 M)

Electrode number	Electrode treatment		αn mean	$E_{\frac{1}{2}}$ mean (V) vs SCE	i_L / AC (10^4 μA cm^{-2} dm^3 mol^{-1}), linearly regressed slope. Correlation coefficient	Level of significance, p
	Polished to a mirror finish		0.26	0.412	12.5	0.9810	$0.001 < p < 0.01$
12	Carbon enrich-ment	Surface 1	0.64	0.636	12.8	0.9909	$0.001 < p < 0.01$
		Surface 2	0.61	0.651	14.0	0.9956	$p < 0.001$
	Re-polished		0.24	0.474	16.6	0.9922	$p < 0.001$
	Polished to a mirror finish		0.64	0.623	18.0	0.9883	$0.01 < p < 0.02$
13	Carbon enrich-ment	Surface 1	0.61	0.652	19.7	0.9974	$0.001 < p < 0.01$
		Surface 2	0.75	0.638	16.0	0.9804	$0.001 < p < 0.01$
	Re-polished		0.26	0.508	16.1	0.9995	$p < 0.001$
Combined standard deviation			0.05	0.010			
Degrees of freedom			28	28			

Table 5-5 Composition of Boron Carbide/Carbon Composite Solid Electrodes.

Electrode number	Extra w% Carbon (lamp black except where indicated) added.	Final w% Carbon	Boron:Carbon ratio
23	0.0	21.8	3.86
24	0.5	22.3	3.77
25	1.0	22.8	3.69
26	1.0 (graphite)	22.8	3.69
27	2.0	23.8	3.53
28	3.0	24.8	3.38
29	4.0	25.8	3.24
30	4.0 (graphite)	25.8	3.24
31	5.0	26.8	3.11
32	6.0	27.8	2.98
33	8.0	29.8	2.76
34	10.0	31.8	2.56

Composition of boron carbide powder: w% Boron = 75.7, w% Carbon = 21.8

Theoretical composition of boron carbide, B_4C: w% Boron = 78.28, w% Carbon = 21.72

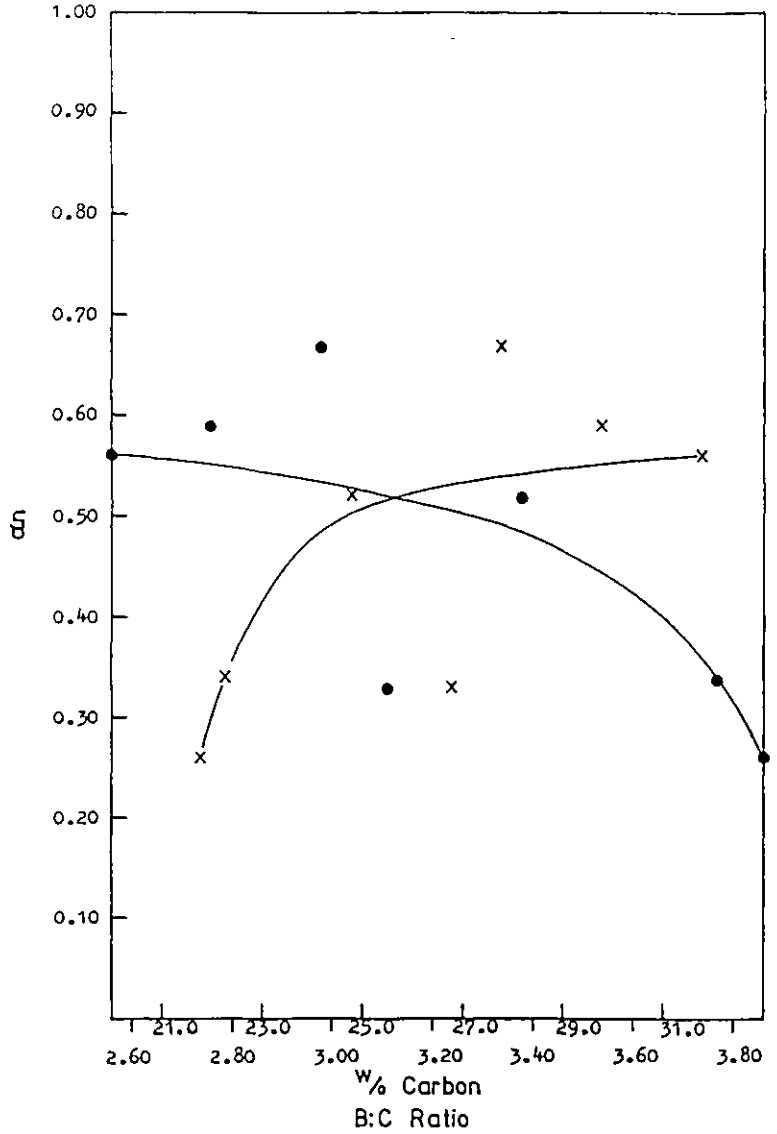

Fig. 5-9 Ir(IV)-Ir(III) Chloroiridate/Perchloric acid supporting electrolyte System: Diagram of values of αn for the electrochemical reduction as a function of weight per cent carbon(X), and boron to carbon ratio(●) of boron carbide/carbon composite solid electrodes.

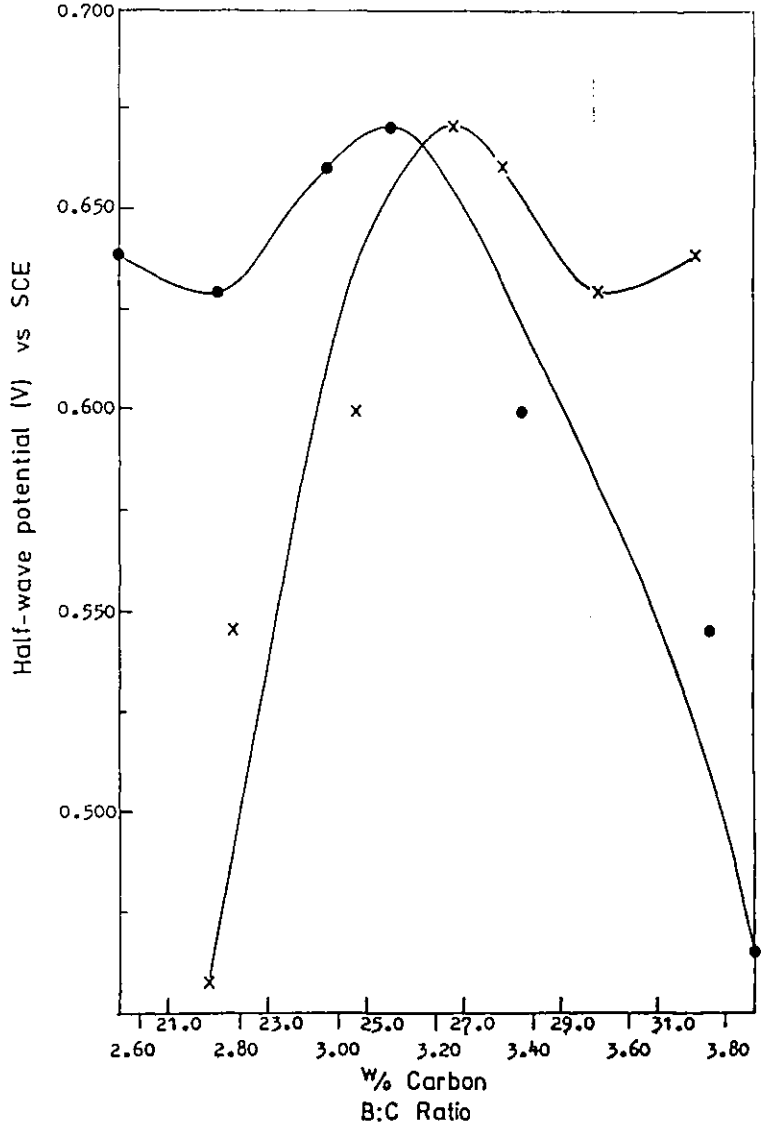

Fig. 5-10 Ir(IV)-Ir(III) Chloroiridate/Perchloric acid supporting electrolyte System: Diagram of values of half-wave potential as a function of weight per cent carbon(X), and boron to carbon ratio(●) of boron carbide/carbon composite solid electrodes.

Table 5-6 Ir(IV)-Ir(III) Chloroiridate System: Values of Limiting Current per unit Area as a function of Concentration of Ammonium Hexachloroiridate obtained at Boron Carbide/Carbon Composite Solid Electrodes.

Electroactive species = $(NH_4)_2IrCl_6$ (1.0×10^{-4} to 5.0×10^{-4} mol dm^{-3})
Supporting electrolyte = $HClO_4$ (0.1 M)

w% Carbon composition	Final Boron:Carbon ratio	i_L / AC (10^4 μA cm^{-2} dm^3 mol^{-1}), linearly regressed slope. Correlation coefficient	Level of significance, p
21.8	3.86	34.1	0.8871	$p > 0.10$
22.3	3.77	20.7	0.9883	$0.01 < p < 0.02$
24.8	3.38	17.2	0.9739	$0.02 < p < 0.05$
26.8	3.11	18.2	0.9824	$p > 0.10$
27.8	2.98	15.0	0.8964	$p > 0.10$
29.8	2.76	11.1	0.9885	$0.05 < p < 0.10$
31.8	2.56	12.1	0.9980	$0.02 < p < 0.05$

5-1.1.(ii) Chemical treatments on electrodes.

Chemical treatment of boron carbide and boron carbide/carbon composite solid electrodes with nitric acid (23%)/hydrofluoric acid (2%)/teepol (2%), hot Sn(II) chloride (25%)/HCl (1+3), hot hydrogen peroxide, hot concentrated nitric acid, or hot aqua regia failed to improve their voltammetric performance.

5-1.1.(iii) Effect of Ir(IV) perchlorate treatment on electrodes.

Treatment of boron carbide and boron carbide/carbon composite solid electrodes with Ir(IV) perchlorate in perchloric acid (section 4-3), however, resulted in a marked improvement in d.c. voltammetric performance for the reduction of chloroiridate. Moreover, the performances of the electrodes were similarly improved irrespective of their chemical compositions (Figures 5-11 to 5-13); thus suggesting a surface phenomenon. Grand mean values for: (i) αn = 0.92 ± 0.04 (29 degrees of freedom), (ii) $E_{\frac{1}{2}}$ = 0.604 V (vs. SCE) ± 0.007 V (29 degrees of freedom), and (iii) i_L/AC = 45.0 x 10^4 ± 5.9 x 10^4 μA cm^{-2} dm^3 mol^{-1} (29 degrees of freedom) were obtained for chloroiridate (1.0 x 10^{-4} mol dm^{-3}) in perchloric acid (0.1 M). Some typical d.c. voltammograms are illustrated in Fig. 5-14.

The results (Figures 5-15 to 5-17) of an investigation into the beneficial effect of Ir(IV) perchlorate treatment solution on the d.c. voltammetric performance, for chloroiridate, of a boron carbide solid electrode (geometric area = 1.13 cm^2) indicate that the improvement in voltammetric performance rapidly reached a plateau when the Ir(IV) perchlorate concentration was increased. This is also evidence of a surface phenomenon. The plateau corresponded to a reversible electrode reaction where the αn value approached unity for the chloroiridate reduction; the $E_{\frac{1}{2}}$ value reaching 0.616 V (vs. SCE) and the sensitivity reaching 51.5 x 10^4 μA cm^{-2} dm^3 mol^{-1}.

Linear sweep voltammetry, in perchloric acid (0.1 M) supporting electrolyte alone, at a boron carbide solid electrode which had been treated with Ir(IV) perchlorate (2.3 x 10^{-3} M) solution confirmed the presence of adsorbed species (Fig. 5-18); initially noticed in d.c. voltammetry (Fig. 5-14, c). Peak 2, in Fig. 5-18, began to merge into Peak 3 at higher sweep rates. Plots of the current function, $i_p/v^{\frac{1}{2}}$, for the measurable peaks against the square root of sweep rate, $v^{\frac{1}{2}}$, (Fig. 5-19) show rising trends which are symptomatic of adsorption systems (section 3-6.2). Plots of the ratio of peak currents against $v^{\frac{1}{2}}$

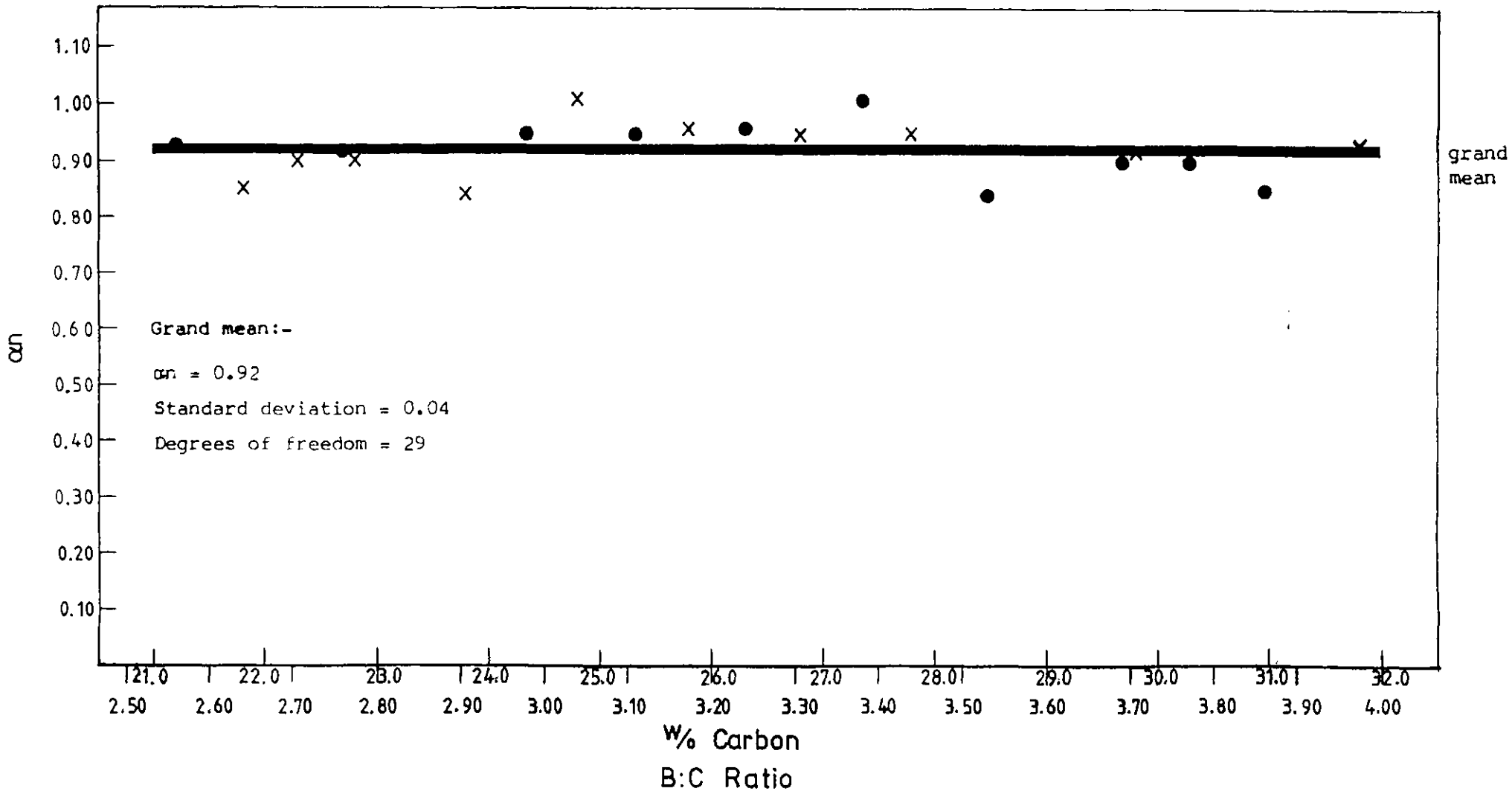

Fig. 5-11 Ir(IV)-Ir(III) Chloroiridate/Perchloric acid supporting electrolyte System: Values of αn for electrochemical reduction as a function of weight per cent carbon(X), and boron to carbon ratio(●) of boron carbide/carbon composite solid electrodes. Electrodes were treated with Ir(IV) Perchlorate(1.0×10^{-4} M) solution.

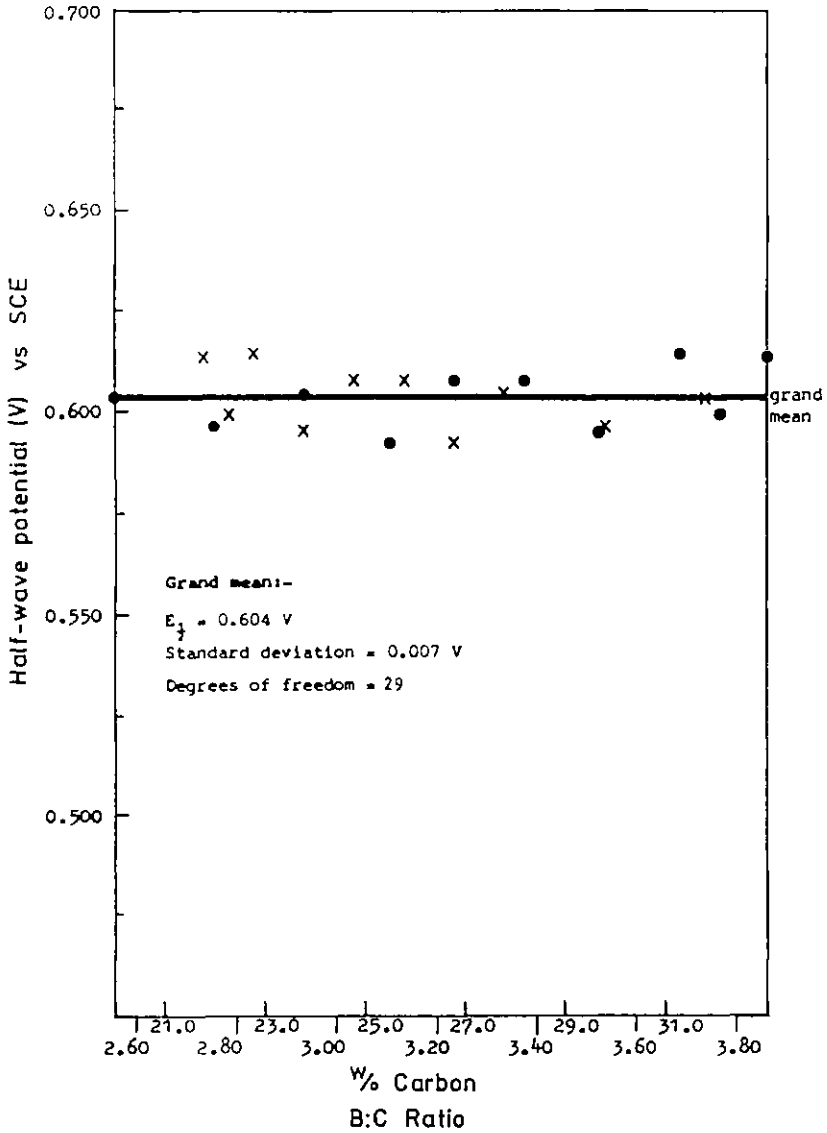

Fig. 5-12 Ir(IV)-Ir(III) Chloroiridate/Perchloric acid supporting electrolyte System: Values of half-wave potential as a function of weight per cent carbon(X), and boron to carbon ratio(●) of boron carbide/carbon composite solid electrodes. Electrodes were treated with Ir(IV) Perchlorate(1.0×10^{-4} M) solution.

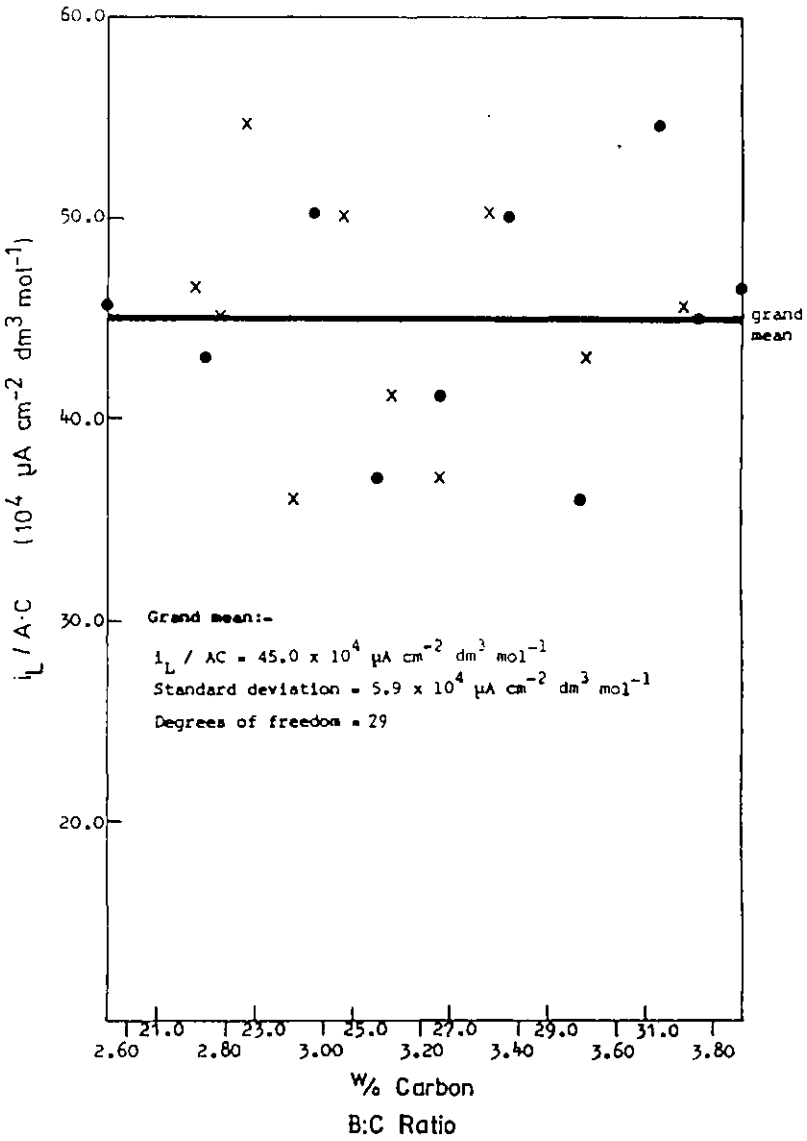

Fig. 5-13 Ir(IV)-Ir(III) Chloroiridate/Perchloric acid supporting electrolyte System: Values of limiting current per unit area divided by concentration as a function of weight per cent carbon(X), and boron to carbon ratio(●) of boron carbide/carbon composite solid electrodes. Electrodes were treated with Ir(IV) Perchlorate(1.0×10^{-4} M) solution.

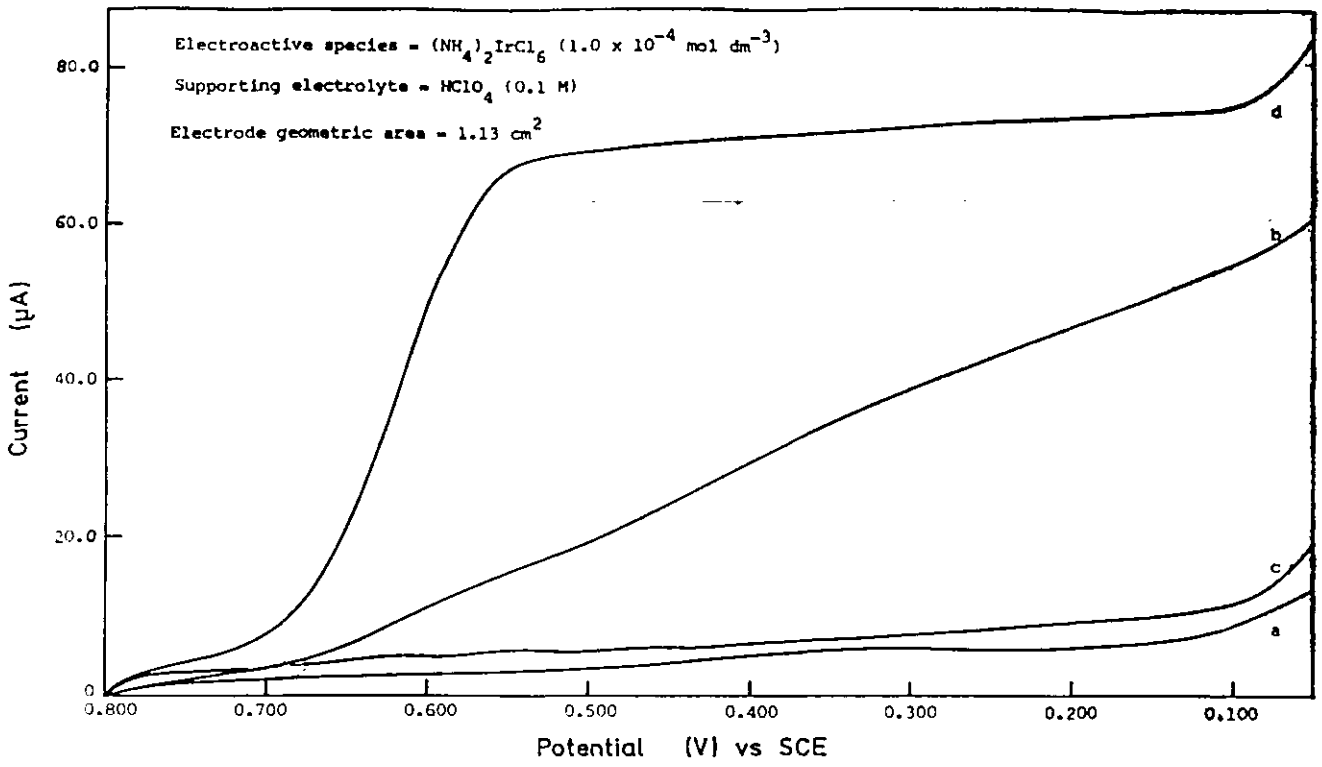

Fig. 5-14 (a) Residual current obtained at anodically stripped boron carbide solid electrode. (b) Voltammogram of the reduction of chloroiridate at anodically stripped boron carbide solid electrode. (c) Residual current obtained after Ir(IV) perchlorate (1.0×10^{-3} M) treatment of boron carbide solid electrode. (d) Voltammogram of the reduction of chloroiridate after Ir(IV) perchlorate treatment of boron carbide solid electrode.

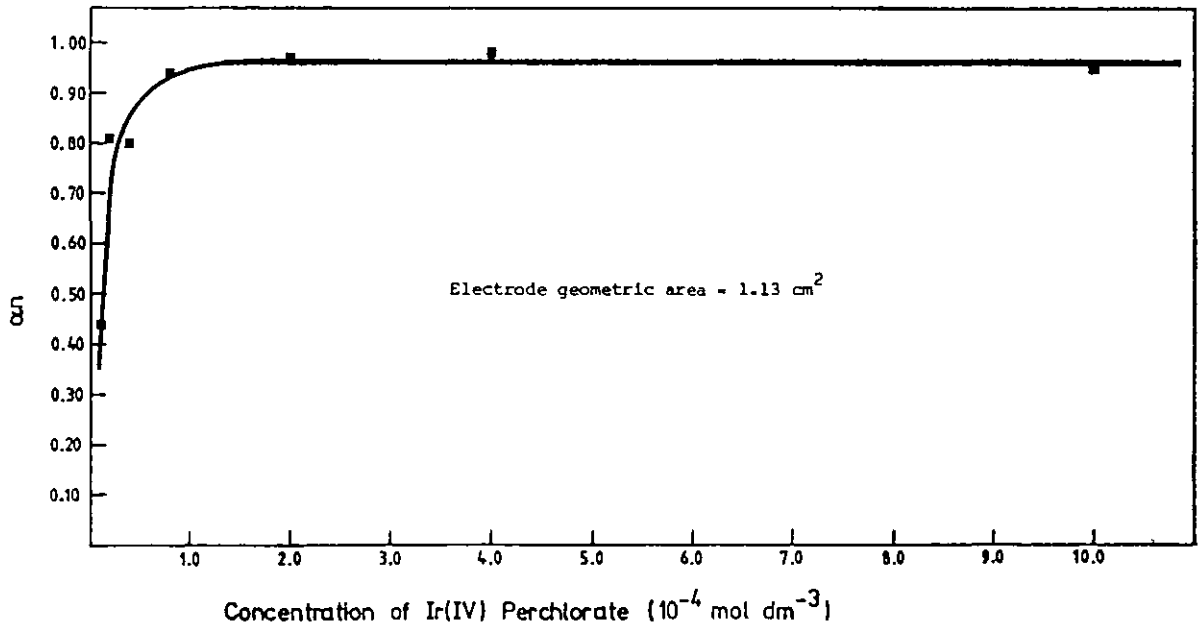

Fig. 5-15 Ir(IV)-Ir(III) Chloroiridate/Perchloric acid supporting electrolyte System: Values of αn for electrochemical reduction as a function of concentration of Ir(IV) Perchlorate treatment solution used for boron carbide solid electrode.

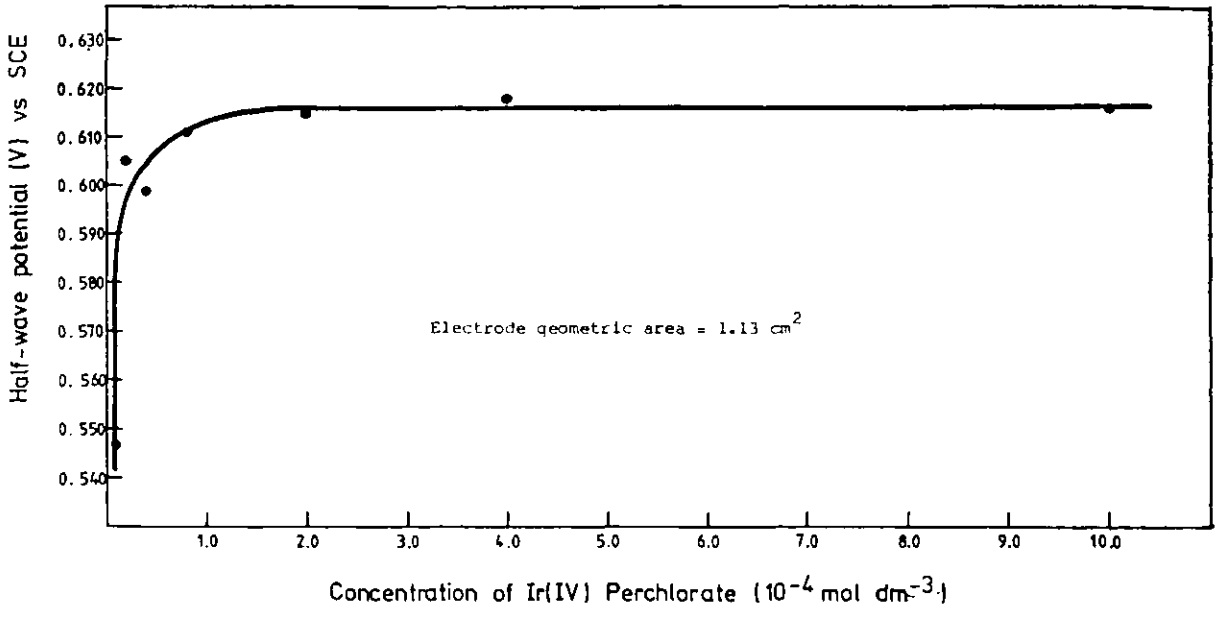

Fig. 5-16 Ir(IV)-Ir(III) Chloroiridate/Perchloric acid supporting electrolyte System: Values of half-wave potentials as a function of concentration of Ir(IV) Perchlorate treatment solution used for boron carbide solid electrode.

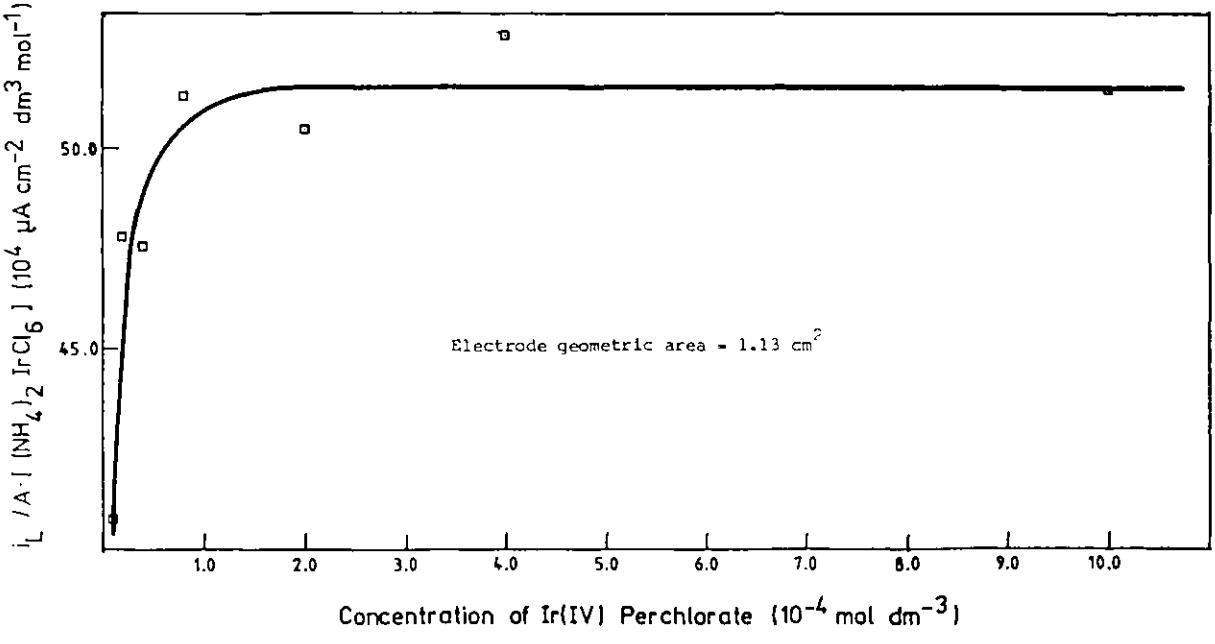

Fig. 5-17 Ir(IV)-Ir(III) Chloroiridate/Perchloric acid supporting electrolyte System: Values of limiting current per unit area divided by concentration of $(NH_4)_2IrCl_6$ as a function of Ir(IV) Perchlorate treatment solution used for boron carbide solid electrode.

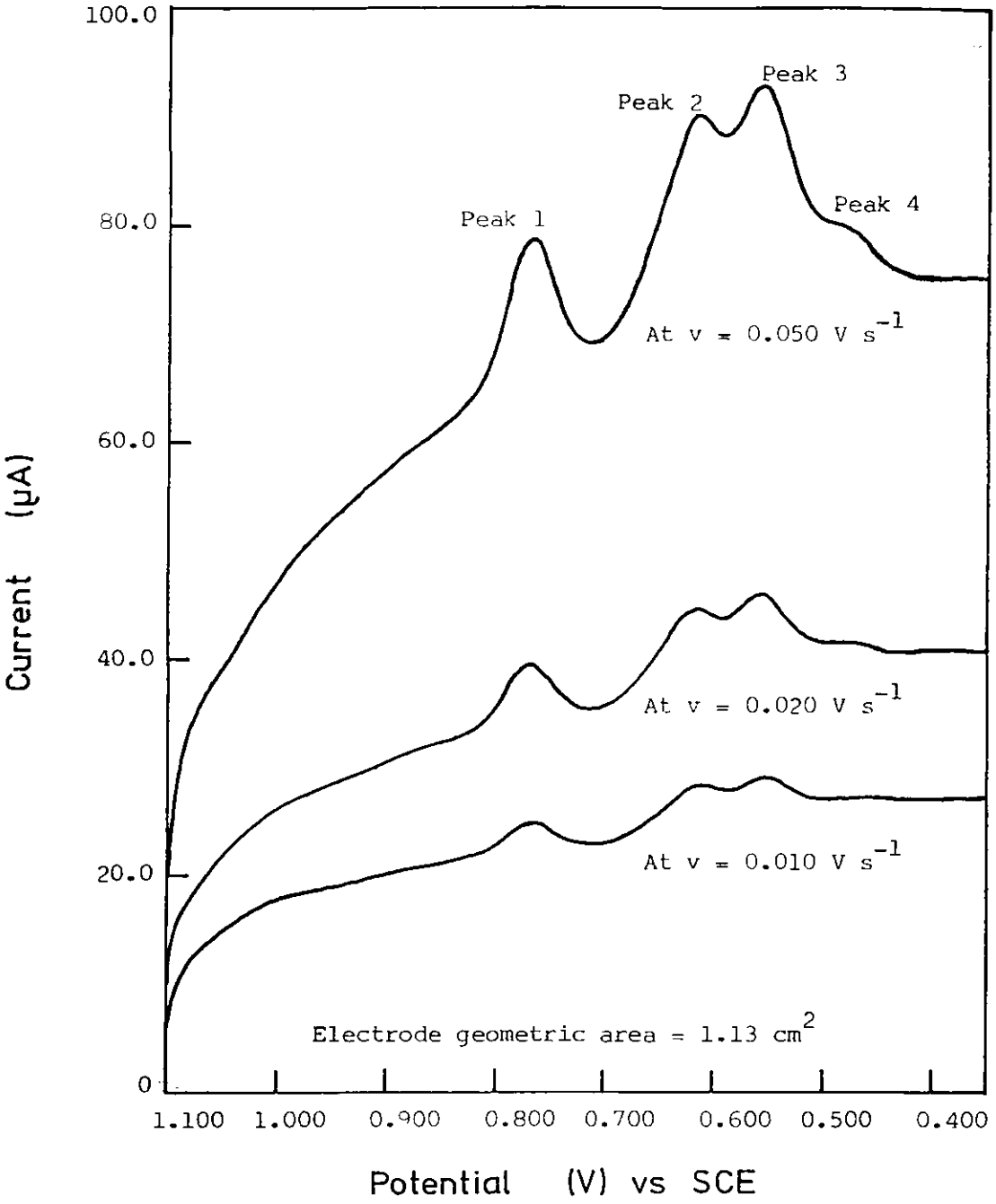

Fig. 5-18 Perchloric acid (0.1 M) supporting electrolyte: Linear sweep voltammograms at different scan rates, v, showing the presence of adsorbed species on the boron carbide solid electrode after treatment with Ir(IV) perchlorate ($9.\cdot \times 10^{-3}$ M) solution.

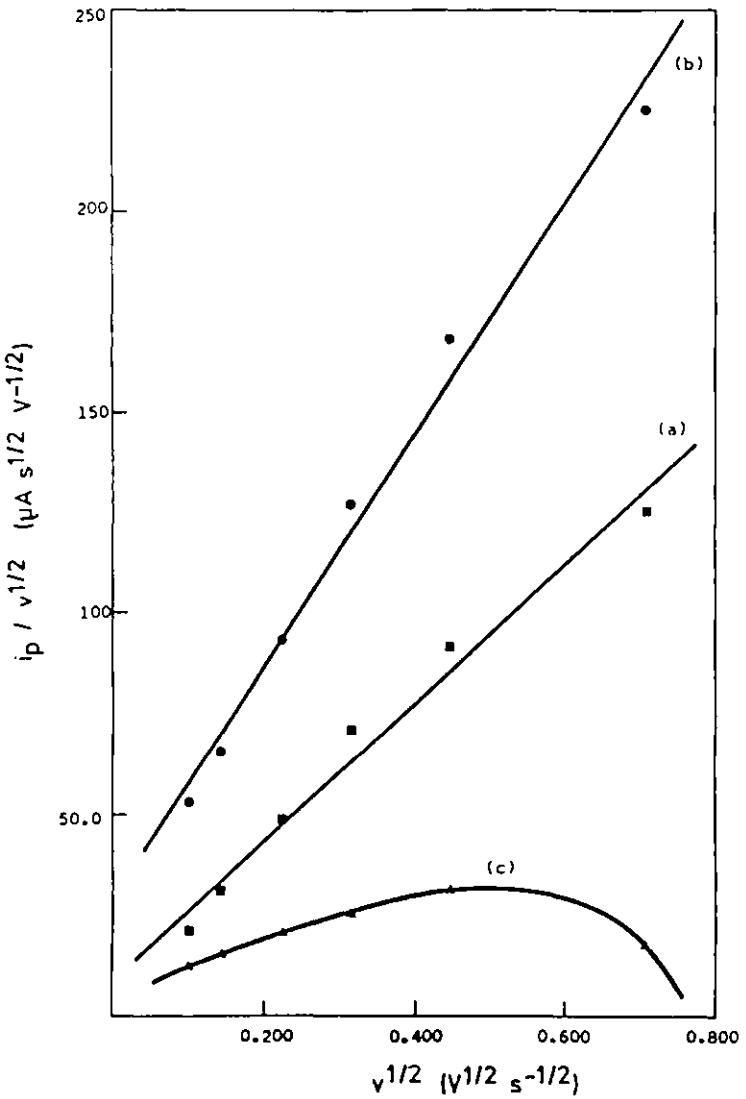

Fig. 5-19 Perchloric acid supporting electrolyte: Background current function, $i_p/v^{\frac{1}{2}}$, for perchloric acid (0.1 M) as a function of square root of potential scan rate, $v^{\frac{1}{2}}$;(a) Peak 1, (b) Peak 2, and (c) Peak 3 in decreasingly less positive peak potentials. Boron carbide solid electrode was treated with Ir(IV) Perchlorate (2.3×10^{-3} M) solution

Fig. 5-19 (continued):-

(a) $i_{p(1)}/v^{\frac{1}{2}} = 9.34 + 172.7\ v^{\frac{1}{2}}$
Correlation coefficient = 0.9898
Level of significance, p = $p < 0.001$
Standard deviation of $i_{p(1)}/v^{\frac{1}{2}}$ from regression = 6.28 μA $s^{\frac{1}{2}}$ $v^{-\frac{1}{2}}$
Degrees of freedom = 4

(b) $i_{p(2)}/v^{\frac{1}{2}} = 29.08 + 289.0\ v^{\frac{1}{2}}$
Correlation coefficient = 0.9940
Level of significance, p = $p < 0.001$
Standard deviation of $i_{p(2)}/v^{\frac{1}{2}}$ from regression = 8.01 μA $s^{\frac{1}{2}}$ $v^{-\frac{1}{2}}$
Degrees of freedom = 4

(Fig. 5-20) show that currents of Peaks 1 and 2 were similarly affected by sweep rate. Fig. 5-21 shows that the peak potentials, E_p's, of the adsorbed species shifted cathodically with increasing sweep rates; thus suggesting the adsorption of reactant in the electrode reduction. However, Fig. 5-22 indicates that an increasing sweep rate affected $E_{p(1)}$ and $E_{p(3)}$ similarly but $E_{p(2)}$ shifted cathodically at a faster rate. this would suggest that Peaks 1 and 3 correspond to strong adsorption whereas Peak 2 included a diffusion element. Cyclic scans (at 0.100 V s^{-1}) showed anodic counterparts for all the cathodic peaks; indicating a degree of reversibility in the electrode reaction (Fig. 5-23).

The effects of the concentration of chloroiridate on the d.c. voltammetric performance of a boron carbide electrode, which was treated first with Ir(IV) perchlorate (1.0×10^{-4} M) solution and then with Ir(IV) perchlorate (2.3×10^{-3} M) solution, were investigated. Linear correlations were found between: (i) decreasing αn values and increasing chloroiridate concentration (Figures 5-24 and 5-25), (ii) decreasing $E_{\frac{1}{2}}$ values and increasing square root value of ionic strength (Figures 5-26 and 5-27), and (iii) increasing limiting current density and increasing chloroiridate concentration (Figures 5-28 and 5-29). However, two-way analysis of variance (two-way ANOVA) on the results plotted in Figures 5-24 to 5-29 indicated that the d.c. voltammetric behaviour of the boron carbide solid electrode did not vary significantly when treated with Ir(IV) perchlorate (2.3×10^{-3} M) solution instead of Ir(IV) perchlorate (1.0×10^{-4} M) solution. Furthermore, two-way ANOVA also indicated that the variations in αn and $E_{\frac{1}{2}}$ values over the concentration range of chloroiridate (1.0×10^{-5} to 1.0×10^{-3} mol dm^{-3}) were not statistically significant at the 0.05 level of significance.

Linear sweep voltammetry (Fig. 5-30) of chloroiridate at the Ir(IV) perchlorate treated boron carbide solid electrode indicated two cathodic peaks. Cyclic voltammetry (Fig. 5-31) produced the anodic counterparts of the two cathodic peaks; suggesting a degree of reversibility. Qualitative comparisons of Figures 5-30 and 5-31 with Figures 5-18 and 5-23 respectively readily show that the underlying charge transfer of the adsorbed Ir(IV) perchlorate species interfered within the potential range for the charge transfer of the chloroiridate anion; Peak 1 (Figures 5-30 and 5-31) being at the potential of the adsorption Peak 1 of the adsorbed Ir(IV) perchlorate species (Figures 5-18 and 5-23) and Peak 2 being the diffusion peak for chloroiridate which enveloped the other adsorption Peaks 2 and 3 of Ir(IV) perchlorate.

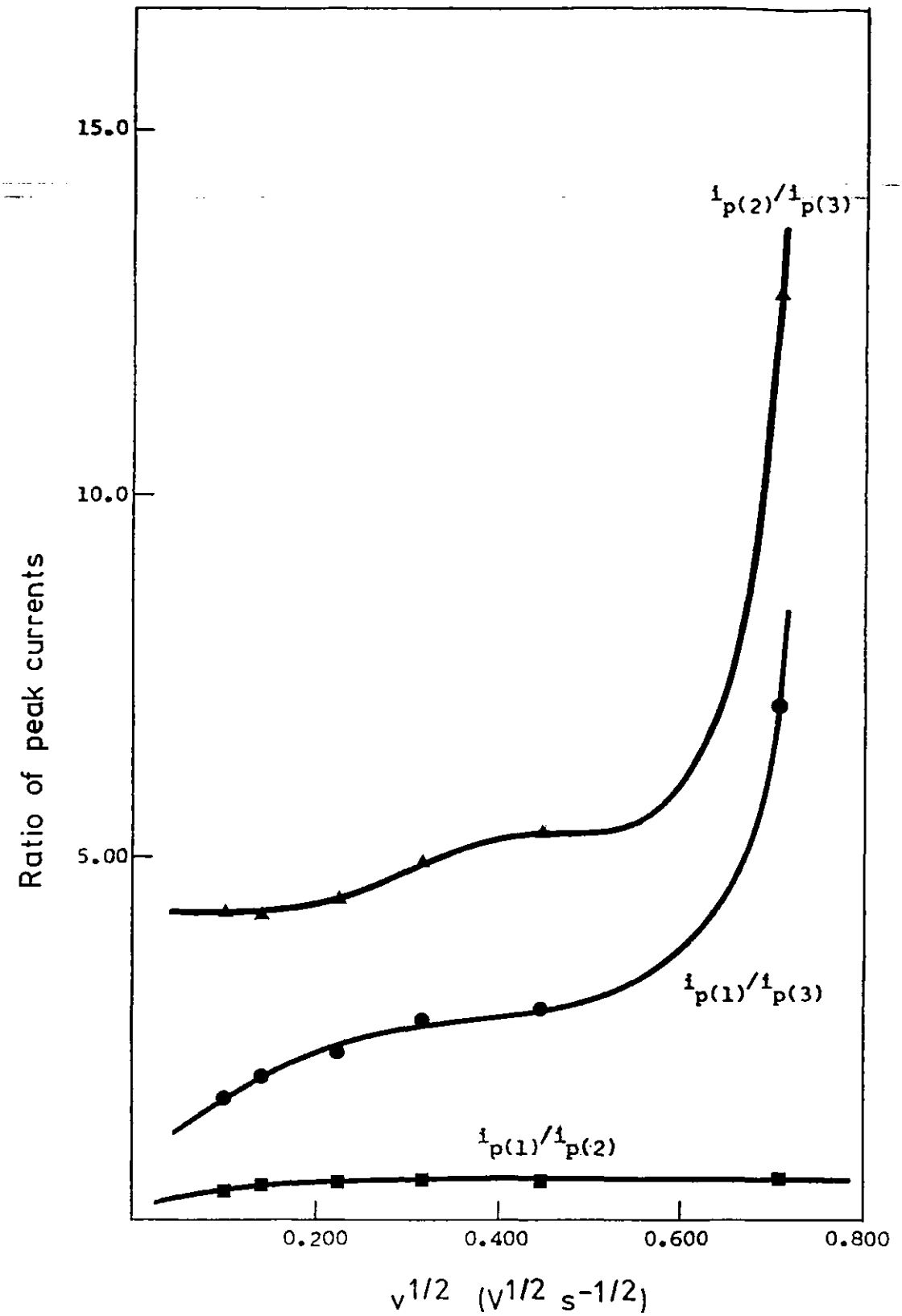

Fig. 5-20 **Perchloric acid supporting electrolyte: Values of ratio of background peak currents for perchloric acid (0.1 M) as a function of square root of potential scan rate, $v^{\frac{1}{2}}$. Boron carbide solid electrode was treated with Ir(IV) Perchlorate (2.3×10^{-3} M) solution.**

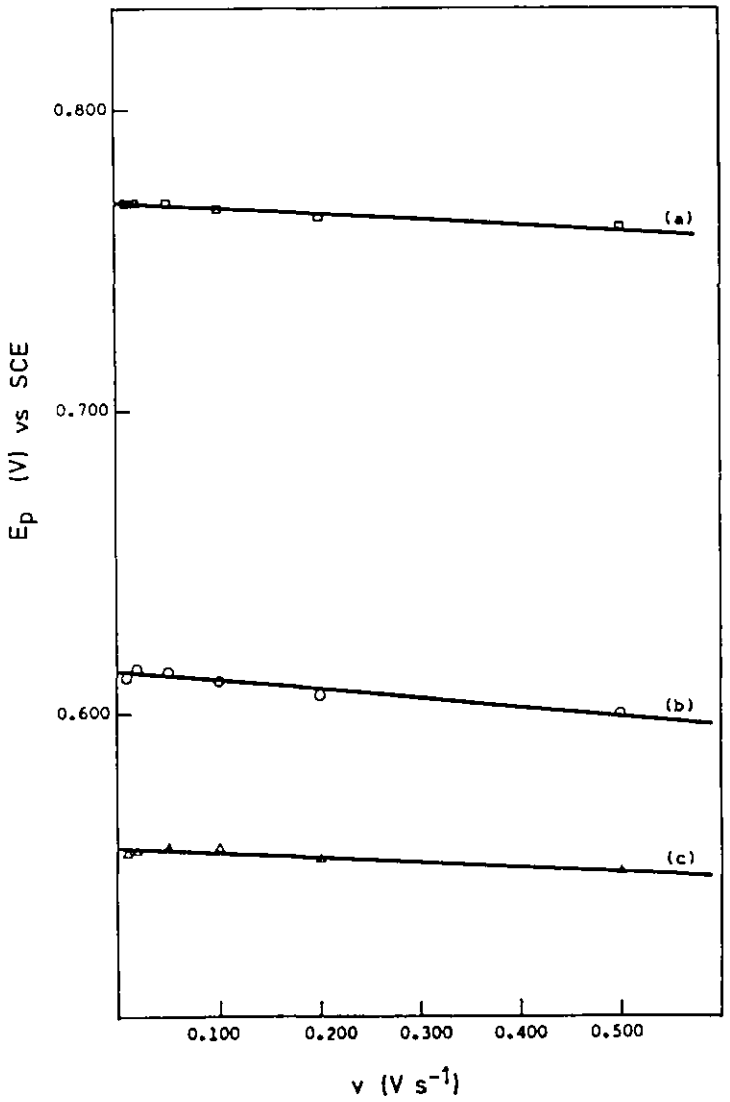

Fig. 5-21 Perchloric acid supporting electrolyte: Background peak potential, E_p, for perchloric acid (0.1 M) as a function of potential scan rate, v; (a) Peak 1, (b) Peak 2, and (c) Peak 3. Boron carbide solid electrode was treated with Ir(IV) Perchlorate (2.3×10^{-3} M)

Fig. 5-21 (continued):-

(a) $E_{p(1)} = 0.769 - 0.018$ v
Correlation coefficient = -0.9499
Level of significance, $p = 0.001 < p < 0.01$
Standard deviation of $E_{p(1)}$ from regression = 0.001 V
Degrees of freedom = 4

(b) $E_{p(2)} = 0.614 - 0.030$ v
Correlation coefficient = -0.9618
Level of significance, $p = 0.001 < p < 0.01$
Standard deviation of $E_{p(2)}$ from regression = 0.002 V
Degrees of freedom = 4

(c) $E_{p(3)} = 0.556 - 0.016$ v
Correlation coefficient = -0.9237
Level of significance, $p = 0.001 < p < 0.01$
Standard deviation of $E_{p(3)}$ from regression = 0.001 V
Degrees of freedom = 4

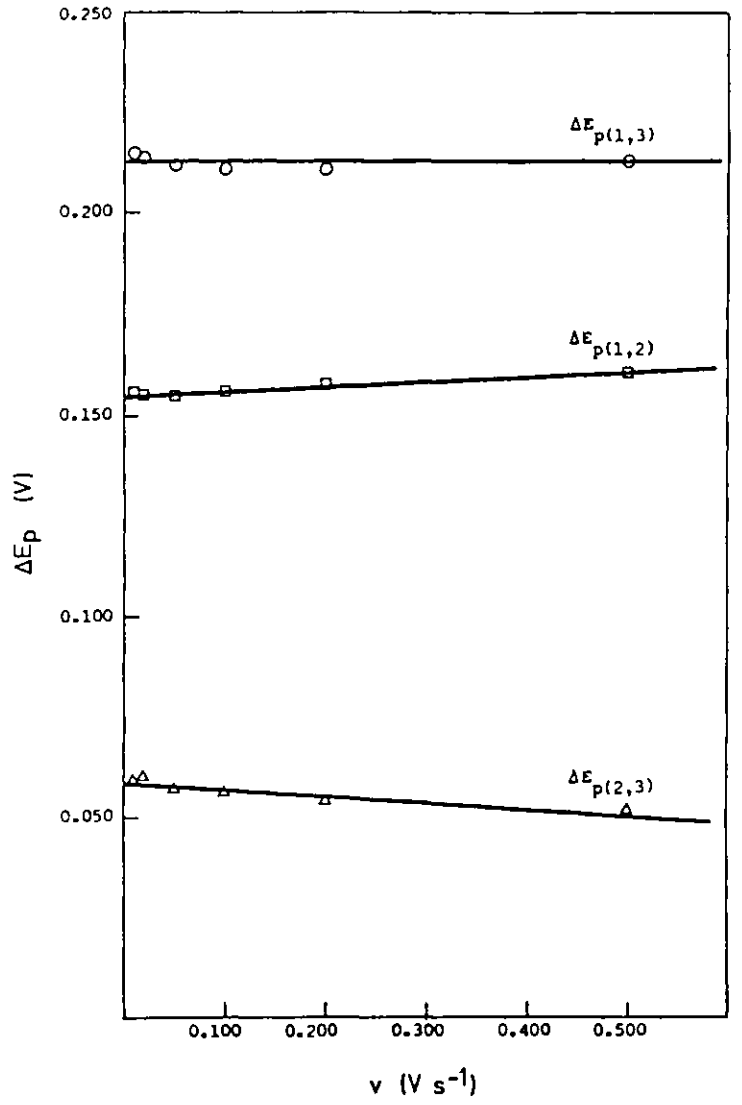

Fig. 5-22 Perchloric acid supporting electrolyte: Difference between background peak potentials, ΔE_p, for perchloric acid (0.1 M) as a function of potential scan rate, v. Boron carbide solid electrode was treated with Ir(IV) Perchlorate (2.3×10^{-3} M) solution.

Fig. 5-22 (continued):-

(a) $\Delta E_{p(1,2)} = 0.155 + 0.012$ v
Correlation coefficient = 0.9295
Level of significance, $p = 0.001 < p < 0.01$.
Standard deviation of $\Delta E_{p(1,2)}$ from regression = 0.001 V
Degrees of freedom = 4

(b) Grand mean of $\Delta E_{p(1,3)}$ = 0.213 V
Standard deviation = 0.001 V
Degrees of freedom = 5

(c) $\Delta E_{p(2,3)} = 0.058 - 0.014$ v
Correlation coefficient = -0.8709
Level of significance, $p = 0.02 < p < 0.05$
Standard deviation of $\Delta E_{p(2,3)}$ from regression = 0.002 V
Degrees of freedom = 4

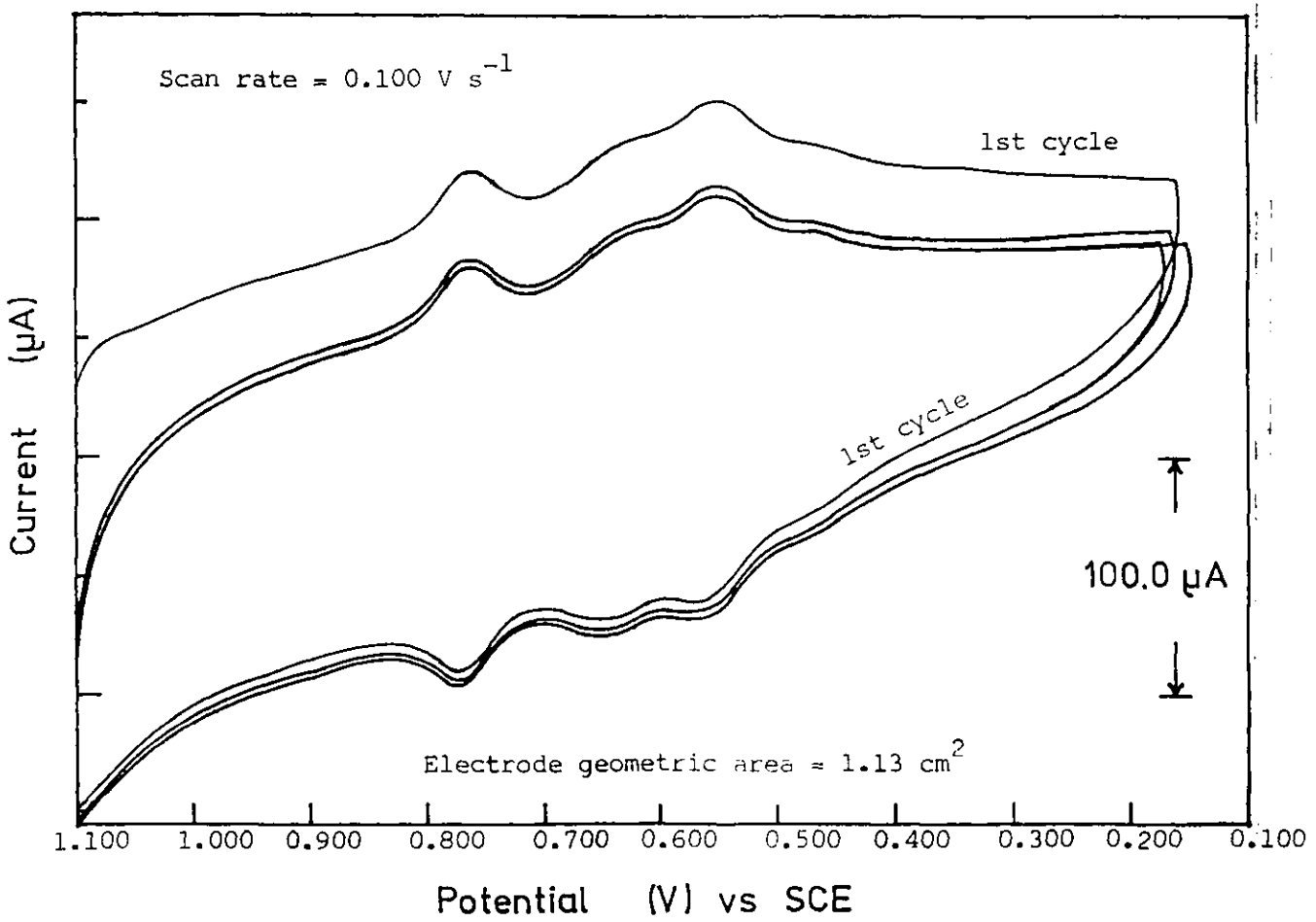

Fig. 5-23 Perchloric acid (0.1 M) supporting electrolyte: Cyclic voltammogram of adsorbed species on the boron carbide solid electrode which had been treated with Ir(IV) perchlorate (2.3×10^{-3} M) solution.

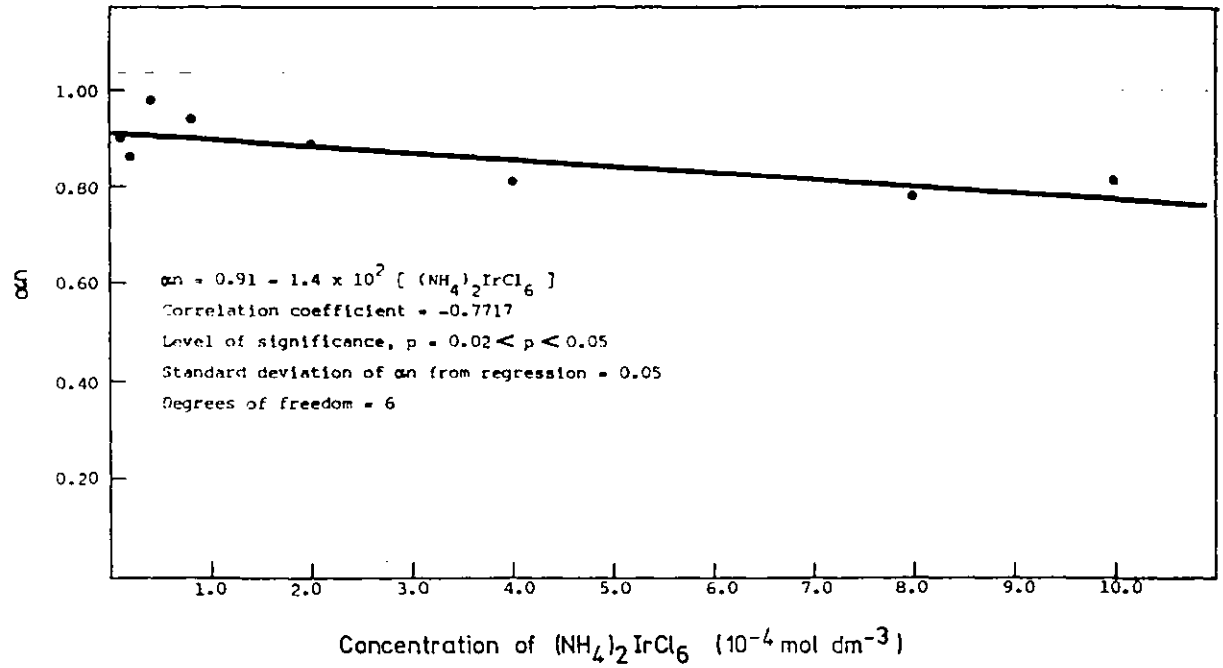

Fig. 5-24 Ir(IV)-Ir(III) Chloroiridate/Perchloric acid supporting electrolyte System: Values of αn as a function of concentration of ammonium hexachloroiridate. Boron carbide solid electrode was treated with Ir(IV) Perchlorate(1.0×10^{-4} M) solution.

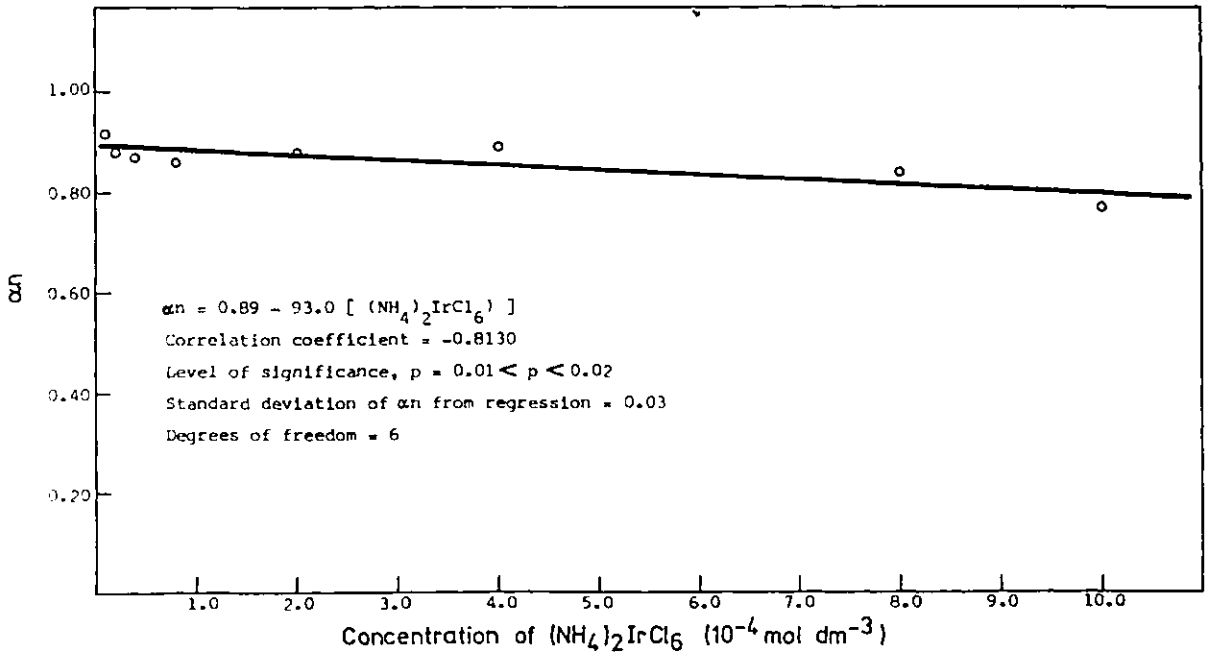

Fig. 5-25 Ir(IV)-Ir(III) Chloroiridate/Perchloric acid supporting electrolyte System: Values of αn as a function of concentration of ammonium hexachloroiridate. Boron carbide solid electrode was treated with Ir(IV) Perchlorate(2.3×10^{-3} M) solution.

Figures 5-24 and 5-25 (continued):-

Two-way Analysis of Variance:

<u>om</u>

Grand mean = 0.87

Standard deviation = 5.4×10^{-2}

Variance ratio due to effects of chloroiridate concentration, $F_1 = 2.09$

Degrees of freedom = 7

Degrees of freedom of the Residual = 7

$F_{0.05}(7,7) = 4.99$ (double-sided)

Therefore, since F_1 does not exceed $F_{0.05}(7,7)$, the effects of chloroiridate concentration are not significant.

Variance ratio due to effects of Ir(IV) perchlorate concentration, $F_2 = 0.142$

Degrees of freedom = 1

Degrees of freedom of the Residual = 7

$F_{0.05}(1,7) = 8.07$ (double-sided)

Therefore, since F_2 does not exceed $F_{0.05}(1,7)$, the effects of Ir(IV) perchlorate concentration are not significant.

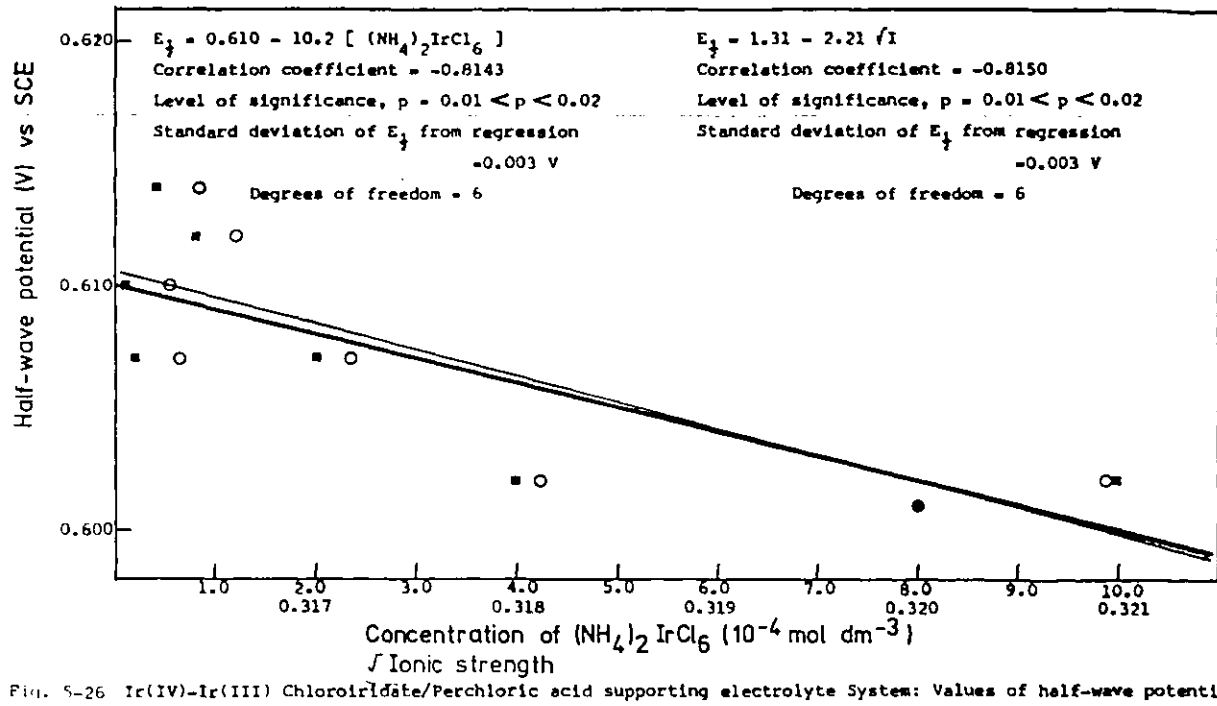

Fig. 5-26 Ir(IV)-Ir(III) Chloroiridate/Perchloric acid supporting electrolyte System: Values of half-wave potential as a function of the concentration of ammonium hexachloroiridate(●), and square root of the total ionic strength(⊖). Boron carbide solid electrode was treated with Ir(IV) Perchlorate(1.0×10^{-4} M) solution.

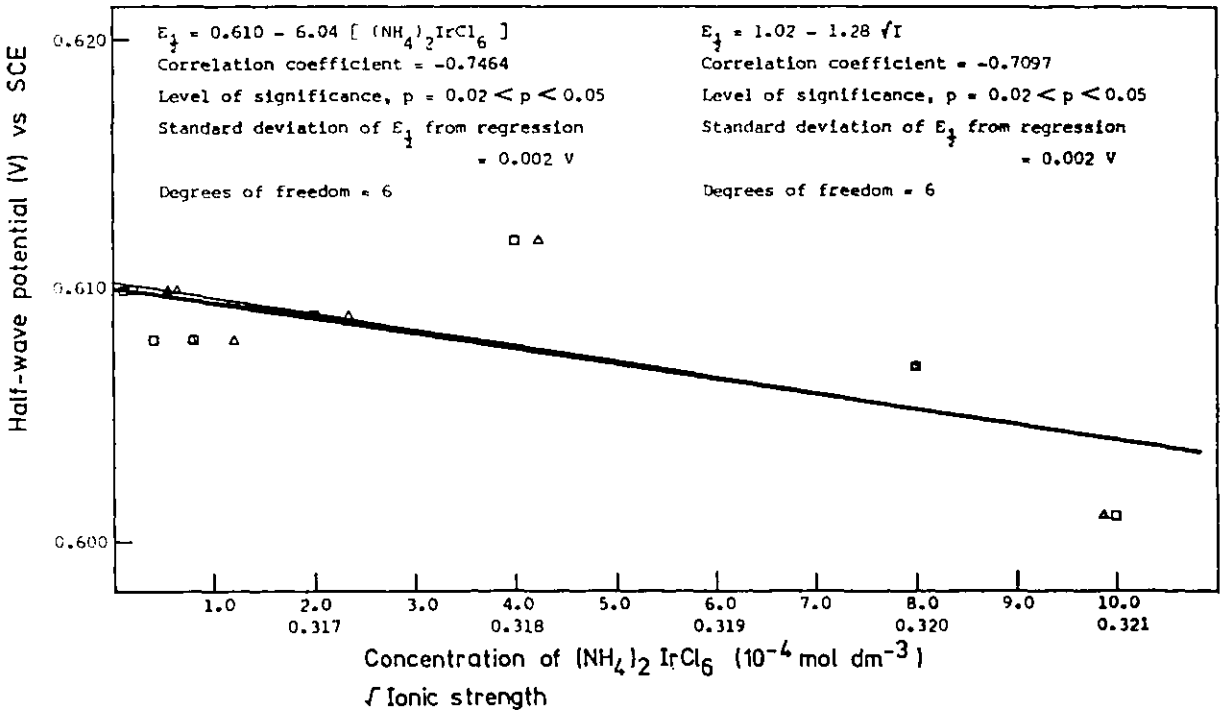

Fig. 5-27 Ir(IV)-Ir(III) Chloroiridate/Perchloric acid supporting electrolyte System: Values of half-wave potential as a function of concentration of ammonium hexachloroiridate(●), and square root of total ionic strength(▲). Boron carbide solid electrode was treated with Ir(IV) Perchlorate(2.3×10^{-3} M) solution.

Figures 5-26 and 5-27 (continued):-

Two-way Analysis of Variance:

$E_{\frac{1}{2}}$

Grand mean = 0.608 V (vs SCE)

Standard deviation = 0.004 V

Variance ratio due to effects of chloroiridate concentration, $F_1 = 4.86$

Degrees of freedom = 7

Degrees of freedom of the Residual = 7

$F_{0.05}(7,7) = 4.99$ (double-sided)

Therefore, since F_1 does not exceed $F_{0.05}(7,7)$, the effects of chloroiridate concentration are not significant.

Variance ratio due to effects of Ir(IV) perchlorate concentration, $F_2 = 1.55$

Degrees of freedom = 1

Degrees of freedom of the Residual = 7

$F_{0.05}(1,7) = 8.07$ (double-sided)

Therefore, since F_2 does not exceed $F_{0.05}(1,7)$, the effects of Ir(IV) perchlorate concentration are not significant.

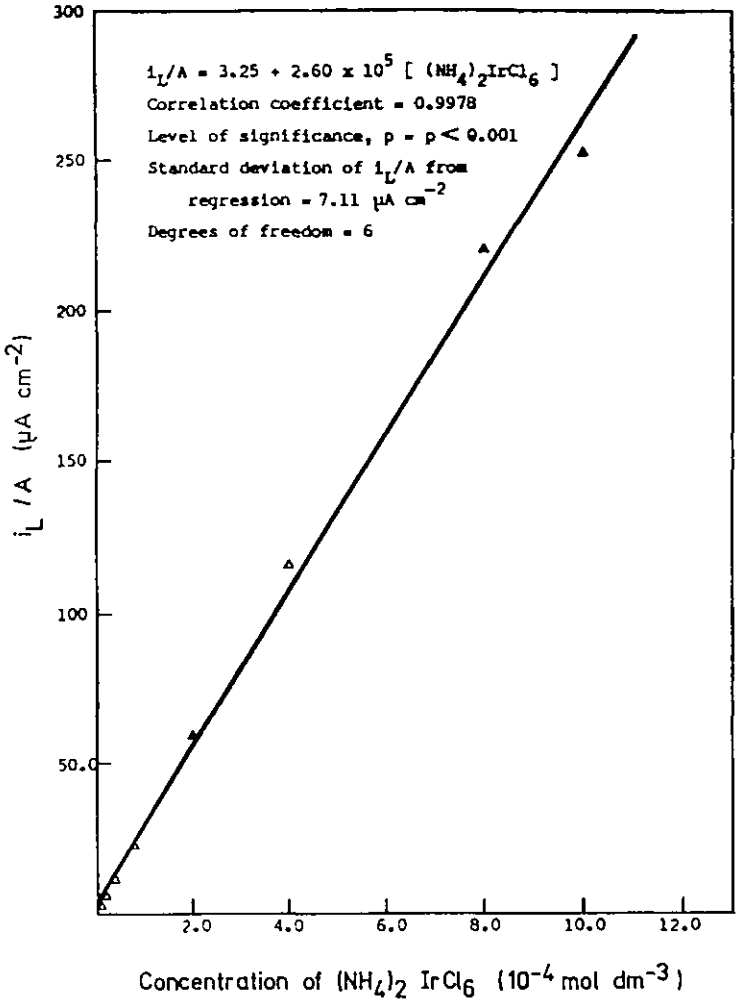

Fig. 5-28 Ir(IV)-Ir(III) Chloroiridate/Perchloric acid supporting electrolyte System: Dependence of limiting current per unit area, i_L/A, on the concentration of ammonium hexachloroiridate. Boron carbide solid electrode was treated with Ir(IV) Perchlorate(1.0×10^{-4} M) solution.

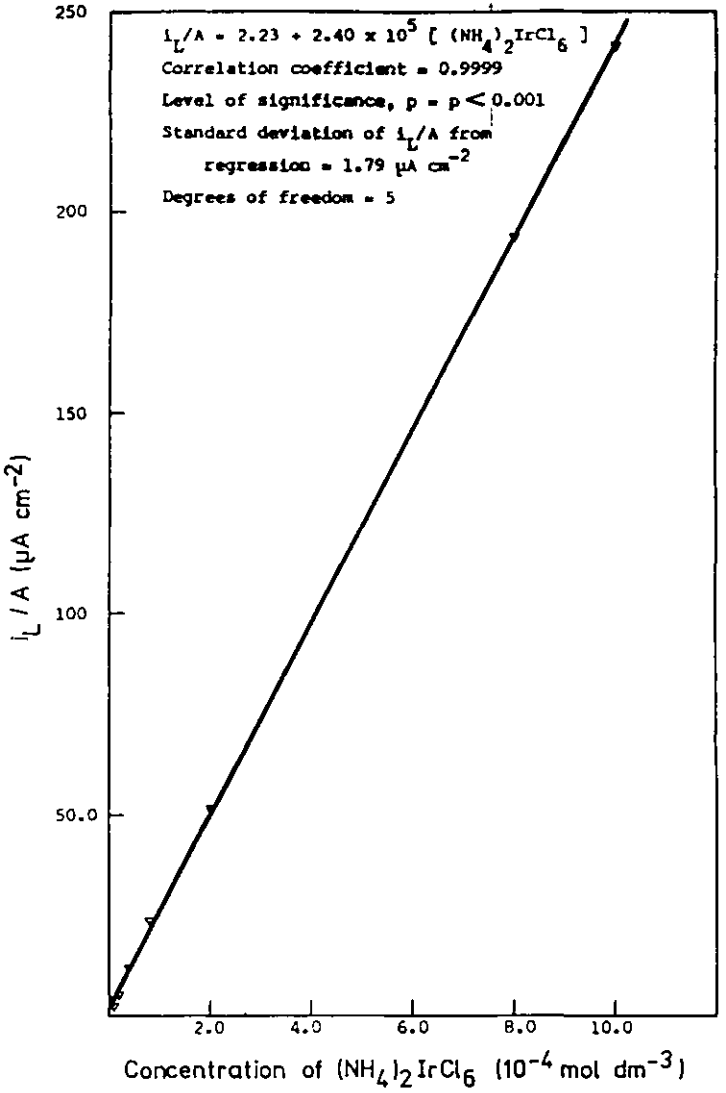

Fig. 5-29 Ir(IV)-Ir(III) Chloroiridate/Perchloric acid supporting electrolyte System: Dependence of limiting current per unit area, i_L/A, on concentration of ammonium hexachloroiridate. Boron carbide solid electrode was treated with Ir(IV) Perchlorate(2.3×10^{-3} M) solution.

Figures 5-28 and 5-29 (continued):-

Two-way Analysis of Variance:

$\underline{i_L/A}$

Grand mean = 83.5 μA cm^{-2}

Standard deviation = 90.5 μA cm^{-2}

Variance ratio due to effects of chloroiridate concentration, F_1 = 410

Degrees of freedom = 7

Degrees of freedom of the Residual = 7

$F_{0.05}(7,7)$ = 4.99 (double-sided)

Therefore, since F_1 exceeds $F_{0.05}(7,7)$, the effects of chloroiridate concentration are significant.

Variance ratio due to effects of Ir(IV) perchlorate concentration, F_2 = 2.60

Degrees of freedom = 1

Degrees of freedom of the Residual = 7

$F_{0.05}(1,7)$ = 8.07 (double-sided)

Therefore, since F_2 does not exceed $F_{0.05}(1,7)$, the effects of Ir(IV) perchlorate concentration are not significant.

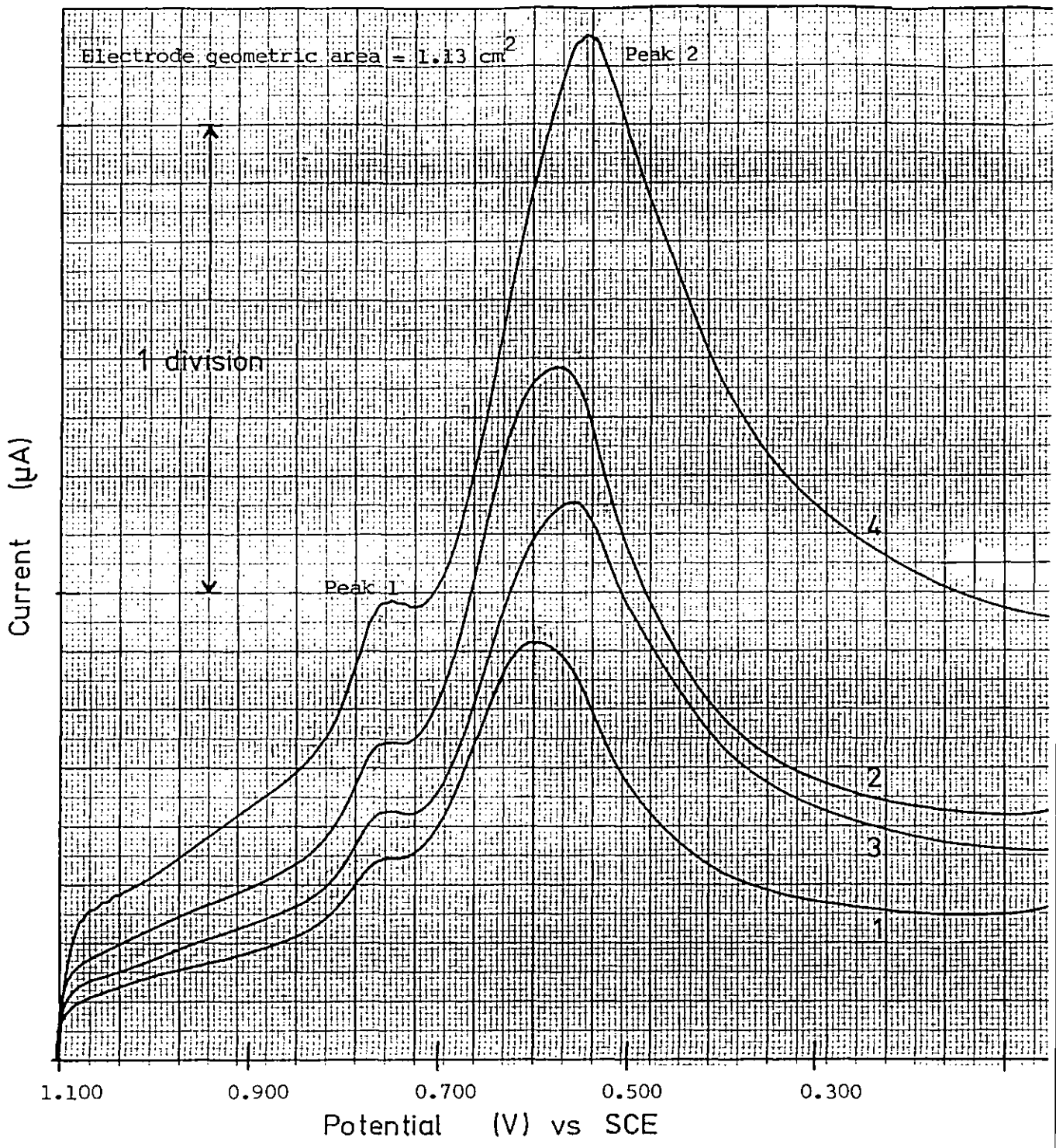

Fig. 5-30 Ir(IV)-Ir(III) Chloroiridate (1.0×10^{-4} mol dm^{-3})/Perchloric acid (0.1 M) supporting electrolyte System: Linear sweep voltammograms at the boron carbide solid electrode which had been treated with Ir(IV) perchlorate (2.3×10^{-3} M) solution. (1) At v = 0.050 V s^{-1}, and current sensitivity = 250 μA per division. (2) At v = 0.100 V s^{-1}, and 250 μA per division. (3) At v = 0.200 V s^{-1}, and 500 μA per division. (4) At v = 0.500 V s^{-1}, and 500 μA per division.

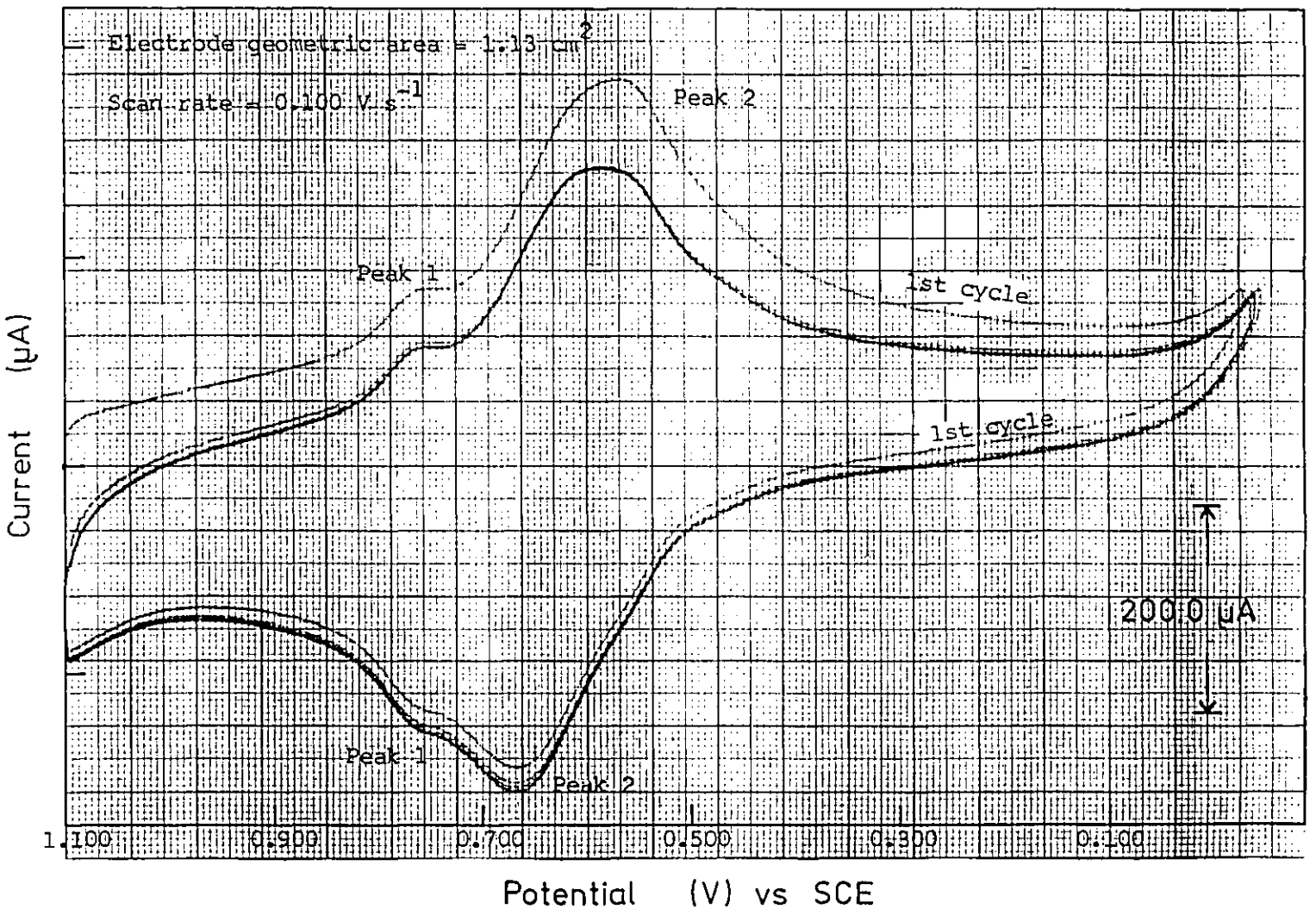

Fig. 5-31 Ir(IV)-Ir(III) Chloroiridate (1.0×10^{-4} mol dm^{-3})/Perchloric acid (0.1 M) supporting electrolyte System: Cyclic voltammogram at the boron carbide solid electrode which had been treated with Ir(IV) perchlorate (2.3×10^{-3} M) solution.

Cyclic scans at sweep rates in excess of 0.200 V s^{-1} revealed the adsorption peaks of Ir(IV) perchlorate which were previously masked by the chloroiridate diffusion peak at slower sweep rates. The anodic adsorption peaks were revealed sooner than the cathodic ones as the sweep rate was increased; thus suggesting reduced reversibility in the chloroiridate charge transfer at higher sweep rates.

Quantitative interpretation (Figures 5-32 and 5-33) of the cyclic voltammograms showed that the cathodic and anodic peak current functions increased with increasing sweep rate and so confirming the presence of adsorption. Contrary to expectations based upon the ratio of cathodic peak currents for the adsorbed species alone (Fig. 5-20), where Peak 1 was the dominant adsorption peak, in the chloroiridate system similar studies (Fig. 5-34) revealed that Peak 1 was affected less than Peak 2 by increasing sweep rates. Moreover, the current function for Peak 1 was also enhanced in the chloroiridate system (Fig. 5-32) when compared with the case of adsorbed species alone (Fig. 5-19, a). These results suggest that chloroiridate was itself also adsorbed and the effects were manifested in Peaks 1 and 2. Plots of the ratio of cathodic:anodic peak currents against increasing square root value of potential sweep rate (Fig. 5-35) indicate that: (i) the anodic current for Peak 1 increased more than the corresponding cathodic current, and (ii) the cathodic current of Peak 2 increased more than the corresponding anodic current at higher sweep rates; thus suggesting strong adsorption of product and weak adsorption of reactant respectively.

Further evidence that the charge transfer for chloroiridate became less reversible at higher sweep rates are shown in Figures 5-36 to 5-38 which indicate that, except for the invariability of the more positive cathodic peak potential, the other cathodic and anodic peak potentials shifted cathodically and anodically respectively as the sweep rate was increased. The less positive peak potential was affected much more than the more positive peak potential by the increasing sweep rate (Fig. 5-38).

The trends, in the cyclic voltammetry of chloroiridate, for the initial cycle were similar to those for the steady state condition (Figures 5-32 to 5-38).

The effects of perchloric acid (0.1 to 2.0 M) supporting electrolyte on the d.c. voltammetric behaviour of Ir(IV) perchlorate (2.3 x 10^{-3} M) treated boron carbide solid electrode are presented in Figures 5-39 to 5-41. The αn value for the reduction of chloroiridate (1.0 x

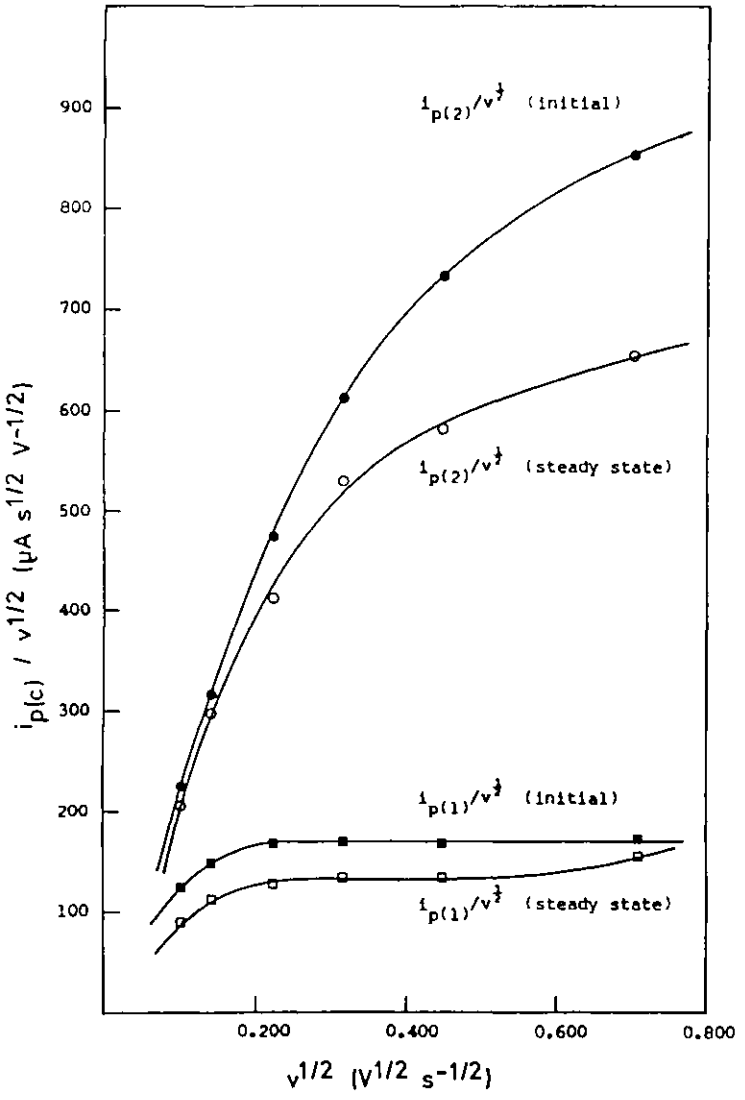

Fig. 5-32 Ir(IV)-Ir(III) Chloroiridate (1.0×10^{-4} mol dm^{-3})/Perchloric acid (0.1 M) supporting electrolyte: Values of cathodic current function, $i_{p(c)}/v^{\frac{1}{2}}$, as a function of square root of potential scan rate, $v^{\frac{1}{2}}$. Boron carbide solid electrode was treated with Ir(IV) Perchlorate (2.3×10^{-3} M) solution.

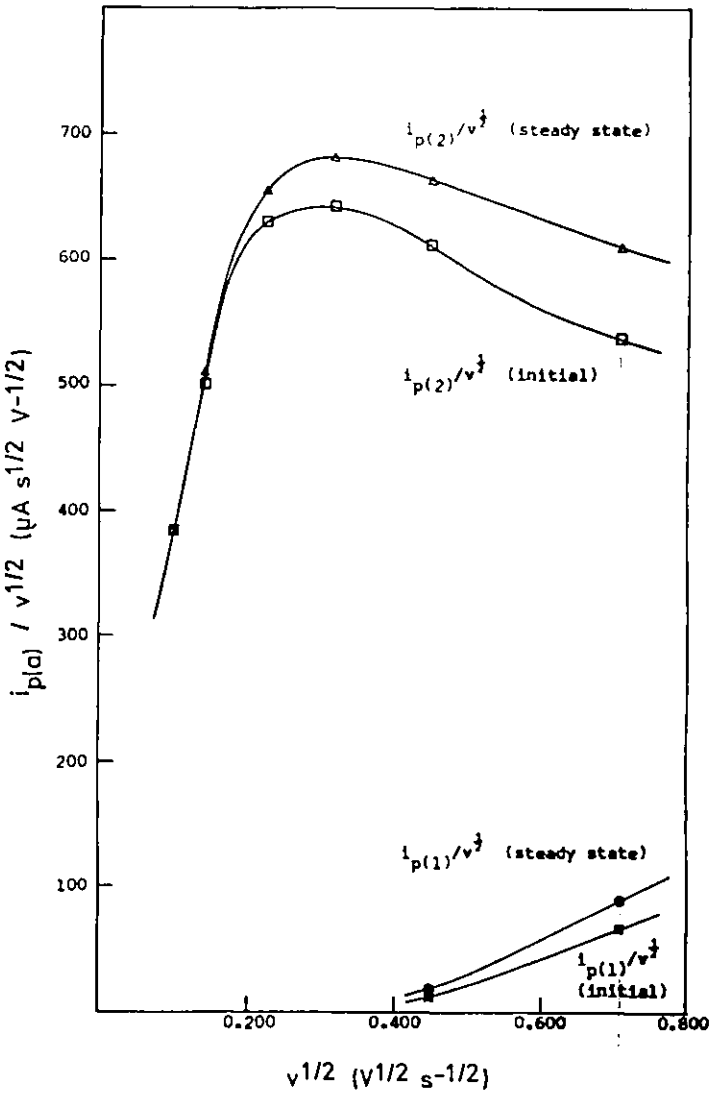

Fig. 5-33 Ir(IV)-Ir(III) Chloroiridate (1.0×10^{-4} mol dm^{-3})/Perchloric acid (0.1 M) supporting electrolyte: Values of anodic current function, $i_{p(a)}/v^{\frac{1}{2}}$, as a function of square root of potential scan rate, $v^{\frac{1}{2}}$. Boron carbide solid electrode was treated with Ir(IV) Perchlorate (2.3×10^{-3} M) solution.

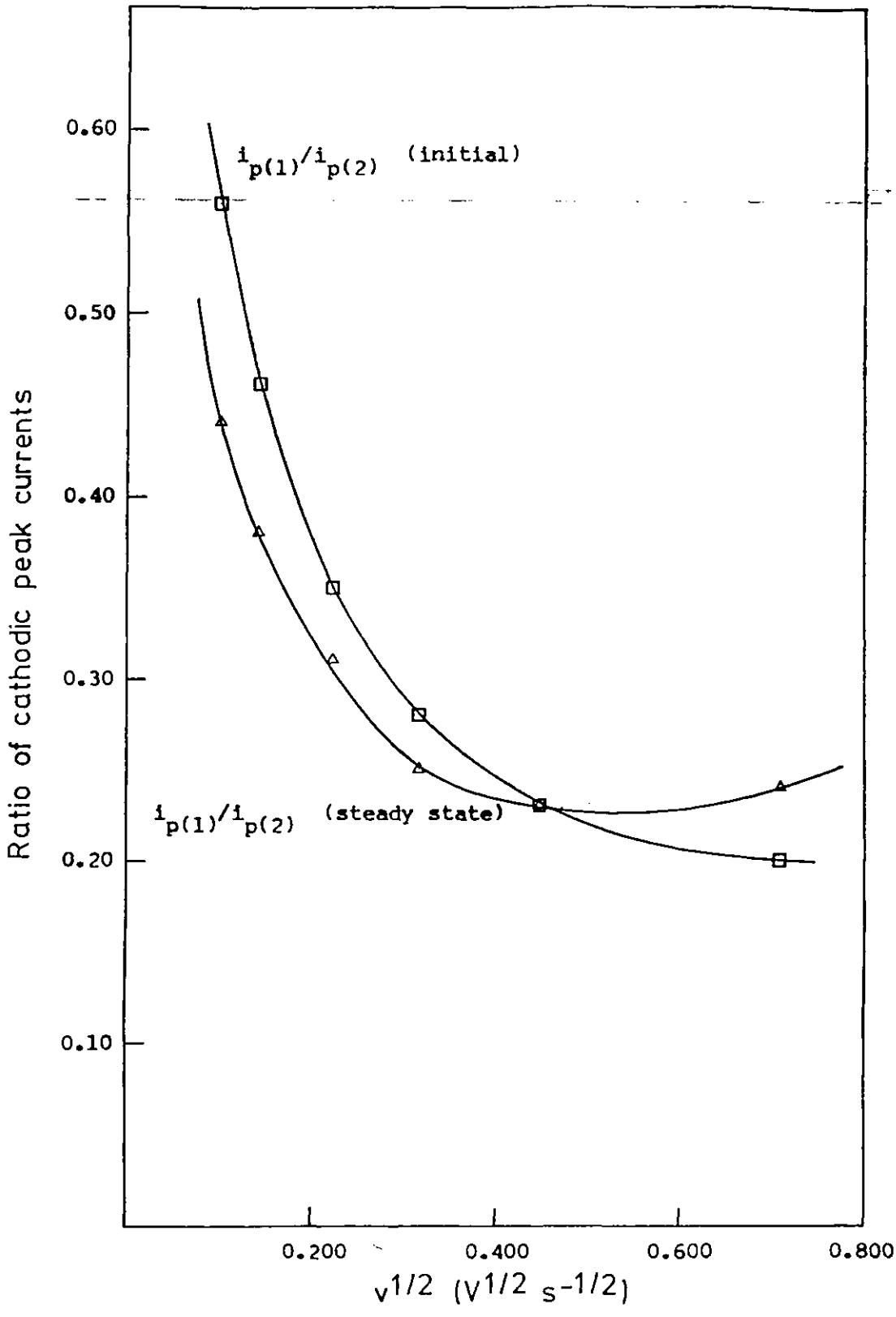

Fig. 5-34 Ir(IV)-Ir(III) Chloroiridate (1.0×10^{-4} mol dm^{-3})/Perchloric acid (0.1 M) supporting electrolyte: Values of ratio of peak currents as a function of square root of potential scan rate, $v^{\frac{1}{2}}$. Boron carbide solid electrode was treated with Ir(IV) Perchlorate (2.3×10^{-3} M) solution.

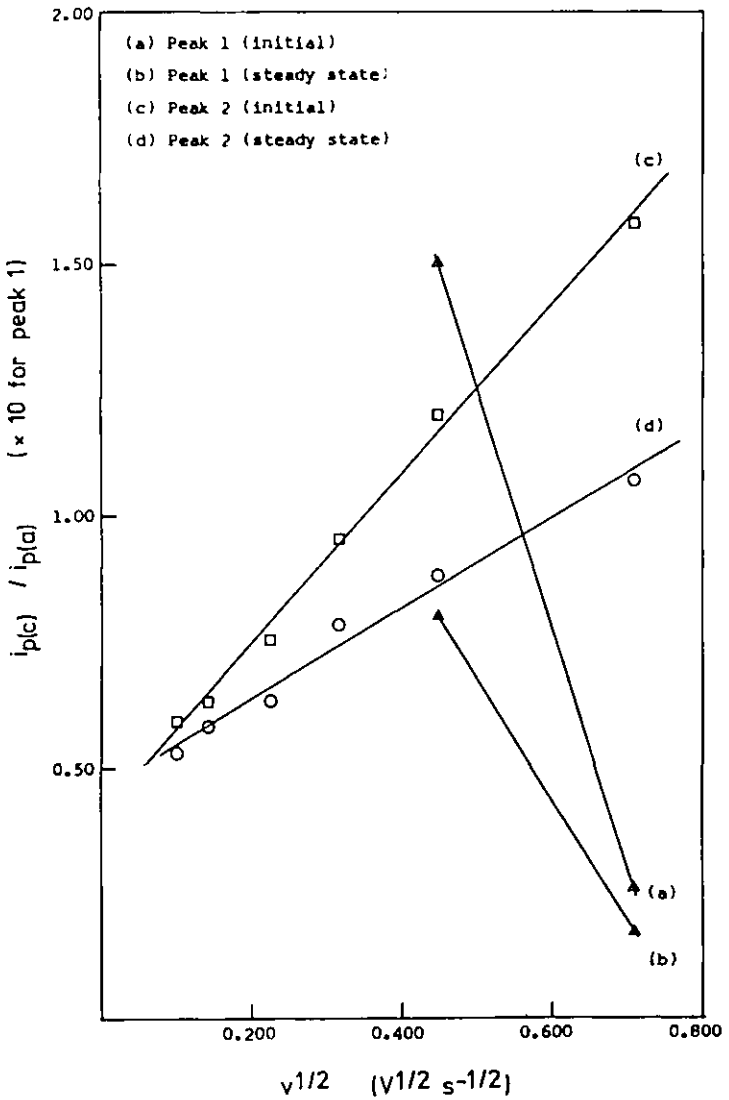

Fig. 5-35 Ir(IV)-Ir(III) Chloroiridate (1.0×10^{-4} mol dm^{-3})/Perchloric acid (0.1 M) supporting electrolyte: Values of the ratio of cathodic to anodic peak currents, $i_{p(c)}/i_{p(a)}$, as a function of square root of potential scan rate, $v^{\frac{1}{2}}$. Boron carbide solid electrode was treated with Ir(IV) Perchlorate (2.3×10^{-3} M) solution.

Fig. 5-35 (continued):-

(a) Cathodic $i_{p(1)}$ (initial)/anodic $i_{p(1)}$ (initial) values were quantifiable only at faster scan rates.

(b) Cathodic $i_{p(1)}$ (steady state)/anodic $i_{p(1)}$ (steady state) values were quantifiable only at faster scan rates.

(c) Cathodic $i_{p(2)}$ (initial)/anodic $i_{p(2)}$ (initial)
$= 0.41 + 1.69\ v^{\frac{1}{2}}$
Correlation coefficient = 0.9979
Level of significance, p = $p < 0.001$
Standard deviation of cathodic $i_{p(2)}$ (initial)/anodic $i_{p(2)}$ (initial) from regression = 0.03
Degrees of freedom = 4

(d) Cathodic $i_{p(2)}$ (steady state)/anodic $i_{p(2)}$ (steady state)
$= 0.46 + 0.90\ v^{\frac{1}{2}}$
Correlation coefficient = 0.9923
Level of significance, p = $p < 0.001$
Standard deviation of cathodic $i_{p(2)}$ (steady state)/anodic $i_{p(2)}$ (steady state) from regression = 0.03
Degrees of freedom = 4

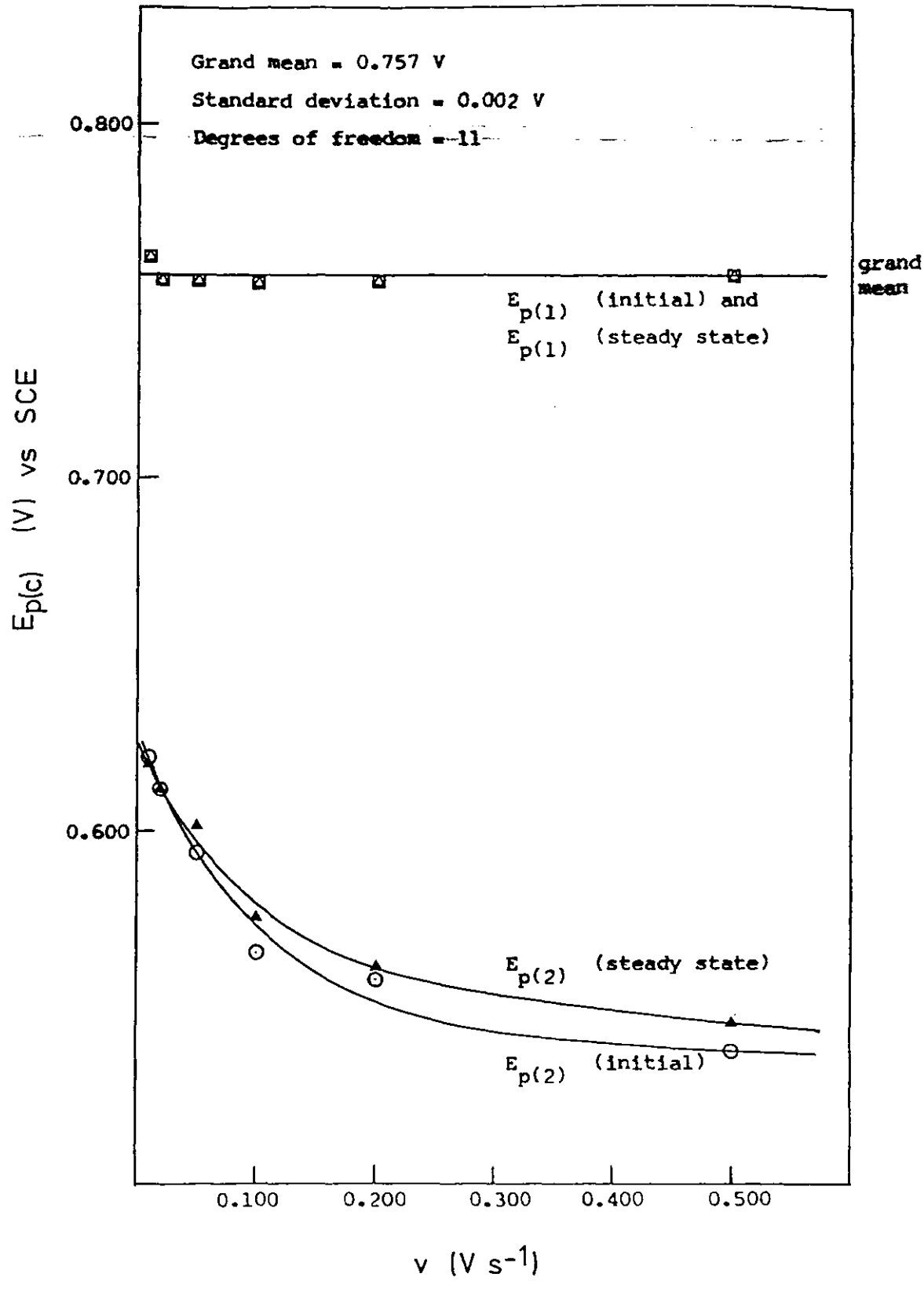

Fig. 5-36 **Ir(IV)-Ir(III) Chloroiridate (1.0×10^{-4} mol dm^{-3})/Perchloric acid (0.1 M) supporting electrolyte: Values of cathodic peak potential, $E_{p(c)}$, as a function of potential scan rate, v. Boron carbide solid electrode was treated with Ir(IV) Perchlorate (2.3×10^{-3} M) solution.**

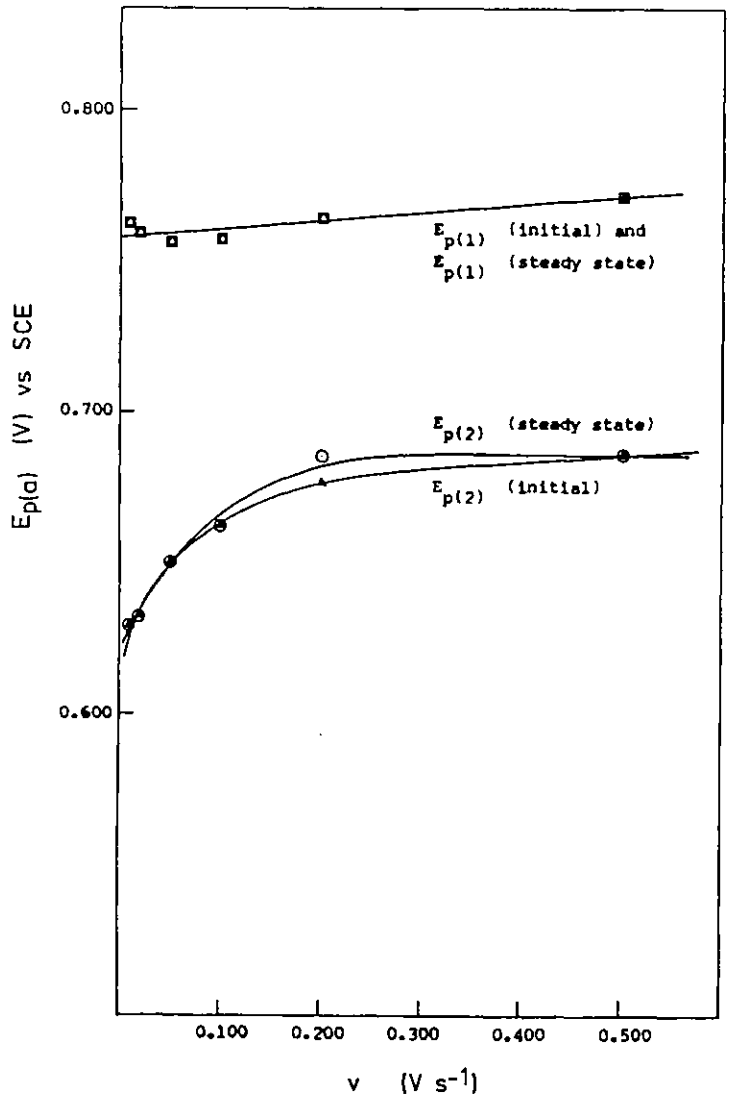

Fig. 5-37 **Ir(IV)-Ir(III) Chloroiridate (1.0×10^{-4} mol dm^{-3})/Perchloric acid (0.1 M) supporting electrolyte: Values of anodic peak potential, $E_{p(a)}$, as a function of potential scan rate, v. Boron carbide solid electrode was treated with Ir(IV) Perchlorate (2.3×10^{-3} M) solution.**

Fig. 5-37 (continued):-

(a) $E_{p(1)}$ (initial) = 0.758 + 0.027 v
Correlation coefficient = 0.8703
Level of significance, $p = 0.02 < p < 0.05$
Standard deviation of $E_{p(1)}$ (initial) from regression = 0.003 V
Degrees of freedom = 4

(b) $E_{p(1)}$ (steady state) = 0.758 + 0.027 v
Correlation coefficient = 0.8703
Level of significance, $p = 0.02 < p < 0.05$
Standard deviation of $E_{p(1)}$ (steady state) from regression = 0.003 V
Degrees of freedom = 4

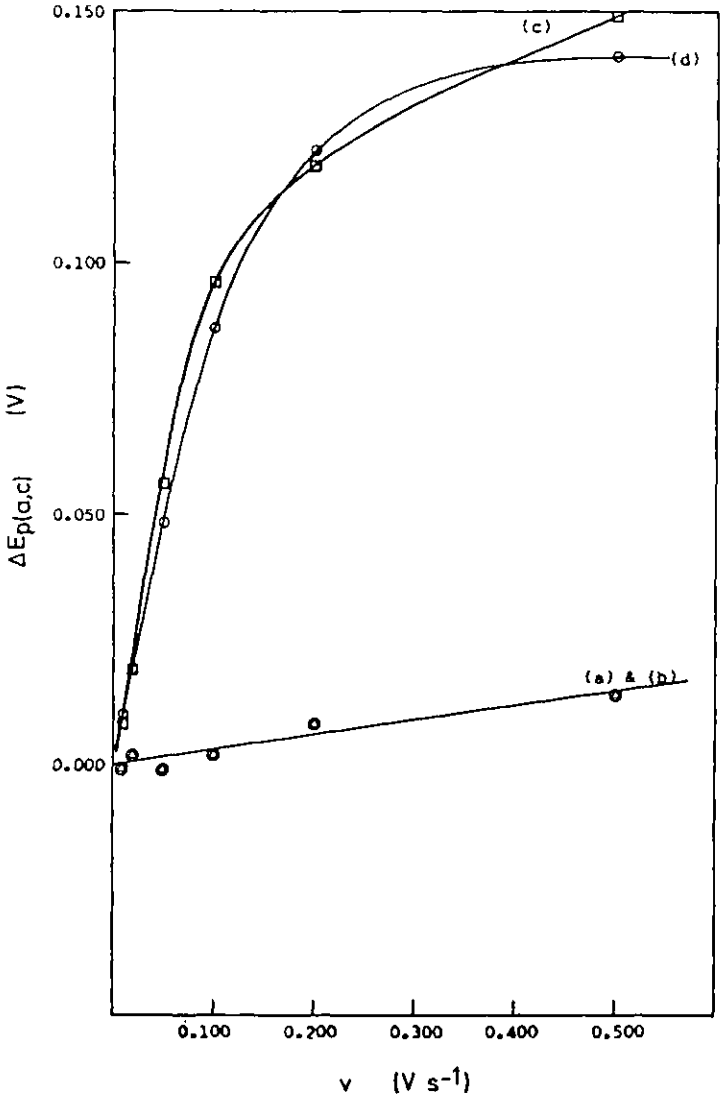

Fig. 5-38 Ir(IV)-Ir(III) Chloroiridate (1.0×10^{-4} mol dm^{-3})/Perchloric acid (0.1 M) supporting electrolyte: Difference between anodic and cathodic peak potentials, $\Delta E_{p(a,c)}$, as a function of potential scan rate, v. Boron carbide solid electrode was treated with Ir(IV) Perchlorate (2.3×10^{-3} M) solution.

Fig. 5-38 (continued):-

(a) Anodic $E_{p(1)}$ (initial) - cathodic $E_{p(1)}$ (initial)
$= 0.030\ v - 2.0 \times 10^{-4}$

Correlation coefficient = 0.9618

Level of significance, $p = 0.001 < p < 0.01$

Standard deviation of anodic $E_{p(1)}$ (initial) - cathodic $E_{p(1)}$ (initial) from regression = 0.002 V

Degrees of freedom = 4

(b) Anodic $E_{p(1)}$ (steady state) - cathodic $E_{p(1)}$ (steady state)
$= 0.030 - 2.0 \times 10^{-4}$

Correlation coefficient = 0.9618

Level of significance, $p = 0.001 < p < 0.01$

Standard deviation of anodic $E_{p(1)}$ (steady state) - cathodic $E_{p(1)}$ (steady state) from regression = 0.002 V

Degrees of freedom = 4

(c) Anodic $E_{p(2)}$ (initial) - cathodic $E_{p(2)}$ (initial)

(d) Anodic $E_{p(2)}$ (steady state) - cathodic $E_{p(2)}$ (steady state)

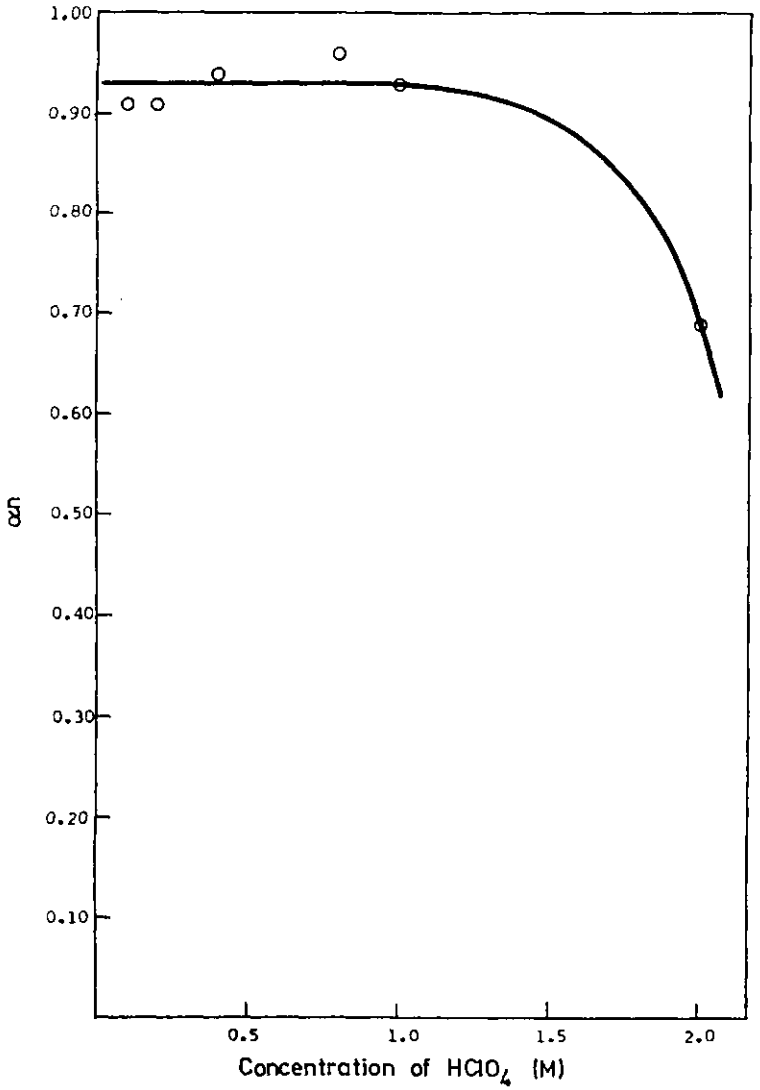

Fig. 5-39 Ir(IV)-Ir(III) Chloroiridate/Perchloric acid supporting electrolyte System: Values of αn as a function of concentration of perchloric acid supporting electrolyte. Boron carbide solid electrode was treated with Ir(IV) Perchlorate(2.3×10^{-3} M) solution.

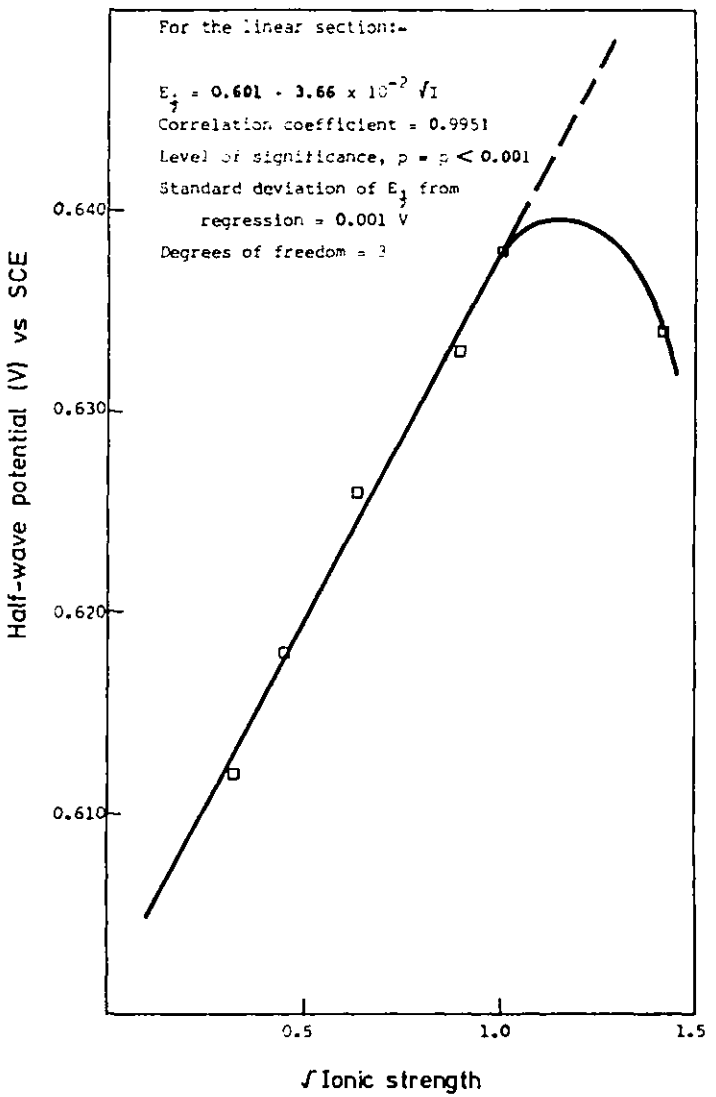

Fig. 5-40 Ir(IV)-Ir(III) Chloroiridate/Perchloric acid supporting electrolyte System: Values of half-wave potential as a function of square root of total ionic strength. Boron carbide solid electrode was treated with Ir(IV) Perchlorate (2.3×10^{-3} M) solution.

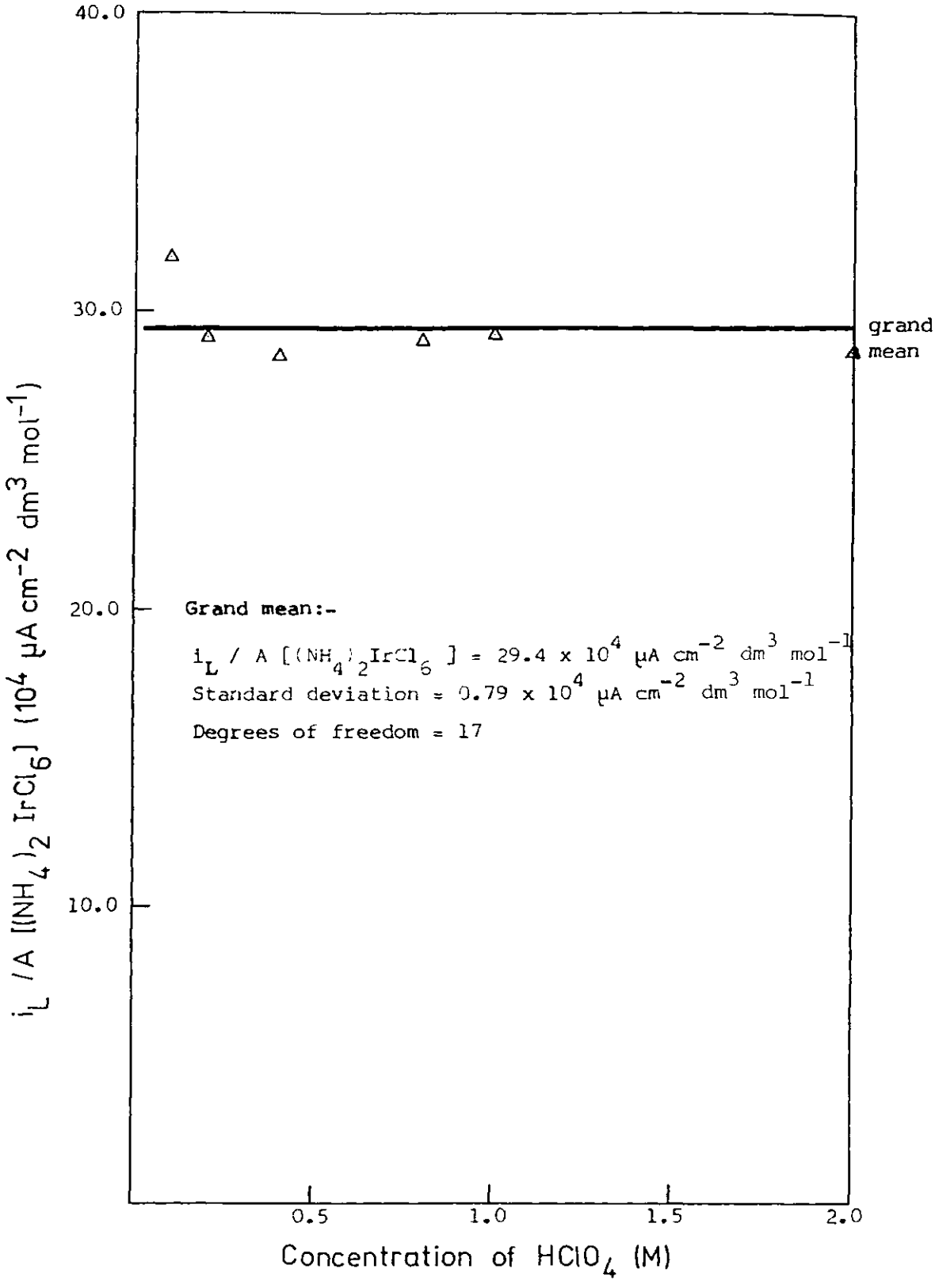

Fig. 5-41 Ir(IV)-Ir(III) Chloroiridate/Perchloric acid supporting electrolyte System: Values of limiting current per unit area divided by concentration of ammonium hexachloroiridate as a function of concentration of perchloric acid supporting electrolyte. Boron carbide solid electrode was treated with Ir(IV) Perchlorate(2.3×10^{-3} M) solution.

10^{-4} mol dm^{-3}) remained essentially constant (grand mean = 0.93 ± 0.05, 15 degrees of freedom) up to 1.0 M perchloric acid but decreased to a value of 0.69 in 2.0 M perchloric acid. The $E_{\frac{1}{2}}$ value increased linearly with increasing (ionic strength)$^{\frac{1}{2}}$, $I^{\frac{1}{2}}$, up to approximately $I^{\frac{1}{2}}$ = 1 before decreasing. This suggests that the electroactive species was anionic (equation 3-10), as expected, despite the earlier apparently anomalous results of Figures 5-26 and 5-27; which may be attributed to a decrease in the reversibility of the electro-reduction of chloroiridate when its concentration was increased. The limiting current was independent of the perchloric acid concentration; within the range investigated.

5-1.1.(iv) Effect of electrochemical treatment on electrodes.

The reversibility of the electro-reduction of chloroiridate at the boron carbide solid electrode was significantly improved (Fig. 5-42) by electrochemical treatment of the electrode (section 4-2.3) prior to d.c. voltammetry. However, the reversibility of the charge transfer deteriorated (as characterised by decreasing αn and $E_{\frac{1}{2}}$ values) with increasing concentration of chloroiridate (Figures 5-43 and 5-44). Electrochemical treatment in more concentrated chloroiridate (2.0 x 10^{-3} M) solution resulted in a greater improvement in electrode performance than when treated in a chloroiridate concentration of the sample itself; although the linear concentration dependences of the limiting current were similar (Fig. 5-45).

Typical linear sweep voltammograms at an electrochemically treated boron carbide solid electrode are presented in Fig. 5-46. Plots of current functions versus (sweep rate)$^{\frac{1}{2}}$ suggest that the diffusion peak of chloroiridate was complicated by a catalytic reaction and very weak adsorption (Fig. 5-47 c.f. Fig. 3-6). Fig. 5-48 shows that the peak potential shifted cathodically whereas the half-peak potential shifted anodically with increasing sweep rate; again suggesting the presence of very weak adsorption. The one-electron charge transfer, however, was not reversible; $|E_p - E_{p/2}|$ values increasing from 0.062 V to 0.095 V with increasing sweep rate (equation 3-32). The anomaly of the half-peak and peak potentials shifting in opposite directions with increasing sweep rate may be explained in terms of weak adsorption of product affecting the half-peak potential position whilst the peak potential was affected by decreasing reversibility.

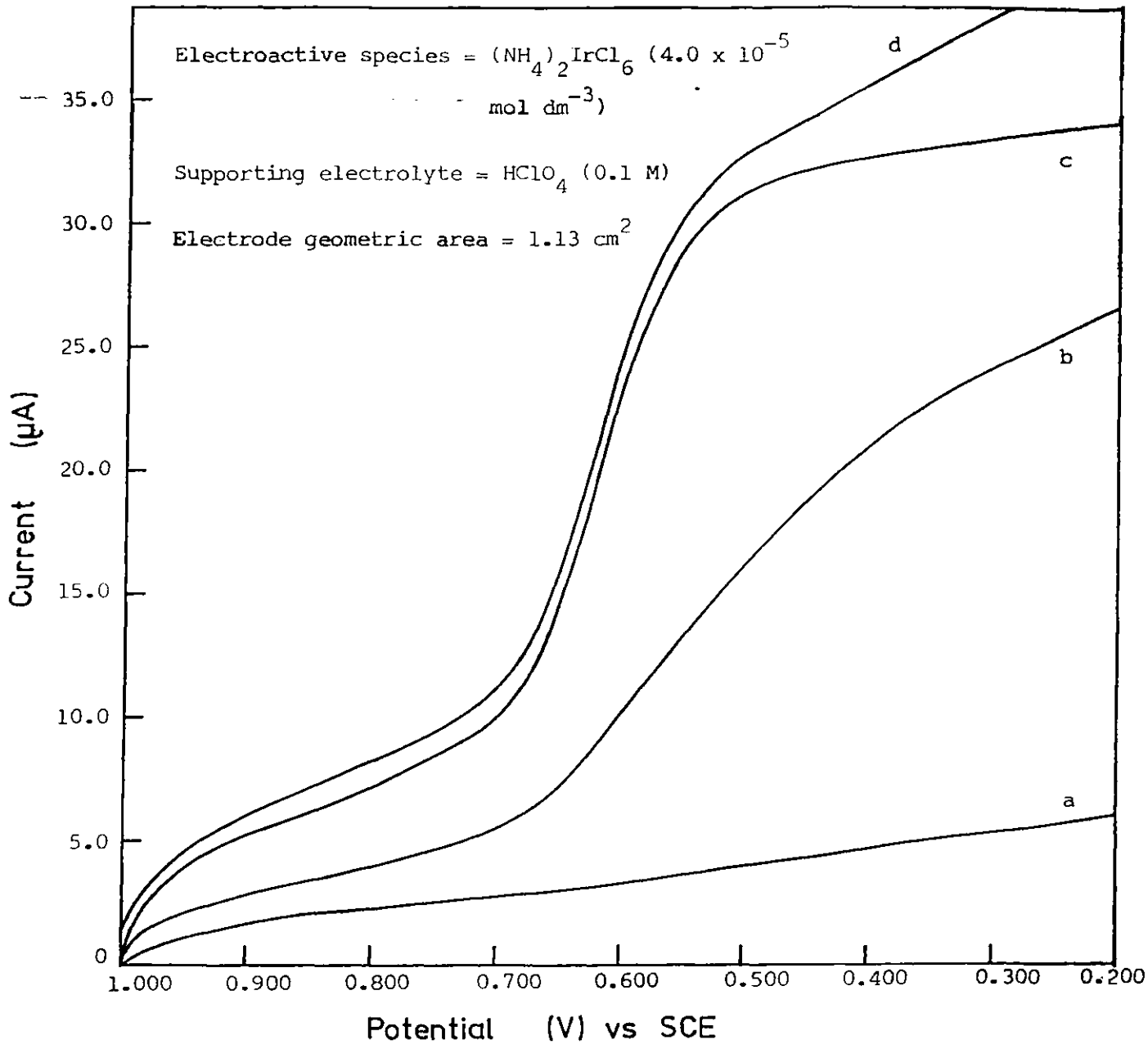

Fig. 5-42 (a) Residual current after cathodic polarisation (at -1 V) in the supporting electrolyte. (b) D.c. voltammogram of the reduction of chloroiridate. (c) Reduction of chloroiridate after the boron carbide solid electrode had been cathodically polarised (at -1 V) in the sample solution. (d) Reduction of chloroiridate after the electrode had been cathodically polarised (at -1 V) in chloroiridate (2.0×10^{-3} M) solution.

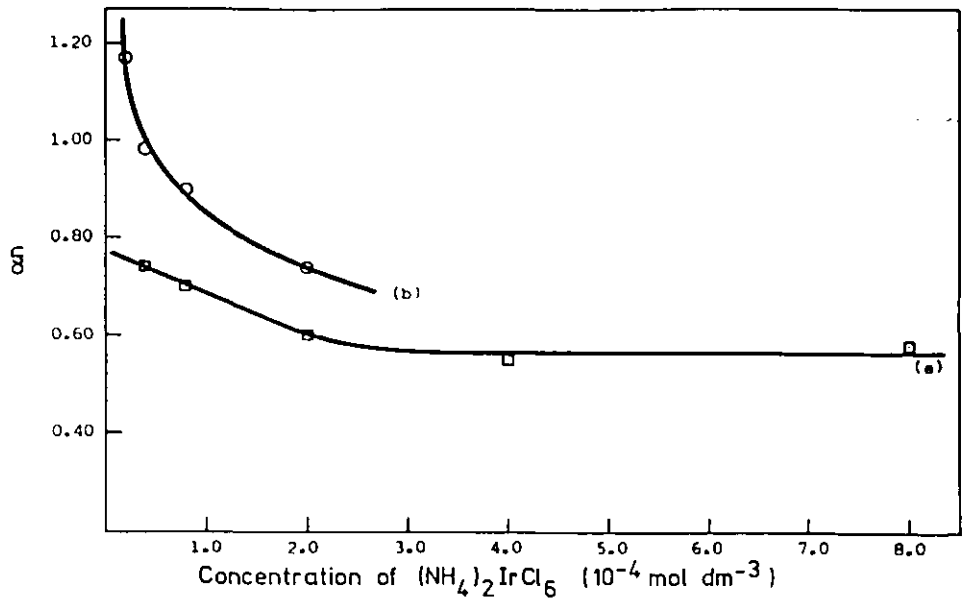

Fig. 5-43 Ir(IV)-Ir(III) Chloroiridate/Perchloric acid supporting electrolyte System: Values of αn as a function of concentration of ammonium hexachloroiridate. Boron carbide solid electrode was treated by cathodic polarisation (at -1 V) in: (a) Sample solution prior to voltammetric scan (□). (b) More concentrated (2.0×10^{-3} M) ammonium hexachloroiridate solution.

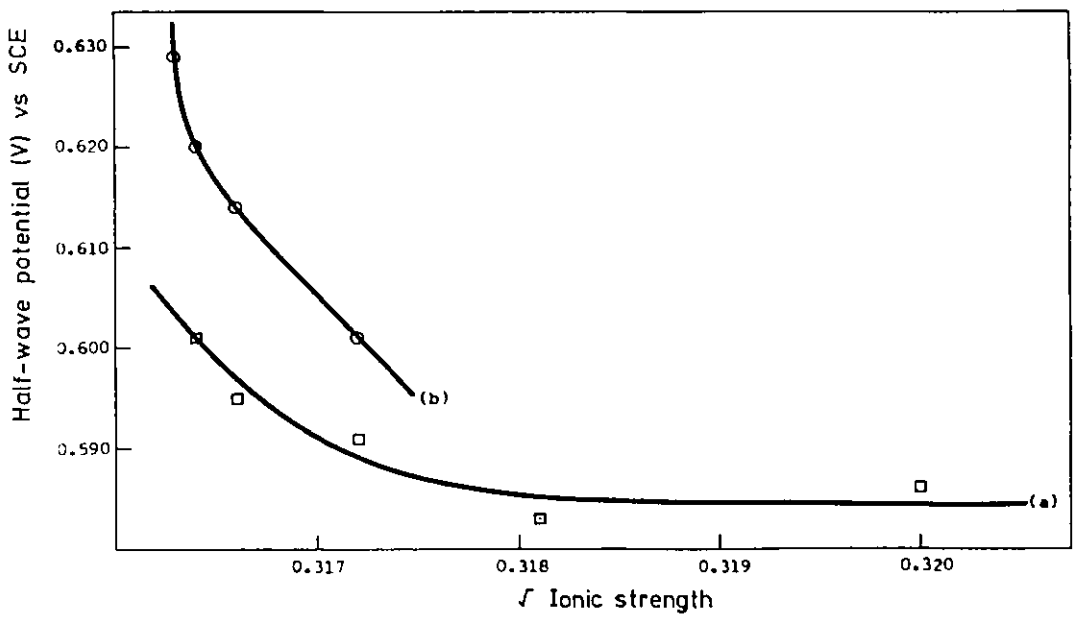

Fig. 5-44 Ir(IV)-Ir(III) Chloroiridate/Perchloric acid supporting electrolyte System: Values of half-wave potential as a function of square root of total ionic strength (where the concentration of ammonium hexachloroiridate was varied). Boron carbide solid electrode was treated by cathodic polarisation (at -1 V) in: (a) Sample solution prior to voltammetric scan. (b) More concentrated (2.0×10^{-3} M) ammonium hexachloroiridate solution.

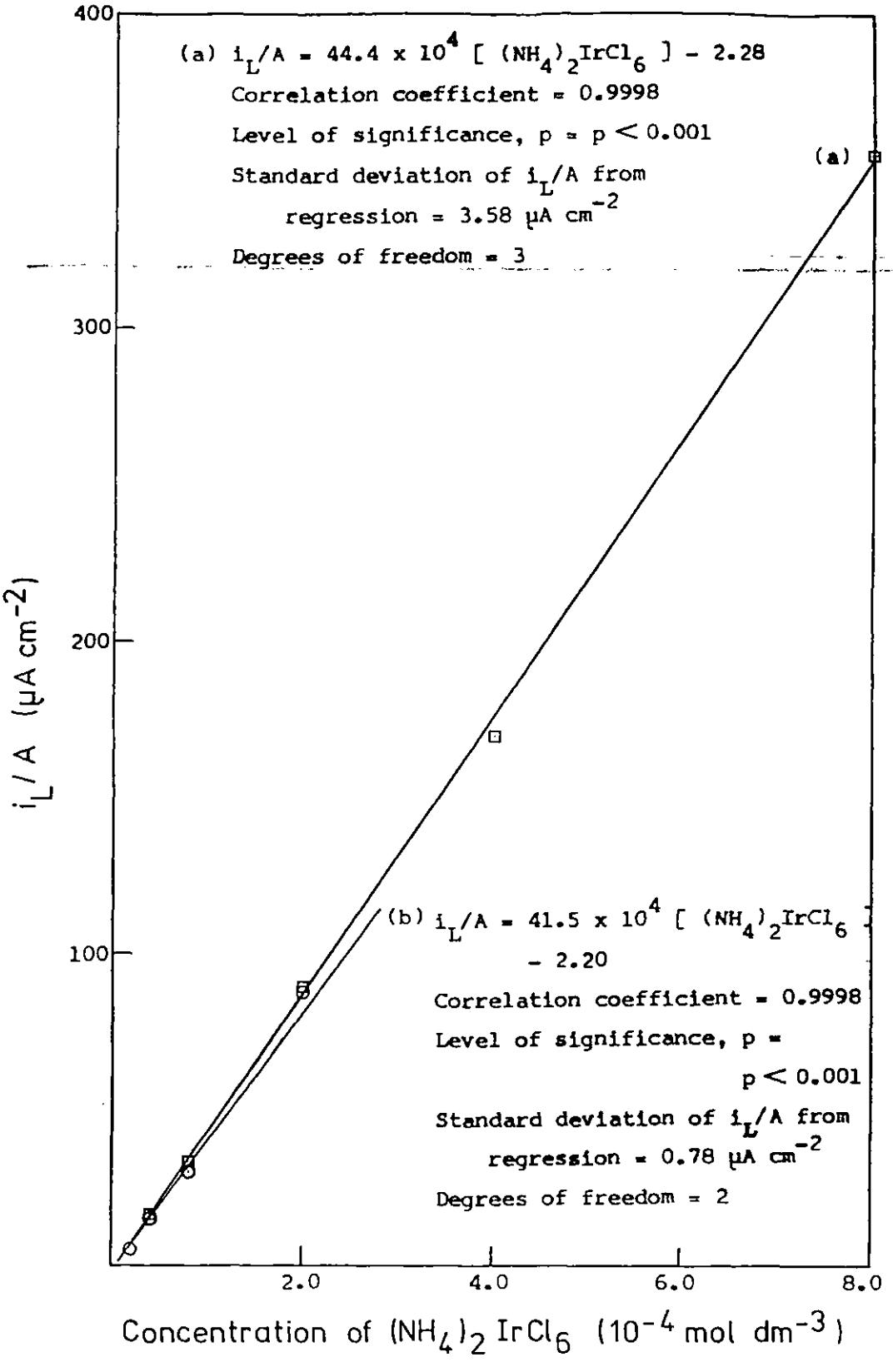

Fig. 5-45 Ir(IV)-Ir(III) Chloroiridate/Perchloric acid supporting electrolyte System: Dependence of limiting current per unit area, i_L/A, on concentration of ammonium hexachloroiridate. Boron carbide solid electrode was treated by cathodic polarisation (at -1 V) in: (a) Sample solution prior to voltammetric scan. (b) More concentrated (2.0×10^{-3} M) ammonium hexachloroiridate solution (-⊖-).

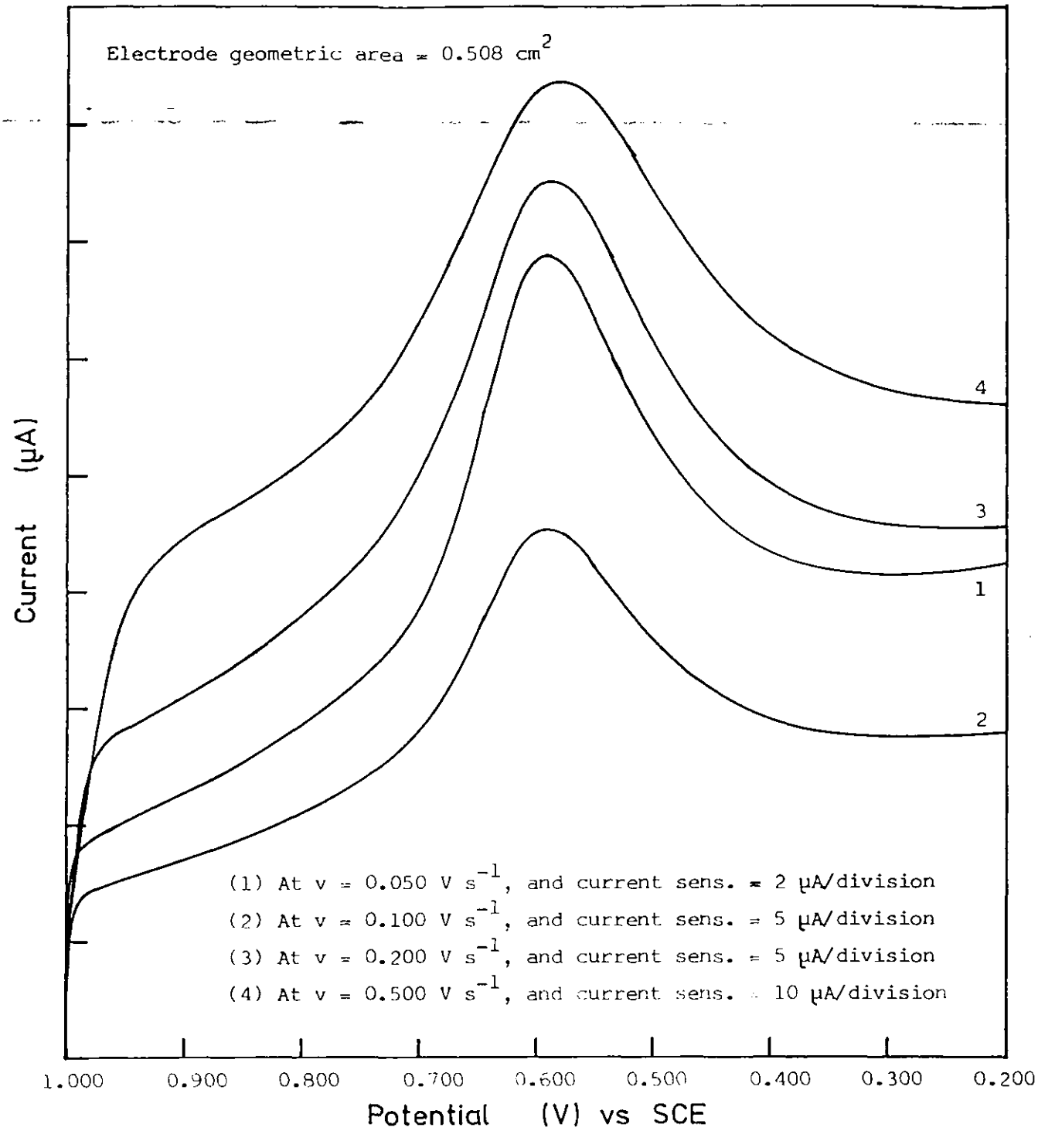

Fig. 5-46 Ir(IV)-Ir(III) Chloroiridate (8.0×10^{-5} mol dm^{-3})/Perchloric acid (0.1 M) supporting electrolyte System: Linear sweep voltammograms at the boron carbide solid electrode which had been treated by cathodic polarisation (at -1 V) in chloroiridate (8.0×10^{-4} M) solution.

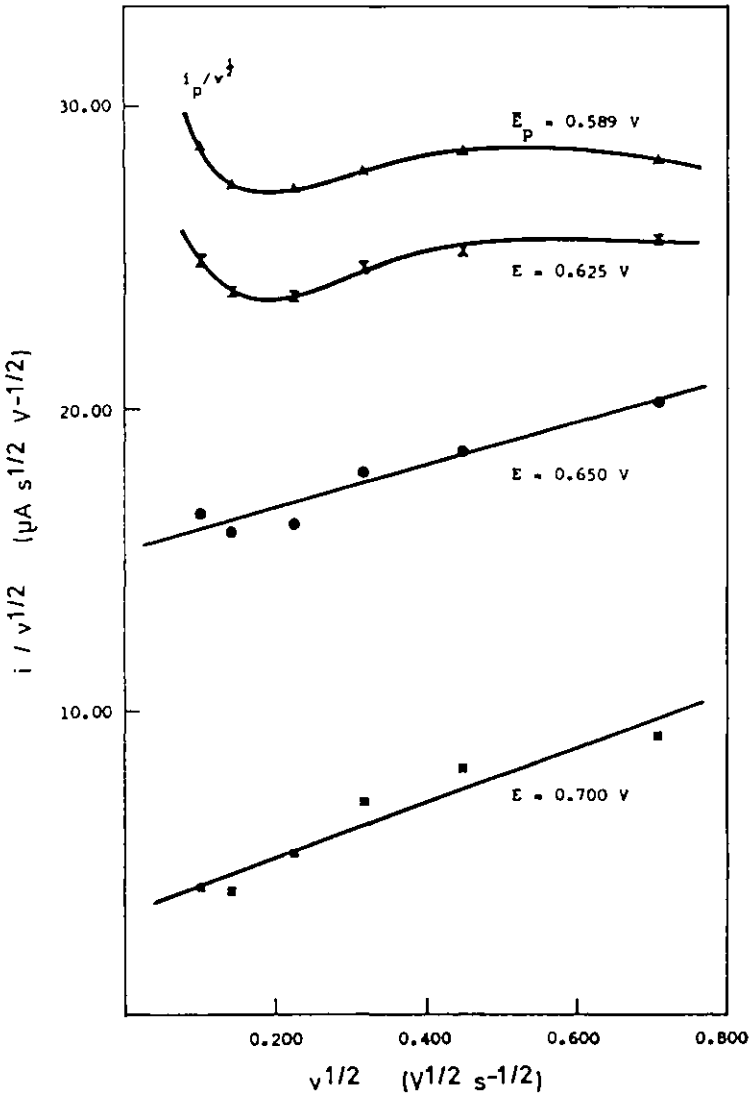

Fig. 5-47 Ir(IV)-Ir(III) Chloroiridate (8.0×10^{-5} mol dm^{-3})/Perchloric acid (0.1 M) supporting electrolyte: Values of current function, $i/v^{\frac{1}{2}}$ (at different potentials along the peak voltammograms), as a function of square root of potential scan rate, $v^{\frac{1}{2}}$. Boron carbide solid electrode was treated by cathodic polarisation (at -1 V) in ammonium hexachloroiridate (8.0×10^{-4} mol dm^{-3}).

Fig. 5-47 (continued):-

(a) At E = 0.700 V:

$i/v^{\frac{1}{2}} = 3.39 + 9.02\ v^{\frac{1}{2}}$

Correlation coefficient = 0.9617

Level of significance, $p = 0.001 < p < 0.01$

Standard deviation of $i/v^{\frac{1}{2}}$ from regression = 0.65 μA $s^{\frac{1}{2}}\ V^{-\frac{1}{2}}$

Degrees of freedom = 4

(b) At E = 0.650 V:

$i/v^{\frac{1}{2}} = 15.3 + 7.10\ v^{\frac{1}{2}}$

Correlation coefficient = 0.9597

Level of significance, $p = 0.001 < p < 0.01$

Standard deviation of $i/v^{\frac{1}{2}}$ from regression = 0.53 μA $s^{\frac{1}{2}}\ V^{-\frac{1}{2}}$

Degrees of freedom = 4

(c) At E = 0.625 V:

$i/v^{\frac{1}{2}}$ mean = 24.71 μA $s^{\frac{1}{2}}\ V^{-\frac{1}{2}}$

Standard deviation = 0.73 μA $s^{\frac{1}{2}}\ V^{-\frac{1}{2}}$

Degrees of freedom = 5

(d) At peak potential (mean value), $\bar{E}_p$ = 0.589 V:

$i_p/v^{\frac{1}{2}}$ mean = 28.01 μA $s^{\frac{1}{2}}\ V^{-\frac{1}{2}}$

Standard deviation = 0.59 μA $s^{\frac{1}{2}}\ V^{-\frac{1}{2}}$

Degrees of freedom = 5

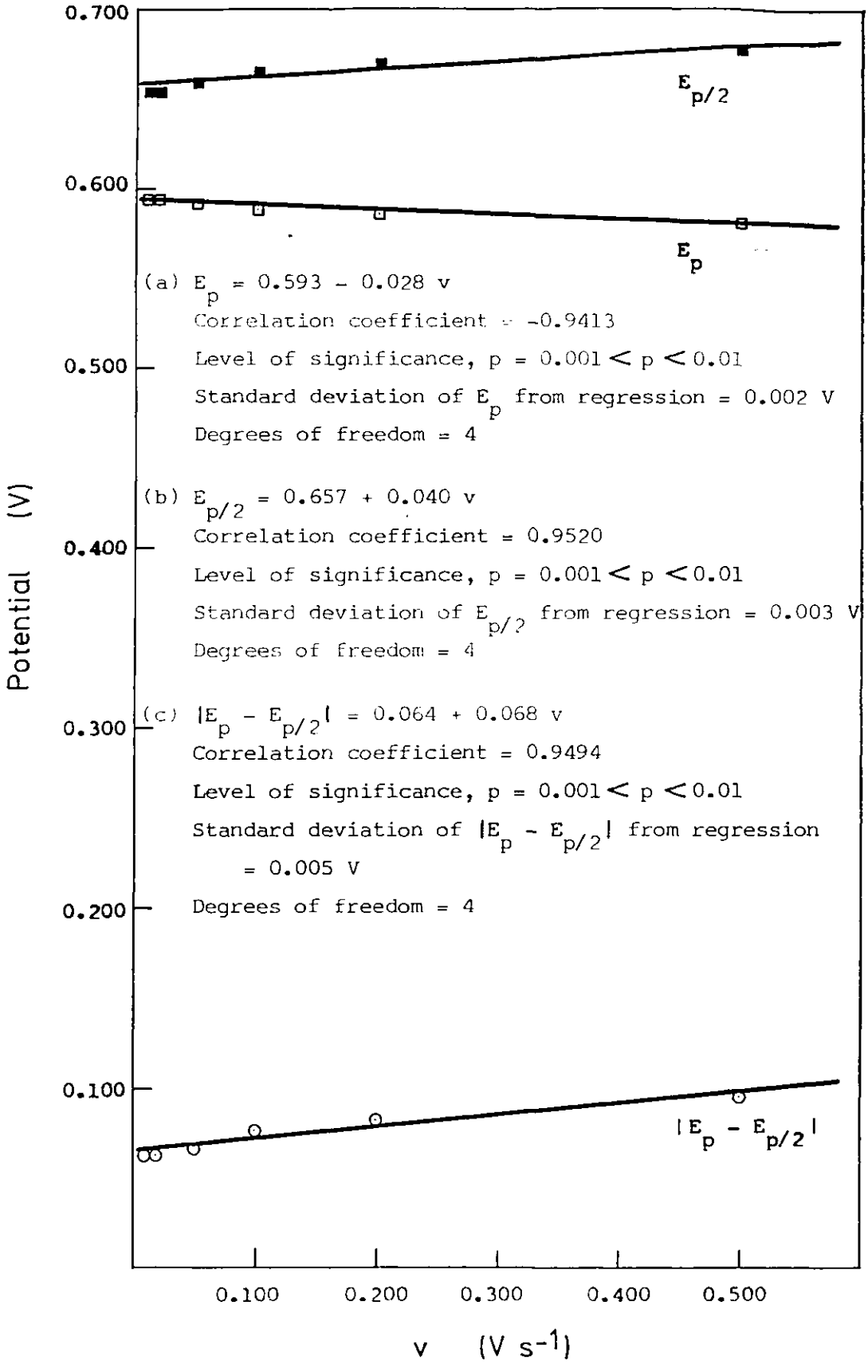

Fig. 5-48 **Ir(IV)-Ir(III) Chloroiridate (8.0 x 10^{-5} mol dm^{-3})/Perchloric acid (0.1 M) supporting electrolyte: Values of peak potential, E_p, half-peak potential, $E_{p/2}$, and absolute difference between peak potential and half-peak potential, $|E_p - E_{p/2}|$, as a function of potential scan rate, v.** Boron carbide solid electrode was treated by cathodic polarisation (at -1 V) in ammonium hexachloroiridate (8.0 x 10^{-4} mol dm^{-3}).

5-1.1.(v) Graphite solid electrode.

Typical d.c. voltammograms for the reduction of chloroiridate (Fig. 5-49) showed a reversible one-electron charge transfer reaction at the graphite solid electrode. The residual current density, however, was larger than that obtained at the boron carbide electrode (Fig. 5-14, a); especially at potentials less anodic than 0.5 V (vs. SCE). Results (Table 5-7) obtained in chloroiridate (1.0×10^{-4} mol dm^{-3}) gave mean values of $\alpha n = 1.11 \pm 0.07$ (10 degrees of freedom) and $E_{\frac{1}{2}} = 0.624$ V (vs. SCE) $\pm$ 0.007 V (10 degrees of freedom).

In linear sweep voltammetry (Fig. 5-50) the peak for the chloroiridate reduction was much smaller than that of the residual current. The cathodic peak current function increased with increasing sweep rate (Fig. 5-51, a); which is characteristic of an adsorbed species. When the electrode was treated with Ir(IV) perchlorate solution the adsorption of chloroiridate was rendered weaker; as reflected in the peaking of the current function at the higher sweep rates (Fig. 5-51, b). The chloroiridate peak potential obtained at the graphite electrode without and with Ir(IV) perchlorate treatment were similar (Fig. 5-52, a, b) and shifted cathodically with increasing sweep rates. Since the value of the difference between peak and half-peak potential (Fig. 5-52, c, d) was close to that for a reversible one-electron charge transfer (equation 3-32) and was not affected by the sweep rates that were applied, this cathodic shift in peak potential signified a weakly adsorbed oxidant (Fig. 3-16).

The peak of the residual current also involved adsorption.

5-1.1.(vi) Summary.

Voltammetry at boron carbide solid electrodes for the charge transfer reaction

$$IrCl_6^{2-} + e^- \rightleftharpoons IrCl_6^{3-}$$

in perchloric acid supporting electrolyte was not reversible (section 5-1.1.(i)). Linear correlations, however, were found between increasing αn value and increasing weight per cent carbon (Fig. 5-1) or decreasing B:C ratio (Fig. 5-2) of the working electrode. Attempts to improve the voltammetric performance of the electrode by carbon enrichment of the electrode surface or by fabrication of boron carbide/carbon composite solid electrodes resulted only in qualified success. Although the better αn values obtained at carbon-rich electrodes confirmed the

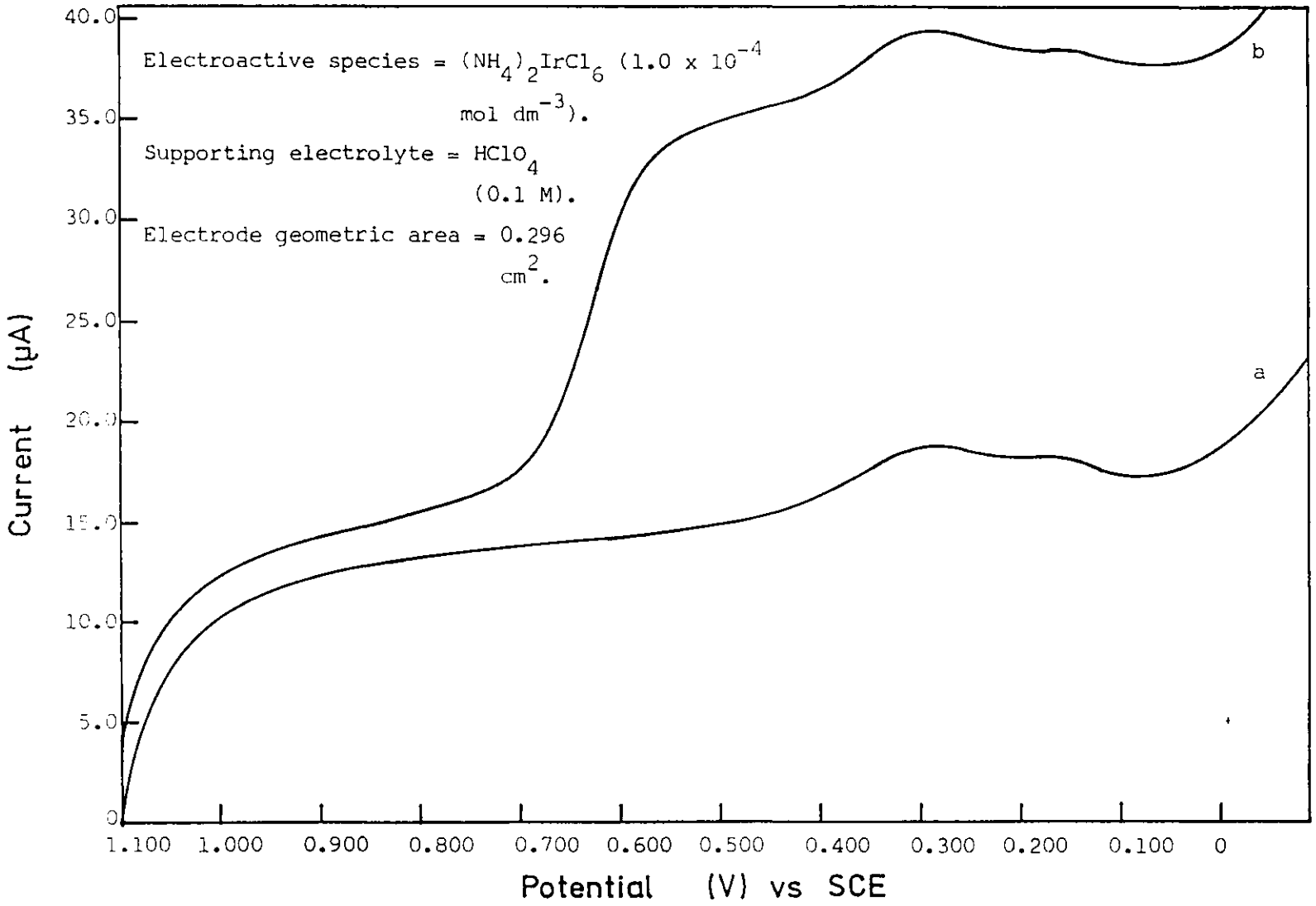

Fig. 5-49 Graphite solid electrode. (a) Residual current. (b) D.c. voltammogram of the reduction of chloroiridate.

Table 5-7 Ir(IV)-Ir(III) Chloroiridate/Perchloric acid supporting electrolyte System: D. C. Voltammetric Performance of Graphite Solid Electrode.

Electroactive species = $(NH_4)_2IrCl_6$ (1.0×10^{-4} mol dm^{-3}) Supporting electrolyte = $HClO_4$ (0.1 M)

Result number	αn	$E_{\frac{1}{2}}$ (V)	i_L / AC (10^4 μA cm^{-2} dm^3 mol^{-1})
1	1.11	0.630	51.6
2	1.28	0.638	49.4
3	1.09	0.625	52.6
4	1.02	0.614	47.3
5	1.11	0.621	46.4
6	1.10	0.628	47.3
7	1.11	0.622	46.1
8	1.11	0.620	44.1
9	1.03	0.617	46.4
10	1.09	0.620	43.1
11	1.11	0.622	42.7
Mean value	1.11	0.624	47.0
Standard deviation	0.07	0.007	3.19
Degrees of freedom	10	10	10

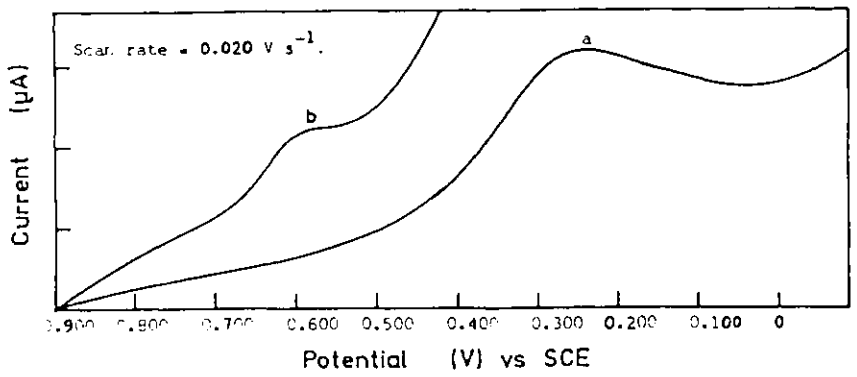

Fig. 5-50 Ir(IV)-Ir(III) Chloroiridate (1.0 x 10^{-4} mol dm^{-3})/Perchloric acid (0.1 M) supporting electrolyte System: Linear sweep voltammetry at the graphite solid electrode. (a) Residual current at current sensitivity = 20 μA/division. (b) Chloroiridate reduction at current sensitivity = 10 μA/division. Electrode geometric area = 0.296 cm^2.

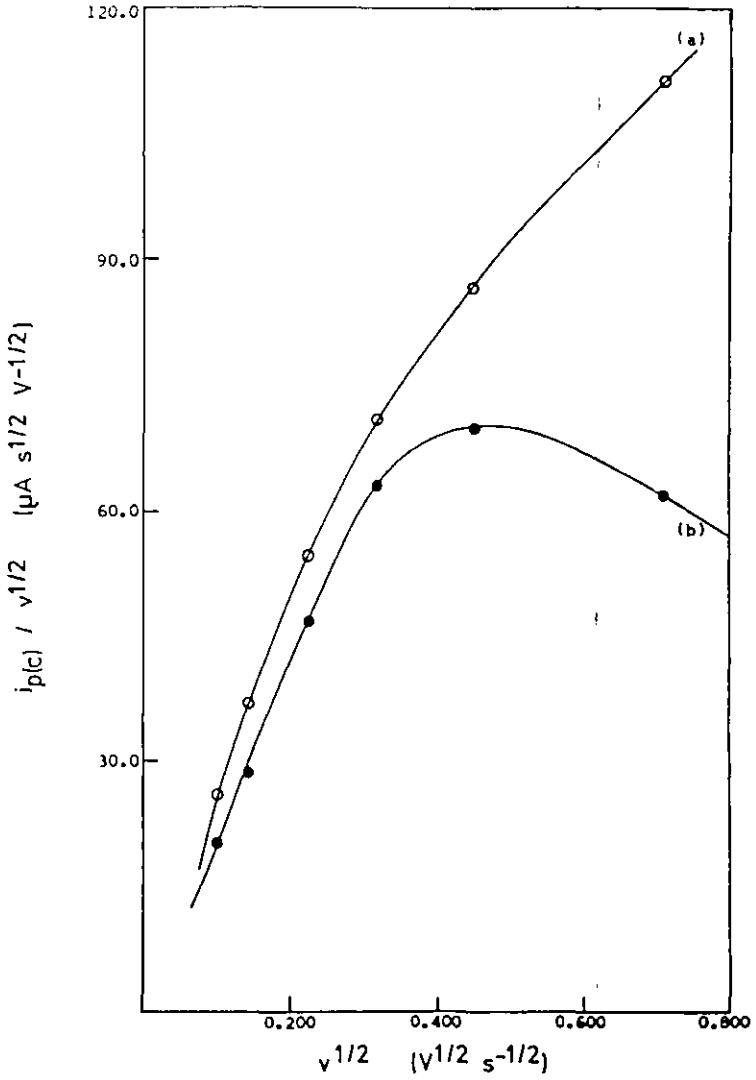

Fig. 5-51 Ir(IV)-Ir(III) Chloroiridate (1.0 x 10^{-4} mol dm^{-3})/Perchloric acid (0.1 M) supporting electrolyte System: Values of cathodic peak current function, $i_{p(c)}/v^{\frac{1}{2}}$, as a function of square root of potential scan rate, $v^{\frac{1}{2}}$. Graphite solid electrode was: (a) polished on hard filter paper, and (b) treated with Ir(IV) Perchlorate

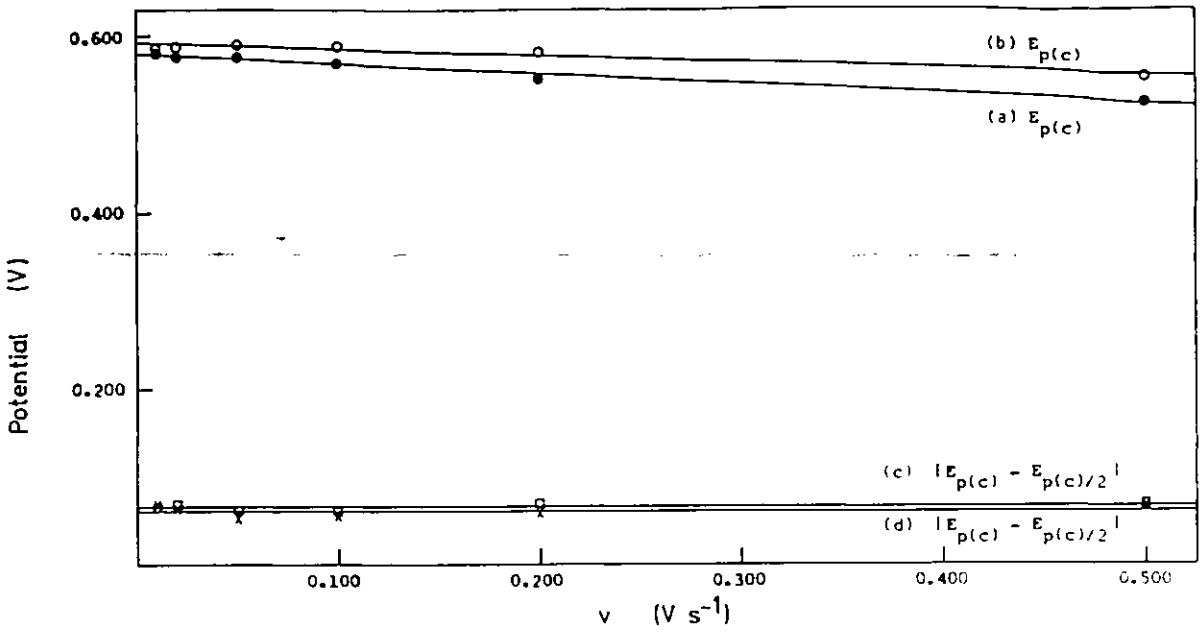

Fig. 5-52 Ir(IV)-Ir(III) Chloroiridate (1.0×10^{-4} mol dm^{-3})/Perchloric acid (0.1 M) supporting electrolyte System: Values of cathodic peak potential, $E_{p(c)}$, and difference between cathodic peak and half-peak potentials, $|E_{p(c)} - E_{p(c)/2}|$, as a function of potential scan rate, v. Graphite solid electrode was: (i) polished on hard filter paper (⊖ and —⊖—), and (ii) treated with Ir(IV) Perchlorate (2.3×10^{-3} M) solution (⊖ and —×—).

(a) $E_{p(c)} = 0.578 - 0.111\ v$
Correlation coefficient = -0.9873
Level of significance, p = $p < 0.001$
Standard deviation of $E_{p(c)}$ from regression = 0.004 V
Degrees of freedom = 4

(b) $E_{p(c)} = 0.590 - 6.90 \times 10^{-2}\ v$
Correlation coefficient = -0.9620
Level of significance, p = $0.001 < p < 0.01$
Standard deviation of $E_{p(c)}$ from regression = 0.004 V
Degrees of freedom = 4

(c) $|E_{p(c)} - E_{p(c)/2}|$ mean = 0.065 V
Standard deviation = 0.004 V
Degrees of freedom = 5

(d) $|E_{p(c)} - E_{p(c)/2}|$ mean = 0.060 V
Standard deviation = 0.007 V
Degrees of freedom = 5

trends of Figures 5-1 and 5-2, the αn value of unity for a reversible charge transfer was still unattainable; the best αn value obtained being below 0.80.

Of the other electrode treatments (sections 5-1.1.(ii), (iii), and (iv)) only treatment with Ir(IV) perchlorate solution and the electrochemical treatment resulted in qualified success. Although electrochemical treatment of the boron carbide solid electrode improved the voltammetric performance (section 5-1.1.(iv), Figures 5-42 and 5-43) as characterised by αn values close to unity, the αn values rapidly deteriorated with increasing chloroiridate concentration. Results of linear sweep voltammetry of chloroiridate (8.0×10^{-5} mol dm^{-3}) at the electrochemically treated electrode indicated that the charge transfer was quasi-reversible and complicated by a catalytic reaction and the weak adsorption of product.

Only the treatment of boron carbide solid electrode with Ir(IV) perchlorate solution (section 5-1.1.(iii)) resulted in consistently reasonable αn values over a concentration range of chloroiridate (1.0×10^{-5} to 1.0×10^{-3} mol dm^{-3}) in perchloric acid (0.1 M) supporting electrolyte; with αn approaching the theoretical unity value at the lower end of the concentration range. The grand mean values obtained were $\alpha n = 0.87 \pm 3.3 \times 10^{-2}$ (63 degrees of freedom) and $E_{\frac{1}{2}} = 0.607$ V (vs. SCE) $\pm 2.33 \times 10^{-3}$V (63 degrees of freedom). The linear concentration dependence of the limiting current was statistically better than at the 0.001 level of significance.

It was also shown that the improvement in electrode performance after treatment with Ir(IV) perchlorate solution was due to strongly adsorbed species from the treatment solution. Furthermore, the chloroiridate reactant was also shown to be weakly adsorbed and the product strongly adsorbed on the treated electrode. Therefore, a possible explanation for the improved reversibility of the chloroiridate charge transfer is that the chloroiridate and chloroiridite anions were preferentially chemisorbed on the adsorbed Ir(IV) perchlorate cations which facilitated the electron transfer. The presence of adsorption, however, confines the quantitative usefulness of the treated electrode to d.c. voltammetry; where the slow scan rates employed will minimise any distortions in the voltammograms caused by adsorption effects.

Boron carbide/carbon composite and boron carbide solid electrodes were similarly affected by the Ir(IV) perchlorate treatment solution irrespective of their chemical compositions (Figures 5-11 to 5-13).

The adsorption of Ir(IV) perchlorate was practically instantaneous on contact. Grand mean values obtained for chloroiridate (1.0×10^{-4} mol dm^{-3}) in perchloric acid (0.1 M) were $\alpha n = 0.92 \pm 0.04$ (29 degrees of freedom), and $E_{\frac{1}{2}} = 0.604$ V (vs. SCE) $\pm$ 0.007 V (29 degrees of freedom).

Voltammetry at the graphite solid electrode in chloroiridate (1.0×10^{-4} mol dm^{-3}) was reversible, but the residual current was much larger than that obtained at boron carbide electrodes and interfered at potentials less anodic than 0.5 V (vs. SCE). Furthermore, the chloroiridate curve and the residual current curve were both affected by the presence of adsorption; the latter being worse affected. Therefore the graphite solid electrode can be useful only in d.c. voltammetry ; where the adsorption effects will be minimised. The voltammetric data obtained for chloroiridate (1.0×10^{-4} mol dm^{-3}) in perchloric acid (0.1 M) were αn mean = 1.11 $\pm$ 0.07 (10 degrees of freedom) and $E_{\frac{1}{2}}$ mean = 0.624 V (vs. SCE) $\pm$ 0.007 V (10 degrees of freedom).

5-1.2 Chloroiridate-chloroiridite in hydrochloric acid supporting electrolyte system

5-1.2.(i) Effect of electrode composition on voltammetric properties.

Linear correlations (Fig. 5-53) were found between increasing αn values and increasing weight per cent carbon composition or decreasing boron:carbon ratio. The charge transfer for the electro-reduction

$$IrCl_6^{2-} + e^- \rightleftharpoons IrCl_6^{3-}$$

in hydrochloric acid (0.1 M) supporting electrolyte was reversible at the electrode with a B:C ratio of 2.56. The half-wave potential, however, increased sharply to a plateau of 0.630 V (vs. SCE) $\pm$ 0.003 V (15 degrees of freedom) at higher carbon contents or lower B:C ratios (Fig. 5-54). Linear dependence of the limiting current on the concentration of chloroiridate was obtained irrespective of the electrode composition (Table 5-8).

5-1.2.(ii) Effects of Ir(IV) perchlorate treatment and electrochemical treatment on the boron carbide solid electrode.

The charge-transfer reaction for chloroiridate was greatly improved when the boron carbide electrode was treated with Ir(IV) perchlorate solution (Fig. 5-55) or was cathodically polarised in chloroiridate solution (Fig. 5-56).

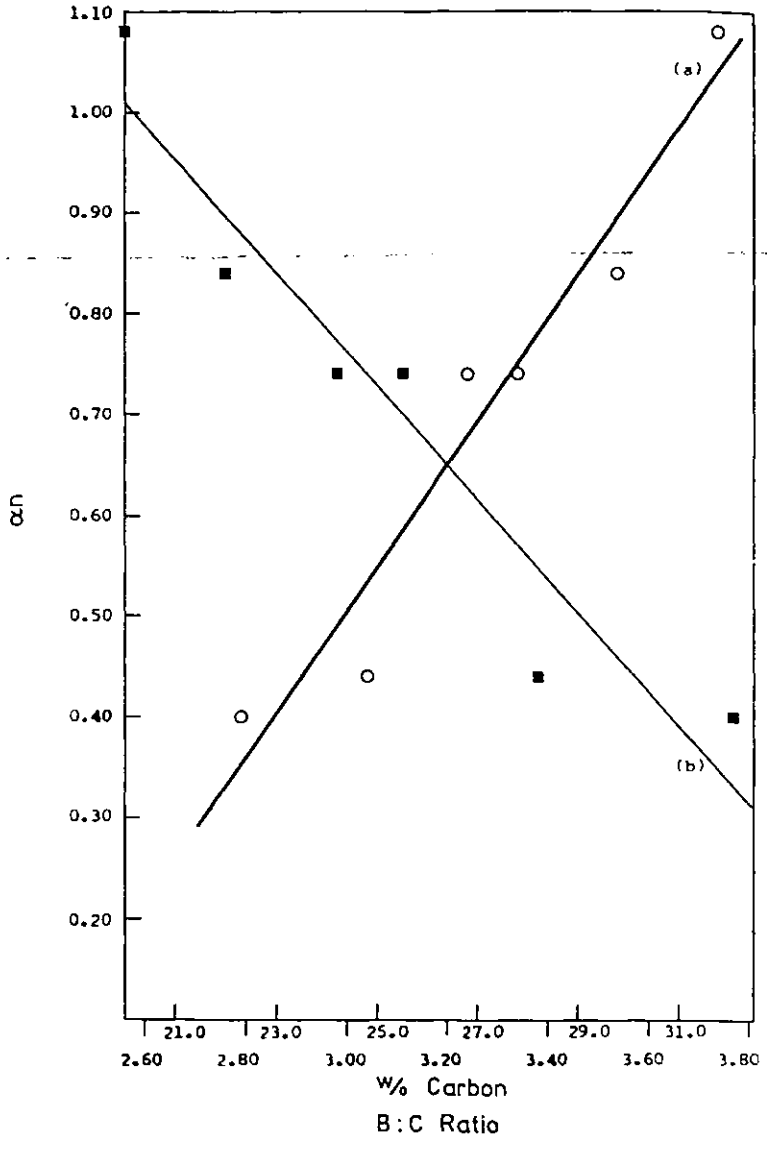

Fig. 5-53 Ir(IV)-Ir(III) Chloroiridate/Hydrochloric acid supporting electrolyte System: Values of αn for electrochemical reduction as a function of (a) weight per cent carbon (-⊖-), and (b) boron to carbon ratio (-■-) of boron carbide/carbon composite solid electrodes.

(a) $\alpha n = 7.24 \times 10^{-2}$ (w% C) - 1.26
Correlation coefficient = 0.9694
Level of significance, $p = 0.001 < p < 0.01$
Standard deviation of αn from regression = 0.07
Degrees of freedom = 4

(b) αn = 2.44 - 0.559 (B:C)
Correlation coefficient = -0.9565
Level of significance, $p = 0.001 < p < 0.01$
Standard deviation of αn from regression = 0.08
Degrees of freedom = 4

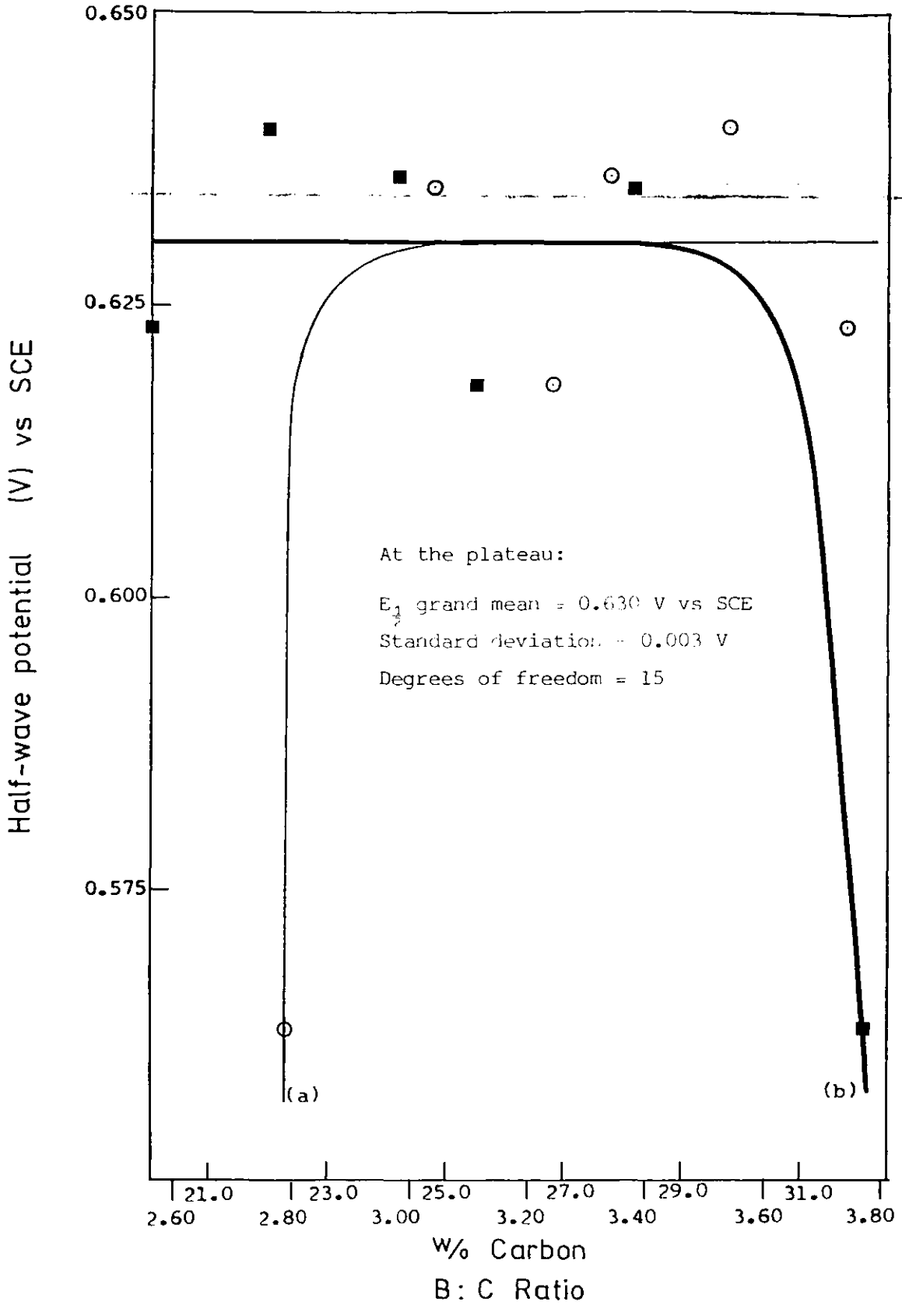

Fig. 5-54 **Ir(IV)-Ir(III) Chloroiridate/Hydrochloric acid supporting electrolyte System: Values of half-wave potential, $E_{\frac{1}{2}}$, as a function of (a) weight per cent carbon (-O-), and (b) boron to carbon ratio (-■-) of boron carbide/carbon composite solid electrodes.**

Table 5-8 Ir(IV)-Ir(III) Chloroiridate/Hydrochloric acid supporting electrolyte System: Values of Limiting Current per unit Area as a function of Concentration of Ammonium Hexachloroiridate obtained at Boron Carbide/Carbon Composite Solid Electrodes.

Electroactive species = $(NH_4)_2IrCl_6$ (1.0×10^{-4} to 4.0×10^{-4} mol dm^{-3})
Supporting electrolyte = HCl (0.1 M)

w% Carbon composition	Final Boron:Carbon ratio	i_L / AC (10^4 μA cm^{-2} dm^3 mol^{-1}), linearly regressed slope. Correlation coefficient	Level of significance, p
22.3	3.77	27.1	0.9957	$0.001 < p < 0.01$
24.8	3.38	19.8	0.9944	$0.001 < p < 0.01$
26.8	3.11	14.8	0.9832	$0.01 < p < 0.02$
27.8	2.98	27.2	0.9984	$0.001 < p < 0.01$
29.8	2.76	18.6	0.9876	$0.01 < p < 0.02$
31.8	2.56	26.1	0.9958	$0.001 < p < 0.01$

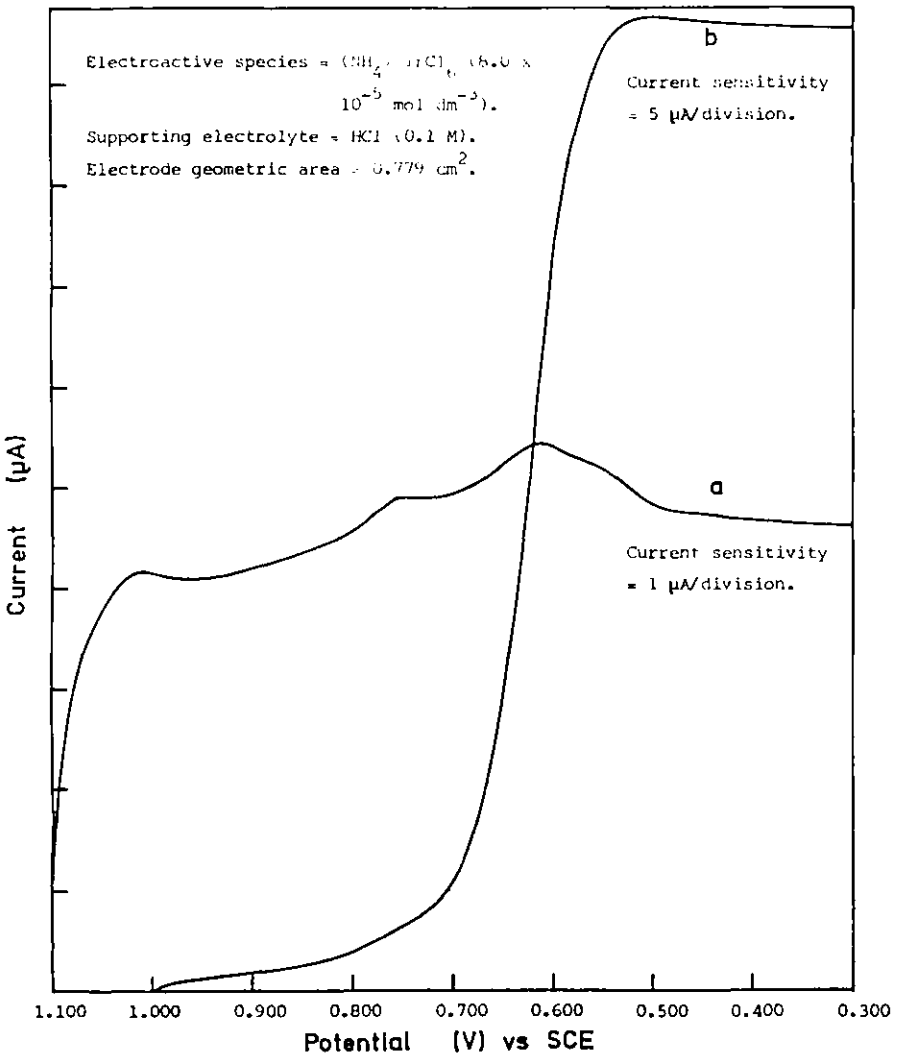

Fig. 5-55 Boron carbide solid electrode treated with Ir(IV) perchlorate (1.0×10^{-3} M) solution. (a) Residual current. (b) D.c. voltammogram of the reduction of chloroiridate.

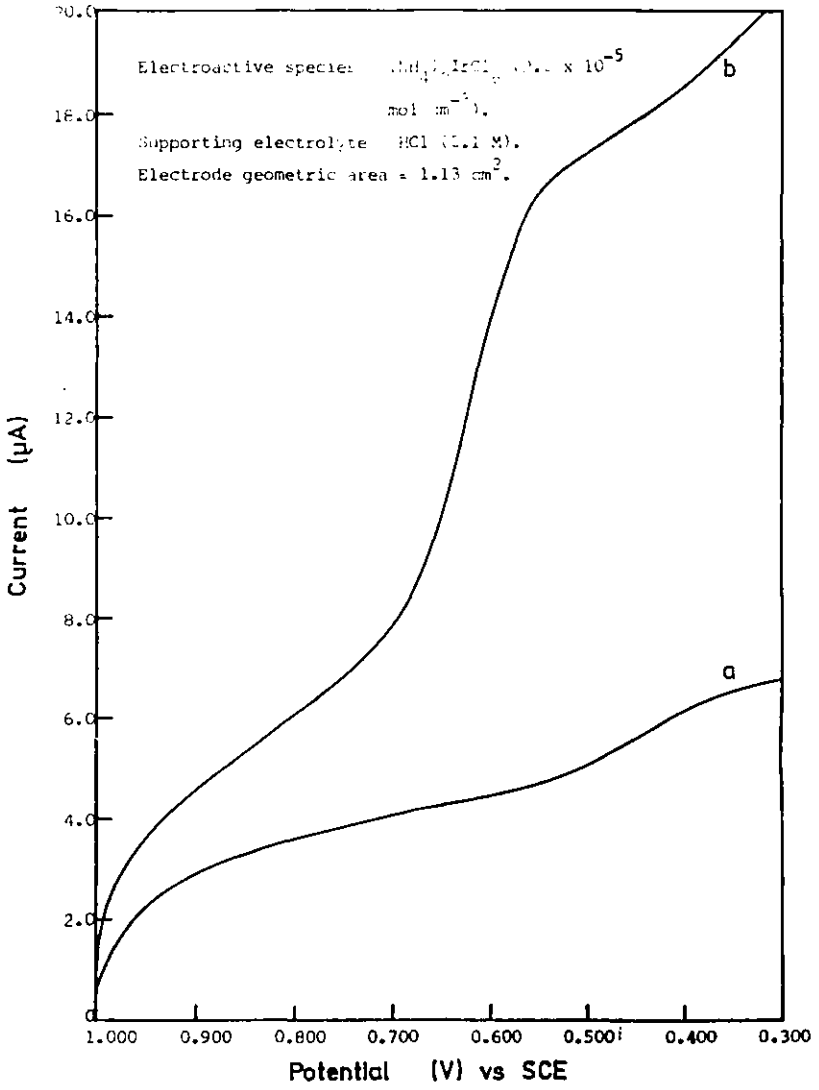

Fig. 5-56 Boron carbide solid electrode treated by cathodic polarisation (at -4 V vs SCE). (a) Residual current. (b) D.c. voltammogram of the reduction of chloroiridate after cathodic polarisation in chloroiridate (8.0×10^{-4} M).

The αn value for the charge transfer declined, with increasing chloroiridate concentration, from that close to unity for a reversible reduction to much lower values for an irreversible reduction (Fig. 5-57). The decline in αn value was steeper at the electrochemically treated electrode than at the Ir(IV) perchlorate treated electrode. Similarly, the half-wave potential shifted cathodically with increasing $(\text{ionic strength})^{\frac{1}{2}}$; when the chloroiridate concentration was increased (Fig. 5-58).

Both methods of electrode treatment showed a linear dependence of limiting current on the concentration of chloroiridate (Fig. 5-59).

The concentration (0.1 to 2.0 M) of hydrochloric acid supporting electrolyte had little effect on αn for the electro-reduction of chloroiridate (1.0×10^{-4} mol dm^{-3}) at the Ir(IV) perchlorate treated boron carbide solid electrode (Fig. 5-60). However, as expected, the increasing ionic strength caused the half-wave potential to shift anodically; thus signifying that the e.a.s. was anionic (Fig. 5-61 and equation 3-10). The limiting current for the reduction of chloroiridate decreased with increasing concentration of hydrochloric acid supporting electrolyte (Fig. 5-62).

Typical linear sweep voltammograms for the residual current and electro-reduction of chloroiridate at the Ir(IV) perchlorate treated boron carbide solid electrode are presented in Fig. 5-63. Plots of residual peak current functions against $(\text{sweep rate})^{\frac{1}{2}}$ indicate that the peaks were complicated by adsorption (Fig. 5-64); Peak 3 being more affected than Peaks 1 and 2. The peak potential of Peaks 1 and 3 shifted cathodically with increasing sweep rate whereas the peak potential of Peak 2 remained relatively constant (Fig. 5-65). Peak 1, however, was not defined at the higher sweep rates; suggesting that it was a diffusion peak which disappeared at the higher sweep rates. The reversibility of charge transfer for all three peaks was reduced at faster sweep rates (Fig. 5-66); as signified by increasing values of $|E_p - E_{p/2}|$ and the disappearance of Peak 1 (although the trend of $|E_{p(1)} - E_{p(1)/2}|$ is anomalous).

For the case of chloroiridate reduction at the Ir(IV) perchlorate treated boron carbide electrode, the increasing trend of peak current functions with increasing $(\text{sweep rate})^{\frac{1}{2}}$ signified the presence of adsorption (Figures 5-67 and 5-68). The adsorption at Peak 1, however, was stronger than at Peak 2 where the peak current function began to

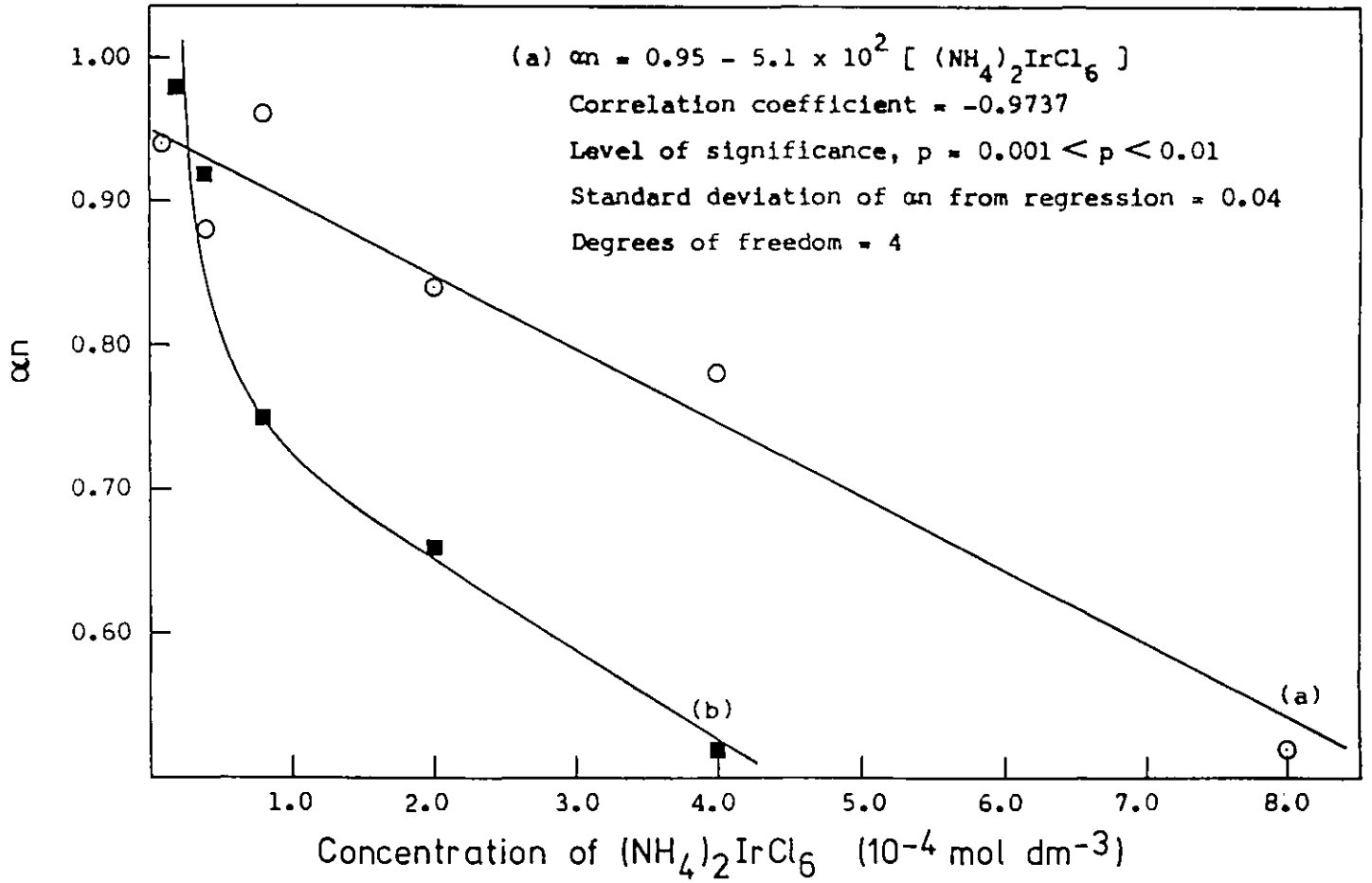

Fig. 5-57 **Ir(IV)-Ir(III) Chloroiridate/Hydrochloric acid supporting electrolyte System: Values of αn as a function of concentration of ammonium hexachloroiridate. Boron carbide solid electrode was treated: (a) With Ir(IV) Perchlorate (1.0×10^{-3} M) solution (-⊖-). (b) By cathodic polarisation (at -4 V) in ammonium hexachloroiridate (8.0×10^{-4} M) solution (-■-).**

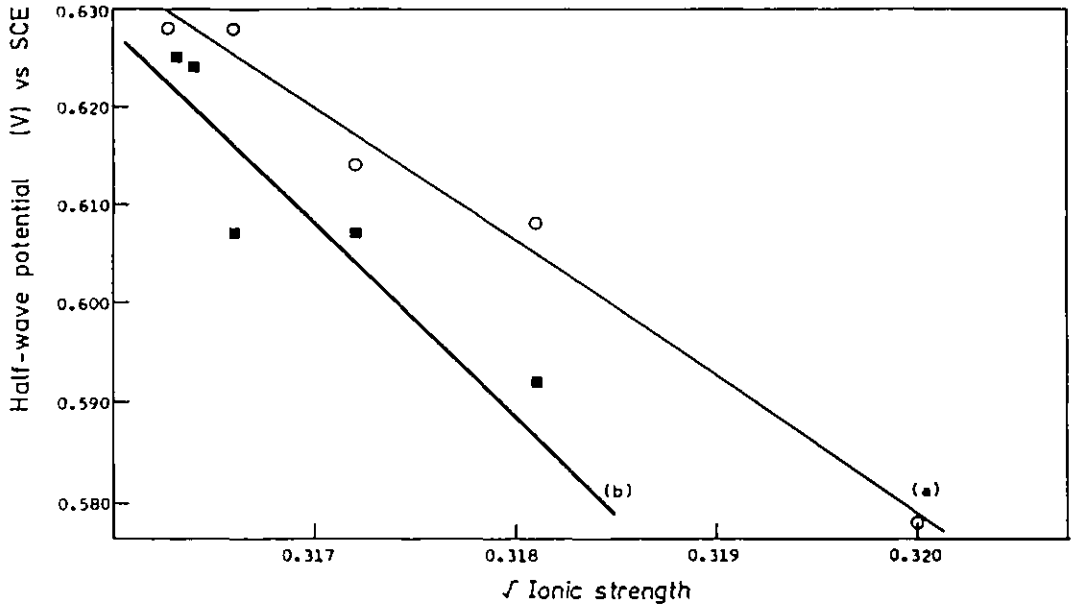

Fig. 5-58 Ir(IV)-Ir(III) Chloroiridate/Hydrochloric acid supporting electrolyte System: Values of half-wave potential as a function of square root of total ionic strength (where the concentration of ammonium hexachloroiridate was varied), $\sqrt{I}$. Boron carbide solid electrode was treated: (a) With Ir(IV) perchlorate (1.0×10^{-3} M) solution (—O—). (b) By cathodic polarisation (at -4 V) in ammonium hexachloroiridate (8.0×10^{-4} M) solution (—■—).

(a) $E_{\frac{1}{2}} = 4.92 - 13.6\ \sqrt{I}$

Correlation coefficient = -0.9895

Level of significance, $p = 0.001 < p < 0.01$

Standard deviation of $E_{\frac{1}{2}}$ from regression = 0.003 V

Degrees of freedom = 3

(b) $E_{\frac{1}{2}} = 6.83 - 19.6\ \sqrt{I}$

Correlation coefficient = -0.9384

Level of significance, $p = 0.01 < p < 0.02$

Standard deviation of $E_{\frac{1}{2}}$ from regression = 0.006 V

Degrees of freedom = 3

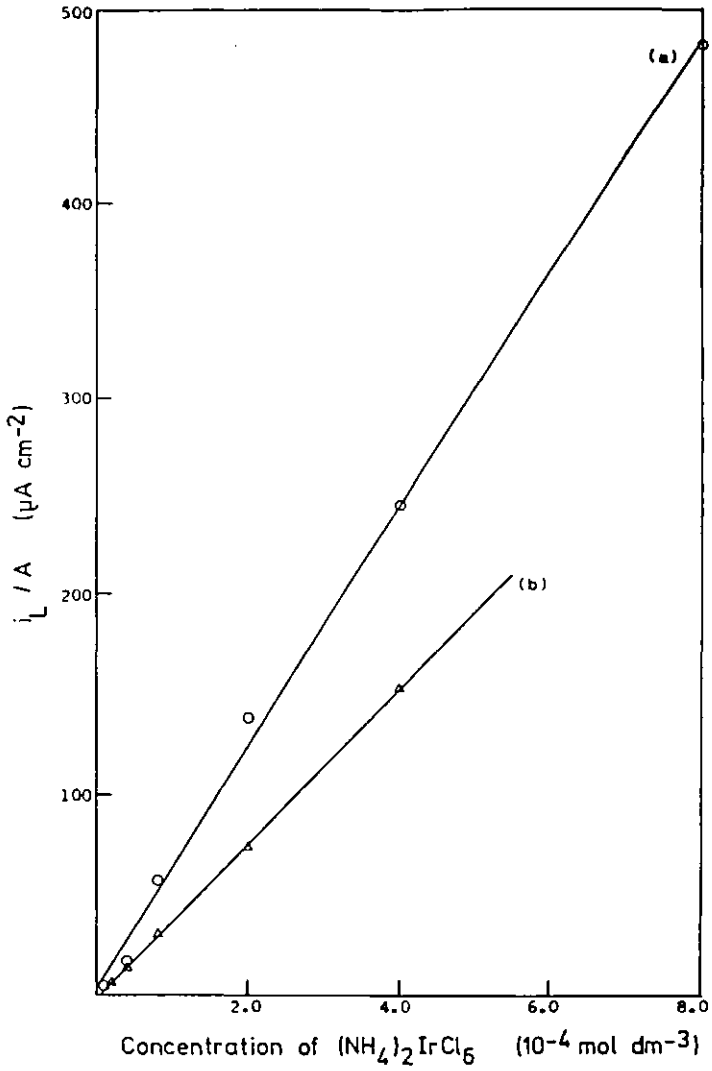

Fig. 5-59 **Ir(IV)-Ir(III) Chloroiridate/Hydrochloric acid supporting electrolyte System: Dependence of limiting current per unit area, i_L/A, on the concentration of ammonium hexachloroiridate. Boron carbide solid electrode was treated: (a) With Ir(IV) Perchlorate (1.0×10^{-3} M) solution (-⊖-). (b) By cathodic polarisation (at -4 V) in ammonium hexachloroiridate (8.0×10^{-4} M) solution (-⊖-).**

(a) $i_L/A = 4.08 + 6.01 \times 10^5 [(NH_4)_2IrCl_6]$
Correlation coefficient = 0.9989
Level of significance, p = $p < 0.001$
Standard deviation of i_L/A from regression = 9.67 μA cm^{-2}
Degrees of freedom = 4

(b) $i_L/A = 3.83 \times 10^5 [(NH_4)_2IrCl_6] - 1.19$
Correlation coefficient = 0.9999
Level of significance, p = $p < 0.001$
Standard deviation of i_L/A from regression = 1.18 μA cm^{-2}
Degrees of freedom = 3

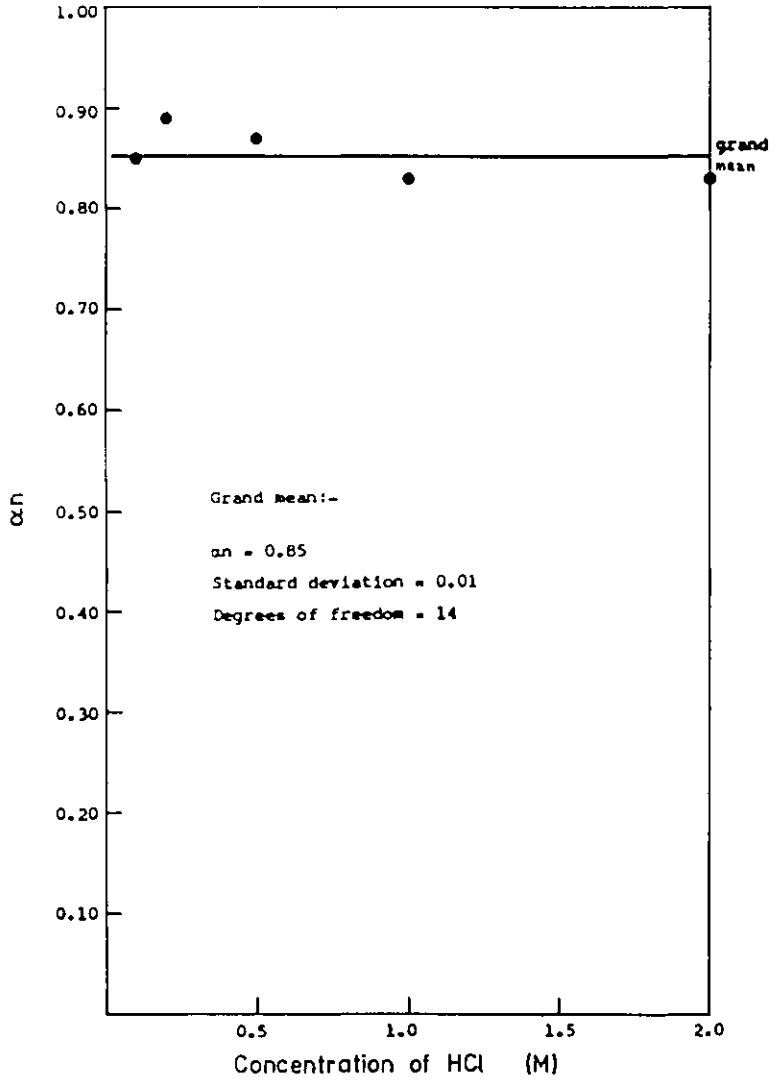

Fig. 5-60 Ir(IV)-Ir(III) Chloroiridate/Hydrochloric acid supporting electrolyte System: Values of αn as a function of concentration of hydrochloric acid supporting electrolyte. Boron carbide solid electrode was treated with Ir(IV) Perchlorate (1.0×10^{-3} M) solution.

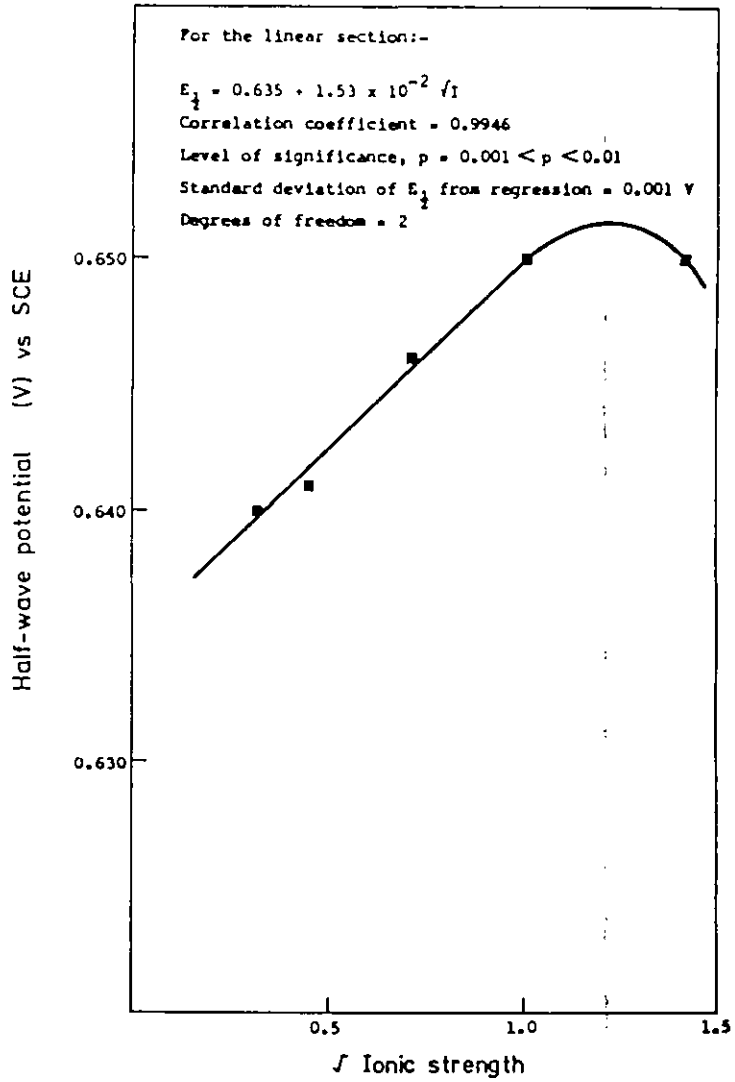

Fig. 5-61 Ir(IV)-Ir(III) Chloroiridate/Hydrochloric acid supporting electrolyte System: Values of half-wave potential, $E_{\frac{1}{2}}$, as a function of square root of total ionic strength (where the concentration of hydrochloric acid supporting electrolyte was varied), $\sqrt{I}$. Boron carbide solid electrode was treated with Ir(IV) Perchlorate (1.0×10^{-3} M) solution.

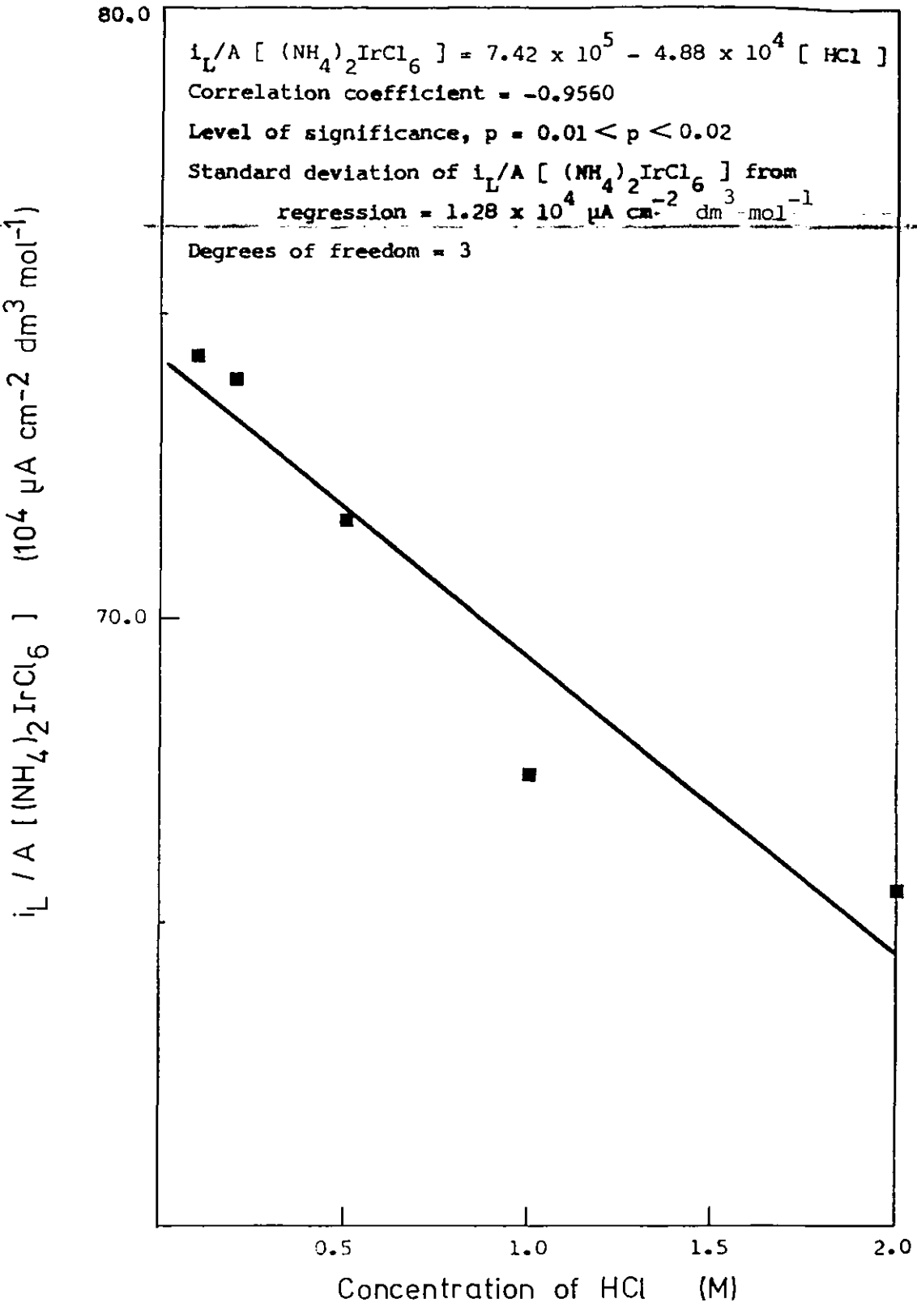

Fig. 5-62 Ir(IV)-Ir(III) Chloroiridate/Hydrochloric acid supporting electrolyte System: Values of limiting current per unit area divided by concentration of ammonium hexachloroiridate, i_L/A [$(NH_4)_2IrCl_6$], as a function of concentration of hydrochloric acid supporting electrolyte, [HCl]. Boron carbide solid electrode was treated with Ir(IV) Perchlorate (1.0×10^{-3} M) solution.

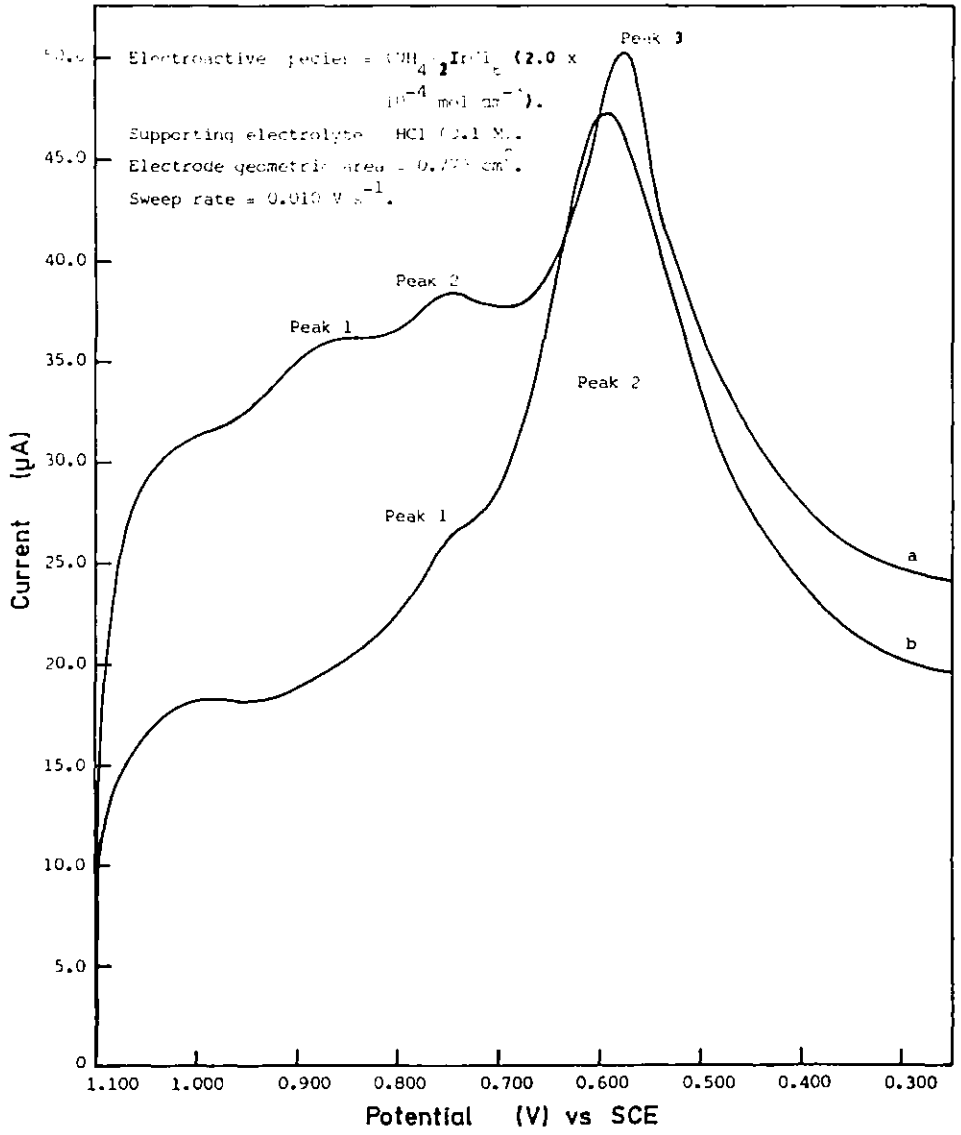

Fig. 5-63 Boron carbide solid electrode treated with Ir(IV) perchlorate (1.0 x 10^{-3} M) solution. Linear sweep voltammetry: (a) Residual current and (b) Electro-reduction of chloroiridate.

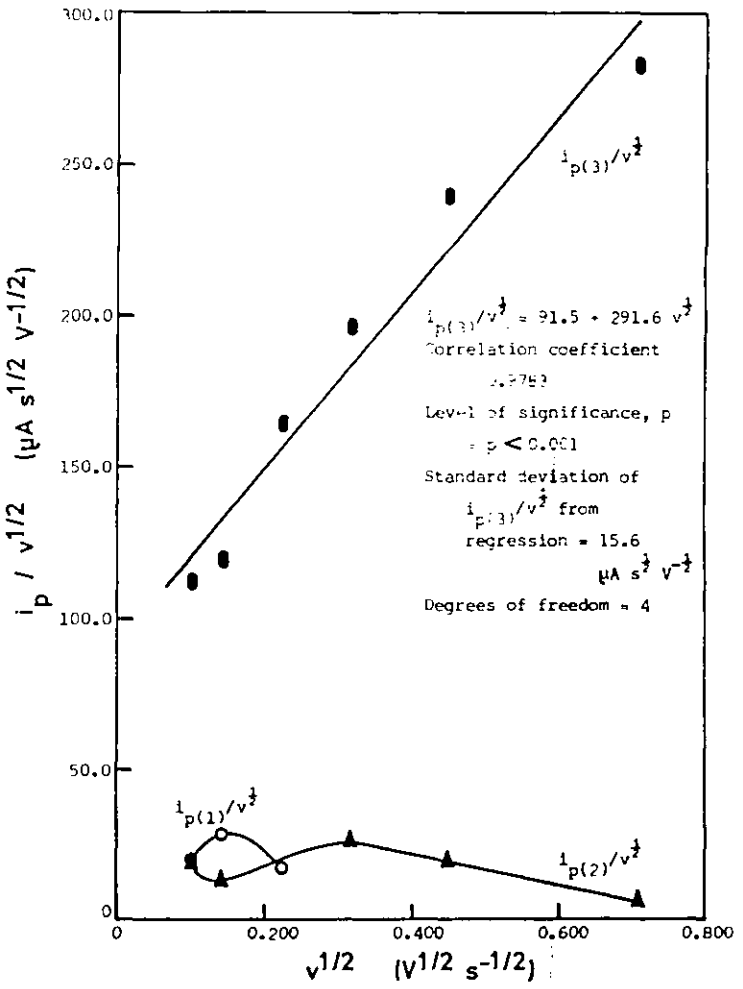

Fig. 5-64 Hydrochloric acid (0.1 M) supporting electrolyte: Residual current function, $i_p/v^{\frac{1}{2}}$, as a function of square root of potential sweep rate, $v^{\frac{1}{2}}$. Boron carbide solid electrode was treated with Ir(IV) perchlorate (1.0 x 10^{-3} M) solution.

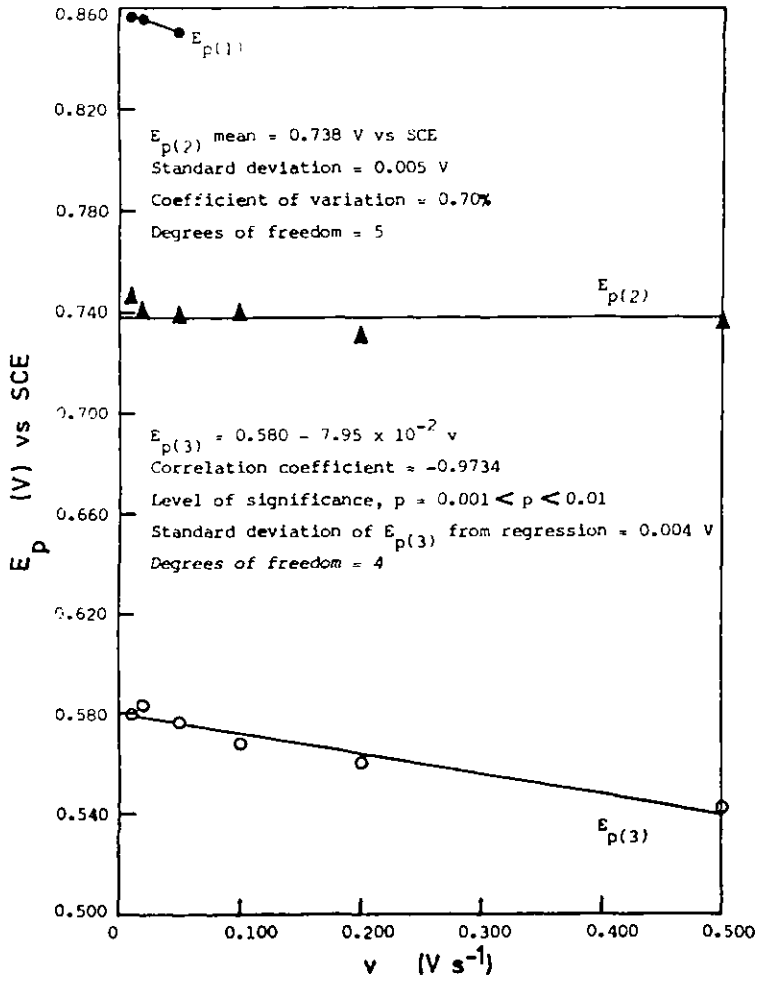

Fig. 5-65 Hydrochloric acid (0.1 M) supporting electrolyte: Residual peak potential, E_p, as a function of potential sweep rate, v. Boron carbide solid electrode was treated with Ir(IV) perchlorate (1.0×10^{-3} M) solution.

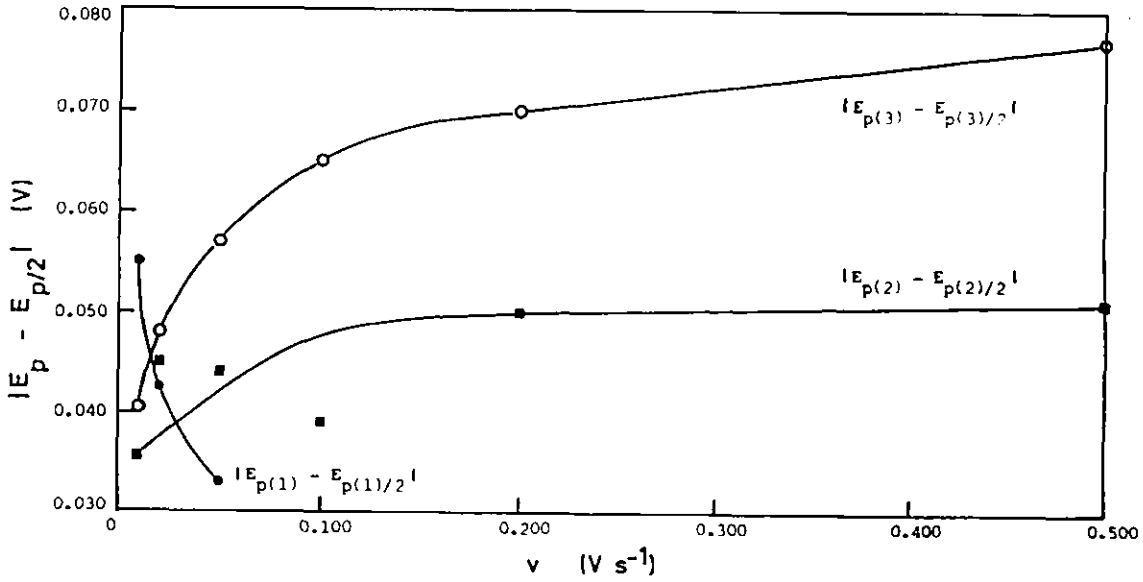

Fig. 5-66 Hydrochloric acid (0.1 M) supporting electrolyte: Values of absolute difference between residual peak and half-peak potential, $|E_p - E_{p/2}|$, as a function of potential sweep rate, v. Boron carbide solid electrode was treated with Ir(IV) perchlorate (1.0×10^{-3} M) solution.

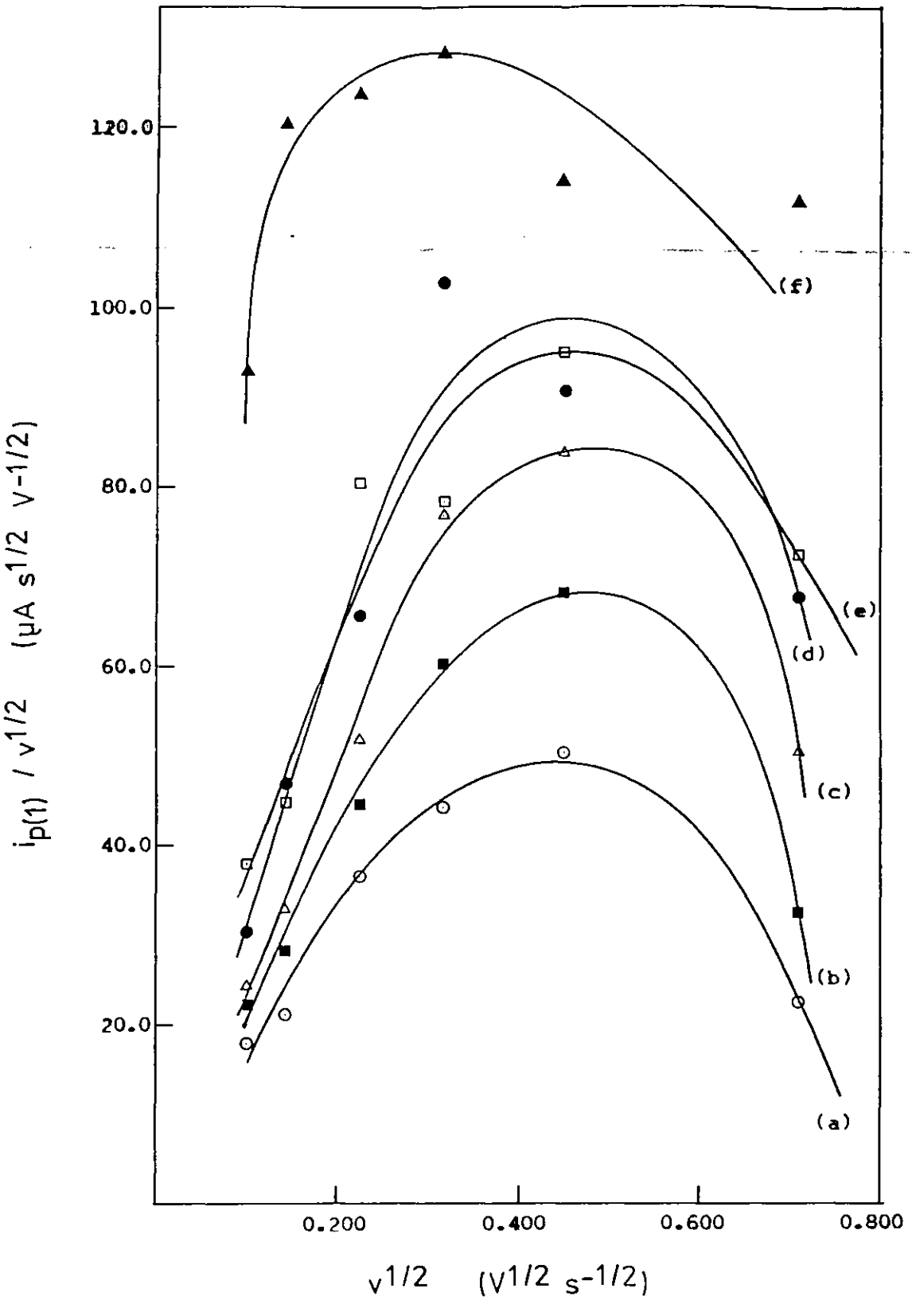

Fig. 5-67 Ir(IV)-Ir(III) Chloroiridate/Hydrochloric acid (0.1 M) supporting electrolyte System: Values of cathodic current function, $i_{p(1)}/v^{\frac{1}{2}}$, (for the more positive peak) as a function of square root of potential scan rate, $v^{\frac{1}{2}}$; at the ammonium hexachloroiridate concentrations (a) 1.0×10^{-5}, (b) 4.0×10^{-5}, (c) 8.0×10^{-5}, (d) 2.0×10^{-4}, (e) 4.0×10^{-4}, and (f) 8.0×10^{-4} mol dm^{-3}. Boron carbide solid electrode was treated with Ir(IV) Perchlorate (1.0×10^{-3} M) solution.

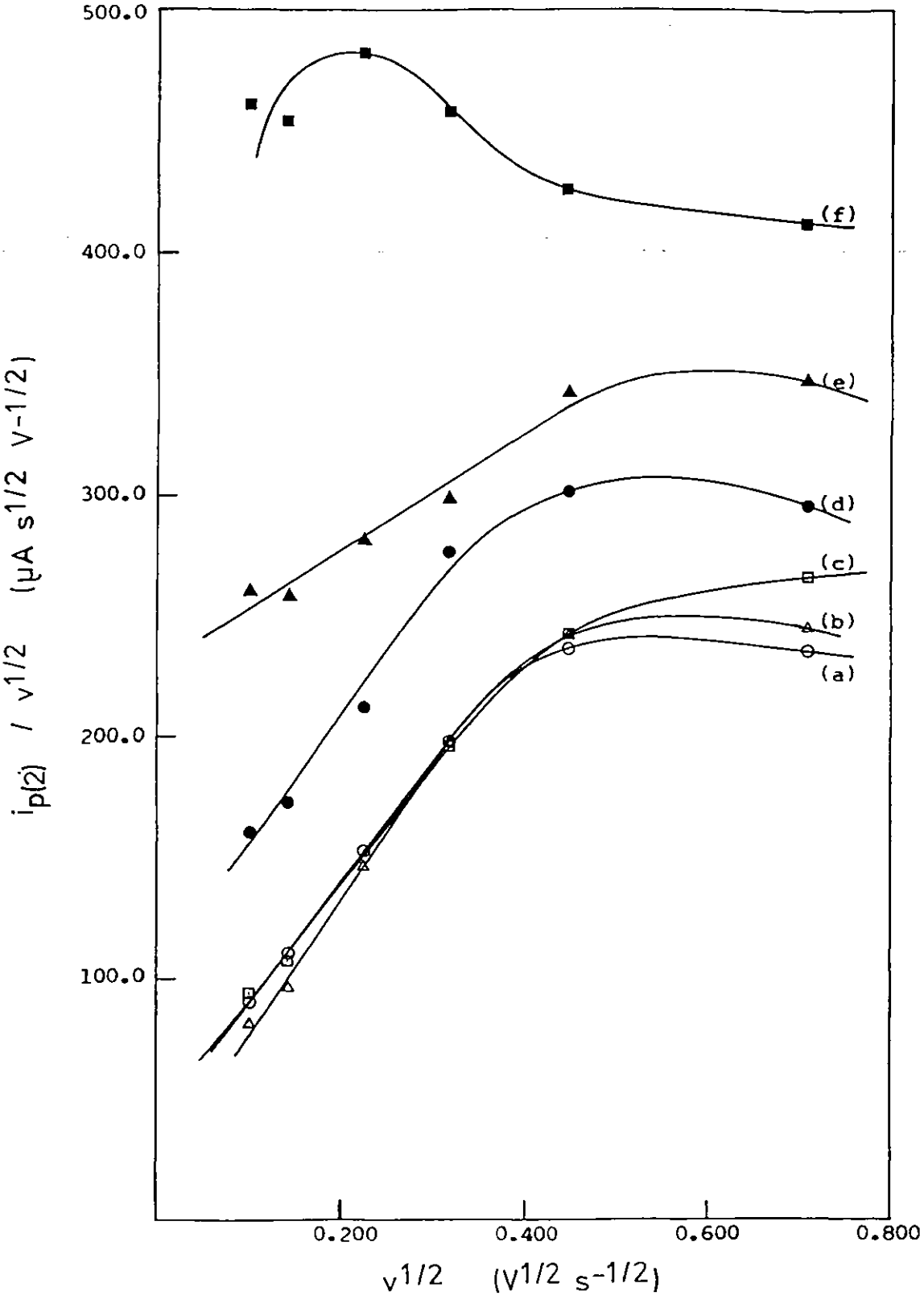

Fig. 5-68 Ir(IV)-Ir(III) Chloroiridate/Hydrochloric acid (0.1 M) supporting electrolyte System: Values of cathodic current function, $i_{p(2)}/v^{\frac{1}{2}}$, (for the less positive peak) as a function of square root of potential scan rate, $v^{\frac{1}{2}}$; at the ammonium hexachloroiridate concentrations (a) 1.0×10^{-5}, (b) 4.0×10^{-5}, (c) 8.0×10^{-5}, (d) 2.0×10^{-4}, (e) 4.0×10^{-4}, and (f) 8.0×10^{-4} mol dm^{-3}. Boron carbide solid electrode was treated with Ir(IV) Perchlorate (1.0×10^{-3} M) solution.

follow the trend for an irreversible charge transfer in the highest concentration of chloroiridate investigated (Fig. 5-68, f). Fig. 5-63 shows that Peaks 1 and 2 for the chloroiridate reduction occurred at potentials close to Peaks 2 and 3 for the underlying reduction of the adsorbed Ir(IV) perchlorate species. Comparison of the values of the peak current functions at these potentials (Fig. 5-64 vs. Figures 5-67 and 5-68) suggests that the chloroiridate Peak 1 was an adsorption peak (superimposed upon the Ir(IV) perchlorate Peak 2) and Peak 2 was a diffusion peak which was grossly distorted by the underlying peak (Peak 3) of the adsorbed Ir(IV) perchlorate species. Further evidence for this hypothesis is furnished by Figures 5-69 and 5-70, where the linear dependence of peak current on the concentration of chloroiridate for Peak 1 became non-linear at the higher sweep rates whilst that of Peak 2 was not affected. The effect of chloroiridate concentration on adsorption is further illustrated in Fig. 5-71 where the ratio of adsorption Peak 1:diffusion Peak 2 increases rapidly to a maximum before decreasing with increasing concentration.

The effect of sweep rate on the peak potentials of chloroiridate reduction is presented in Fig. 5-72. The potential of Peak 1 remained constant ($E_{p(1)}$ mean = 0.744 V vs SCE ± 0.007 V, 35 degrees of freedom) but the potential of Peak 2 shifted cathodically with increasing sweep rate. Plots of the absolute difference between peak and half-peak potential as a function of sweep rate show that $|E_{p(1)} - E_{p(1)/2}|$ was relatively constant (mean value = 0.033 V ± 0.003 V, 32 degrees of freedom), but $|E_{p(2)} - E_{p(2)/2}|$ increased with sweep rate (Fig. 5-73) thus signifying a decreasing reversibility of the charge transfer. This is further evidence that Peak 1 was an adsorption peak whereas Peak 2 was a diffusion peak. Since the adsorption peak was a pre-peak, it signified the strong adsorption of product (Fig. 3-15, d).

The effect of chloroiridate concentration on the peak potentials is illustrated in Fig. 5-74 where $E_{p(1)}$ shifted anodically with increasing $I^{\frac{1}{2}}$, but $E_{p(2)}$ shifted cathodically after the initial anodic shifts at lower chloroiridate concentrations. The absolute difference between peak and half-peak potential, however, was independent of chloroiridate concentration for both peaks (Fig. 5-75). An increase in the concentration of hydrochloric acid supporting electrolyte caused both peak potentials to shift anodically (Fig. 5-76) with increasing $I^{\frac{1}{2}}$; signifying that the e.a.s. was anionic. However, the adsorption peak (Peak 1) was not defined at high hydrochloric acid concentrations; suggesting

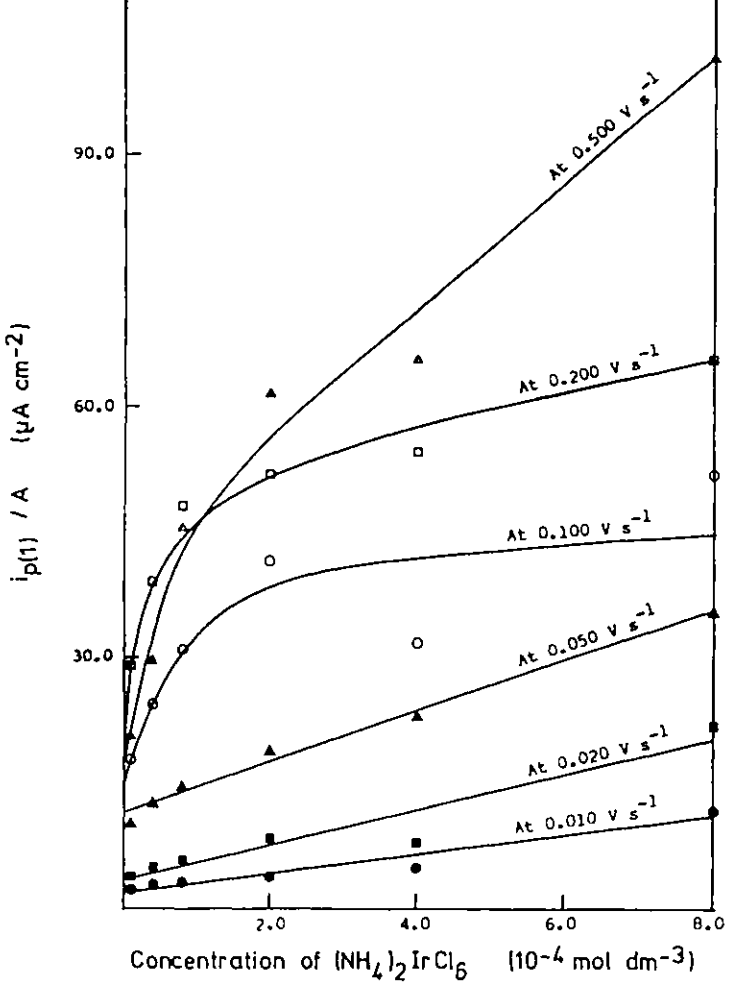

Fig. 5-6 Ir(IV)-Ir(III) Chloroiridate/Hydrochloric acid (0.1 M) supporting electrolyte System: Values of peak current per unit area, $i_{p(1)}/A$, (for the more positive peak) as a function of concentration of ammonium hexachloroiridate; at different potential scan rates. Boron carbide solid electrode was treated with Ir(IV) Perchlorate (1.0×10^{-3} M) solution.

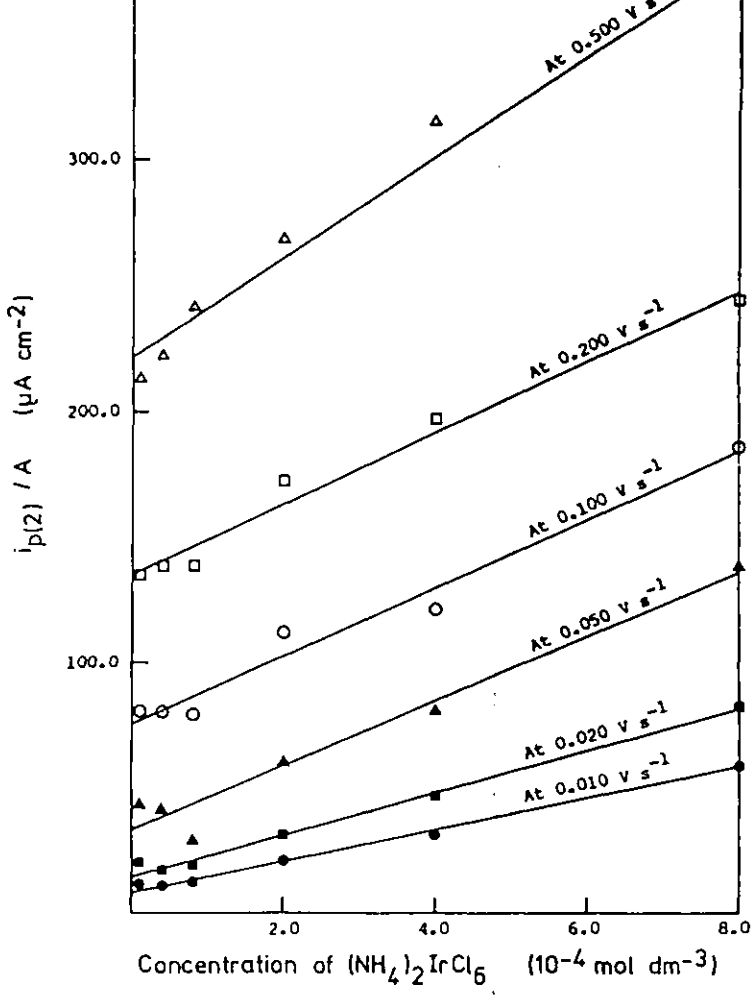

Fig. 5-7 Ir(IV)-Ir(III) Chloroiridate/Hydrochloric acid (0.1 M) supporting electrolyte System: Dependence of peak current per unit area, $i_{p(2)}/A$, (for the less positive peak) as a function of concentration of ammonium hexachloroiridate; at different potential scan rates. Boron carbide solid electrode was treated with Ir(IV) Perchlorate (1.0×10^{-3} M) solution.

Fig. 5-69 (continued):-

(a) At $v = 0.010\ V\ s^{-1}$:

$i_{p(1)}/A = 1.92 + 1.15 \times 10^4\ [\ (NH_4)_2IrCl_6\ ]$
Correlation coefficient = 0.9693
Level of significance, $p = 0.001 < p < 0.01$
Standard deviation of $i_{p(1)}/A$ from regression = 0.986 $\mu A\ cm^{-2}$
Degrees of freedom = 4

(b) At $v = 0.020\ V\ s^{-1}$:

$i_{p(1)}/A = 3.59 + 2.08 \times 10^4\ [\ (NH_4)_2IrCl_6\ ]$
Correlation coefficient = 0.9558
Level of significance, $p = 0.001 < p < 0.01$
Standard deviation of $i_{p(1)}/A$ from regression = 2.16 $\mu A\ cm^{-2}$
Degrees of freedom = 4

(c) At $v = 0.050\ V\ s^{-1}$:

$i_{p(1)}/A = 11.6 + 3.00 \times 10^4\ [\ (NH_4)_2IrCl_6\ ]$
Correlation coefficient = 0.9946
Level of significance, $p = p < 0.001$
Standard deviation of $i_{p(1)}/A$ from regression = 1.06 $\mu A\ cm^{-2}$
Degrees of freedom = 4

Fig. 5-70 (continued):-

(a) At $v = 0.010\ V\ s^{-1}$:

$i_{p(2)}/A = 8.60 + 6.28 \times 10^4\ [\ (NH_4)_2IrCl_6\ ]$
Correlation coefficient = 0.9976
Level of significance, $p = p < 0.001$
Standard deviation of $i_{p(2)}/A$ from regression = 1.48 $\mu A\ cm^{-2}$
Degrees of freedom = 4

(b) At $v = 0.020\ V\ s^{-1}$:

$i_{p(2)}/A = 15.2 + 8.25 \times 10^4\ [\ (NH_4)_2IrCl_6\ ]$
Correlation coefficient = 0.9960
Level of significance, $p = p < 0.001$
Standard deviation of $i_{p(2)}/A$ from regression = 2.49 $\mu A\ cm^{-2}$
Degrees of freedom = 4

(c) At $v = 0.050\ V\ s^{-1}$:

$i_{p(2)}/A = 33.2 + 1.28 \times 10^5\ [\ (NH_4)_2IrCl_6\ ]$
Correlation coefficient = 0.9798
Level of significance, $p = p < 0.001$
Standard deviation of $i_{p(2)}/A$ from regression = 8.88 $\mu A\ cm^{-2}$
Degrees of freedom = 4

(d) At $v = 0.100\ V\ s^{-1}$:

$i_{p(2)}/A = 75.5 + 1.35 \times 10^5\ [\ (NH_4)_2IrCl_6\ ]$
Correlation coefficient = 0.9871
Level of significance, $p = p < 0.001$
Standard deviation of $i_{p(2)}/A$ from regression = 7.38 $\mu A\ cm^{-2}$
Degrees of freedom = 4

(e) At $v = 0.200\ V\ s^{-1}$:

$i_{p(2)}/A = 135.0 + 1.41 \times 10^5\ [\ (NH_4)_2IrCl_6\ ]$
Correlation coefficient = 0.9899
Level of significance, $p = p < 0.001$
Standard deviation of $i_{p(2)}/A$ from regression = 6.84 $\mu A\ cm^{-2}$
Degrees of freedom = 4

(f) At $v = 0.500\ V\ s^{-1}$:

$i_{p(2)}/A = 220.9 + 2.00 \times 10^5\ [\ (NH_4)_2IrCl_6\ ]$
Correlation coefficient = 0.9872
Level of significance, $p = p < 0.001$
Standard deviation of $i_{p(2)}/A$ from regression = 10.9 $\mu A\ cm^{-2}$
Degrees of freedom = 4

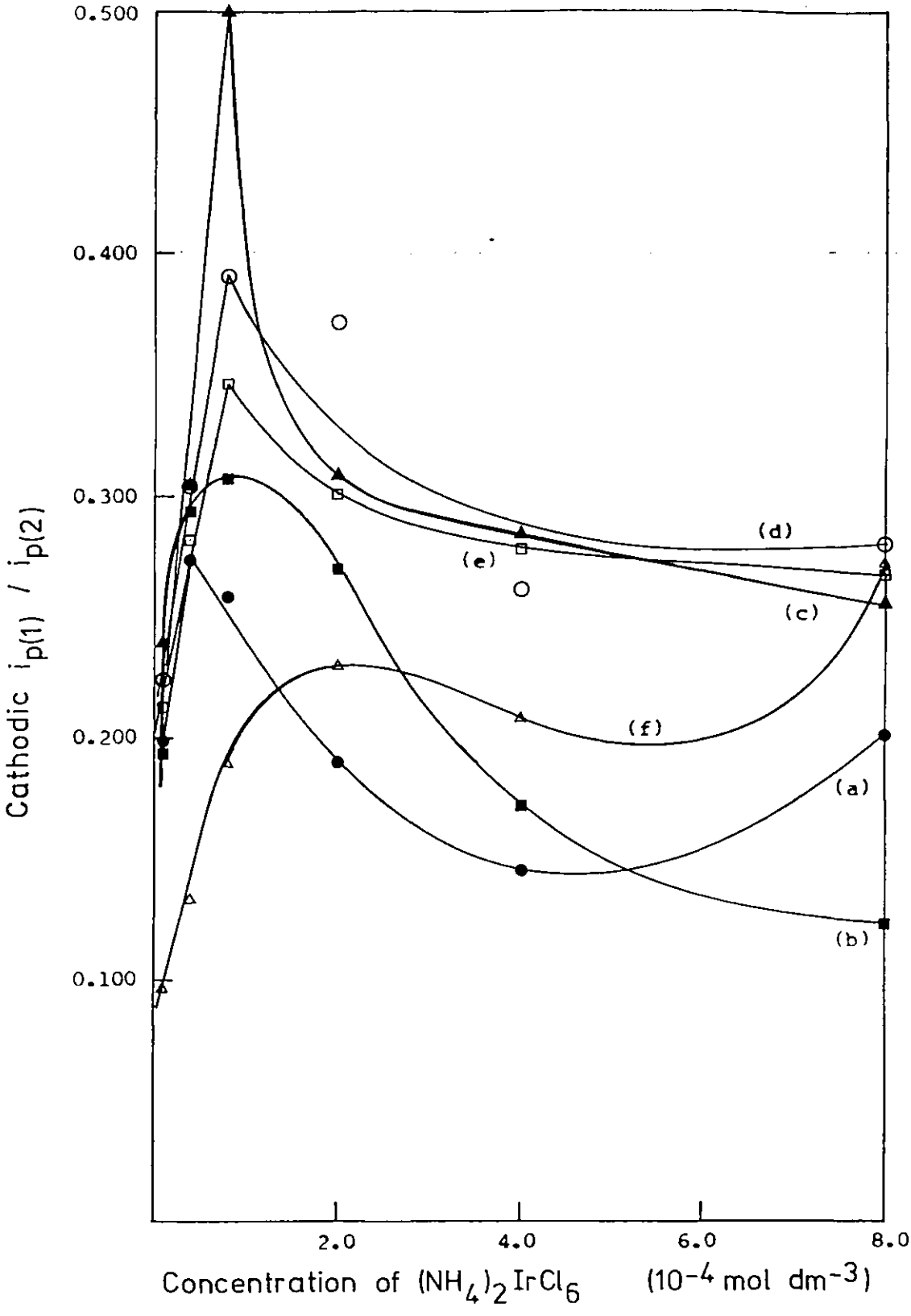

Fig. 5-71 Ir(IV)-Ir(III) Chloroiridate/Hydrochloric acid (0.1 M) supporting electrolyte System: Values of ratio of cathodic peak currents, $i_{p(1)}/i_{p(2)}$, as a function of concentration of ammonium hexachloroiridate; at the potential scan rates (a) 0.010 V s^{-1}, (b) 0.020 V s^{-1}, (c) 0.050 V s^{-1}, (d) 0.100 V s^{-1}, (e) 0.200 V s^{-1}, and (f) 0.500 V s^{-1}. Boron carbide solid electrode was treated with Ir(IV) Perchlorate (1.0 x 10^{-3} M) solution.

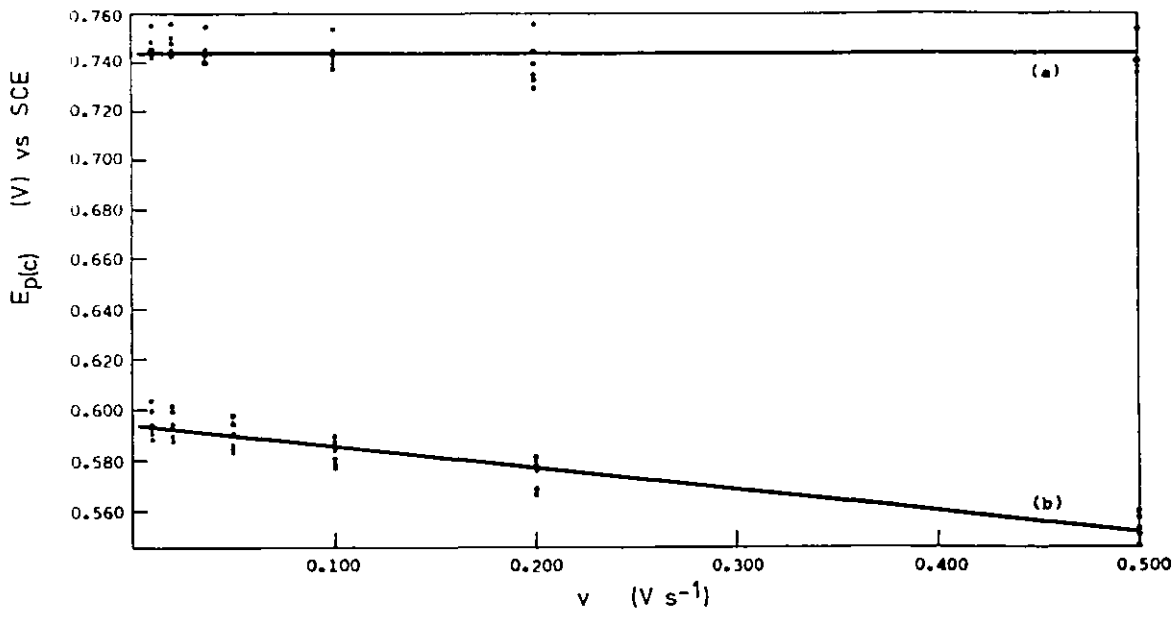

Fig. 5-72 Ir(IV)-Ir(III) Chloroiridate/Hydrochloric acid (0.1 M) supporting electrolyte System: Values of cathodic peak potential, $E_{p(c)}$, as a function of potential scan rate, v; at ammonium hexachloroiridate concentrations of 1.0×10^{-5} to 8.0×10^{-4} mol dm^{-3}. Boron carbide solid electrode was treated with Ir(IV) perchlorate (1.0×10^{-3} M) solution.

(a) For the more positive peak potential, $E_{p(1)}$:

Grand mean, $\bar{E}_{p(1)} = 0.744$ V (vs SCE)
Standard deviation = 0.007 V
Degrees of freedom = 35

(b) For the less positive peak potential, $E_{p(2)}$:

$E_{p(2)} = 0.594 - 8.41 \times 10^{-2}$ v
Correlation coefficient = -0.9383
Level of significance, p = $p < 0.001$
Standard deviation of $E_{p(2)}$ from regression = 0.005 V
Degrees of freedom = 34

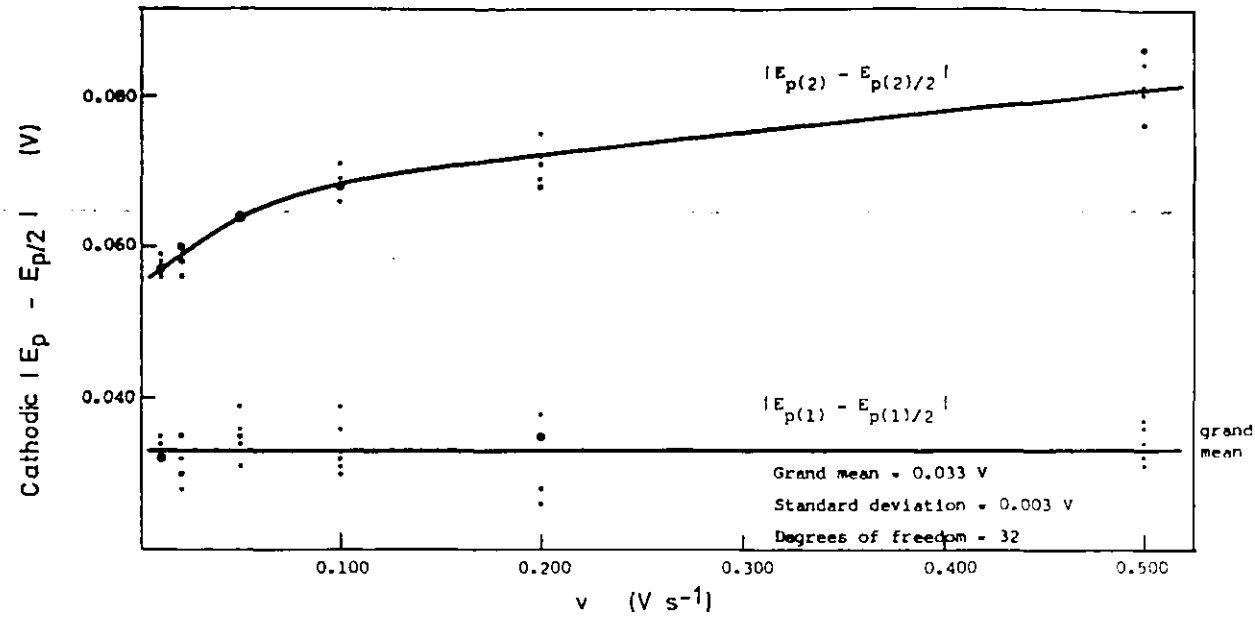

Fig. 5-73 Ir(IV)-Ir(III) Chloroiridate/Hydrochloric acid (0.1 M) supporting electrolyte System: Values of absolute difference between cathodic peak and cathodic half-peak potential, $|E_p - E_{p/2}|$, as a function of potential scan rate, v; at ammonium hexachloroiridate concentrations of 1.0×10^{-5} to 8.0×10^{-4} mol dm^{-3}. Boron carbide solid electrode was treated with Ir(IV) Perchlorate (1.0×10^{-3} M) solution.

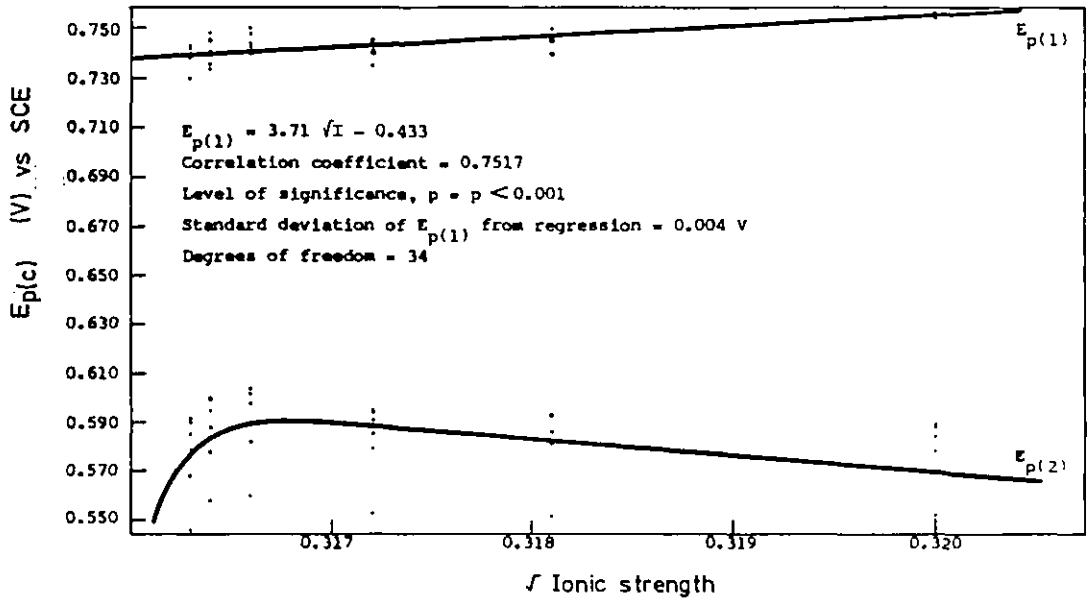

Fig. 5-74 Ir(IV)-Ir(III) Chloroiridate/Hydrochloric acid (0.1 M) supporting electrolyte System: Values of cathodic peak potential, $E_{p(c)}$, as a function of square root of total ionic strength (where the concentration of ammonium hexachloroiridate was varied), $\sqrt{I}$; at potential scan rates of 0.010 V s^{-1} to 0.500 V s^{-1}. Boron carbide solid electrode was treated with Ir(IV) Perchlorate (1.0×10^{-3} M) solution.

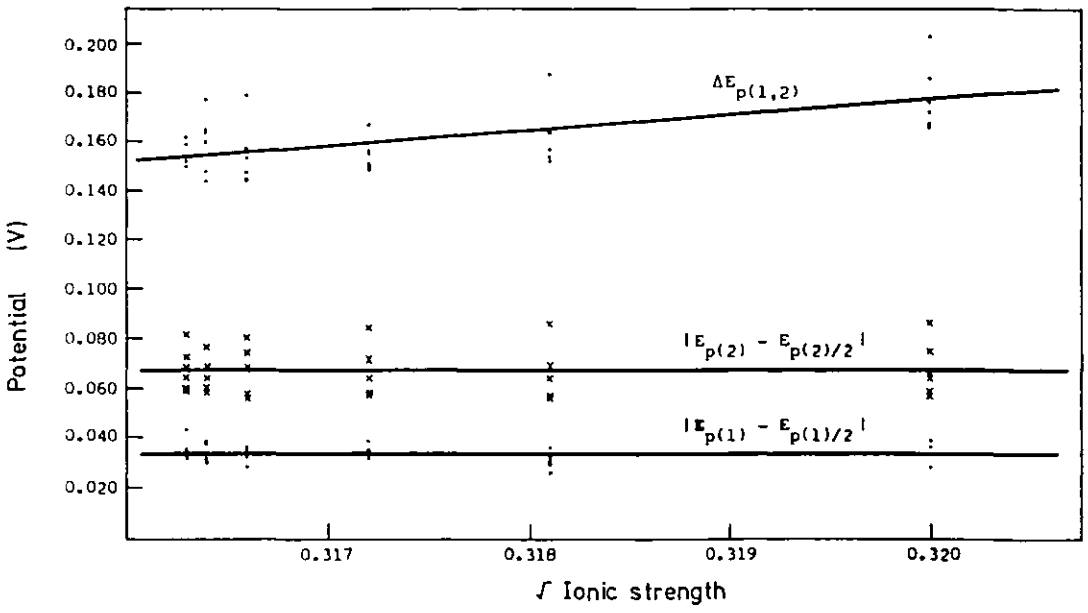

Fig. 5-75 Ir(IV)-Ir(III) Chloroiridate/Hydrochloric acid (0.1 M) supporting electrolyte System: Values of the difference between peak potentials, $\Delta E_{p(1,2)}$, difference between peak and half-peak potentials, $|E_{p(1)} - E_{p(1)/2}|$ and $|E_{p(2)} - E_{p(2)/2}|$, as functions of the square root of total ionic strength (where the concentration of ammonium hexachloroiridate was varied), $\sqrt{I}$; at potential scan rates of 0.010 V s^{-1} to 0.500 V s^{-1}. Boron carbide solid electrode was treated with Ir(IV) perchlorate (1.0×10^{-3} M) solution.

(a) $\Delta E_{p(1,2)} = 6.37\ \sqrt{I} - 1.86$
Correlation coefficient = 0.5842
Level of significance, p = $p < 0.001$
Standard deviation of $\Delta E_{p(1,2)}$ from regression = 0.012 V
Degrees of freedom = 33

(b) $|E_{p(1)} - E_{p(1)/2}|$ mean = 0.034 V
Standard deviation = 0.003 V
Degrees of freedom = 33

(c) $|E_{p(2)} - E_{p(2)/2}|$ mean = 0.067 V
Standard deviation = 0.009 V
Degrees of freedom = 35

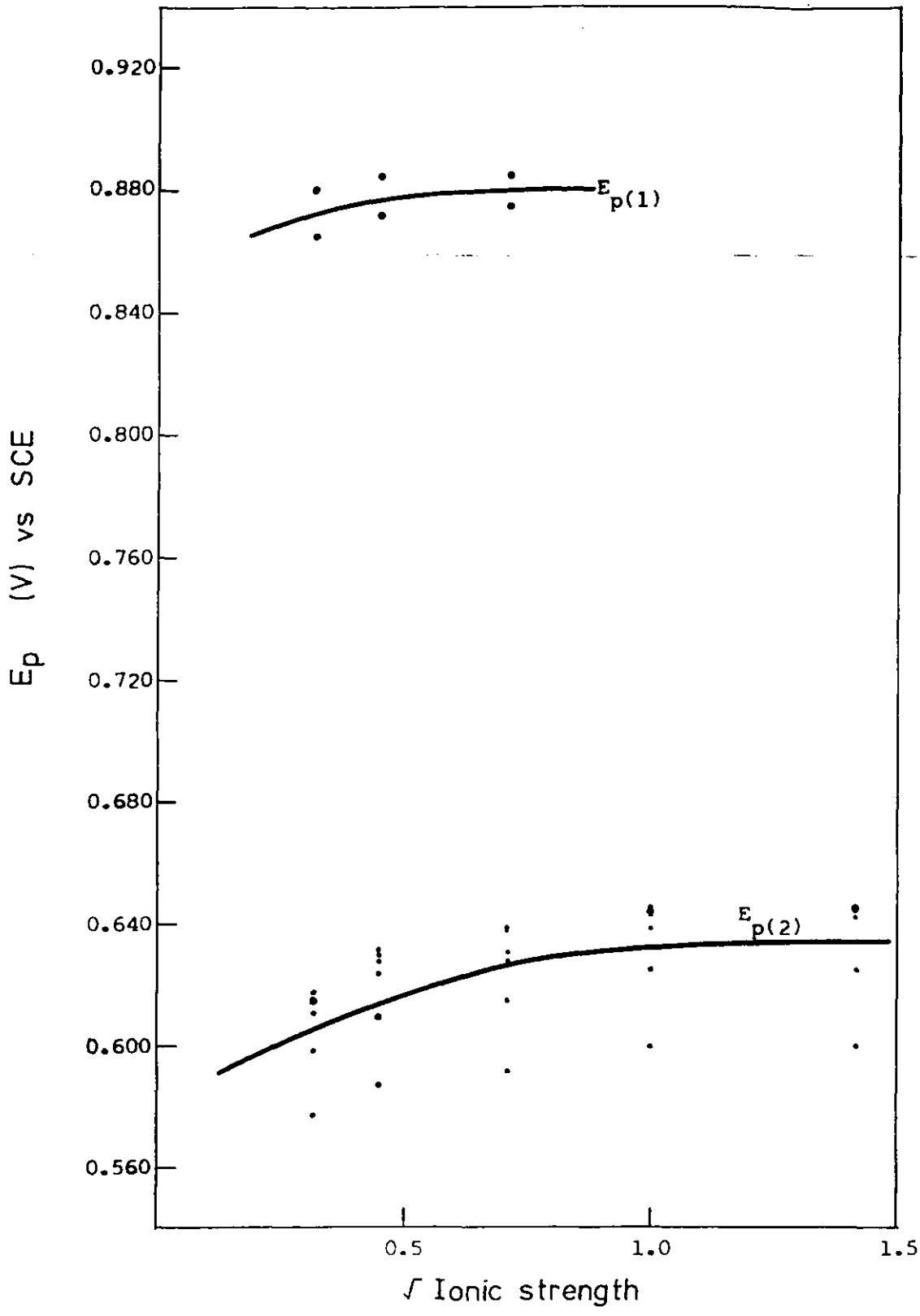

Fig. 5-76 Ir(IV)-Ir(III) Chloroiridate (1.0×10^{-4} mol dm^{-3})/Hydrochloric acid supporting electrolyte System: Values of cathodic peak potential, $E_{p(1)}$ and $E_{p(2)}$, as a function of square root of total ionic strength (where the concentration of hydrochloric acid supporting electrolyte was varied), $\sqrt{I}$; at potential scan rates of 0.010 V s^{-1} to 0.500 V s^{-1}. Boron carbide solid electrode was treated with Ir(IV) Perchlorate (1.0×10^{-3} M) solution.

that the adsorption of product was greatly reduced or even inhibited. This is illustrated further by Fig. 5-77 which shows that the peak current density for the diffusion peak (Peak 2) was independent of the concentration of hydrochloric acid whereas that for the adsorption peak (Peak 1) decreased to zero with increasing concentration of hydrochloric acid supporting electrolyte.

5-1.2.(iii) Summary.

The charge transfer for the d.c. voltammetric reaction

$$IrCl_6^{2-} + e^- \rightleftharpoons IrCl_6^{3-}$$

in hydrochloric acid (0.1 M) supporting electrolyte was found to be reversible only at the boron carbide/carbon composite solid electrode with the B:C ratio of 2.56 (section 5-1.2.(i) and Fig. 5-53).

Attempts to improve the voltammetric performance of the boron carbide solid electrode by treatment with Ir(IV) perchlorate solution or cathodic polarisation (at -4 V vs. SCE) in chloroiridate solution resulted only in qualified success (section 5-1.2.(ii)). The values of αn obtained were only close to the reversible unity value at the lower end of the concentration range of the chloroiridate (1.0×10^{-5} to 8.0×10^{-4} mol dm^{-3}) e.a.s. The decline in αn value with increasing chloroiridate concentration was steeper at the electrochemically treated electrode than at the Ir(IV) perchlorate treated electrode.

Linear sweep voltammetry at the Ir(IV) perchlorate treated electrode in hydrochloric acid (0.1 M) supporting electrolyte alone showed that the Ir(IV) perchlorate species was adsorbed on the electrode surface (Figures 5-63, a and 5-64). When this treated electrode was applied to the linear sweep voltammetry of chloroiridate (Fig. 5-63, b), it was shown that the more positive peak (Peak 1) was due to strong adsorption of product (Fig. 5-69) whilst the less positive peak (Peak 2) was due to diffusion of chloroiridate (Figures 5-70 and 5-71); although both peaks suffered interference from the underlying peaks of the adsorbed Ir(IV) perchlorate species (Fig. 5-63). The adsorption pre-peak was not defined at higher concentrations of hydrochloric acid supporting electrolyte; whilst the diffusion peak was relatively unaffected (Fig. 5-77).

The presence of adsorption effects confines the quantitative application of the Ir(IV) perchlorate treated electrode to d.c. volt-

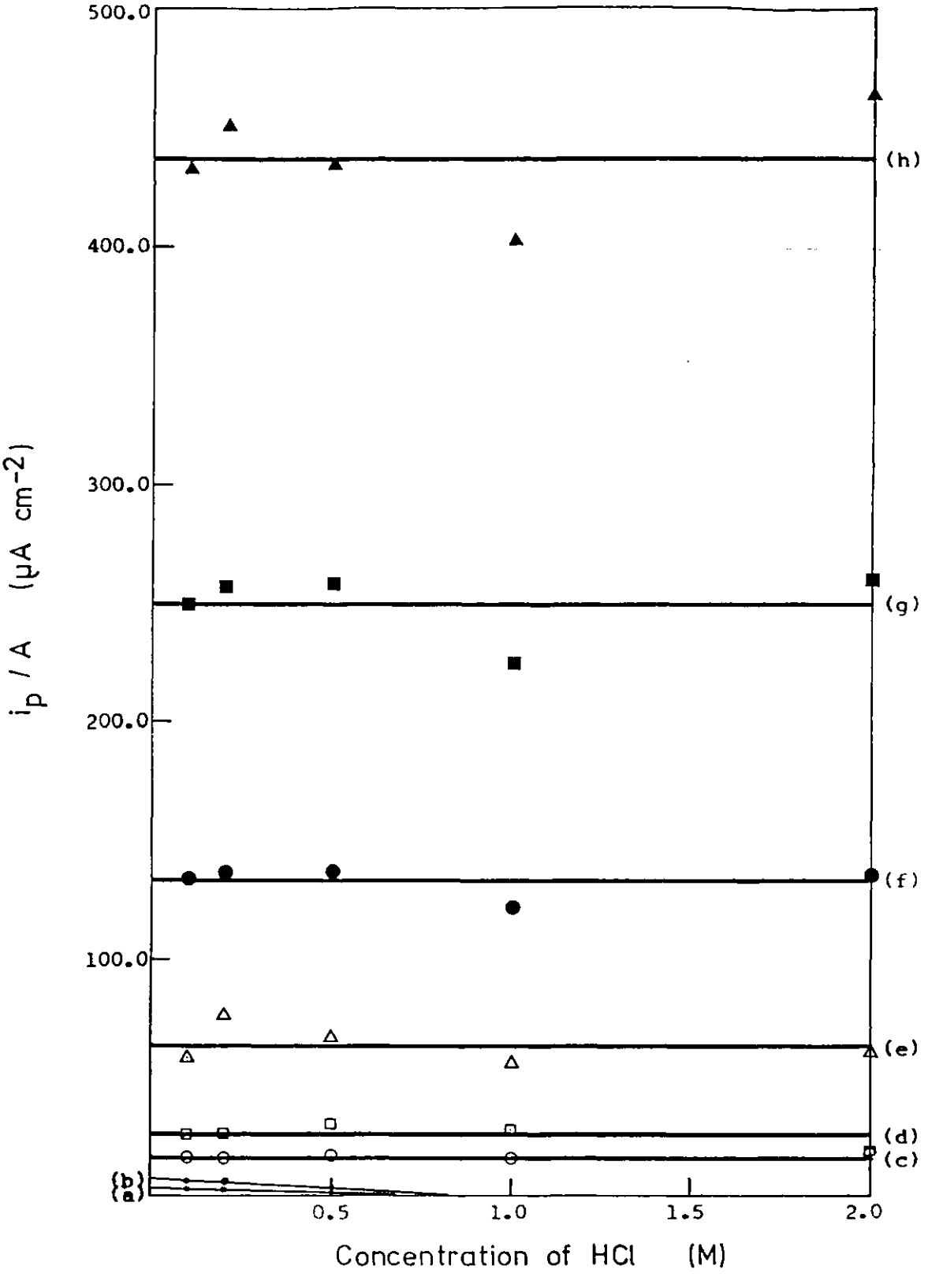

Fig. 5-77 Ir(IV)-Ir(III) Chloroiridate (1.0×10^{-4} mol dm^{-3})/Hydrochloric acid supporting electrolyte System: Values of peak current per unit area, i_p/A, as a function of concentration of hydrochloric acid supporting electrolyte. (a) $i_{p(\underline{1})}/A$ at 0.010 V s^{-1}, (b) $i_{p(\underline{1})}/A$ at 0.020 V s^{-1}, (c) $i_{p(\underline{2})}/A$ at 0.010 V s^{-1}, (d) $i_{p(\underline{2})}/A$ at 0.020 V s^{-1}, (e) $i_{p(\underline{2})}/A$ at 0.050 V s^{-1}, (f) $i_{p(2)}/A$ at 0.100 V s^{-1}, (g) $i_{p(2)}/A$ at 0.200 V s^{-1}, (h) $i_{p(2)}/A$ at 0.500 V s^{-1}. Boron carbide solid electrode was treated with Ir(IV) Perchlorate (1.0×10^{-3} M) solution.

Fig. 5-77 (continued):-

(c) At $v = 0.010$ V s^{-1}:

$i_{p(2)}/A$ mean = 16.5 μA cm^{-2}
Standard deviation = 1.07 μA cm^{-2}
Degrees of freedom = 4

(d) At $v = 0.020$ V s^{-1}:

$i_{p(2)}/A$ mean = 26.1 μA cm^{-2}
Standard deviation = 4.47 μA cm^{-2}
Degrees of freedom = 4

(e) At $v = 0.050$ V s^{-1}:

$i_{p(2)}/A$ mean = 63.8 μA cm^{-2}
Standard deviation = 7.66 μA cm^{-2}
Degrees of freedom = 4

(f) At $v = 0.100$ V s^{-1}:

$i_{p(2)}/A$ mean = 133.1 μA cm^{-2}
Standard deviation = 6.37 μA cm^{-2}
Degrees of freedom = 4

(g) At $v = 0.200$ V s^{-1}:

$i_{p(2)}/A$ mean = 249.8 μA cm^{-2}
Standard deviation = 14.6 μA cm^{-2}
Degrees of freedom = 4

(h) At $v = 0.500$ V s^{-1}:

$i_{p(2)}/A$ mean = 436.9 μA cm^{-2}
Standard deviation = 23.3 μA cm^{-2}
Degrees of freedom = 4

ammetry (Fig. 5-59); although linear sweep voltammetry at slow sweep rates has been shown to be quantitative (Figures 5-69 and 5-70).

5-1.3 Chloroiridate-chloroiridite in sodium perchlorate supporting electrolyte system

5-1.3.(i) Effect of electrochemical treatment on the boron carbide solid electrode.

The d.c voltammetric performance of the boron carbide solid electrode for the reduction of chloroiridate was significantly improved by electrochemical treatment of the electrode (Fig. 5-78). Consistently high αn values were obtained irrespective of the chloroiridate (4.0×10^{-5} to 8.0×10^{-4} mol dm^{-3}) concentration (Fig. 5-79) in sodium perchlorate (0.1 M) supporting electrolyte; αn grand mean = 0.85 ± 0.04 (20 degrees of freedom). The half-wave potential, however, shifted anodically with increasing $I^{\frac{1}{2}}$ when the concentration of chloroiridate was increased (Fig. 5-80); as expected of an anionic e.a.s. However, the extreme non-linearity of the anodic shift might be indicative of an adsorbed reactant. Fig. 5-81 shows the linear dependence of limiting current density on the concentration of chloroiridate e.a.s., with a correlation coefficient better than that at the 0.001 level of significance.

Typical linear sweep and cyclic voltammograms are presented in Figures 5-82 and 5-83 respectively. Plots of cathodic current function against $(\text{sweep rate})^{\frac{1}{2}}$ for chloroiridate (2.0×10^{-4} to 2.0×10^{-3} mol dm^{-3}) show that the charge transfer was complicated by a catalytic reaction and weak adsorption at low and high sweep rates respectively (Figures 5-84 to 5-87, c.f. Fig 3-6). This hypothesis is confirmed by the plots of anodic current functions (Fig. 5-88) and ratio of cathodic: anodic peak currents (Fig. 5-89 c.f. Fig. 3-8) against $(\text{sweep rate})^{\frac{1}{2}}$.

The second anodic peak (Fig. 5-83, Peak 2) was an adsorption peak which disappeared at high sweep rates (Fig. 5-88) and did not have a cathodic counterpart. This suggests that Peak 2 was due to an e.a.s. which was formed by a chemical reaction following the electro-reduction of chloroiridate. The adsorption effect for Peak 2 was stronger than for Peak 1 (Fig. 5-90).

The dependence of cathodic peak current density on the concentration of chloroiridate was linear at slower sweep rates but became non-linear at high sweep rates (Fig. 5-91); confirming the presence of weak

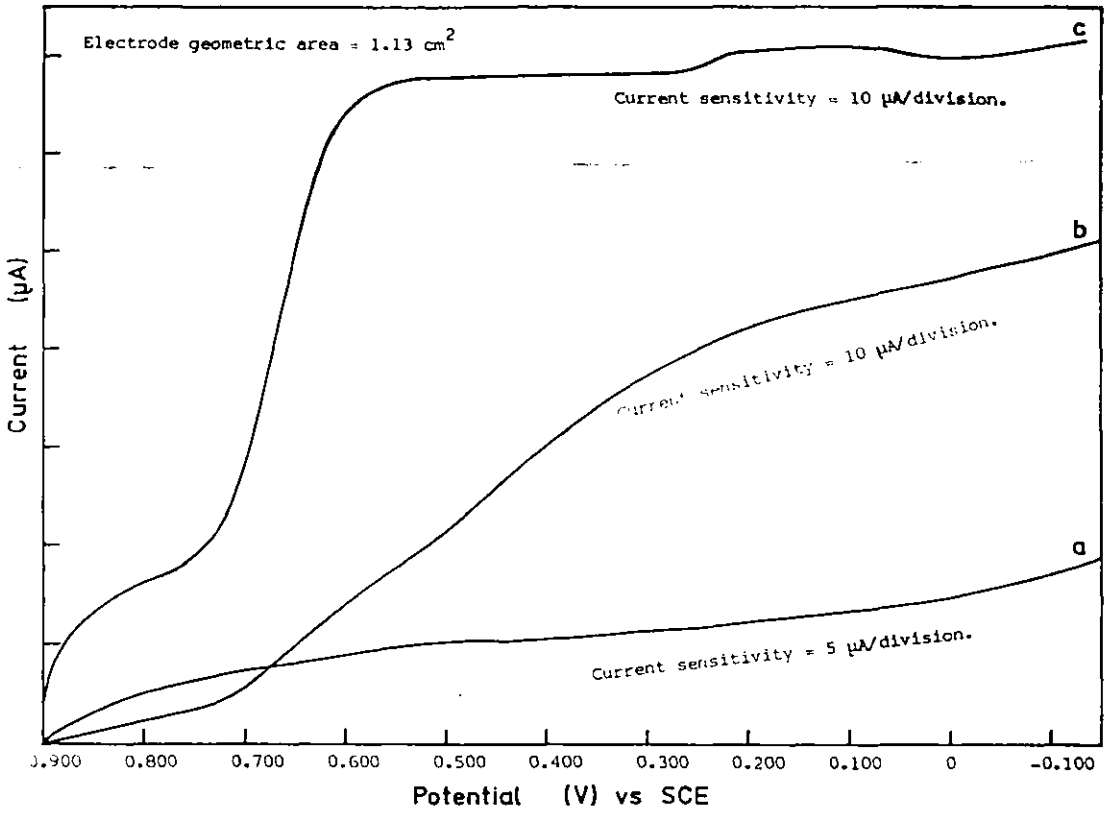

Fig. 5-78 Ir(IV)-Ir(III) Chloroiridate (1.0×10^{-4} mol dm^{-3})/Sodium perchlorate (0.1 M) supporting electrolyte System: (a) Residual current. (b) D.c. voltammogram of chloroiridate. (c) D.c. voltammogram of chloroiridate after the boron carbide solid electrode had been treated by cathodic polarisation (at -1 V vs SCE) in chloroiridate solution.

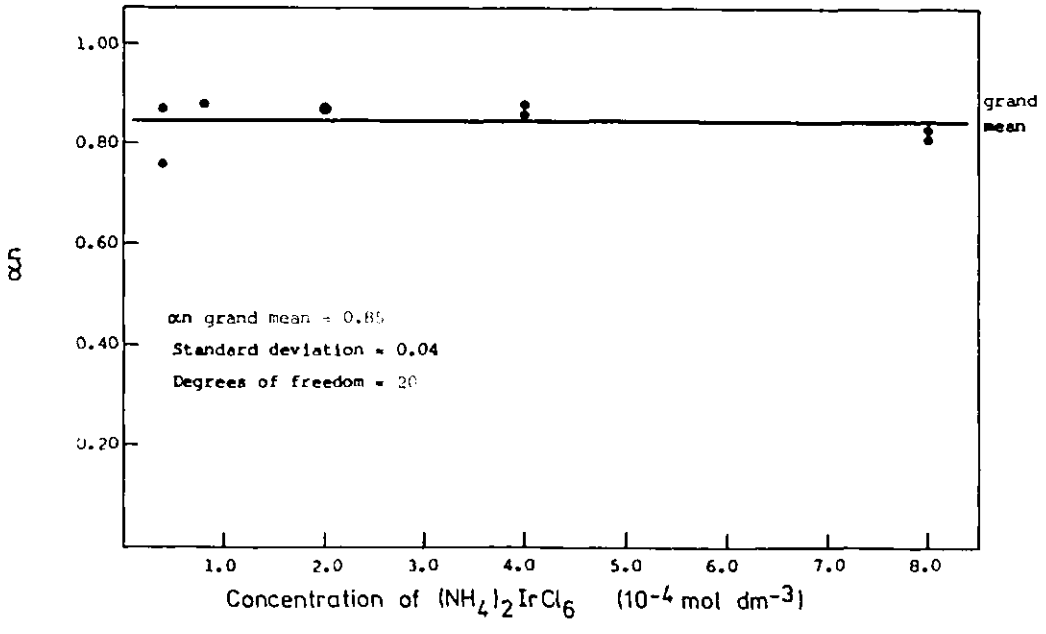

Fig. 5-79 Ir(IV)-Ir(III) Chloroiridate/Sodium perchlorate (0.1 M) supporting electrolyte System: Values of αn as a function of concentration of ammonium hexachloroiridate. Boron carbide solid electrode was treated by cathodic polarisation (at -1 V) in sample solution prior to voltammetric scan.

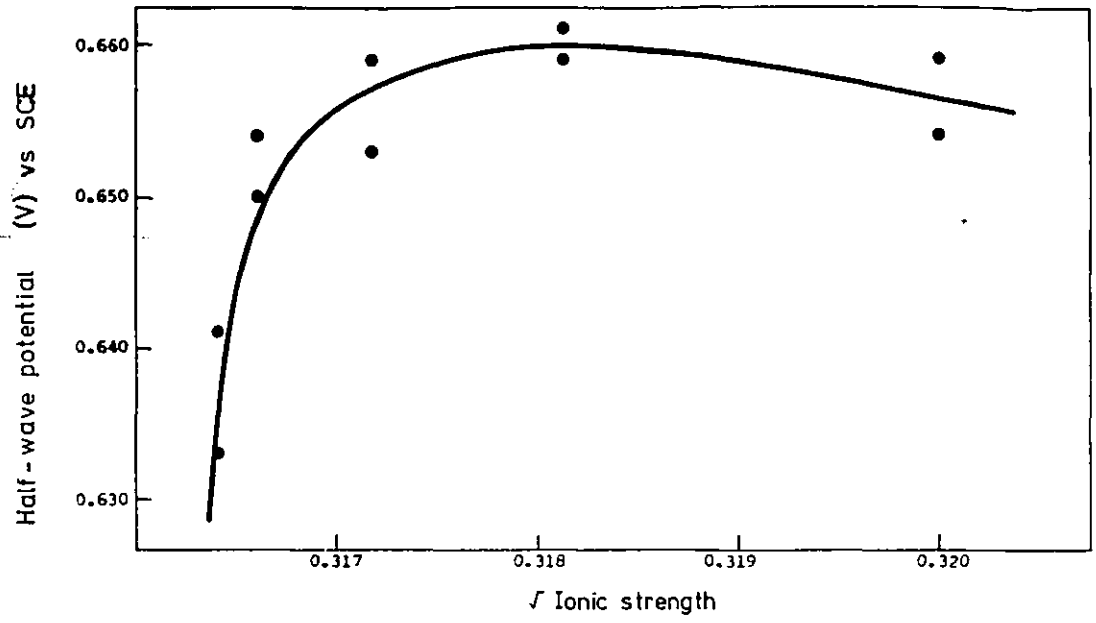

Fig. 5-80 Ir(IV)-Ir(III) Chloroiridate/Sodium perchlorate (0.1 M) supporting electrolyte System: Values of half-wave potential, $E_{\frac{1}{2}}$, as a function of square root of total ionic strength (where the concentration of ammonium hexachloroiridate was varied), √I. Boron carbide solid electrode was treated by cathodic polarisation (at -1 V) in sample solution prior to voltammetric scan.

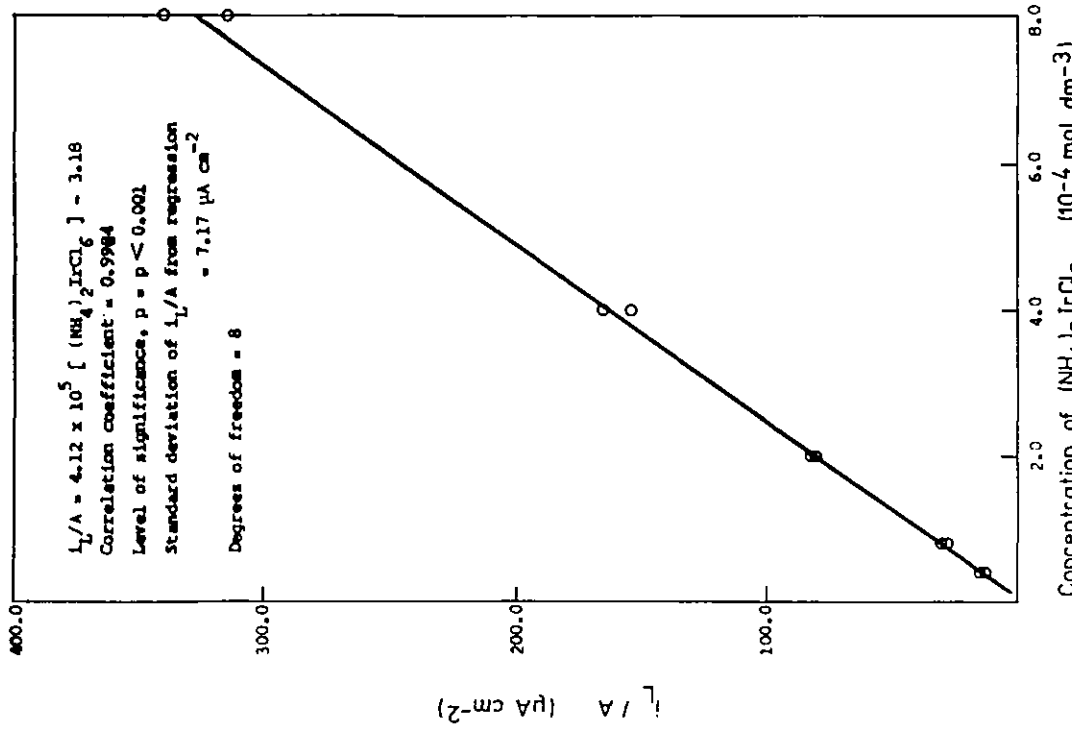

Fig. 5-81 Ir(IV)-Ir(III) Chloroiridate/Sodium perchlorate (0.1 M) supporting electrolyte System: Dependence of limiting current per unit area, i_L/A, on the concentration of ammonium hexachloroiridate. Boron carbide solid electrode was treated by cathodic polarisation (at -1 V) in sample solution prior to voltammetric scan.

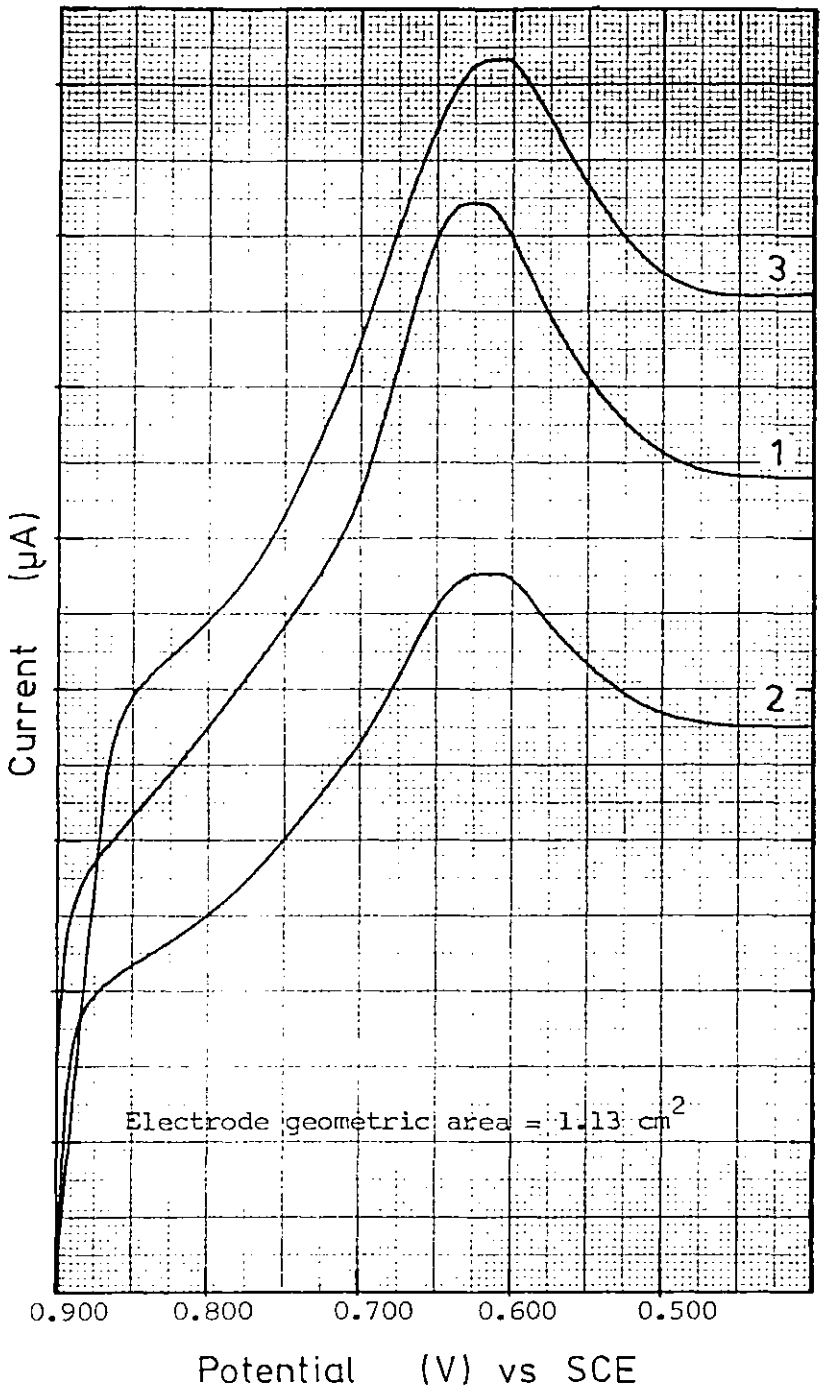

Fig. 5-82 Ir(IV)-Ir(III) Chloroiridate (4.0×10^{-4} mol dm^{-3})/Sodium perchlorate (0.1 M) supporting electrolyte System: Linear sweep voltammograms at the boron carbide solid electrode which had been treated by cathodic polarisation (at -1 V vs SCE) in chloroiridate.
(1) At v = [illegible] V s^{-1}, and current sens. = 20 μA/division.
(2) At v = [illegible] V s^{-1}, and current sens. = 50 μA/division.
(3) At v = [illegible] V s^{-1}, and current sens. = 50 μA/division.

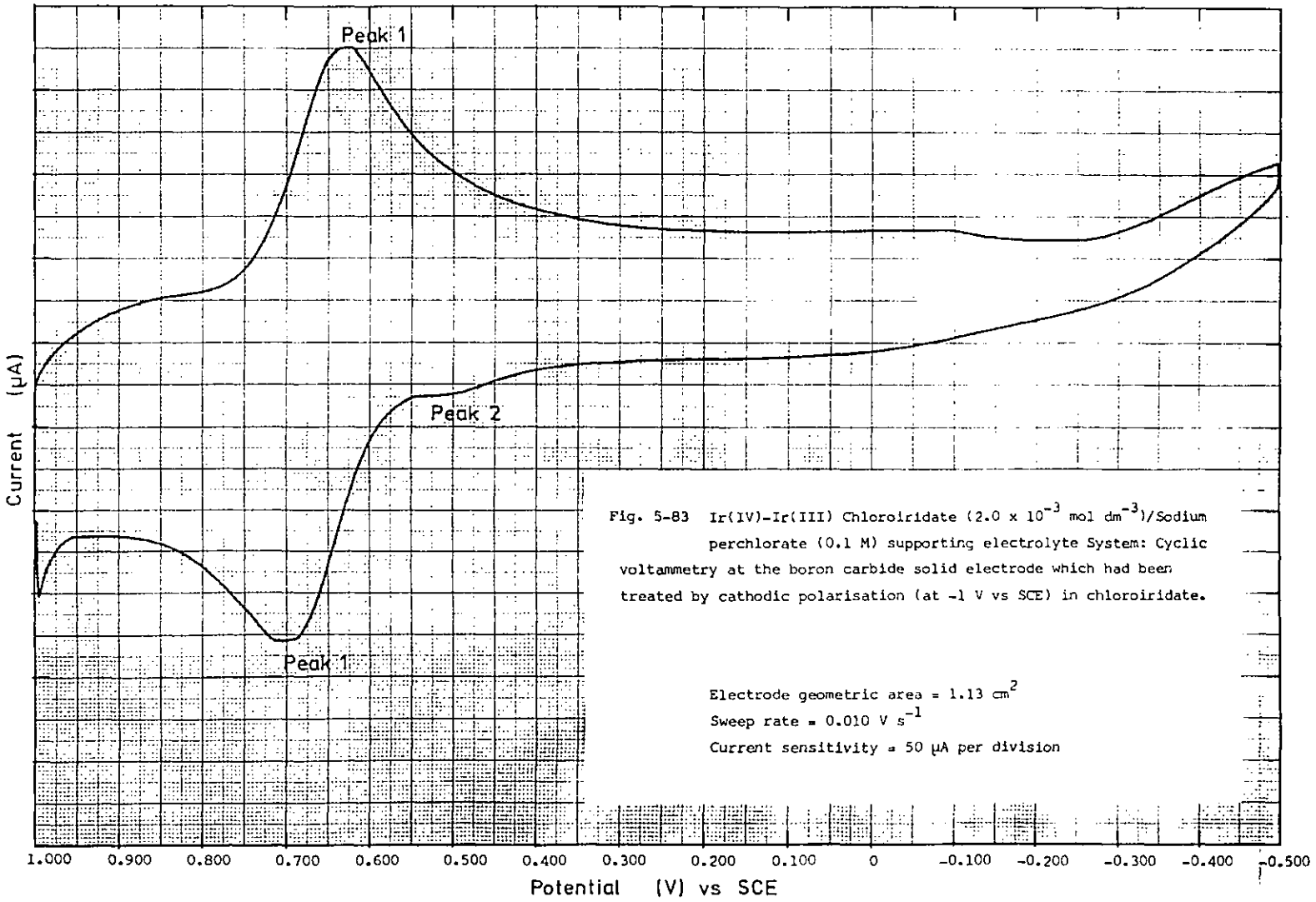

Fig. 5-83 Ir(IV)-Ir(III) Chloroiridate (2.0×10^{-3} mol dm^{-3})/Sodium perchlorate (0.1 M) supporting electrolyte System: Cyclic voltammetry at the boron carbide solid electrode which had been treated by cathodic polarisation (at -1 V vs SCE) in chloroiridate.

Electrode geometric area = 1.13 cm^2
Sweep rate = 0.010 V s^{-1}
Current sensitivity = 50 μA per division

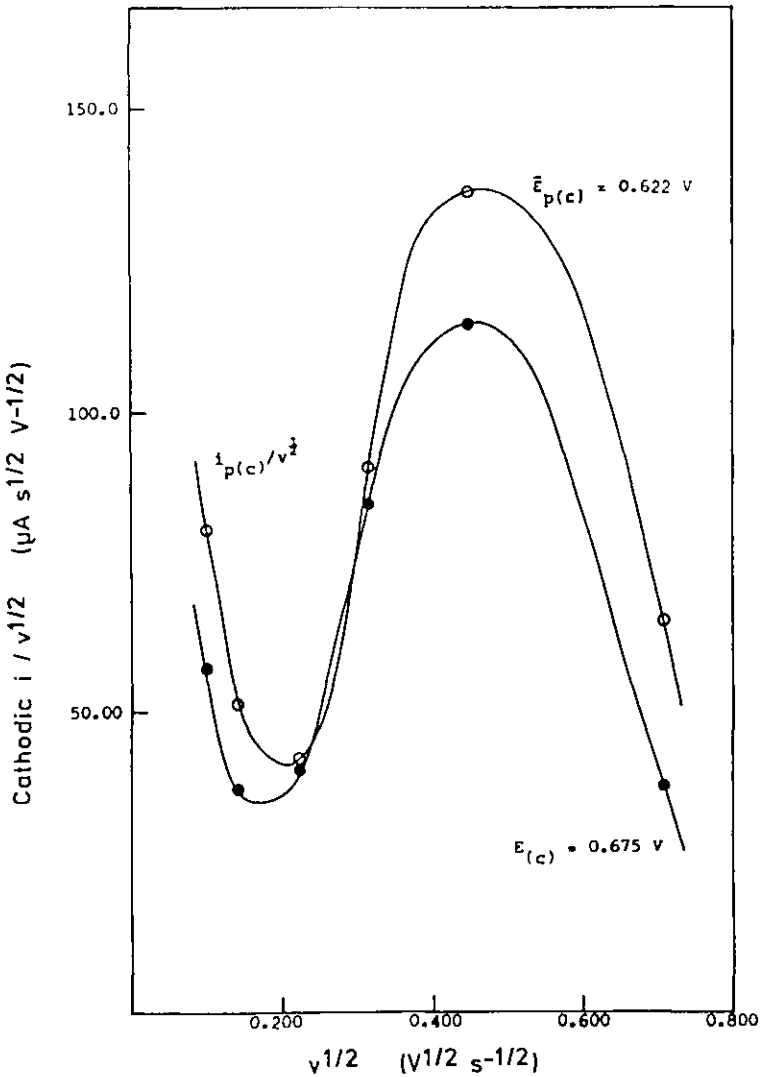

Fig. 5-84 Ir(IV)-Ir(III) Chloroiridate (2.0×10^{-4} mol dm^{-3})/Sodium perchlorate (0.1 M) supporting electrolyte System: Values of current function, $i/v^{\frac{1}{2}}$ (at different potentials along the peak voltammograms), as a function of square root of potential scan rate, $v^{\frac{1}{2}}$. Boron carbide solid electrode was treated by cathodic polarisation (at -1 V) in sample solution prior to voltammetric scan.

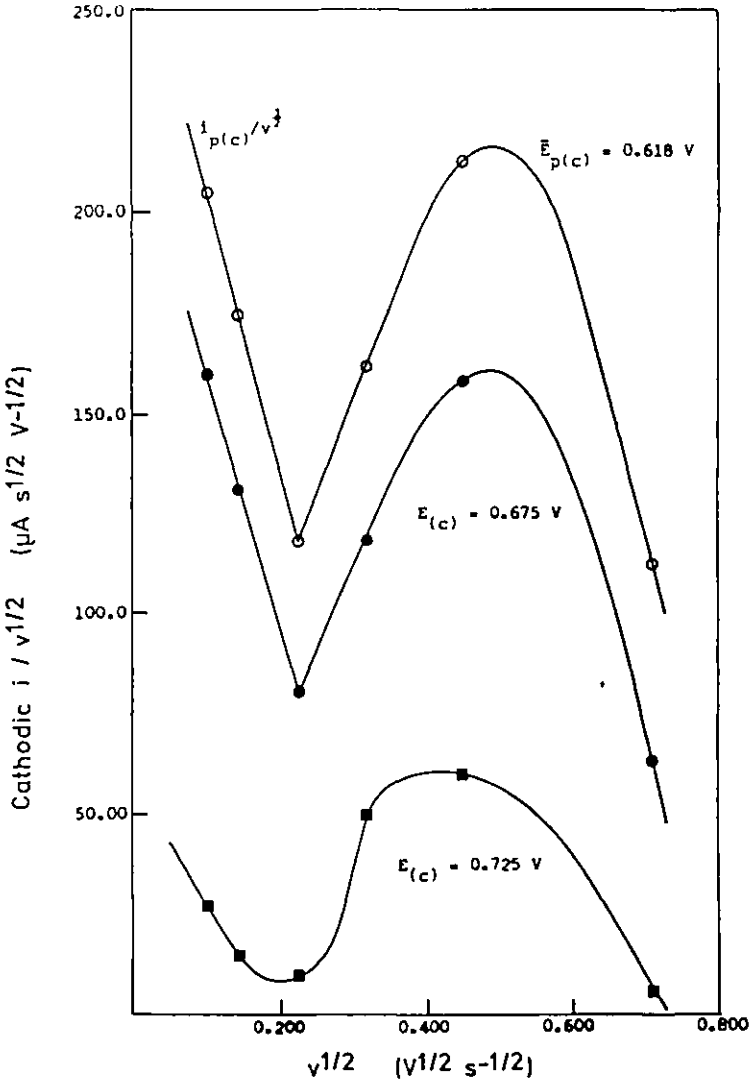

Fig. 5-85 Ir(IV)-Ir(III) Chloroiridate (4.0×10^{-4} mol dm^{-3})/Sodium perchlorate (0.1 M) supporting electrolyte System: Values of current function, $i/v^{\frac{1}{2}}$ (at different potentials along the peak voltammograms), as a function of square root of potential scan rate, $v^{\frac{1}{2}}$. Boron carbide solid electrode was treated by cathodic polarisation (at -1 V) in the sample solution prior to voltammetric scan.

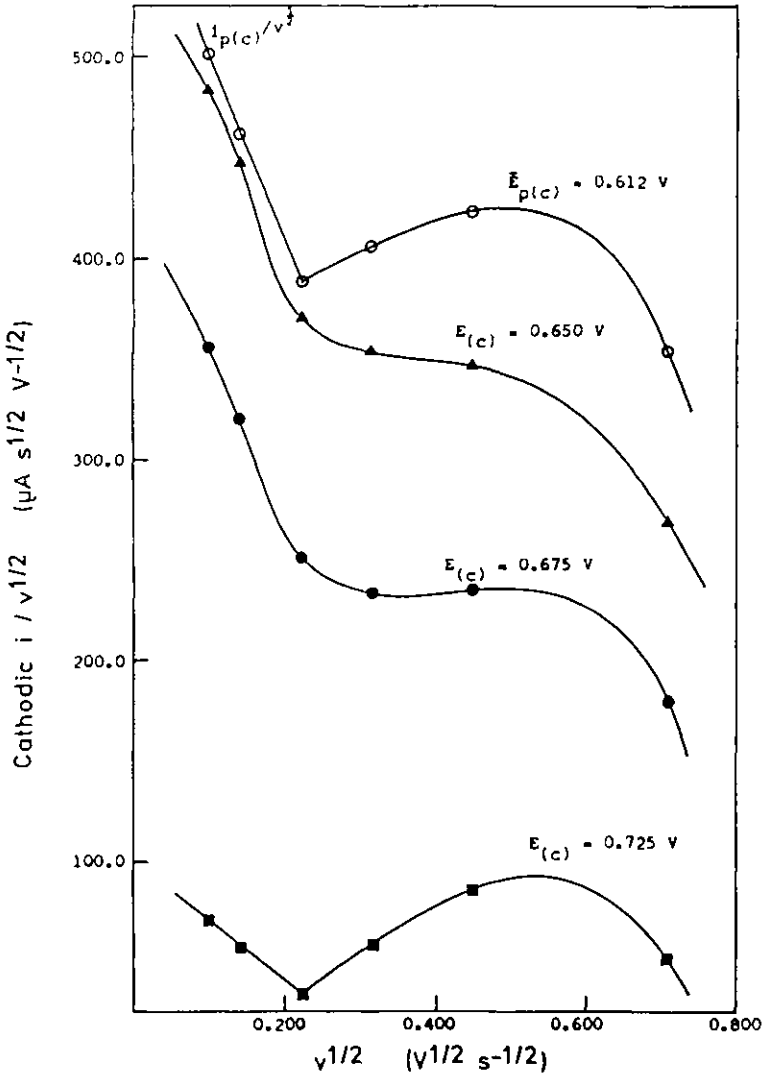

Fig. 5-86 Ir(IV)-Ir(III) Chloroiridate (8.0×10^{-4} mol dm^{-3})/Sodium perchlorate (0.1 M) supporting electrolyte System: Values of current function, $i/v^{\frac{1}{2}}$ (at different potentials along the peak voltammograms), as a function of square root of potential scan rate, $v^{\frac{1}{2}}$. Boron carbide solid electrode was treated by cathodic polarisation (at -1 V) in sample solution prior to voltammetric scan.

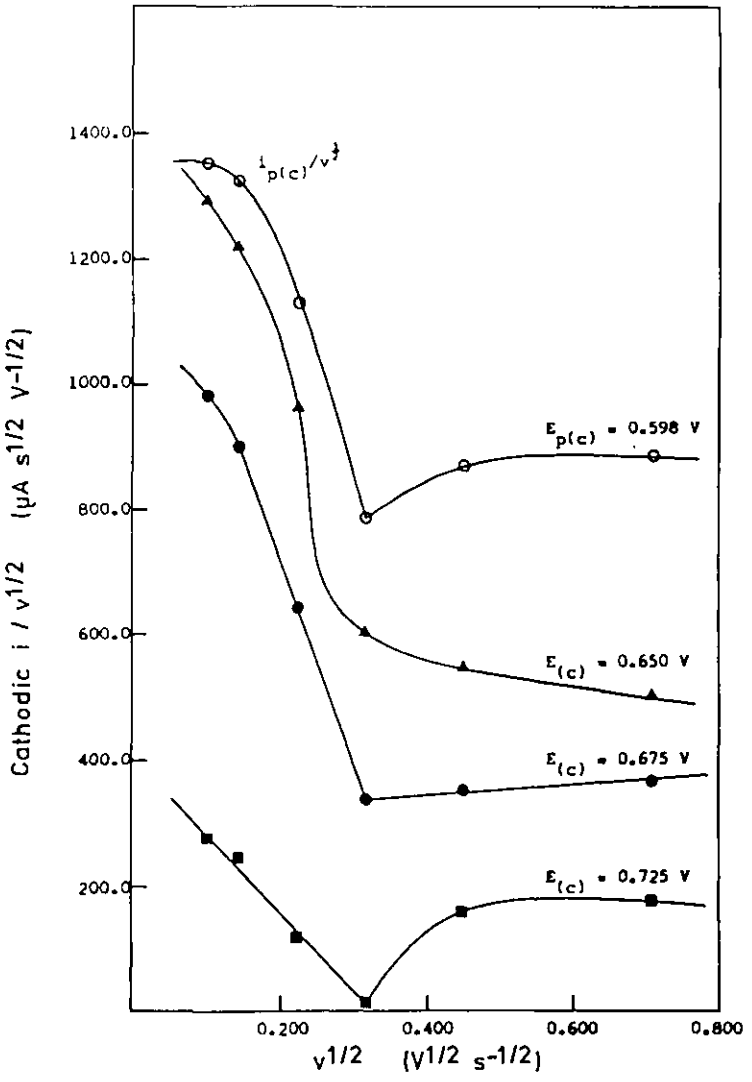

Fig. 5-87 Ir(IV)-Ir(III) Chloroiridate (2.0×10^{-3} mol dm^{-3})/Sodium perchlorate (0.1 M) supporting electrolyte System: Values of current function, $i/v^{\frac{1}{2}}$ (at different potentials along the peak voltammograms), as a function of square root of potential scan rate, $v^{\frac{1}{2}}$. Boron carbide solid electrode was treated by cathodic polarisation (at -1 V) in sample solution prior to voltammetric scan.

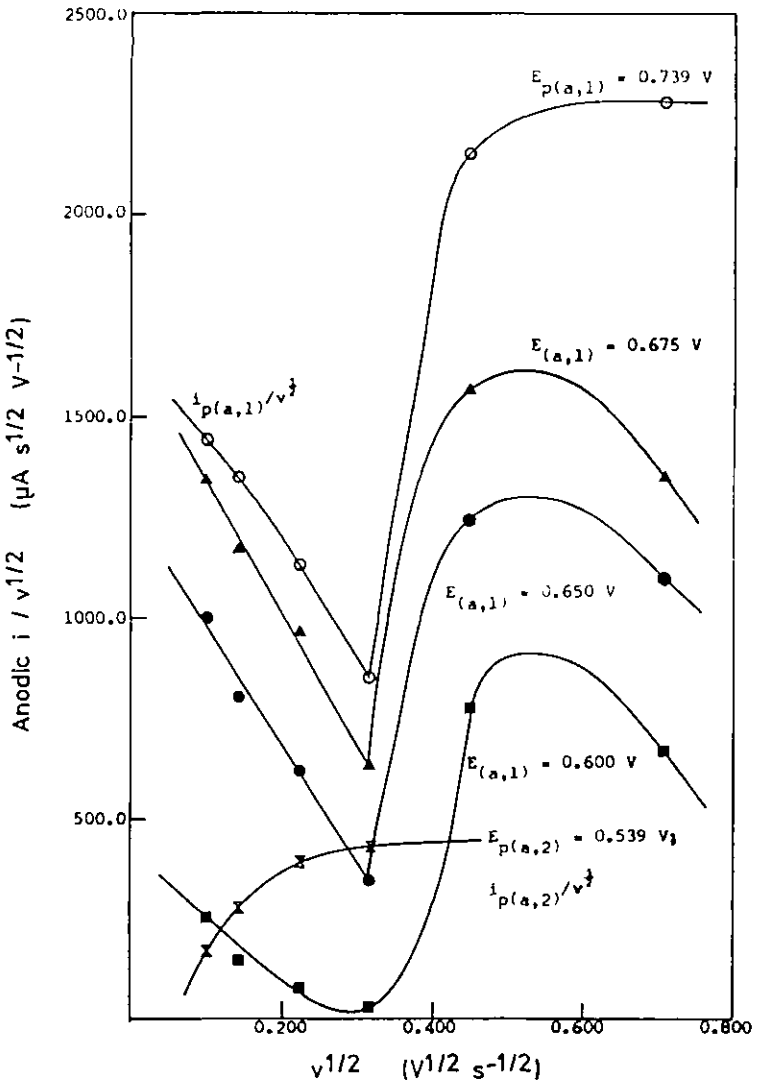

Fig. 5-88 Ir(IV)-Ir(III) Chloroiridate (2.0×10^{-3} mol dm^{-3})/Sodium perchlorate (0.1 M) supporting electrolyte System: Values of anodic current function, $i/v^{\frac{1}{2}}$ (at different potentials along the peak voltammograms), as a function of square root of potential scan rate, $v^{\frac{1}{2}}$. Boron carbide solid electrode was treated by cathodic polarisation (at -1 V) in sample solution prior to voltammetric scan.

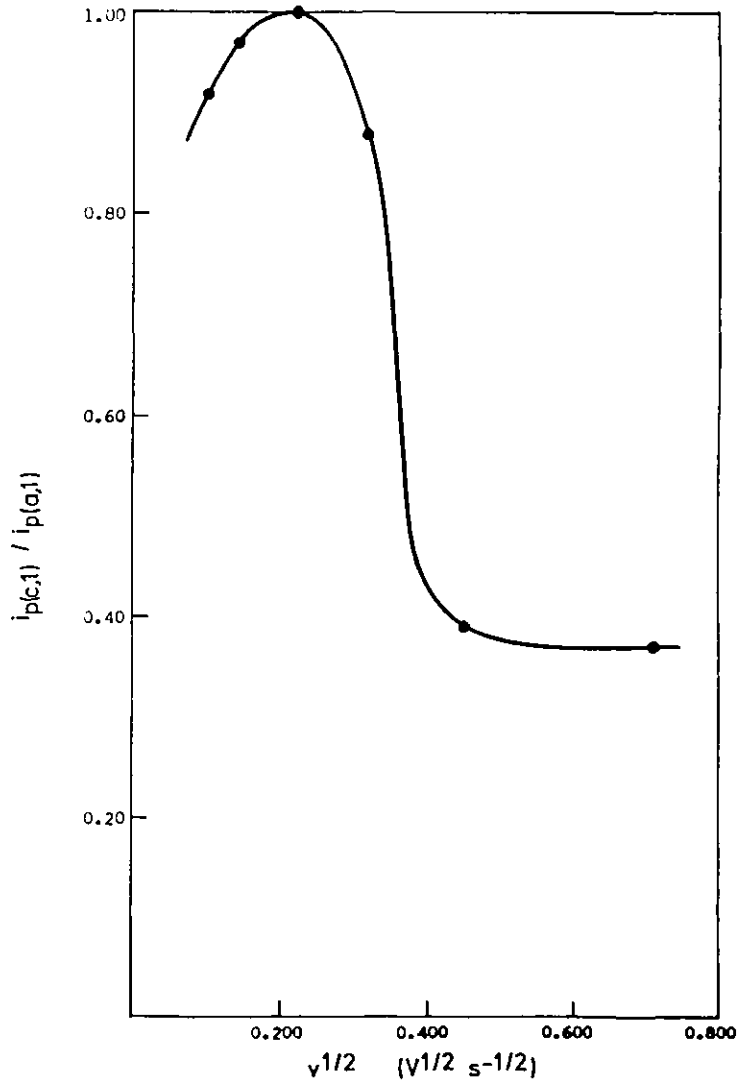

Fig. 5-89 Ir(IV)-Ir(III) Chloroiridate (2.0×10^{-3} mol dm^{-3})/Sodium perchlorate (0.1 M) supporting electrolyte System: Values of ratio of cathodic to anodic peak currents (for the more positive peaks), $i_{p(c,1)}/i_{p(a,1)}$, as a function of square root of potential scan rate, $v^{\frac{1}{2}}$. Boron carbide solid electrode was treated by cathodic polarisation (at -1 V) in sample solution prior to voltammetric scan.

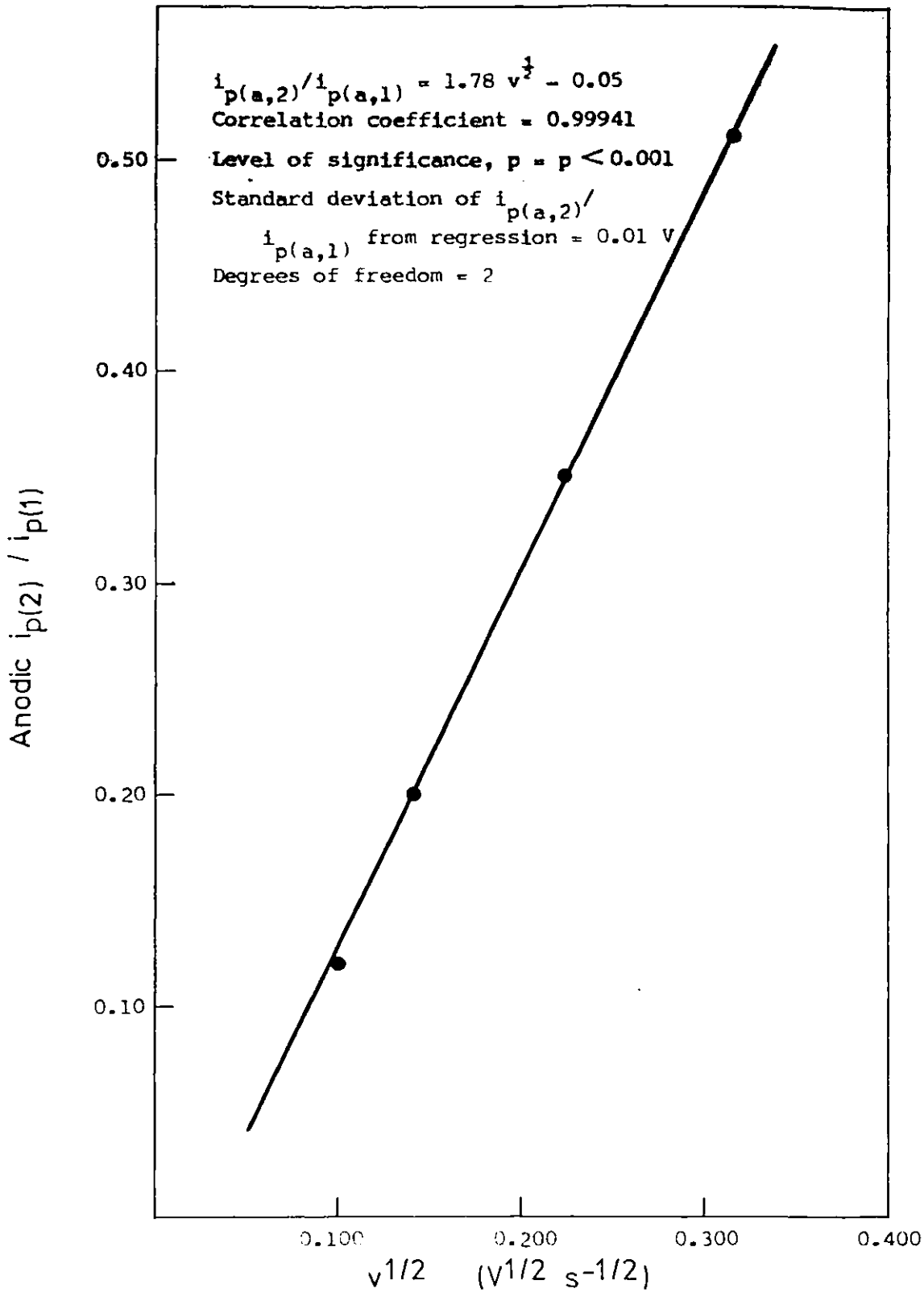

Fig. 5-90 Ir(IV)-Ir(III) Chloroiridate (2.0×10^{-3} mol dm^{-3})/Sodium perchlorate (0.1 M) supporting electrolyte System: Values of ratio of anodic peak currents, $i_{p(a,2)}/i_{p(a,1)}$, as a function of square root of potential scan rate, $v^{\frac{1}{2}}$. Boron carbide solid electrode was treated by cathodic polarisation (at -1 V) in sample solution prior to voltammetric scan.

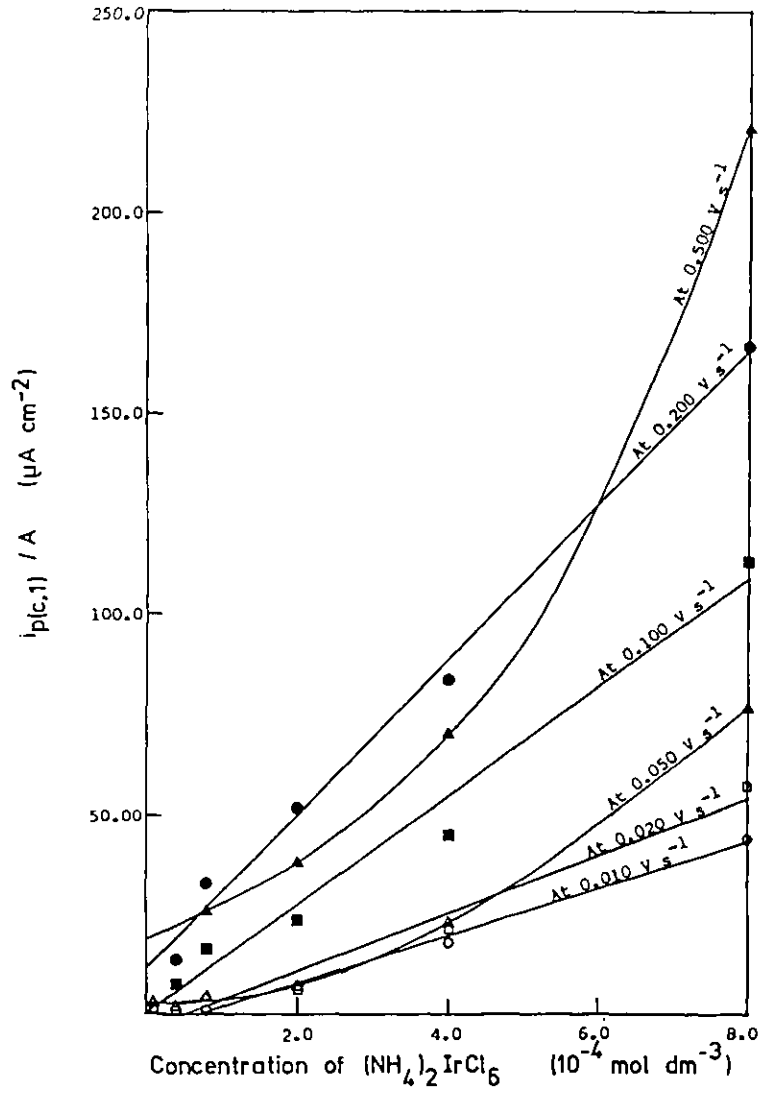

Fig. 5-91 Ir(IV)-Ir(III) Chloroiridate/Sodium perchlorate (0.1 M) supporting electrolyte System: Values of cathodic peak current per unit area, $i_{p(c,1)}/A$, as a function of concentration of ammonium hexachloiridate; at different potential scan rates. Boron carbide solid electrode was treated by cathodic polarisation (at -1 V) in sample solution prior to voltammetric scan.

Fig. 5-91 (continued):-

(a) At 0.010 V s^{-1}:

$i_{p(c,1)}/A = 6.04 \times 10^4 [(NH_4)_2IrCl_6] - 4.70$
Correlation coefficient = 0.99846
Level of significance, $p = 0.001 < p < 0.01$
Standard deviation of $i_{p(c,1)}/A$ from regression = 1.30 μA cm^{-2}
Degrees of freedom = 2

(b) At 0.020 V s^{-1}:

$i_{p(c,1)}/A = 7.26 \times 10^4 [(NH_4)_2IrCl_6] - 3.46$
Correlation coefficient = 0.98498
Level of significance, $p = 0.001 < p < 0.01$
Standard deviation of $i_{p(c,1)}/A$ from regression = 4.77 μA cm^{-2}
Degrees of freedom = 3

(c) At 0.050 V s^{-1}:

$i_{p(c,1)}/A$ is a nonlinear function of $[(NH_4)_2IrCl_6]$.

(d) At 0.100 V s^{-1}:

$i_{p(c,1)}/A = 0.11 + 1.36 \times 10^5 [(NH_4)_2IrCl_6]$
Correlation coefficient = 0.98906
Level of significance, $p = 0.001 < p < 0.01$
Standard deviation of $i_{p(c,1)}/A$ from regression = 7.27 μA cm^{-2}
Degrees of freedom = 3

(e) At 0.200 V s^{-1}:

$i_{p(c,1)}/A = 11.4 + 1.93 \times 10^5 [(NH_4)_2IrCl_6]$
Correlation coefficient = 0.99672
Level of significance, $p = p < 0.001$
Standard deviation of $i_{p(c,1)}/A$ from regression = 5.61 μA cm^{-2}
Degrees of freedom = 3

(f) At 0.500 V s^{-1}:

$i_{p(c,1)}/A$ is a nonlinear function of $[(NH_4)_2IrCl_6]$.

adsorption.

The cathodic peak potential shifted cathodically with increasing sweep rate (Fig. 5-92) or increasing chloroiridate concentration (Fig. 5-94) which indicated a decreasing reversibility in the charge transfer ; as confirmed by Fig. 5-93, where $|E_p - E_{p/2}|$ increased with increasing sweep rate, and Fig. 5-94 where the $|E_p - E_{p/2}|$ value was greater than that for a reversible charge transfer (equation 3-32). Further evidence that the charge transfer of chloroiridate was quasi-reversible is furnished by Figures 5-95 to 5-97.

Figures 5-95 and 5-96 also show that the anodic Peak 2 was affected by the weak adsorption of reductant since the peak potential, $E_{p(a,2)}$, shifted anodically whilst $|E_{p(a,2)} - E_{p(a,2)/2}|$ decreased with increasing sweep rate.

5-1.3.(ii) Summary.

The charge transfer for the d.c. voltammetric reaction

$$IrCl_6^{2-} + e^- \rightleftharpoons IrCl_6^{3-}$$

in sodium perchlorate (0.1 M) supporting electrolyte at a boron carbide solid electrode was significantly improved when the working electrode was electrochemically treated in chloroiridate solution (Fig. 5-78). A grand mean value for αn of 0.85 ± 0.04 (20 degrees of freedom) was obtained for chloroiridate (4.0×10^{-5} to 8.0×10^{-4} mol dm^{-3}). The half-wave potential shifted anodically in an extremely non-linear fashion from 0.637 V to a maximum of 0.660 V (vs. SCE) with increasing $(\text{ionic strength})^{\frac{1}{2}}$ as the chloroiridate concentration was increased (Fig. 5-80); thus suggesting that the e.a.s. was anionic and very weakly adsorbed. The dependence of limiting current density on the chloroiridate concentration was linear with a correlation coefficient better than that at the 0.001 level of significance (Fig. 5-81).

Linear sweep and cyclic voltammetric studies revealed that the quasi-reversible charge transfer was complicated by a catalytic reaction and weak adsorption as well as the weak adsorption of the product of a following chemical reaction.

5-1.4 Spectrophotometry of chloroiridate

The absorption spectra of chloroiridate were similar irrespective of the supporting electrolyte employed (Fig. 5-98) and compare well with the spectrum obtained by Jorgensen[5.1] (Fig. 5-98, inset).

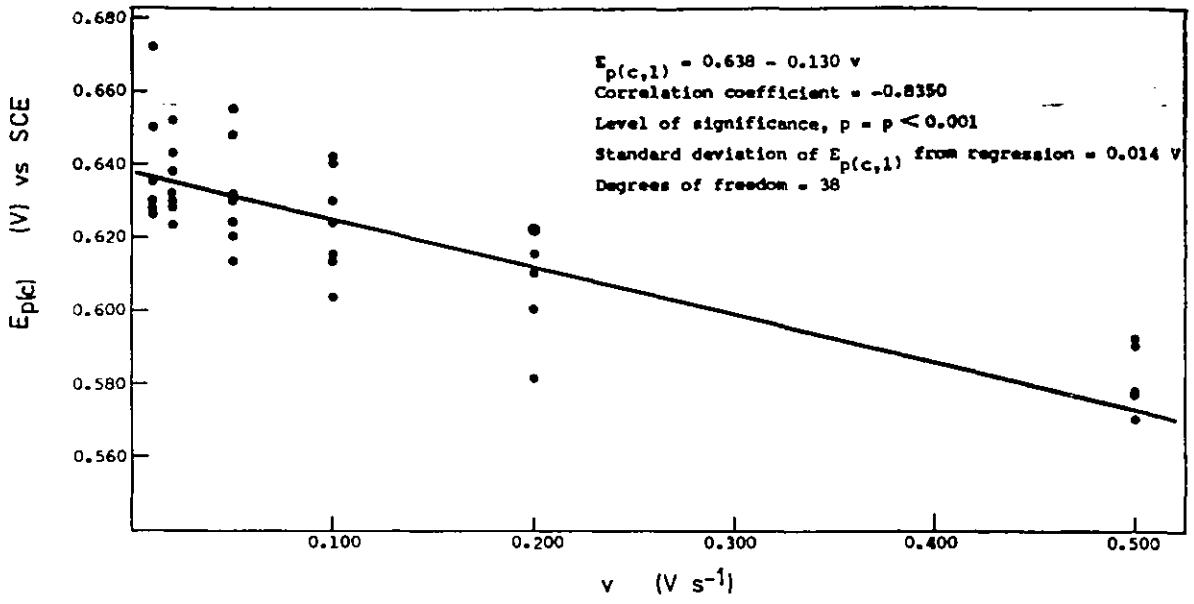

Fig. 5-92 Ir(IV)-Ir(III) Chloroiridate/Sodium perchlorate (0.1 M) supporting electrolyte System: Values of cathodic peak potential, $E_{p(c)}$, as a function of potential scan rate, v; at ammonium hexachloroiridate concentrations of 1.0×10^{-5} to 2.0×10^{-3} mol dm^{-3}. Boron carbide solid electrode was treated by cathodic polarisation (at -1 V) in the sample solution prior to voltammetric scan.

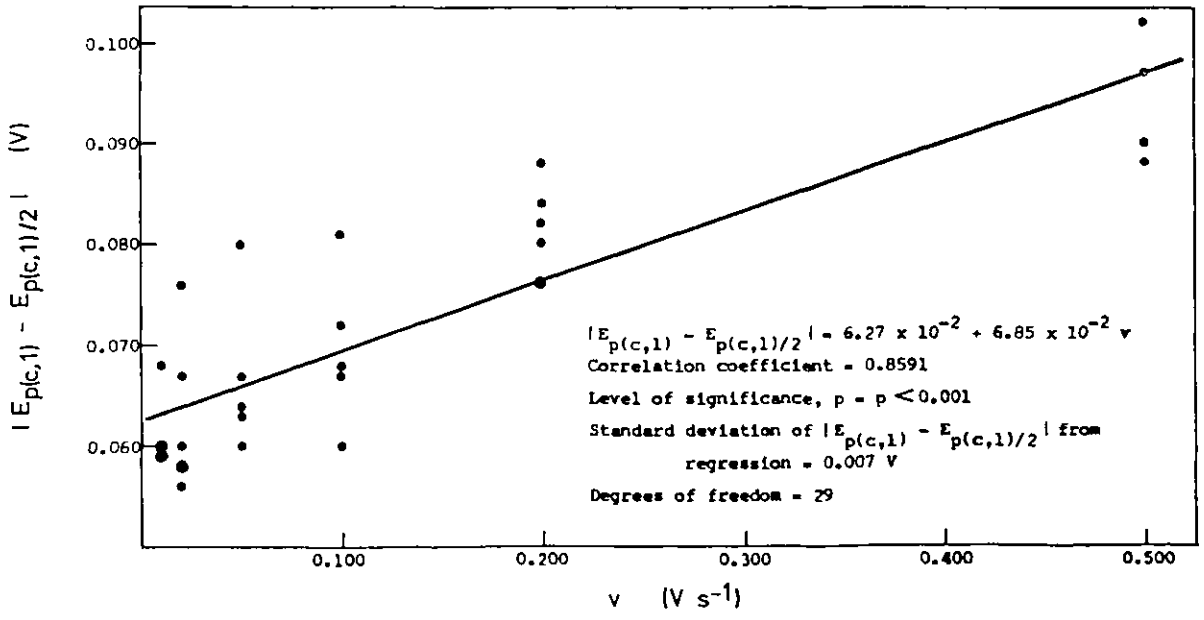

Fig. 5-93 Ir(IV)-Ir(III) Chloroiridate/Sodium perchlorate (0.1 M) supporting electrolyte System: Values of difference between cathodic peak and half-peak potentials, $|E_{p(c,1)} - E_{p(c,1)/2}|$, as a function of potential scan rate, v; at ammonium hexachloroiridate concentrations of 1.0×10^{-5} to 2.0×10^{-3} mol dm^{-3}. Boron carbide solid electrode was treated by cathodic polarisation (at -1 V) in sample solution prior to voltammetric scan.

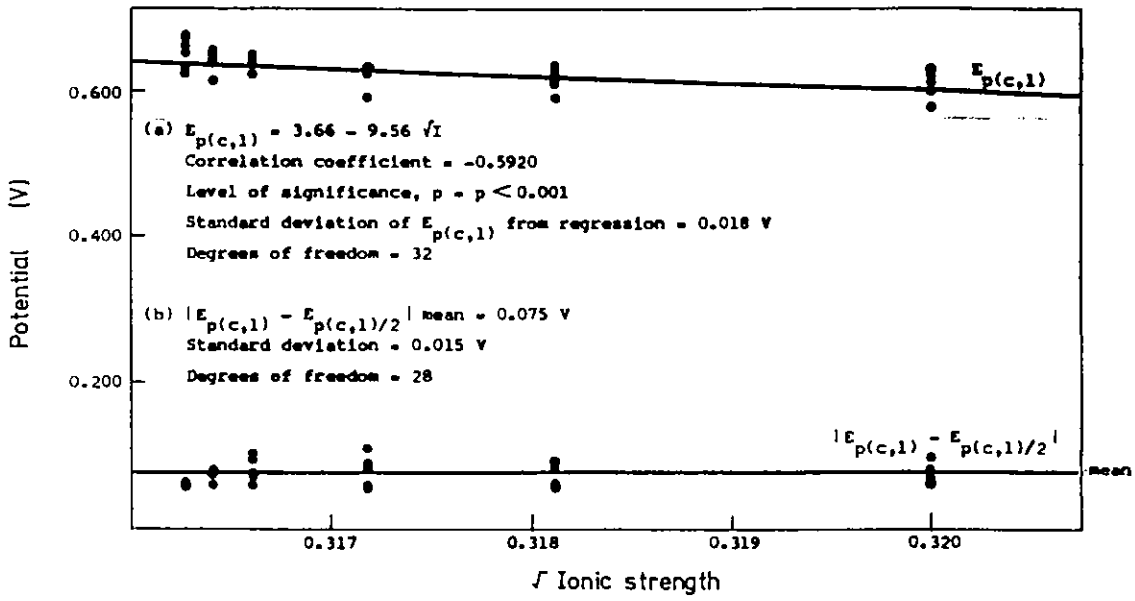

Fig. 5-94 Ir(IV)-Ir(III) Chloroiridate/Sodium perchlorate (0.1 M) supporting electrolyte System: Values of cathodic peak potential, $E_{p(c,1)}$, and difference between cathodic peak and half-peak potential, $|E_{p(c,1)} - E_{p(c,1)/2}|$, as a function of square root of total ionic strength (where the concentration of ammonium hexachloroiridate was varied), $\sqrt{I}$; at potential scan rates of 0.010 V s^{-1} to 0.500 V s^{-1}. Boron carbide solid electrode was treated by cathodic polarisation (at -1 V) in sample solution prior to voltammetric scan.

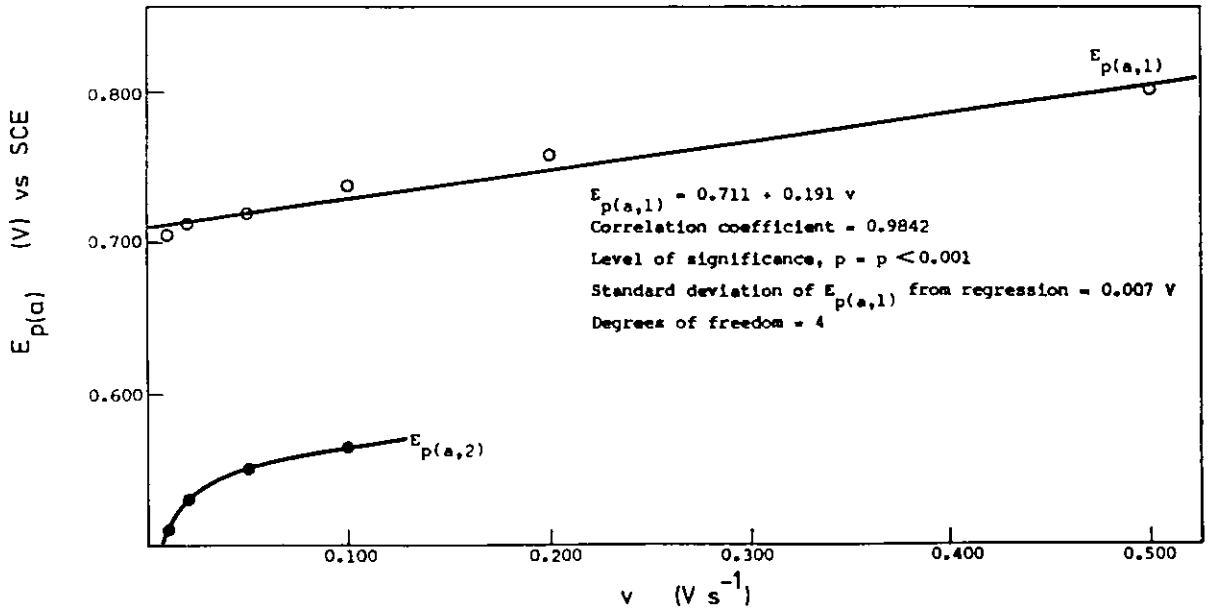

Fig. 5-95 Ir(IV)-Ir(III) Chloroiridate (2.0×10^{-3} mol dm^{-3}/Sodium perchlorate (0.1 M) supporting electrolyte System: Values of anodic peak potentials for the more positive and less positive peaks, $E_{p(a,1)}$ and $E_{p(a,2)}$ respectively, as a function of potential scan rate, v. Boron carbide solid electrode was treated by cathodic polarisation (at -1 V) in sample solution prior to cyclic voltammetry.

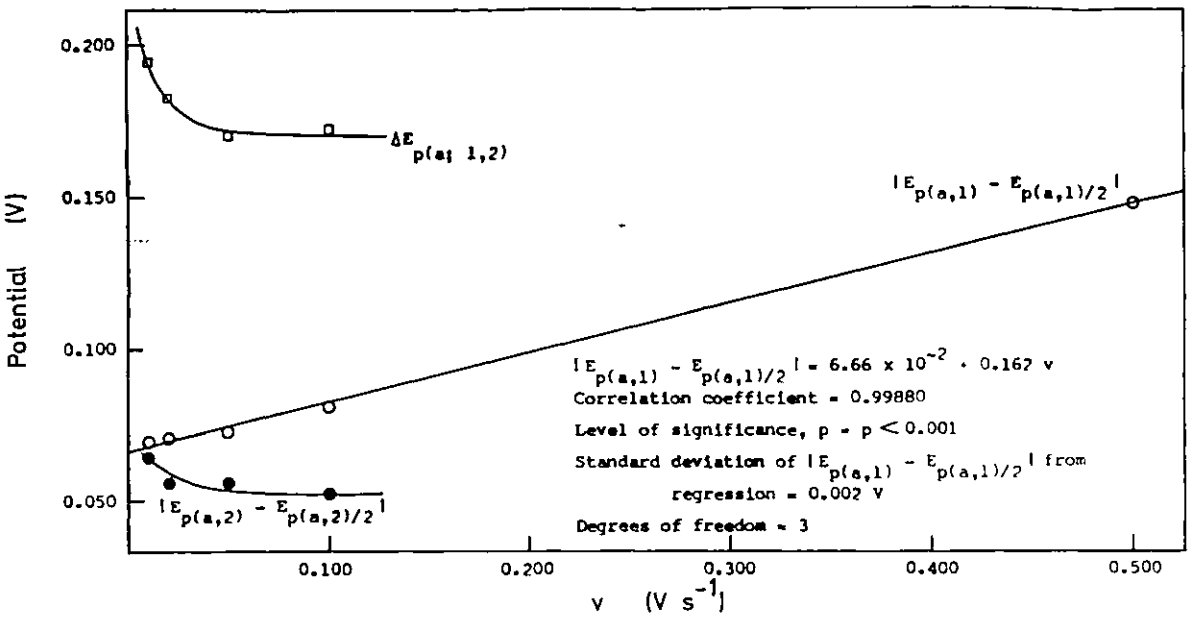

Fig. 5-96 Ir(IV)-Ir(III) Chloroiridate (2.0×10^{-3} mol dm^{-3}/Sodium perchlorate (0.1 M) supporting electrolyte System: Values of difference between anodic peak potentials, $\Delta E_{p(a;\,1,2)}$, difference between anodic peak and half-peak potentials, $|E_{p(a,1)} - E_{p(a,1)/2}|$ and $|E_{p(a,2)} - E_{p(a,2)/2}|$, as a function of potential scan rate, v. Boron carbide solid electrode was treated by cathodic polarisation (at -1 V) in sample solution prior to cyclic voltammetry.

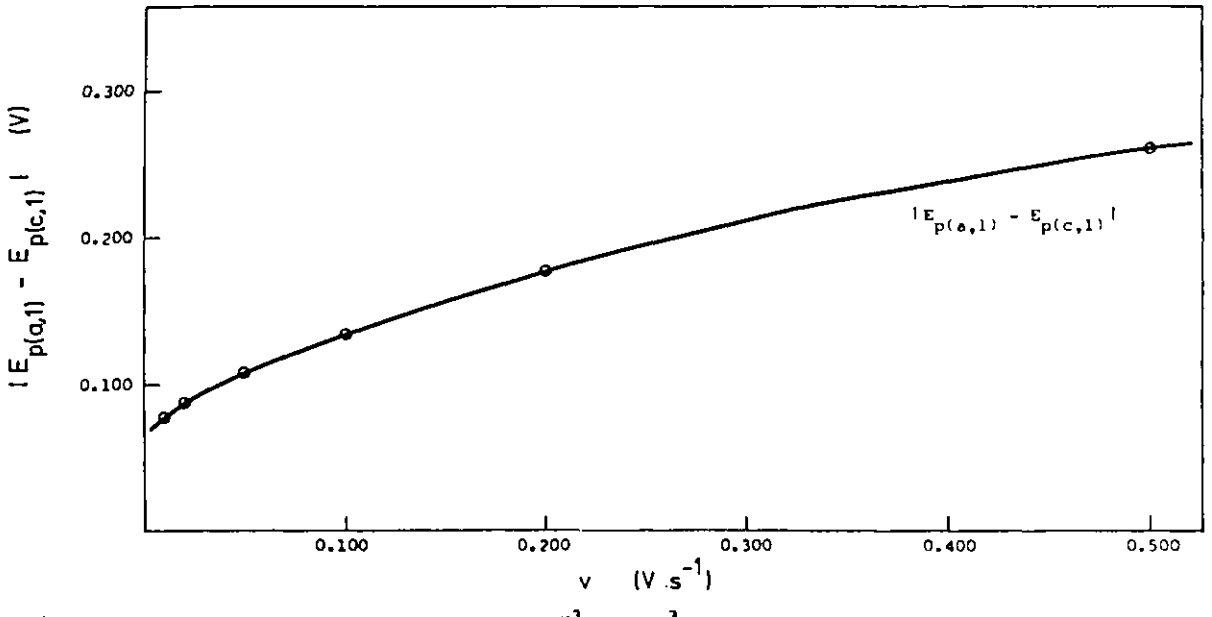

Fig. 5-97 Ir(IV)-Ir(III) Chloroiridate (2.0×10^{-3} mol dm^{-3}/Sodium perchlorate (0.1 M) supporting electrolyte System: Values of difference between anodic and cathodic peak potentials for the more positive peak, $|E_{p(a,1)} - E_{p(c,1)}|$, as a function of potential scan rate, v. Boron carbide solid electrode was treated by cathodic polarisation (at -1 V) in sample solution prior to cyclic voltammetry.

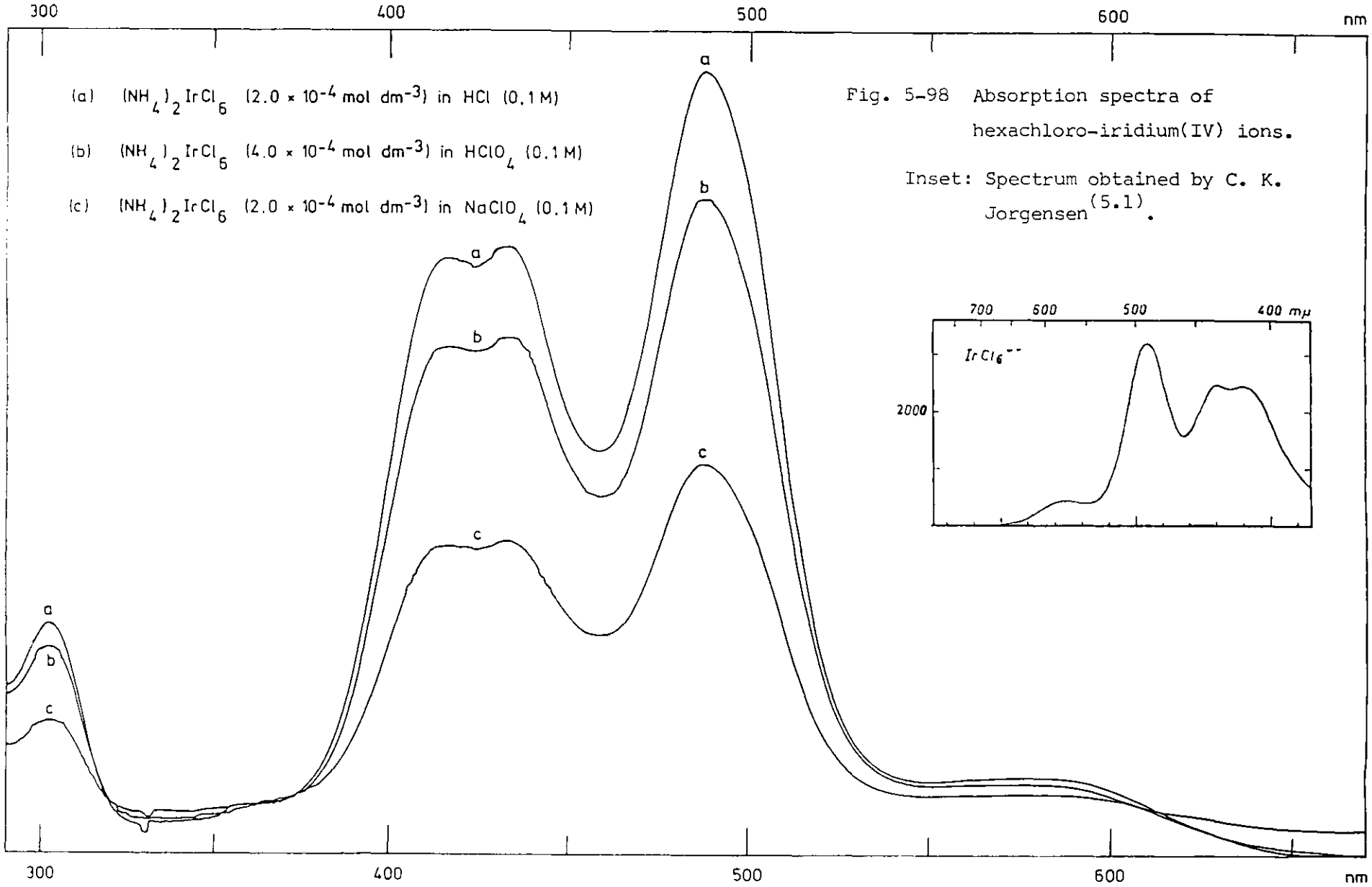

Fig. 5-98 Absorption spectra of hexachloro-iridium(IV) ions.

Inset: Spectrum obtained by C. K. Jorgensen[5.1].

5-1.5 Ir(IV) perchlorate system

5-1.5.(i) D.c. voltammetry.

Typical d.c. voltammograms of Ir(IV) perchlorate (1.0×10^{-4} mol dm^{-3}) in perchloric acid (0.1 M) supporting electrolyte obtained at boron carbide, boron carbide/carbon composite, and graphite solid electrodes are presented in Figures 5-99 and 5-100. It can be clearly seen that Wave 3 obtained at the boron carbide electrode $B_{4.05}C$ (Fig. 5-99, a) was split into two waves (Waves 3 and 4) at boron carbide/carbon composite solid electrodes of higher carbon contents (e.g. $B_{3.38}C$; Fig. 5-99, f); with Wave 3 gaining dominance over Wave 4 as the carbon content increased (Figures 5-99, c-f, and 5-100, g-k). The voltammetric curve obtained at the graphite solid electrode also shows that Wave 3 dominated Wave 4 (Fig. 5-100, l), but an extra wave, ß, was also present. When the d.c. voltammograms obtained with a slower scan rate (0.001 V s^{-1}) at a selection of these electrodes (Fig. 5-101) are compared with the corresponding curves obtained with the faster scan rate of 0.002 V s^{-1} (Figures 5-99 and 5-100), it can be seen that Wave 3 became less prominent at the slower scan rate; thus suggesting that Wave 3 was an adsorption wave. Furthermore, Wave ß at the graphite electrode was also an adsorption wave because it was not exhibited when the slower scan rate was used.

The values of αn as a function of boron:carbon ratio are plotted in Fig. 5-102; consisting of values of interpretable waves. The value of αn for: Wave 1, $\alpha n_{(1)}$, varied within the range 1.09 to 1.81; Wave 3, $\alpha n_{(3)}$, varied within the range 1.68 to 3.06; Wave 4, $\alpha n_{(4)}$, varied within the range 3.37 to 4.85. Little emphasis, however, can be placed on these actual αn values because of the presence of adsorption.

The half-wave potentials, or "peak" potentials where peaks were exhibited rather than waves, generally remained relatively constant irrespective of the boron:carbon ratio of the working electrode (Fig. 5-103). The only exception was the half-wave potential of Wave 3, $E_{\frac{1}{2}(3)}$, which was more anodic at lower B:C ratios; reflecting the resulting prominence of Wave 3.

5-1.5.(i).a Boron carbide solid electrode $B_{4.05}C$

D.c. voltammograms obtained over a concentration range of Ir(IV) perchlorate in perchloric acid (0.1 M) supporting electrolyte show that Wave 2 and the maximum on Wave 3 disappeared at higher concentrations of

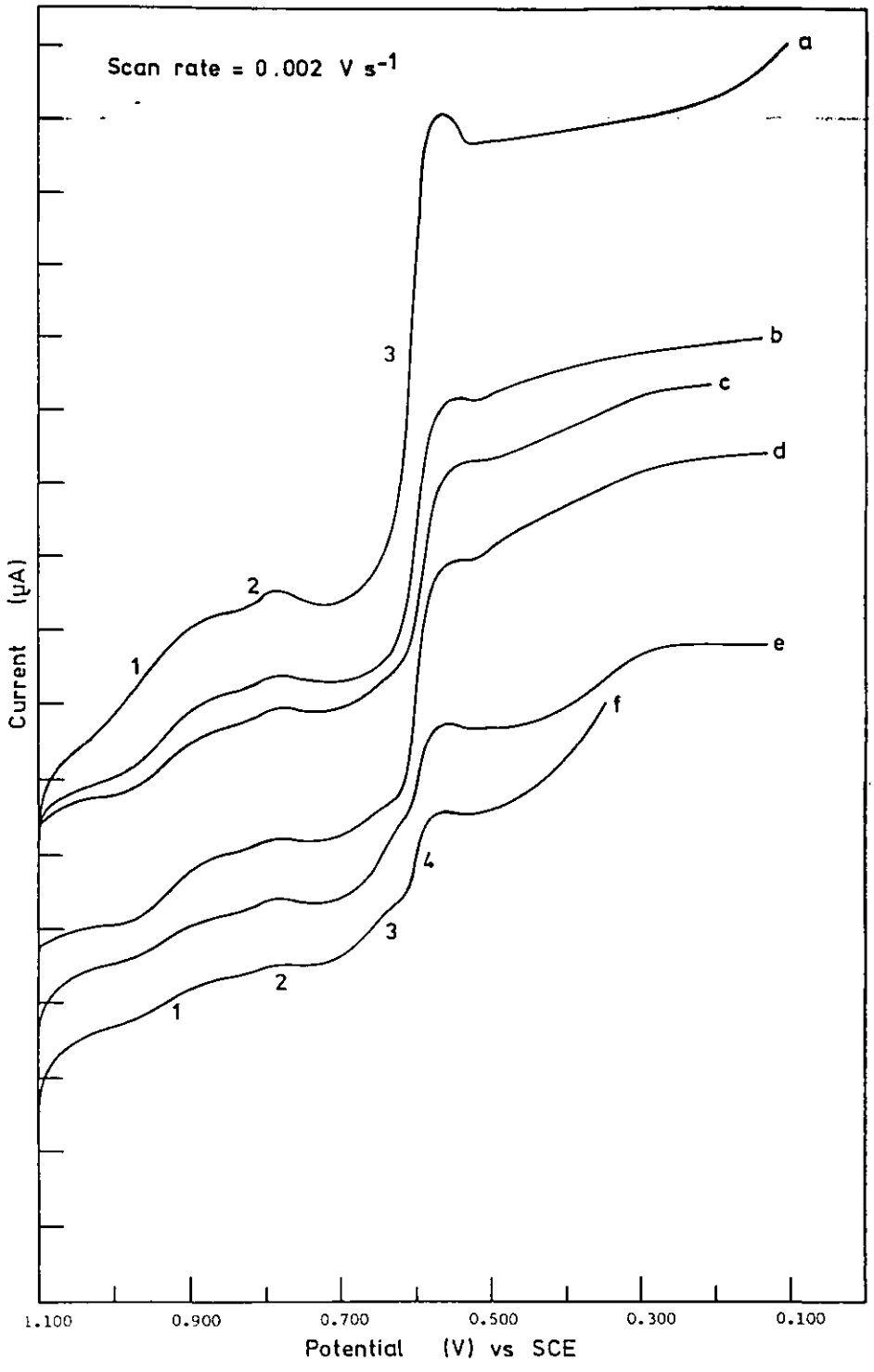

Fig. 5-99 Ir(IV) perchlorate (1.0×10^{-4} mol dm^{-3})/Perchloric acid (0.1 M) supporting electrolyte System: D.c. voltammograms obtained at boron carbide solid electrodes, (a) $B_{4.05}C$ and (b) $B_{3.86}C$; and boron carbide/carbon composite solid electrodes, (c) $B_{3.77}C$, (d) $B_{3.69}C$, (e) $B_{3.53}C$, and (f) $B_{3.38}C$. The current sensitivities were: (a) to (d) 5 μA per division; (e) and (f) 10 μA per division.

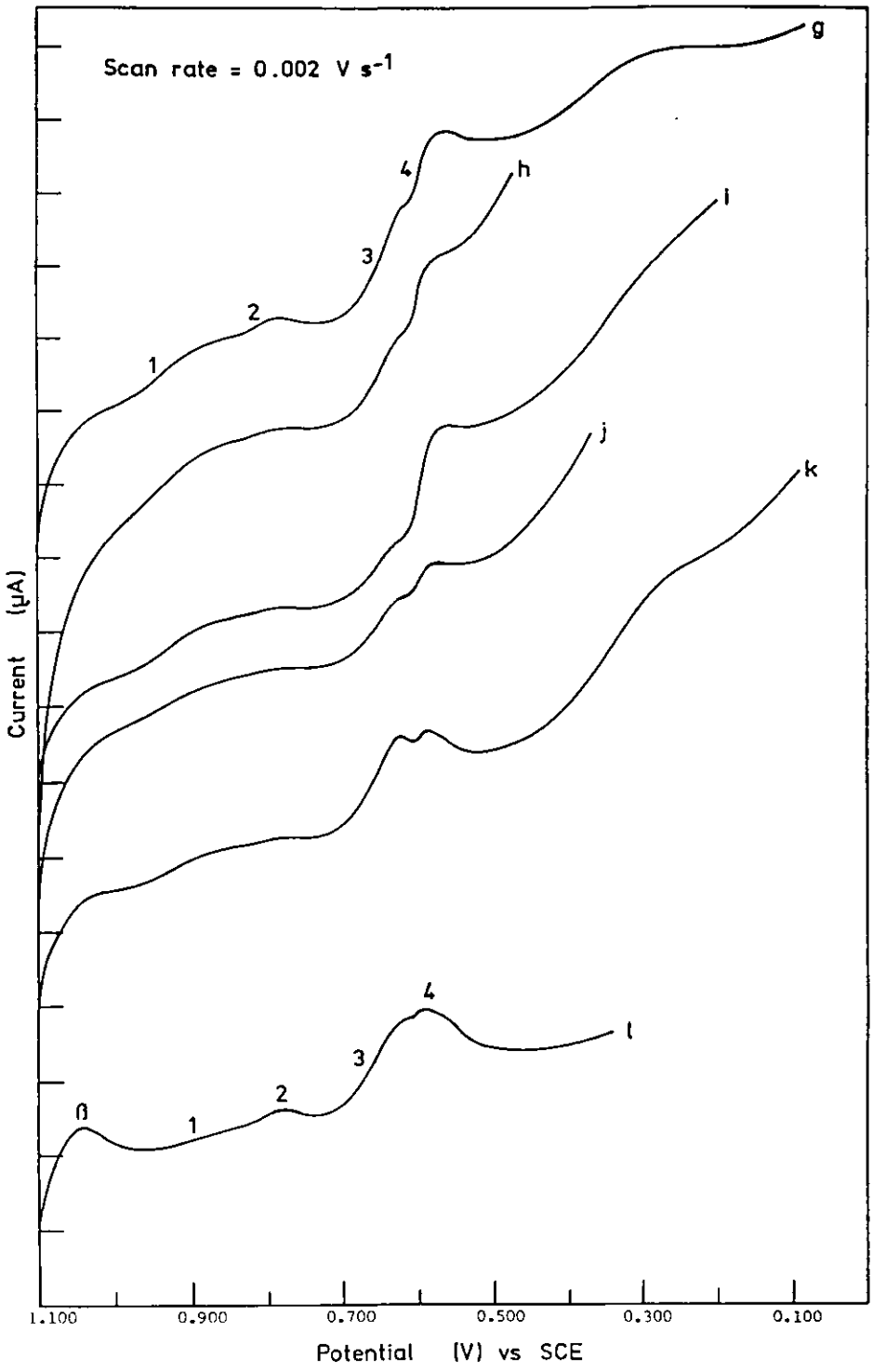

Fig. 5-100 Ir(IV) perchlorate (1.0×10^{-4} mol dm^{-3})/Perchloric acid (0.1 M) supporting electrolyte System: D.c. voltammograms obtained at boron carbide/carbon composite solid electrodes, (g) $B_{3.24}C$, (h) $B_{3.11}C$, (i) $B_{2.98}C$, (j) $B_{2.76}C$, and (k) $B_{2.56}C$; and graphite solid electrode, (l). The current sensitivities were: (g) to (i) plus (l) 10 μA per division; (j) and (k) 20 μA per division.

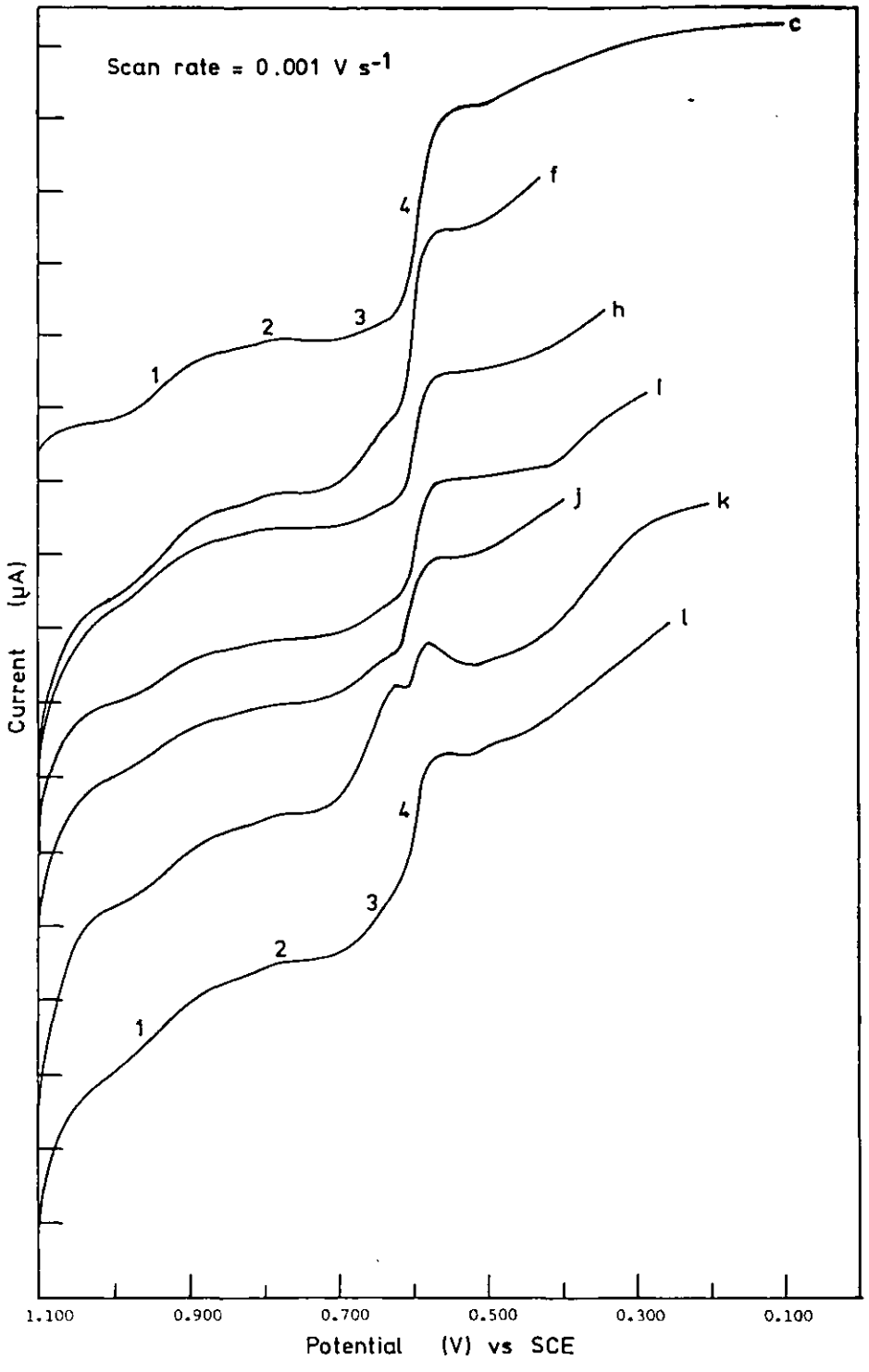

Fig. 5-101 Ir(IV) perchlorate (1.0×10^{-4} mol dm^{-3})/Perchloric acid (0.1 M) supporting electrolyte System: D.c. voltammograms obtained at boron carbide/carbon composite solid electrodes, (c) $B_{3.77}C$, (f) $B_{3.38}C$, (h) $B_{3.11}C$, (i) $B_{2.98}C$, (j) $B_{2.76}C$, and (k) $B_{2.56}C$; and graphite solid electrode, (l). The current sensitivities were: (c), (f), and (l) 5 μA per division; (h) to (k) 10 μA per division.

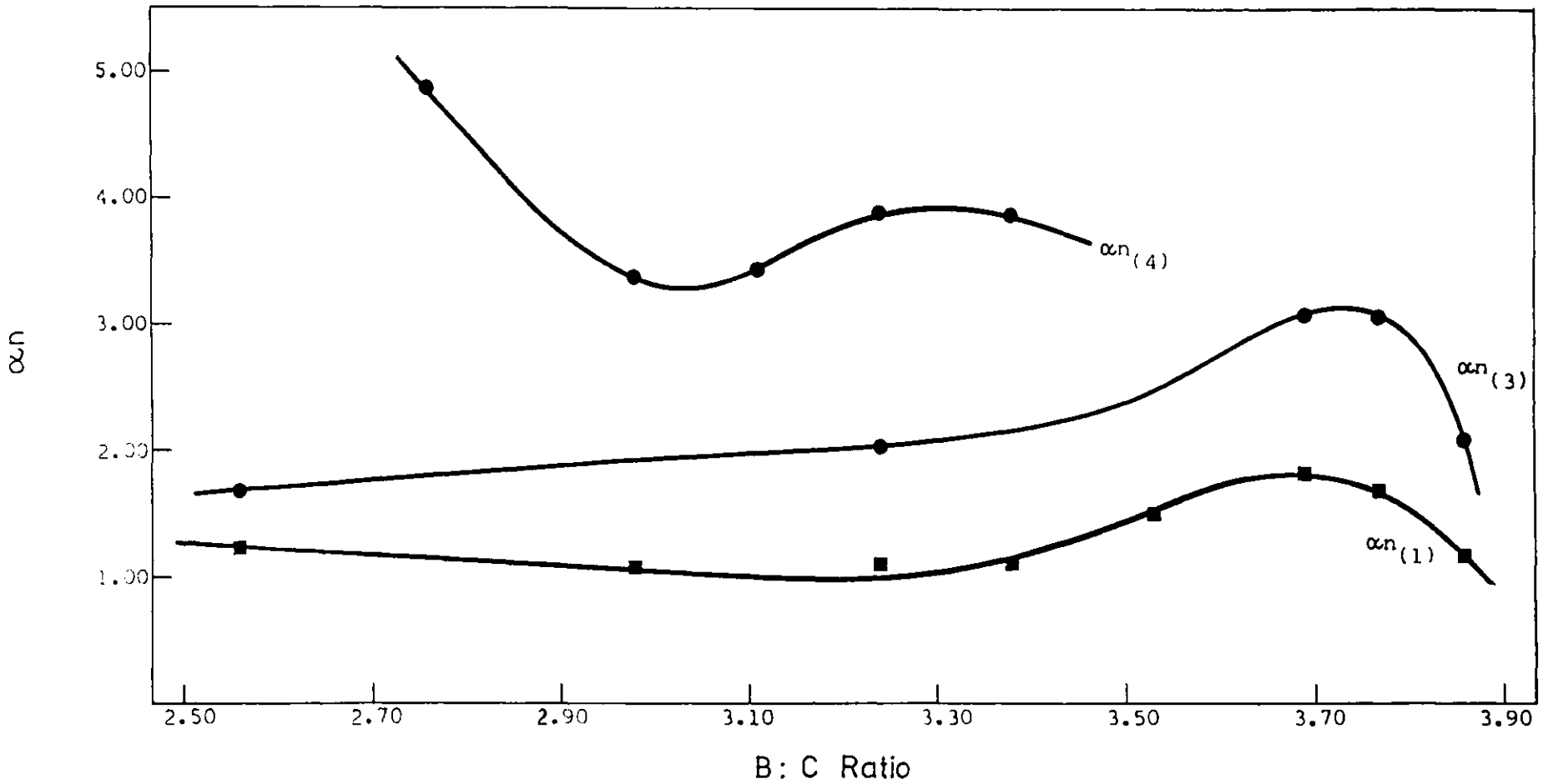

Fig. 3-102 Ir(IV) Perchlorate (1.0×10^{-4} mol dm^{-3})/Perchloric acid (0.1 M) supporting electrolyte System: Values of αn for electrochemical reduction as a function of boron to carbon ratio of boron carbide/carbon composite solid electrodes.

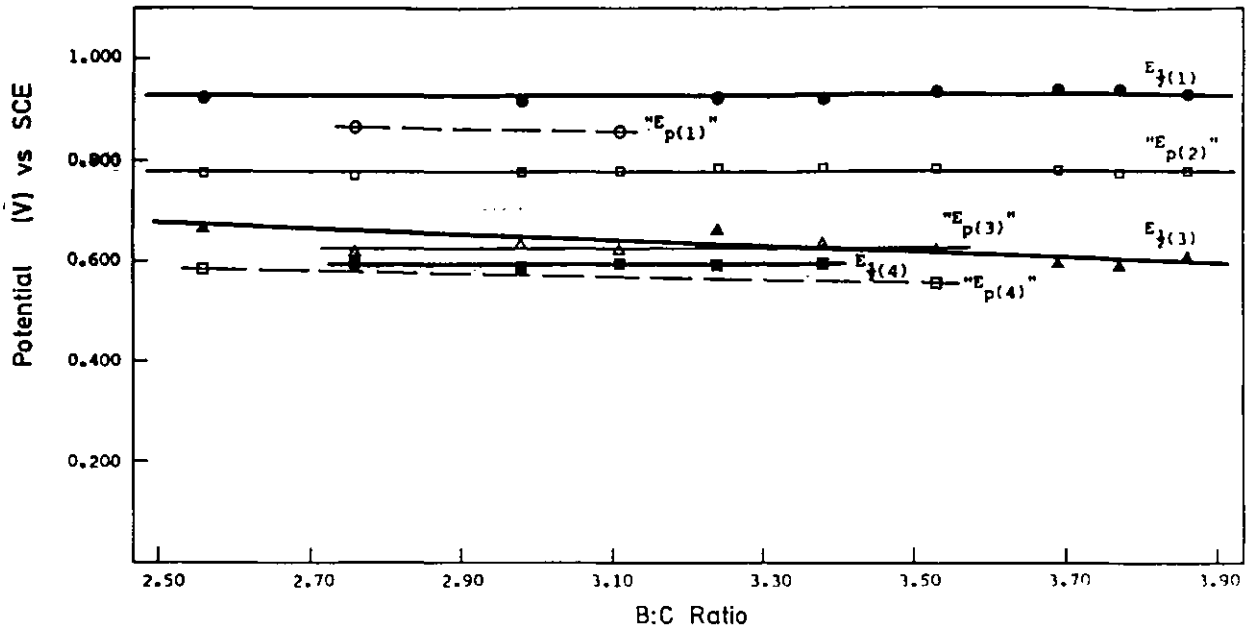

Fig. 5-103 Ir(IV) Perchlorate (1.0×10^{-4} mol dm^{-3})/Perchloric acid (0.1 M) supporting electrolyte System: Values of half-wave potential, $E_{\frac{1}{2}}$, or "peak potential", "E_p" (when the voltammogram exhibits a peak rather than a wave), as a function of boron to carbon ratio of boron carbide/carbon composite solid electrodes.

(a) $E_{\frac{1}{2}(1)}$ mean = 0.927 V
Standard deviation = 0.008 V
Degrees of freedom = 7

(b) "$E_{p(1)}$" is plotted when the voltammogram exhibits a peak rather than a wave (as in (a)).

(c) "$E_{p(2)}$" mean = 0.776 V
Standard deviation = 0.005 V
Degrees of freedom = 9

(d) $E_{\frac{1}{2}(3)} = 0.834 - 6.24 \times 10^{-2}$ (B:C)
Correlation coefficient = -0.88111
Level of significance, $p = 0.02 < p < 0.05$
Standard deviation of $E_{\frac{1}{2}(3)}$ from regression = 0.021 V
Degrees of freedom = 3

(e) "$E_{p(3)}$" is plotted when the voltammogram exhibits a peak rather than a wave (as in (d)):

"$E_{p(3)}$" mean = 0.624 V
Standard deviation = 0.007 V
Degrees of freedom = 4

(f) $E_{\frac{1}{2}(4)}$ mean = 0.591 V
Standard deviation = 0.002 V
Degrees of freedom = 4

(g) "$E_{p(4)}$" is plotted when the voltammogram exhibits a peak rather than a wave (as in (f)).

e.a.s. (Fig. 5-104). This signifies that Wave 2 was an adsorption wave and Wave 3 was a diffusion wave complicated by weak adsorption. The effect of Ir(IV) perchlorate concentration on αn values is presented in Fig. 5-105 which shows that the range of αn values for Wave 1 was 0.94-1.42 ± 0.07 (17 degrees of freedom) and Wave 3 was 1.36-2.98 ± 0.10 (23 degrees of freedom). The variation of half-wave potentials with $(\text{ionic strength})^{\frac{1}{2}}$, as the Ir(IV) perchlorate concentration was increased, is shown in Fig. 5-106 where the range of $E_{\frac{1}{2}(1)}$ was 0.915-0.958 V (vs. SCE) ± 0.003 V (16 degrees of freedom) and $E_{\frac{1}{2}(3)}$ was 0.598-0.672 V (vs. SCE) ± 0.001 V (23 degrees of freedom). Fig. 5-107 illustrates the linear dependence of limiting current density on Ir(IV) perchlorate concentration for Wave 1 and Wave 3 (when the maximum was excluded by the usual method).

Typical voltammograms of Ir(IV) perchlorate (1.0×10^{-4} mol dm^{-3}) in a concentration range of perchloric acid supporting electrolyte show that the maximum on Wave 3 disappeared at higher perchloric acid concentrations (Fig. 5-108). The variation of αn values with increasing concentration of perchloric acid supporting electrolyte is shown in Fig. 5-109. Irrespective of the two scan rates, αn for Wave 1 remained relatively similar ($\alpha n_{(1)}$ grand mean = 1.14 ± 0.11, 17 degrees of freedom). For Wave 3, however, $\alpha n_{(3)}$ was smaller at high perchloric acid concentration; the trends being similar for the two scan rates.

Plots of half-wave potentials and peak potentials (where a peak was exhibited rather than a wave) against $(\text{ionic strength})^{\frac{1}{2}}$ show that the potentials shifted anodically as the perchloric acid concentration was increased (Fig. 5-110). This seems to suggest that the e.a.s. was anionic despite the result from paper electrophoresis (section 4-12.3) which showed that the Ir(IV) perchlorate migrated towards the cathode and, therefore, was cationic. Furthermore, the difference in potentials between the waves narrowed with increasing ionic strength; albeit to different degrees (Fig. 5-110) because the anodic shift, in ascending order, was $E_{\frac{1}{2}(1)} < "E_{p(2)}" < E_{\frac{1}{2}(3)}$.

An explanation for the apparent discrepancy of the anodic shift in potentials with increasing ionic strength despite a cationic e.a.s. might be the decrease in the strength of adsorption of reactant with increasing perchloric acid concentration. Thus the waves which were initially shifted cathodically by the adsorption of reactant were merely gradually returning to the potentials corresponding to pure diffusion control as the adsorption effect was reduced. Support for this hypo-

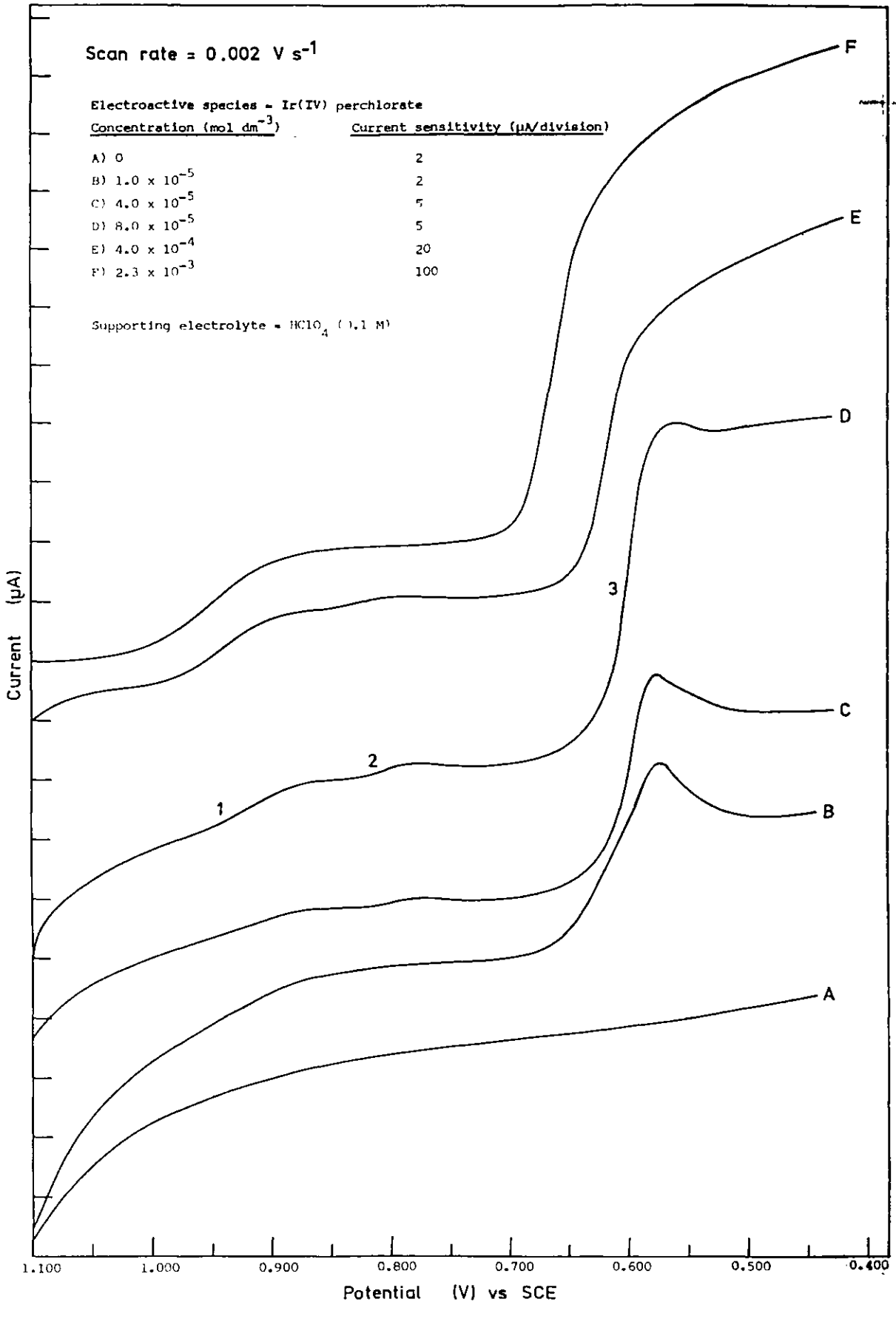

Fig. 5-104 D.c. voltammograms obtained at the boron carbide solid electrode $B_{4.05}C$ for a concentration range of Ir(IV) perchlorate.

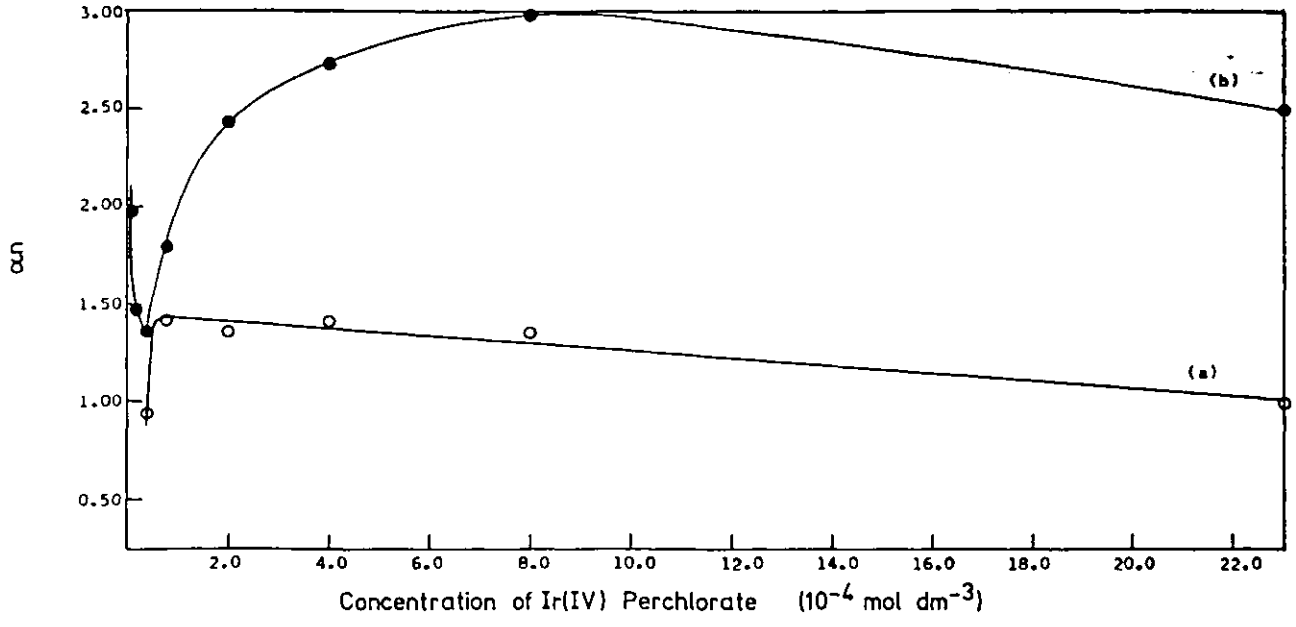

Fig. 5-105 Ir(IV) Perchlorate/Perchloric acid (0.1 M) supporting electrolyte System: Values of αn as a function of concentration of Ir(IV) Perchlorate. D. C. voltammetric performance at boron carbide solid electrode, where (a) is the first cathodic wave and (b) is the third cathodic wave.

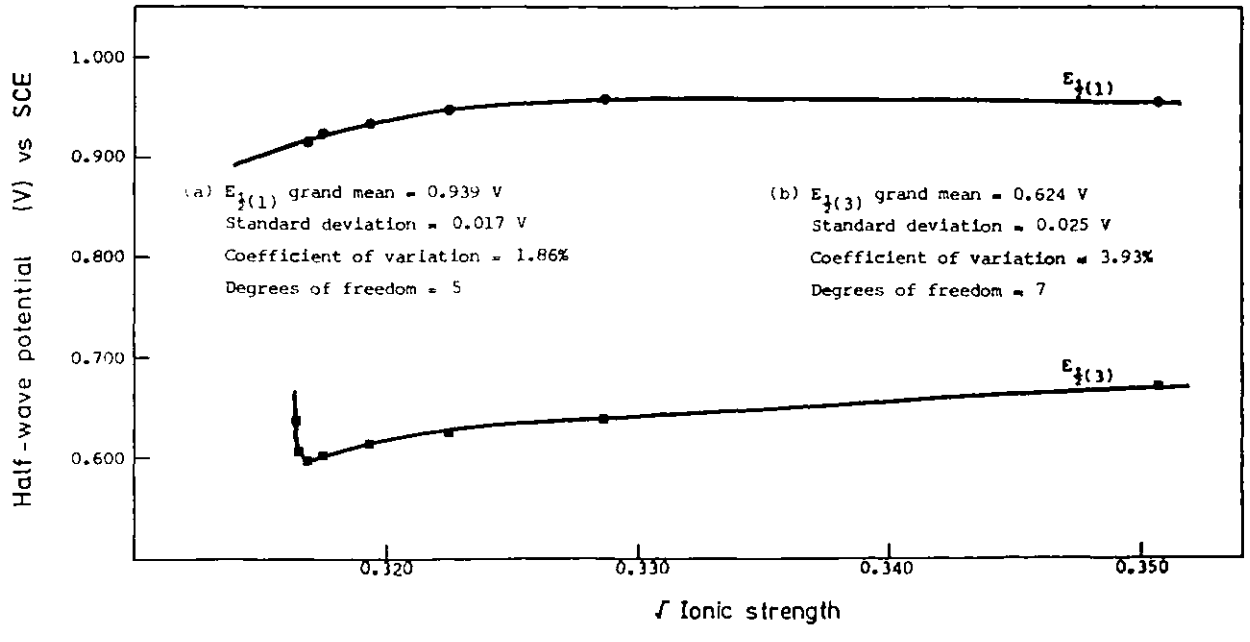

Fig. 5-106 Ir(IV) Perchlorate/Perchloric acid (0.1 M) supporting electrolyte System: Values of half-wave potential, $E_{\frac{1}{2}}$, as a function of square root of total ionic strength, $\sqrt{I}$ (where the concentration of Ir(IV) Perchlorate was varied).

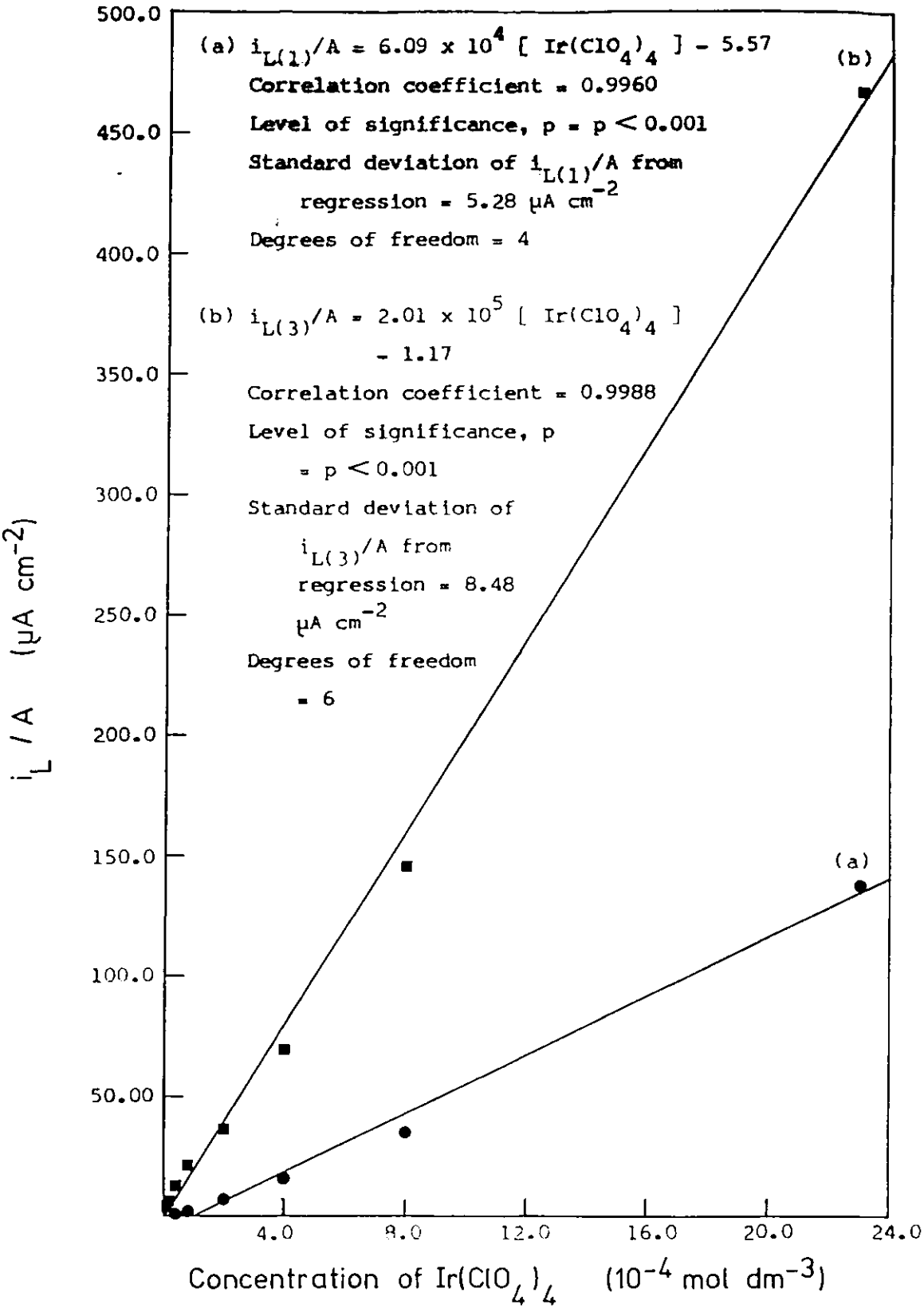

Fig. 5-107 Ir(IV) Perchlorate/Perchloric acid (0.1 M) supporting electrolyte System: Dependence of limiting current per unit area, i_L/A, on the concentration of Ir(IV) Perchlorate.

N.B. $i_{L(3)}/A$ values are exclusive of the maximum on the wave.

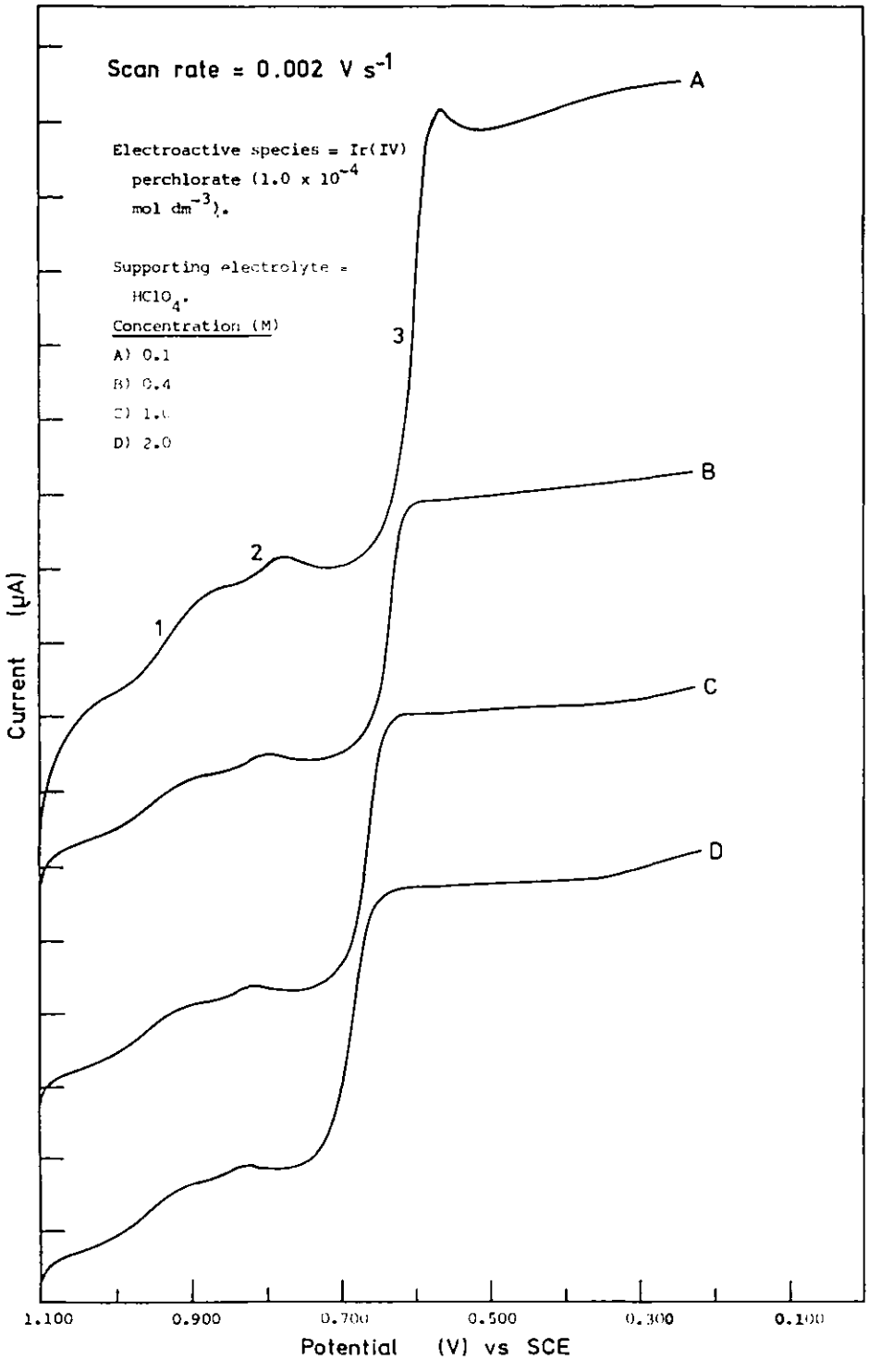

Fig. 5-108 D.c. voltammograms of Ir(IV) perchlorate (1.0×10^{-4} mol dm^{-3}) at the boron carbide solid electrode $B_{4.0}C$ in a concentration range of perchloric acid supporting electrolyte. The current sensitivities were: A) 5 μA per division, and B) to D) 10 μA per division.

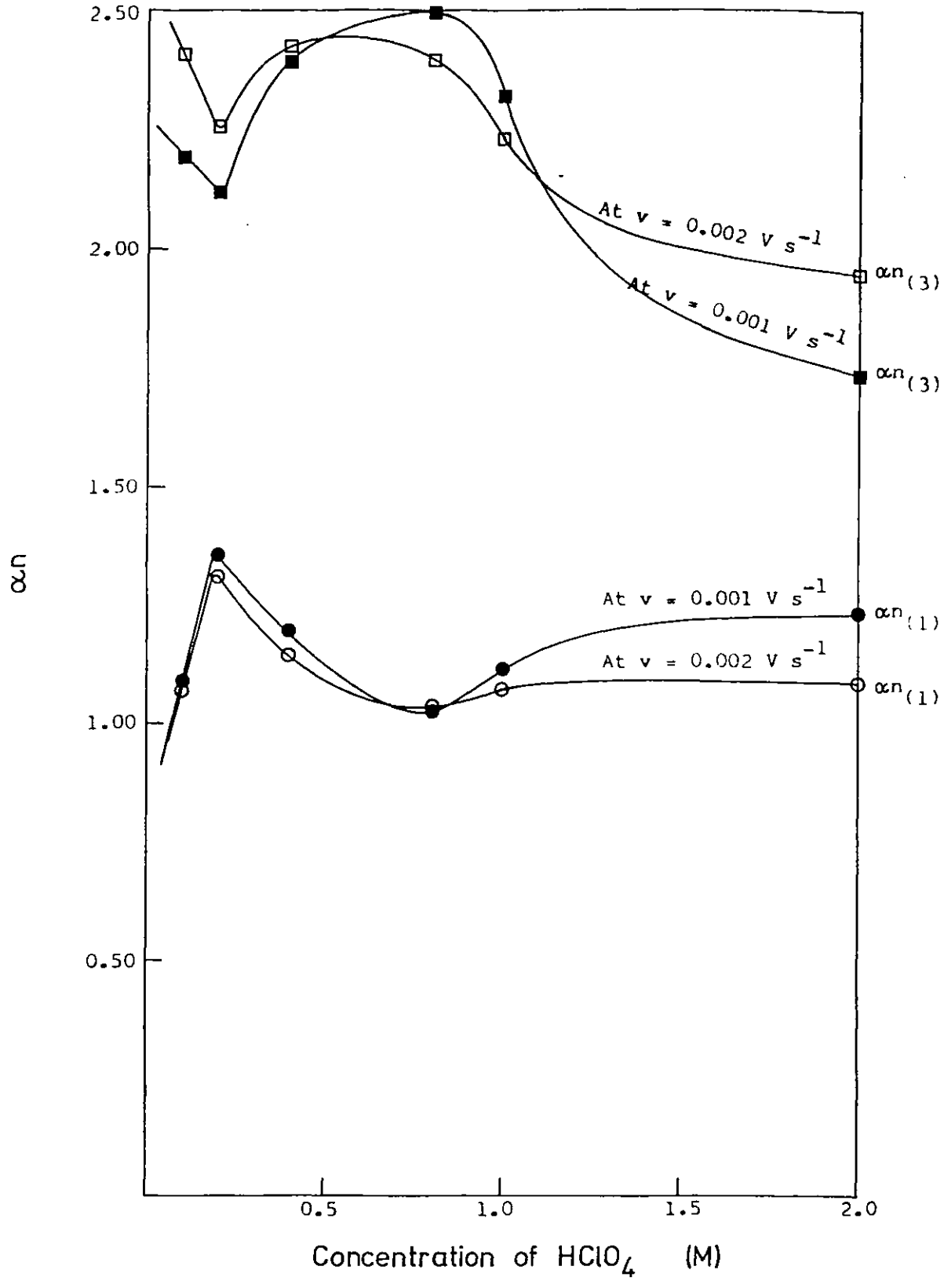

Fig. 5-109 **Ir(IV) Perchlorate (1.0×10^{-4} mol dm^{-3})/Perchloric acid supporting electrolyte System: Values of αn as a function of concentration of perchloric acid; at scan rates, v, of 0.001 and 0.002 V s^{-1}. Boron carbide solid electrode composition was $B_{4.05}C$.**

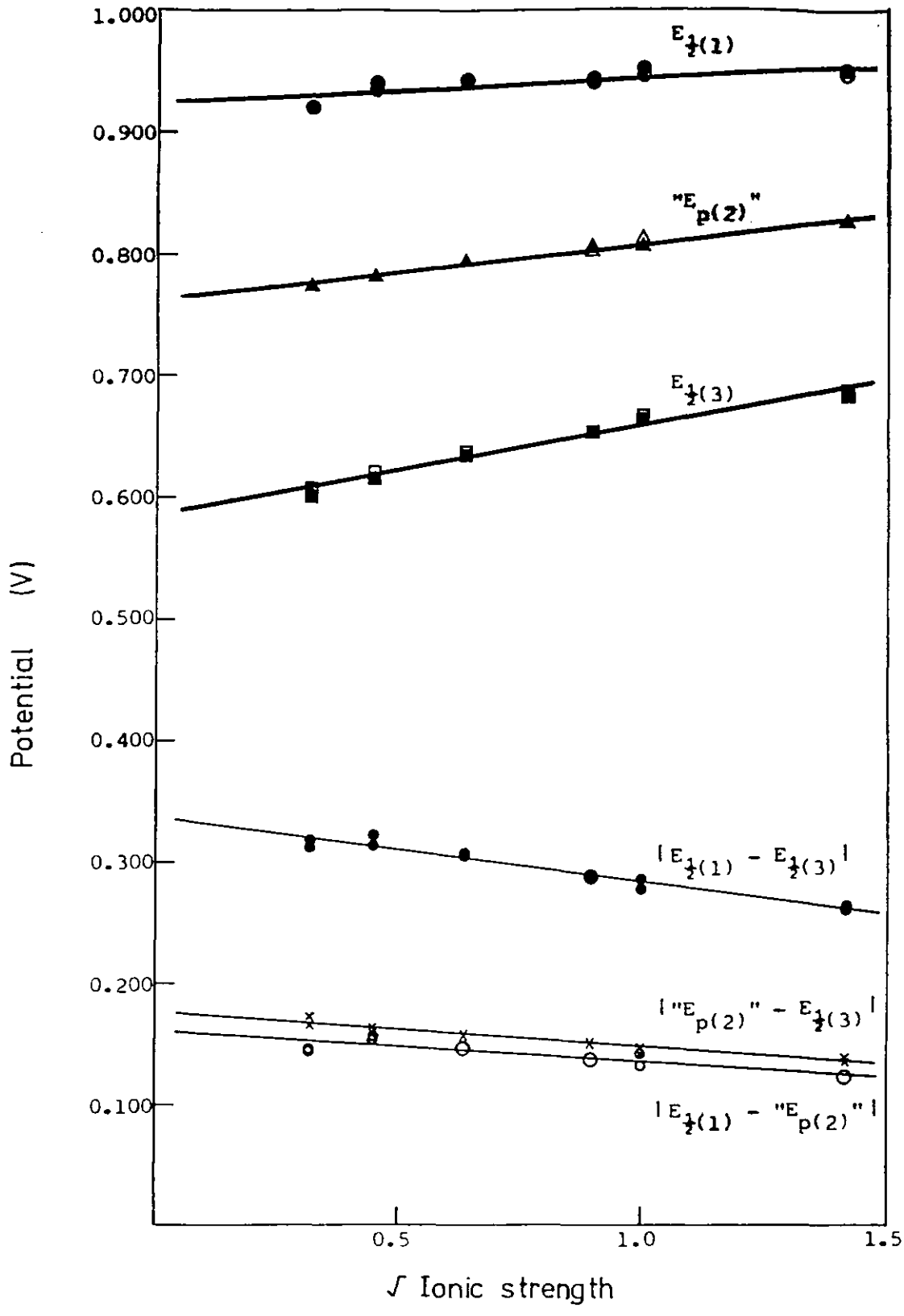

Fig. 5-110 Ir(IV) Perchlorate (1.0×10^{-4} mol dm^{-3})/Perchloric acid (0.1 to 2.0 M) supporting electrolyte System: Values of half-wave potential, $E_{\frac{1}{2}}$, or "peak potential", "E_p" (when the voltammogram exhibits a peak rather than a wave), and the difference between these potentials as a function of square root of total ionic strength, $\sqrt{I}$ (where the concentration of perchloric acid was varied). Boron carbide solid electrode $B_{4.05}C$.

Fig. 5-110 (continued):-

(a) $E_{\frac{1}{2}(1)} = 0.924 + 2.11 \times 10^{-2} \sqrt{I}$

Correlation coefficient = 0.8029

Level of significance, $p = 0.001 < p < 0.01$

Standard deviation of $E_{\frac{1}{2}(1)}$ from regression = 0.006 V

Degrees of freedom = 10

(b) $"E_{p(2)}" = 0.762 + 4.67 \times 10^{-2} \sqrt{I}$

Correlation coefficient = 0.9882

Level of significance, $p = p < 0.001$

Standard deviation of $"E_{p(2)}"$ from regression = 0.003 V

Degrees of freedom = 10

(c) $E_{\frac{1}{2}(3)} = 0.585 + 7.53 \times 10^{-2} \sqrt{I}$

Correlation coefficient = 0.9871

Level of significance, $p = p < 0.001$

Standard deviation of $E_{\frac{1}{2}(3)}$ from regression = 0.005 V

Degrees of freedom = 10

(d) $|E_{\frac{1}{2}(1)} - "E_{p(2)}"| = 0.162 - 2.56 \times 10^{-2} \sqrt{I}$

Correlation coefficient = - 0.8837

Level of significance, $p = p < 0.001$

Standard deviation of $|E_{\frac{1}{2}(1)} - "E_{p(2)}"|$ from regression = 0.005 V

Degrees of freedom = 10

(e) $|"E_{p(2)}" - E_{\frac{1}{2}(3)}| = 0.177 - 2.85 \times 10^{-2} \sqrt{I}$

Correlation coefficient = -0.9590

Level of significance, $p = p < 0.001$

Standard deviation of $|"E_{p(2)}" - E_{\frac{1}{2}(3)}|$ from regression = 0.003 V

Degrees of freedom = 10

(f) $|E_{\frac{1}{2}(1)} - E_{\frac{1}{2}(3)}| = 0.339 - 5.41 \times 10^{-2} \sqrt{I}$

Correlation coefficient = -0.9774

Level of significance, $p = p < 0.001$

Standard deviation of $|E_{\frac{1}{2}(1)} - E_{\frac{1}{2}(3)}|$ from regression = 0.005 V

Degrees of freedom = 10

thesis is given by Fig. 5-111 which shows the trends of the current function, $i_{max}/A\ [Ir(ClO_4)_4]$ (where i_{max} is the limiting current or "peak" current), with increasing perchloric acid concentration. The current function of Wave 1, which was least affected by adsorption and so experienced the smallest anodic shift in potential, remained relatively constant (Fig. 5-111, a). For Wave 2, the current function decreased at high perchloric acid concentration (Fig. 5-111, c); and actually disappeared for the slower scan rate of 0.001 V s^{-1} (Fig. 5-111, b). Wave 3 had a current function which increased non-linearly with increasing perchloric acid concentration despite the disappearance of the maximum (Fig. 5-111, e). However, this increase was gradual and linear for the slower scan rate of 0.001 V s^{-1} (Fig. 5-111, d). Thus, although the adsorption effect on Wave 3 was debilitated, a catalytic reaction was enhanced by the increasing perchloric acid concentration.

5-1.5.(i).b Boron carbide solid electrode $B_{3.86}C$

D.c. voltammograms of Ir(IV) perchlorate (1.0×10^{-4} mol dm^{-3}) obtained at the boron carbide electrode $B_{3.86}C$ show that the maximum on Wave 3 disappeared at higher concentrations of perchloric acid supporting electrolyte (Fig. 5-112); but the wave height was enhanced. The αn values of interpretable waves are plotted as functions of perchloric acid concentration in Fig. 5-113 and show the variations obtained. The half-wave potential or peak potential (where a peak was defined rather than a wave) shifted anodically with increasing $(\text{ionic strength})^{\frac{1}{2}}$ as the perchloric acid concentration was increased (Fig. 5-114). The differences between these potentials, however, were smaller at higher ionic strengths (Fig. 5-114). Plots of the current function, $i_L/A\ [Ir(ClO_4)_4]$, against perchloric acid concentration show that it was generally constant for Wave 1 but Wave 3 had a current function that varied (Fig. 5-115). The variation in the current function for Wave 3 suggests that, when the perchloric acid concentration was increased, the adsorption effect was decreasing whilst the catalytic reaction was being enhanced.

Therefore, in general, the results obtained at the boron carbide electrode $B_{3.86}C$ are similar to the corresponding results obtained at the $B_{4.05}C$ electrode (section 5-1.5.(i).a). Thus the diagnoses of the reactions that occurred at the electrode-solution interface are mutually applicable.

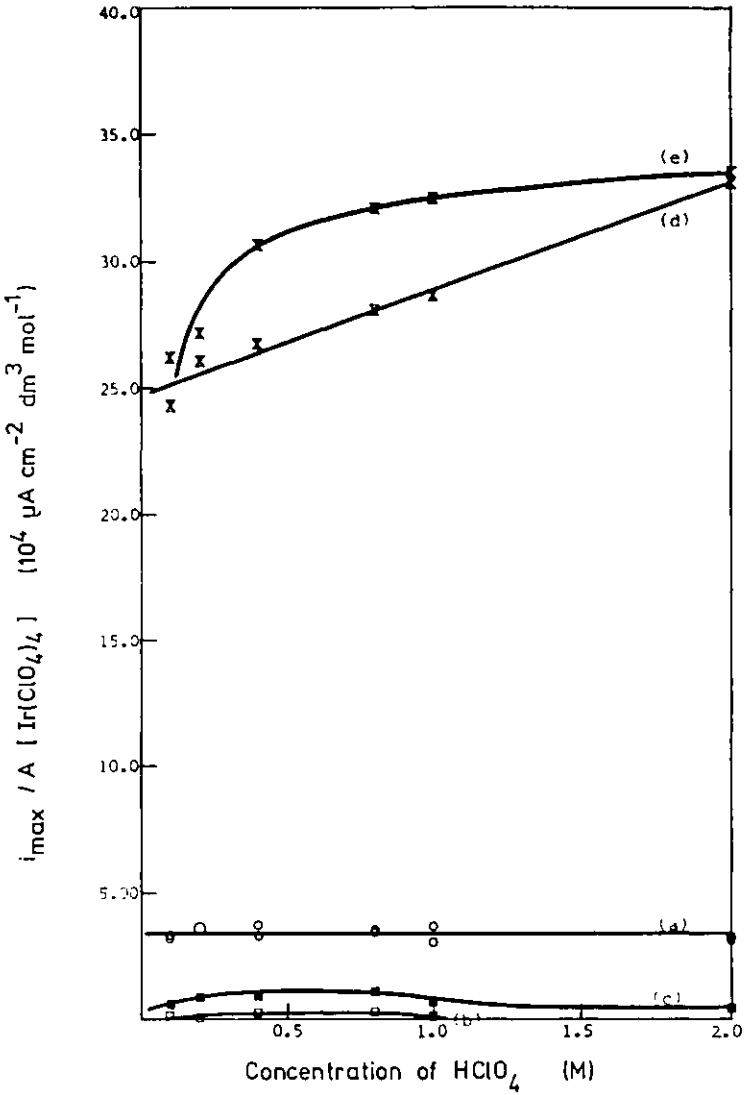

Fig. 5-111 Ir(IV) Perchlorate (1.0×10^{-4} mol dm^{-3})/Perchloric acid (0.1 to 2.0 M) supporting electrolyte System: Values of limiting or "peak" current per unit area divided by concentration of Ir(IV) Perchlorate as a function of concentration of perchloric acid supporting electrolyte. Boron carbide solid electrode $B_{4.05}C$.

Fig. 5-111 (continued):-

(a) At scan rate, v = 0.001 and 0.002 V s^{-1}:

$i_{L(1)}/A$ [$Ir(ClO_4)_4$] mean = 3.42×10^4 µA cm^{-2} dm^3 mol^{-1}
Standard deviation = 0.23×10^4 µA cm^{-2} dm^3 mol^{-1}
Degrees of freedom = 11

(b) At scan rate, v = 0.001 V s^{-1}:

Values of "$i_{p(2)}$"/A [$Ir(ClO_4)_4$].

(c) At scan rate, v = 0.002 V s^{-1}:

Values of "$i_{p(2)}$"/A [$Ir(ClO_4)_4$].

(d) At scan rate, v = 0.001 V s^{-1}:

$i_{L(3)}/A$ [$Ir(ClO_4)_4$] = $2.47 \times 10^5 + 4.25 \times 10^4$ [$HClO_4$]
Correlation coefficient = 0.9877
Level of significance, p = $p < 0.001$
Standard deviation of $i_{L(3)}/A$ [$Ir(ClO_4)_4$] from regression
= 5.30×10^3 µA cm^{-2} dm^3 mol^{-1}
Degrees of freedom = 4

(e) At scan rate, v = 0.002 V s^{-1}:

Values of $i_{L(3)}/A$ [$Ir(ClO_4)_4$].

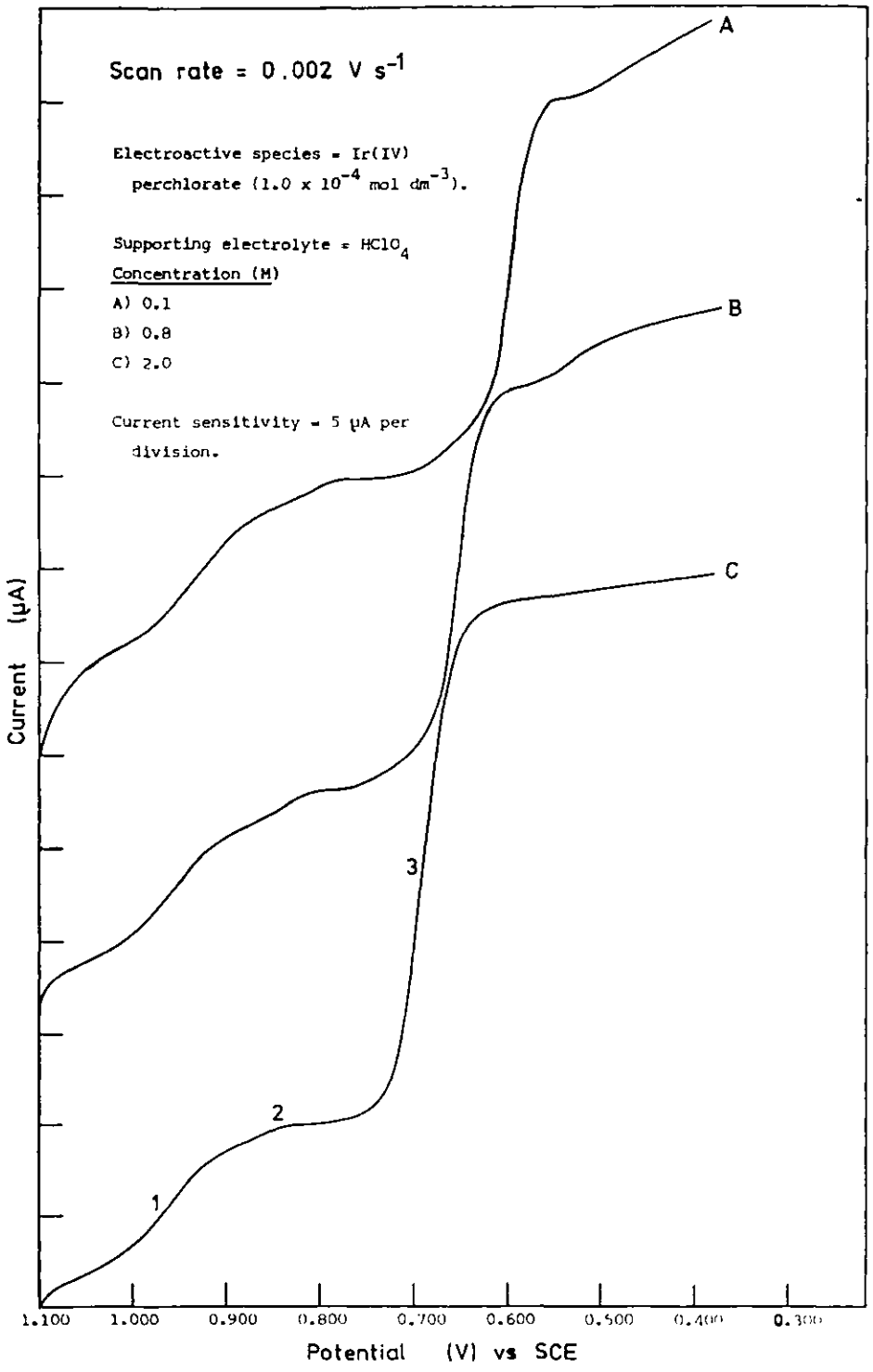

Fig. 5-112 D.c. voltammograms of Ir(IV) perchlorate (1.0 x 10^{-4} mol cm^{-3}) at the boron carbide solid electrode $B_{3.86}C$ in a concentration range of perchloric acid supporting electrolyte.

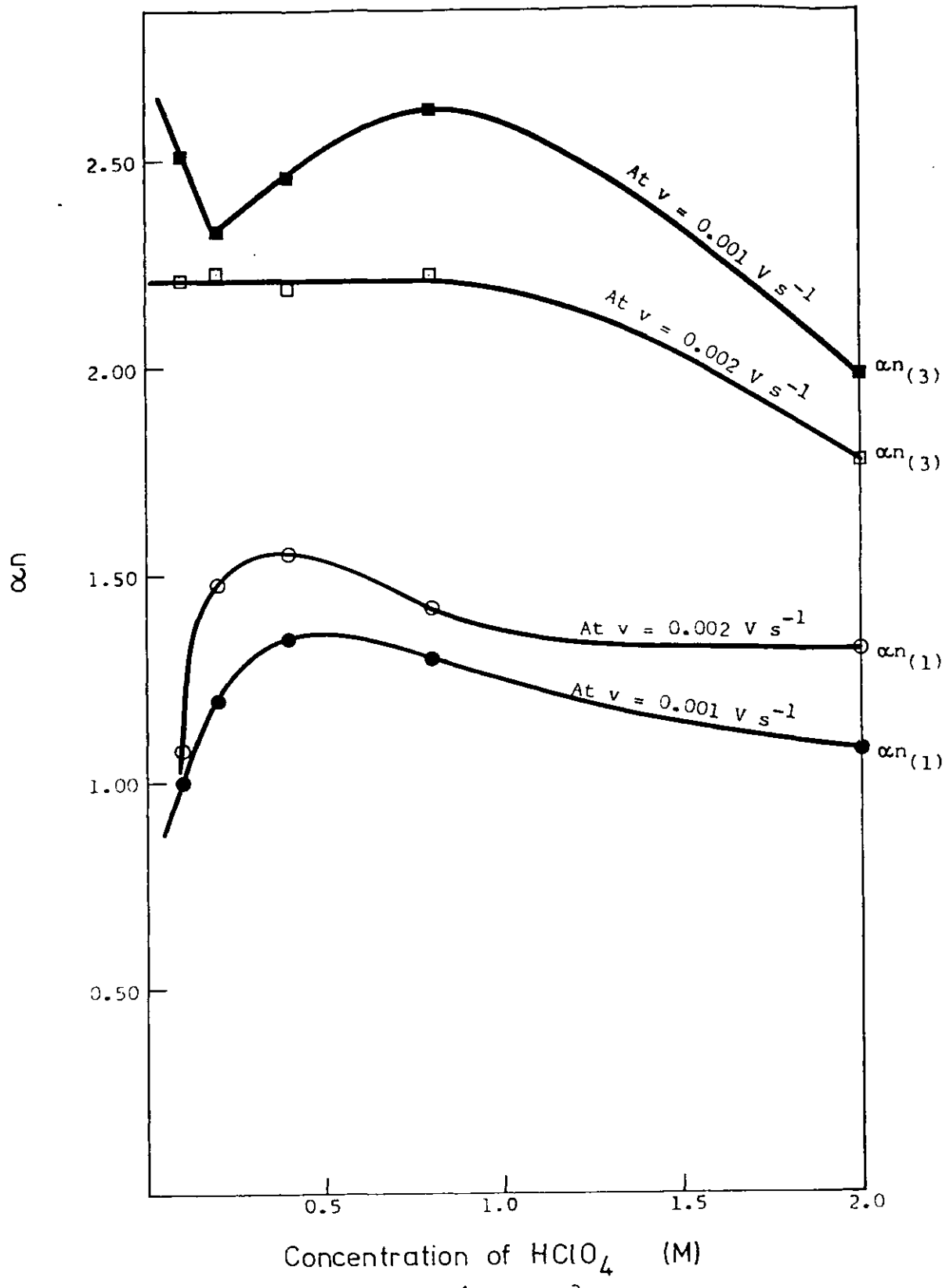

Fig. 5-113 Ir(IV) Perchlorate (1.0×10^{-4} mol dm^{-3})/Perchloric acid supporting electrolyte System: Values of αn as a function of concentration of perchloric acid; at scan rates, v, of 0.001 and 0.002 V s^{-1}. Boron carbide solid electrode $B_{3.86}C$.

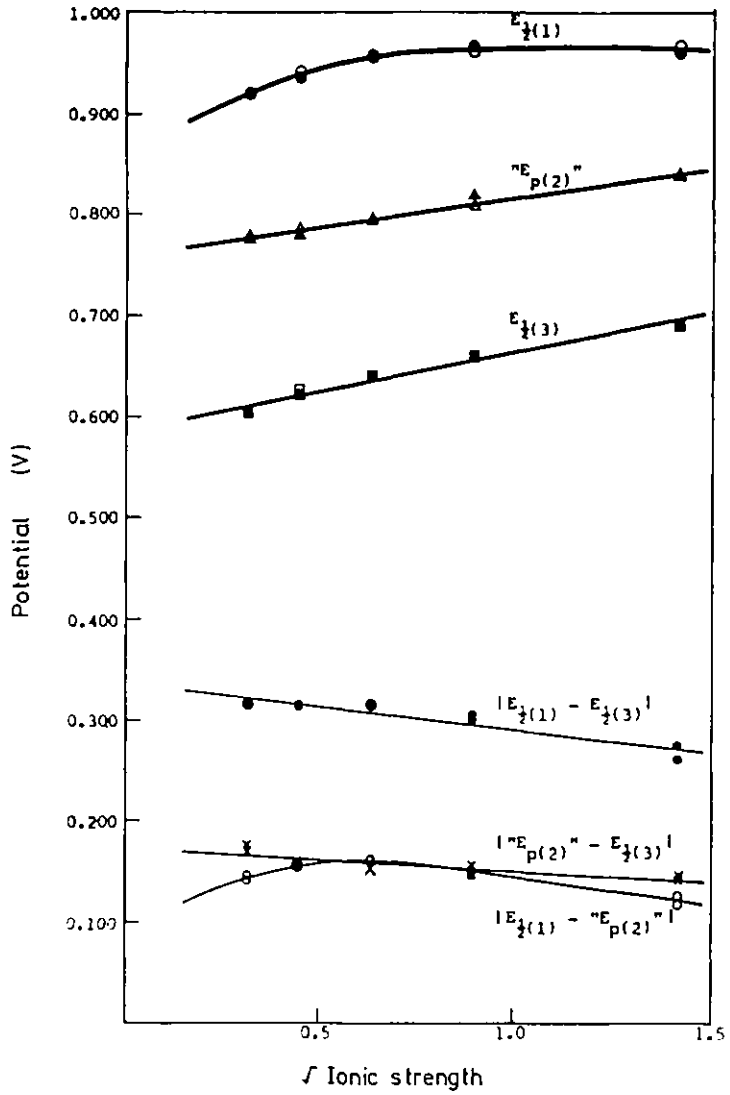

Fig. 5-114 Ir(IV) perchlorate (1.0×10^{-4} mol dm^{-3})/Perchloric acid (0.1 to 2.0 M) supporting electrolyte System: Values of half-wave potential, $E_{\frac{1}{2}}$, or "peak potential", "E_p" (when the voltammogram exhibits a peak rather than a wave), and the difference between these potentials as functions of the square root of total ionic strength, $\sqrt{I}$ (when the concentration of perchloric acid was varied). Boron carbide solid electrode $B_{3.86}C$.

Fig. 5-114 (continued):-

(a) At scan rate, v = 0.001 and 0.002 V s^{-1}:

Values of $E_{\frac{1}{2}(1)}$.

(b) At scan rate, v = 0.001 and 0.002 V s^{-1}:

$"E_{p(2)}" = 0.759 + 5.98 \times 10^{-2} \sqrt{I}$
Correlation coefficient = 0.9898
Level of significance, p = $p < 0.001$
Standard deviation of "$E_{p(2)}$" from regression = 0.004 V
Degrees of freedom = 8

(c) At scan rate, v = 0.001 and 0.002 V s^{-1}:

$E_{\frac{1}{2}(3)} = 0.586 + 8.03 \times 10^{-2} \sqrt{I}$
Correlation coefficient = 0.9887
Level of significance, p = $p < 0.001$
Standard deviation of $E_{\frac{1}{2}(3)}$ from regression = 0.005 V
Degrees of freedom = 8

(d) At scan rate, v = 0.001 and 0.002 V s^{-1}:

Values of $|E_{\frac{1}{2}(1)} - "E_{p(2)}"|$.

(e) At scan rate, v = 0.001 and 0.002 V s^{-1}:

$|E_{\frac{1}{2}(1)} - E_{\frac{1}{2}(3)}| = 0.338 - 4.52 \times 10^{-2} \sqrt{I}$
Correlation coefficient = -0.9345
Level of significance, p = $p < 0.001$
Standard deviation of $|E_{\frac{1}{2}(1)} - E_{\frac{1}{2}(3)}|$ from regression = 0.007 V
Degrees of freedom = 8

(f) At scan rate, v = 0.001 and 0.002 V s^{-1}:

$|"E_{p(2)}" - E_{\frac{1}{2}(3)}| = 0.173 - 2.06 \times 10^{-2} \sqrt{I}$
Correlation coefficient = -0.8367
Level of significance, p = $0.001 < p < 0.01$
Standard deviation of $|"E_{p(2)}" - E_{\frac{1}{2}(3)}|$ from regression = 0.006 V
Degrees of freedom = 8

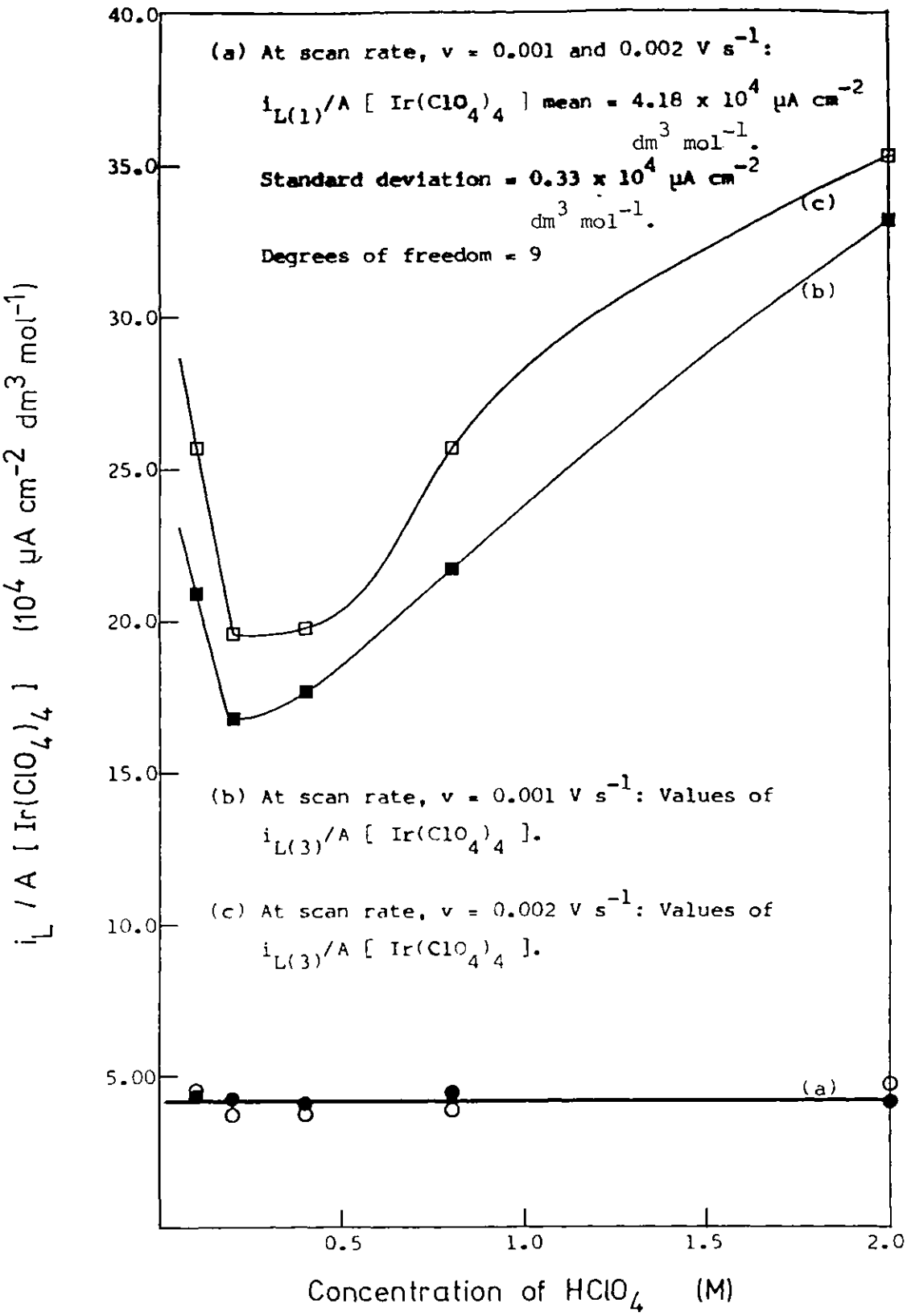

Fig. 5-119 Ir(IV) Perchlorate (1.0 x 10^{-4} mol dm^{-3})/Perchloric acid supporting electrolyte System: Values of limiting current per unit area divided by concentration of Ir(IV) Perchlorate as a function of concentration of perchloric acid; at scan rates, v, of 0.001 and 0.002 V s^{-1}. Boron carbide solid eletrode $B_{3.86}C$.

5-1.5.(i).c Boron carbide/carbon composite solid electrode $B_{3.11}C$

D.c. voltammograms of Ir(IV) perchlorate (1.0×10^{-4} mol dm^{-3}), in perchloric acid (0.1 to 2.0 M), obtained at the boron carbide/carbon composite solid electrode $B_{3.11}C$ exhibited four waves (Fig. 5-116). The definition of Waves 1 and 2 deteriorated with increasing perchloric acid concentration; which also caused the maximum on Wave 4 to decrease. The variations of αn values (for interpretable waves) with increasing perchloric acid concentration are presented in Fig. 5-117.

The half-wave potentials shifted anodically with increasing $(\text{ionic strength})^{\frac{1}{2}}$ as the concentration of perchloric acid was increased (Fig. 5-118). The differences between the half-wave potentials of Wave 1 and Waves 3 and 4 were reduced at high ionic strength, but the difference between the half-wave potentials of Wave 3 and Wave 4 remained relatively constant (Fig. 5-118). Plots of the limiting current function, i_L/A [$Ir(ClO_4)_4$], against the concentration of perchloric acid supporting electrolyte show that Waves 1, 3, and 4 were not only affected by adsorption but also by catalytic reactions (Fig. 5-119). Wave 1 had a limiting current function which increased to a maximum value before decreasing with increasing perchloric acid concentration until no wave was defined (Fig. 5-119, a and b); higher values were obtained for the faster scan rate of 0.002 V s^{-1}. This suggests that the adsorption effect was more important than the catalytic effect. Similarly, Wave 3 was affected more by adsorption than by the catalytic reaction (Fig. 5-119, c and d). Wave 4, however, was strongly affected by the catalytic reaction (Fig. 5-119, e and f); especially at the slower scan rate of 0.001 V s^{-1}. The debilitating effect of high perchloric acid concentration on adsorption, however, eventually caused the limiting current function to decrease.

5-1.5.(i).d Boron carbide/carbon composite solid electrode $B_{2.56}C$

Fig. 5-120 illustrates the effect of perchloric acid supporting electrolyte on the d.c. voltammograms of Ir(IV) perchlorate (1.0×10^{-4} mol dm^{-3}) obtained at the boron carbide/carbon composite solid electrode $B_{2.56}C$. Four waves, 1 to 4 inclusive, were exhibited along with the wave of the residual current, r. When the concentration of perchloric acid was increased, Waves 1 and 2 became less defined, the maximum on Wave 4 decreased, and Wave r increased. The variations of αn values (for the interpretable waves) with perchloric acid concentration are

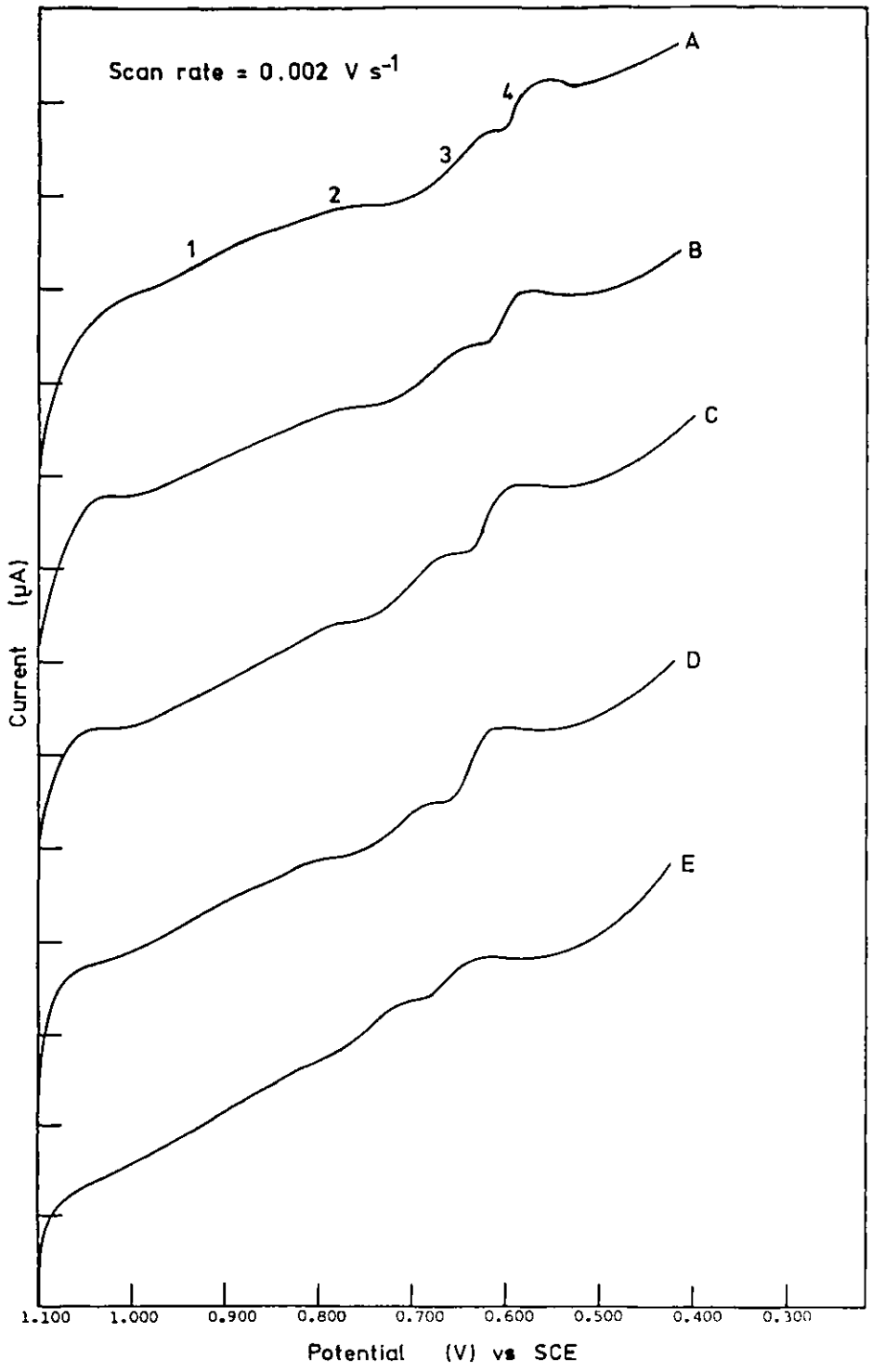

Fig. 5-116 *Ir*(IV) perchlorate (1.0×10^{-4} mol dm^{-3})/Perchloric acid (0.1 to 2.0 M) supporting electrolyte System: D.c. voltammograms at the boron carbide/carbon composite solid electrode $B_{3.11}C$. Concentration of $HClO_4$: A) 0.1 M, B) 0.2 M, C) 0.4 M, D) 0.8 M, and E) 2.0 M. Current sensitivity = 20 μA per division.

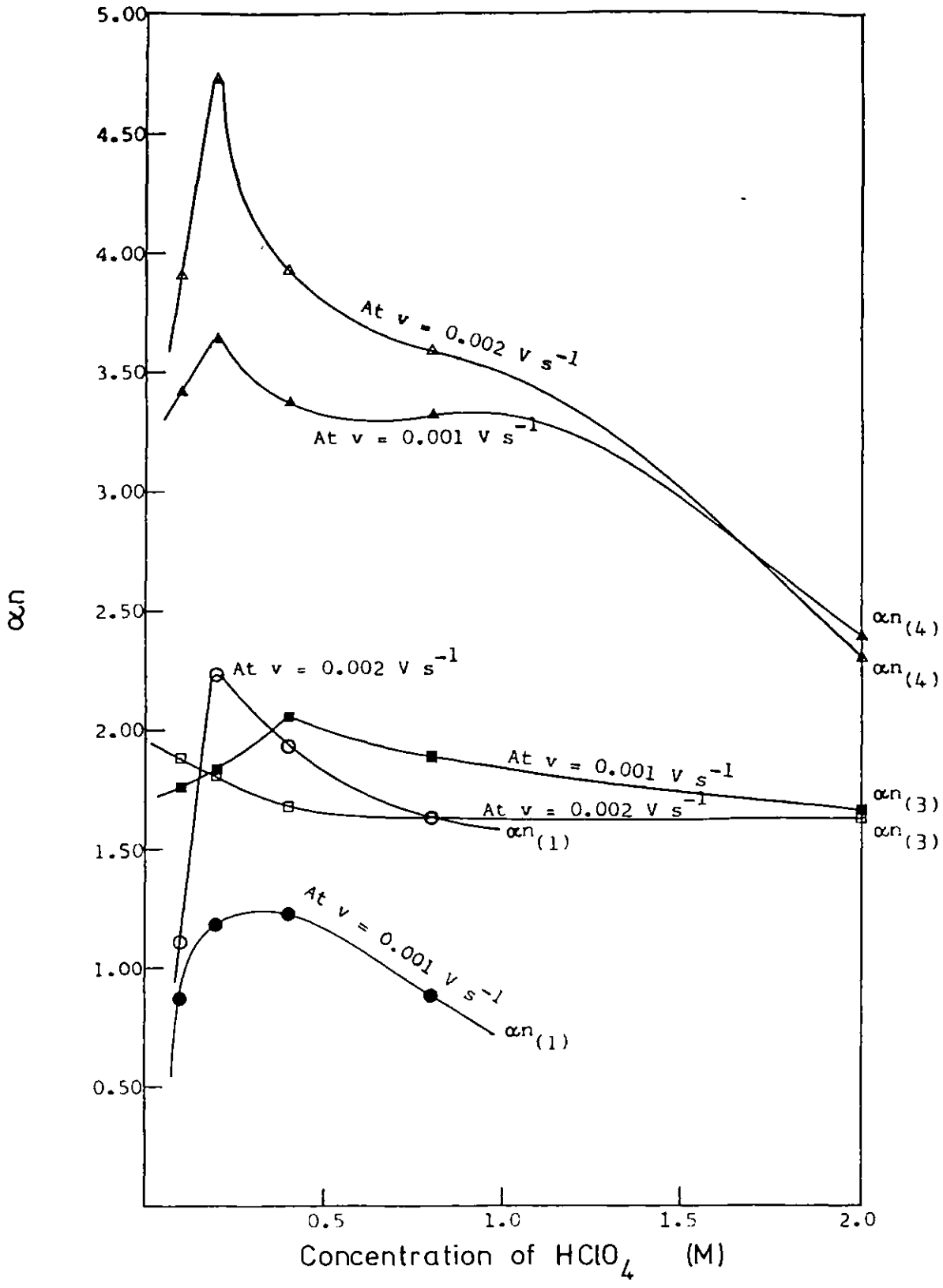

Fig. 5-117 Ir(IV) Perchlorate (1.0×10^{-4} mol dm^{-3})/Perchloric acid supporting electrolyte System: Values of αn as a function of concentration of perchloric acid; at scan rates, v, of 0.001 and 0.002 V s^{-1}. Boron carbide/carbon composite solid electrode $B_{3.11}C$.

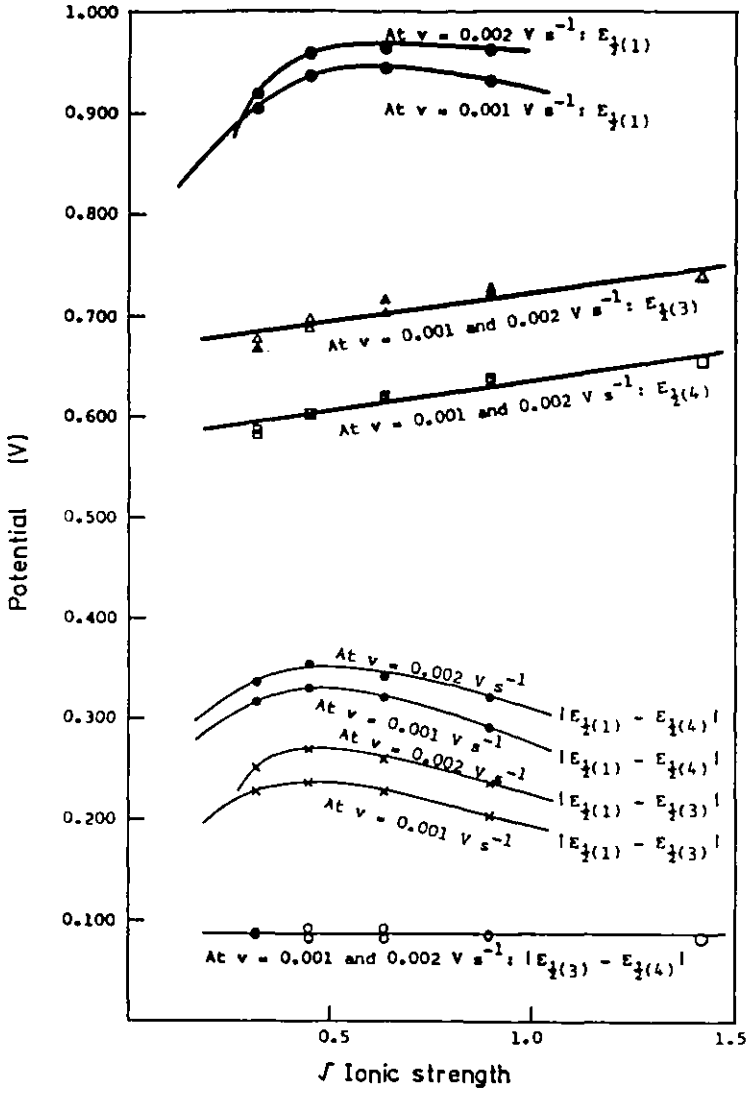

Fig. 5-118 Ir(IV) perchlorate (1.0×10^{-4} mol dm^{-3})/Perchloric acid (0.1 to 2.0 M) supporting electrolyte System: Values of half-wave potential, $E_{\frac{1}{2}}$, and the difference between these potentials as functions of the square root of total ionic strength, $\sqrt{I}$ (where the concentration of perchloric acid was varied). Boron carbide/carbon composite solid electrode $^{B}_{3.11}{}^{C}$.

(a) At scan rate, v = 0.001 and 0.002 V s^{-1}:

$E_{\frac{1}{2}(3)} = 0.666 + 5.67 \times 10^{-2} \sqrt{I}$
Correlation coefficient = 0.9266
Level of significance, p = $p < 0.001$
Standard deviation of $E_{\frac{1}{2}(3)}$ from regression = 0.010 V
Degrees of freedom = 8

(b) At scan rate, v = 0.001 and 0.002 V s^{-1}:

$E_{\frac{1}{2}(4)} = 0.576 + 6.10 \times 10^{-2} \sqrt{I}$
Correlation coefficient = 0.9559
Level of significance, p = $p < 0.001$
Standard deviation of $E_{\frac{1}{2}(4)}$ from regression = 0.008 V
Degrees of freedom = 8

(c) At scan rate, v = 0.001 and 0.002 V s^{-1}:

$|E_{\frac{1}{2}(3)} - E_{\frac{1}{2}(4)}|$ mean = 8.69×10^{-2} V
Standard deviation = 3.92×10^{-3} V
Degrees of freedom = 9

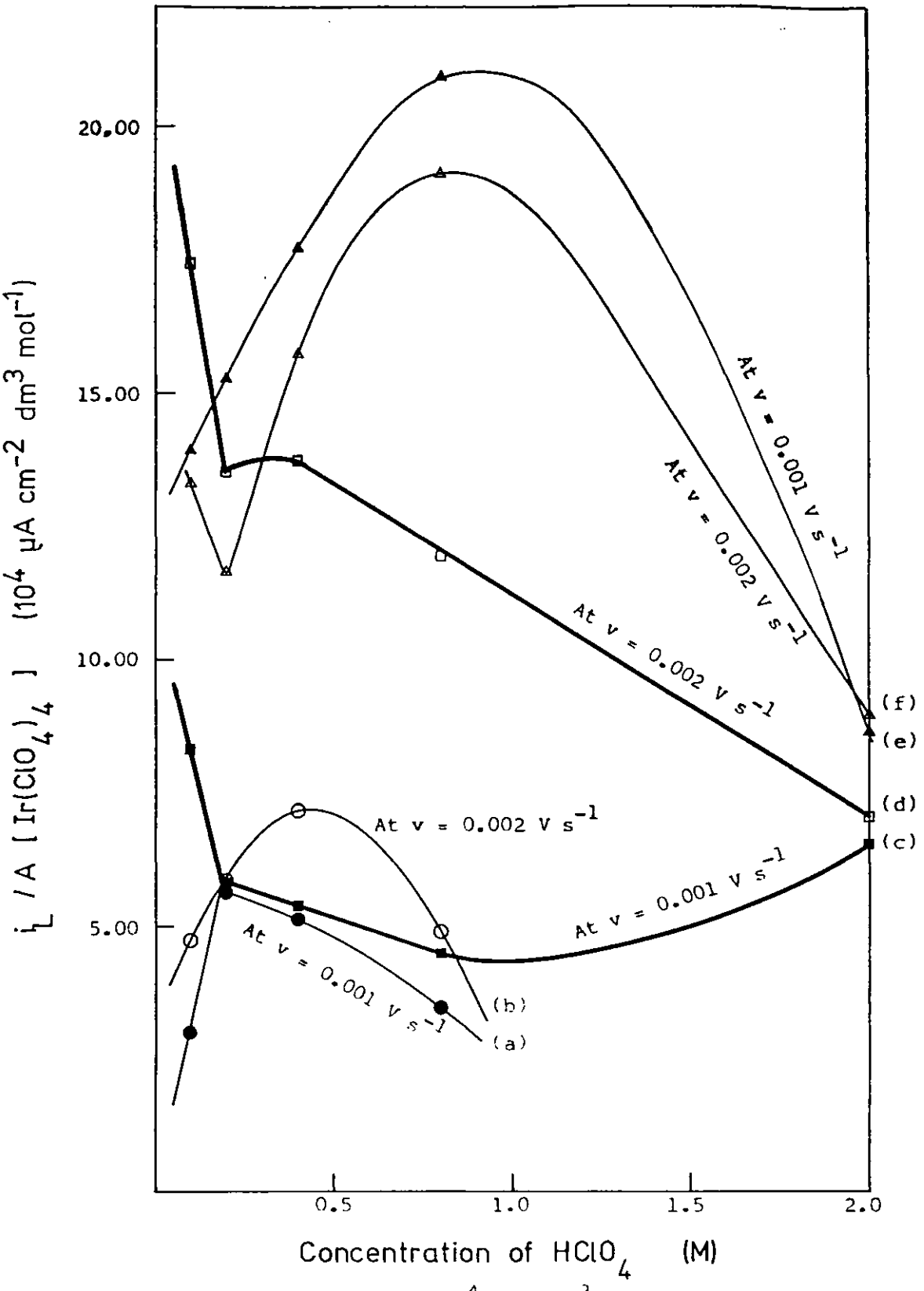

Fig. 5-119 Ir(IV) Perchlorate (1.0×10^{-4} mol dm^{-3})/Perchloric acid supporting electrolyte System: Values of limiting current per unit area divided by concentration of Ir(IV) Perchlorate as a function of concentration of perchloric acid; at scan rates, v, of 0.001 and 0.002 V s^{-1}. Boron carbide/carbon composite solid electrode $B_{3.11}C$. (a) & (b) $i_{L(1)}/A$ [$Ir(ClO_4)_4$], (c) & (d) $i_{L(3)}/A$ [$Ir(ClO_4)_4$], and (e) & (f) $i_{L(4)}/A$ [$Ir(ClO_4)_4$].

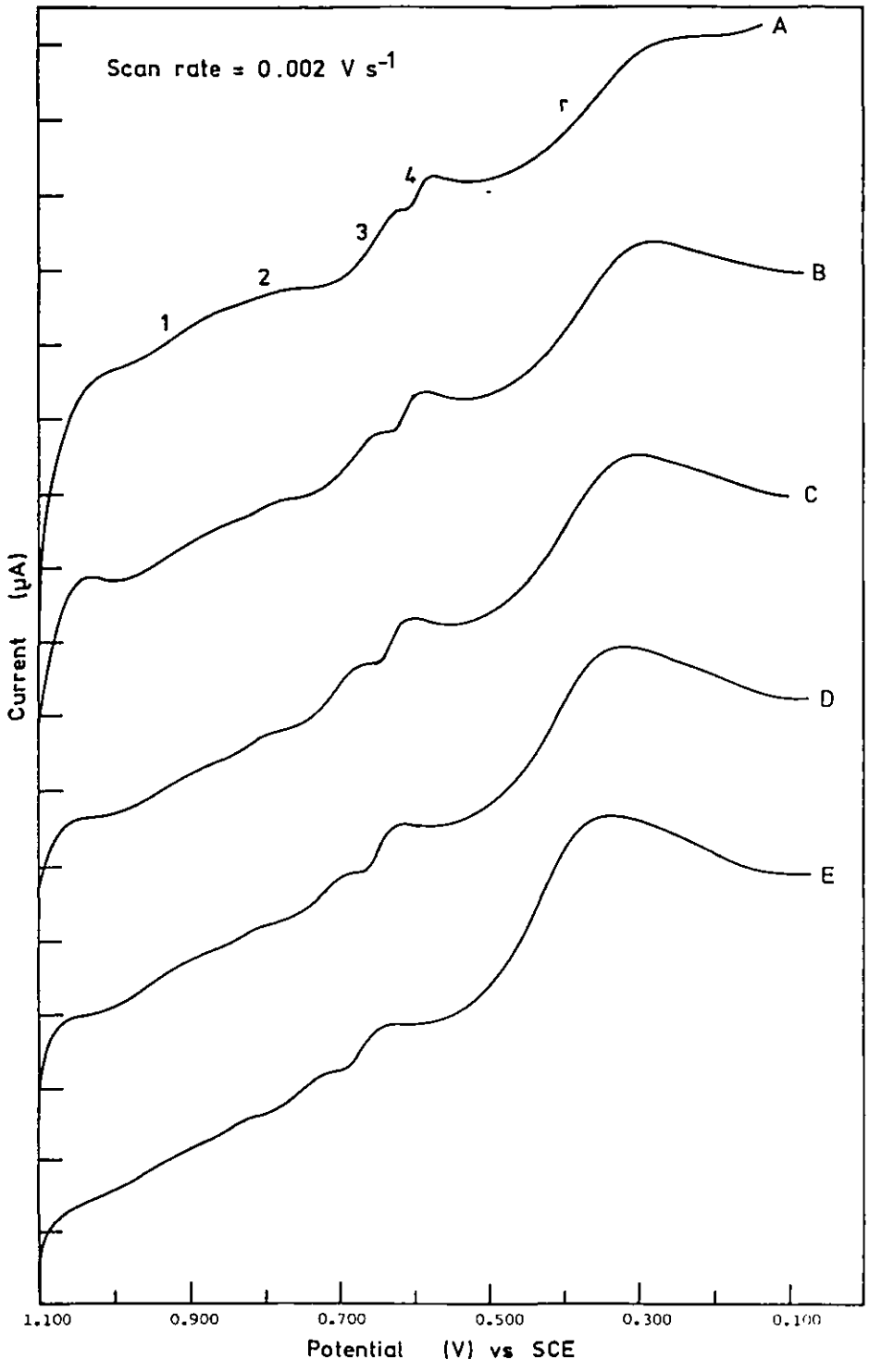

Fig. 5-120 Ir(IV) perchlorate (1.0×10^{-4} mol dm^{-3})/Perchloric acid (0.1 to 2.0 M) supporting electrolyte System: D.c. voltammograms at the boron carbide/carbon composite solid electrode $B_{2.56}C$. Concentration of $HClO_4$: A) 0.1 M, B) 0.2 M, C) 0.4 M, D) 0.8 M, and E) 2.0 M. Current sensitivity = 20 μA per division.

presented in Fig. 5-121; which also shows that, in general, values obtained at the faster scan rate of 0.002 V s^{-1} were higher than those obtained at 0.001 V s^{-1}.

The potentials, half-wave or peak, shifted anodically with increasing (ionic strength)$^{\frac{1}{2}}$ as the concentration of perchloric acid was increased (Fig. 5-122). The absolute difference between the potentials are also included in Fig. 5-122. Only $|E_{\frac{1}{2}(3)} - E_{\frac{1}{2}(4)}|$ remained constant ; signifying that the behaviour of these two waves was related.

The trends of the limiting current function, $i_L/A\ [Ir(ClO_4)_4]$, with increasing perchloric acid concentration show the reduction in the adsorption effect whereas the catalytic reaction was enhanced (Fig. 5-123). The behaviour of Wave 1, although affected by a catalytic reaction, was more affected by the adsorption effect; hence the correspondingly higher values for the current function at the faster scan rate of 0.002 V s^{-1} (Fig. 5-123, a and b). Wave 3, however, was completely dominated by the adsorption effect (Fig. 5-123, c and d); again resulting in higher values of the limiting current function at the faster scan rate. In contrast, Wave 4 was more affected by the catalytic reaction than by the adsorption effect and so the limiting current function generally increased with increasing perchloric acid concentration or decreased scan rate, 0.001 V s^{-1}, (Fig. 5-123, e and f).

5-1.5.(i).e Graphite solid electrode

The d.c. voltammogram of Ir(IV) perchlorate (1.0×10^{-4} mol dm^{-3}), in perchloric acid supporting electrolyte, obtained at the graphite solid electrode exhibited five waves, 1 to 5 inclusive, and two residual current waves, r (Fig. 5-124, C). When the concentration of perchloric acid was increased, however, Waves 1 and 2 became less defined and the maximum on Wave 5 decreased (Fig. 5-124). The αn values of interpretable waves are plotted as a function of perchloric acid concentration in Fig. 5-125.

In general the potentials, half-wave or peak, of all five waves shifted anodically with increasing (ionic strength)$^{\frac{1}{2}}$ as the perchloric acid concentration was increased (Fig. 5-126); although $E_{\frac{1}{2}(2)}$ obtained at the slower scan rate of 0.001 V s^{-1} remained relatively constant (Fig. 5-126, c). Fig. 5-127 shows that the difference between potentials tended to be less at high ionic strength, although notable exceptions are $|E_{\frac{1}{2}(4)} - E_{\frac{1}{2}(5)}|$ and $|E_{\frac{1}{2}(4)} - "E_{p(5)}"|$ (Fig. 5-127, p and q respectively).

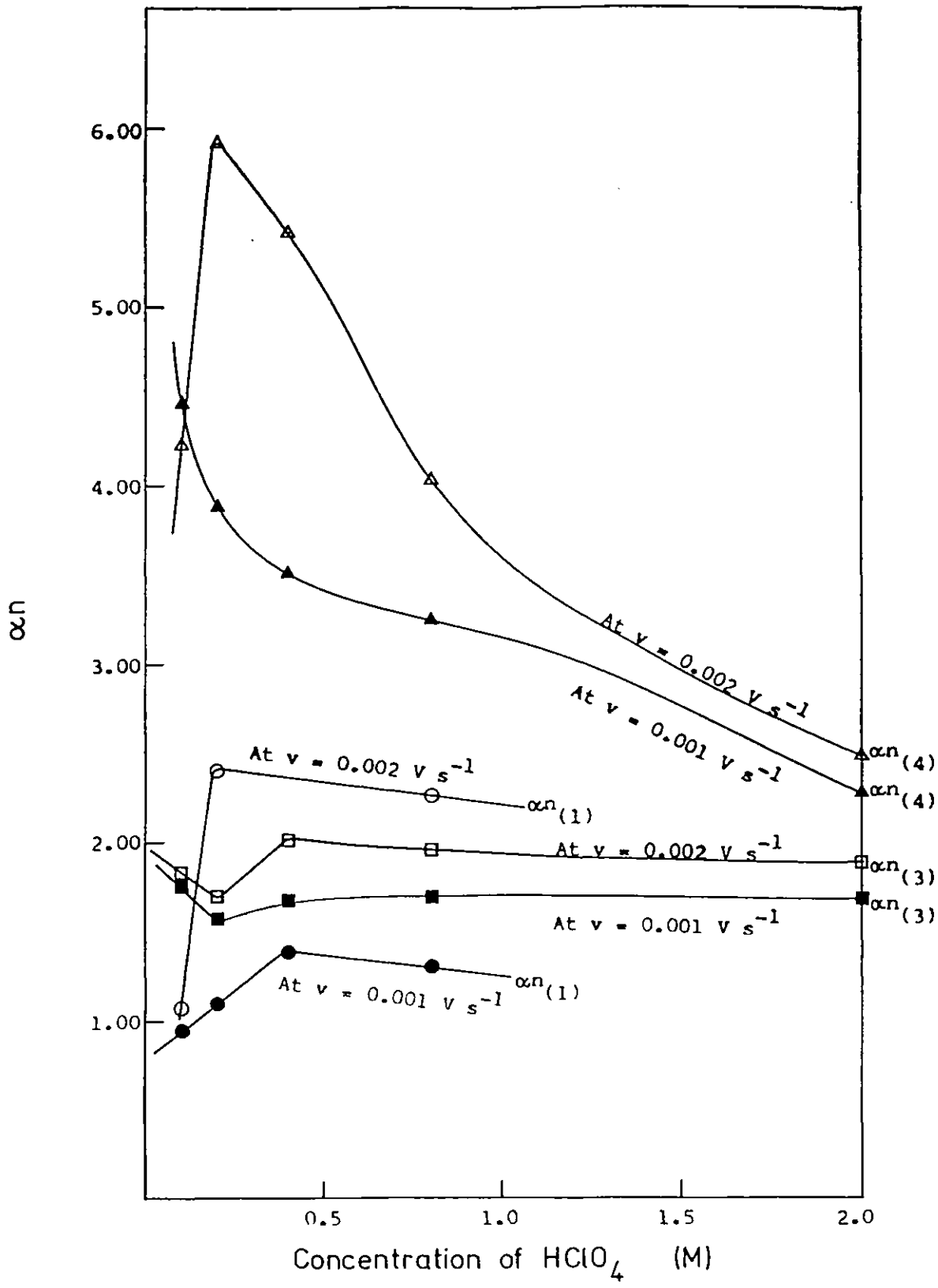

Fig. 5-121 Ir(IV) Perchlorate (1.0×10^{-4} mol dm^{-3})/Perchloric acid supporting electrolyte System: Values of αn as a function of concentration of perchloric acid; at scan rates, v, of 0.001 and 0.002 V s^{-1}. Boron carbide/carbon composite solid electrode $B_{2.56}C$.

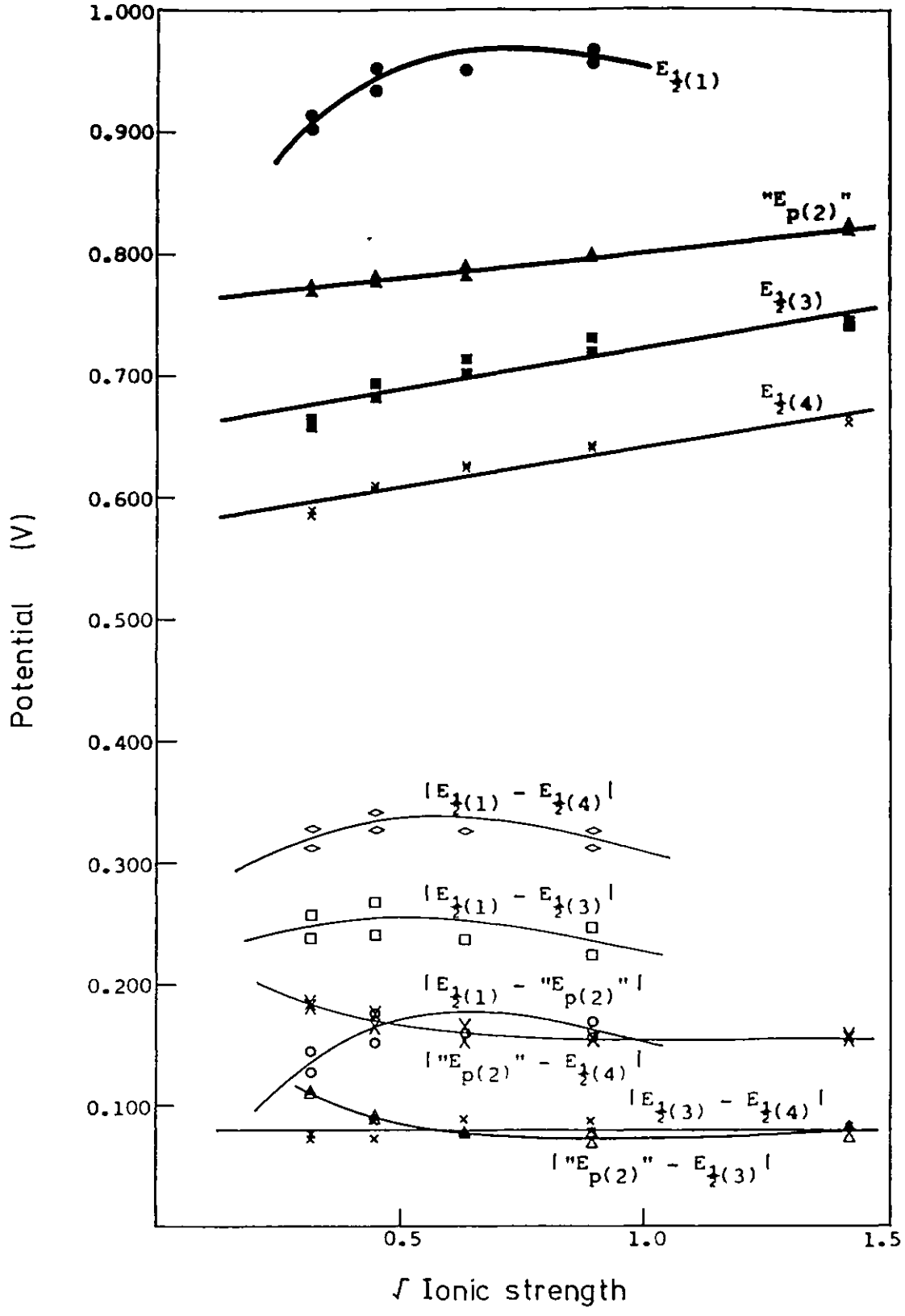

Fig. 5-122 Ir(IV) Perchlorate (1.0×10^{-4} mol dm^{-3})/Perchloric acid (0.1 to 2.0 M) supporting electrolyte System: Values of half-wave potential, $E_{\frac{1}{2}}$, or "peak potential", "E_p" (when the voltammogram exhibits a peak rather than a wave), and the difference between these potentials as a function of square root of total ionic strength, $\sqrt{I}$ (where the concentration of perchloric acid was varied). Boron carbide/carbon composite solid electrode $B_{2.56}C$.

Fig. 5-122 (continued):-

(a) At scan rate, $v = 0.001$ and 0.002 V s^{-1}:

$"E_{p(2)}" = 0.758 + 4.51 \times 10^{-2} \sqrt{I}$

Correlation coefficient = 0.9826

Level of significance, $p = p < 0.001$

Standard deviation of $"E_{p(2)}"$ from regression = 0.004 V

Degrees of freedom = 8

(b) At scan rate, $v = 0.001$ and 0.002 V s^{-1}:

$E_{\frac{1}{2}(3)} = 0.654 + 6.96 \times 10^{-2} \sqrt{I}$

Correlation coefficient = 0.9234

Level of significance, $p = p < 0.001$

Standard deviation of $E_{\frac{1}{2}(3)}$ from regression = 0.013 V

Degrees of freedom = 8

(c) At scan rate, $v = 0.001$ and 0.002 V s^{-1}:

$E_{\frac{1}{2}(4)} = 0.577 + 6.56 \times 10^{-2} \sqrt{I}$

Correlation coefficient = 0.9622

Level of significance, $p = p < 0.001$

Standard deviation of $E_{\frac{1}{2}(4)}$ from regression = 0.008 V

Degrees of freedom = 8

(d) At scan rate, $v = 0.001$ and 0.002 V s^{-1}:

$|E_{\frac{1}{2}(3)} - E_{\frac{1}{2}(4)}|$ mean $= 7.99 \times 10^{-2}$ V

Standard deviation $= 6.40 \times 10^{-3}$ V

Degrees of freedom = 9

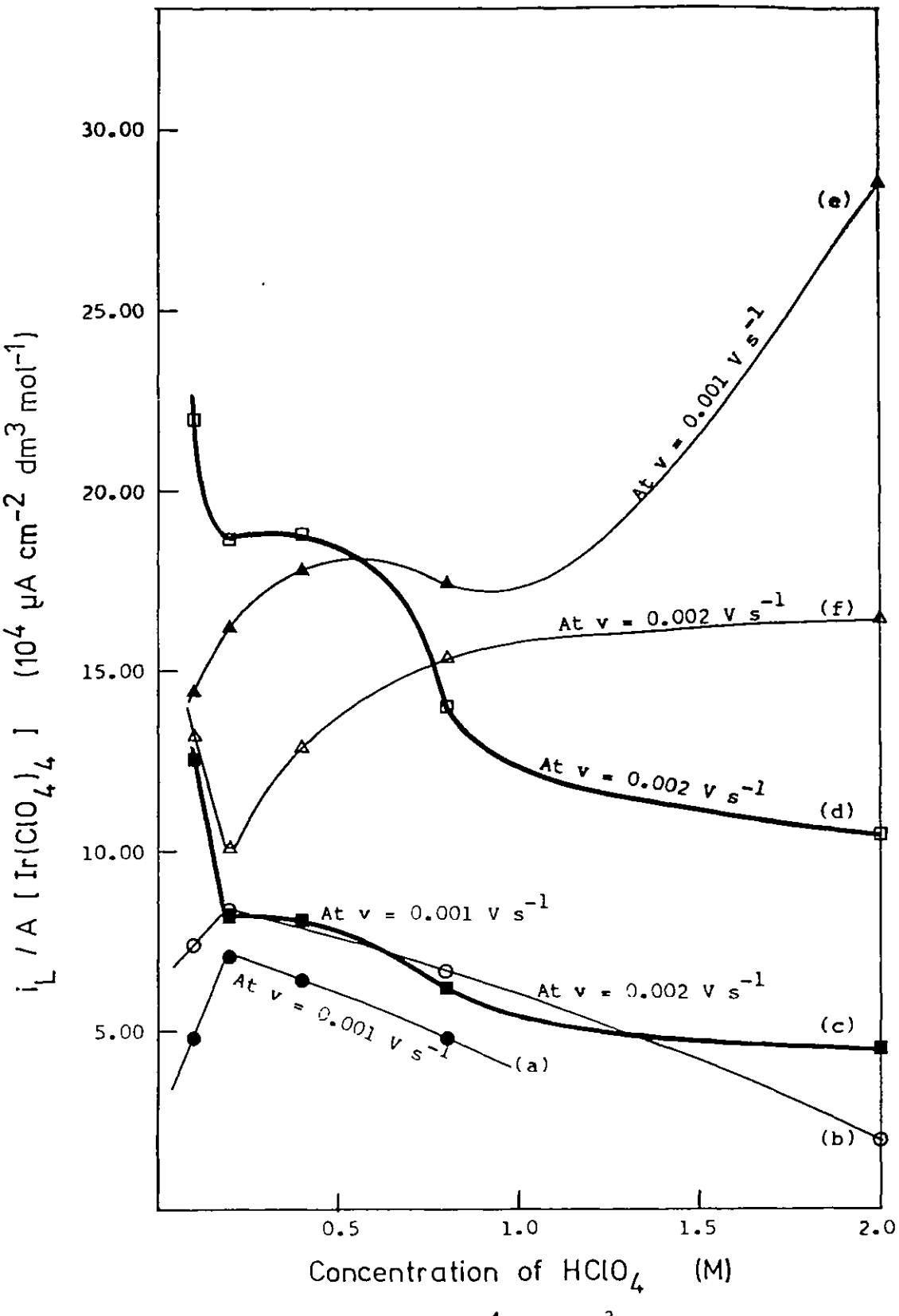

Fig. 5-123 Ir(IV) Perchlorate (1.0×10^{-4} mol dm^{-3})/Perchloric acid supporting electrolyte System: Values of limiting current per unit area divided by concentration of Ir(IV) Perchlorate as a function of concentration of perchloric acid; at scan rates, v, of 0.001 and 0.002 V s^{-1}. (a) & (b) $i_{L(1)}/A$ [$Ir(ClO_4)_4$], (c) & (d) $i_{L(3)}/A$ [$Ir(ClO_4)_4$], and (e) & (f) $i_{L(4)}/A$ [$Ir(ClO_4)_4$]. Boron carbide/carbon composite solid electrode $B_{2.56}C$.

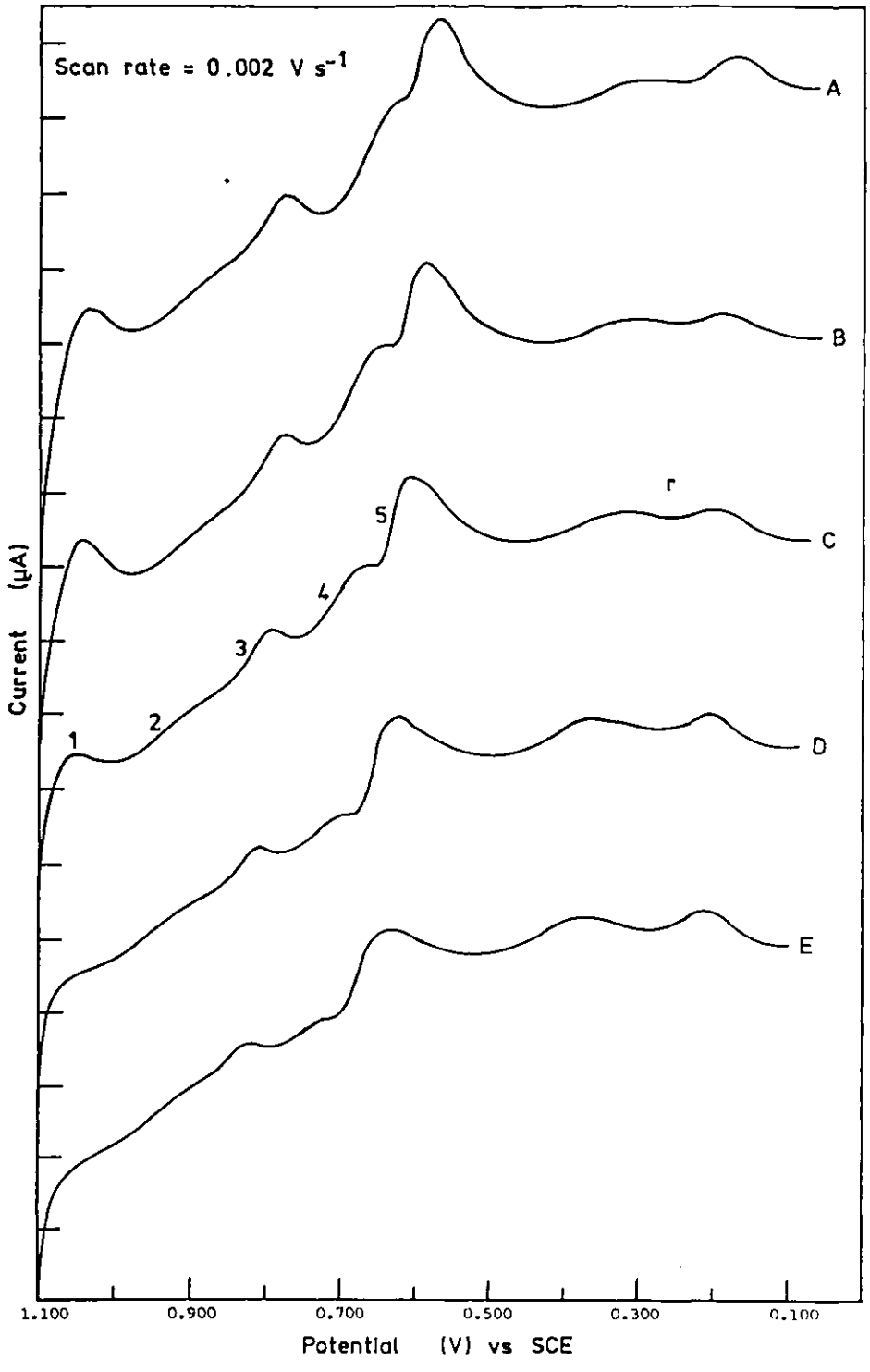

Fig. 5-124 Ir(IV) perchlorate (1.0×10^{-4} mol dm^{-3})/Perchloric acid (0.1 to 2.0 M) supporting electrolyte System: D.c. voltammograms at the graphite solid electrode. Concentration of $HClO_4$: A) 0.1 M, B) 0.2 M, C) 0.4 M, D) 1.0 M, and E) 2.0 M. Current sensitivity = 5 μA per division.

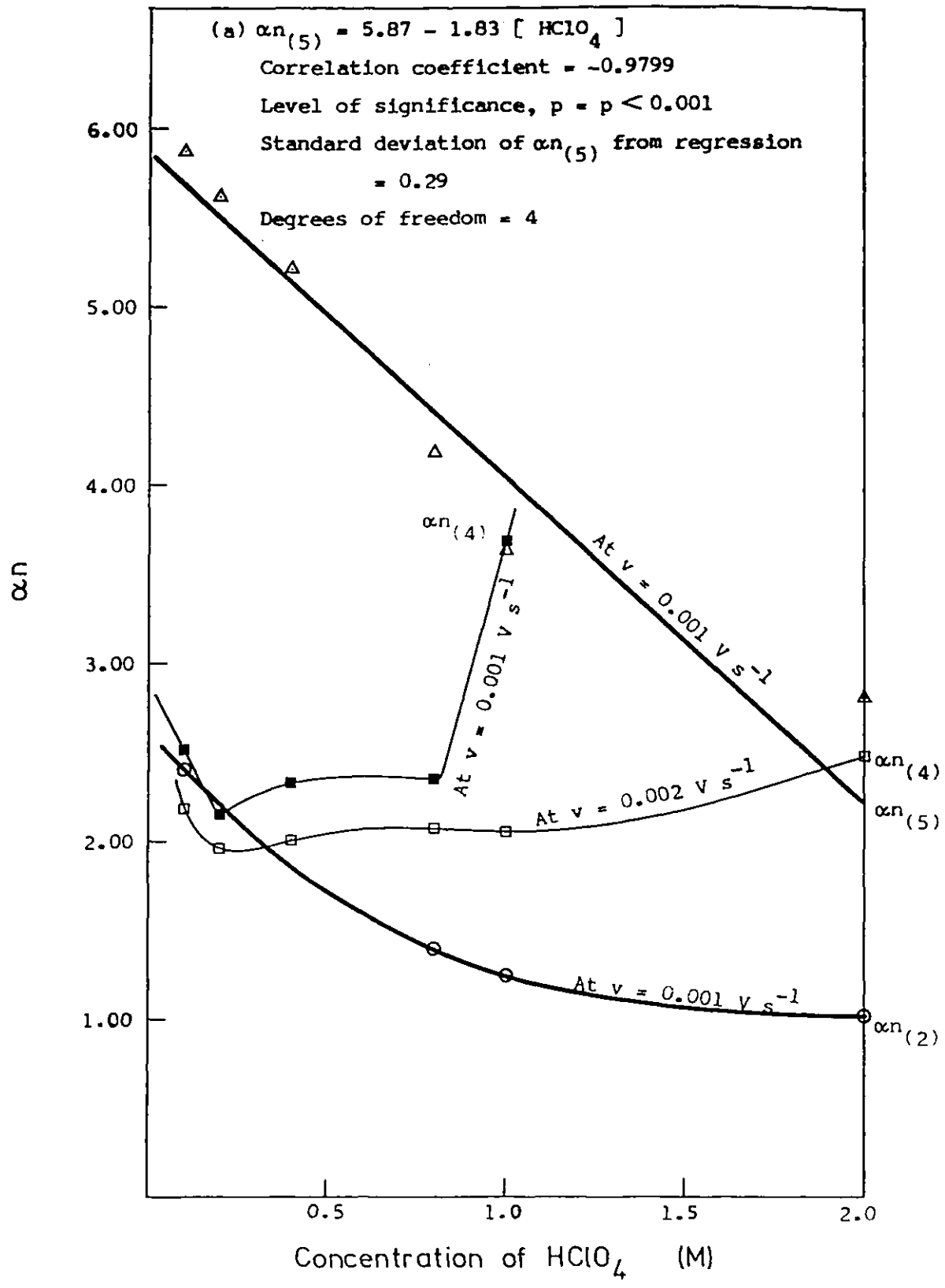

Fig. 5-125 Ir(IV) Perchlorate (1.0×10^{-4} mol dm^{-3})/Perchloric acid supporting electrolyte System: Values of αn as a function of concentration of perchloric acid; at scan rates, v, of 0.001 and 0.002 V s^{-1}. Graphite solid electrode.

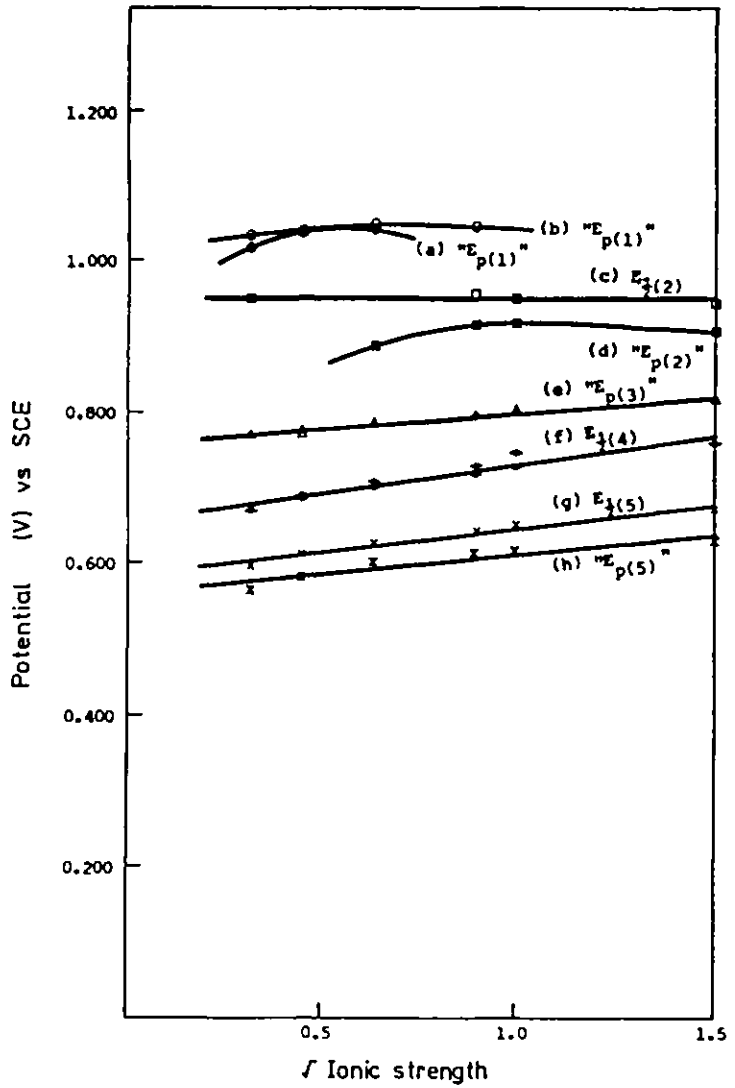

Fig. 5-126 Ir(IV) Perchlorate (1.0×10^{-4} mol dm^{-3})/Perchloric acid (0.1 to 2.0 M) supporting electrolyte System: Values of half-wave potential, $E_{\frac{1}{2}}$, or "peak potential", "E_p" (when the voltammogram exhibits a peak rather than a wave), as a function of square root of total ionic strength, $\sqrt{I}$ (where the concentration of perchloric acid was varied). Graphite solid electrode.

Fig. 5-126 (continued):-

(a) At scan rate, v = 0.001 V s^{-1}: Values of "$E_{p(1)}$".

(b) At scan rate, v = 0.002 V s^{-1}: Values of "$E_{p(1)}$".

(c) At scan rate, v = 0.001 V s^{-1}:
$E_{\frac{1}{2}(2)}$ mean = 0.950 V
Standard deviation = 0.005 V
Degrees of freedom = 3

(d) At scan rate, v = 0.002 V s^{-1}: Values of "$E_{p(2)}$".

(e) At scan rate, v = 0.001 and 0.002 V s^{-1}:
"$E_{p(3)}$" = $0.755 + 4.58 \times 10^{-2} \sqrt{I}$
Correlation coefficient = 0.9913
Level of significance, p = $p < 0.001$
Standard deviation of "$E_{p(3)}$" from regression = 0.002 V
Degrees of freedom = 10

(f) At scan rate, v = 0.001 and 0.002 V s^{-1}:
$E_{\frac{1}{2}(4)} = 0.651 + 8.36 \times 10^{-2} \sqrt{I}$
Correlation coefficient = 0.9761
Level of significance, p = $p < 0.001$
Standard deviation of $E_{\frac{1}{2}(4)}$ from regression = 0.007 V
Degrees of freedom = 9

(g) At scan rate, v = 0.001 V s^{-1}:
$E_{\frac{1}{2}(5)} = 0.580 + 6.94 \times 10^{-2} \sqrt{I}$
Correlation coefficient = 0.9879
Level of significance, p = $p < 0.001$
Standard deviation of $E_{\frac{1}{2}(5)}$ from regression = 0.005 V
Degrees of freedom = 4

(h) At scan rate, v = 0.002 V s^{-1}:
"$E_{p(5)}$" = $0.556 + 5.89 \times 10^{-2} \sqrt{I}$
Correlation coefficient = 0.9580
Level of significance, p = $0.001 < p < 0.01$
Standard deviation of "$E_{p(5)}$" from regression = 0.008 V
Degrees of freedom = 4

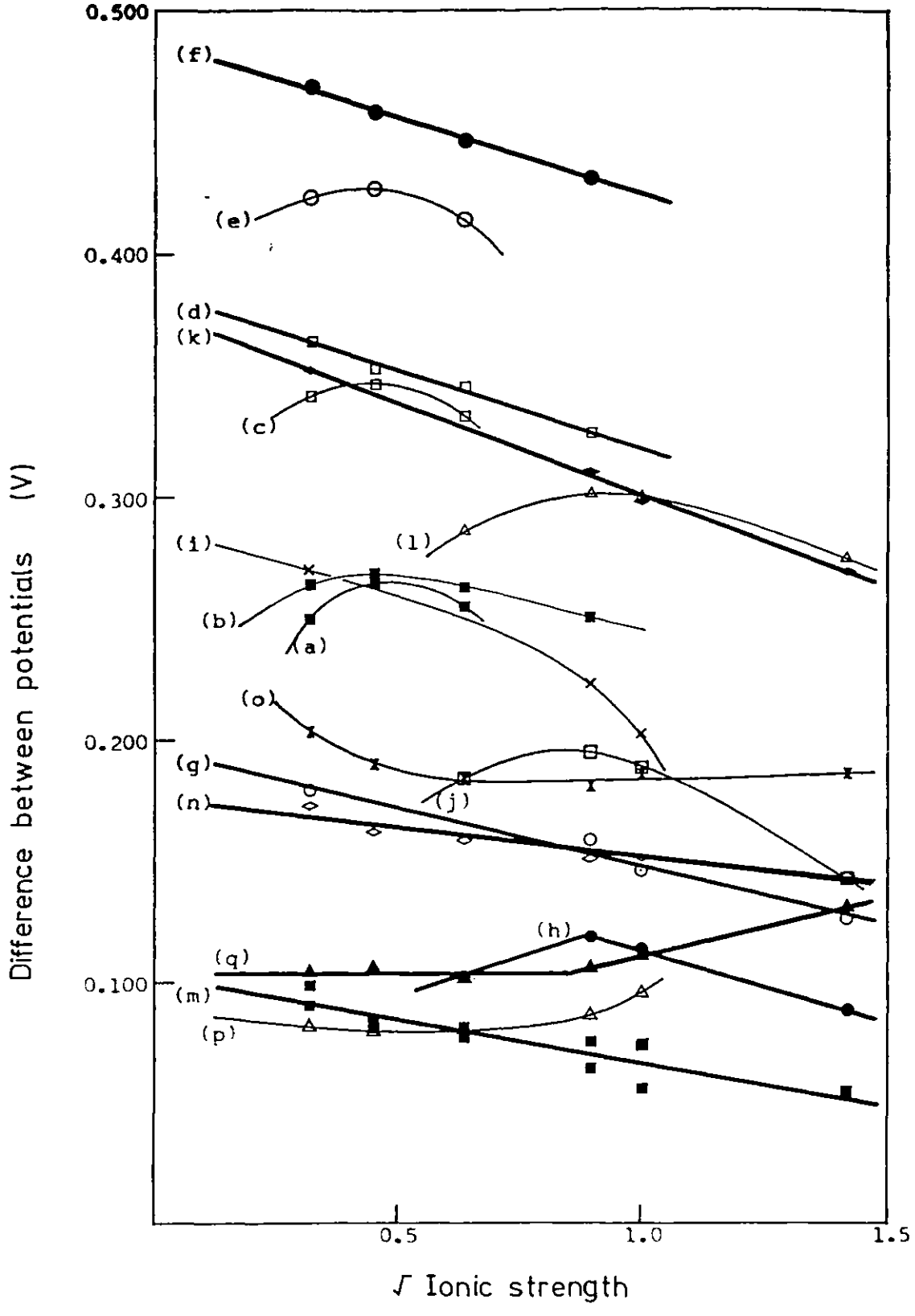

Fig. 5-127 Ir(IV) Perchlorate (1.0×10^{-4} mol dm^{-3})/Perchloric acid (0.1 to 2.0 M) supporting electrolyte System: Values of difference between potentials as a function of square root of total ionic strength, $\sqrt{I}$ (where the concentration of perchloric acid was varied). Graphite solid electrode.

Fig. 5-127 (continued):-

(a) At scan rate, $v = 0.001$ V s^{-1}: Values of $|"E_{p(1)}" - "E_{p(3)}"|$.

(b) At scan rate, $v = 0.002$ V s^{-1}: Values of $|"E_{p(1)}" - "E_{p(3)}"|$.

(c) At scan rate, $v = 0.001$ V s^{-1}: Values of $|"E_{p(1)}" - E_{\frac{1}{2}(4)}|$.

(d) At scan rate, $v = 0.002$ V s^{-1}:

$|"E_{p(1)}" - E_{\frac{1}{2}(4)}| = 0.383 - 6.32 \times 10^{-2} \sqrt{I}$
Correlation coefficient = -0.9939
Level of significance, $p = 0.001 < p < 0.01$
Standard deviation of $|"E_{p(1)}" - E_{\frac{1}{2}(4)}|$ from regression = 0.002 V
Degrees of freedom = 2

(e) At scan rate, $v = 0.001$ V s^{-1}: Values of $|"E_{p(1)}" - E_{\frac{1}{2}(5)}|$.

(f) At scan rate, $v = 0.002$ V s^{-1}:

$|"E_{p(1)}" - "E_{p(5)}"| = 0.487 - 6.25 \times 10^{-2} \sqrt{I}$
Correlation coefficient = -0.9986
Level of significance, $p = 0.001 < p < 0.01$
Standard deviation of $|"E_{p(1)}" - "E_{p(5)}"|$ from regression
= 0.001 V
Degrees of freedom = 2

(g) At scan rate, $v = 0.001$ V s^{-1}:

$|E_{\frac{1}{2}(2)} - "E_{p(3)}"| = 0.197 - 4.89 \times 10^{-2} \sqrt{I}$
Correlation coefficient = -0.9854
Level of significance, $p = 0.01 < p < 0.02$
Standard deviation of $|E_{\frac{1}{2}(2)} - "E_{p(3)}"|$ from regression = 0.005 V
Degrees of freedom = 2

(h) At scan rate, $v = 0.002$ V s^{-1}: Values of $|"E_{p(2)}" - "E_{p(3)}"|$.

(i) At scan rate, $v = 0.001$ V s^{-1}: Values of $|E_{\frac{1}{2}(2)} - E_{\frac{1}{2}(4)}|$.

(j) At scan rate, $v = 0.002$ V s^{-1}: Values of $|"E_{p(2)}" - E_{\frac{1}{2}(4)}|$.

(k) At scan rate, $v = 0.001$ V s^{-1}:

$|E_{\frac{1}{2}(2)} - E_{\frac{1}{2}(5)}| = 0.377 - 7.61 \times 10^{-2} \sqrt{I}$
Correlation coefficient = -0.9985
Level of significance, $p = 0.001 < p < 0.01$
Standard deviation of $|E_{\frac{1}{2}(2)} - E_{\frac{1}{2}(5)}|$ from regression = 0.002 V
Degrees of freedom = 2

(l) At scan rate, $v = 0.002$ V s^{-1}: Values of $|"E_{p(2)}" - "E_{p(5)}"|$.

(m) At scan rate, $v = 0.001$ and 0.002 V s^{-1}:

$|"E_{p(3)}" - E_{\frac{1}{2}(4)}| = 0.103 - 3.60 \times 10^{-2} \sqrt{I}$
Correlation coefficient = -0.9053
Level of significance, $p = p < 0.001$
Standard deviation of $|"E_{p(3)}" - E_{\frac{1}{2}(4)}|$ from regression
= 0.006 V
Degrees of freedom = 9

(n) At scan rate, $v = 0.001$ V s^{-1}:

$|"E_{p(3)}" - E_{\frac{1}{2}(5)}| = 0.176 - 2.46 \times 10^{-2} \sqrt{I}$
Correlation coefficient = -0.9597
Level of significance, $p = 0.001 < p < 0.01$
Standard deviation of $|"E_{p(3)}" - E_{\frac{1}{2}(5)}|$ from regression
= 0.003 V
Degrees of freedom = 4

(o) At scan rate, $v = 0.002$ V s^{-1}: Values of $|"E_{p(3)}" - "E_{p(5)}"|$.

(p) At scan rate, $v = 0.001$ V s^{-1}: Values of $|E_{\frac{1}{2}(4)} - E_{\frac{1}{2}(5)}|$.

(q) At scan rate, $v = 0.002$ V s^{-1}: Values of $|E_{\frac{1}{2}(4)} - "E_{p(5)}"|$.

The current function, $i_{max}/A\ [Ir(ClO_4)_4]$ (where i_{max} is the limiting or peak current), is plotted against increasing concentration of perchloric acid in Fig. 5-128. Wave 1 could not be quantitatively interpreted, but its disappearance at high perchloric acid concentrations (Fig. 5-124) or slower scan rate (Fig 5-101, 1) suggests the presence of adsorption. The current function for Wave 2 decreased with increasing perchloric acid concentration (Fig. 5-128, a and b), with the values being higher at the faster scan rate of 0.002 V s^{-1}, thus signifying a weakening in the adsorption effect. Wave 3, although weakly affected by a catalytic reaction, was more influenced by adsorption and so its current function initially increased but retreated later to end at lower values (Fig. 5-128, c and d). The effects of perchloric acid concentration and scan rate on Wave 4 (Fig. 5-128, e and f) were generally similar to that on Wave 3. Wave 5 was greatly influenced by a catalytic reaction, as signified by the increased value of the current function at higher perchloric acid concentrations (Fig. 5-128, g and h) or slower scan rate (0.001 V s^{-1}), although it was also influenced by adsorption.

5-1.5.(i).f Summary

D.c. voltammetric studies of Ir(IV) perchlorate in perchloric acid supporting electrolyte have shown that the reactions and phenomena which occurred at boron carbide, boron carbide/carbon composite, and graphite solid electrodes were generally similar in nature and that any differences that have occurred were due mainly to the difference in the degree of the adsorption effects on these electrodes; adsorption being stronger on electrodes of higher carbon content (Figures 5-99, 5-100, and 5-101). The extremely strong physical adsorption of Ir(IV) perchlorate on these electrodes has already been encountered in voltammetric studies of the chloroiridate- chloroiridite system (section 5-1.1.(iii)).

The evidence suggests that, for the boron carbide solid electrode, three waves were obtained (Fig. 5-104) of which Wave 1, the most anodic, was mainly diffusion controlled and thus yielded a linear dependence of limiting current density on the concentration of Ir(IV) perchlorate (Fig. 5-107, a). The variations in αn and $E_{\frac{1}{2}}$ values with Ir(IV) perchlorate concentration (Fig. 5-105, a and Fig. 5-106, a respectively), however, do suggest the influence of a very weak adsorption effect on Wave 1. Wave 2 was a post-wave, due to the strong adsorption of reactant, which disappeared at high Ir(IV) perchlorate concentration. Wave 3, however,

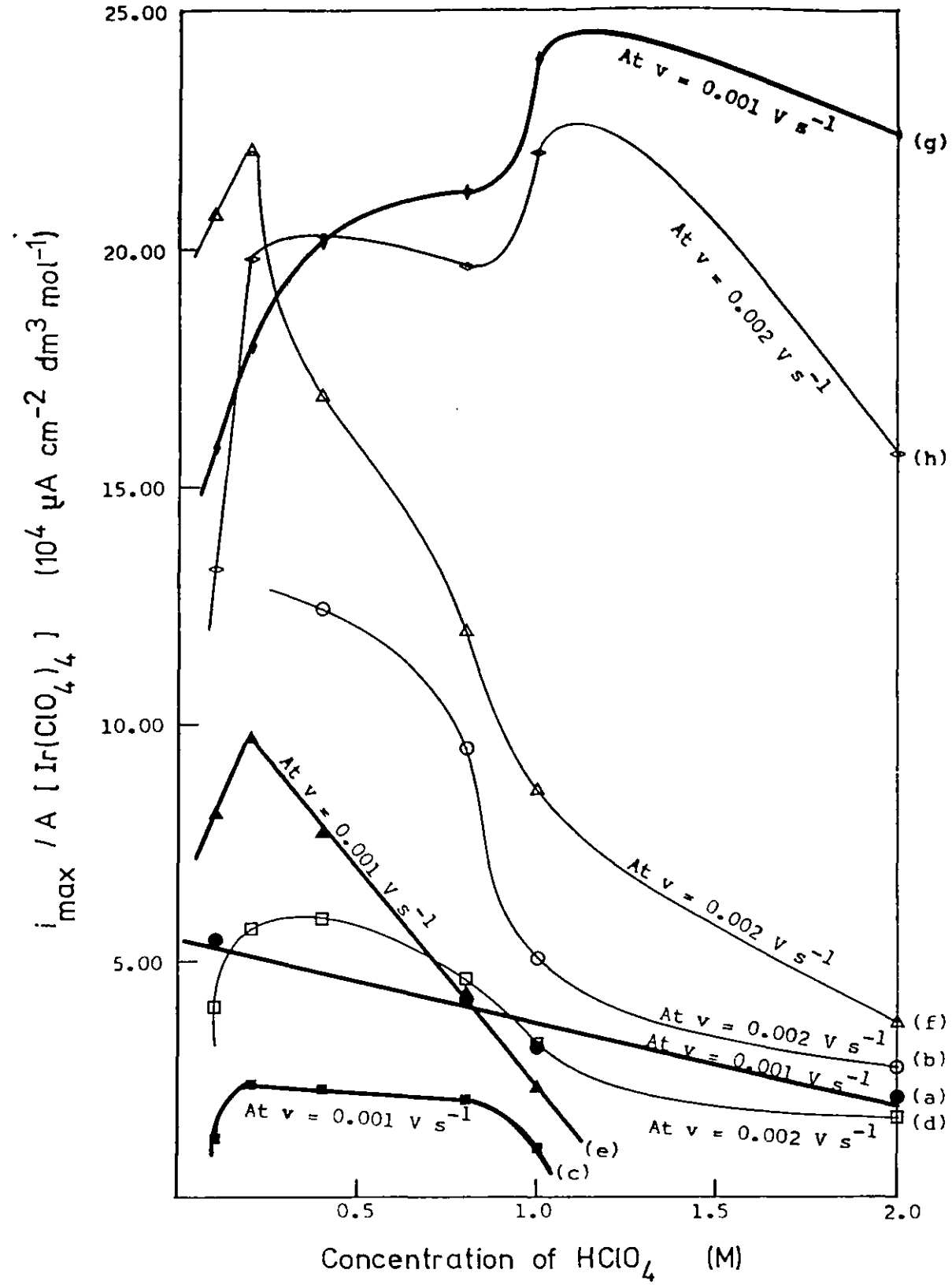

Fig. 5-128 Ir(IV) Perchlorate (1.0×10^{-4} mol dm^{-3})/Perchloric acid supporting electrolyte System: Values of maximum current per unit area divided by concentration of Ir(IV) Perchlorate as a function of concentration of perchloric acid; at scan rates, v, of 0.001 and 0.002 V s^{-1}. (a) $i_{L(2)}/A$ [$Ir(ClO_4)_4$], (b) "$i_{p(2)}$"/A [$Ir(ClO_4)_4$], (c) & (d) "$i_{p(3)}$"/A [$Ir(ClO_4)_4$], (e) & (f) $i_{L(4)}/A$ [$Ir(ClO_4)_4$], (g) $i_{L(5)}/A$ [$Ir(ClO_4)_4$], (h) "$i_{p(5)}$"/A [$Ir(ClO_4)_4$]. Graphite solid electrode.

was influenced both by adsorption and a catalytic reaction. The limiting current density of Wave 3 was linearly dependent on Ir(IV) perchlorate concentration only when the maximum on the wave was excluded (Fig. 5-107, b). The αn and $E_{\frac{1}{2}}$ values varied with increasing Ir(IV) perchlorate concentration (Fig. 5-105, b and Fig. 5-106, b respectively). Furthermore, the limiting current function, $i_{L(3)}/A\ [Ir(ClO_4)_4]$, increased with increasing perchloric acid concentration (Fig. 5-111, d and e).

At the highest concentration of Ir(IV) perchlorate, 2.3×10^{-3} mol dm^{-3}, in perchloric acid (0.1 M) supporting electrolyte studied: $\alpha n_{(1)} = 0.99 \pm 0.07$ (17 degrees of freedom), $E_{\frac{1}{2}(1)} = 0.955$ V (vs. SCE) $\pm$ 0.003 V (16 degrees of freedom); $\alpha n_{(3)} = 2.49 \pm 0.10$ (23 degrees of freedom), and $E_{\frac{1}{2}(3)} = 0.672$ V (vs. SCE) $\pm$ 0.001 V (23 degrees of freedom).

The increase in the concentration of perchloric acid supporting electrolyte, apart from enhancing the catalytic reaction, also debilitated the adsorption effects and caused the potentials of all the waves to be shifted anodically, but the differences between these potentials were narrowed (Fig. 5-110). The anodic shift of all the potentials with increasing ionic strength is anomalous because Ir(IV) perchlorate was found to be cationic by studies with paper electrophoresis. A possible explanation for this anomalous behaviour might be that the waves, initially shifted to less anodic potentials by the extremely strong physical adsorption of Ir(IV) perchlorate reactant, were merely gradually returning to potentials corresponding to pure diffusion control as the adsorption effect was debilitated by the increasing perchloric acid concentration.

At boron carbide/carbon composite solid electrodes, three voltammetric waves (similar to those at the boron carbide electrodes) were obtained when the carbon content of the electrodes was low. When the carbon content of the electrodes was increased, however, the least anodic wave was split into two waves, Waves 3 and 4 (Figures 5-99 and 5-100). Studies of the effects of scan rate and perchloric acid concentration on the voltammograms for Ir(IV) perchlorate show that Wave 1 was affected by weak adsorption and a catalytic reaction, Wave 2 was an adsorption post-wave due to the reactant, Wave 3 was affected mainly by adsorption, and Wave 4 was affected mainly by a catalytic reaction.

D.c. voltammetry of Ir(IV) perchlorate at the graphite solid electrode exhibited five waves; consisting of the four waves already obtained

at boron carbide/carbon composite electrodes of high carbon content, and an additional wave (labelled ß in Fig. 5-100, 1) which appeared at a potential more anodic than for all the other waves. The effects of scan rate and perchloric acid concentration (Fig. 5-124) on the waves indicate that Wave 1 was an adsorption pre-wave due to the product, Wave 2 was a diffusion wave complicated by adsorption, Wave 3 was an adsorption post-wave weakly complicated by a catalytic reaction, Wave 4 was also an adsorption wave weakly complicated by a catalytic reaction, and Wave 5 was a catalytic wave complicated by adsorption.

The anodic shift of the potentials of the voltammetric waves for Ir(IV) perchlorate, obtained at boron carbide/carbon composite and graphite solid electrodes, with increasing ionic strength (as the perchloric acid concentration was increased) was similar to the phenomenon encountered with boron carbide solid electrodes and thus may be similarly explained.

5-1.5.(ii) Linear sweep and cyclic voltammetry.

5-1.5.(ii).a Boron carbide solid electrode $B_{4.05}C$

Cyclic voltammograms of Ir(IV) perchlorate (1.0×10^{-4} mol dm^{-3}), in perchloric acid (0.1 M) supporting electrolyte, obtained at the boron carbide solid electrode $B_{4.05}C$ over a range of sweep rates are presented in Fig. 5-129. As can be seen, Peak 4 increased in height and became better defined at faster sweep rates; thus suggesting the presence of adsorption. Quantitative treatment of the interpretable peaks is presented in Fig. 5-130, which shows that the cathodic and anodic current functions of all four peaks were influenced by adsorption; with Peak 1 being least affected. The ratios of cathodic to anodic peak currents as functions of $(\text{sweep rate})^{\frac{1}{2}}$ are plotted in Fig. 5-131 which shows that, generally, the sweep rate affected the cathodic currents more than the anodic counterparts. Although actual values for the ratios cannot be considered to be quantitative, because of the difficulty in establishing comparable cathodic and anodic base lines, the trends obtained suggest the influence of weak adsorption of reactant on Peaks 1 and 3 (Fig. 5-131, a and c respectively) and that Peak 2 was due to the strong adsorption of reactant (Fig. 5-131, b).

Fig. 5-132 shows that at the low Ir(IV) perchlorate concentration of 2.0×10^{-5} mol dm^{-3} Peak 1 was probably affected initially by a

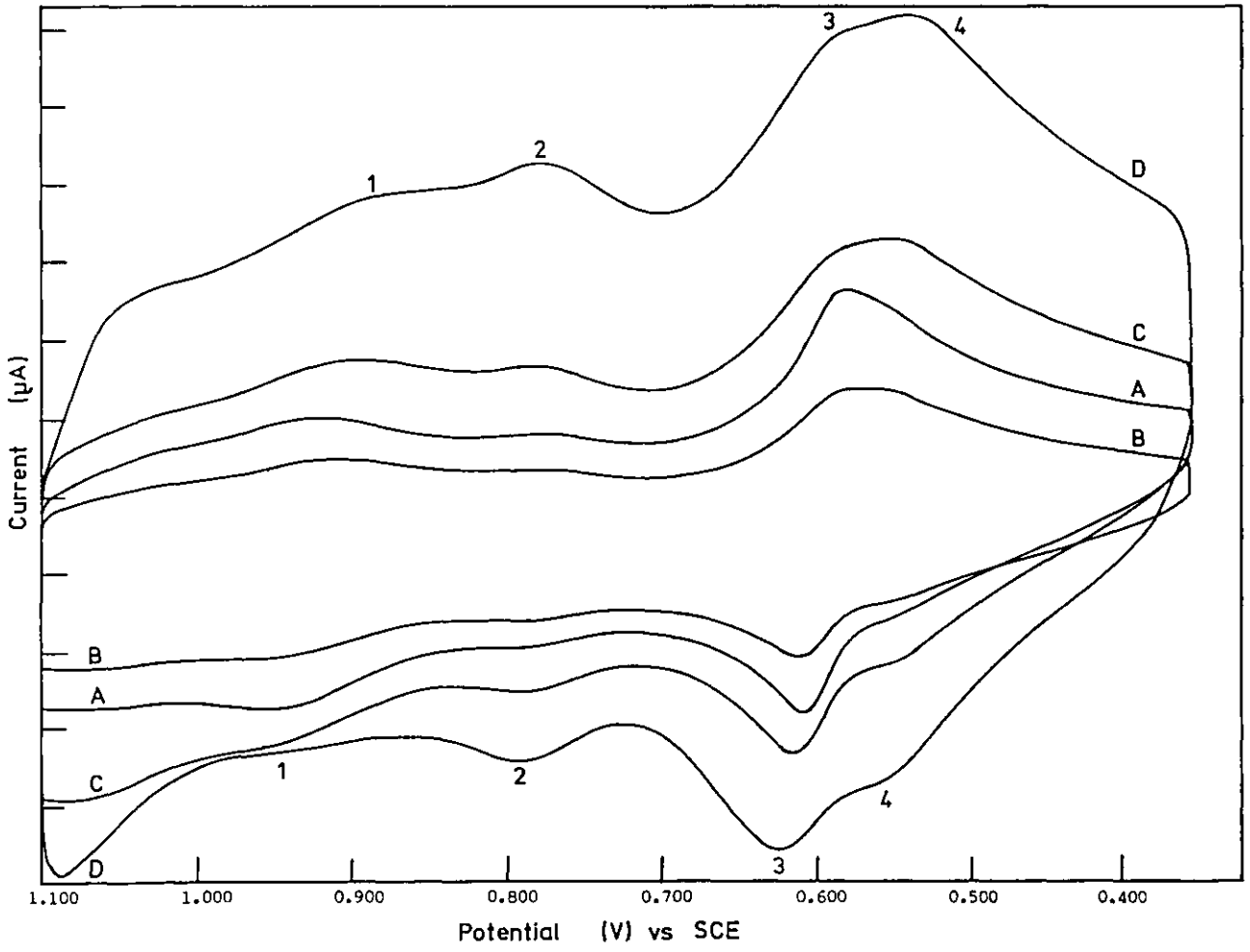

Fig. 5-129 Ir(IV) perchlorate (1.0×10^{-4} mol dm^{-3})/Perchloric acid (0.1 M) supporting electrolyte System: Cyclic voltammograms obtained at the boron carbide solid electrode $B_{4.05}C$ over a range of potential sweep rates, v. A) v = 0.010 V s^{-1}, current sensitivity = 20 μA/division; B) v = 0.020 V s^{-1}, current sensitivity = 50 μA/division; C) v = 0.050 V s^{-1}, current sensitivity = 50 μA/division; and D) v = 0.500 V s^{-1}, current sensitivity = 200 μA/division.

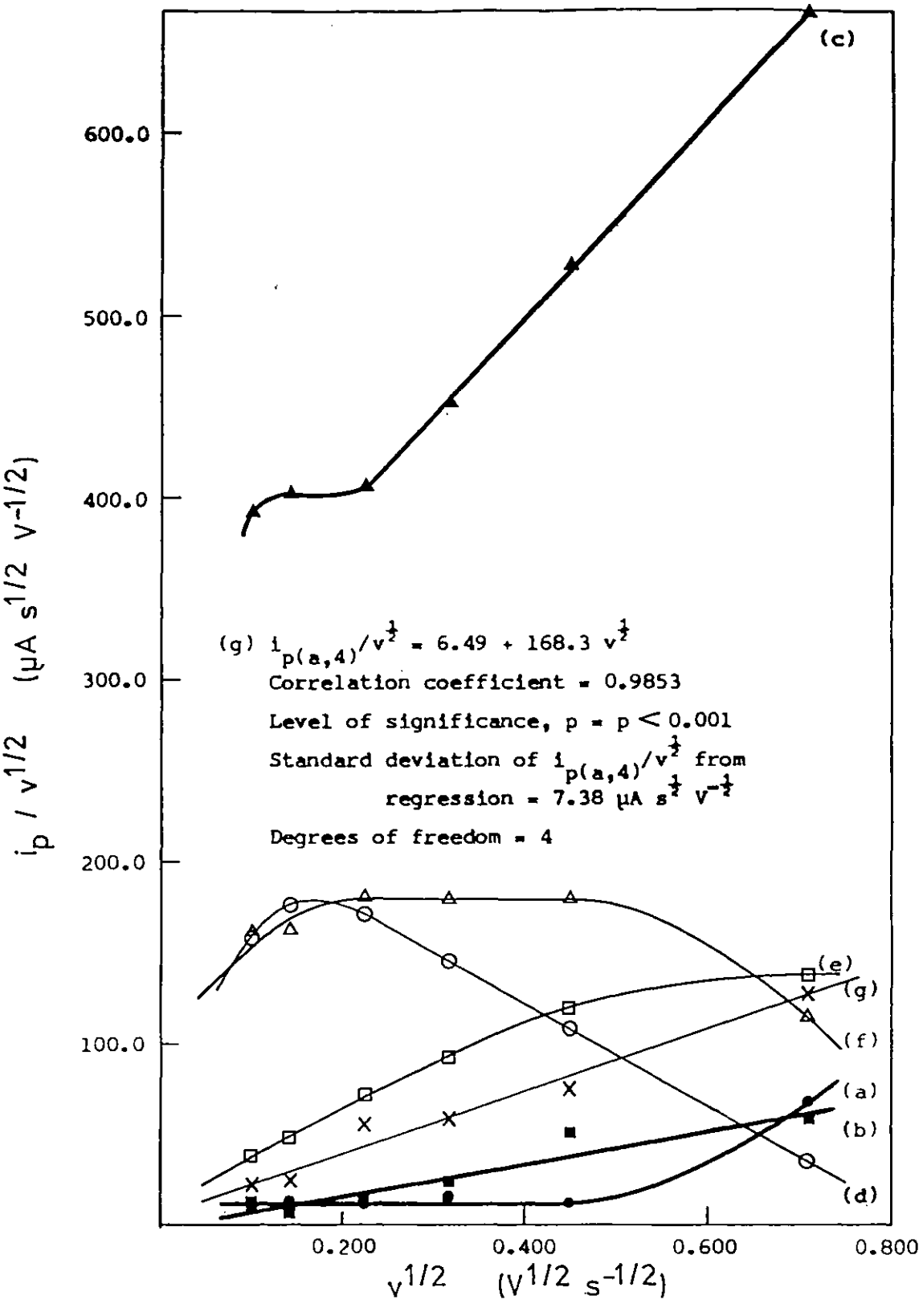

Fig. 5-130 Ir(IV) Perchlorate (1.0×10^{-4} mol dm^{-3})/Perchloric acid (0.1 M) supporting electrolyte System: Values of cathodic and anodic current functions, $i_{p(c)}/v^{\frac{1}{2}}$ and $i_{p(a)}/v^{\frac{1}{2}}$ respectively, as a function of square root of potential scan rate, $v^{\frac{1}{2}}$. (a) $i_{p(c,1)}/v^{\frac{1}{2}}$, (b) $i_{p(c,2)}/v^{\frac{1}{2}}$, (c) $i_{p(c,3)}/v^{\frac{1}{2}}$, (d) $i_{p(a,1)}/v^{\frac{1}{2}}$, (e) $i_{p(a,2)}/v^{\frac{1}{2}}$, (f) $i_{p(a,3)}/v^{\frac{1}{2}}$, (g) $i_{p(a,4)}/v^{\frac{1}{2}}$. Boron carbide solid electrode $B_{4.05}C$.

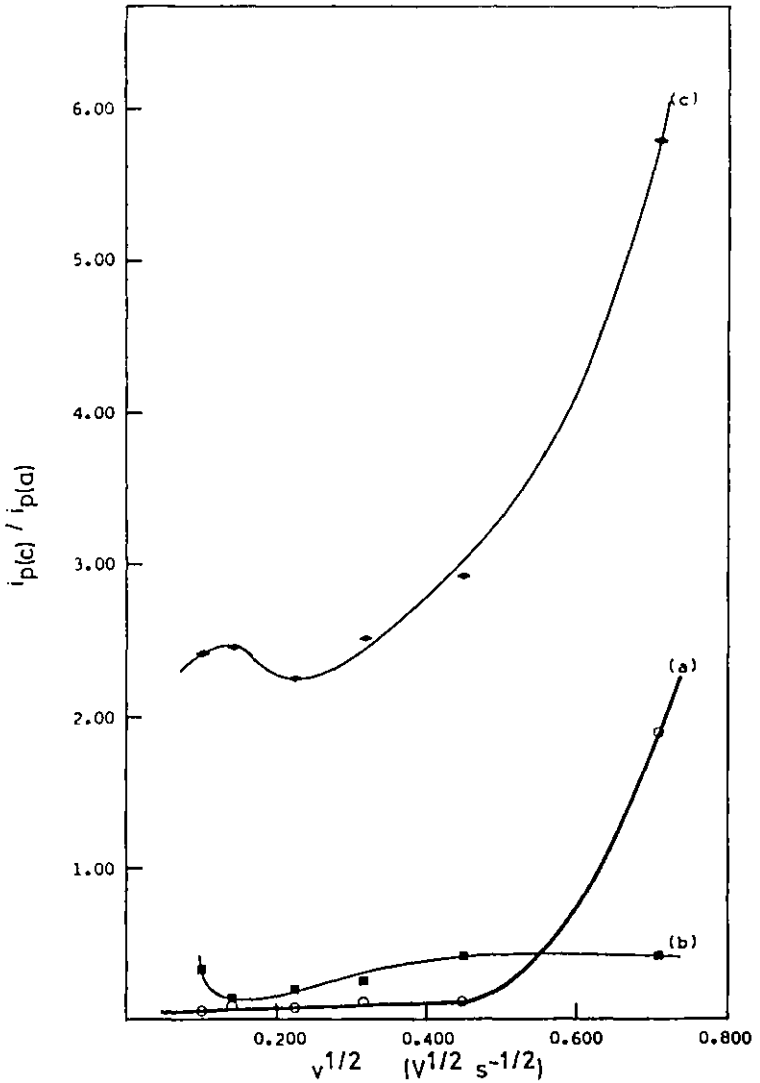

Fig. 5-131 Ir(IV) Perchlorate (1.0×10^{-4} mol dm^{-3})/Perchloric acid (0.1 M) supporting electrolyte System: Values of ratio of cathodic to anodic peak currents, $i_{p(c)}/i_{p(a)}$, as a function of square root of potential scan rate, $v^{\frac{1}{2}}$. (a) $i_{p(c,1)}/i_{p(a,1)}$, (b) $i_{p(c,2)}/i_{p(a,2)}$, and (c) $i_{p(c,3)}/i_{p(a,3)}$. Boron carbide solid electrode $B_{4.05}C$.

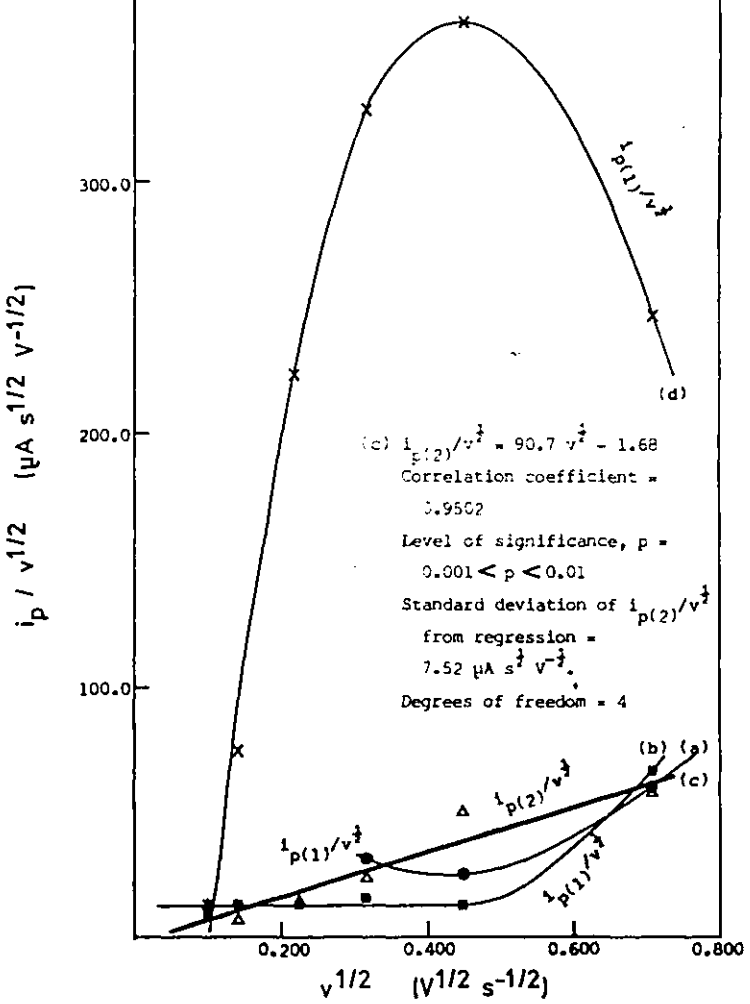

Fig. 5-132 Ir(IV) Perchlorate/Perchloric acid (0.1 M) supporting electrolyte System: Values of cathodic current function, $i_p/v^{\frac{1}{2}}$, as a function of square root of potential scan rate, $v^{\frac{1}{2}}$, at the Ir(IV) Perchlorate concentrations (a) 2.0×10^{-5}, (b) & (c) 1.0×10^{-4}, and (d) 2.3×10^{-3} mol dm^{-3}. Boron carbide solid electrode $B_{4.05}C$.

catalytic reaction whereas at 1.0×10^{-4} mol dm^{-3} Peak 1 was initially diffusion controlled; but both cases show the influence of adsorption at the faster sweep rates. The influence of adsorption on Peak 1 was more pronounced at the higher Ir(IV) perchlorate concentration of 2.3×10^{-3} mol dm^{-3}. Peak 2 was not defined at the low concentration of 2.0×10^{-5} mol dm^{-3}; which is consistent with Henry's Law behaviour (equation 3-67) for low concentrations when separate peaks for strong adsorption are not exhibited. At the Ir(IV) perchlorate concentration of 1.0×10^{-4} mol dm^{-3}, however, Peak 2 showed the current function characteristic of adsorption (Fig. 5-132, c); but the definition of Peak 2 deteriorated at much higher concentrations of e.a.s., another symptom of adsorption. Adsorption effects on Peaks 1 and 2 cause the respective peak current densities to increase non-linearly with concentration (Fig. 5-134).

Peak 3 was exhibited over the entire range of Ir(IV) perchlorate concentration investigated. The variations in Peak 3 current function with changes in sweep rate (Fig. 5-133) show that at low concentrations and sweep rates Peak 3 was almost diffusion controlled with slight complication by a catalytic reaction. At higher concentrations and sweep rates, however, the adsorption effect became dominant. Although the dependence of cathodic Peak 3 current density, $i_{p(3)}/A$, on the Ir(IV) perchlorate concentration was generally linear (Fig. 5-134), a closer examination of the lower end of the concentration range shows a distinct non-linearity typical of the influence of weak adsorption.

Linear sweep voltammograms of Ir(IV) perchlorate (1.0×10^{-4} mol dm^{-3}) in perchloric acid (0.1 M) supporting electrolyte, which have been monitored by a cathode ray oscilloscope for sweep rates up to 5 V s^{-1}, confirm the trends already noted previously in cyclic voltammetry (Fig. 5-135 c.f. Fig. 5-129).

The cathodic peak potentials are plotted against sweep rate in Fig. 5-136 and show that $E_{p(c,1)}$, $E_{p(c,3)}$, and $E_{p(c,4)}$ were shifted cathodically by increasing sweep rate but $E_{p(c,2)}$ remained steady (mean value = 0.793 V (vs SCE) ± 0.017 V, 35 degrees of freedom). However, Fig. 5-137 shows that the cathodic $|E_p - E_{p/2}|$ values for Peaks 1 and 3 increased with increasing sweep rate and thus their cathodic shift in potential was the result of decreasing reversibility of the charge transfer. $|E_{p(c,2)} - E_{p(c,2)/2}|$ values decreased initially with increasing sweep rate but later recovered to approximately former levels at faster rates; indicating adsorption influences. The effect of Ir(IV) perchlorate concentration on cathodic peak potentials was to shift them to more anodic values with increasing $I^{\frac{1}{2}}$ (Fig. 5-138).

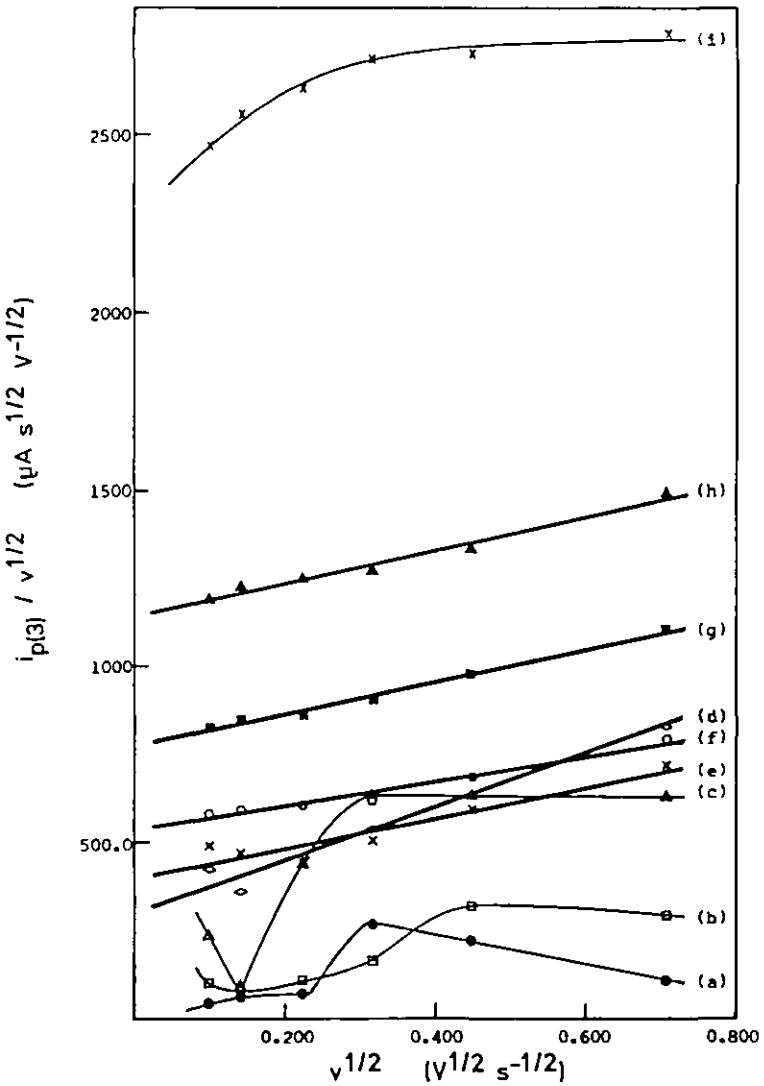

Fig. 5-133 Ir(IV) Perchlorate/Perchloric acid (0.1 M) supporting electrolyte System: Values of cathodic current function, $i_{p(3)}/v^{\frac{1}{2}}$, as a function of square root of potential scan rate, $v^{\frac{1}{2}}$; at the Ir(IV) Perchlorate concentrations (a) 4.0×10^{-6}, (b) 1.0×10^{-5}, (c) 2.0×10^{-5}, (d) 4.0×10^{-5}, (e) 8.0×10^{-5}, (f) 2.0×10^{-4}, (g) 4.0×10^{-4}, (h) 8.0×10^{-4}, and (i) 2.3×10^{-3} mol dm^{-3}. Boron carbide solid electrode $B_{4.05}C$.

Fig. 5-133 (continued):-

(d) $i_{p(3)}/v^{\frac{1}{2}} = 303.3 + 764.7\ v^{\frac{1}{2}}$
Correlation coefficient = 0.9766
Level of significance, p = $p < 0.001$
Standard deviation of $i_{p(3)}/v^{\frac{1}{2}}$ from regression = 42.6 μA $s^{\frac{1}{2}}$ $V^{-\frac{1}{2}}$
Degrees of freedom = 4

(e) $i_{p(3)}/v^{\frac{1}{2}} = 396.5 + 433.3\ v^{\frac{1}{2}}$
Correlation coefficient = 0.9312
Level of significance, $0.001 < p < 0.01$
Standard deviation of $i_{p(3)}/v^{\frac{1}{2}}$ from regression = 42.8 μA $s^{\frac{1}{2}}$ $V^{-\frac{1}{2}}$
Degrees of freedom = 4

(f) $i_{p(3)}/v^{\frac{1}{2}} = 537.2 + 348.1\ v^{\frac{1}{2}}$
Correlation coefficient = 0.9828
Level of significance, p = $p < 0.001$
Standard deviation of $i_{p(3)}/v^{\frac{1}{2}}$ from regression = 16.5 μA $s^{\frac{1}{2}}$ $V^{-\frac{1}{2}}$
Degrees of freedom = 4

(g) $i_{p(3)}/v^{\frac{1}{2}} = 775.7 + 455.6\ v^{\frac{1}{2}}$
Correlation coefficient = 0.9936
Level of significance, p = $p < 0.001$
Standard deviation of $i_{p(3)}/v^{\frac{1}{2}}$ from regression = 13.1 μA $s^{\frac{1}{2}}$ $V^{-\frac{1}{2}}$
Degrees of freedom = 4

(h) $i_{p(3)}/v^{\frac{1}{2}} = 1145.6 + 464.7\ v^{\frac{1}{2}}$
Correlation coefficient = 0.9890
Level of significance, p = $p < 0.001$
Standard deviation of $i_{p(3)}/v^{\frac{1}{2}}$ from regression = 17.5 μA $s^{\frac{1}{2}}$ $V^{-\frac{1}{2}}$
Degrees of freedom = 4

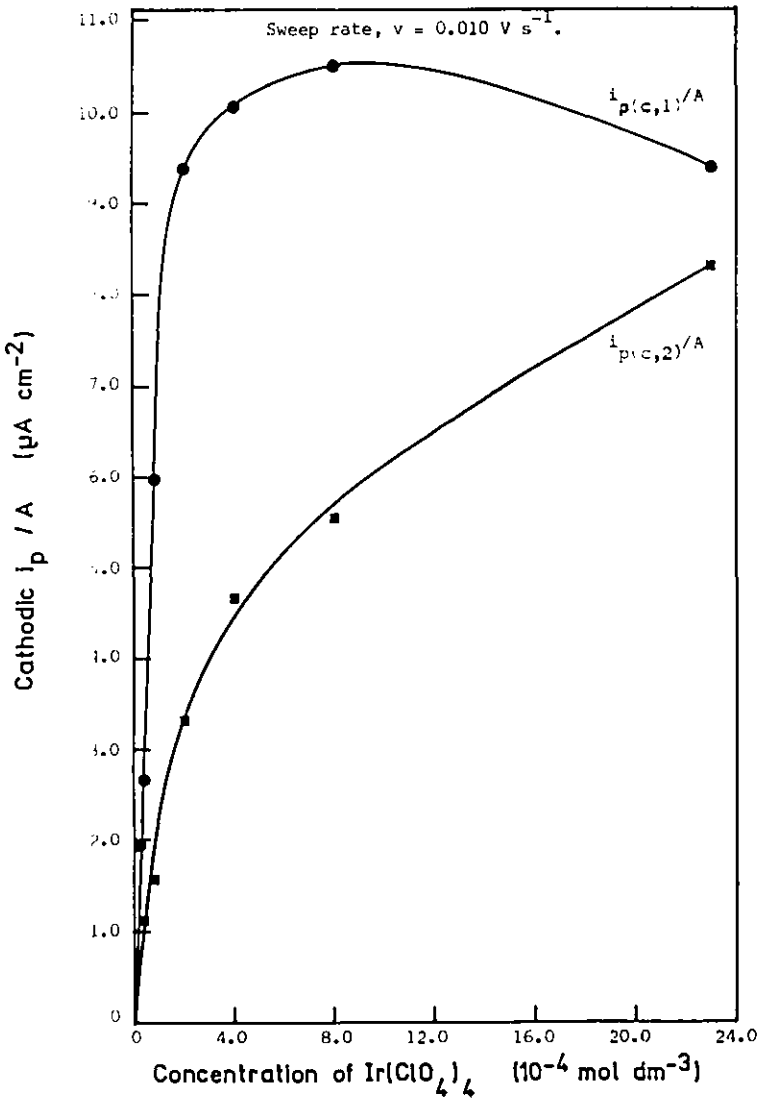

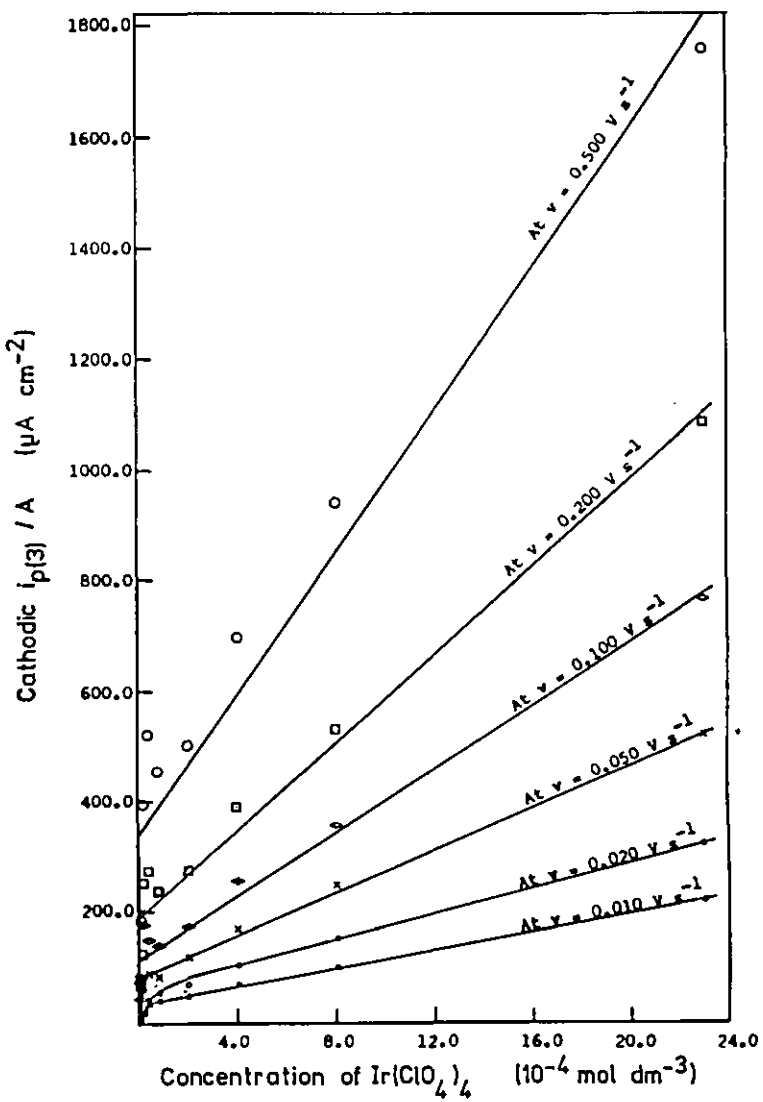

Fig. 5-134 Ir(IV) perchlorate (4.0×10^{-6} to 2.3×10^{-3} mol dm^{-3})/Perchloric acid (0.1 M) supporting electrolyte System: Dependence of the cathodic peak current densities, $i_{p(c,1)}/A$, $i_{p(c,2)}/A$, and $i_{p(c,3)}/A$, on the concentration of Ir(IV) perchlorate electroactive species. Boron carbide solid working electrode $B_{4.05}C$.

Fig. 5-134 (continued):-

(a) At $v = 0.010$ V s^{-1}:

$i_{p(c,3)}/A = 25.4 + 8.70 \times 10^4$ [$Ir(ClO_4)_4$]
Correlation coefficient = 0.9796
Level of significance, $p = p < 0.001$
Standard deviation of $i_{p(c,3)}/A$ from regression = 14.3 μA cm^{-2}
Degrees of freedom = 7

(b) At $v = 0.020$ V s^{-1}:

$i_{p(c,3)}/A = 34.5 + 1.29 \times 10^5$ [$Ir(ClO_4)_4$]
Correlation coefficient = 0.9823
Level of significance, $p = p < 0.001$
Standard deviation of $i_{p(c,3)}/A$ from regression = 19.6 μA cm^{-2}
Degrees of freedom = 7

(c) At $v = 0.050$ V s^{-1}:

$i_{p(c,3)}/A = 63.4 + 2.04 \times 10^5$ [$Ir(ClO_4)_4$]
Correlation coefficient = 0.9826
Level of significance, $p = p < 0.001$
Standard deviation of $i_{p(c,3)}/A$ from regression = 30.9 μA cm^{-2}
Degrees of freedom = 7

(d) At $v = 0.100$ V s^{-1}:

$i_{p(c,3)}/A = 115.4 + 2.84 \times 10^5$ [$Ir(ClO_4)_4$]
Correlation coefficient = 0.9843
Level of significance, $p = p < 0.001$
Standard deviation of $i_{p(c,3)}/A$ from regression = 40.8 μA cm^{-2}
Degrees of freedom = 7

(e) At $v = 0.200$ V s^{-1}:

$i_{p(c,3)}/A = 191.4 + 3.92 \times 10^5$ [$Ir(ClO_4)_4$]
Correlation coefficient = 0.9822
Level of significance, $p = p < 0.001$
Standard deviation of $i_{p(c,3)}/A$ from regression = 60.2 μA cm^{-2}
Degrees of freedom = 7

(f) At $v = 0.500$ V s^{-1}:

$i_{p(c,3)}/A = 336.5 + 6.34 \times 10^5$ [$Ir(ClO_4)_4$]
Correlation coefficient = 0.9607
Level of significance, $p = p < 0.001$
Standard deviation of $i_{p(c,3)}/A$ from regression = 146.8 μA cm^{-2}
Degrees of freedom = 7

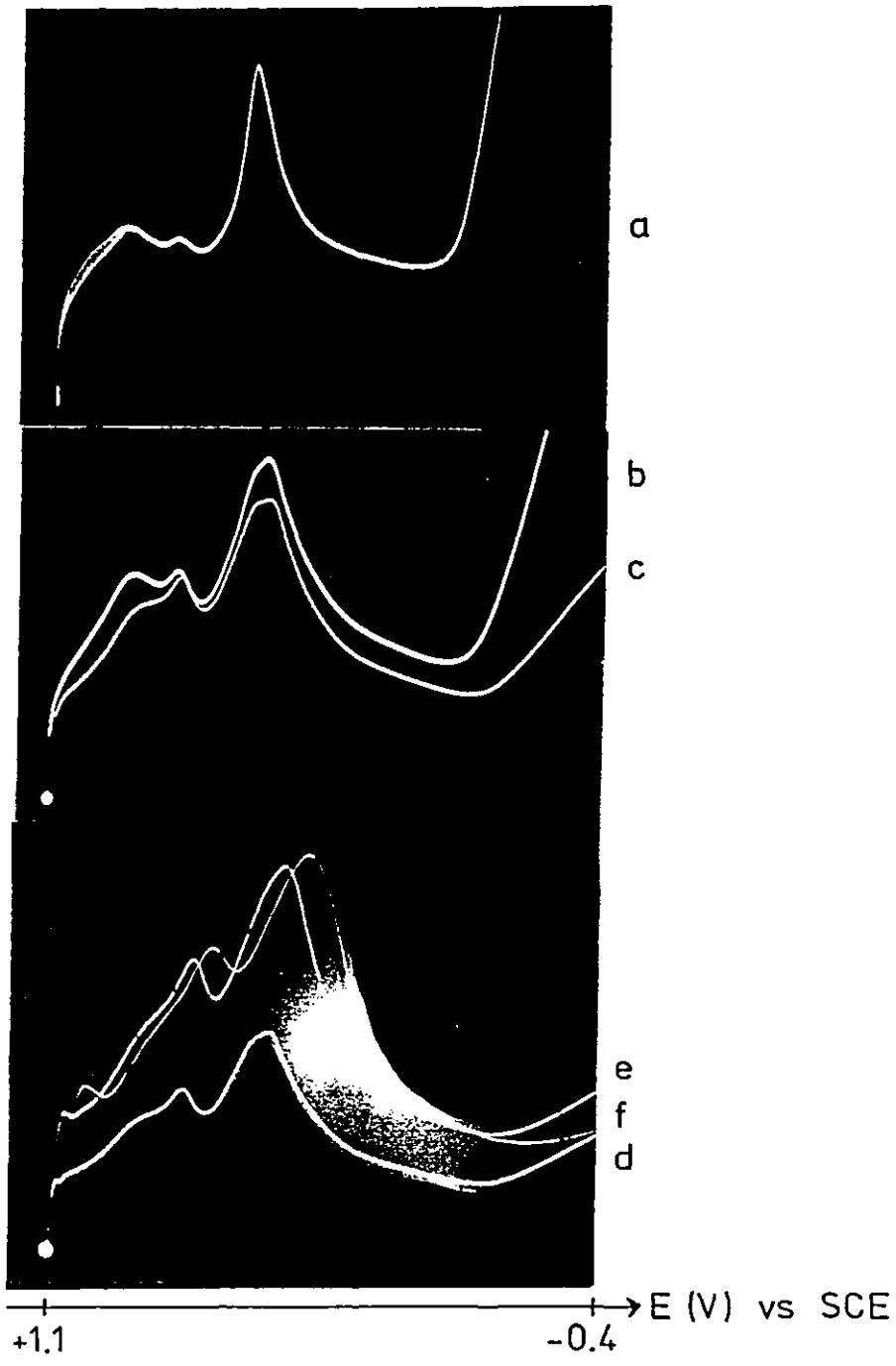

Fig. 5-135 Ir(IV) perchlorate (1.0×10^{-4} mol dm^{-3})/Perchloric acid (0.1 M) supporting electrolyte System: Linear sweep voltammograms obtained at the boron carbide solid electrode $B_{4.05}C$ - variation with sweep rate, v.

	v ($V\ s^{-1}$)	Current sensitivity (mA f.s.d.)
(a)	0.010	0.1
(b)	0.100	0.5
(c)	0.500	2
(d)	1	5
(e)	2	5
(f)	5	10

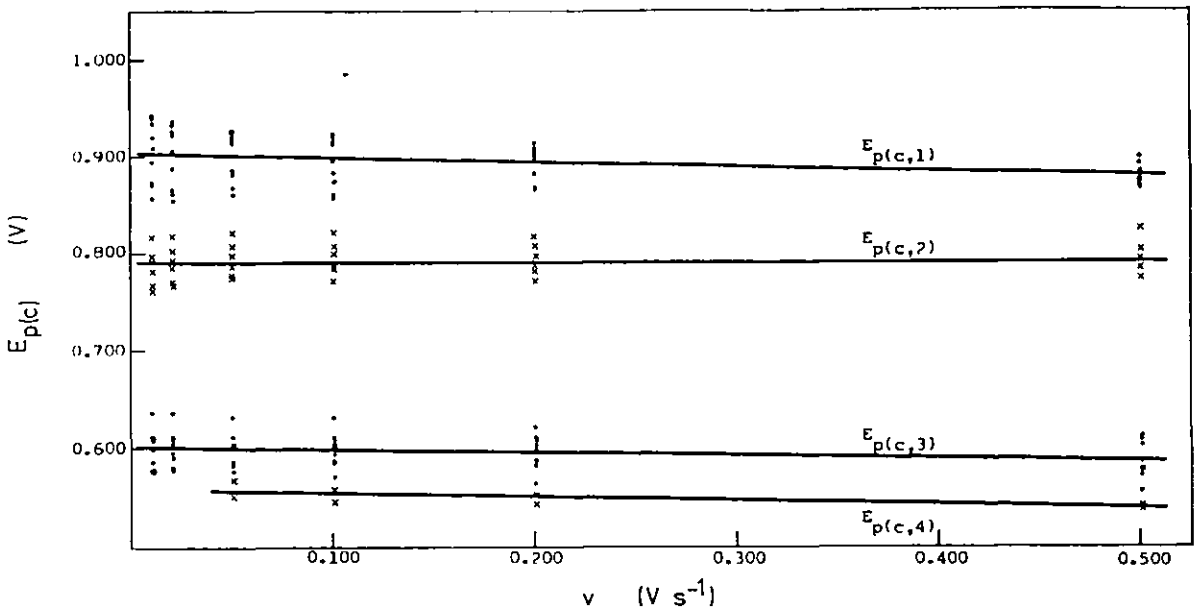

Fig. 5-136 Ir(IV) Perchlorate/Perchloric acid (0.1 M) supporting electrolyte System: Values of cathodic peak potential, $E_{p(c)}$, as a function of potential scan rate, v; at Ir(IV) Perchlorate concentrations of 4.0×10^{-6} to 2.3×10^{-3} mol dm^{-3}. Boron carbide solid electrode $B_{4.05}C$.

(a) $E_{p(c,1)} = 0.904 - 4.92 \times 10^{-2}$ v
Correlation coefficient = -0.3388
Level of significance, $p = 0.01 < p < 0.02$
Standard deviation of $E_{p(c,1)}$ from regression = 0.024 V
Degrees of freedom = 52

(b) $E_{p(c,2)}$ mean = 0.793 V
Standard deviation = 0.017 V
Degrees of freedom = 35

(c) $E_{p(c,3)} = 0.603 - 3.11 \times 10^{-2}$ v
Correlation coefficient = -0.3028
Level of significance, $p = 0.02 < p < 0.05$
Standard deviation of $E_{p(c,3)}$ from regression = 0.017 V
Degrees of freedom = 52

(d) $E_{p(c,4)} = 0.559 - 4.18 \times 10^{-2}$ v
Correlation coefficient = -0.7647
Level of significance, $p = 0.02 < p < 0.05$
Standard deviation of $E_{p(c,4)}$ from regression = 0.007 V
Degrees of freedom = 6

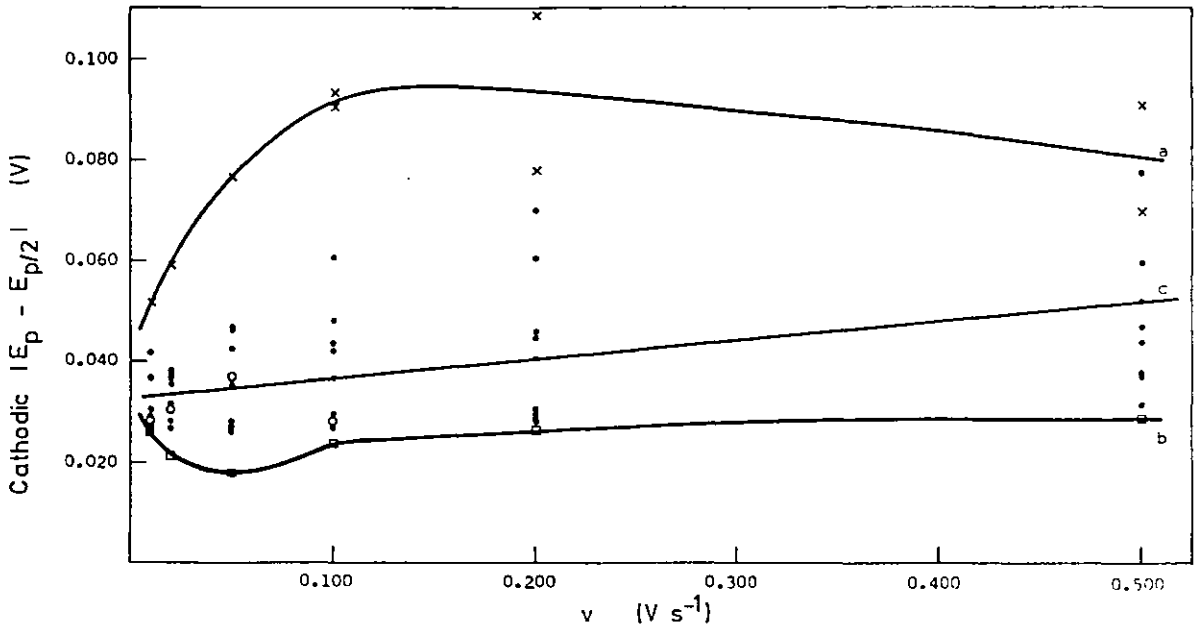

Fig. 5-137 Ir(IV) Perchlorate/Perchloric acid (0.1 M) supporting electrolyte System: Values of the absolute difference between cathodic peak and half-peak potential, $|E_{p(c)} - E_{p(c)/2}|$, as a function of potential scan rate, v; at Ir(IV) Perchlorate concentrations of 4.0×10^{-6} to 2.3×10^{-3} mol dm^{-3}. (a) $|E_{p(c,1)} - E_{p(c,1)/2}|$, (b) $|E_{p(c,2)} - E_{p(c,2)/2}|$, and (c) $|E_{p(c,3)} - E_{p(c,3)/2}|$. Boron carbide solid electrode $B_{4.05}C$.

(c) $|E_{p(c,3)} - E_{p(c,3)/2}| = 0.033 + 0.037\ v$

Correlation coefficient = 0.5219

Level of significance, $p = p < 0.001$

Standard deviation of $|E_{p(c,3)} - E_{p(c,3)/2}|$ from regression
= 0.011 V

Degrees of freedom = 52

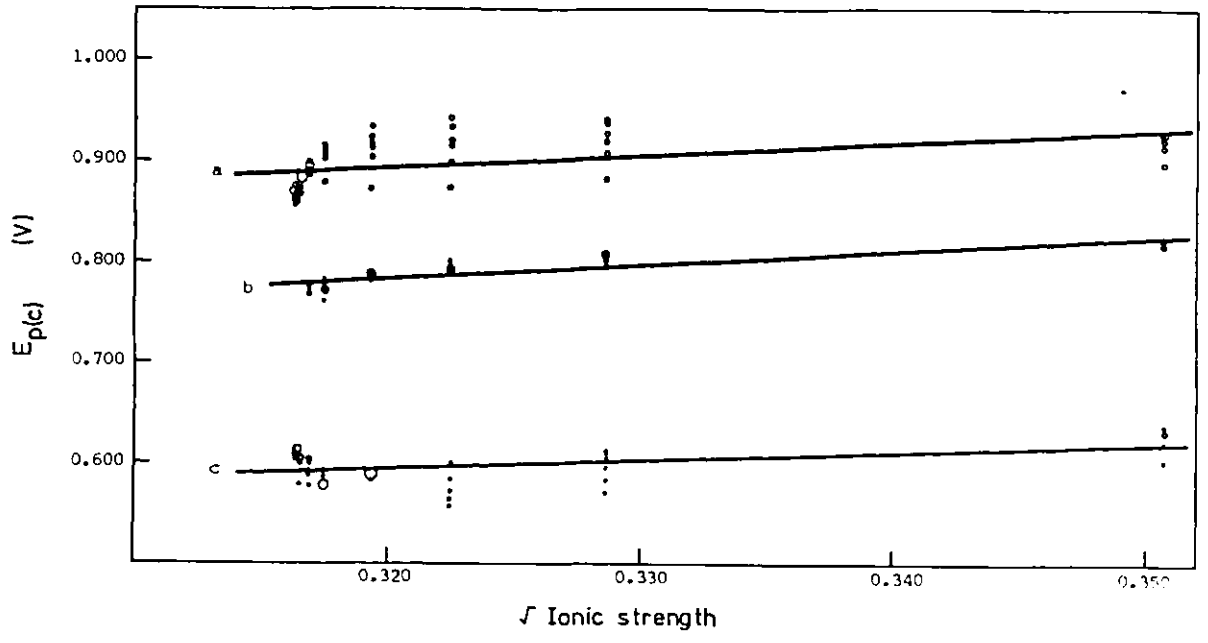

Fig. 5-138 Ir(IV) Perchlorate (4.0×10^{-6} to 2.3×10^{-3} mol dm^{-3})/Perchloric acid (0.1 M) supporting electrolyte System: Values of cathodic peak potential, $E_{p(c)}$, as a function of square root of total ionic strength, $\sqrt{I}$ (where the concentration of Ir(IV) Perchlorate was varied); at potential scan rates of 0.010 to 0.500 V s^{-1}. (a) $E_{p(c,1)}$, (b) $E_{p(c,2)}$, and (c) $E_{p(c,3)}$. Boron carbide solid electrode $B_{4.05}C$.

(a) $E_{p(c,1)} = 0.523 + 1.16\ \sqrt{I}$
Correlation coefficient = 0.4975
Level of significance, p = $p < 0.001$
Standard deviation of $E_{p(c,1)}$ from regression = 0.022 V
Degrees of freedom = 52

(b) $E_{p(c,2)} = 0.371 + 1.29\ \sqrt{I}$
Correlation coefficient = 0.8901
Level of significance, p = $p < 0.001$
Standard deviation of $E_{p(c,2)}$ from regression = 0.008 V
Degrees of freedom = 34

(c) $E_{p(c,3)} = 0.343 + 0.791\ \sqrt{I}$
Correlation coefficient = 0.4787
Level of significance, p = $p < 0.001$
Standard deviation of $E_{p(c,3)}$ from regression = 0.016 V
Degrees of freedom = 52

Linear regression analysis of the results indicates that the anodic shift in cathodic peak potentials was, in ascending order, $E_{p(c,3)} < E_{p(c,1)} < E_{p(c,2)}$ (Fig. 5-138). The differences between these potentials are plotted against $I^{\frac{1}{2}}$ in Fig. 5-139 which also shows that $|E_{p(c,3)} - E_{p(c,3)/2}|$ was relatively steady (mean value = 0.038 V ± 0.012 V, 53 degrees of freedom). These anodic shifts of the cathodic peak potentials with increasing Ir(IV) perchlorate concentration are consistent with the expected shifts for the system where the reactant is adsorbed (Fig. 3-22); especially when the Ir(IV) perchlorate species has been shown to be cationic by paper electrophoresis.

The trends of anodic peak potentials with increasing sweep rate (Fig. 5-140) show that $E_{p(a,1)}$ was shifted cathodically, $E_{p(a,2)}$ was constant (mean value = 0.791 V (vs. SCE) ± 0.002 V, 5 degrees of freedom), and $E_{p(a,3)}$ and $E_{p(a,4)}$ were both shifted anodically. Plots of anodic $|E_p - E_{p/2}|$ versus sweep rate (Fig. 5-141), however, reveal that: (i) $|E_{p(a,1)} - E_{p(a,1)/2}|$ decreased with increasing sweep rate and so the cathodic shift in potential for Peak 1 was due to the weak adsorption of reactant (Fig. 3-16), (ii) $|E_{p(a,2)} - E_{p(a,2)/2}|$ was independent of sweep rate (mean value = 0.037 V ± 0.002 V, 5 degrees of freedom) and thus the behaviour of Peak 2 was consistent with a strong adsorption peak, (iii) $|E_{p(a,3)} - E_{p(a,3)/2}|$ and $|E_{p(a,4)} - E_{p(a,4)/2}|$ both increased with increasing sweep rate which indicate that the anodic shift in the potentials of Peaks 3 and 4 was due to the decrease in the reversibility of the corresponding charge transfers.

The absolute difference between corresponding anodic and cathodic peak potentials, $|E_{p(a)} - E_{p(c)}|$, as a function of the sweep rate, v, is shown in Fig. 5-142 which indicates that, except for Peak 2, the values of the absolute difference increased with increasing sweep rate for Peaks 1, 3, and 4. This is evidence for the decreasing reversibility of the charge transfer for Peaks 1, 3, and 4 as v increased. $|E_{p(a,2)} - E_{p(c,2)}|$, however, initially decreased with increasing v but later reverted gradually to approximately former levels at higher sweep rates; thus reflecting the influence of adsorption.

The influence of perchloric acid concentration on the adsorption effect for the cathodic Peaks 1, 2, and 3 are presented in Figures 5-143, 5-144, and 5-145 respectively. The adsorption effect on Peaks 1 and 3 was debilitated by increasing perchloric acid concentration (Fig. 5-143 and Fig. 5-145 respectively). For Peak 2, however, the adsorption increased with increasing perchloric acid concentration initially before

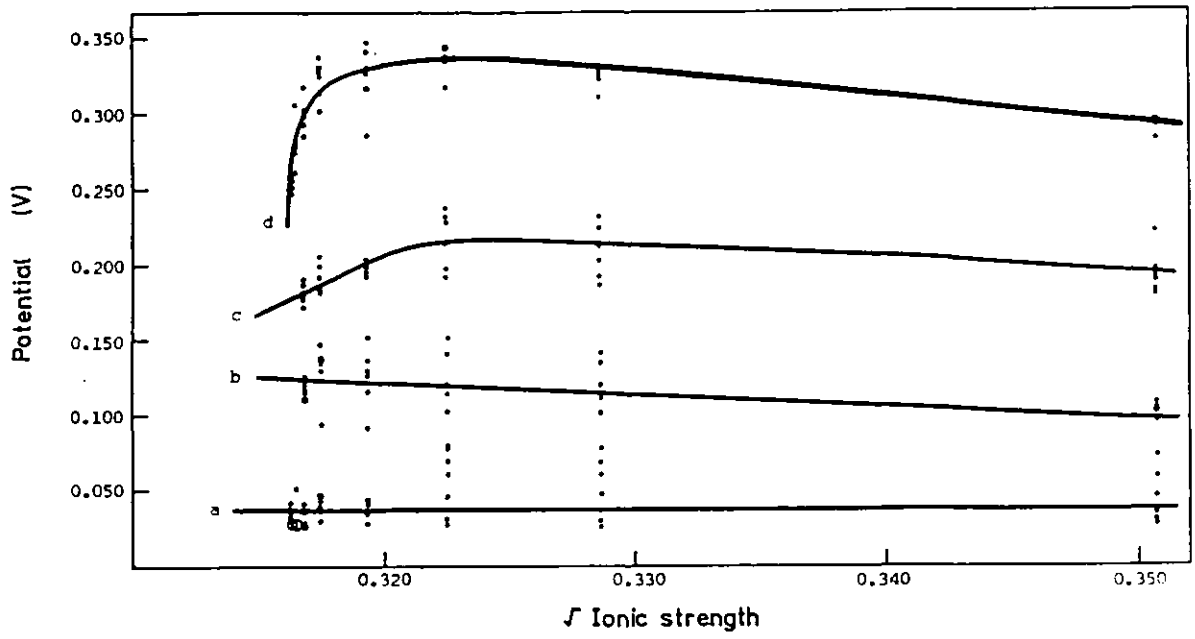

Fig. 5-139 Ir(IV) Perchlorate (4.0×10^{-6} to 2.3×10^{-3} mol dm^{-3})/Perchloric acid (0.1 M) supporting electrolyte System: Values of the difference between cathodic peak and half-peak potential, $|E_{p(c)} - E_{p(c)/2}|$, and the difference between cathodic peak potentials, $\Delta E_{p(c)}$, as a function of square root of total ionic strength (where the concentration of Ir(IV) Perchlorate was varied), $\sqrt{I}$; at potential scan rates of 0.010 to 0.500 V s^{-1}. (a) $|E_{p(c,3)} - E_{p(c,3)/2}|$, (b) $\Delta E_{p(c;\ 1,2)}$, (c) $\Delta E_{p(c;\ 2,3)}$, and (d) $\Delta E_{p(c;\ 1,3)}$. Boron carbide solid electrode $B_{4.05}C$.

(a) $|E_{p(c,3)} - E_{p(c,3)/2}|$ mean = 0.038 V
Standard deviation = 0.012 V
Degrees of freedom = 53

(b) $\Delta E_{p(c;\ 1,2)} = 0.378 - 0.798\ \sqrt{I}$
Correlation coefficient = -0.4664
Level of significance, $p = 0.001 < p < 0.01$
Standard deviation of $\Delta E_{p(c;\ 1,2)}$ from regression = 0.018 V
Degrees of freedom = 34

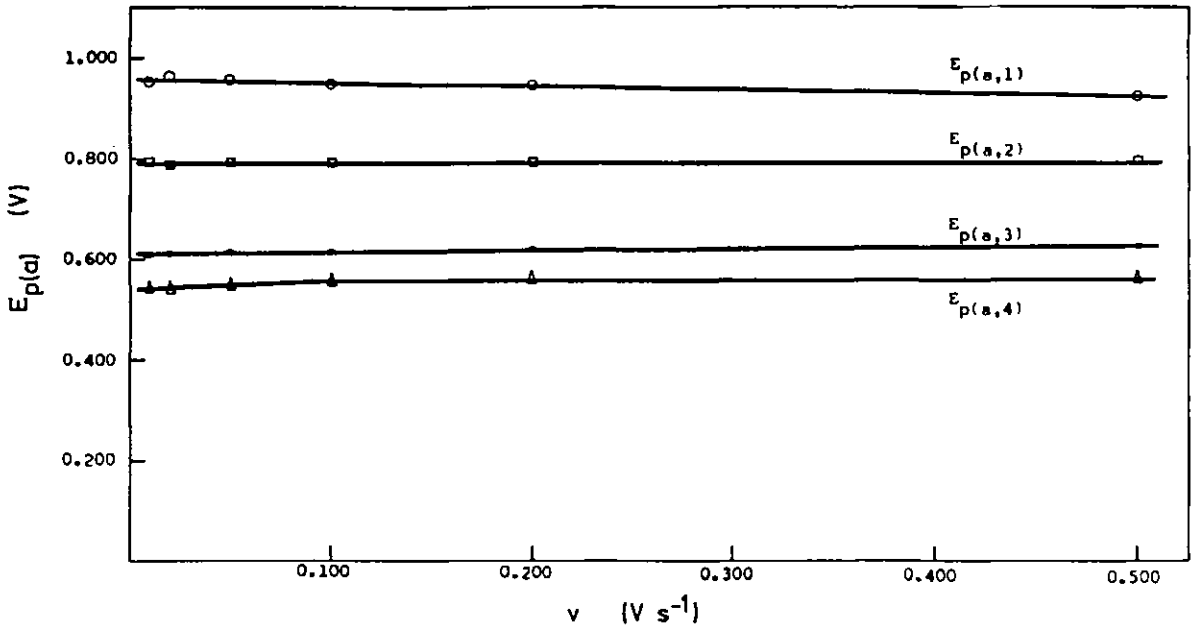

Fig. 5-140 Ir(IV) Perchlorate (1.0×10^{-4} mol dm^{-3})/Perchloric acid (0.1 M) supporting electrolyte System: Values of anodic peak potential, $E_{p(a)}$, as a function of potential scan rate, v. Boron carbide solid electrode $B_{4.05}C$.

(a) $E_{p(a,1)} = 0.958 - 7.34 \times 10^{-2}$ v
Correlation coefficient = -0.9660
Level of significance, $p = 0.001 < p < 0.01$
Standard deviation of $E_{p(a,1)}$ from regression = 0.004 V
Degrees of freedom = 4

(b) $E_{p(a,2)}$ mean = 0.791 V
Standard deviation = 0.002 V
Degrees of freedom = 5

(c) $E_{p(a,3)} = 0.612 + 3.16 \times 10^{-2}$ v
Correlation coefficient = 0.9150
Level of significance, $p = 0.01 < p < 0.02$
Standard deviation of $E_{p(a,3)}$ from regression = 0.003 V
Degrees of freedom = 4

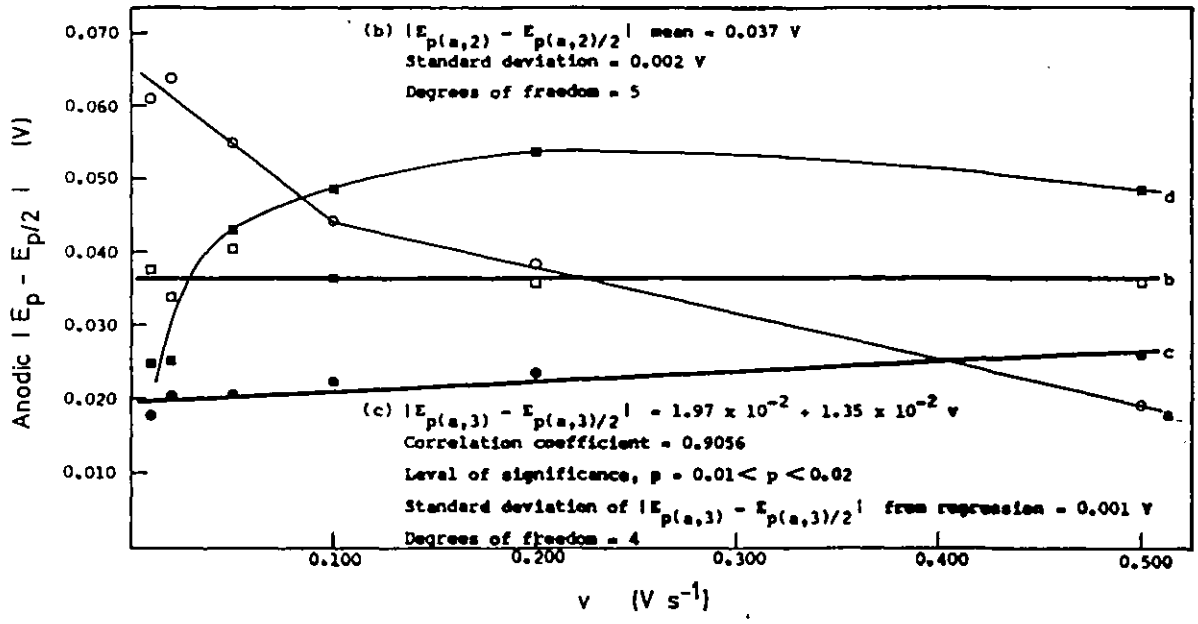

Fig. 5-141 Ir(IV) Perchlorate (1.0×10^{-4} mol dm^{-3})/Perchloric acid (0.1 M) supporting electrolyte System: Values of the absolute difference between anodic peak and half-peak potential, $|E_{p(a)} - E_{p(a)/2}|$, as a function of potential scan rate, v. (a) $|E_{p(a,1)} - E_{p(a,1)/2}|$, (b) $|E_{p(a,2)} - E_{p(a,2)/2}|$, (c) $|E_{p(a,3)} - E_{p(a,3)/2}|$, and (d) $|E_{p(a,4)} - E_{p(a,4)/2}|$. Boron carbide solid electrode $B_{4.05}C$.

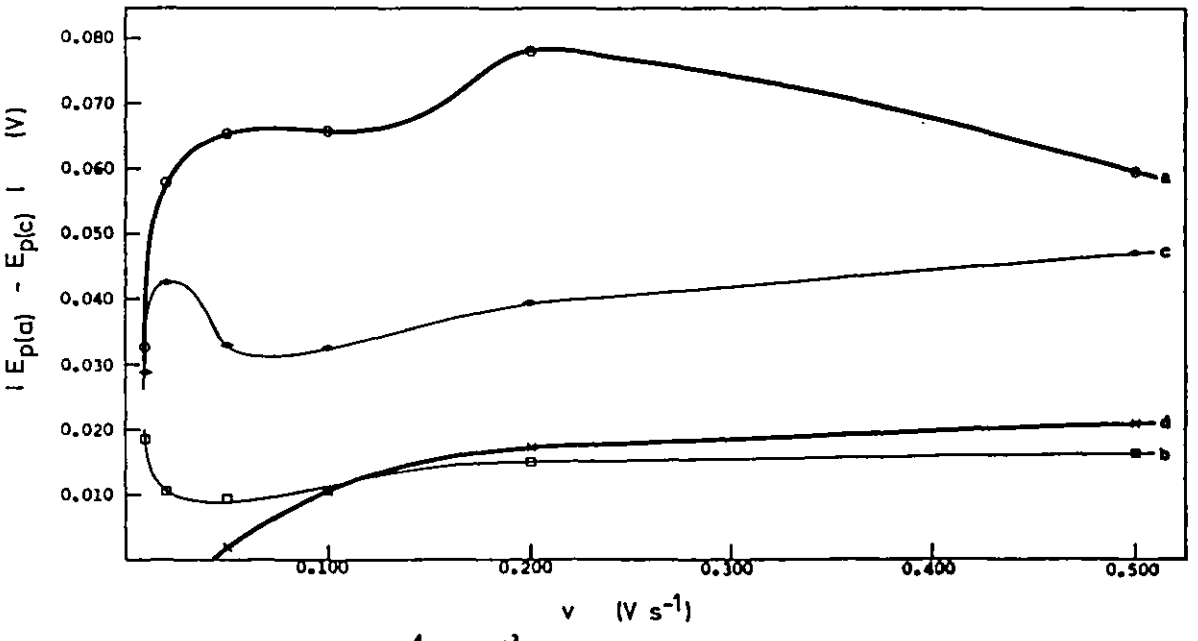

Fig. 5-142 Ir(IV) Perchlorate (1.0×10^{-4} mol dm^{-3})/Perchloric acid (0.1 M) supporting electrolyte System: Values of the difference between anodic and cathodic peak potential, $|E_{p(a)} - E_{p(c)}|$, as a function of potential scan rate, v. (a) $|E_{p(a,1)} - E_{p(c,1)}|$, (b) $|E_{p(a,2)} - E_{p(c,2)}|$, (c) $|E_{p(a,3)} - E_{p(c,3)}|$, and (d) $|E_{p(a,4)} - E_{p(c,4)}|$. Boron carbide solid electrode $B_{4.05}C$.

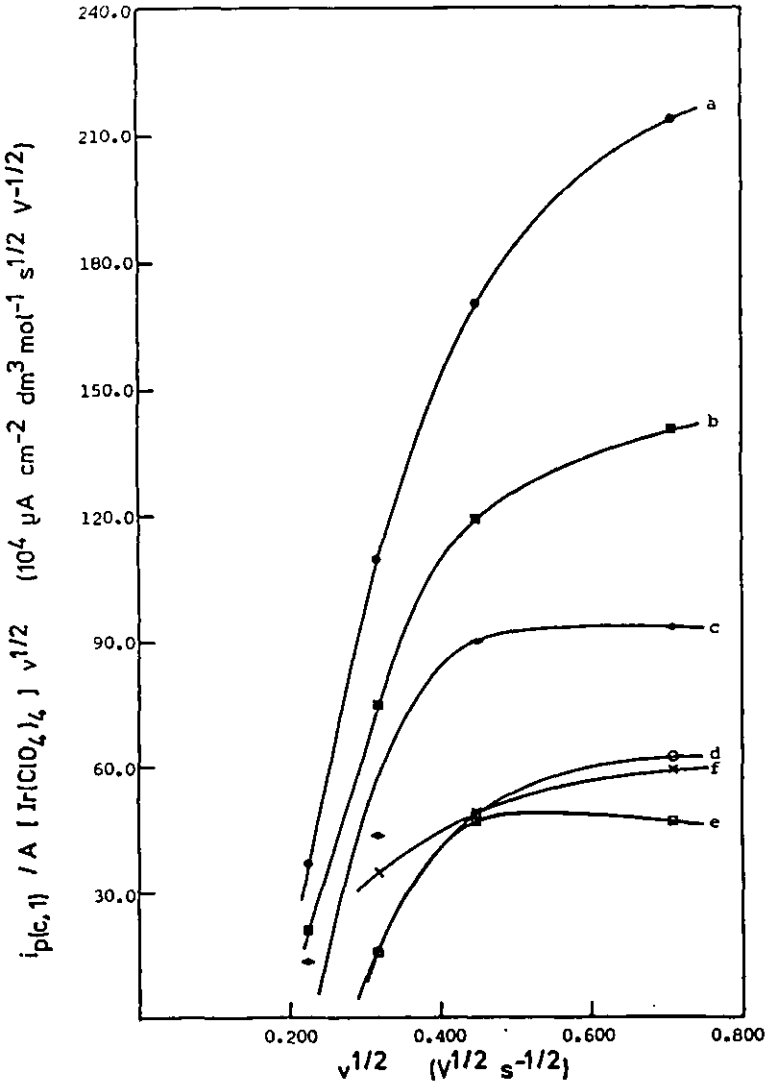

Fig. 5-143 Ir(IV) Perchlorate (1.0×10^{-4} mol dm^{-3})/Perchloric acid supporting electrolyte System: Values of cathodic current function, $i_{p(c,1)}/A\ [\ Ir(ClO_4)_4\ ]\ v^{\frac{1}{2}}$, as a function of square root of potential scan rate, $v^{\frac{1}{2}}$; at the perchloric acid concentrations (a) 0.1, (b) 0.2, (c) 0.4, (d) 0.8, (e) 1.0, and (f) 2.0 M. Boron carbide solid electrode $B_{4.05}C$.

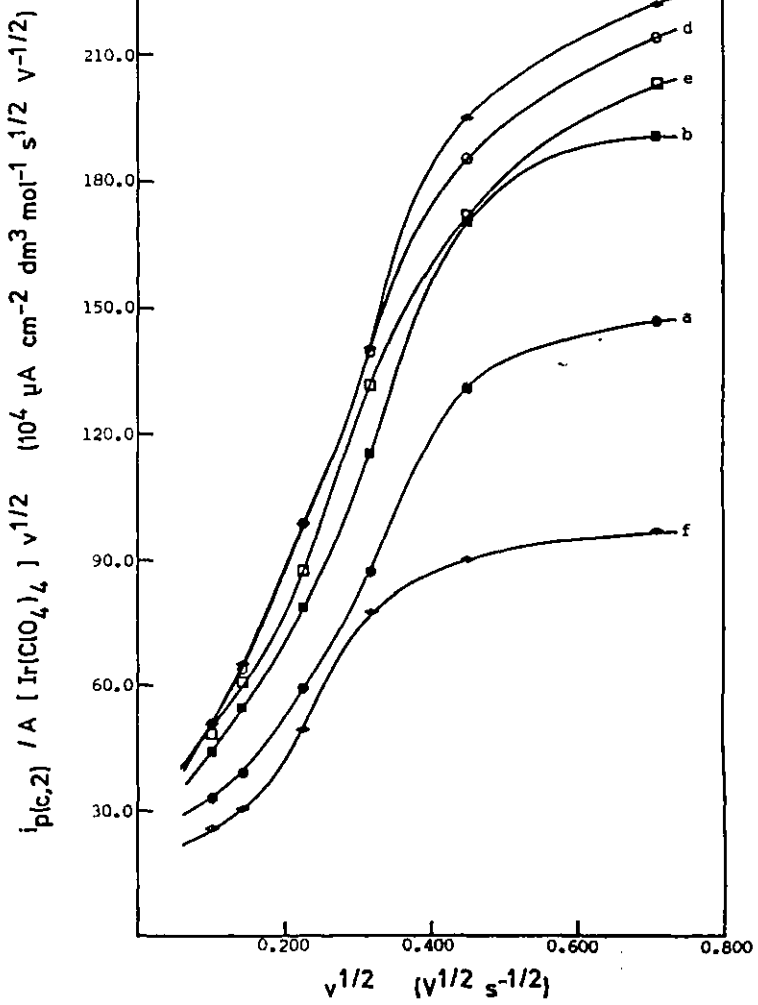

Fig. 5-144 Ir(IV) Perchlorate (1.0×10^{-4} mol dm^{-3})/Perchloric acid supporting electrolyte System: Values of cathodic current function, $i_{p(c,2)}/A\ [\ Ir(ClO_4)_4\ ]\ v^{\frac{1}{2}}$, as a function of square root of potential scan rate, $v^{\frac{1}{2}}$; at the perchloric acid concentrations (a) 0.1, (b) 0.2, (c) 0.4, (d) 0.8, (e) 1.0, and (f) 2.0 M. Boron carbide solid electrode $B_{4.05}C$.

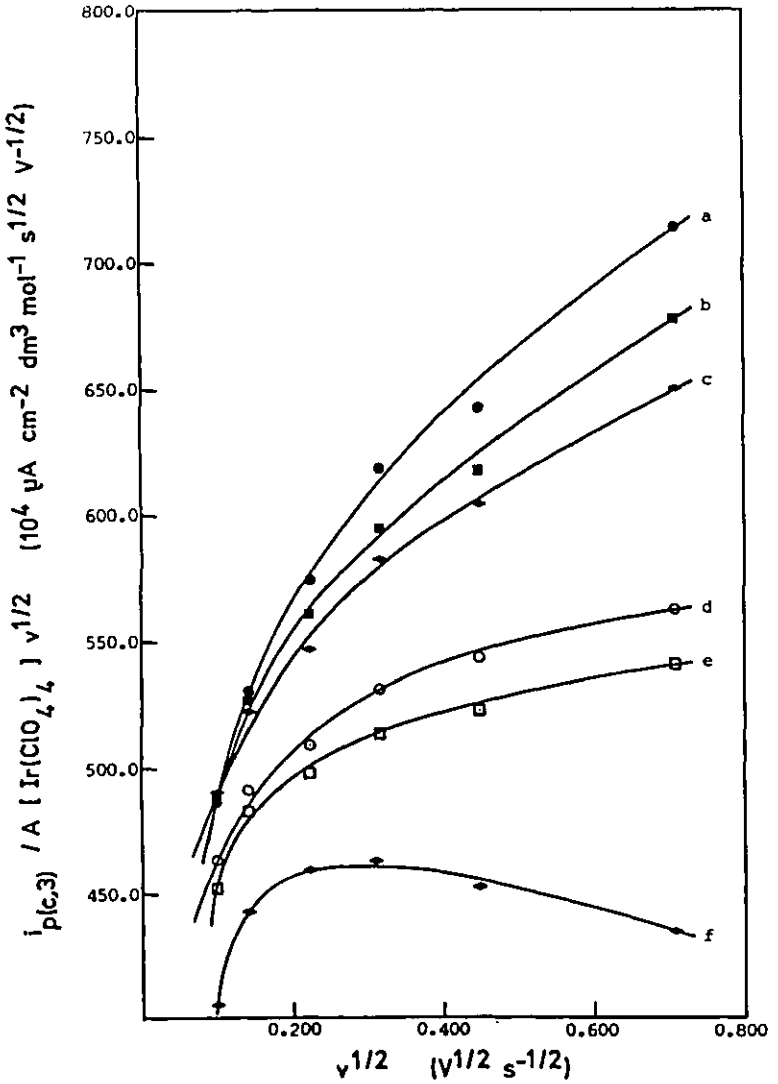

Fig. 5-145 Ir(IV) Perchlorate (1.0×10^{-4} mol dm^{-3})/Perchloric acid supporting electrolyte System: Values of cathodic current function, $i_{p(c,3)}/A\ [\ Ir(ClO_4)_4\ ]\ v^{\frac{1}{2}}$, as a function of square root of potential scan rate, $v^{\frac{1}{2}}$; at the perchloric acid concentrations (a) 0.1, (b) 0.2, (c) 0.4, (d) 0.8, (e) 1.0, and (f) 2.0 M. Boron carbide solid electrode $B_{4.05}C$.

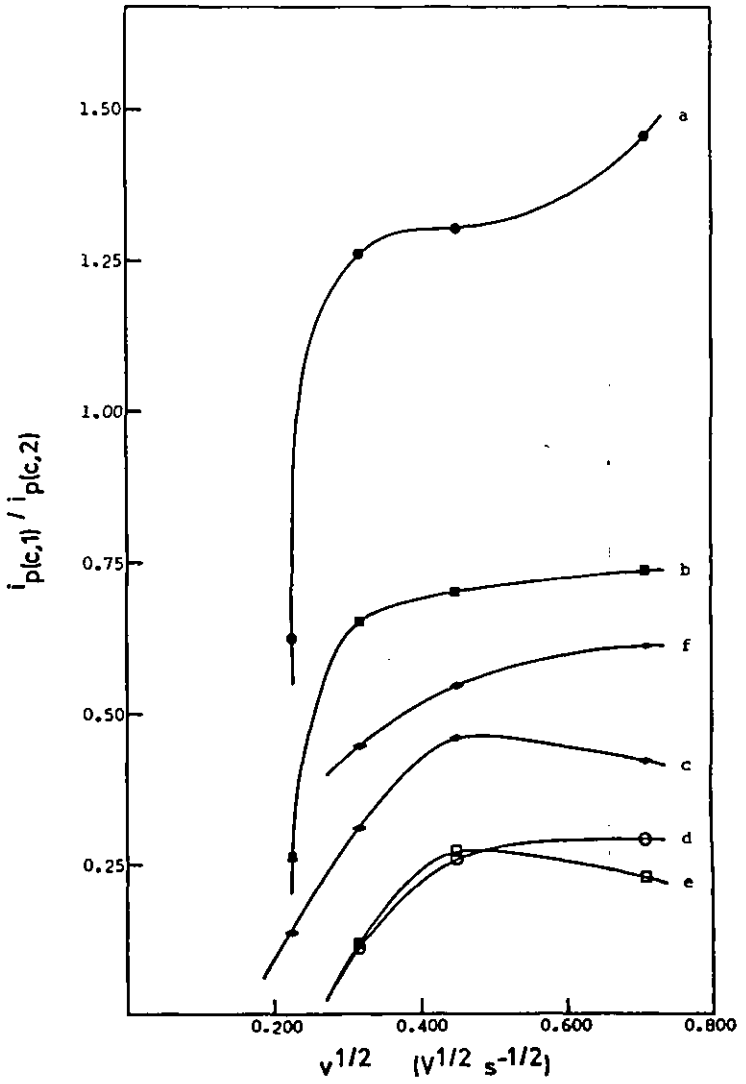

Fig. 5-146 Ir(IV) Perchlorate (1.0×10^{-4} mol dm^{-3})/Perchloric acid supporting electrolyte System: Values of the ratio of cathodic peak currents, $i_{p(c,1)}/i_{p(c,2)}$, as a function of square root of potential scan rate, $v^{\frac{1}{2}}$; at the perchloric acid concentrations (a) 0.1, (b) 0.2, (c) 0.4, (d) 0.8, (e) 1.0, and (f) 2.0 M. Boron carbide solid electrode $B_{4.05}C$.

decreasing to a weaker effect at 2.0 M perchloric acid (Fig. 5-144). The ratios of cathodic peak currents as functions of potential (sweep rate)$^{\frac{1}{2}}$ at different perchloric acid concentrations are plotted in Figures 5-146 to 5-148 and show that the increasing sweep rate increased the peak currents in the order $i_{p(c,1)} > i_{p(c,2)} > i_{p(c,3)}$. However, the increasing perchloric acid concentration decreased $i_{p(c,1)}$ and $i_{p(c,3)}$; the trends being emphasised at faster sweep rates (Figures 5-149 and 5-151 respectively). This effect indicates that the adsorption influences at Peaks 1 and 3 were weakened by higher perchloric acid concentrations. Fig. 5-150, in contrast, shows that $i_{p(c,2)}$ initially was enhanced by increasing perchloric acid concentration before it declined to end at lower values; thus reflecting the influence of a catalytic reaction together with adsorption.

In general, the cathodic peak potentials were shifted anodically by the increasing $I^{\frac{1}{2}}$ as the perchloric acid concentration was increased (Fig. 5-152). Furthermore, Fig. 5-153 shows that the differences between these peak potentials narrowed as $I^{\frac{1}{2}}$ increased whilst $|E_p - E_{p/2}|$ values either remained steady or decreased. Therefore, as was experienced with d.c. voltammetry (section 5-1.5.(i).a), the anodic shift in peak potentials for the cationic Ir(IV) perchlorate species with increasing perchloric acid concentration may be explained in terms of a decrease in the adsorption effect on these potentials at higher perchloric acid concentrations. Thus the peak potentials, which were initially shifted to less anodic values by the extremely strong physical adsorption of Ir(IV) perchlorate reactant, were gradually reverting to potentials corresponding to diffusion controlled reductions as the adsorption effect was debilitated by the increasing perchloric acid concentration.

5-1.5.(ii).b Boron carbide solid electrode $B_{3.86}C$

Typical linear sweep voltammograms for Ir(IV) perchlorate (1.0×10^{-4} mol dm^{-3}) in perchloric acid (0.1 M) supporting electrolyte which were obtained at the boron carbide solid electrode $B_{3.86}C$ over a range of sweep rates are presented in Fig. 5-154. Three cathodic peaks were exhibited and plots of their peak current functions as functions of potential (sweep rate)$^{\frac{1}{2}}$, $v^{\frac{1}{2}}$, revealed the influence of adsorption on all the peaks; the adsorption effect being generally weaker at higher concentrations of perchloric acid supporting electrolyte (Figures 5-155, 5-156, and 5-157). The most anodic peak, Peak 1 (Fig. 5-154), was not quantifiable over the entire range of perchloric acid concentration but

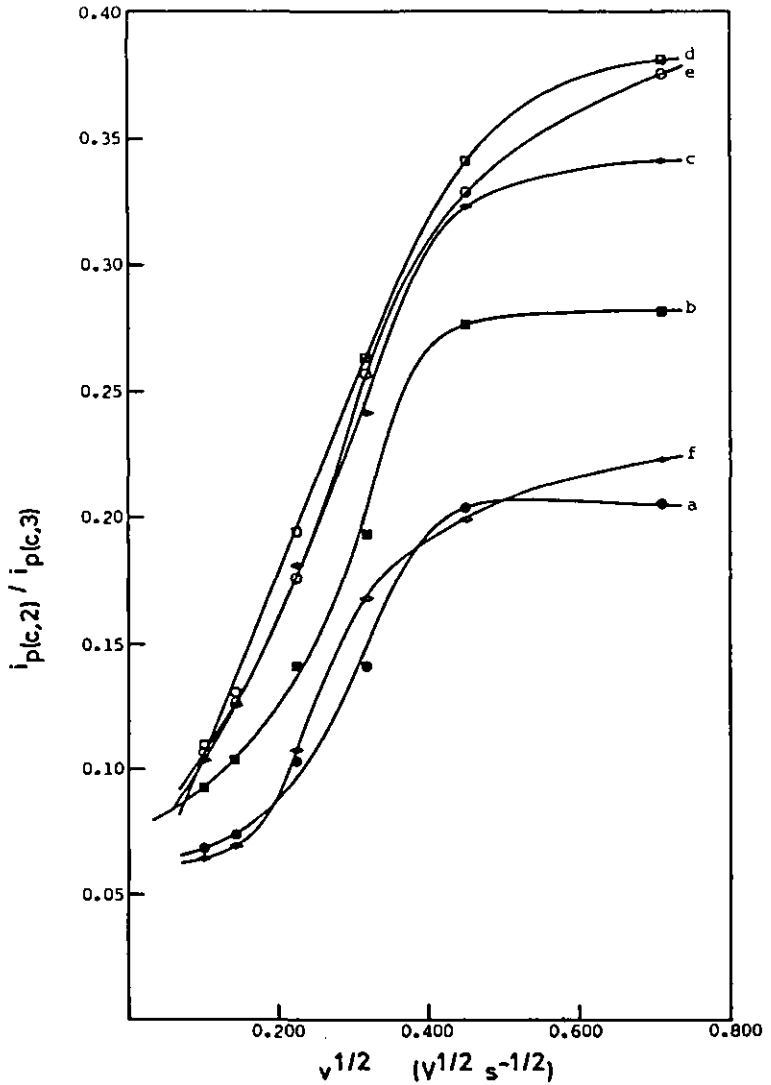

Fig. 5-147 Ir(IV) Perchlorate (1.0×10^{-4} mol dm^{-3})/Perchloric acid supporting electrolyte System: Values of the ratio of cathodic peak currents, $i_{p(c,2)}/i_{p(c,3)}$, as a function of square root of potential scan rate, $v^{\frac{1}{2}}$; at the perchloric acid concentrations (a) 0.1, (b) 0.2, (c) 0.4, (d) 0.8, (e) 1.0, and (f) 2.0 M. Boron carbide solid electrode $B_{4.05}C$.

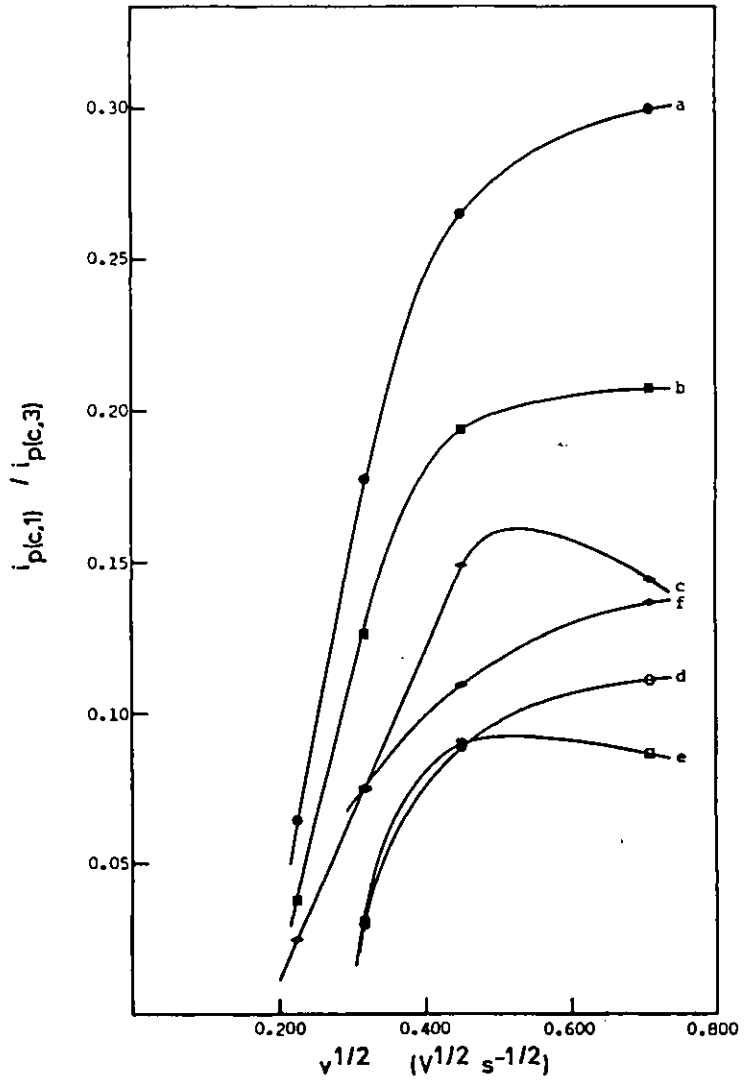

Fig. 5-148 Ir(IV) Perchlorate (1.0×10^{-4} mol dm^{-3})/Perchloric acid supporting electrolyte System: Values of the ratio of cathodic peak currents, $i_{p(c,1)}/i_{p(c,3)}$, as a function of square root of potential scan rate, $v^{\frac{1}{2}}$; at the perchloric acid concentrations (a) 0.1, (b) 0.2, (c) 0.4, (d) 0.8, (e) 1.0, and (f) 2.0 M. Boron carbide solid electrode $B_{4.05}C$.

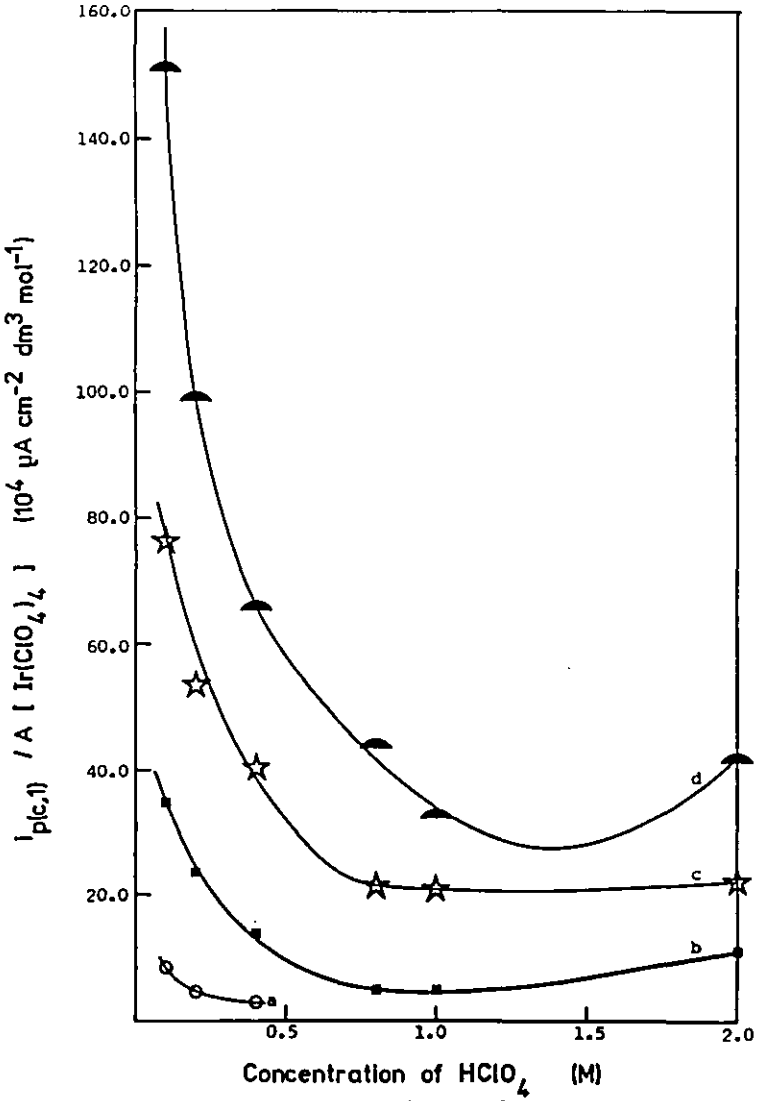

Fig. 5-149 Ir(IV) Perchlorate (1.0×10^{-4} mol dm^{-3})/Perchloric acid supporting electrolyte System: Values of cathodic peak current per unit area divided by concentration of Ir(IV) Perchlorate, $i_{p(c,1)}/A$ [$Ir(ClO_4)_4$], as a function of concentration of perchloric acid; at potential scan rates (a) 0.050, (b) 0.100, (c) 0.200, and (d) 0.500 V s^{-1}. Boron carbide solid electrode $B_{4.05}C$.

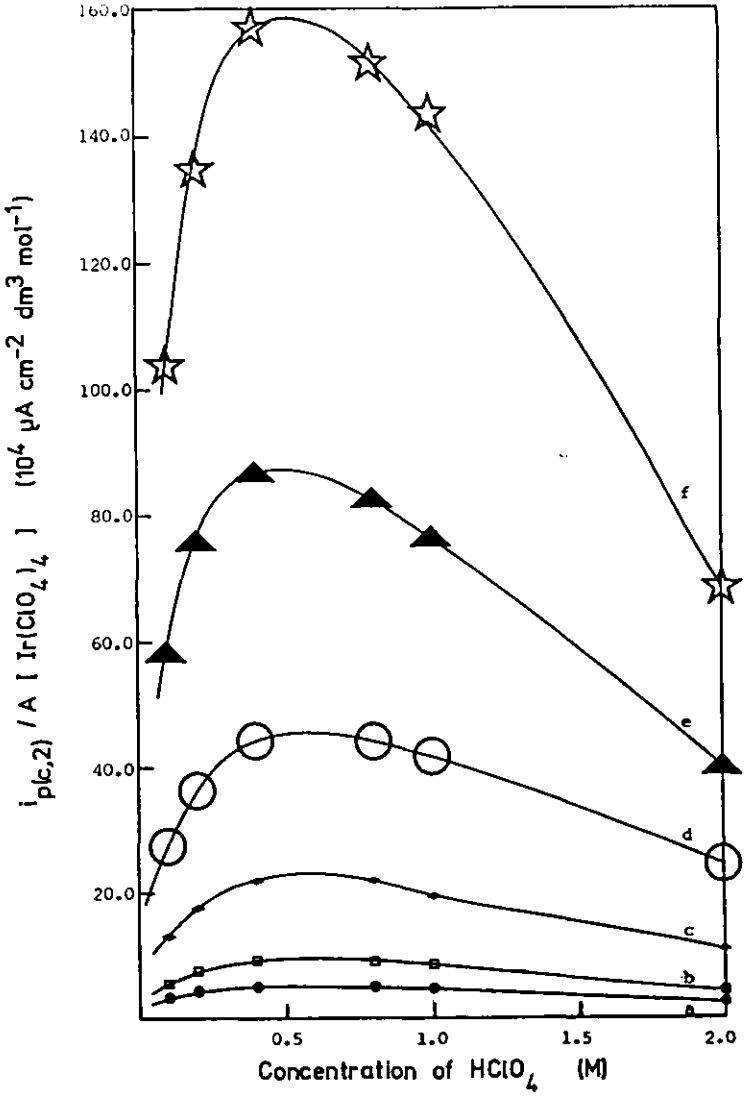

Fig. 5-150 Ir(IV) Perchlorate (1.0×10^{-4} mol dm^{-3})/Perchloric acid supporting electrolyte System: Values of cathodic peak current per unit area divided by concentration of Ir(IV) Perchlorate, $i_{p(c,2)}/A$ [$Ir(ClO_4)_4$], as a function of concentration of perchloric acid; at potential scan rates (a) 0.010, (b) 0.020, (c) 0.050, (d) 0.100, (e) 0.200, and (f) 0.500 V s^{-1}. Boron carbide solid electrode $B_{4.05}C$.

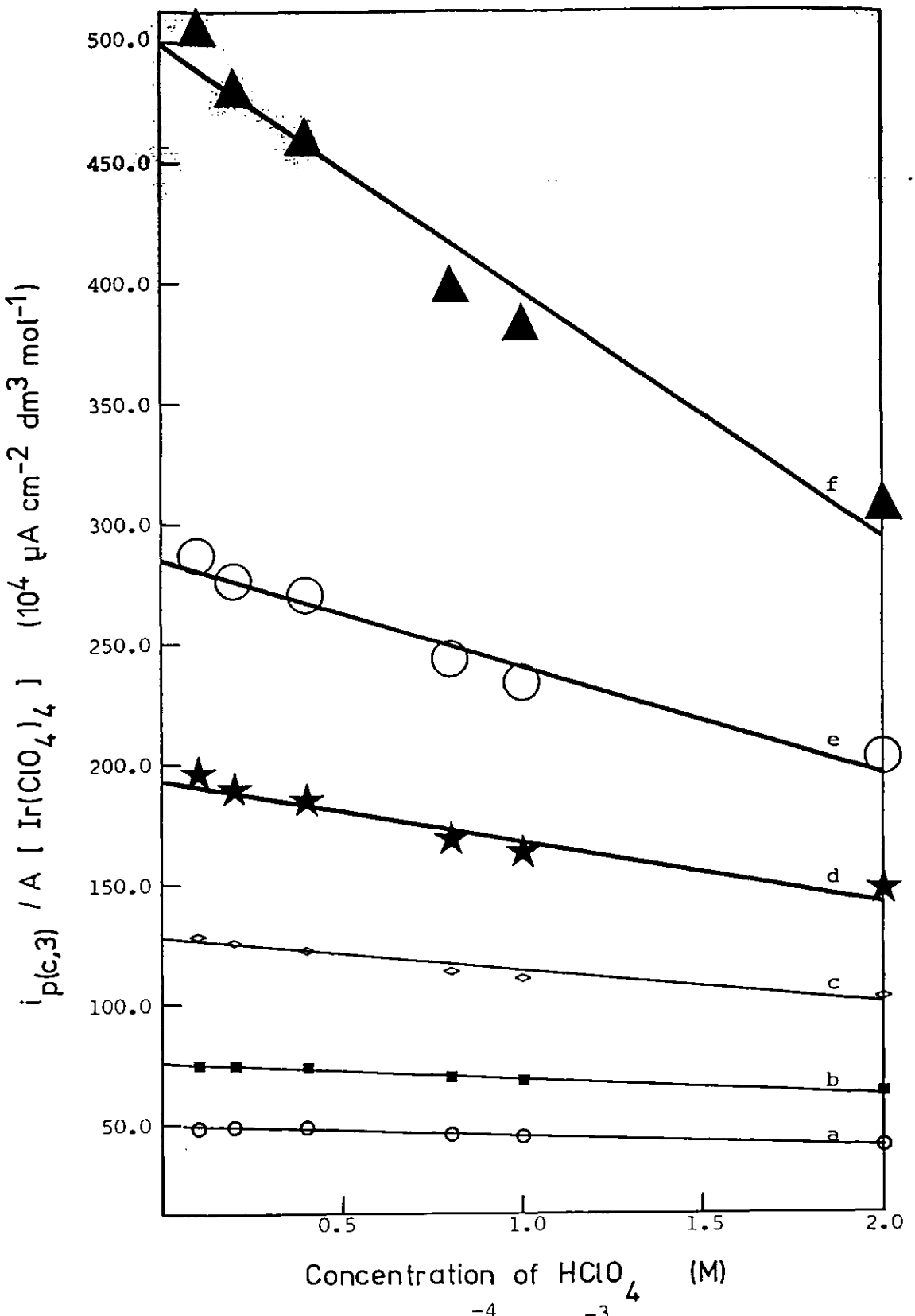

Fig. 5-151 Ir(IV) Perchlorate (1.0×10^{-4} mol dm^{-3})/Perchloric acid supporting electrolyte System: Values of cathodic peak current per unit area divided by concentration of Ir(IV) Perchlorate, $i_{p(c,3)}/A$ [$Ir(ClO_4)_4$], as a function of concentration of perchloric acid; at potential scan rates (a) 0.010, (b) 0.020, (c) 0.050, (d) 0.100, (e) 0.200, and (f) 0.500 V s^{-1}. Boron carbide solid electrode $B_{4.05}C$.

Fig. 5-151 (continued):-

(a) $i_{p(c,3)}/A\ [\ Ir(ClO_4)_4\ ] = 4.99 \times 10^5 - 4.64 \times 10^4\ [\ HClO_4\ ]$
Correlation coefficient = -0.9858
Level of significance, $p = p < 0.001$
Standard deviation of $i_{p(c,3)}/A\ [\ Ir(ClO_4)_4\ ]$ from regression
$= 6.22 \times 10^3\ \mu A\ cm^{-2}\ dm^3\ mol^{-1}$.
Degrees of freedom = 4

(b) $i_{p(c,3)}/A\ [\ Ir(ClO_4)_4\ ] = 7.57 \times 10^5 - 6.75 \times 10^4\ [\ HClO_4\ ]$
Correlation coefficient = -0.9914
Level of significance, $p = p < 0.001$
Standard deviation of $i_{p(c,3)}/A\ [\ Ir(ClO_4)_4\ ]$ from regression
$= 7.01 \times 10^3\ \mu A\ cm^{-2}\ dm^3\ mol^{-1}$
Degrees of freedom = 4

(c) $i_{p(c,3)}/A\ [\ Ir(ClO_4)_4\ ] = 1.27 \times 10^6 - 1.35 \times 10^5\ [\ HClO_4\ ]$
Correlation coefficient = -0.9719
Level of significance, $p = 0.001 < p < 0.01$
Standard deviation of $i_{p(c,3)}/A\ [\ Ir(ClO_4)_4\ ]$ from regression
$= 2.57 \times 10^4\ \mu A\ cm^{-2}\ dm^3\ mol^{-1}$
Degrees of freedom = 4

(d) $i_{p(c,3)}/A\ [\ Ir(ClO_4)_4\ ] = 1.93 \times 10^6 - 2.55 \times 10^5\ [\ HClO_4\ ]$
Correlation coefficient = -0.9718
Level of significance, $p = 0.001 < p < 0.01$
Standard deviation of $i_{p(c,3)}/A\ [\ Ir(ClO_4)_4\ ]$ from regression
$= 4.87 \times 10^4\ \mu A\ cm^{-2}\ dm^3\ mol^{-1}$
Degrees of freedom = 4

(e) $i_{p(c,3)}/A\ [\ Ir(ClO_4)_4\ ] = 2.85 \times 10^6 - 4.44 \times 10^5\ [\ HClO_4\ ]$
Correlation coefficient = -0.9823
Level of significance, $p = p < 0.001$
Standard deviation of $i_{p(c,3)}/A\ [\ Ir(ClO_4)_4\ ]$ from regression
$= 6.66 \times 10^4\ \mu A\ cm^{-2}\ dm^3\ mol^{-1}$
Degrees of freedom = 4

(f) $i_{p(c,3)}/A\ [\ Ir(ClO_4)_4\ ] = 4.99 \times 10^6 - 1.02 \times 10^6\ [\ HClO_4\ ]$
Correlation coefficient = -0.9811
Level of significance, $p = p < 0.001$
Standard deviation of $i_{p(c,3)}/A\ [\ Ir(ClO_4)_4\ ]$ from regression
$= 1.59 \times 10^5\ \mu A\ cm^{-2}\ dm^3\ mol^{-1}$
Degrees of freedom = 4

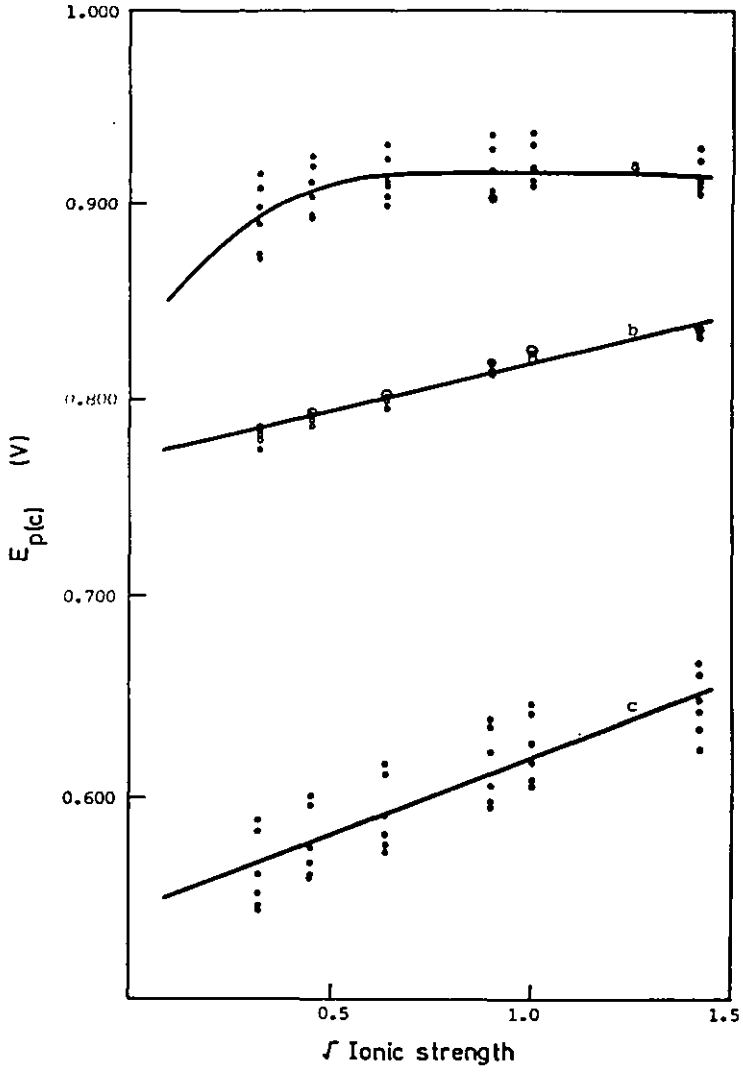

Fig. 5-152 Ir(IV) Perchlorate (1.0×10^{-4} mol dm^{-3})/Perchloric acid (0.1 to 2.0 M) supporting electrolyte System: Values of cathodic peak potential, $E_{p(c)}$, as a function of square root of total ionic strength, $\sqrt{I}$ (where the concentration of perchloric acid was varied); at potential scan rates of 0.010 to 0.500 V s^{-1}. (a) $E_{p(c,1)}$, (b) $E_{p(c,2)}$, and (c) $E_{p(c,3)}$. Boron carbide solid electrode $B_{4.05}C$.

(a) $E_{p(c,1)}$ mean = 0.912 V
Standard deviation = 0.015 V
Degrees of freedom = 35

(b) $E_{p(c,2)} = 0.770 + 4.98 \times 10^{-2} \sqrt{I}$
Correlation coefficient = 0.9781
Level of significance, p = $p < 0.001$
Standard deviation of $E_{p(c,2)}$ from regression = 0.004 V
Degrees of freedom = 34

(c) $E_{p(c,3)} = 0.543 + 7.72 \times 10^{-2} \sqrt{I}$
Correlation coefficient = 0.8622
Level of significance, p = $p < 0.001$
Standard deviation of $E_{p(c,3)}$ from regression = 0.017 V
Degrees of freedom = 34

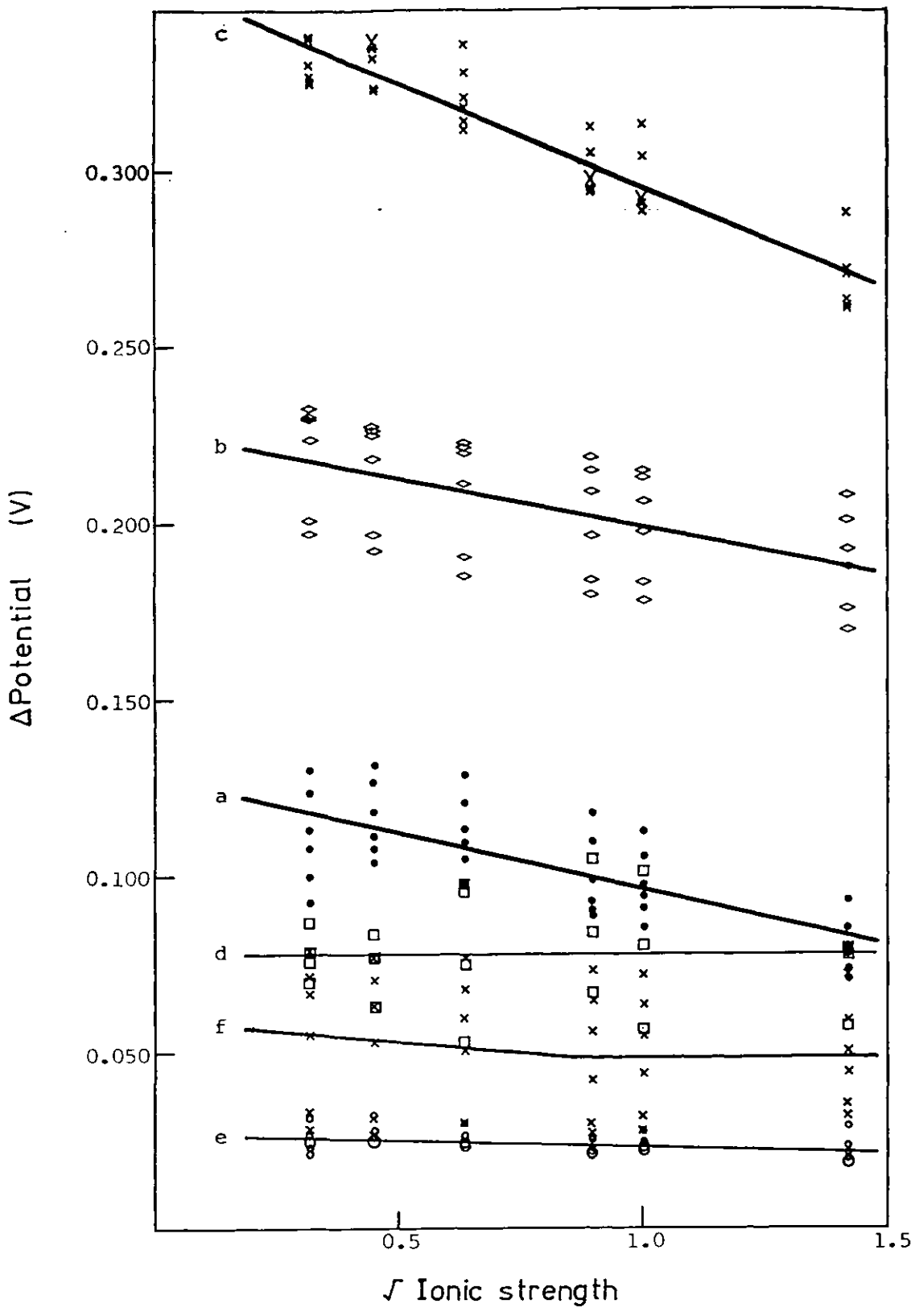

Fig. 5-153 Ir(IV) Perchlorate (1.0×10^{-4} mol dm^{-3})/Perchloric acid (0.1 to 2.0 M) supporting electrolyte System: Values of the difference between cathodic peak potentials, $\Delta E_{p(c)}$, and the difference between cathodic peak and half-peak potential, $|E_{p(c)} - E_{p(c)/2}|$, as a function of square root of total ionic strength, $\sqrt{I}$ (where the concentration of perchloric acid was varied); at potential scan rates of 0.010 to 0.500 V s^{-1}. (a) $\Delta E_{p(c;\ 1,2)}$, (b) $\Delta E_{p(c;\ 2,3)}$, (c) $\Delta E_{p(c;\ 1,3)}$, (d) $|E_{p(c,1)} - E_{p(c,1)/2}|$, (e) $|E_{p(c,2)} - E_{p(c,2)/2}|$, and (f) $|E_{p(c,3)} - E_{p(c,3)/2}|$.

Fig. 5-153 (continued):-

(a) $\Delta E_{p(c;\ 1,2)} = 0.128 - 3.19 \times 10^{-2} \sqrt{I}$
Correlation coefficient = -0.7351
Level of significance, p = $p < 0.001$
Standard deviation of $\Delta E_{p(c;\ 1,2)}$ from regression = 0.011 V
Degrees of freedom = 34

(b) $\Delta E_{p(c;\ 2,3)} = 0.226 - 2.74 \times 10^{-2} \sqrt{I}$
Correlation coefficient = -0.5730
Level of significance, p = $p < 0.001$
Standard deviation of $\Delta E_{p(c;\ 2,3)}$ from regression = 0.015 V
Degrees of freedom = 34

(c) $\Delta E_{p(c;\ 1,3)} = 0.354 - 5.93 \times 10^{-2} \sqrt{I}$
Correlation coefficient = -0.9374
Level of significance, p = $p < 0.001$
Standard deviation of $\Delta E_{p(c;\ 1,3)}$ from regression = 0.008 V
Degrees of freedom = 34

(d) $|E_{p(c,1)} - E_{p(c,1)/2}|$ mean = 0.078 V
Standard deviation = 0.014 V
Degrees of freedom = 20

(e) $|E_{p(c,2)} - E_{p(c,2)/2}| = 2.75 \times 10^{-2} - 4.22 \times 10^{-3} \sqrt{I}$
Correlation coefficient = -0.4853
Level of significance, p = $0.001 < p < 0.01$
Standard deviation of $|E_{p(c,2)} - E_{p(c,2)/2}|$ from regression
= 0.003 V
Degrees of freedom = 34

(f) $|E_{p(c,3)} - E_{p(c,3)/2}|$ mean = 0.051 V
Standard deviation = 0.018 V
Degrees of freedom = 35

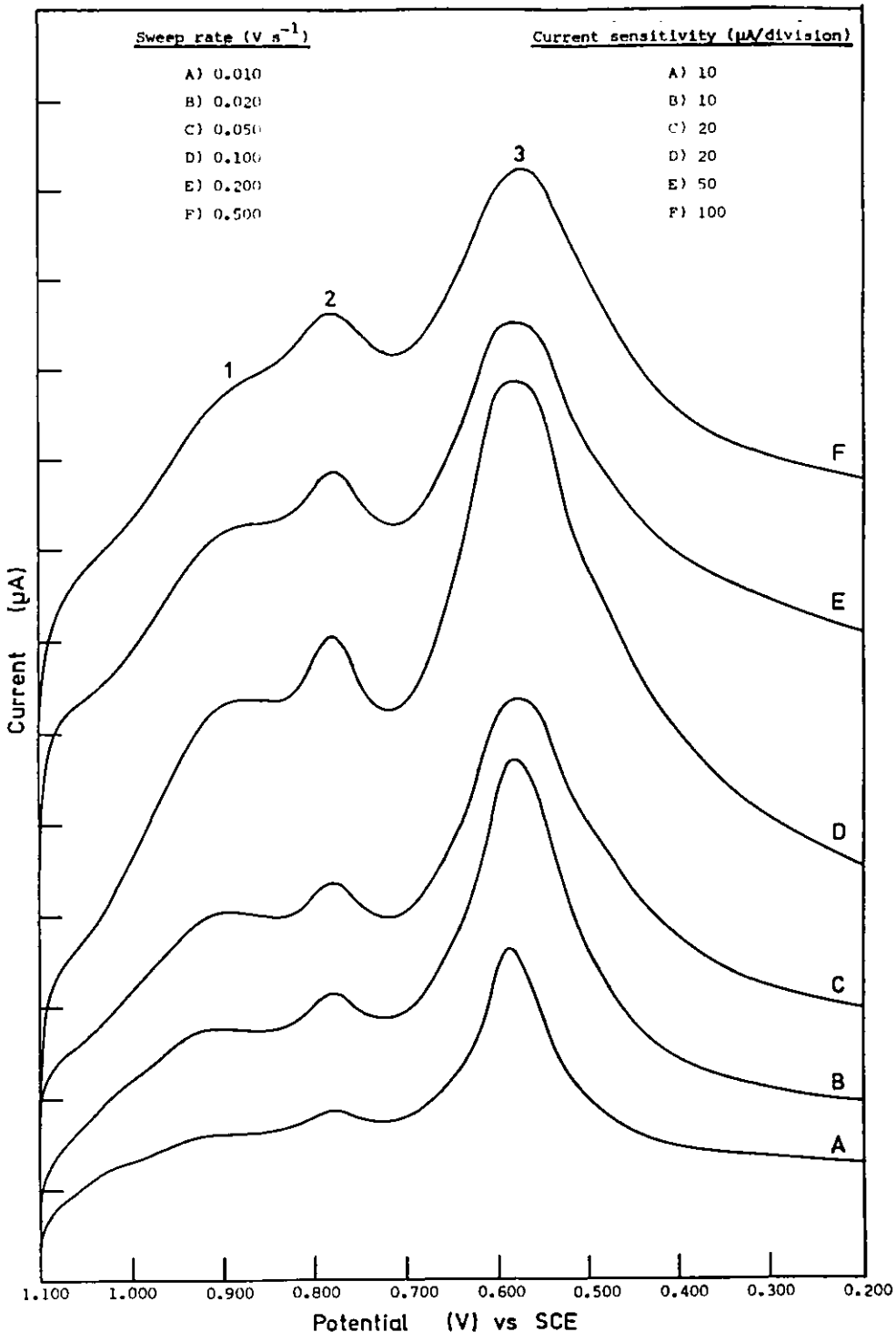

Fig. 5-154 Ir(IV) perchlorate (1.0×10^{-4} mol dm^{-3})/Perchloric acid (0.1 M) supporting electrolyte System: Linear sweep voltammograms obtained at the boron carbide solid electrode $B_{3.86}C$ over a range of sweep rates (0.010 to 0.500 V s^{-1}).

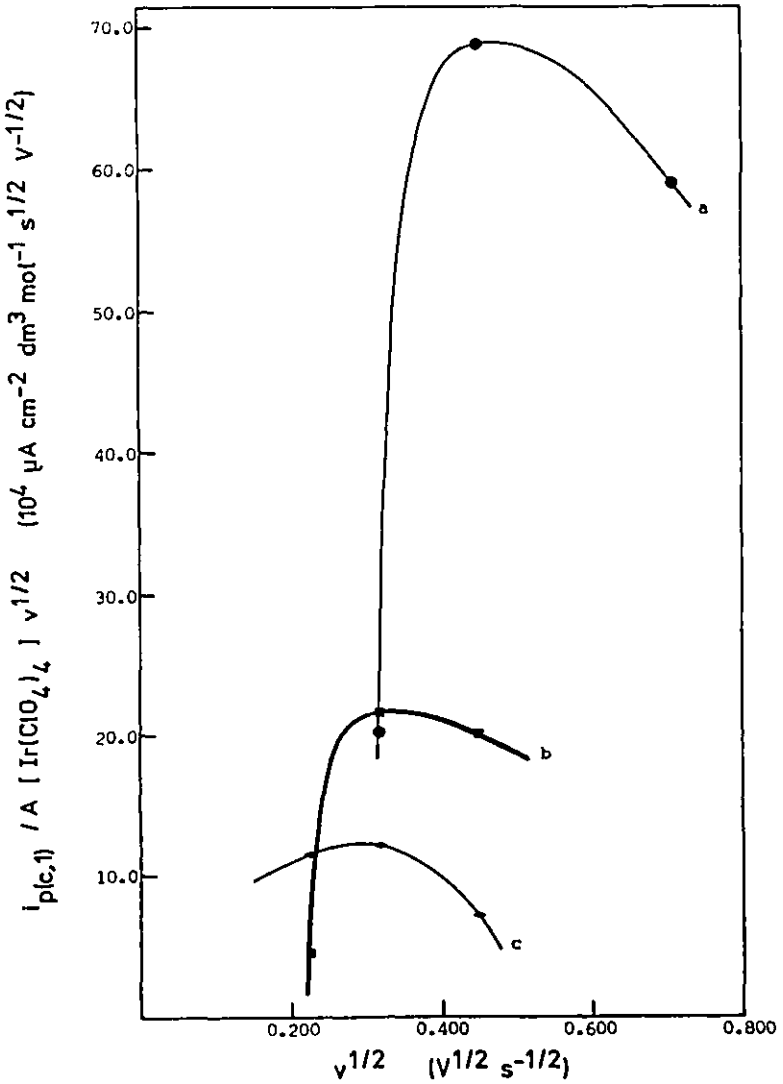

Fig. 5-155 Ir(IV) Perchlorate (1.0×10^{-4} mol dm^{-3})/Perchloric acid supporting electrolyte System: Values of cathodic current function, $i_{p(c,1)}/A$ [$Ir(ClO_4)_4$] $v^{\frac{1}{2}}$, as a function of square root of potential scan rate, $v^{\frac{1}{2}}$; at perchloric acid concentrations (a) 0.1, (b) 0.8, and (c) 2.0 M. Boron carbide solid electrode $B_{3.86}C$.

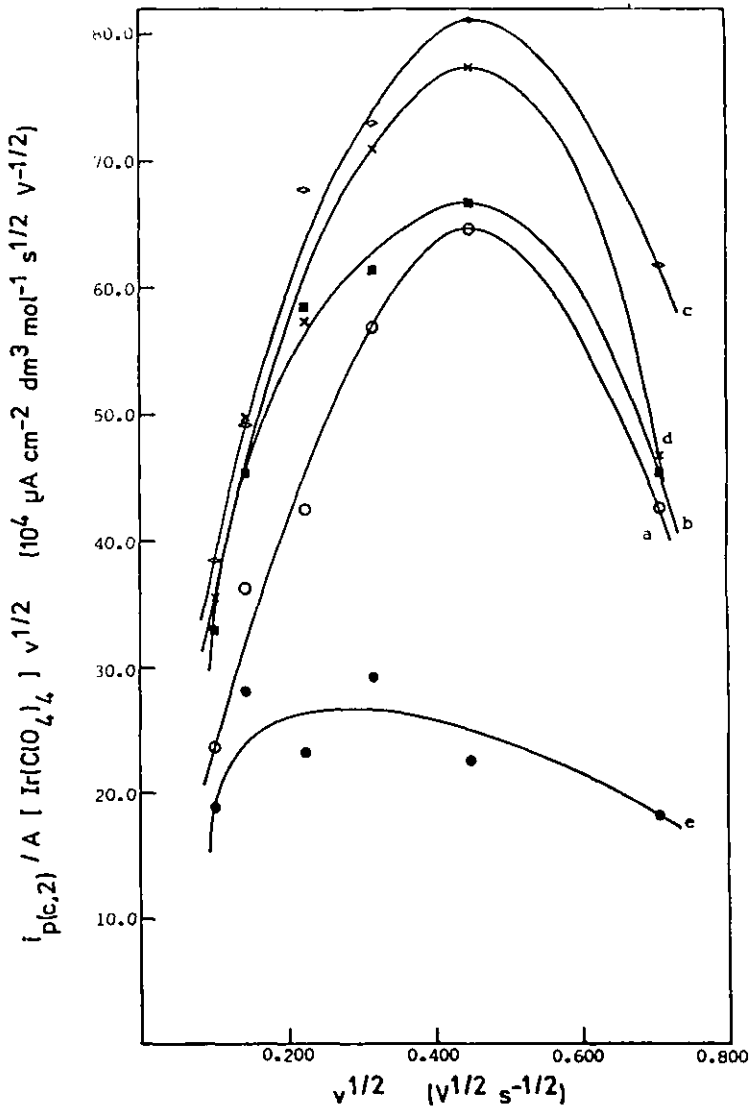

Fig. 5-156 Ir(IV) Perchlorate (1.0×10^{-4} mol dm^{-3})/Perchloric acid supporting electrolyte System: Values of cathodic current function, $i_{p(c,2)}/A$ [$Ir(ClO_4)_4$] $v^{\frac{1}{2}}$, as a function of square root of potential scan rate, $v^{\frac{1}{2}}$; at perchloric acid concentrations (a) 0.1, (b) 0.2, (c) 0.4, (d) 0.8, and (e) 2.0 M. Boron carbide solid electrode $B_{3.86}C$.

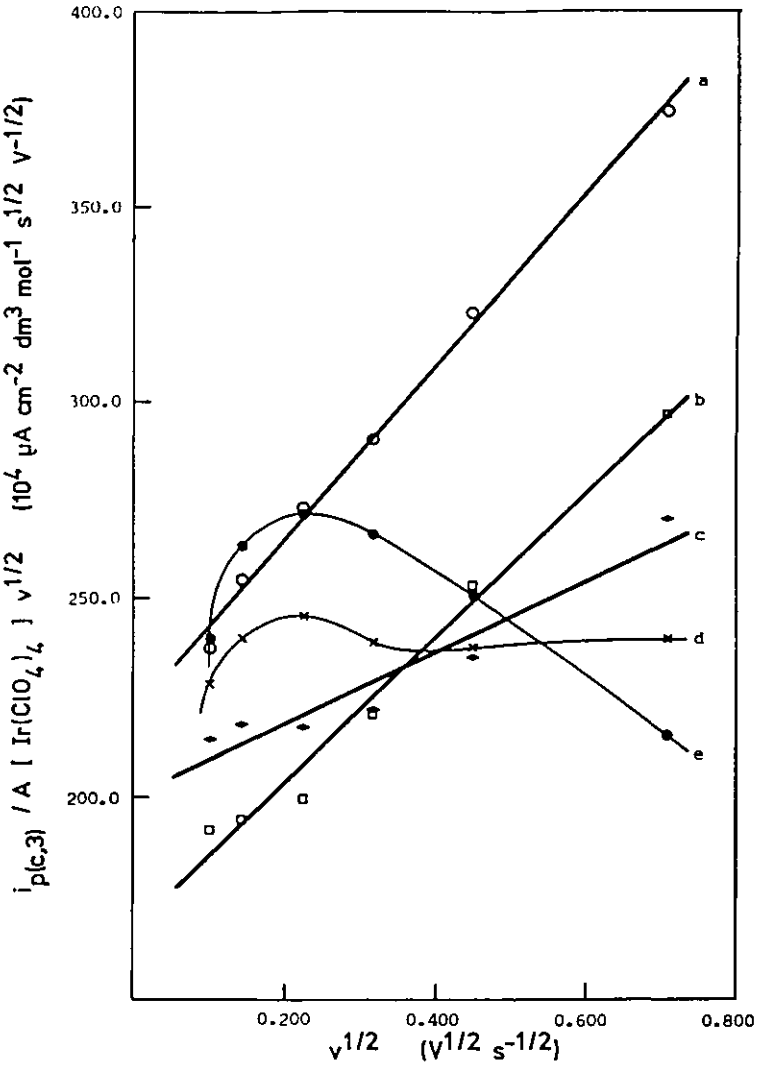

Fig. 5-157 Ir(IV) Perchlorate (1.0×10^{-4} mol dm^{-3})/Perchloric acid supporting electrolyte System: Values of cathodic current function, $i_{p(c,3)}/A\ [\ Ir(ClO_4)_4\ ]\ v^{\frac{1}{2}}$, as a function of square root of potential scan rate, $v^{\frac{1}{2}}$; at perchloric acid concentrations (a) 0.1, (b) 0.2, (c) 0.4, (d) 0.8, and (e) 2.0 M. Boron carbide solid electrode $B_{3.86}C$.

(a) $i_{p(c,3)}/A\ [\ Ir(ClO_4)_4\ ]\ v^{\frac{1}{2}} = 2.21 \times 10^6 + 2.21 \times 10^6\ v^{\frac{1}{2}}$
Correlation coefficient = 0.9977
Level of significance, p = $p < 0.001$
Standard deviation of $i_{p(c,3)}/A\ [\ Ir(ClO_4)_4\ ]\ v^{\frac{1}{2}}$ from regression = 3.80×10^4 μA cm^{-2} dm^3 mol^{-1} $s^{\frac{1}{2}}$ $V^{-\frac{1}{2}}$
Degrees of freedom = 4

(b) $i_{p(c,3)}/A\ [\ Ir(ClO_4)_4\ ]\ v^{\frac{1}{2}} = 1.68 \times 10^6 + 1.82 \times 10^6\ v^{\frac{1}{2}}$
Correlation coefficient = 0.9912
Level of significance, p = $p < 0.001$
Standard deviation of $i_{p(c,3)}/A\ [\ Ir(ClO_4)_4\ ]\ v^{\frac{1}{2}}$ from regression = 6.14×10^4 μA cm^{-2} dm^3 mol^{-1} $s^{\frac{1}{2}}$ $V^{-\frac{1}{2}}$
Degrees of freedom = 4

(c) $i_{p(c,3)}/A\ [\ Ir(ClO_4)_4\ ]\ v^{\frac{1}{2}} = 2.01 \times 10^6 + 8.95 \times 10^5\ v^{\frac{1}{2}}$
Correlation coefficient = 0.9589
Level of significance, p = $0.001 < p < 0.01$
Standard deviation of $i_{p(c,3)}/A\ [\ Ir(ClO_4)_4\ ]\ v^{\frac{1}{2}}$ from regression = 6.70×10^4 μA cm^{-2} dm^3 mol^{-1} $s^{\frac{1}{2}}$ $V^{-\frac{1}{2}}$
Degrees of freedom = 4

it can be inferred from Fig. 5-155 that the increasing perchloric acid concentration reduced the Peak 1 current. Fig. 5-158, however, shows that Peak 2 was initially enhanced by the increasing perchloric acid concentration before declining to end at lower values of peak current; thus reflecting the influence of adsorption coupled with a catalytic reaction. Peak 3 declined with increasing perchloric acid concentration (Fig. 5-159) because the adsorption effect was weakened.

The cathodic peak potentials generally remained steady as the sweep rate was increased (Fig. 5-160); when considering the results obtained over the entire range of perchloric acid concentration studied. Plots of $|E_p - E_{p/2}|$ as a function of sweep rate show that the charge transfers became less reversible at faster rates (Fig. 5-161). Cathodic peak potentials when plotted as functions of (ionic strength)$^{\frac{1}{2}}$, $I^{\frac{1}{2}}$, (when the perchloric acid concentration was increased) exhibited shifts to more anodic potentials despite the Ir(IV) perchlorate species being cationic (Fig. 5-162). Fig. 5-163 shows that the differences between these peak potentials narrowed as $I^{\frac{1}{2}}$ increased, $|E_{p(c,2)} - E_{p(c,2)/2}|$ was relatively independent of $I^{\frac{1}{2}}$, and $|E_{p(c,3)} - E_{p(c,3)/2}|$ was reduced at high values of $I^{\frac{1}{2}}$. Therefore, the anodic shift in peak potentials with increasing $I^{\frac{1}{2}}$ may be attributed to the weakening of the effect of strong adsorption of reactant.

5-1.5.(ii).c Boron carbide/carbon composite solid electrode $B_{3.77}C$

Linear sweep voltammograms for Ir(IV) perchlorate (1.0×10^{-4} mol dm^{-3}), in perchloric acid (0.1 M) supporting electrolyte, obtained at the boron carbide/carbon composite solid electrode $B_{3.77}C$ over a range of sweep rates are presented in Fig. 5-164. As can be seen, the charge transfers became less reversible as the sweep rate was increased; hence the peaks broadened and were shifted to less anodic potentials. Of the three cathodic peaks, the most anodic peak (Peak 1) was a charge transfer of low reversibility complicated by a chemical reaction (Fig. 5-165); hence Peak 1 was not defined at higher sweep rates. Fig. 5-165 also shows that Peaks 2 and 3 were influenced by adsorption.

The cathodic peak potentials were cathodically shifted by increasing sweep rate (Fig. 5-166). Fig. 5-167 shows that the differences between these potentials increased with increasing sweep rate, and $|E_p - E_{p/2}|$ values for Peaks 2 and 3 also increased; reflecting the decrease in the reversibility of the charge transfers.

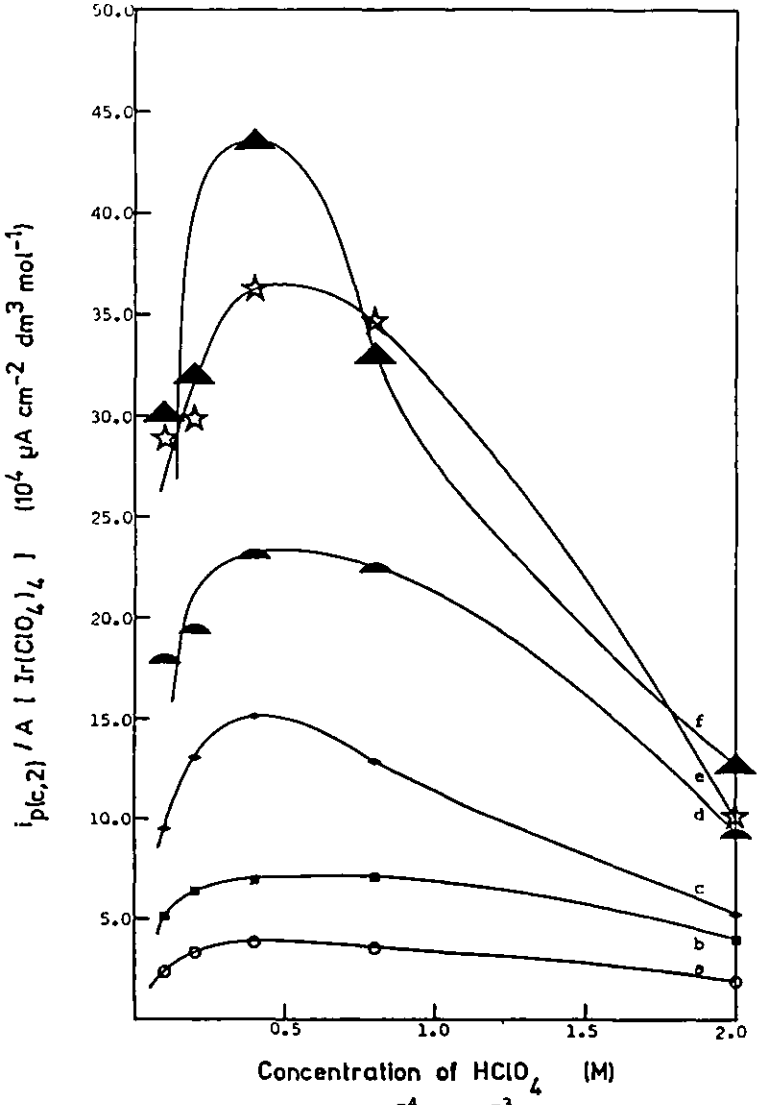

Fig. 5-158 Ir(IV) Perchlorate (1.0×10^{-4} mol dm^{-3})/Perchloric acid supporting electrolyte System: Values of cathodic peak current per unit area divided by concentration of Ir(IV) Perchlorate, $i_{p(c,2)}/A$ [$Ir(ClO_4)_4$], as a function of concentration of perchloric acid; at potential scan rates (a) 0.010, (b) 0.020, (c) 0.050, (d) 0.100, (e) 0.200, and (f) 0.500 V s^{-1}. Boron carbide solid electrode $B_{3.86}C$.

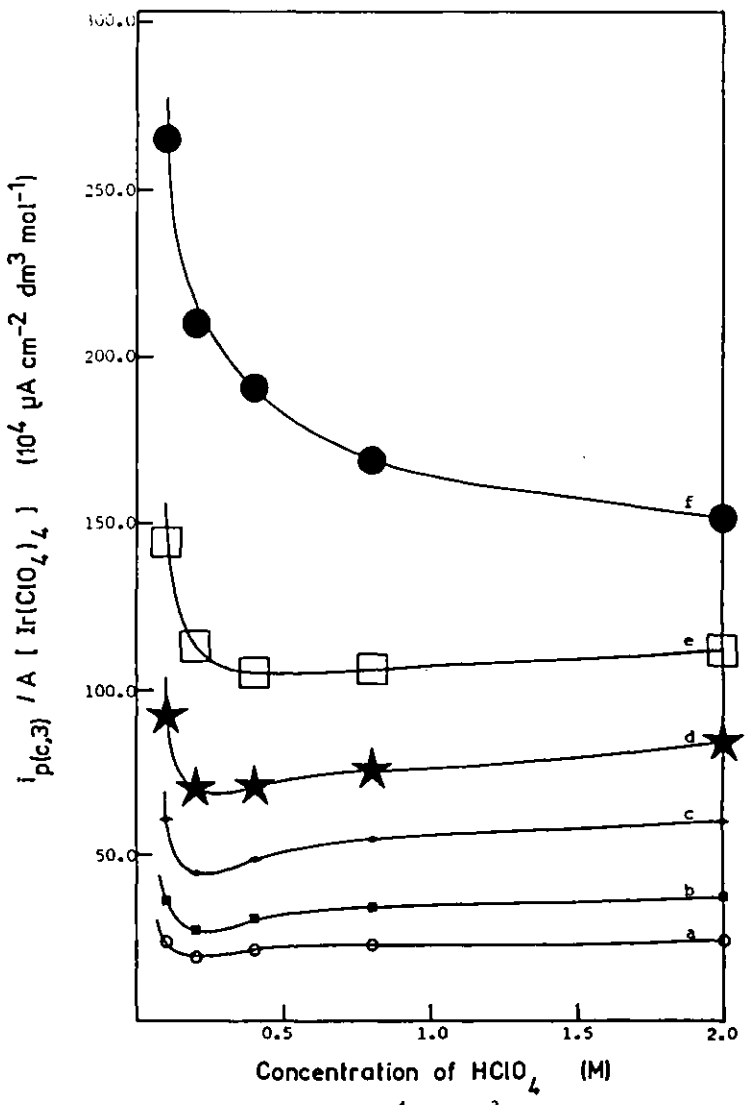

Fig. 5-159 Ir(IV) Perchlorate (1.0×10^{-4} mol dm^{-3})/Perchloric acid supporting electrolyte System: Values of cathodic peak current per unit area divided by concentration of Ir(IV) Perchlorate, $i_{p(c,3)}/A$ [$Ir(ClO_4)_4$], as a function of concentration of perchloric acid; at potential scan rates (a) 0.010, (b) 0.020, (c) 0.050, (d) 0.100, (e) 0.200, and (f) 0.500 V s^{-1}. Boron carbide solid electrode $B_{3.86}C$.

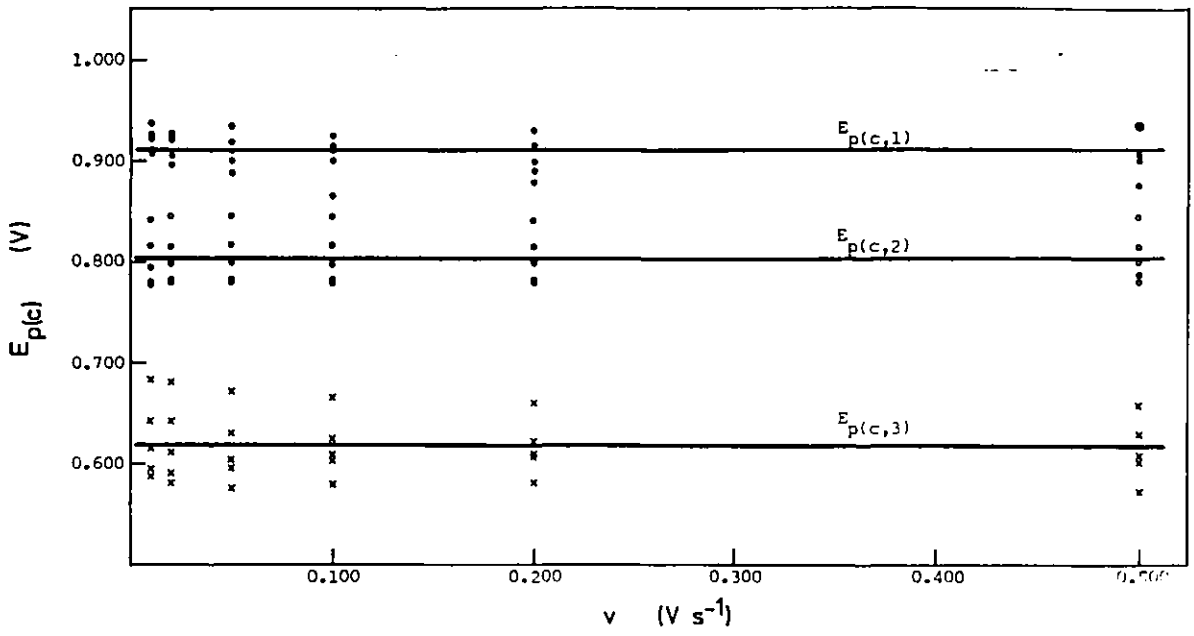

Fig. 5-160 Ir(IV) Perchlorate (1.0×10^{-4} mol dm^{-3})/Perchloric acid supporting electrolyte System: Values of cathodic peak potential, $E_{p(c)}$, as a function of potential scan rate, v; at perchloric acid concentrations of 0.1 to 2.0 M. Boron carbide solid electrode $B_{3.86}C$.

(a) $E_{p(c,1)}$ mean = 0.910 V
Standard deviation = 0.019 V
Degrees of freedom = 29

(b) $E_{p(c,2)}$ mean = 0.804 V
Standard deviation = 0.024 V
Degrees of freedom = 29

(c) $E_{p(c,3)}$ mean = 0.618 V
Standard deviation = 0.032 V
Degrees of freedom = 29

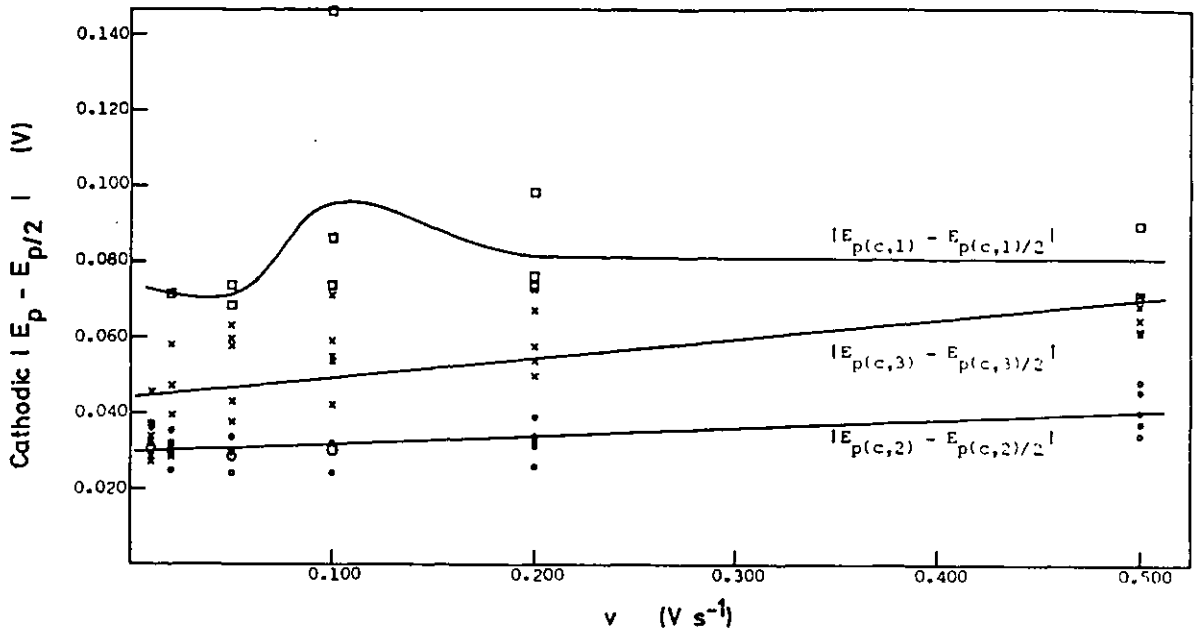

Fig. 5-161 Ir(IV) Perchlorate (1.0×10^{-4} mol dm^{-3})/Perchloric acid supporting electrolyte System: Values of the absolute difference between cathodic peak and half-peak potential, $|E_{p(c)} - E_{p(c)/2}|$, as a function of potential scan rate, v; at perchloric acid concentrations of 0.1 to 2.0 M. Boron carbide solid electrode $B_{3.86}C$.

(a) $|E_{p(c,2)} - E_{p(c,2)/2}| = 2.97 \times 10^{-2} + 2.10 \times 10^{-2}$ v
Correlation coefficient = 0.6508
Level of significance, p = $p < 0.001$
Standard deviation of $|E_{p(c,2)} - E_{p(c,2)/2}|$ from regression
= 0.004 V
Degrees of freedom = 28

(b) $|E_{p(c,3)} - E_{p(c,3)/2}| = 4.43 \times 10^{-2} + 5.07 \times 10^{-2}$ v
Correlation coefficient = 0.6240
Level of significance, p = $p < 0.001$
Standard deviation of $|E_{p(c,3)} - E_{p(c,3)/2}|$ from regression
= 0.011 V
Degrees of freedom = 28

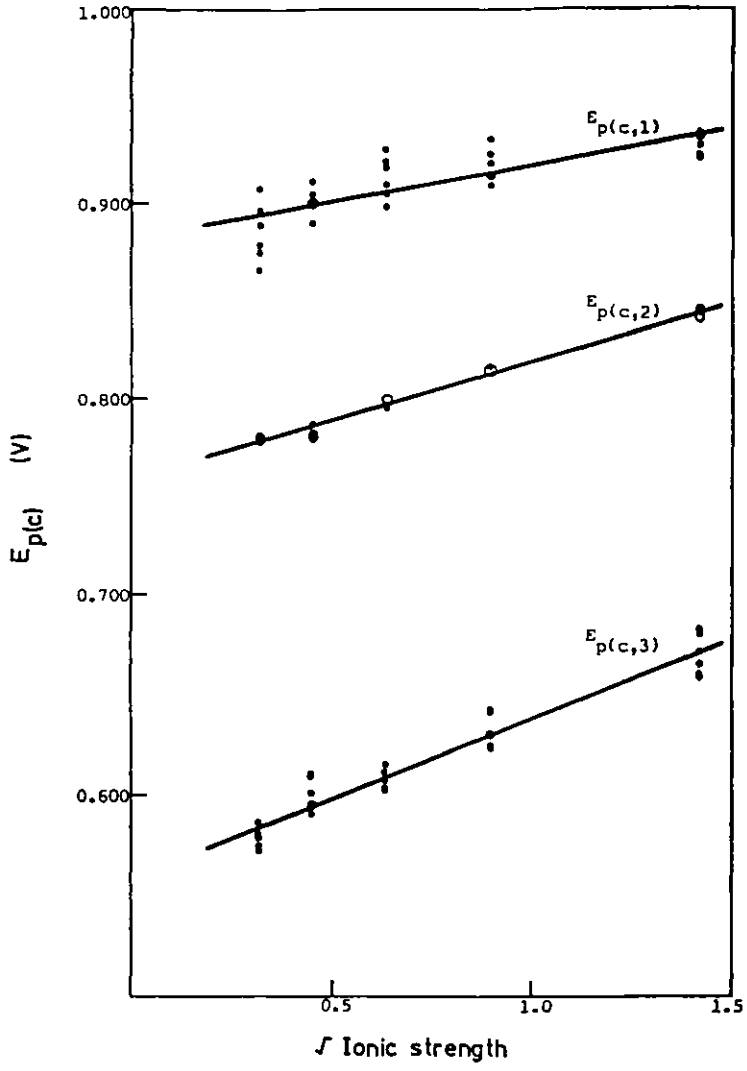

Fig. 5-162 Ir(IV) Perchlorate (1.0×10^{-4} mol dm^{-3})/Perchloric acid (0.1 to 2.0 M) supporting electrolyte System: Values of cathodic peak potential, $E_{p(c)}$, as a function of square root of total ionic strength, $\sqrt{I}$ (where the concentration of perchloric acid was varied); at potential scan rates of 0.010 to 0.500 V s^{-1}. Boron carbide solid electrode $B_{3.86}C$.

(a) $E_{p(c,1)} = 0.882 + 3.76 \times 10^{-2} \sqrt{I}$
Correlation coefficient = 0.7969
Level of significance, p = $p < 0.001$
Standard deviation of $E_{p(c,1)}$ from regression = 0.012 V
Degrees of freedom = 28

(b) $E_{p(c,2)} = 0.759 + 6.07 \times 10^{-2} \sqrt{I}$
Correlation coefficient = 0.9941
Level of significance, p = $p < 0.001$
Standard deviation of $E_{p(c,2)}$ from regression = 0.003 V
Degrees of freedom = 28

(c) $E_{p(c,3)} = 0.559 + 7.91 \times 10^{-2} \sqrt{I}$
Correlation coefficient = 0.9692
Level of significance, p = $p < 0.001$
Standard deviation of $E_{p(c,3)}$ from regression = 0.008 V
Degrees of freedom = 28

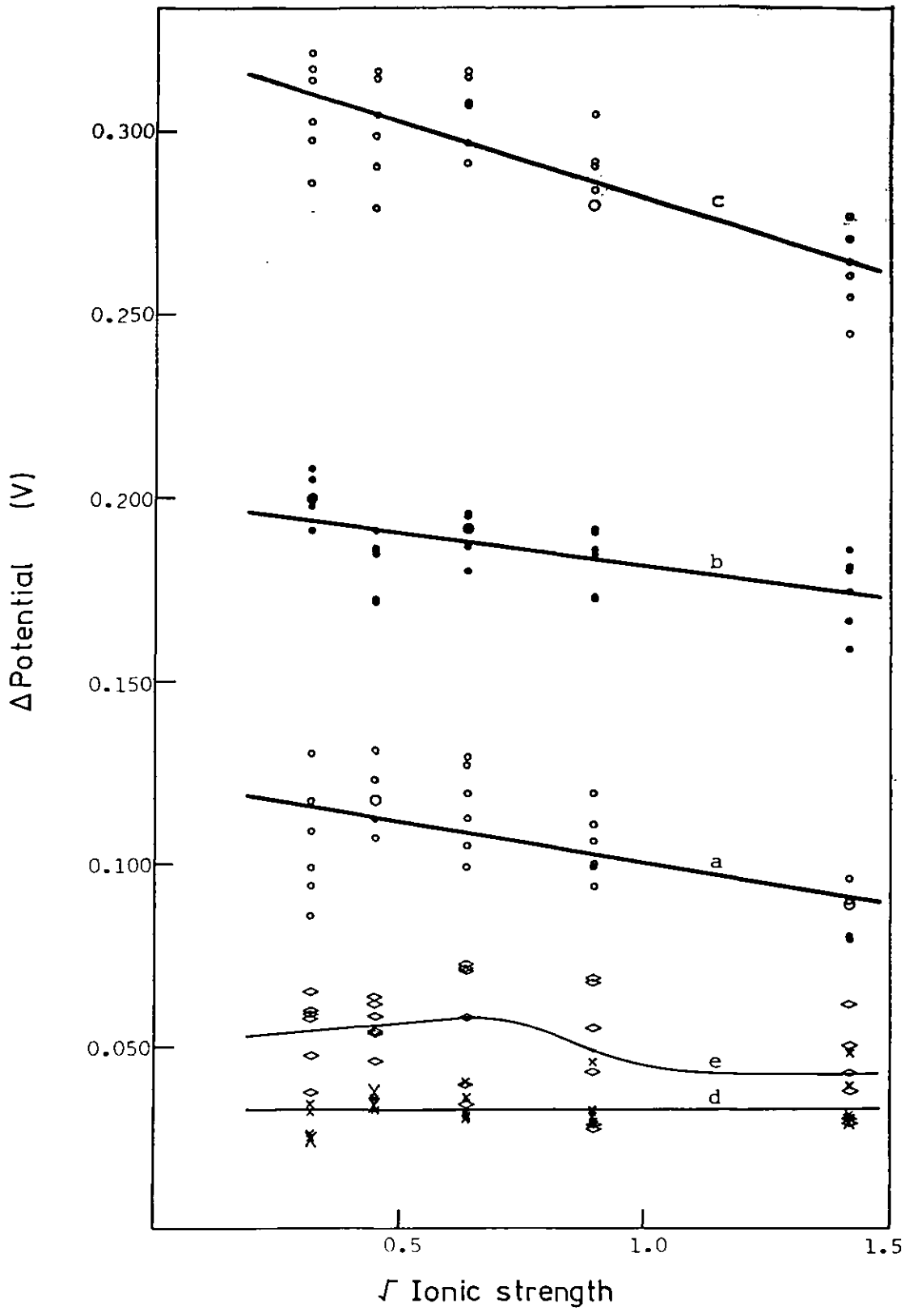

Fig. 5-163 Ir(IV) Perchlorate (1.0×10^{-4} mol dm^{-3})/Perchloric acid (0.1 to 2.0 M) supporting electrolyte System: Values of the difference between cathodic peak potentials, $\Delta E_{p(c)}$, and the difference between cathodic peak and half-peak potential, $|E_{p(c)} - E_{p(c)/2}|$, as a function of square root of total ionic strength, $\sqrt{I}$ (where the concentration of perchloric acid was varied); at potential scan rates of 0.010 to 0.500 V s^{-1}. (a) $\Delta E_{p(c;\ 1,2)}$, (b) $\Delta E_{p(c;\ 2,3)}$, (c) $\Delta E_{p(c;\ 1,3)}$, (d) $|E_{p(c,2)} - E_{p(c,2)/2}|$, and (e) $|E_{p(c,3)} - E_{p(c,3)/2}|$.

Fig. 5-163 (continued):-

(a) $\Delta E_{p(c;\ 1,2)} = 0.124 - 2.31 \times 10^{-2} \sqrt{I}$
Correlation coefficient = -0.6055
Level of significance, p = $p < 0.001$
Standard deviation of $\Delta E_{p(c;\ 1,2)}$ from regression = 0.012 V
Degrees of freedom = 28

(b) $\Delta E_{p(c;\ 2,3)} = 0.200 - 1.84 \times 10^{-2} \sqrt{I}$
Correlation coefficient = -0.6296
Level of significance, p = $p < 0.001$
Standard deviation of $\Delta E_{p(c;\ 2,3)}$ from regression = 0.009 V
Degrees of freedom = 28

(c) $\Delta E_{p(c;\ 1,3)} = 0.323 - 4.15 \times 10^{-2} \sqrt{I}$
Correlation coefficient = -0.8057
Level of significance, p = $p < 0.001$
Standard deviation of $\Delta E_{p(c;\ 1,3)}$ from regression = 0.012 V
Degrees of freedom = 28

(d) $|E_{p(c,2)} - E_{p(c,2)/2}|$ mean = 0.033 V
Standard deviation = 0.006 V
Degrees of freedom = 29

(e) $|E_{p(c,3)} - E_{p(c,3)/2}|$ mean = 0.052 V
Standard deviation = 0.014 V
Degrees of freedom = 29

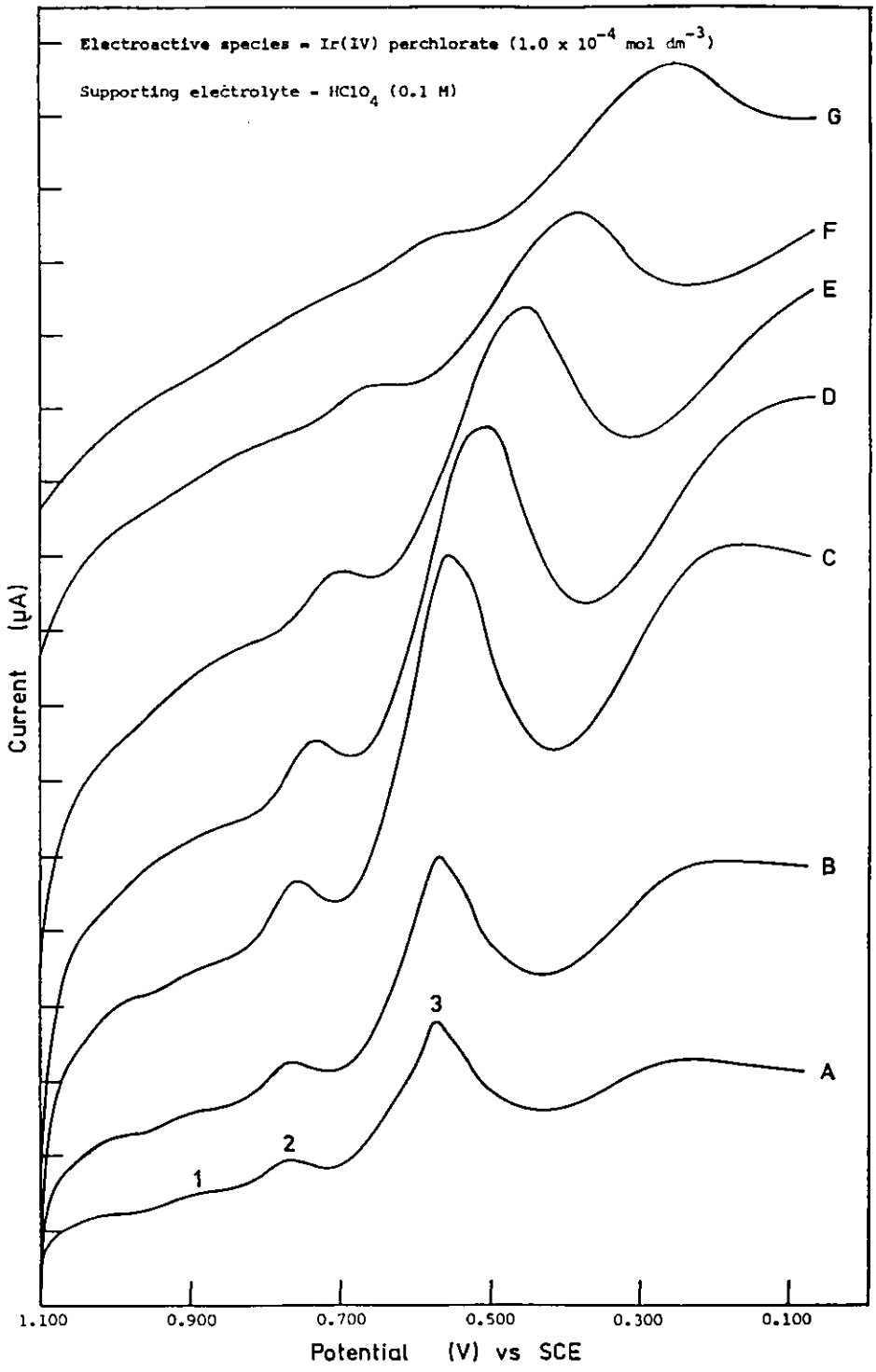

Fig. 5-164 Linear sweep voltammograms obtained at the boron carbide/carbon composite solid electrode $B_{3.77}C$ over a range of sweep rates.

	Sweep rate (V s^{-1})	Current sensitivity (μA/division)
A)	0.005	5
B)	0.010	5
C)	0.020	5
D)	0.050	10
E)	0.100	20
F)	0.200	50
G)	0.500	100

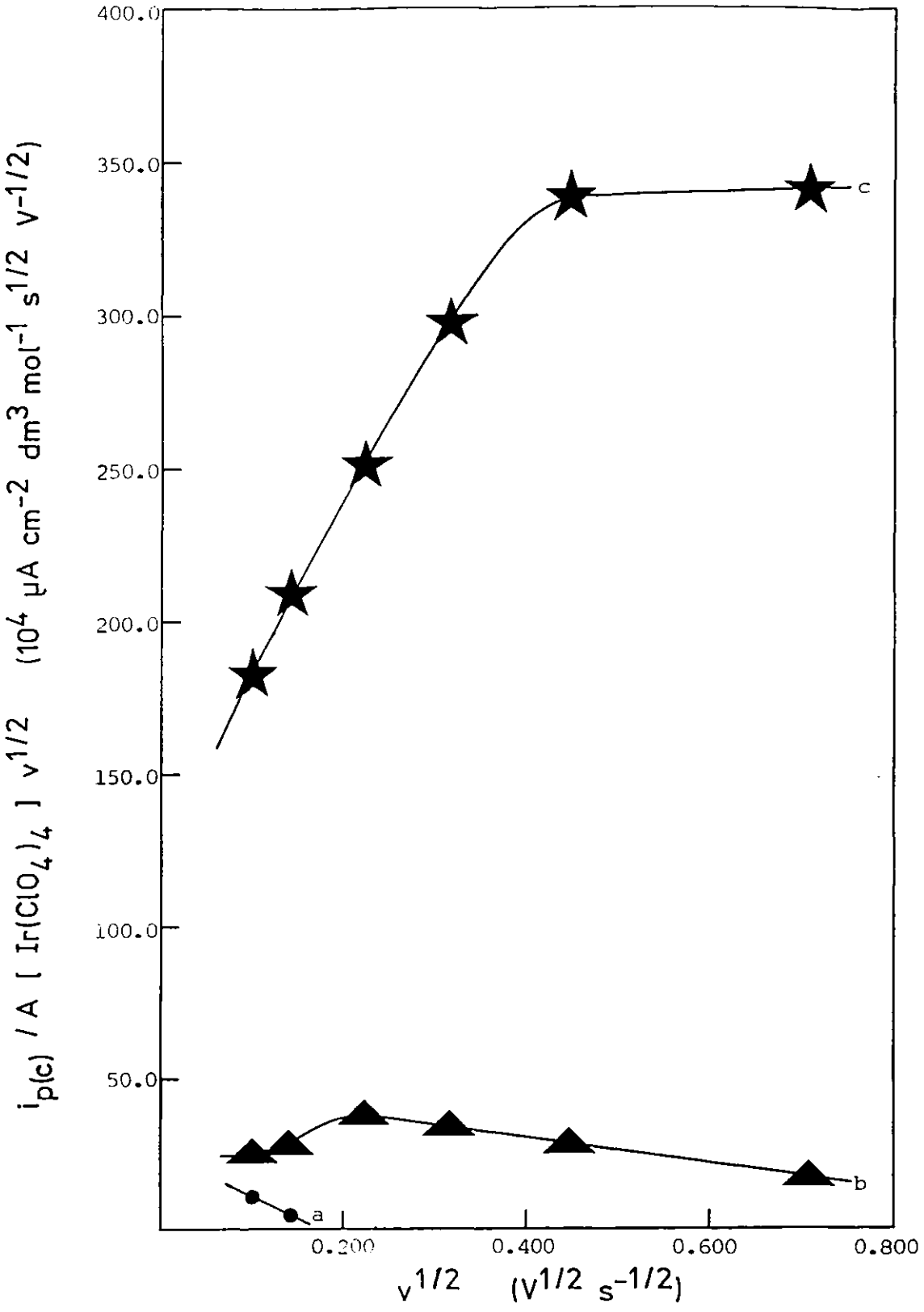

Fig. 5-165 Ir(IV) Perchlorate (1.0×10^{-4} mol dm^{-3})/Perchloric acid (0.1 M) supporting electrolyte System: Values of cathodic current function, $i_{p(c)}/A\ [\ Ir(ClO_4)_4\ ]\ v^{\frac{1}{2}}$, as a function of square root of potential scan rate, $v^{\frac{1}{2}}$. (a) $i_{p(c,1)}/A\ [Ir(ClO_4)_4\ ]\ v^{\frac{1}{2}}$, (b) $i_{p(c,2)}/A\ [\ Ir(ClO_4)_4\ ]\ v^{\frac{1}{2}}$, and (c) $i_{p(c,3)}/A\ [\ Ir(ClO_4)_4\ ]\ v^{\frac{1}{2}}$. Boron carbide/carbon composite solid electrode $B_{3.77}C$.

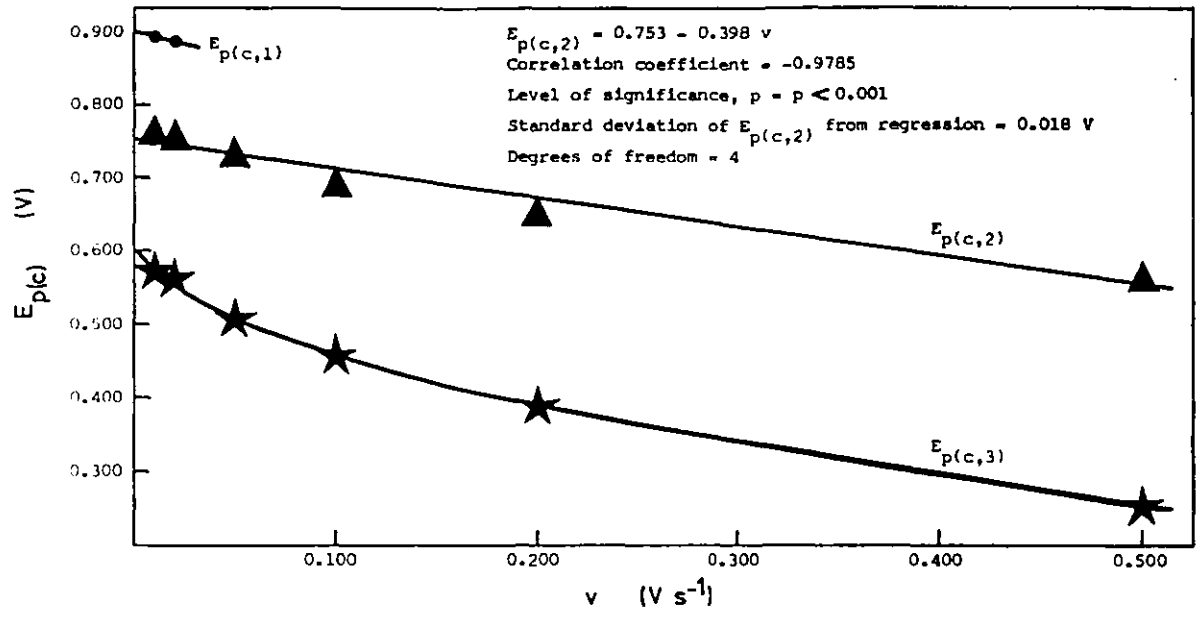

Fig. 5-166 Ir(IV) Perchlorate (1.0×10^{-4} mol dm^{-3})/Perchloric acid (0.1 M) supporting electrolyte System: Values of cathodic peak potential, $E_{p(c)}$, as a function of potential scan rate, v. Boron carbide/carbon composite solid electrode $B_{3.77}C$.

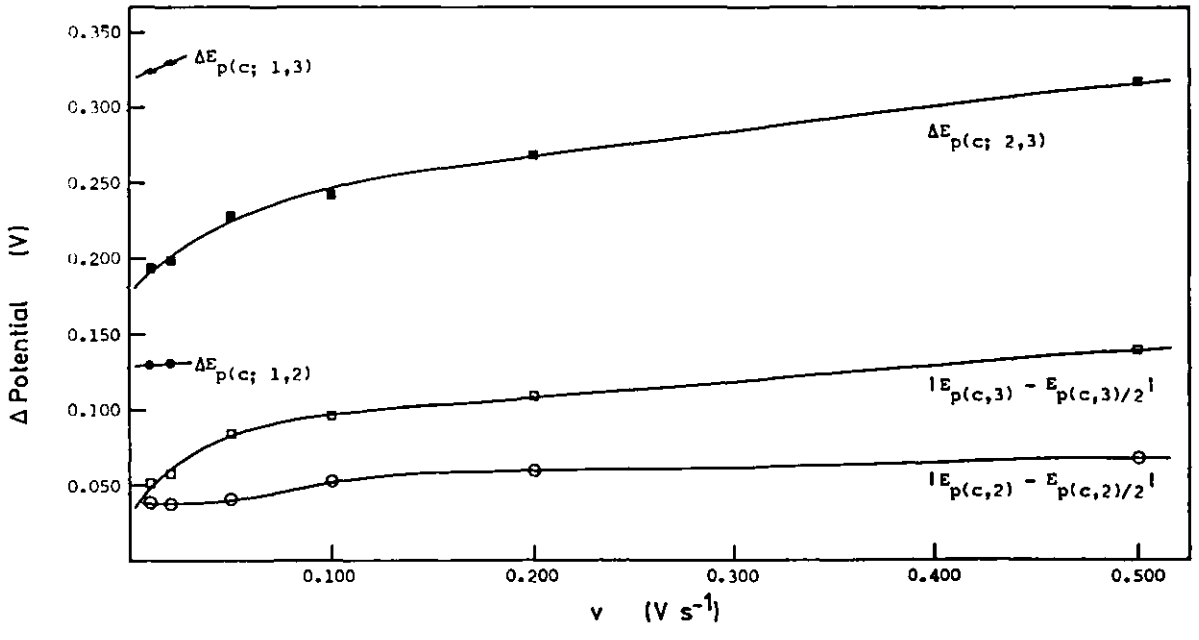

Fig. 5-167 Ir(IV) Perchlorate (1.0×10^{-4} mol dm^{-3})/Perchloric acid (0.1 M) supporting electrolyte System: Values of the difference between cathodic peak potentials, $\Delta E_{p(c)}$, and the absolute difference between cathodic peak and half-peak potential, $|E_{p(c)} - E_{p(c)/2}|$, as a function of potential scan rate, v. Boron carbide/carbon composite solid electrode $B_{3.77}C$.

5-1.5.(ii).d Boron carbide/carbon composite solid electrode $B_{3.69}C$

Typical linear sweep voltammograms, using a range of sweep rates, and a cyclic voltammogram for Ir(IV) perchlorate (1.0×10^{-4} mol dm^{-3}) in perchloric acid (0.1 M) supporting electrolyte obtained at the boron carbide/carbon composite solid electrode $B_{3.69}C$ are presented in Fig. 5-168. Qualitative examination of the cyclic voltammogram shows that Peak 1 was irreversible whereas Peaks 2 and 3 were reversible and so anodic counterparts of Peaks 2 and 3 were exhibited. All the voltammograms indicate that Peak 3 was distorted by other processes which occurred at nearly the same potential as Peak 3. Quantitative treatment of the linear sweep voltammograms reveals that the peak current function of all three peaks increased with increasing (sweep rate)$^{\frac{1}{2}}$, $v^{\frac{1}{2}}$; thus suggesting that the charge transfers were complicated by adsorption (Fig. 5-169).

The influence of sweep rate on the peak potentials is shown in Fig. 5-170. $E_{p(c,2)}$ was constant whereas $E_{p(c,1)}$ and $E_{p(c,3)}$ were initially shifted to more anodic values by increasing sweep rate before cathodic shifts at faster sweep rates returned them to approximately initial values. Fig. 5-171 shows the trends of the differences between the peak potentials as functions of the sweep rate, v, and also reveals that the $|E_p - E_{p/2}|$ values for Peak 2 was constant but values for Peaks 1 and 3 widened with increasing sweep rate.

The evidence suggests that Peaks 1 and 3 were diffusion peaks which were complicated by the adsorption of reactant and possibly a weaker adsorption of product; hence the initial anodic shift in their peak potentials with increasing sweep rate. Peak 2, however, was the strong adsorption post-peak of Ir(IV) perchlorate reactant.

5-1.5.(ii).e Boron carbide/carbon composite solid electrode $B_{3.53}C$

Linear sweep and cyclic voltammograms were obtained at the boron carbide/carbon composite solid electrode $B_{3.53}C$ for the electro-reduction of Ir(IV) perchlorate (1.0×10^{-4} mol dm^{-3}) in perchloric acid (0.1 M) supporting electrolyte (Fig. 5-172). The three cathodic peaks, Peaks 1, 2, and 3, were reversible; hence their anodic counterparts were exhibited in the cyclic voltammogram. Peak 1, however, was poorly defined; especially at slower sweep rates. The peak current function, for interpretable peaks, as a function of (sweep rate)$^{\frac{1}{2}}$ is plotted in Fig. 5-173 and shows that Peaks 2 and 3 were influenced by adsorption; Peak 2

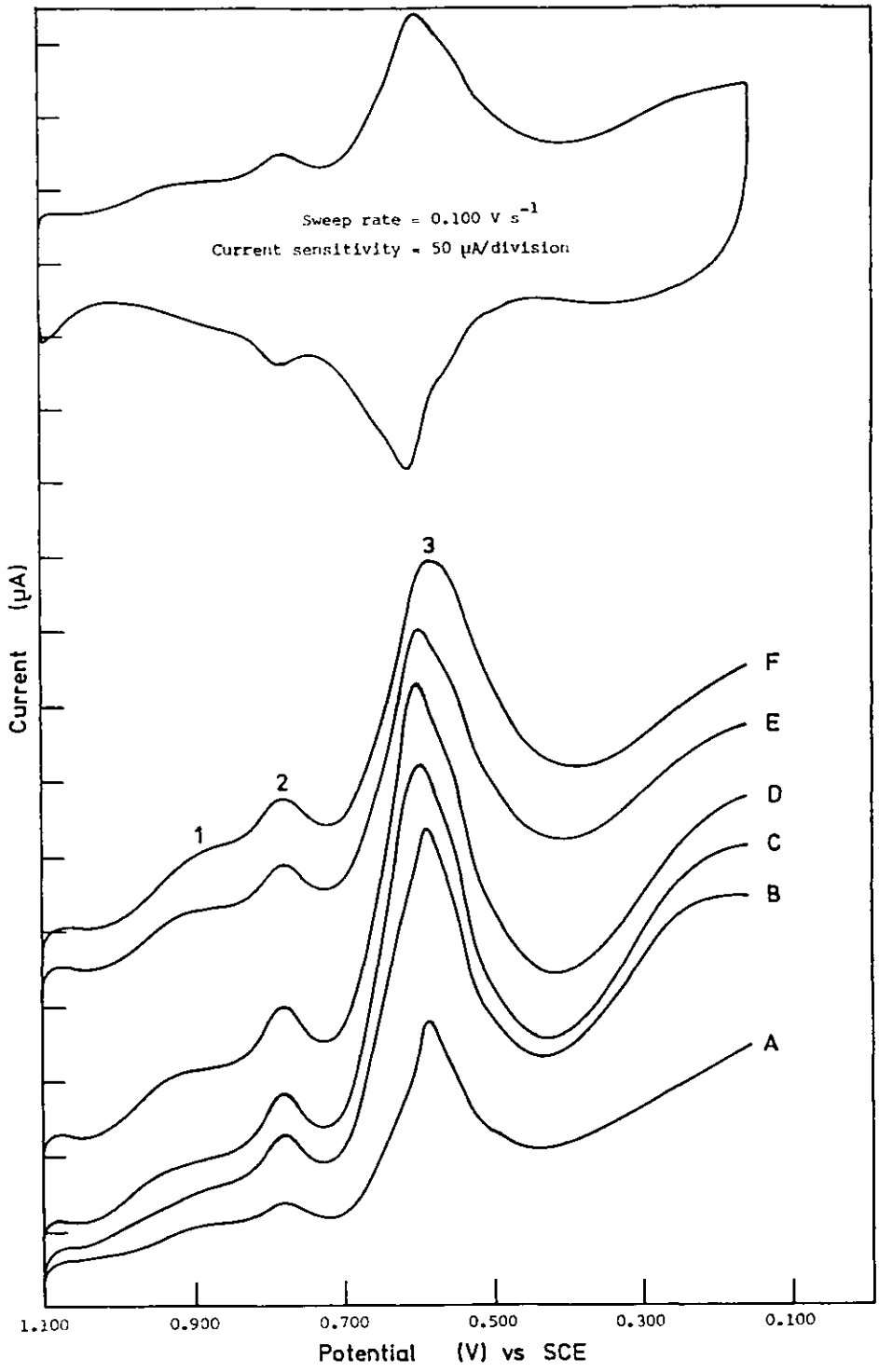

Fig. 5-168 Ir(IV) perchlorate (1.0×10^{-4} mol dm^{-3})/Perchloric acid (0.1 M) supporting electrolyte System: Cyclic and linear sweep voltammograms obtained at the boron carbide/carbon composite solid electrode $B_{3.69}C$.

	Sweep rate (V s^{-1})	Current sensitivity (μA/division)
A)	0.010	5
B)	0.020	5
C)	0.050	10
D)	0.100	20
E)	0.200	50
F)	0.500	100

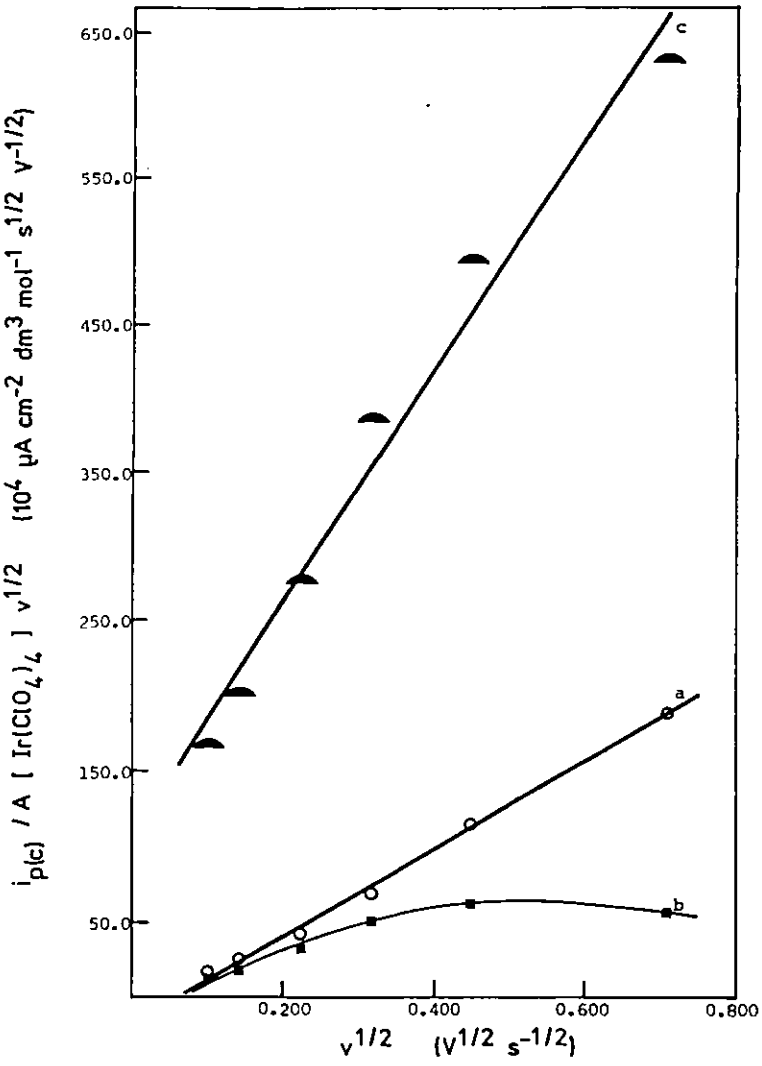

Fig. 5-169 Ir(IV) Perchlorate (1.0×10^{-4} mol dm^{-3})/Perchloric acid (0.1 M) supporting electrolyte System: Values of cathodic current function, $i_{p(c)}/A\ [\ Ir(ClO_4)_4\ ]\ v^{\frac{1}{2}}$, as a function of square root of potential scan rate, $v^{\frac{1}{2}}$. (a) $i_{p(c,1)}/A\ [\ Ir(ClO_4)_4\ ]\ v^{\frac{1}{2}}$, (b) $i_{p(c,2)}/A\ [\ Ir(ClO_4)_4\ ]\ v^{\frac{1}{2}}$, and (c) $i_{p(c,3)}/A\ [\ Ir(ClO_4)_4\ ]\ v^{\frac{1}{2}}$. Boron carbide/carbon composite solid electrode $B_{3.69}C$.

(a) $i_{p(c,1)}/A\ [\ Ir(ClO_4)_4\ ]\ v^{\frac{1}{2}} = 2.89 \times 10^6\ v^{\frac{1}{2}} - 1.71 \times 10^5$
Correlation coefficient = 0.9977
Level of significance, $p = p < 0.001$
Standard deviation of $i_{p(c,1)}/A\ [\ Ir(ClO_4)_4\ ]\ v^{\frac{1}{2}}$ from regression = 4.99×10^4 µA cm^{-2} dm^3 mol^{-1} $s^{\frac{1}{2}}$ $v^{-\frac{1}{2}}$
Degrees of freedom = 4

(c) $i_{p(c,3)}/A\ [\ Ir(ClO_4)_4\ ]\ v^{\frac{1}{2}} = 1.07 \times 10^6 + 7.87 \times 10^6\ v^{\frac{1}{2}}$
Correlation coefficient = 0.9883
Level of significance, $p = p < 0.001$
Standard deviation of $i_{p(c,3)}/A\ [\ Ir(ClO_4)_4\ ]\ v^{\frac{1}{2}}$ from regression = 3.08×10^5 µA cm^{-2} dm^3 mol^{-1} $s^{\frac{1}{2}}$ $v^{-\frac{1}{2}}$
Degrees of freedom = 4

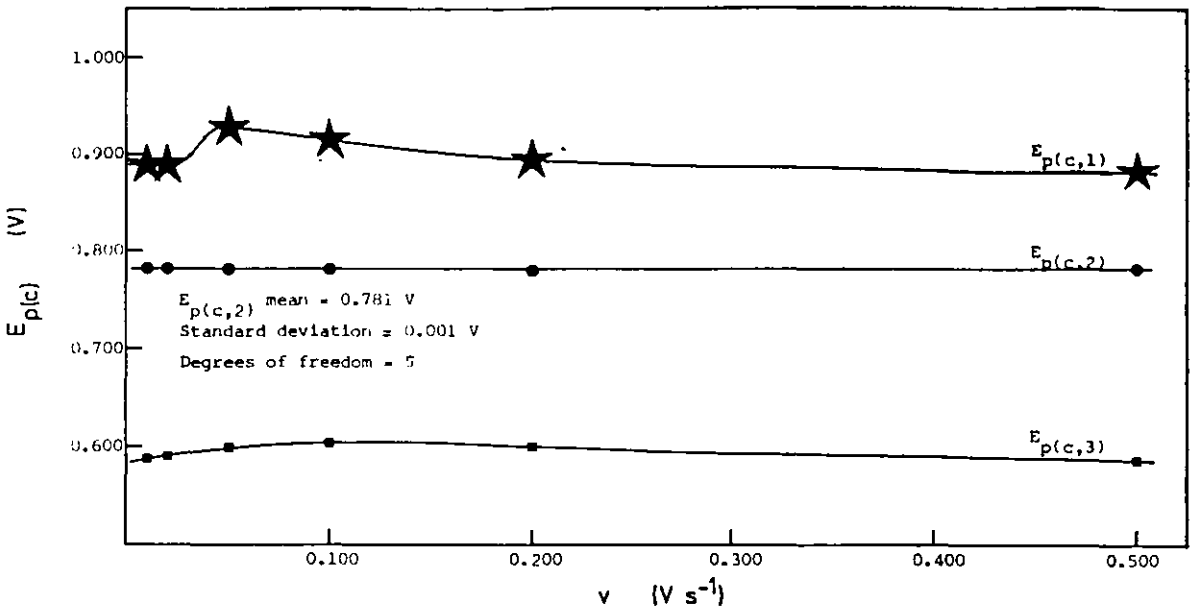

Fig. 5-170 Ir(IV) Perchlorate (1.0×10^{-4} mol dm^{-3})/Perchloric acid (0.1 M) supporting electrolyte System: Values of cathodic peak potential, $E_{p(c)}$, as a function of potential scan rate, v. Boron carbide/carbon composite solid electrode $B_{3.69}C$.

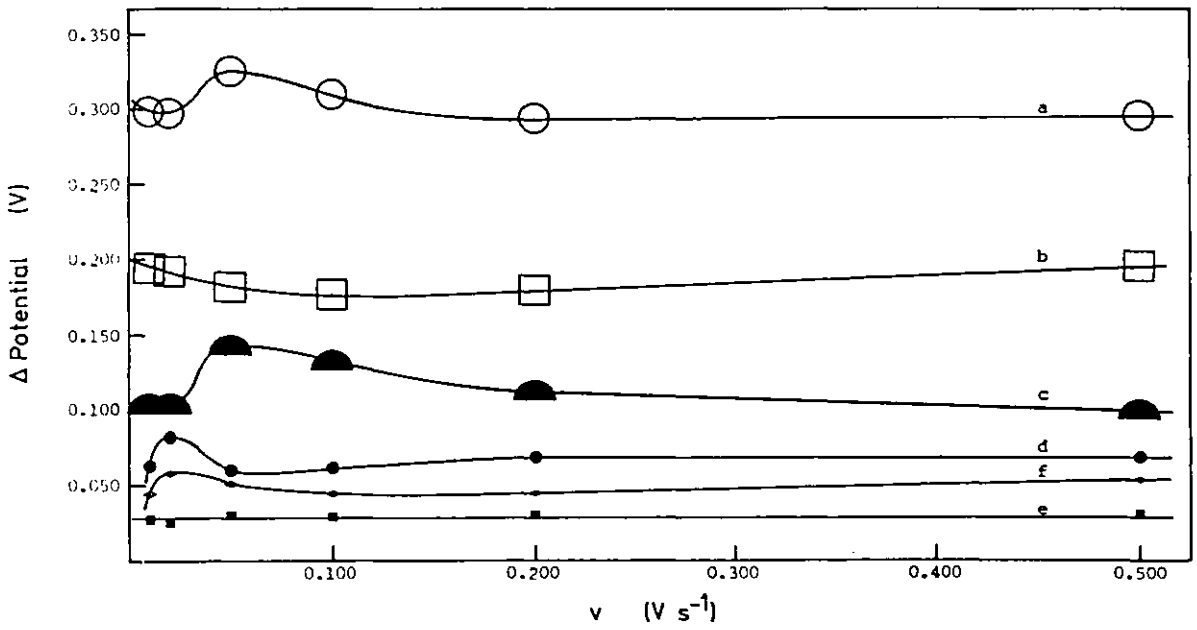

Fig. 5-171 Ir(IV) Perchlorate (1.0×10^{-4} mol dm^{-3})/Perchloric acid (0.1 M) supporting electrolyte System: Values of the difference between cathodic peak potentials, $\Delta E_{p(c)}$, and the absolute difference between cathodic peak and half-peak potential, $|E_{p(c)} - E_{p(c)/2}|$, as a function of potential scan rate, v. (a) $\Delta E_{p(c;\,1,2)}$, (b) $\Delta E_{p(c;\,2,3)}$, (c) $\Delta E_{p(c;\,1,3)}$, (d) $|E_{p(c,1)} - E_{p(c,1)/2}|$, (e) $|E_{p(c,2)} - E_{p(c,2)/2}|$, and (f) $|E_{p(c,3)} - E_{p(c,3)/2}|$. Boron carbide/carbon composite solid electrode $B_{3.69}C$.

(e) $|E_{p(c,2)} - E_{p(c,2)/2}|$ mean = 0.029 V
Standard deviation = 0.002 V
Degrees of freedom = 5

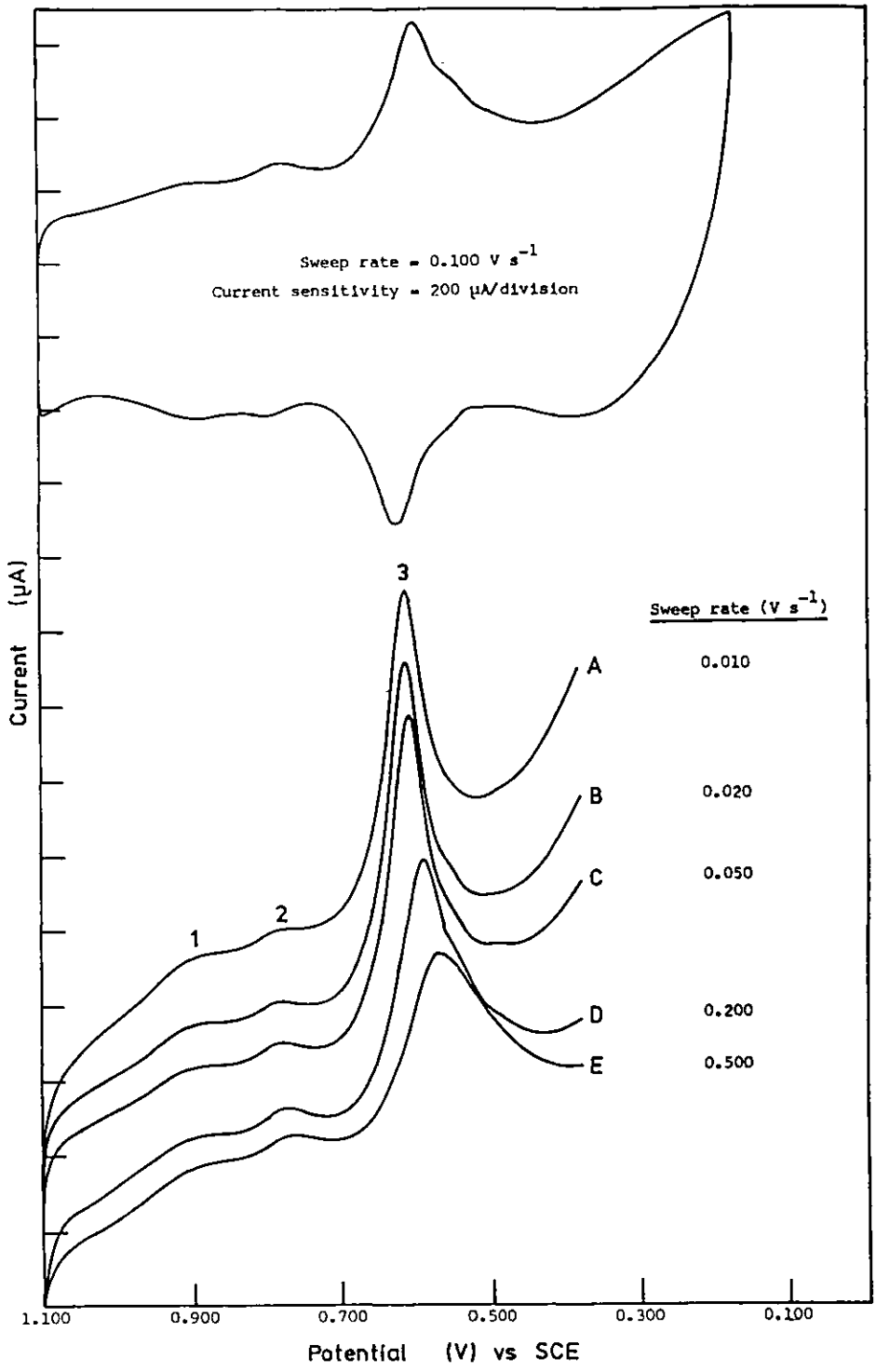

Fig. 5-172 Ir(IV) perchlorate (1.0×10^{-4} mol dm^{-3})/Perchloric acid (0.1 M) supporting electrolyte System: Cyclic and linear sweep voltammograms obtained at the boron carbide/carbon composite solid electrode $B_{3.53}C$. Current sensitivity (μA/division): A) 10, B) 20, C) 50, D) 200, and E) 500.

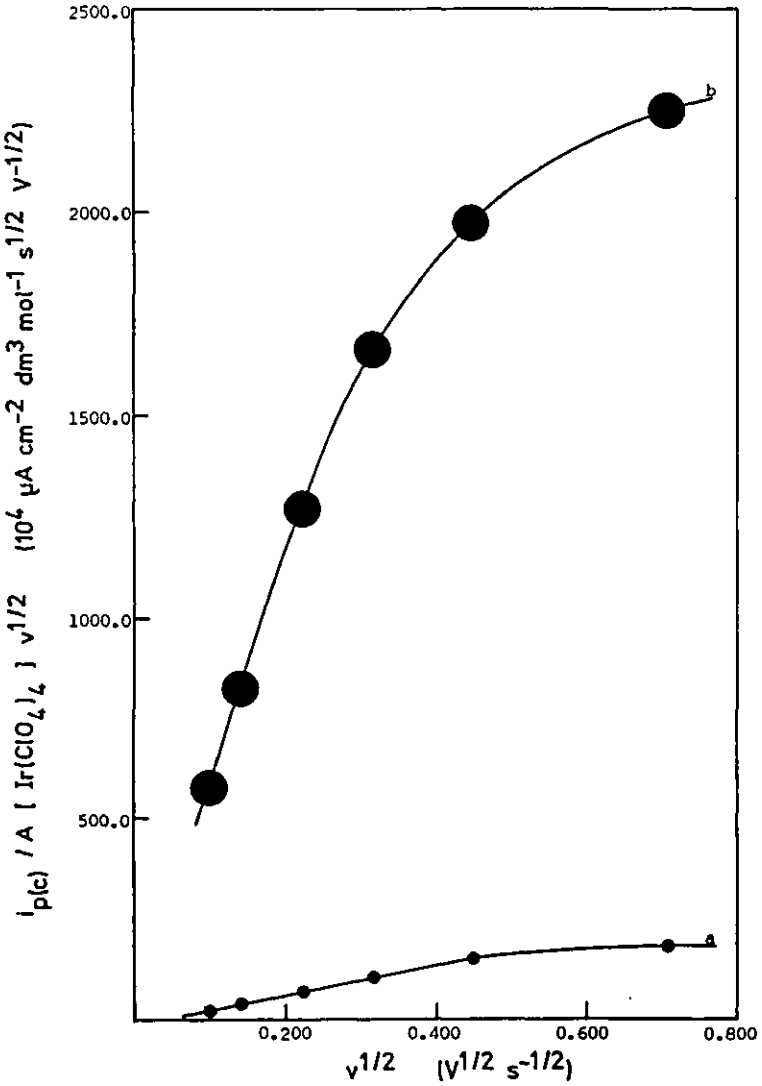

Fig. 5-173 Ir(IV) Perchlorate (1.0×10^{-4} mol dm^{-3})/Perchloric acid (0.1 M) supporting electrolyte System: Values of cathodic current function, $i_{p(c)}/A\,[Ir(ClO_4)_4]\,v^{\frac{1}{2}}$, as a function of square root of potential scan rate, $v^{\frac{1}{2}}$. (a) $i_{p(c,2)}/A\,[Ir(ClO_4)_4]\,v^{\frac{1}{2}}$, and (b) $i_{p(c,3)}/A\,[Ir(ClO_4)_4]\,v^{\frac{1}{2}}$. Boron carbide/carbon composite solid electrode $B_{3.53}C$.

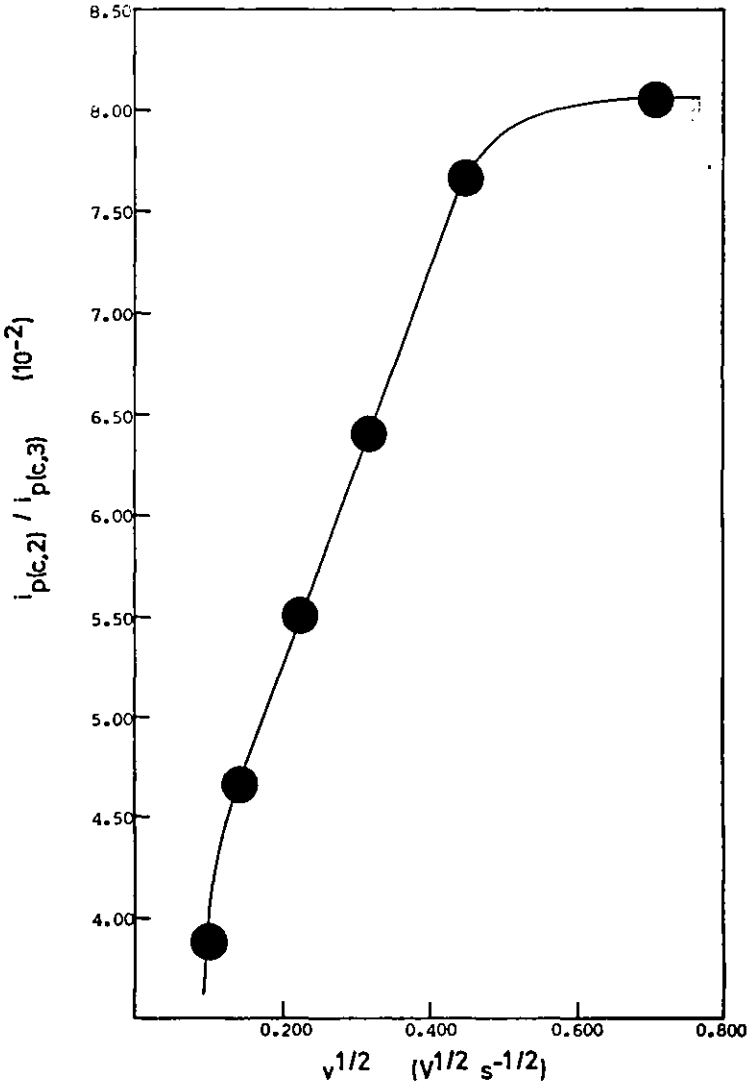

Fig. 5-174 Ir(IV) Perchlorate (1.0×10^{-4} mol dm^{-3})/Perchloric acid (0.1 M) supporting electrolyte System: Values of the ratio of cathodic peak currents, $i_{p(c,2)}/i_{p(c,3)}$, as a function of square root of potential scan rate, $v^{\frac{1}{2}}$. Boron carbide/carbon composite solid electrode $B_{3.53}C$.

being affected more than Peak 3 (Fig. 5-174).

The effect of increasing sweep rate on the cathodic peak potentials of Peaks 2 and 3 was to shift them to less anodic potentials (Fig. 5-175). $E_{p(c,1)}$ remained constant irrespective of the sweep rate. The differences between these cathodic peak potentials are plotted as functions of sweep rate in Fig. 5-176 which also shows that $|E_p - E_{p/2}|$ values for Peaks 2 and 3 increased slightly with increasing sweep rate. No half-peak potential was obtainable for Peak 1 because of the poor definition of the peak.

The evidence indicates that Peaks 1 and 3 were complicated by the weak adsorption of reactant whereas Peak 2 was a post-peak due to the strong adsorption of reactant. Qualitatively, it can be seen from Fig. 5-172 that Peak 3 was also complicated by another process occurring slightly cathodic of $E_{p(c,3)}$.

5-1.5.(ii).f Boron carbide/carbon composite solid electrode $B_{3.38}C$

Cyclic and linear sweep voltammograms obtained at the boron carbide/carbon composite solid electrode $B_{3.38}C$ for the electro-reduction of Ir(IV) perchlorate (1.0×10^{-4} mol dm^{-3}) in perchloric acid (0.1 M) supporting electrolyte are presented in Fig. 5-177. Three cathodic peaks, 1 to 3 inclusive, were exhibited and their anodic counterparts were present in cyclic voltammetry; reflecting a degree of reversibility in the charge transfers. Qualitatively, it can be seen that Peak 3 was enhanced by increasing sweep rate and, therefore, was influenced by the presence of moderately strong adsorption of reactant; Peak 3 being the post-peak relative to Peak 2. Quantitative treatment of the interpretable peaks reveals that Peak 2 was affected by weak adsorption (Fig. 5-178).

The peak potentials, as functions of the sweep rate, are plotted in Fig. 5-179 which shows that $E_{p(c,1)}$ and $E_{p(c,2)}$ remained constant but $E_{p(c,3)}$ shifted cathodically with increasing sweep rate. Fig. 5-180, however, shows that the differences between the potentials of Peaks 1 and 3 and Peaks 2 and 3 increased with increasing sweep rate whereas the difference between $E_{p(c,1)}$ and $E_{p(c,2)}$ remained relatively constant, as was to be expected from the results of Fig. 5-179. Fig. 5-180 also shows that $|E_{p(c,2)} - E_{p(c,2)/2}|$ was relatively independent of the sweep rate.

The evidence suggests that Peak 1 was exhibited at a potential

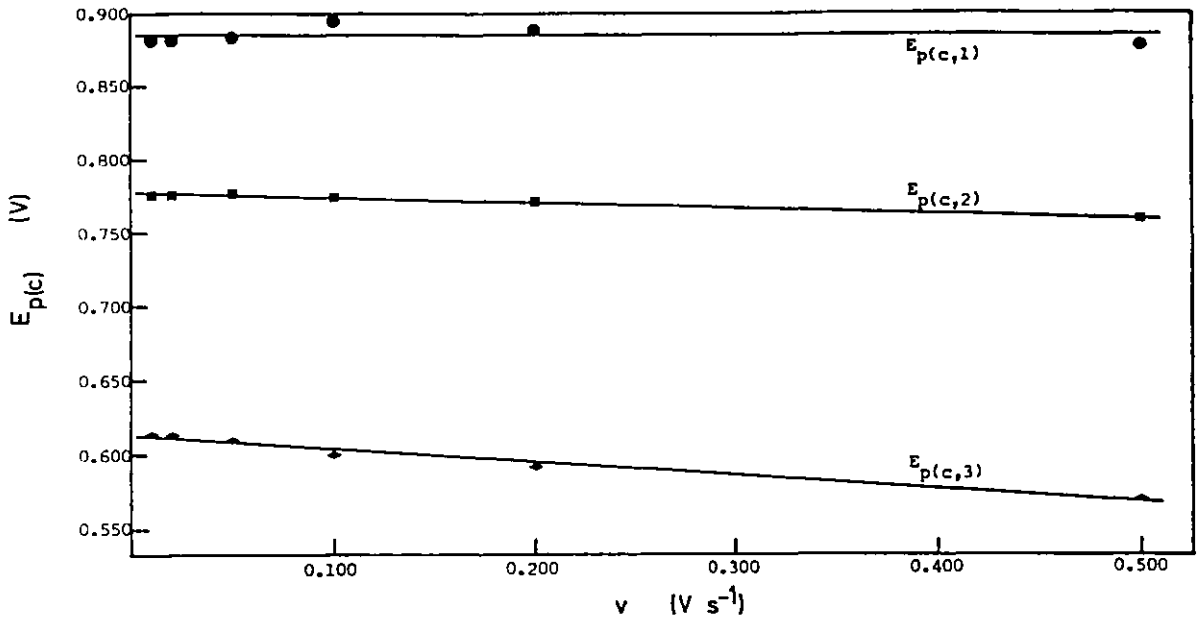

Fig. 5-175 Ir(IV) Perchlorate (1.0×10^{-4} mol dm^{-3})/Perchloric acid (0.1 M) supporting electrolyte System: Values of cathodic peak potential, $E_{p(c)}$, as a function of potential scan rate, v. Boron carbide/carbon composite solid electrode $B_{3.53}C$.

(a) $E_{p(c,1)}$ mean = 0.885 V
Standard deviation = 0.006 V
Degrees of freedom = 5

(b) $E_{p(c,2)} = 0.778 - 3.57 \times 10^{-2}$ v
Correlation coefficient = -0.9925
Level of significance, p = $p < 0.001$
Standard deviation of $E_{p(c,2)}$ from regression = 0.001 V
Degrees of freedom = 4

(c) $E_{p(c,3)} = 0.613 - 9.01 \times 10^{-2}$ v
Correlation coefficient = -0.9842
Level of significance, p = $p < 0.001$
Standard deviation of $E_{p(c,3)}$ from regression = 0.003 V
Degrees of freedom = 4

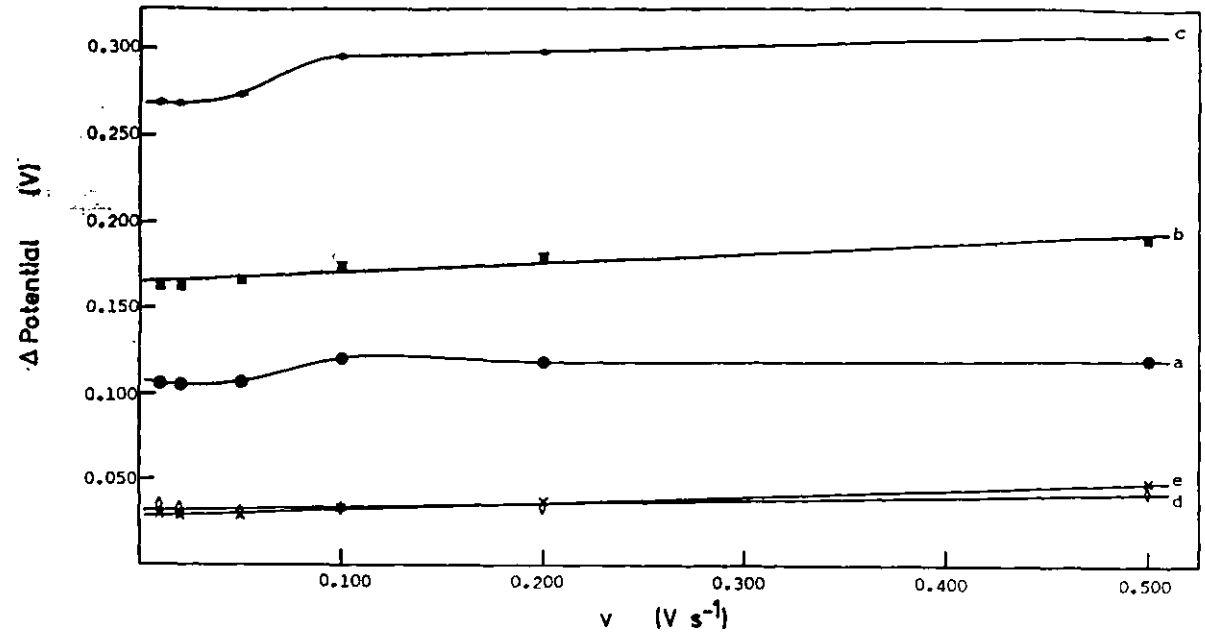

Fig. 5-176 Ir(IV) Perchlorate (1.0×10^{-4} mol dm^{-3})/Perchloric acid (0.1 M) supporting electrolyte System: Values of the difference between cathodic peak potentials, $\Delta E_{p(c)}$, and the absolute difference between cathodic peak and half-peak potential, $|E_{p(c)} - E_{p(c)/2}|$, as a function of potential scan rate, v. (a) $\Delta E_{p(c;\ 1,2)}$, (b) $\Delta E_{p(c;\ 2,3)}$, (c) $\Delta E_{p(c;\ 1,3)}$, (d) $|E_{p(c,2)} - E_{p(c,2)/2}|$, and (e) $|E_{p(c,3)} - E_{p(c,3)/2}|$. Boron carbide/carbon composite solid electrode $B_{3.53}C$.

(a) $\Delta E_{p(c;\ 1,2)}$ mean = 0.113 V
Standard deviation = 0.007 V
Degrees of freedom = 5

(b) $\Delta E_{p(c;\ 2,3)} = 0.165 + 5.44 \times 10^{-2}\ v$
Correlation coefficient = 0.9442
Level of significance, $p = 0.001 < p < 0.01$
Standard deviation of $\Delta E_{p(c;\ 2,3)}$ from regression = 0.004 V
Degrees of freedom = 4

(c) $\Delta E_{p(c;\ 1,3)}$ mean = 0.285 V
Standard deviation = 0.017 V
Degrees of freedom = 5

(d) $|E_{p(c,2)} - E_{p(c,2)/2}| = 3.20 \times 10^{-2} + 1.88 \times 10^{-2}\ v$
Correlation coefficient = 0.8826
Level of significance, $p = 0.01 < p < 0.02$
Standard deviation of $|E_{p(c,2)} - E_{p(c,2)/2}|$ from regression
= 0.002 V
Degrees of freedom = 4

(e) $|E_{p(c,3)} - E_{p(c,3)/2}| = 2.81 \times 10^{-2} + 4.04 \times 10^{-2}\ v$
Correlation coefficient = 0.9948
Level of significance, $p = p < 0.001$
Standard deviation of $|E_{p(c,3)} - E_{p(c,3)/2}|$ from regression
= 0.001 V
Degrees of freedom = 4

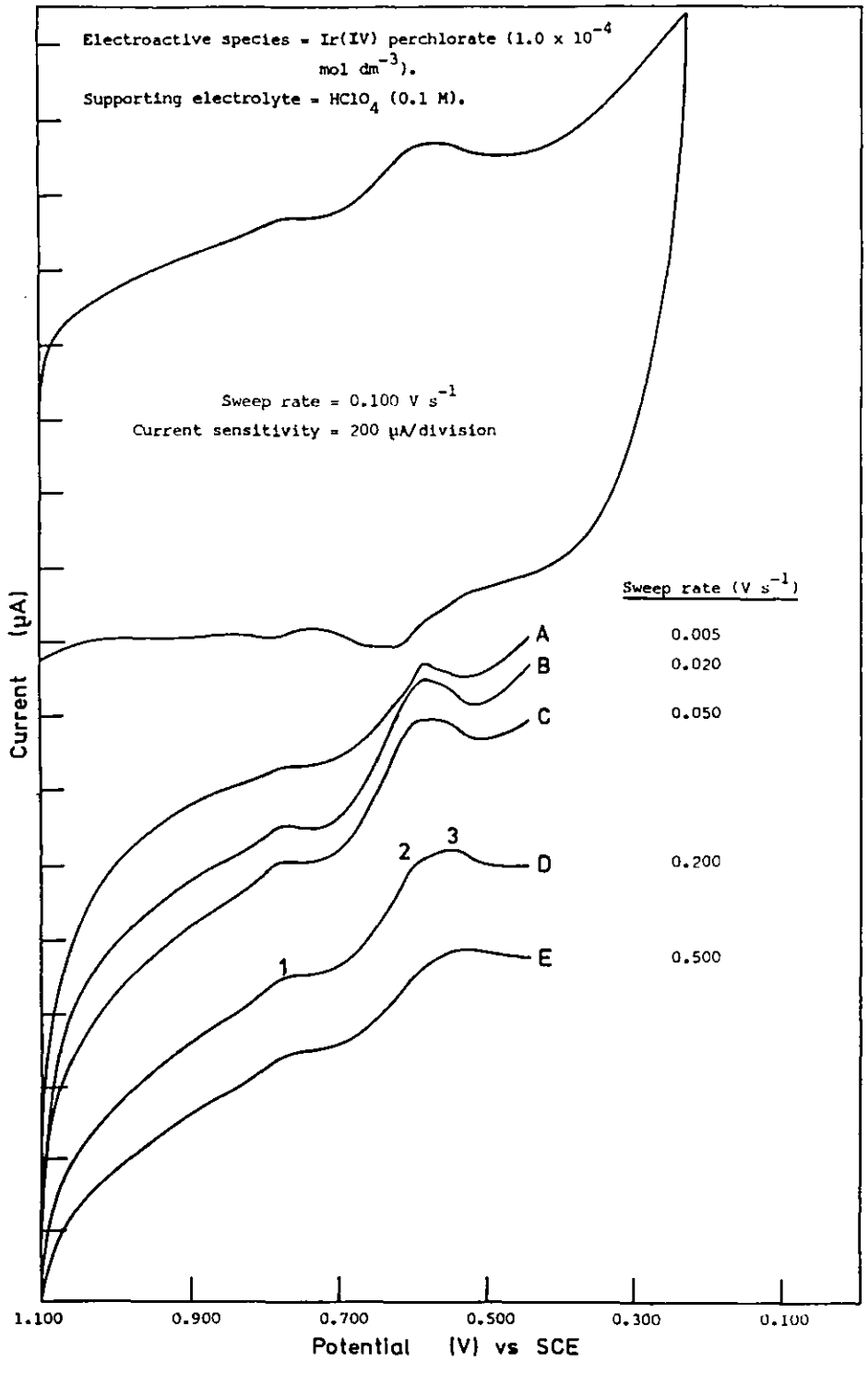

Fig. 5-177 Cyclic and linear sweep voltammograms obtained at the boron carbide/carbon composite solid electrode $B_{3.38}C$. Current sensitivity (µA/division): A) 10, B) 20, C) 50, D) 200, and E) 500.

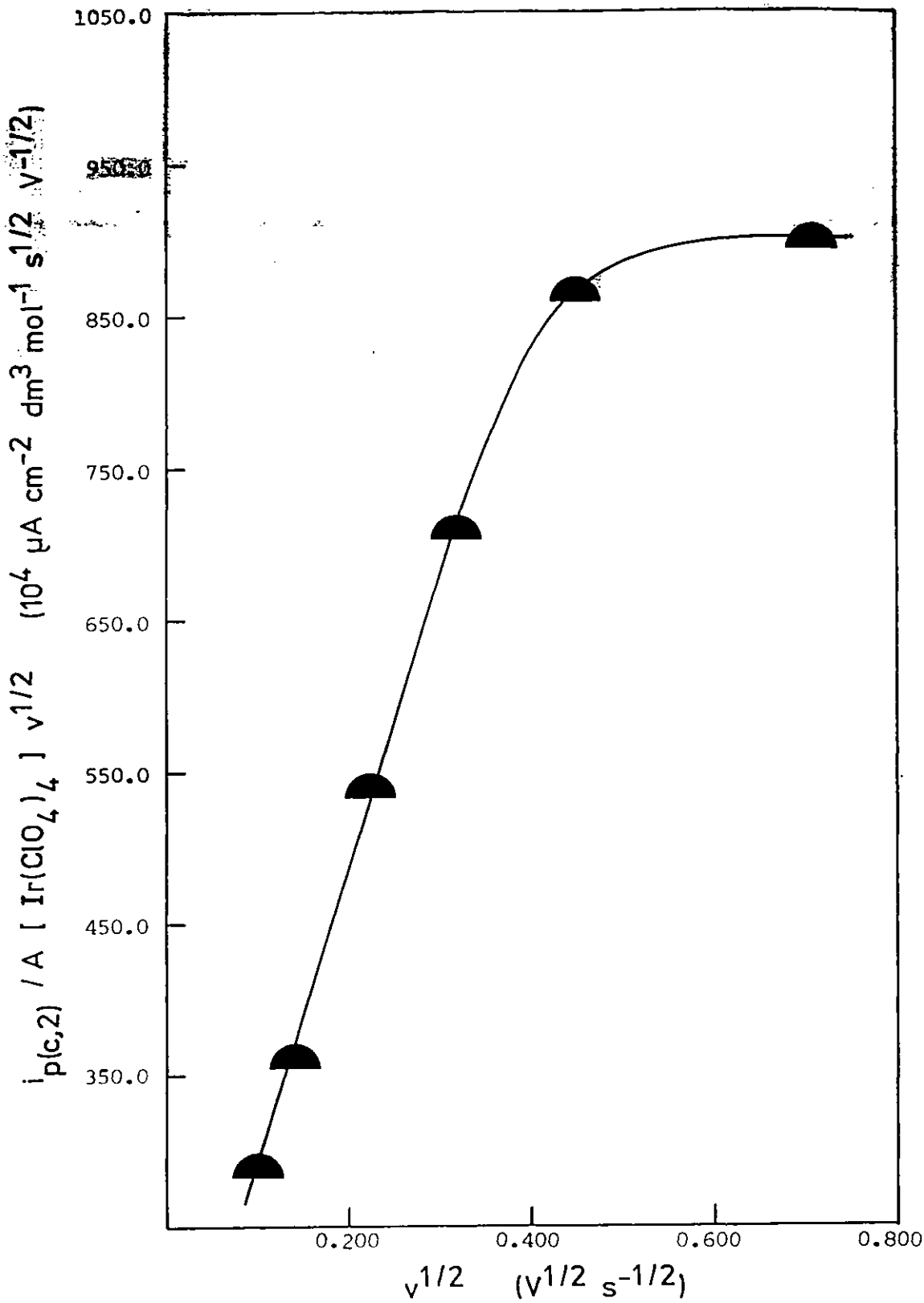

Fig. 5-178 Ir(IV) Perchlorate (1.0×10^{-4} mol dm^{-3})/Perchloric acid (0.1 M) supporting electrolyte System: Values of cathodic current function, $i_{p(c,2)}/A\ [\ Ir(ClO_4)_4\ ]\ v^{\frac{1}{2}}$, as a function of square root of potential scan rate, $v^{\frac{1}{2}}$. Boron carbide/carbon composite solid electrode $B_{3.38}C$.

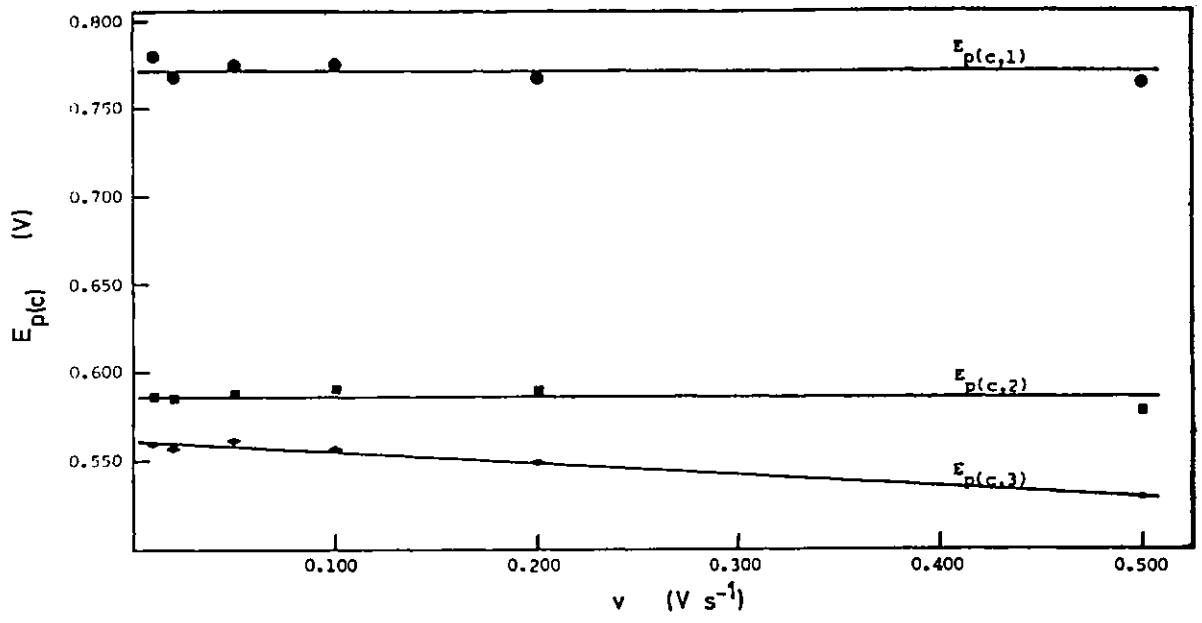

Fig. 5-179 Ir(IV) Perchlorate (1.0×10^{-4} mol dm^{-3})/Perchloric acid (0.1 M) supporting electrolyte System: Values of cathodic peak potential, $E_{p(c)}$, as a function of potential scan rate, v. Boron carbide/carbon composite solid electrode $B_{3.38}C$.

(a) $E_{p(c,1)}$ mean = 0.771 V
Standard deviation = 0.006 V
Degrees of freedom = 5

(b) $E_{p(c,2)}$ mean = 0.586 V
Standard deviation = 0.004 V
Degrees of freedom = 5

(c) $E_{p(c,3)} = 0.561 - 6.34 \times 10^{-2}$ v
Correlation coefficient = -0.9807
Level of significance, p = $p < 0.001$
Standard deviation of $E_{p(c,3)}$ from regression = 0.003 V
Degrees of freedom = 4

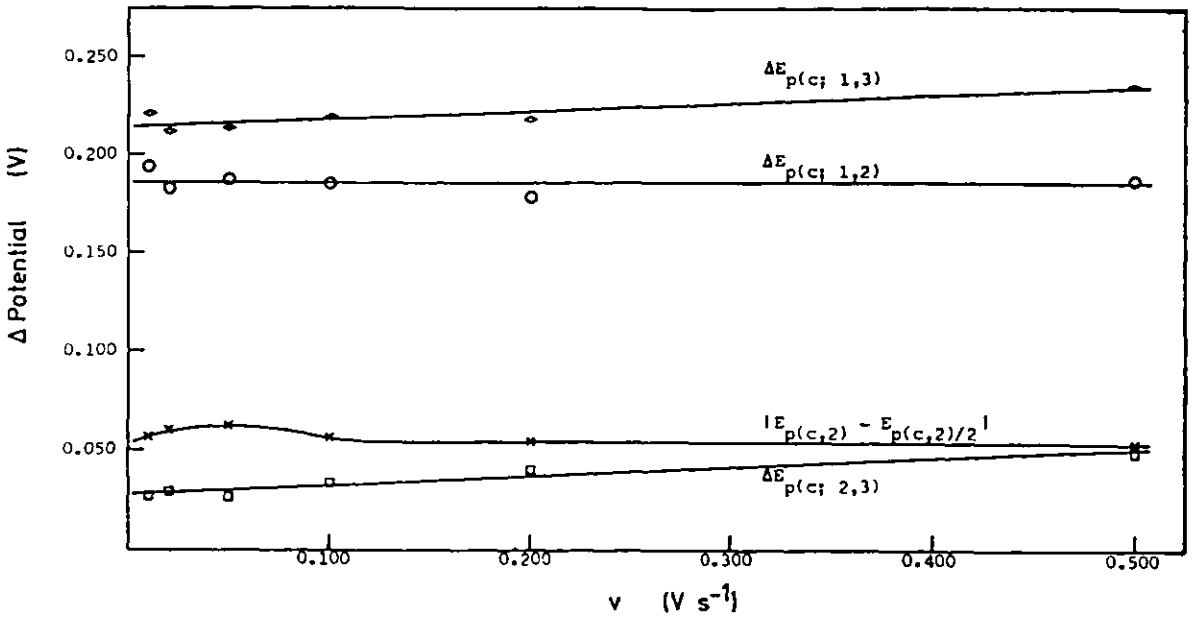

Fig. 5-180 Ir(IV) Perchlorate (1.0×10^{-4} mol dm^{-3})/Perchloric acid (0.1 M) supporting electrolyte System: Values of the difference between cathodic peak potentials, $\Delta E_{p(c)}$, and the absolute difference between cathodic peak and half-peak potential, $|E_{p(c)} - E_{p(c)/2}|$, as a function of potential scan rate, v. Boron carbide/carbon composite solid electrode $B_{3.38}C$.

(a) $\Delta E_{p(c;\ 1,2)}$ mean = 0.186 V
Standard deviation = 0.005 V
Degrees of freedom = 5

(b) $\Delta E_{p(c;\ 2,3)} = 2.75 \times 10^{-2} + 4.51 \times 10^{-2}$ v
Correlation coefficient = 0.9585
Level of significance, $p = 0.001 < p < 0.01$
Standard deviation of $\Delta E_{p(c;\ 2,3)}$ from regression = 0.003 V
Degrees of freedom = 4

(c) $\Delta E_{p(c;\ 1,3)} = 0.214 + 4.08 \times 10^{-2}$ v
Correlation coefficient = 0.8927
Level of significance, $p = 0.01 < p < 0.02$
Standard deviation of $\Delta E_{p(c;\ 1,3)}$ from regression = 0.004 V
Degrees of freedom = 4

(d) $|E_{p(c,2)} - E_{p(c,2)/2}|$ mean = 0.057 V
Standard deviation = 0.003 V
Degrees of freedom = 5

similar to the potential of the peak which has been associated with the strong adsorption of Ir(IV) perchlorate reactant at all the other electrodes investigated prior to this $B_{3.38}C$ electrode (e.g. Fig. 5-177 c.f. Fig. 5-172). Therefore, Peak 1 was probably due to the strong adsorption of Ir(IV) perchlorate reactant, Peak 2 was affected by the weak adsorption of product, and Peak 3 was due to moderately strong adsorption of reactant.

5-1.5.(ii).g Boron carbide/carbon composite solid electrode $B_{3.24}C$

Fig. 5-181 shows that the cyclic and linear sweep voltammograms for Ir(IV) perchlorate (1.0×10^{-4} mol dm^{-3}) in perchloric acid (0.1 M) supporting electrolyte exhibited three cathodic peaks, Peaks 1 to 3 inclusive; the anodic counterparts being also exhibited for the cyclic scan. Qualitatively, the charge transfers were reversible, as can be seen from the cyclic voltammogram, and also the linear sweep voltammograms show that the cathodic peaks were cathodically shifted by the increasing sweep rate; probably a symptom of the adsorption of reactant. Quantitative studies of the interpretable peaks reveal the influence of adsorption on Peaks 2 and 3 (Fig. 5-182), with Peak 2 being more affected (Fig. 5-183).

The cathodic peak potentials were cathodically shifted by the increasing sweep rate in the order $E_{p(c,3)} > E_{p(c,1)} > E_{p(c,2)}$ (Fig. 5-184). Fig. 5-185 shows that, although the difference between Peaks 1 and 2 was quite steady, the differences between Peaks 1 and 3, and Peaks 2 and 3 widened with increasing sweep rate. Furthermore, $|E_{p(c,2)} - E_{p(c,2)/2}|$ was constant but $|E_{p(c,3)} - E_{p(c,3)/2}|$ increased with increasing sweep rate.

The evidence suggests that Peaks 1 and 3 were influenced by the weak adsorption of reactant whereas Peak 2 was a post-peak due to the extremely strong adsorption of Ir(IV) perchlorate reactant.

5-1.5.(ii).h Boron carbide/carbon composite solid electrode $B_{3.11}C$

Linear sweep voltammograms for Ir(IV) perchlorate (1.0×10^{-4} mol dm^{-3}) in a concentration range of perchloric acid supporting electrolyte obtained at the boron carbide/carbon composite solid electrode $B_{3.11}C$ are presented in Fig. 5-186. Qualitatively, it can be seen that Peak 4 was defined at higher perchloric acid concentrations and its definition continued to improve with increasing perchloric acid concentration.

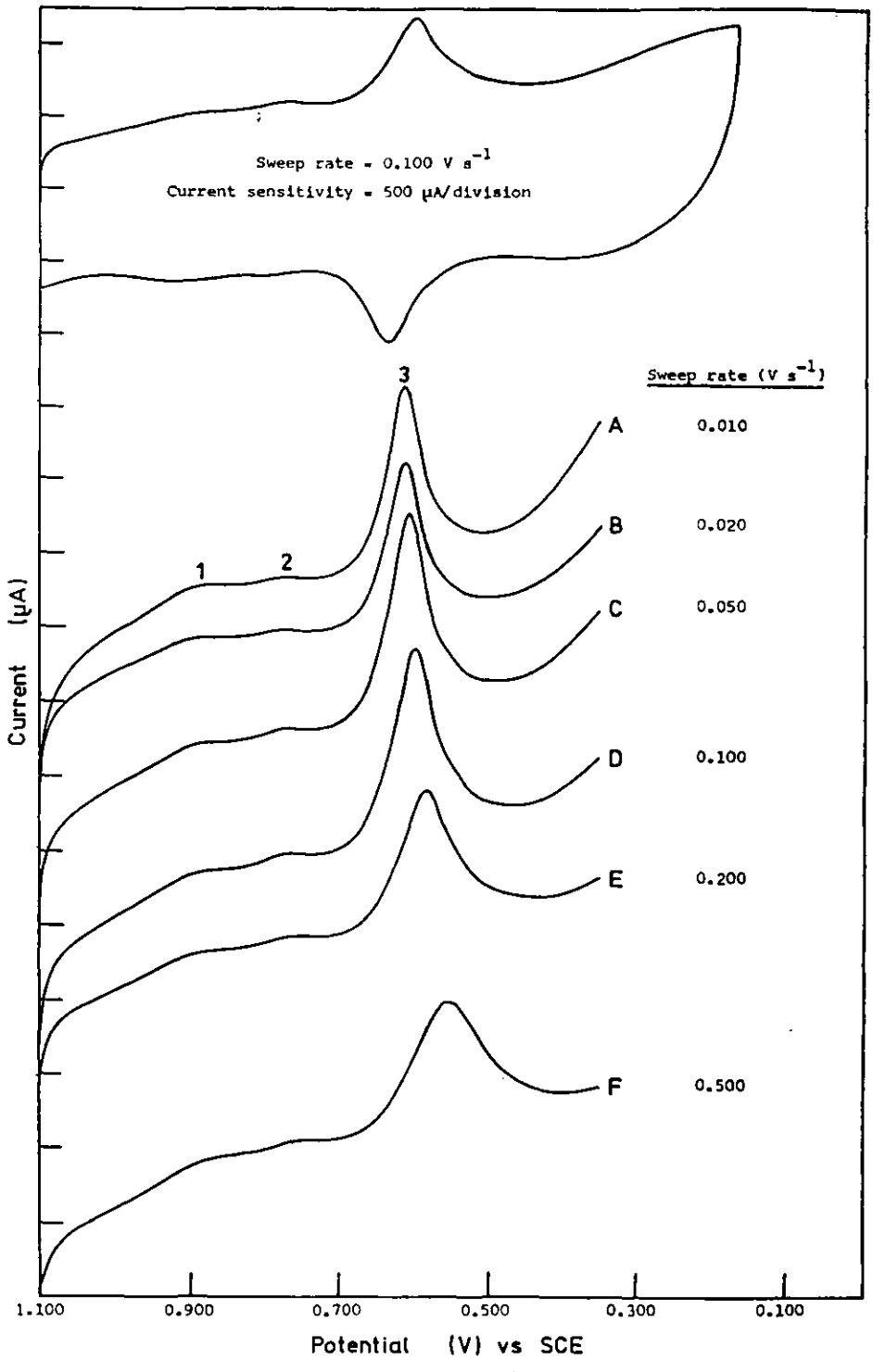

Fig. 5-181 Ir(IV) perchlorate (1.0×10^{-4} mol dm^{-3})/Perchloric acid (0.1 M) supporting electrolyte System: Cyclic and Linear sweep voltammograms obtained at the boron carbide/carbon composite solid electrode $B_{3.24}C$. Current sensitivity (μA/division): A) 20, B) 50, C) 100, D) 200, E) 500, and F) 1000.

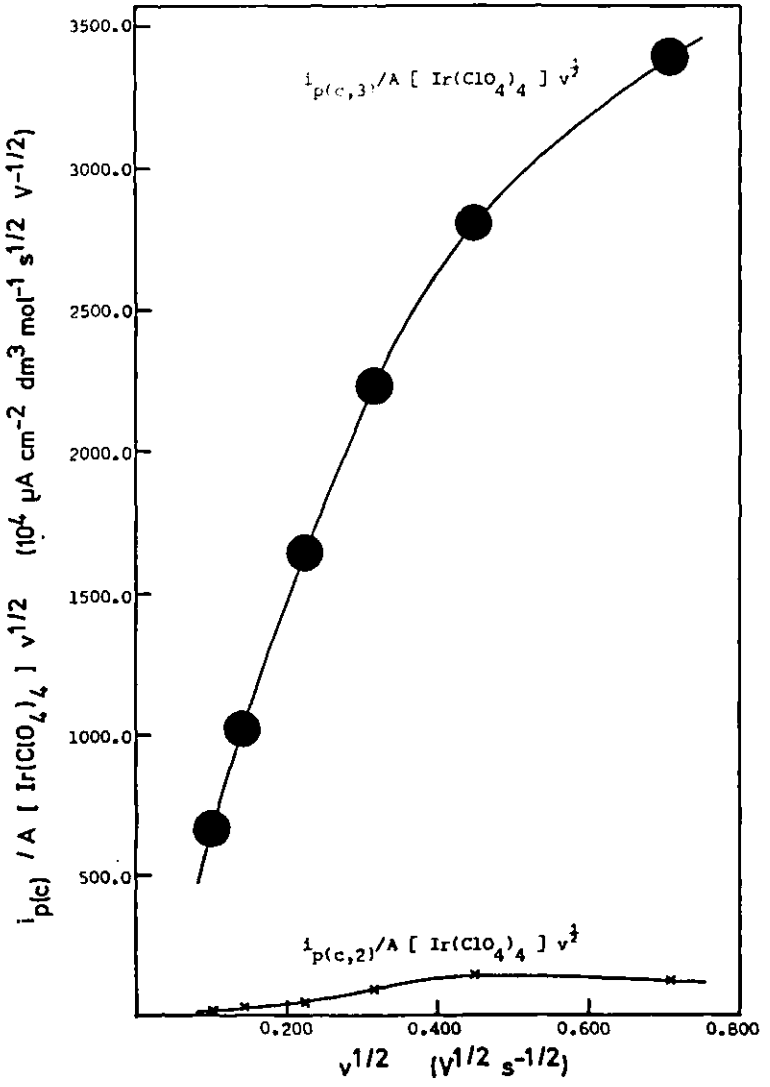

Fig. 5-182 Ir(IV) Perchlorate (1.0×10^{-4} mol dm^{-3})/Perchloric acid (0.1 M) supporting electrolyte System: Values of cathodic current function, $i_{p(c)}/A\ [\ Ir(ClO_4)_4\ ]\ v^{\frac{1}{2}}$, as a function of square root of potential scan rate, $v^{\frac{1}{2}}$. Boron carbide/carbon composite solid electrode $B_{3.24}C$.

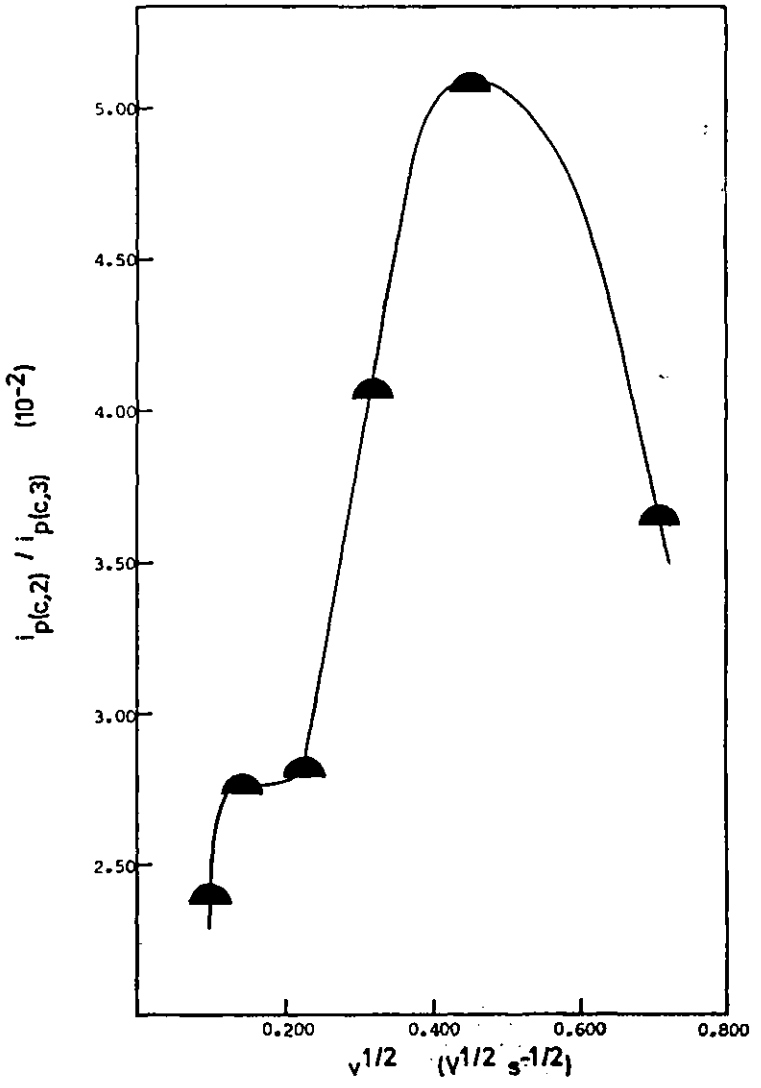

Fig. 5-183 Ir(IV) Perchlorate (1.0×10^{-4} mol dm^{-3})/Perchloric acid (0.1 M) supporting electrolyte System: Values of the ratio of cathodic peak currents, $i_{p(c,2)}/i_{p(c,3)}$, as a function of square root of potential scan rate, $v^{\frac{1}{2}}$. Boron carbide/carbon composite solid electrode $B_{3.24}C$.

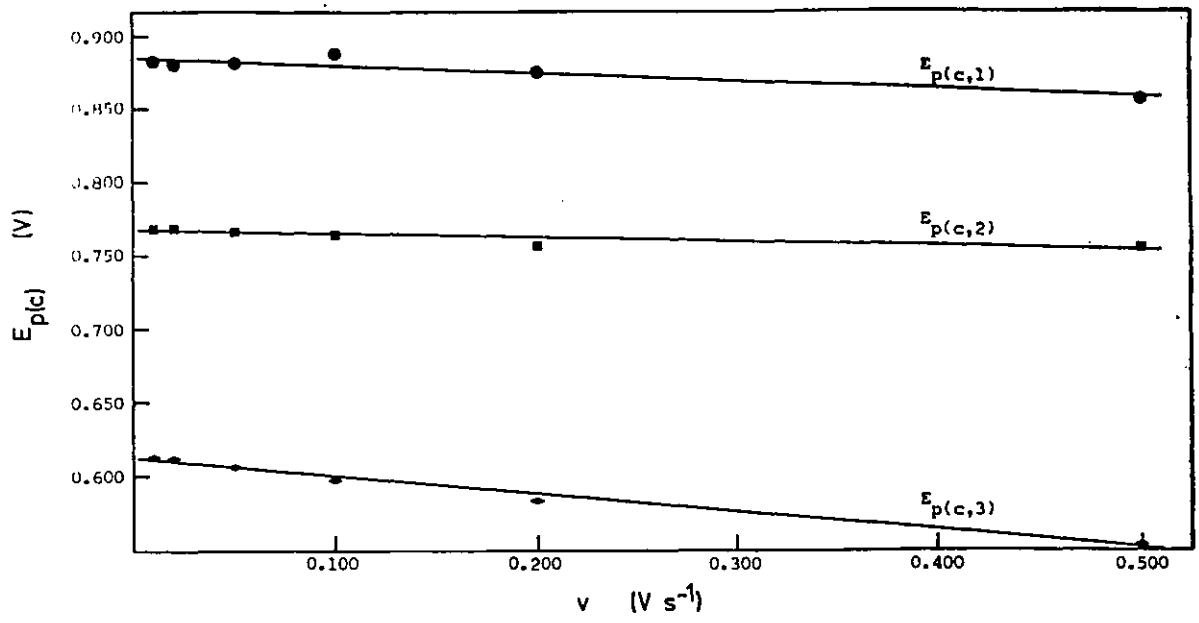

Fig. 5-184 Ir(IV) Perchlorate (1.0×10^{-4} mol dm^{-3})/Perchloric acid (0.1 M) supporting electrolyte System: Values of cathodic peak potential, $E_{p(c)}$, as a function of potential scan rate, v. Boron carbide/carbon composite solid electrode $B_{3.24}C$.

(a) $E_{p(c,1)} = 0.884 - 5.21 \times 10^{-2}$ v
Correlation coefficient = -0.8945
Level of significance, $p = 0.01 < p < 0.02$
Standard deviation of $E_{p(c,1)}$ from regression = 0.005 V
Degrees of freedom = 4

(b) $E_{p(c,2)} = 0.768 - 2.88 \times 10^{-2}$ v
Correlation coefficient = -0.8740
Level of significance, $p = 0.02 < p < 0.05$
Standard deviation of $E_{p(c,2)}$ from regression = 0.003 V
Degrees of freedom = 4

(c) $E_{p(c,3)} = 0.612 - 0.121$ v
Correlation coefficient = -0.9908
Level of significance, $p = p < 0.001$
Standard deviation of $E_{p(c,3)}$ from regression = 0.003 V
Degrees of freedom = 4

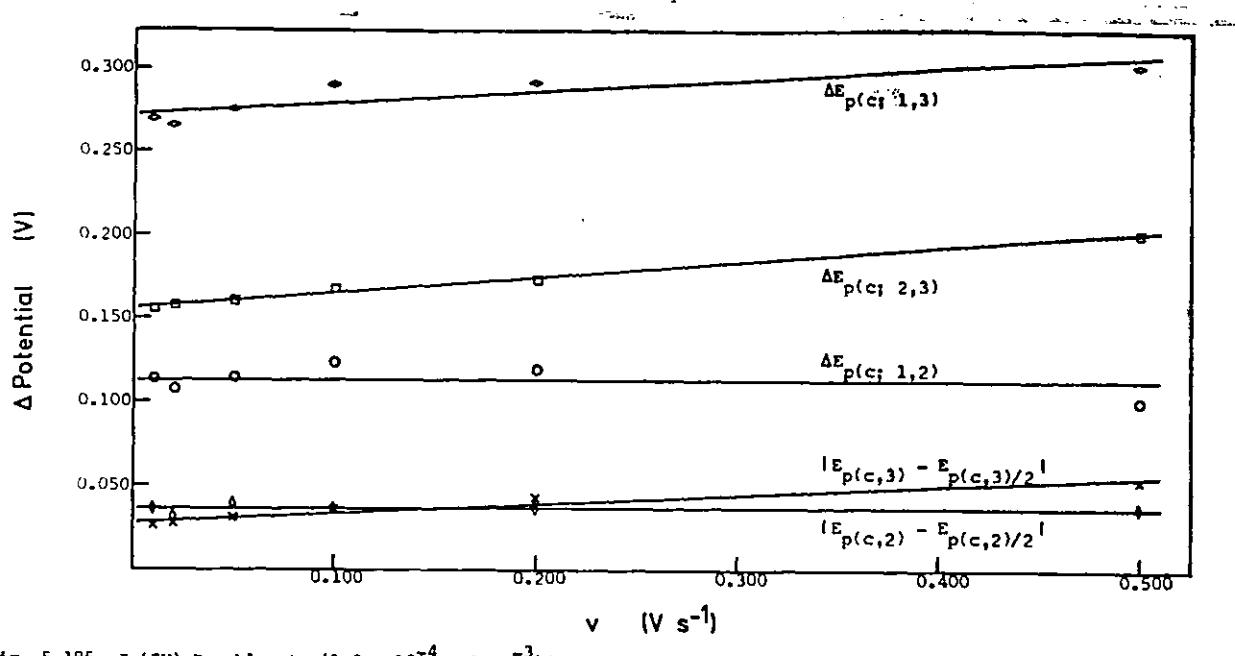

Fig. 5-185 Ir(IV) Perchlorate (1.0×10^{-4} mol dm^{-3})/Perchloric acid (0.1 M) supporting electrolyte System: Values of the difference between cathodic peak potentials, $\Delta E_{p(c)}$, and the absolute difference between cathodic peak and half-peak potential, $|E_{p(c)} - E_{p(c)/2}|$, as a function of potential scan rate, v. Boron carbide/carbon composite solid electrode $B_{3.24}C$.

(a) $\Delta E_{p(c;\ 1,2)}$ mean = 0.113 V
Standard deviation = 0.008 V
Degrees of freedom = 5

(b) $\Delta E_{p(c;\ 2,3)} = 0.156 + 9.18 \times 10^{-2}$ v
Correlation coefficient = 0.9972
Level of significance, p = $p < 0.001$
Standard deviation of $\Delta E_{p(c;\ 2,3)}$ from regression = 0.001 V
Degrees of freedom = 4

(c) $\Delta E_{p(c;\ 1,3)} = 0.272 + 6.85 \times 10^{-2}$ v
Correlation coefficient = 0.8666
Level of significance, p = $0.02 < p < 0.05$
Standard deviation of $\Delta E_{p(c;\ 1,3)}$ from regression = 0.008 V
Degrees of freedom = 4

(d) $|E_{p(c,2)} - E_{p(c,2)/2}|$ mean = 0.036 V
Standard deviation = 0.002 V
Degrees of freedom = 5

(e) $|E_{p(c,3)} - E_{p(c,3)/2}| = 2.81 \times 10^{-2} + 5.36 \times 10^{-2}$ v
Correlation coefficient = 0.9716
Level of significance, p = $0.001 < p < 0.01$
Standard deviation of $|E_{p(c,3)} - E_{p(c,3)/2}|$ from regression
= 0.003 V
Degrees of freedom = 4

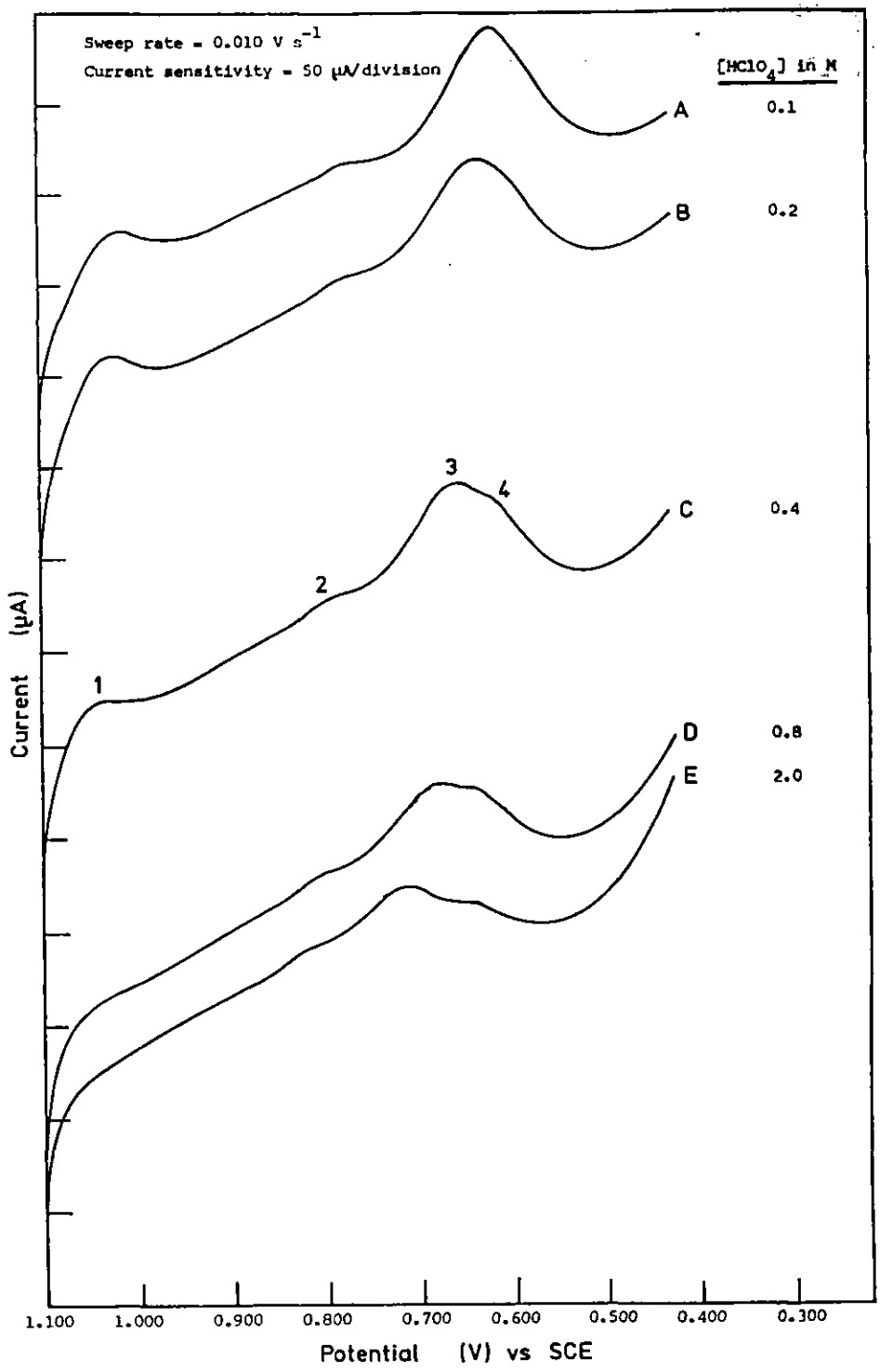

Fig. 5-186 Ir(IV) perchlorate (1.0×10^{-4} mol dm^{-3})/Perchloric acid (0.1 to 2.0 M) supporting electrolyte System: Linear sweep voltammograms obtained at the boron carbide/carbon composite solid electrode $B_{3.11}C$.

The definition of Peak 1, however, deteriorated with increasing perchloric acid concentration; resulting in its disappearance at high concentrations. All the peaks were shifted anodically by the increasing ionic strength. Quantitative treatment of the interpretable peaks shows that Peak 2 (Fig. 5-187) and Peak 3 (Fig. 5-188) were influenced by adsorption which was debilitated by the increasing perchloric acid concentration. The adsorption at Peak 2 was stronger than at Peak 3; as is evident from the effect of sweep rate on the peak current ratio $i_{p(c,2)}/i_{p(c,3)}$ in Fig. 5-189.

Fig. 5-190 shows that the peak potential of Peak 1, $E_{p(c,1)}$, was shifted to less anodic potentials by increasing sweep rate, v, when exhibited. The rapid disappearance of Peak 1 with increasing sweep rate indicates that the related charge transfer was quasi-reversible. $E_{p(c,2)}$, however, remained relatively constant although Peak 2 was not defined at high sweep rates; a symptom of poor reversibility in the charge transfer reaction. $E_{p(c,3)}$ was cathodically shifted with increasing sweep rate, and similarly for $E_{p(c,4)}$ although the increasing prominence of Peak 4 with increasing sweep rate eventually caused Peaks 3 and 4 to merge. The behaviour of cathodic $|E_p - E_{p/2}|$ with increasing sweep rate (Fig. 5-191) suggests that Peak 2 was influenced by adsorption whilst Peak 3 became less reversible at faster sweep rates.

The effect of perchloric acid supporting electrolyte on Peaks 2 and 3 (Figures 5-192 and 5-193 respectively) suggests that, despite the presence of a catalytic reaction involving perchloric acid, the overriding factor was the debilitating influence of increasing perchloric acid concentration on the adsorption effects. The anodic shifts of all the peak potentials with increasing $(\text{ionic strength})^{\frac{1}{2}}$ are plotted in Fig. 5-194. Fig. 5-195 indicates that, in general, $|E_p - E_{p/2}|$ values for Peaks 2 and 3 narrowed as the ionic strength increased.

The evidence suggests that Peak 1 was associated with a quasi-reversible charge transfer, Peak 2 was due to the strong adsorption of reactant coupled with a weak catalytic reaction involving perchloric acid, Peak 3 was a quasi-reversible charge transfer complicated by weak adsorption and weak catalytic effects, and Peak 4 was due to the moderately strong adsorption of reactant which was revealed at higher ionic strengths because Peak 3 was anodically shifted at a greater rate than Peak 4 by the increasing ionic strength.

The anodic shift in peak potentials with increasing ionic strength, as the perchloric acid concentration was increased, despite the cationic

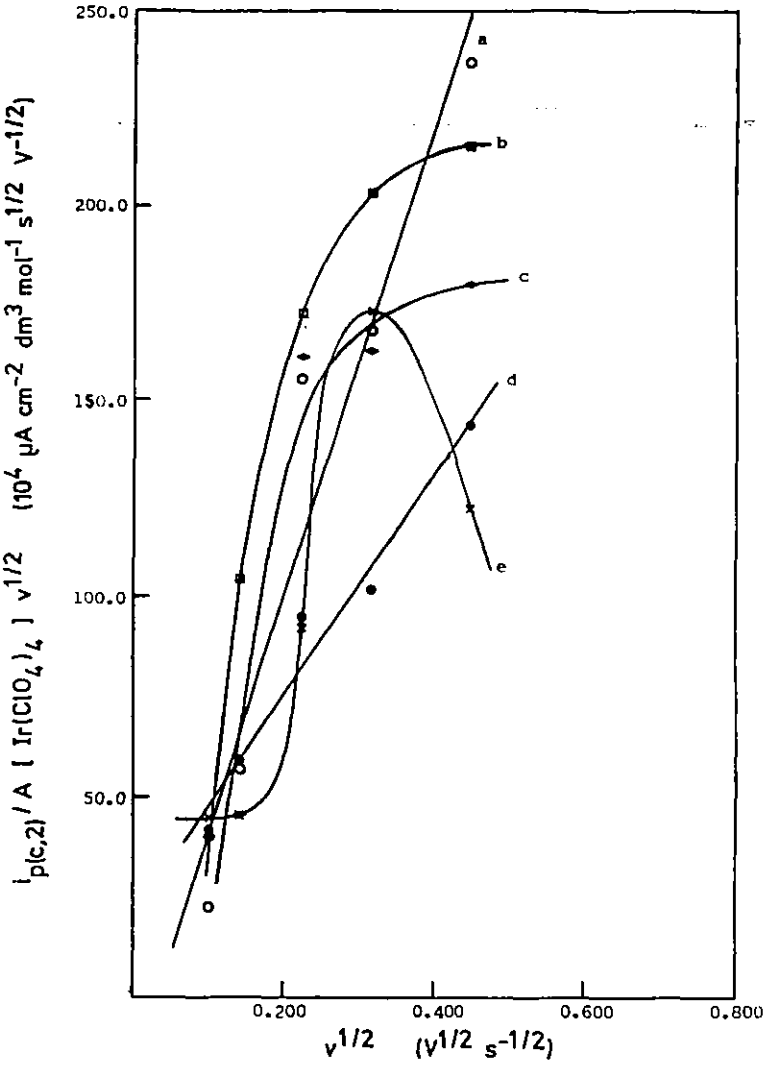

Fig. 5-187 Ir(IV) Perchlorate (1.0×10^{-4} mol dm^{-3})/Perchloric acid supporting electrolyte System: Values of cathodic current function, $i_{p(c,2)}/A\ [\ Ir(ClO_4)_4\ ]\ v^{\frac{1}{2}}$, as a function of square root of potential scan rate, $v^{\frac{1}{2}}$; at perchloric acid concentrations (a) 0.1, (b) 0.2, (c) 0.4, (d) 0.8, and (e) 2.0 M. Boron carbide/carbon composite solid electrode $B_{3.11}C$.

(a) $i_{p(c,2)}/A\ [\ Ir(ClO_4)_4\ ]\ v^{\frac{1}{2}} = 6.00 \times 10^6\ v^{\frac{1}{2}} - 1.98 \times 10^5$
Correlation coefficient = 0.9635
Level of significance, $p = 0.001 < p < 0.01$
Standard deviation of $i_{p(c,2)}/A\ [\ Ir(ClO_4)_4\ ]\ v^{\frac{1}{2}}$ from regression = 2.69×10^5 μA cm^{-2} dm^3 mol^{-1} s$^{\frac{1}{2}}$ V$^{-\frac{1}{2}}$
Degrees of freedom = 3

(d) $i_{p(c,2)}/A\ [\ Ir(ClO_4)_4\ ]\ v^{\frac{1}{2}} = 1.97 \times 10^5 + 2.78 \times 10^6\ v^{\frac{1}{2}}$
Correlation coefficient = 0.9810
Level of significance, $p = 0.001 < p < 0.01$
Standard deviation of $i_{p(c,2)}/A\ [\ Ir(ClO_4)_4\ ]\ v^{\frac{1}{2}}$ from regression = 8.88×10^4 μA cm^{-2} dm^3 mol^{-1} s$^{\frac{1}{2}}$ V$^{-\frac{1}{2}}$
Degrees of freedom = 3

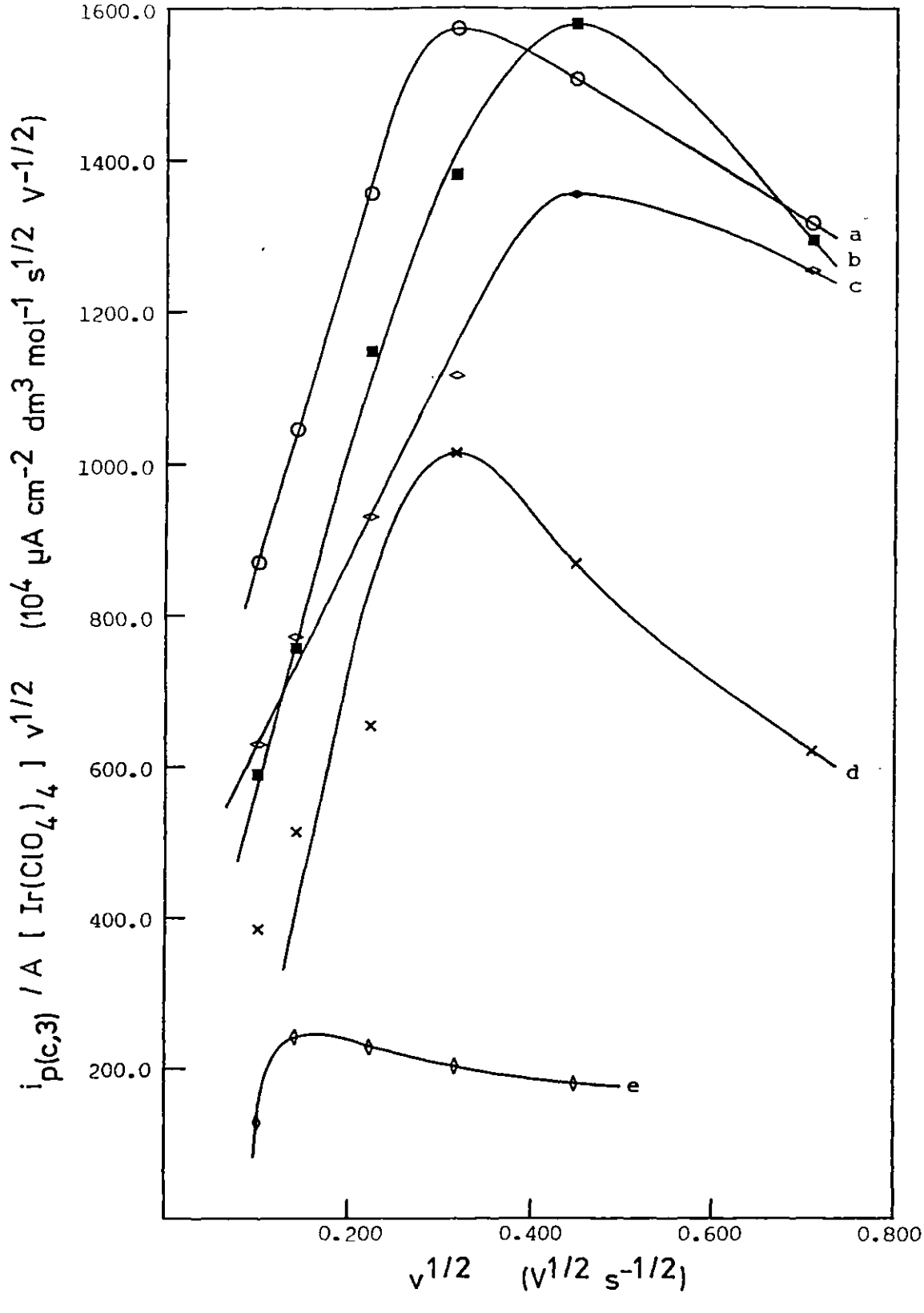

Fig. 5-188 Ir(IV) Perchlorate (1.0×10^{-4} mol dm^{-3})/Perchloric acid supporting electrolyte System: Values of cathodic current function, $i_{p(c,3)}/A\ [\ Ir(ClO_4)_4\ ]\ v^{\frac{1}{2}}$, as a function of square root of potential scan rate, $v^{\frac{1}{2}}$; at perchloric acid concentrations (a) 0.1, (b) 0.2, (c) 0.4, (c) 0.8, and (e) 2.0 M. Boron carbide/carbon composite solid electrode $B_{3.11}C$.

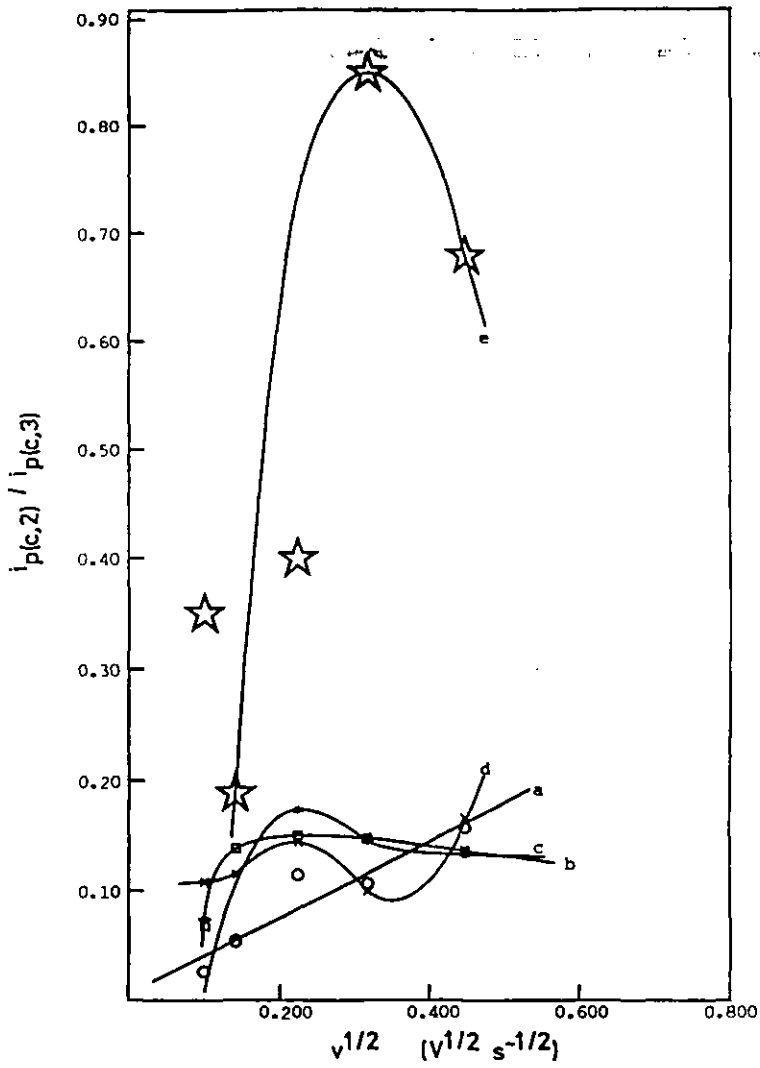

Fig. 5-189 Ir(IV) Perchlorate (1.0×10^{-4} mol dm^{-3})/Perchloric acid supporting electrolyte System: Values of the ratio of cathodic peak currents, $i_{p(c,2)}/i_{p(c,3)}$, as a function of square root of potential scan rate, $v^{\frac{1}{2}}$; at perchloric acid concentrations (a) 0.1, (b) 0.2, (c) 0.4, (d) 0.8, and (e) 2.0 M. Boron carbide/carbon composite solid electrode $B_{3.11}C$.

(a) $i_{p(c,2)}/i_{p(c,3)} = 5.95 \times 10^{-3} + 0.348\ v^{\frac{1}{2}}$

Correlation coefficient = 0.9397

Level of significance, $p = 0.01 < p < 0.02$

Standard deviation of $i_{p(c,2)}/i_{p(c,3)}$ from regression $= 2.05 \times 10^{-2}$

Degrees of freedom = 3

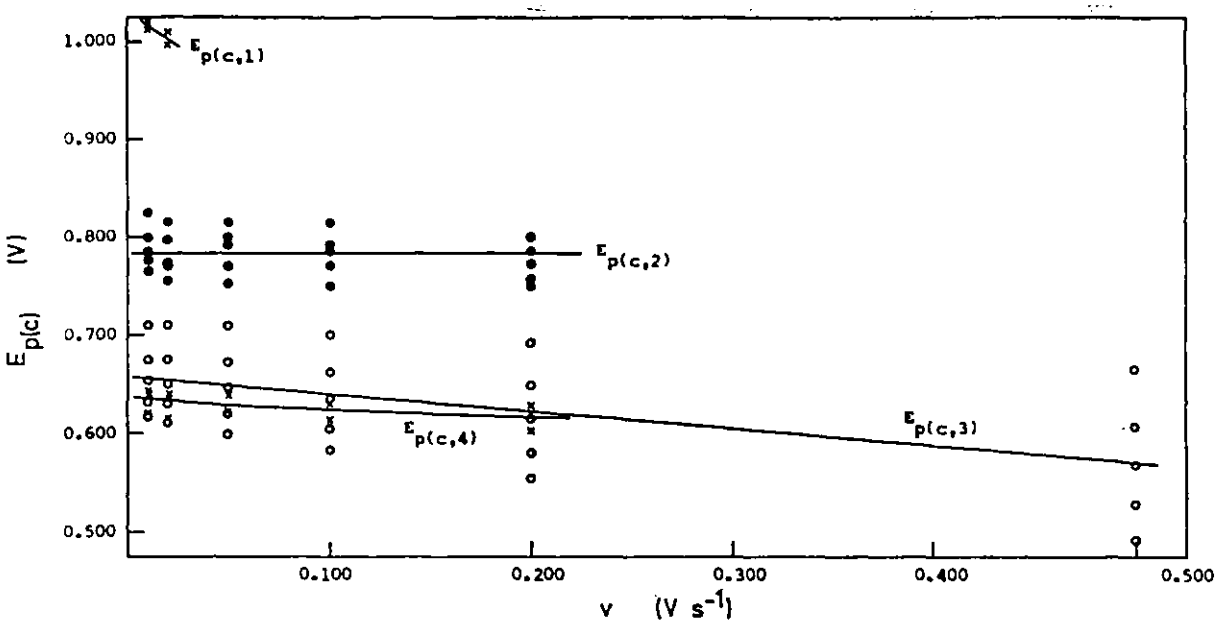

Fig. 5-190 Ir(IV) Perchlorate (1.0×10^{-4} mol dm^{-3})/Perchloric acid supporting electrolyte System: Values of cathodic peak potential, $E_{p(c)}$, as a function of potential scan rate, v; at perchloric acid concentrations of 0.1 to 2.0 M. Boron carbide/carbon composite solid electrode $B_{3.11}C$.

(a) $E_{p(c,1)}$ mean = 1.010 V
Standard deviation = 0.010 V
Coefficient of variation = 1.01%
Degrees of freedom = 3

(b) $E_{p(c,2)}$ mean = 0.783 V
Standard deviation = 0.022 V
Coefficient of variation = 2.83%
Degrees of freedom = 24

(c) $E_{p(c,3)} = 0.657 - 0.176\ v$
Correlation coefficient = -0.5610
Level of significance, $p = 0.001 < p < 0.01$
Standard deviation of $E_{p(c,3)}$ from regression = 0.046 V
Degrees of freedom = 28

(d) $E_{p(c,4)}$ mean = 0.627 V
Standard deviation = 0.013 V
Coefficient of variation = 2.04%
Degrees of freedom = 11

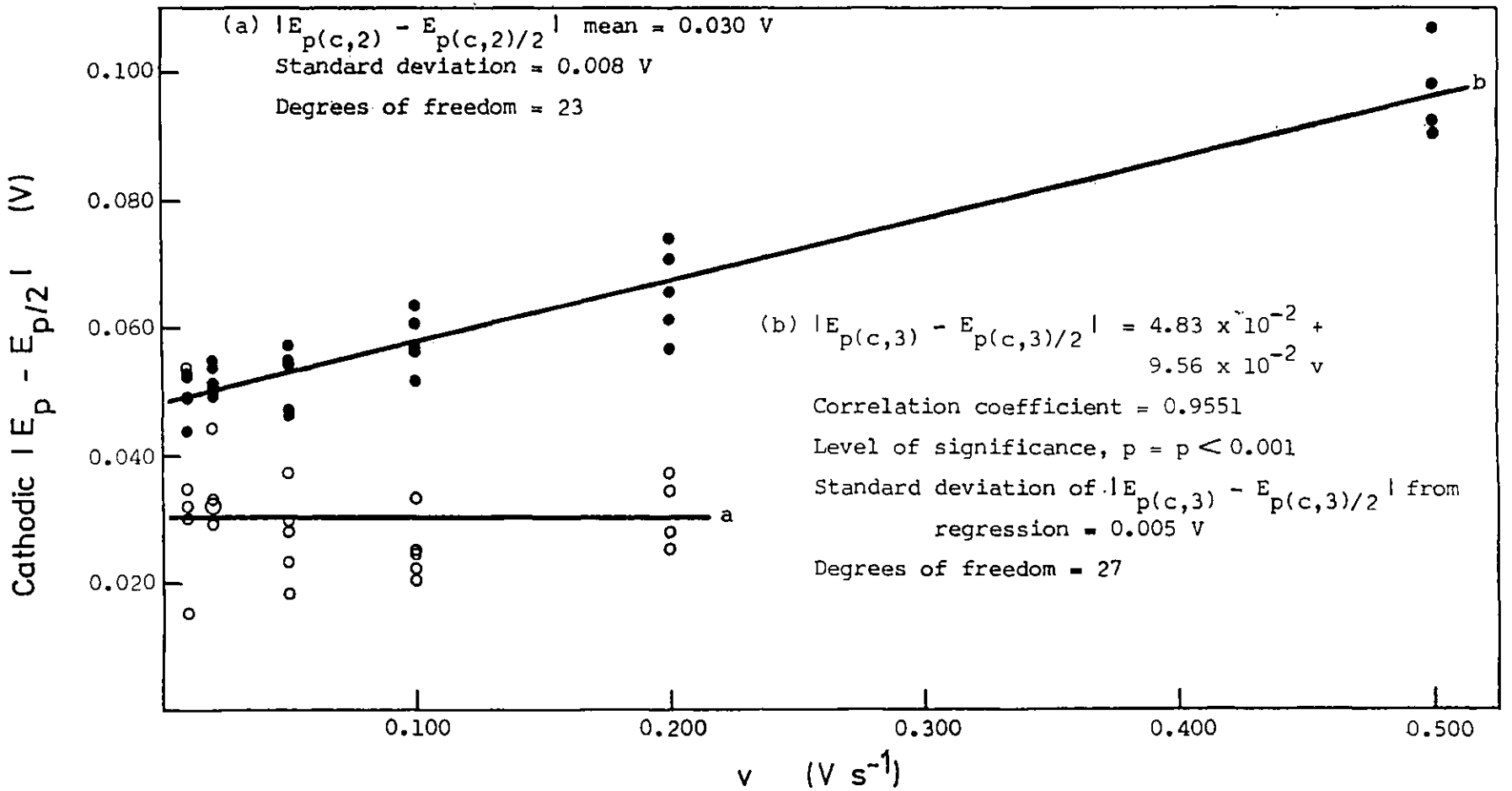

Fig. 5-191 Ir(IV) Perchlorate (1.0×10^{-4} mol dm^{-3})/Perchloric acid supporting electrolyte System: Values of the absolute difference between cathodic peak and half-peak potential, $|E_{p(c)} - E_{p(c)/2}|$, as a function of potential scan rate, v; at perchloric acid concentrations of 0.1 to 2.0 M. Boron carbide/carbon composite solid electrode $B_{3.11}C$.

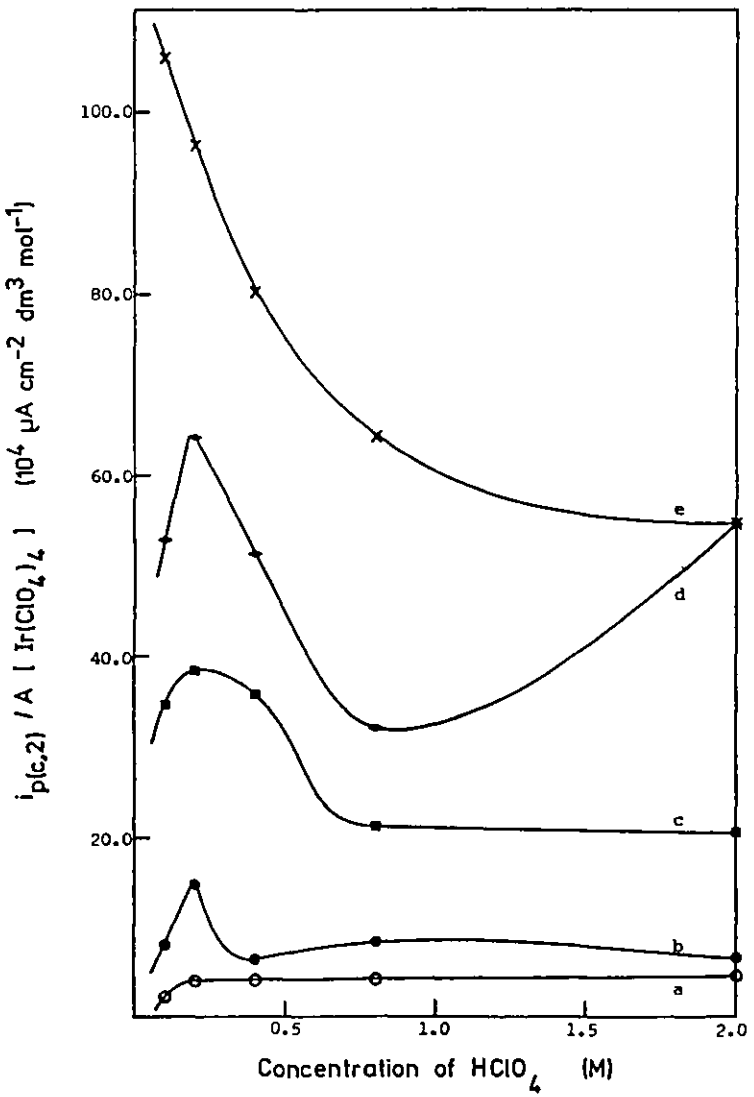

Fig. 5-192 Ir(IV) Perchlorate (1.0×10^{-4} mol dm^{-3})/Perchloric acid supporting electrolyte System: Values of cathodic peak current per unit area divided by concentration of Ir(IV) Perchlorate, $i_{p(c,2)}/A$ [$Ir(ClO_4)_4$], as a function of concentration of perchloric acid; at potential scan rates (a) 0.010, (b) 0.020, (c) 0.050, (d) 0.100, and (e) 0.200 $V\,s^{-1}$. Boron carbide/carbon composite solid electrode $B_{3.11}C$.

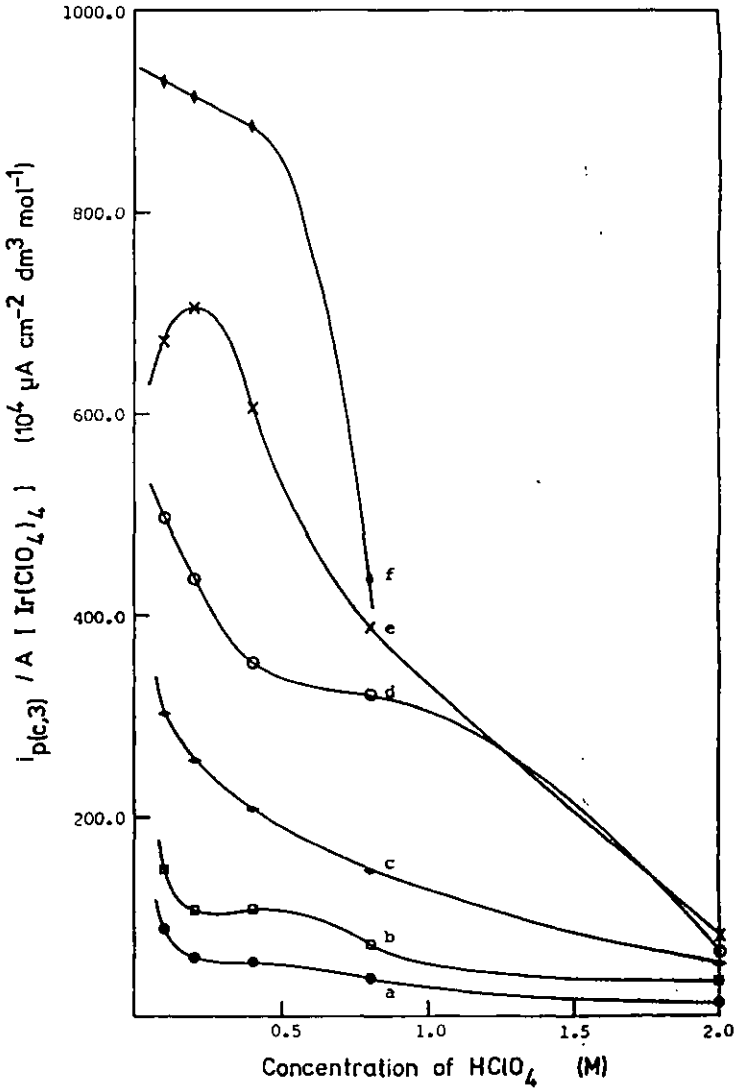

Fig. 5-193 Ir(IV) Perchlorate (1.0×10^{-4} mol dm^{-3})/Perchloric acid supporting electrolyte System: Values of cathodic peak current per unit area divided by concentration of Ir(IV) Perchlorate, $i_{p(c,3)}/A$ [$Ir(ClO_4)_4$], as a function of concentration of perchloric acid; at potential scan rates (a) 0.010, (b) 0.020, (c) 0.050, (d) 0.100, (e) 0.200, and (f) 0.500 $V\,s^{-1}$. Boron carbide/carbon composite solid electrode $B_{3.11}C$.

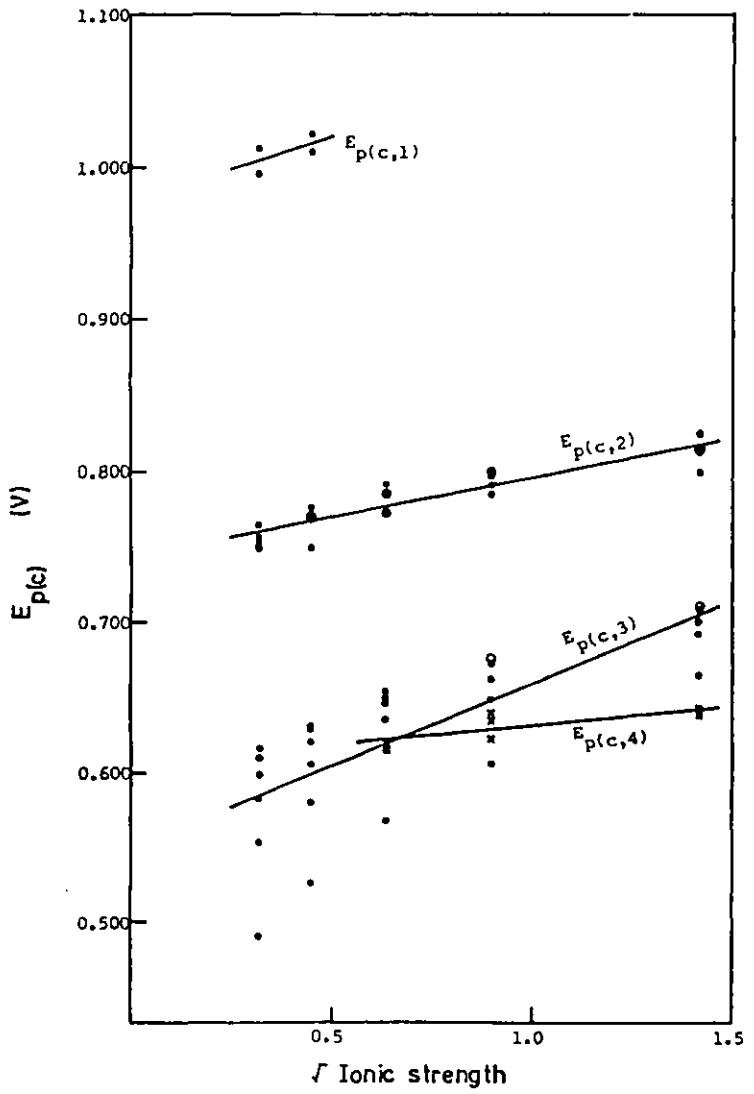

Fig. 5-194 Ir(IV) Perchlorate (1.0×10^{-4} mol dm^{-3})/Perchloric acid (0.1 to 2.0 M) supporting electrolyte System: Values of cathodic peak potential, $E_{p(c)}$, as a function of square root of total ionic strength, $\sqrt{I}$ (where the concentration of perchloric acid was varied); at potential scan rates of 0.010 to 0.500 V s^{-1}. Boron carbide/carbon composite solid electrode $B_{3.11}C$.

(a) $E_{p(c,1)}$ mean = 1.010 V
Standard deviation = 0.010 V
Coefficient of variation = 1.01%
Degrees of freedom = 3

(b) $E_{p(c,2)} = 0.744 + 5.18 \times 10^{-2} \sqrt{I}$
Correlation coefficient = 0.9260
Level of significance, p = $p < 0.001$
Standard deviation of $E_{p(c,2)}$ from regression = 0.009 V
Degrees of freedom = 23

(c) $E_{p(c,3)} = 0.550 + 0.109 \sqrt{I}$
Correlation coefficient = 0.7941
Level of significance, p = $p < 0.001$
Standard deviation of $E_{p(c,3)}$ from regression = 0.034 V
Degrees of freedom = 28

(d) $E_{p(c,4)} = 0.605 + 2.65 \times 10^{-2} \sqrt{I}$
Correlation coefficient = 0.8282
Level of significance, p = $0.01 < p < 0.02$
Standard deviation of $E_{p(c,4)}$ from regression = 0.007 V
Degrees of freedom = 6

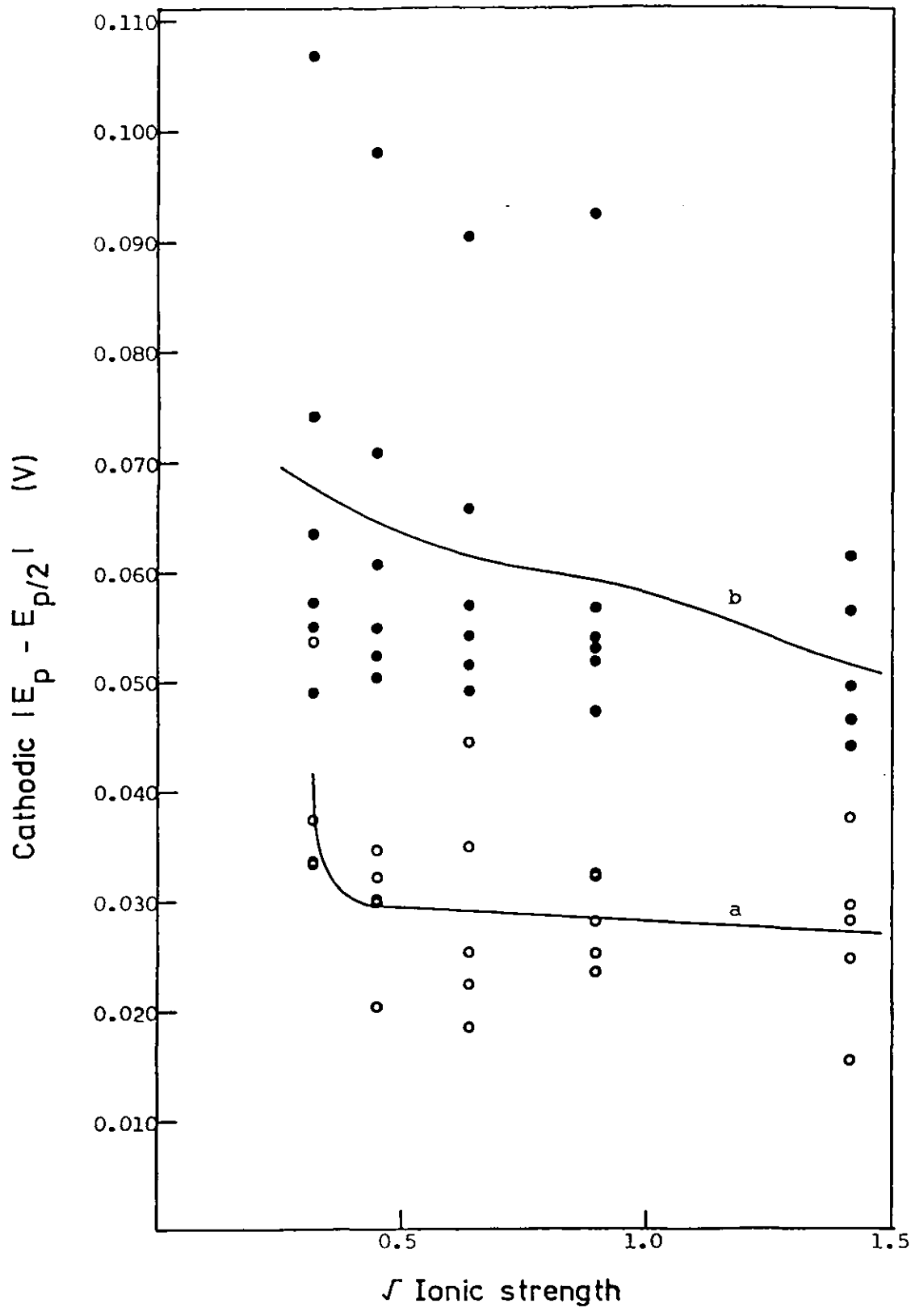

Fig. 5-195 Ir(IV) Perchlorate (1.0×10^{-4} mol dm^{-3})/Perchloric acid (0.1 to 2.0 M) supporting electrolyte System: Values of the absolute difference between cathodic peak and half-peak potential, $|E_{p(c)} - E_{p(c)/2}|$, as a function of square root of total ionic strength, $\sqrt{I}$ (where the concentration of perchloric acid was varied); at potential scan rates of 0.010 to 0.500 V s^{-1}. Boron carbide/carbon composite solid electrode $B_{3.11}C$. (a) $|E_{p(c,2)} - E_{p(c,2)/2}|$, and (b) $|E_{p(c,3)} - E_{p(c,3)/2}|$.

nature of the Ir(IV) perchlorate species may again be explained in terms of the weakening of the adsorption effect by the increase in perchloric acid concentration (section 5-1.5.(ii).a). Thus the peak potentials, which were initially shifted to less anodic values by the extremely strong physical adsorption of Ir(IV) perchlorate reactant, were merely reverting gradually to potential values corresponding to adsorption-free charge transfers as the adsorption effect was debilitated by the increasing perchloric acid concentration.

5-1.5.(ii).i Boron carbide/carbon composite solid electrode $B_{2.98}C$

The linear sweep voltammograms for Ir(IV) perchlorate (1.0×10^{-4} mol dm^{-3}), in perchloric acid (0.1 M) supporting electrolyte, obtained at the boron carbide/carbon composite solid electrode $B_{2.98}C$ reveal that three peaks were exhibited at slow sweep rates (Fig. 5-196). As the sweep rate was increased, however, Peak 2 was enhanced until it merged with Peak 3. The cyclic scan shows that the charge transfers were qualitatively reversible, as measured by the presence of the anodic counterparts for the cathodic peaks. Quantitative studies of the interpretable peaks reveal that Peak 2 was affected by adsorption (Fig. 5-197). The effect of sweep rate on the peak potentials is shown in Fig. 5-198; $E_{p(c,1)}$ and $E_{p(c,2)}$ being cathodically shifted by increasing sweep rates. Fig. 5-199 shows the differences between the peak potentials as functions of the sweep rate, and that $|E_{p(c,2)} - E_{p(c,2)/2}|$ widened with increasing sweep rates.

The evidence suggests that Peak 1, being exhibited at potentials previously associated with the post-peak due to the strong adsorption of reactant, was a post-peak relative to a diffusion peak which was too irreversible to be exhibited under the prevailing experimental conditions. Peak 2, however, was a quasi-reversible charge transfer which was complicated by weak adsorption of reactant whereas Peak 3 was due to moderately strong adsorption of reactant and therefore appeared as a post-peak.

5-1.5.(ii).j Boron carbide/carbon composite solid electrode $B_{2.76}C$

Cyclic and linear sweep voltammograms for Ir(IV) perchlorate (1.0×10^{-4} mol dm^{-3}), in perchloric acid (0.1 M) supporting electrolyte, obtained at the boron carbide/carbon composite solid electrode $B_{2.76}C$ are presented in Fig. 5-200. It can be seen that at slow sweep rates

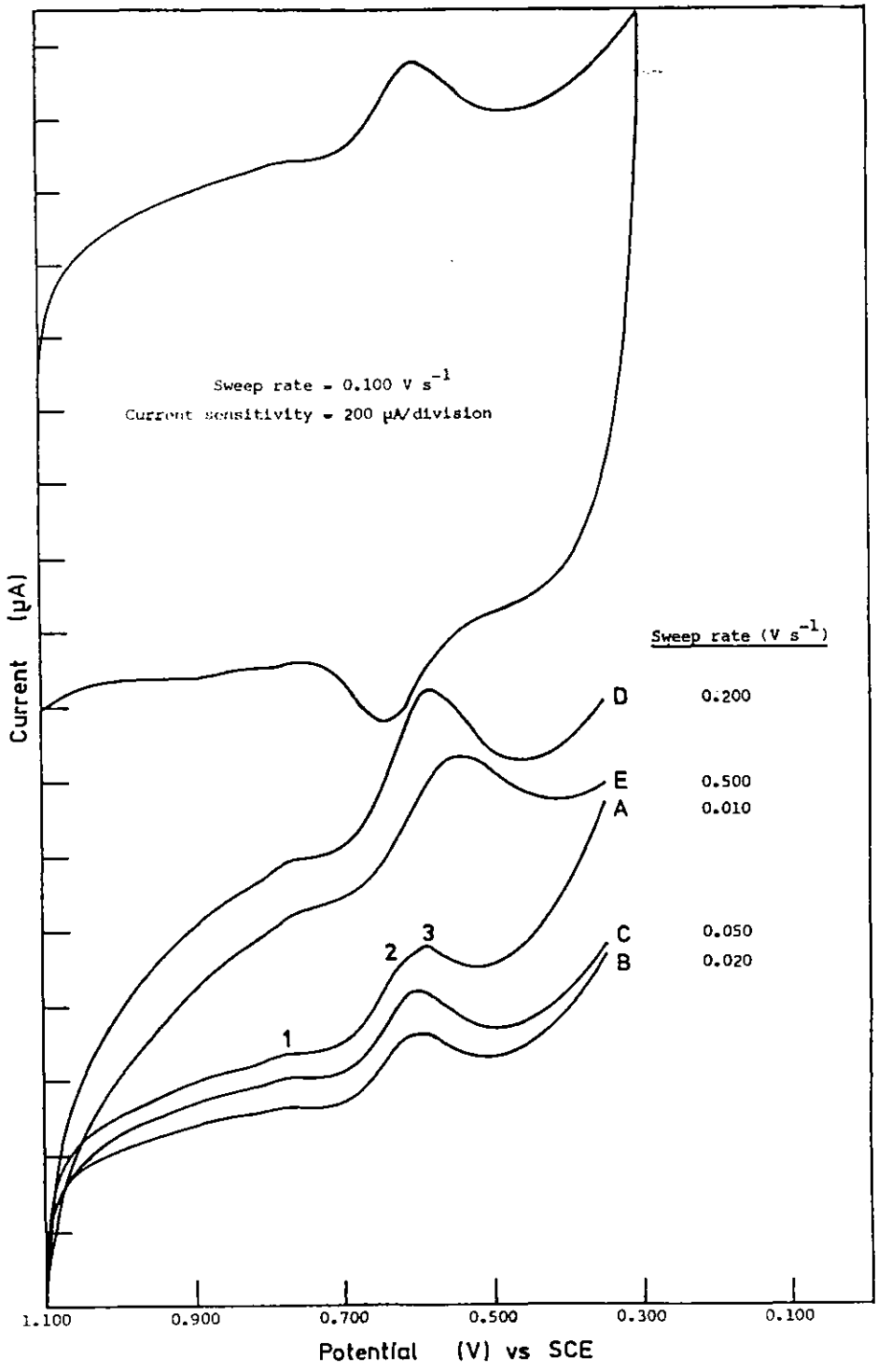

Fig. 5-196 Ir(IV) perchlorate (1.0×10^{-4} mol dm^{-3})/Perchloric acid (0.1 M) supporting electrolyte System: Cyclic and linear sweep voltammograms obtained at the boron carbide/carbon composite solid electrode $B_{2.98}C$. Current sensitivity (μA/division): A) 20, B) 50, C) 100, D) 200, and E) 500.

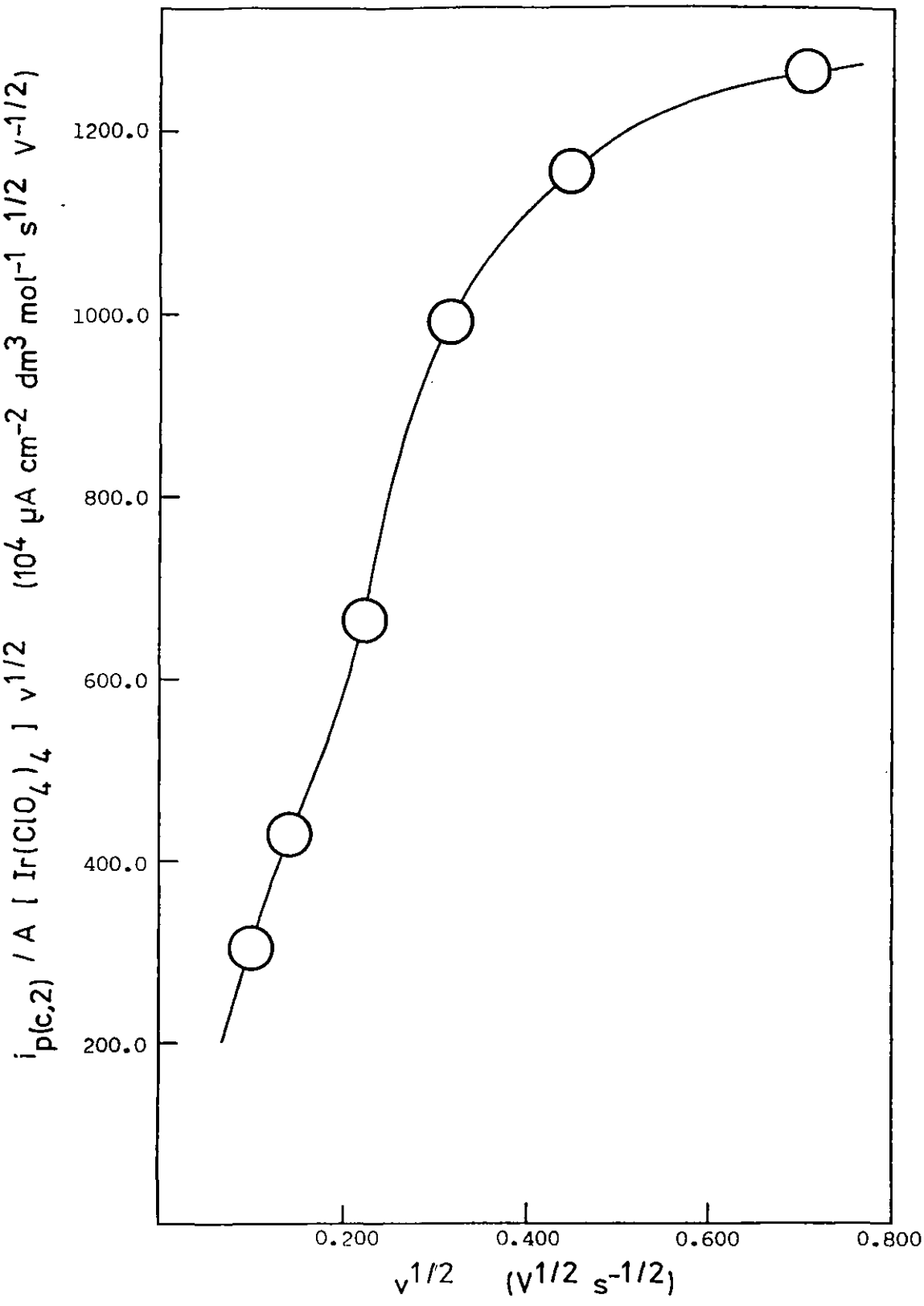

Fig. 5-197 Ir(IV) Perchlorate (1.0×10^{-4} mol dm^{-3})/Perchloric acid (0.1 M) supporting electrolyte System: Values of cathodic current function, $i_{p(c,2)}/A\ [\ Ir(ClO_4)_4\ ]\ v^{\frac{1}{2}}$, as a function of square root of potential scan rate, $v^{\frac{1}{2}}$. Boron carbide/carbon composite solid electrode $B_{2.98}C$.

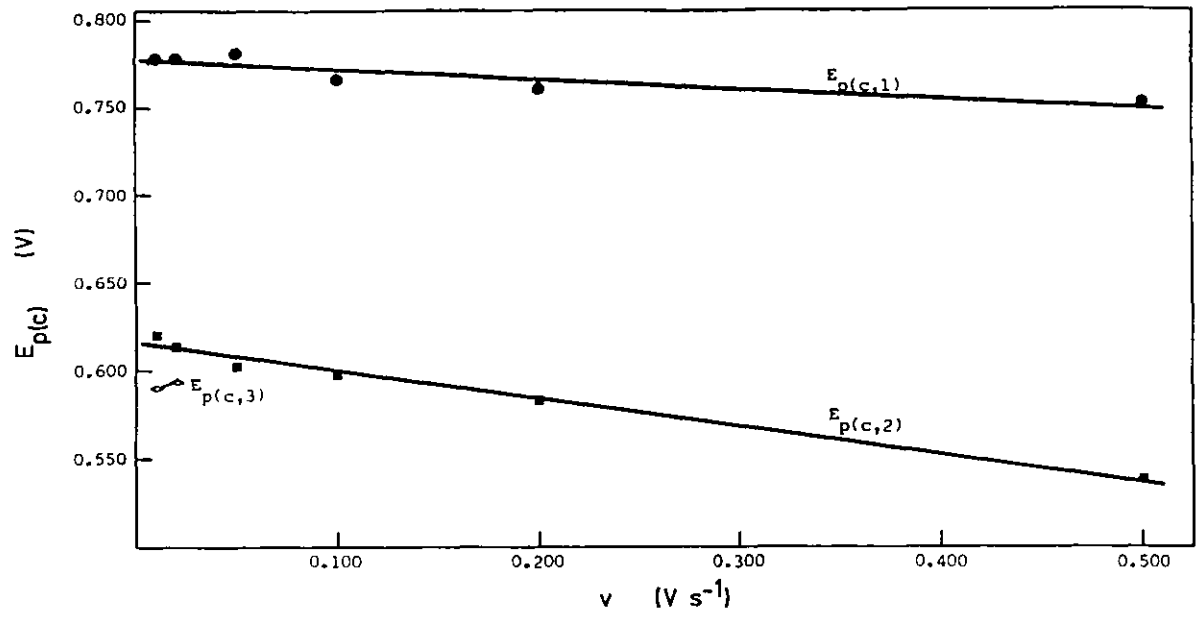

Fig. 5-198 Ir(IV) Perchlorate (1.0×10^{-4} mol dm^{-3})/Perchloric acid (0.1 M) supporting electrolyte System: Values of cathodic peak potential, $E_{p(c)}$, as a function of potential scan rate, v. Boron carbide/carbon composite solid electrode $B_{2.98}C$.

(a) $E_{p(c,1)} = 0.778 - 5.72 \times 10^{-2}$ v
Correlation coefficient = -0.9106
Level of significance, $p = 0.01 < p < 0.02$
Standard deviation of $E_{p(c,1)}$ from regression = 0.005 V
Degrees of freedom = 4

(b) $E_{p(c,2)} = 0.615 - 0.158$ v
Correlation coefficient = -0.9919
Level of significance, $p = p < 0.001$
Standard deviation of $E_{p(c,2)}$ from regression = 0.004 V
Degrees of freedom = 4

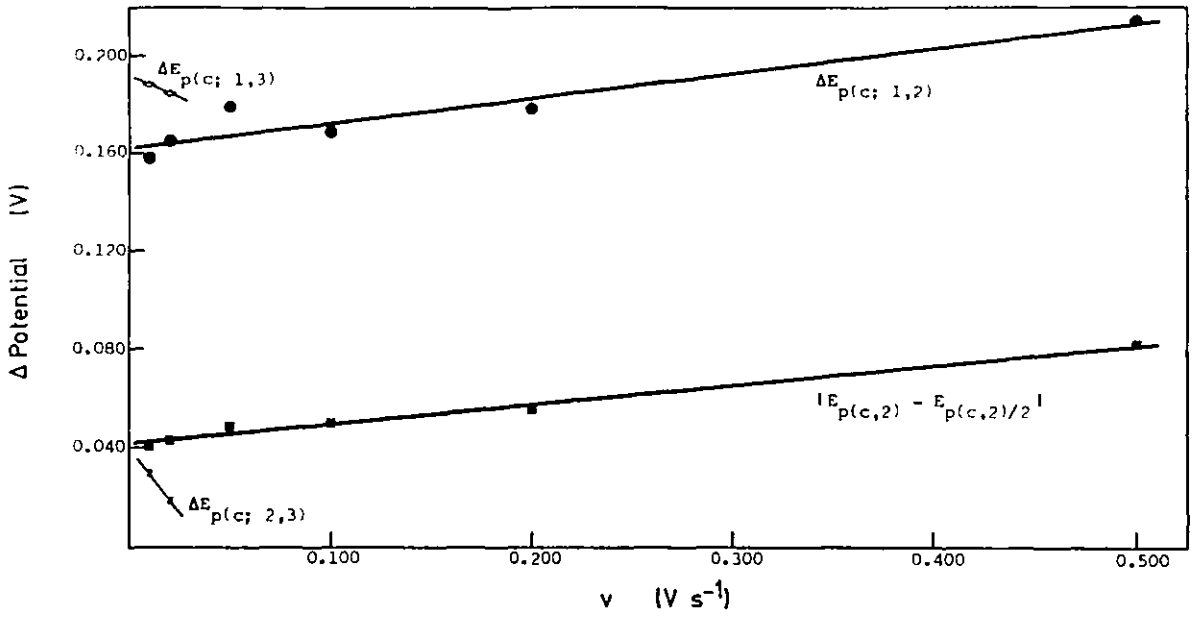

Fig. 5-199 Ir(IV) Perchlorate (1.0×10^{-4} mol dm^{-3})/Perchloric acid (0.1 M) supporting electrolyte System: Values of the difference between cathodic peak potentials, $\Delta E_{p(c)}$, and the absolute difference between cathodic peak and half-peak potential, $|E_{p(c)} - E_{p(c)/2}|$, as a function of potential scan rate, v. Boron carbide/carbon composite solid electrode $B_{2.98}C$.

(a) $\Delta E_{p(c;\ 1,2)} = 0.162 + 0.101\ v$
Correlation coefficient = 0.9496
Level of significance, $p = 0.001 < p < 0.01$
Standard deviation of $\Delta E_{p(c;\ 1,2)}$ from regression = 0.007 V
Degrees of freedom = 4

(b) $|E_{p(c,2)} - E_{p(c,2)/2}| = 4.18 \times 10^{-2} + 7.83 \times 10^{-2}\ v$
Correlation coefficient = 0.9920
Level of significance, $p = p < 0.001$
Standard deviation of $|E_{p(c,2)} - E_{p(c,2)/2}|$ from regression = 0.002 V
Degrees of freedom = 4

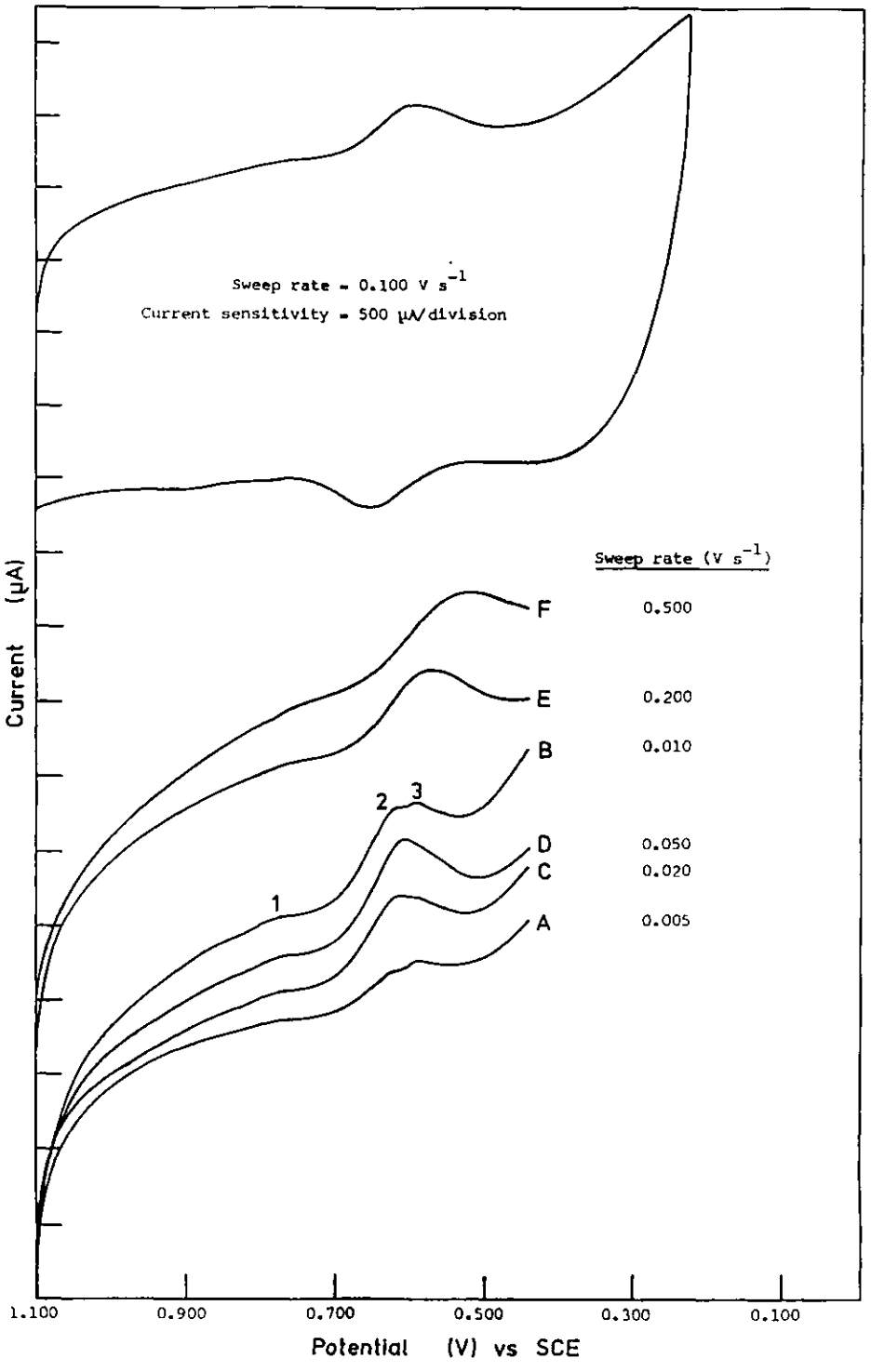

Fig. 5-200 Ir(IV) perchlorate (1.0×10^{-4} mol dm^{-3})/Perchloric acid (0.1 M) supporting electrolyte System: Cyclic and linear sweep voltammograms obtained at the boron carbide/carbon composite solid electrode $B_{2.76}C$. Current sensitivity (μA/division) : A) 20, B) 20, C) 50, D) 100, E) 500, and F) 1000.

three peaks, 1 to 3 inclusive, were exhibited. With increasing sweep rate, however, Peak 2 was enhanced and it eventually merged with Peak 3. The cyclic scan shows that anodic counterparts were exhibited for the cathodic peaks which were displayed; thus indicating some degree of reversibility in the related charge transfers. Plots of peak current function against $(\text{sweep rate})^{\frac{1}{2}}$ for interpretable peaks reveal that Peak 2 was influenced by adsorption (Fig. 5-201). The effect of increasing sweep rates on the peak potentials is shown in Fig. 5-202, which indicates that $E_{p(c,1)}$ and $E_{p(c,2)}$ were shifted cathodically. The absolute differences between the peak potentials as functions of the sweep rate are presented in Fig. 5-203; which also shows that $|E_{p(c,2)} - E_{p(c,2)/2}|$ widened with increasing sweep rate.

The evidence suggests that Peak 1, being of a similar character to the post-peak previously attributed to the strong adsorption of Ir(IV) perchlorate reactant (section 5-1.5.(ii).d), was a post-peak relative to a diffusion peak which was too irreversible to be defined under the prevailing experimental conditions. Peak 2 was a quasi-reversible charge transfer complicated by weak adsorption whereas Peak 3 was a post-peak, relative to Peak 2, reflecting the moderately strong adsorption of reactant.

5-1.5.(ii).k Boron carbide/carbon composite solid electrode $B_{2.56}C$

Linear sweep voltammograms for Ir(IV) perchlorate (1.0×10^{-4} mol dm^{-3}), in a concentration range of perchloric acid supporting electrolyte, obtained at the boron carbide/carbon composite solid electrode $B_{2.56}C$ are presented in Fig. 5-204. Qualitatively, it can be seen that all the peaks were anodically shifted by the increase in perchloric acid concentration. At higher perchloric acid concentrations, Peak 1 was not defined but Peak 4 became more distinct. Quantitative treatment of the interpretable peaks reveals that Peak 2 (Fig. 5-205) and Peak 3 (Fig. 5-206) were affected by adsorption; with Peak 2 being more influenced than Peak 3 (Fig. 5-207). The peak potentials are plotted as functions of the sweep rate in Fig. 5-208 which shows that $E_{p(c,1)}$ and $E_{p(c,3)}$ were cathodically shifted whereas $E_{p(c,2)}$ and $E_{p(c,4)}$ remained relatively constant. Furthermore, Fig. 5-209 indicates that $|E_{p(c,2)} - E_{p(c,2)/2}|$ was quite independent of the sweep rate but $|E_{p(c,3)} - E_{p(c,3)/2}|$ widened with increasing sweep rate; thus reflecting the decreasing reversibility in the charge transfer corresponding to Peak 3.

Fig. 5-210 shows that Peak 2 was enhanced at high perchloric acid

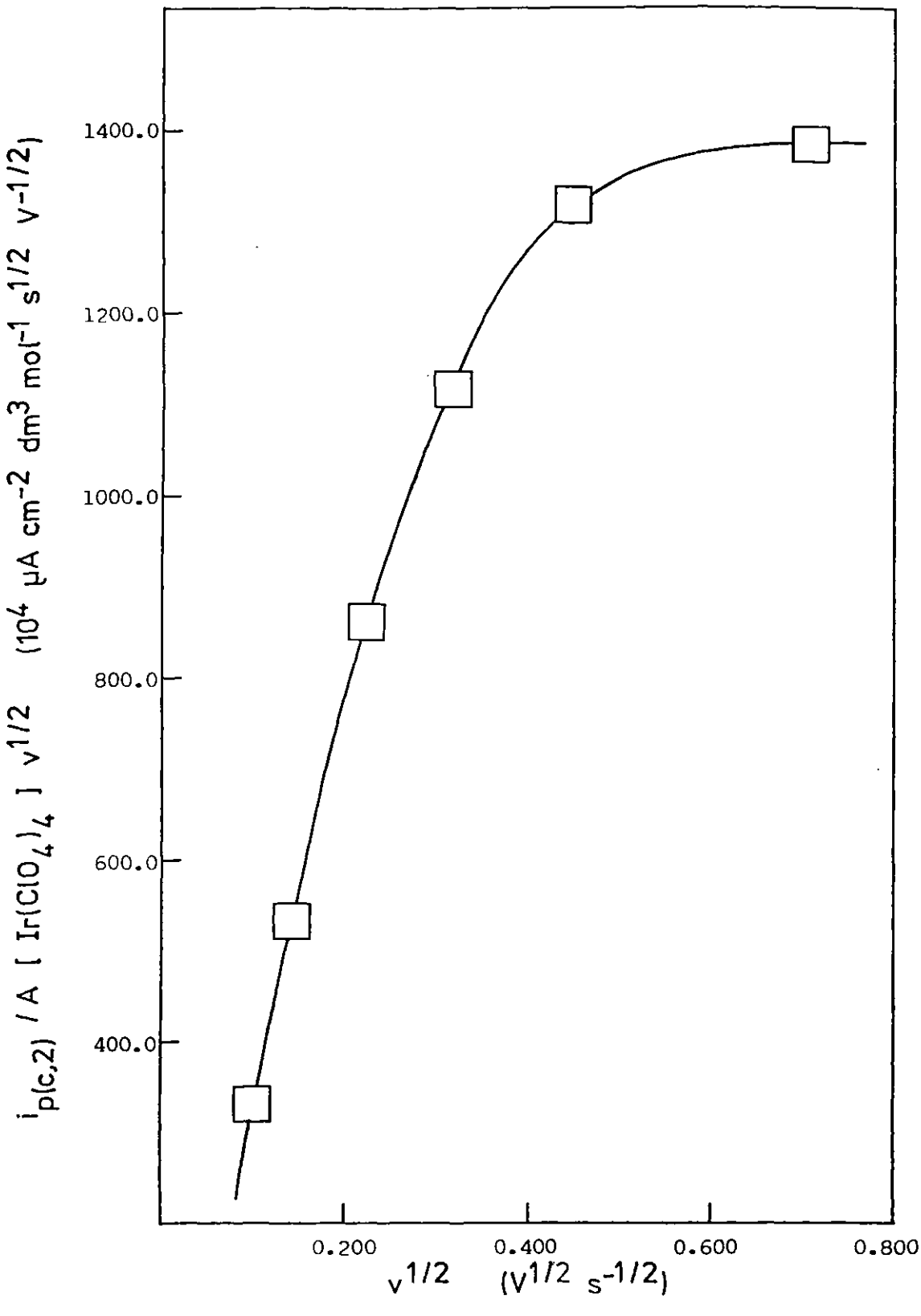

Fig. 5-201 Ir(IV) Perchlorate (1.0×10^{-4} mol dm^{-3})/Perchloric acid (0.1 M) supporting electrolyte System: Values of cathodic current function, $i_{p(c,2)}/A\ [\ Ir(ClO_4)_4\ ]\ v^{\frac{1}{2}}$, as a function of square root of potential scan rate, $v^{\frac{1}{2}}$. Boron carbide/carbon composite solid electrode $B_{2.76}C$.

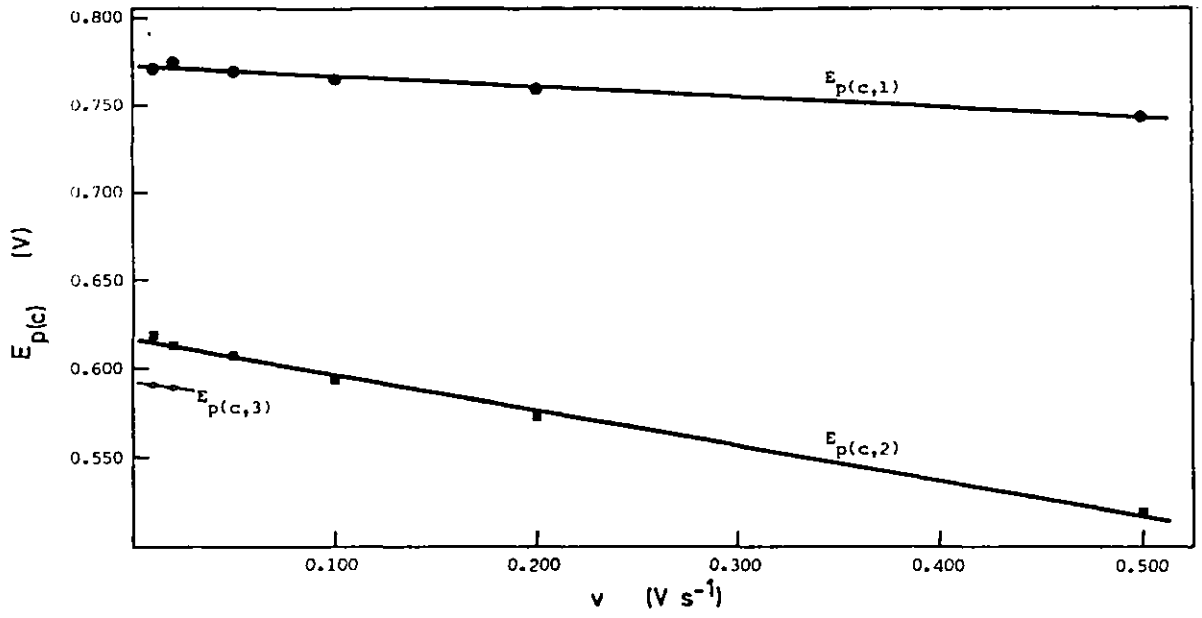

Fig. 5-202 Ir(IV) Perchlorate (1.0×10^{-4} mol dm^{-3})/Perchloric acid (0.1 M) supporting electrolyte System: Values of cathodic peak potential, $E_{p(c)}$, as a function of potential scan rate, v. Boron carbide/carbon composite solid electrode $B_{2.76}C$.

(a) $E_{p(c,1)} = 0.773 - 6.09 \times 10^{-2}$ v
Correlation coefficient = -0.9866
Level of significance, p = $p < 0.001$
Standard deviation of $E_{p(c,1)}$ from regression = 0.002 V
Degrees of freedom = 4

(b) $E_{p(c,2)} = 0.617 - 0.199$ v
Correlation coefficient = -0.9966
Level of significance, p = $p < 0.001$
Standard deviation of $E_{p(c,2)}$ from regression = 0.003 V
Degrees of freedom = 4

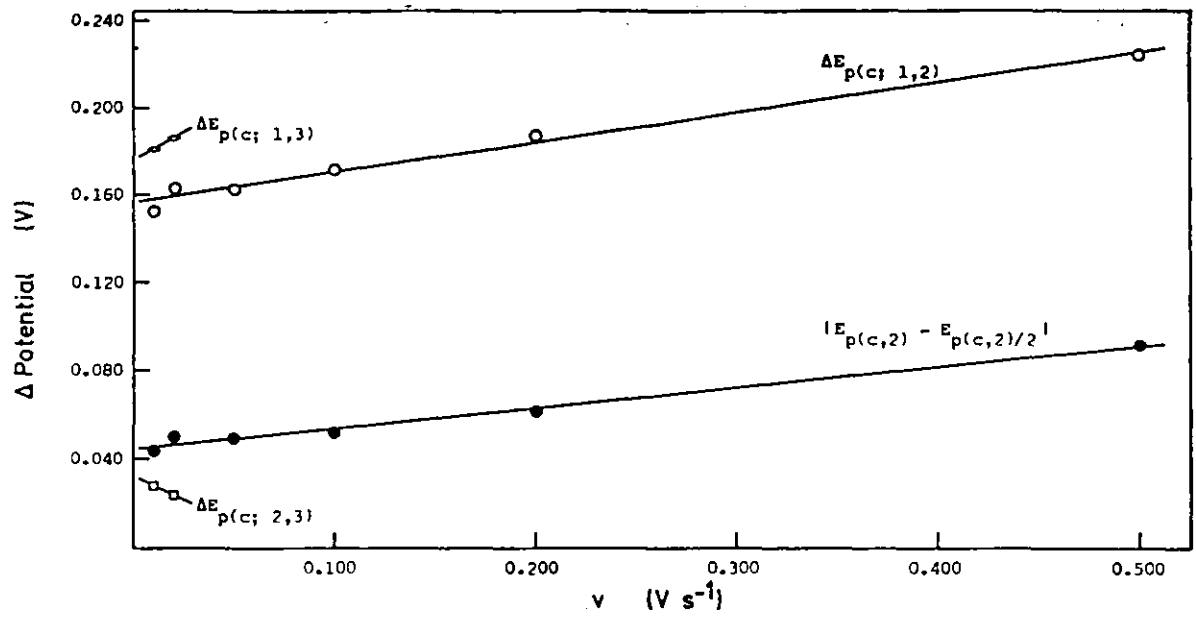

Fig. 5-203 Ir(IV) Perchlorate (1.0×10^{-4} mol dm^{-3})/Perchloric acid (0.1 M) supporting electrolyte System: Values of the difference between cathodic peak potentials, $\Delta E_{p(c)}$, and the absolute difference between cathodic peak and half-peak potential, $|E_{p(c)} - E_{p(c)/2}|$, as a function of potential scan rate, v. Boron carbide/carbon composite solid electrode $B_{2.76}C$.

(a) $\Delta E_{p(c;\ 1,2)} = 0.156 + 0.139\ v$
Correlation coefficient = 0.9926
Level of significance, p = $p < 0.001$
Standard deviation of $\Delta E_{p(c;\ 1,2)}$ from regression = 0.004 V
Degrees of freedom = 4

(b) $|E_{p(c,2)} - E_{p(c,2)/2}| = 4.44 \times 10^{-2} + 9.20 \times 10^{-2}\ v$
Correlation coefficient = 0.9923
Level of significance, p = $p < 0.001$
Standard deviation of $|E_{p(c,2)} - E_{p(c,2)/2}|$ from regression = 0.002 V
Degrees of freedom = 4

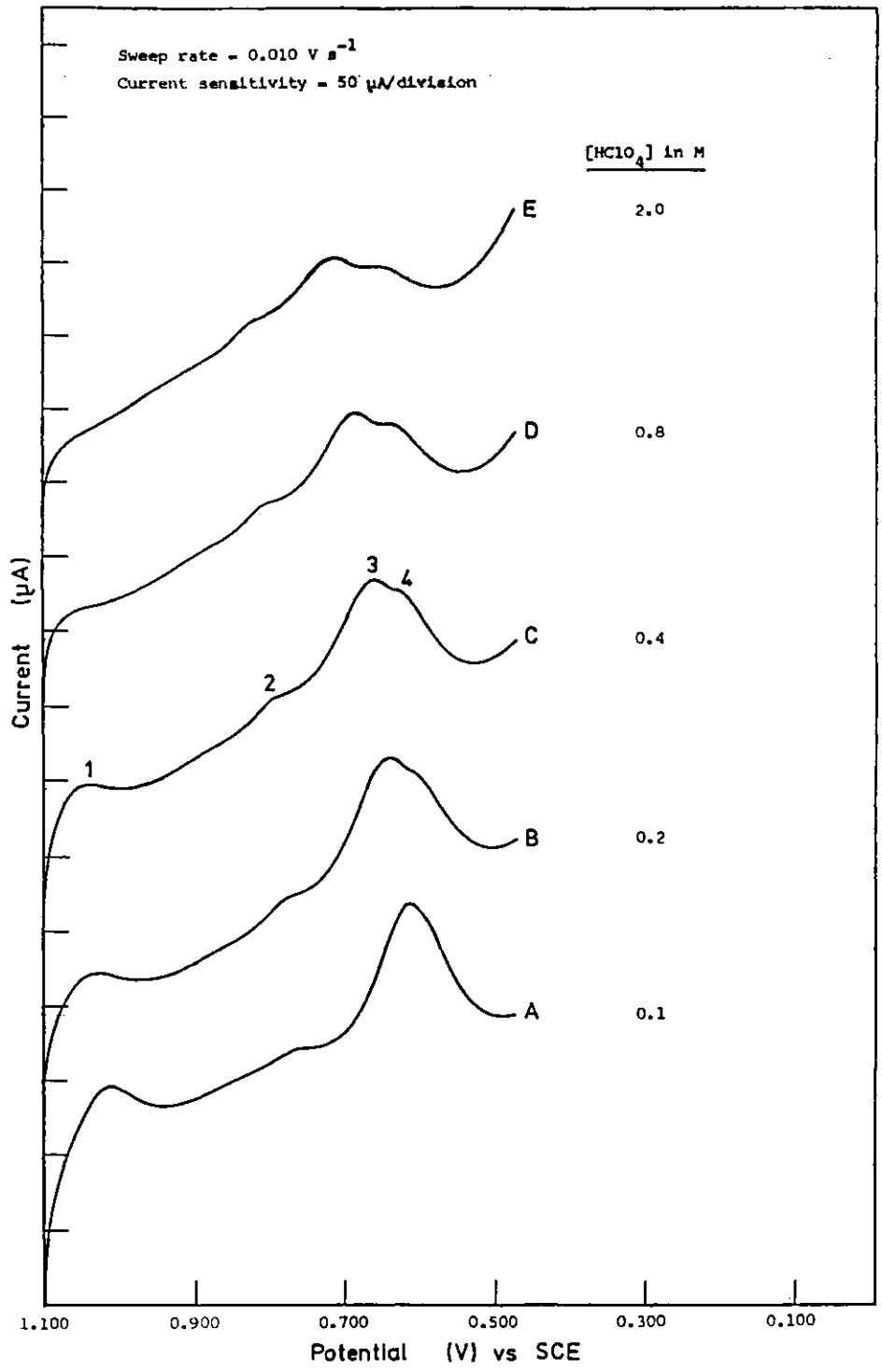

Fig. 5-204 Ir(IV) perchlorate (1.0×10^{-4} mol dm^{-3})/Perchloric acid (0.1 to 2.0 M) supporting electrolyte System: Linear sweep voltammograms obtained at the boron carbide/carbon composite solid electrode $B_{2.56}C$.

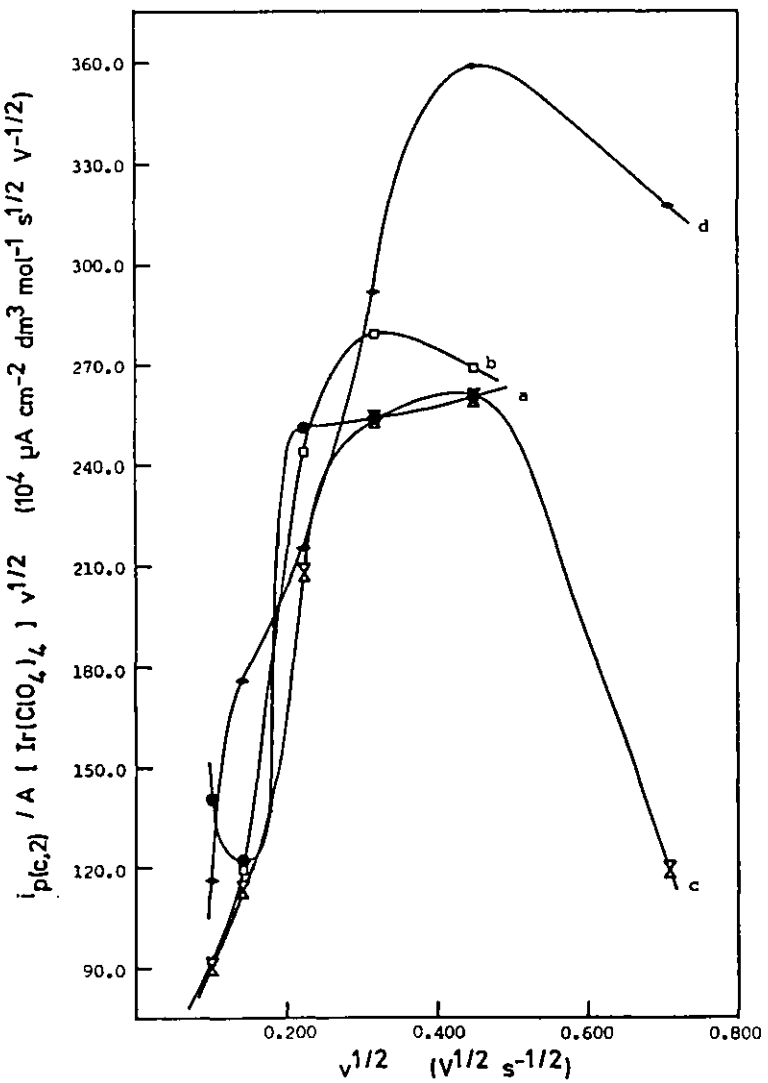

Fig. 5-205 Ir(IV) Perchlorate (1.0×10^{-4} mol dm^{-3})/Perchloric acid supporting electrolyte System: Values of cathodic current function, $i_{p(c,2)}/A$ [$Ir(ClO_4)_4$] $v^{\frac{1}{2}}$, as a function of square root of potential scan rate, $v^{\frac{1}{2}}$; at perchloric acid concentrations (a) 0.2, (b) 0.4, (c) 0.8, and (d) 2.0 M. Boron carbide/carbon composite solid electrode $B_{2.56}C$.

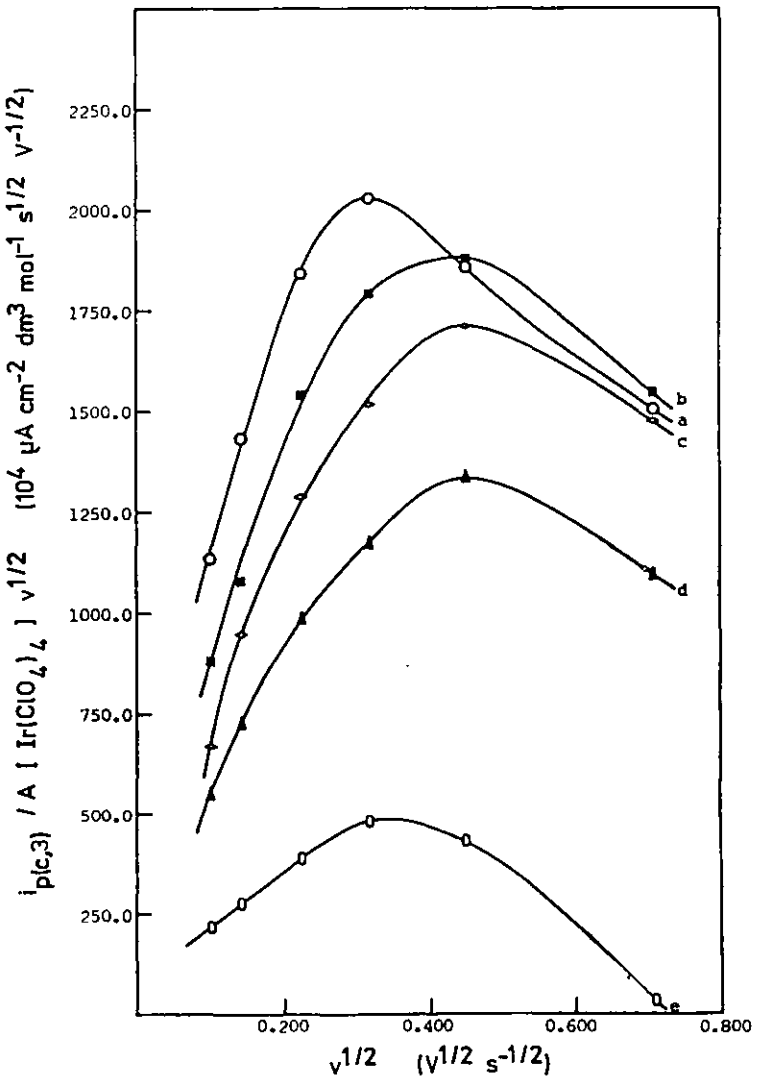

Fig. 5-206 Ir(IV) Perchlorate (1.0×10^{-4} mol dm^{-3})/Perchloric acid supporting electrolyte System: Values of cathodic current function, $i_{p(c,3)}/A$ [$Ir(ClO_4)_4$] $v^{\frac{1}{2}}$, as a function of square root of potential scan rate, $v^{\frac{1}{2}}$; at perchloric acid concentrations (a) 0.1, (b) 0.2, (c) 0.4, (d) 0.8, and (e) 2.0 M. Boron carbide/carbon composite solid electrode $B_{2.56}C$.

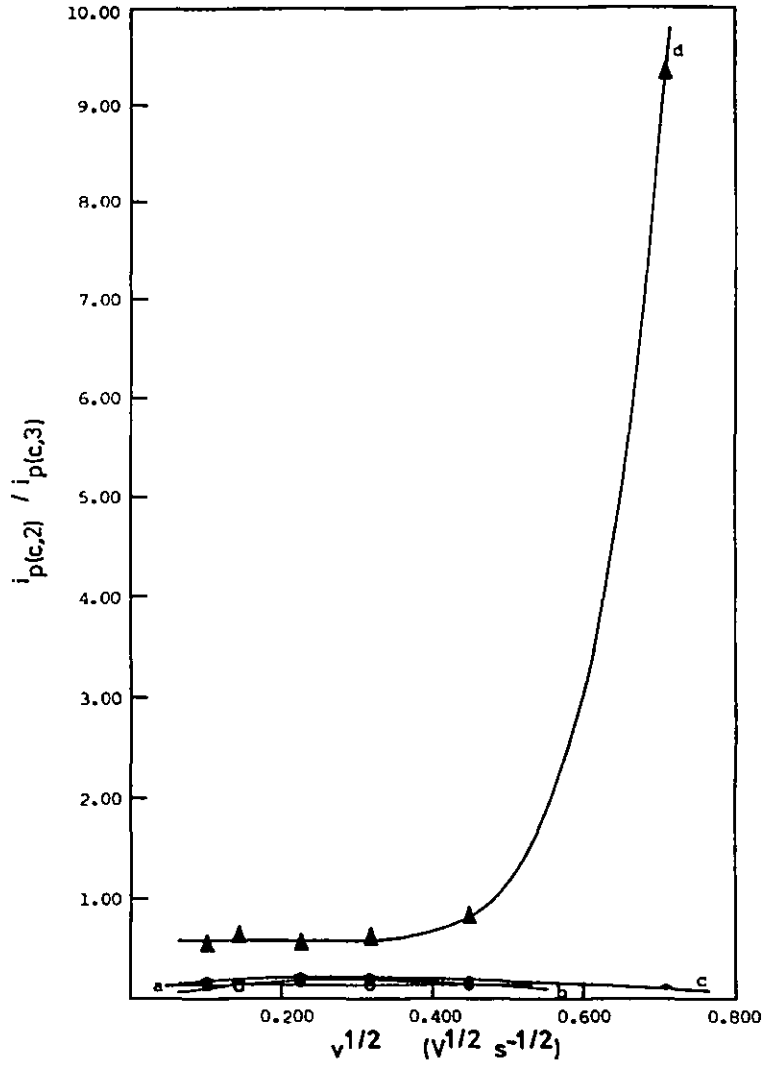

Fig. 5-207 Ir(IV) Perchlorate (1.0×10^{-4} mol dm^{-3})/Perchloric acid supporting electrolyte System: Values of the ratio of cathodic peak currents, $i_{p(c,2)}/i_{p(c,3)}$, as a function of square root of potential scan rate, $v^{\frac{1}{2}}$; at perchloric acid concentrations (a) 0.2, (b) 0.4, (c) 0.8, and (d) 2.0 M. Boron carbide/carbon composite solid electrode $B_{2.56}C$.

(a) $i_{p(c,2)}/i_{p(c,3)}$ mean = 0.14
Standard deviation = 0.02
Coefficient of variation = 13.8%
Degrees of freedom = 4

(b) $i_{p(c,2)}/i_{p(c,3)}$ mean = 0.16
Standard deviation = 0.03
Coefficient of variation = 17.6%
Degrees of freedom = 4

(c) $i_{p(c,2)}/i_{p(c,3)}$ mean = 0.18
Standard deviation = 0.04
Coefficient of variation = 23.2%
Degrees of freedom = 5

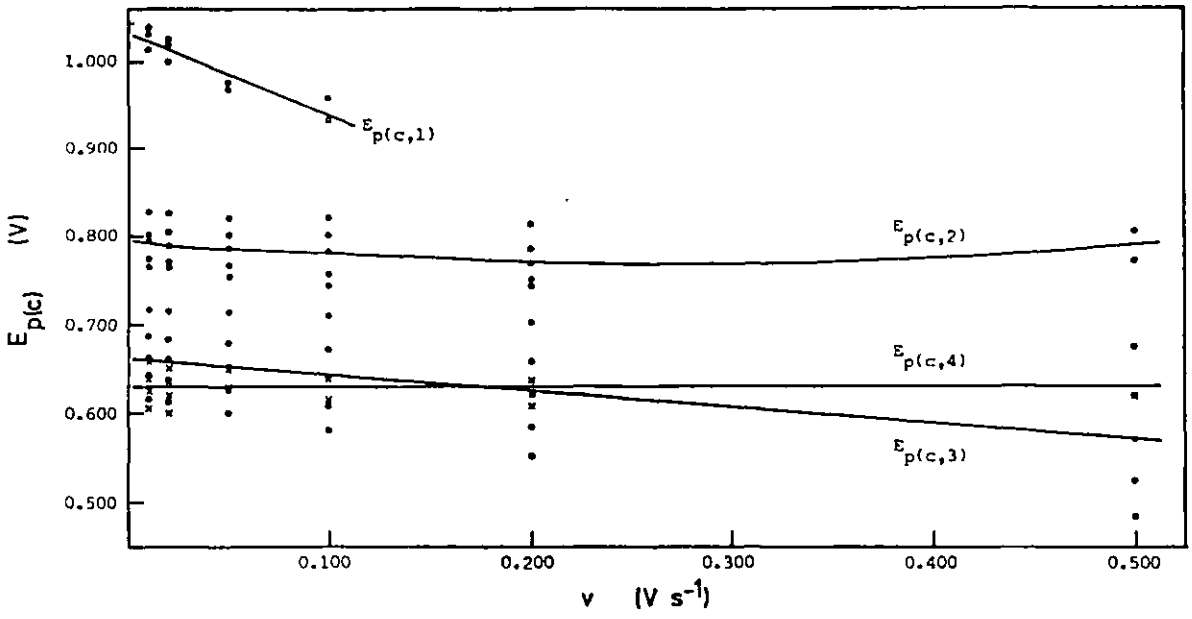

Fig. 5-208 Ir(IV) Perchlorate (1.0×10^{-4} mol dm^{-3})/Perchloric acid supporting electrolyte System: Values of cathodic peak potential, $E_{p(c)}$, as a function of potential scan rate, v; at perchloric acid concentrations of 0.1 to 2.0 M. Boron carbide/carbon composite solid electrode $B_{2.56}C$.

(a) $E_{p(c,1)} = 1.033 - 0.949\ v$
Correlation coefficient = -0.9281
Level of significance, $p = p < 0.001$
Standard deviation of $E_{p(c,1)}$ from regression = 0.014 V
Degrees of freedom = 8

(b) $E_{p(c,2)}$ mean = 0.784 V
Standard deviation = 0.025 V
Coefficient of variation = 3.22%
Degrees of freedom = 26

(c) $E_{p(c,3)} = 0.663 - 0.182\ v$
Correlation coefficient = -0.5433
Level of significance, $p = 0.001 < p < 0.01$
Standard deviation of $E_{p(c,3)}$ from regression = 0.049 V
Degrees of freedom = 28

(d) $E_{p(c,4)}$ mean = 0.629 V
Standard deviation = 0.017 V
Coefficient of variation = 2.73%
Degrees of freedom = 14

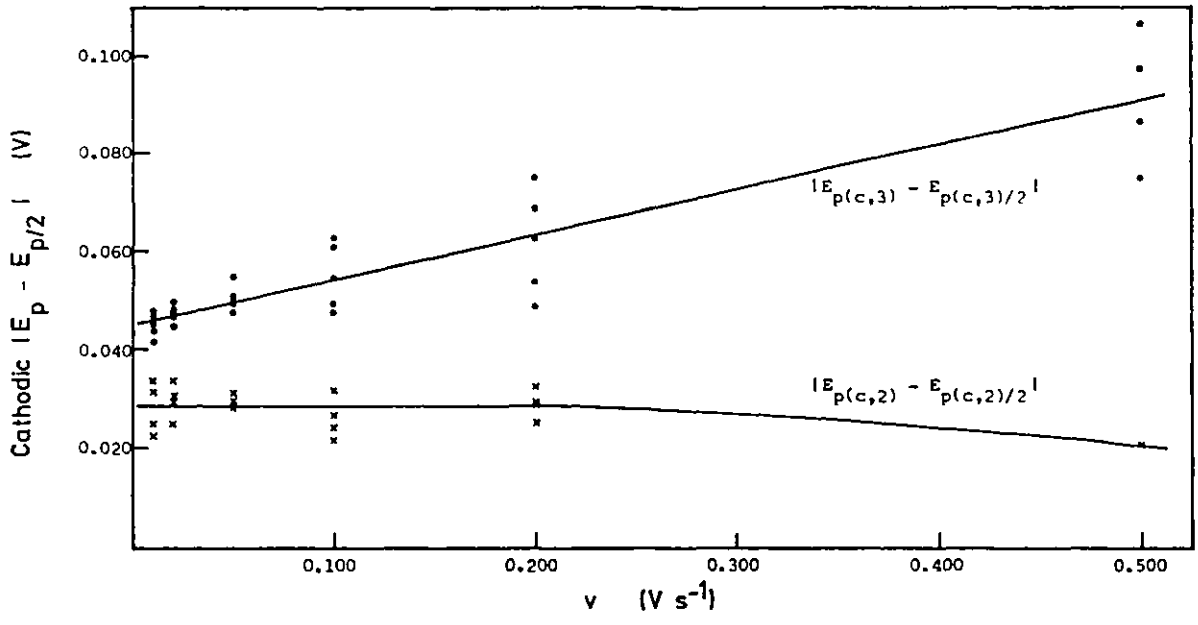

Fig. 5-209 Ir(IV) Perchlorate (1.0×10^{-4} mol dm^{-3})/Perchloric acid supporting electrolyte System: Values of the absolute difference between cathodic peak and half-peak potential, $|E_{p(c)} - E_{p(c)/2}|$, as a function of potential scan rate, v; at perchloric acid concentrations of 0.1 to 2.0 M. Boron carbide/carbon composite solid electrode $B_{2.56}C$.

(a) $|E_{p(c,2)} - E_{p(c,2)/2}|$ mean = 0.028 V
Standard deviation = 0.004 V
Coefficient of variation = 14.0%
Degrees of freedom = 20

(b) $|E_{p(c,3)} - E_{p(c,3)/2}| = 4.50 \times 10^{-2} + 9.19 \times 10^{-2}$ v
Correlation coefficient = 0.9103
Level of significance, p = $p < 0.001$
Standard deviation of $|E_{p(c,3)} - E_{p(c,3)/2}|$ from regression
= 0.007 V
Degrees of freedom = 27

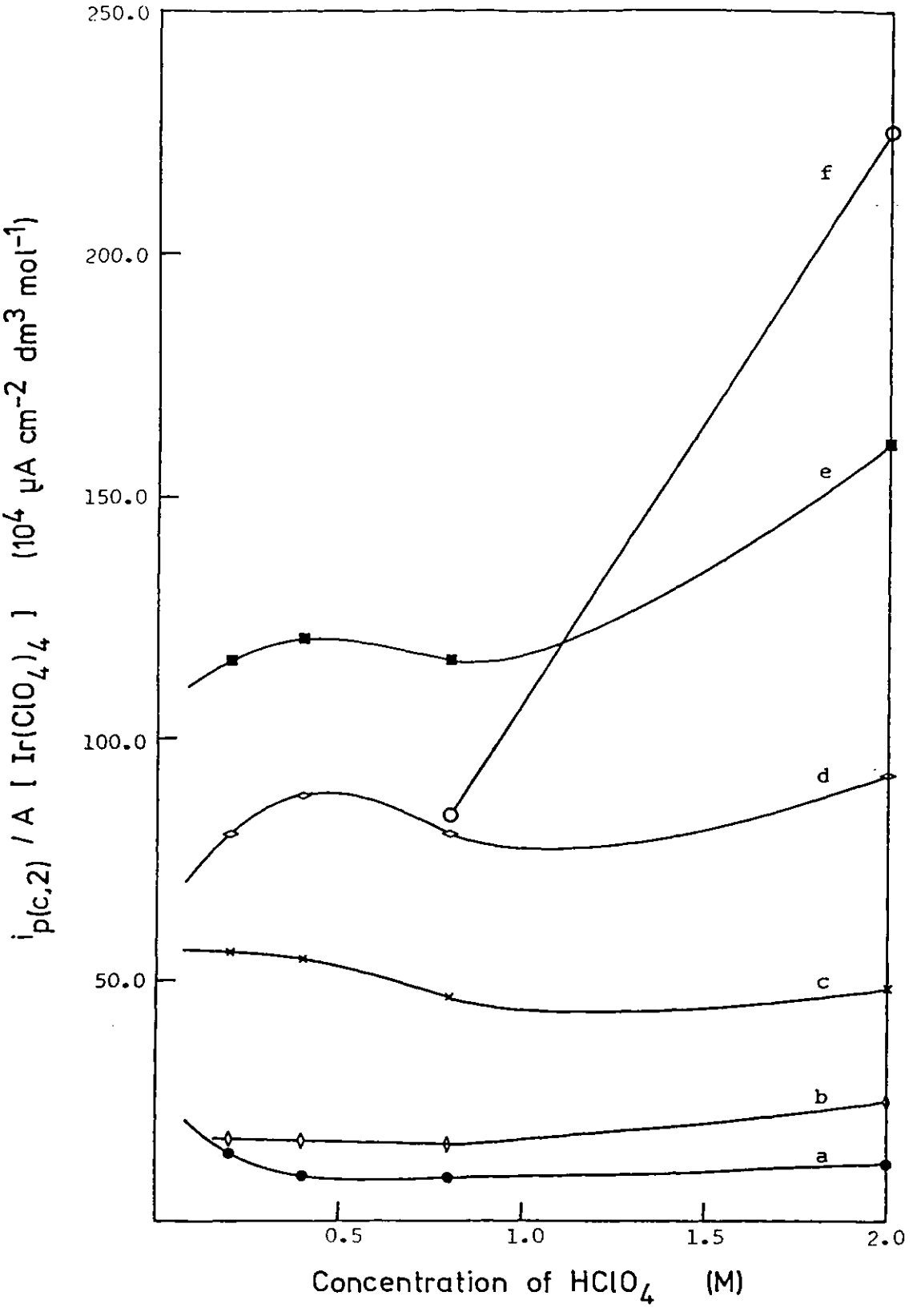

Fig. 5-210 Ir(IV) Perchlorate (1.0×10^{-4} mol dm^{-3})/Perchloric acid supporting electrolyte System: Values of cathodic peak current per unit area divided by concentration of Ir(IV) Perchlorate, $i_{p(c,2)}/A$ [$Ir(ClO_4)_4$], as a function of concentration of perchloric acid; at potential scan rates (a) 0.010, (b) 0.020, (c) 0.050, (d) 0.100, (e) 0.200, and (f) 0.500 V s^{-1}. Boron carbide/carbon composite solid electrode $B_{2.56}C$.

concentrations; especially when coupled with fast sweep rates. These results when considered in conjunction with those in Fig. 5-205 suggest that the increase in perchloric acid concentration influences the strong adsorption and the weak catalytic reaction for Peak 2 in different and opposing manners; depending on the prevailing sweep rate. Peak 3, however, was debilitated by the increasing perchloric acid concentration (Fig. 5-211); reflecting the weakening of the adsorption effect.

All the cathodic peak potentials were anodically shifted by the increasing ionic strength (Fig. 5-212); whilst $|E_{p(c,2)} - E_{p(c,2)/2}|$ and $|E_{p(c,3)} - E_{p(c,3)/2}|$ narrowed (Fig. 5-213).

The evidence suggests that Peak 1, being inhibited by both fast sweep rates and high perchloric acid concentration, was associated with a quasi-reversible charge transfer. Peak 2 was a post-peak due to the strong adsorption of Ir(IV) perchlorate reactant, although the related diffusion peak was too irreversible to be defined, which was slightly complicated by a very weak catalytic reaction. Peak 3 was a quasi-reversible charge transfer which was complicated by adsorption. Peak 4 was a moderately strong adsorption peak due to the adsorption of reactant; but became distinct only at higher ionic strength when Peak 3 was anodically shifted to a greater degree than Peak 4. The quasi-reversible nature of Peak 3, however, resulted in cathodic shifts in its peak potential with increasing sweep rate and thus led to the eventual coalescence of Peaks 3 and 4.

The apparently anomalous anodic shift in peak potentials with increasing ionic strength, although the Ir(IV) perchlorate species was shown to be cationic by paper electrophoresis, may again be explained in terms of the debilitating influence of the increasing perchloric acid concentration on the extremely strong physical adsorption of the Ir(IV) perchlorate reactant onto the electrode (section 5-1.5.(ii).h).

5-1.5.(ii).1 Graphite solid electrode

Cyclic and linear sweep voltammograms for Ir(IV) perchlorate (1.0×10^{-4} mol dm^{-3}), in perchloric acid (0.1 M) supporting electrolyte, obtained at the graphite solid electrode are presented in Fig. 5-214. Qualitatively, it can be seen that the four cathodic peaks displayed were reversible to some degree at slow sweep rates; as is evident from the presence of the anodic counterparts for the reverse scan in cyclic voltammetry. The definition of Peak 1, however, deteriorated with

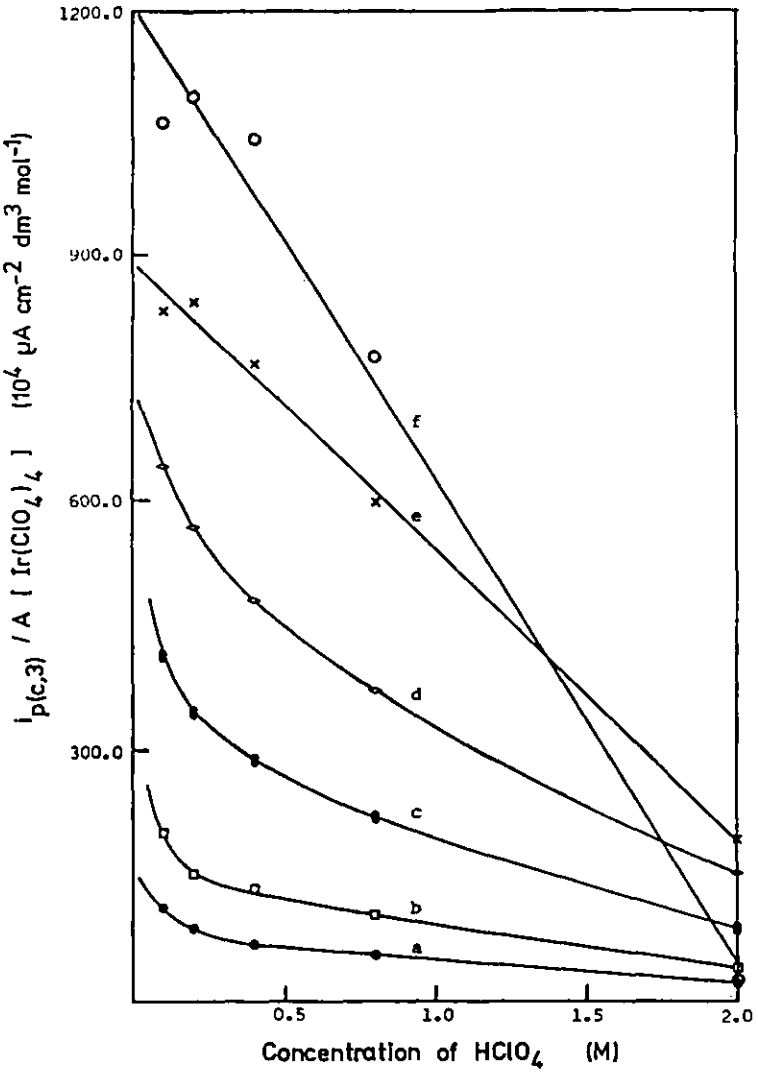

Fig. 5-211 Ir(IV) Perchlorate (1.0×10^{-4} mol dm^{-3})/Perchloric acid supporting electrolyte System: Values of cathodic peak current per unit area divided by concentration of Ir(IV) Perchlorate, $i_{p(c,3)}/A$ [$Ir(ClO_4)_4$], as a function of concentration of perchloric acid; at potential scan rates (a) 0.010, (b) 0.020, (c) 0.050, (d) 0.100, (e) 0.200, and (f) 0.500 V s^{-1}. Boron carbide/carbon composite solid electrode $B_{2.56}C$.

(e) $i_{p(c,3)}/A$ [$Ir(ClO_4)_4$] = $8.91 \times 10^6 - 3.50 \times 10^6$ [$HClO_4$]
Correlation coefficient = -0.9976
Level of significance, p = $p < 0.001$
Standard deviation of $i_{p(c,3)}/A$ [$Ir(ClO_4)_4$] from regression
= 2.18×10^5 μA cm^{-2} dm^3 mol^{-1}
Degrees of freedom = 3

(f) $i_{p(c,3)}/A$ [$Ir(ClO_4)_4$] = $1.20 \times 10^7 - 5.79 \times 10^6$ [$HClO_4$]
Correlation coefficient = -0.9917
Level of significance, p = $p < 0.001$
Standard deviation of $i_{p(c,3)}/A$ [$Ir(ClO_4)_4$] from regression
= 6.71×10^5 μA cm^{-2} dm^3 mol^{-1}
Degrees of freedom = 3

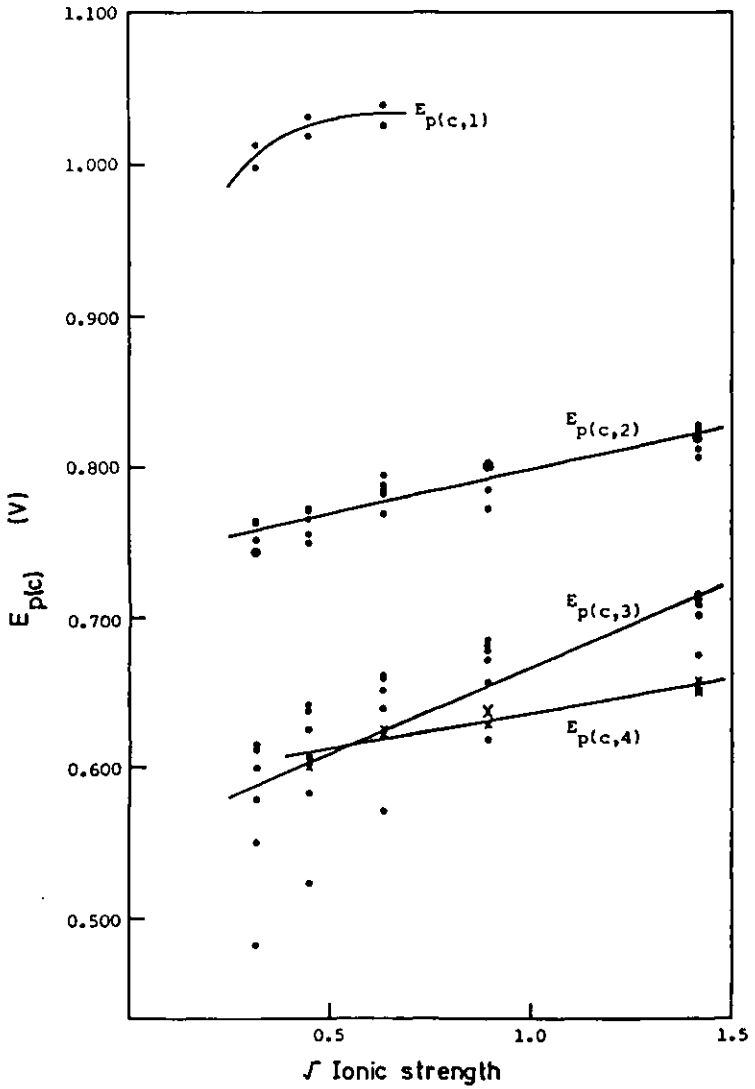

Fig. 5-212 Ir(IV) Perchlorate (1.0×10^{-4} mol dm^{-3})/Perchloric acid (0.1 to 2.0 M) supporting electrolyte System: Values of cathodic peak potential, $E_{p(c)}$, as a function of square root of total ionic strength, $\sqrt{I}$ (where the concentration of perchloric acid was varied); at potential scan rates of 0.010 to 0.500 V s^{-1}. Boron carbide/carbon composite solid electrode $B_{2.56}C$.

(a) $E_{p(c,1)}$ mean = 1.021 V
Standard deviation = 0.014 V
Coefficient of variation = 1.40%
Degrees of freedom = 5

(b) $E_{p(c,2)} = 0.740 + 5.75 \times 10^{-2} \sqrt{I}$
Correlation coefficient = 0.9177
Level of significance, p = $p < 0.001$
Standard deviation of $E_{p(c,2)}$ from regression = 0.010 V
Degrees of freedom = 25

(c) $E_{p(c,3)} = 0.550 + 0.116 \sqrt{I}$
Correlation coefficient = 0.7926
Level of significance, p = $p < 0.001$
Standard deviation of $E_{p(c,3)}$ from regression = 0.036 V
Degrees of freedom = 28

(d) $E_{p(c,4)} = 0.589 + 4.71 \times 10^{-2} \sqrt{I}$
Correlation coefficient = 0.9537
Level of significance, p = $p < 0.001$
Standard deviation of $E_{p(c,4)}$ from regression = 0.006 V
Degrees of freedom = 8

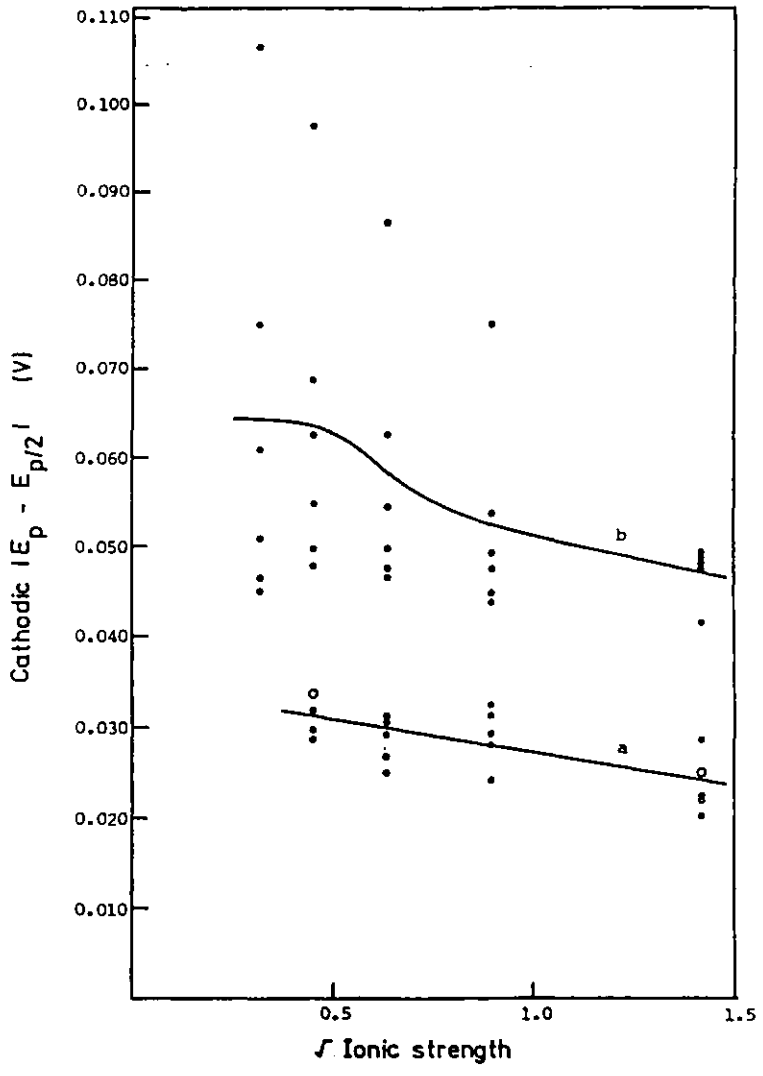

Fig. 5-213 Ir(IV) Perchlorate (1.0×10^{-4} mol dm^{-3})/Perchloric acid (0.1 to 2.0 M) supporting electrolyte System: Values of the absolute difference between cathodic peak and half-peak potential, $|E_{p(c)} - E_{p(c)/2}|$, as a function of square root of total ionic strength, $\sqrt{I}$ (where the concentration of perchloric acid was varied); at potential scan rates of 0.010 to 0.500 V s^{-1}. Boron carbide/carbon composite solid electrode $B_{2.56}C$. (a) $|E_{p(c,2)} - E_{p(c,2)/2}|$, and (b) $|E_{p(c,3)} - E_{p(c,3)/2}|$.

(a) $|E_{p(c,2)} - E_{p(c,2)/2}| = 3.45 \times 10^{-2} - 7.32 \times 10^{-3} \sqrt{I}$
Correlation coefficient = -0.7143
Level of significance, p = $p < 0.001$
Standard deviation of $|E_{p(c,2)} - E_{p(c,2)/2}|$ from regression
= 0.003 V
Degrees of freedom = 19

(b) $|E_{p(c,3)} - E_{p(c,3)/2}|$ mean = 0.057 V
Standard deviation = 0.016 V
Coefficient of variation = 28.7%
Degrees of freedom = 28

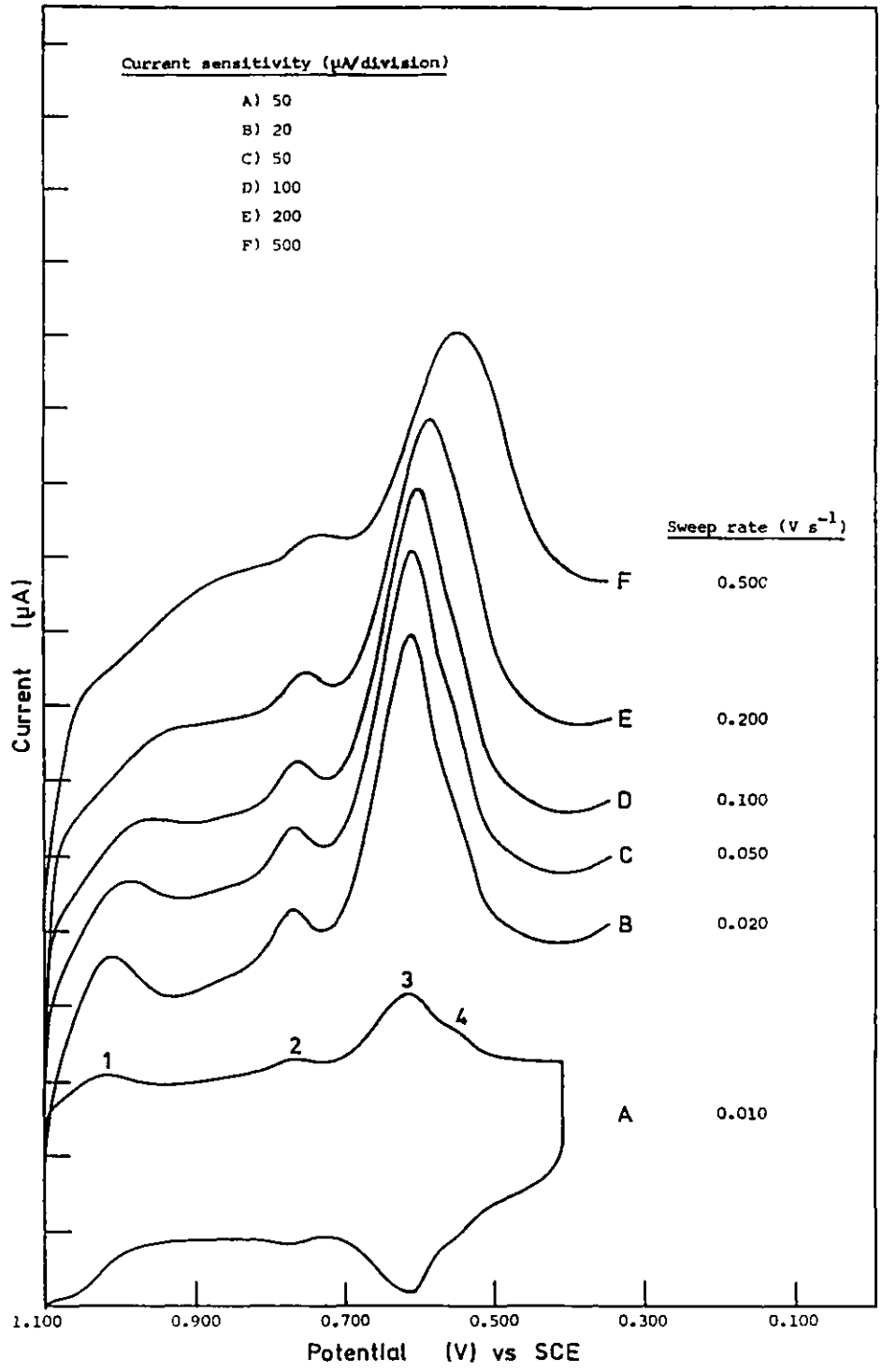

Fig. 5-214 Ir(IV) perchlorate (1.0×10^{-4} mol dm^{-3})/Perchloric acid (0.1 M) supporting electrolyte System: Cyclic and linear sweep voltammograms obtained at the graphite solid electrode.

increasing sweep rate whilst its peak potential was shifted cathodically; thus indicating a quasi-reversible charge transfer. Quantitative treatment of the interpretable peaks reveals that Peak 2 (Fig. 5-215) and Peak 3 (Fig. 5-216) were influenced by adsorption which was debilitated by the increase in the perchloric acid concentration. Generally, the increase in sweep rate enhanced Peak 3 to a greater degree than Peak 2 (Fig. 5-217).

The cathodic peak potentials were all cathodically shifted by the increasing sweep rate (Fig. 5-218) whilst $|E_p - E_{p/2}|$ values for Peaks 2 and 3 widened. Thus the charge transfer corresponding to Peaks 2 and 3 became less reversible with increasing sweep rate (Fig. 5-219). The definition of Peak 4 deteriorated with increasing sweep rate because Peak 3 was cathodically shifted to a greater degree than Peak 4 and so eventually leading to the merger of the two peaks.

The influence of perchloric acid supporting electrolyte on the linear sweep voltammograms for Ir(IV) perchlorate (1.0×10^{-4} mol dm^{-3}) is displayed in Fig. 5-220. Qualitatively, it can be seen that all the peaks were shifted anodically by the increasing perchloric acid concentration whilst the definition of Peak 1 deteriorated but that of Peak 4 improved. The peaks for the residual current, labelled r, were anodically shifted and enhanced by increasing perchloric acid concentration. Quantitatively, Peaks 2 and 3 were diminished by increasing perchloric acid concentration (Figures 5-221 and 5-222 respectively).

The anodic shift in peak potentials with increasing $(\text{ionic strength})^{\frac{1}{2}}$ is plotted in Fig. 5-223 which reveals that the shift for Peaks 1 and 3 was greater than for Peaks 2 and 4; thus explaining the improved definition of Peak 4 at high perchloric acid concentrations. Fig. 5-224 indicates that $|E_p - E_{p/2}|$ values for Peaks 2 and 3 narrowed with increasing perchloric acid concentration.

The evidence suggests that Peak 1 was a quasi-reversible charge transfer, Peak 2 was a post-peak of the strong adsorption of Ir(IV) perchlorate reactant, Peak 3 was a quasi-reversible charge transfer complicated by weak adsorption, and Peak 4 was a post-peak of the moderately strong adsorption of reactant. The apparently anomalous anodic shift in peak potentials with increasing ionic strength, notwithstanding the cationic nature of the Ir(IV) perchlorate reactant, may again be the consequence of the debilitating effect of increasing perchloric acid concentration on the strength of adsorption (section 5-1.5.(ii).h).

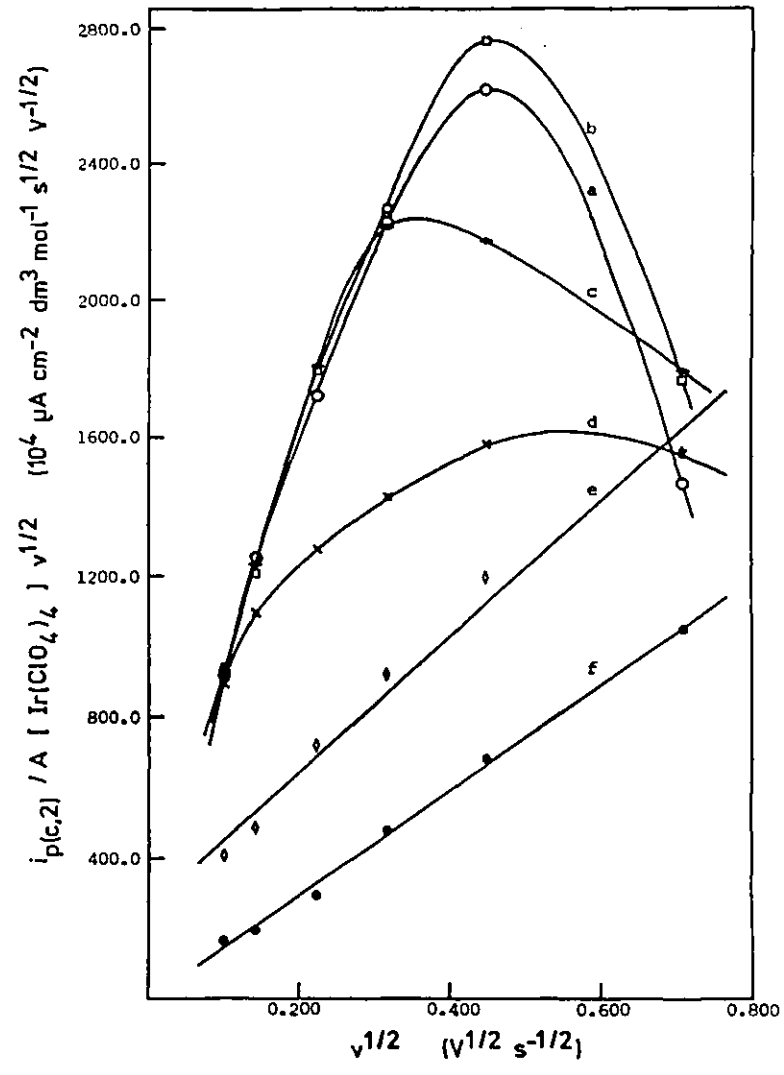

Fig. 5-215 Ir(IV) Perchlorate (1.0×10^{-4} mol dm^{-3})/Perchloric acid supporting electrolyte System: Values of cathodic current function, $i_{p(c,2)}/A\ [\ Ir(ClO_4)_4\ ]\ v^{\frac{1}{2}}$, as a function of square root of potential scan rate, $v^{\frac{1}{2}}$; at perchloric acid concentrations (a) 0.1, (b) 0.2, (c) 0.4, (d) 0.8, (e) 1.0, and (f) 2.0 M. Graphite solid electrode.

(e) $i_{p(c,2)}/A\ [\ Ir(ClO_4)_4\ ]\ v^{\frac{1}{2}} = 2.62 \times 10^6 + 1.92 \times 10^7\ v^{\frac{1}{2}}$

Correlation coefficient = 0.9904

Level of significance, $p = p < 0.001$

Standard deviation of $i_{p(c,2)}/A\ [\ Ir(ClO_4)_4\ ]\ v^{\frac{1}{2}}$ from regression = 6.77×10^5 μA cm^{-2} dm^3 mol^{-1} $s^{\frac{1}{2}}$ $v^{-\frac{1}{2}}$

Degrees of freedom = 4

(f) $i_{p(c,2)}/A\ [\ Ir(ClO_4)_4\ ]\ v^{\frac{1}{2}} = 1.50 \times 10^7\ v^{\frac{1}{2}} - 5.68 \times 10^4$

Correlation coefficient = 0.9980

Level of significance, $p = p < 0.001$

Standard deviation of $i_{p(c,2)}/A\ [\ Ir(ClO_4)_4\ ]\ v^{\frac{1}{2}}$ from regression = 2.39×10^5 μA cm^{-2} dm^3 mol^{-1} $s^{\frac{1}{2}}$ $v^{-\frac{1}{2}}$

Degrees of freedom = 4

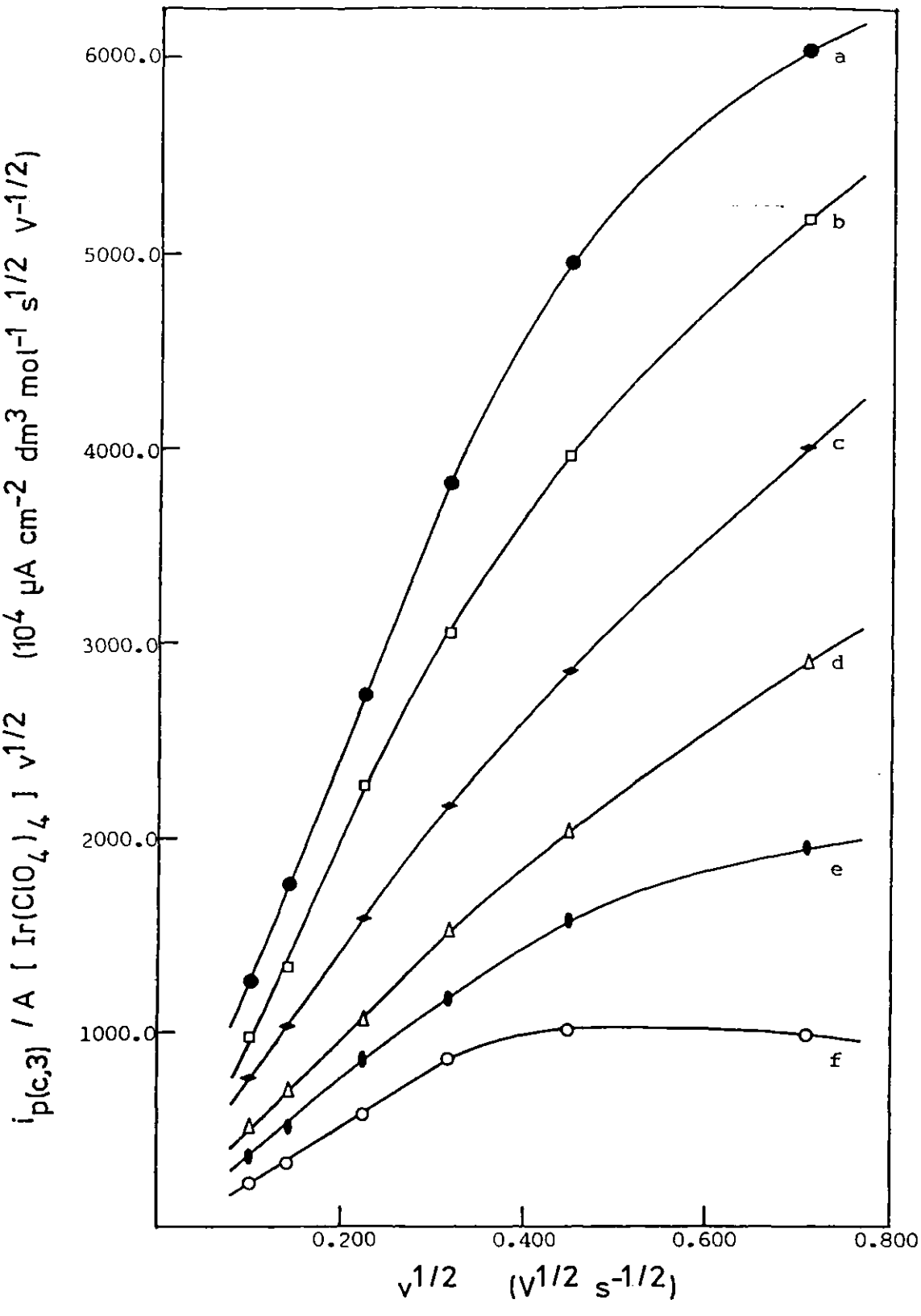

Fig. 5-216 Ir(IV) Perchlorate (1.0×10^{-4} mol dm^{-3})/Perchloric acid supporting electrolyte System: Values of cathodic current function, $i_{p(c,3)}/A\ [\ Ir(ClO_4)_4\ ]\ v^{\frac{1}{2}}$, as a function of square root of potential scan rate, $v^{\frac{1}{2}}$; at perchloric acid concentrations (a) 0.1, (b) 0.2, (c) 0.4, (d) 0.8, (e) 1.0, and (f) 2.0 M. Graphite solid electrode.

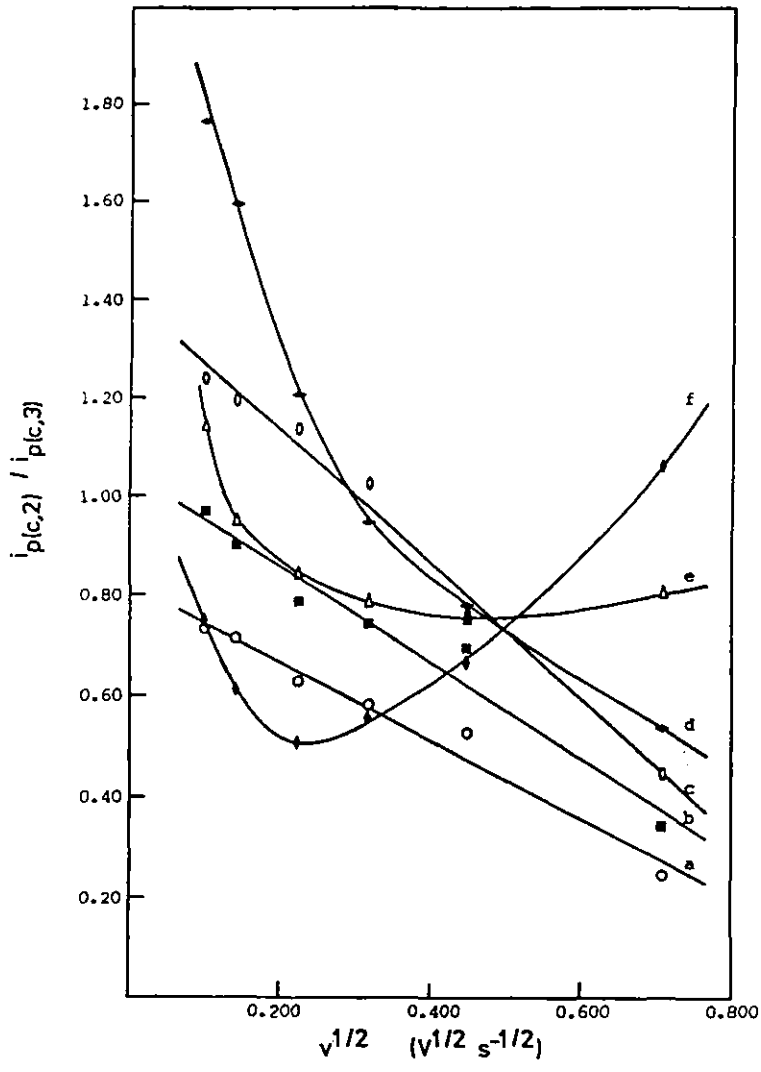

Fig. 5-217 Ir(IV) Perchlorate (1.0×10^{-4} mol dm^{-3})/Perchloric acid supporting electrolyte System: Values of the ratio of cathodic peak currents, $i_{p(c,2)}/i_{p(c,3)}$, as a function of square root of potential scan rate, $v^{\frac{1}{2}}$; at perchloric acid concentrations (a) 0.1, (b) 0.2, (c) 0.4, (d) 0.8, (e) 1.0, and (f) 2.0 M. Graphite solid electrode.

(a) $i_{p(c,2)}/i_{p(c,3)} = 0.822 - 0.777\ v^{\frac{1}{2}}$
Correlation coefficient = -0.9858
Level of significance, p = $p < 0.001$
Standard deviation of $i_{p(c,2)}/i_{p(c,3)}$ from regression = 0.033
Degrees of freedom = 4

(b) $i_{p(c,2)}/i_{p(c,3)} = 1.05 - 0.954\ v^{\frac{1}{2}}$
Correlation coefficient = -0.9806
Level of significance, p = $p < 0.001$
Standard deviation of $i_{p(c,2)}/i_{p(c,3)}$ from regression = 0.048
Degrees of freedom = 4

(c) $i_{p(c,2)}/i_{p(c,3)} = 1.40 - 1.35\ v^{\frac{1}{2}}$
Correlation coefficient = -0.9934
Level of significance, p = $p < 0.001$
Standard deviation of $i_{p(c,2)}/i_{p(c,3)}$ from regression = 0.039
Degrees of freedom = 4

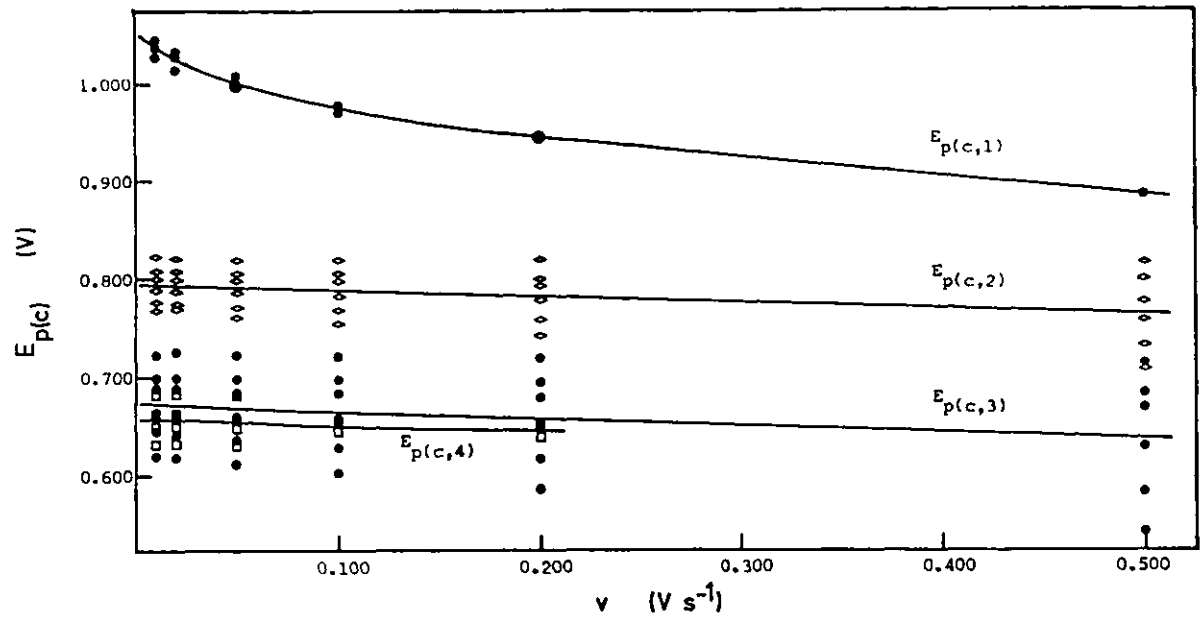

Fig. 5-218 Ir(IV) Perchlorate (1.0×10^{-4} mol dm^{-3})/Perchloric acid supporting electrolyte System: Values of cathodic peak potential, $E_{p(c)}$, as a function of potential scan rate, v; at perchloric acid concentrations of 0.1 to 2.0 M. Graphite solid electrode.

(a) $E_{p(c,1)}$ mean = 0.993 V
Standard deviation = 0.045 V
Coefficient of variation = 4.55%
Degrees of freedom = 13

(b) $E_{p(c,2)} = 0.793 - 5.91 \times 10^{-2}$ v
Correlation coefficient = -0.3761
Level of significance, $p = 0.02 < p < 0.05$
Standard deviation of $E_{p(c,2)}$ from regression = 0.026 V
Degrees of freedom = 34

(c) $E_{p(c,3)}$ mean = 0.661 V
Standard deviation = 0.045 V
Coefficient of variation = 6.85%
Degrees of freedom = 35

(d) $E_{p(c,4)}$ mean = 0.653 V
Standard deviation = 0.017 V
Coefficient of variation = 2.63%
Degrees of freedom = 15

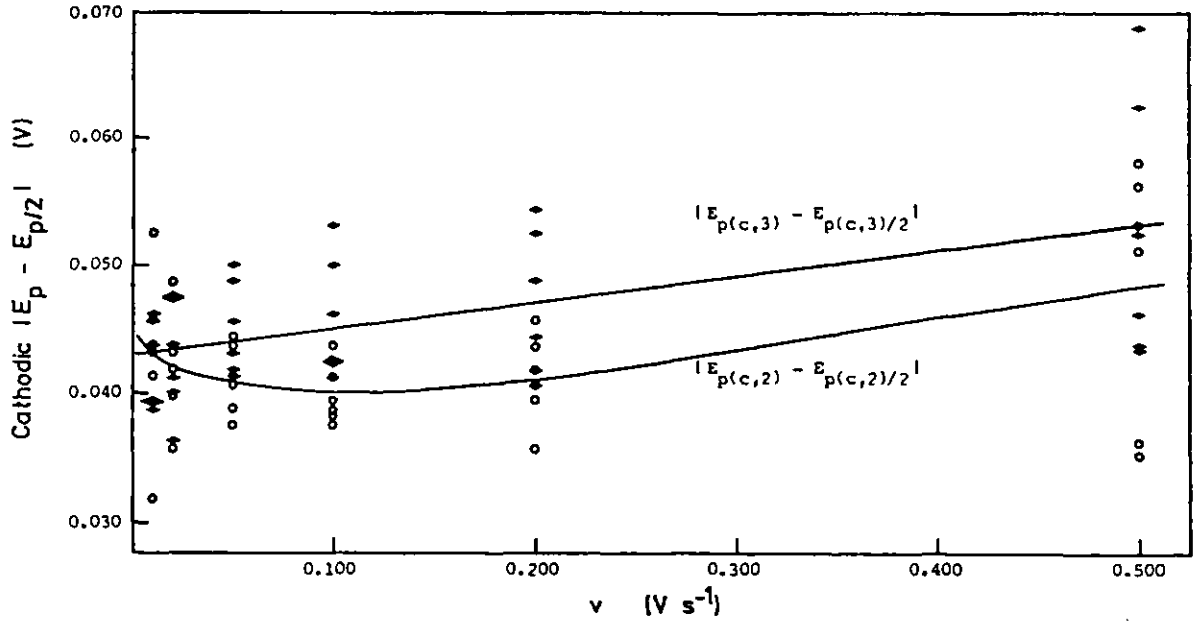

Fig. 5-219 Ir(IV) Perchlorate (1.0×10^{-4} mol dm^{-3})/Perchloric acid supporting electrolyte System: Values of the absolute difference between cathodic peak and half-peak potential, $|E_{p(c)} - E_{p(c)/2}|$, as a function of potential scan rate, v; at perchloric acid concentrations of 0.1 to 2.0 M. Graphite solid electrode.

(a) $|E_{p(c,2)} - E_{p(c,2)/2}|$ mean = 0.043 V
Standard deviation = 0.006 V
Coefficient of variation = 13.9%
Degrees of freedom = 35

(b) $|E_{p(c,3)} - E_{p(c,3)/2}| = 4.30 \times 10^{-2} + 2.02 \times 10^{-2}$ v
Correlation coefficient = 0.5312
Level of significance, $p = p < 0.001$
Standard deviation of $|E_{p(c,3)} - E_{p(c,3)/2}|$ from regression
= 0.006 V
Degrees of freedom = 34

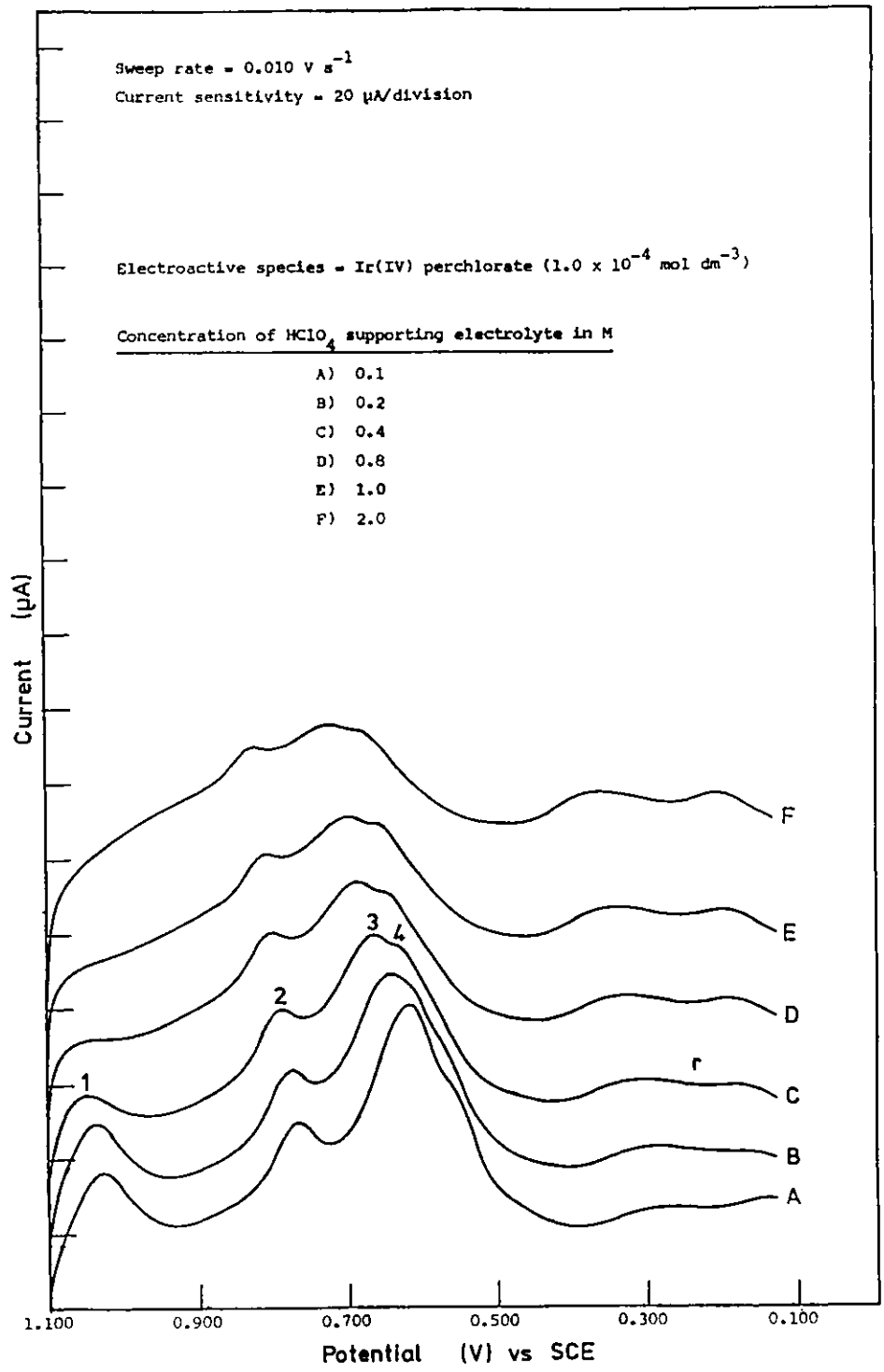

Fig. 5-220 Linear sweep voltammograms obtained at the graphite solid electrode — Variation with concentration of perchloric acid supporting electrolyte.

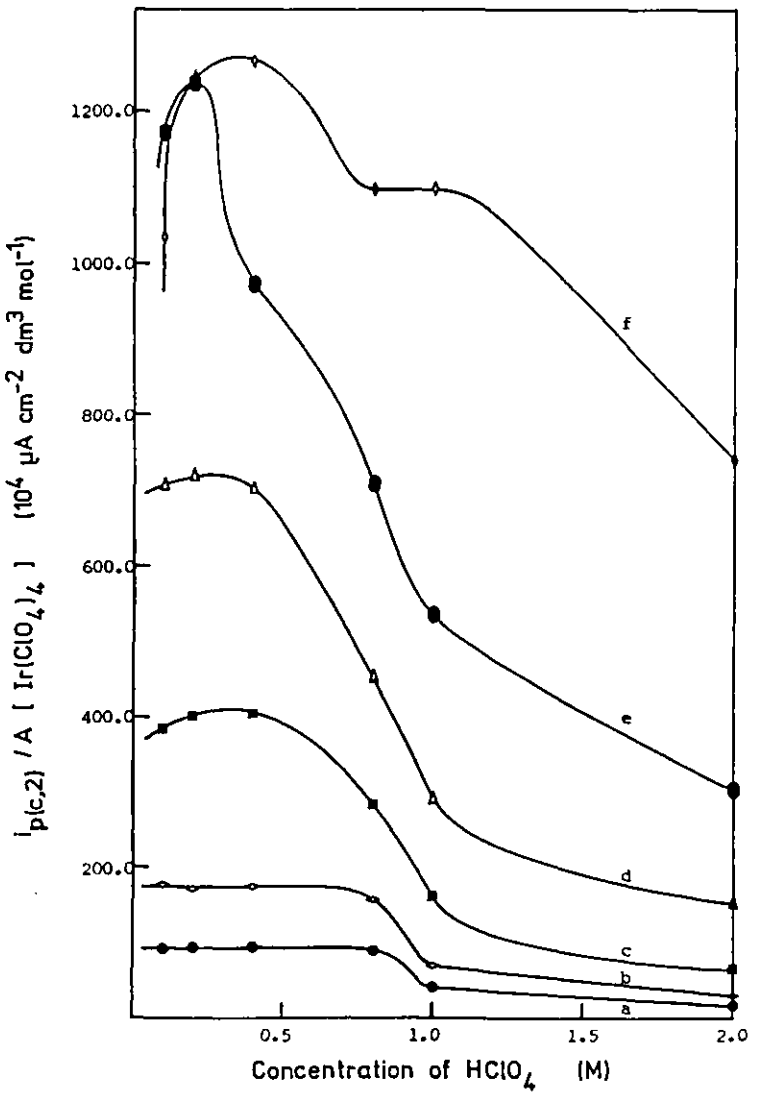

Fig. 5-221 Ir(IV) Perchlorate (1.0×10^{-4} mol dm^{-3})/Perchloric acid supporting electrolyte System: Values of cathodic peak current per unit area divided by concentration of Ir(IV) Perchlorate, $i_{p(c,2)}/A$ [$Ir(ClO_4)_4$], as a function of concentration of perchloric acid; at potential scan rates (a) 0.010, (b) 0.020, (c) 0.050, (d) 0.100, (e) 0.200, and (f) 0.500 V s^{-1}. Graphite solid electrode.

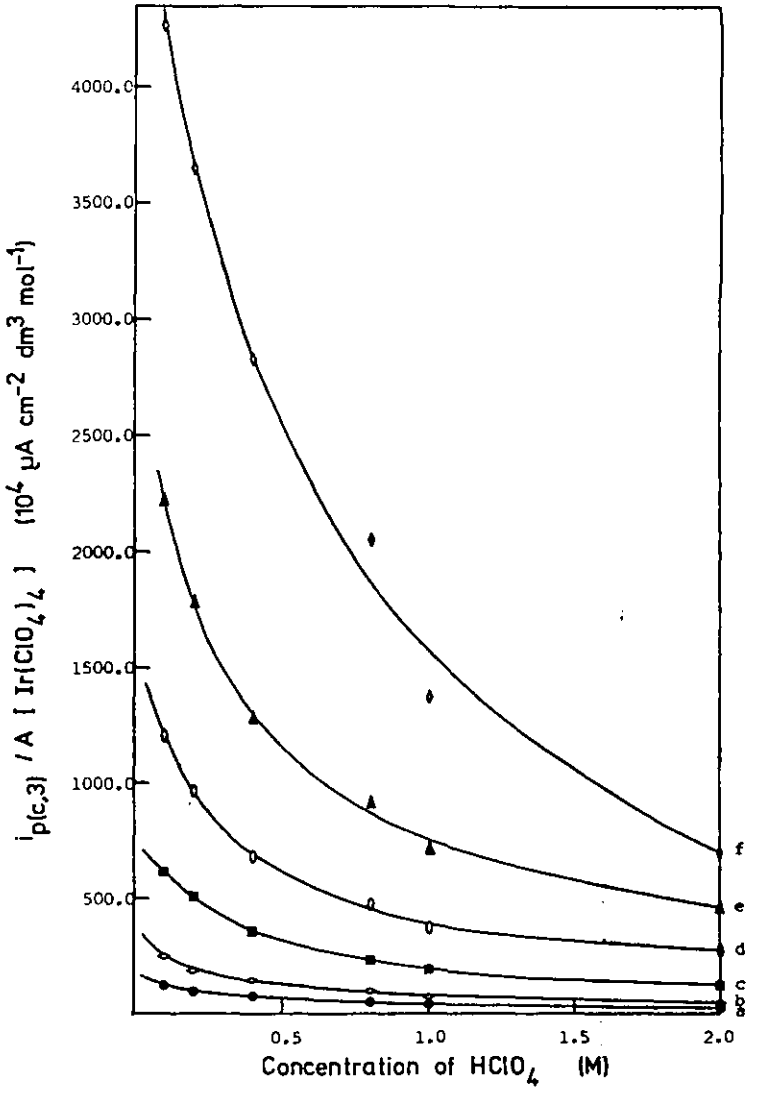

Fig. 5-222 Ir(IV) Perchlorate (1.0×10^{-4} mol dm^{-3})/Perchloric acid supporting electrolyte System: Values of cathodic peak current per unit area divided by concentration of Ir(IV) Perchlorate, $i_{p(c,3)}/A$ [$Ir(ClO_4)_4$], as a function of concentration of perchloric acid; at potential scan rates (a) 0.010, (b) 0.020, (c) 0.050, (d) 0.100, (e) 0.200, and (f) 0.500 V s^{-1}. Graphite solid electrode.

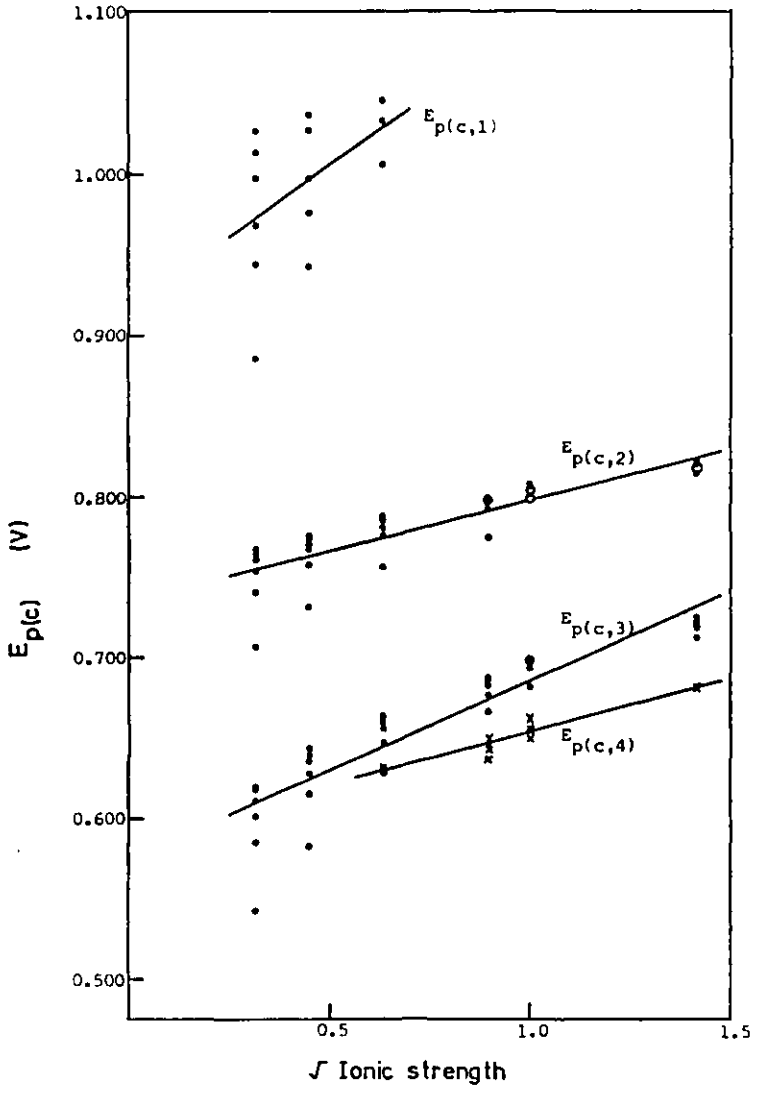

Fig. 5-223 Ir(IV) Perchlorate (1.0×10^{-4} mol dm^{-3})/Perchloric acid (0.1 to 2.0 M) supporting electrolyte System: Values of cathodic *peak potential*, $E_{p(c)}$, *as a function of square root of total ionic* strength, $\sqrt{I}$ (where the concentration of perchloric acid was varied); at potential scan rates of 0.010 to 0.500 V s^{-1}. Graphite solid electrode.

(a) $E_{p(c,1)}$ mean = 0.993 V
Standard deviation = 0.045 V
Coefficient of variation = 4.55%
Degrees of freedom = 13

(b) $E_{p(c,2)} = 0.734 + 6.39 \times 10^{-2} \sqrt{I}$
Correlation coefficient = 0.8774
Level of significance, p = $p < 0.001$
Standard deviation of $E_{p(c,2)}$ from regression = 0.013 V
Degrees of freedom = 34

(c) $E_{p(c,3)} = 0.574 + 0.112 \sqrt{I}$
Correlation coefficient = 0.9169
Level of significance, p = $p < 0.001$
Standard deviation of $E_{p(c,3)}$ from regression = 0.018 V
Degrees of freedom = 34

(d) $E_{p(c,4)} = 0.589 + 6.56 \times 10^{-2} \sqrt{I}$
Correlation coefficient = 0.9681
Level of significance, p = $p < 0.001$
Standard deviation of $E_{p(c,4)}$ from regression = 0.004 V
Degrees of freedom = 14

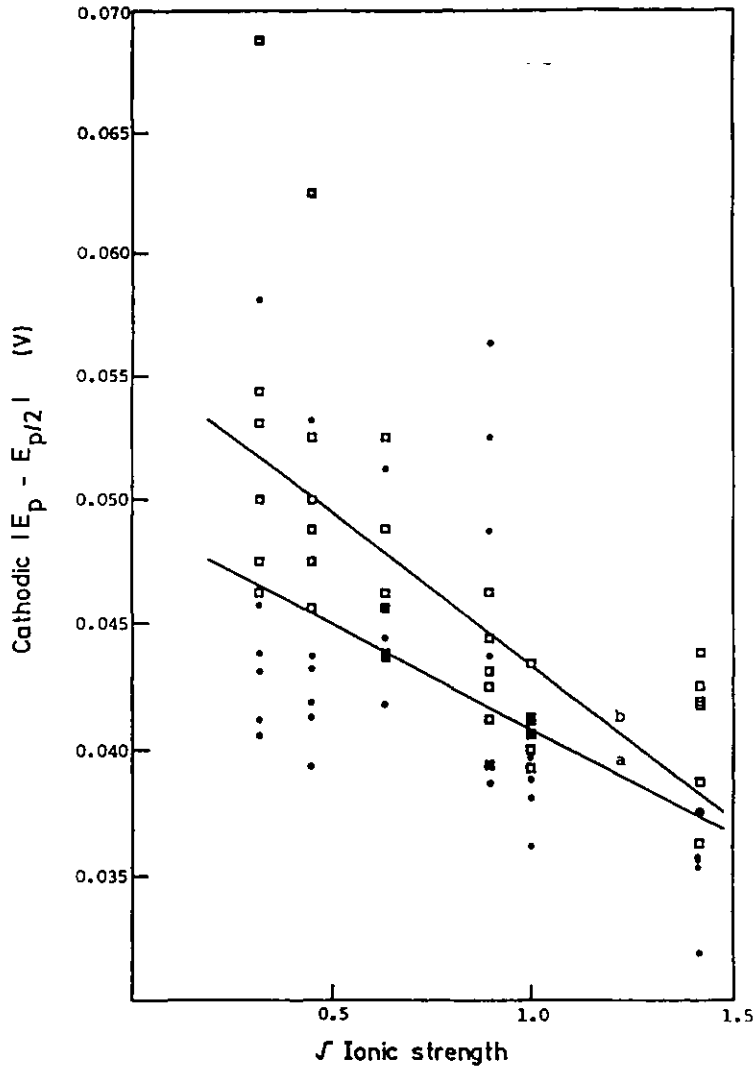

Fig. 5-224 Ir(IV) Perchlorate (1.0×10^{-4} mol dm^{-3})/Perchloric acid (0.1 to 2.0 M) supporting electrolyte System: Values of the absolute difference between cathodic peak and half-peak potential, $|E_{p(c)} - E_{p(c)/2}|$, as a function of square root of total ionic strength, $\sqrt{I}$ (where the concentration of perchloric acid was varied); at potential scan rates of 0.010 to 0.500 V s^{-1}. Graphite solid electrode. (a) $|E_{p(c,2)} - E_{p(c,2)/2}|$, and (b) $|E_{p(c,3)} - E_{p(c,3)/2}|$.

(a) $|E_{p(c,2)} - E_{p(c,2)/2}| = 4.92 \times 10^{-2} - 8.43 \times 10^{-3} \sqrt{I}$
Correlation coefficient = -0.5299
Level of significance, p = $p < 0.001$
Standard deviation of $|E_{p(c,2)} - E_{p(c,2)/2}|$ from regression = 0.005 V
Degrees of freedom = 34

(b) $|E_{p(c,3)} - E_{p(c,3)/2}| = 5.56 \times 10^{-2} - 1.23 \times 10^{-2} \sqrt{I}$
Correlation coefficient = -0.6980
Level of significance, p = $p < 0.001$
Standard deviation of $|E_{p(c,3)} - E_{p(c,3)/2}|$ from regression = 0.005 V
Degrees of freedom = 34

5-1.5.(ii).m Effect of Ir(IV) perchlorate adsorption on the residual current at the working electrode

Variation of the residual current with sweep rate is shown by the linear sweep voltammograms obtained at the boron carbide solid electrode $B_{4.05}C$ (Fig. 5-225, Peak r). After treatment with Ir(IV) perchlorate (2.3×10^{-3} mol dm^{-3})/perchloric acid (0.1 M) solution, the $B_{4.05}C$ electrode was adsorbed with the Ir(IV) perchlorate species which was manifested in the cyclic and linear sweep voltammograms for the solution consisting of perchloric acid (0.1 M) alone (Fig. 5-226). Qualitatively, it can be seen that three cathodic peaks, Peaks 1, 2, and 3, were obtained for the Ir(IV) perchlorate species and their anodic counterparts were also exhibited in cyclic voltammetry; thus suggesting some degree of reversibility in the respective charge transfers. Increasing sweep rates caused Peak 3 to dominate Peak 2; indicating that Peak 3 was a post-peak due to the strong adsorption of reactant.

Quantitative treatment of the interpretable peaks shows that all the peaks exhibited, including the residual current peak, were influenced by adsorption (Fig. 5-227). The peak potentials and the limiting background potential (where the residual current exceeds 1 μA) are plotted against sweep rate in Fig. 5-228. In general, all the peak potentials were cathodically shifted by the increasing sweep rate whilst the limiting background potential was anodically shifted. The differences between the Ir(IV) perchlorate peak potentials as functions of the sweep rate are shown in Fig. 5-229, which also indicates that $|E_{p(c,1)} - E_{p(c,1)/2}|$ and $|E_{p(c,2)} - E_{p(c,2)/2}|$ were independent of sweep rate. Thus it is reasonable to conclude that Peaks 1 and 2 were affected by the adsorption of reactant (c.f. Fig. 3-16). $|E_{p(c,r)} - E_{p(c,r)/2}|$ for the residual current, however, initially narrowed with increasing sweep rate before faster rates reversed the trend to end with wider values (Fig. 5-229).

The evidence suggests that the voltammograms for the adsorbed Ir(IV) perchlorate species (Fig. 5-226) were similar to the voltammograms obtained for Ir(IV) perchlorate (1.0×10^{-4} mol dm^{-3}) in perchloric acid (0.1 M) supporting electrolyte (Fig. 5-129); except that the diffusion peak complicated by weak adsorption which was exhibited (at approximately 0.9 V vs. SCE) for the Ir(IV) perchlorate solution was absent when only the species adsorbed onto the electrode was considered. The behaviour and characteristics of the mutually exhibited peaks, however, clearly

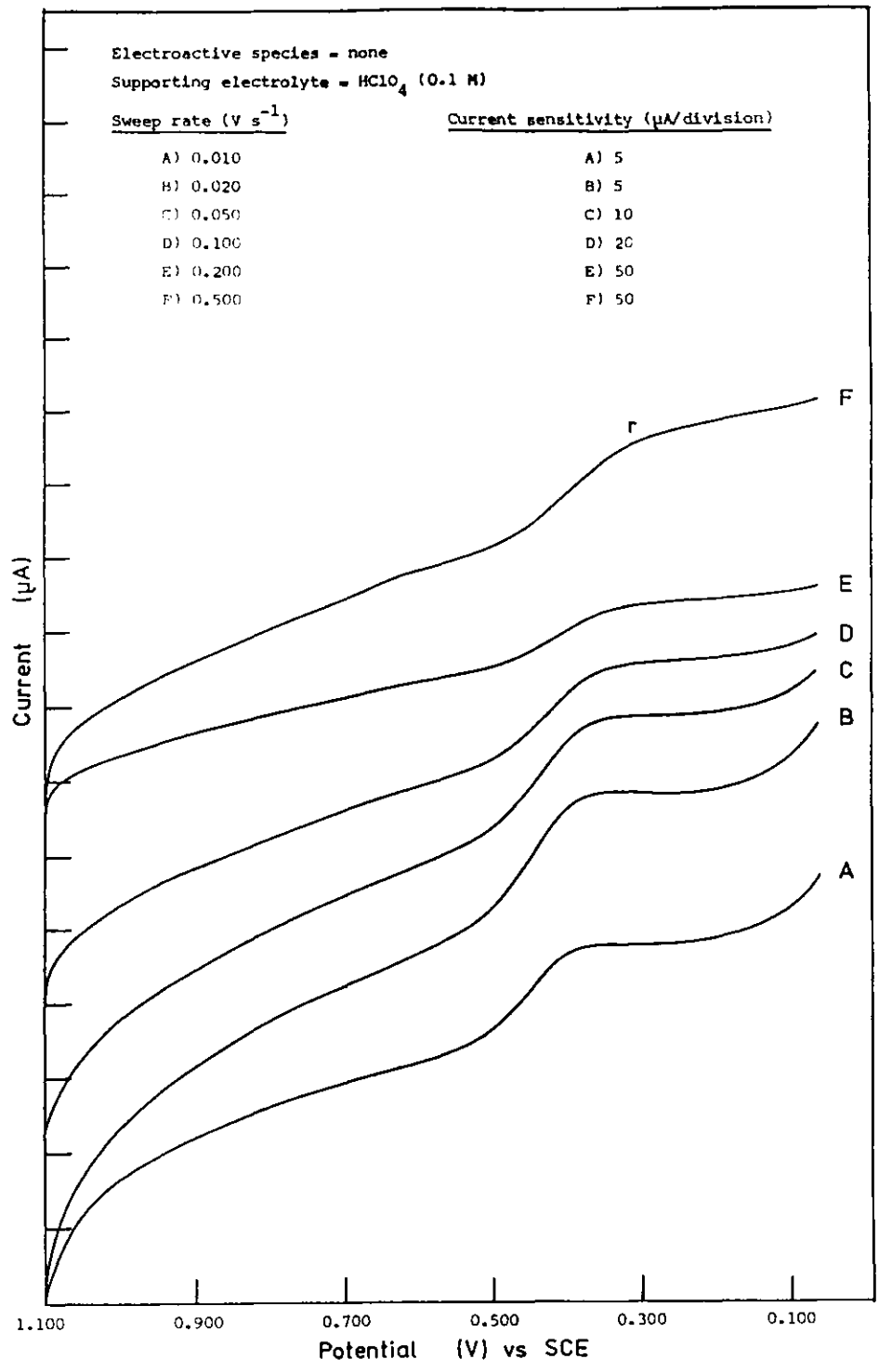

Fig. 5-225 Linear sweep voltammograms for the residual current obtained at the boron carbide solid electrode $B_{4.05}C$ — Variation with sweep rate.

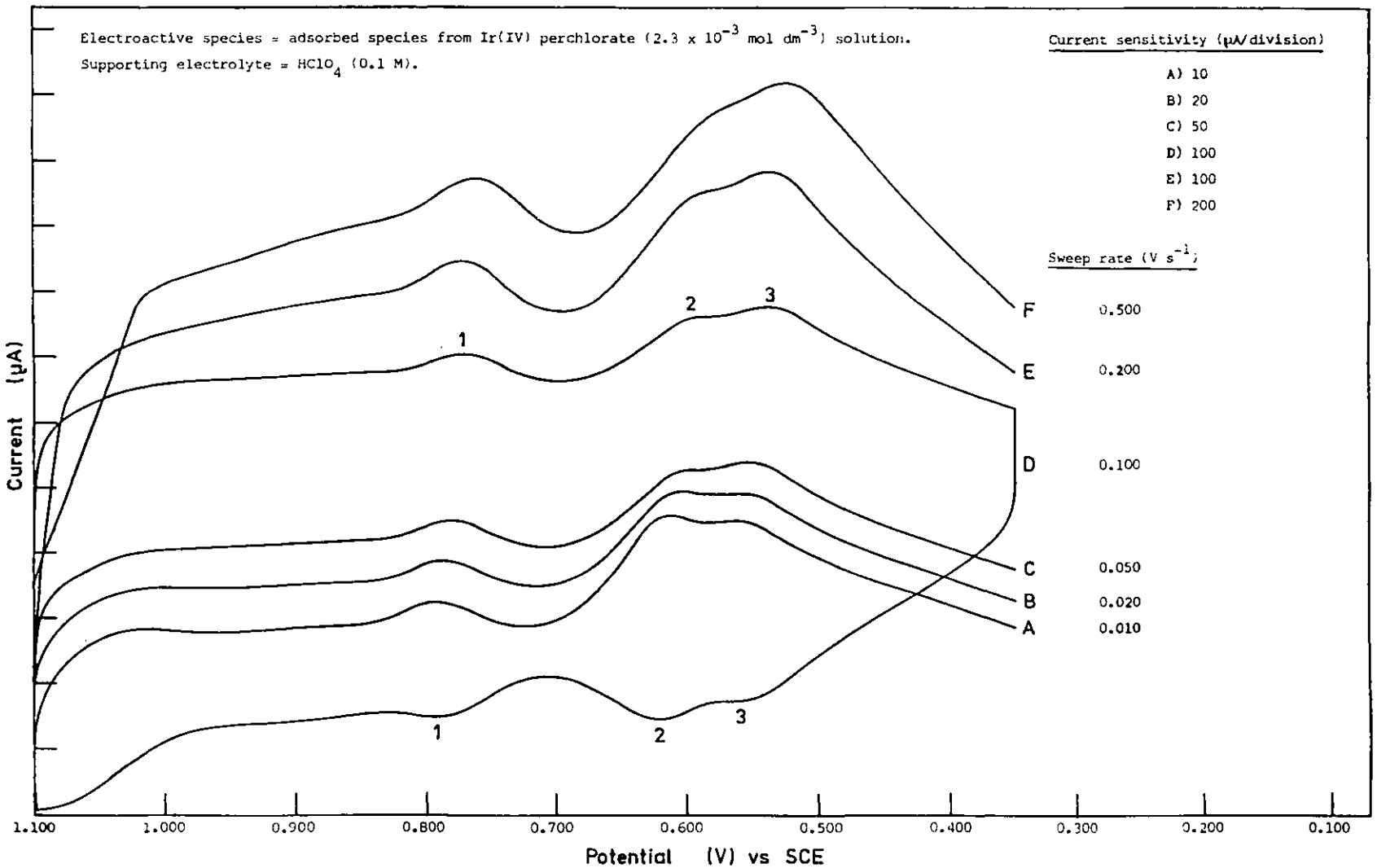

Fig. S-226 Perchloric acid (0.1 M) supporting electrolyte: Cyclic and linear sweep voltammograms obtained at the boron carbide solid electrode $b_{4.05}C$ which had been treated with Ir(IV) perchlorate.

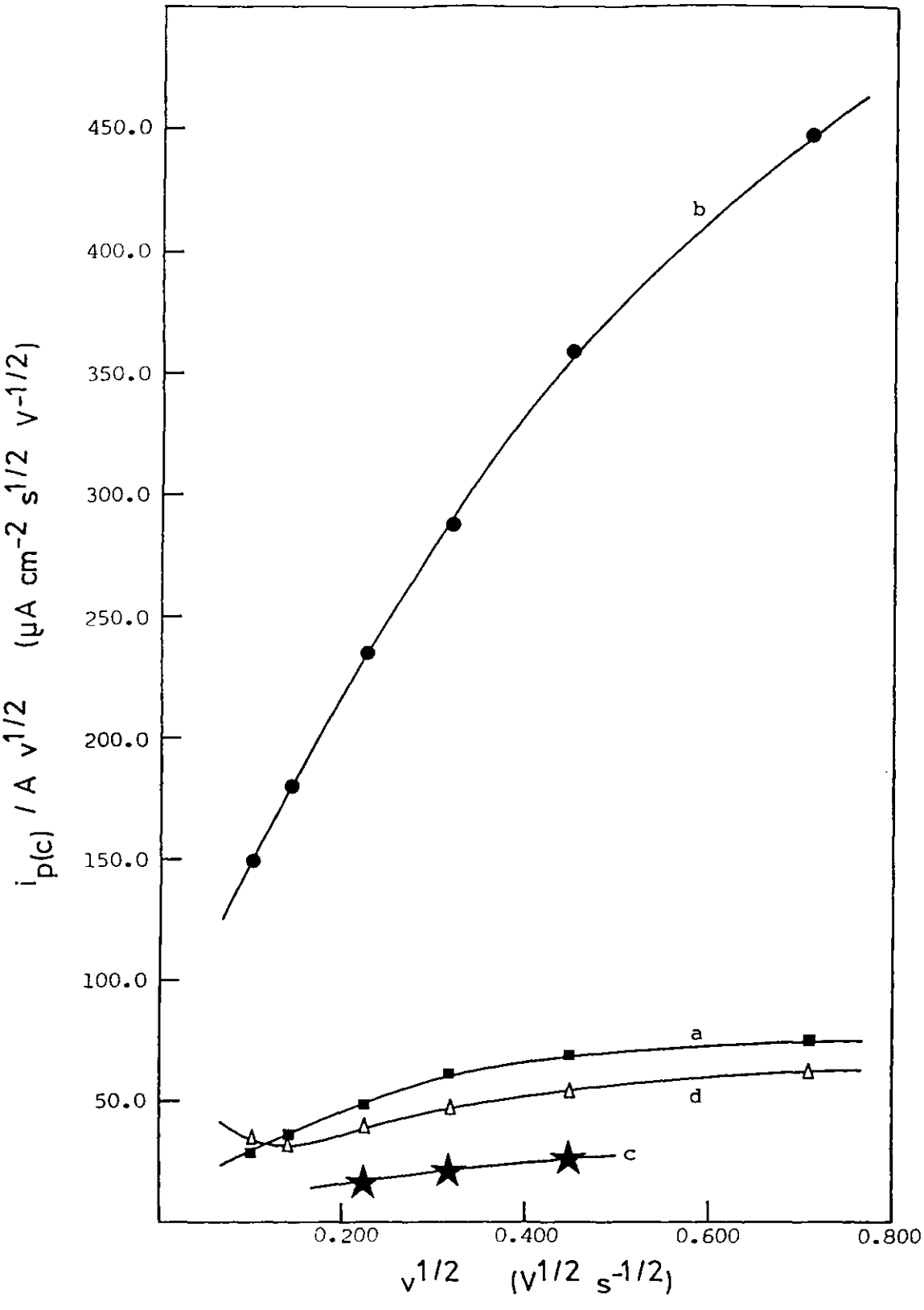

Fig. 5-227 Perchloric acid (0.1 M) supporting electrolyte: Values of cathodic current function, $i_{p(c)}/A\ v^{\frac{1}{2}}$, as a function of square root of potential scan rate, $v^{\frac{1}{2}}$. Boron carbide solid electrode, $B_{4.05}C$, was treated with Ir(IV) Perchlorate (2.3×10^{-3} M): (a) $i_{p(c,1)}/A\ v^{\frac{1}{2}}$, (b) $i_{p(c,2)}/A\ v^{\frac{1}{2}}$, and (c) $i_{p(c,3)}/A\ v^{\frac{1}{2}}$. (d) Residual current function, $i_{p(c,r)}/A\ v^{\frac{1}{2}}$, of untreated electrode.

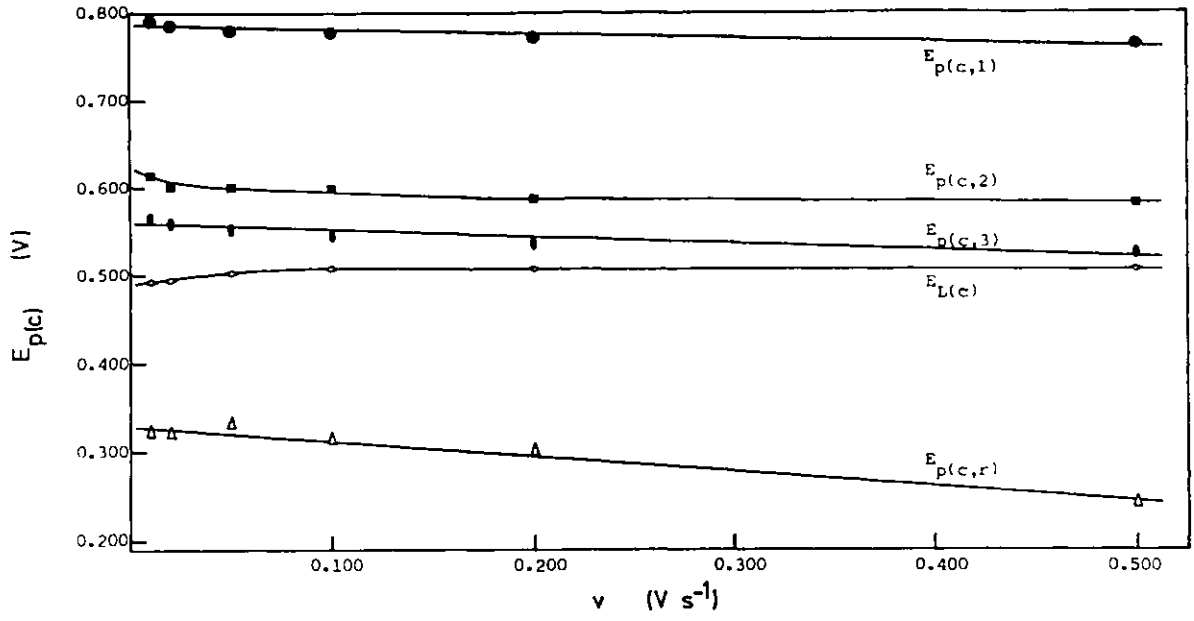

Fig. 5-228 Perchloric acid (0.1 M) supporting electrolyte: Values of cathodic peak potential, $E_{p(c)}$, as a function of potential scan rate, v. (i) Boron carbide solid electrode $B_{4.05}C$ was treated with Ir(IV) Perchlorate (2.3×10^{-3} M): $E_{p(c,1)}$, $E_{p(c,2)}$, and $E_{p(c,3)}$. (ii) Untreated electrode: $E_{p(c,r)}$, and background cathodic limiting potential, $E_{L(c)}$.

(a) $E_{p(c,1)} = 0.786 - 5.10 \times 10^{-2}$ v
Correlation coefficient = -0.9254
Level of significance, $p = 0.001 < p < 0.01$
Standard deviation of $E_{p(c,1)}$ from regression = 0.004 V
Degrees of freedom = 4

(b) $E_{p(c,2)}$ mean = 0.597 V
Standard deviation = 0.012 V
Coefficient of variation = 1.93%
Degrees of freedom = 5

(c) $E_{p(c,3)} = 0.558 - 7.54 \times 10^{-2}$ v
Correlation coefficient = -0.9247
Level of significance, $p = 0.001 < p < 0.01$
Standard deviation of $E_{p(c,3)}$ from regression = 0.006 V
Degrees of freedom = 4

(d) $E_{p(c,r)} = 0.329 - 0.172$ v
Correlation coefficient = -0.9779
Level of significance, $p = p < 0.001$
Standard deviation of $E_{p(c,r)}$ from regression = 0.008 V
Degrees of freedom = 4

(e) $E_{L(c)}$ mean = 0.501 V
Standard deviation = 0.006 V
Coefficient of variation = 1.29%
Degrees of freedom = 5

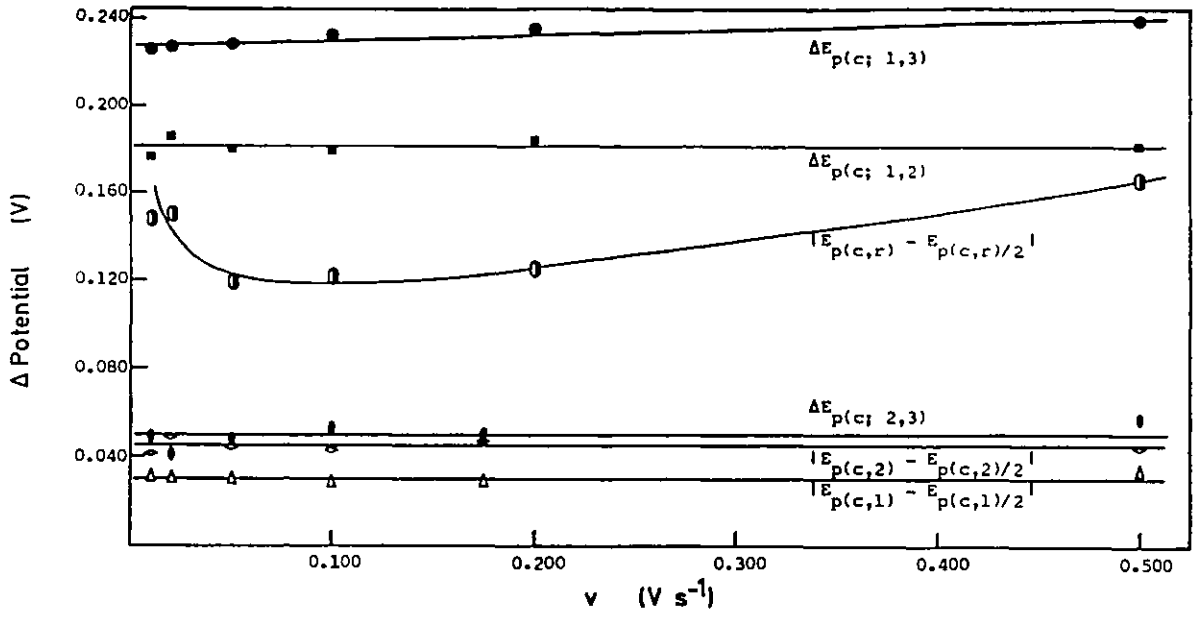

Fig. 5-229 Perchloric acid (0.1 M) supporting electrolyte: Values of the difference between cathodic peak potentials, $\Delta E_{p(c)}$, and the absolute difference between cathodic peak and half-peak potential, $|E_{p(c)} - E_{p(c)/2}|$, as a function of potential scan rate, v. Boron carbide solid electrode $B_{4.05}C$ was treated with Ir(IV) Perchlorate (2.3×10^{-3} M).

(a) $\Delta E_{p(c;\ 1,2)}$ mean = 0.181 V
Standard deviation = 0.003 V
Coefficient of variation = 1.79%
Degrees of freedom = 5

(b) $\Delta E_{p(c;\ 2,3)}$ mean = 0.050 V
Standard deviation = 0.005 V
Coefficient of variation = 10.0%
Degrees of freedom = 5

(c) $\Delta E_{p(c;\ 1,3)} = 0.228 + 2.44 \times 10^{-2}\ v$
Correlation coefficient = 0.9076
Level of significance, $p = 0.01 < p < 0.02$
Standard deviation of $\Delta E_{p(c;\ 1,3)}$ from regression = 0.002 V
Degrees of freedom = 4

(d) $|E_{p(c,1)} - E_{p(c,1)/2}|$ mean = 0.030 V
Standard deviation = 0.002 V
Coefficient of variation = 5.88%
Degrees of freedom = 5

(e) $|E_{p(c,2)} - E_{p(c,2)/2}|$ mean = 0.045 V
Standard deviation = 0.003 V
Coefficient of variation = 6.04%
Degrees of freedom = 5

indicate that for the voltammograms of the adsorbed Ir(IV) perchlorate species alone (Fig. 5-226): Peak 1 was a post-peak (relative to the diffusion peak which was not exhibited) due to the extremely strong physical adsorption of Ir(IV) perchlorate reactant, Peak 2 was a diffusion peak complicated by weak adsorption, and Peak 3 was a post-peak due to the strong adsorption of reactant. The similarities can be further noticed by comparing the peak potentials in Fig. 5-228 with those in Fig. 5-136 for the $B_{4.05}C$ electrode.

For the graphite solid electrode, linear sweep voltammograms of the residual current for perchloric acid (0.1 M) supporting electrolyte and cyclic voltammograms of the adsorbed Ir(IV) perchlorate species are presented in Fig. 5-230. When compared with the voltammograms of Ir(IV) perchlorate (1.0×10^{-4} mol dm^{-3}) solution (Fig. 5-214), it can clearly be seen that the voltammograms for the adsorbed species from the Ir(IV) perchlorate (1.0×10^{-4} mol dm^{-3}) treatment solution (Fig. 5-230) are very similar to the voltammograms for the Ir(IV) perchlorate solution itself. Plots of the peak current function, for the interpretable peaks, against $(\text{sweep rate})^{\frac{1}{2}}$ show that Peaks 2 and 3 as well as the residual current peak, Peak r, were influenced by adsorption (Fig. 5-231). The peak potentials and the limiting background potential, $E_{L(c)}$ (where the residual current exceeds 1 μA), are plotted as functions of the sweep rate in Fig. 5-232. The cathodic peak potentials were cathodically shifted whilst the anodic peak potentials were anodically shifted by increasing sweep rate; thus reflecting a decrease in the reversibility of the charge transfers. This conclusion about decreased reversibility is reinforced by Fig. 5-233 which shows that, in general, $|E_p - E_{p/2}|$ values widened with increasing sweep rate.

The evidence suggests that the characteristics and behaviour of the voltammograms for the adsorbed Ir(IV) perchlorate species were very similar to the voltammograms for Ir(IV) perchlorate solution itself; for example when comparing the respective peak potentials (Fig. 5-232 c.f. Fig. 5-218) obtained for the two different experimental conditions at the graphite solid electrode.

5-1.5.(ii).n Summary

Linear sweep and cyclic voltammetric investigations of the Ir(IV) perchlorate/perchloric acid supporting electrolyte system have served to emphasise the dominance of the extremely strong physical adsorption of Ir(IV) perchlorate reactant on the electrochemistry of the system at

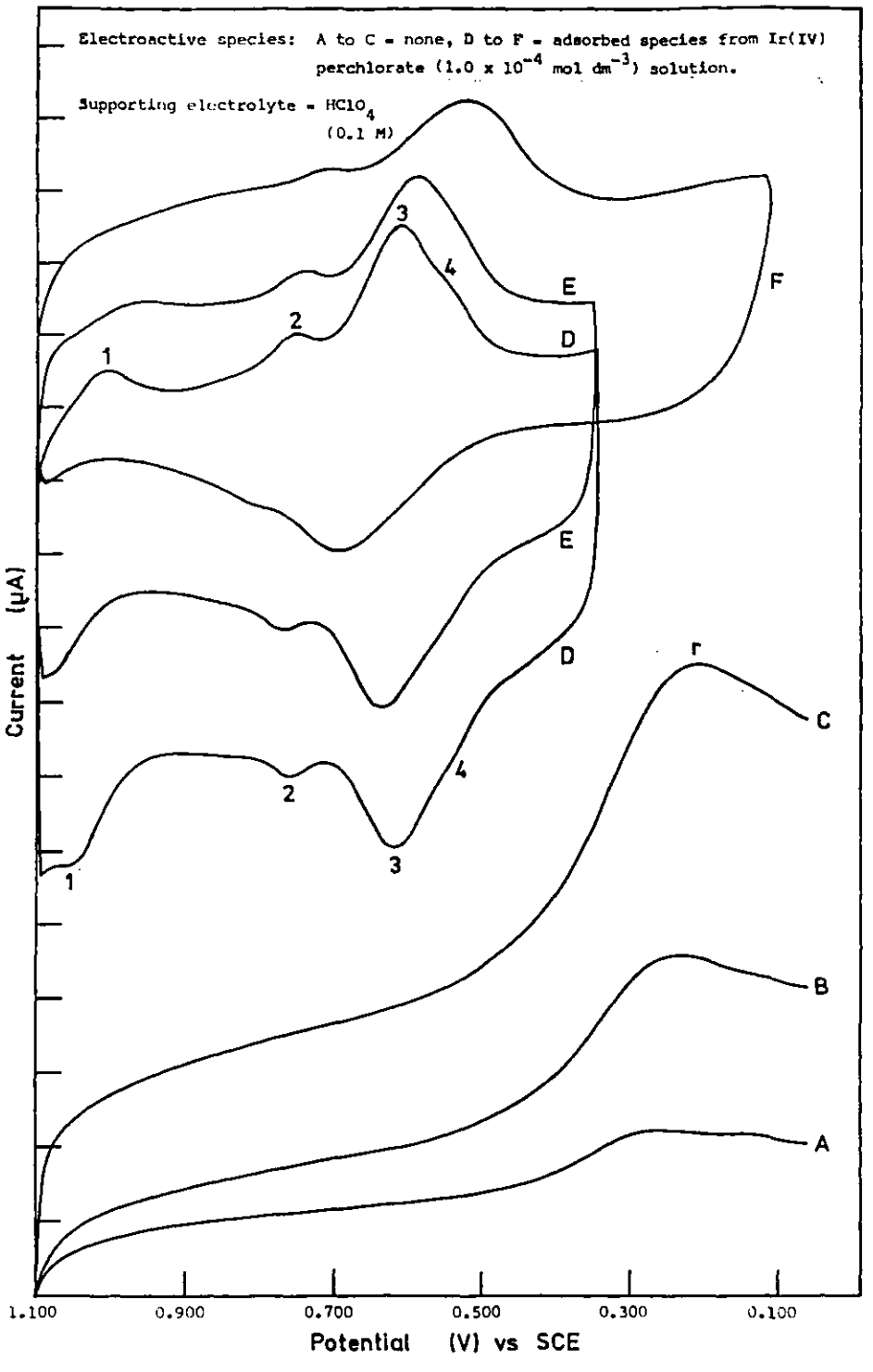

Fig. 5-230 Perchloric acid (0.1 M): Linear sweep voltammograms for the residual current (A to C) and cyclic voltammograms for the adsorbed Ir(IV) perchlorate species (D to F) obtained at the graphite solid electrode.

	Sweep rate (V s^{-1})	Current sensitivity (μA/division)
A)	0.010	20
B)	0.020	20
C)	0.100	50
D)	0.010	20
E)	0.100	200
F)	0.500	1000

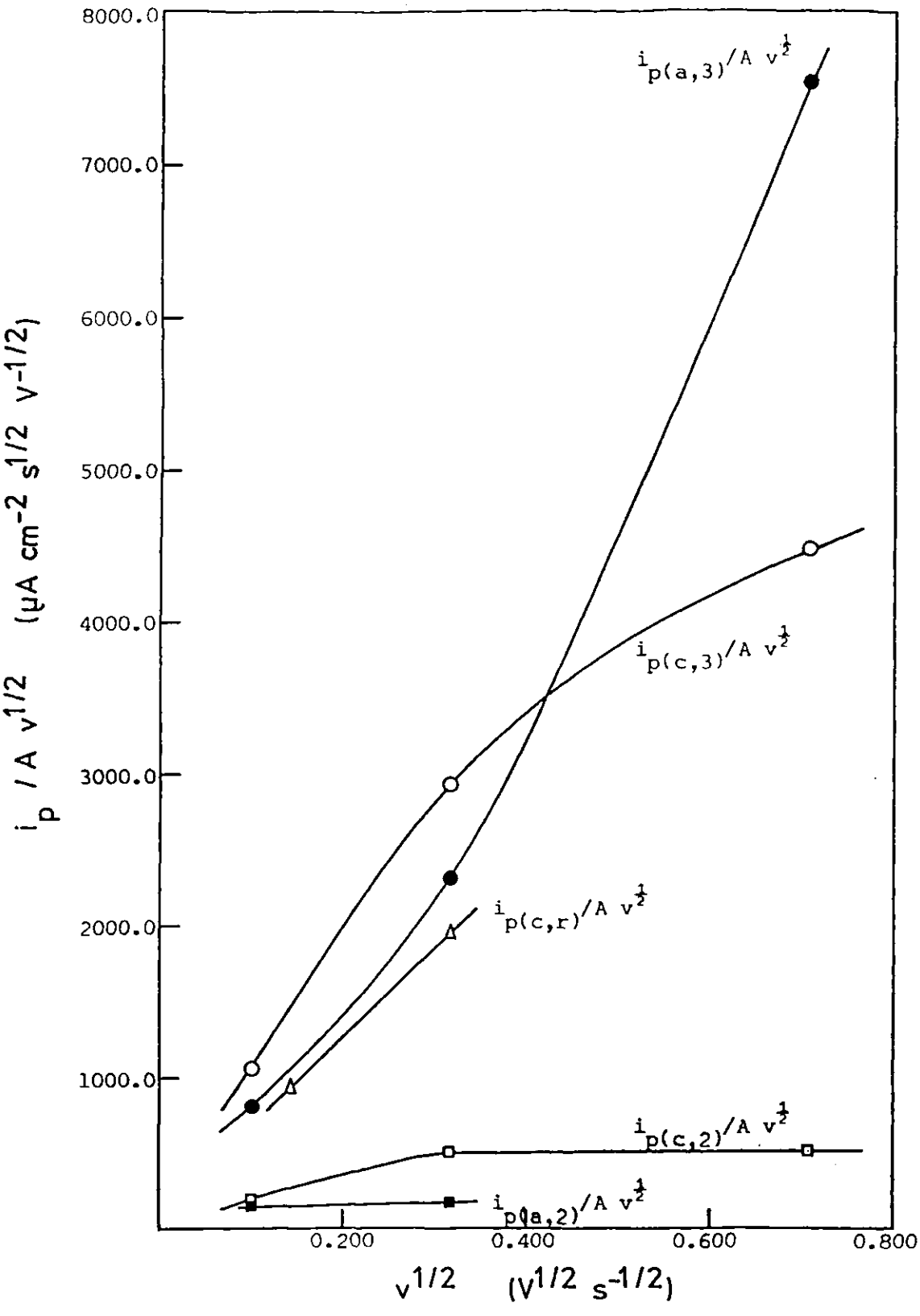

Fig. 5-231 Perchloric acid (0.1 M) supporting electrolyte: Values of cathodic and anodic current functions, $i_{p(c)}/A\ v^{\frac{1}{2}}$ and $i_{p(a)}/A\ v^{\frac{1}{2}}$ respectively, as a function of square root of potential scan rate. (i) Graphite solid electrode was treated with Ir(IV) Perchlorate (1.0×10^{-4} M) solution: $i_{p(c,2)}/A\ v^{\frac{1}{2}}$, $i_{p(c,3)}/A\ v^{\frac{1}{2}}$, $i_{p(a,2)}/A\ v^{\frac{1}{2}}$, and $i_{p(a,3)}/A\ v^{\frac{1}{2}}$. (ii) Untreated electrode: $i_{p(c,r)}/A\ v^{\frac{1}{2}}$.

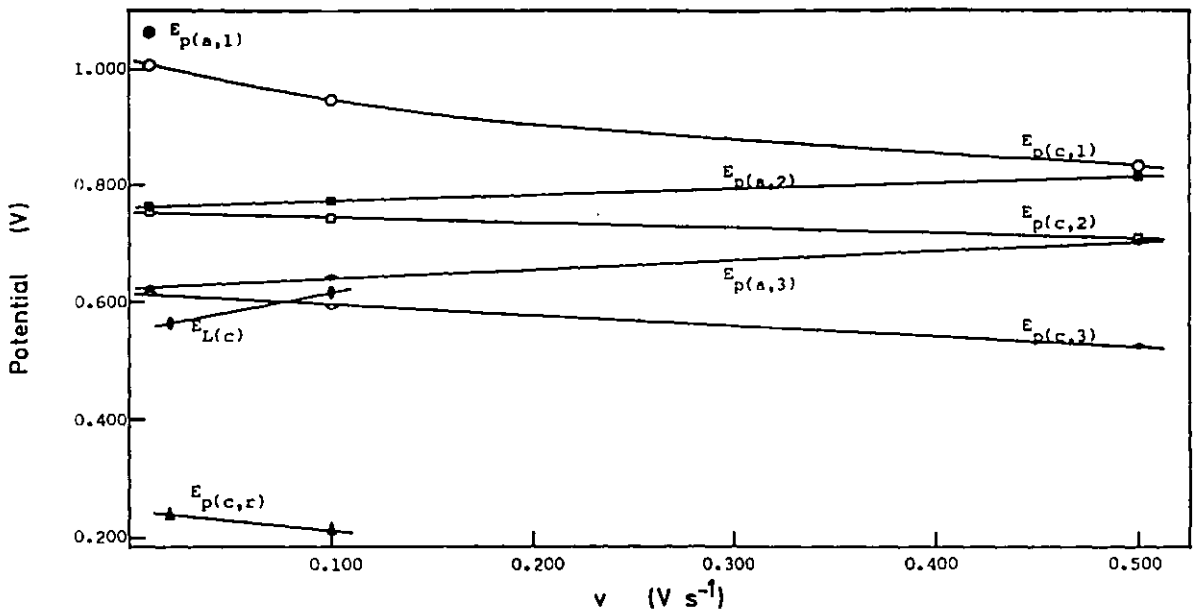

Fig. 5-232 Perchloric acid (0.1 M) supporting electrolyte: Values of cathodic peak potential, $E_{p(c)}$, background cathodic limiting potential, $E_{L(c)}$, and anodic peak potential, $E_{p(a)}$, as functions of potential scan rate, v. (i) Graphite solid electrode was treated with Ir(IV) Perchlorate (1.0×10^{-4} M) solution: $E_{p(c,1)}$, $E_{p(c,2)}$, $E_{p(c,3)}$, $E_{p(a,1)}$, $E_{p(a,2)}$, and $E_{p(a,3)}$. (ii) Untreated electrode: $E_{p(c,r)}$, and $E_{L(c)}$.

(a) $E_{p(c,1)}$ mean = 0.928 V
Standard deviation = 0.090 V
Coefficient of variation = 9.67%
Degrees of freedom = 2

(b) $E_{p(c,2)} = 0.753 - 9.32 \times 10^{-2}$ v
Correlation coefficient = -0.99733
Level of significance, $p = 0.02 < p < 0.05$
Standard deviation of $E_{p(c,2)}$ from regression = 0.002 V
Degrees of freedom = 1

(c) $E_{p(c,3)} = 0.612 - 0.181$ v
Correlation coefficient = -0.99730
Level of significance, $p = 0.02 < p < 0.05$
Standard deviation of $E_{p(c,3)}$ from regression = 0.005 V
Degrees of freedom = 1

(d) $E_{p(a,2)} = 0.762 + 0.101$ v
Correlation coefficient = 0.99998
Level of significance, $p = 0.001 < p < 0.01$
Standard deviation of $E_{p(a,2)}$ from regression = 0.0003 V
Degrees of freedom = 1

(e) $E_{p(a,3)} = 0.623 + 0.154$ v
Correlation coefficient = 0.99758
Level of significance, $p = 0.02 < p < 0.05$
Standard deviation of $E_{p(a,3)}$ from regression = 0.004 V
Degrees of freedom = 1

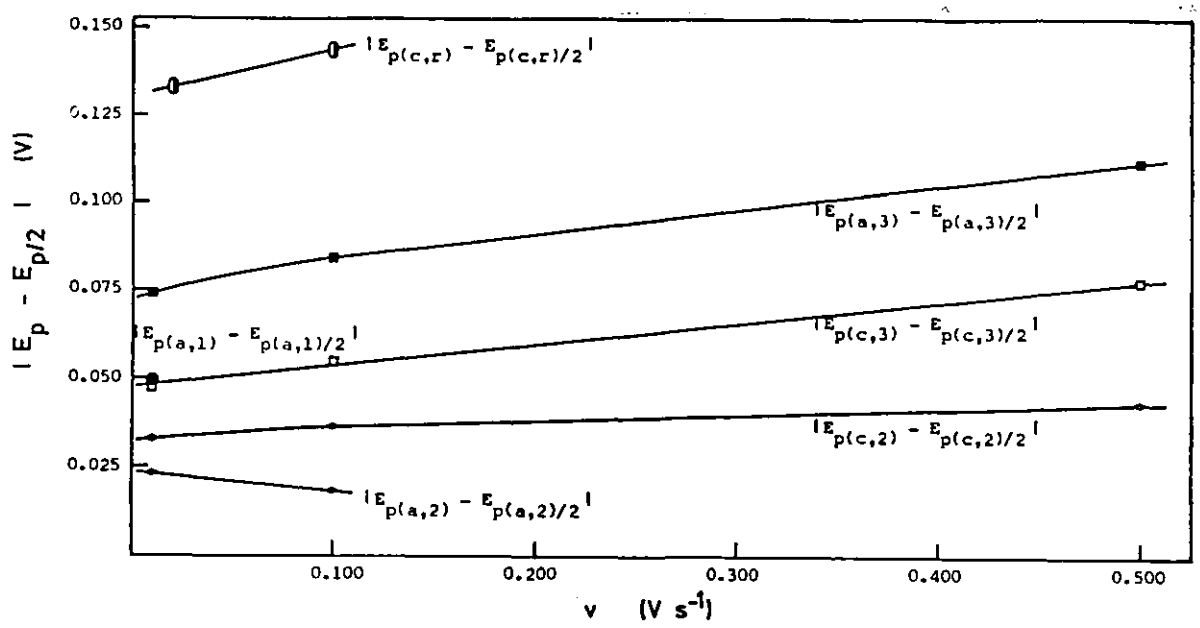

Fig. 5-233 Perchloric acid (0.1 M) supporting electrolyte: Values of the absolute difference between peak and half-peak potential, $|E_p - E_{p/2}|$, as a function of potential scan rate, v. (i) Graphite solid electrode was treated with Ir(IV) Perchlorate (1.0×10^{-4} M) solution: $|E_{p(c,2)} - E_{p(c,2)/2}|$, $|E_{p(c,3)} - E_{p(c,3)/2}|$, $|E_{p(a,1)} - E_{p(a,1)/2}|$, $|E_{p(a,2)} - E_{p(a,2)/2}|$, and $|E_{p(a,3)} - E_{p(a,3)/2}|$. (ii) Untreated electrode: $|E_{p(c,r)} - E_{p(c,r)/2}|$

(a) $|E_{p(c,3)} - E_{p(c,3)/2}| = 4.76 \times 10^{-2} + 6.02 \times 10^{-2}\ v$

Correlation coefficient = 0.99885

Level of significance, $p = 0.02 < p < 0.05$

Standard deviation of $|E_{p(c,3)} - E_{p(c,3)/2}|$ from regression = 0.001 V

Degrees of freedom = 1

boron carbide, boron carbide/carbon composite, and graphite solid electrodes. In general, the voltammograms obtained at all the electrodes investigated were similar and the observed differences were merely reflections of the relative importance of the adsorption effects with respect to the other processes of diffusion, rate of charge transfer, and catalytic reaction with perchloric acid that also occurred. It has been observed that the strength of adsorption was greater at electrodes of higher carbon composition. Thus, at the low end of the scale for carbon composition, the voltammograms obtained at the $B_{4.05}C$ electrode (Fig. 5-129 and Fig. 5-135) exhibited three peaks at slow sweep rates but four peaks at faster rates. The evidence (section 5-1.5.(ii).a) suggests that Peak 1 (at approximately 0.9 V vs. SCE) was a reversible charge transfer complicated by a weak adsorption effect (probably due to the strong adsorption post-peak, Peak 2) and, when the concentration of e.a.s. was low, also by a weak catalytic reaction. The reversibility of the charge transfer for Peak 1 deteriorated with increasing sweep rate. Peak 2 (at approximately 0.8 V vs. SCE) was the post-peak, relative to Peak 1, due to the strong adsorption of Ir(IV) perchlorate reactant; but it was also complicated by a catalytic reaction involving perchloric acid. Peak 3 (at approximately 0.6 V vs. SCE) was a reversible charge transfer complicated by a weak adsorption effect (probably as a result of the moderately strong adsorption post-peak, Peak 4) and, at low concentrations of e.a.s., it was also affected by a catalytic reaction. The reversibility of the charge transfer for Peak 3 also deteriorated with increasing sweep rate. Finally, Peak 4 (at approximately 0.56 V vs. SCE) was a post-peak, relative to Peak 3, due to the moderately strong adsorption of reactant. The extremely strong adsorption of Ir(IV) perchlorate onto the $B_{4.05}C$ electrode is clearly emphasised in Fig. 5-226 which presents the linear sweep and cyclic voltammograms obtained in perchloric acid (0.1 M) solution alone at the boron carbide electrode treated with Ir(IV) perchlorate beforehand. The adsorbed Ir(IV) species displayed only the latter three peaks above; that is, the peaks at approximately 0.8 V, 0.6 V, and 0.56 V (vs. SCE). The diffusion peak at approximately 0.9 V (vs. SCE) was absent (section 5-1.5.(ii).m).

When the carbon composition of the working electrode was increased, the voltammograms for Ir(IV) perchlorate/perchloric acid supporting electrolyte solution generally displayed an enhancement of the adsorption peaks at the expense of the diffusion peaks (e.g. Fig. 5-196);

although there were variations, within the general trend, between individual electrodes. Thus the diffusion peak (at approximately 0.9 V vs. SCE) was absent whilst the strong adsorption peak, the diffusion peak, and the moderately strong adsorption peak (at approximately 0.78 V, 0.62 V, and 0.59 V vs. SCE respectively) were exhibited even at slow sweep rates. The increasing relative importance of adsorption effects over other processes for the voltammograms of Ir(IV) perchlorate/perchloric acid supporting electrolyte solution culminated at the boron carbide/carbon composite solid electrode $B_{2.56}C$ (Fig. 5-204); which is at the high end of the scale for carbon composition. Thus not only were the strong adsorption post-peak, diffusion peak, and moderately strong adsorption post-peak (at approximately 0.8 V, 0.66 V, and 0.63 V vs. SCE respectively) exhibited, coupled with the absence of the diffusion peak at approximately 0.9 V vs. SCE, but a quasi-reversible peak (at approximately 1.03 V vs. SCE) was also displayed. Despite the deterioration of this quasi-reversible peak with increasing sweep rate or increasing concentration of perchloric acid supporting electrolyte, its anodic position (at approximately 1.03 V vs. SCE) relative to the unexhibited diffusion peak (at approximately 0.9 V vs. SCE when displayed) suggests that this quasi-reversible peak could have been a pre-peak due to the strong adsorption of product.

The voltammograms for Ir(IV) perchlorate/perchloric acid supporting electrolyte solution obtained at the graphite solid electrode were similar to those obtained at the $B_{2.56}C$ electrode but the adsorption peaks were more prominent (Fig. 5-214 and Fig. 5-220). Thus the probable adsorption pre-peak, the adsorption post-peak, the diffusion peak, and the adsorption post-peak due to moderately strong adsorption of reactant were exhibited at approximately 1.04 V, 0.79 V, 0.66 V, and 0.65 V vs. SCE respectively. Further evidence that these peaks were adsorption and adsorption related peaks is furnished by Fig. 5-230 which presents the cyclic voltammograms obtained in perchloric acid (0.1 M) supporting electrolyte alone by use of the Ir(IV) perchlorate treated graphite solid electrode (section 5-1.5.(ii).m). As can be clearly seen, all the peaks obtained for Ir(IV) perchlorate/perchloric acid supporting electrolyte solution were also exhibited by the Ir(IV) perchlorate treated graphite solid electrode in perchloric acid supporting electrolyte alone.

The apparent anomaly of the anodic shift of all the peaks for Ir(IV) perchlorate with increasing ionic strength (as the concentration of perchloric acid supporting electrolyte was raised), despite the

cationic nature of the Ir(IV) species detected by paper electrophoresis, may be explained in terms of the debilitating influence of increasing perchloric acid concentration on the strength of the adsorption of Ir(IV) perchlorate onto the working electrode (boron carbide, boron carbide/carbon composite, or graphite solid electrode). Thus the peaks, which were initially shifted to less anodic potentials by the extremely strong adsorption of Ir(IV) perchlorate reactant, were merely reverting gradually to the more anodic potentials corresponding to adsorption-free charge transfers as the perchloric acid concentration was increased.

5-1.5.(iii) The influence of nitrogen aeration on the Ir(IV) perchlorate system.

D.c. voltammograms for nitrogen aerated (16 hours) Ir(IV) perchlorate (8.0×10^{-4} mol dm^{-3})/$HClO_4$ (0.1 M) supporting electrolyte solution were obtained at boron carbide, boron carbide/carbon composite, and graphite solid electrodes (Fig. 5-234). The effect of nitrogen aeration on αn values for Waves 1 and 2 (Fig. 5-234) is shown in Fig. 5-235. Statistical analysis of the results did not indicate any significant differences in αn values as a consequence of nitrogen aeration; thus $\alpha n_{(1)}$ grand mean = 1.08 ± 0.11 (12 degrees of freedom), and $\alpha n_{(2)}$ grand mean = 2.88 ± 0.18 (14 degrees of freedom). Neither was there any significant effect from nitrogen aeration on $E_{\frac{1}{2}}$ values (Fig. 5-236) nor on the limiting current density function, $i_L/A\ [Ir(ClO_4)_4]$ (Fig. 5-237); $E_{\frac{1}{2}(1)}$ grand mean = 0.953 V (vs. SCE) ± 0.006 V (12 degrees of freedom), and $E_{\frac{1}{2}(2)}$ grand mean = 0.640 V (vs. SCE) ± 0.003 V (14 degrees of freedom).

5-1.5.(iii).a Boron carbide solid electrode $B_{4.05}C$

Linear sweep voltammograms for nitrogen aerated (16 hours) Ir(IV) perchlorate (8.0×10^{-4} mol dm^{-3}), in perchloric acid (0.1 M) supporting electrolyte, obtained at the boron carbide solid electrode $B_{4.05}C$ are presented in Fig. 5-238. The three peaks exhibited, Peaks 1, 2, and 3, were influenced by adsorption (Fig. 5-239); Peak 2 being the post-peak, relative to Peak 1, due to the strong adsorption of Ir(IV) perchlorate reactant. The increasing dominance of Peak 2 over Peak 1 with increasing sweep rate is well illustrated by Fig. 5-238. Thus Peak 1 was a diffusion peak complicated by weak adsorption influences emanating from the strong adsorption post-peak, Peak 2. Peak 3, however, was a diffusion peak complicated by weak adsorption.

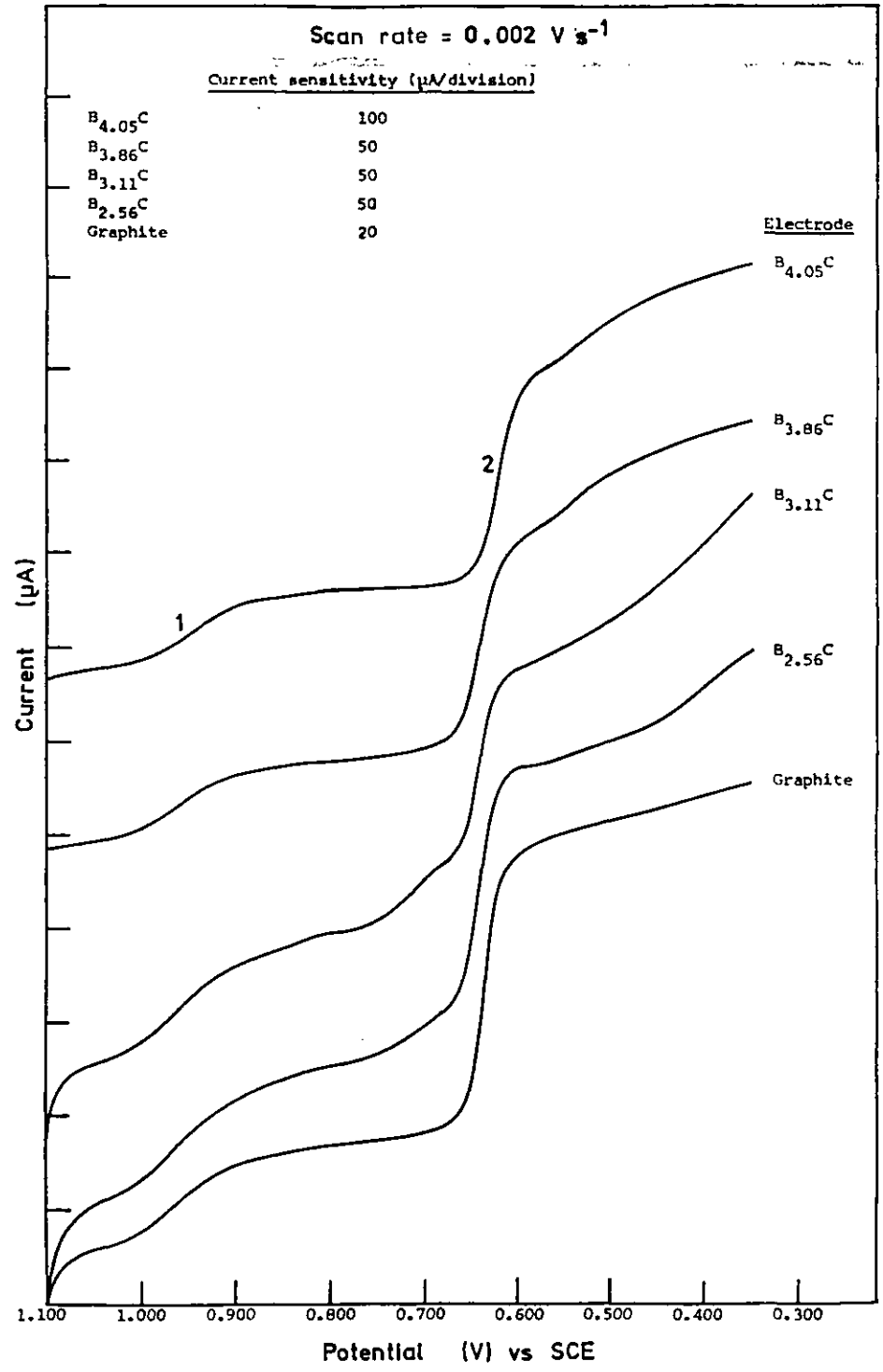

Fig. 5-234 Nitrogen aerated (16 hours) Ir(IV) perchlorate (8.0×10^{-4} mol dm^{-3})/Perchloric acid (0.1 M) supporting electrolyte System: D.c. voltammograms obtained at boron carbide, boron carbide/carbon composite, and graphite solid electrodes.

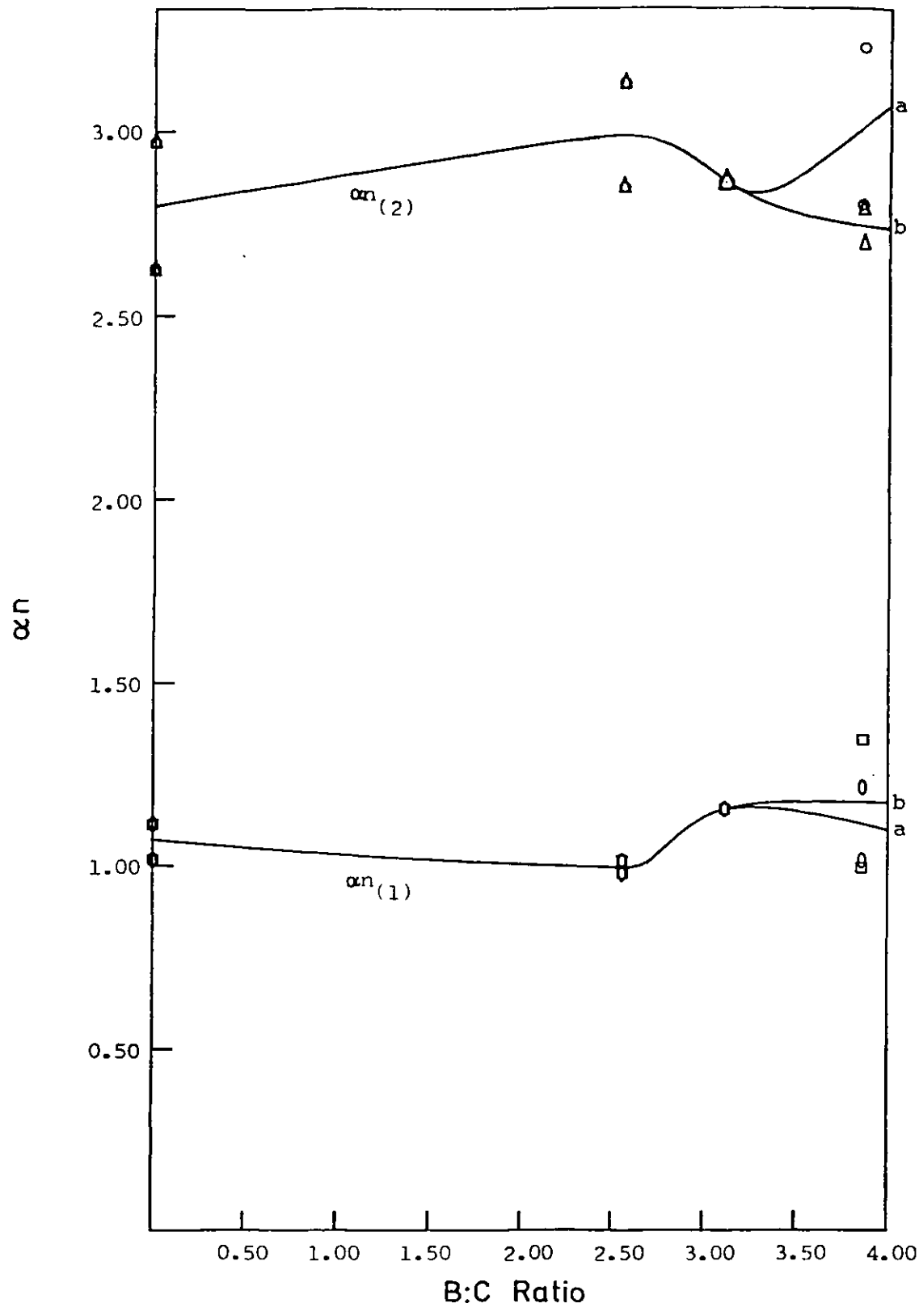

Fig. 5-235 Ir(IV) Perchlorate (8.0×10^{-4} mol dm^{-3})/Perchloric acid (0.1 M) supporting electrolyte System: Values of αn for voltammetric waves, (1) more positive and (2) less positive, as functions of the boron to carbon ratio of boron carbide/carbon composite solid electrodes. Graphite solid electrode is plotted as B:C = 0. (a) Sample solution as prepared, and (b) Sample solution aerated with nitrogen for 16 hours.

Fig. 5-235 (continued):-

(a) Sample solution as prepared:

$\alpha n_{(1)}$ mean = 1.07
Standard deviation = 8.88×10^{-2}
Coefficient of variation = 8.29%
Degrees of freedom = 6

$\alpha n_{(2)}$ mean = 2.92
Standard deviation = 0.190
Coefficient of variation = 6.52%
Degrees of freedom = 7

(b) Sample solution aerated with nitrogen for 16 hours:

$\alpha n_{(1)}$ mean = 1.09
Standard deviation = 0.128
Coefficient of variation = 11.8%
Degrees of freedom = 6

$\alpha n_{(2)}$ mean = 2.85
Standard deviation = 0.158
Coefficient of variation = 5.56%
Degrees of freedom = 7

Statistical Analysis: Comparison of αn values obtained at (a) with those at (b).

(i) For $\alpha n_{(1)}$ values:

F Test

$F = (0.128)^2/(8.88 \times 10^{-2})^2 = 2.09$

$F_{0.05}(6,6) = 5.82$ (double-sided)

Therefore, since F does not exceed $F_{0.05}(6,6)$, the variances are not significantly different.

t Test

Combined standard deviation = 0.110
Combined degrees of freedom = 12
Standard error = 5.89×10^{-2}
$t = (1.09 - 1.07)/(5.89 \times 10^{-2}) = 0.261$
$t_{0.05}(12) = 2.18$ (double-sided)

Therefore, since t does not exceed $t_{0.05}(12)$, the $\alpha n_{(1)}$ values of (a) and (b) are not significantly different.

Hence: $\alpha n_{(1)}$ grand mean = 1.08
Standard deviation = 0.110
Coefficient of variation = 10.2%
Degrees of freedom = 12

(ii) For $\alpha n_{(2)}$ values:

F Test

$F = (0.190)^2/(0.158)^2 = 1.45$

$F_{0.05}(7,7) = 4.99$ (double-sided)

Therefore, since F does not exceed $F_{0.05}(7,7)$, the variances are not significantly different.

t Test

Combined standard deviation = 0.175
Combined degrees of freedom = 14
Standard error = 8.75×10^{-2}
$t = (2.92 - 2.85)/(8.75 \times 10^{-2}) = 0.777$
$t_{0.05}(14) = 2.14$ (double-sided)

Therefore, since t does not exceed $t_{0.05}(14)$, the $\alpha n_{(2)}$ values of (a) and (b) are not significantly different.

Hence: $\alpha n_{(2)}$ grand mean = 2.88
Standard deviation = 0.175
Coefficient of variation = 6.07%
Degrees of freedom = 14

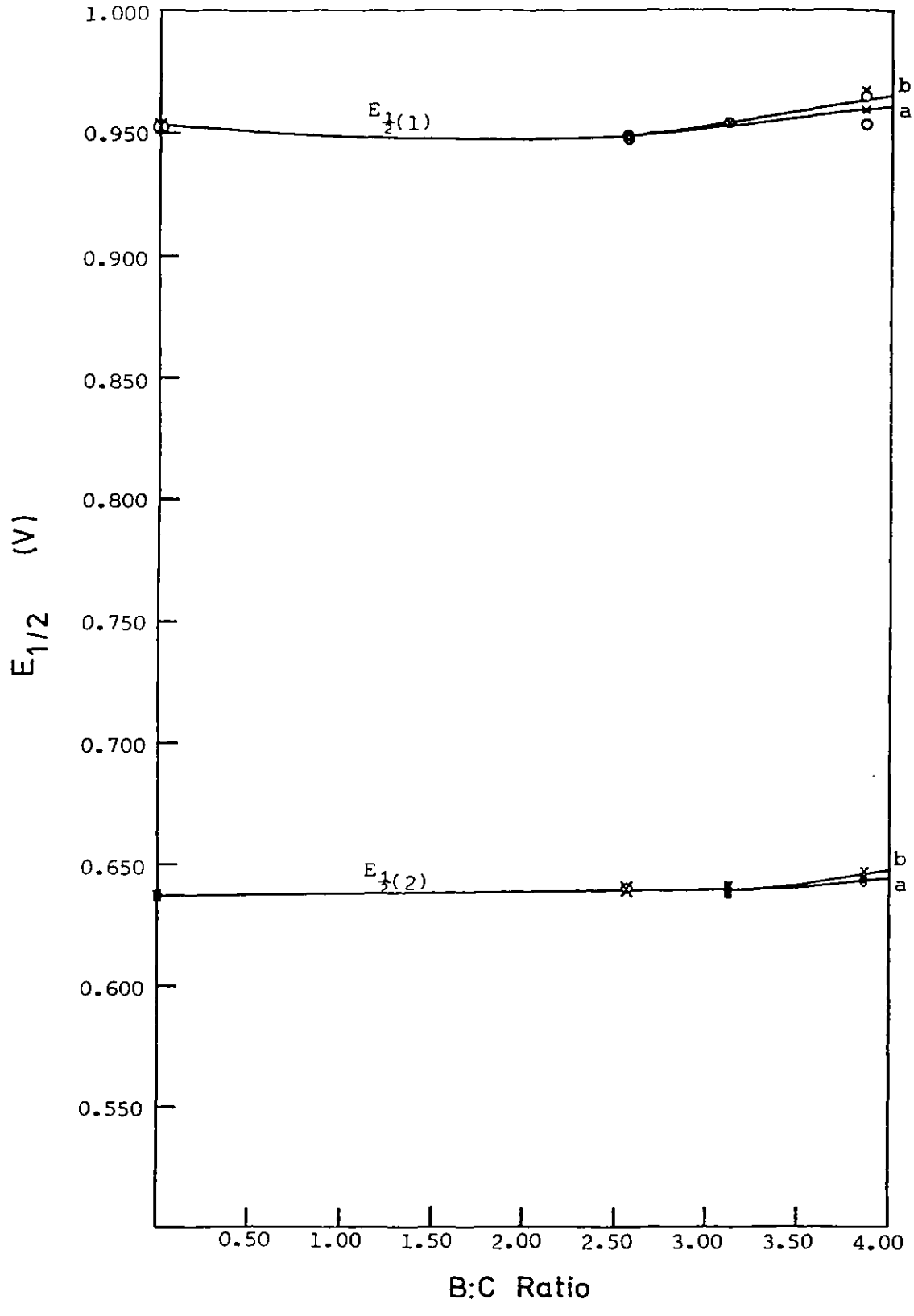

Fig. 5-236 Ir(IV) Perchlorate (8.0×10^{-4} mol dm^{-3})/Perchloric acid (0.1 M) supporting electrolyte System: Values of half-wave potential, $E_{\frac{1}{2}}$, as a function of boron to carbon ratio of boron carbide/carbon composite solid electrodes; graphite solid electrode is plotted as B:C = 0. (a) Sample solution as prepared, and (b) Sample solution aerated with nitrogen for 16 hours.

Fig. 5-236 (continued):-

(a) Sample solution as prepared:

$E_{\frac{1}{2}(1)}$ mean = 0.953 V
Standard deviation = 0.006 V
Coefficient of variation = 0.597%
Degrees of freedom = 6

$E_{\frac{1}{2}(2)}$ mean = 0.639 V
Standard deviation = 0.003 V
Coefficient of variation = 0.395%
Degrees of freedom = 7

(b) Sample solution aerated with nitrogen for 16 hours:

$E_{\frac{1}{2}(1)}$ mean =0.954 V
Standard deviation = 0.007 V
Coefficient of variation = 0.726%
Degrees of freedom = 6

$E_{\frac{1}{2}(2)}$ mean = 0.640 V
Standard deviation = 0.004 V
Coefficient of variation = 0.593%
Degrees of freedom = 7

Statistical Analysis: Comparison of $E_{\frac{1}{2}}$ values obtained at (a) with those at (b).

(i) For $E_{\frac{1}{2}(1)}$ values:

F Test

F = 1.48

$F_{0.05}(6,6)$ = 5.82 (double-sided)

Therefore, since F does not exceed $F_{0.05}(6,6)$, the variances are not significantly different.

t Test

Combined standard deviation = 6.33×10^{-3} V

Combined degrees of freedom = 12

Standard error = 3.39×10^{-3}

t = 0.362

$t_{0.05}(12)$ = 2.18 (double-sided)

Therefore, since t does not exceed $t_{0.05}(12)$, the $E_{\frac{1}{2}(1)}$ values of (a) and (b) are not significantly different.

Hence: $E_{\frac{1}{2}(1)}$ grand mean = 0.953 V
Standard deviation = 0.006 V
Coefficient of variation = 0.665%
Degrees of freedom = 12

(ii) For $E_{\frac{1}{2}(2)}$ values:

F Test

F = 2.26

$F_{0.05}(7,7)$ = 4.99 (double-sided)

Therefore, since F does not exceed $F_{0.05}(7,7)$, the variances are not significantly different.

t Test

Combined standard deviation = 3.22×10^{-3} V

Combined degrees of freedom = 14

Standard error = 1.61×10^{-3}

t = 0.481

$t_{0.05}(14)$ = 2.14 (double-sided)

Therefore, since t does not exceed $t_{0.05}(14)$, the $E_{\frac{1}{2}(2)}$ values of (a) and (b) are not significantly different.

Hence: $E_{\frac{1}{2}(2)}$ grand mean = 0.640 V
Standard deviation = 0.003 V
Coefficient of variation = 0.503%
Degrees of freedom = 14

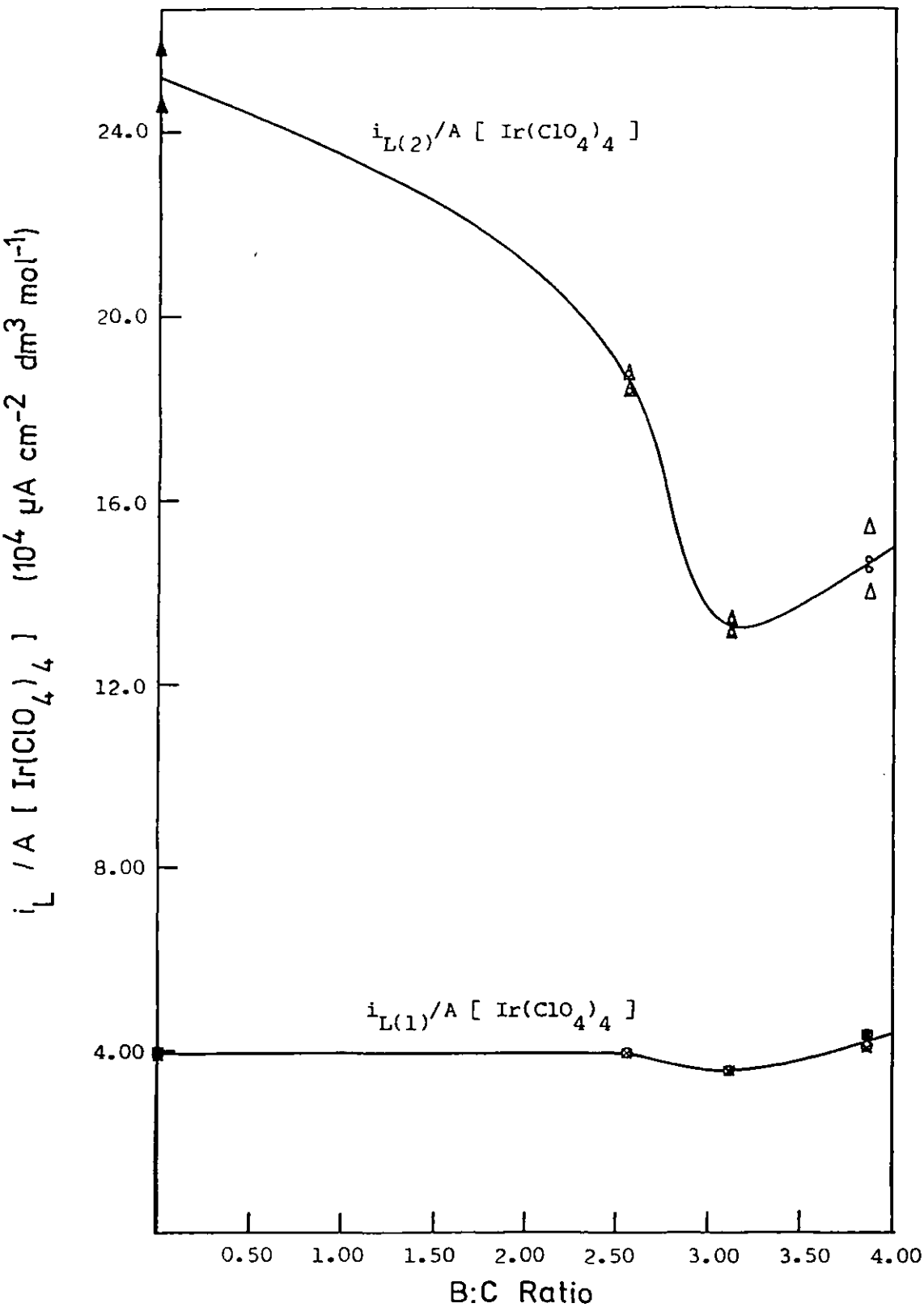

Fig. 5-237 Ir(IV) Perchlorate (8.0×10^{-4} mol dm^{-3})/Perchloric acid (0.1 M) supporting electrolyte System: Values of limiting current per unit area divided by concentration of Ir(IV) Perchlorate, i_L/A [$Ir(ClO_4)_4$], as a function of boron to carbon ratio of boron carbide/carbon composite solid electrode (graphite solid electrode is plotted as B:C = 0); at potential scan rates of 0.001 and 0.002 V s^{-1}. (a) Sample solution as prepared (o and ∘), and (b) Sample solution aerated with nitrogen for 16 hours (x and Δ).

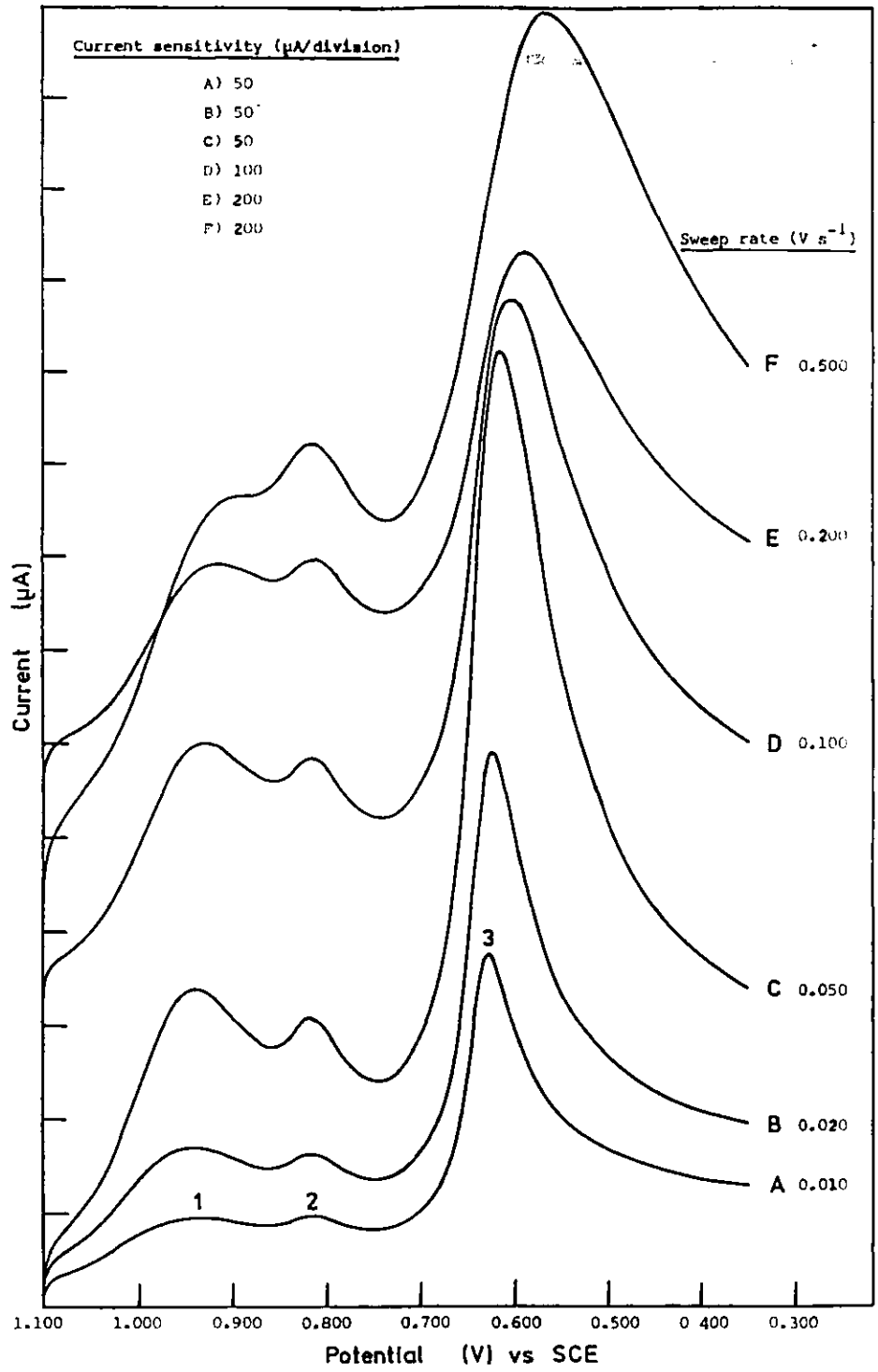

Fig. 5-238 Nitrogen aerated (16 hours) Ir(IV) perchlorate (8.0×10^{-4} mol dm^{-3})/Perchloric acid (0.1 M) supporting electrolyte System: Linear sweep voltammograms obtained at the boron carbide solid electrode $B_{4.0S}C$ — variation with sweep rate.

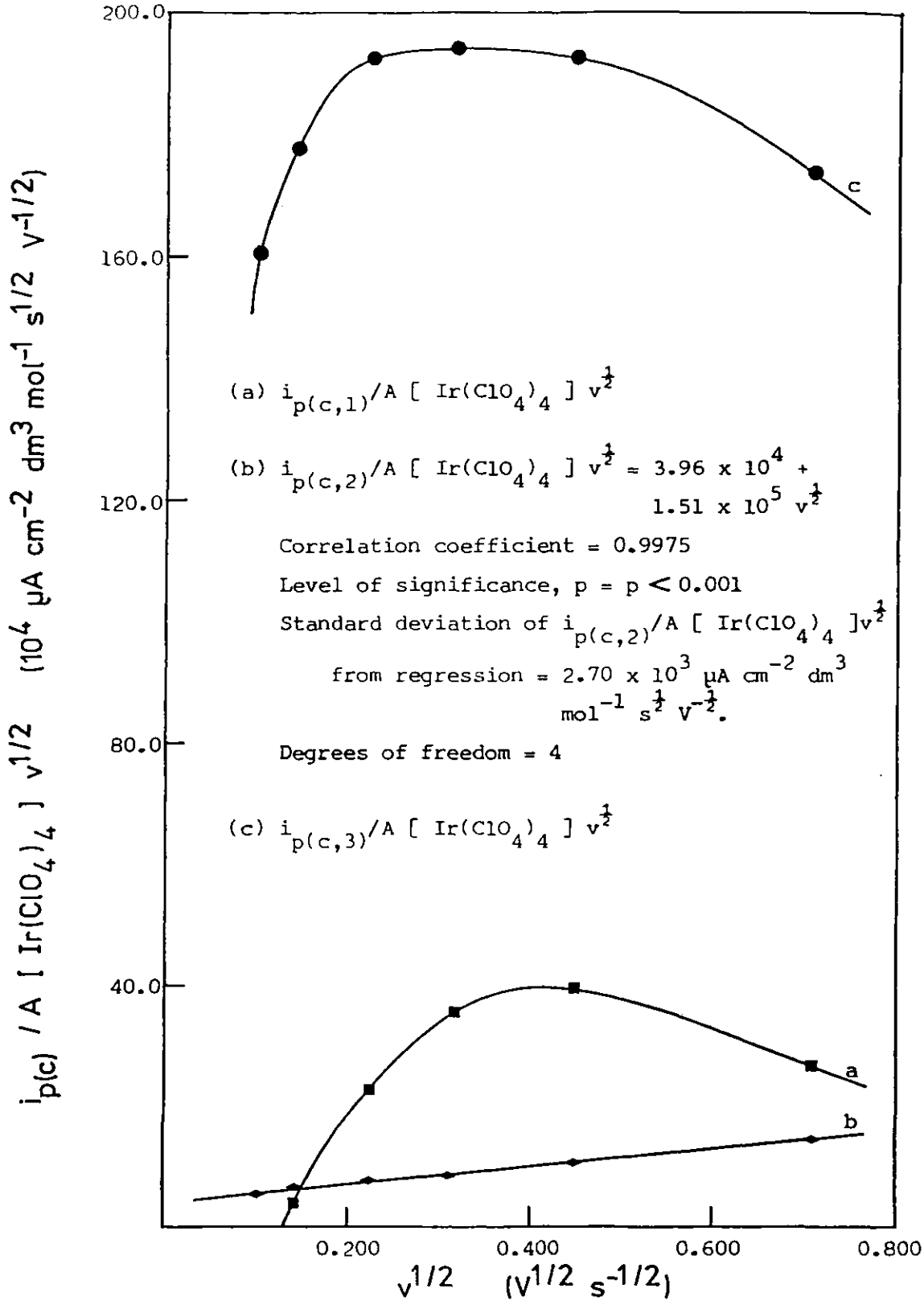

Fig. 5-239 Ir(IV) Perchlorate (8.0 x 10^{-4} mol dm^{-3})/Perchloric acid (0.1 M) supporting electrolyte System: Values of cathodic current function, $i_{p(c)}/A$ [$Ir(ClO_4)_4$] $v^{\frac{1}{2}}$, as a function of square root of potential scan rate, $v^{\frac{1}{2}}$. Sample solution was aerated with nitrogen for 16 hours. Boron carbide solid electrode $B_{4.05}C$.

The cathodic peak potentials for Ir(IV) perchlorate (8.0×10^{-4} mol dm^{-3}), before and after nitrogen aeration, are plotted as functions of sweep rate in Fig. 5-240. Although the general trends are similar, two-way ANOVA indicated that nitrogen aeration significantly affected $E_{p(c,2)}$ and $E_{p(c,3)}$ but not $E_{p(c,1)}$. In general, increasing sweep rate caused the charge transfers to become less reversible; thus $|E_p - E_{p/2}|$ values widened with increasing sweep rate for all the peaks (Fig. 5-241).

5-1.5.(iii).b Boron carbide solid electrode $B_{3.86}C$

Linear sweep voltammograms (Fig. 5-242) obtained at the boron carbide solid electrode $B_{3.86}C$ for Ir(IV) perchlorate (8.0×10^{-4} mol dm^{-3})/$HClO_4$ (0.1 M) supporting electrolyte solution do not show any fundamental differences between the sample solution as prepared and the sample solution after nitrogen aeration (16 hours). Thus, in general, three cathodic peaks (Peaks 1, 2, and 3) were exhibited for either case. Quantitative treatment of the peaks reveals that all the peaks were influenced by adsorption (Fig. 5-243). Two-way ANOVA indicated that nitrogen aeration significantly affected the peak current function for Peak 3 but not Peaks 1 and 2.

The cathodic peak potentials are plotted as functions of the sweep rate in Fig. 5-244. Two-way ANOVA indicated that nitrogen aeration significantly affected $E_{p(c,2)}$ and $E_{p(c,3)}$ but not $E_{p(c,1)}$. Increasing sweep rate caused the charge transfers for all three peaks to become less reversible; as reflected by widening $|E_p - E_{p/2}|$ values (Fig. 5-245). Nitrogen aeration significantly affected the values of $|E_{p(c,2)} - E_{p(c,2)/2}|$ and $|E_{p(c,3)} - E_{p(c,3)/2}|$ but not $|E_{p(c,1)} - E_{p(c,1)/2}|$, as shown by two-way ANOVA.

The evidence suggests that Peak 1 was a diffusion peak complicated by weak adsorption influences emanating from the strong adsorption post-peak , Peak 2, of Ir(IV) perchlorate reactant. Peak 3 was a diffusion peak coupled with weak adsorption.

5-1.5.(iii).c Boron carbide/carbon composite solid electrode $B_{3.11}C$

Linear sweep voltammograms (Fig. 5-246) for Ir(IV) perchlorate (8.0×10^{-4} mol dm^{-3})/$HClO_4$ (0.1 M) supporting electrolyte solution, obtained at the boron carbide/carbon composite solid electrode $B_{3.11}C$, do not show any fundamental differences between the sample solution as

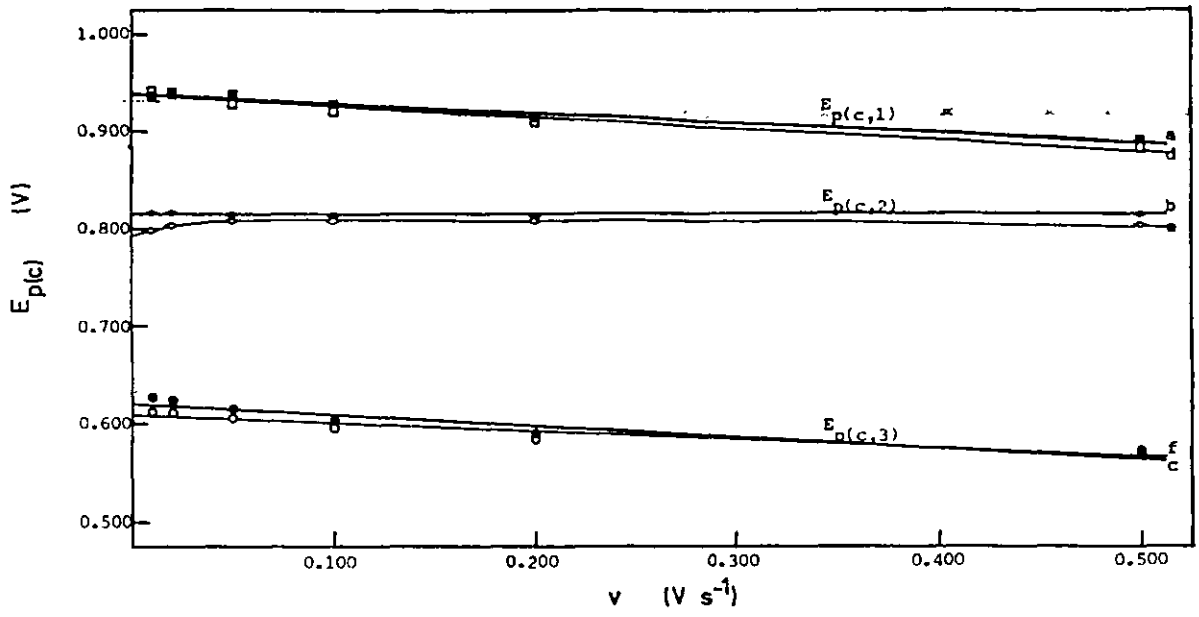

Fig. 5-240 Ir(IV) Perchlorate (8.0×10^{-4} mol dm^{-3})/Perchloric acid (0.1 M) supporting electrolyte System: Values of cathodic peak potential, $E_{p(c)}$, as a function of potential scan rate, v. (i) Sample solution aerated with nitrogen for 16 hours: a, b, and c. (ii) Sample solution as prepared: d, e, and f. Boron carbide solid electrode $B_{4.05}C$.

(i) Sample solution aerated with nitrogen for 16 hours:

(a) $E_{p(c,1)} = 0.940 - 0.102\ v$
Correlation coefficient = -0.9824
Level of significance, p = $p < 0.001$
Standard deviation of $E_{p(c,1)}$ from regression = 0.004 V
Degrees of freedom = 4

(b) $E_{p(c,2)}$ mean = 0.815 V
Standard deviation = 0.001 V
Coefficient of variation = 0.144%
Degrees of freedom = 5

(c) $E_{p(c,3)} = 0.621 - 0.113\ v$
Correlation coefficient = -0.9543
Level of significance, $0.001 < p < 0.01$
Standard deviation of $E_{p(c,3)}$ from regression = 0.007 V
Degrees of freedom = 4

(ii) Sample solution as prepared:

(d) $E_{p(c,1)} = 0.937 - 0.116\ v$
Correlation coefficient = -0.9805
Level of significance, p = $p < 0.001$
Standard deviation of $E_{p(c,1)}$ from regression = 0.005 V
Degrees of freedom = 4

(e) $E_{p(c,2)}$ mean = 0.805 V
Standard deviation = 0.004 V
Coefficient of variation = 0.483%
Degrees of freedom = 5

(f) $E_{p(c,3)} = 0.608 - 8.26 \times 10^{-2}\ v$
Correlation coefficient = -0.9425
Level of significance, $0.001 < p < 0.01$
Standard deviation of $E_{p(c,3)}$ from regression = 0.006 V
Degrees of freedom = 4

Fig. 5-240 (continued):-

Two-way Analysis of Variance:

$E_{p(c,1)}$

Grand mean = 0.922 V

Standard deviation = 0.019 V

Variance ratio due to effects of scan rate, F(v) = 50.2

Degrees of freedom = 5

Degrees of freedom of the Residual = 5

$F_{0.05}(5,5)$ = 7.15 (double-sided)

Therefore, since F(v) exceeds $F_{0.05}(5,5)$. the effects of scan rate are significant.

Variance ratio due to effects of nitrogen aeration, $F(N_2)$ = 4.69

Degrees of freedom = 1

Degrees of freedom of the Residual = 5

$F_{0.05}(1,5)$ = 10.0 (double-sided)

Therefore, since $F(N_2)$ does not exceed $F_{0.05}(1,5)$, the effects of nitrogen aeration are not significant.

$E_{p(c,2)}$

Grand mean = 0.810 V

Standard deviation = 0.006 V

Variance ratio due to effects of scan rate, F(v) = 0.424

Degrees of freedom = 5

Degrees of freedom of the Residual = 5

Therefore, since F(v) does not exceed $F_{0.05}(5,5)$, the effects of scan rate are not significant.

Variance ratio due to effects of nitrogen aeration, $F(N_2)$ = 26.1

Degrees of freedom = 1

Degrees of freedom of the Residual = 5

Therefore, since $F(N_2)$ exceeds $F_{0.05}(1,5)$, the effects of nitrogen aeration are significant.

$E_{p(c,3)}$

Grand mean = 0.600 V

Standard deviation = 0.018 V

Variance ratio due to effects of scan rate, F(v) = 42.6

Degrees of freedom = 5

Degrees of freedom of the Residual = 5

Therefore, since F(v) exceeds $F_{0.05}(5,5)$, the effects of scan rate are significant.

Variance ratio due to effects of nitrogen aeration, $F(N_2)$ = 11.7

Degrees of freedom = 1

Degrees of freedom of the Residual = 5

Therefore, since $F(N_2)$ exceeds $F_{0.05}(1,5)$, the effects of nitrogen aeration are significant.

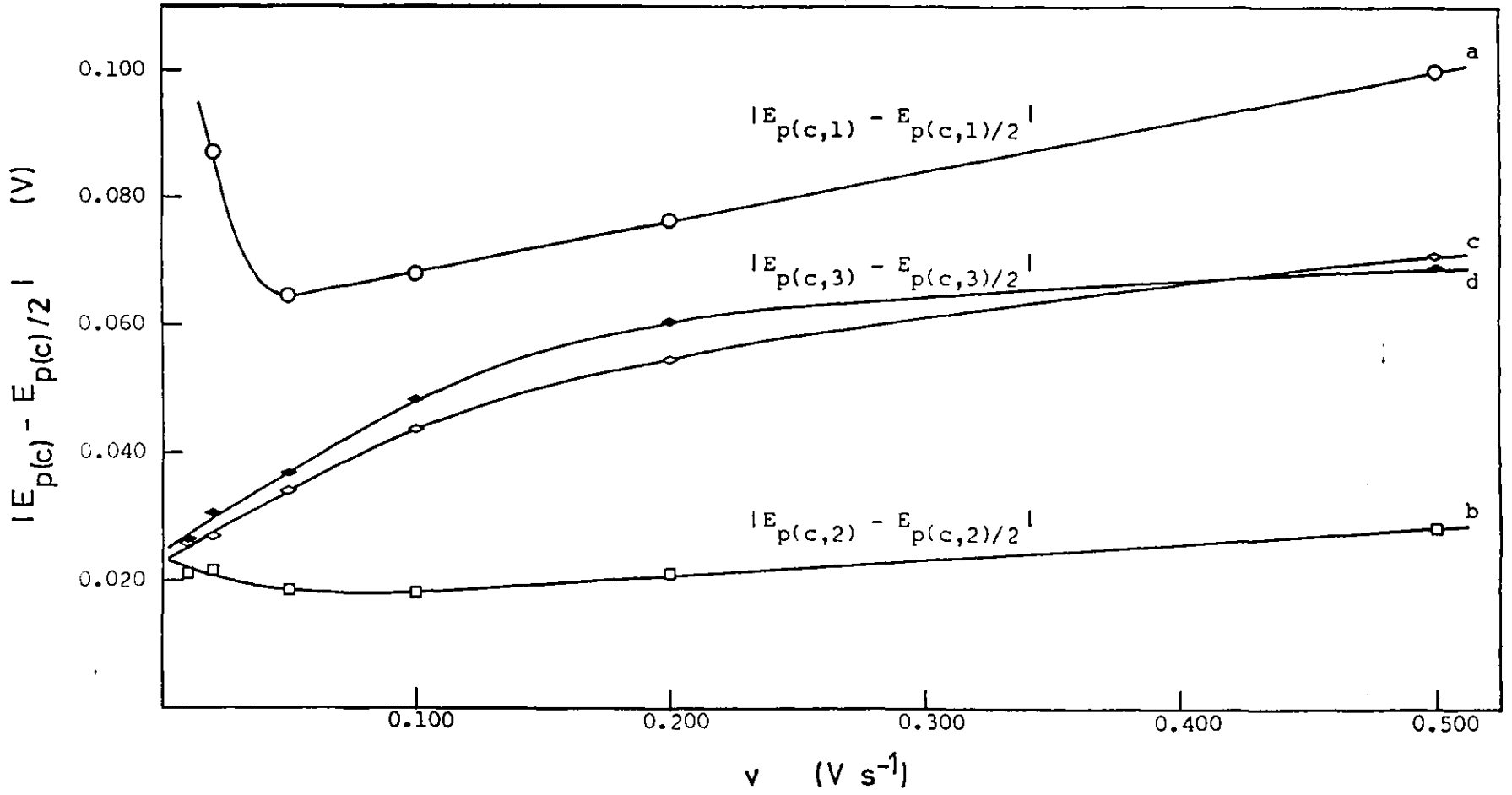

Fig. 5-241 Ir(IV) Perchlorate (8.0×10^{-4} mol dm^{-3})/Perchloric acid (0.1 M) supporting electrolyte System: Values of the difference between cathodic peak and half-peak potential, $|E_{p(c)} - E_{p(c)/2}|$, as a function of potential scan rate, v. (i) Sample solution aerated with nitrogen for 16 hours: a, b, and c. (ii) Sample solution as prepared: d. Boron carbide solid electrode $B_{4.05}C$.

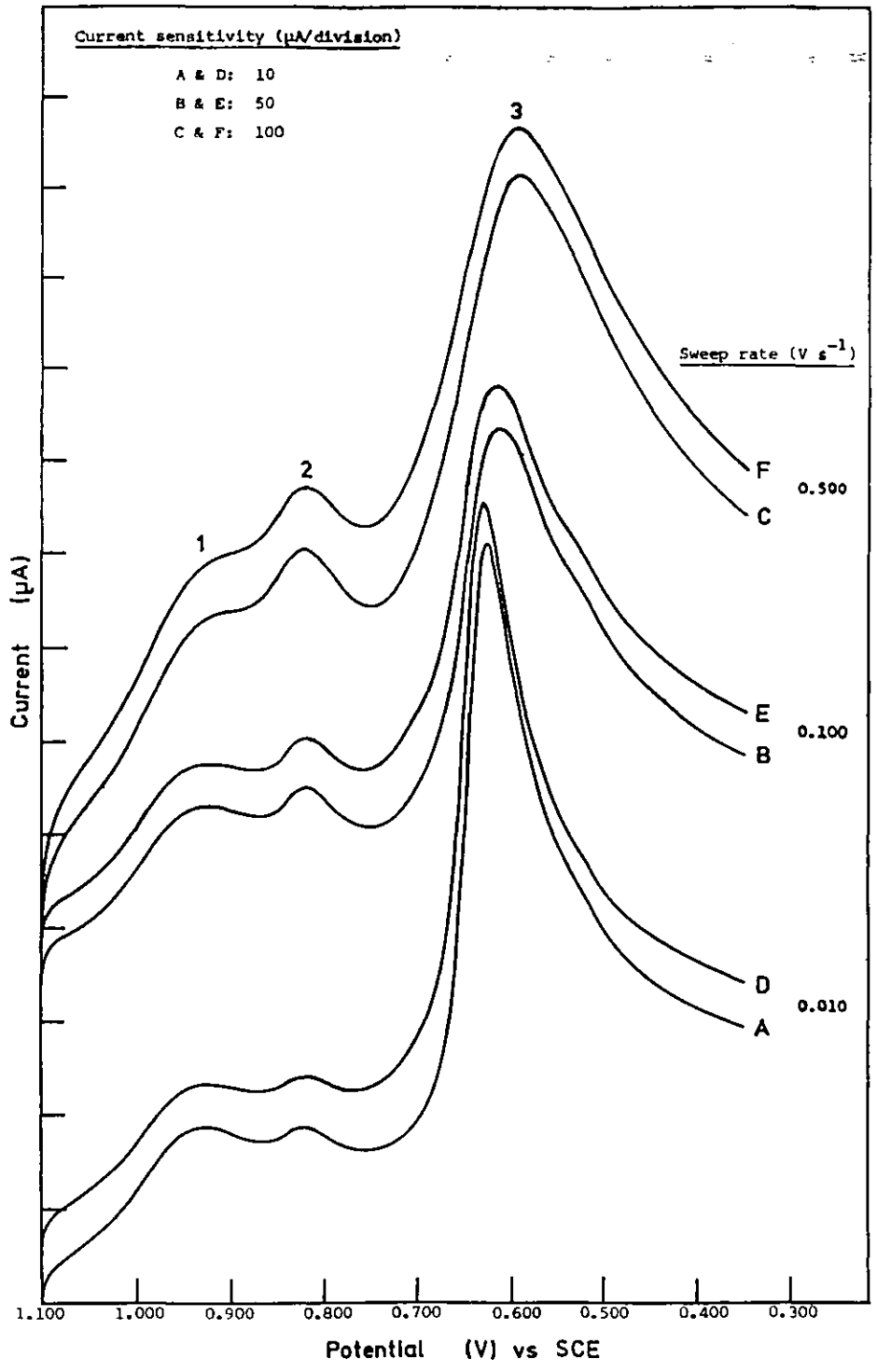

Fig. 5-242 Ir(IV) perchlorate (8.0×10^{-4} mol dm^{-3})/Perchloric acid (0.1 M) supporting electrolyte System: Linear sweep voltammograms obtained at the boron carbide solid electrode $B_{3.86}C$ — variation with sweep rate. A, B, and C: sample as prepared. D, E, and F: sample aerated with nitrogen for 16 hours.

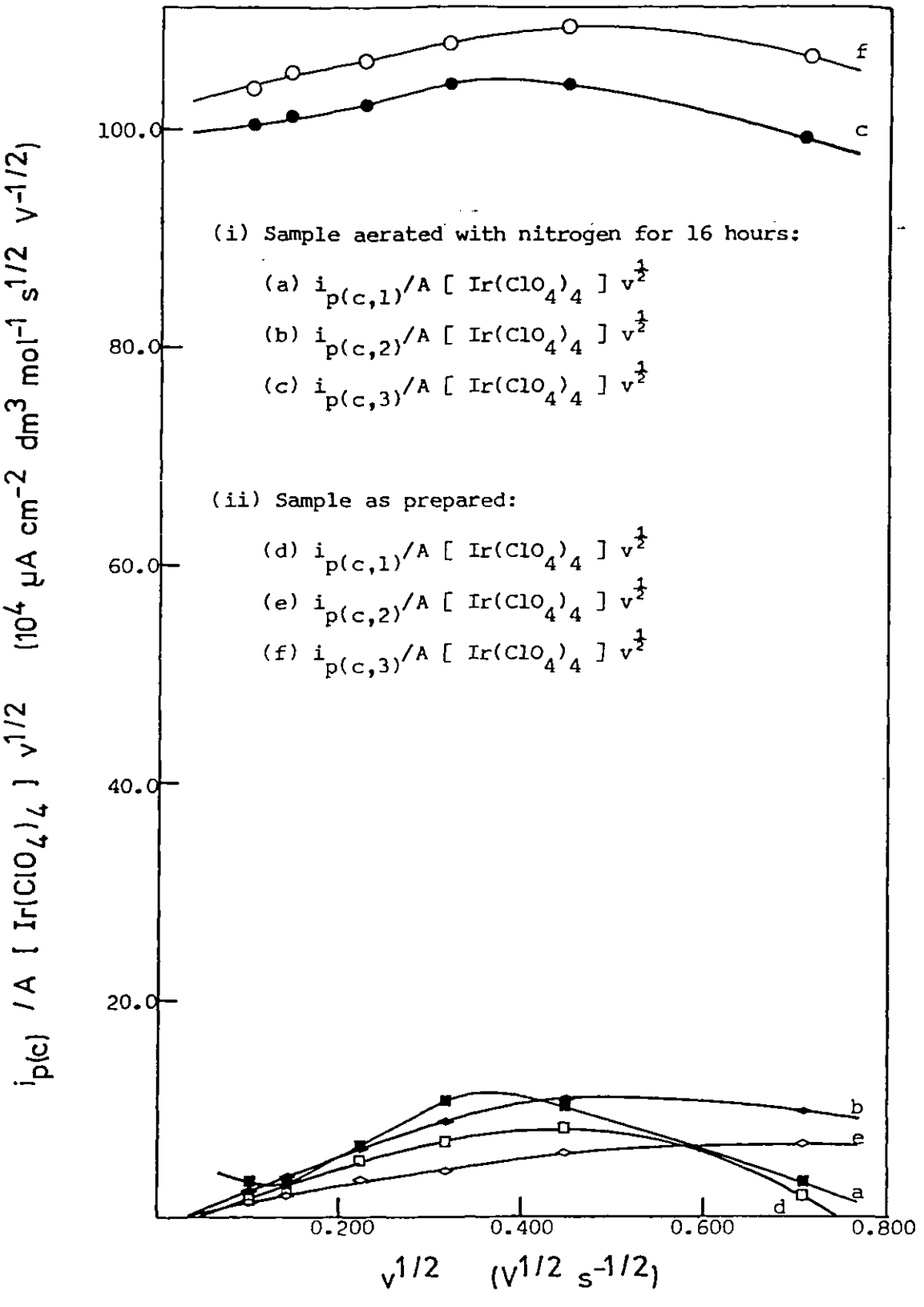

Fig. 5-243 Ir(IV) Perchlorate (8.0×10^{-4} mol dm^{-3})/Perchloric acid (0.1 M) supporting electrolyte System: Values of cathodic current function, $i_{p(c)}/A\ [\ Ir(ClO_4)_4\ ]\ v^{\frac{1}{2}}$, as a function of square root of potential scan rate, $v^{\frac{1}{2}}$. Boron carbide solid electrode $B_{3.86}C$.

Fig. 5-243 (continued):-

Two-way Analysis of Variance:

$\frac{i_{p(c,1)}}{A\,[\,Ir(ClO_4)_4\,]\,v^{\frac{1}{2}}}$

Grand mean = 7.06×10^4 μA cm^{-2} dm^3 mol^{-1} $s^{\frac{1}{2}}$ $V^{-\frac{1}{2}}$

Standard deviation = 4.11×10^4 μA cm^{-2} dm^3 mol^{-1} $s^{\frac{1}{2}}$ $V^{-\frac{1}{2}}$

Variance ratio due to effects of scan rate, F(v) = 22.5

Degrees of freedom = 5

Degrees of freedom of the Residual = 5

$F_{0.05}(5,5)$ = 7.15 (double-sided)

Therefore, since F(v) exceeds $F_{0.05}(5,5)$, the effects of scan rate are significant.

Variance ratio due to effects of nitrogen aeration, $F(N_2)$ = 6.34

Degrees of freedom = 1

Degrees of freedom of the Residual = 5

$F_{0.05}(1,5)$ = 10.0 (double-sided)

Therefore, since $F(N_2)$ does not exceed $F_{0.05}(1,5)$, the effects of nitrogen aeration are not significant.

$\frac{i_{p(c,2)}}{A\,[\,Ir(ClO_4)_4\,]\,v^{\frac{1}{2}}}$

Grand mean = 6.97×10^4 μA cm^{-2} dm^3 mol^{-1} $s^{\frac{1}{2}}$ $V^{-\frac{1}{2}}$

Standard deviation = 3.28×10^4 μA cm^{-2} dm^3 mol^{-1} $s^{\frac{1}{2}}$ $V^{-\frac{1}{2}}$

Variance ratio due to effects of scan rate, F(v) = 36.8

Degrees of freedom = 5

Degrees of freedom of the Residual = 5

Therefore, since F(v) exceeds $F_{0.05}(5,5)$, the effects of scan rate are significant.

Variance ratio due to effects of nitrogen aeration, $F(N_2)$ = 4.97×10^{-2}

Degrees of freedom = 1

Degrees of freedom of the Residual = 5

Therefore, since $F(N_2)$ does not exceed $F_{0.05}(1,5)$, the effects of nitrogen aeration are not significant.

$\frac{i_{p(c,3)}}{A\,[\,Ir(ClO_4)_4\,]\,v^{\frac{1}{2}}}$

Grand mean = 1.04×10^6 μA cm^{-2} dm^3 mol^{-1} $s^{\frac{1}{2}}$ $V^{-\frac{1}{2}}$

Standard deviation = 2.94×10^4 μA cm^{-2} dm^3 mol^{-1} $s^{\frac{1}{2}}$ $V^{-\frac{1}{2}}$

Variance ratio due to effects of scan rate, F(v) = 6.20

Degrees of freedom = 5

Degrees of freedom of the Residual = 5

Therefore, since F(v) does not exceed $F_{0.05}(5,5)$, the effects of scan rate are not significant.

Variance ratio due to effects of nitrogen aeration, $F(N_2)$ = 61.3

Degrees of freedom = 1

Degrees of freedom of the Residual = 5

Therefore, since $F(N_2)$ exceeds $F_{0.05}(1,5)$, the effects of nitrogen aeration are significant.

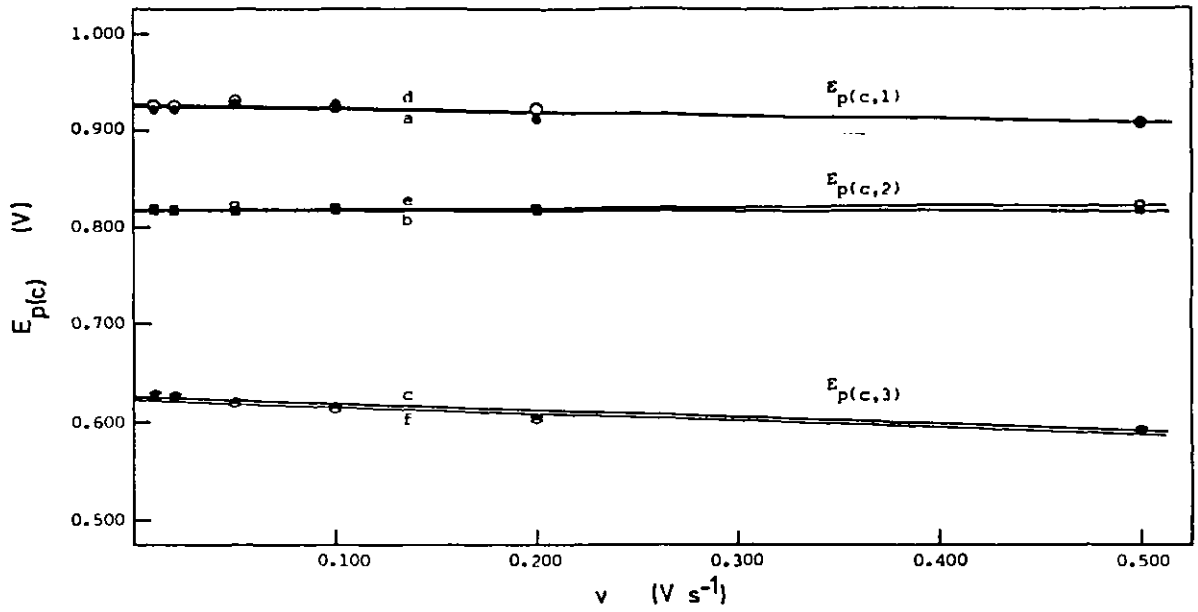

Fig. 5-244 Ir(IV) Perchlorate (8.0×10^{-4} mol dm^{-3})/Perchloric acid (0.1 M) supporting electrolyte System: Values of cathodic peak potential, $E_{p(c)}$, as a function of potential scan rate, v. (i) Sample solution aerated with nitrogen for 16 hours: a, b, and c. (ii) Sample solution as prepared: d, e, and f. Boron carbide solid electrode $B_{3.86}C$.

(i) Sample solution aerated with nitrogen for 16 hours:

(a) $E_{p(c,1)} = 0.925 - 3.42 \times 10^{-2}$ v
Correlation coefficient = -0.8130
Level of significance, $p = 0.02 < p < 0.05$
Standard deviation of $E_{p(c,1)}$ from regression = 0.005 V
Degrees of freedom = 4

(b) $E_{p(c,2)}$ mean = 0.817 V
Standard deviation = 0.001 V
Coefficient of variation = 8.25×10^{-2}%
Degrees of freedom = 5

(c) $E_{p(c,3)} = 0.626 - 6.94 \times 10^{-2}$ v
Correlation coefficient = -0.9415
Level of significance, $0.001 < p < 0.01$
Standard deviation of $E_{p(c,3)}$ from regression = 0.005 V
Degrees of freedom = 4

(ii) Sample solution as prepared:

(d) $E_{p(c,1)} = 0.927 - 3.68 \times 10^{-2}$ v
Correlation coefficient = -0.9294
Level of significance, $0.001 < p < 0.01$
Standard deviation of $E_{p(c,1)}$ from regression = 0.003 V
Degrees of freedom = 4

(e) $E_{p(c,2)} = 0.818 + 8.08 \times 10^{-3}$ v
Correlation coefficient = 0.8557
Level of significance, $0.02 < p < 0.05$
Standard deviation of $E_{p(c,2)}$ from regression = 0.001 V
Degrees of freedom = 4

(f) $E_{p(c,3)} = 0.622 - 6.89 \times 10^{-2}$ v
Correlation coefficient = -0.9470
Level of significance, $0.001 < p < 0.01$
Standard deviation of $E_{p(c,3)}$ from regression = 0.005 V
Degrees of freedom = 4

Fig. 5-244 (continued):-

Two-way Analysis of Variance:

$E_{p(c,1)}$

Grand mean = 0.921 V

Standard deviation = 0.007 V

Variance ratio due to effects of scan rate, F(v) = 8.42

Degrees of freedom = 5

Degrees of freedom of the Residual = 5

$F_{0.05}(5,5)$ = 7.15 (double-sided)

Therefore, since F(v) exceeds $F_{0.05}(5,5)$, the effects of scan rate are significant.

Variance ratio due to effects of nitrogen aeration, $F(N_2)$ = 1.34

Degrees of freedom = 1

Degrees of freedom of the Residual = 5

$F_{0.05}(1,5)$ = 10.0 (double-sided)

Therefore, since $F(N_2)$ does not exceed $F_{0.05}(1,5)$, the effects of nitrogen aeration are not significant.

$E_{p(c,2)}$

Grand mean = 0.818 V

Standard deviation = 0.002 V

Variance ratio due to effects of scan rate, F(v) = 1.85

Degrees of freedom = 5

Degrees of freedom of the Residual = 5

Therefore, since F(v) does not exceed $F_{0.05}(5,5)$, the effects of scan rate are not significant.

Variance ratio due to effects of nitrogen aeration, $F(N_2)$ = 11.5

Degrees of freedom = 1

Degrees of freedom of the Residual = 5

Therefore, since $F(N_2)$ exceeds $F_{0.05}(1,5)$, the effects of nitrogen aeration are significant.

$E_{p(c,3)}$

Grand mean = 0.614 V

Standard deviation = 0.013 V

Variance ratio due to effects of scan rate, $F(v) = 2.43 \times 10^3$

Degrees of freedom = 5

Degrees of freedom of the Residual = 5

Therefore, since F(v) exceeds $F_{0.05}(5,5)$, the effects of scan rate are significant.

Variance ratio due to effects of nitrogen aeration, $F(N_2) = 3.08 \times 10^2$

Degrees of freedom = 1

Degrees of freedom of the Residual = 5

Therefore, since $F(N_2)$ exceeds $F_{0.05}(1,5)$, the effects of nitrogen aeration are significant.

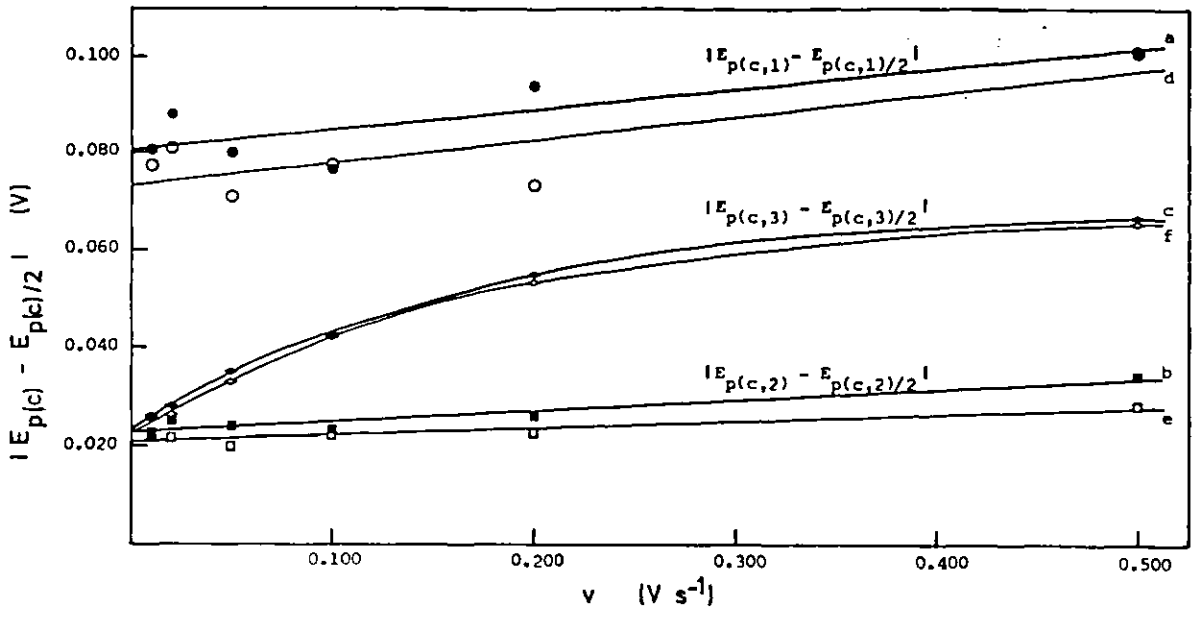

Fig. 5-245 Ir(IV) Perchlorate (8.0×10^{-4} mol dm^{-3})/Perchloric acid (0.1 M) supporting electrolyte System: Values of the difference between cathodic peak and half-peak potential, $|E_{p(c)} - E_{p(c)/2}|$, as a function of potential scan rate, v. (i) Sample solution aerated with nitrogen for 16 hours: a, b, and c. (ii) Sample solution as prepared: d, e, and f. Boron carbide solid electrode $B_{3.86}C$.

(i) Sample solution aerated with nitrogen for 16 hours:

(a) $|E_{p(c,1)} - E_{p(c,1)/2}| = 8.06 \times 10^{-2} + 4.19 \times 10^{-2}$ v
Correlation coefficient = 0.8267
Level of significance, $p = 0.02 < p < 0.05$
Standard deviation of $|E_{p(c,1)} - E_{p(c,1)/2}|$ from regression
= 0.006 V
Degrees of freedom = 4

(b) $|E_{p(c,2)} - E_{p(c,2)/2}| = 2.27 \times 10^{-2} + 2.14 \times 10^{-2}$ v
Correlation coefficient = 0.9555
Level of significance, $p = 0.001 < p < 0.01$
Standard deviation of $|E_{p(c,2)} - E_{p(c,2)/2}|$ from regression
= 0.001 V
Degrees of freedom = 4

(ii) Sample solution as prepared:

(d) $|E_{p(c,1)} - E_{p(c,1)/2}| = 7.33 \times 10^{-2} + 4.76 \times 10^{-2}$ v
Correlation coefficient = 0.8257
Level of significance, $p = 0.02 < p < 0.05$
Standard deviation of $|E_{p(c,1)} - E_{p(c,1)/2}|$ from regression
= 0.007 V
Degrees of freedom = 4

(e) $|E_{p(c,2)} - E_{p(c,2)/2}| = 2.07 \times 10^{-2} + 1.36 \times 10^{-2}$ v
Correlation coefficient = 0.9249
Level of significance, $p = 0.001 < p < 0.01$
Standard deviation of $|E_{p(c,2)} - E_{p(c,2)/2}|$ from regression
= 0.001 V
Degrees of freedom = 4

Fig. 5-245 (continued):-

Two-way Analysis of Variance:

$|E_{p(c,1)} - E_{p(c,1)/2}|$

Grand mean = 0.084 V

Standard deviation = 0.010 V

Variance ratio due to effects of scan rate, F(v) = 5.68

Degrees of freedom = 5

Degrees of freedom of the Residual = 5

$F_{0.05}(5,5)$ = 7.15 (double-sided)

Therefore, since F(v) does not exceed $F_{0.05}(5,5)$, the effects of scan rate are not significant.

Variance ratio due to effects of nitrogen aeration, $F(N_2)$ = 4.16

Degrees of freedom = 1

Degrees of freedom of the Residual = 5

$F_{0.05}(1,5)$ = 10.0 (double-sided)

Therefore, since $F(N_2)$ does not exceed $F_{0.05}(1,5)$, the effects of nitrogen aeration are not significant.

$|E_{p(c,2)} - E_{p(c,2)/2}|$

Grand mean = 0.024 V

Standard deviation = 0.004 V

Variance ratio due to effects of scan rate, F(v) = 11.2

Degrees of freedom = 5

Degrees of freedom of the Residual = 5

Therefore, since F(v) exceeds $F_{0.05}(5,5)$, the effects of scan rate are significant.

Variance ratio due to effects of nitrogen aeration, $F(N_2)$ = 14.1

Degrees of freedom = 1

Degrees of freedom of the Residual = 5

Therefore, since $F(N_2)$ exceeds $F_{0.05}(1,5)$, the effects of nitrogen aeration are significant.

$|E_{p(c,3)} - E_{p(c,3)/2}|$

Grand mean = 0.042 V

Standard deviation = 0.015 V

Variance ratio due to effects of scan rate, $F(v) = 1.98 \times 10^3$

Degrees of freedom = 5

Degrees of freedom of the Residual = 5

Therefore, since F(v) exceeds $F_{0.05}(5,5)$, the effects of scan rate are significant.

Variance ratio due to effects of nitrogen aeration, $F(N_2)$ = 17.2

Degrees of freedom = 1

Degrees of freedom of the Residual = 5

Therefore, since $F(N_2)$ exceeds $F_{0.05}(1,5)$, the effects of nitrogen aeration are significant.

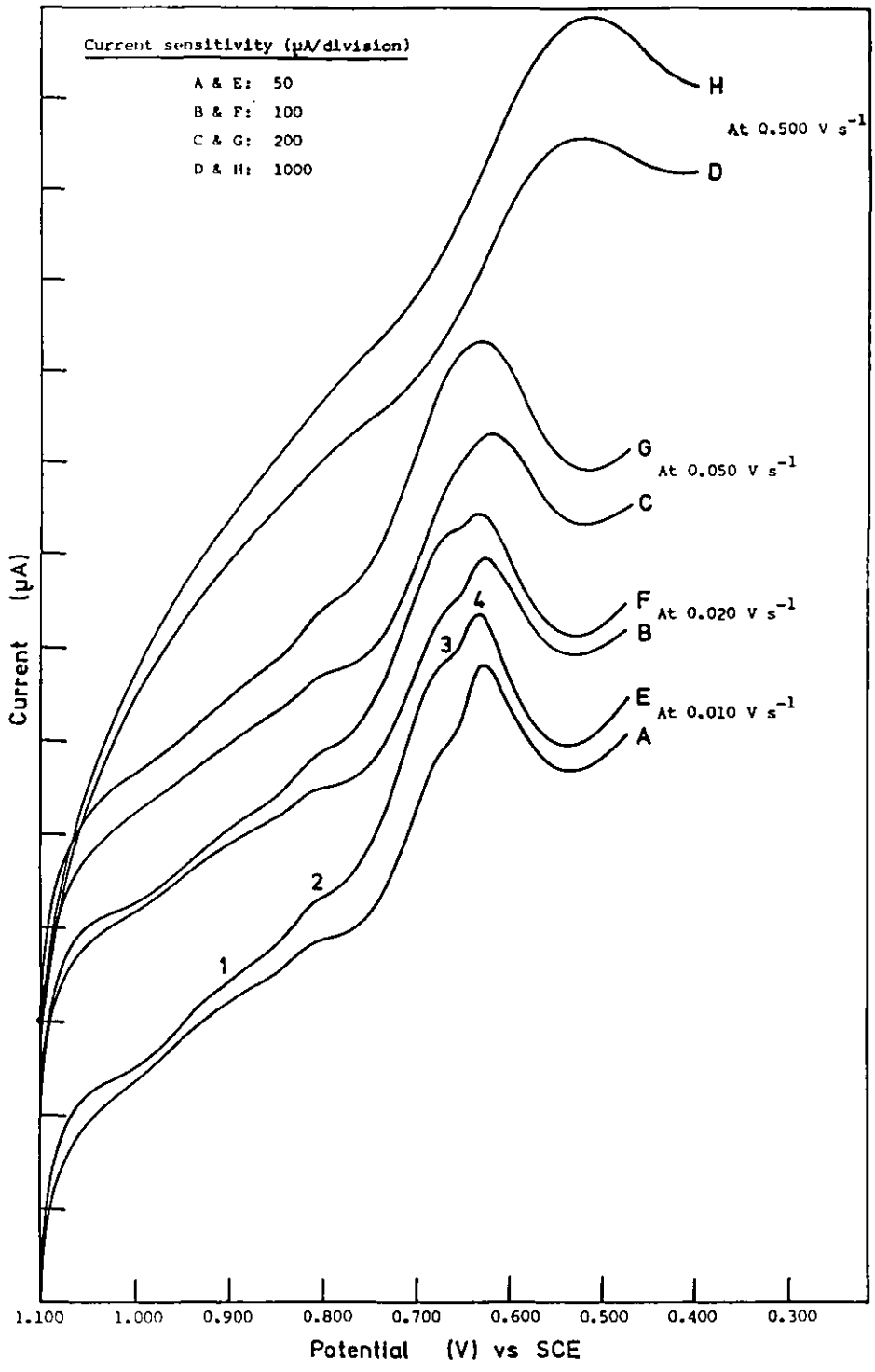

Fig. 5-246 Ir(IV) perchlorate (8.0×10^{-4} mol dm^{-3})/Perchloric acid (0.1 M) supporting electrolyte System: Linear sweep voltammograms obtained at the boron carbide/carbon composite solid electrode $B_{3.11}C$ — variation with sweep rate. A to D inclusive: sample as prepared. E to H inclusive: sample aerated with nitrogen for 16 hours.

prepared and the sample solution after nitrogen aeration (16 hours). Thus the same peaks were exhibited irrespective of nitrogen aeration. Quantitative treatment of the interpretable peaks shows that Peaks 1, 2, and 3 were influenced by adsorption; as reflected in the increase in the peak current function with increasing sweep rate (Fig. 5-247). Peak 4, however, had a peak current function which decreased with increasing sweep rate; but this could be attributed to the cathodic shift in Peak 3 with increasing sweep rate that eventually lead to the merger of Peaks 3 and 4. Thus Peak 1 was a diffusion peak affected by weak adsorption influences emanating from the strong adsorption post-peak, Peak 2, of Ir(IV) perchlorate reactant; whereas Peak 3 was a diffusion peak affected by weak adsorption influences emanating from the moderately strong adsorption post-peak, Peak 4, for the reactant. Qualitatively, it can be seen in Fig. 5-246 that nitrogen aeration improved the definition of the diffusion peaks; often at the expense of the related adsorption peaks. Two-way ANOVA of the peak current functions, however, did not reveal any statistically significant difference between the nitrogen-aerated and untreated samples; within the number of degrees of freedom available.

Two-way ANOVA of the cathodic peak potentials, plotted as functions of sweep rate (Fig. 5-248), did not show any statistically significant difference between the values obtained for nitrogen-aerated and untreated samples. Neither were there any statistically significant differences for the $|E_p - E_{p/2}|$ values due to nitrogen aeration (Fig. 5-249).

5-1.5.(iii).d Boron carbide/carbon composite solid electrode $B_{2.56}C$

The linear sweep voltammograms, obtained at the boron carbide/carbon composite solid electrode $B_{2.56}C$, for Ir(IV) perchlorate (8.0×10^{-4} mol dm^{-3})/$HClO_4$ (0.1 M) supporting electrolyte solution showed no fundamental differences between nitrogen-aerated and untreated samples (Fig. 5-250). Thus, at slow sweep rates, four peaks were exhibited (Peaks 1 to 4 inclusive). Quantitative treatment of the interpretable peaks shows that Peaks 2 and 3 were influenced by adsorption (Fig. 5-251). Two-way ANOVA on the peak current function for Peaks 2 and 3 indicated that the influence of nitrogen aeration was statistically significant.

The cathodic peak potentials are plotted as functions of sweep rate in Fig. 5-252. Two-way ANOVA indicated that nitrogen aeration

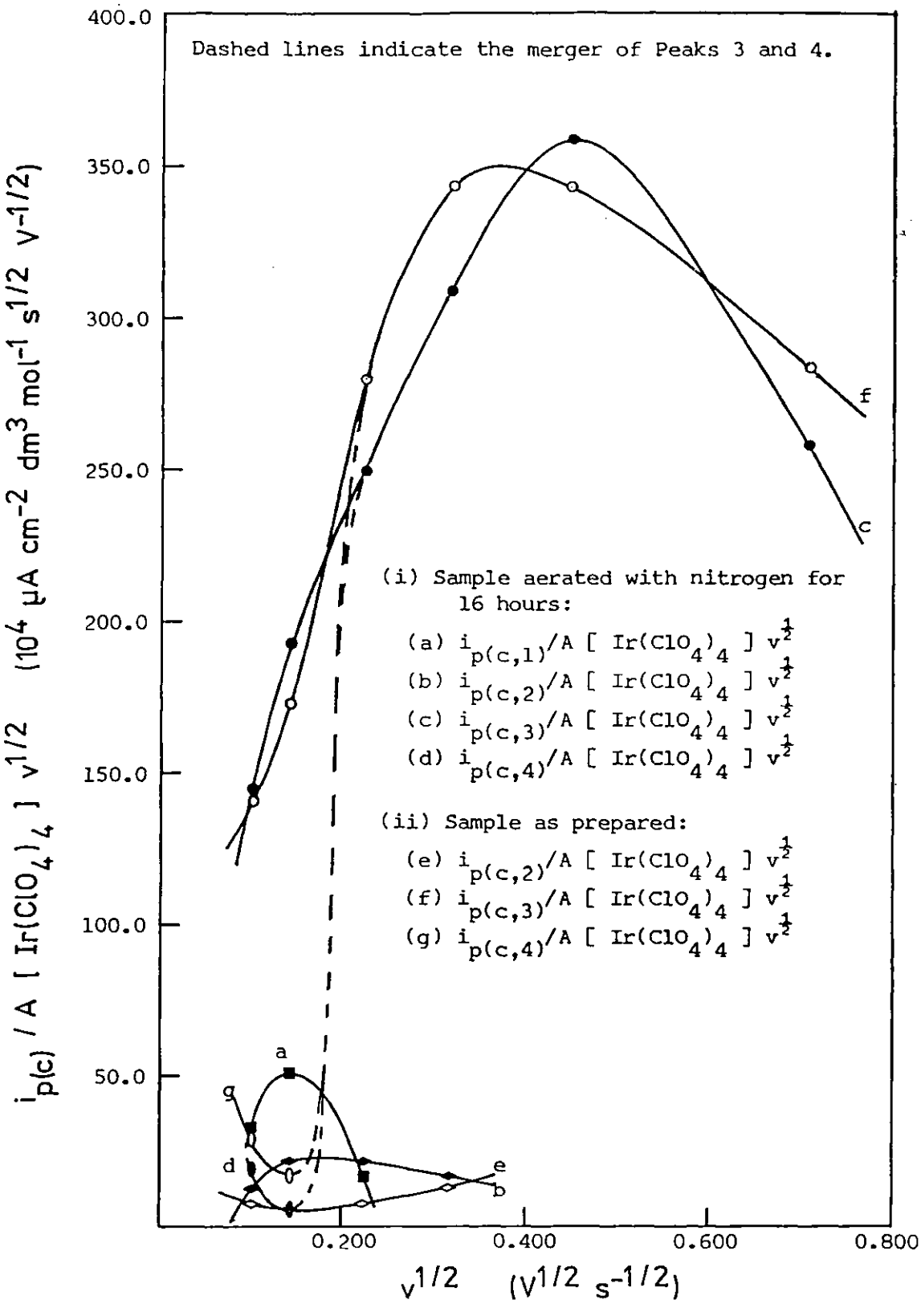

Fig. 5-247 Ir(IV) Perchlorate (8.0×10^{-4} mol dm^{-3})/Perchloric acid (0.1 M) supporting electrolyte System: Values of cathodic current function, $i_{p(c)}/A\ [\ Ir(ClO_4)_4\ ]\ v^{\frac{1}{2}}$, as a function of square root of potential scan rate, $v^{\frac{1}{2}}$. Boron carbide/carbon composite solid electrode $B_{3.11}C$.

Fig. 5-247 (continued):-

Two-way Analysis of Variance:

$\frac{i_{p(c,2)}}{A\,[\,Ir(ClO_4)_4\,]\,v^{\frac{1}{2}}}$

Grand mean = 1.31×10^5 μA cm^{-2} dm^3 mol^{-1} $s^{\frac{1}{2}}$ $V^{-\frac{1}{2}}$

Standard deviation = 5.92×10^4 μA cm^{-2} dm^3 mol^{-1} $s^{\frac{1}{2}}$ $V^{-\frac{1}{2}}$

Variance ratio due to effects of scan rate, F(v) = 0.550

Degrees of freedom = 3

Degrees of freedom of the Residual = 3

$F_{0.05}(3,3)$ = 15.4 (double-sided)

Therefore, since F(v) does not exceed $F_{0.05}(3,3)$, the effects of scan rate are not significant.

Variance ratio due to effects of nitrogen aeration, $F(N_2)$ = 9.75

Degrees of freedom = 1

Degrees of freedom of the Residual = 3

$F_{0.05}(1,3)$ = 17.4 (double-sided)

Therefore, since $F(N_2)$ does not exceed $F_{0.05}(1,3)$, the effects of nitrogen aeration are not significant.

$\frac{i_{p(c,3)}}{A\,[\,Ir(ClO_4)_4\,]\,v^{\frac{1}{2}}}$

Grand mean = 2.56×10^6 μA cm^{-2} dm^3 mol^{-1} $s^{\frac{1}{2}}$ $V^{-\frac{1}{2}}$

Standard deviation = 7.43×10^5 μA cm^{-2} dm^3 mol^{-1} $s^{\frac{1}{2}}$ $V^{-\frac{1}{2}}$

Variance ratio due to effects of scan rate, F(v) = 42.8

Degrees of freedom = 5

Degrees of freedom of the Residual = 5

$F_{0.05}(5,5)$ = 7.15 (double-sided)

Therefore, since F(v) exceeds $F_{0.05}(5,5)$, the effects of scan rate are significant.

Variance ratio due to effects of nitrogen aeration, $F(N_2)$ = 0.694

Degrees of freedom = 1

Degrees of freedom of the Residual = 5

$F_{0.05}(1,5)$ = 10.0 (double-sided)

Therefore, since $F(N_2)$ does not exceed $F_{0.05}(1,5)$, the effects of nitrogen aeration are not significant.

$\frac{i_{p(c,4)}}{A\,[\,Ir(ClO_4)_4\,]\,v^{\frac{1}{2}}}$

Grand mean = 1.78×10^5 μA cm^{-2} dm^3 mol^{-1} $s^{\frac{1}{2}}$ $V^{-\frac{1}{2}}$

Standard deviation = 8.38×10^4 μA cm^{-2} dm^3 mol^{-1} $s^{\frac{1}{2}}$ $V^{-\frac{1}{2}}$

Variance ratio due to the effects of scan rate, F(v) = 517

Degrees of freedom = 1

Degrees of freedom of the Residual = 1

$F_{0.05}(1,1)$ = 648 (double-sided)

Therefore, since F(v) does not exceed $F_{0.05}(1,1)$, the effects of scan rate are not significant.

Variance ratio due to effects of nitrogen aeration, $F(N_2)$ = 366

Degrees of freedom = 1

Degrees of freedom of the Residual = 1

Therefore, since $F(N_2)$ does not exceed $F_{0.05}(1,1)$, the effects of nitrogen aeration are not significant.

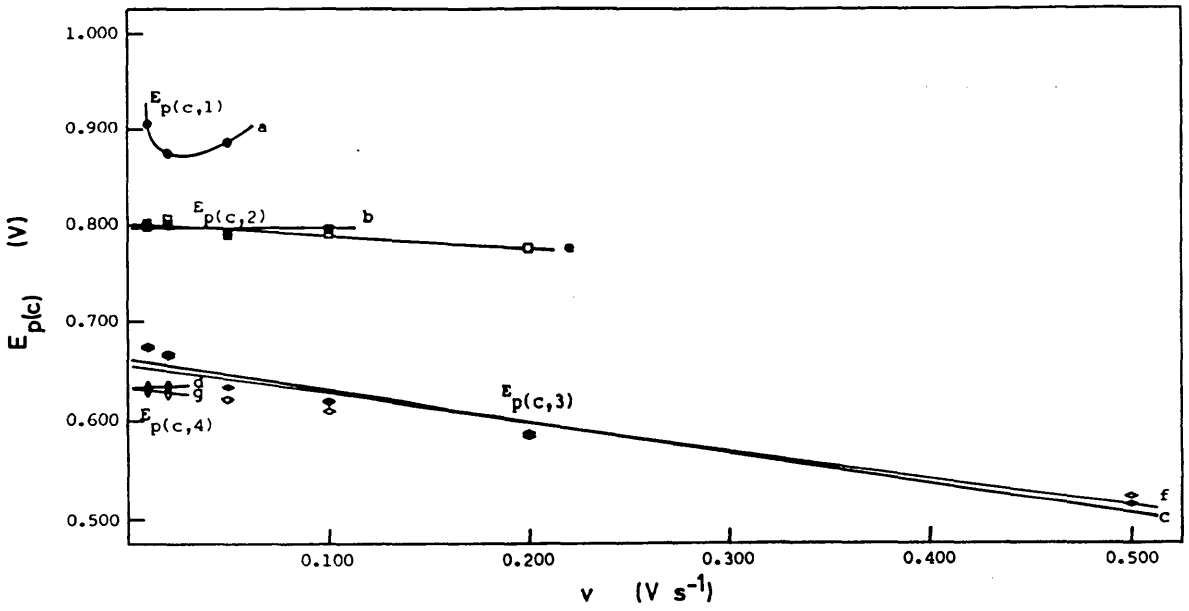

Fig. 5-248 Ir(IV) Perchlorate (8.0×10^{-4} mol dm^{-3})/Perchloric acid (0.1 M) supporting electrolyte System: Values of cathodic peak potential, $E_{p(c)}$, as a function of potential scan rate, v. (i) Sample solution aerated with nitrogen for 16 hours: a, b, c, and d. (ii) Sample solution as prepared: e, f, and g. Boron carbide/carbon composite solid electrode $B_{3.11}C$.

(i) Sample solution aerated with nitrogen for 16 hours:

(a) $E_{p(c,1)}$ mean = 0.888 V
Standard deviation = 0.015 V
Coefficient of variation = 1.74%
Degrees of freedom = 2

(b) $E_{p(c,2)}$ mean = 0.797 V
Standard deviation = 0.004 V
Coefficient of variation = 0.520%
Degrees of freedom = 3

(c) $E_{p(c,3)} = 0.661 - 0.312$ v
Correlation coefficient = -0.9730
Level of significance, $p = 0.001 < p < 0.01$
Standard deviation of $E_{p(c,3)}$ from regression = 0.015 V
Degrees of freedom = 4

(d) $E_{p(c,4)}$ mean = 0.632 V
Standard deviation = 0.001 V
Coefficient of variation = 0.201%
Degrees of freedom = 1

(ii) Sample solution as prepared:

(e) $E_{p(c,2)} = 0.802 - 0.137$ v
Correlation coefficient = -0.9088
Level of significance, $p = 0.02 < p < 0.05$
Standard deviation of $E_{p(c,2)}$ from regression = 0.006 V
Degrees of freedom = 3

(f) $E_{p(c,3)} = 0.654 - 0.282$ v
Correlation coefficient = -0.9426
Level of significance, $p = 0.001 < p < 0.01$
Standard deviation of $E_{p(c,3)}$ from regression = 0.021 V
Degrees of freedom = 4

Fig. 5-248 (continued):-

(g) $E_{p(c,4)}$ mean = 0.627 V
Standard deviation = 0.002 V
Coefficient of variation = 0.361%
Degrees of freedom = 1

Two-way Analysis of Variance:

$E_{p(c,2)}$

Grand mean = 0.796 V
Standard deviation = 0.006 V

Variance ratio due to effects of scan rate, F(v) = 6.68
Degrees of freedom = 3
Degrees of freedom of the Residual = 3
$F_{0.05}(3,3)$ = 15.4 (double-sided)
Therefore, since F(v) does not exceed $F_{0.05}(3,3)$, the effects of scan rate are not significant.

Variance ratio due to effects of nitrogen aeration, $F(N_2)$ = 0.446
Degrees of freedom = 1
Degrees of freedom of the Residual = 3
$F_{0.05}(1,3)$ = 17.4 (double-sided)
Therefore, since $F(N_2)$ does not exceed $F_{0.05}(1,3)$, the effects of nitrogen aeration are not significant.

$E_{p(c,3)}$

Grand mean = 0.614 V
Standard deviation = 0.053 V

Variance ratio due to effects of scan rate, F(v) = 241
Degrees of freedom = 5
Degrees of freedom of the Residual = 5
$F_{0.05}(5,5)$ = 7.15 (double-sided)
Therefore, since F(v) exceeds $F_{0.05}(5,5)$, the effects of scan rate are significant.

Variance ratio due to effects of nitrogen aeration, $F(N_2)$ = 0.706
Degrees of freedom = 1
Degrees of freedom of the Residual = 5
$F_{0.05}(1,5)$ = 10.0 (double-sided)
Therefore, since $F(N_2)$ does not exceed $F_{0.05}(1,5)$, the effects of nitrogen aeration are not significant.

$E_{p(c,4)}$

Grand mean = 0.630 V
Standard deviation = 0.003 V

Variance ratio due to effects of scan rate, F(v) = 784
Degrees of freedom = 1
Degrees of freedom of the Residual = 1
$F_{0.05}(1,1)$ = 648 (double-sided)
Therefore, since F(v) exceeds $F_{0.05}(1,1)$, the effects of scan rate are significant.

Variance ratio due to effects of nitrogen aeration, $F(N_2)$ = 4.00
Degrees of freedom = 1
Degrees of freedom of the Residual = 1
Therefore, since $F(N_2)$ does not exceed $F_{0.05}(1,1)$, the effects of nitrogen aeration are not significant.

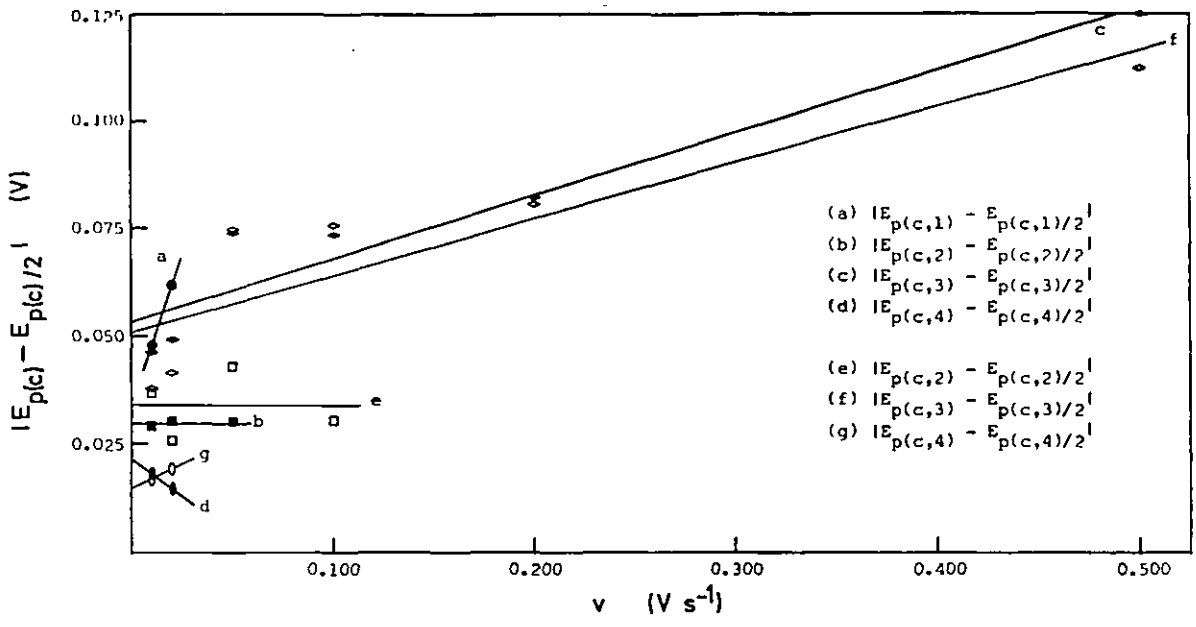

Fig. 5-249 Ir(IV) Perchlorate (8.0×10^{-4} mol dm^{-3})/Perchloric acid (0.1 M) supporting electrolyte System: Values of the difference between cathodic peak and half-peak potential, $|E_{p(c)} - E_{p(c)/2}|$, as a function of potential scan rate, v. (i) Sample solution aerated with nitrogen for 16 hours: a, b, c, and d. (ii) Sample solution as prepared: e, f, and g. Boron carbide/carbon composite solid electrode $B_{3.11}C$.

(i) Sample solution aerated with nitrogen for 16 hours:

(b) $|E_{p(c,2)} - E_{p(c,2)/2}|$ mean = 0.030 V
Standard deviation = 0.001 V
Coefficient of variation = 2.54%
Degrees of freedom = 2

(c) $|E_{p(c,3)} - E_{p(c,3)/2}| = 5.33 \times 10^{-2} + 0.147\ v$
Correlation coefficient = 0.9584
Level of significance, $p = 0.001 < p < 0.01$
Standard deviation of $|E_{p(c,3)} - E_{p(c,3)/2}|$ from regression = 0.009 V
Degrees of freedom = 4

(ii) Sample solution as prepared:

(e) $|E_{p(c,2)} - E_{p(c,2)/2}|$ mean = 0.034 V
Standard deviation = 0.008 V
Coefficient of variation = 2.26%
Degrees of freedom = 3

(f) $|E_{p(c,3)} - E_{p(c,3)/2}| = 5.10 \times 10^{-2} + 0.132.v$
Correlation coefficient = 0.8881
Level of significance, $p = 0.01 < p < 0.02$
Standard deviation of $|E_{p(c,3)} - E_{p(c,3)/2}|$ from regression = 0.014 V
Degrees of freedom = 4

Fig. 5-249 (continued):-

Two-way Analysis of Variance:

$|E_{p(c,2)} - E_{p(c,2)/2}|$

Grand mean = 0.032 V

Standard deviation = 0.006 V

Variance ratio due to effects of scan rate, F(v) = 0.952

Degrees of freedom = 2

Degrees of freedom of the Residual = 2

$F_{0.05}(2,2)$ = 39.0 (double-sided)

Therefore, since F(v) does not exceed $F_{0.05}(2,2)$, the effects of scan rate are not significant.

Variance ratio due to effects of nitrogen aeration, $F(N_2)$ = 1.10

Degrees of freedom = 1

Degrees of freedom of the Residual = 2

$F_{0.05}(1,2)$ = 38.5 (double-sided)

Therefore, since $F(N_2)$ does not exceed $F_{0.05}(1,2)$, the effects of nitrogen aeration sre not significant.

$|E_{p(c,3)} - E_{p(c,3)/2}|$

Grand mean = 0.073 V

Standard deviation = 0.026 V

Variance ratio due to effects of scan rate, F(v) = 91.5

Degrees of freedom = 5

Degrees of freedom of the Residual = 5

$F_{0.05}(5,5)$ = 7.15 (double-sided)

Therefore, since F(v) exceeds $F_{0.05}(5,5)$, the effects of scan rate are significant.

Variance ratio due to effects of nitrogen aeration, $F(N_2)$ = 3.55

Degrees of freedom = 1

Degrees of freedom of the Residual = 5

$F_{0.05}(1,5)$ = 10.0 (double-sided)

Therefore, since $F(N_2)$ does not exceed $F_{0.05}(1,5)$, the effects of nitrogen aeration are not significant.

$|E_{p(c,4)} - E_{p(c,4)/2}|$

Grand mean = 0.017 V

Standard deviation = 0.002 V

Variance ratio due to effects of scan rate, F(v) = 2.49×10^{-2}

Degrees of freedom = 1

Degrees of freedom of the Residual = 1

$F_{0.05}(1,1)$ = 648 (double-sided)

Therefore, since F(v) does not exceed $F_{0.05}(1,1)$, the effects of scan rate are not significant.

Variance ratio due to effects of nitrogen aeration, $F(N_2)$ = 0.335

Degrees of freedom = 1

Degrees of freedom of the Residual = 1

Therefore, since $F(N_2)$ does not exceed $F_{0.05}(1,1)$, the effects of nitrogen aeration are not significant.

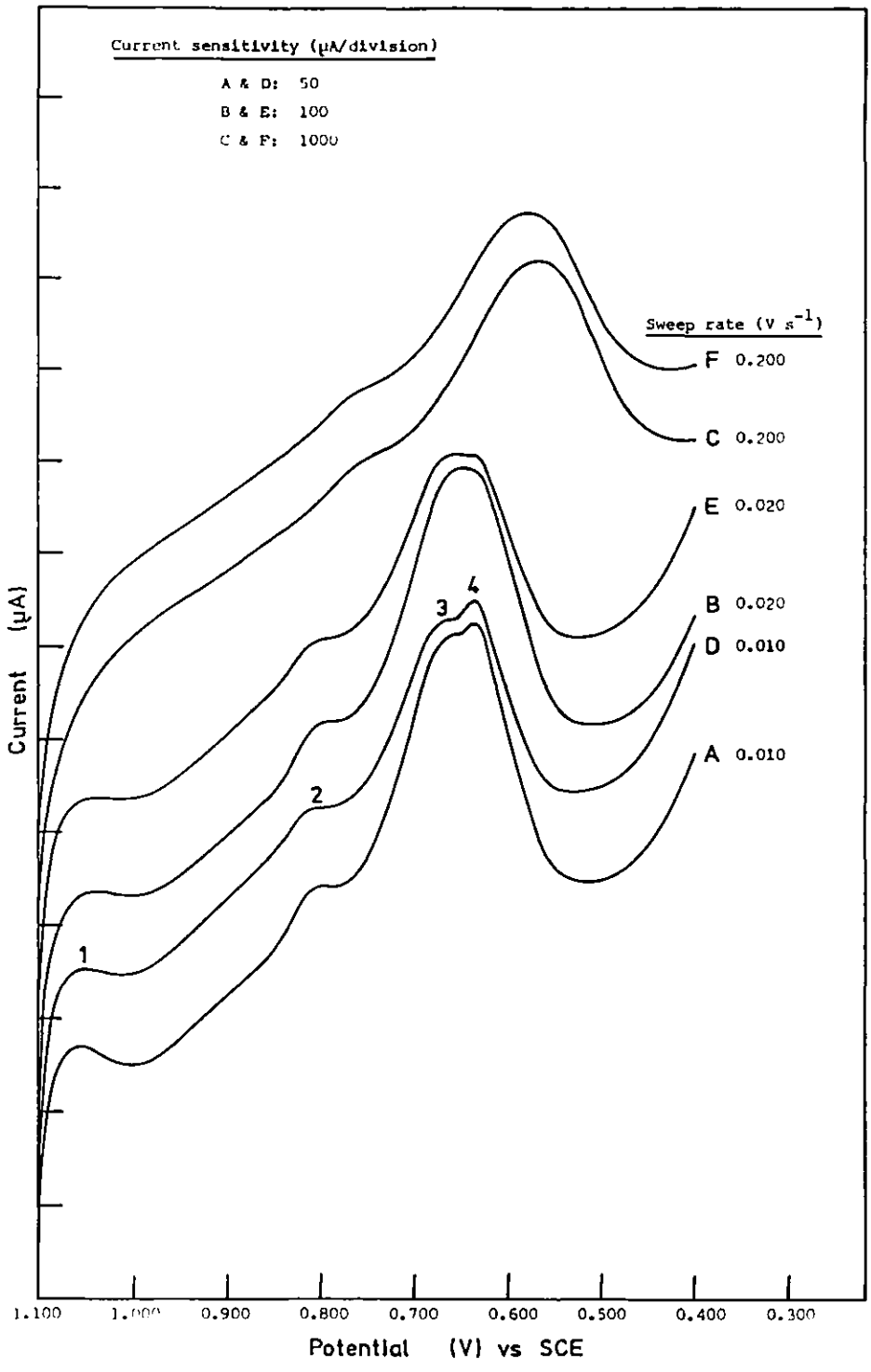

Fig. 5-250 Ir(IV) perchlorate (8.0×10^{-4} mol dm^{-3})/Perchloric acid (0.1 M) supporting electrolyte System: Linear sweep voltammograms obtained at the boron carbide/carbon composite solid electrode $B_{2.56}C$ — variation with sweep rate. A to C inclusive: sample as prepared. D to F inclusive: sample aerated with nitrogen for 16 hours.

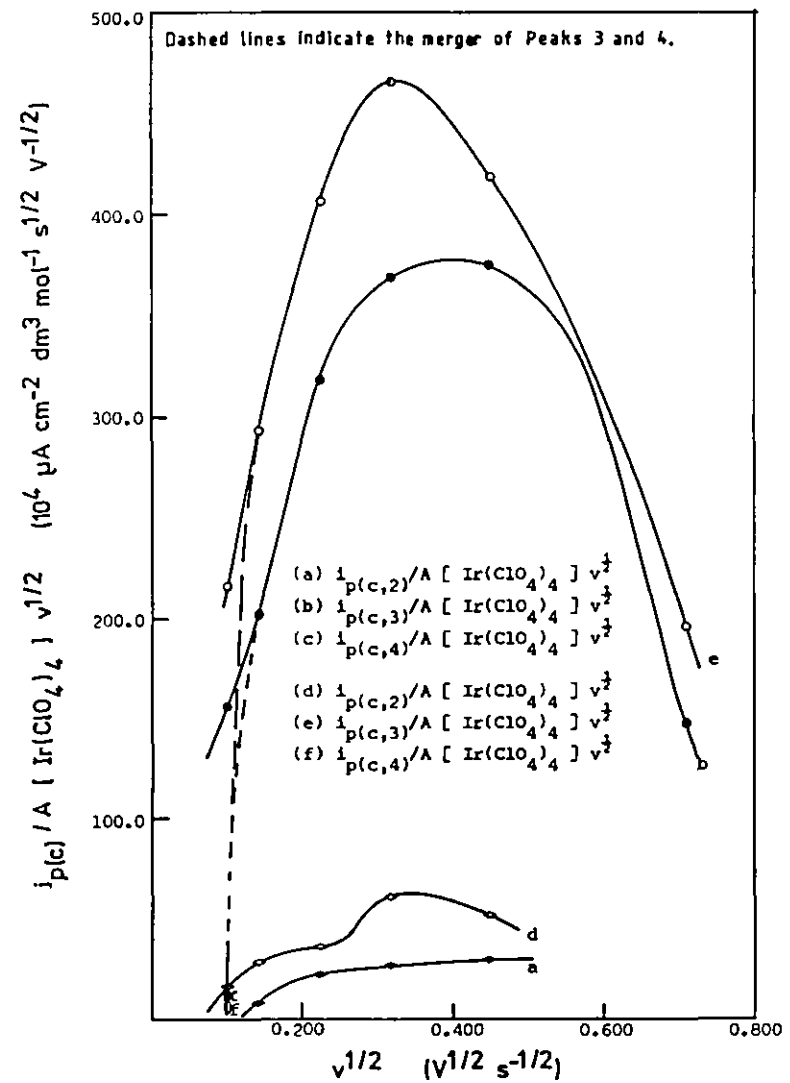

Fig. 5-251 Ir(IV) Perchlorate (8.0×10^{-4} mol dm^{-3})/Perchloric acid (0.1 M) supporting electrolyte System: Values of cathodic current function, $i_{p(c)}/A$ [$Ir(ClO_4)_4$] $v^{\frac{1}{2}}$, as a function of square root of potential scan rate, $v^{\frac{1}{2}}$. (i) Sample solution aerated with nitrogen for 16 hours: a, b, and c. (ii) Sample solution as prepared: d, e, and f. Boron carbide/carbon composite solid electrode $B_{2.56}C$.

Two-way Analysis of Variance:

$\frac{i_{p(c,2)}/A \text{ [} Ir(ClO_4)_4 \text{] } v^{\frac{1}{2}}}{}$

Grand mean = 3.30×10^5 µA cm^{-2} dm^3 mol^{-1} s$^{\frac{1}{2}}$ v$^{-\frac{1}{2}}$

Standard deviation = 1.57×10^5 µA cm^{-2} dm^3 mol^{-1} s$^{\frac{1}{2}}$ v$^{-\frac{1}{2}}$

Variance ratio due to effects of scan rate, F(v) = 7.46

Degrees of freedom = 3

Degrees of freedom of the Residual = 3

$F_{0.05}(3,3)$ = 15.4 (double-sided)

Therefore, since F(v) does not exceed $F_{0.05}(3,3)$, the effects of scan rate are not significant.

Variance ratio due to effects of nitrogen aeration, $F(N_2)$ = 28.3

Degrees of freedom = 1

Degrees of freedom of the Residual = 3

$F_{0.05}(1,3)$ = 17.4 (double-sided)

Therefore, since $F(N_2)$ exceeds $F_{0.05}(1,3)$, the effects of nitrogen aeration are significant.

$\frac{i_{p(c,3)}/A \text{ [} Ir(ClO_4)_4 \text{] } v^{\frac{1}{2}}}{}$

Grand mean = 2.97×10^6 µA cm^{-2} dm^3 mol^{-1} s$^{\frac{1}{2}}$ v$^{-\frac{1}{2}}$

Standard deviation = 1.06×10^6 µA cm^{-2} dm^3 mol^{-1} s$^{\frac{1}{2}}$ v$^{-\frac{1}{2}}$

Variance ratio due to effects of scan rate, F(v) = 84.7

Degrees of freedom = 5

Degrees of freedom of the Residual = 5

$F_{0.05}(5,5)$ = 7.15 (double-sided)

Therefore, since F(v) exceeds $F_{0.05}(5,5)$, the effects of scan rate are significant.

Variance ratio due to effects of nitrogen aeration, $F(N_2)$ = 54.6

Degrees of freedom = 1

Degrees of freedom of the Residual = 5

$F_{0.05}(1,5)$ = 10.0 (double-sided)

Therefore, since $F(N_2)$ exceeds $F_{0.05}(1,5)$, the effects of nitrogen aeration are significant.

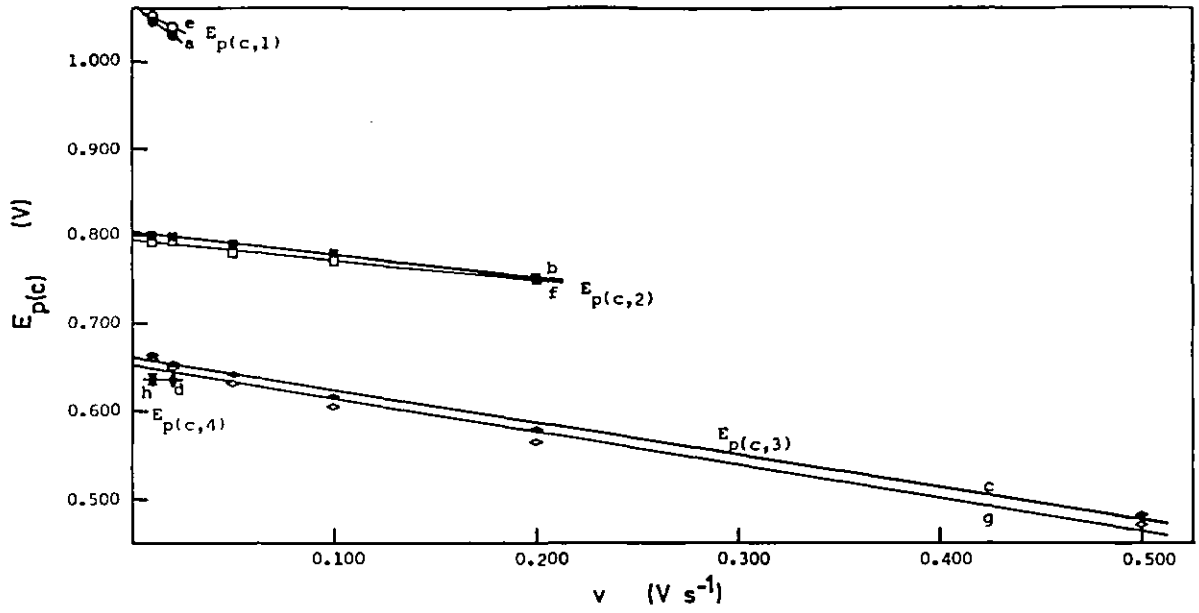

Fig. 5-252 Ir(IV) Perchlorate (8.0×10^{-4} mol dm^{-3})/Perchloric acid (0.1 M) supporting electrolyte System: Values of cathodic peak potential, $E_{p(c)}$, as a function of potential scan rate, v. (i) Sample solution aerated with nitrogen for 16 hours: a, b, c, and d. (ii) Sample solution as prepared: e, f, g, and h. Boron carbide/carbon composite solid electrode $B_{2.56}C$.

(i) Sample solution aerated with nitrogen for 16 hours:

(a) $E_{p(c,1)}$ mean = 1.038 V
Standard deviation = 0.012 V
Coefficient of variation = 1.11%
Degrees of freedom = 1

(b) $E_{p(c,2)} = 0.804 - 0.256\ v$
Correlation coefficient = -0.9975
Level of significance, p = $p < 0.001$
Standard deviation of $E_{p(c,2)}$ from regression = 0.002 V
Degrees of freedom = 3

(c) $E_{p(c,3)} = 0.660 - 0.365\ v$
Correlation coefficient = -0.9952
Level of significance, p = $p < 0.001$
Standard deviation of $E_{p(c,3)}$ from regression = 0.008 V
Degrees of freedom = 4

(d) $E_{p(c,4)}$ mean = 0.635 V
Standard deviation = 0.000 V
Degrees of freedom = 1

(ii) Sample solution as prepared:

(e) $E_{p(c,1)}$ mean = 1.045 V
Standard deviation = 0.007 V
Coefficient of variation = 0.711%
Degrees of freedom = 1

(f) $E_{p(c,2)} = 0.795 - 0.231\ v$
Correlation coefficient = -0.9898
Level of significance, p = $0.001 < p < 0.01$
Standard deviation of $E_{p(c,2)}$ from regression = 0.003 V
Degrees of freedom = 3

Fig. 5-252 (continued):-

(g) $E_{p(c,3)} = 0.652 - 0.377\ v$
Correlation coefficient = -0.9916
Level of significance, p = $p < 0.001$
Standard deviation of $E_{p(c,3)}$ from regression = 0.010 V
Degrees of freedom = 4

Two-way Analysis of Variance:

$E_{p(c,1)}$

Grand mean = 1.041 V
Standard deviation = 0.008 V

Variance ratio due to effects of scan rate, F(v) = 21.4
Degrees of freedom = 1
Degrees of freedom of the Residual = 1
$F_{0.05}(1,1)$ = 648 (double-sided)
Therefore, since F(v) does not exceed $F_{0.05}(1,1)$, the effects of scan rate are not significant.

Variance ratio due to effects of nitrogen aeration, $F(N_2)$ = 5.18
Degrees of freedom = 1
Degrees of freedom of the Residual = 1
Therefore, since $F(N_2)$ does not exceed $F_{0.05}(1,1)$, the effects of nitrogen aeration are not significant.

$E_{p(c,2)}$

Grand mean = 0.781 V
Standard deviation = 0.017 V

Variance ratio due to effects of scan rate, F(v) = 154
Degrees of freedom = 4
Degrees of freedom of the Residual = 4
$F_{0.05}(4,4)$ = 9.60 (double-sided)
Therefore, since F(v) exceeds $F_{0.05}(4,4)$, the effects of scan rate are significant.

Variance ratio due to effects of nitrogen aeration, $F(N_2)$ = 24.2
Degrees of freedom = 1
Degrees of freedom of the Residual = 4
$F_{0.05}(1,4)$ = 12.2 (double-sided)
Therefore, since $F(N_2)$ exceeds $F_{0.05}(1,4)$, the effects of nitrogen aeration are significant.

$E_{p(c,3)}$

Grand mean = 0.602 V
Standard deviation = 0.064 V

Variance ratio due to effects of scan rate, F(v) = 1.59×10^3
Degrees of freedom = 5
Degrees of freedom of the Residual = 5
$F_{0.05}(5,5)$ = 7.15 (double-sided)
Therefore, since F(v) exceeds $F_{0.05}(5,5)$, the effects of scan rate are significant.

Variance ratio due to effects of nitrogen aeration, $F(N_2)$ = 44.4
Degrees of freedom = 1
Degrees of freedom of the Residual = 5
$F_{0.05}(1,5)$ = 10.0 (double-sided)
Therefore, since $F(N_2)$ exceeds $F_{0.05}(1,5)$, the effects of nitrogen aeration are significant.

significantly affected the values of $E_{p(c,2)}$ and $E_{p(c,3)}$ but not the values of $E_{p(c,1)}$ with respect to the degrees of freedom available. $|E_{p(c,2)} - E_{p(c,2)/2}|$ and $|E_{p(c,3)} - E_{p(c,3)/2}|$ values did not show any significant differences attributable to nitrogen aeration (Fig. 5-253).

5-1.5.(iii).e Graphite solid electrode

Linear sweep voltammograms, obtained at the graphite solid electrode, for nitrogen aerated (16 hours) Ir(IV) perchlorate (8.0×10^{-4} mol dm^{-3})/$HClO_4$ (0.1 M) supporting electrolyte solution are presented in Fig. 5-254; four peaks, Peaks 1 to 4 inclusive, being exhibited at slow sweep rates. Qualitatively, it can be seen that Peaks 2 and 4 predominate at high sweep rates. Quantitative treatment shows the influence of adsorption on Peaks 1 to 3 inclusive, but the peak current function for Peak 4 decreased with increasing sweep rate (Fig. 5-255). Fig. 5-254, however, qualitatively reveals that the peak current function for Peak 4 decreased because Peak 3 was cathodically shifted by the increasing sweep rate and thus intensified the deformation of Peak 4. The cathodic peak potentials are plotted as functions of sweep rate in Fig. 5-256 which shows that $E_{p(c,1)}$, $E_{p(c,2)}$, and $E_{p(c,4)}$ remained relatively constant whilst $E_{p(c,3)}$ was cathodically shifted by increasing sweep rate. Plots of the values of $|E_p - E_{p/2}|$ as functions of sweep rate indicate that the charge transfer for Peak 3 became less reversible at faster sweep rates (Fig. 5-257).

The evidence suggests that Peak 1 was a diffusion wave complicated by weak adsorption influences emanating from the strong adsorption post-peak of Ir(IV) perchlorate reactant, Peak 2, whilst Peak 3 was a diffusion peak complicated by weak adsorption effects emanating from the moderately strong adsorption post-peak, Peak 4, of the reactant. Thus, at fast sweep rates the strong adsorption post-peaks, Peaks 2 and 4, predominated over the related diffusion peaks, Peaks 1 and 3 respectively.

5-1.5.(iii).f Summary

Nitrogen aeration (16 hours) of the Ir(IV) perchlorate sample did not result in any fundamental differences in the voltammograms obtained at the same working electrode. Thus, for comparable concentrations of Ir(IV) perchlorate reactant/perchloric acid supporting electrolyte solution, the same characteristic peaks were exhibited before and after

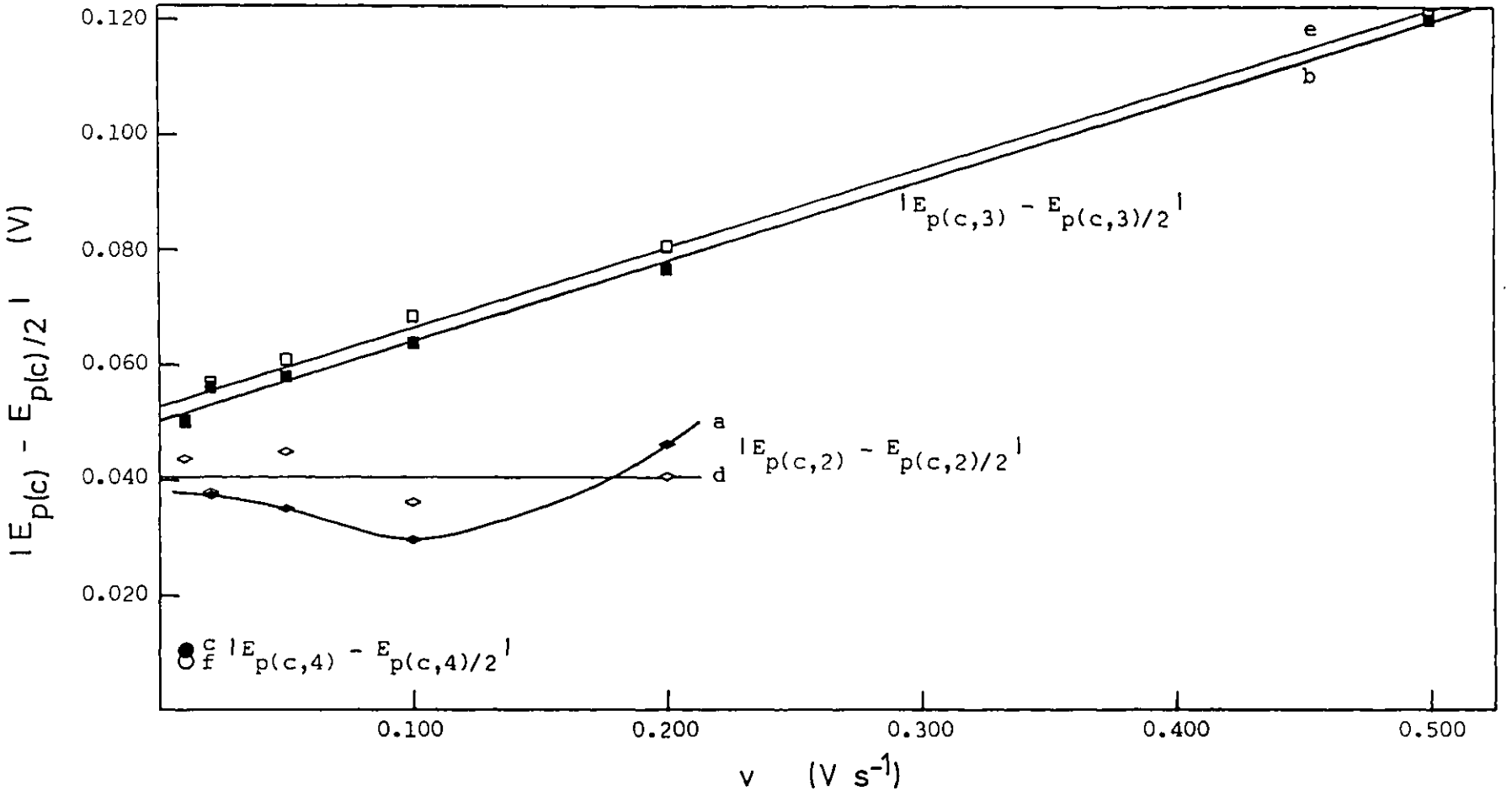

Fig. 5-253 Ir(IV) Perchlorate (8.0×10^{-4} mol dm^{-3})/Perchloric acid (0.1 M) supporting electrolyte System: Values of the difference between cathodic peak and half-peak potential, $|E_{p(c)} - E_{p(c)/2}|$, as a function of potential scan rate, v. (i) Sample solution aerated with nitrogen for 16 hours: a, b, and c. (ii) Sample solution as prepared: d, e, and f. Boron carbide/carbon composite solid electrode $B_{2.56}C$.

Fig. 5-253 (continued):-

(i) Sample solution aerated with nitrogen for 16 hours:

(a) $|E_{p(c,2)} - E_{p(c,2)/2}|$ mean = 0.037 V
Standard deviation = 0.007 V
Coefficient of variation = 18.3%
Degrees of freedom = 3

(b) $|E_{p(c,3)} - E_{p(c,3)/2}| = 5.03 \times 10^{-2} + 0.138$ v
Correlation coefficient = 0.9980
Level of significance, p = p $<$ 0.001
Standard deviation of $|E_{p(c,3)} - E_{p(c,3)/2}|$ from regression = 0.002 V
Degrees of freedom = 4

(ii) Sample solution as prepared:

(d) $|E_{p(c,2)} - E_{p(c,2)/2}|$ mean = 0.041 V
Standard deviation = 0.004 V
Coefficient of variation = 9.29%
Degrees of freedom = 4

(e) $|E_{p(c,3)} - E_{p(c,3)/2}| = 5.27 \times 10^{-2} + 0.138$ v
Correlation coefficient = 0.9964
Level of significance, p = p $<$ 0.001
Standard deviation of $|E_{p(c,3)} - E_{p(c,3)/2}|$ from regression = 0.002 V
Degrees of freedom = 4

Two-way Analysis of Variance:

$\underline{|E_{p(c,2)} - E_{p(c,2)/2}|}$

Grand mean = 0.039 V
Standard deviation = 0.005 V

Variance ratio due to effects of scan rate, F(v) = 1.56
Degrees of freedom = 3
Degrees of freedom of the Residual = 3
$F_{0.05}(3,3)$ = 15.4 (double-sided)

Therefore, since F(v) does not exceed $F_{0.05}(3,3)$, the effects of scan rate are not significant.

Variance ratio due to effects of nitrogen aeration, $F(N_2)$ = 0.559
Degrees of freedom = 1
Degrees of freedom of the Residual = 3
$F_{0.05}(1,3)$ = 17.4 (double-sided)
Therefore, since $F(N_2)$ does not exceed $F_{0.05}(1,3)$, the effects of nitrogen aeration are not significant.

$\underline{|E_{p(c,3)} - E_{p(c,3)/2}|}$

Grand mean = 0.072 V
Standard deviation = 0.024 V

Variance ratio due to effects of scan rate, F(v) = 648
Degrees of freedom = 5
Degrees of freedom of the Residual = 5
$F_{0.05}(5,5)$ = 7.15 (double-sided)
Therefore, since F(v) exceeds $F_{0.05}(5,5)$, the effects of scan rate are significant.

Variance ratio due to effects of nitrogen aeration, $F(N_2)$ = 7.84
Degrees of freedom = 1
Degrees of freedom of the Residual = 5
$F_{0.05}(1,5)$ = 10.0 (double-sided)
Therefore, since $F(N_2)$ does not exceed $F_{0.05}(1,5)$, the effects of nitrogen aeration are not significant.

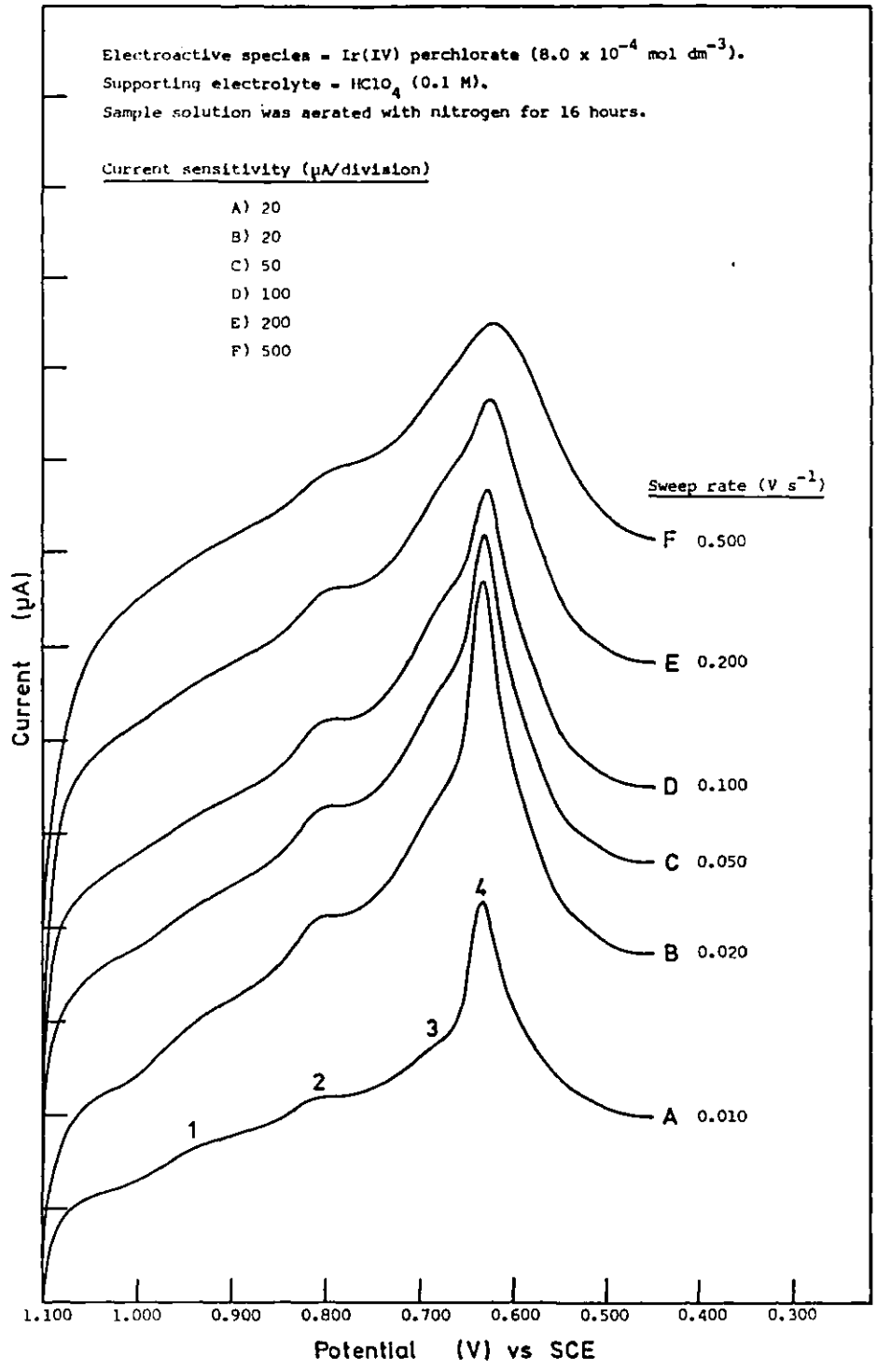

Fig. 5-254 Linear sweep voltammograms obtained at the graphite solid electrode — variation with sweep rate.

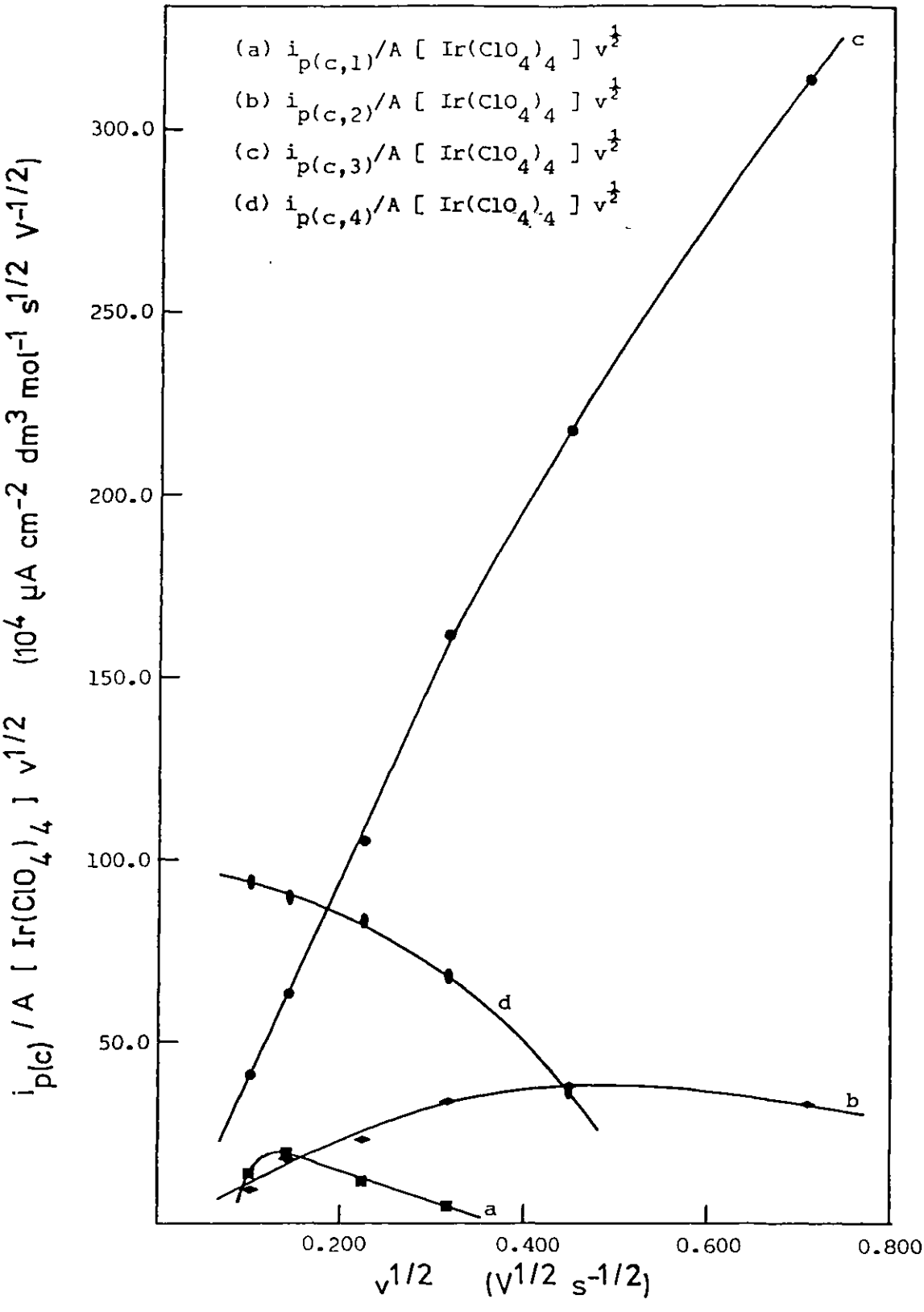

Fig. 5-255 Ir(IV) Perchlorate (8.0×10^{-4} mol dm^{-3})/Perchloric acid (0.1 M) supporting electrolyte System: Values of cathodic current function, $i_{p(c)}/A\ [\ Ir(ClO_4)_4\ ]\ v^{\frac{1}{2}}$, as a function of square root of potential scan rate, $v^{\frac{1}{2}}$. Sample solution was aerated with nitrogen for 16 hours. Graphite solid electrode.

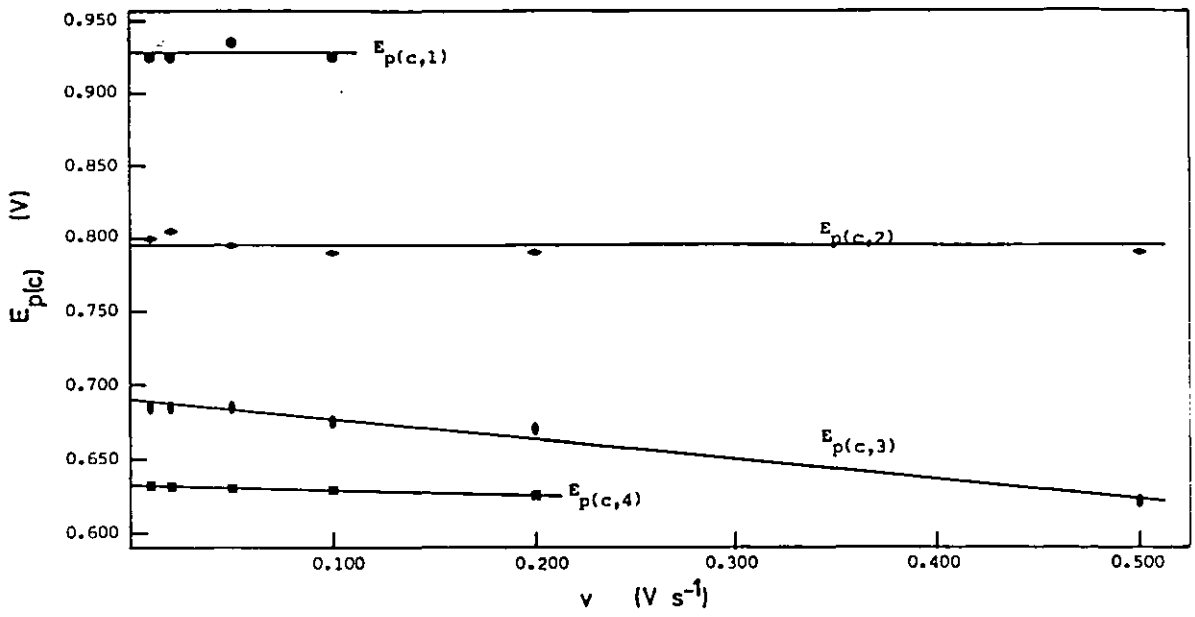

Fig. 5-256 Ir(IV) Perchlorate (8.0×10^{-4} mol dm^{-3})/Perchloric acid (0.1M) supporting electrolyte System: Values of cathodic peak potential, $E_{p(c)}$, as a function of potential scan rate, v. Sample solution was aerated with nitrogen for 16 hours. Graphite solid electrode.

(a) $E_{p(c,1)}$ mean = 0.928 V
Standard deviation = 0.005 V
Coefficient of variation = 0.539%
Degrees of freedom = 3

(b) $E_{p(c,2)}$ mean = 0.795 V
Standard deviation = 0.006 V
Coefficient of variation = 0.796%
Degrees of freedom = 5

(c) $E_{p(c,3)} = 0.690 - 0.134\ v$
Correlation coefficient = -0.9876
Level of significance, p = $p < 0.001$
Standard deviation of $E_{p(c,3)}$ from regression = 0.004 V
Degrees of freedom = 4

(d) $E_{p(c,4)} = 0.632 - 3.43 \times 10^{-2}\ v$
Correlation coefficient = -0.9835
Level of significance, p = $0.001 < p < 0.01$
Standard deviation of $E_{p(c,4)}$ from regression = 0.001 V
Degrees of freedom = 3

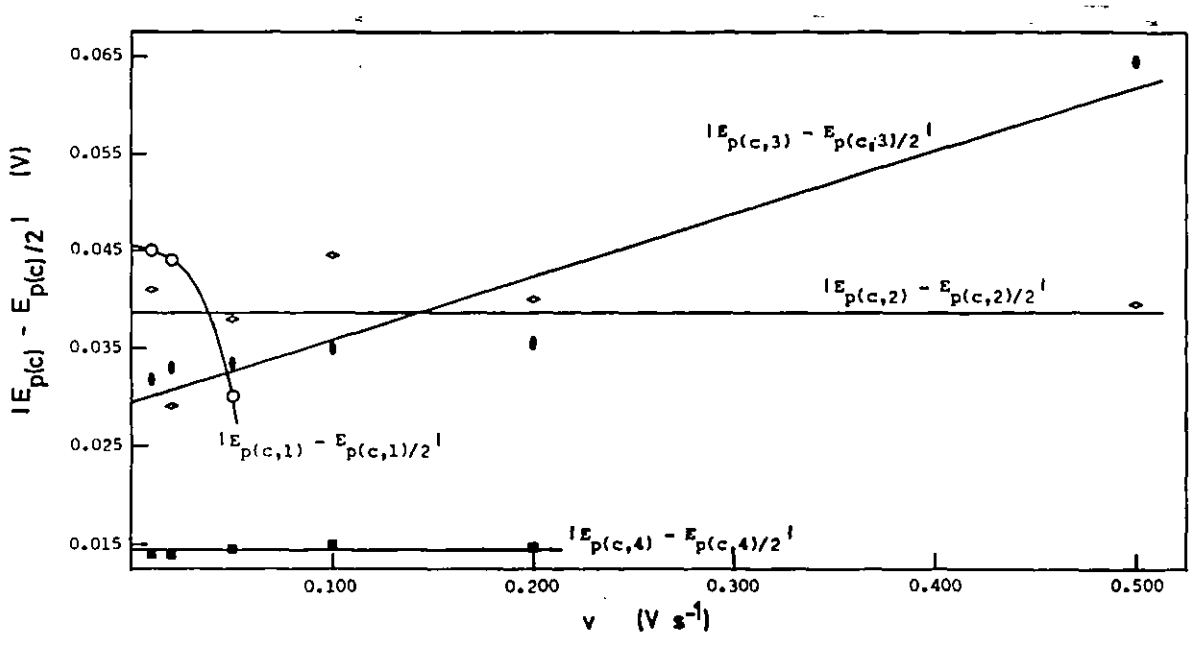

Fig. 5-257 Ir(IV) Perchlorate (8.0×10^{-4} mol dm^{-3})/Perchloric acid (0.1 M) supporting electrolyte System: Values of the difference between cathodic peak and half-peak potential, $|E_{p(c)} - E_{p(c)/2}|$, as a function of potential scan rate, v. Sample solution was aerated with nitrogen for 16 hours. Graphite solid electrode.

(a) $|E_{p(c,2)} - E_{p(c,2)/2}|$ mean = 0.039 V
Standard deviation = 0.005 V
Coefficient of variation = 13.4%
Degrees of freedom = 5

(b) $|E_{p(c,3)} - E_{p(c,3)/2}| = 2.94 \times 10^{-2} + 6.49 \times 10^{-2}$ v
Correlation coefficient = 0.9588
Level of significance, $p = 0.001 < p < 0.01$
Standard deviation of $|E_{p(c,3)} - E_{p(c,3)/2}|$ from regression
= 0.004 V
Degrees of freedom = 4

(c) $|E_{p(c,4)} - E_{p(c,4)/2}|$ mean = 0.014 V
Standard deviation = 4.39×10^{-4} V
Coefficient of variation = 3.04%
Degrees of freedom = 4

nitrogen aeration in linear sweep voltammetric studies. Similar behaviour was noticed in d.c. voltammetry.

Quantitative treatment coupled with statistical analysis, however, revealed some statistically significant differences in peak currents and peak potentials attributable to nitrogen aeration. In general, nitrogen aeration when shown to have a statistically significant effect caused a drop in the peak current, and an anodic shift in the corresponding peak potential; but the general trends with increasing sweep rate were unaltered.

5-1.5.(iv) The influence of boron carbide treatment on the Ir(IV) perchlorate system.

5-1.5.(iv).a Without nitrogen aeration

Linear sweep voltammograms for Ir(IV) perchlorate (2.3×10^{-3} mol dm^{-3}) in perchloric acid (0.1 M) supporting electrolyte, obtained at the boron carbide solid electrode $B_{3.86}C$, show qualitatively that treatment of the sample solution with boron carbide prior to voltammetry resulted in decreased peak currents coupled with cathodic shifts in peak potentials (Fig. 5-258). Quantitative treatment revealed that all three peaks exhibited, Peaks 1 to 3 inclusive, were influenced by adsorption (Fig. 5-259). Two-way ANOVA for the peak current functions confirmed that treatment of the sample with boron carbide significantly affected the peak currents of Peaks 1 and 3, but not Peak 2. The peak potentials are plotted as functions of sweep rate in Fig. 5-260 which illustrates the cathodic shifts caused by boron carbide treatment of the sample; as confirmed by two-way ANOVA of the results. Generally, the values of $|E_p - E_{p/2}|$ were widened by boron carbide treatment (Fig. 5-261); although two-way ANOVA confirmed this observation only for Peak 1.

5-1.5.(iv).b With nitrogen aeration

Linear sweep and cyclic voltammograms for Ir(IV) perchlorate (2.0×10^{-4} mol dm^{-3})/$HClO_4$ (0.1 M) supporting electrolyte solution, corresponding to the sample as prepared, sample aerated with nitrogen (16 hours), and nitrogen aerated sample treated with boron carbide (2 minutes), which were obtained at the boron carbide solid electrode $B_{3.86}C$

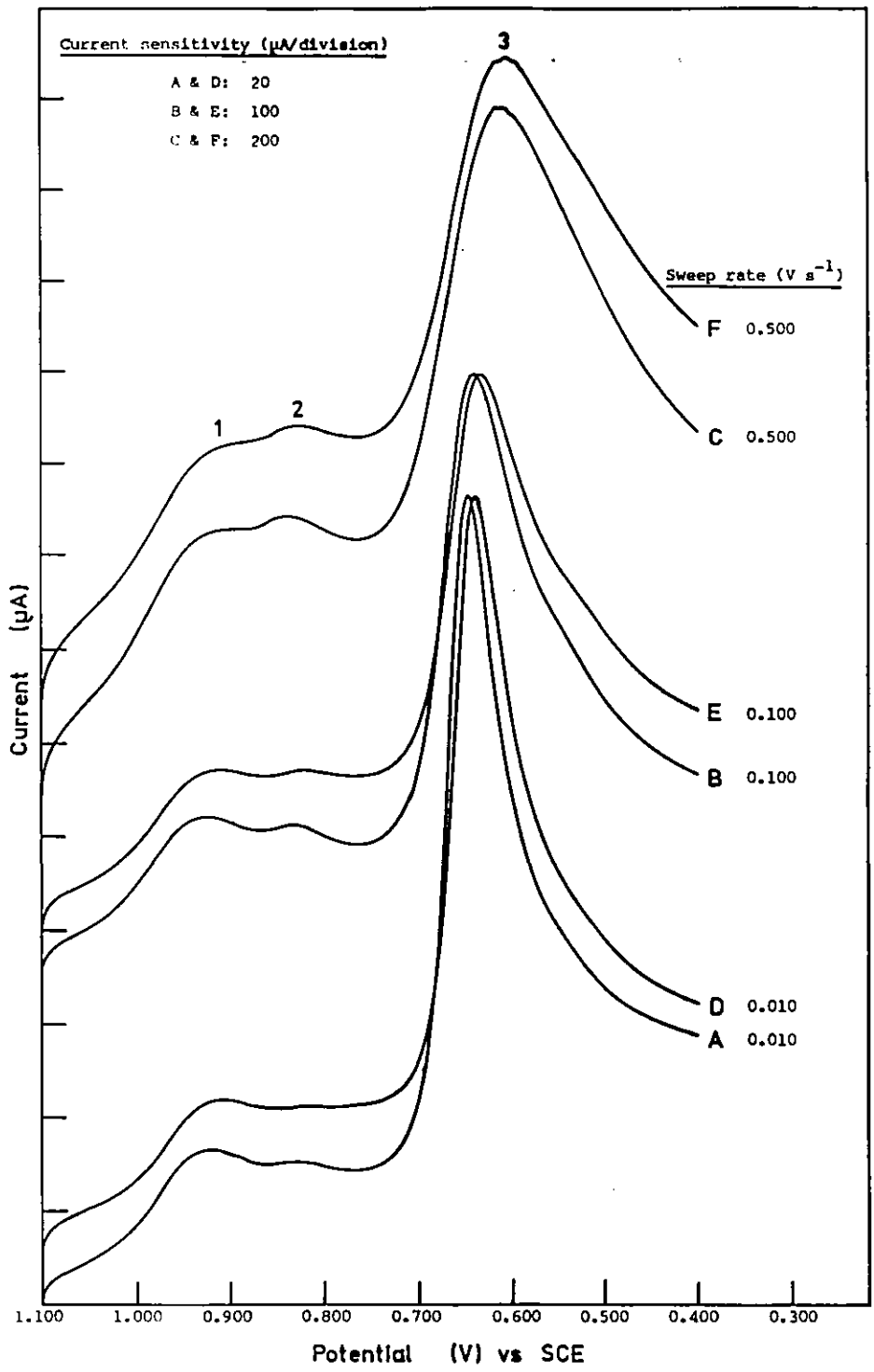

Fig. 5-258 Ir(IV) perchlorate (2.3×10^{-3} mol dm^{-3})/Perchloric acid (0.1 M) supporting electrolyte System: Linear sweep voltammograms obtained at the boron carbide solid electrode $B_{3.86}C$ — variation with sweep rate. A to C inclusive: sample as prepared. D to F inclusive: sample treated by prolonged contact with boron carbide.

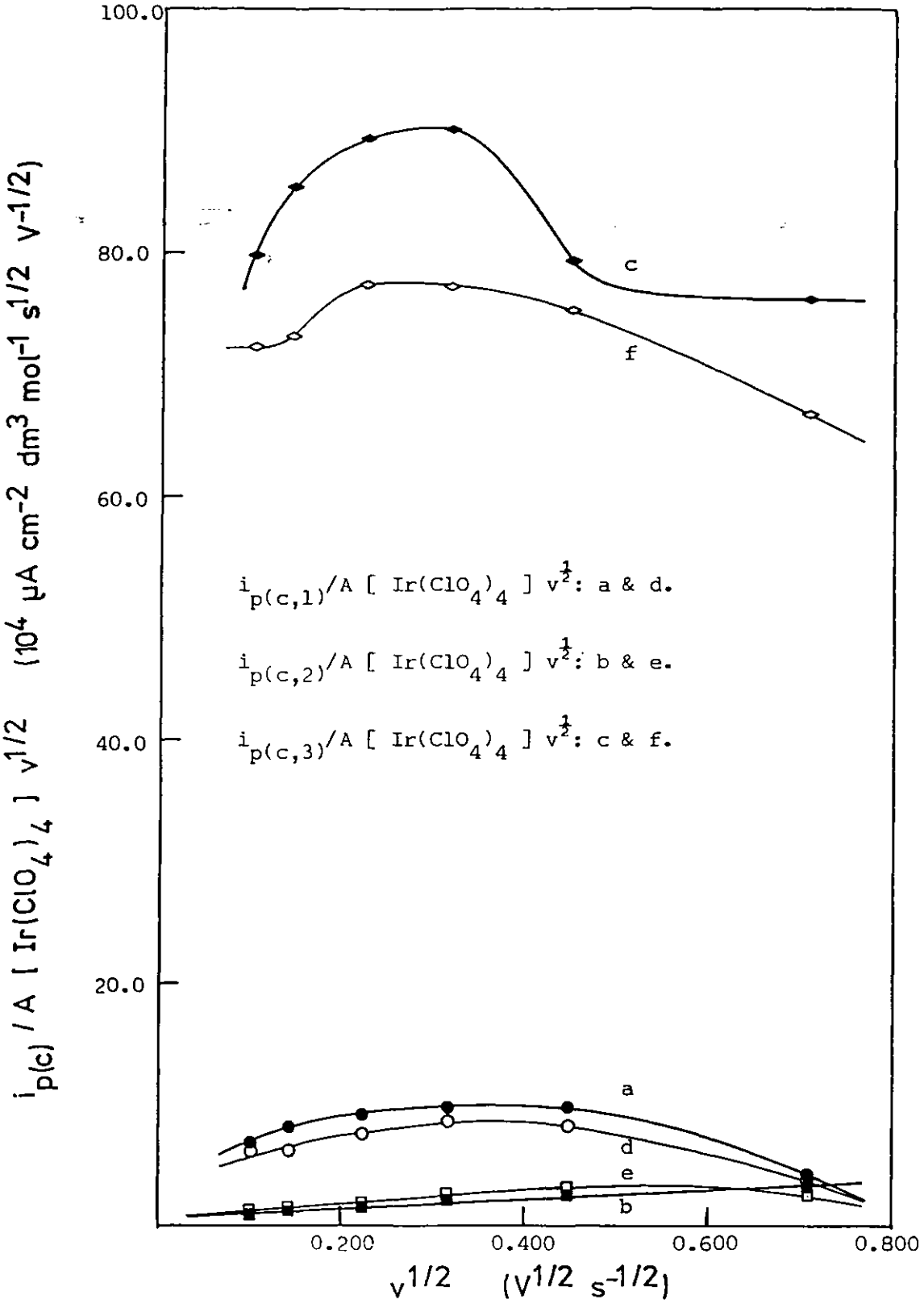

Fig. 5-259 Ir(IV) Perchlorate (2.3×10^{-3} mol dm^{-3})/Perchloric acid (0.1 M) supporting electrolyte System: Values of cathodic current function, $i_{p(c)}/A$ [$Ir(ClO_4)_4$] $v^{\frac{1}{2}}$, as a function of square root of potential scan rate, $v^{\frac{1}{2}}$. (i) Sample solution as prepared: a, b, and c. (ii) Sample solution after prolonged treatment with boron carbide: d, e, and f. Boron carbide solid electrode $B_{3.86}C$.

Fig. 5-259 (continued):-

(i) Sample solution as prepared:

(b) $i_{p(c,2)}/A\ [\ Ir(ClO_4)_4\ ]\ v^{\frac{1}{2}} = 5.92 \times 10^3 + 3.84 \times 10^4\ v^{\frac{1}{2}}$

Correlation coefficient = 0.9839

Level of significance, p = $p < 0.001$

Standard deviation of $i_{p(c,2)}/A\ [\ Ir(ClO_4)_4\ ]\ v^{\frac{1}{2}}$ from regression = 1.77×10^3 μA cm^{-2} dm^3 mol^{-1} $s^{\frac{1}{2}}$ $V^{-\frac{1}{2}}$

Degrees of freedom = 4

Two-way Analysis of Variance:

$\underline{i_{p(c,1)}/A\ [\ Ir(ClO_4)_4\ ]\ v^{\frac{1}{2}}}$

Grand mean = 7.35×10^4 μA cm^{-2} dm^3 mol^{-1} $s^{\frac{1}{2}}$ $V^{-\frac{1}{2}}$

Standard deviation = 1.93×10^4 μA cm^{-2} dm^3 mol^{-1} $s^{\frac{1}{2}}$ $V^{-\frac{1}{2}}$

Variance ratio due to effects of scan rate, F(v) = 52.8

Degrees of freedom = 5

Degrees of freedom of the Residual = 5

$F_{0.05}(5,5)$ = 7.15 (double-sided)

Therefore, since F(v) exceeds $F_{0.05}(5,5)$, the effects of scan rate are significant.

Variance ratio due to effects of boron carbide, F(boron carbide) = 34.8

Degrees of freedom = 1

Degrees of freedom of the Residual = 5

$F_{0.05}(1,5)$ = 10.0 (double-sided)

Therefore, since F(boron carbide) exceeds $F_{0.05}(1,5)$, the effects of boron carbide are significant.

$\underline{i_{p(c,2)}/A\ [\ Ir(ClO_4)_4\ ]\ v^{\frac{1}{2}}}$

Grand mean = 1.97×10^4 μA cm^{-2} dm^3 mol^{-1} $s^{\frac{1}{2}}$ $V^{-\frac{1}{2}}$

Standard deviation = 7.67×10^3 μA cm^{-2} dm^3 mol^{-1} $s^{\frac{1}{2}}$ $V^{-\frac{1}{2}}$

Variance ratio due to effects of scan rate, F(v) = 11.3

Degrees of freedom = 5

Degrees of freedom of the Residual = 5

Therefore, since F(v) exceeds $F_{0.05}(5,5)$, the effects of scan rate are significant.

Variance ratio due to effects of boron carbide, F(boron carbide) = 1.97

Degrees of freedom = 1

Degrees of freedom of the Residual = 5

Therefore, since F(boron carbide) does not exceed $F_{0.05}(1,5)$, the effects of boron carbide are not significant.

$\underline{i_{p(c,3)}/A\ [\ Ir(ClO_4)_4\ ]\ v^{\frac{1}{2}}}$

Grand mean = 7.85×10^5 μA cm^{-2} dm^3 mol^{-1} $s^{\frac{1}{2}}$ $V^{-\frac{1}{2}}$

Standard deviation = 6.65×10^4 μA cm^{-2} dm^3 mol^{-1} $s^{\frac{1}{2}}$ $V^{-\frac{1}{2}}$

Variance ratio due to effects of scan rate, F(v) = 7.37

Degrees of freedom = 5

Degrees of freedom of the Residual = 5

Therefore, since F(v) exceeds $F_{0.05}(5,5)$, the effects of scan rate are significant.

Variance ratio due to effects of boron carbide, F(boron carbide) = 48.3

Degrees of freedom = 1

Degrees of freedom of the Residual = 5

Therefore, since F(boron carbide) exceeds $F_{0.05}(1,5)$, the effects of boron carbide are significant.

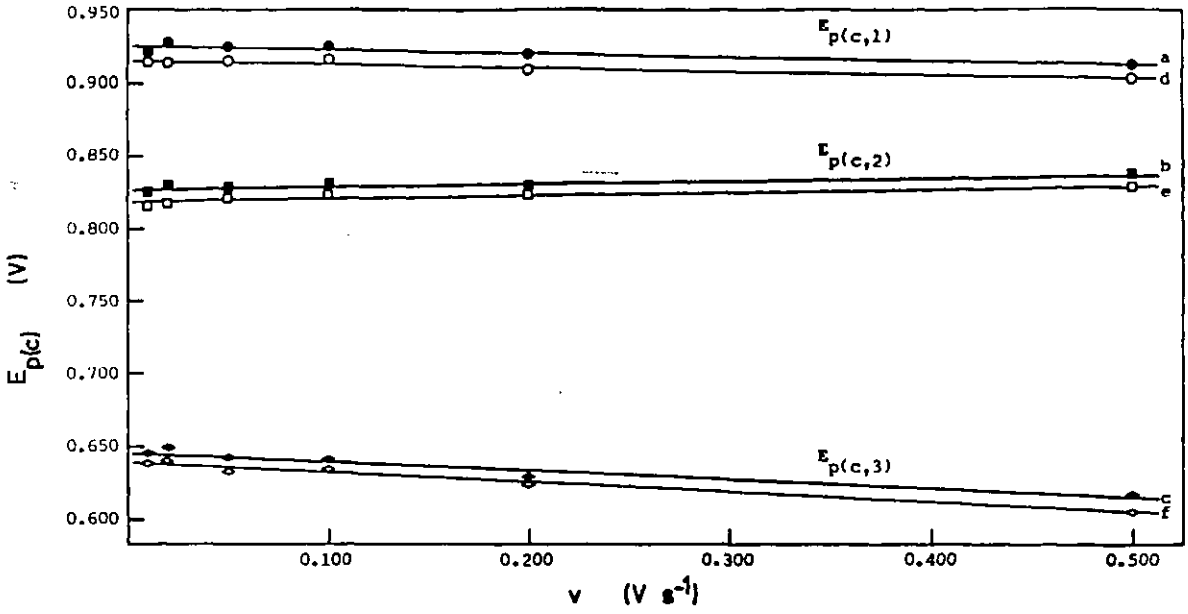

Fig. 5-260 Ir(IV) Perchlorate (2.3×10^{-3} mol dm^{-3})/Perchloric acid (0.1 M) supporting electrolyte System: Values of cathodic peak potential, $E_{p(c)}$, as a function of potential scan rate, v. (i) Sample solution as prepared: a, b, and c. (ii) Sample solution after prolonged treatment with boron carbide: d, e, and f. Boron carbide solid electrode $B_{3.86}C$.

(i) Sample solution as prepared:

(a) $E_{p(c,1)} = 0.925 - 2.57 \times 10^{-2}$ v
Correlation coefficient = -0.9072
Level of significance, p = 0.01 p 0.02
Standard deviation of $E_{p(c,1)}$ from regression = 0.002 V
Degrees of freedom = 4

(b) $E_{p(c,2)} = 0.827 + 1.91 \times 10^{-2}$ v
Correlation coefficient = 0.9002
Level of significance, p = 0.01 p 0.02
Standard deviation of $E_{p(c,2)}$ from regression = 0.002 V
Degrees of freedom = 4

(c) $E_{p(c,3)} = 0.646 - 6.16 \times 10^{-2}$ v
Correlation coefficient = -0.9671
Level of significance, p = 0.001 p 0.01
Standard deviation of $E_{p(c,3)}$ from regression = 0.003 V
Degrees of freedom = 4

(ii) Sample solution after prolonged treatment with boron carbide:

(d) $E_{p(c,1)} = 0.916 - 2.54 \times 10^{-2}$ v
Correlation coefficient = -0.9352
Level of significance, p = 0.001 p 0.01
Standard deviation of $E_{p(c,1)}$ from regression = 0.002 V
Degrees of freedom = 4

(e) $E_{p(c,2)} = 0.818 + 1.95 \times 10^{-2}$ v
Correlation coefficient = 0.9029
Level of significance, p = 0.01 p 0.02
Standard deviation of $E_{p(c,2)}$ from regression = 0.002 V
Degrees of freedom = 4

(f) $E_{p(c,3)} = 0.639 - 6.77 \times 10^{-2}$ v
Correlation coefficient = -0.9860
Level of significance, p = p 0.001
Standard deviation of $E_{p(c,3)}$ from regression = 0.002 V
Degrees of freedom = 4

Fig. 5-260 (continued):-

Two-way Analysis of Variance:

$E_{p(c,1)}$

Grand mean = 0.917 V

Standard deviation = 6.69×10^{-3} V

Variance ratio due to effects of scan rate, F(v) = 17.1

Degrees of freedom = 5

Degrees of freedom of the Residual = 5

$F_{0.05}(5,5)$ = 7.15 (double-sided)

Therefore, since F(v) exceeds $F_{0.05}(5,5)$, the effects of scan rate are significant.

Variance ratio due to effects of boron carbide, F(boron carbide) = 90.0

Degrees of freedom = 1

Degrees of freedom of the Residual = 5

$F_{0.05}(1,5)$ = 10.0 (double-sided)

Therefore, since F(boron carbide) exceeds $F_{0.05}(1,5)$, the effects of boron carbide are significant.

$E_{p(c,2)}$

Grand mean = 0.825 V

Standard deviation = 5.72×10^{-3} V

Variance ratio due to effects of scan rate, F(v) = 15.8

Degrees of freedom = 5

Degrees of freedom of the Residual = 5

Therefore, since F(v) exceeds $F_{0.05}(5,5)$, the effects of scan rate are significant.

Variance ratio due to effects of boron carbide, F(boron carbide) = 122

Degrees of freedom = 1

Degrees of freedom of the Residual = 5

Therefore, since F(boron carbide) exceeds $F_{0.05}(1,5)$, the effects of boron carbide are significant.

$E_{p(c,3)}$

Grand mean = 0.633 V

Standard deviation = 1.20×10^{-2} V

Variance ratio due to effects of scan rate, F(v) = 133

Degrees of freedom = 5

Degrees of freedom of the Residual = 5

Therefore, since F(v) exceeds $F_{0.05}(5,5)$, the effects of scan rate are significant.

Variance ratio due to effects of boron carbide, F(boron carbide) = 84.6

Degrees of freedom = 1

Degrees of freedom of the Residual = 5

Therefore, since F(boron carbide) exceeds $F_{0.05}(1,5)$, the effects of boron carbide are significant.

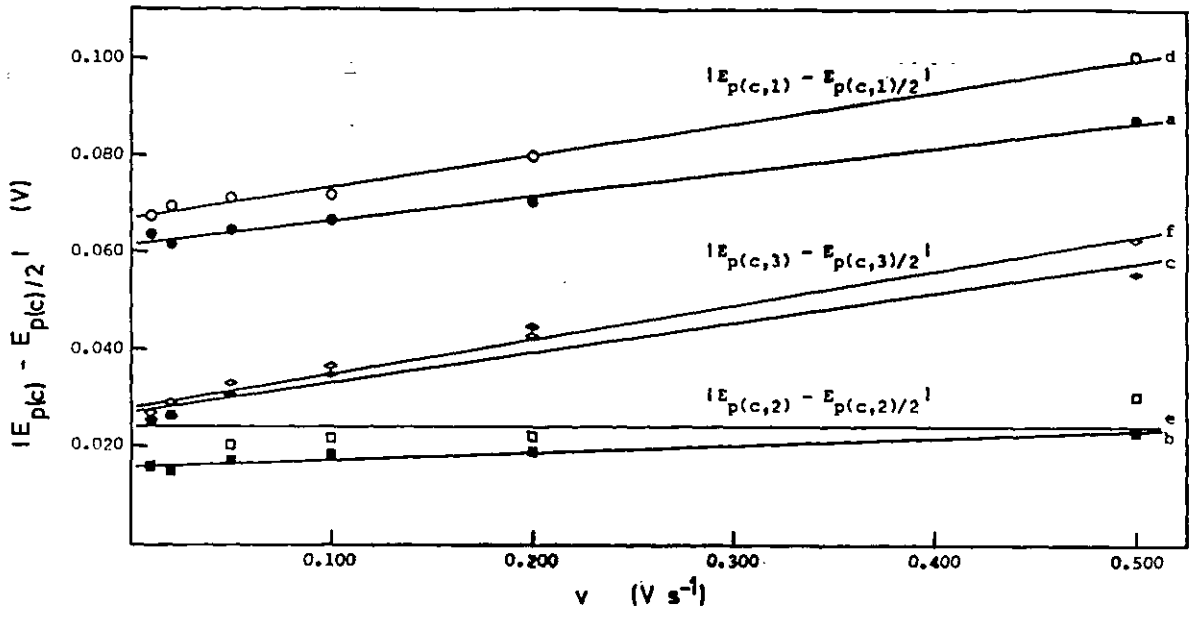

Fig. 5-261 Ir(IV) Perchlorate (2.3×10^{-3} mol dm^{-3})/Perchloric acid (0.1 M) supporting electrolyte System: Values of the difference between cathodic peak and half-peak potentials, $|E_{p(c)} - E_{p(c)/2}|$, as a function of potential scan rate, v. (i) Sample solution as prepared: a, b, and c. (ii) Sample solution after prolonged treatment with boron carbide: d, e, and f. Boron carbide solid electrode $B_{3.86}C$.

(i) Sample solution as prepared:

(a) $|E_{p(c,1)} - E_{p(c,1)/2}| = 6.15 \times 10^{-2} + 5.02 \times 10^{-2}$ v
Correlation coefficient = 0.9929
Level of significance, p = p < 0.001
Standard deviation of $|E_{p(c,1)} - E_{p(c,1)/2}|$ from regression = 0.001 V
Degrees of freedom = 4

(b) $|E_{p(c,2)} - E_{p(c,2)/2}| = 1.58 \times 10^{-2} + 1.46 \times 10^{-2}$ v
Correlation coefficient = 0.9688
Level of significance, p = 0.001 < p < 0.01
Standard deviation of $|E_{p(c,2)} - E_{p(c,2)/2}|$ from regression = 0.001 V
Degrees of freedom = 4

(c) $|E_{p(c,3)} - E_{p(c,3)/2}| = 2.69 \times 10^{-2} + 6.17 \times 10^{-2}$ v
Correlation coefficient = 0.9676
Level of significance, p = 0.001 < p < 0.01
Standard deviation of $|E_{p(c,3)} - E_{p(c,3)/2}|$ from regression = 0.003 V
Degrees of freedom = 4

(ii) Sample solution after prolonged treatment with boron carbide:

(d) $|E_{p(c,1)} - E_{p(c,1)/2}| = 6.69 \times 10^{-2} + 6.59 \times 10^{-2}$ v
Correlation coefficient = 0.9967
Level of significance, p = p < 0.001
Standard deviation of $|E_{p(c,1)} - E_{p(c,1)/2}|$ from regression = 0.001 V
Degrees of freedom = 4

(e) $|E_{p(c,2)} - E_{p(c,2)/2}|$ mean = 2.41×10^{-2} V
Standard deviation = 0.004 V
Coefficient of variation = 15.5%
Degrees of freedom = 5

Fig. 5-261 (continued):-

(f) $|E_{p(c,3)} - E_{p(c,3)/2}| = 2.79 \times 10^{-2} + 7.02 \times 10^{-2}$ v

Correlation coefficient = 0.9951

Level of significance, p = $p < 0.001$

Standard deviation of $|E_{p(c,3)} - E_{p(c,3)/2}|$ from regression = 0.001 V

Degrees of freedom = 4

Two-way Analysis of Variance:

$\underline{|E_{p(c,1)} - E_{p(c,1)/2}|}$

Grand mean = 7.27×10^{-2} V

Standard deviation = 1.07×10^{-2} V

Variance ratio due to effects of scan rate, F(v) = 41.9

Degrees of freedom = 5

Degrees of freedom of the Residual = 5

$F_{0.05}(5,5)$ = 7.15 (double-sided)

Therefore, since F(v) exceeds $F_{0.05}(5,5)$, the effects of scan rate are significant.

Variance ratio due to effects of boron carbide, F(boron carbide) = 31.4

Degrees of freedom = 1

Degrees of freedom of the Residual = 5

$F_{0.05}(1,5)$ = 10.0 (double-sided)

Therefore, since F(boron carbide) exceeds $F_{0.05}(1,5)$, the effects of boron carbide are significant.

$\underline{|E_{p(c,2)} - E_{p(c,2)/2}|}$

Grand mean = 2.10×10^{-2} V

Standard deviation = 4.28×10^{-3} V

Variance ratio due to effects of scan rate, F(v) = 2.51

Degrees of freedom = 5

Degrees of freedom of the Residual = 5

Therefore, since F(v) does not exceed $F_{0.05}(5,5)$, the effects of scan rate are not significant.

Variance ratio due to effects of boron carbide, F(boron carbide) = 17.8

Degrees of freedom = 1

Degrees of freedom of the Residual = 5

Therefore, since F(boron carbide) exceeds $F_{0.05}(1,5)$, the effects of boron carbide are significant.

$\underline{|E_{p(c,3)} - E_{p(c,3)/2}|}$

Grand mean = 3.71×10^{-2} V

Standard deviation = 1.15×10^{-2} V

Variance ratio due to effects of scan rate, F(v) = 73.0

Degrees of freedom = 5

Degrees of freedom of the Residual = 5

Therefore, since F(v) exceeds $F_{0.05}(5,5)$, the effects of scan rate are significant.

Variance ratio due to effects of boron carbide, F(boron carbide) = 3.58

Degrees of freedom = 1

Degrees of freedom of the Residual = 5

Therefore, since F(boron carbide) does not exceed $F_{0.05}(1,5)$, the effects of boron carbide are not significant.

are presented in Fig. 5-262. It can be seen that no fundamental change to the voltammograms had occurred from the sample treatments; the same peaks being exhibited.

Quantitative studies on the cathodic peaks, however, indicate that nitrogen aeration enhanced Peaks 1 and 3 whilst depressing Peak 2; the effects being confirmed by two-way ANOVA only for Peaks 2 and 3 (Fig. 5-263). Boron carbide treatment of the nitrogen aerated sample prior to voltammetry resulted in decreased peak currents for all three peaks; but confirmed by two-way ANOVA only for Peak 2. The general trends of peak current functions with increasing sweep rate, however, remained unaltered by the sample treatments and show the influence of adsorption on all the peaks.

Fig. 5-264 shows that nitrogen aeration enhanced the anodic peak current function of Peaks 1 and 3; as confirmed by two-way ANOVA. Boron carbide treatment of the nitrogen aerated sample prior to voltammetry decreased the anodic peak current function of Peaks 1 and 2; but confirmed by two-way ANOVA only for Peak 2. The trends of the anodic peak current functions with increasing sweep rate show the influence of adsorption on all three peaks, regardless of any sample treatments.

The cathodic peak potentials are plotted as functions of sweep rate in Fig. 5-265. Two-way ANOVA on the results indicated that nitrogen aeration affected $E_{p(c,1)}$ and $E_{p(c,2)}$ whereas none of the cathodic peak potentials was affected by boron carbide treatment of the nitrogen aerated sample. The anodic peak potentials were not affected by boron carbide treatment, and nitrogen aeration affected only $E_{p(a,2)}$; as shown by two-way ANOVA (Fig. 5-266). Boron carbide treatment of the nitrogen aerated Ir(IV) perchlorate sample solution did not affect the cathodic or anodic $|E_p - E_{p/2}|$ values (Figures 5-267 and 5-268), nor the $|E_{p(c)} - E_{p(a)}|$ values (Fig. 5-269); as shown by two-way ANOVA.

5-1.5.(iv).c Summary

Boron carbide treatment of the Ir(IV) perchlorate/$HClO_4$ (0.1 M) supporting electrolyte solution, without and with nitrogen aeration, resulted in decreases for the peak currents (Figures 5-259 and 5-263); thus furnishing more evidence for the strong physical adsorption of Ir(IV) perchlorate reactant on boron carbide. The decrements were shown, by two-way ANOVA, to be statistically significant for Peaks 1

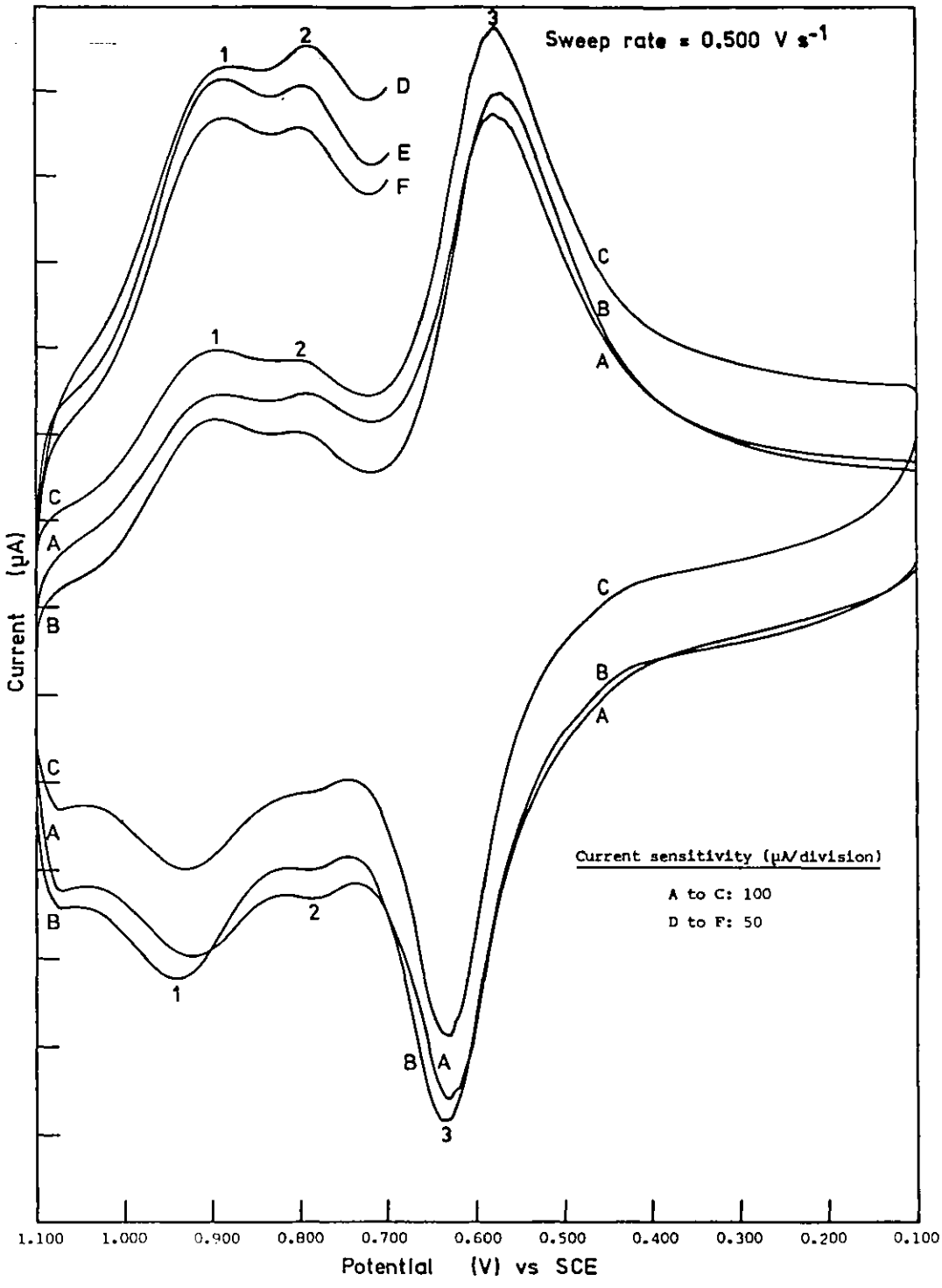

Fig. 5-262 Ir(IV) perchlorate (2.0×10^{-4} mol dm^{-3})/Perchloric acid (0.1 M) supporting electrolyte System: Linear sweep and cyclic voltammograms obtained at the boron carbide solid electrode $B_{3.86}C$. A & D: sample solution as prepared. B & E: sample solution aerated with nitrogen for 16 hours. C & F: nitrogen aerated sample was treated with boron carbide for 2 minutes.

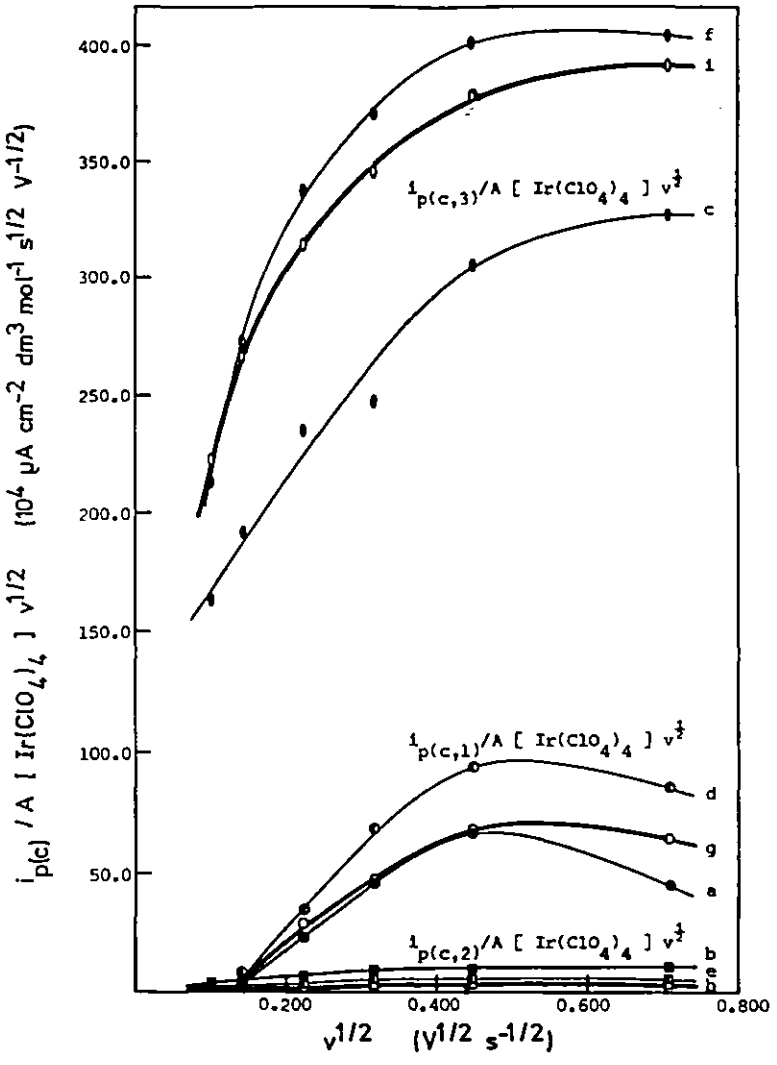

Fig. 5-263 Ir(IV) Perchlorate (2.0×10^{-4} mol dm^{-3})/Perchloric acid (0.1 M) supporting electrolyte System: Values of cathodic current function, $i_{p(c)}/A$ [$Ir(ClO_4)_4$] $v^{\frac{1}{2}}$, as a function of square root of potential scan rate, $v^{\frac{1}{2}}$. (i) Sample solution as prepared: a, b, and c. (ii) Sample solution aerated with nitrogen for 16 hours: d, e, and f. (iii) Nitrogen aerated solution treated with boron carbide: g, h, and i. Boron carbide solid electrode $B_{3.86}C$.

Two-way Analysis of Variance:

$\frac{i_{p(c,1)}/A\ [\ Ir(ClO_4)_4\ ]\ v^{\frac{1}{2}}}{}$

(1) Grand mean = 4.72×10^5 μA cm^{-2} dm^3 mol^{-1} $s^{\frac{1}{2}}$ $v^{-\frac{1}{2}}$

Standard deviation = 2.93×10^5 μA cm^{-2} dm^3 mol^{-1} $s^{\frac{1}{2}}$ $v^{-\frac{1}{2}}$

Variance ratio due to effects of scan rate, F(v) = 19.2

Degrees of freedom = 4

Degrees of freedom of the Residual = 4

$F_{0.05}(4,4)$ = 9.60 (double-sided)

Therefore, since F(v) exceeds $F_{0.05}(4,4)$, the effects of scan rate are significant.

Variance ratio due to effects of nitrogen aeration, $F(N_2)$ = 12.0

Degrees of freedom = 1

Degrees of freedom of the Residual = 4

$F_{0.05}(1,4)$ = 12.2 (double-sided)

Therefore, since $F(N_2)$ does not exceed $F_{0.05}(1,4)$, the effects of nitrogen aeration are not significant.

Fig. 5-263 (continued):-

(2) Grand mean = 5.00×10^5 μA cm^{-2} dm^3 mol^{-1} $s^{\frac{1}{2}}$ $V^{-\frac{1}{2}}$
Standard deviation = 2.89×10^5 μA cm^{-2} dm^3 mol^{-1} $s^{\frac{1}{2}}$ $V^{-\frac{1}{2}}$

Variance ratio due to effects of scan rate, F(v) = 34.1
Degrees of freedom = 4
Degrees of freedom of the Residual = 4
Therefore, since F(v) exceeds $F_{0.05}(4,4)$, the effects of scan rate are significant.

Variance ratio due to effects of boron carbide, F(boron carbide) = 10.6
Degrees of freedom = 1
Degrees of freedom of the Residual = 4
Therefore, since F(boron carbide) does not exceed $F_{0.05}(1,4)$, the effects of boron carbide are not significant.

$\frac{i_{p(c,2)}/A\ [\ Ir(ClO_4)_4\ ]\ v^{\frac{1}{2}}}{}$

(1) Grand mean = 5.84×10^4 μA cm^{-2} dm^3 mol^{-1} $s^{\frac{1}{2}}$ $V^{-\frac{1}{2}}$
Standard deviation = 2.61×10^4 μA cm^{-2} dm^3 mol^{-1} $s^{\frac{1}{2}}$ $V^{-\frac{1}{2}}$

Variance ratio due to effects of scan rate, F(v) = 7.33
Degrees of freedom = 5
Degrees of freedom of the Residual = 5
$F_{0.05}(5,5)$ = 7.15 (double-sided)
Therefore, since F(v) exceeds $F_{0.05}(5,5)$, the effects of scan rate are significant.

Variance ratio due to effects of nitrogen aeration, $F(N_2)$ = 38.0
Degrees of freedom = 1
Degrees of freedom of the Residual = 5
$F_{0.05}(1,5)$ = 10.0 (double-sided)
Therefore, since $F(N_2)$ exceeds $F_{0.05}(1,5)$, the effects of nitrogen aeration are significant.

(2) Grand mean = 3.26×10^4 μA cm^{-2} dm^3 mol^{-1} $s^{\frac{1}{2}}$ $V^{-\frac{1}{2}}$
Standard deviation = 1.13×10^4 μA cm^{-2} dm^3 mol^{-1} $s^{\frac{1}{2}}$ $V^{-\frac{1}{2}}$

Variance ratio due to effects of scan rate, F(v) = 2.62
Degrees of freedom = 5
Degrees of freedom of the Residual = 5
Therefore, since F(v) does not exceed $F_{0.05}(5,5)$, the effects of scan rate are not significant.

Variance ratio due to effects of boron carbide, F(boron carbide) = 16.0
Degrees of freedom = 1
Degrees of freedom of the Residual = 5
Therefore, since F(boron carbide) exceeds $F_{0.05}(1,5)$, the effects of boron carbide are significant.

$\frac{i_{p(c,3)}/A\ [\ Ir(ClO_4)_4\ ]\ v^{\frac{1}{2}}}{}$

(1) Grand mean = 2.89×10^6 μA cm^{-2} dm^3 mol^{-1} $s^{\frac{1}{2}}$ $V^{-\frac{1}{2}}$
Standard deviation = 7.78×10^5 μA cm^{-2} dm^3 mol^{-1} $s^{\frac{1}{2}}$ $V^{-\frac{1}{2}}$

Variance ratio due to effects of scan rate, F(v) = 29.9
Degrees of freedom = 5
Degrees of freedom of the Residual = 5
Therefore, since F(v) exceeds $F_{0.05}(5,5)$, the effects of scan rate are significant.

Variance ratio due to effects of nitrogen aeration, $F(N_2)$ = 73.0
Degrees of freedom = 1
Degrees of freedom of the Residual = 5
Therefore, since $F(N_2)$ exceeds $F_{0.05}(1,5)$, the effects of nitrogen aeration are significant.

(2) Grand mean = 3.26×10^6 μA cm^{-2} dm^3 mol^{-1} $s^{\frac{1}{2}}$ $V^{-\frac{1}{2}}$
Standard deviation = 6.55×10^5 μA cm^{-2} dm^3 mol^{-1} $s^{\frac{1}{2}}$ $V^{-\frac{1}{2}}$

Variance ratio due to effects of scan rate, F(v) = 112
Degrees of freedom = 5
Degrees of freedom of the Residual = 5
Therefore, since F(v) exceeds $F_{0.05}(5,5)$, the effects of scan rate are significant.

Variance ratio due to effects of boron carbide, F(boron carbide) = 6.17
Degrees of freedom = 1
Degrees of freedom of the Residual = 5
Therefore, since F(boron carbide) does not exceed $F_{0.05}(1,5)$, the effects of boron carbide are not significant.

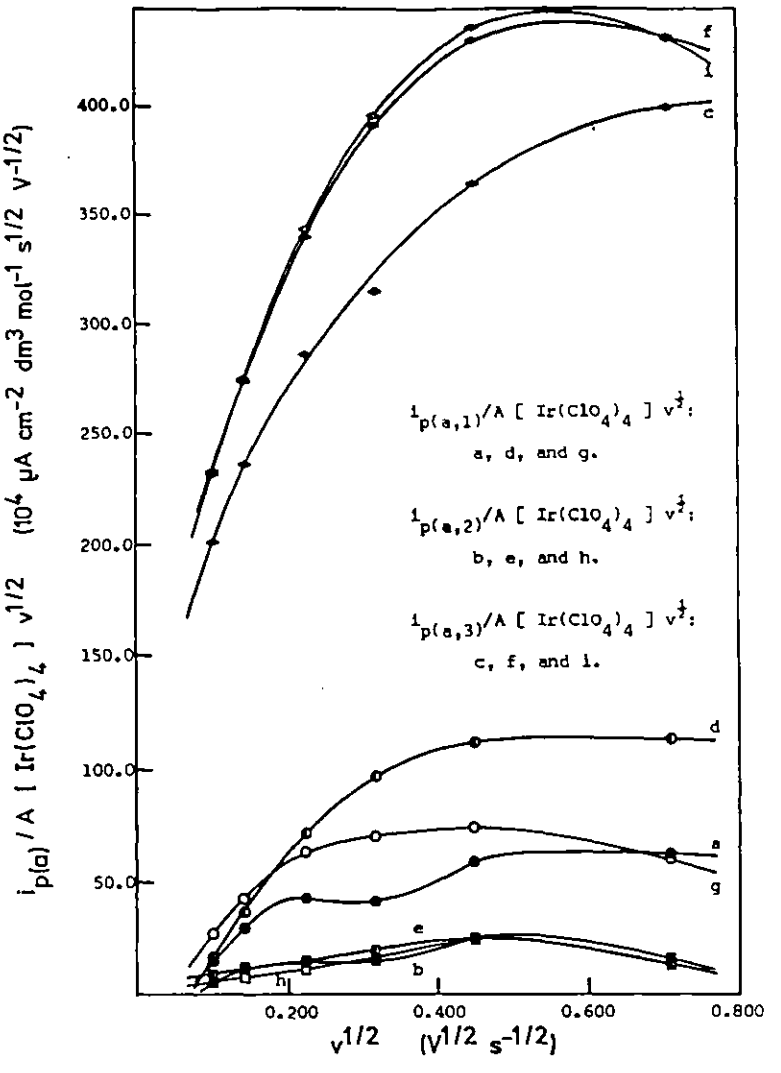

Fig. 5-264 Ir(IV) Perchlorate (2.0×10^{-4} mol dm^{-3})/Perchloric acid (0.1 M) supporting electrolyte System: Values of anodic current function, $i_{p(a)}/A$ [$Ir(ClO_4)_4$] $v^{\frac{1}{2}}$, as a function of square root of potential scan rate, $v^{\frac{1}{2}}$. (i) Sample solution as prepared: a, b, and c. (ii) Sample solution aerated with nitrogen for 16 hours: d, e, and f. (iii) Nitrogen aerated solution treated with boron carbide: g, h, and i. Boron carbide solid electrode $B_{3.86}C$.

Two-way Analysis of Variance:

$\frac{i_{p(a,1)}/A \text{ [} Ir(ClO_4)_4 \text{] } v^{\frac{1}{2}}}{}$

(1) Grand mean = 5.83×10^5 μA cm^{-2} dm^3 mol^{-1} $s^{\frac{1}{2}}$ $V^{-\frac{1}{2}}$

Standard deviation = 3.31×10^5 μA cm^{-2} dm^3 mol^{-1} $s^{\frac{1}{2}}$ $V^{-\frac{1}{2}}$

Variance ratio due to effects of scan rate, F(v) = 5.91

Degrees of freedom = 5

Degrees of freedom of the Residual = 5

$F_{0.05}(5,5)$ = 7.15 (double-sided)

Therefore, since F(v) does not exceed $F_{0.05}(5,5)$, the effects of scan rate are not significant.

Variance ratio due to effects of nitrogen aeration, $F(N_2)$ = 11.4

Degrees of freedom = 1

Degrees of freedom of the Residual = 5

$F_{0.05}(1,5)$ = 10.0 (double-sided)

Therefore, since $F(N_2)$ exceeds $F_{0.05}(1,5)$, the effects of nitrogen aeration are significant.

Fig. 5-264 (continued):-

(2) Grand mean = 6.57×10^5 μA cm^{-2} dm^3 mol^{-1} $s^{\frac{1}{2}}$ $v^{-\frac{1}{2}}$
Standard deviation = 3.01×10^5 μA cm^{-2} dm^3 mol^{-1} $s^{\frac{1}{2}}$ $v^{-\frac{1}{2}}$

Variance ratio due to effects of scan rate, F(v) = 5.13
Degrees of freedom = 5
Degrees of freedom of the Residual = 5
Therefore, since F(v) does not exceed $F_{0.05}(5,5)$, the effects of scan rate are not significant.

Variance ratio due to effects of boron carbide, F(boron carbide) = 3.04
Degrees of freedom = 1
Degrees of freedom of the Residual = 5
Therefore, since F(boron carbide) does not exceed $F_{0.05}(1,5)$, the effects of boron carbide are not significant.

$\frac{i_{p(a,2)}}{A\ [\ Ir(ClO_4)_4\ ]\ v^{\frac{1}{2}}}$

(1) Grand mean = 1.50×10^5 μA cm^{-2} dm^3 mol^{-1} $s^{\frac{1}{2}}$ $v^{-\frac{1}{2}}$
Standard deviation = 5.62×10^4 μA cm^{-2} dm^3 mol^{-1} $s^{\frac{1}{2}}$ $v^{-\frac{1}{2}}$

Variance ratio due to effects of scan rate, F(v) = 21.9
Degrees of freedom = 5
Degrees of freedom of the Residual = 5
Therefore, since F(v) exceeds $F_{0.05}(5,5)$, the effects of scan rate are significant.

Variance ratio due to effects of nitrogen aeration, $F(N_2)$ = 1.73
Degrees of freedom = 1
Degrees of freedom of the Residual = 5
Therefore, since $F(N_2)$ does not exceed $F_{0.05}(1,5)$, the effects of nitrogen aeration are not significant.

(2) Grand mean = 1.44×10^5 μA cm^{-2} dm^3 mol^{-1} $s^{\frac{1}{2}}$ $v^{-\frac{1}{2}}$
Standard deviation = 5.85×10^4 μA cm^{-2} dm^3 mol^{-1} $s^{\frac{1}{2}}$ $v^{-\frac{1}{2}}$

Variance ratio due to effects of scan rate, F(v) = 56.2
Degrees of freedom = 5
Degrees of freedom of the Residual = 5
Therefore, since F(v) exceeds $F_{0.05}(5,5)$, the effects of scan rate are significant.

Variance ratio due to effects of boron carbide, F(boron carbide) = 14.6
Degrees of freedom = 1
Degrees of freedom of the Residual = 5
Therefore, since F(boron carbide) exceeds $F_{0.05}(1,5)$, the effects of boron carbide are significant.

$\frac{i_{p(a,3)}}{A\ [\ Ir(ClO_4)_4\ ]\ v^{\frac{1}{2}}}$

(1) Grand mean = 3.25×10^6 μA cm^{-2} dm^3 mol^{-1} $s^{\frac{1}{2}}$ $v^{-\frac{1}{2}}$
Standard deviation = 7.64×10^5 μA cm^{-2} dm^3 mol^{-1} $s^{\frac{1}{2}}$ $v^{-\frac{1}{2}}$

Variance ratio due to effects of scan rate, F(v) = 73.1
Degrees of freedom = 5
Degrees of freedom of the Residual = 5
Therefore, since F(v) exceeds $F_{0.05}(5,5)$, the effects of scan rate are significant.

Variance ratio due to effects of nitrogen aeration, $F(N_2)$ = 44.5
Degrees of freedom = 1
Degrees of freedom of the Residual = 5
Therefore, since $F(N_2)$ exceeds $F_{0.05}(1,5)$, the effects of nitrogen aeration are significant.

(2) Grand mean = 3.51×10^6 μA cm^{-2} dm^3 mol^{-1} $s^{\frac{1}{2}}$ $v^{-\frac{1}{2}}$
Standard deviation = 7.63×10^5 μA cm^{-2} dm^3 mol^{-1} $s^{\frac{1}{2}}$ $v^{-\frac{1}{2}}$

Variance ratio due to effects of scan rate, F(v) = 2.78×10^3
Degrees of freedom = 5
Degrees of freedom of the Residual = 5
Therefore, since F(v) exceeds $F_{0.05}(5,5)$, the effects of scan rate are significant.

Variance ratio due to effects of boron carbide, F(boron carbide) = 1.62
Degrees of freedom = 1
Degrees of freedom of the Residual = 5
Therefore, since F(boron carbide) does not exceed $F_{0.05}(1,5)$, the effects of boron carbide are not significant.

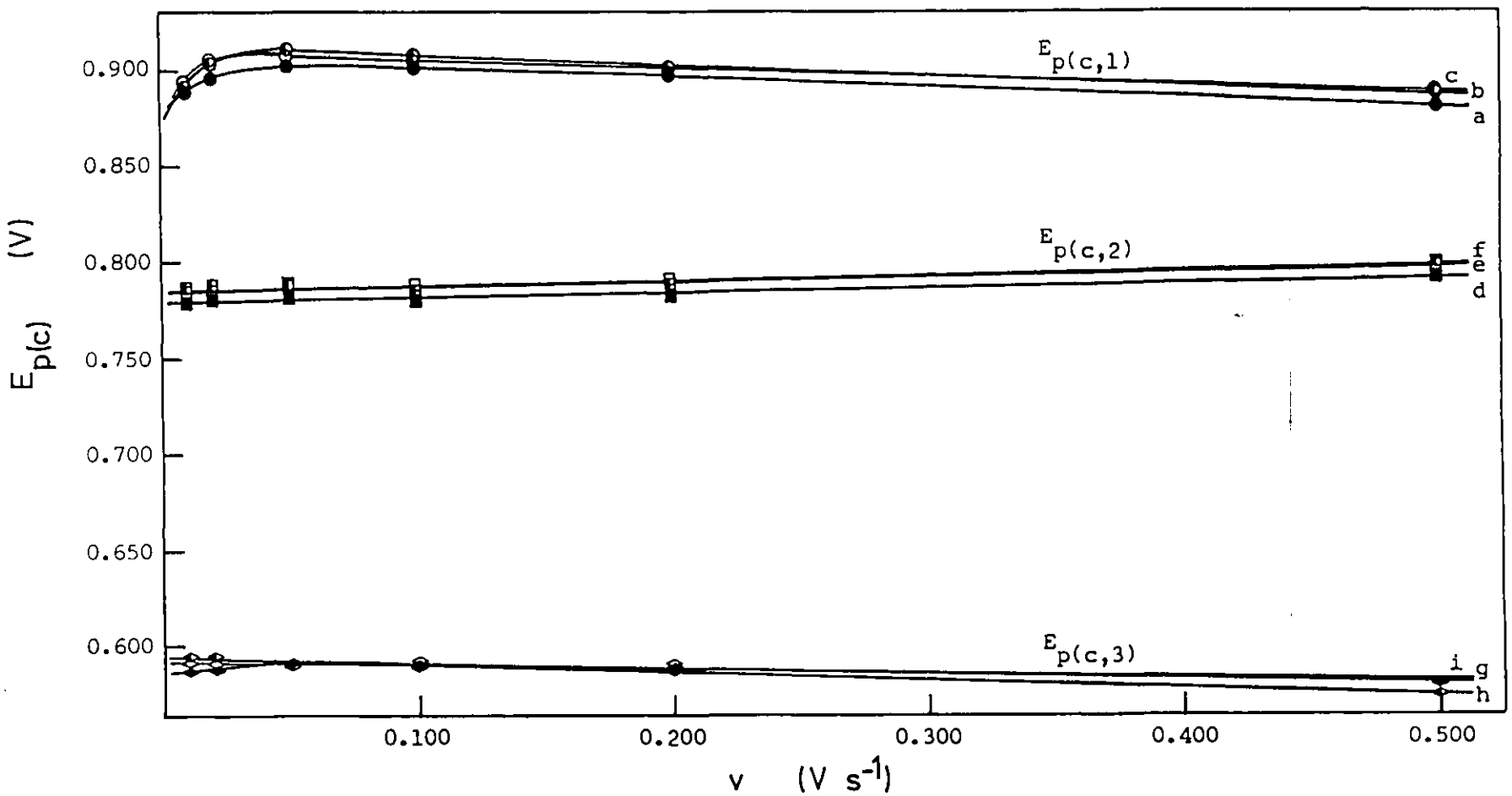

Fig. 5-265 Ir(IV) Perchlorate (2.0×10^{-4} mol dm^{-3})/Perchloric acid (0.1 M) supporting electrolyte System: Values of cathodic peak potential, $E_{p(c)}$, as a function of potential scan rate, v. (i) Sample as prepared: a, d, and g. (ii) Sample solution aerated with nitrogen for 16 hours: b, e, and h. (iii) Nitrogen aerated solution treated with boron carbide: c, f, and i. Boron carbide solid electrode $B_{3.86}C$.

Fig. 5-265 (continued):-

(i) Sample solution as prepared:

(a) $E_{p(c,1)}$ mean = 0.894 V
Standard deviation = 0.008 V
Coefficient of variation = 0.915%
Degrees of freedom = 5

(d) $E_{p(c,2)} = 0.779 + 2.35 \times 10^{-2}$ v
Correlation coefficient = 0.9565
Level of significance, $p = 0.001 < p < 0.01$
Standard deviation of $E_{p(c,2)}$ from regression = 0.002 V
Degrees of freedom = 4

(g) $E_{p(c,3)}$ mean = 0.587 V
Standard deviation = 0.004 V
Coefficient of variation = 0.674%
Degrees of freedom = 5

(ii) Sample solution aerated with nitrogen for 16 hours:

(b) $E_{p(c,1)}$ mean = 0.901 V
Standard deviation = 0.009 V
Coefficient of variation = 1.00%
Degrees of freedom = 5

(e) $E_{p(c,2)} = 0.785 + 2.45 \times 10^{-2}$ v
Correlation coefficient = 0.9349
Level of significance, $p = 0.001 < p < 0.01$
Standard deviation of $E_{p(c,2)}$ from regression = 0.002 V
Degrees of freedom = 4

(h) $E_{p(c,3)} = 0.595 - 4.12 \times 10^{-2}$ v
Correlation coefficient = -0.9832
Level of significance, $p = p < 0.001$
Standard deviation of $E_{p(c,3)}$ from regression = 0.002 V
Degrees of freedom = 4

(iii) Nitrogen aerated solution treated with boron carbide:

(c) $E_{p(c,1)}$ mean = 0.900 V
Standard deviation = 0.007 V
Coefficient of variation = 0.818%
Degrees of freedom = 5

(f) $E_{p(c,2)} = 0.786 + 2.53 \times 10^{-2}$ v
Correlation coefficient = 0.9855
Level of significance, $p = p < 0.001$
Standard deviation of $E_{p(c,2)}$ from regression = 0.001 V
Degrees of freedom = 4

(i) $E_{p(c,3)} = 0.593 - 2.29 \times 10^{-2}$ v
Correlation coefficient = -0.9231
Level of significance, $p = 0.001 < p < 0.01$
Standard deviation of $E_{p(c,3)}$ from regression = 0.002 V
Degrees of freedom = 4

Two-way Analysis of Variance:

$\underline{E_{p(c,1)}}$

(1) Grand mean = 0.898 V
Standard deviation = 0.008 V

Variance ratio due to effects of scan rate, F(v) = 98.0
Degrees of freedom = 5
Degrees of freedom of the Residual = 5
$F_{0.05}(5,5) = 7.15$ (double-sided)
Therefore, since F(v) exceeds $F_{0.05}(5,5)$, the effects of scan rate are significant.

Variance ratio due to effects of nitrogen aeration, $F(N_2)$ = 81.9
Degrees of freedom = 1
Degrees of freedom of the Residual = 5
$F_{0.05}(1,5) = 10.0$ (double-sided)
Therefore, since $F(N_2)$ exceeds $F_{0.05}(1,5)$, the effects of nitrogen aeration are significant.

Fig. 5-265 (continued):-

(2) Grand mean = 0.900 V

Standard deviation = 0.008 V

Variance ratio due to effects of scan rate, F(v) = 35.3

Degrees of freedom = 5

Degrees of freedom of the Residual = 5

Therefore, since F(v) exceeds $F_{0.05}(5,5)$, the effects of scan rate are significant.

Variance ratio due to effects of boron carbide, F(boron carbide) = 0.432

Degrees of freedom = 1

Degrees of freedom of the Residual = 5

Therefore, since F(boron carbide) does not exceed $F_{0.05}(1,5)$, the effects of boron carbide are not significant.

$\underline{E_{p(c,2)}}$

(1) Grand mean = 0.786 V

Standard deviation = 0.005 V

Variance ratio due to effects of scan rate, F(v) = 120

Degrees of freedom = 5

Degrees of freedom of the Residual = 5

Therefore, since F(v) exceeds $F_{0.05}(5,5)$, the effects of scan rate are significant.

Variance ratio due to effects of nitrogen aeration, $F(N_2)$ = 331

Degrees of freedom = 1

Degrees of freedom of the Residual = 5

Therefore, since $F(N_2)$ exceeds $F_{0.05}(1,5)$, the effects of nitrogen aeration are significant.

(2) Grand mean = 0.789 V

Standard deviation = 0.004 V

Variance ratio due to effects of scan rate, F(v) = 20.6

Degrees of freedom = 5

Degrees of freedom of the Residual = 5

Therefore, since F(v) exceeds $F_{0.05}(5,5)$, the effects of scan rate are significant.

Variance ratio due to effects of boron carbide, F(boron carbide) = 0.239

Degrees of freedom = 1

Degrees of freedom of the Residual = 5

Therefore, since F(boron carbide) does not exceed $F_{0.05}(1,5)$, the effects of boron carbide are not significant.

$\underline{E_{p(c,3)}}$

(1) Grand mean = 0.588 V

Standard deviation = 0.006 V

Variance ratio due to effects of scan rate, F(v) = 3.93

Degrees of freedom = 5

Degrees of freedom of the Residual = 5

Therefore, since F(v) does not exceed $F_{0.05}(5,5)$, the effects of scan rate are not significant.

Variance ratio due to effects of nitrogen aeration, $F(N_2)$ = 0.277

Degrees of freedom = 1

Degrees of freedom of the Residual = 5

Therefore, since $F(N_2)$ does not exceed $F_{0.05}(1,5)$, the effects of nitrogen aeration are not significant.

(2) Grand mean = 0.589 V

Standard deviation = 0.006 V

Variance ratio due to effects of scan rate, F(v) = 8.90

Degrees of freedom = 5

Degrees of freedom of the Residual = 5

Therefore, since F(v) exceeds $F_{0.05}(5,5)$, the effects of scan rate are significant.

Variance ratio due to effects of boron carbide, F(boron carbide) = 0.220

Degrees of freedom = 1

Degrees of freedom of the Residual = 5

Therefore, since F(boron carbide) does not exceed $F_{0.05}(1,5)$, the effects of boron carbide are not significant.

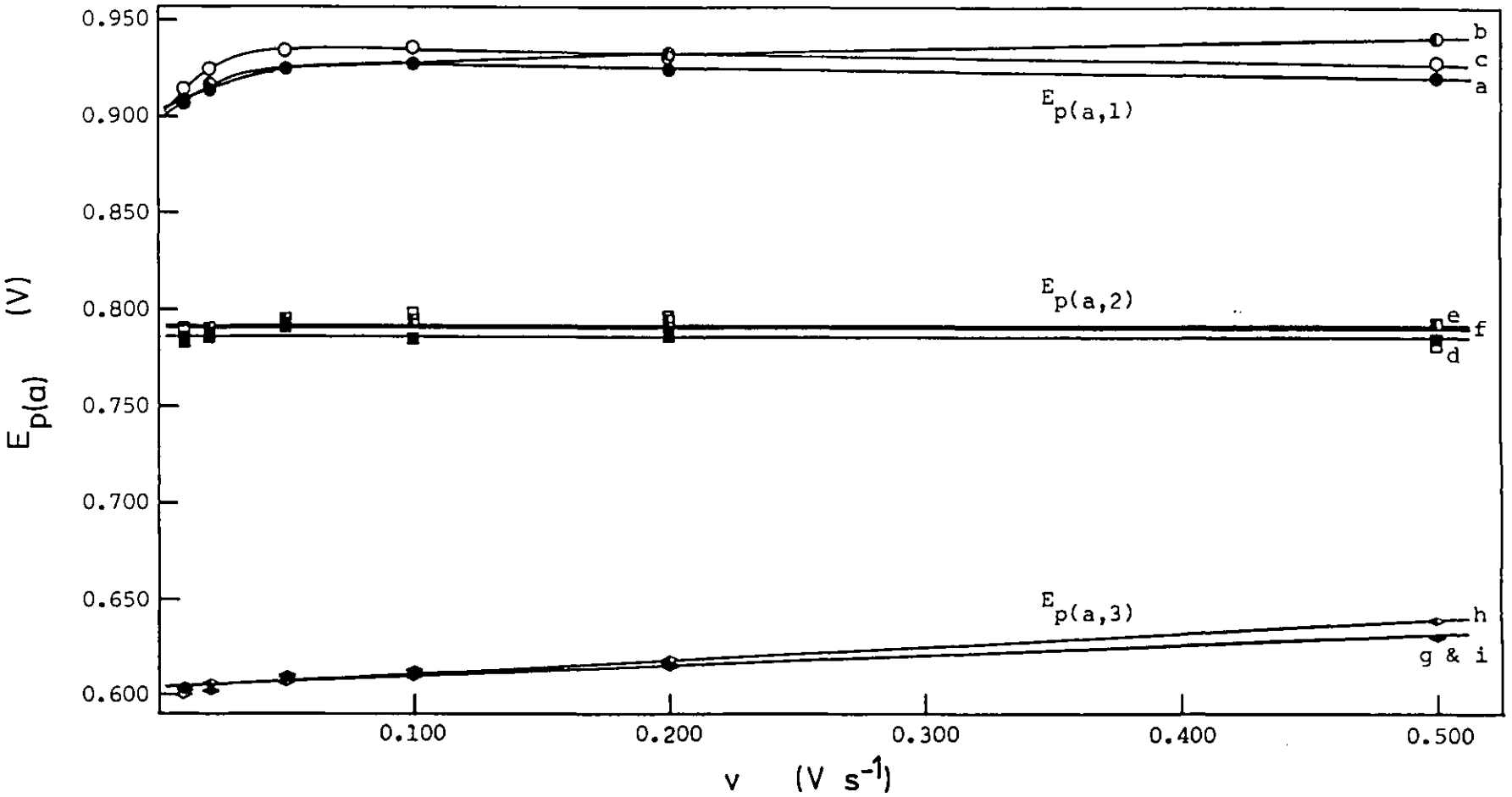

Fig. 5-266 Ir(IV) Perchlorate (2.0×10^{-4} mol dm^{-3})/Perchloric acid (0.1 M) supporting electrolyte System: Values of anodic peak potential, $E_{p(a)}$, as a function of potential scan rate, v. (i) Sample as prepared: a, d, and g. (ii) Sample solution aerated with nitrogen for 16 hours: b, e, and h. (iii) Nitrogen aerated solution treated with boron carbide: c, f, and i. Boron carbide solid electrode $B_{3.86}C$.

Fig. 5-266 (continued):-

(i) Sample solution as prepared:

(a) $E_{p(a,1)}$ mean = 0.920 V
Standard deviation = 0.007 V
Coefficient of variation = 0.795%
Degrees of freedom = 5

(d) $E_{p(a,2)}$ mean = 0.786 V
Standard deviation = 0.003 V
Coefficient of variation = 0.402%
Degrees of freedom = 5

(g) $E_{p(a,3)} = 0.604 + 5.31 \times 10^{-2}$ v
Correlation coefficient = 0.9660
Level of significance, $p = 0.001 < p < 0.01$
Standard deviation of $E_{p(a,3)}$ from regression = 0.003 V
Degrees of freedom = 4

(ii) Sample solution aerated with nitrogen for 16 hours:

(b) $E_{p(a,1)}$ mean = 0.925 V
Standard deviation = 0.012 V
Coefficient of variation = 1.27%
Degrees of freedom = 5

(e) $E_{p(a,2)}$ mean = 0.791 V
Standard deviation = 0.003 V
Coefficient of variation = 0.441%
Degrees of freedom = 5

(h) $E_{p(a,3)} = 0.604 + 7.00 \times 10^{-2}$ v
Correlation coefficient = 0.9989
Level of significance, $p = p < 0.001$
Standard deviation of $E_{p(a,3)}$ from regression = 0.001 V
Degrees of freedom = 4

(iii) Nitrogen aerated solution treated with boron carbide:

(c) $E_{p(a,1)}$ mean = 0.928 V
Standard deviation = 0.008 V
Coefficient of variation = 0.840%
Degrees of freedom = 5

(f) $E_{p(a,2)}$ mean = 0.791 V
Standard deviation = 0.006 V
Coefficient of variation = 0.748%
Degrees of freedom = 5

(i) $E_{p(a,3)} = 0.604 + 5.50 \times 10^{-2}$ v
Correlation coefficient = 0.9528
Level of significance, $p = 0.001 < p < 0.01$
Standard deviation of $E_{p(a,3)}$ from regression = 0.004 V
Degrees of freedom = 4

Two-way Analysis of Variance:

$\underline{E_{p(a,1)}}$

(1) Grand mean = 0.922 V
Standard deviation = 0.009 V

Variance ratio due to effects of scan rate, F(v) = 4.97
Degrees of freedom = 5
Degrees of freedom of the Residual = 5
$F_{0.05}(5,5) = 7.15$ (double-sided)
Therefore, since F(v) does not exceed $F_{0.05}(5,5)$, the effects of scan rate are not significant.

Variance ratio due to effects of nitrogen aeration, $F(N_2) = 2.58$
Degrees of freedom = 1
Degrees of freedom of the Residual = 5
$F_{0.05}(1,5) = 10.0$ (double-sided)
Therefore, since $F(N_2)$ does not exceed $F_{0.05}(1,5)$, the effects of nitrogen aeration are not significant.

Fig. 5-266 (continued):-

(2) Grand mean = 0.926 V
Standard deviation = 0.009 V

Variance ratio due to effects of scan rate, F(v) = 4.90
Degrees of freedom = 5
Degrees of freedom of the Residual = 5
Therefore, since F(v) does not exceed $F_{0.05}(5,5)$, the effects of scan rate are not significant.

Variance ratio due to effects of boron carbide, F(boron carbide) = 0.680
Degrees of freedom = 1
Degrees of freedom of the Residual = 5
Therefore, since F(boron carbide) does not exceed $F_{0.05}(1,5)$, the effects of boron carbide are not significant.

$E_{p(a,2)}$

(1) Grand mean = 0.789 V
Standard deviation = 0.004 V

Variance ratio due to effects of scan rate, F(v) = 3.24
Degrees of freedom = 5
Degrees of freedom of the Residual = 5
Therefore, since F(v) does not exceed $F_{0.05}(5,5)$, the effects of scan rate are not significant.

Variance ratio due to effects of nitrogen aeration, $F(N_2)$ = 14.6
Degrees of freedom = 1
Degrees of freedom of the Residual = 5
Therefore, since $F(N_2)$ exceeds $F_{0.05}(1,5)$, the effects of nitrogen aeration are significant.

(2) Grand mean = 0.791 V
Standard deviation = 0.004 V

Variance ratio due to effects of scan rate, F(v) = 1.84
Degrees of freedom = 5
Degrees of freedom of the Residual = 5
Therefore, since F(v) does not exceed $F_{0.05}(5,5)$, the effects of scan rate are not significant.

Variance ratio due to effects of boron carbide, F(boron carbide) = 0.115
Degrees of freedom = 1
Degrees of freedom of the Residual = 5
Therefore, since F(boron carbide) does not exceed $F_{0.05}(1,5)$, the effects of boron carbide are not significant.

$E_{p(a,3)}$

(1) Grand mean = 0.613 V
Standard deviation = 0.011 V

Variance ratio due to effects of scan rate, F(v) = 26.2
Degrees of freedom = 5
Degrees of freedom of the Residual = 5
Therefore, since F(v) exceeds $F_{0.05}(5,5)$, the effects of scan rate are significant.

Variance ratio due to effects of nitrogen aeration, $F(N_2)$ = 1.14
Degrees of freedom = 1
Degrees of freedom of the Residual = 5
Therefore, since $F(N_2)$ does not exceed $F_{0.05}(1,5)$, the effects of nitrogen aeration are not significant.

(2) Grand mean = 0.613 V
Standard deviation = 0.011 V

Variance ratio due to effects of scan rate, F(v) = 25.0
Degrees of freedom = 5
Degrees of freedom of the Residual = 5
Therefore, since F(v) exceeds $F_{0.05}(5,5)$, the effects of scan rate are significant.

Variance ratio due to effects of boron carbide, F(boron carbide) = 1.05
Degrees of freedom = 1
Degrees of freedom of the Residual = 5
Therefore, since F(boron carbide) does not exceed $F_{0.05}(1,5)$, the effects of boron carbide are not significant.

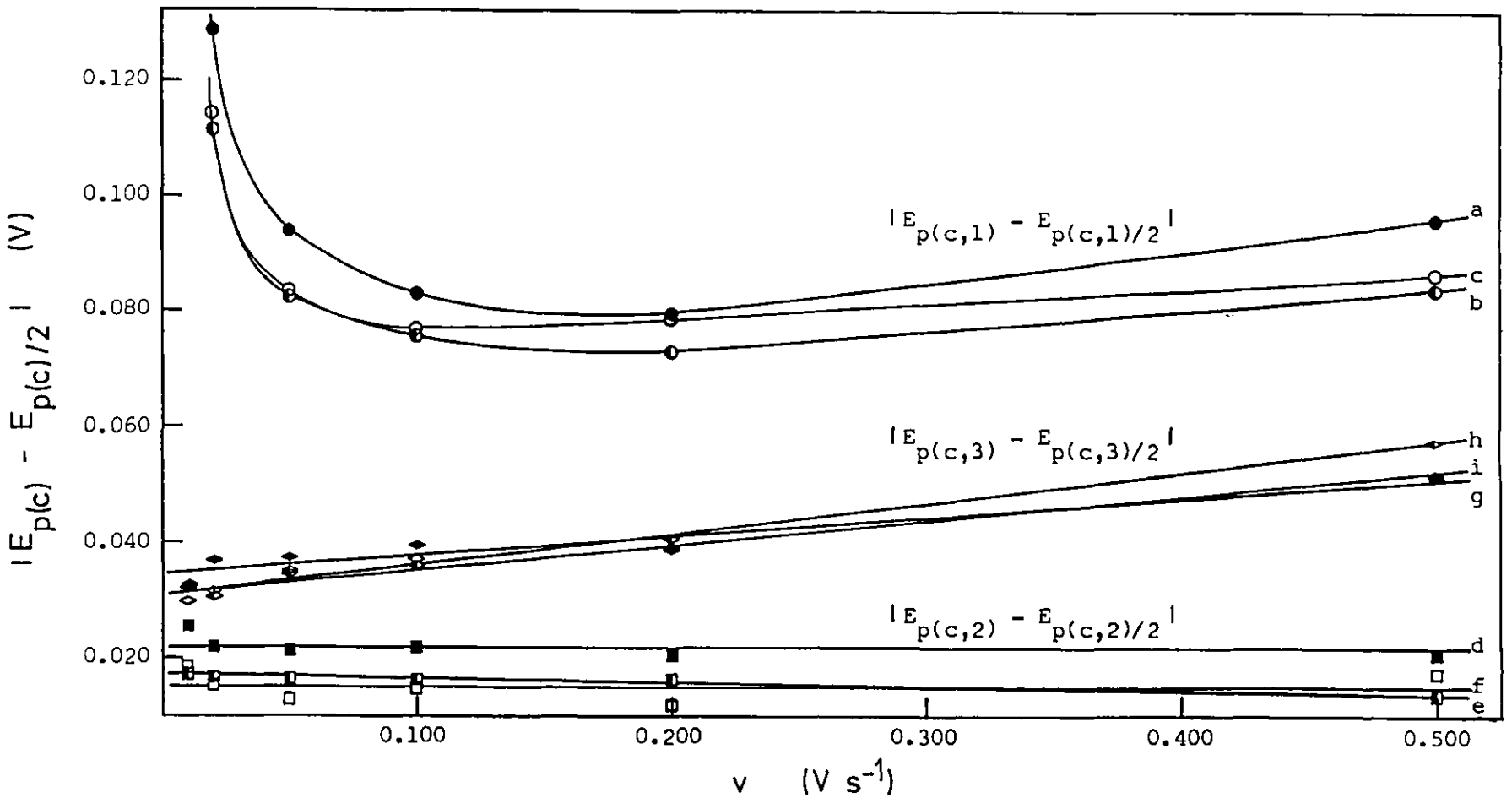

Fig. 5-267 Ir(IV) Perchlorate (2.0×10^{-4} mol dm^{-3})/Perchloric acid (0.1 M) supporting electrolyte System: Values of the difference between cathodic peak and half-peak potentials, $|E_{p(c)} - E_{p(c)/2}|$, as a function of potential scan rate, v. (i) Sample as prepared: a, d, and g. (ii) Sample solution aerated with nitrogen for 16 hours: b, e, and h. (iii) Nitrogen aerated solution treated with boron carbide: c, f, and i. Boron carbide solid electrode $B_{3.86}C$.

Fig. 5-267 (continued):-

(i) Sample solution as prepared:

(d) $|E_{p(c,2)} - E_{p(c,2)/2}|$ mean = 0.022 V
Standard deviation = 0.002 V
Coefficient of variation = 8.77%
Degrees of freedom = 5

(g) $|E_{p(c,3)} - E_{p(c,3)/2}| = 3.46 \times 10^{-2} + 3.27 \times 10^{-2}$ v
Correlation coefficient = 0.9620
Level of significance, $p = 0.001 < p < 0.01$
Standard deviation of $|E_{p(c,3)} - E_{p(c,3)/2}|$ from regression
= 0.002 V
Degrees of freedom = 4

(ii) Sample solution aerated with nitrogen for 16 hours:

(e) $|E_{p(c,2)} - E_{p(c,2)/2}| = 1.71 \times 10^{-2} - 6.93 \times 10^{-3}$ v
Correlation coefficient = -0.9303
Level of significance, $p = 0.001 < p < 0.01$
Standard deviation of $|E_{p(c,2)} - E_{p(c,2)/2}|$ from regression
= 0.001 V
Degrees of freedom = 4

(h) $|E_{p(c,3)} - E_{p(c,3)/2}| = 3.08 \times 10^{-2} + 5.31 \times 10^{-2}$ v
Correlation coefficient = 0.9946
Level of significance, $p = p < 0.001$
Standard deviation of $|E_{p(c,3)} - E_{p(c,3)/2}|$ from regression
= 0.001 V
Degrees of freedom = 4

(iii) Nitrogen aerated solution treated with boron carbide:

(f) $|E_{p(c,2)} - E_{p(c,2)/2}|$ mean = 0.015 V
Standard deviation = 0.002 V
Coefficient of variation = 16.7%
Degrees of freedom = 5

(i) $|E_{p(c,3)} - E_{p(c,3)/2}| = 3.12 \times 10^{-2} + 4.19 \times 10^{-2}$ v
Correlation coefficient = 0.9849
Level of significance, $p = p < 0.001$
Standard deviation of $|E_{p(c,3)} - E_{p(c,3)/2}|$ from regression
= 0.002 V
Degrees of freedom = 4

Two-way Analysis of Variance:

$\underline{|E_{p(c,1)} - E_{p(c,1)/2}|}$

(1) Grand mean = 9.08×10^{-2} V
Standard deviation = 1.66×10^{-2} V
Variance ratio due to effects of scan rate, F(v) = 63.3
Degrees of freedom = 4
Degrees of freedom of the Residual = 4
$F_{0.05}(4,4) = 9.60$ (double-sided)
Therefore, since F(v) exceeds $F_{0.05}(4,4)$, the effects of scan rate are significant.
Variance ratio due to effects of nitrogen aeration, $F(N_2)$ = 32.1
Degrees of freedom = 1
Degrees of freedom of the Residual = 4
$F_{0.05}(1,4) = 12.2$ (double-sided)
Therefore, since $F(N_2)$ exceeds $F_{0.05}(1,4)$, the effects of nitrogen aeration are significant.

(2) Grand mean = 8.67×10^{-2} V
Standard deviation = 1.39×10^{-2} V
Variance ratio due to effects of scan rate, F(v) = 219
Degrees of freedom = 4
Degrees of freedom of the Residual = 4
Therefore, since F(v) exceeds $F_{0.05}(4,4)$, the effects of scan rate are significant.
Variance ratio due to effects of boron carbide,
F(boron carbide) = 10.1
Degrees of freedom = 1
Degrees of freedom of the Residual = 4
Therefore, since F(boron carbide) does not exceed $F_{0.05}(1,4)$, the effects of boron carbide are not significant.

Fig. 5-267 (continued):-

$\underline{|E_{p(c,2)} - E_{p(c,2)/2}|}$

(1) Grand mean = 1.90×10^{-2} V

Standard deviation = 3.29×10^{-3} V

Variance ratio due to effects of scan rate, F(v) = 3.00

Degrees of freedom = 5

Degrees of freedom of the Residual = 5

$F_{0.05}(5,5) = 7.15$ (double-sided)

Therefore, since F(v) does not exceed $F_{0.05}(5,5)$, the effects of scan rate are not significant.

Variance ratio due to effects of nitrogen aeration, $F(N_2) = 72.6$

Degrees of freedom = 1

Degrees of freedom of the Residual = 5

$F_{0.05}(1,5) = 10.0$ (double-sided)

Therefore, since $F(N_2)$ exceeds $F_{0.05}(1,5)$, the effects of nitrogen aeration are significant.

(2) Grand mean = 1.55×10^{-2} V

Standard deviation = 1.92×10^{-3} V

Variance ratio due to effects of scan rate, F(v) = 0.618

Degrees of freedom = 5

Degrees of freedom of the Residual = 5

Therefore, since F(v) does not exceed $F_{0.05}(5,5)$, the effects of scan rate are not significant.

Variance ratio due to effects of boron carbide, F(boron carbide) = 0.696

Degrees of freedom = 1

Degrees of freedom of the Residual = 5

Therefore, since F(boron carbide) does not exceed $F_{0.05}(1,5)$, the effects of boron carbide are not significant.

$\underline{|E_{p(c,3)} - E_{p(c,3)/2}|}$

(1) Grand mean = 3.90×10^{-2} V

Standard deviation = 7.62×10^{-3} V

Variance ratio due to effects of scan rate, F(v) = 13.4

Degrees of freedom = 5

Degrees of freedom of the Residual = 5

Therefore, since F(v) exceeds $F_{0.05}(5,5)$, the effects of scan rate are significant.

Variance ratio due to effects of nitrogen aeration, $F(N_2) = 0.191$

Degrees of freedom = 1

Degrees of freedom of the Residual = 5

Therefore, since $F(N_2)$ does not exceed $F_{0.05}(1,5)$, the effects of nitrogen aeration are not significant.

(2) Grand mean = 3.80×10^{-2} V

Standard deviation = 8.23×10^{-3} V

Variance ratio due to effects of scan rate, F(v) = 45.0

Degrees of freedom = 5

Degrees of freedom of the Residual = 5

Therefore, since F(v) exceeds $F_{0.05}(5,5)$, the effects of scan rate are significant.

Variance ratio due to effects of boron carbide, F(boron carbide) = 1.30

Degrees of freedom = 1

Degrees of freedom of the Residual = 5

Therefore, since F(boron carbide) does not exceed $F_{0.05}(1,5)$, the effects of boron carbide are not significant.

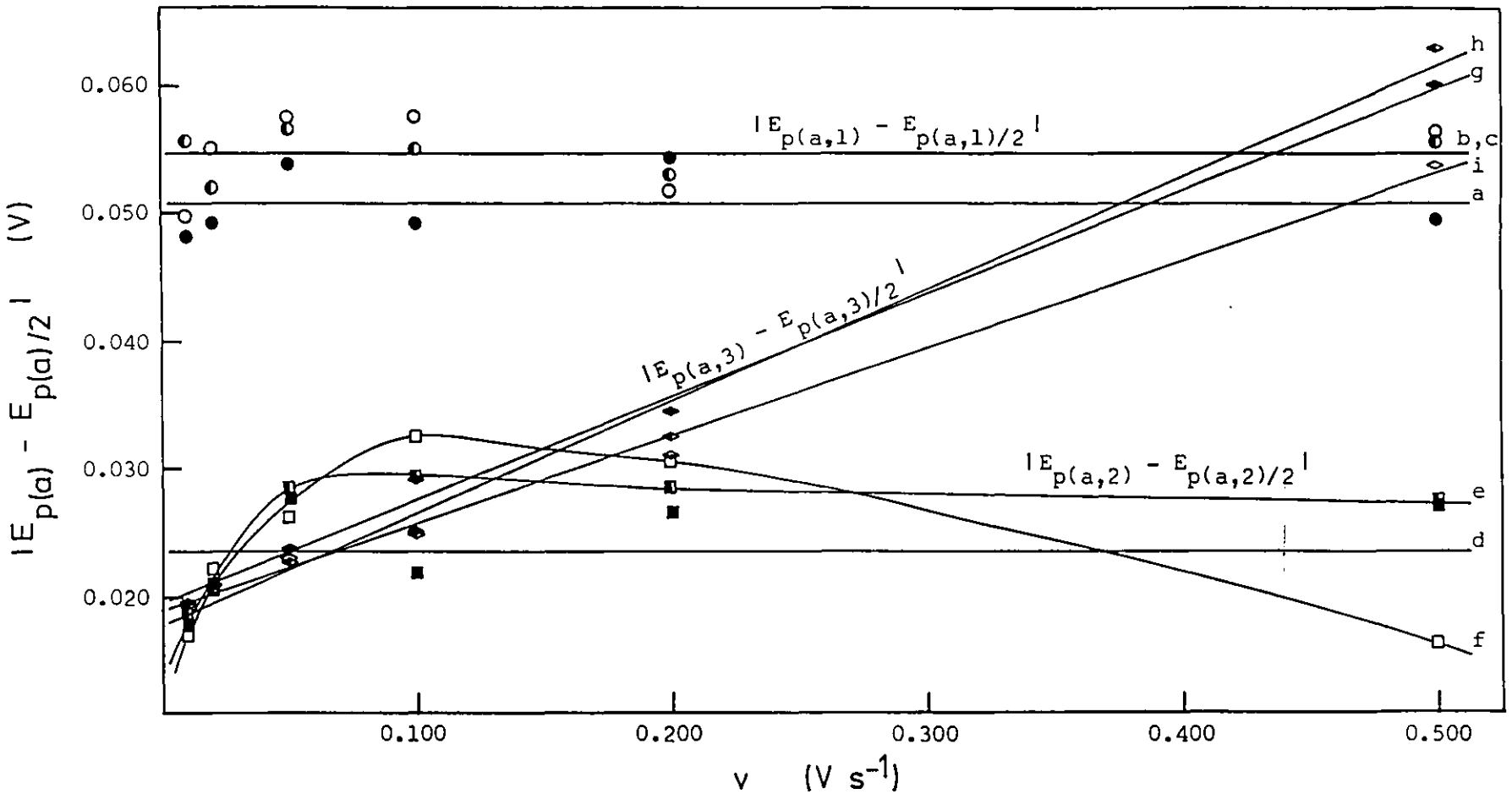

Fig. 5-268 Ir(IV) Perchlorate (2.0×10^{-4} mol dm^{-3})/Perchloric acid (0.1 M) supporting electrolyte System: Values of the difference between anodic peak and half-peak potentials, $|E_{p(a)} - E_{p(a)/2}|$, as a function of potential scan rate, v. (i) Sample as prepared: a, d, and g. (ii) Sample solution aerated with nitrogen for 16 hours: b, e, and h. (iii) Nitrogen aerated solution treated with boron carbide: c, f, and i. Boron carbide solid electrode $B_{3.86}C$.

Fig. 5-268 (continued):-

(i) Sample solution as prepared:

(a) $|E_{p(a,1)} - E_{p(a,1)/2}|$ mean = 0.051 V
Standard deviation = 0.003 V
Coefficient of variation = 5.24%
Degrees of freedom = 5

(d) $|E_{p(a,2)} - E_{p(a,2)/2}|$ mean = 0.024 V
Standard deviation = 0.004 V
Coefficient of variation = 16.8%
Degrees of freedom = 5

(g) $|E_{p(a,3)} - E_{p(a,3)/2}| = 1.95 \times 10^{-2} + 8.07 \times 10^{-2}$ v
Correlation coefficient = 0.9982
Level of significance, p = $p < 0.001$
Standard deviation of $|E_{p(a,3)} - E_{p(a,3)/2}|$ from regression
= 0.001 V
Degrees of freedom = 4

(ii) Sample solution aerated with nitrogen for 16 hours:

(b) $|E_{p(a,1)} - E_{p(a,1)/2}|$ mean = 0.055 V
Standard deviation = 0.002 V
Coefficient of variation = 3.18%
Degrees of freedom = 5

(h) $|E_{p(a,3)} - E_{p(a,3)/2}| = 1.78 \times 10^{-2} + 8.75 \times 10^{-2}$ v
Correlation coefficient = 0.9947
Level of significance, p = $p < 0.001$
Standard deviation of $|E_{p(a,3)} - E_{p(a,3)/2}|$ from regression
= 0.002 V
Degrees of freedom = 4

(iii) Nitrogen aerated solution treated with boron carbide:

(c) $|E_{p(a,1)} - E_{p(a,1)/2}|$ mean = 0.055 V
Standard deviation = 0.003 V
Coefficient of variation = 5.86%
Degrees of freedom = 5

(i) $|E_{p(a,3)} - E_{p(a,3)/2}| = 1.89 \times 10^{-2} + 6.83 \times 10^{-2}$ v
Correlation coefficient = 0.9971
Level of significance, p = $p < 0.001$
Standard deviation of $|E_{p(a,3)} - E_{p(a,3)/2}|$ from regression
= 0.001 V
Degrees of freedom = 4

Two-way Analysis of Variance:

$\underline{|E_{p(a,1)} - E_{p(a,1)/2}|}$

(1) Grand mean = 5.27×10^{-2} V
Standard deviation = 2.84×10^{-3} V

Variance ratio due to effects of scan rate, F(v) = 0.960
Degrees of freedom = 5
Degrees of freedom of the Residual = 5
$F_{0.05}(5,5)$ = 7.15 (double-sided)
Therefore, since F(v) does not exceed $F_{0.05}(5,5)$, the effects of scan rate are not significant.

Variance ratio due to effects of nitrogen aeration, $F(N_2)$ = 9.03
Degrees of freedom = 1
Degrees of freedom of the Residual = 5
$F_{0.05}(1,5)$ = 10.0 (double-sided)
Therefore, since $F(N_2)$ does not exceed $F_{0.05}(1,5)$, the effects of nitrogen aeration are not significant.

(2) Grand mean = 5.46×10^{-2} V
Standard deviation = 2.35×10^{-3} V

Variance ratio due to effects of scan rate, F(v) = 1.49
Degrees of freedom = 5
Degrees of freedom of the Residual = 5
Therefore, since F(v) does not exceed $F_{0.05}(5,5)$, the effects of scan rate are not significant.

Fig. 5-268 (continued):-

Variance ratio due to effects of boron carbide,
F(boron carbide) = 1.56×10^{-4}
Degrees of freedom = 1
Degrees of freedom of the Residual = 5
Therefore, since F(boron carbide) does not exceed $F_{0.05}(1,5)$, the effects of boron carbide are not significant.

$|E_{p(a,2)} - E_{p(a,2)/2}|$

(1) Grand mean = 2.45×10^{-2} V
Standard deviation = 4.04×10^{-3} V

Variance ratio due to effects of scan rate, F(v) = 7.95
Degrees of freedom = 5
Degrees of freedom of the Residual = 5
Therefore, since F(v) exceeds $F_{0.05}(5,5)$, the effects of scan rate are significant.

Variance ratio due to effects of nitrogen aeration, $F(N_2)$ = 2.52
Degrees of freedom = 1
Degrees of freedom of the Residual = 5
Therefore, since $F(N_2)$ does not exceed $F_{0.05}(1,5)$, the effects of nitrogen aeration are not significant.

(2) Grand mean = 2.48×10^{-2} V
Standard deviation = 5.35×10^{-3} V

Variance ratio due to effects of scan rate, F(v) = 3.99
Degrees of freedom = 5
Degrees of freedom of the Residual = 5
Therefore, since F(v) does not exceed $F_{0.05}(5,5)$, the effects of scan rate are not significant.

Variance ratio due to effects of boron carbide,
F(boron carbide) = 0.404
Degrees of freedom = 1
Degrees of freedom of the Residual = 5
Therefore, since F(boron carbide) does not exceed $F_{0.05}(1,5)$, the effects of boron carbide are not significant.

$|E_{p(a,3)} - E_{p(a,3)/2}|$

(1) Grand mean = 3.10×10^{-2} V
Standard deviation = 1.44×10^{-2} V

Variance ratio due to effects of scan rate, F(v) = 196
Degrees of freedom = 5
Degrees of freedom of the Residual = 5
Therefore, since F(v) exceeds $F_{0.05}(5,5)$, the effects of scan rate are significant.

Variance ratio due to effects of nitrogen aeration, $F(N_2)$ = 0.612
Degrees of freedom = 1
Degrees of freedom of the Residual = 5
Therefore, since $F(N_2)$ does not exceed $F_{0.05}(1,5)$, the effects of nitrogen aeration are not significant.

(2) Grand mean = 2.98×10^{-2} V
Standard deviation = 1.35×10^{-2} V

Variance ratio due to effects of scan rate, F(v) = 63.1
Degrees of freedom = 5
Degrees of freedom of the Residual = 5
Therefore, since F(v) exceeds $F_{0.05}(5,5)$, the effects of scan rate are significant.

Variance ratio due to effects of boron carbide,
F(boron carbide) = 1.31
Degrees of freedom = 1
Degrees of freedom of the Residual = 5
Therefore, since F(boron carbide) does not exceed $F_{0.05}(1,5)$, the effects of boron carbide are not significant.

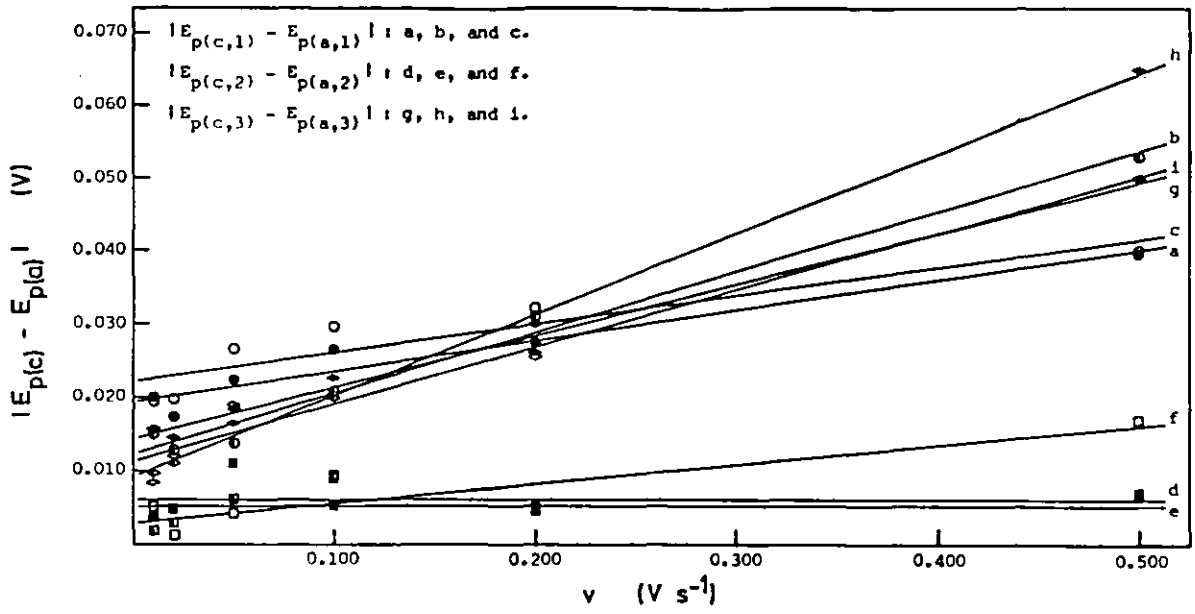

Fig. 5-269 Ir(IV) Perchlorate (2.0×10^{-4} mol dm^{-3})/Perchloric acid (0.1 M) supporting electrolyte System: Values of the difference between cathodic and anodic peak potentials, $|E_{p(c)} - E_{p(a)}|$, as a function of potential scan rate, v. (i) Sample as prepared: a, d, and g. (ii) Sample solution aerated with nitrogen for 16 hours: b, e, and h. (iii) Nitrogen aerated solution treated with boron carbide: c, f, and i. Boron carbide solid electrode $B_{3.86}C$.

(i) Sample solution as prepared:

(a) $|E_{p(c,1)} - E_{p(a,1)}| = 1.95 \times 10^{-2} + 4.13 \times 10^{-2}$ v
Correlation coefficient = 0.9696
Level of significance, $p = 0.001 < p < 0.01$
Standard deviation of $|E_{p(c,1)} - E_{p(a,1)}|$ from regression
= 0.002 V
Degrees of freedom = 4

(d) $|E_{p(c,2)} - E_{p(a,2)}|$ mean $= 6.07 \times 10^{-3}$ V
Standard deviation $= 2.60 \times 10^{-3}$ V
Coefficient of variation = 42.9%
Degrees of freedom = 5

(g) $|E_{p(c,3)} - E_{p(a,3)}| = 1.43 \times 10^{-2} + 7.03 \times 10^{-2}$ v
Correlation coefficient = 0.9941
Level of significance, $p = p < 0.001$
Standard deviation of $|E_{p(c,3)} - E_{p(a,3)}|$ from regression
= 0.002 V
Degrees of freedom = 4

(ii) Sample solution aerated with nitrogen for 16 hours:

(b) $|E_{p(c,1)} - E_{p(a,1)}| = 1.22 \times 10^{-2} + 8.29 \times 10^{-2}$ v
Correlation coefficient = 0.9927
Level of significance, $p = p < 0.001$
Standard deviation of $|E_{p(c,1)} - E_{p(a,1)}|$ from regression
= 0.002 V
Degrees of freedom = 4

(e) $|E_{p(c,2)} - E_{p(a,2)}|$ mean $= 5.17 \times 10^{-3}$ V
Standard deviation $= 2.70 \times 10^{-3}$ V
Coefficient of variation = 52.3%
Degrees of freedom = 5

Fig. 5-269 (continued):-

(h) $|E_{p(c,3)} - E_{p(a,3)}| = 9.02 \times 10^{-3} + 0.111$ v

Correlation coefficient = 0.9986

Level of significance, p = $p < 0.001$

Standard deviation of $|E_{p(c,3)} - E_{p(a,3)}|$ from regression = 0.001 V

Degrees of freedom = 4

(iii) Nitrogen aerated solution treated with boron carbide:

(c) $|E_{p(c,1)} - E_{p(a,1)}| = 2.22 \times 10^{-2} + 3.88 \times 10^{-2}$ v

Correlation coefficient = 0.9232

Level of significance, $0.001 < p < 0.01$

Standard deviation of $|E_{p(c,1)} - E_{p(a,1)}|$ from regression = 0.003 V

Degrees of freedom = 4

(f) $|E_{p(c,2)} - E_{p(a,2)}| = 3.02 \times 10^{-3} + 2.61 \times 10^{-2}$ v

Correlation coefficient = 0.8811

Level of significance, $0.02 < p < 0.05$

Standard deviation of $|E_{p(c,2)} - E_{p(a,2)}|$ from regression = 0.003 V

Degrees of freedom = 4

(i) $|E_{p(c,3)} - E_{p(a,3)}| = 1.12 \times 10^{-2} + 7.79 \times 10^{-2}$ v

Correlation coefficient = 0.9852

Level of significance, p = $p < 0.001$

Standard deviation of $|E_{p(c,3)} - E_{p(a,3)}|$ from regression = 0.003 V

Degrees of freedom = 4

Two-way Analysis of Variance:

$|E_{p(c,1)} - E_{p(a,1)}|$

(1) Grand mean = 2.49×10^{-2} V

Standard deviation = 1.13×10^{-2} V

Variance ratio due to effects of scan rate, F(v) = 8.17

Degrees of freedom = 5

Degrees of freedom of the Residual = 5

$F_{0.05}(5,5) = 7.15$ (double-sided)

Therefore, since F(v) exceeds $F_{0.05}(5,5)$, the effects of scan rate are significant.

Variance ratio due to effects of nitrogen aeration, $F(N_2) = 0.119$

Degrees of freedom = 1

Degrees of freedom of the Residual = 5

$F_{0.05}(1,5) = 10.0$ (double-sided)

Therefore, since $F(N_2)$ does not exceed $F_{0.05}(1,5)$, the effects of nitrogen aeration are not significant.

(2) Grand mean = 2.61×10^{-2} V

Standard deviation = 1.14×10^{-2} V

Variance ratio due to effects of scan rate, F(v) = 6.48

Degrees of freedom = 5

Degrees of freedom of the Residual = 5

Therefore, since F(v) does not exceed $F_{0.05}(5,5)$, the effects of scan rate are not significant.

Variance ratio due to effects of boron carbide, F(boron carbide) = 0.903

Degrees of freedom = 1

Degrees of freedom of the Residual = 5

Therefore, since F(boron carbide) does not exceed $F_{0.05}(1,5)$, the effects of boron carbide are not significant.

Fig. 5-269 (continued):-

$|E_{p(c,2)} - E_{p(a,2)}|$

(1) Grand mean = 5.62×10^{-3} V

Standard deviation = 2.46×10^{-3} V

Variance ratio due to effects of scan rate, F(v) = 2.15

Degrees of freedom = 5

Degrees of freedom of the Residual = 5

Therefore, since F(v) does not exceed $F_{0.05}(5,5)$, the effects of scan rate are not significant.

Variance ratio due to effects of nitrogen aeration, $F(N_2)$ = 0.543

Degrees of freedom = 1

Degrees of freedom of the Residual = 5

Therefore, since $F(N_2)$ does not exceed $F_{0.05}(1,5)$, the effects of nitrogen aeration are not significant.

(2) Grand mean = 6.01×10^{-3} V

Standard deviation = 4.06×10^{-3} V

Variance ratio due to effects of scan rate, F(v) = 2.41

Degrees of freedom = 5

Degrees of freedom of the Residual = 5

Therefore, since F(v) does not exceed $F_{0.05}(5,5)$, the effects of scan rate are not significant.

Variance ratio due to effects of boron carbide, F(boron carbide) = 0.766

Degrees of freedom = 1

Degrees of freedom of the Residual = 5

Therefore, since F(boron carbide) does not exceed $F_{0.05}(1,5)$, the effects of boron carbide are not significant.

$|E_{p(c,3)} - E_{p(a,3)}|$

(1) Grand mean = 2.50×10^{-2} V

Standard deviation = 1.59×10^{-2} V

Variance ratio due to effects of scan rate, F(v) = 19.2

Degrees of freedom = 5

Degrees of freedom of the Residual = 5

Therefore, since F(v) exceeds $F_{0.05}(5,5)$, the effects of scan rate are significant.

Variance ratio due to effects of nitrogen aeration, $F(N_2) = 5.89 \times 10^{-2}$

Degrees of freedom = 1

Degrees of freedom of the Residual = 5

Therefore, since $F(N_2)$ does not exceed $F_{0.05}(1,5)$, the effects of nitrogen aeration are not significant.

(2) Grand mean = 2.40×10^{-2} V

Standard deviation = 1.65×10^{-2} V

Variance ratio due to effects of scan rate, F(v) = 30.2

Degrees of freedom = 5

Degrees of freedom of the Residual = 5

Therefore, since F(v) exceeds $F_{0.05}(5,5)$, the effects of scan rate are significant.

Variance ratio due to effects of boron carbide, F(boron carbide) = 1.09

Degrees of freedom = 1

Degrees of freedom of the Residual = 5

Therefore, since F(boron carbide) does not exceed $F_{0.05}(1,5)$, the effects of boron carbide are not significant.

and 3 at high concentration of Ir(IV) perchlorate (i.e. 2.3 x 10^{-3} mol dm^{-3}), and for Peak 2 at lower concentration (i.e. 2.0 x 10^{-4} mol dm^{-3}). This is consistent with the hypothesis that Peak 2 was the strong adsorption post-peak of Ir(IV) perchlorate reactant; whereas Peak 1 was a diffusion peak complicated by weak adsorption influences emanating from Peak 2, and Peak 3 was a diffusion peak coupled with weak adsorption. The cathodic shifts in peak potentials (Fig. 5-260) due to boron carbide treatment of the sample prior to voltammetry are consistent with the loss of electroactive species, removed as adsorbate on the boron carbide surface, for a system where the reactants are adsorbed on the working electrode (Fig. 3-22). The composition of the boron carbide solid electrode employed was $B_{3.86}C$.

5-1.5.(v) Spectrophotometry of Ir(IV) perchlorate.

The absorption spectra of Ir(IV) perchlorate in perchloric acid (0.1 M) show the expected falls in absorbance after the sample had been treated by nitrogen aeration and/or contact with boron carbide (Fig. 5-270). The trends are consistent with those obtained in voltammetry (sections 5-1.5.(iii).f and 5-1.5.(iv).c) for peak currents.

5-1.6 Ir(IV) sulphate system

Cyclic voltammograms for Ir(IV) sulphate (1.0 x 10^{-4} mol dm^{-3}), in sulphuric acid (0.05 to 0.4 M) supporting electrolyte, were obtained at the boron carbide solid electrode using a range of potential sweep rates (Figures 5-271 and 5-272). It can be seen that at low sulphuric acid concentration (i.e. 0.05 M) only two cathodic and three anodic peaks were exhibited for Ir(IV) sulphate (Fig. 5-272). At higher sulphuric acid concentrations, however, three cathodic and four anodic peaks were obtained. The presence of an extra anodic peak for the reverse sweep strongly suggests that the system involved a follow-up chemical reaction.

When the concentration of sulphuric acid supporting electrolyte was 0.05 M, the peak current functions for Ir(IV) sulphate as functions of $(\text{sweep rate})^{\frac{1}{2}}$ show that the cathodic Peak 1 was probably the sum of

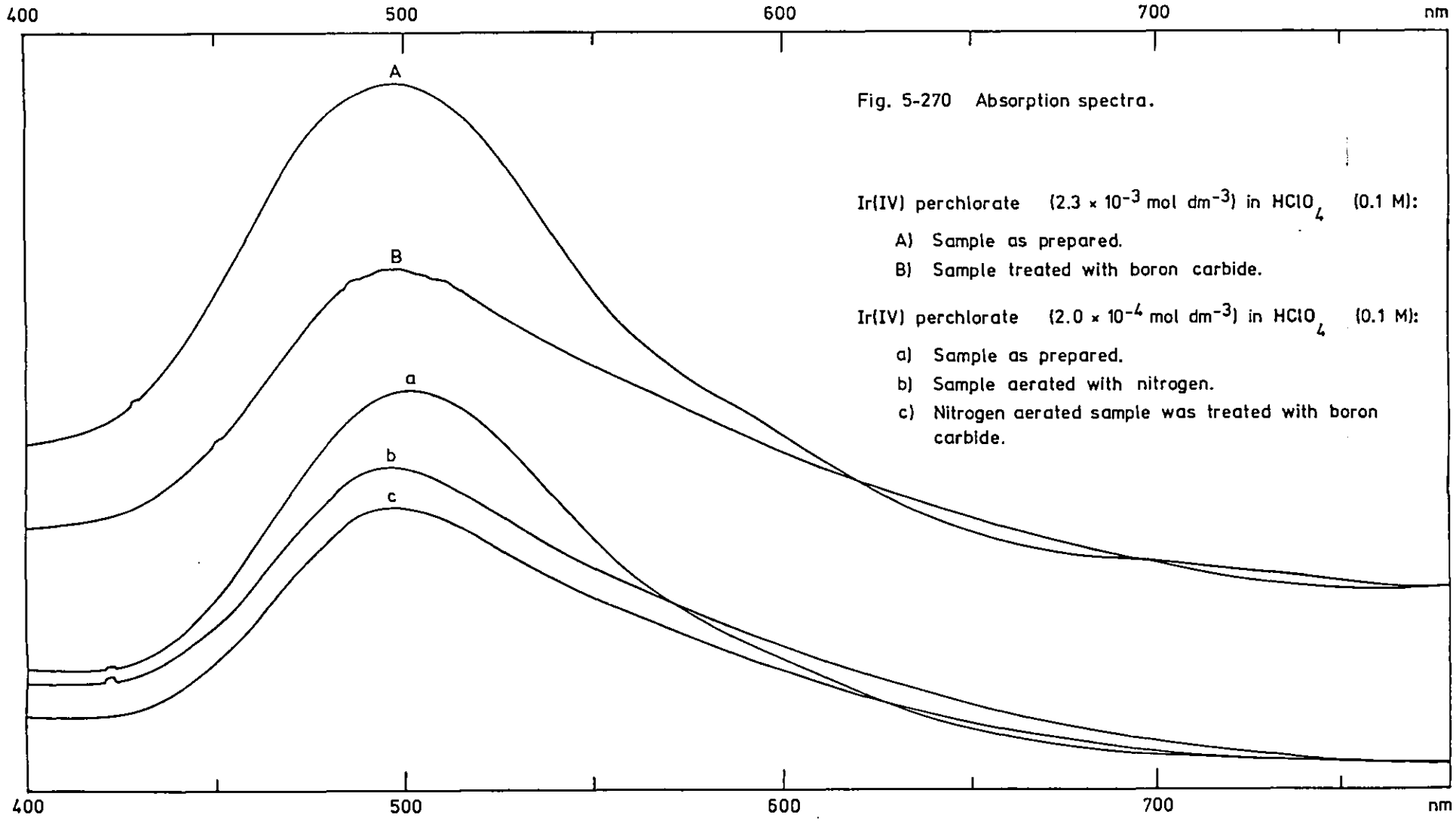

Fig. 5-270 Absorption spectra.

Ir(IV) perchlorate (2.3×10^{-3} mol dm^{-3}) in $HClO_4$ (0.1 M):

A) Sample as prepared.

B) Sample treated with boron carbide.

Ir(IV) perchlorate (2.0×10^{-4} mol dm^{-3}) in $HClO_4$ (0.1 M):

a) Sample as prepared.

b) Sample aerated with nitrogen.

c) Nitrogen aerated sample was treated with boron carbide.

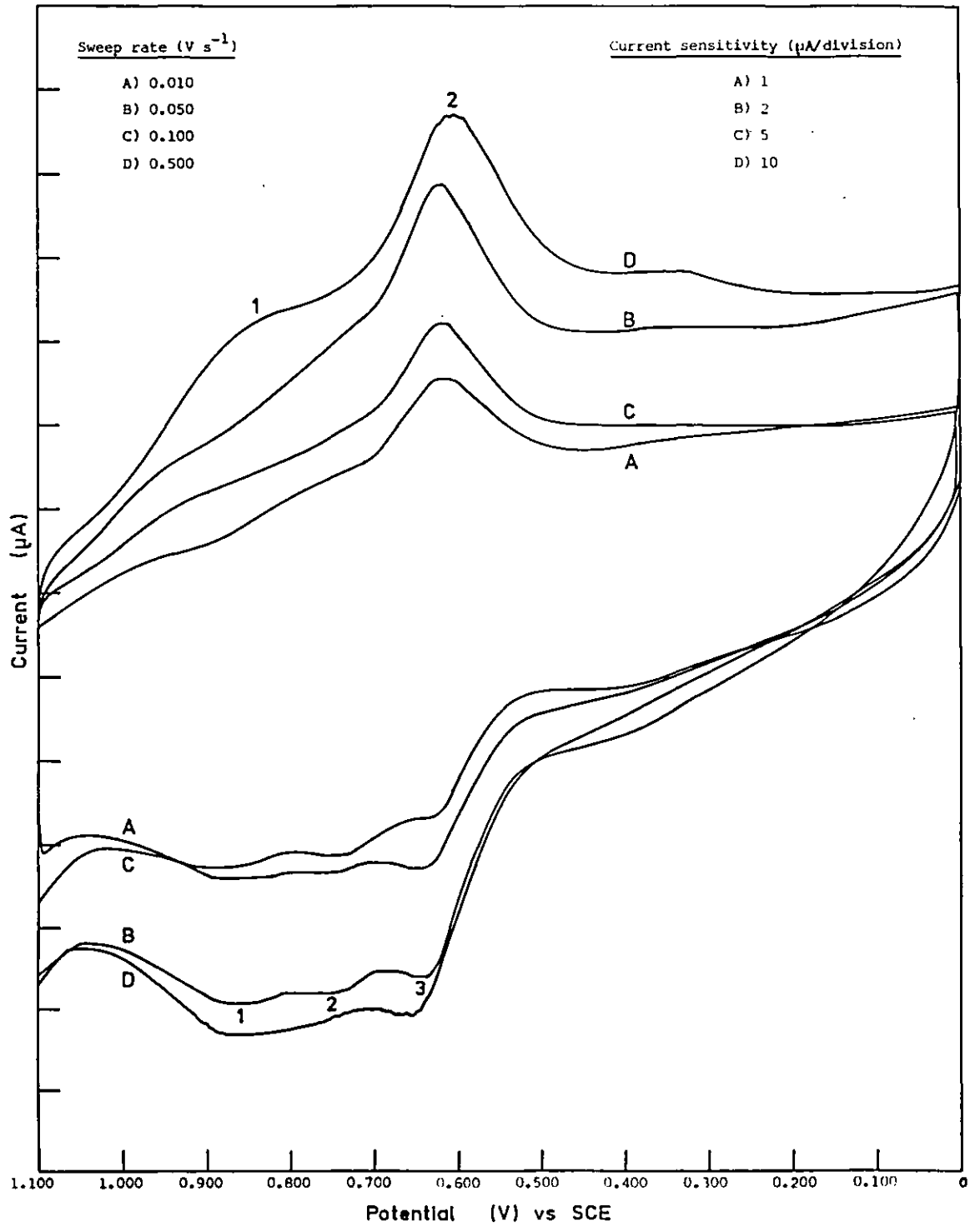

Fig. 5-271 Ir(IV) sulphate (1.0×10^{-4} mol dm^{-3})/Sulphuric acid (0.05 M) supporting electrolyte System: Cyclic voltammograms obtained at the boron carbide solid electrode — variation with sweep rate.

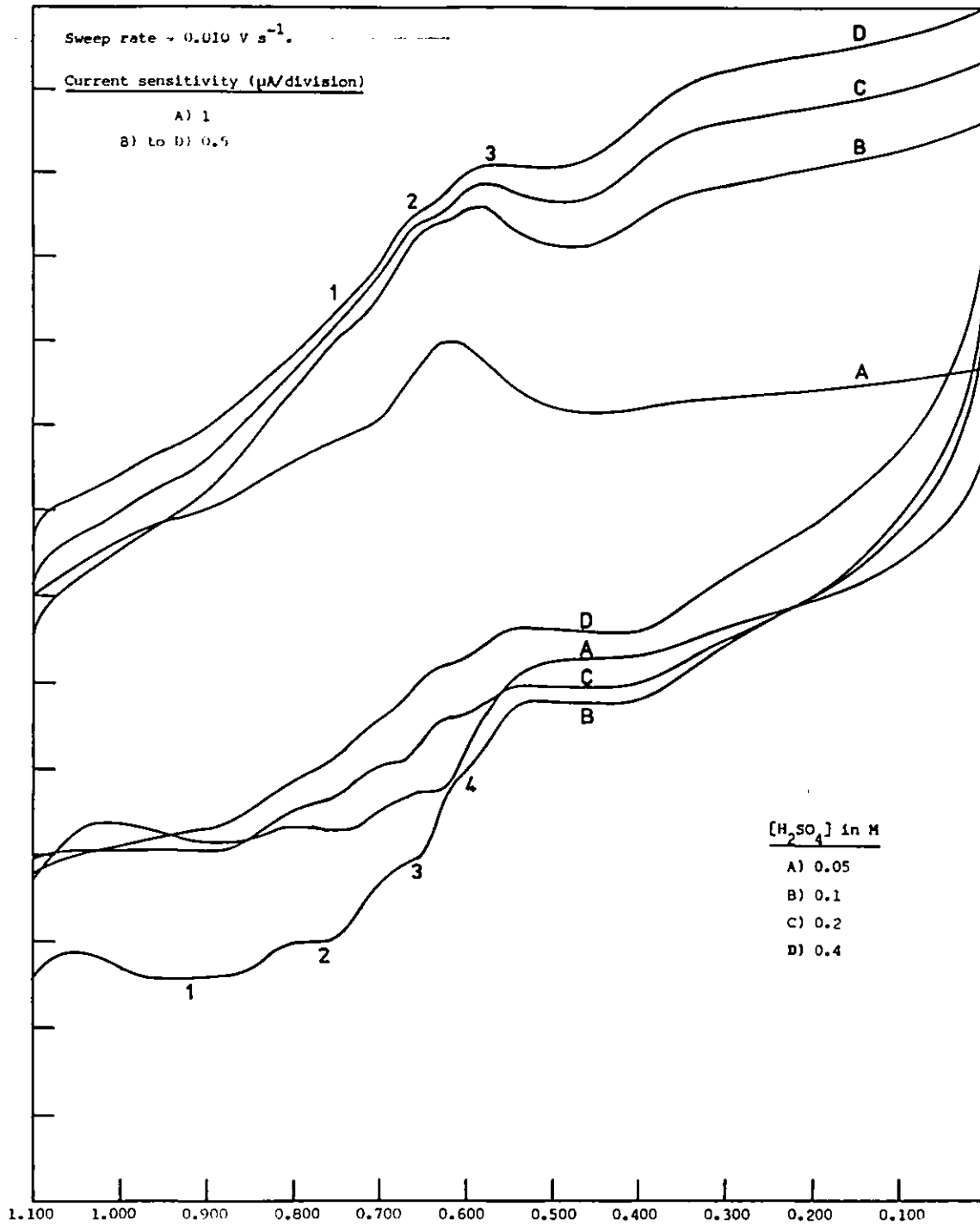

Fig. 5-272 Ir(IV) sulphate (1.0×10^{-4} mol dm^{-3})/Sulphuric acid (0.05 to 0.4 M) supporting electrolyte System: Cyclic voltammograms obtained at the boron carbide solid electrode.

two charge transfers where the individual peaks had merged (Fig. 5-273). Thus the trend of $i_{p(c,1)}/v^{\frac{1}{2}}$ with increasing $v^{\frac{1}{2}}$ reflected the presence of an irreversible follow-up chemical reaction at slow sweep rates but the presence of adsorption was reflected at fast sweep rates. Furthermore, the reverse sweep exhibited two anodic counterparts, anodic Peaks 1 and 2, for the cathodic Peak 1; where $i_{p(a,1)}/v^{\frac{1}{2}}$ and $i_{p(a,2)}/v^{\frac{1}{2}}$, as functions of $(\text{sweep rate})^{\frac{1}{2}}$, reflected the presence of adsorption and the presence of the irreversible follow-up chemical reaction respectively (Fig. 5-273 c.f. Fig. 3-6). Cathodic Peak 2 and anodic Peak 3 represent the cycle of a charge transfer which was influenced by adsorption; thus $i_{p(c,2)}/v^{\frac{1}{2}}$ and $i_{p(a,3)}/v^{\frac{1}{2}}$ show similar trends with increasing sweep rate (Fig. 5-273).

The peak current functions for Ir(IV) sulphate, when the concentration of sulphuric acid supporting electrolyte was 0.1 M, show that all the cathodic and anodic peaks were influenced by adsorption (Fig. 5-274). Furthermore, the cathodic Peaks 1 and 2 were also complicated by catalytic reactions at the slower sweep rates (c.f. Fig. 3-6). As the concentration of sulphuric acid supporting electrolyte was increased the influence of adsorption was diminished (Figures 5-275 and 5-276), and cathodic Peak 1 and anodic Peak 2 became too poorly defined to be quantified (Fig. 5-272).

The peak potentials of the interpretable peaks for Ir(IV) sulphate (1.0×10^{-4} mol dm^{-3}) in sulphuric acid (0.05 to 0.4 M) supporting electrolyte are presented as functions of sweep rate in Figures 5-277 to 5-280 inclusive. The corresponding $|E_p - E_{p/2}|$ values are plotted in Figures 5-281 to 5-284 inclusive. In general, the peak potentials were anodically shifted by the increase in ionic strength; even though some of the charge transfers became less reversible, as reflected in wider $|E_p - E_{p/2}|$ values. In the case for cathodic Peak 3, $E_{p(c,3)}$, the increase in ionic strength decreased the reversibility of the charge transfer to the extent of causing the peak potential to be shifted cathodically.

The evidence suggests that the Ir(IV) sulphate reactant was adsorbed and that the anodic shift in the peak potentials with increasing ionic strength (as the concentration of H_2SO_4 was increased) was mainly due to the weakening of the adsorption influences. Although such anodic shifts in peak potentials with increasing ionic strength also suggest that the electroactive species was anionic, this is not clear because of the adsorption effects.

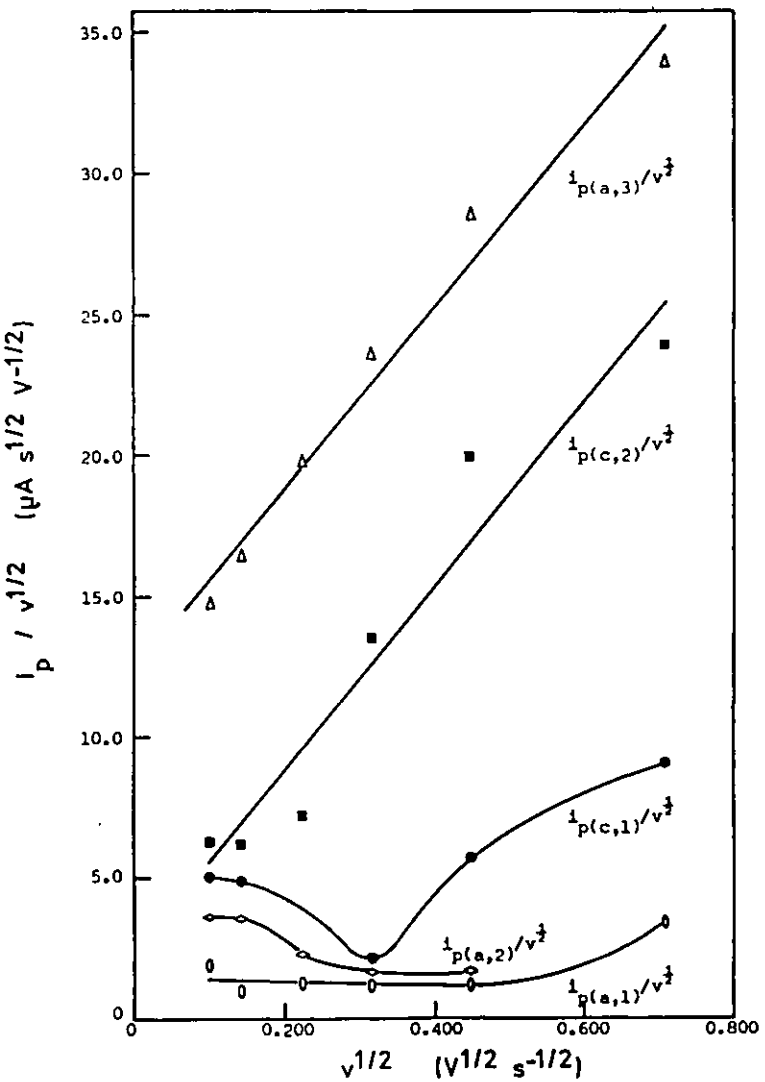

Fig. 5-273 Ir(IV) sulphate (1.0×10^{-4} mol dm^{-3})/Sulphuric acid (0.05 M) supporting electrolyte System: Values of peak current function, $i_p/v^{\frac{1}{2}}$, as a function of square root of potential sweep rate, $v^{\frac{1}{2}}$. Boron carbide solid electrode.

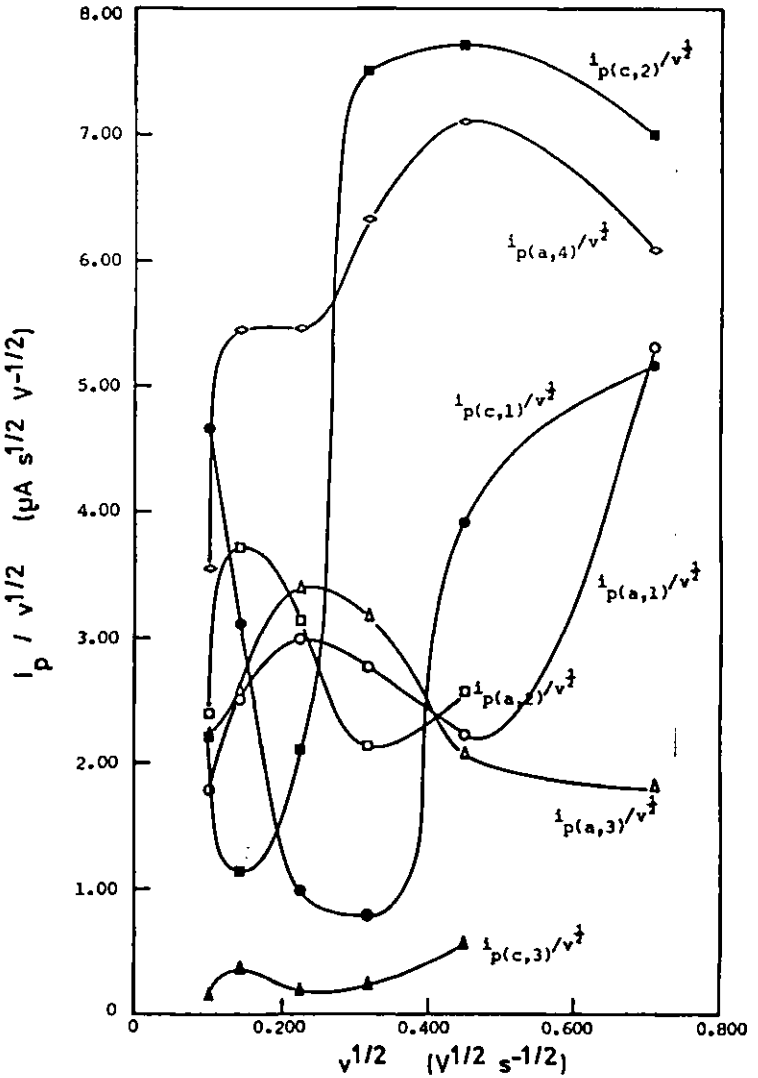

Fig. 5-274 Ir(IV) sulphate (1.0×10^{-4} mol dm^{-3})/Sulphuric acid (0.1 M) supporting electrolyte System: Values of peak current function, $i_p/v^{\frac{1}{2}}$, as a function of square root of potential sweep rate, $v^{\frac{1}{2}}$. Boron carbide solid electrode.

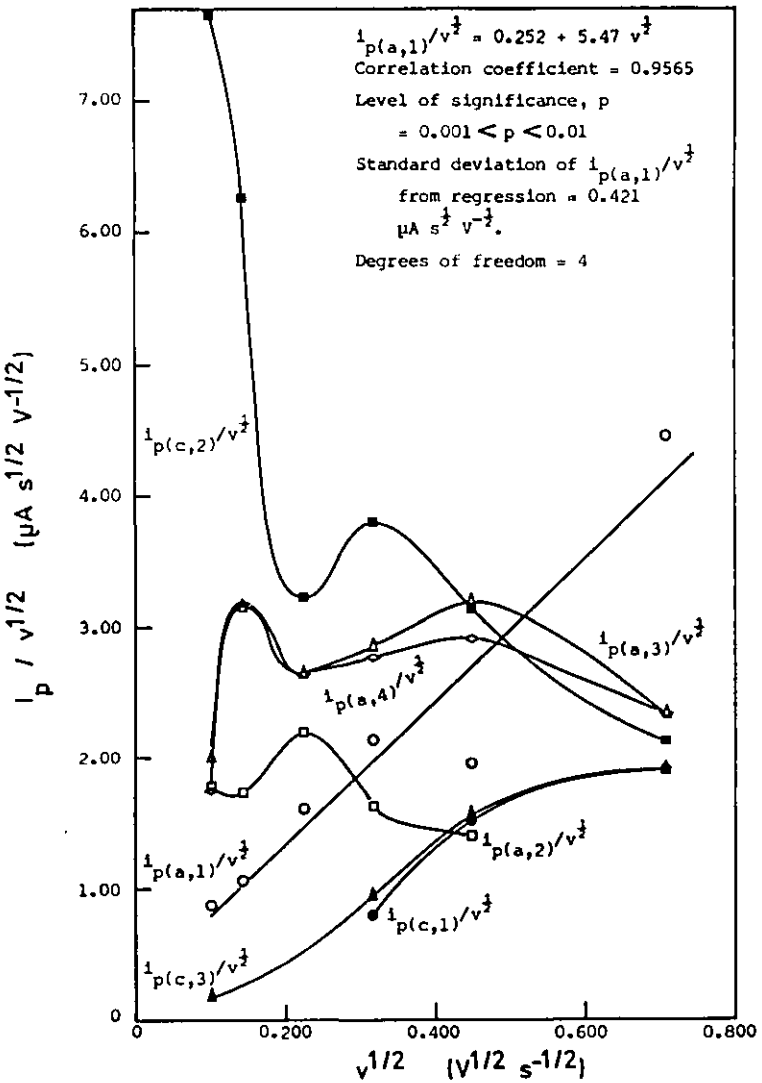

Fig. 5-275 Ir(IV) sulphate (1.0×10^{-4} mol dm^{-3})/Sulphuric acid (0.2 M) supporting electrolyte System: Values of peak current function, $i_p/v^{\frac{1}{2}}$, as a function of square root of potential sweep rate, $v^{\frac{1}{2}}$. Boron carbide solid electrode.

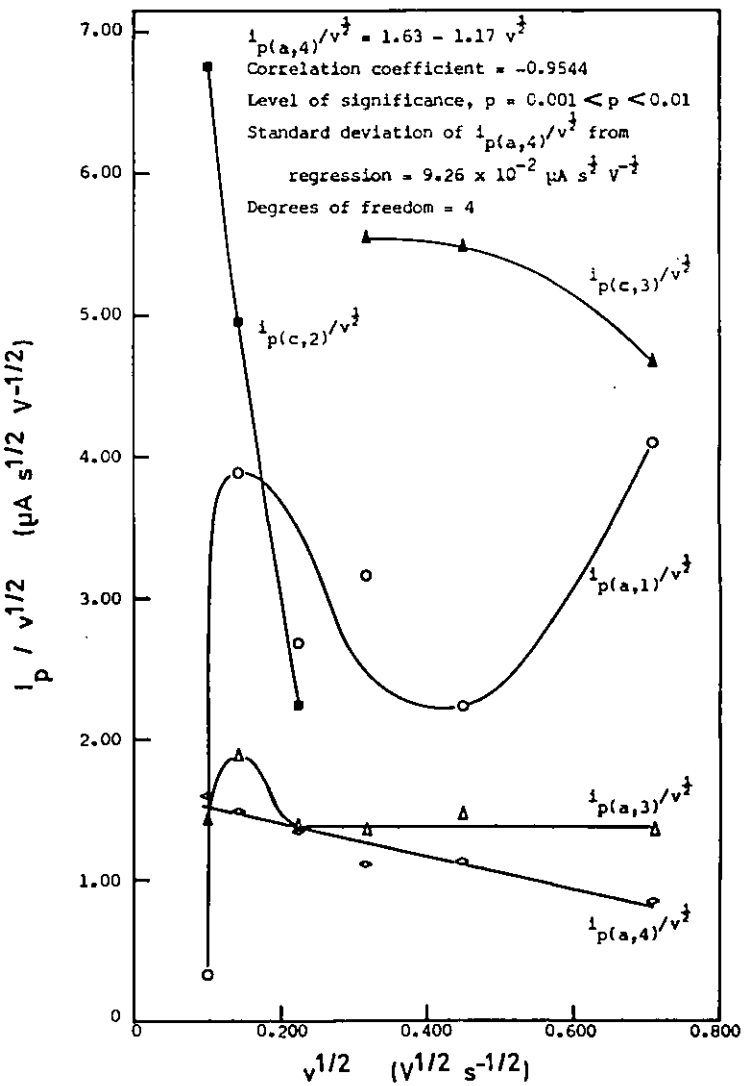

Fig. 5-276 Ir(IV) sulphate (1.0×10^{-4} mol dm^{-3})/Sulphuric acid (0.4 M) supporting electrolyte System: Values of peak current function, $i_p/v^{\frac{1}{2}}$, as a function of square root of potential sweep rate, $v^{\frac{1}{2}}$. Boron carbide solid electrode.

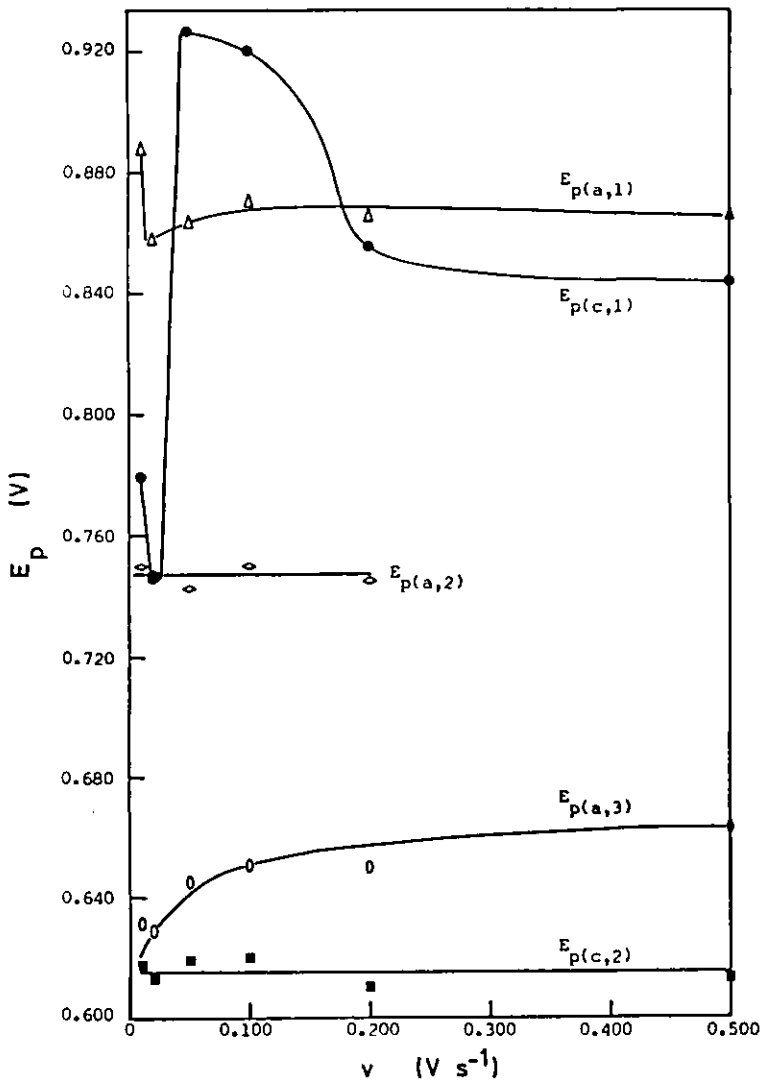

Fig. 5-277 Ir(IV) sulphate (1.0×10^{-4} mol dm^{-3})/Sulphuric acid (0.05 M) supporting electrolyte System: Values of peak potential, E_p, as a function of potential sweep rate, v. Boron carbide solid electrode.

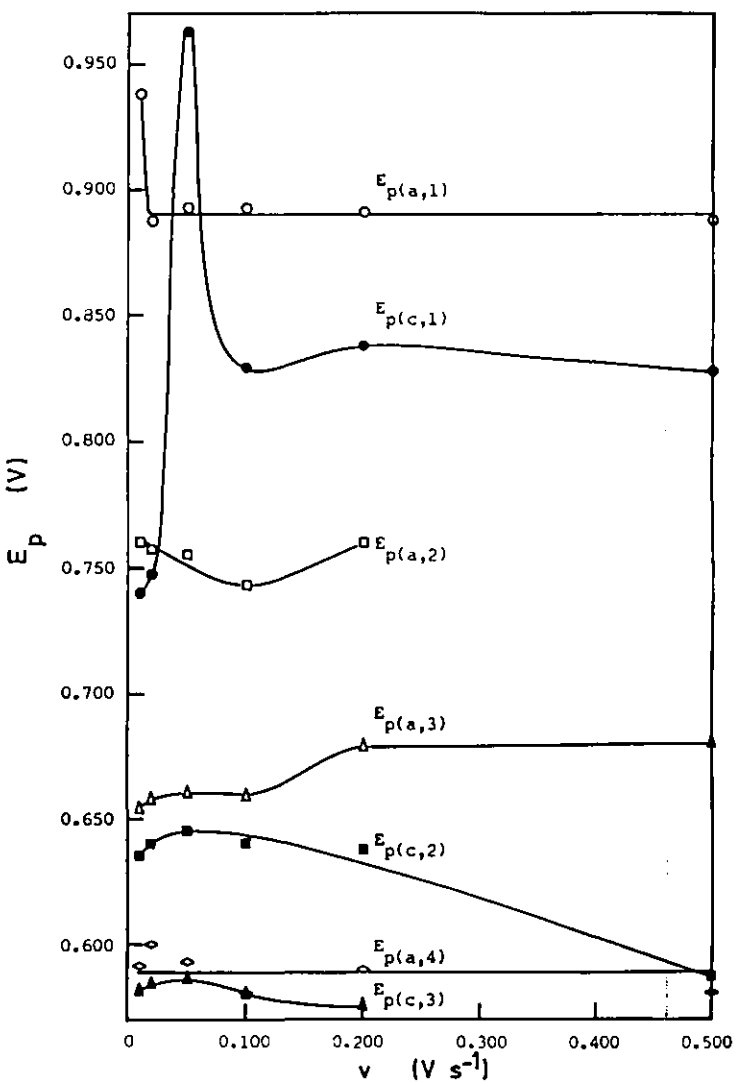

Fig. 5-278 Ir(IV) sulphate (1.0×10^{-4} mol dm^{-3})/Sulphuric acid (0.1 M) supporting electrolyte System: Values of peak potential, E_p, as a function of potential sweep rate, v. Boron carbide solid electrode.

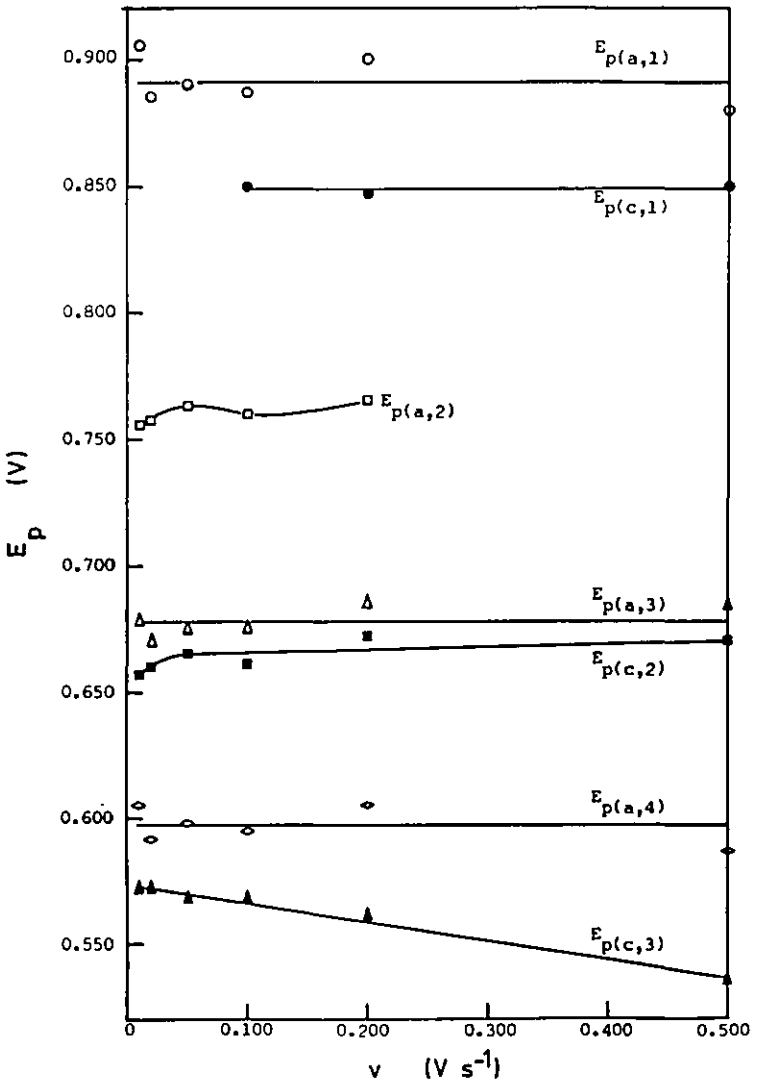

Fig. 5-279 Ir(IV) sulphate (1.0×10^{-4} mol dm^{-3})/Sulphuric acid (0.2 M) supporting electrolyte System: Values of peak potential, E_p, as a function of potential sweep rate, v. Boron carbide solid electrode.

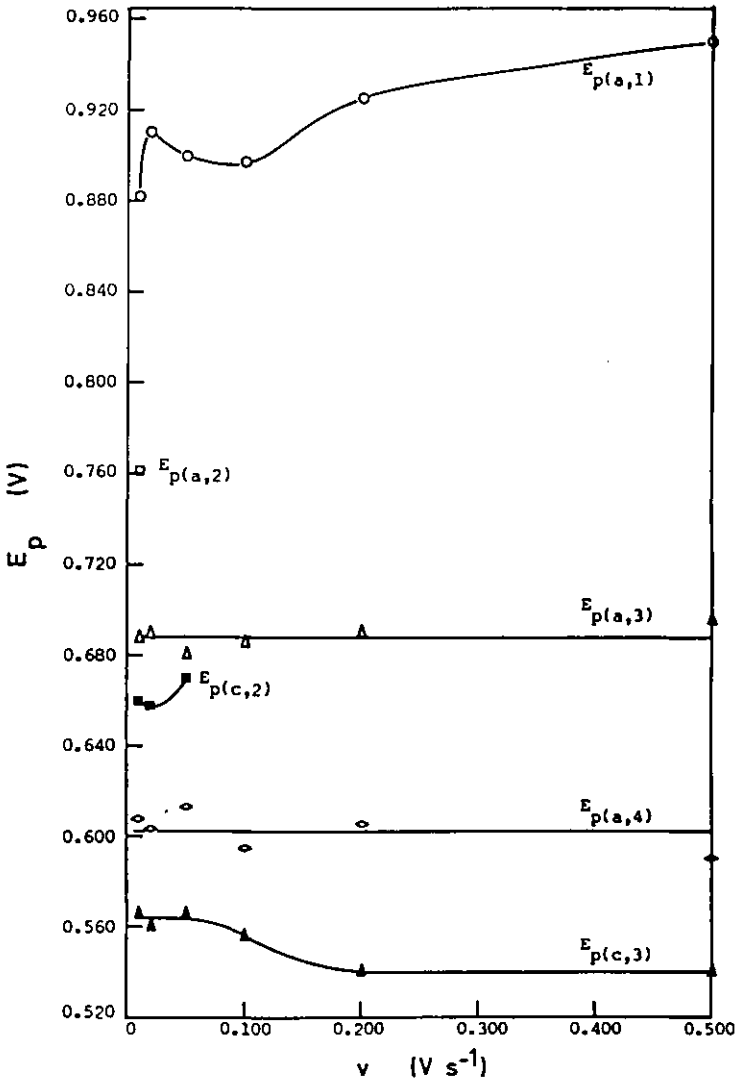

Fig. 5-280 Ir(IV) sulphate (1.0×10^{-4} mol dm^{-3})/Sulphuric acid (0.4 M) supporting electrolyte System: Values of peak potential, E_p, as a function of potential sweep rate, v. Boron carbide solid electrode.

Figures 5-277 to 5-280 (continued):-

Regression Analysis of Peak Potential Values as Functions of Square Root Value of Ionic Strength, $\sqrt{I}$.

1) $E_{p(c,1)} = 0.835 + 1.26 \times 10^{-2} \sqrt{I}$
Correlation coefficient = 0.2041
Level of significance, p = $p > 0.10$
Standard deviation of $E_{p(c,1)}$ from regression = 1.10×10^{-2} V
Degrees of freedom = 6

$E_{p(c,1)}$ grand mean = 0.842 V (vs SCE) ± 0.010 V
Coefficient of variation = 1.19%
Degrees of freedom = 7

2) $E_{p(c,2)} = 0.594 + 7.55 \times 10^{-2} \sqrt{I}$
Correlation coefficient = 0.8638
Level of significance, p = $p < 0.001$
Standard deviation of $E_{p(c,2)}$ from regression = 1.11×10^{-2} V
Degrees of freedom = 18

3) $E_{p(c,3)} = 0.607 - 4.85 \times 10^{-2} \sqrt{I}$
Correlation coefficient = -0.8328
Level of significance, p = $p < 0.001$
Standard deviation of $E_{p(c,3)}$ from regression = 7.86×10^{-3} V
Degrees of freedom = 14

4) $E_{p(a,1)} = 0.857 + 4.38 \times 10^{-2} \sqrt{I}$
Correlation coefficient = 0.7190
Level of significance, p = $p < 0.001$
Standard deviation of $E_{p(a,1)}$ from regression = 1.16×10^{-2} V
Degrees of freedom = 20

5) $E_{p(a,2)} = 0.739 + 2.52 \times 10^{-2} \sqrt{I}$
Correlation coefficient = 0.7150
Level of significance, p = $0.001 < p < 0.01$
Standard deviation of $E_{p(a,2)}$ from regression = 5.26×10^{-3} V
Degrees of freedom = 14

6) $E_{p(a,3)} = 0.637 + 4.85 \times 10^{-2} \sqrt{I}$
Correlation coefficient = 0.8554
Level of significance, p = $p < 0.001$
Standard deviation of $E_{p(a,3)}$ from regression = 7.99×10^{-3} V
Degrees of freedom = 20

7) $E_{p(a,4)} = 0.577 + 2.34 \times 10^{-2} \sqrt{I}$
Correlation coefficient = 0.5891
Level of significance, p = $0.01 < p < 0.02$
Standard deviation of $E_{p(a,4)}$ from regression = 7.64×10^{-3} V
Degrees of freedom = 16

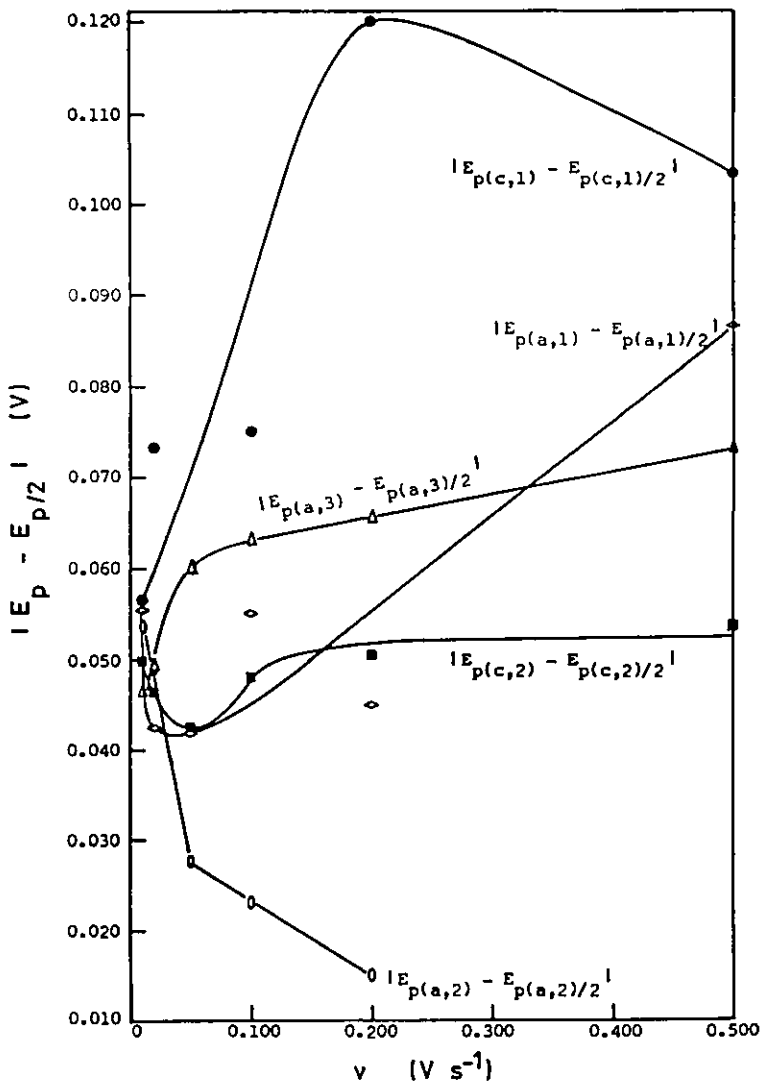

Fig. 5-281 Ir(IV) sulphate (1.0×10^{-4} mol dm^{-3})/Sulphuric acid (0.05 M) supporting electrolyte System: Values of the absolute difference between peak and half-peak potential, $|E_p - E_{p/2}|$, as a function of potential sweep rate, v. Boron carbide solid electrode.

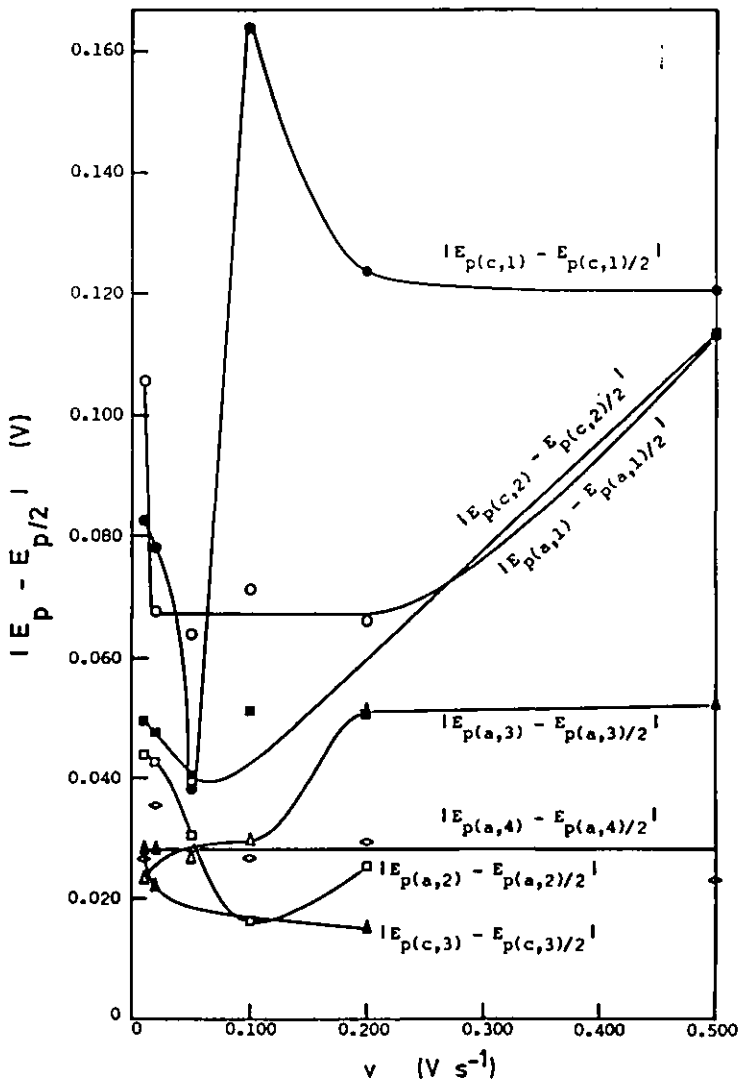

Fig. 5-282 Ir(IV) sulphate (1.0×10^{-4} mol dm^{-3})/Sulphuric acid (0.1 M) supporting electrolyte System: Values of the absolute difference between peak and half-peak potential, $|E_p - E_{p/2}|$, as a function of potential sweep rate, v. Boron carbide solid electrode.

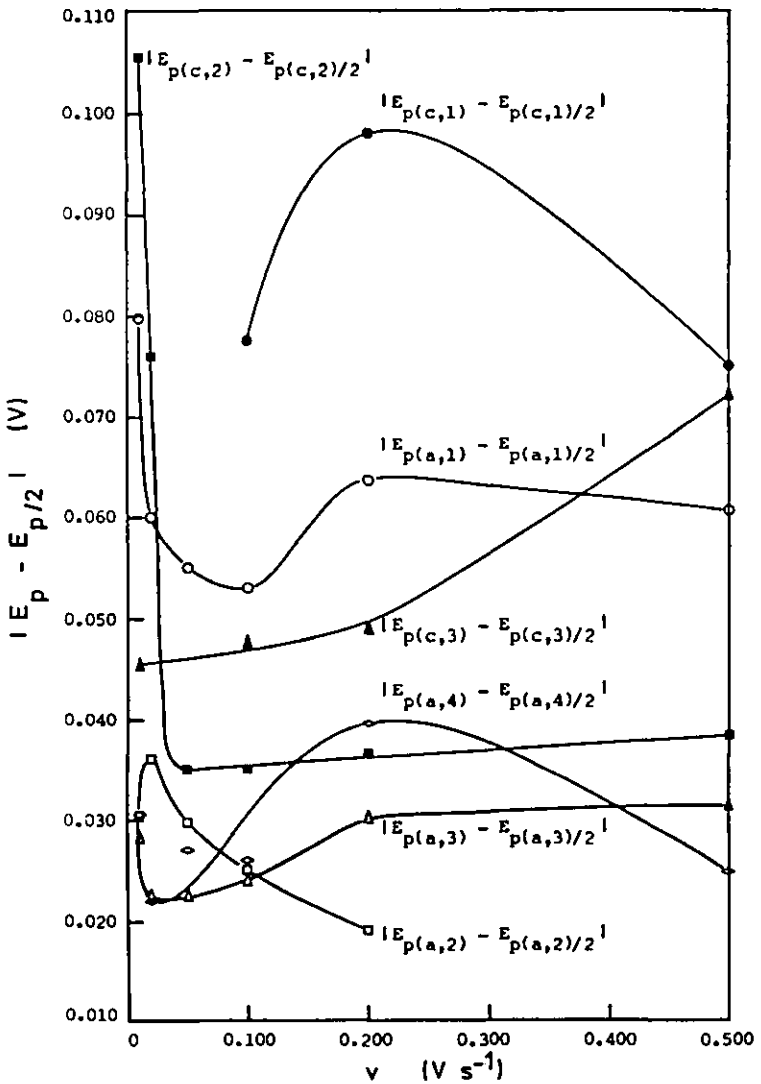

Fig. 5-283 Ir(IV) sulphate (1.0×10^{-4} mol dm^{-3})/Sulphuric acid (0.2 M) supporting electrolyte System: Values of the absolute difference between peak and half-peak potential, $|E_p - E_{p/2}|$, as a function of potential sweep rate, v. Boron carbide solid electrode.

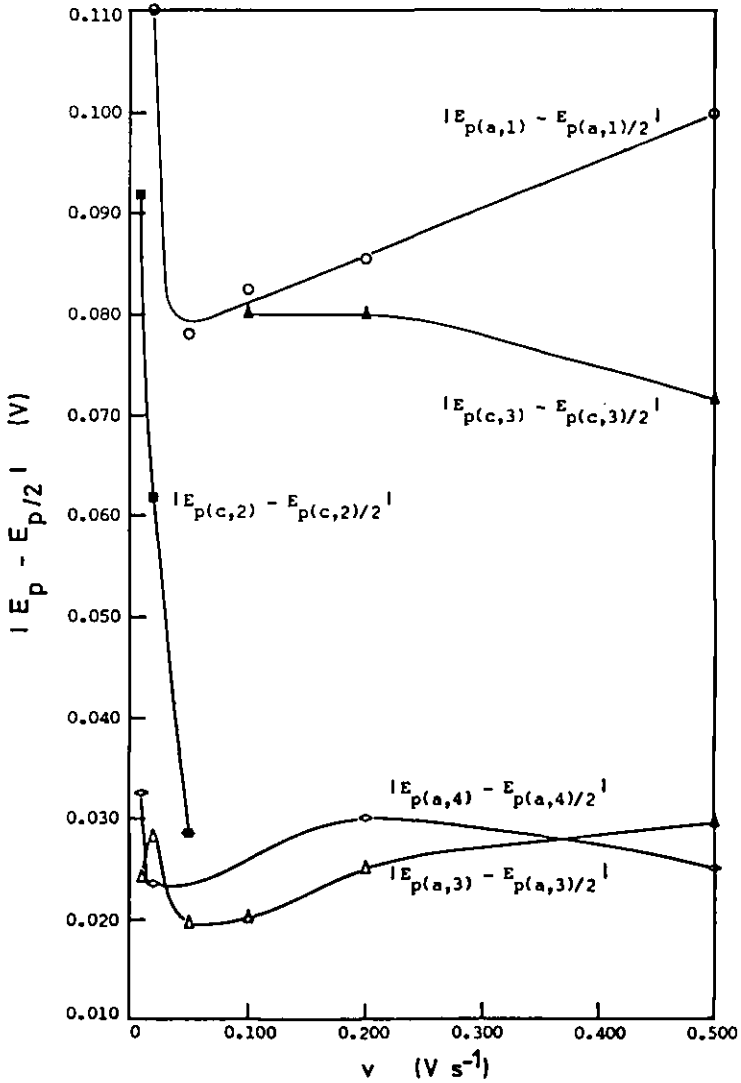

Fig. 5-284 Ir(IV) sulphate (1.0×10^{-4} mol dm^{-3})/Sulphuric acid (0.4 M) supporting electrolyte System: Values of the absolute difference between peak and half-peak potential, $|E_p - E_{p/2}|$, as a function of potential sweep rate, v. Boron carbide solid electrode.

Figures 5-281 to 5-284 (continued):-

Regression Analysis of Values of $|E_p - E_{p/2}|$ as Functions of Square Root Value of Ionic Strength, $\sqrt{I}$.

1) $|E_{p(c,1)} - E_{p(c,1)/2}| = 9.31 \times 10^{-2} - 2.51 \times 10^{-3} \sqrt{I}$
Correlation coefficient = -0.01147
Level of significance, p = p > 0.10
Standard deviation of $|E_{p(c,1)} - E_{p(c,1)/2}|$ from regression = 3.35×10^{-2} V
Degrees of freedom = 12

$|E_{p(c,1)} - E_{p(c,1)/2}|$ grand mean = 9.17×10^{-2} V ± 3.22×10^{-2} V
Coefficient of variation = 35.1%
Degrees of freedom = 13

2) $|E_{p(c,2)} - E_{p(c,2)/2}| = 6.18 \times 10^{-2} - 3.07 \times 10^{-2} \sqrt{I}$
Correlation coefficient = -0.8576
Level of significance, p = p < 0.001
Standard deviation of $|E_{p(c,2)} - E_{p(c,2)/2}|$ from regression = 3.95×10^{-3} V
Degrees of freedom = 14

3) $|E_{p(c,3)} - E_{p(c,3)/2}| = 0.101 \sqrt{I} - 3.27 \times 10^{-2}$
Correlation coefficient = 0.9839
Level of significance, p = p < 0.001
Standard deviation of $|E_{p(c,3)} - E_{p(c,3)/2}|$ from regression = 4.66×10^{-3} V
Degrees of freedom = 7

4) $|E_{p(a,1)} - E_{p(a,1)/2}| = 2.82 \times 10^{-2} + 5.41 \times 10^{-2} \sqrt{I}$
Correlation coefficient = 0.8055
Level of significance, p = p < 0.001
Standard deviation of $|E_{p(a,1)} - E_{p(a,1)/2}|$ from regression = 1.10×10^{-2} V
Degrees of freedom = 18

5) $|E_{p(a,2)} - E_{p(a,2)/2}| = 3.94 \times 10^{-2} - 1.46 \times 10^{-2} \sqrt{I}$
Correlation coefficient = -0.2050
Level of significance, p = p > 0.10
Standard deviation of $|E_{p(a,2)} - E_{p(a,2)/2}|$ from regression = 1.19×10^{-2} V
Degrees of freedom = 13

$|E_{p(a,2)} - E_{p(a,2)/2}|$ grand mean = 3.11×10^{-2} V ± 1.17×10^{-2} V
Coefficient of variation = 37.6%
Degrees of freedom = 14

6) $|E_{p(a,3)} - E_{p(a,3)/2}| = 6.75 \times 10^{-2} - 4.44 \times 10^{-2} \sqrt{I}$
Correlation coefficient = -0.7334
Level of significance, p = p < 0.001
Standard deviation of $|E_{p(a,3)} - E_{p(a,3)/2}|$ from regression = 1.14×10^{-2} V
Degrees of freedom = 22

7) $|E_{p(a,4)} - E_{p(a,4)/2}| = 2.89 \times 10^{-2} - 2.40 \times 10^{-3} \sqrt{I}$
Correlation coefficient = -0.1471
Level of significance, p = p > 0.10
Standard deviation of $|E_{p(a,4)} - E_{p(a,4)/2}|$ from regression = 3.96×10^{-3} V
Degrees of freedom = 15

$|E_{p(a,4)} - E_{p(a,4)/2}|$ grand mean = 2.69×10^{-2} V ± 3.88×10^{-3} V
Coefficient of variation = 14.4%
Degrees of freedom = 16

5-1.7 Ir(IV) phosphate system

D.c. and linear sweep voltammograms for Ir(IV) phosphate (5.2×10^{-4} mol dm^{-3}), in phosphoric acid (0.32 M) - perchloric acid (0.1 M) supporting electrolyte, obtained at the boron carbide solid electrode are presented in Fig. 5-285. As can be seen, the d.c. wave shows poor reversibility for the charge transfer; αn and $E_{\frac{1}{2}}$ values are given in Table 5-9.

Quantitative treatment of the linear sweep voltammograms reveals that Peaks 1 and 2 were both influenced by catalytic reactions (Fig. 5-286 c.f. Fig. 3-6). The cathodic peak potentials are plotted as functions of sweep rate in Fig. 5-287, and show that $E_{p(c,1)}$ remained relatively constant whereas $E_{p(c,2)}$ was shifted cathodically. The $|E_p - E_{p/2}|$ values, as functions of sweep rate, are plotted in Fig. 5-288 and indicate the decreasing reversibility for the charge transfer of Peak 2.

The evidence suggests that Peak 1 was a catalytic wave which was not exhibited at faster sweep rates whereas Peak 2 was a charge transfer of poor reversibility which was complicated by a catalytic reaction.

5-2 Iron

5-2.1 Fe(III)-Fe(II) perchlorate system

D.c. and cyclic voltammograms for the ferric perchlorate (1.0×10^{-3} mol dm^{-3})/perchloric acid (0.1 M) supporting electrolyte system, obtained at the boron carbide solid electrode $B_{3.86}C$, are presented in Fig. 5-289.

5-2.1.(i) Effect of electrode composition on voltammetric properties.

Although the residual current increased with increase in carbon content of the working electrode (boron carbide, boron carbide/carbon composite, and graphite solid electrodes), the reversible one-electron charge transfer for the electrochemical reduction of ferric perchlorate was not influenced by the B:C ratio of the working electrode (Figures 5-290 and 5-291). Thus αn grand mean = 1.01 ± 0.05 (31 degrees of freedom), and $E_{\frac{1}{2}}$ grand mean = 0.466 V (vs SCE) ± 0.005 V (32 degrees of

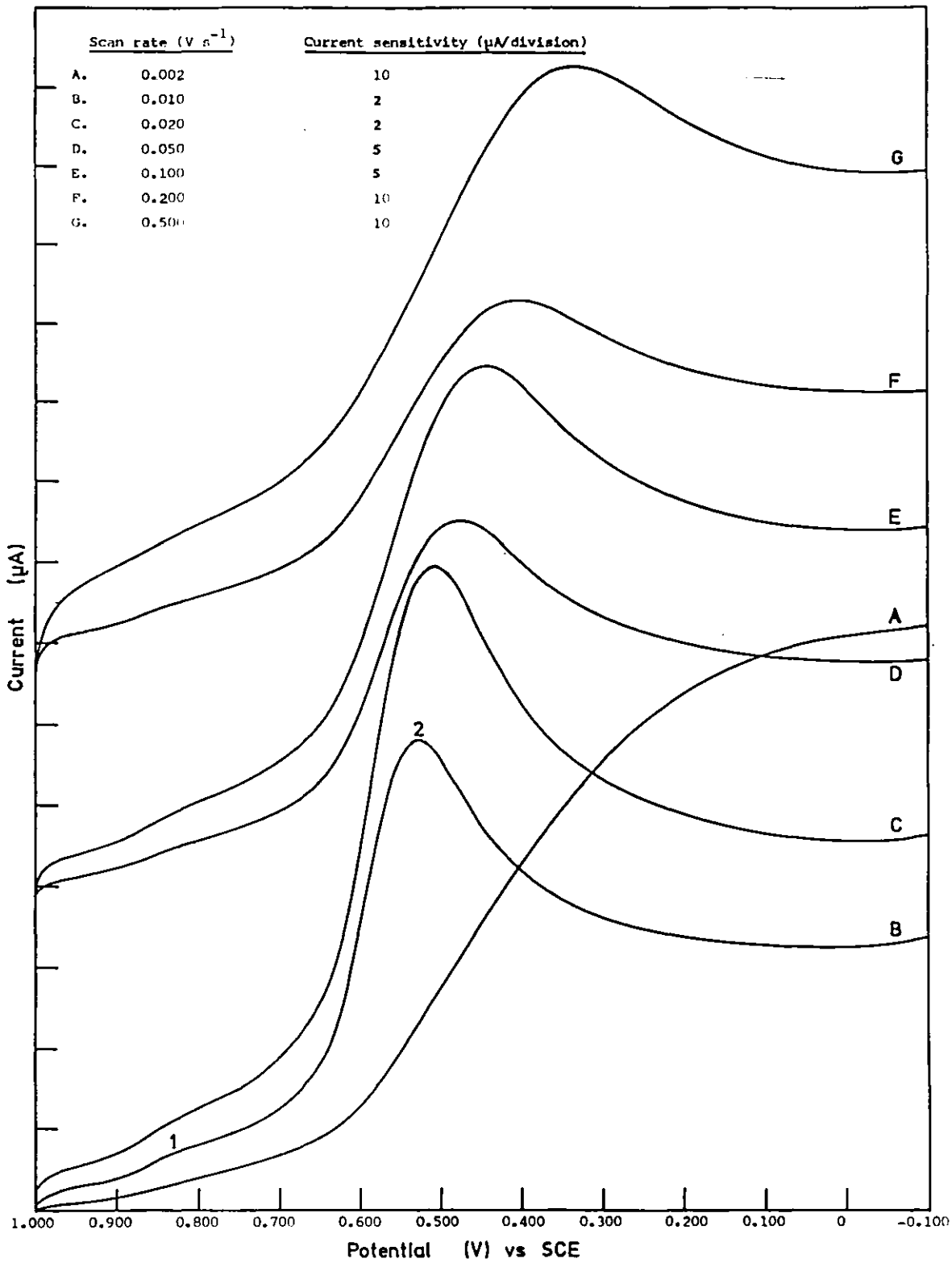

Fig. 5-285 Ir(IV) phosphate (5.2×10^{-4} mol dm^{-3})/Phosphoric acid (0.32 M) - Perchloric acid (0.1 M) supporting electrolyte System: A. D.c. voltammogram; B-G. Linear sweep voltammograms obtained at the boron carbide solid electrode.

Table 5-9 Ir(IV) Phosphate/Phosphoric acid-Perchloric acid supporting electrolyte System: D. C. Voltammetry at the Boron Carbide Solid Electrode.

Electroactive species = Ir(IV) Phosphate (5.2×10^{-4} mol dm^{-3})
Supporting electrolyte = H_3PO_4 (0.32 M)/$HClO_4$ (0.1 M)

	αn	$E_{\frac{1}{2}}$ (V)	i_L/A [Ir(IV) Phosphate] (10^4 μA cm^{-2} dm^3 mol^{-1}).
Mean value	0.25	0.427	18.8
Standard deviation	6.14×10^{-3}	3.78×10^{-2}	0.535
Coefficient of variation	2.41%	8.86%	2.84%
Degrees of freedom	3	3	3

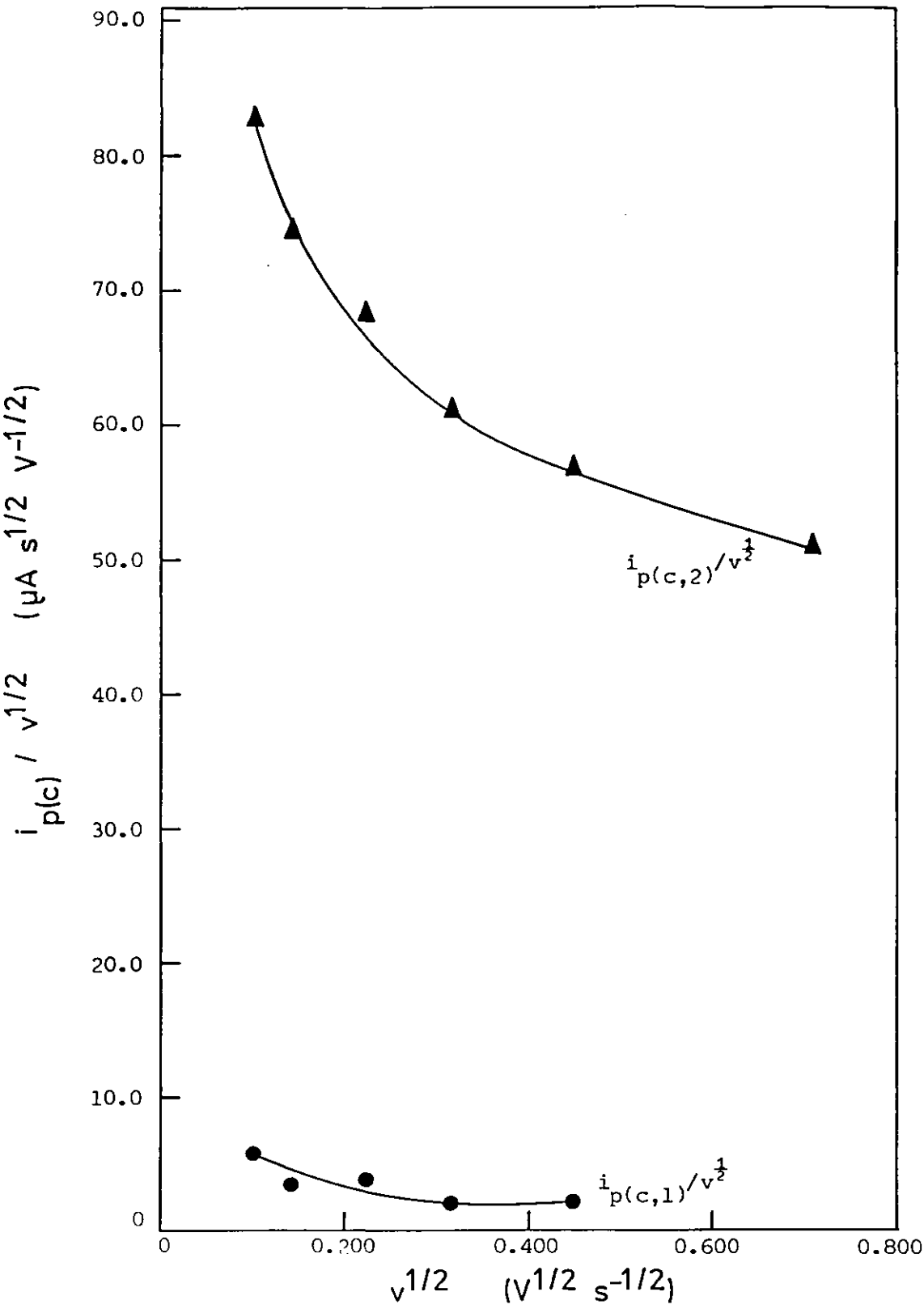

Fig. 5-286 Ir(IV) phosphate (5.2×10^{-4} mol dm^{-3})/Phosphoric acid (0.32 M) - Perchloric acid (0.1 M) supporting electrolyte System: Values of peak current function, $i_{p(c)}/v^{\frac{1}{2}}$, as a function of square root of potential sweep rate, $v^{\frac{1}{2}}$. Boron carbide solid electrode.

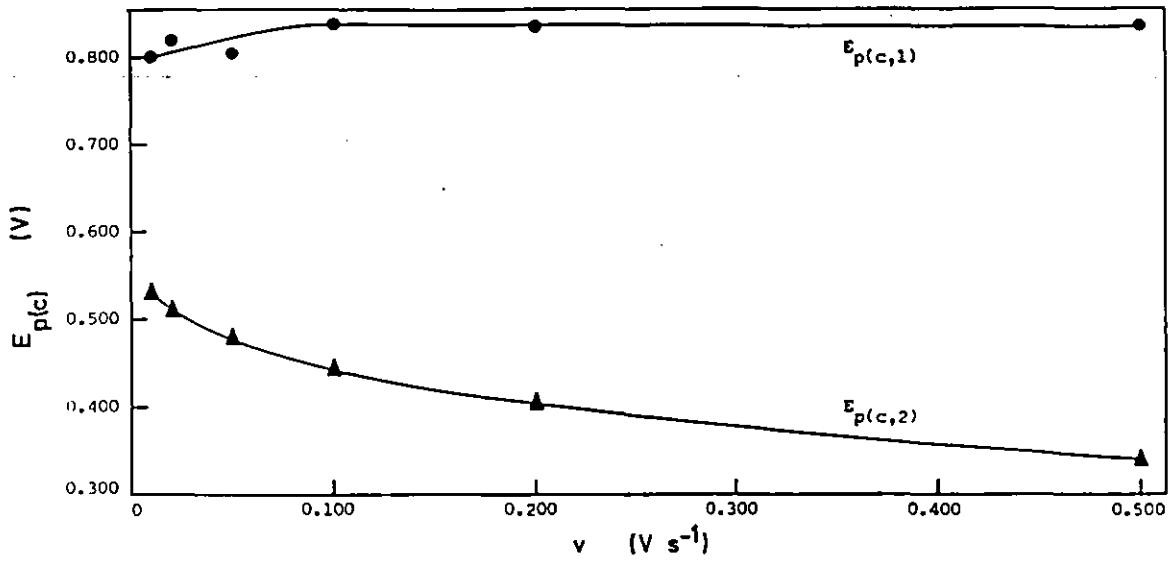

Fig. 5-287 Ir(IV) phosphate (5.2×10^{-4} mol dm^{-3})/Phosphoric acid (0.32 M) - Perchloric acid (0.1 M) supporting electrolyte System: Values of cathodic peak potential, $E_{p(c)}$, as a function of potential sweep rate, v. Boron carbide solid electrode.

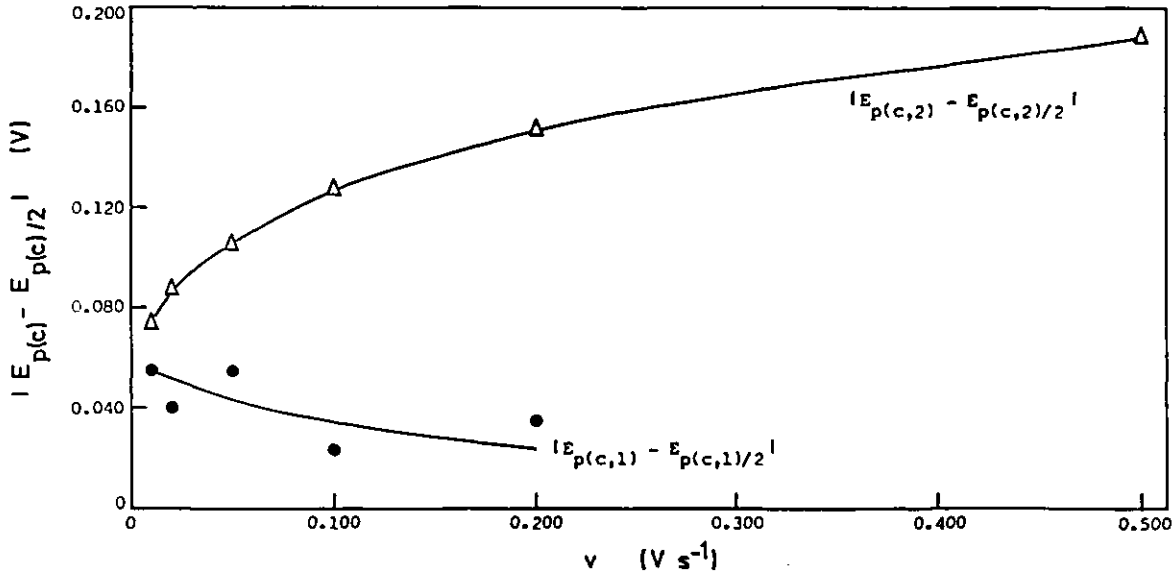

Fig. 5-288 Ir(IV) phosphate (5.2×10^{-4} mol dm^{-3})/Phosphoric acid (0.32 M) - Perchloric acid (0.1 M) supporting electrolyte System: Values of the absolute difference between peak and half-peak potential, $|E_{p(c)} - E_{p(c)/2}|$, as a function of potential sweep rate, v. Boron carbide solid electrode.

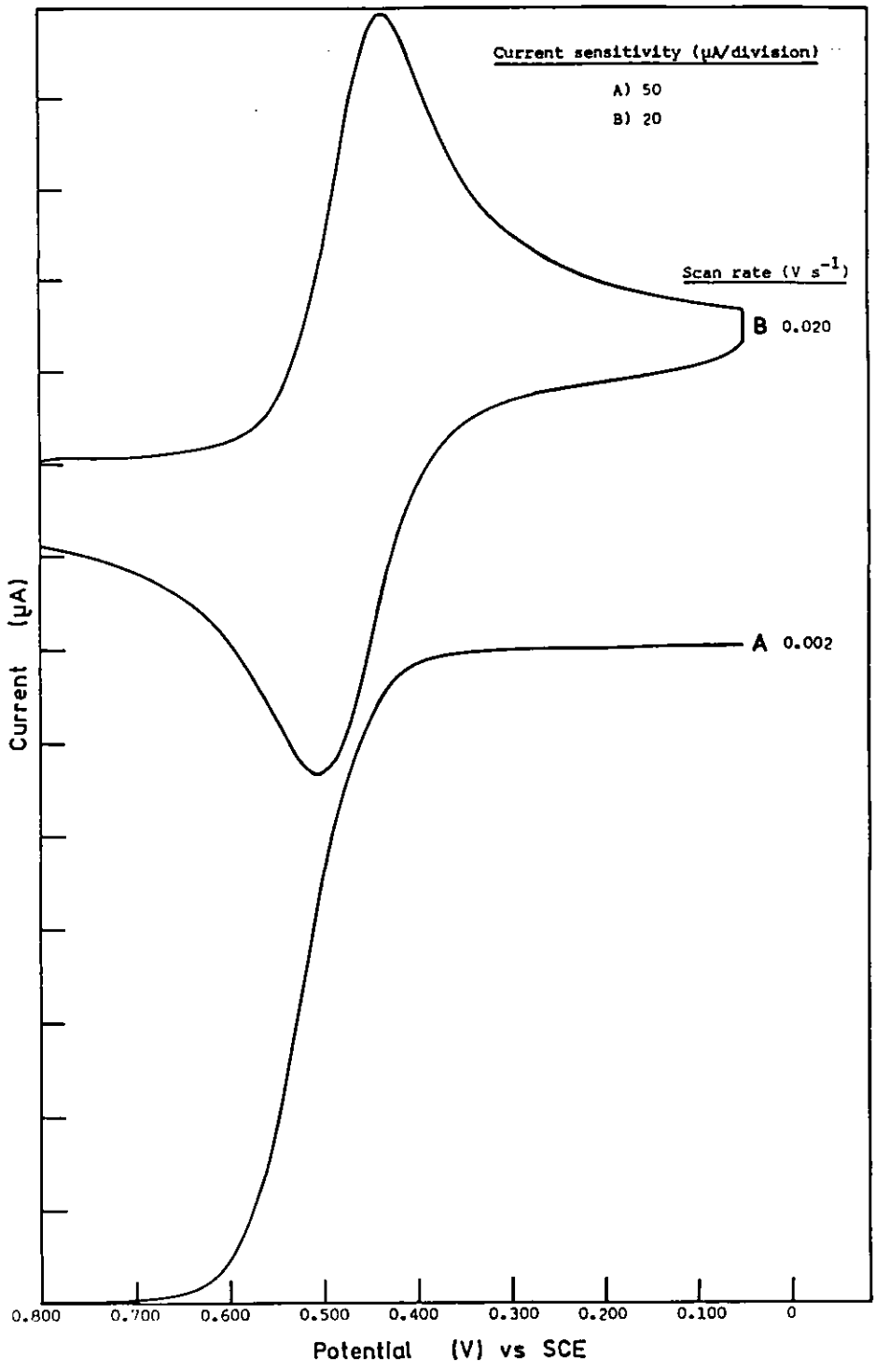

Fig. 5-289 Fe(III) perchlorate (1.0×10^{-3} mol dm^{-3})/Perchloric acid (0.1 M) supporting electrolyte System: (A) d.c. voltammogram, and (B) cyclic voltammogram obtained at the boron carbide solid electrode $B_{3.86}C$.

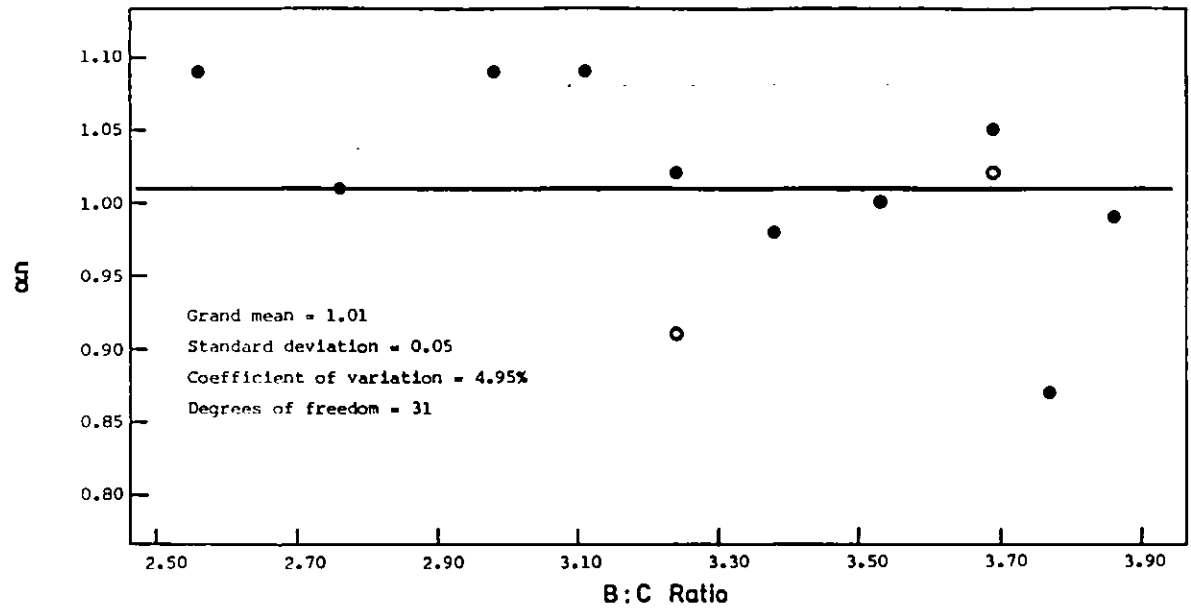

Fig. 5-290 Fe(III) Perchlorate (1.0×10^{-4} mol dm^{-3})/Perchloric acid (0.1 M) supporting electrolyte System: Value of αn as a function of boron to carbon ratio, B:C, of boron carbide/carbon composite solid electrodes. (O): Graphite, instead of the usual lampblack, was used to prepare the required B:C ratio.

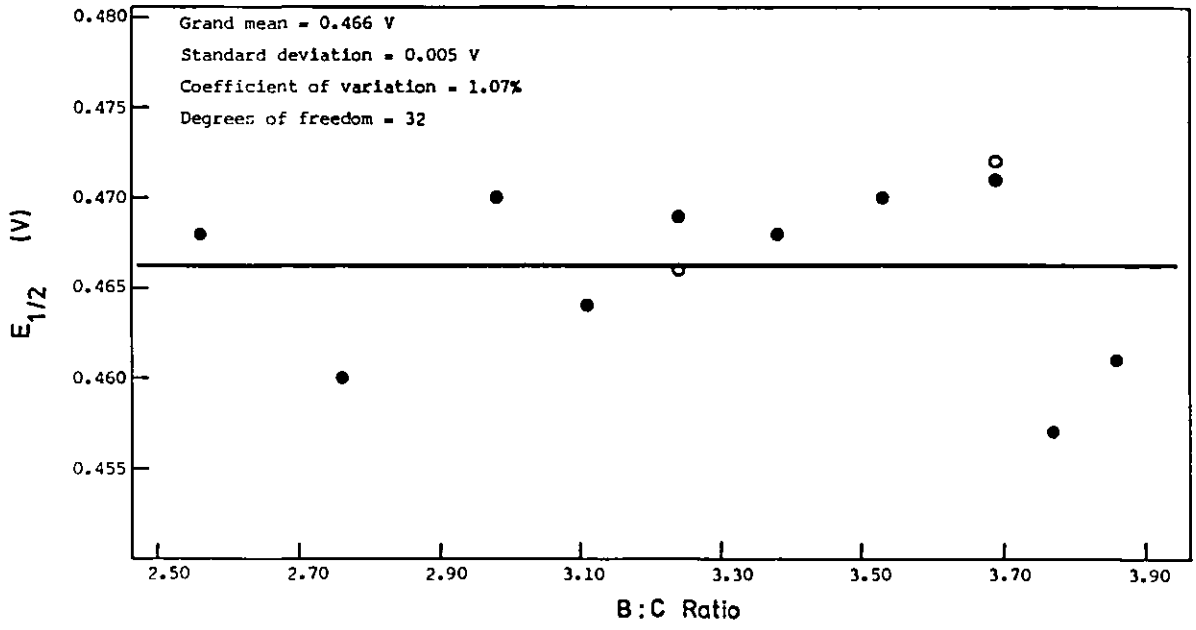

Fig. 5-291 Fe(III) Perchlorate (1.0×10^{-4} mol dm^{-3})/Perchloric acid (0.1 M) supporting electrolyte System: Value of half-wave potential, $E_{\frac{1}{2}}$, as a function of boron to carbon ratio, B:C, of boron carbide/carbon composite solid electrodes. (O): Graphite, instead of the usual lampblack, was used to prepare the required B:C ratio.

Figures 5-290 and 5-291 (continued):-

Fe(III) Perchlorate (1.0×10^{-4} mol dm^{-3})/Perchloric acid (0.1 M) supporting electrolyte System: Graphite solid electrode.

(i) Limiting current plateau as in voltammetric scan:

αn mean = 1.36

Standard deviation = 0.08

Coefficient of variation = 5.50%

Degrees of freedom = 3

$E_{\frac{1}{2}}$ mean = 0.486 V

Standard deviation = 0.002 V

Coefficient of variation = 0.486%

Degrees of freedom = 3

(ii) Limiting current plateau was constructed from the voltammetrically scanned plateau but was drawn parallel to the base line and through the Limiting Background Potential:

αn mean = 1.04

Standard deviation = 0.02

Coefficient of variation = 1.71%

Degrees of freedom = 3

$E_{\frac{1}{2}}$ mean = 0.469 V

Standard deviation = 0.001 V

Coefficient of variation = 0.142%

Degrees of freedom = 3

freedom). The limiting current function, $i_L/A\ [Fe(ClO_4)_3]$, when plotted as a function of B:C ratio shows that the sensitivity of the working electrode with respect to ferric perchlorate was higher for the electrode compositions between approximately $B_{3.20}C$ and $B_{3.70}C$ (Fig. 5-292).

Further investigations of the Fe(III)-Fe(II) perchlorate system were done with boron carbide solid electrodes because the residual currents were lower. It was found that αn and $E_{\frac{1}{2}}$ values were relatively unaffected by the concentration of ferric perchlorate electroactive species (Figures 5-293 and 5-294). Thus, for Fe(III) perchlorate (1.0×10^{-5} to 1.0×10^{-3} mol dm^{-3}) in perchloric acid (0.1 M) supporting electrolyte, αn grand mean = 0.98 ± 0.04 (86 degrees of freedom) and $E_{\frac{1}{2}}$ grand mean = 0.462 V (vs SCE) ± 0.003 V (85 degrees of freedom). The limiting current density was linearly dependent on the concentration of ferric perchlorate to a level of significance better than 0.001 (Fig. 5-295).

The effect of perchloric acid supporting electrolyte on the charge transfer was also investigated. Thus, for Fe(III) perchlorate (1.0×10^{-4} mol dm^{-3}) in perchloric acid (0.1 to 1.0 M) supporting electrolyte, it was found that αn values remained constant prior to declining as the concentration of perchloric acid exceeded approximately 0.8 M (Fig. 5-296). Similarly, the $E_{\frac{1}{2}}$ values remained constant until $(\text{ionic strength})^{\frac{1}{2}}$ exceeded approximately 0.8; when $E_{\frac{1}{2}}$ was cathodically shifted by further increases in ionic strength (Fig. 5-297). Despite these deviations over the concentration range of perchloric acid studied, the grand mean values were: αn = 0.98 ± 0.03 (17 degrees of freedom), and $E_{\frac{1}{2}}$ = 0.450 V (vs SCE) ± 0.005 V (18 degrees of freedom). The limiting current, however, declined with increasing concentration of perchloric acid supporting electrolyte (Fig. 5-298).

Cyclic voltammetry of Fe(III) perchlorate (1.0×10^{-4} mol dm^{-3}), in perchloric acid (0.1 M) supporting electrolyte, revealed that the charge transfer was complicated by the weak adsorption of reactant (Fig. 5-299). Furthermore, the anodic peak current function also indicated that at slow sweep rates a chemical reaction preceding the anodic charge transfer was able to proceed (Fig. 5-299 c.f. Fig. 3-6). At faster sweep rates, however, the electrochemical re-oxidation of Fe(II) perchlorate was able to occur before the chemical reaction could proceed; and the adsorption effect became dominant. The chemical reaction probably involved the conversion of Fe(II) to Fe(III) species by molecular oxygen in acid solution. The peak potentials are plotted as functions

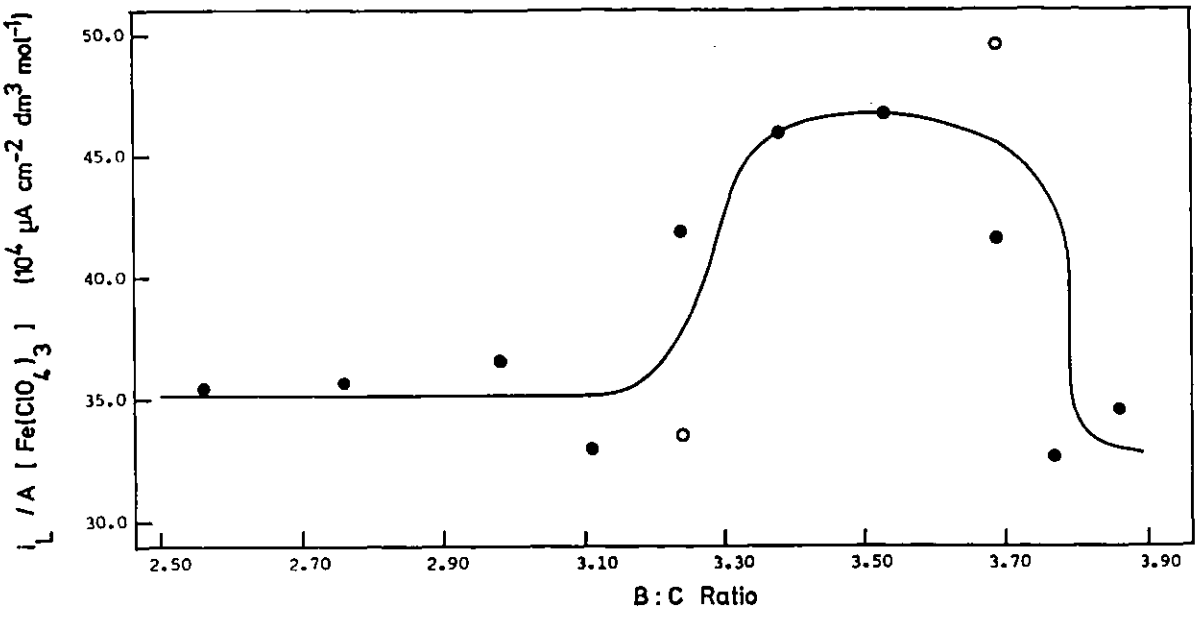

Fig. 5-292 Fe(III) Perchlorate (1.0×10^{-4} mol dm^{-3})/Perchloric acid (0.1 M) supporting electrolyte System: Values of limiting current per unit area divided by concentration of ferric perchlorate, i_L/A [$Fe(ClO_4)_3$], as a function of boron to carbon ratio, B:C, of boron carbide/carbon composite solid electrodes.
(O): Graphite, instead of the usual lampblack, was used to prepare the required B:C ratio.

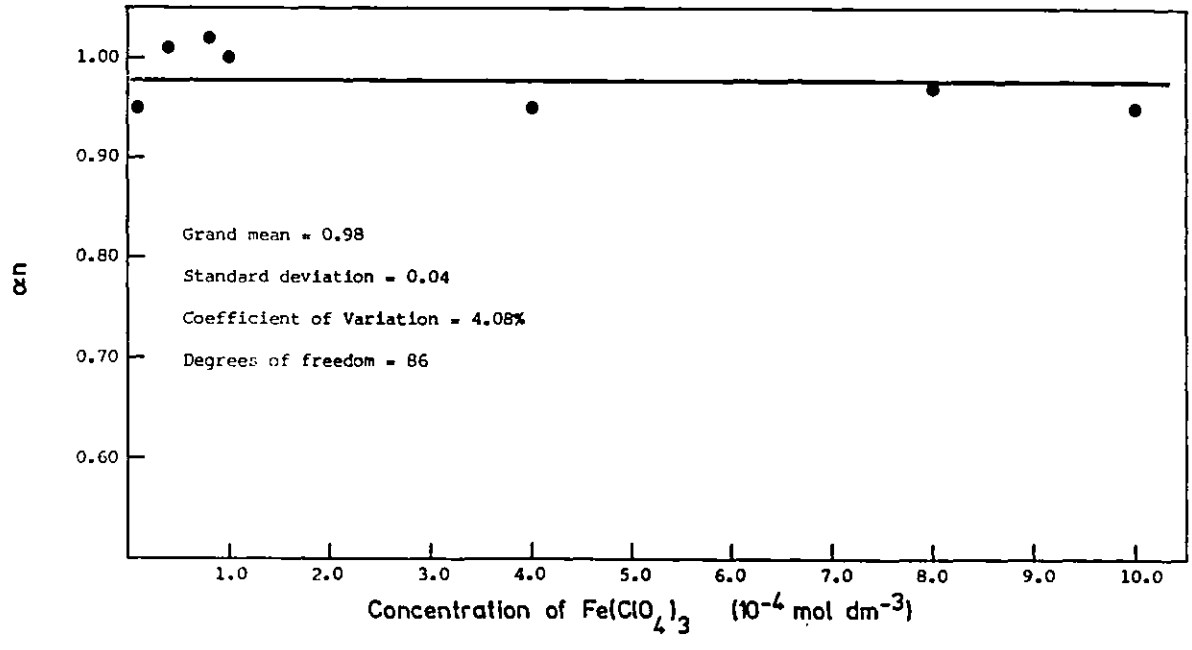

Fig. 5-293 Fe(III) Perchlorate/Perchloric acid (0.1 M) supporting electrolyte System: Values of αn as a function of concentration of ferric perchlorate, [$Fe(ClO_4)_3$]. Boron carbide solid electrode $B_{4.05}C$.

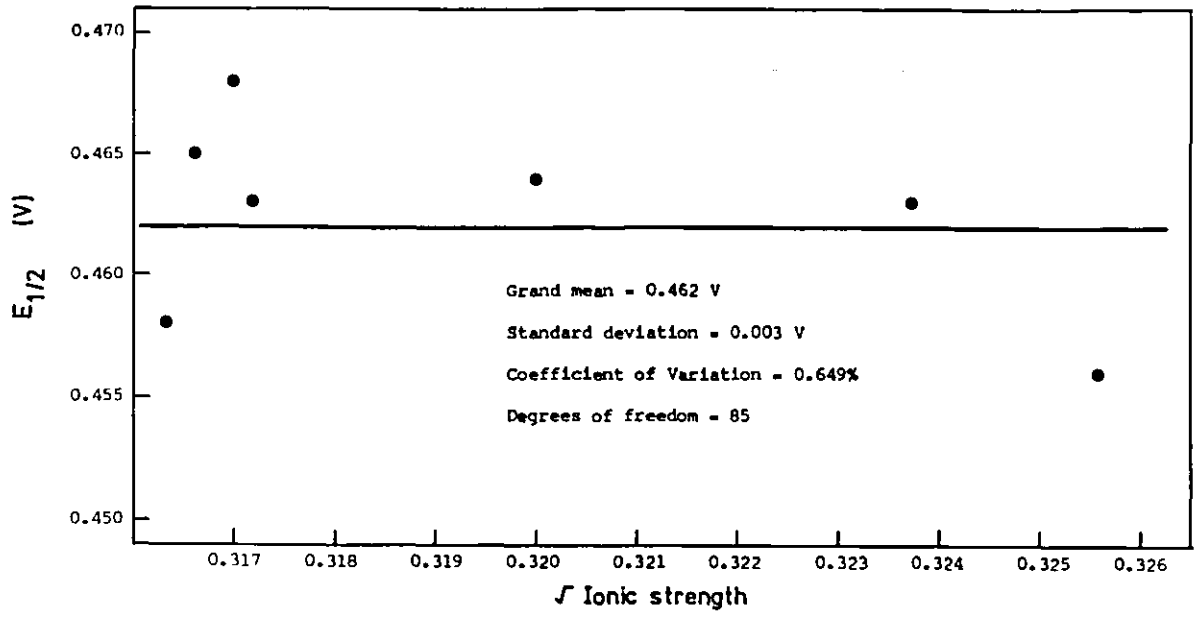

Fig. 5-294 Fe(III) Perchlorate (1.0×10^{-5} to 1.0×10^{-3} mol dm^{-3})/Perchloric acid (0.1M) supporting electrolyte System: Values of half-wave potential, $E_{\frac{1}{2}}$, as a function of square root of total ionic strength (where the concentration of ferric perchlorate was varied), $\sqrt{I}$. Boron carbide solid electrode $B_{4.05}C$.

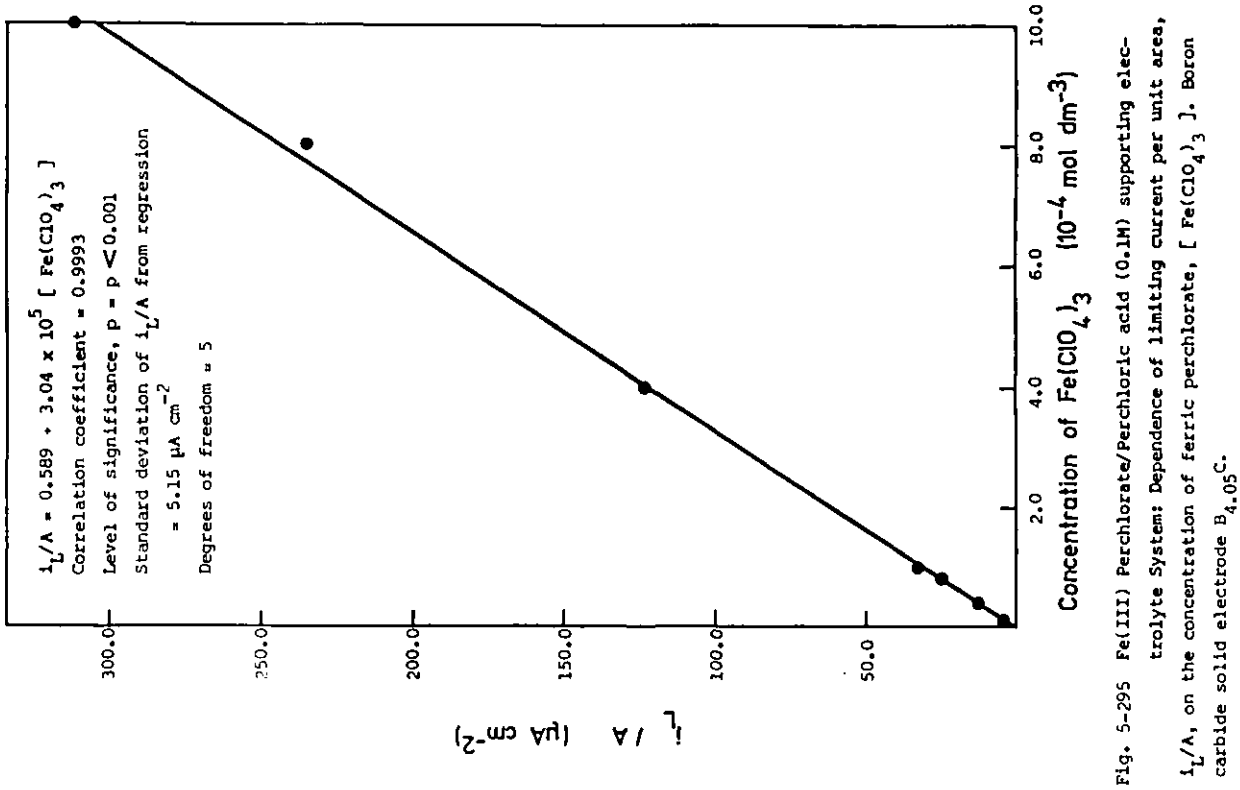

Fig. 5-295 Fe(III) Perchlorate/Perchloric acid (0.1M) supporting electrolyte System: Dependence of limiting current per unit area, i_L/A, on the concentration of ferric perchlorate, [$Fe(ClO_4)_3$]. Boron carbide solid electrode $B_{4.05}C$.

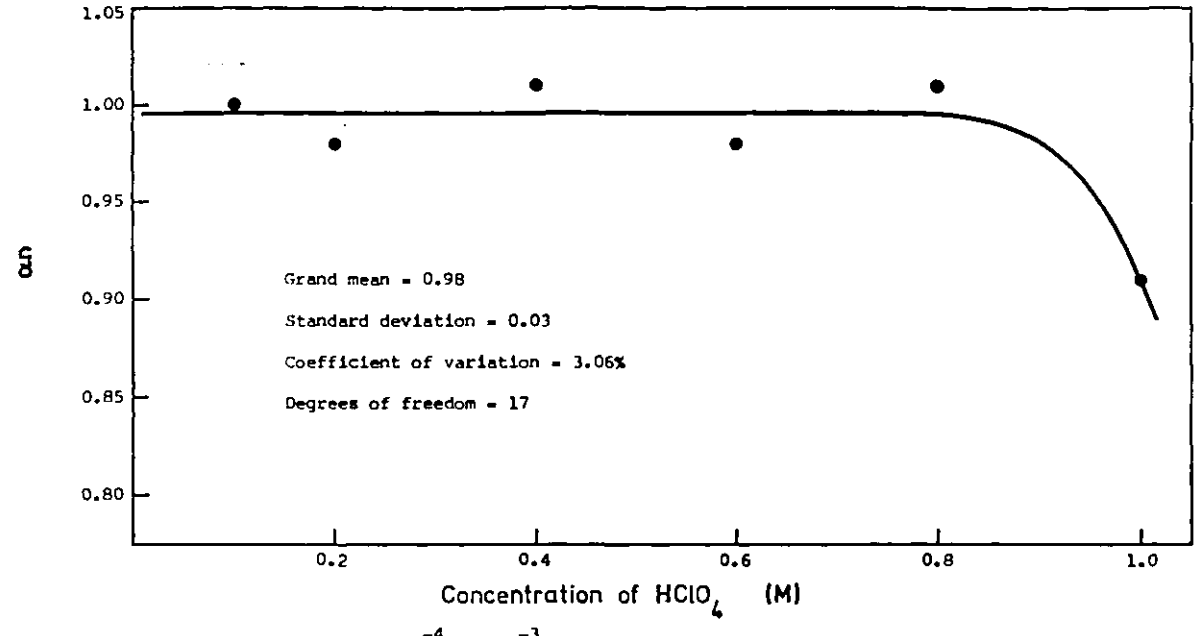

Fig. 5-296 Fe(III) Perchlorate (1.0×10^{-4} mol dm^{-3})/Perchloric acid supporting electrolyte System: Values of αn as a function of concentration of perchloric acid supporting electrolyte, [$HClO_4$]. Boron carbide solid electrode $B_{4.05}C$.

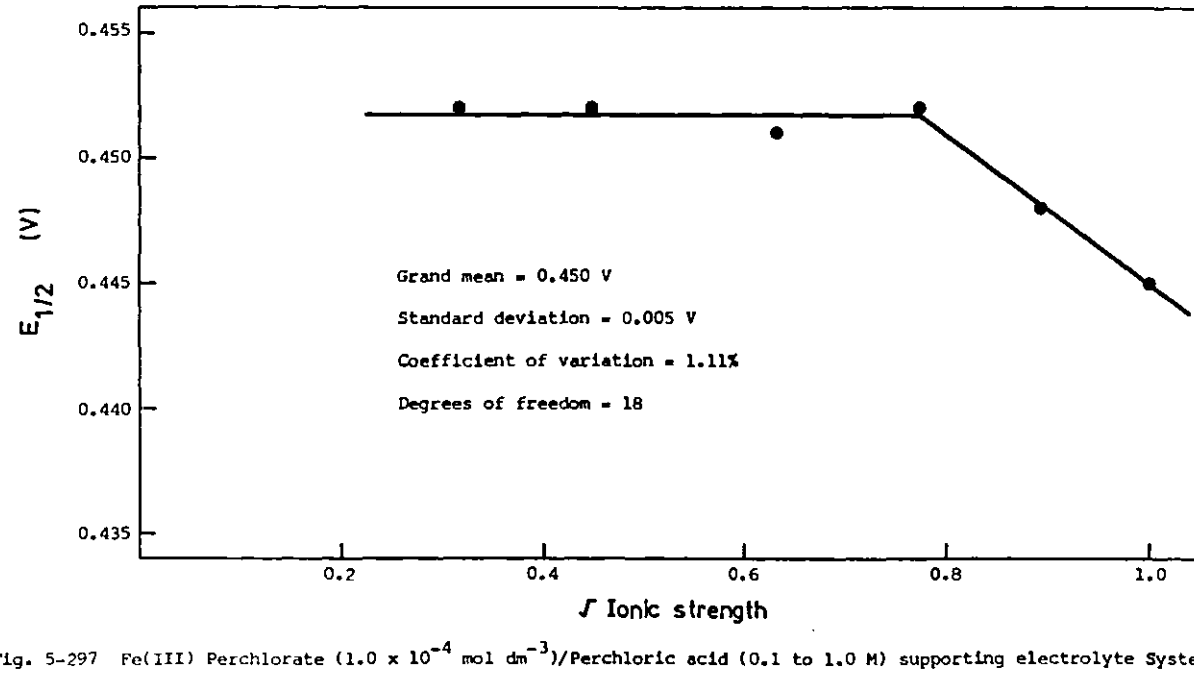

Fig. 5-297 Fe(III) Perchlorate (1.0×10^{-4} mol dm^{-3})/Perchloric acid (0.1 to 1.0 M) supporting electrolyte System: Values of half-wave potential, $E_{\frac{1}{2}}$, as a function of square root of total ionic strength (where the concentration of perchloric acid supporting electrolyte was varied), $\sqrt{I}$. Boron carbide solid electrode $B_{4.05}C$.

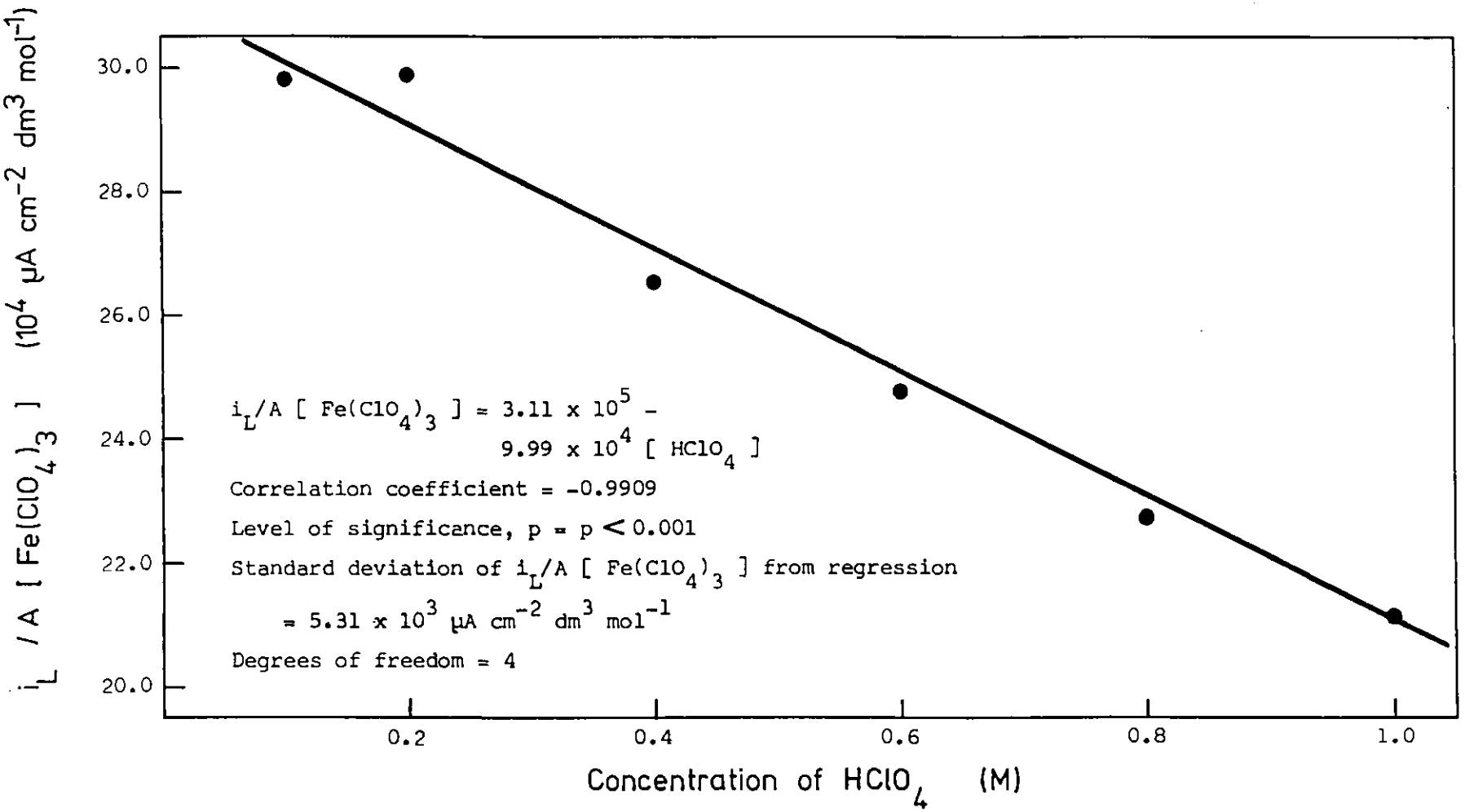

Fig. 5-298 Fe(III) Perchlorate (1.0 x 10^{-4} mol dm^{-3})/Perchloric acid supporting electrolyte System: Values of limiting current per unit area divided by concentration of ferric perchlorate, i_L/A [$Fe(ClO_4)_3$], as a function of concentration of perchloric acid supporting electrolyte, [$HClO_4$]. Boron carbide solid electrode $B_{4.05}C$.

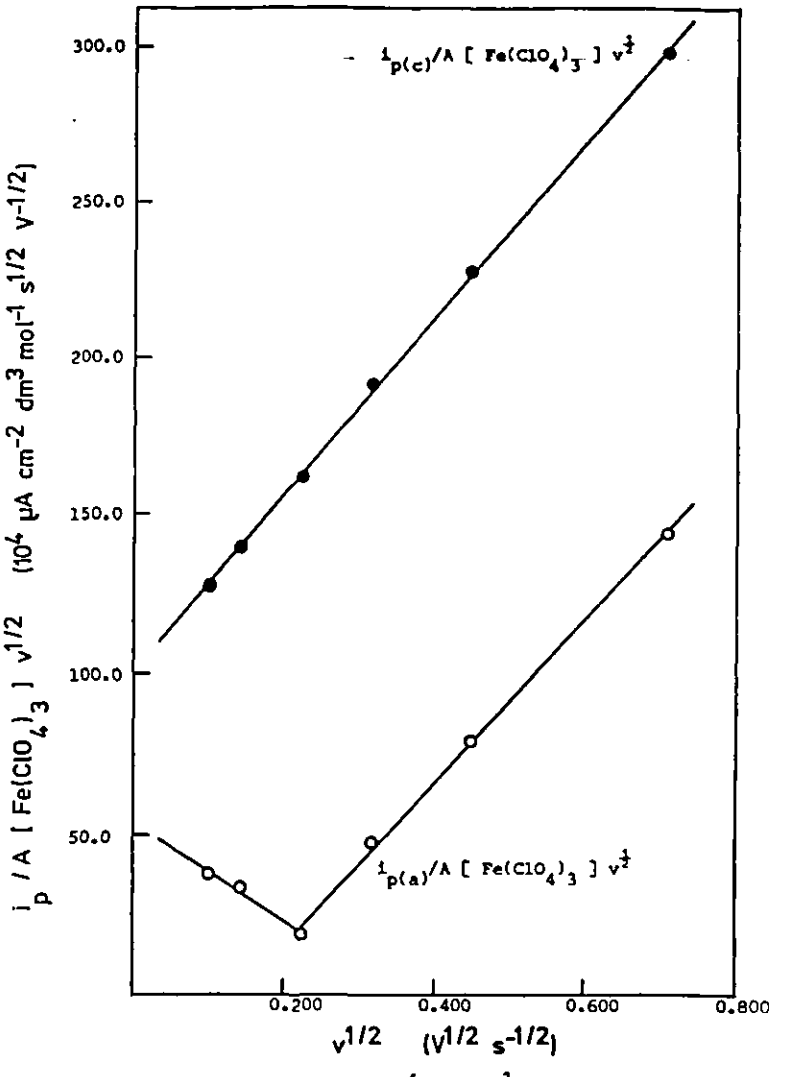

Fig. 5-299 Fe(III) Perchlorate (1.0×10^{-4} mol dm^{-3})/Perchloric acid (0.1 M) supporting electrolyte System: Values of cathodic and anodic current functions, $i_{p(c)}/A\ [\ Fe(ClO_4)_3\ ]\ v^{\frac{1}{2}}$ and $i_{p(a)}/A\ [\ Fe(ClO_4)_3\ ]\ v^{\frac{1}{2}}$ respectively, as functions of the square root of potential scan rate, $v^{\frac{1}{2}}$. Boron carbide solid electrode $B_{4.04}C$.

(a) $i_{p(c)}/A\ [\ Fe(ClO_4)_3\ ]\ v^{\frac{1}{2}} = 9.99 \times 10^5 + 2.82 \times 10^6\ v^{\frac{1}{2}}$

Correlation coefficient = 0.9998

Level of significance, p = $p < 0.001$

Standard deviation of $i_{p(c)}/A\ [\ Fe(ClO_4)_3\ ]\ v^{\frac{1}{2}}$ from regression

$= 1.55 \times 10^4$ μA cm^{-2} dm^3 mol^{-1} s$^{\frac{1}{2}}$ v$^{-\frac{1}{2}}$

Degrees of freedom = 4

(b) For the increasing trend line:

$i_{p(a)}/A\ [\ Fe(ClO_4)_3\ ]\ v^{\frac{1}{2}} = 2.55 \times 10^6\ v^{\frac{1}{2}} - 3.56 \times 10^5$

Correlation coefficient = 0.99920

Level of significance, p = $p < 0.001$

Standard deviation of $i_{p(a)}/A\ [\ Fe(ClO_4)_3\ ]\ v^{\frac{1}{2}}$ from regression

$= 2.62 \times 10^4$ μA cm^{-2} dm^3 mol^{-1} s$^{\frac{1}{2}}$ v$^{-\frac{1}{2}}$

Degrees of freedom = 2

of sweep rate in Fig. 5-300, and the corresponding $|E_p - E_{p/2}|$ and $|E_{p(c)} - E_{p(a)}|$ values are plotted in Fig. 5-301. It can be seen that $E_{p(c)}$ was cathodically shifted by increasing sweep rate whilst $|E_{p(c)} - E_{p(c)/2}|$ remained constant; thus confirming the weak adsorption of Fe(III) perchlorate reactant. $E_{p(a)}$ was also shifted cathodically by increasing sweep rate, but to a greater degree, and when coupled with the behaviour of the $|E_{p(a)} - E_{p(a)/2}|$ and $|E_{p(c)} - E_{p(a)}|$ values the evidence supports the hypothesis that the anodic charge transfer was complicated by a preceding chemical reaction and weak adsorption.

Linear sweep voltammetry of Fe(III) perchlorate (1.0×10^{-3} mol dm^{-3}), in perchloric acid (0.1 M) supporting electrolyte, revealed that the influence of the weak adsorption of ferric perchlorate reactant was still dominant at this higher concentration of e.a.s. (Fig. 5-302). $E_{p(c)}$ was shifted to less anodic values by increasing sweep rate (Fig. 5-303), but this was partly caused by the deterioration in the reversibility of the charge transfer; as evidenced by the widening in $|E_{p(c)} - E_{p(c)/2}|$ values (Fig. 5-304).

5-2.1.(ii) Effect of Ir(IV) perchlorate treatment on the working electrode.

The influence of Ir(IV) perchlorate treatment on the working boron carbide solid electrode was investigated by use of Fe(III) perchlorate (1.0×10^{-4} mol dm^{-3}) in perchloric acid (0.1 M) supporting electrolyte. In general, higher concentrations of Ir(IV) perchlorate treatment solution resulted in the working electrode giving voltammograms of lower αn values and less anodic $E_{\frac{1}{2}}$ values for Fe(III) perchlorate (Figures 5-305 and 5-306 respectively). The grand mean values, however, are $\alpha n = 0.94 \pm 0.03$ (23 degrees of freedom) and $E_{\frac{1}{2}} = 0.466$ V (vs SCE) $\pm$ 0.003 (24 degrees of freedom). When these values were compared with those obtained at the untreated working electrode (Figures 5-293 and 5-294) by use of the t-test, the following results were obtained: (a) For αn values, t = 5.06 (109 degrees of freedom); (b) For $E_{\frac{1}{2}}$ values, t = 6.50 (109 degrees of freedom). The literature values[5.1] for t, however, are: $t_{0.001} = 3.46$ (double-sided, 60 degrees of freedom), and $t_{0.001} = 3.373$ (double-sided, 120 degrees of freedom). Therefore, since the calculated t-values exceeded the literature t-values for the 0.001 level of significance, treatment of the working electrode with Ir(IV) perchlorate affected the αn and $E_{\frac{1}{2}}$ values for Fe(III) perchlorate to a highly significant degree. Fig. 5-307 shows that the

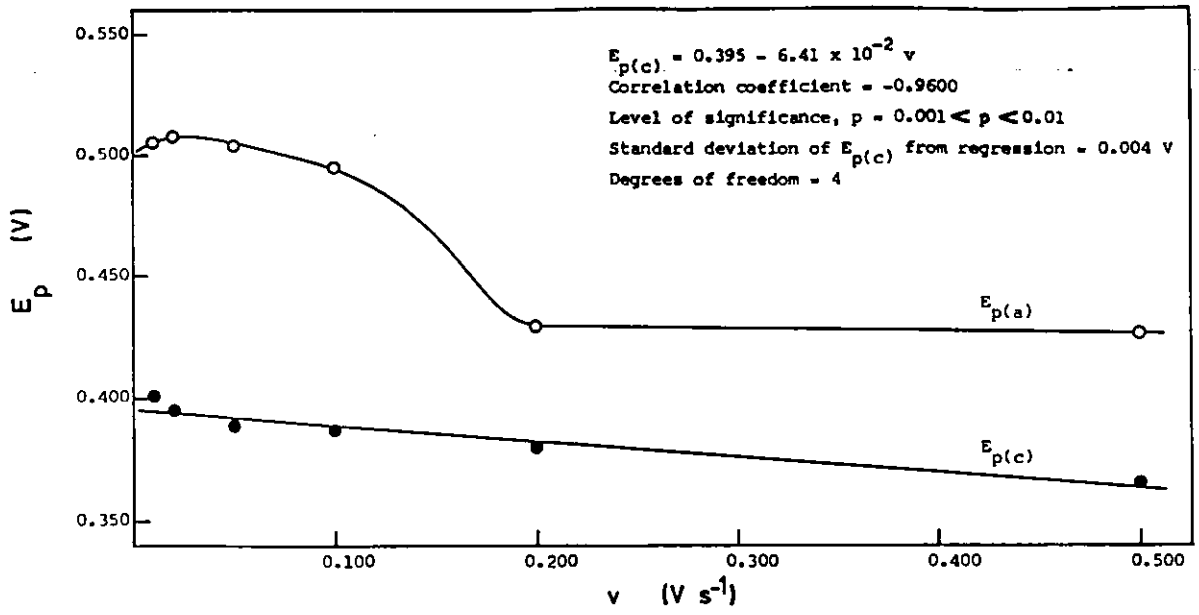

Fig. 5-300 Fe(III) Perchlorate (1.0×10^{-4} mol dm^{-3})/Perchloric acid (0.1 M) supporting electrolyte System: Values of cathodic and anodic peak potentials, $E_{p(c)}$ and $E_{p(a)}$ respectively, as functions of the potential scan rate, v. Boron carbide solid electrode $B_{4.04}C$.

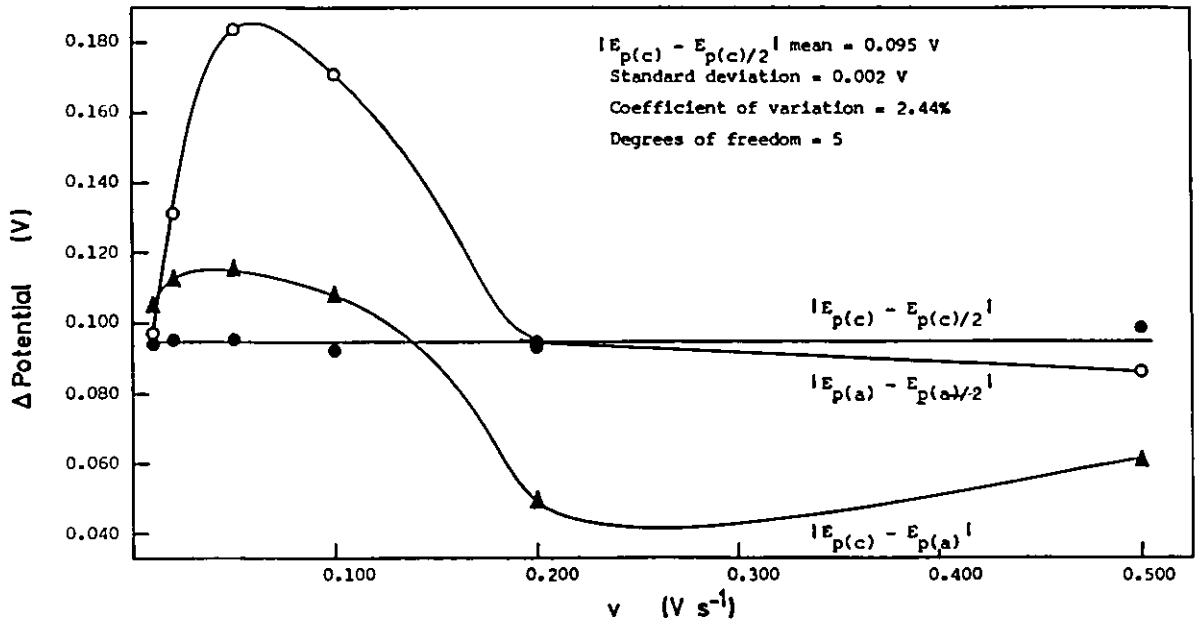

Fig. 5-301 Fe(III) Perchlorate (1.0×10^{-4} mol dm^{-3})/Perchloric acid (0.1 M) supporting electrolyte System: Values of the difference between peak and half-peak potentials for the cathodic and anodic scans, $|E_{p(c)} - E_{p(c)/2}|$ and $|E_{p(a)} - E_{p(a)/2}|$ respectively, and the difference between cathodic and anodic peak potentials, $|E_{p(c)} - E_{p(a)}|$, as functions of the potential scan rate, v. Boron carbide solid electrode $B_{4.04}C$.

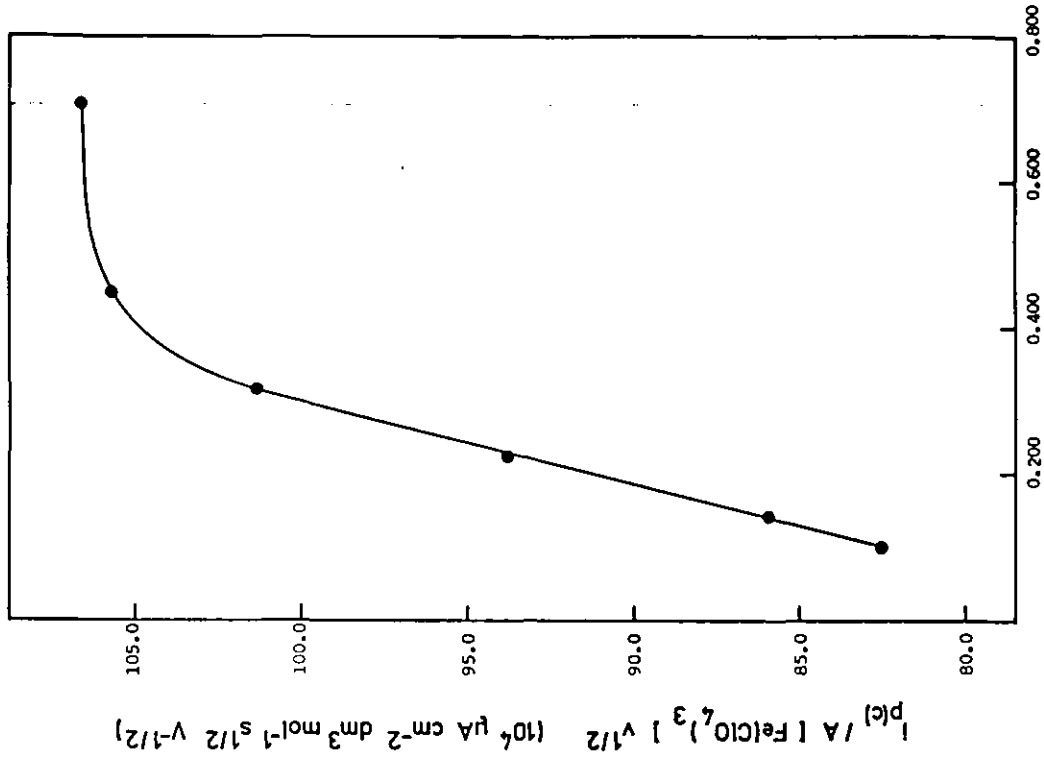

Fig. 5-302 Fe(III) Perchlorate (1.0×10^{-3} mol dm^{-3})/Perchloric acid (0.1M) supporting electrolyte System: Values of cathodic current function, $i_{p(c)}/A\ [\ Fe(ClO_4)_3\ ]\ v^{\frac{1}{2}}$, as a function of square root of potential scan rate, $v^{\frac{1}{2}}$. Boron carbide solid electrode $B_{3.86}C$.

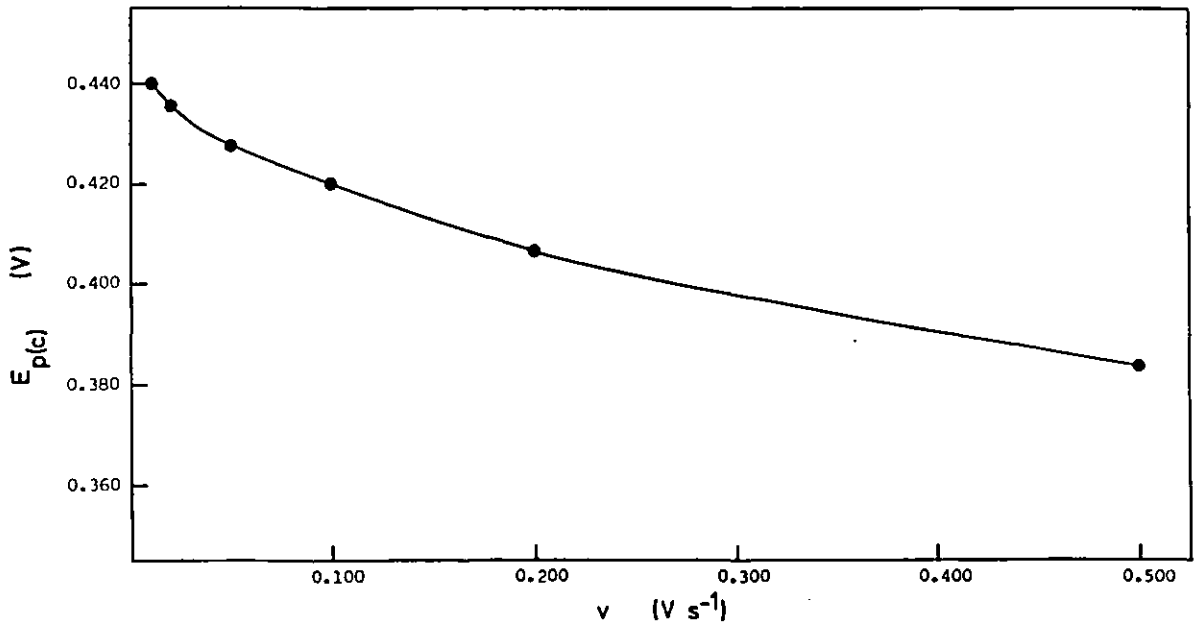

Fig. 5-303 Fe(III) Perchlorate (1.0×10^{-3} mol dm^{-3})/Perchloric acid (0.1 M) supporting electrolyte System: Values of cathodic peak potential, $E_{p(c)}$, as a function of potential scan rate, v. Boron carbide solid electrode $B_{3.86}C$.

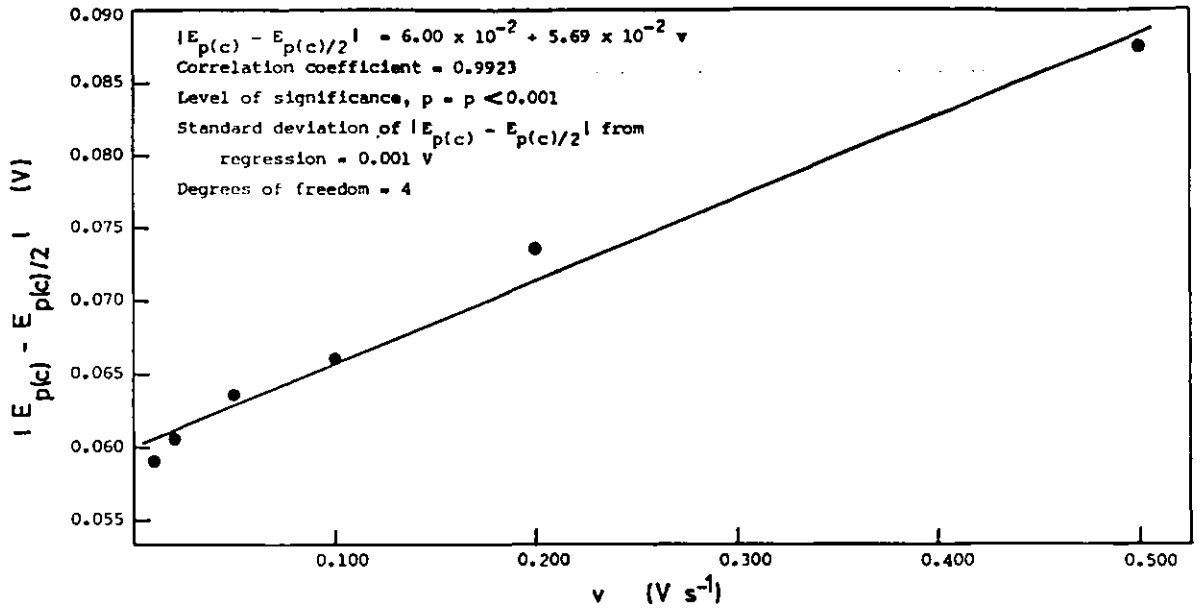

Fig. 5-304 Fe(III) Perchlorate (1.0×10^{-3} mol dm^{-3})/Perchloric acid (0.1 M) supporting electrolyte System: Values of the difference between cathodic peak and half-peak potentials, $|E_{p(c)} - E_{p(c)/2}|$, as a function of potential scan rate, v. Boron carbide solid electrode $B_{3.86}C$.

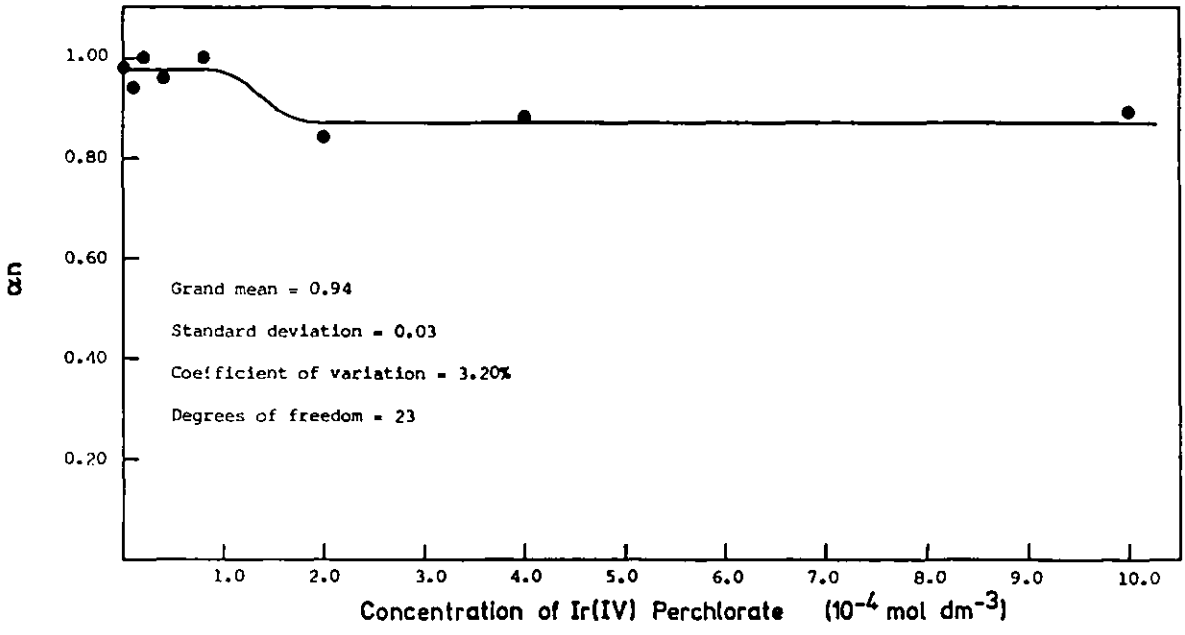

Fig. 5-305 Fe(III) Perchlorate (1.0×10^{-4} mol dm^{-3})/Perchloric acid (0.1 M) supporting electrolyte System: Values of αn as a function of concentration of Ir(IV) Perchlorate treatment solution. Boron carbide solid electrode $B_{4.05}C$.

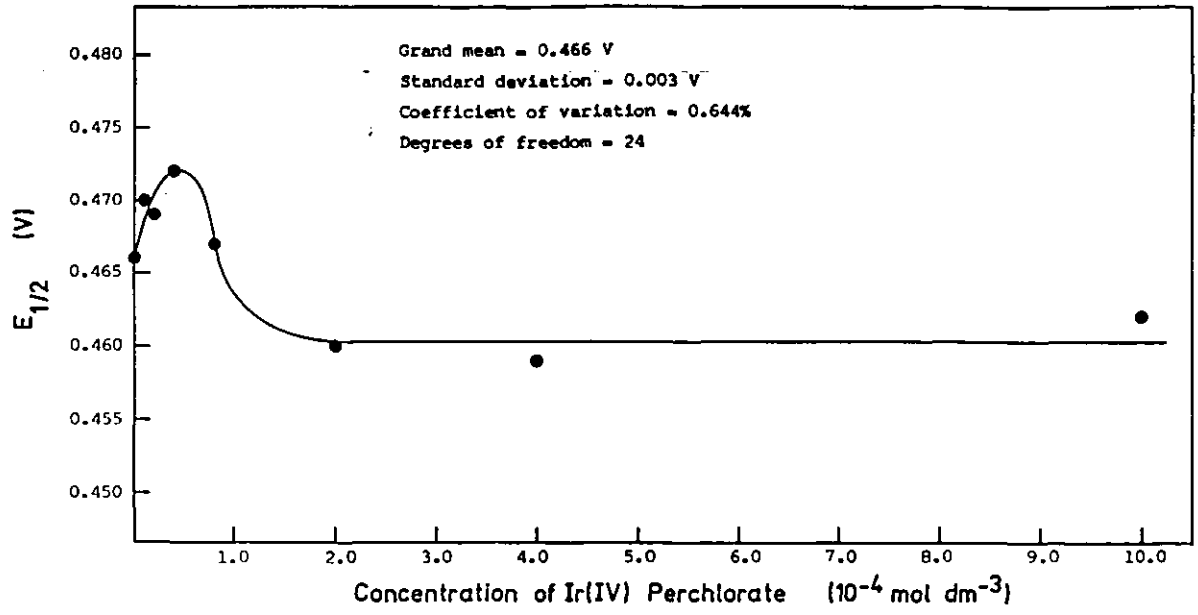

Fig. 5-306 Fe(III) Perchlorate (1.0×10^{-4} mol dm^{-3})/Perchloric acid (0.1 M) supporting electrolyte System: Values of half-wave potential, $E_{\frac{1}{2}}$, as a function of concentration of Ir(IV) Perchlorate treatment solution. Boron carbide solid electrode $B_{4.05}C$.

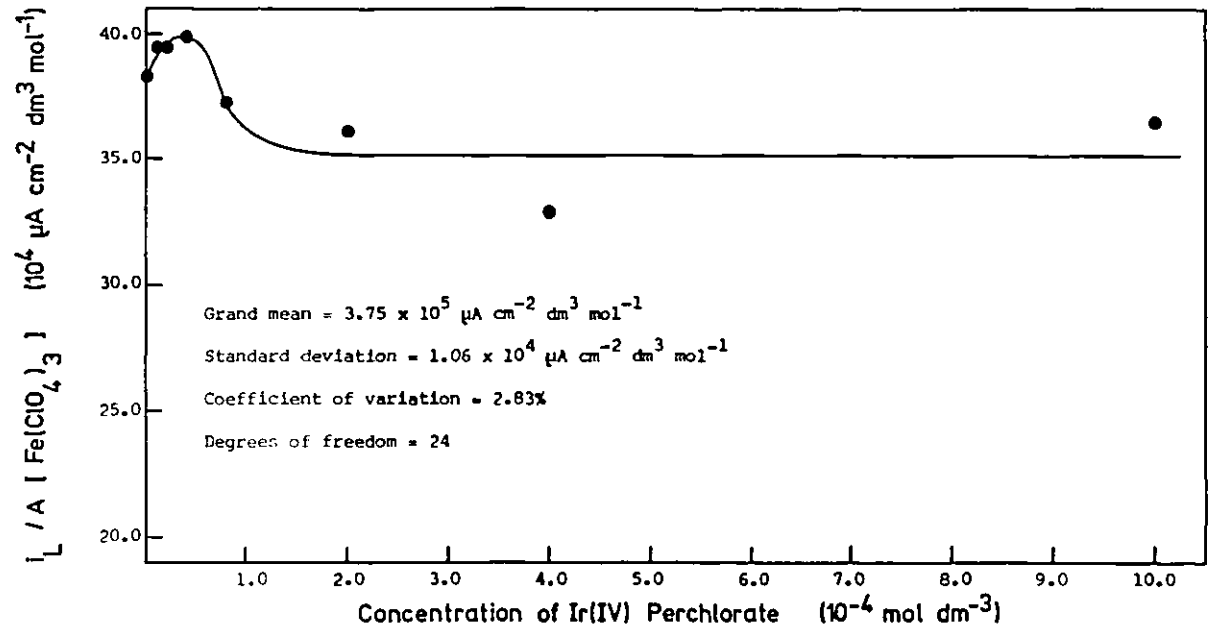

Fig. 5-307 Fe(III) Perchlorate (1.0×10^{-4} mol dm^{-3})/Perchloric acid (0.1 M) supporting electrolyte System: Values of limiting current per unit area divided by concentration of ferric perchlorate, i_L/A [$Fe(ClO_4)_3$], as a function of concentration of Ir(IV) Perchlorate treatment solution. Boron carbide solid electrode $B_{4.05}C$.

sensitivity of the boron carbide solid electrode towards Fe(III) perchlorate was slightly decreased after it had been treated by higher concentrations of Ir(IV) perchlorate.

5-2.1.(iii) Summary.

Under d.c. voltammetric conditions, the charge transfer in the electrochemical reduction of Fe(III) to Fe(II) perchlorate was found to be reversible irrespective of the B:C ratio of the working electrode (boron carbide, boron carbide/carbon composite, or graphite solid electrodes; Fig. 5-290). A linear concentration dependence of the limiting current density was obtained at the boron carbide solid electrode (Fig. 5-295). Increasing concentration of perchloric acid supporting electrolyte, however, depressed the limiting current for ferric perchlorate (Fig. 5-298).

Linear sweep and cyclic voltammetry at the boron carbide solid electrode revealed that the charge transfer was complicated by weak adsorption of Fe(III) reactant as well as a following reversible chemical reaction. Thus the reaction scheme may be represented as:

$$Fe^{3+}_{soln} \rightleftharpoons Fe^{3+}_{ads}$$

$$Fe^{3+} + e^- \rightleftharpoons Fe^{2+}$$

$$2Fe^{2+} + \tfrac{1}{2}O_2 + 2H^+ \rightleftharpoons 2Fe^{3+} + H_2O \quad \text{(i.e. catalytic reaction)}$$

The catalytic reaction might also involve oxidation by perchlorate.

Treatment of the boron carbide solid electrode with Ir(IV) perchlorate affected its d.c. voltammetric performance for Fe(III) perchlorate to a highly significant degree (Figures 5-305 to 5-307 inclusive). As to be expected, the strongly adsorbed Ir(IV) species occupied the adsorption sites and thus weakened the Fe(III) adsorption; hence lower αn and limiting current values.

5-2.2 Fe(III)-Fe(II) chloride system

D.c. and cyclic voltammograms for Fe(III) chloride (2×10^{-3} M), in hydrochloric acid (0.1 M) supporting electrolyte, obtained at the boron carbide solid electrode $B_{4.04}C$ are presented in Fig. 5-308.

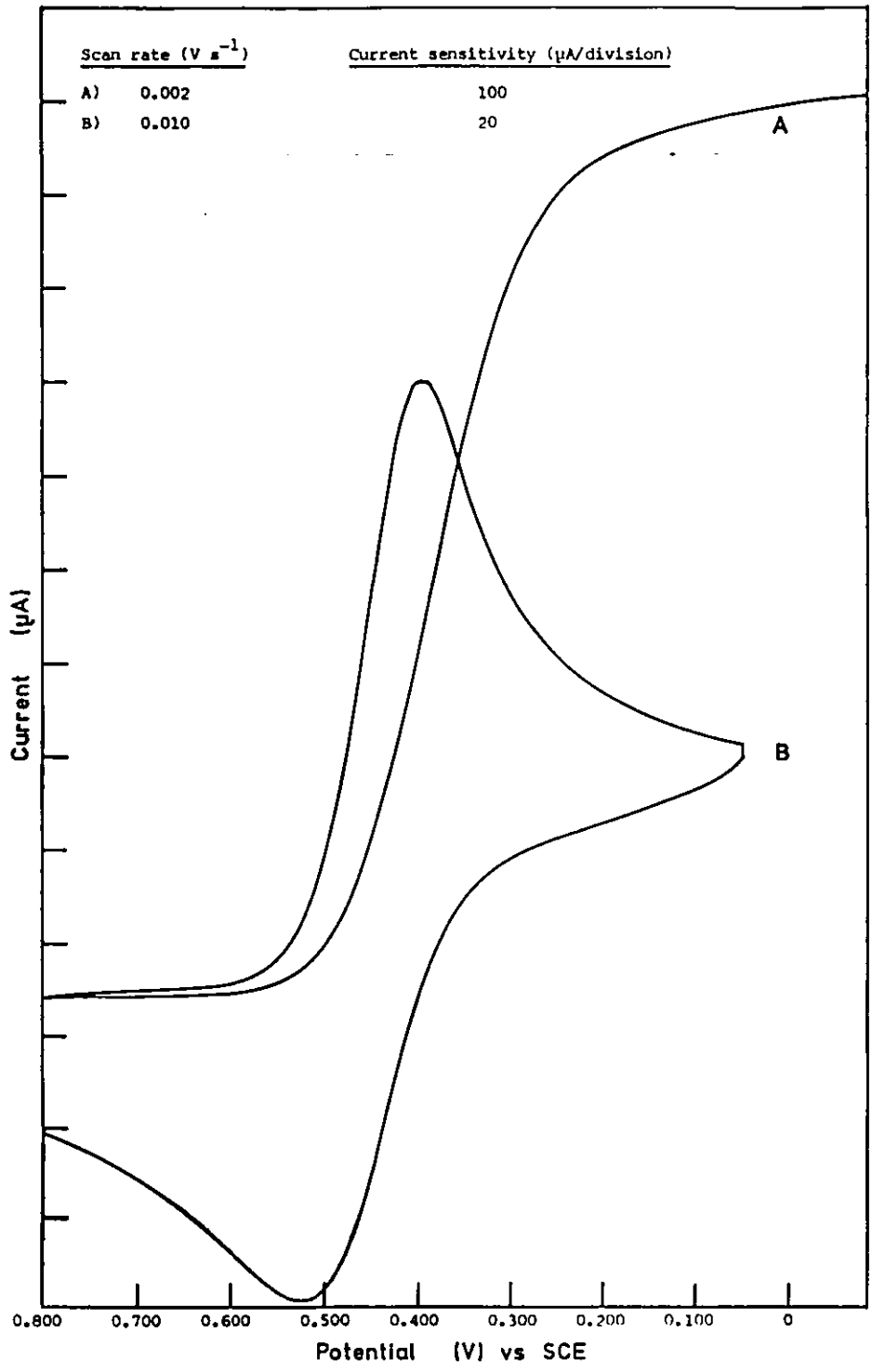

Fig. 5-308 Fe(III) chloride (2 x 10^{-3} M)/Hydrochloric acid (0.1 M) supporting electrolyte System: A) d.c. voltammogram, and B) cyclic voltammogram obtained at the boron carbide solid electrode $B_{4.04}C$.

5-2.2.(i) D.c. voltammetry.

D.c. voltammetry of Fe(III) chloride (4×10^{-5} to 2×10^{-3} M), in hydrochloric acid (0.1 M) supporting electrolyte, revealed that the reversibility of the charge transfer deteriorated with increasing concentration of e.a.s.; as characterised by decreasing αn values (Fig. 5-309) and the cathodic shift in $E_{\frac{1}{2}}$ values (Fig. 5-310). The limiting current density, however, was found to be linearly dependent on the concentration of Fe(III) chloride to a level of significance better than 0.001 (Fig. 5-311).

The influence of hydrochloric acid on the electrochemical reduction of ferric chloride is shown in Figures 5-312 to 5-314 inclusive. In general, αn and limiting current values decreased with increasing concentration of hydrochloric acid supporting electrolyte whilst the corresponding $E_{\frac{1}{2}}$ was cathodically shifted.

5-2.2.(ii) Linear sweep and cyclic voltammetry.

The cathodic current function, as a function of $(\text{sweep rate})^{\frac{1}{2}}$, suggests that the electrochemical reduction was complicated by weak adsorption (Fig. 5-315); but at high concentration of e.a.s. (2×10^{-3} M) the influence of adsorption was negligible and there was a hint of the presence of a following irreversible chemical reaction (Fig. 5-315, f c.f. Fig. 3-6). The anodic current function readily confirmed that the charge transfer was complicated by both weak adsorption and a catalytic reaction (Fig. 5-316). The cathodic and anodic peak potentials were both cathodically shifted by increasing sweep rate (Fig. 5-317) despite the poor reversibility of the charge transfer as indicated by the widening of $|E_p - E_{p/2}|$ values (Fig. 5-318). This suggests that it was the Fe(III) chloride reactant which was weakly adsorbed.

Dependence of the cathodic peak current density on the concentration of ferric chloride was linear (Fig. 5-319) at sweep rates of 0.010 to 0.500 V s^{-1}. The anodic peak current density, however, as a function of ferric chloride concentration became non-linear at the sweep rate of 0.500 V s^{-1} (Fig. 5-320); thus reflecting the diminished influence of adsorption at high concentrations of e.a.s. (ferric chloride). The increasing ferric chloride concentration did not affect the cathodic peak potential very much ($E_{p(c)}$ mean = 0.374 V (vs SCE) ± 0.021 V, 59 degrees of freedom), but the anodic peak potential was anodically shifted (Fig. 5-321). The effect of ferric chloride concentration on

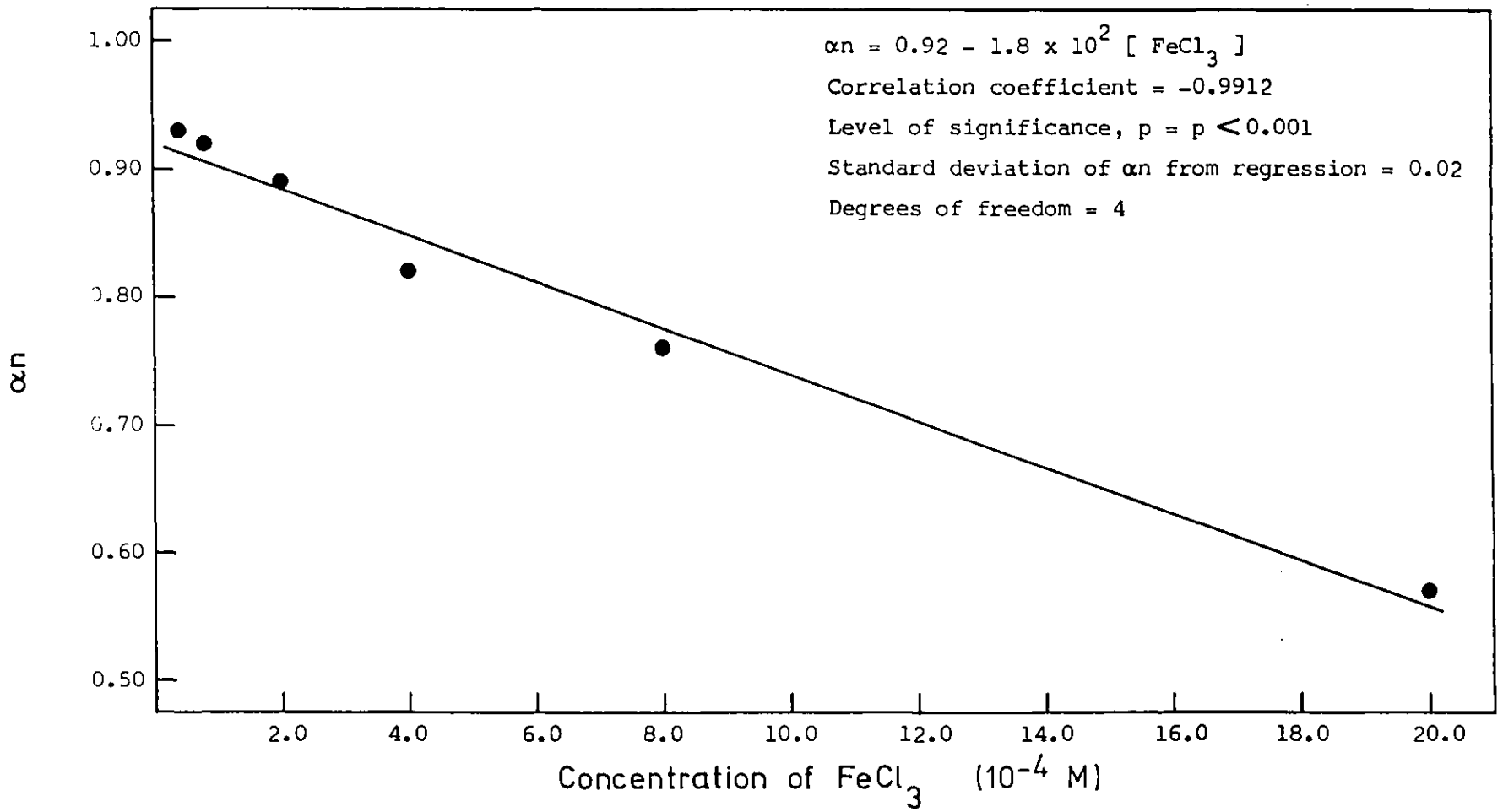

Fig. 5-309 Fe(III) chloride (4×10^{-5} to 2×10^{-3} M)/Hydrochloric acid (0.1 M) supporting electrolyte System: Values of αn as a function of concentration of ferric chloride, [$FeCl_3$]. Boron carbide solid electrode $B_{4.04}C$.

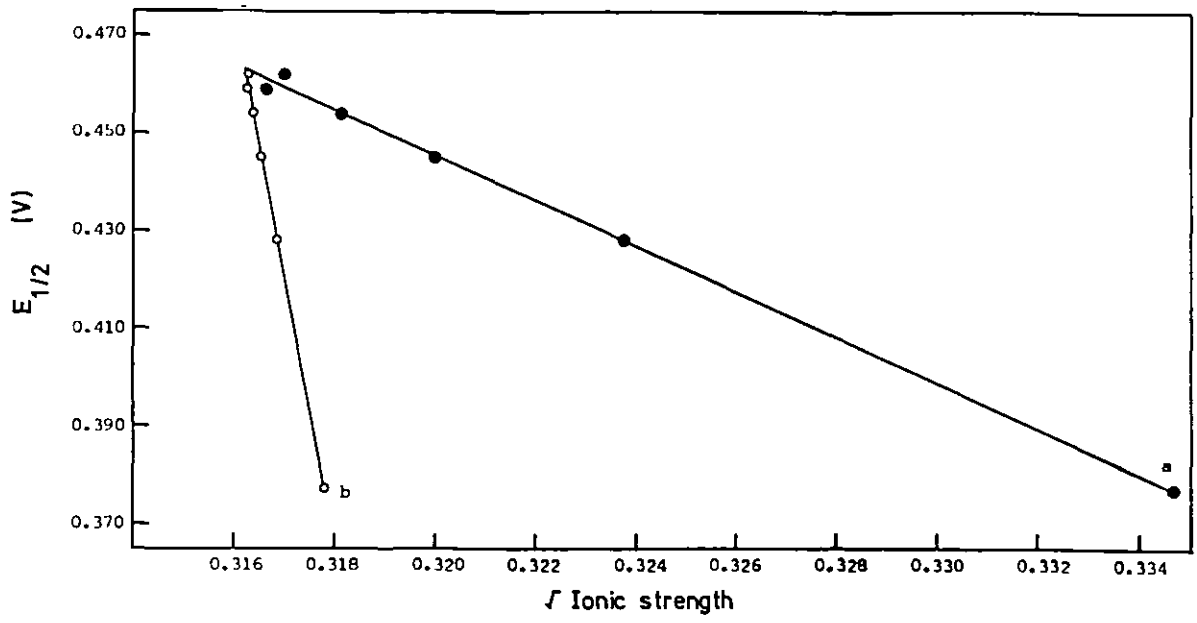

Fig. 5-310 Fe(III) chloride (4×10^{-5} to 2×10^{-3} M)/Hydrochloric acid (0.1 M) supporting electrolyte System: Values of half-wave potential, $E_{\frac{1}{2}}$, as a function of square root of total ionic strength (where the concentration of ferric chloride was varied), $\sqrt{I}$. Boron carbide solid electrode $B_{4.04}C$.

(a) Assuming that the main Fe(III) species was Fe^{3+}:

$E_{\frac{1}{2}} = 1.94 - 4.66\ \sqrt{I}$
Correlation coefficient = -0.9989
Level of significance, p = $p < 0.001$
Standard deviation of $E_{\frac{1}{2}}$ from regression = 0.002 V
Degrees of freedom = 4

(b) Assuming that the main Fe(III) species was $FeCl_4^-$:

$E_{\frac{1}{2}} = 17.7 - 54.4\ \sqrt{I}$
Correlation coefficient = -0.9989
Level of significance, p = $p < 0.001$
Standard deviation of $E_{\frac{1}{2}}$ from regression = 0.002 V
Degrees of freedom = 4

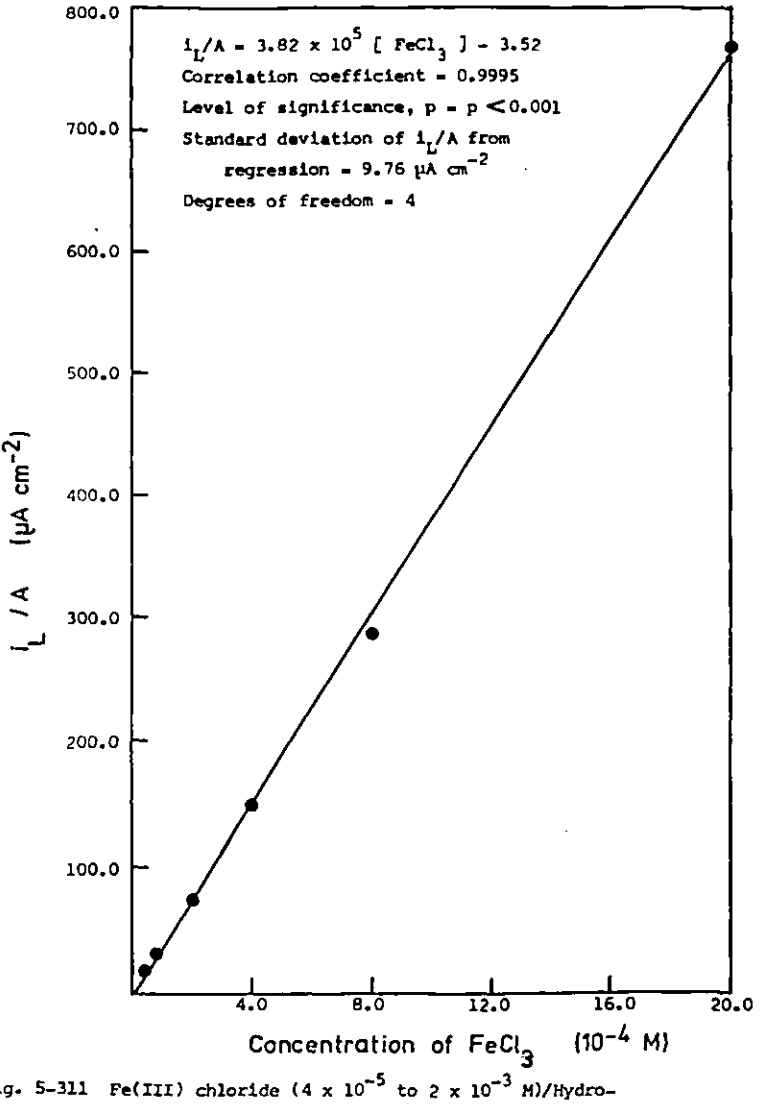

Fig. 5-311 Fe(III) chloride (4×10^{-5} to 2×10^{-3} M)/Hydrochloric acid (0.1 M) supporting electrolyte System: Dependence of limiting current per unit area, i_L/A, on the concentration of ferric chloride, [$FeCl_3$]. Boron carbide solid electrode $B_{4.04}C$.

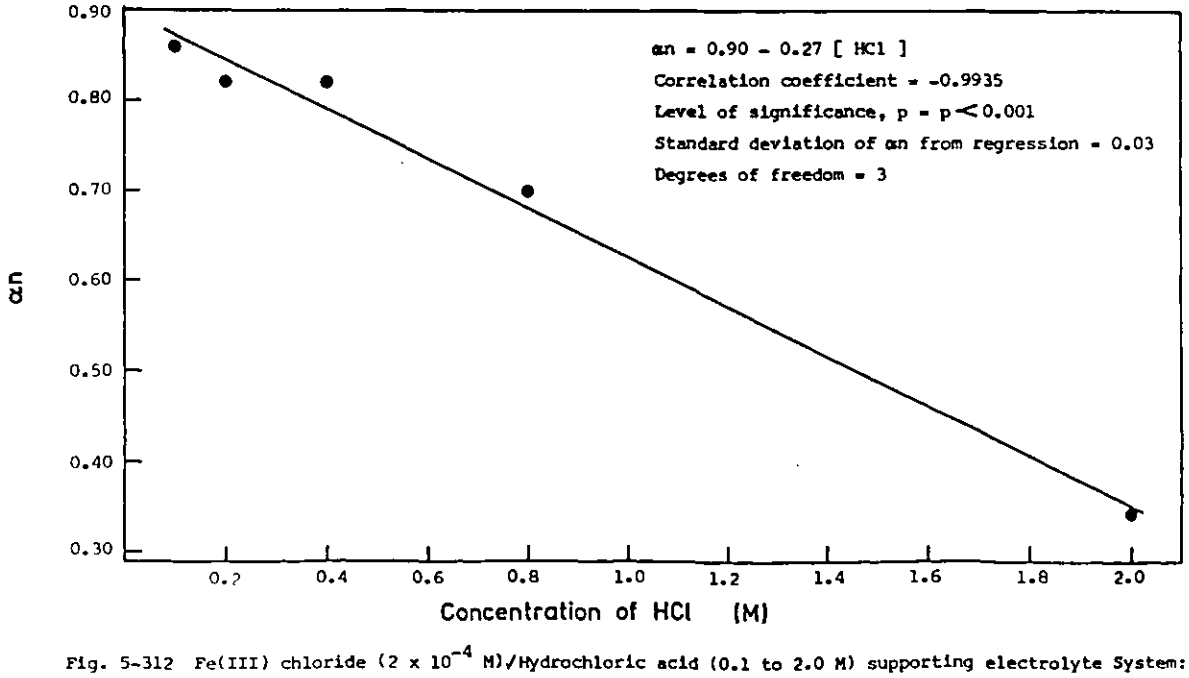

Fig. 5-312 Fe(III) chloride (2×10^{-4} M)/Hydrochloric acid (0.1 to 2.0 M) supporting electrolyte System: Values of αn as a function of concentration of hydrochloric acid supporting electrolyte, [HCl]. Boron carbide solid electrode $B_{4.04}C$.

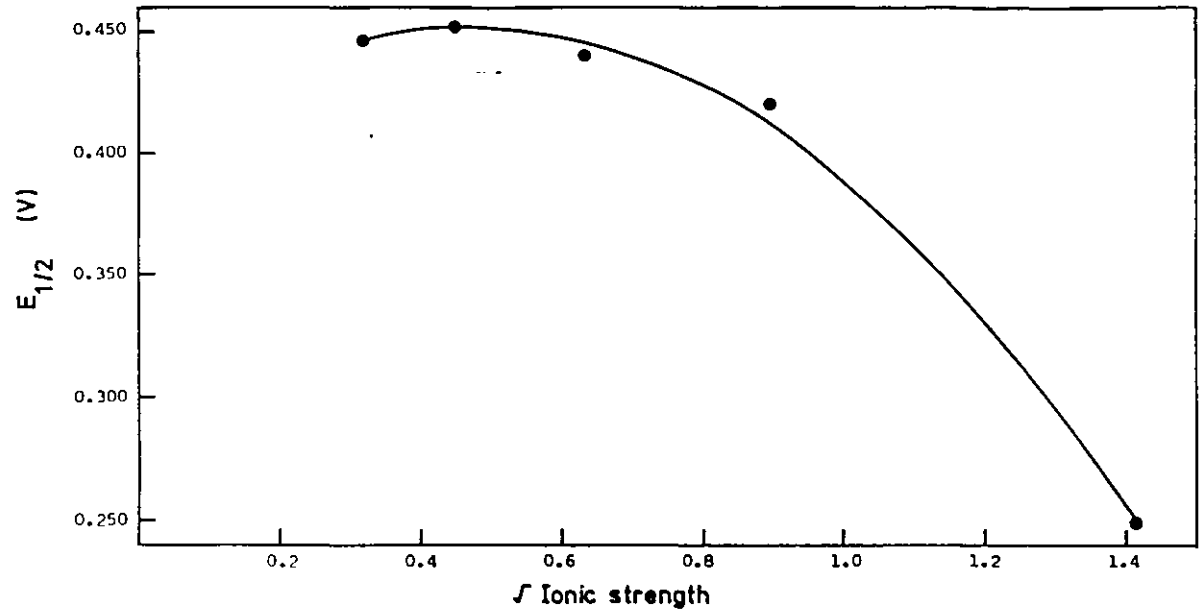

Fig. 5-313 Fe(III) chloride (2×10^{-4} M)/Hydrochloric acid (0.1 to 2.0 M) supporting electrolyte System: Values of half-wave potential, $E_{\frac{1}{2}}$, as a function of square root of total ionic strength (where the concentration of hydrochloric acid supporting electrolyte was varied), $\sqrt{I}$. Boron carbide solid electrode $B_{4.04}C$.

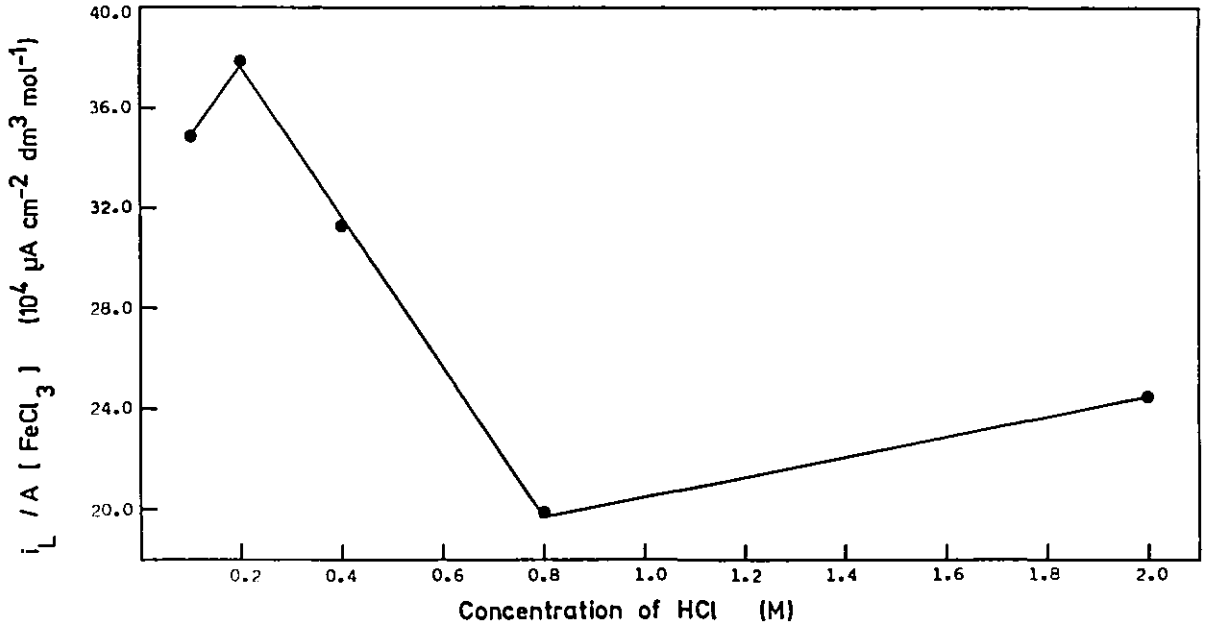

Fig. 5-314 Fe(III) chloride (2×10^{-4} M)/Hydrochloric acid (0.1 to 2.0 M) supporting electrolyte System: Values of limiting current per unit area divided by concentration of ferric chloride, i_L/A [$FeCl_3$], as a function of concentration of hydrochloric acid supporting electrolyte, [HCl]. Boron carbide solid electrode $B_{4.04}C$.

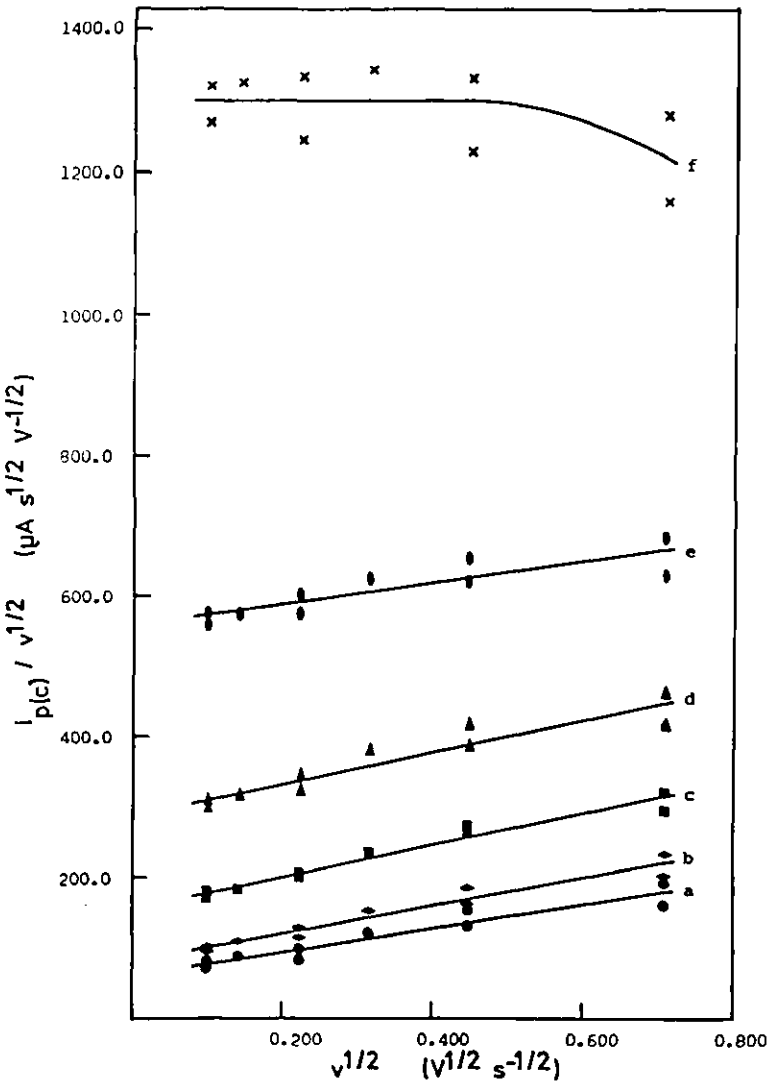

Fig. 5-315 Fe(III) chloride (4×10^{-5} to 2×10^{-3} M)/Hydrochloric acid (0.1 M) supporting electrolyte System: Values of cathodic current function, $i_{p(c)}/v^{\frac{1}{2}}$, as a function of square root of potential scan rate, $v^{\frac{1}{2}}$; at the ferric chloride concentrations (a) 4×10^{-5}, (b) 8×10^{-5}, (c) 2×10^{-4}, (d) 4×10^{-4}, (e) 8×10^{-4}, and (f) 2×10^{-3} M. Boron carbide solid electrode $B_{4.04}C$.

(a) $i_{p(c)}/v^{\frac{1}{2}} = 60.4 + 168.6\ v^{\frac{1}{2}}$
Correlation coefficient = 0.9581
Level of significance, p = $p < 0.001$
Standard deviation of $i_{p(c)}/v^{\frac{1}{2}}$ from regression = 12.3 μA $s^{\frac{1}{2}}$ $V^{-\frac{1}{2}}$
Degrees of freedom = 8

(b) $i_{p(c)}/v^{\frac{1}{2}} = 81.5 + 196.6\ v^{\frac{1}{2}}$
Correlation coefficient = 0.9726
Level of significance, p = $p < 0.001$
Standard deviation of $i_{p(c)}/v^{\frac{1}{2}}$ from regression = 11.4 μA $s^{\frac{1}{2}}$ $V^{-\frac{1}{2}}$
Degrees of freedom = 8

(c) $i_{p(c)}/v^{\frac{1}{2}} = 156.0 + 224.6\ v^{\frac{1}{2}}$
Correlation coefficient = 0.9813
Level of significance, p = $p < 0.001$
Standard deviation of $i_{p(c)}/v^{\frac{1}{2}}$ from regression = 10.7 μA $s^{\frac{1}{2}}$ $V^{-\frac{1}{2}}$
Degrees of freedom = 8

(d) $i_{p(c)}/v^{\frac{1}{2}} = 287.9 + 228.5\ v^{\frac{1}{2}}$
Correlation coefficient = 0.9460
Level of significance, p = $p < 0.001$
Standard deviation of $i_{p(c)}/v^{\frac{1}{2}}$ from regression = 19.1 μA $s^{\frac{1}{2}}$ $V^{-\frac{1}{2}}$
Degrees of freedom = 8

(e) $i_{p(c)}/v^{\frac{1}{2}} = 558.0 + 152.7\ v^{\frac{1}{2}}$
Correlation coefficient = 0.8734
Level of significance, p = $p < 0.001$
Standard deviation of $i_{p(c)}/v^{\frac{1}{2}}$ from regression = 20.7 μA $s^{\frac{1}{2}}$ $V^{-\frac{1}{2}}$
Degrees of freedom = 8

(f) $i_{p(c)}/v^{\frac{1}{2}}$ mean = 1283.9 μA $s^{\frac{1}{2}}$ $V^{-\frac{1}{2}}$
Standard deviation = 59.1 μA $s^{\frac{1}{2}}$ $V^{-\frac{1}{2}}$
Coefficient of variation = 4.60%
Degrees of freedom = 9

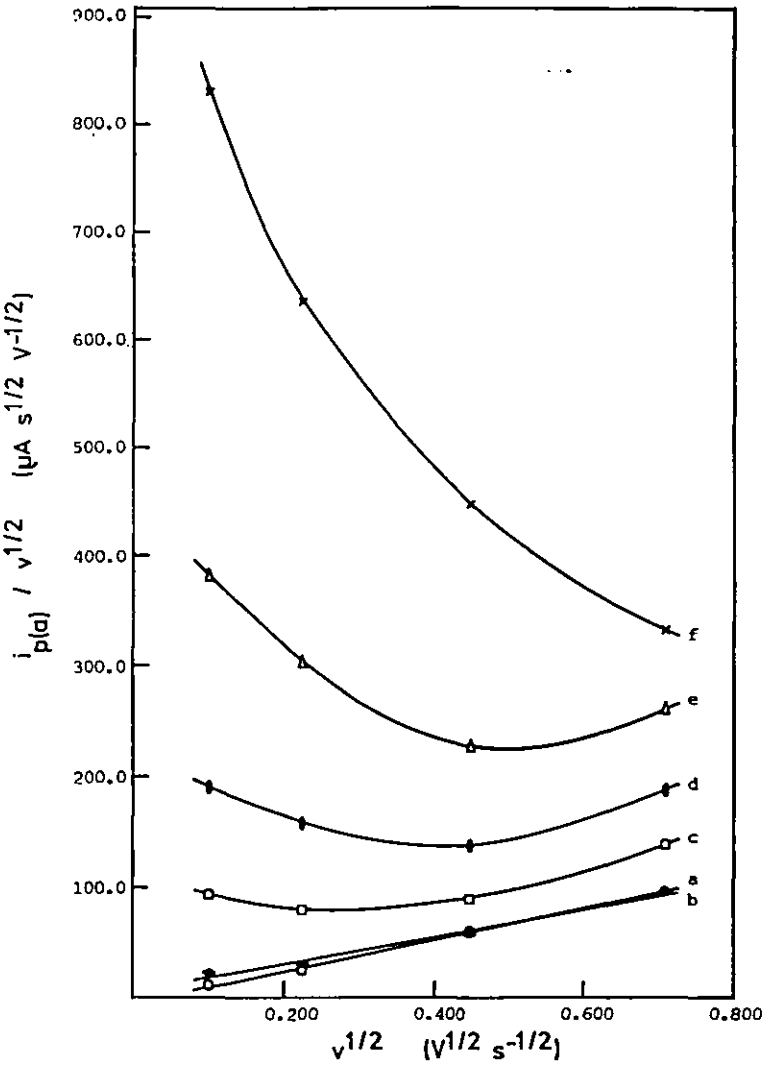

Fig. 5-316 Fe(III) chloride (4×10^{-5} to 2×10^{-3} M)/Hydrochloric acid (0.1 M) supporting electrolyte System: Values of anodic current function, $i_{p(a)}/v^{\frac{1}{2}}$, as a function of square root of potential scan rate, $v^{\frac{1}{2}}$; at ferric chloride concentrations (a) 4×10^{-5}, (b) 8×10^{-5}, (c) 2×10^{-4}, (d) 4×10^{-4}, (e) 8×10^{-4}, and (f) 2×10^{-3} M. Boron carbide solid electrode $B_{4.04}C$.

(a) $i_{p(a)}/v^{\frac{1}{2}} = 144.1\ v^{\frac{1}{2}} - 5.57$
Correlation coefficient = 0.9987
Level of significance, $p = 0.001 < p < 0.01$
Standard deviation of $i_{p(a)}/v^{\frac{1}{2}}$ from regression = 2.39 μA $s^{\frac{1}{2}}$ $V^{-\frac{1}{2}}$
Degrees of freedom = 2

(b) $i_{p(a)}/v^{\frac{1}{2}} = 5.66 + 125.8\ v^{\frac{1}{2}}$
Correlation coefficient = 0.9929
Level of significance, $p = 0.001 < p < 0.01$
Standard deviation of $i_{p(a)}/v^{\frac{1}{2}}$ from regression = 4.92 μA $s^{\frac{1}{2}}$ $V^{-\frac{1}{2}}$
Degrees of freedom = 2

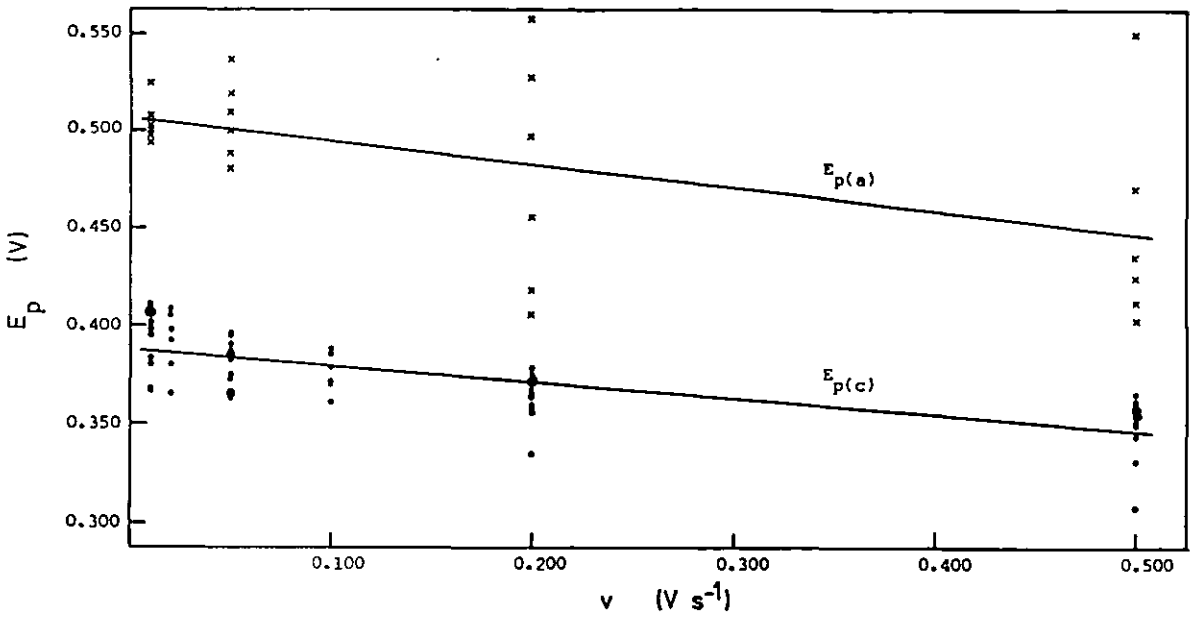

Fig. 5-317 Fe(III) chloride (4×10^{-5} to 2×10^{-3} M)/Hydrochloric acid (0.1 M) supporting electrolyte System: Values of cathodic and anodic peak potentials, $E_{p(c)}$ and $E_{p(a)}$ respectively, as functions of potential sweep rate, v; at ferric chloride concentrations of 4×10^{-5} to 2×10^{-3} M. Boron carbide solid electrode $B_{4.04}C$.

(a) $E_{p(c)} = 0.388 - 8.33 \times 10^{-2}$ v
Correlation coefficient = -0.7311
Level of significance, p = $p < 0.001$
Standard deviation of $E_{p(c)}$ from regression = 1.43×10^{-2} V
Degrees of freedom = 58

(b) $E_{p(a)} = 0.506 - 0.118$ v
Correlation coefficient = -0.5032
Level of significance, p = $0.01 < p < 0.02$
Standard deviation of $E_{p(a)}$ from regression = 4.09×10^{-2} V
Degrees of freedom = 22

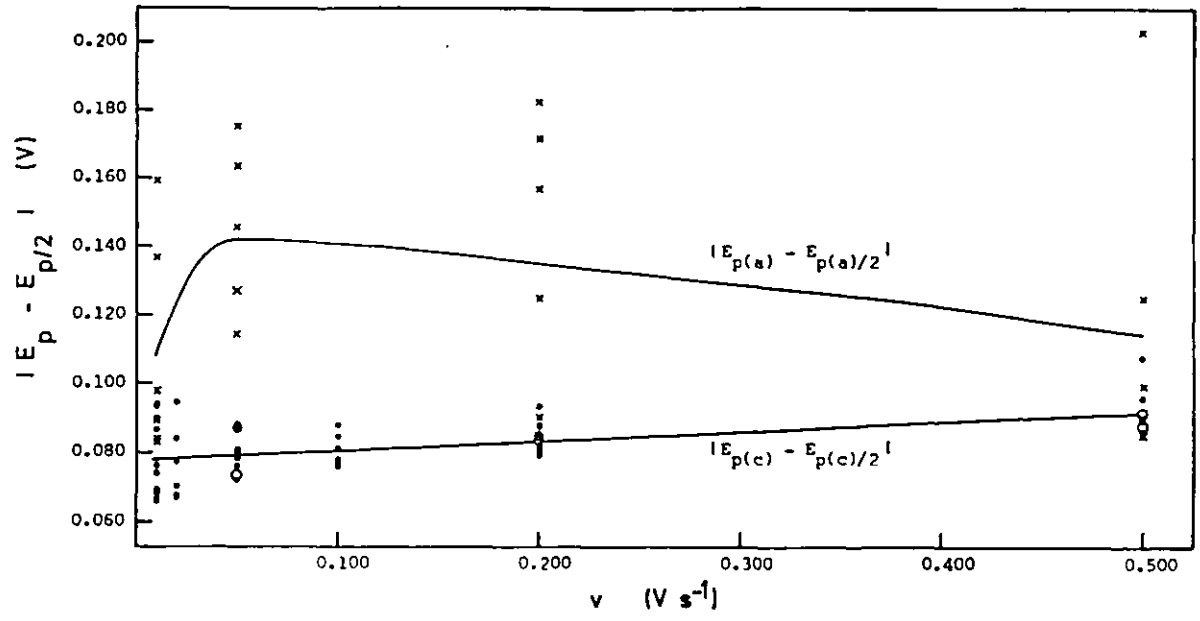

Fig. 5-318 Fe(III) chloride (4×10^{-5} to 2×10^{-3} M)/Hydrochloric acid (0.1 M) supporting electrolyte System: Values of the absolute difference between cathodic peak and half-peak potentials and between anodic peak and half-peak potentials, $|E_{p(c)} - E_{p(c)/2}|$ and $|E_{p(a)} - E_{p(a)/2}|$ respectively, as functions of potential sweep rate, v; at ferric chloride concentrations of 4×10^{-5} to 2×10^{-3} M. Boron carbide solid electrode $B_{4.04}C$.

(a) $|E_{p(c)} - E_{p(c)/2}| = 7.74 \times 10^{-2} + 2.83 \times 10^{-2}$ v
Correlation coefficient = 0.5780
Level of significance, p = p < 0.001
Standard deviation of $|E_{p(c)} - E_{p(c)/2}|$ from regression = 7.35×10^{-3} V
Degrees of freedom = 58

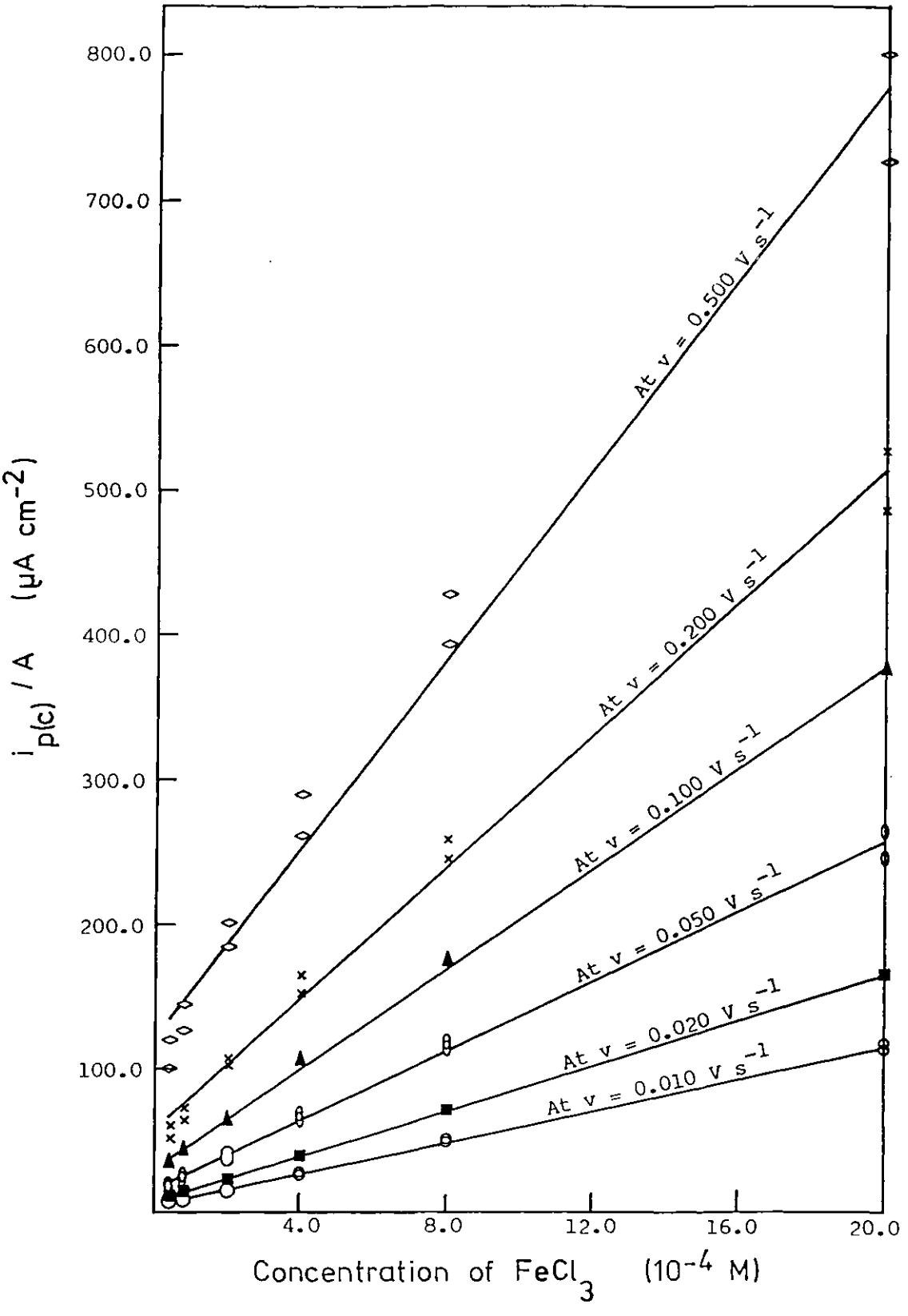

Fig. 5-319 Fe(III) chloride (4×10^{-5} to 2×10^{-3} M)/Hydrochloric acid (0.1 M) supporting electrolyte System: Dependence of cathodic peak current per unit area, $i_{p(c)}/A$, on the concentration of ferric chloride, [$FeCl_3$]; at sweep rate, v, of 0.010 to 0.500 V s^{-1}. Boron carbide solid electrode $B_{4.04}C$.

Fig. 5-319 (continued):-

(a) At v = 0.010 V s^{-1}:

$i_{p(c)}/A = 4.72 + 5.52 \times 10^4$ [$FeCl_3$]
Correlation coefficient = 0.9995
Level of significance, p = p < 0.001
Standard deviation of $i_{p(c)}/A$ from regression = 1.29 μA cm^{-2}
Degrees of freedom = 10

(b) At v= 0.020 V s^{-1}:

$i_{p(c)}/A = 7.69 + 7.91 \times 10^4$ [$FeCl_3$]
Correlation coefficient = 0.99997
Level of significance, p = p < 0.001
Standard deviation of $i_{p(c)}/A$ from regression = 0.544 μA cm^{-2}
Degrees of freedom = 4

(c) At v = 0.050 V s^{-1}:

$i_{p(c)}/A = 16.0 + 1.20 \times 10^5$ [$FeCl_3$]
Correlation coefficient = 0.9984
Level of significance, p = p < 0.001
Standard deviation of $i_{p(c)}/A$ from regression = 5.13 μA cm^{-2}
Degrees of freedom = 10

(d) At v= 0.100 V s^{-1}:

$i_{p(c)}/A = 31.5 + 1.73 \times 10^5$ [$FeCl_3$]
Correlation coefficient = 0.9995
Level of significance, p = p < 0.001
Standard deviation of $i_{p(c)}/A$ from regression = 4.52 μA cm^{-2}
Degrees of freedom = 4

(e) At v = 0.200 V s^{-1}:

$i_{p(c)}/A = 57.9 + 2.27 \times 10^5$ [$FeCl_3$]
Correlation coefficient = 0.9965
Level of significance, p = p < 0.001
Standard deviation of $i_{p(c)}/A$ from regression = 14.2 μA cm^{-2}
Degrees of freedom = 10

(f) At v = 0.500 V s^{-1}:

$i_{p(c)}/A = 1.22 \times 10^2 + 3.27 \times 10^5$ [$FeCl_3$]
Correlation coefficient = 0.9927
Level of significance, p = p < 0.001
Standard deviation of $i_{p(c)}/A$ from regression = 29.6 μA cm^{-2}
Degrees of freedom = 10

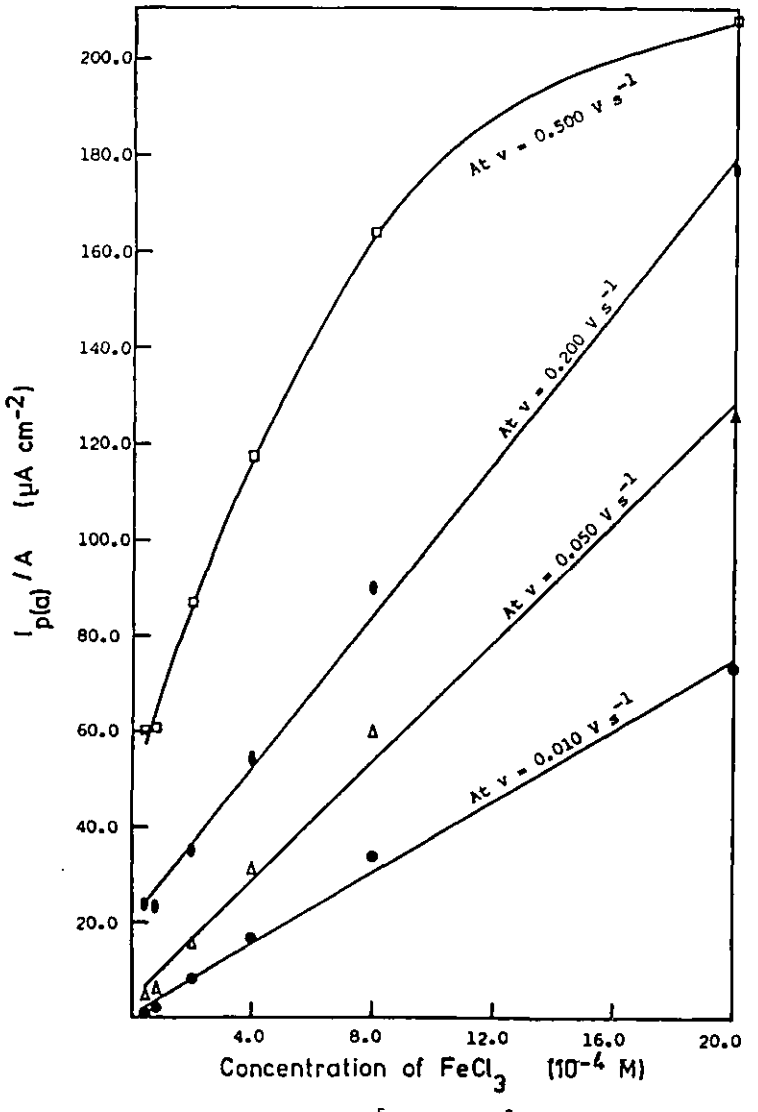

Fig. 5-320 Fe(III) chloride (4×10^{-5} to 2×10^{-3} M)/Hydrochloric acid (0.1 M) supporting electrolyte System: Dependence of anodic peak current per unit area, $i_{p(a)}/A$, on the concentration of ferric chloride, [$FeCl_3$]; at scan rate, v, of 0.010 to 0.500 V s^{-1}. Boron carbide solid electrode $B_{4.04}C$.

(a) At v = 0.010 V s^{-1}:

$i_{p(a)}/A = 0.762 + 3.70 \times 10^4$ [$FeCl_3$]
Correlation coefficient = 0.9975
Level of significance, p = $p < 0.001$
Standard deviation of $i_{p(a)}/A$ from regression = 2.19 μA cm^{-2}
Degrees of freedom = 4

(b) At v = 0.050 V s^{-1}:

$i_{p(a)}/A = 4.06 + 6.21 \times 10^4$ [$FeCl_3$]
Correlation coefficient = 0.9971
Level of significance, p = $p < 0.001$
Standard deviation of $i_{p(a)}/A$ from regression = 3.93 μA cm^{-2}
Degrees of freedom = 4

(c) At v = 0.200 V s^{-1}:

$i_{p(a)}/A = 20.7 + 7.93 \times 10^4$ [$FeCl_3$]
Correlation coefficient = 0.9984
Level of significance, p = $p < 0.001$
Standard deviation of $i_{p(a)}/A$ from regression = 3.79 μA cm^{-2}
Degrees of freedom = 4

(d) At v = 0.500 V s^{-1}:

$i_{p(a)}/A = 71.9 + 7.52 \times 10^4$ [$FeCl_3$]
Correlation coefficient = 0.9435
Level of significance, p = $0.001 < p < 0.01$
Standard deviation of $i_{p(a)}/A$ from regression = 22.0 μA cm^{-2}
Degrees of freedom = 4

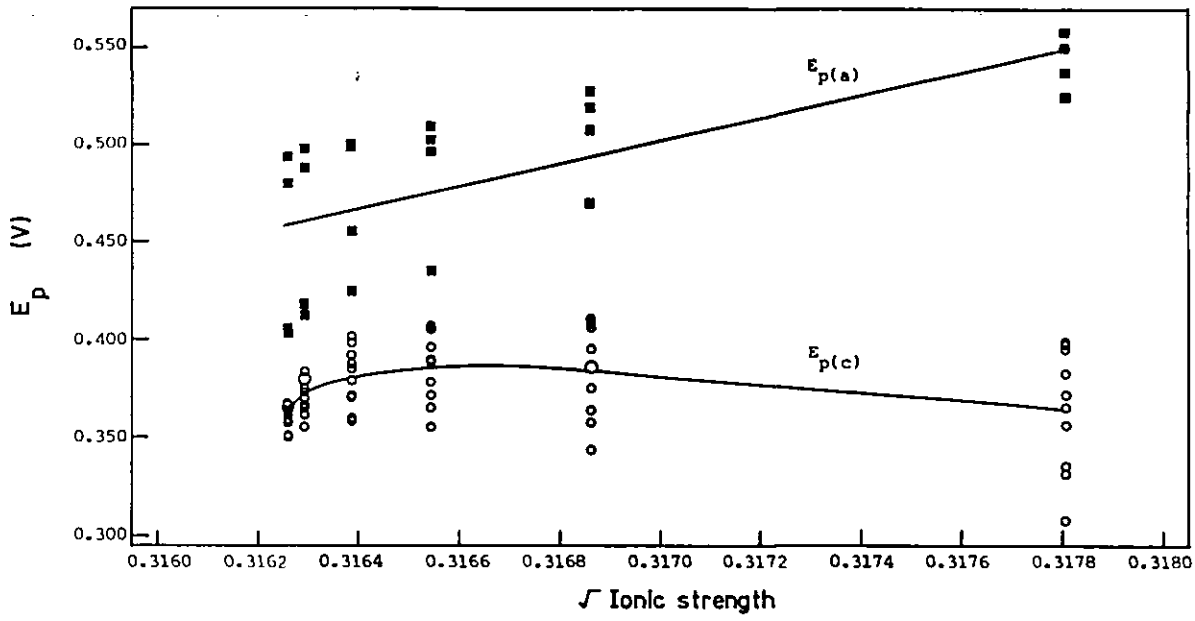

Fig. 5-321 Fe(III) chloride (4×10^{-5} to 2×10^{-3} M)/Hydrochloric acid (0.1 M) supporting electrolyte System: Values of cathodic and anodic peak potentials, $E_{p(c)}$ and $E_{p(a)}$ respectively, as functions of square root of total ionic strength (where the concentration of ferric chloride was varied), $\sqrt{I}$; at sweep rates of 0.010 to 0.500 V s^{-1}. The predominant Fe(III) species is assumed to be $FeCl_4^-$. Boron carbide solid electrode $B_{4.04}C$.

(a) $E_{p(c)}$ mean = 0.374 V (vs SCE)
Standard deviation = 2.08×10^{-2} V
Coefficient of variation = 5.55%
Degrees of freedom = 59

(b) $E_{p(a)} = 58.7\ \sqrt{I} - 18.1$
Correlation coefficient = 0.6958
Level of significance, p = $p < 0.001$
Standard deviation of $E_{p(a)}$ from regression = 3.40×10^{-2} V
Degrees of freedom = 22

cathodic and anodic $|E_p - E_{p/2}|$ values are shown in Figures 5-322 and 5-323 respectively.

Fig. 5-324 reveals that for the electrochemical reduction of Fe(III) chloride (2×10^{-4} M) the weak adsorption of reactant was the predominant factor when the concentration of hydrochloric acid supporting electrolyte was within the approximate range of 0.1 to 0.4 M. When the hydrochloric acid concentration was 0.8 M the adsorption effect was not apparent but there was indication of a catalytic reaction which persisted at higher concentrations of hydrochloric acid supporting electrolyte (Fig. 5-324, d and e, c.f. Fig. 3-6). For the anodic scan, however, the influence of the catalytic reaction persisted throughout the entire concentration range of hydrochloric acid supporting electrolyte employed (Fig. 5-325) whilst the weak adsorption was not evident at high hydrochloric acid concentration (e.g. 2.0 M). At HCl (0.2 M), the anodic curve for Fe(III) chloride exhibited two peaks (1 and 2) when the potential sweep rate did not exceed 0.1 V s^{-1}; where Peak 1 was affected by the catalytic reaction and Peak 2 was affected by the adsorption of ferric chloride reactant. Peaks 1 and 2 merged at faster sweep rates and only the adsorption effect complicated the charge transfer.

The effect of hydrochloric acid concentration on the cathodic peak current for ferric chloride is presented in Fig. 5-326; the increase in concentration causing the peak current to fall. The anodic peak current, however, was enhanced by increasing concentration of hydrochloric acid supporting electrolyte until the situation was reached when further increase in the concentration of hydrochloric acid weakened the adsorption factor to a greater extent than could be compensated for by the enhancement of the catalytic reaction (Fig. 5-327). Fig. 5-328 shows that the cathodic peak potential was cathodically shifted whilst the anodic peak potential was anodically shifted by increasing (ionic strength)$^{\frac{1}{2}}$; although the main Fe(III) species was expected to be the anion $FeCl_4^-$. The potential shifts, however, were caused by the deteriorating reversibility of the charge transfer when the concentration of hydrochloric acid supporting electrolyte was increased; as evidenced by widening $|E_p - E_{p/2}|$ values (Fig. 5-329).

5-2.2.(iii) Summary.

The voltammetric investigations were carried out on Fe(III) chloride (4×10^{-5} to 2×10^{-3} M) in hydrochloric acid (0.1 to 2.0 M)

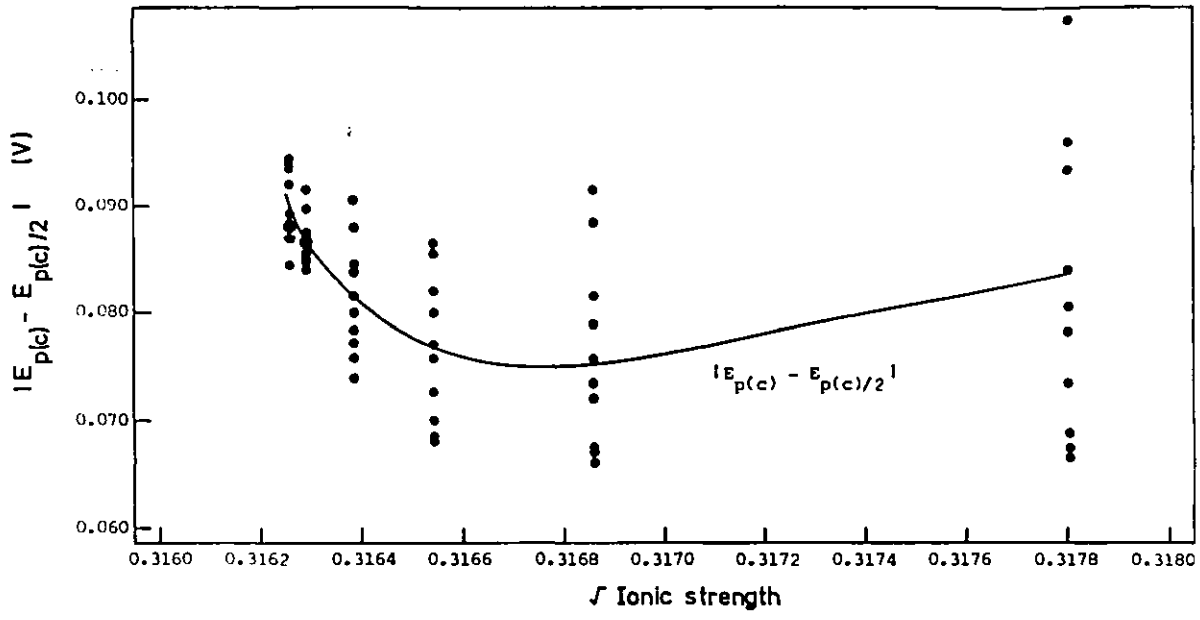

Fig. 5-322 Fe(III) chloride (4×10^{-5} to 2×10^{-3} M)/Hydrochloric acid (0.1 M) supporting electrolyte System: Values of the absolute difference between cathodic peak and half-peak potentials, $|E_{p(c)} - E_{p(c)/2}|$, as a function of square root of total ionic strength (where the concentration of ferric chloride was varied), $\sqrt{I}$; at potential sweep rates of 0.010 to 0.500 V s^{-1}. The predominant Fe(III) species is assumed to be $FeCl_4^-$. Boron carbide solid electrode $B_{4.04}C$.

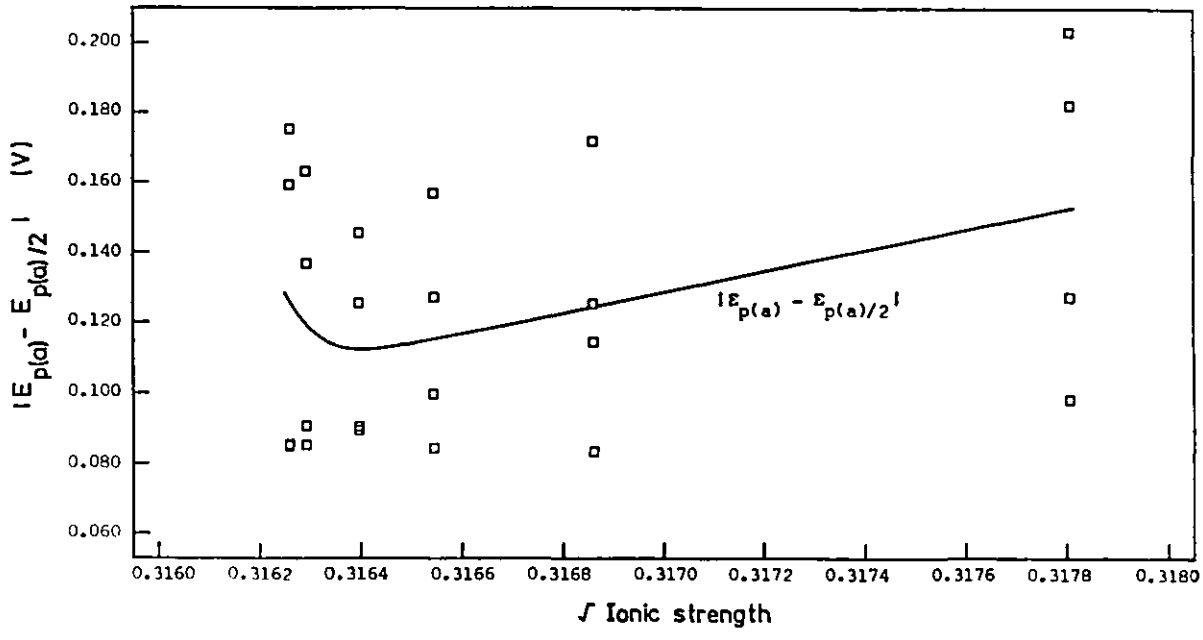

Fig. 5-323 Fe(III) chloride (4×10^{-5} to 2×10^{-3} M)/Hydrochloric acid (0.1 M) supporting electrolyte System: Values of the absolute difference between anodic peak and half-peak potentials, $|E_{p(a)} - E_{p(a)/2}|$, as a function of square root of total ionic strength (where the concentration of ferric chloride was varied), $\sqrt{I}$; at potential sweep rates of 0.010 to 0.500 V s^{-1}. The predominant Fe(III) species is assumed to be $FeCl_4^-$. Boron carbide solid electrode $B_{4.04}C$.

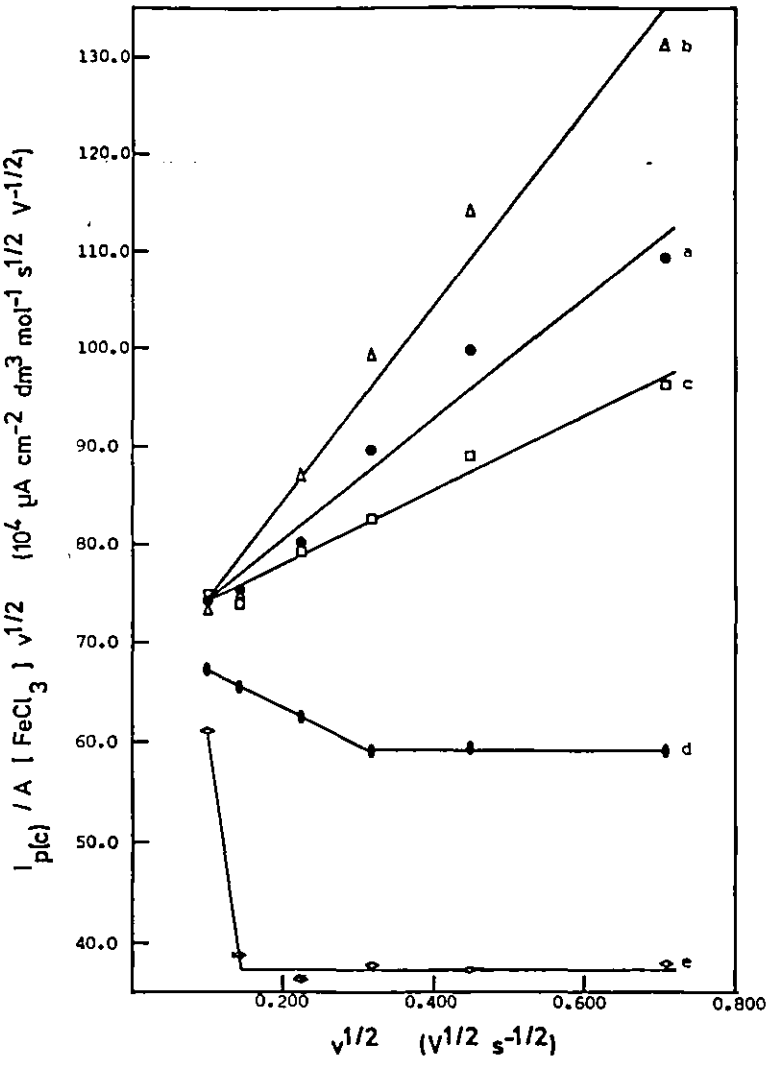

Fig. 5-324 Fe(III) chloride (2×10^{-4} M)/Hydrochloric acid (0.1 to 2.0 M) supporting electrolyte System: Values of cathodic current function, $i_{p(c)}/A\ [\ FeCl_3\ ]\ v^{\frac{1}{2}}$, as a function of square root of potential sweep rate, $v^{\frac{1}{2}}$; at hydrochloric acid concentrations (a) 0.1, (b) 0.2, (c) 0.4, (d) 0.8, and (e) 2.0 M. Boron carbide solid electrode $B_{4.04}C$.

(a) $i_{p(c)}/A\ [\ FeCl_3\ ]\ v^{\frac{1}{2}} = 6.80 \times 10^5 + 6.19 \times 10^5\ v^{\frac{1}{2}}$
Correlation coefficient = 0.9850
Level of significance, p = $p < 0.001$
Standard deviation of $i_{p(c)}/A\ [\ FeCl_3\ ]\ v^{\frac{1}{2}}$ from regression
$= 2.74 \times 10^4$ μA cm^{-2} dm^3 mol^{-1} $s^{\frac{1}{2}}$ $V^{-\frac{1}{2}}$
Degrees of freedom = 4

(b) $i_{p(c)}/A\ [\ FeCl_3\ ]\ v^{\frac{1}{2}} = 6.43 \times 10^5 + 1.00 \times 10^6\ v^{\frac{1}{2}}$
Correlation coefficient = 0.9880
Level of significance, p = $p < 0.001$
Standard deviation of $i_{p(c)}/A\ [\ FeCl_3\ ]\ v^{\frac{1}{2}}$ from regression
$= 3.95 \times 10^4$ μA cm^{-2} dm^3 mol^{-1} $s^{\frac{1}{2}}$ $V^{-\frac{1}{2}}$
Degrees of freedom = 4

(c) $i_{p(c)}/A\ [\ FeCl_3\ ]\ v^{\frac{1}{2}} = 7.03 \times 10^5 + 3.78 \times 10^5\ v^{\frac{1}{2}}$
Correlation coefficient = 0.9894
Level of significance, p = $p < 0.001$
Standard deviation of $i_{p(c)}/A\ [\ FeCl_3\ ]\ v^{\frac{1}{2}}$ from regression
$= 1.40 \times 10^4$ μA cm^{-2} dm^3 mol^{-1} $s^{\frac{1}{2}}$ $V^{-\frac{1}{2}}$
Degrees of freedom = 4

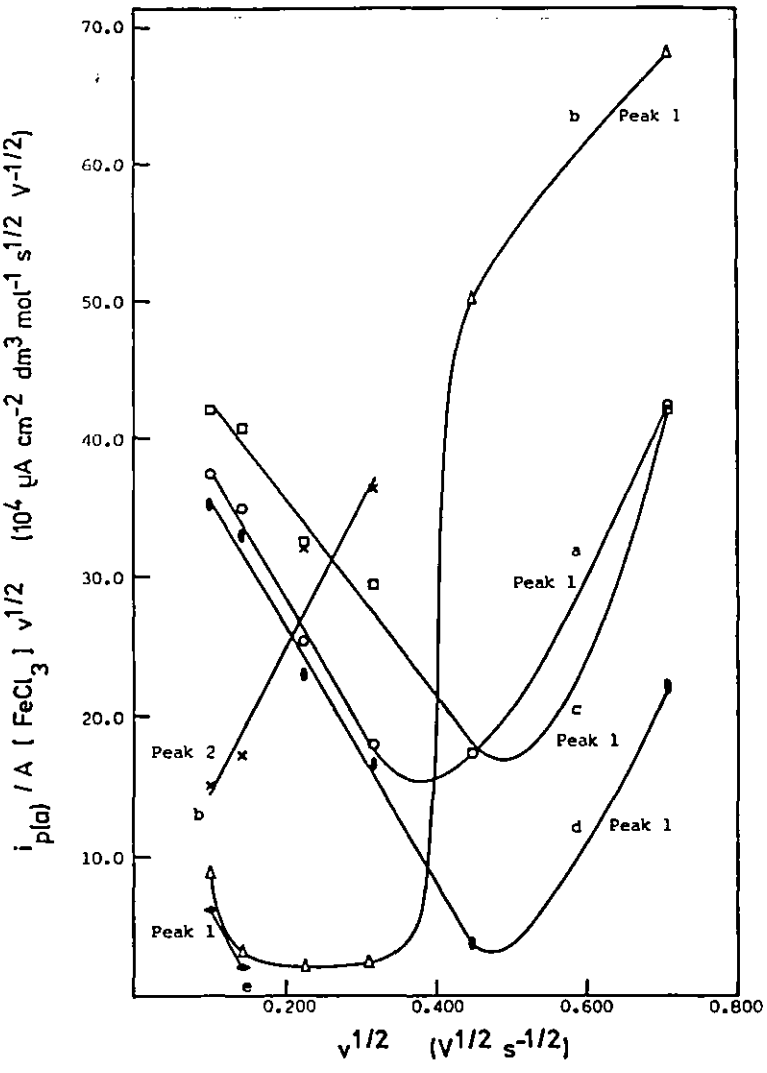

Fig. 5-325 Fe(III) chloride (2×10^{-4} M)/Hydrochloric acid (0.1 to 2.0 M) supporting electrolyte System: Values of anodic current function, $i_{p(a)}/A$ [$FeCl_3$] $v^{\frac{1}{2}}$, as a function of square root of potential sweep rate, $v^{\frac{1}{2}}$; at hydrochloric acid concentrations (a) 0.1, (b) 0.2, (c) 0.4, (d) 0.8, and (e) 2.0 M. Boron carbide solid electrode $B_{4.04}C$.

(b) Peak 2:

$i_{p(a)}/A$ [$FeCl_3$] $v^{\frac{1}{2}} = 4.01 \times 10^4 + 1.04 \times 10^6\ v^{\frac{1}{2}}$

Correlation coefficient = 0.9925

Level of significance, $p = 0.001 < p < 0.01$

Standard deviation of $i_{p(a)}/A$ [$FeCl_3$] $v^{\frac{1}{2}}$ from regression

$= 1.49 \times 10^4$ µA cm^{-2} dm^3 mol^{-1} $s^{\frac{1}{2}}$ $V^{-\frac{1}{2}}$

Degrees of freedom = 2

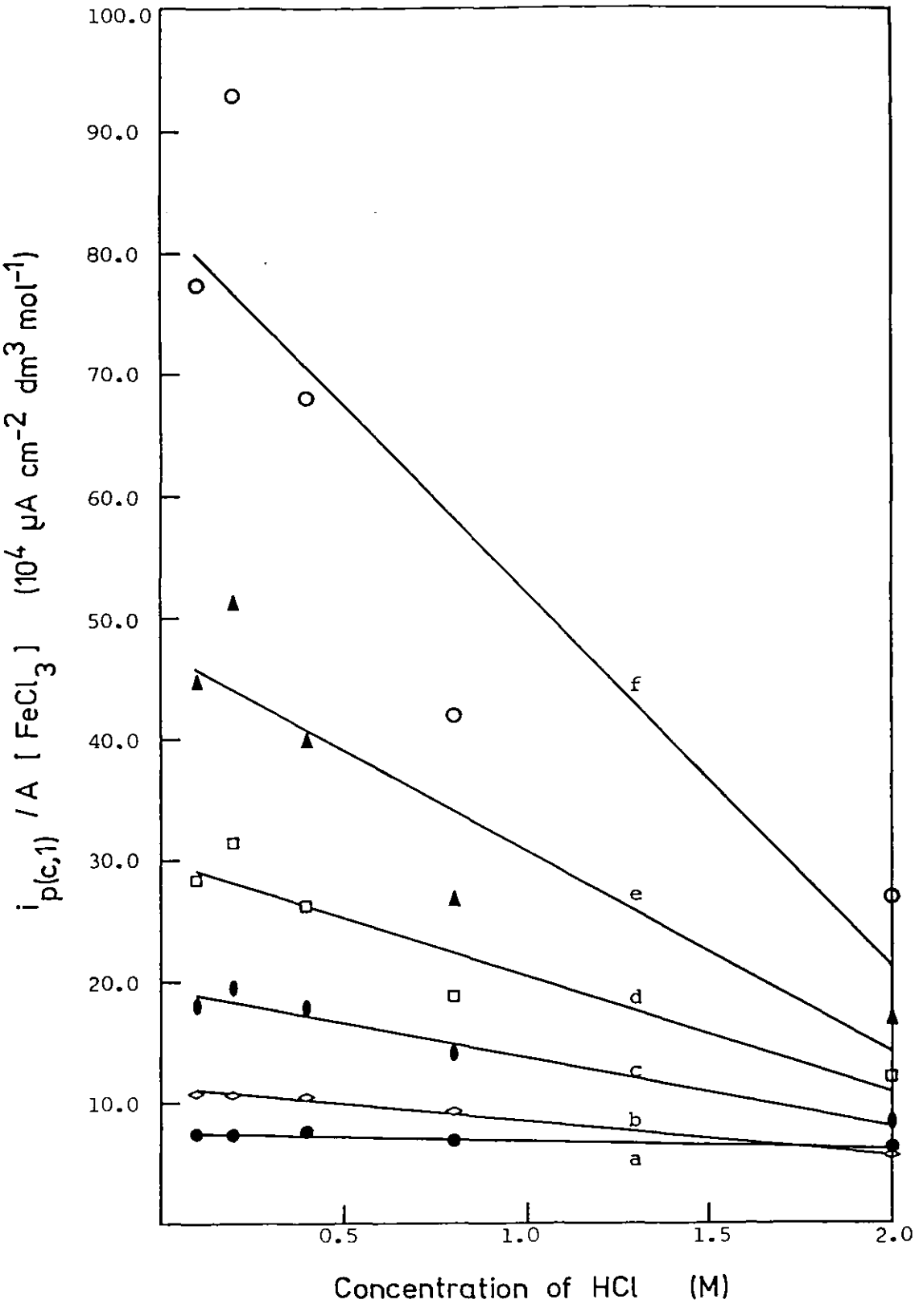

Fig. 5-326 Fe(III) chloride (2×10^{-4} M)/Hydrochloric acid (0.1 to 2.0 M) supporting electrolyte System: Values of cathodic peak current per unit area divided by concentration of ferric chloride, $i_{p(c,1)}/A$ [$FeCl_3$], as a function of concentration of hydrochloric acid; at potential scan rates (a) 0.010, (b) 0.020, (c) 0.050, (d) 0.100, (e) 0.200, and (f) 0.500 V s^{-1}. Boron carbide solid electrode $B_{4.04}C$.

Fig. 5-326 (continued):-

(a) $i_{p(c,1)}/A\ [\ FeCl_3\ ] = 7.52 \times 10^4 - 7.29 \times 10^3\ [\ HCl\ ]$
Correlation coefficient = -0.9574
Level of significance, $p = 0.01 < p < 0.02$
Standard deviation of $i_{p(c,1)}/A\ [\ FeCl_3\ ]$ from regression
$= 1.97 \times 10^3\ \mu A\ cm^{-2}\ dm^3\ mol^{-1}$
Degrees of freedom = 3

(b) $i_{p(c,1)}/A\ [\ FeCl_3\ ] = 1.13 \times 10^5 - 2.82 \times 10^4\ [\ HCl\ ]$
Correlation coefficient = -0.9923
Level of significance, $p = p < 0.001$
Standard deviation of $i_{p(c,1)}/A\ [\ FeCl_3\ ]$ from regression
$= 3.16 \times 10^3\ \mu A\ cm^{-2}\ dm^3\ mol^{-1}$
Degrees of freedom = 3

(c) $i_{p(c,1)}/A\ [\ FeCl_3\ ] = 1.95 \times 10^5 - 5.75 \times 10^4\ [\ HCl\ ]$
Correlation coefficient = -0.9795
Level of significance, $p = 0.001 < p < 0.01$
Standard deviation of $i_{p(c,1)}/A\ [\ FeCl_3\ ]$ from regression
$= 1.06 \times 10^4\ \mu A\ cm^{-2}\ dm^3\ mol^{-1}$
Degrees of freedom = 3

(d) $i_{p(c,1)}/A\ [\ FeCl_3\ ] = 3.00 \times 10^5 - 9.63 \times 10^4\ [\ HCl\ ]$
Correlation coefficient = -0.9464
Level of significance, $p = 0.01 < p < 0.02$
Standard deviation of $i_{p(c,1)}/A\ [\ FeCl_3\ ]$ from regression
$= 2.94 \times 10^4\ \mu A\ cm^{-2}\ dm^3\ mol^{-1}$
Degrees of freedom = 3

(e) $i_{p(c,1)}/A\ [\ FeCl_3\ ] = 4.73 \times 10^5 - 1.66 \times 10^5\ [\ HCl\ ]$
Correlation coefficient = -0.9233
Level of significance, $p = 0.02 < p < 0.05$
Standard deviation of $i_{p(c,1)}/A\ [\ FeCl_3\ ]$ from regression
$= 6.17 \times 10^4\ \mu A\ cm^{-2}\ dm^3\ mol^{-1}$
Degrees of freedom = 3

(f) $i_{p(c,1)}/A\ [\ FeCl_3\ ] = 8.30 \times 10^5 - 3.09 \times 10^5\ [\ HCl\ ]$
Correlation coefficient = -0.8941
Level of significance, $p = 0.02 < p < 0.05$
Standard deviation of $i_{p(c,1)}/A\ [\ FeCl_3\ ]$ from regression
$= 1.39 \times 10^5\ \mu A\ cm^{-2}\ dm^3\ mol^{-1}$
Degrees of freedom = 3

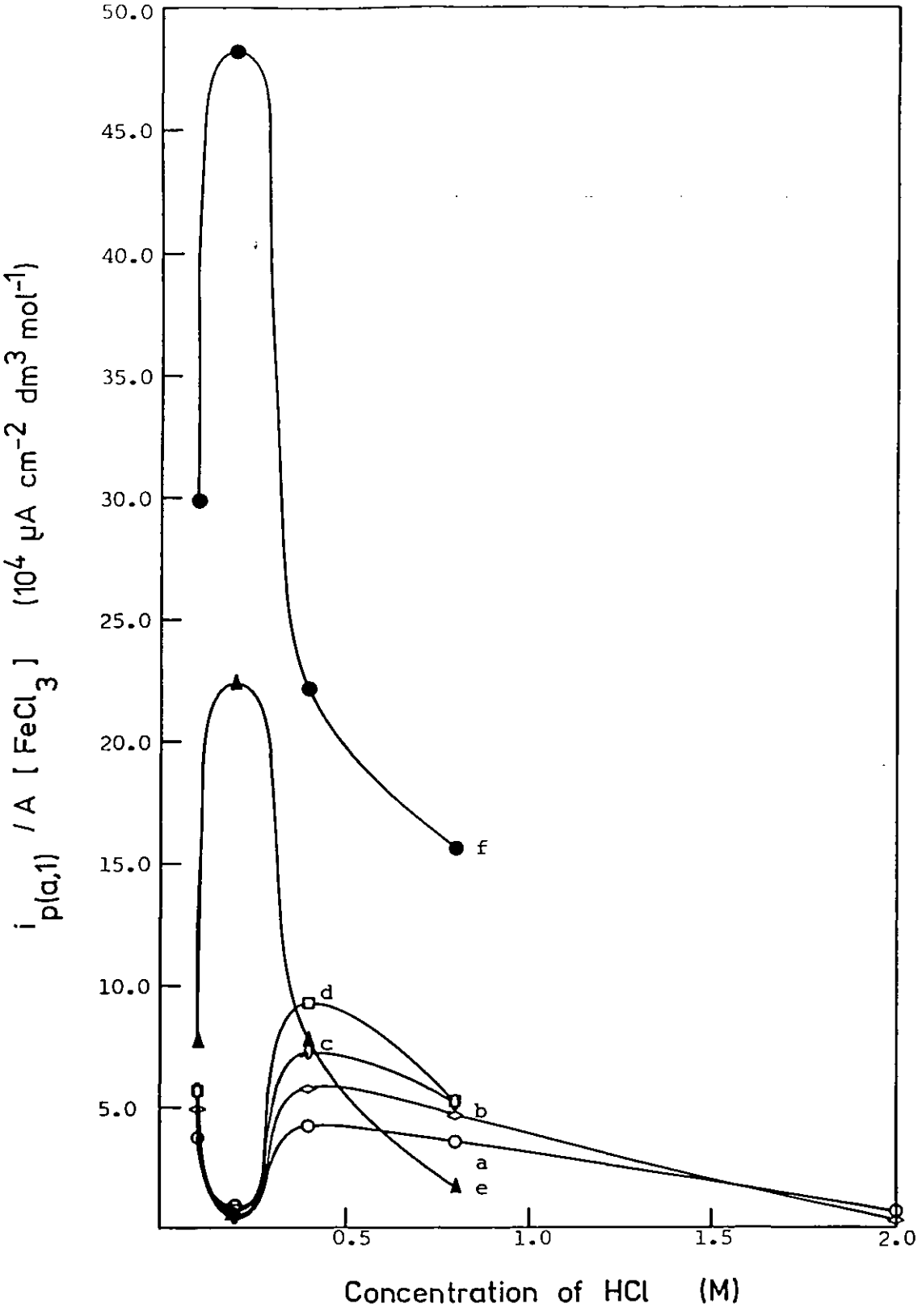

Fig. 5-327 Fe(III) chloride (2×10^{-4} M)/Hydrochloric acid (0.1 to 2.0 M) supporting electrolyte System: Values of anodic peak current per unit area divided by concentration of ferric chloride, $i_{p(a,1)}/A$ [$FeCl_3$], as a function of concentration of hydrochloric acid; at potential scan rates (a) 0.010, (b) 0.020, (c) 0.050, (d) 0.100, (e) 0.200 and (f) 0.500 V s^{-1}. Boron carbide solid electrode $B_{4.04}C$.

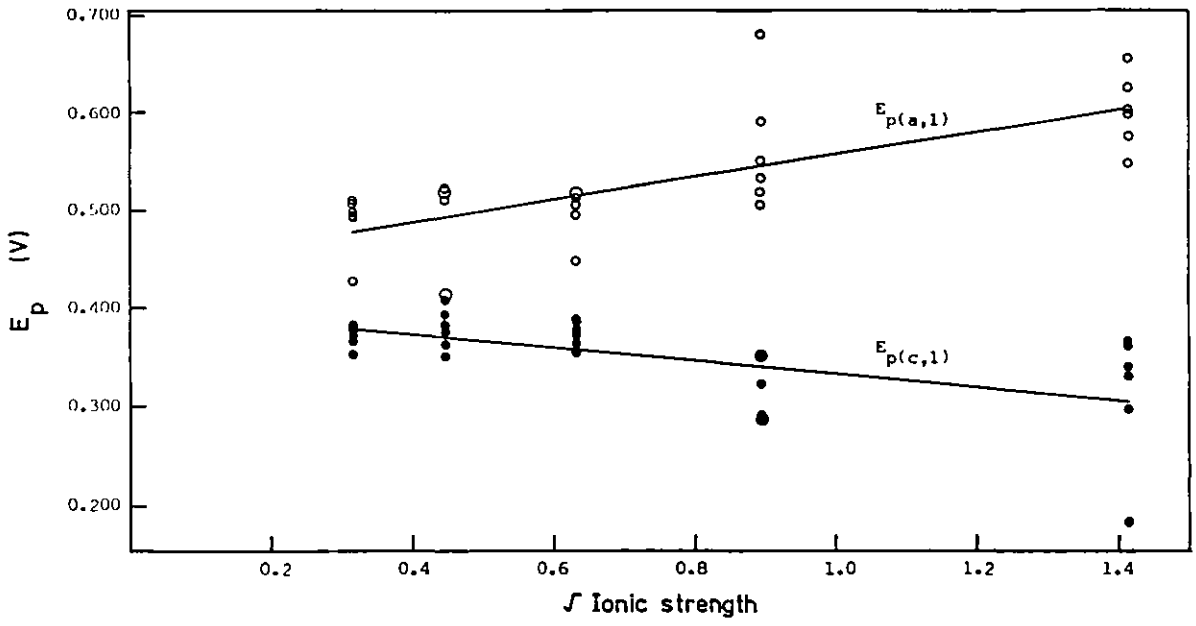

Fig. 5-328 Fe(III) chloride (2×10^{-4} M)/Hydrochloric acid (0.1 to 2.0 M) supporting electrolyte System: Values of cathodic and anodic peak potentials, $E_{p(c,1)}$ and $E_{p(a,1)}$ respectively, as functions of square root of total ionic strength (where the concentration of hydrochloric acid supporting electrolyte was varied), $\sqrt{I}$; at scan rates of 0.010 to 0.500 V s^{-1}. Boron carbide solid electrode $B_{4.04}C$.

(a) $E_{p(c,1)} = 0.400 - 6.74 \times 10^{-2} \sqrt{I}$
Correlation coefficient = -0.5898
Level of significance, p = $p < 0.001$
Standard deviation of $E_{p(c,1)}$ from regression = 3.71×10^{-2} V
Degrees of freedom = 28

(b) $E_{p(a,1)} = 0.441 + 0.116 \sqrt{I}$
Correlation coefficient = 0.7231
Level of significance, p = $p < 0.001$
Standard deviation of $E_{p(a,1)}$ from regression = 4.45×10^{-2} V
Degrees of freedom = 28

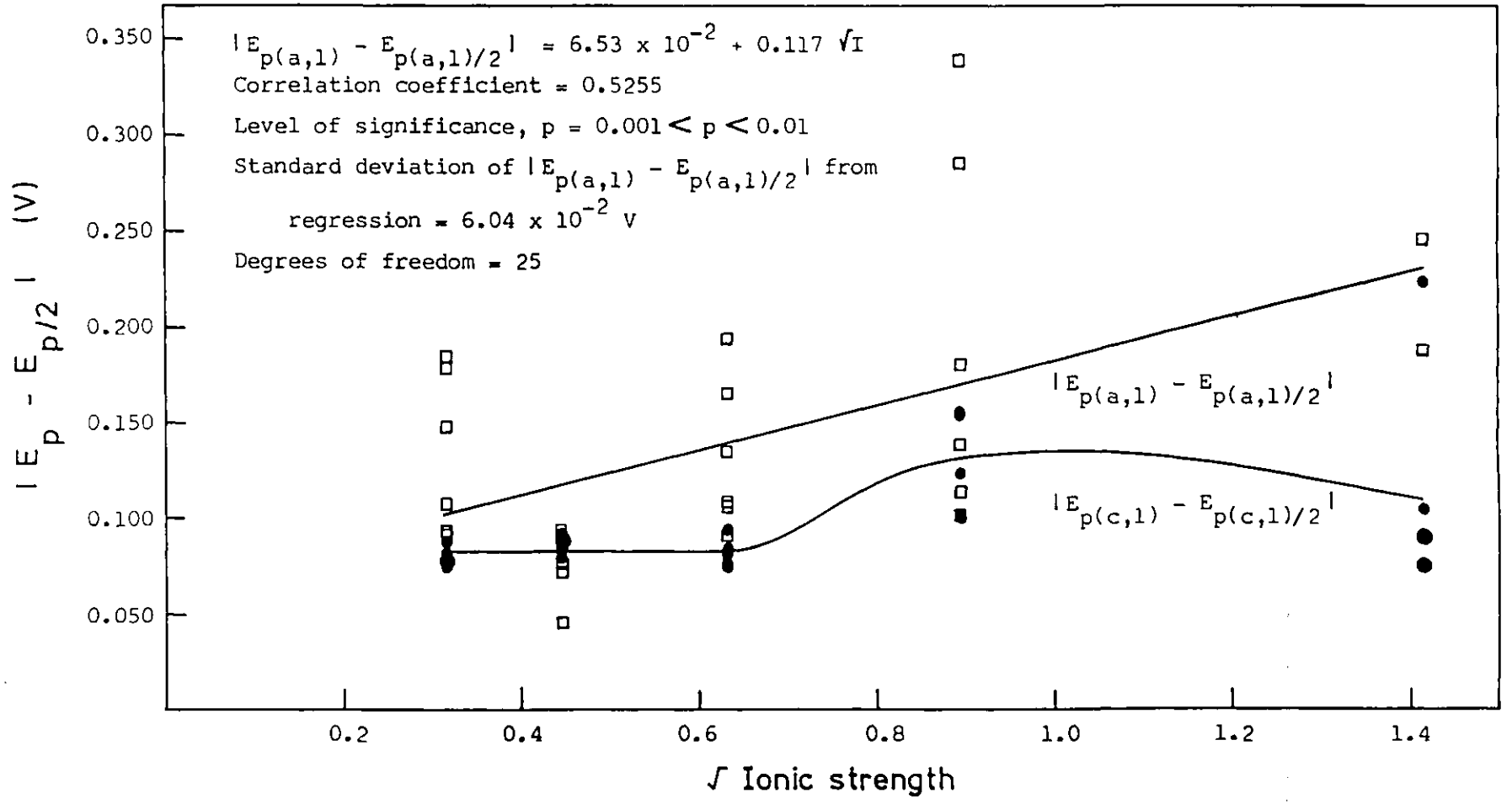

Fig. 5-329 Fe(III) chloride (2×10^{-4} M)/Hydrochloric acid (0.1 to 2.0 M) supporting electrolyte System:

Values of the absolute difference between cathodic peak and half-peak and between anodic peak and half-peak potentials, $|E_{p(c,1)} - E_{p(c,1)/2}|$ and $|E_{p(a,1)} - E_{p(a,1)/2}|$ respectively, as functions of square root of total ionic strength (where the concentration of hydrochloric acid supporting electrolyte was varied), $\sqrt{I}$; at scan rates of 0.010 to 0.500 V s^{-1}. Boron carbide solid electrode $B_{4.04}C$.

supporting electrolyte. Therefore, since a large excess of HCl was maintained, the main Fe(III) species may be considered to have been $FeCl_4^-$.

D.c. voltammetry of Fe(III) chloride (4×10^{-5} to 2×10^{-3} M) in hydrochloric acid (0.1 M) supporting electrolyte indicated that the charge transfer was nearly reversible at the low end of the concentration range but became increasingly less reversible with increasing concentration of e.a.s.; αn varied from 0.93 to 0.57 (Fig. 5-309), and $E_{\frac{1}{2}}$ shifted cathodically from 0.462 to 0.377 V vs SCE (Fig. 5-310). The limiting current density, however, was linearly dependent upon the concentration of Fe(III) chloride (Fig. 5-311). The reversibility of the charge transfer was also reduced by increasing concentration of HCl supporting electrolyte (0.1 to 2.0 M); αn varied from 0.86 to 0.34, and $E_{\frac{1}{2}}$ shifted cathodically from 0.452 to 0.249 V vs SCE (Figures 5-312 and 5-313 respectively).

The evidence from linear sweep and cyclic voltammetry of the Fe (III) chloride/HCl system suggests that the charge transfer was complicated by both weak adsorption of reactant and catalytic reaction. The reaction scheme, therefore, may be represented by:

$$FeCl_{4\,soln}^- \rightleftharpoons FeCl_{4\,ads}^-$$

$$FeCl_4^- + e^- \rightleftharpoons FeCl_4^{2-}$$

$$2FeCl_4^{2-} + \tfrac{1}{2}O_2 + 2H^+ \rightleftharpoons 2FeCl_4^- + H_2O$$

Although the cathodic peak current density was linearly dependent on the concentration of Fe(III) chloride over a range of sweep rates (Fig. 5-319), it would be better to employ slow rates of potential sweep so that the influence of weak adsorption of reactant will be minimised in quantitative analysis.

5-2.3 Fe(III)-Fe(II) cyanide system

D.c. and cyclic voltammograms for Fe(III) cyanide (2.0×10^{-4} mol dm^{-3}), in potassium chloride (0.5 M) supporting electrolyte, obtained at the boron carbide solid electrode are presented in Fig. 5-330. It is immediately apparent that the charge transfer for Fe(III) cyanide

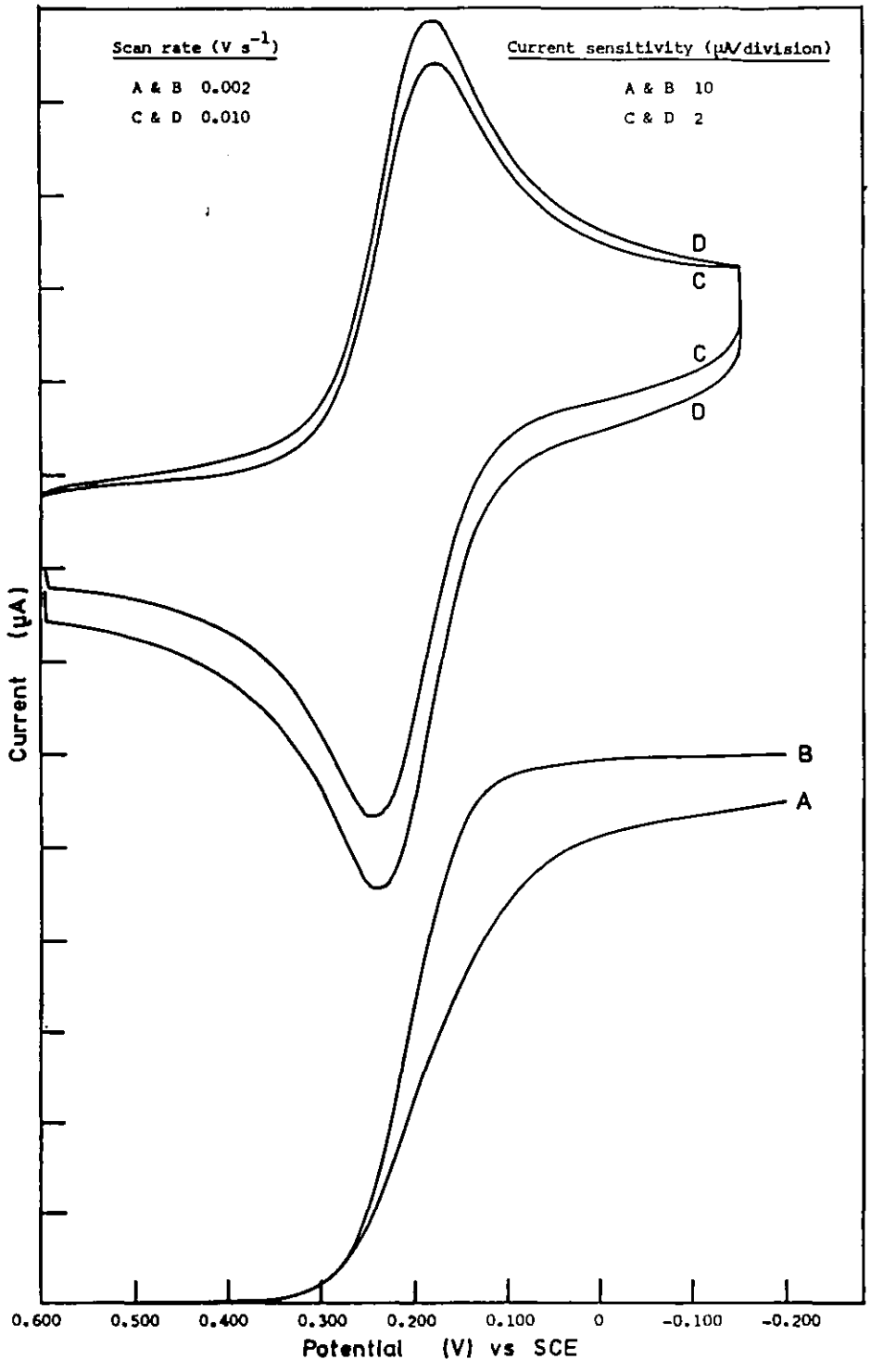

Fig. 5-330 Fe(III) cyanide (2.0×10^{-4} mol dm^{-3})/Potassium chloride (0.5 M) supporting electrolyte System: D.c. voltammograms (A & B) and cyclic voltammograms (C & D) obtained at the boron carbide solid electrode. (A) & (C): Boron carbide solid electrode as prepared. (B) & (D): Boron carbide solid electrode treated with Ir(IV) perchlorate (1.0×10^{-4} mol dm^{-3}).

was more reversible at the boron carbide solid electrode which had been treated with Ir(IV) perchlorate.

5-2.3.(i) D.c. voltammetry.

The charge transfer for the electrochemical reduction of potassium ferricyanide, in potassium chloride (0.5 M) supporting electrolyte, at the boron carbide solid electrode was poorly reversible and became increasingly less reversible as the concentration of e.a.s. was increased (Fig. 5-331, a). After treatment of the boron carbide solid electrode with Ir(IV) perchlorate, however, the charge transfer was significantly more reversible; αn varying from 0.96 to 0.76 over the concentration range (8.0×10^{-5} to 2.0×10^{-3} mol dm^{-3}) of potassium ferricyanide investigated (Fig. 5-331, b). This improvement in the reversibility of the charge transfer was also reflected in the more anodic $E_{\frac{1}{2}}$ values obtained, as compared with those obtained at the untreated electrode; although values of $E_{\frac{1}{2}}$ were also cathodically shifted by increasing concentration of Fe(III) cyanide (Fig. 5-332). The limiting current density was linearly dependent upon the concentration of potassium ferricyanide to a level of significance better than 0.001, for the boron carbide solid electrode as prepared or after Ir(IV) perchlorate treatment (Fig. 5-333).

D.c. voltammetry of $K_3Fe(CN)_6$ (2.0×10^{-4} mol dm^{-3}) in KCl (0.1 to 2.0 M) supporting electrolyte shows that, at the boron carbide solid electrode as prepared, the reversibility of the charge transfer was much poorer when the concentration of KCl supporting electrolyte was low (i.e. 0.1 M). The αn value increased from 0.44, at KCl (0.1 M), to 0.67, at KCl (0.5 M), but subsequently declined to 0.57 at KCl (2.0 M). At the Ir(IV)-perchlorate treated boron carbide solid electrode, however, the αn values were only slightly affected by KCl concentration; αn values were 0.88, 0.88, and 0.82 at the KCl concentration of 0.1, 0.5, and 2.0 M respectively (Fig. 5-334). Fig. 5-335 indicates that, regardless of the electrode treatment, $E_{\frac{1}{2}}$ values were anodically shifted by increasing $(\text{ionic strength})^{\frac{1}{2}}$; thus suggesting, as expected, that the e.a.s. was anionic (equation 3-10). Higher concentrations of KCl supporting electrolyte enhanced the sensitivity of the working electrode towards $K_3Fe(CN)_6$ (Fig. 5-336).

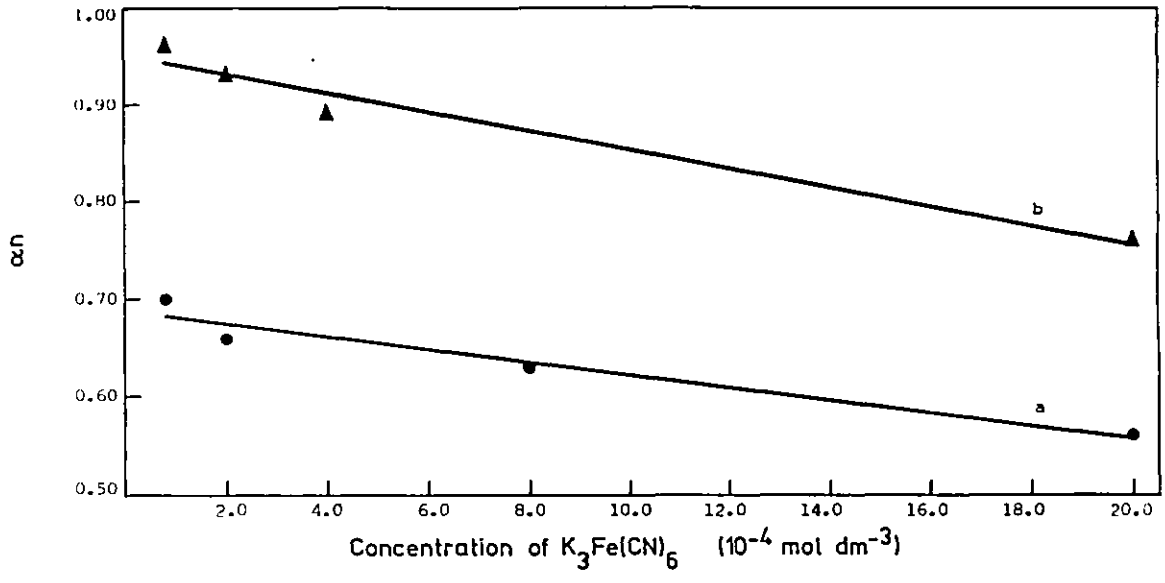

Fig. 5-331 Fe(III) cyanide (8.0×10^{-5} to 2.0×10^{-3} mol dm^{-3})/Potassium chloride (0.5 M) supporting electrolyte System: Values of αn as a function of concentration of potassium ferricyanide, [$K_3Fe(CN)_6$]. (a) Boron carbide solid electrode. (b) Boron carbide solid electrode treated with Ir(IV) perchlorate (1.0×10^{-4} mol dm^{-3}).

(a) Boron carbide solid electrode:

$\alpha n = 0.69 - 65 [K_3Fe(CN)_6]$
Correlation coefficient = -0.9569
Level of significance, $p = 0.02 < p < 0.05$
Standard deviation of αn from regression = 0.02
Degrees of freedom = 2

(b) Boron carbide solid electrode treated with Ir(IV) Perchlorate (1.0×10^{-4} mol dm^{-3}):

$\alpha n = 0.95 - 97 [K_3Fe(CN)_6]$
Correlation coefficient = -0.9793
Level of significance, $p = 0.02 < p < 0.05$
Standard deviation of αn from regression = 0.02
Degrees of freedom = 2

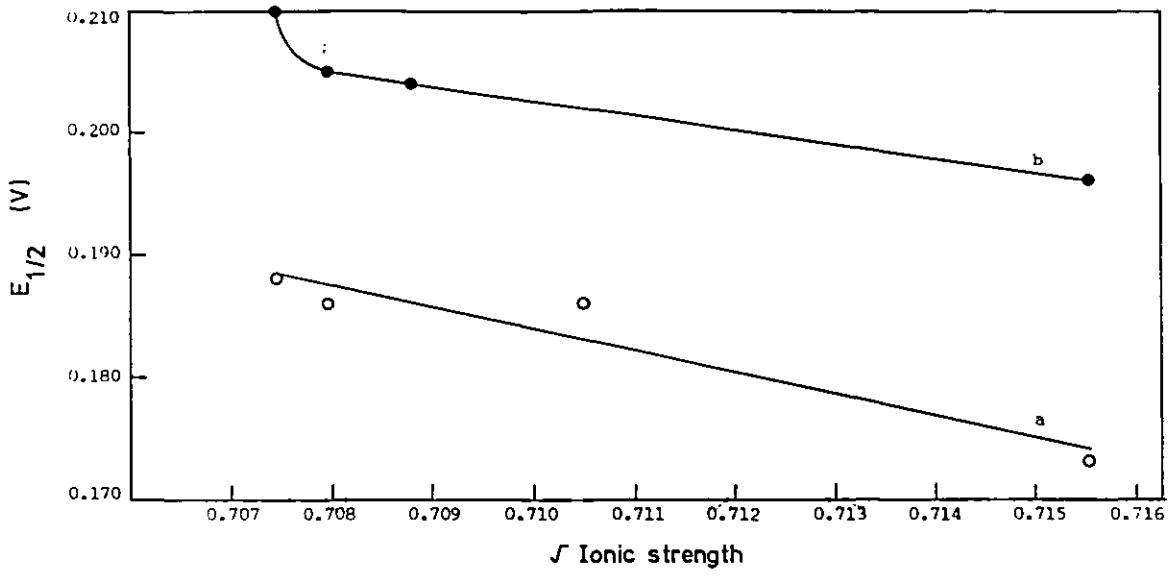

Fig. 5-332 Fe(III) cyanide (8.0×10^{-5} to 2.0×10^{-3} mol dm^{-3})/Potassium chloride (0.5 M) supporting electrolyte System: Values of half-wave potential, $E_{\frac{1}{2}}$, as a function of square root of total ionic strength (where the concentration of potassium ferricyanide was varied), $\sqrt{I}$. (a) Boron carbide solid electrode. (b) Boron carbide solid electrode treated with Ir(IV) perchlorate (1.0×10^{-4} mol dm^{-3}).

(a) Boron carbide solid electrode:

$E_{\frac{1}{2}} = 1.45 - 1.78\ \sqrt{I}$

Correlation coefficient = -0.95519

Level of significance, $p = 0.02 < p < 0.05$

Standard deviation of $E_{\frac{1}{2}}$ from regression = 0.003 V

Degrees of freedom = 2

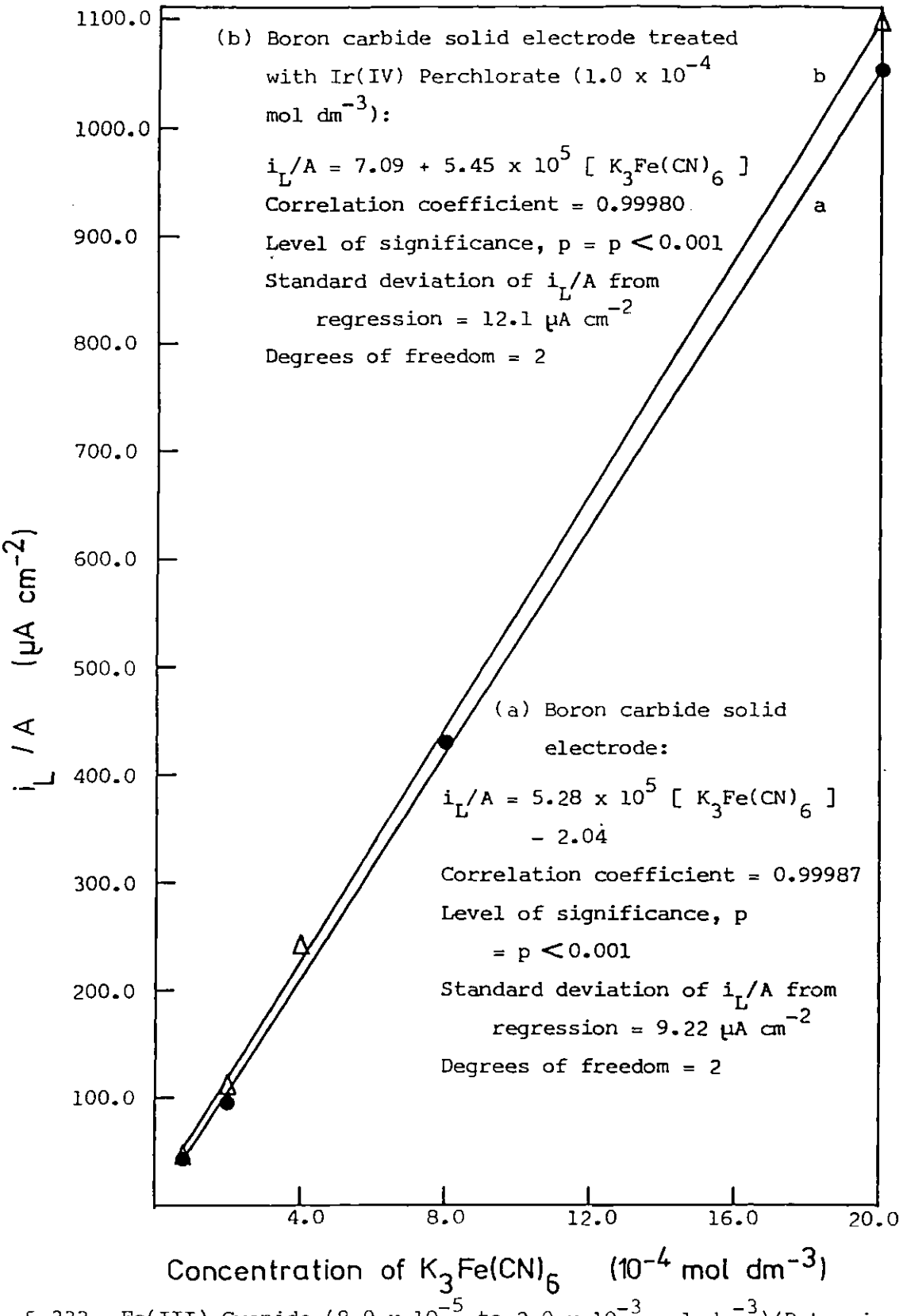

Fig. 5-333 Fe(III) Cyanide (8.0×10^{-5} to 2.0×10^{-3} mol dm^{-3})/Potassium chloride (0.5 M) supporting electrolyte System: Dependence of limiting current per unit area, i_L/A, on the concentration of potassium ferricyanide, [$K_3Fe(CN)_6$].

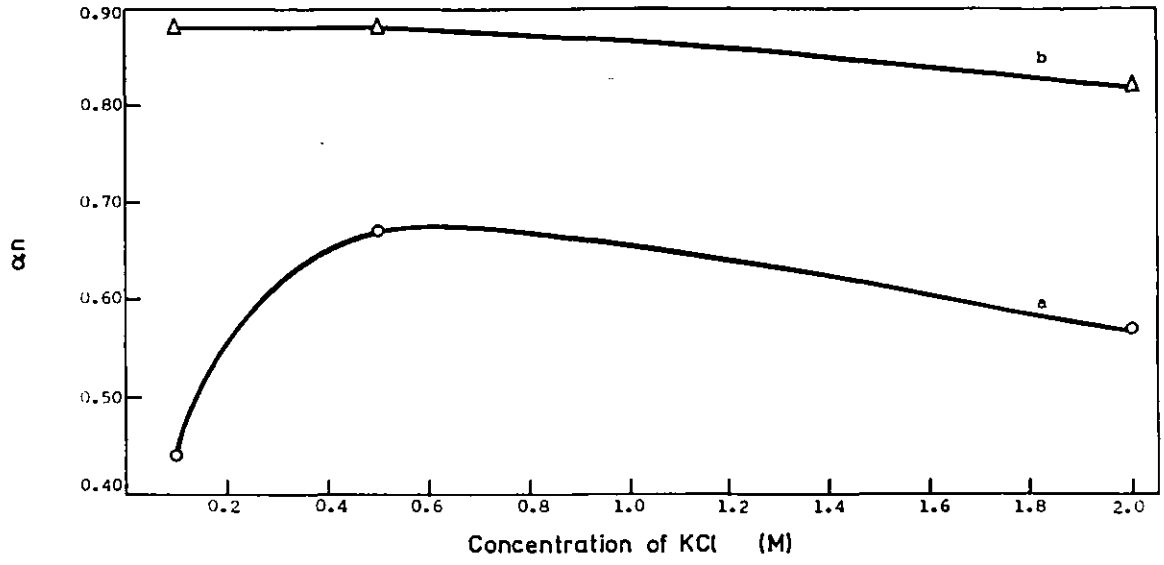

Fig. 5-334 Fe(III) cyanide (2.0×10^{-4} mol dm^{-3})/Potassium chloride (0.1 to 2.0 M) supporting electrolyte System: Values of αn as a function of concentration of potassium chloride supporting electrolyte, [KCl]. (a) Boron carbide solid electrode. (b) Boron carbide solid electrode treated with Ir(IV) perchlorate (1.0×10^{-4} mol dm^{-3}).

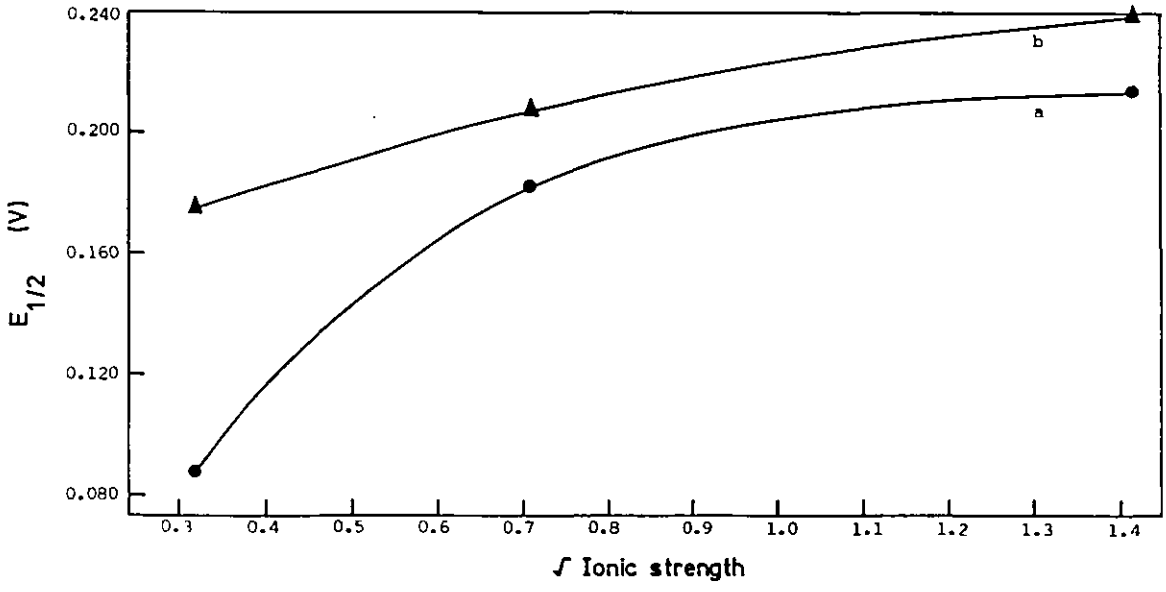

Fig. 5-335 Fe(III) cyanide (2.0×10^{-4} mol dm^{-3})/Potassium chloride (0.1 to 2.0 M) supporting electrolyte System: Values of half-wave potential, $E_{\frac{1}{2}}$, as a function of square root of total ionic strength (where the concentration of potassium chloride supporting electrolyte was varied), $\sqrt{I}$. (a) Boron carbide solid electrode. (b) Boron carbide solid electrode treated with Ir(IV) perchlorate (1.0×10^{-4} mol dm^{-3}).

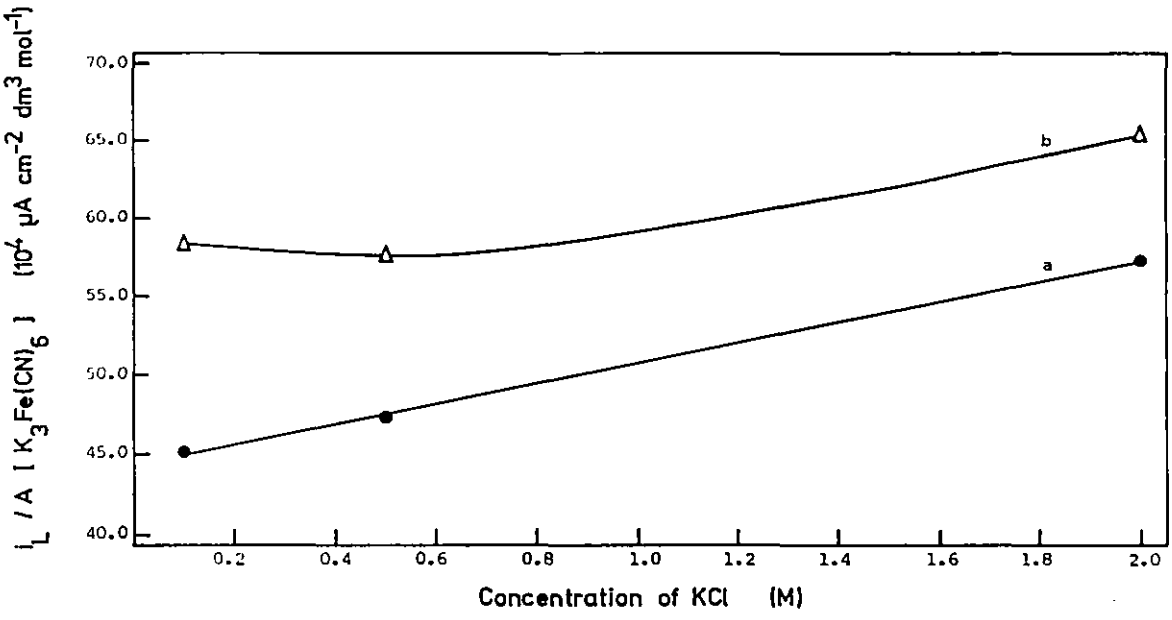

Fig. 5-336 Fe(III) cyanide (2.0×10^{-4} mol dm^{-3})/Potassium chloride (0.1 to 2.0 M) supporting electrolyte System: Values of limiting current per unit area divided by concentration of potassium ferricyanide, i_L/A [$K_3Fe(CN)_6$], as a function of concentration of potassium chloride supporting electrolyte, [KCl]. (a) Boron carbide solid electrode. (b) Boron carbide solid electrode treated with Ir(IV) perchlorate (1.0×10^{-4} mol dm^{-3}).

(a) i_L/A [$K_3Fe(CN)_6$] = $4.43 \times 10^5 + 6.50 \times 10^4$ [KCl]
Correlation coefficient = 0.999423
Level of significance, $p = 0.02 < p < 0.05$
Standard deviation of i_L/A [$K_3Fe(CN)_6$] from regression
= 3.13×10^3 μA cm^{-2} dm^3 mol^{-1}
Degrees of freedom = 1

5-2.3.(ii) Cyclic voltammetry.

The cathodic current functions, $i_{(c)}/v^{\frac{1}{2}}$, as functions of (sweep rate)$^{\frac{1}{2}}$, $v^{\frac{1}{2}}$, for the cyclic voltammograms of $K_3Fe(CN)_6$ (8.0×10^{-5} to 2.0×10^{-3} mol dm^{-3})/KCl (0.5 M) supporting electrolyte obtained at the boron carbide solid electrode are presented in Figures 5-337 to 5-340 inclusive. When compared with Figures 3-2 and 3-6, these experimental current functions suggest that the electrochemical reduction of Fe(III) cyanide involved not only slow electron transfer but also a chemical reaction; especially at higher concentrations of Fe(III) cyanide e.a.s.. The anodic current functions (Figures 5-341 to 5-344 inclusive), however, confirm that the chemical reaction was catalytic; especially at the top end of the concentration range investigated (Fig. 5-344).

After the boron carbide solid electrode had been treated with Ir (IV) perchlorate (1.0×10^{-4} mol dm^{-3}), the cathodic current functions as functions of (sweep rate)$^{\frac{1}{2}}$ reveal the influence of adsorption as well as the other factors of slow electron transfer and chemical reaction (Figures 5-345 to 5-348 inclusive). The anodic current functions also reveal that the charge transfer was slow and complicated by adsorption and catalytic reaction (Figures 5-349 to 5-352). The adsorption effect predominated at lower concentrations of Fe(III) cyanide, whereas the charge transfer became less reversible and the catalytic reaction became the dominant complication at higher concentrations of Fe(III) cyanide.

The peak potentials, plotted as functions of potential sweep rate, show that the cathodic peak potentials were cathodically shifted while the anodic peak potentials were anodically shifted by increasing sweep rate (Fig. 5-353); the potential shifts being smaller after the boron carbide solid electrode had been treated with Ir(IV) perchlorate. Thus the $|E_{p(c)} - E_{p(a)}|$ values obtained at the Ir(IV)-perchlorate treated electrode were less affected by sweep rate (Fig. 5-354); indicating an improvement in the reversibility of the charge transfer reaction. This is confirmed by Figures 5-355 and 5-356 which show that values of the absolute difference between peak and half-peak potentials, $|E_p - E_{p/2}|$, as functions of sweep rate, were narrower after the boron carbide solid electrode had been treated with Ir(IV) perchlorate.

The cathodic peak current density and the anodic peak current density were both linearly dependent upon the concentration of potassium ferricyanide to levels of significance better than 0.001; irrespective

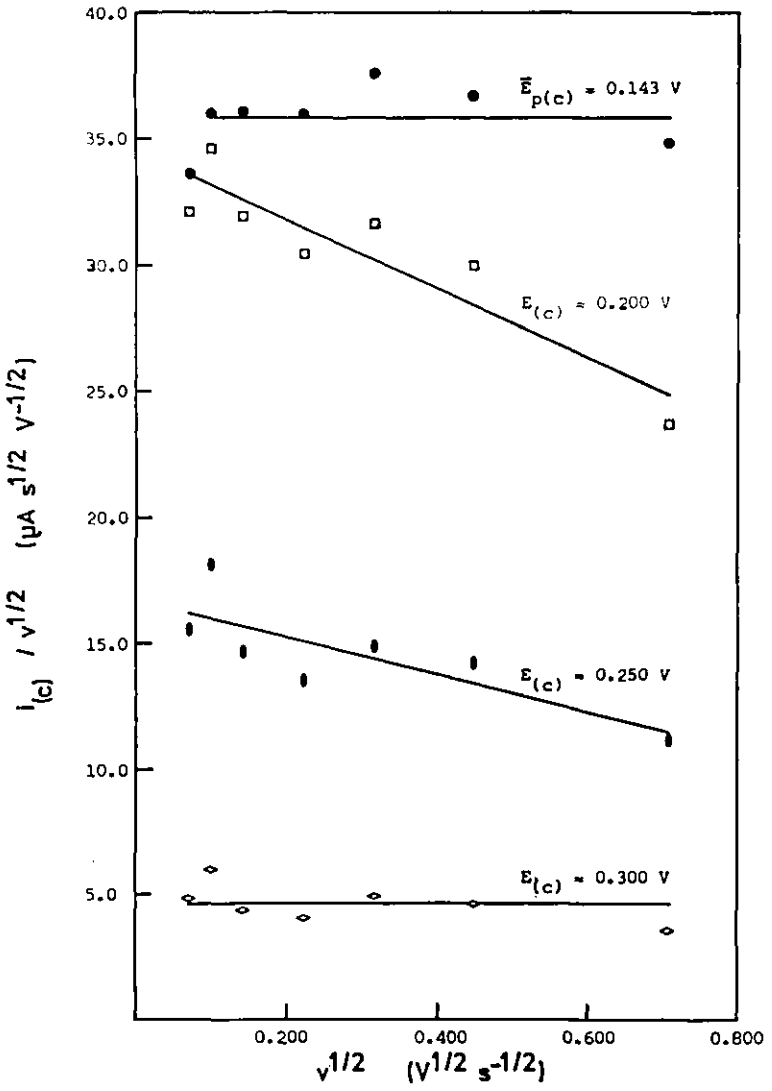

Fig. 5-337 Fe(III) Cyanide (8.0×10^{-5} mol dm^{-3})/Potassium chloride (0.5M) supporting electrolyte System: Values of cathodic current function, $i_{(c)}/v^{\frac{1}{2}}$ (at different potentials along the peak voltammograms), as a function of square root of potential scan rate, $v^{\frac{1}{2}}$. Boron carbide solid electrode.

(a) At $E_{(c)}$ = 0.300 V:

$i_{(c)}/v^{\frac{1}{2}}$ mean = 4.60 μA $s^{\frac{1}{2}}$ $V^{-\frac{1}{2}}$

Standard deviation = 0.775 μA $s^{\frac{1}{2}}$ $V^{-\frac{1}{2}}$

Coefficient of variation = 16.8%

Degrees of freedom = 6

(b) At $E_{(c)}$ = 0.250 V:

$i_{(c)}/v^{\frac{1}{2}} = 16.7 - 7.45\ v^{\frac{1}{2}}$

Correlation coefficient = -0.8027

Level of significance, $p = 0.02 < p < 0.05$

Standard deviation of $i_{(c)}/v^{\frac{1}{2}}$ from regression = 1.38 μA $s^{\frac{1}{2}}$ $V^{-\frac{1}{2}}$

Degrees of freedom = 5

(c) At $E_{(c)}$ = 0.200 V:

$i_{(c)}/v^{\frac{1}{2}} = 34.6 - 13.8\ v^{\frac{1}{2}}$

Correlation coefficient = -0.9135

Level of significance, $p = 0.001 < p < 0.01$

Standard deviation of $i_{(c)}/v^{\frac{1}{2}}$ from regression = 1.53 μA $s^{\frac{1}{2}}$ $V^{-\frac{1}{2}}$

Degrees of freedom = 5

(d) At $\bar{E}_{p(c)}$ = 0.143 V:

$i_{p(c)}/v^{\frac{1}{2}}$ mean = 35.8 μA $s^{\frac{1}{2}}$ $V^{-\frac{1}{2}}$

Standard deviation = 1.29 μA $s^{\frac{1}{2}}$ $V^{-\frac{1}{2}}$

Coefficient of variation = 3.59%

Degrees of freedom = 6

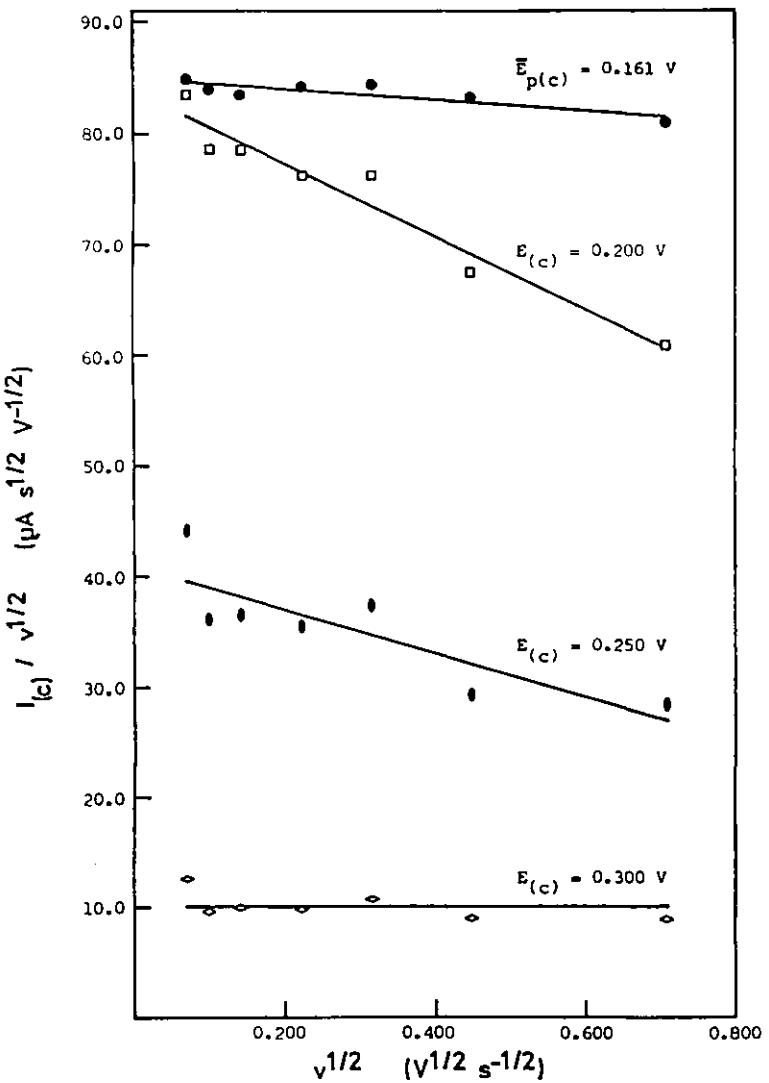

Fig. 5-338 Fe(III) Cyanide (2.0×10^{-4} mol dm^{-3})/Potassium chloride (0.5 M) supporting electrolyte System: Values of cathodic current function, $i_{(c)}/v^{\frac{1}{2}}$ (at different potentials along the peak voltammograms), as a function of square root of potential scan rate, $v^{\frac{1}{2}}$. Boron carbide solid electrode.

(a) At $E_{(c)}$ = 0.300 V:

$i_{(c)}/v^{\frac{1}{2}}$ mean = 10.0 μA $s^{\frac{1}{2}}$ $V^{-\frac{1}{2}}$

Standard deviation = 1.29 μA $s^{\frac{1}{2}}$ $V^{-\frac{1}{2}}$

Coefficient of variation = 12.9%

Degrees of freedom = 6

(b) At $E_{(c)}$ = 0.250 V:

$i_{(c)}/v^{\frac{1}{2}} = 40.9 - 19.7\ v^{\frac{1}{2}}$

Correlation coefficient = -0.8420

Level of significance, $p = 0.01 < p < 0.02$

Standard deviation of $i_{(c)}/v^{\frac{1}{2}}$ from regression = 3.14 μA $s^{\frac{1}{2}}$ $V^{-\frac{1}{2}}$

Degrees of freedom = 5

(c) At $E_{(c)}$ = 0.200 V:

$i_{(c)}/v^{\frac{1}{2}} = 83.9 - 33.1\ v^{\frac{1}{2}}$

Correlation coefficient = -0.9729

Level of significance, $p = p < 0.001$

Standard deviation of $i_{(c)}/v^{\frac{1}{2}}$ from regression = 1.96 μA $s^{\frac{1}{2}}$ $V^{-\frac{1}{2}}$

Degrees of freedom = 5

(d) At $\bar{E}_{p(c)}$ = 0.161 V:

$i_{p(c)}/v^{\frac{1}{2}} = 85.0 - 4.97\ v^{\frac{1}{2}}$

Correlation coefficient = -0.8627

Level of significance, $p = 0.01 < p < 0.02$

Standard deviation of $i_{p(c)}/v^{\frac{1}{2}}$ from regression = 0.72 μA $s^{\frac{1}{2}}$ $V^{-\frac{1}{2}}$

Degrees of freedom = 5

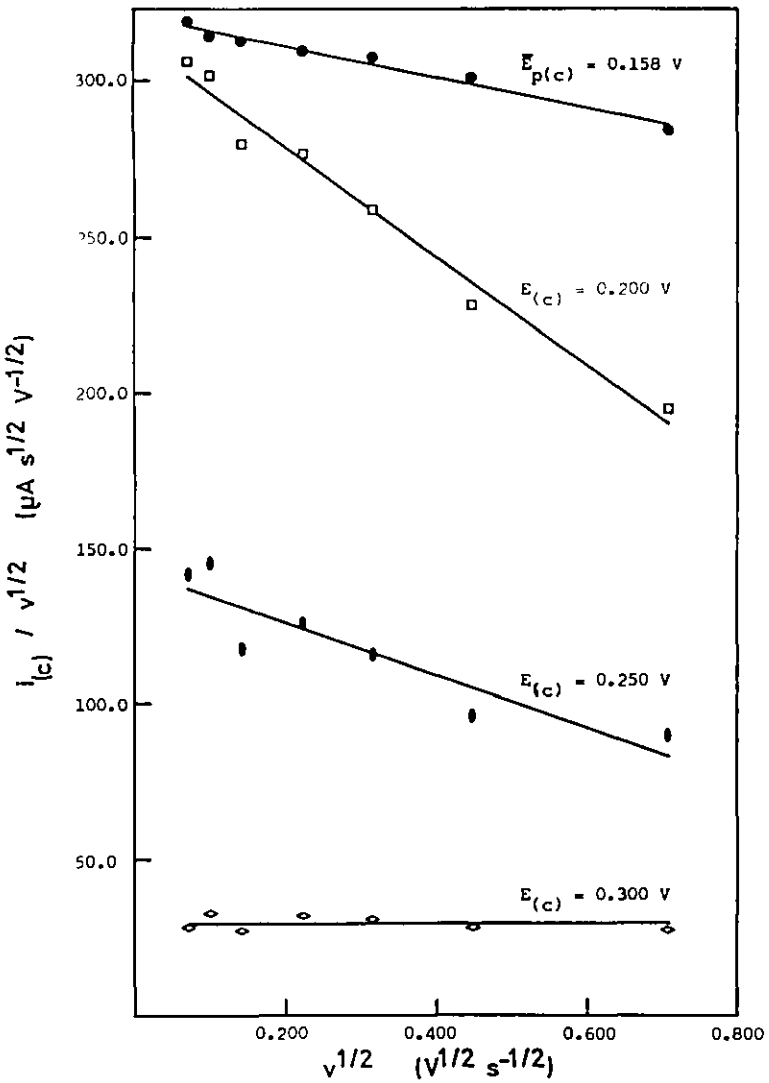

Fig. 5-339 Fe(III) Cyanide (8.0×10^{-4} mol dm^{-3})/Potassium chloride (0.5 M) supporting electrolyte System: Values of cathodic current function, $i_{(c)}/v^{\frac{1}{2}}$ (at different potentials along the peak voltammograms), as a function of square root of potential scan rate, $v^{\frac{1}{2}}$. Boron carbide solid electrode.

(a) At $E_{(c)}$ = 0.300 V:

$i_{(c)}/v^{\frac{1}{2}}$ mean = 29.4 μA $s^{\frac{1}{2}}$ $V^{-\frac{1}{2}}$

Standard deviation = 2.24 μA $s^{\frac{1}{2}}$ $V^{-\frac{1}{2}}$

Coefficient of variation = 7.61%

Degrees of freedom = 6

(b) At $E_{(c)}$ = 0.250 V:

$i_{(c)}/v^{\frac{1}{2}} = 142.8 - 84.9\ v^{\frac{1}{2}}$

Correlation coefficient = -0.9130

Level of significance, $p = 0.02 < p < 0.01$

Standard deviation of $i_{(c)}/v^{\frac{1}{2}}$ from regression = 9.40 μA $s^{\frac{1}{2}}$ $V^{-\frac{1}{2}}$

Degrees of freedom = 5

(c) At $E_{(c)}$ = 0.200 V:

$i_{(c)}/v^{\frac{1}{2}} = 313.8 - 175.5\ v^{\frac{1}{2}}$

Correlation coefficient = -0.9878

Level of significance, $p = p < 0.001$

Standard deviation of $i_{(c)}/v^{\frac{1}{2}}$ from regression = 6.90 μA $s^{\frac{1}{2}}$ $V^{-\frac{1}{2}}$

Degrees of freedom = 5

(d) At $\bar{E}_{p(c)}$ = 0.158 V:

$i_{p(c)}/v^{\frac{1}{2}} = 320.8 - 49.6\ v^{\frac{1}{2}}$

Correlation coefficient = -0.9873

Level of significance, $p = p < 0.001$

Standard deviation of $i_{p(c)}/v^{\frac{1}{2}}$ from regression = 2.00 μA $s^{\frac{1}{2}}$ $V^{-\frac{1}{2}}$

Degrees of freedom = 5

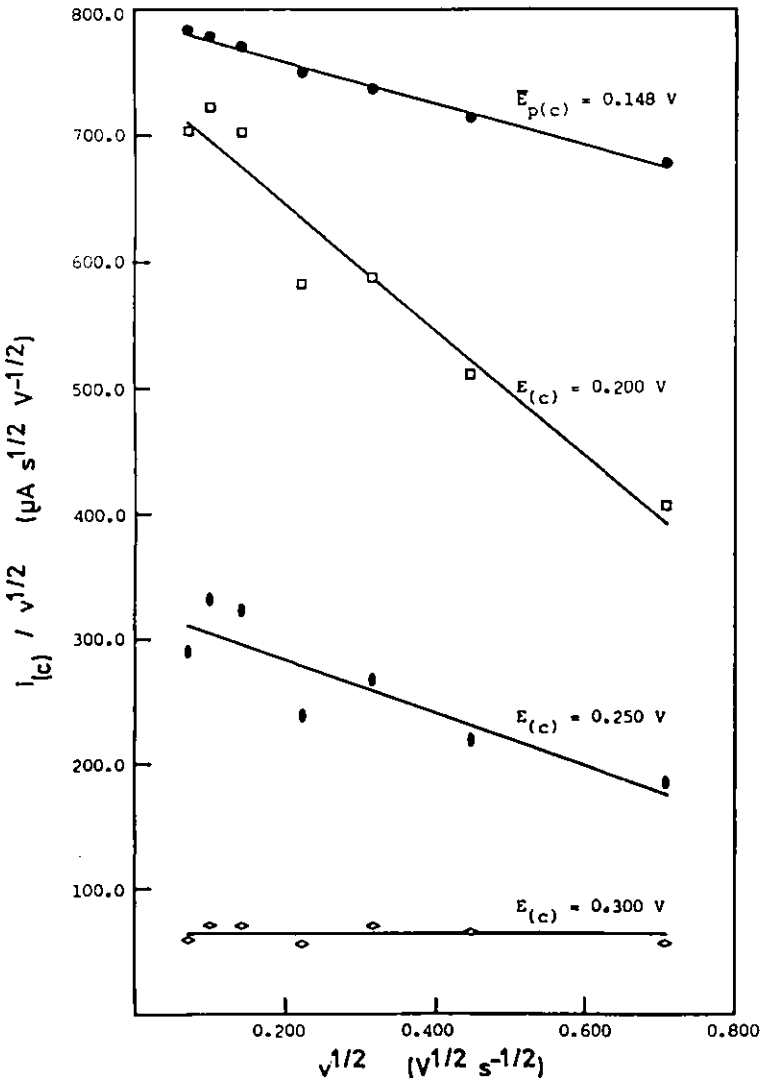

Fig. 5-340 Fe(III) Cyanide (2.0×10^{-3} mol dm^{-3})/Potassium chloride (0.5 M) supporting electrolyte System: Values of cathodic current function, $i_{(c)}/v^{\frac{1}{2}}$ (at different potentials along the peak voltammograms), as a function of square root of potential scan rate, $v^{\frac{1}{2}}$. Boron carbide solid electrode.

(a) At $E_{(c)}$ = 0.300 V:

$i_{(c)}/v^{\frac{1}{2}}$ mean = 64.1 μA $s^{\frac{1}{2}}$ $V^{-\frac{1}{2}}$

Standard deviation = 6.80 μA $s^{\frac{1}{2}}$ $V^{-\frac{1}{2}}$

Coefficient of variation = 10.6%

Degrees of freedom = 6

(b) At $E_{(c)}$ = 0.250 V:

$i_{(c)}/v^{\frac{1}{2}}$ = 326.0 - 213.3 $v^{\frac{1}{2}}$

Correlation coefficient = -0.8881

Level of significance, $p = 0.001 < p < 0.01$

Standard deviation of $i_{(c)}/v^{\frac{1}{2}}$ from regression = 27.5 μA $s^{\frac{1}{2}}$ $V^{-\frac{1}{2}}$

Degrees of freedom = 5

(c) At $E_{(c)}$ = 0.200 V:

$i_{(c)}/v^{\frac{1}{2}}$ = 745.3 - 500.2 $v^{\frac{1}{2}}$

Correlation coefficient = -0.9728

Level of significance, $p = p < 0.001$

Standard deviation of $i_{(c)}/v^{\frac{1}{2}}$ from regression = 29.6 μA $s^{\frac{1}{2}}$ $V^{-\frac{1}{2}}$

Degrees of freedom = 5

(d) At $E_{p(c)}$ = 0.148 V:

$i_{p(c)}/v^{\frac{1}{2}}$ = 793.2 - 169.5 $v^{\frac{1}{2}}$

Correlation coefficient = -0.9960

Level of significance, $p = p < 0.001$

Standard deviation of $i_{p(c)}/v^{\frac{1}{2}}$ from regression = 3.80 μA $s^{\frac{1}{2}}$ $V^{-\frac{1}{2}}$

Degrees of freedom = 5

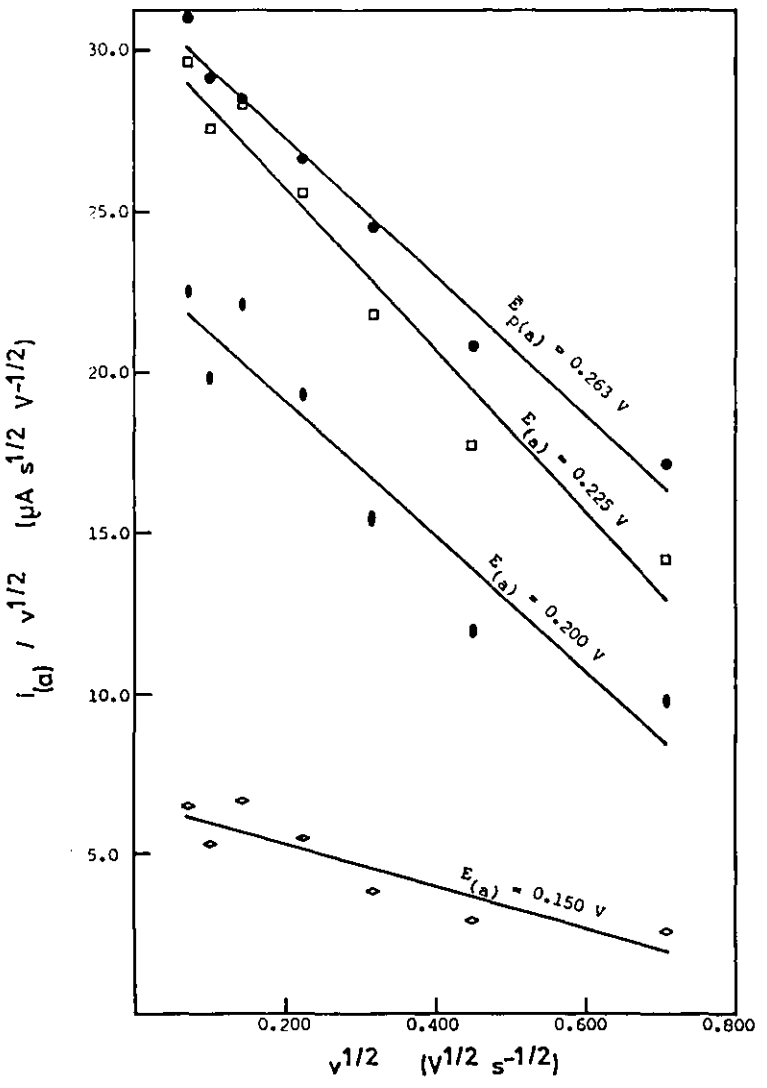

Fig. 5-341 Fe(III) Cyanide (8.0×10^{-5} mol dm^{-3})/Potassium chloride (0.5 M) supporting electrolyte System: Values of anodic current function, $i_{(a)}/v^{\frac{1}{2}}$ (at different potentials along the peak voltammograms), as a function of square root of potential scan rate, $v^{\frac{1}{2}}$. Boron carbide solid electrode.

(a) At $E_{(a)}$ = 0.150 V:

$i_{(a)}/v^{\frac{1}{2}} = 6.63 - 6.61\ v^{\frac{1}{2}}$

Correlation coefficient = -0.9025

Level of significance, $p = 0.001 < p < 0.01$

Standard deviation of $i_{(a)}/v^{\frac{1}{2}}$ from regression = 0.790 μA $s^{\frac{1}{2}}$ $V^{-\frac{1}{2}}$

Degrees of freedom = 5

(b) At $E_{(a)}$ = 0.200 V:

$i_{(a)}/v^{\frac{1}{2}} = 23.3 - 21.0\ v^{\frac{1}{2}}$

Correlation coefficient = -0.9554

Level of significance, $p = p < 0.001$

Standard deviation of $i_{(a)}/v^{\frac{1}{2}}$ from regression = 1.62 μA $s^{\frac{1}{2}}$ $V^{-\frac{1}{2}}$

Degrees of freedom = 5

(c) At $E_{(a)}$ = 0.225 V:

$i_{(a)}/v^{\frac{1}{2}} = 30.8 - 25.3\ v^{\frac{1}{2}}$

Correlation coefficient = -0.9800

Level of significance, $p = p < 0.001$

Standard deviation of $i_{(a)}/v^{\frac{1}{2}}$ from regression = 1.28 μA $s^{\frac{1}{2}}$ $V^{-\frac{1}{2}}$

Degrees of freedom = 5

(d) At $E_{p(a)}$ = 0.263 V:

$i_{p(a)}/v^{\frac{1}{2}} = 31.6 - 21.5\ v^{\frac{1}{2}}$

Correlation coefficient = -0.9901

Level of significance, $p = p < 0.001$

Standard deviation of $i_{p(a)}/v^{\frac{1}{2}}$ from regression = 0.760 μA $s^{\frac{1}{2}}$ $V^{-\frac{1}{2}}$

Degrees of freedom = 5

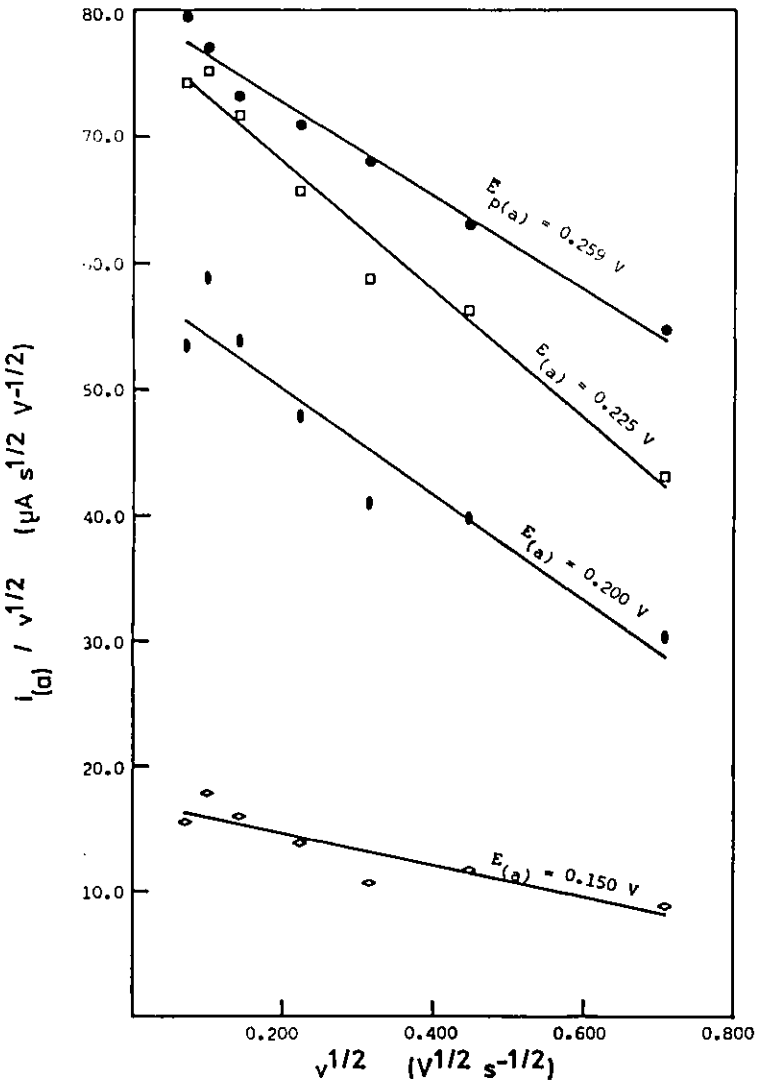

Fig. 5-342 Fe(III) Cyanide (2.0×10^{-4} mol dm^{-3})/Potassium chloride (0.5 M) supporting electrolyte System: Values of anodic current function, $i_{(a)}/v^{\frac{1}{2}}$ (at different potentials along the peak voltammograms), as a function of square root of potential scan rate, $v^{\frac{1}{2}}$. Boron carbide solid electrode.

(a) At $E_{(a)}$ = 0.150 V:

$i_{(a)}/v^{\frac{1}{2}} = 17.1 - 12.9\ v^{\frac{1}{2}}$

Correlation coefficient = -0.9029

Level of significance, $p = 0.001 < p < 0.01$

Standard deviation of $i_{(a)}/v^{\frac{1}{2}}$ from regression = 1.52 μA $s^{\frac{1}{2}}$ $V^{-\frac{1}{2}}$

Degrees of freedom = 5

(b) At $E_{(a)}$ = 0.200 V:

$i_{(a)}/v^{\frac{1}{2}} = 58.5 - 42.1\ v^{\frac{1}{2}}$

Correlation coefficient = -0.9580

Level of significance, $p = p < 0.001$

Standard deviation of $i_{(a)}/v^{\frac{1}{2}}$ from regression = 3.13 μA $s^{\frac{1}{2}}$ $V^{-\frac{1}{2}}$

Degrees of freedom = 5

(c) At $E_{(a)}$ = 0.225 V:

$i_{(a)}/v^{\frac{1}{2}} = 78.1 - 50.8\ v^{\frac{1}{2}}$

Correlation coefficient = -0.9884

Level of significance, $p = p < 0.001$

Standard deviation of $i_{(a)}/v^{\frac{1}{2}}$ from regression = 1.95 μA $s^{\frac{1}{2}}$ $V^{-\frac{1}{2}}$

Degrees of freedom = 5

(d) At $E_{p(a)}$ = 0.259 V:

$i_{p(a)}/v^{\frac{1}{2}} = 80.1 - 37.0\ v^{\frac{1}{2}}$

Correlation coefficient = -0.9895

Level of significance, $p = p < 0.001$

Standard deviation of $i_{p(a)}/v^{\frac{1}{2}}$ from regression = 1.35 μA $s^{\frac{1}{2}}$ $V^{-\frac{1}{2}}$

Degrees of freedom = 5

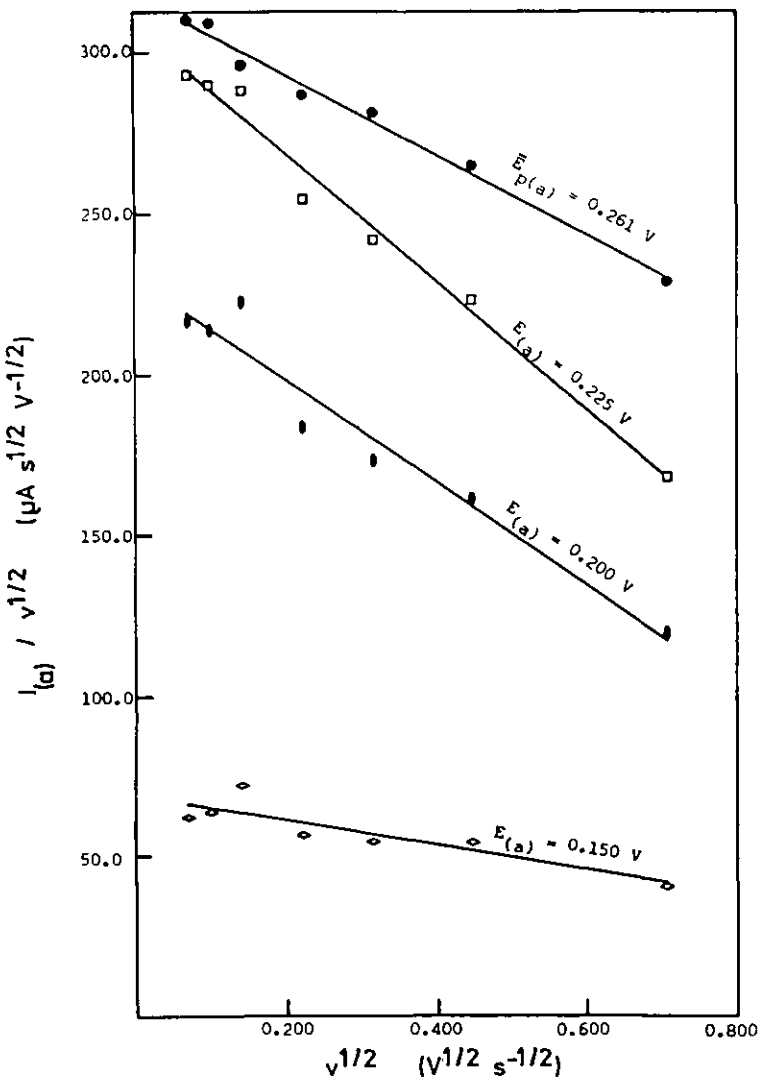

Fig. 5-343 Fe(III) Cyanide (8.0×10^{-4} mol dm^{-3})/Potassium chloride (0.5 M) supporting electrolyte System: Values of anodic current function, $i_{(a)}/v^{\frac{1}{2}}$ (at different potentials along the peak voltammograms), as a function of square root of potential scan rate, $v^{\frac{1}{2}}$. boron carbide solid electrode.

(a) At $E_{(a)}$ = 0.150 V:

$i_{(a)}/v^{\frac{1}{2}} = 68.6 - 38.6\ v^{\frac{1}{2}}$

Correlation coefficient = -0.8899

Level of significance, $p = 0.001 < p < 0.01$

Standard deviation of $i_{(a)}/v^{\frac{1}{2}}$ from regression = 4.92 μA $s^{\frac{1}{2}}$ $V^{-\frac{1}{2}}$

Degrees of freedom = 5

(b) At $E_{(a)}$ = 0.200 V:

$i_{(a)}/v^{\frac{1}{2}} = 230.2 - 159.8\ v^{\frac{1}{2}}$

Correlation coefficient = -0.9769

Level of significance, $p = p < 0.001$

Standard deviation of $i_{(a)}/v^{\frac{1}{2}}$ from regression = 8.70 μA $s^{\frac{1}{2}}$ $V^{-\frac{1}{2}}$

Degrees of freedom = 5

(c) At $E_{(a)}$ = 0.225 V:

$i_{(a)}/v^{\frac{1}{2}} = 308.3 - 199.6\ v^{\frac{1}{2}}$

Correlation coefficient = -0.9931

Level of significance, $p = p < 0.001$

Standard deviation of $i_{(a)}/v^{\frac{1}{2}}$ from regression = 5.89 μA $s^{\frac{1}{2}}$ $V^{-\frac{1}{2}}$

Degrees of freedom = 5

(d) At $\bar{E}_{p(a)}$ = 0.261 V:

$i_{p(a)}/v^{\frac{1}{2}} = 318.2 - 124.9\ v^{\frac{1}{2}}$

Correlation coefficient = -0.9943

Level of significance, $p = p < 0.001$

Standard deviation of $i_{p(a)}/v^{\frac{1}{2}}$ from regression = 3.30 μA $s^{\frac{1}{2}}$ $V^{-\frac{1}{2}}$

Degrees of freedom = 5

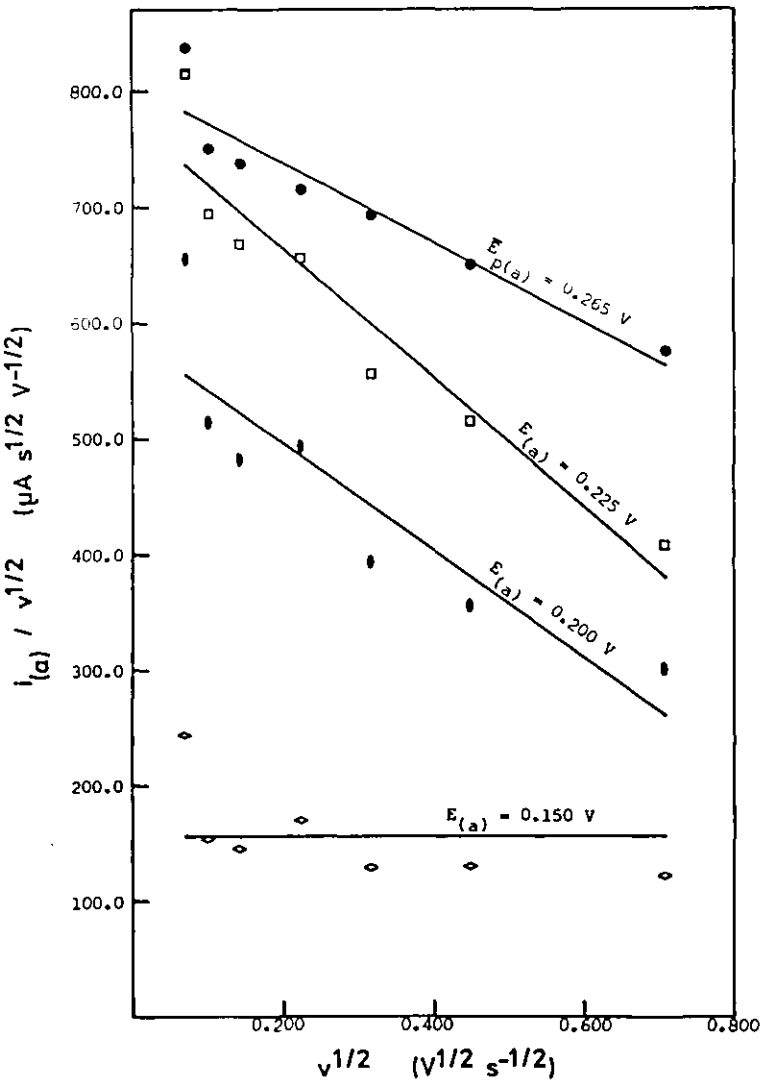

Fig. 5-344 Fe(III) Cyanide (2.0×10^{-3} mol dm^{-3})/Potassium chloride (0.5 M) supporting electrolyte System: Values of anodic current function, $i_{(a)}/v^{\frac{1}{2}}$ (at different potentials along the peak voltammograms), as a function of square root of potential scan rate, $v^{\frac{1}{2}}$. Boron carbide solid electrode.

(a) At $E_{(a)}$ = 0.150 V:

$i_{(a)}/v^{\frac{1}{2}}$ mean = 156.0 μA $s^{\frac{1}{2}}$ $V^{-\frac{1}{2}}$

Standard deviation = 42.0 μA $s^{\frac{1}{2}}$ $V^{-\frac{1}{2}}$

Coefficient of variation = 26.9%

Degrees of freedom = 6

(b) At $E_{(a)}$ = 0.200 V:

$i_{(a)}/v^{\frac{1}{2}}$ = 588.8 − 463.7 $v^{\frac{1}{2}}$

Correlation coefficient = -0.8920

Level of significance, $p = 0.001 < p < 0.01$

Standard deviation of $i_{(a)}/v^{\frac{1}{2}}$ from regression = 58.5 μA $s^{\frac{1}{2}}$ $V^{-\frac{1}{2}}$

Degrees of freedom = 5

(c) At $E_{(a)}$ = 0.225 V:

$i_{(a)}/v^{\frac{1}{2}}$ = 776.2 − 560.1 $v^{\frac{1}{2}}$

Correlation coefficient = -0.9500

Level of significance, $p = 0.001 < p < 0.01$

Standard deviation of $i_{(a)}/v^{\frac{1}{2}}$ from regression = 45.8 μA $s^{\frac{1}{2}}$ $V^{-\frac{1}{2}}$

Degrees of freedom = 5

(d) At $\bar{E}_{p(a)}$ = 0.265 V:

$i_{p(a)}/v^{\frac{1}{2}}$ = 806.8 − 343.5 $v^{\frac{1}{2}}$

Correlation coefficient = -0.9477

Level of significance, $p = 0.001 < p < 0.01$

Standard deviation of $i_{p(a)}/v^{\frac{1}{2}}$ from regression = 28.8 μA $s^{\frac{1}{2}}$ $V^{-\frac{1}{2}}$

Degrees of freedom = 5

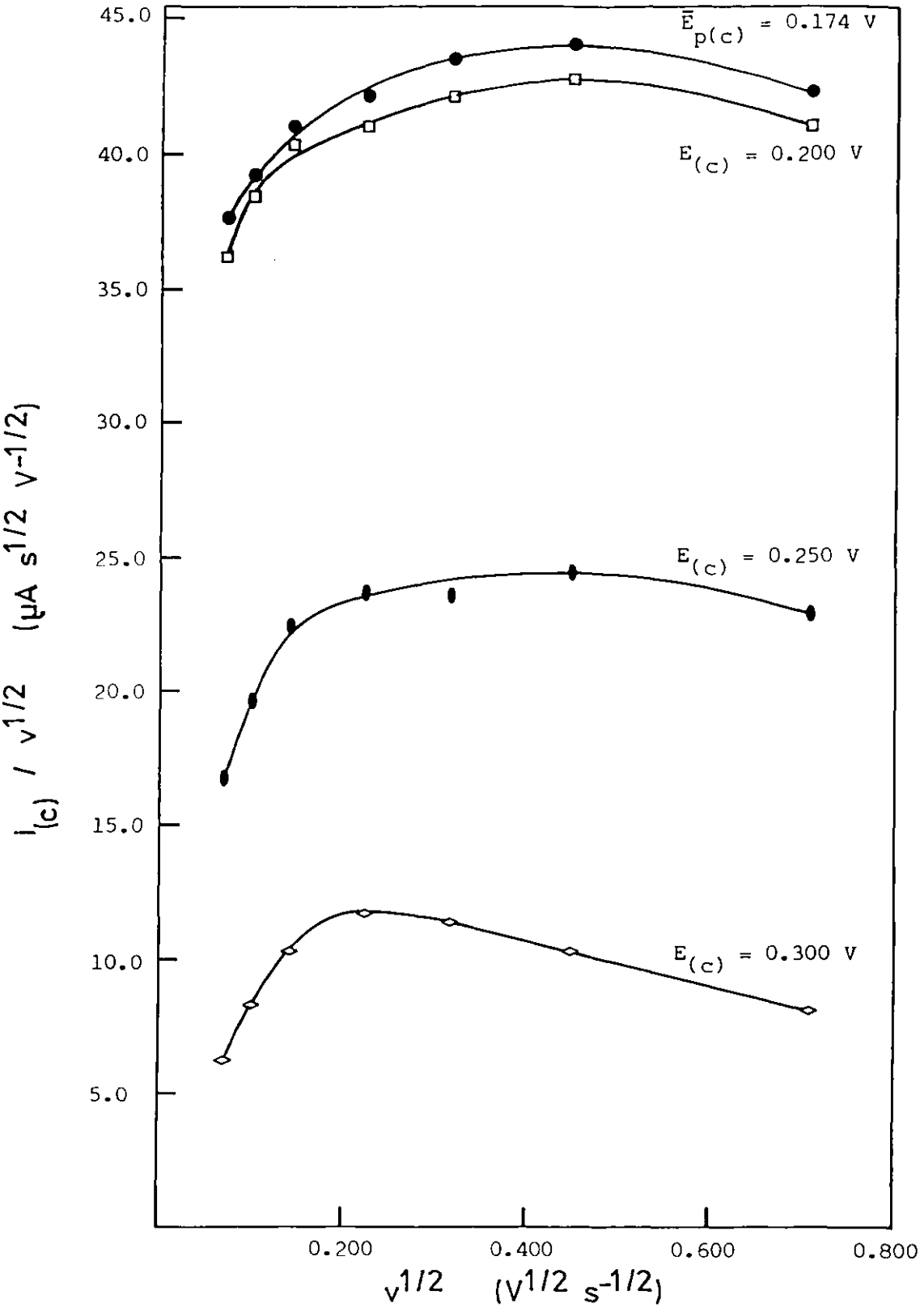

Fig. 5-345 Fe(III) Cyanide (8.0×10^{-5} mol dm^{-3})/Potassium chloride (0.5 M) supporting electrolyte System: Values of cathodic current function, $i_{(c)}/v^{\frac{1}{2}}$ (at different potentials along the peak voltammograms), as a function of square root of potential scan rate, $v^{\frac{1}{2}}$. Boron carbide solid electrode treated with Ir(IV) Perchlorate (1.0×10^{-4} mol dm^{-3}).

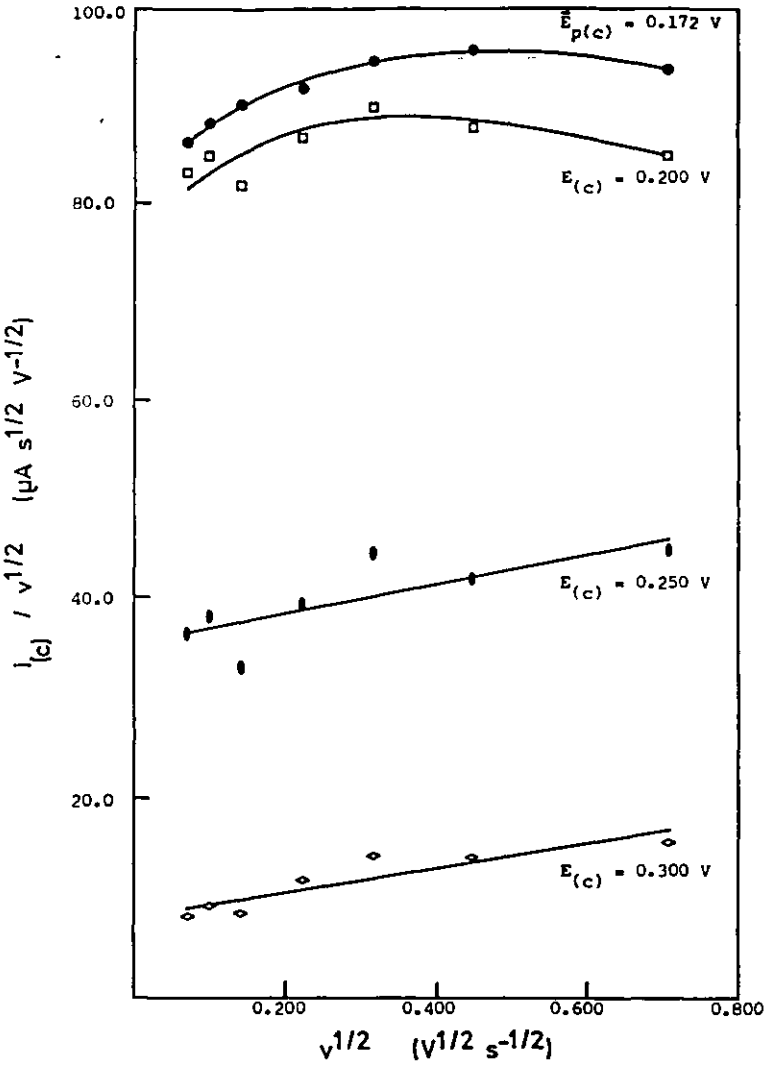

Fig. 5-346 Fe(III) Cyanide (2.0×10^{-4} mol dm^{-3})/Potassium chloride (0.5 M) supporting electrolyte System: Values of cathodic current function, $i_{(c)}/v^{\frac{1}{2}}$ (at different potentials along the peak voltammograms), as a function of square root of potential scan rate, $v^{\frac{1}{2}}$. Boron carbide solid electrode treated with Ir(IV) Perchlorate (1.0×10^{-4} mol dm^{-3}).

(a) At $E_{(c)}$ = 0.300 V:

$i_{(c)}/v^{\frac{1}{2}} = 8.13 + 12.2\ v^{\frac{1}{2}}$

Correlation coefficient = 0.9035

Level of significance, $p = 0.001 < p < 0.01$

Standard deviation of $i_{(c)}/v^{\frac{1}{2}}$ from regression = 1.45 μA $s^{\frac{1}{2}}$ $V^{-\frac{1}{2}}$

Degrees of freedom = 5

(b) At $E_{(c)}$ = 0.250 V:

$i_{(c)}/v^{\frac{1}{2}} = 35.4 + 14.7\ v^{\frac{1}{2}}$

Correlation coefficient = 0.7816

Level of significance, $p = 0.02 < p < 0.05$

Standard deviation of $i_{(c)}/v^{\frac{1}{2}}$ from regression = 2.93 μA $s^{\frac{1}{2}}$ $V^{-\frac{1}{2}}$

Degrees of freedom = 5

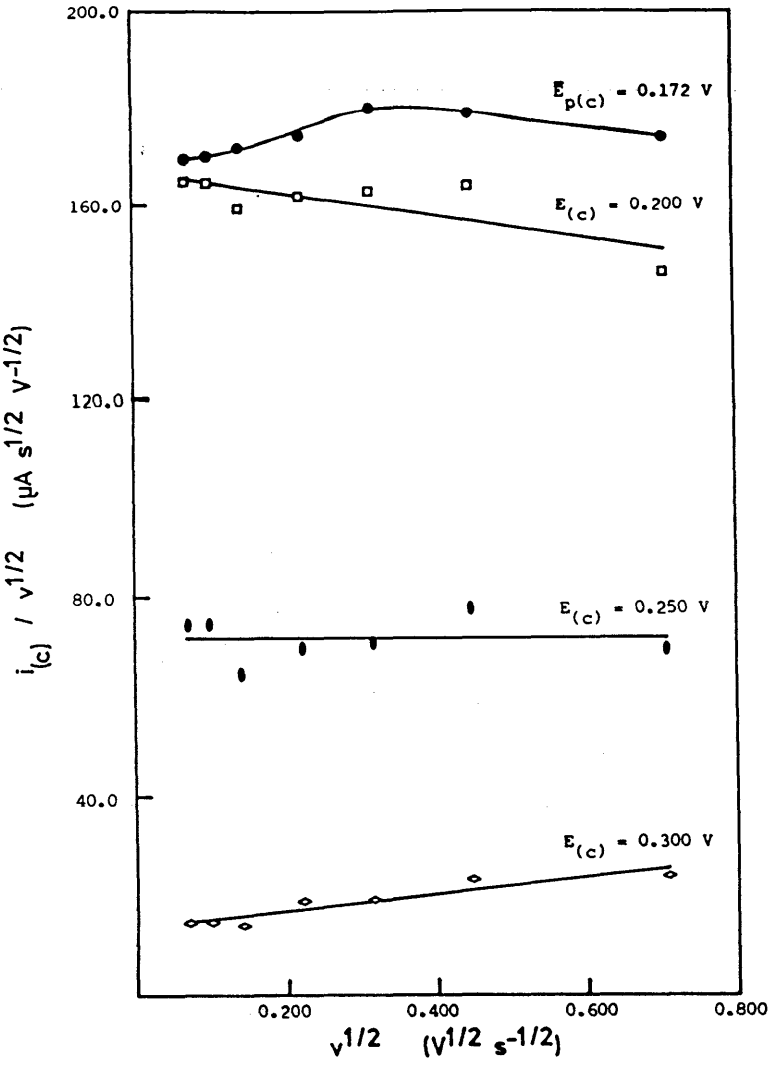

Fig. 5-347 Fe(III) Cyanide (4.0×10^{-4} mol dm^{-3})/Potassium chloride (0.5 M) supporting electrolyte System: Values of cathodic current function, $i_{(c)}/v^{\frac{1}{2}}$ (at different potentials along the peak voltammograms), as a function of square root of potential scan rate, $v^{\frac{1}{2}}$. Boron carbide solid electrode treated with Ir(IV) Perchlorate (1.0×10^{-4} mol dm^{-3}).

(a) At $E_{(c)}$ = 0.300 V:

$i_{(c)}/v^{\frac{1}{2}} = 13.8 + 16.6\ v^{\frac{1}{2}}$

Correlation coefficient = 0.9299

Level of significance, $p = 0.001 < p < 0.01$

Standard deviation of $i_{(c)}/v^{\frac{1}{2}}$ from regression = 1.64 μA $s^{\frac{1}{2}}$ $V^{-\frac{1}{2}}$

Degrees of freedom = 5

(b) At $E_{(c)}$ = 0.250 V:

$i_{(c)}/v^{\frac{1}{2}}$ mean = 71.5 μA $s^{\frac{1}{2}}$ $V^{-\frac{1}{2}}$

Standard deviation = 4.42 μA $s^{\frac{1}{2}}$ $V^{-\frac{1}{2}}$

Coefficient of variation = 6.18%

Degrees of freedom = 6

(c) At $E_{(c)}$ = 0.200 V:

$i_{(c)}/v^{\frac{1}{2}} = 167.0 - 23.2\ v^{\frac{1}{2}}$

Correlation coefficient = -0.7830

Level of significance, $p = 0.02 < p < 0.05$

Standard deviation of $i_{(c)}/v^{\frac{1}{2}}$ from regression = 4.60 μA $s^{\frac{1}{2}}$ $V^{-\frac{1}{2}}$

Degrees of freedom = 5

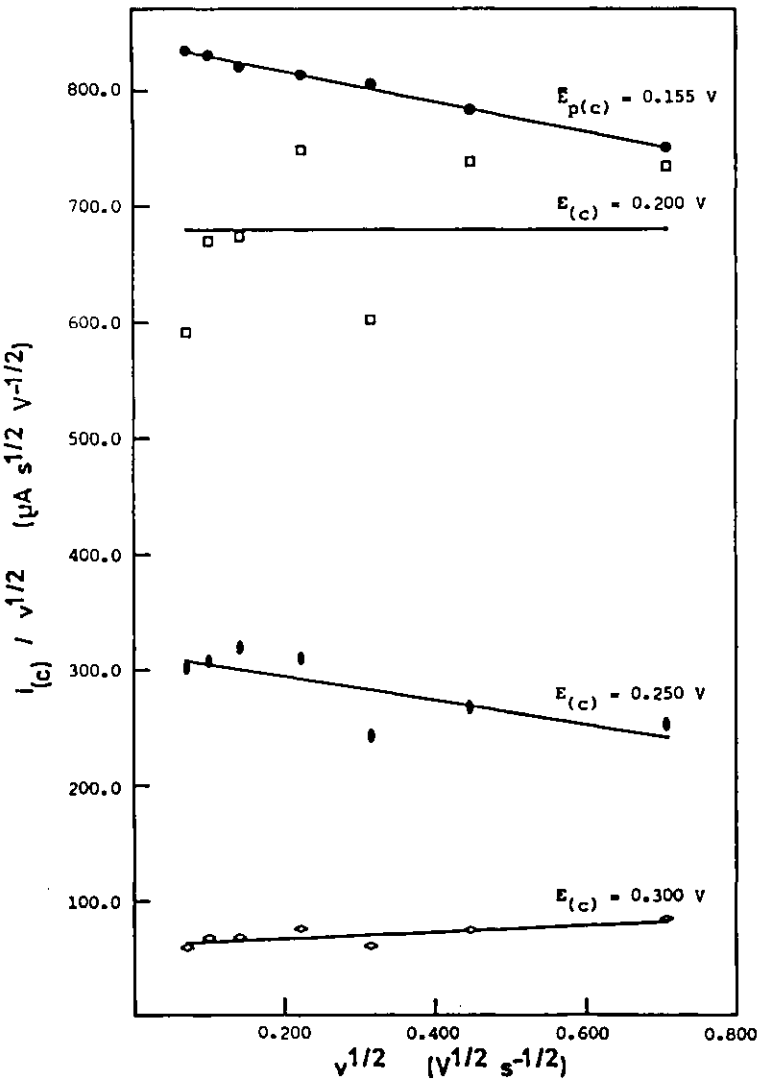

Fig. 5-348 Fe(III) Cyanide (2.0×10^{-3} mol dm^{-3})/Potassium chloride (0.5 M) supporting electrolyte System: Values of cathodic current function, $i_{(c)}/v^{\frac{1}{2}}$ (at different potentials along the peak voltammograms), as a function of square root of potential scan rate, $v^{\frac{1}{2}}$. Boron carbide solid electrode treated with Ir(IV) Perchlorate (1.0×10^{-4} mol dm^{-3}).

(a) At $E_{(c)}$ = 0.300 V:

$i_{(c)}/v^{\frac{1}{2}} = 61.1 + 28.9\ v^{\frac{1}{2}}$

Correlation coefficient = 0.7616

Level of significance, $p = 0.02 < p < 0.05$

Standard deviation of $i_{(c)}/v^{\frac{1}{2}}$ from regression = 6.13 μA $s^{\frac{1}{2}}$ $V^{-\frac{1}{2}}$

Degrees of freedom = 5

(b) At $E_{(c)}$ = 0.250 V:

$i_{(c)}/v^{\frac{1}{2}} = 315.5 - 105.1\ v^{\frac{1}{2}}$

Correlation coefficient = -0.7649

Level of significance, $p = 0.02 < p < 0.05$

Standard deviation of $i_{(c)}/v^{\frac{1}{2}}$ from regression = 22.0 μA $s^{\frac{1}{2}}$ $V^{-\frac{1}{2}}$

Degrees of freedom = 5

(c) At $E_{(c)}$ = 0.200 V:

$i_{(c)}/v^{\frac{1}{2}}$ mean = 679.6 μA $s^{\frac{1}{2}}$ $V^{-\frac{1}{2}}$

Standard deviation = 64.7 μA $s^{\frac{1}{2}}$ $V^{-\frac{1}{2}}$

Coefficient of variation = 9.52%

Degrees of freedom = 6

(d) At $\bar{E}_{p(c)}$ = 0.155 V:

$i_{p(c)}/v^{\frac{1}{2}} = 842.0 - 130.2\ v^{\frac{1}{2}}$

Correlation coefficient = -0.9972

Level of significance, $p = p < 0.001$

Standard deviation of $i_{p(c)}/v^{\frac{1}{2}}$ from regression = 2.44 μA $s^{\frac{1}{2}}$ $V^{-\frac{1}{2}}$

Degrees of freedom = 5

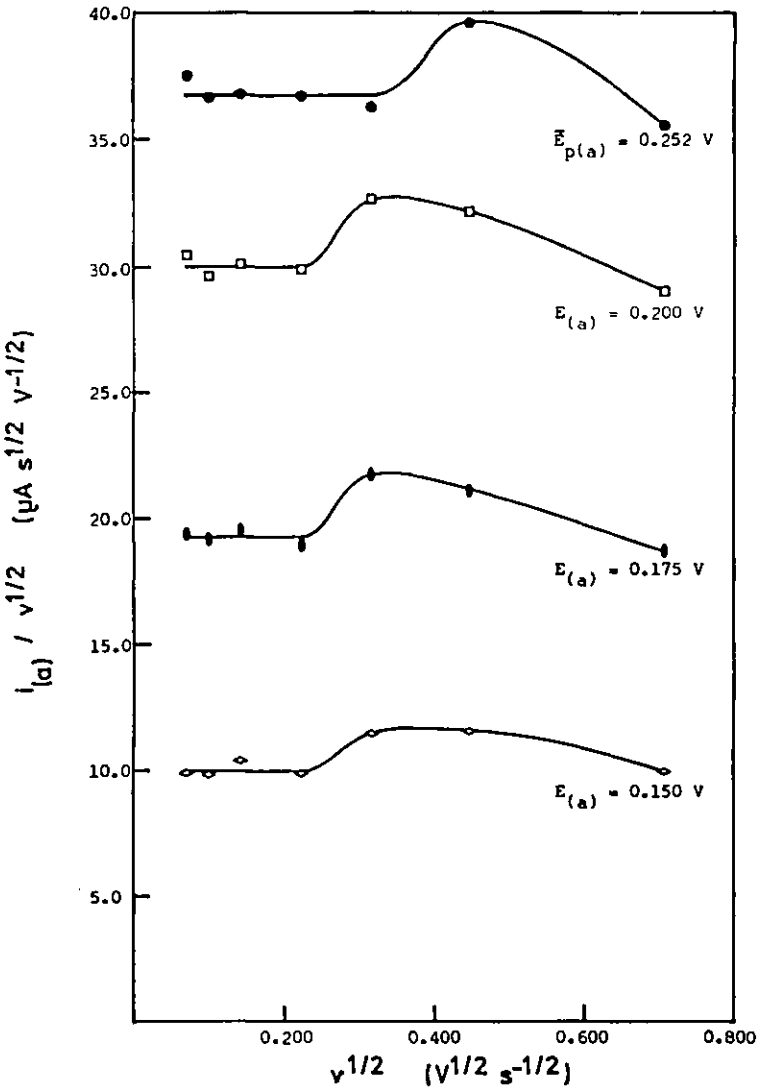

Fig. 5-349 Fe(III) Cyanide (8.0×10^{-5} mol dm^{-3})/Potassium chloride (0.5 M) supporting electrolyte System: Values of anodic current function, $i_{(a)}/v^{\frac{1}{2}}$ (at different potentials along the peak voltammograms), as a function of square root of potential scan rate, $v^{\frac{1}{2}}$. Boron carbide solid electrode treated with Ir(IV) Perchlorate (1.0×10^{-4} mol dm^{-3}).

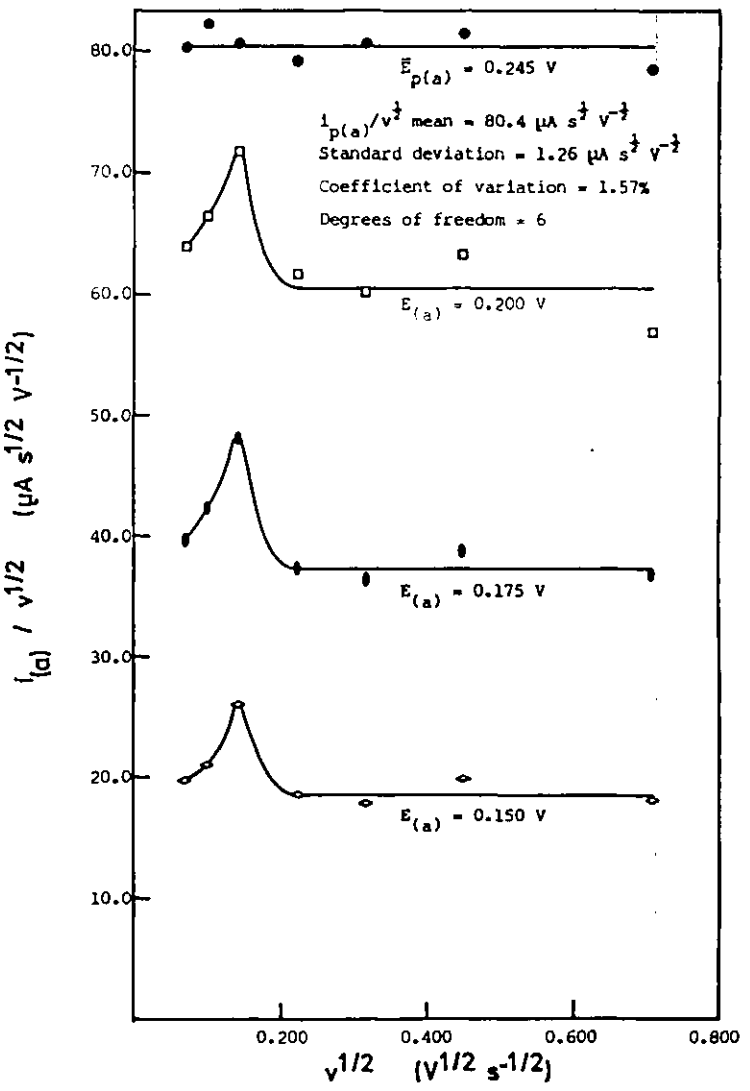

Fig. 5-350 Fe(III) Cyanide (2.0×10^{-4} mol dm^{-3})/Potassium chloride (0.5 M) supporting electrolyte System: Values of anodic current function, $i_{(a)}/v^{\frac{1}{2}}$ (at different potentials along the peak voltammograms), as a function of square root of potential scan rate, $v^{\frac{1}{2}}$. Boron carbide solid electrode treated with Ir(IV) Perchlorate (1.0×10^{-4} mol dm^{-3}).

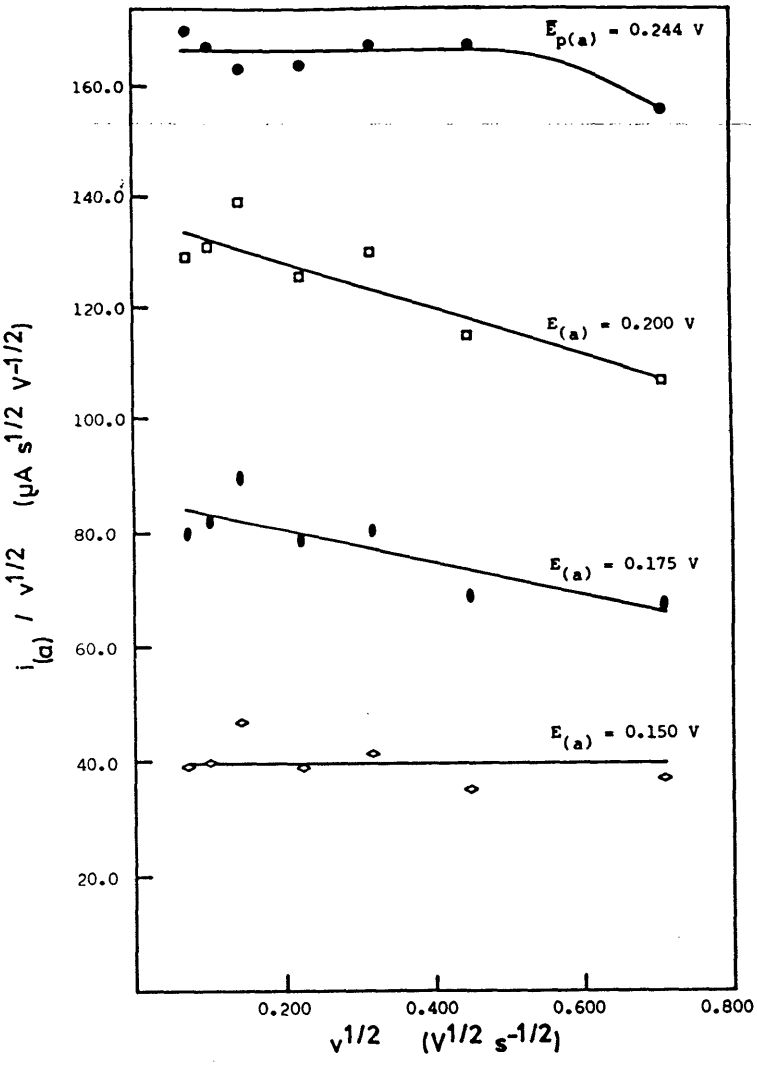

Fig. 5-351 Fe(III) Cyanide (4.0 x 10^{-4} mol dm^{-3})/Potassium chloride (0.5 M) supporting electrolyte System: Values of anodic current function, $i_{(a)}/v^{\frac{1}{2}}$ (at different potentials along the peak voltammograms), as a function of square root of potential scan rate, $v^{\frac{1}{2}}$. Boron carbide solid electrode treated with Ir(IV) Perchlorate (1.0 x 10^{-4} mol dm^{-3}).

(a) At $E_{(a)}$ = 0.150 V:

$i_{(a)}/v^{\frac{1}{2}}$ mean = 39.6 μA $s^{\frac{1}{2}}$ $V^{-\frac{1}{2}}$

Standard deviation = 3.77 μA $s^{\frac{1}{2}}$ $V^{-\frac{1}{2}}$

Coefficient of variation = 9.52%

Degrees of freedom = 6

(b) At $E_{(a)}$ = 0.175 V:

$i_{(a)}/v^{\frac{1}{2}}$ = 86.4 - 28.8 $v^{\frac{1}{2}}$

Correlation coefficient = -0.8347

Level of significance, $p = 0.01 < p < 0.02$

Standard deviation of $i_{(a)}/v^{\frac{1}{2}}$ from regression = 4.73 μA $s^{\frac{1}{2}}$ $V^{-\frac{1}{2}}$

Degrees of freedom = 5

(c) At $E_{(a)}$ = 0.200 V:

$i_{(a)}/v^{\frac{1}{2}}$ = 137.4 - 43.3 $v^{\frac{1}{2}}$

Correlation coefficient = -0.8941

Level of significance, $p = 0.001 < p < 0.01$

Standard deviation of $i_{(a)}/v^{\frac{1}{2}}$ from regression = 5.40 μA $s^{\frac{1}{2}}$ $V^{-\frac{1}{2}}$

Degrees of freedom = 5

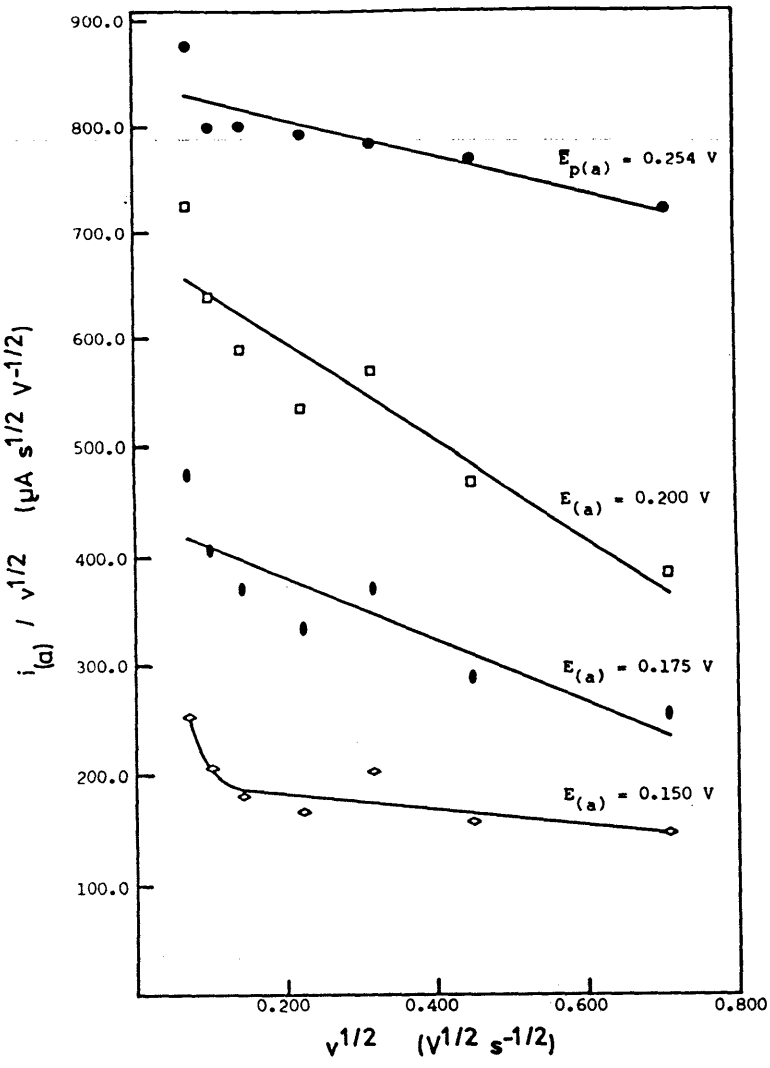

Fig. 5-352 Fe(III) Cyanide (2.0×10^{-3} mol dm^{-3})/Potassium chloride (0.5 M) supporting electrolyte System: Values of anodic current function, $i_{(a)}/v^{\frac{1}{2}}$ (at different potentials along the peak voltammograms), as a function of square root of potential scan rate, $v^{\frac{1}{2}}$. Boron carbide solid electrode treated with Ir(IV) Perchlorate (1.0×10^{-4} mol dm^{-3}).

(b) At $E_{(a)}$ = 0.175 V:

$i_{(a)}/v^{\frac{1}{2}} = 438.9 - 286.8\ v^{\frac{1}{2}}$

Correlation coefficient = -0.8860

Level of significance, $p = 0.001 < p < 0.01$

Standard deviation of $i_{(a)}/v^{\frac{1}{2}}$ from regression = 37.3 μA $s^{\frac{1}{2}}$ $V^{-\frac{1}{2}}$

Degrees of freedom = 5

(c) At $E_{(a)}$ = 0.200 V:

$i_{(a)}/v^{\frac{1}{2}} = 688.3 - 456.1\ v^{\frac{1}{2}}$

Correlation coefficient = -0.9315

Level of significance, $p = 0.001 < p < 0.01$

Standard deviation of $i_{(a)}/v^{\frac{1}{2}}$ from regression = 44.3 μA $s^{\frac{1}{2}}$ $V^{-\frac{1}{2}}$

Degrees of freedom = 5

(d) At $\bar{E}_{p(a)}$ = 0.254 V:

$i_{p(a)}/v^{\frac{1}{2}} = 842.6 - 176.2\ v^{\frac{1}{2}}$

Correlation coefficient = -0.8634

Level of significance, $p = 0.01 < p < 0.02$

Standard deviation of $i_{p(a)}/v^{\frac{1}{2}}$ from regression = 25.6 μA $s^{\frac{1}{2}}$ $V^{-\frac{1}{2}}$

Degrees of freedom = 5

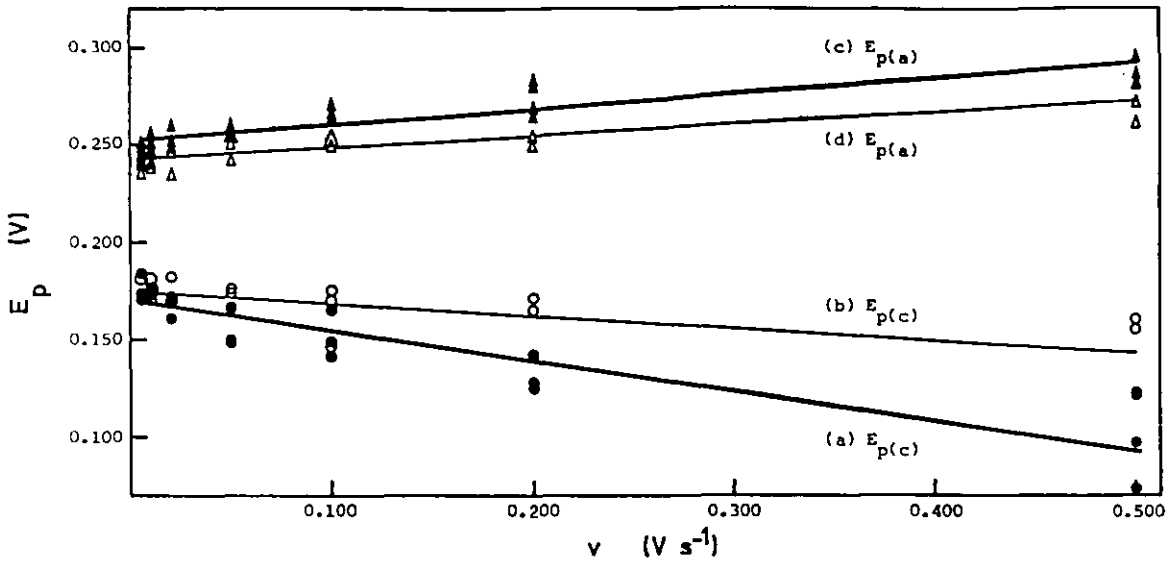

Fig. 5-353 Fe(III) cyanide (8.0×10^{-5} to 2.0×10^{-3} mol dm^{-3})/Potassium chloride (0.5 M) supporting electrolyte System: Values of cathodic and anodic peak potentials, $E_{p(c)}$ and $E_{p(a)}$ respectively, as functions of potential sweep rate, v; at potassium ferricyanide concentrations of 8.0×10^{-5} to 2.0×10^{-3} mol dm^{-3}. (a) & (c): Boron carbide solid electrode. (b) & (d): Boron carbide solid electrode treated with Ir(IV) perchlorate (1.0×10^{-4} mol dm^{-3}).

(a) $E_{p(c)} = 0.170 - 0.154\ v$
Correlation coefficient = -0.9161
Level of significance, p = $p < 0.001$
Standard deviation of $E_{p(c)}$ from regression = 1.17×10^{-2} V
Degrees of freedom = 19

(b) $E_{p(c)} = 0.175 - 6.32 \times 10^{-2}\ v$
Correlation coefficient = -0.7082
Level of significance, p = $p < 0.001$
Standard deviation of $E_{p(c)}$ from regression = 1.09×10^{-2} V
Degrees of freedom = 19

(c) $E_{p(a)} = 0.252 + 8.07 \times 10^{-2}\ v$
Correlation coefficient = 0.8923
Level of significance, p = $p < 0.001$
Standard deviation of $E_{p(a)}$ from regression = 7.09×10^{-3} V
Degrees of freedom = 19

(d) $E_{p(a)} = 0.242 + 6.14 \times 10^{-2}\ v$
Correlation coefficient = 0.8550
Level of significance, p = $p < 0.001$
Standard deviation of $E_{p(a)}$ from regression = 6.47×10^{-3} V
Degrees of freedom = 19

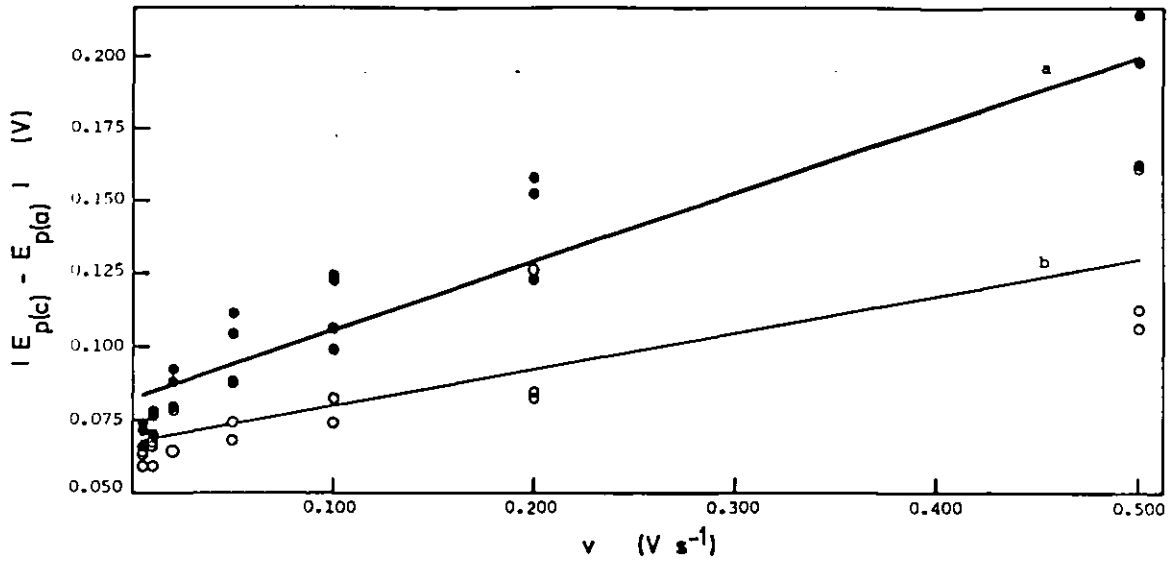

Fig. 5-354 Fe(III) cyanide (8.0×10^{-5} to 2.0×10^{-3} mol dm^{-3})/Potassium chloride (0.5 M) supporting electrolyte System: Values of the absolute difference between cathodic and anodic peak potentials, $|E_{p(c)} - E_{p(a)}|$, as a function of potential sweep rate, v; at potassium ferricyanide concentrations of 8.0×10^{-5} to 2.0×10^{-3} mol dm^{-3}. (a) Boron carbide solid electrode. (b) Boron carbide solid electrode treated with Ir(IV) perchlorate (1.0×10^{-4} mol dm^{-3}).

(a) Boron carbide solid electrode:

$|E_{p(c)} - E_{p(a)}| = 8.21 \times 10^{-2} + 0.235\ v$
Correlation coefficient = 0.9286
Level of significance, p = $p < 0.001$
Standard deviation of $|E_{p(c)} - E_{p(a)}|$ from regression
$= 1.63 \times 10^{-2}$ V
Degrees of freedom = 19

(b) Boron carbide solid electrode treated with Ir(IV) Perchlorate (1.0×10^{-4} mol dm^{-3}):

$|E_{p(c)} - E_{p(a)}| = 6.74 \times 10^{-2} + 0.125\ v$
Correlation coefficient = 0.8164
Level of significance, p = $p < 0.001$
Standard deviation of $|E_{p(c)} - E_{p(a)}|$ from regression
$= 1.54 \times 10^{-2}$ V
Degrees of freedom = 19

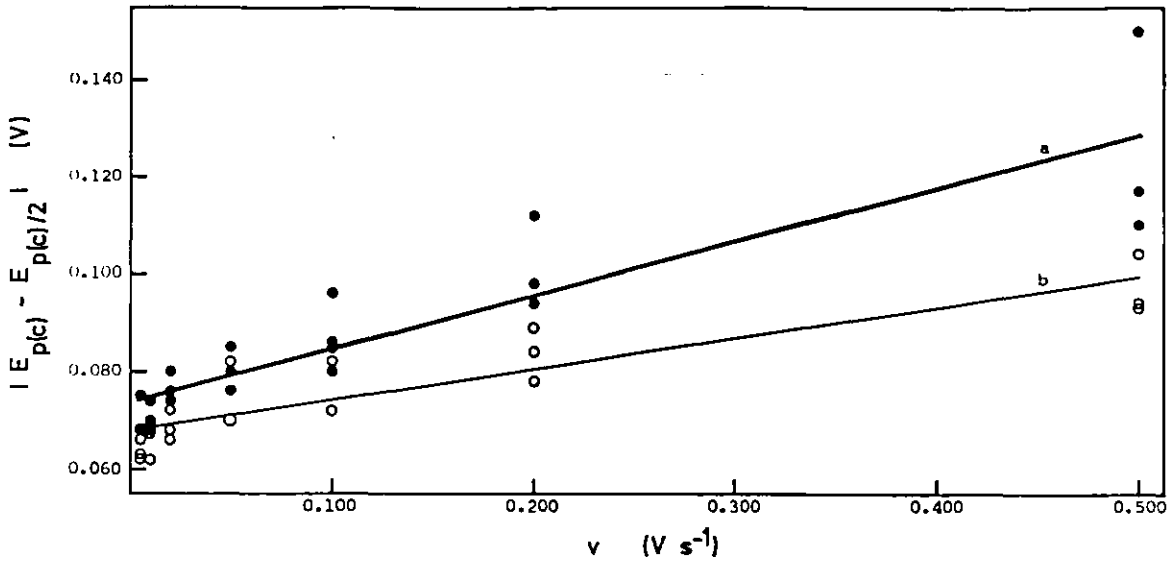

Fig. 5-355 Fe(III) cyanide (8.0×10^{-5} to 2.0×10^{-3} mol dm^{-3})/Potassium chloride (0.5 M) supporting electrolyte System: Values of the absolute difference between cathodic peak and half-peak potentials, $|E_{p(c)} - E_{p(c)/2}|$, as a function of potential sweep rate, v; at potassium ferricyanide concentrations of 8.0×10^{-5} to 2.0×10^{-3} mol dm^{-3}. (a) Boron carbide solid electrode. (b) Boron carbide solid electrode treated with Ir(IV) perchlorate (1.0×10^{-4} mol dm^{-3}).

(a) Boron carbide solid electrode:

$|E_{p(c)} - E_{p(c)/2}| = 7.36 \times 10^{-2} + 0.110\ v$
Correlation coefficient = 0.9026
Level of significance, p = $p < 0.001$
Standard deviation of $|E_{p(c)} - E_{p(c)/2}|$ from regression
$= 9.12 \times 10^{-3}$ V
Degrees of freedom = 19

(b) Boron carbide solid electrode treated with Ir(IV) Perchlorate (1.0×10^{-4} mol dm^{-3}):

$|E_{p(c)} - E_{p(c)/2}| = 6.82 \times 10^{-2} + 6.23 \times 10^{-2}\ v$
Correlation coefficient = 0.8843
Level of significance, p = $p < 0.001$
Standard deviation of $|E_{p(c)} - E_{p(c)/2}|$ from regression
$= 5.71 \times 10^{-3}$ V
Degrees of freedom = 19

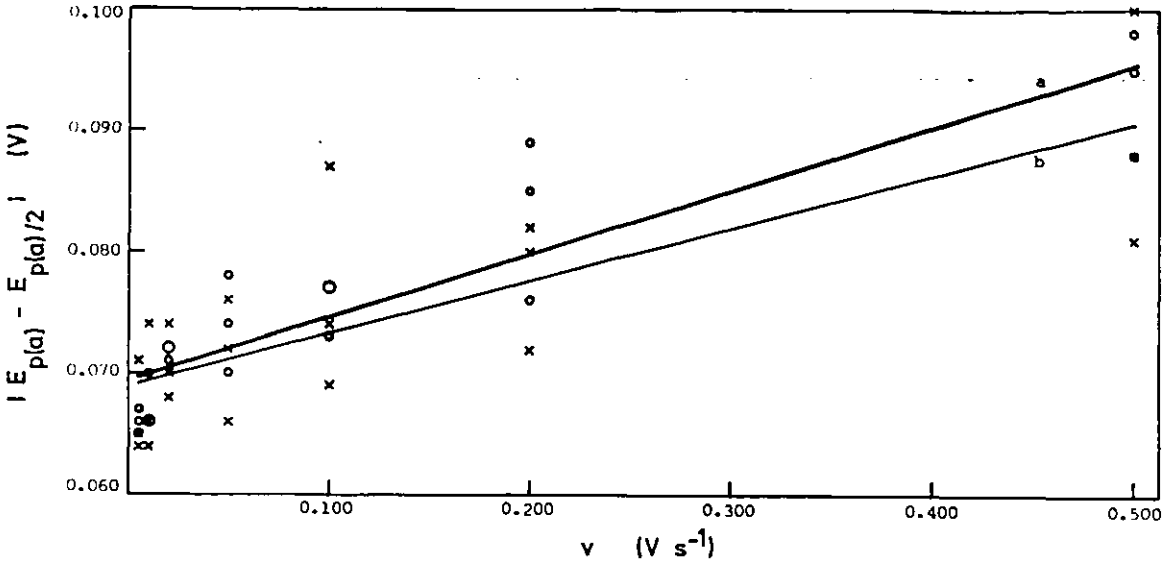

Fig. 5-356 Fe(III) cyanide (8.0×10^{-5} to 2.0×10^{-3} mol dm^{-3})/Potassium chloride (0.5 M) supporting electrolyte System: Values of the absolute difference between anodic peak and half-peak potentials, $|E_{p(a)} - E_{p(a)/2}|$, as a function of potential sweep rate, v; at potassium ferricyanide concentrations of 8.0×10^{-5} to 2.0×10^{-3} mol dm^{-3}. (a) Boron carbide solid electrode: (o). (b) Boron carbide solid electrode treated with Ir(IV) perchlorate (1.0×10^{-4} mol dm^{-3}): (×).

(a) Boron carbide solid electrode:

$|E_{p(a)} - E_{p(a)/2}| = 6.93 \times 10^{-2} + 5.22 \times 10^{-2}$ v
Correlation coefficient = 0.9102
Level of significance, p = $p < 0.001$
Standard deviation of $|E_{p(a)} - E_{p(a)/2}|$ from regression
$= 4.13 \times 10^{-3}$ V
Degrees of freedom = 19

(b) Boron carbide solid electrode treated with Ir(IV) Perchlorate (1.0×10^{-4} mol dm^{-3}):

$|E_{p(a)} - E_{p(a)/2}| = 6.90 \times 10^{-2} + 4.30 \times 10^{-2}$ v
Correlation coefficient = 0.7918
Level of significance, p = $p < 0.001$
Standard deviation of $|E_{p(a)} - E_{p(a)/2}|$ from regression
$= 5.77 \times 10^{-3}$ V
Degrees of freedom = 19

of Ir(IV)-perchlorate treatment of the boron carbide solid working electrode (Figures 5-357 and 5-359 c.f. Figures 5-358 and 5-360 respectively). Fig. 5-361 illustrates the effect of the concentration of Fe (III) cyanide on the peak potentials. In general, $|E_{p(c)} - E_{p(a)}|$ values widened with increasing concentration of Fe(III) cyanide (Fig. 5-362). The $|E_{p(c)} - E_{p(c)/2}|$ and $|E_{p(a)} - E_{p(a)/2}|$ values (Figures 5-363 and 5-364 respectively), as functions of $(\text{ionic strength})^{\frac{1}{2}}$, generally show that initially an increase in the concentration of Fe(III) cyanide caused the charge transfer to become more reversible; but this reversibility deteriorated with further increases in concentration. Although Ir(IV)-perchlorate treatment of the boron carbide solid working electrode improved the reversibility of the charge transfer for Fe(III) cyanide, a completely reversible electrochemical reaction was not achieved; best $|E_p - E_{p/2}|$ value obtained was 0.062 V as compared with the theoretical 0.056 V for a reversible one-electron charge transfer at 25 °C (equation 3-32).

Figures 5-365 and 5-366 show the enhancement of the cathodic and anodic peak current functions, respectively, by: (i) Ir(IV)-perchlorate treatment of the working electrode, and (ii) increase in concentration of KCl supporting electrolyte; although only a slight enhancement was encountered beyond 0.5 M. The effect of KCl supporting electrolyte on the peak currents is well illustrated by Figures 5-367 and 5-368. The influence of KCl concentration on the ratio of cathodic peak current to anodic peak current, $i_{p(c)}/i_{p(a)}$, was significant (Fig. 5-369); but not if the working electrode had been treated with Ir(IV) perchlorate (Fig. 5-370).

The influence of KCl supporting electrolyte on the peak potentials is presented in Fig. 5-371. As expected of an anionic e.a.s., the peak potentials were anodically shifted by increasing ionic strength. The $|E_{p(c)} - E_{p(a)}|$ and $|E_p - E_{p/2}|$ values narrowed as the concentration of KCl was increased from 0.1 M to 0.5 M, suggesting an improvement in the reversibility of the charge transfer, but remained constant beyond the concentration of 0.5 M KCl (Figures 5-372 and 5-373 respectively).

5-2.3.(iii) Summary.

D.c. voltammetry of $K_3Fe(CN)_6$ (8.0×10^{-5} to 2.0×10^{-3} mol dm^{-3})/ KCl (0.5 M) supporting electrolyte solutions, at the boron carbide solid electrode, was poorly reversible; αn values ranged from 0.70 to 0.56 (Fig. 5-331, a). After the boron carbide electrode had been treated

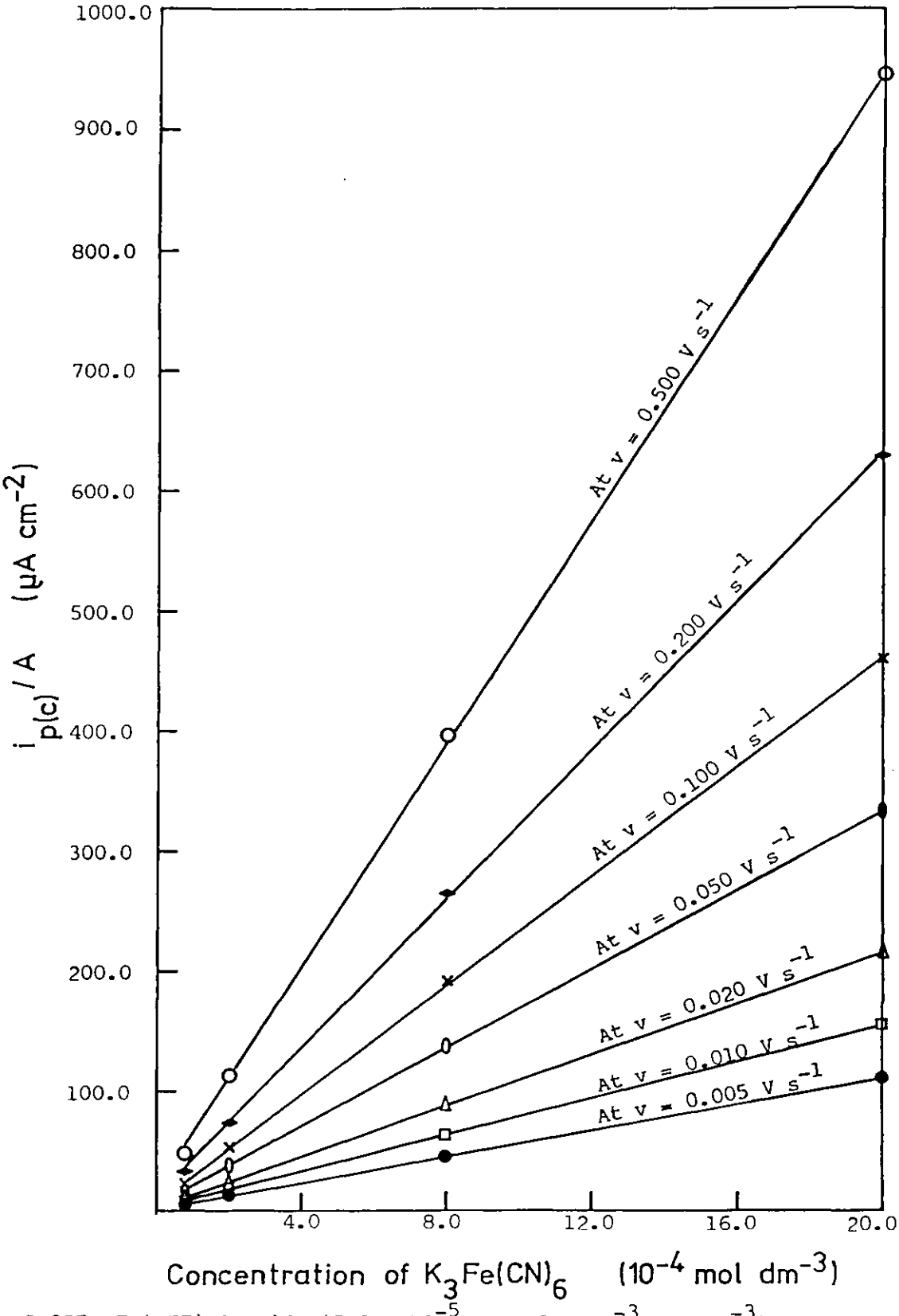

Fig. 5-357 Fe(III) Cyanide (8.0×10^{-5} to 2.0×10^{-3} mol dm^{-3})/Potassium chloride (0.5 M) supporting electrolyte System: Dependence of cathodic peak current per unit area, $i_{p(c)}/A$, on the concentration of potassium ferricyanide, $[K_3Fe(CN)_6]$; at scan rates of 0.005 to 0.500 V s^{-1}. Boron carbide solid electrode.

Fig. 5-357 (continued):-

(a) At $v = 0.005\ V\ s^{-1}$:

$i_{p(c)}/A = 0.709 + 5.42 \times 10^4\ [\ K_3Fe(CN)_6\ ]$
Correlation coefficient = 0.99998
Level of significance, p = $p < 0.001$
Standard deviation of $i_{p(c)}/A$ from regression = 0.358 $\mu A\ cm^{-2}$
Degrees of freedom = 2

(b) At $v = 0.010\ V\ s^{-1}$:

$i_{p(c)}/A = 1.10 + 7.61 \times 10^4\ [\ K_3Fe(CN)_6\ ]$
Correlation coefficient = 0.999997
Level of significance, p = $p < 0.001$
Standard deviation of $i_{p(c)}/A$ from regression = 0.209 $\mu A\ cm^{-2}$
Degrees of freedom = 2

(c) At $v = 0.020\ V\ s^{-1}$:

$i_{p(c)}/A = 1.76 + 1.07 \times 10^5\ [\ K_3Fe(CN)_6\ ]$
Correlation coefficient = 0.999998
Level of significance, p = $p < 0.001$
Standard deviation of $i_{p(c)}/A$ from regression = 0.227 $\mu A\ cm^{-2}$
Degrees of freedom = 2

(d) At $v = 0.050\ V\ s^{-1}$:

$i_{p(c)}/A = 3.95 + 1.64 \times 10^5\ [\ K_3Fe(CN)_6\ ]$
Correlation coefficient = 0.99997
Level of significance, p = $p < 0.001$
Standard deviation of $i_{p(c)}/A$ from regression = 1.36 $\mu A\ cm^{-2}$
Degrees of freedom = 2

(e) At $v = 0.100\ V\ s^{-1}$:

$i_{p(c)}/A = 7.28 + 2.27 \times 10^5\ [\ K_3Fe(CN)_6\ ]$
Correlation coefficient = 0.99994
Level of significance, p = $p < 0.001$
Standard deviation of $i_{p(c)}/A$ from regression = 2.76 $\mu A\ cm^{-2}$
Degrees of freedom = 2

(f) At $v = 0.200\ V\ s^{-1}$:

$i_{p(c)}/A = 11.3 + 3.10 \times 10^5\ [\ K_3Fe(CN)_6\ ]$
Correlation coefficient = 0.99988
Level of significance, p = $p < 0.001$
Standard deviation of $i_{p(c)}/A$ from regression = 5.20 $\mu A\ cm^{-2}$
Degrees of freedom = 2

(g) At $v = 0.500\ V\ s^{-1}$:

$i_{p(c)}/A = 17.5 + 4.64 \times 10^5\ [\ K_3Fe(CN)_6\ ]$
Correlation coefficient = 0.99991
Level of significance, p = $p < 0.001$
Standard deviation of $i_{p(c)}/A$ from regression = 6.85 $\mu A\ cm^{-2}$
Degrees of freedom = 2

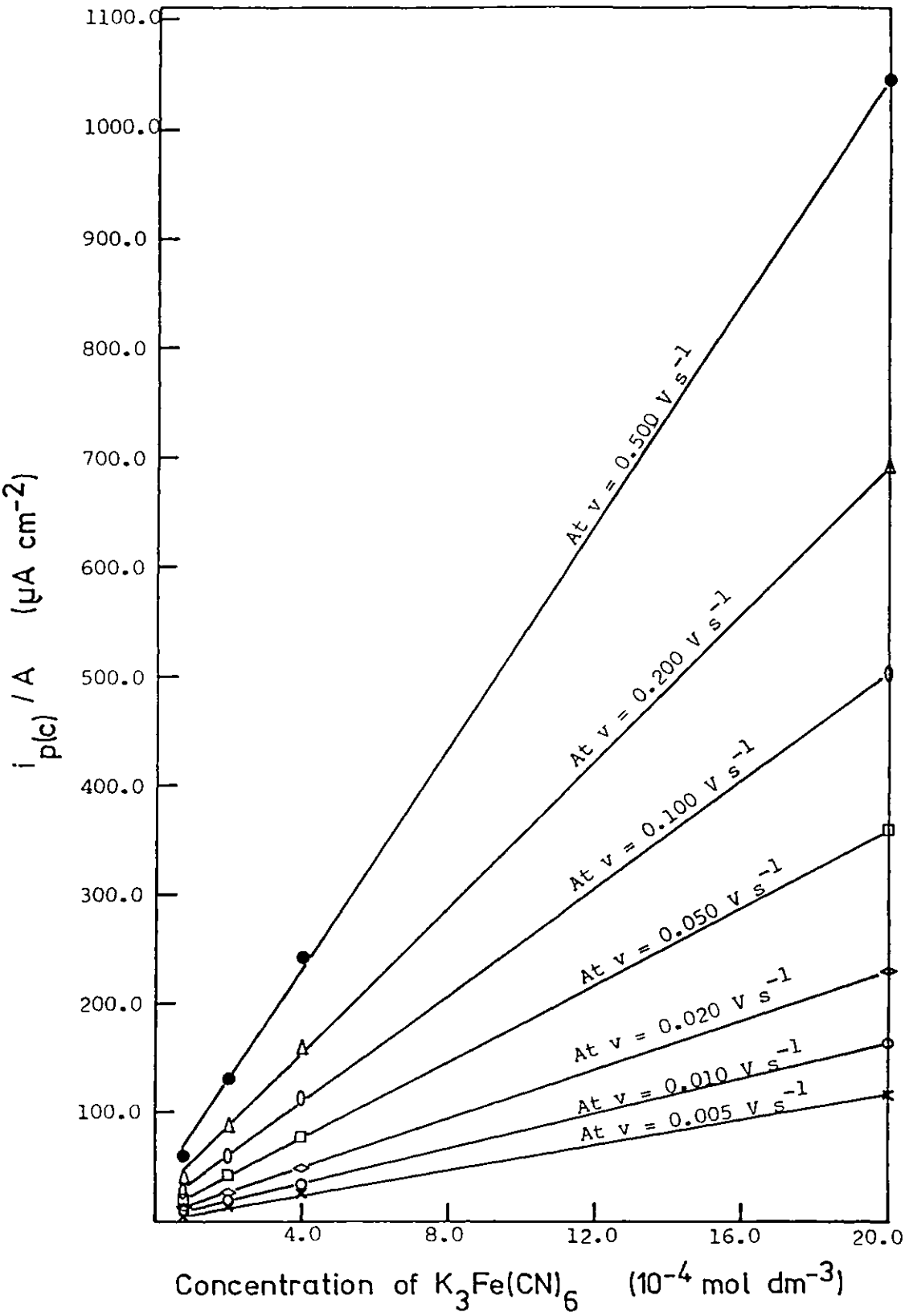

Fig. 5-358 Fe(III) Cyanide (8.0 x 10^{-5} to 2.0 x 10^{-3} mol dm^{-3})/Potassium chloride (0.5 M) supporting electrolyte System: Dependence of cathodic peak current per unit area, $i_{p(c)}/A$, on the concentration of potassium ferricyanide, [$K_3Fe(CN)_6$]; at scan rates of 0.005 to 0.500 V s^{-1}. Boron carbide solid electrode treated with Ir(IV) Perchlorate (1.0 x 10^{-4} mol dm^{-3}).

Fig. 5-358 (continued):-

(a) At $v = 0.005$ V s^{-1}:

$i_{p(c)}/A = 0.533 + 5.77 \times 10^4$ [$K_3Fe(CN)_6$]
Correlation coefficient = 0.9999992
Level of significance, $p = p < 0.001$
Standard deviation of $i_{p(c)}/A$ from regression
$= 8.04 \times 10^{-2}$ μA cm^{-2}
Degrees of freedom = 2

(b) At $v = 0.010$ V s^{-1}:

$i_{p(c)}/A = 1.14 + 8.12 \times 10^4$ [$K_3Fe(CN)_6$]
Correlation coefficient = 0.9999993
Level of significance, $p = p < 0.001$
Standard deviation of $i_{p(c)}/A$ from regression = 0.106 μA cm^{-2}
Degrees of freedom = 2

(c) At $v = 0.020$ V s^{-1}:

$i_{p(c)}/A = 2.51 + 1.13 \times 10^5$ [$K_3Fe(CN)_6$]
Correlation coefficient = 0.9999993
Level of significance, $p = p < 0.001$
Standard deviation of $i_{p(c)}/A$ from regression = 0.142 μA cm^{-2}
Degrees of freedom = 2

(d) At $v = 0.050$ V s^{-1}:

$i_{p(c)}/A = 5.19 + 1.77 \times 10^5$ [$K_3Fe(CN)_6$]
Correlation coefficient = 0.99999
Level of significance, $p = p < 0.001$
Standard deviation of $i_{p(c)}/A$ from regression = 0.903 μA cm^{-2}
Degrees of freedom = 2

(e) At $v = 0.100$ V s^{-1}:

$i_{p(c)}/A = 10.1 + 2.46 \times 10^5$ [$K_3Fe(CN)_6$]
Correlation coefficient = 0.99993
Level of significance, $p = p < 0.001$
Standard deviation of $i_{p(c)}/A$ from regression = 3.23 μA cm^{-2}
Degrees of freedom = 2

(f) At $v = 0.200$ V s^{-1}:

$i_{p(c)}/A = 16.9 + 3.37 \times 10^5$ [$K_3Fe(CN)_6$]
Correlation coefficient = 0.99989
Level of significance, $p = p < 0.001$
Standard deviation of $i_{p(c)}/A$ from regression = 5.57 μA cm^{-2}
Degrees of freedom = 2

(g) At $v = 0.500$ V s^{-1}:

$i_{p(c)}/A = 27.9 + 5.09 \times 10^5$ [$K_3Fe(CN)_6$]
Correlation coefficient = 0.99983
Level of significance, $p = p < 0.001$
Standard deviation of $i_{p(c)}/A$ from regression = 10.4 μA cm^{-2}
Degrees of freedom = 2

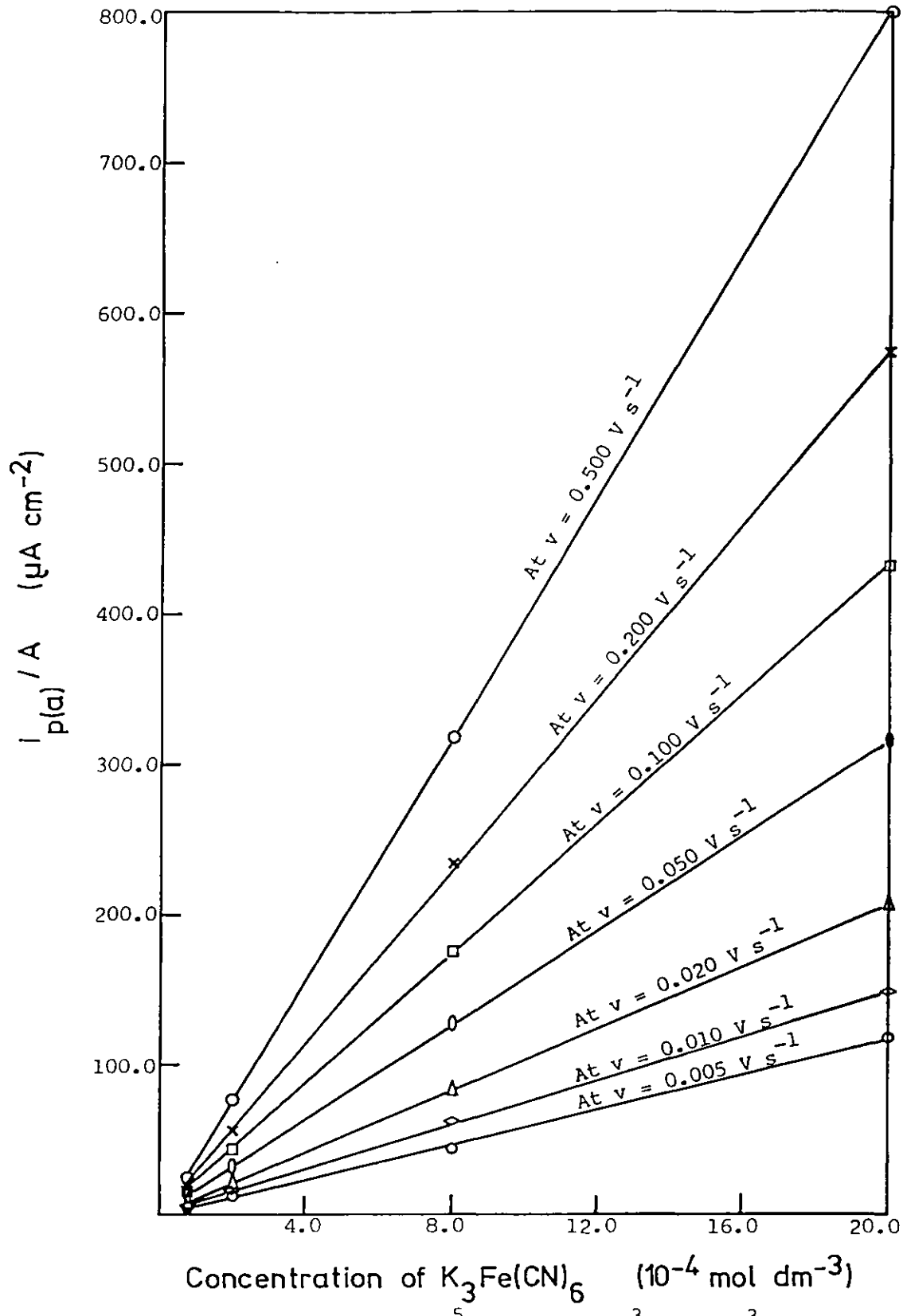

Fig. 5-359 Fe(III) Cyanide (8.0 x 10^{-5} to 2.0 x 10^{-3} mol dm^{-3})/Potassium chloride (0.5 M) supporting electrolyte System: Dependence of anodic peak current per unit area, $i_{p(a)}/A$, on the concentration of potassium ferricyanide, [$K_3Fe(CN)_6$]; at scan rates of 0.005 to 0.500 V s^{-1}. Boron carbide solid electrode.

Fig. 5-359 (continued):-

(a) At $v = 0.005\ V\ s^{-1}$:

$i_{p(a)}/A = 5.85 \times 10^4\ [\ K_3Fe(CN)_6\ ] - 1.25$
Correlation coefficient = 0.99952
Level of significance, $p = p < 0.001$
Standard deviation of $i_{p(a)}/A$ from regression = 1.94 $\mu A\ cm^{-2}$
Degrees of freedom = 2

(b) At $v = 0.010\ V\ s^{-1}$:

$i_{p(a)}/A = 0.518 + 7.38 \times 10^4\ [\ K_3Fe(CN)_6\ ]$
Correlation coefficient = 0.99991
Level of significance, $p = p < 0.001$
Standard deviation of $i_{p(a)}/A$ from regression = 1.08 $\mu A\ cm^{-2}$
Degrees of freedom = 2

(c) At $v = 0.020\ V\ s^{-1}$:

$i_{p(a)}/A = 1.03 \times 10^5\ [\ K_3Fe(CN)_6\ ] - 0.181$
Correlation coefficient = 0.999998
Level of significance, $p = p < 0.001$
Standard deviation of $i_{p(a)}/A$ from regression = 0.222 $\mu A\ cm^{-2}$
Degrees of freedom = 2

(d) At $v = 0.050\ V\ s^{-1}$:

$i_{p(a)}/A = 1.58 \times 10^5\ [\ K_3Fe(CN)_6\ ] - 0.460$
Correlation coefficient = 0.99999
Level of significance, $p = p < 0.001$
Standard deviation of $i_{p(a)}/A$ from regression = 0.549 $\mu A\ cm^{-2}$
Degrees of freedom = 2

(e) At $v = 0.100\ V\ s^{-1}$:

$i_{p(a)}/A = 2.17 \times 10^5\ [\ K_3Fe(CN)_6\ ] - 0.638$
Correlation coefficient = 0.99995
Level of significance, $p = p < 0.001$
Standard deviation of $i_{p(a)}/A$ from regression = 2.30 $\mu A\ cm^{-2}$
Degrees of freedom = 2

(f) At $v = 0.200\ V\ s^{-1}$:

$i_{p(a)}/A = 2.88 \times 10^5\ [\ K_3Fe(CN)_6\ ] - 2.00$
Correlation coefficient = 0.99992
Level of significance, $p = p < 0.001$
Standard deviation of $i_{p(a)}/A$ from regression = 4.01 $\mu A\ cm^{-2}$
Degrees of freedom = 2

(g) At $v = 0.500\ V\ s^{-1}$:

$i_{p(a)}/A = 4.03 \times 10^5\ [\ K_3Fe(CN)_6\ ] - 5.98$
Correlation coefficient = 0.99999
Level of significance, $p = p < 0.001$
Standard deviation of $i_{p(a)}/A$ from regression = 2.37 $\mu A\ cm^{-2}$
Degrees of freedom = 2

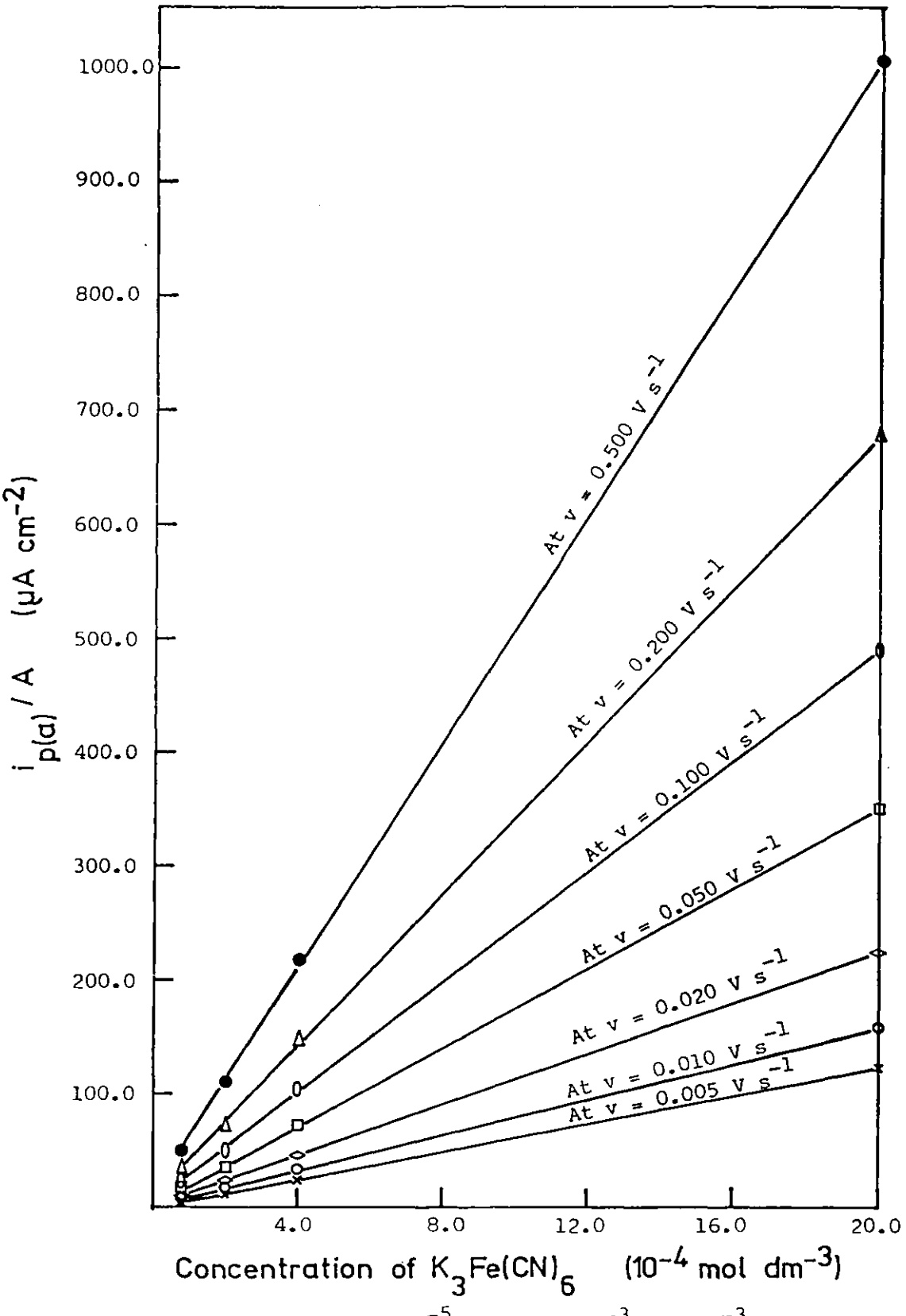

Fig. 5-360 Fe(III) Cyanide (8.0×10^{-5} to 2.0×10^{-3} mol dm^{-3})/Potassium chloride (0.5 M) supporting electrolyte System: Dependence of anodic peak current per unit area, $i_{p(a)}/A$, on the concentration of potassium ferricyanide, [$K_3Fe(CN)_6$]; at scan rates of 0.005 to 0.500 V s^{-1}. Boron carbide solid electrode treated with Ir(IV) Perchlorate (1.0×10^{-4} mol dm^{-3}).

Fig. 5-360 (continued):-

(a) At $v = 0.005$ V s^{-1}:

$i_{p(a)}/A = 6.13 \times 10^4 [K_3Fe(CN)_6] - 0.507$
Correlation coefficient = 0.99994
Level of significance, $p = p < 0.001$
Standard deviation of $i_{p(a)}/A$ from regression = 0.753 μA cm^{-2}
Degrees of freedom = 2

(b) At $v = 0.010$ V s^{-1}:

$i_{p(a)}/A = 1.01 + 7.82 \times 10^4 [K_3Fe(CN)_6]$
Correlation coefficient = 0.99998
Level of significance, $p = p < 0.001$
Standard deviation of $i_{p(a)}/A$ from regression = 0.538 μA cm^{-2}
Degrees of freedom = 2

(c) At $v = 0.020$ V s^{-1}:

$i_{p(a)}/A = 0.902 + 1.11 \times 10^5 [K_3Fe(CN)_6]$
Correlation coefficient = 0.99999
Level of significance, $p = p < 0.001$
Standard deviation of $i_{p(a)}/A$ from regression = 0.579 μA cm^{-2}
Degrees of freedom = 2

(d) At $v = 0.050$ V s^{-1}:

$i_{p(a)}/A = 1.56 + 1.74 \times 10^5 [K_3Fe(CN)_6]$
Correlation coefficient = 0.99998
Level of significance, $p = p < 0.001$
Standard deviation of $i_{p(a)}/A$ from regression = 1.33 μA cm^{-2}
Degrees of freedom = 2

(e) At $v = 0.100$ V s^{-1}:

$i_{p(a)}/A = 3.95 + 2.42 \times 10^5 [K_3Fe(CN)_6]$
Correlation coefficient = 0.99994
Level of significance, $p = p < 0.001$
Standard deviation of $i_{p(a)}/A$ from regression = 2.97 μA cm^{-2}
Degrees of freedom = 2

(f) At $v = 0.200$ V s^{-1}:

$i_{p(a)}/A = 8.55 + 3.35 \times 10^5 [K_3Fe(CN)_6]$
Correlation coefficient = 0.99993
Level of significance, $p = p < 0.001$
Standard deviation of $i_{p(a)}/A$ from regression = 4.40 μA cm^{-2}
Degrees of freedom = 2

(g) At $v = 0.500$ V s^{-1}:

$i_{p(a)}/A = 12.3 + 4.97 \times 10^5 [K_3Fe(CN)_6]$
Correlation coefficient = 0.99996
Level of significance, $p = p < 0.001$
Standard deviation of $i_{p(a)}/A$ from regression = 4.78 μA cm^{-2}
Degrees of freedom = 2

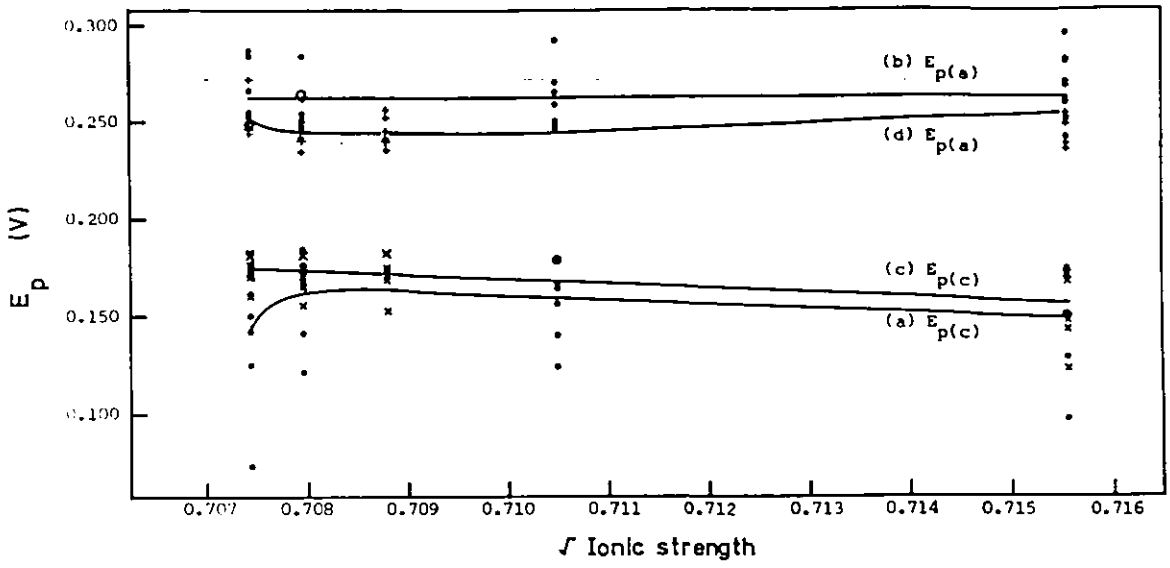

Fig. 5-361 Fe(III) cyanide (8.0×10^{-5} to 2.0×10^{-3} mol dm^{-3})/Potassium chloride (0.5 M) supporting electrolyte System: Values of cathodic and anodic peak potentials, $E_{p(c)}$ and $E_{p(a)}$ respectively, as functions of square root of total ionic strength (where the concentration of $K_3Fe(CN)_6$ was varied), $\sqrt{I}$. (a) & (b) Boron carbide solid electrode: (—•—) & (—•—) respectively. (c) & (d) Boron carbide solid electrode treated with Ir(IV) perchlorate (1.0×10^{-4} mol dm^{-3}): (—×—) & (—•—) respectively. Sweep rates: 0.005 to 0.500 V s^{-1}.

(a) $E_{p(c)}$ mean = 0.152 V
Standard deviation = 2.65×10^{-2} V
Coefficient of variation = 17.4%
Degrees of freedom = 27

(b) $E_{p(a)}$ mean = 0.262 V
Standard deviation = 1.53×10^{-2} V
Coefficient of variation = 5.82%
Degrees of freedom = 27

(c) $E_{p(c)} = 1.80 - 2.30\sqrt{I}$
Correlation coefficient = -0.5470
Level of significance, $p = 0.001 < p < 0.01$
Standard deviation of $E_{p(c)}$ from regression = 1.19×10^{-2} V
Degrees of freedom = 26

(d) $E_{p(a)}$ mean = 0.249 V
Standard deviation = 1.14×10^{-2} V
Coefficient of variation = 4.57%
Degrees of freedom = 27

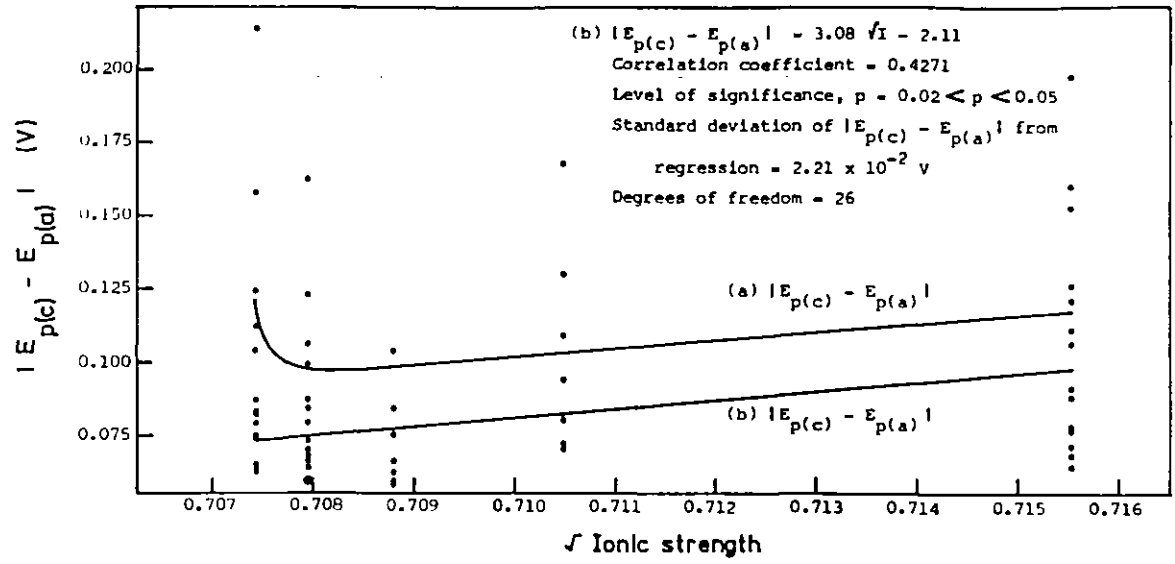

Fig. 5-362 Fe(III) Cyanide (8.0×10^{-5} to 2.0×10^{-3} mol dm^{-3})/Potassium chloride (0.5 M) supporting electrolyte System: Values of the absolute difference between cathodic and anodic peak potentials, $|E_{p(c)} - E_{p(a)}|$, as a function of square root of total ionic strength (where the concentration of potassium ferricyanide was varied), $\sqrt{I}$; at scan rates of 0.005 to 0.500 V s^{-1}. (a) Boron carbide solid electrode: (—•—). (b) Boron carbide solid electrode treated with Ir(IV) Perchlorate (1.0×10^{-4} mol dm^{-3}): (—•—).

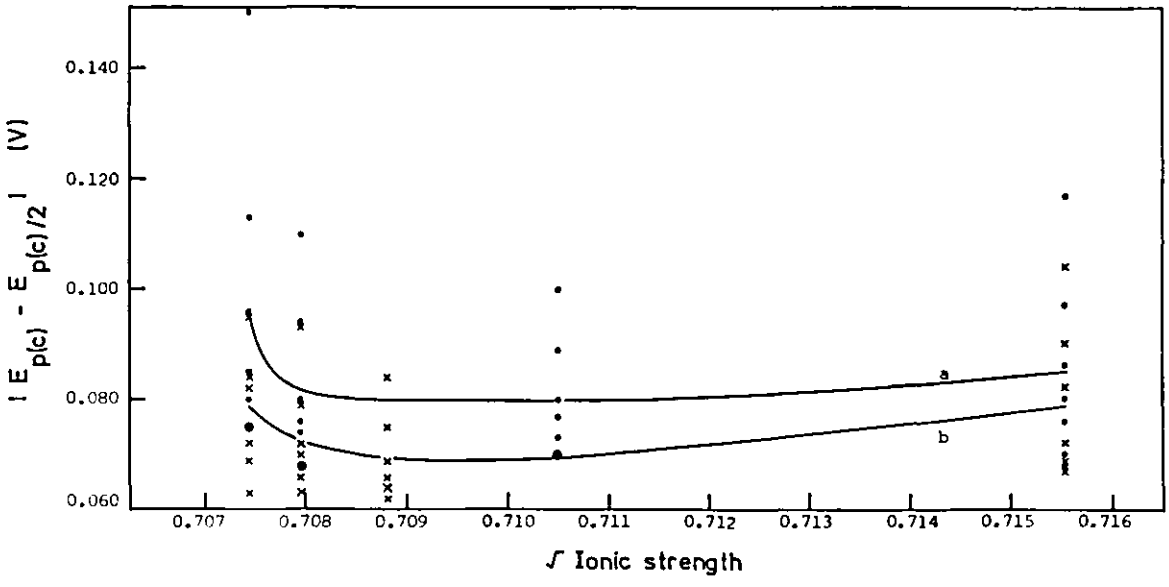

Fig. 5-363 Fe(III) Cyanide (8.0×10^{-5} to 2.0×10^{-3} mol dm^{-3})/Potassium chloride (0.5 M) supporting electrolyte System: Values of the absolute difference between cathodic peak and half-peak potentials, $|E_{p(c)} - E_{p(c)/2}|$, as a function of square root of total ionic strength (where the concentration of potassium ferricyanide was varied), $\sqrt{I}$; at scan rates of 0.005 to 0.500 V s^{-1}. (a) Boron carbide solid electrode: (—•—). (b) Boron carbide solid electrode treated with Ir(IV) Perchlorate (1.0×10^{-4} mol dm^{-3}): (—×—).

Fig. 5-363 (continued):-

(a) $|E_{p(c)} - E_{p(c)/2}|$ mean = 8.56×10^{-2} V
Standard deviation = 1.88×10^{-2} V
Coefficient of variation = 22.0%
Degrees of freedom = 27

(b) $|E_{p(c)} - E_{p(c)/2}|$ mean = 7.47×10^{-2} V
Standard deviation = 1.13×10^{-2} V
Coefficient of variation = 15.1%
Degrees of freedom = 27

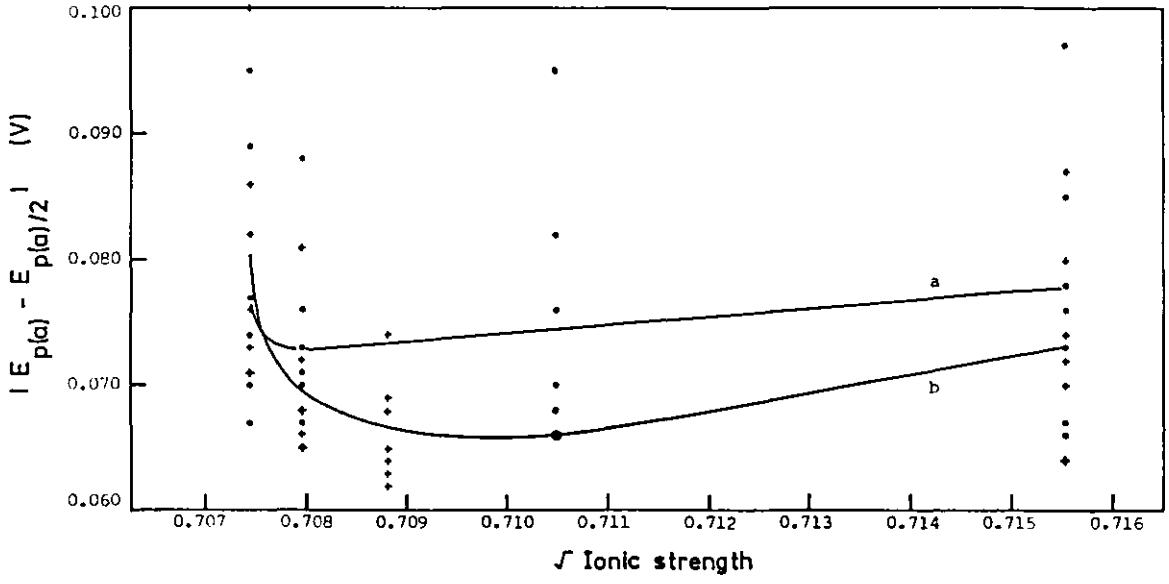

Fig. 5-364 Fe(III) Cyanide (8.0×10^{-5} to 2.0×10^{-3} mol dm^{-3})/Potassium chloride (0.5 M) supporting electrolyte System: Values of the absolute difference between anodic peak and half-peak potentials, $|E_{p(a)} - E_{p(a)/2}|$, as a function of square root of total ionic strength (where the concentration of potassium ferricyanide was varied), $\sqrt{I}$; at scan rates of 0.005 to 0.500 V s^{-1}. (a) Boron carbide solid electrode: (—•—). (b) Boron carbide solid electrode treated with Ir(IV) Perchlorate (1.0×10^{-4} mol dm^{-3}): (–•–).

(a) $|E_{p(a)} - E_{p(a)/2}|$ mean = 7.56×10^{-2} V
Standard deviation = 9.63×10^{-3} V
Coefficient of variation = 12.7%
Degrees of freedom = 27

(b) $|E_{p(a)} - E_{p(a)/2}|$ mean = 7.23×10^{-2} V
Standard deviation = 8.81×10^{-3} V
Coefficient of variation = 12.2%
Degrees of freedom = 27

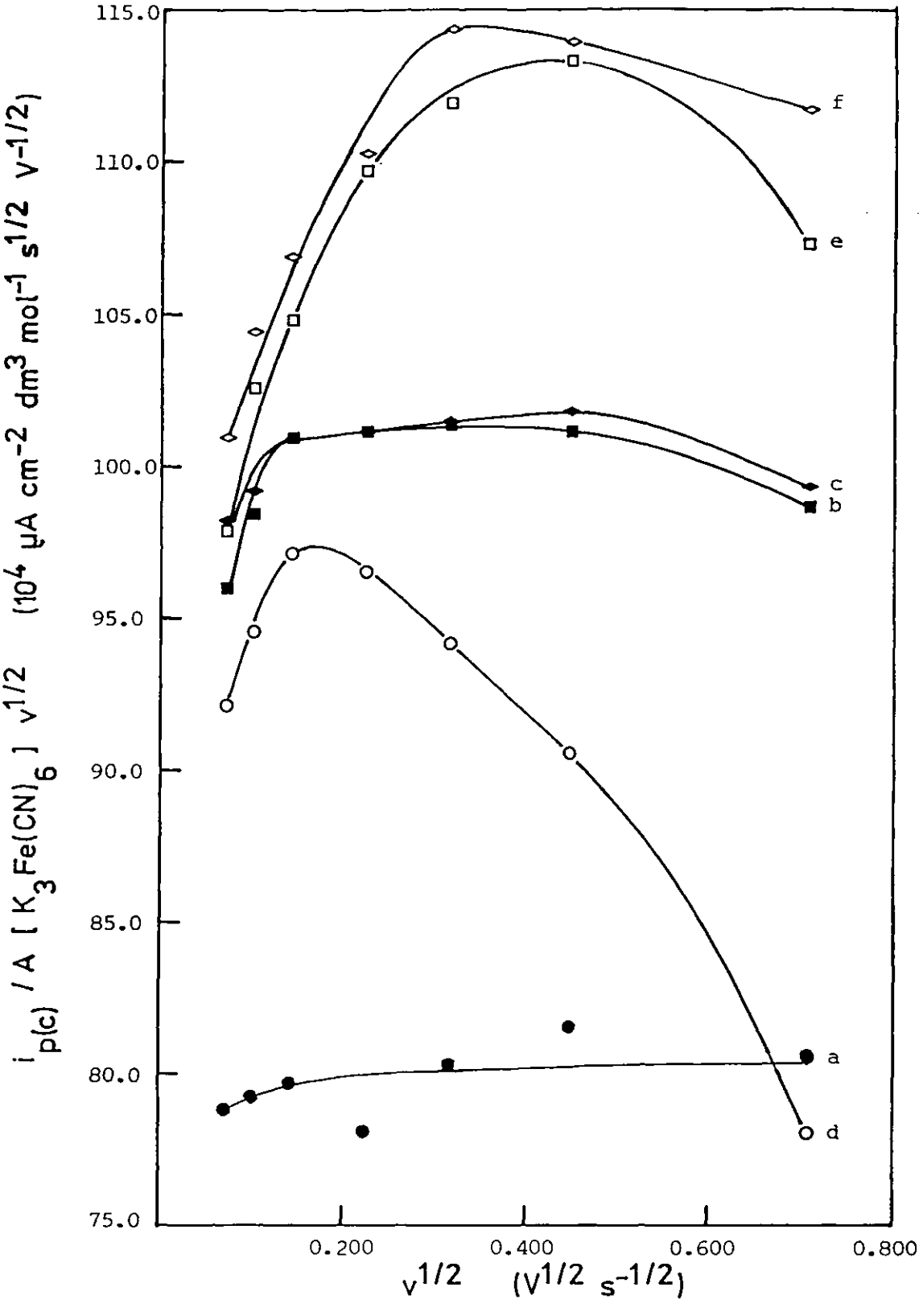

Fig. 5-365 Fe(III) Cyanide (2.0×10^{-4} mol dm^{-3})/Potassium chloride (0.1 to 2.0 M) supporting electrolyte System: Values of cathodic current function, $i_{p(c)}/A\,[\,K_3Fe(CN)_6\,]\,v^{\frac{1}{2}}$, as a function of square root of potential scan rate, $v^{\frac{1}{2}}$; at potassium chloride concentrations (a) & (d) 0.1, (b) & (e) 0.5, and (c) & (f) 2.0 M. Boron carbide solid electrode: a, b, and c. Boron carbide solid electrode treated with Ir(IV) Perchlorate (1.0×10^{-4} mol dm^{-3}): d, e, and f.

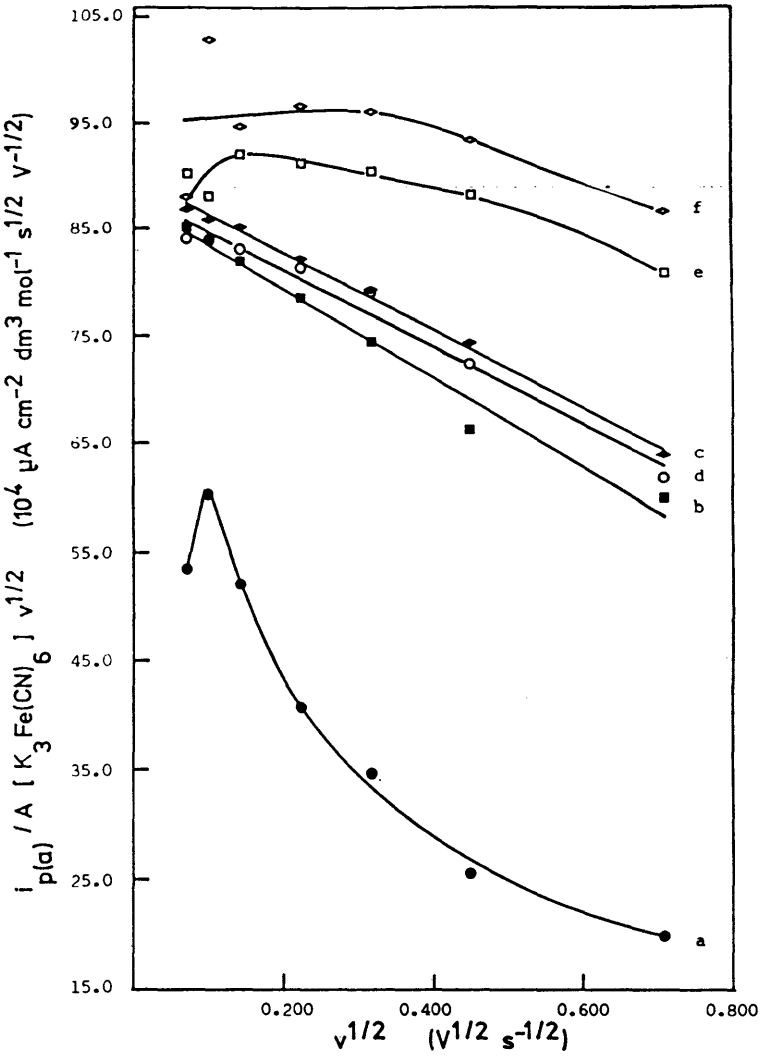

Fig. 5-366 Fe(III) Cyanide (2.0×10^{-4} mol dm^{-3})/Potassium chloride (0.1 to 2.0 M) supporting electrolyte System: Values of anodic current function, $i_{p(a)}/A\ [\ K_3Fe(CN)_6\ ]\ v^{\frac{1}{2}}$, as a function of square root of potential scan rate, $v^{\frac{1}{2}}$; at potassium chloride concentrations (a) & (d) 0.1, (b) & (e) 0.5, and (c) & (f) 2.0 M. Boron carbide solid electrode: a, b, and c. Boron carbide solid electrode treated with Ir(IV) Perchlorate (1.0×10^{-4}mol dm^{-3}): d, e, and f.

(b) $i_{p(a)}/A\ [\ K_3Fe(CN)_6\ ]\ v^{\frac{1}{2}} = 8.75 \times 10^5 - 4.14 \times 10^5\ v^{\frac{1}{2}}$
Correlation coefficient = -0.9889
Level of significance, p = $p < 0.001$
Standard deviation of $i_{p(a)}/A\ [\ K_3Fe(CN)_6\ ]\ v^{\frac{1}{2}}$ from regression
$= 1.55 \times 10^4$ μA cm^{-2} dm^3 mol^{-1} s$^{\frac{1}{2}}$ v$^{-\frac{1}{2}}$
Degrees of freedom = 5

(c) $i_{p(a)}/A\ [\ K_3Fe(CN)_6\ ]\ v^{\frac{1}{2}} = 9.00 \times 10^5 - 3.62 \times 10^5\ v^{\frac{1}{2}}$
Correlation coefficient = -0.9980
Level of significance, p = $p < 0.001$
Standard deviation of $i_{p(a)}/A\ [\ K_3Fe(CN)_6\ ]\ v^{\frac{1}{2}}$ from regression
$= 5.71 \times 10^3$ μA cm^{-2} dm^3 mol^{-1} s$^{\frac{1}{2}}$ v$^{-\frac{1}{2}}$
Degrees of freedom = 5

(d) $i_{p(a)}/A\ [\ K_3Fe(CN)_6\ ]\ v^{\frac{1}{2}} = 8.82 \times 10^5 - 3.59 \times 10^5\ v^{\frac{1}{2}}$
Correlation coefficient = -0.9881
Level of significance, p = $p < 0.001$
Standard deviation of $i_{p(a)}/A\ [\ K_3Fe(CN)_6\ ]\ v^{\frac{1}{2}}$ from regression
$= 1.39 \times 10^4$ μA cm^{-2} dm^3 mol^{-1} s$^{\frac{1}{2}}$ v$^{-\frac{1}{2}}$
Degrees of freedom = 5

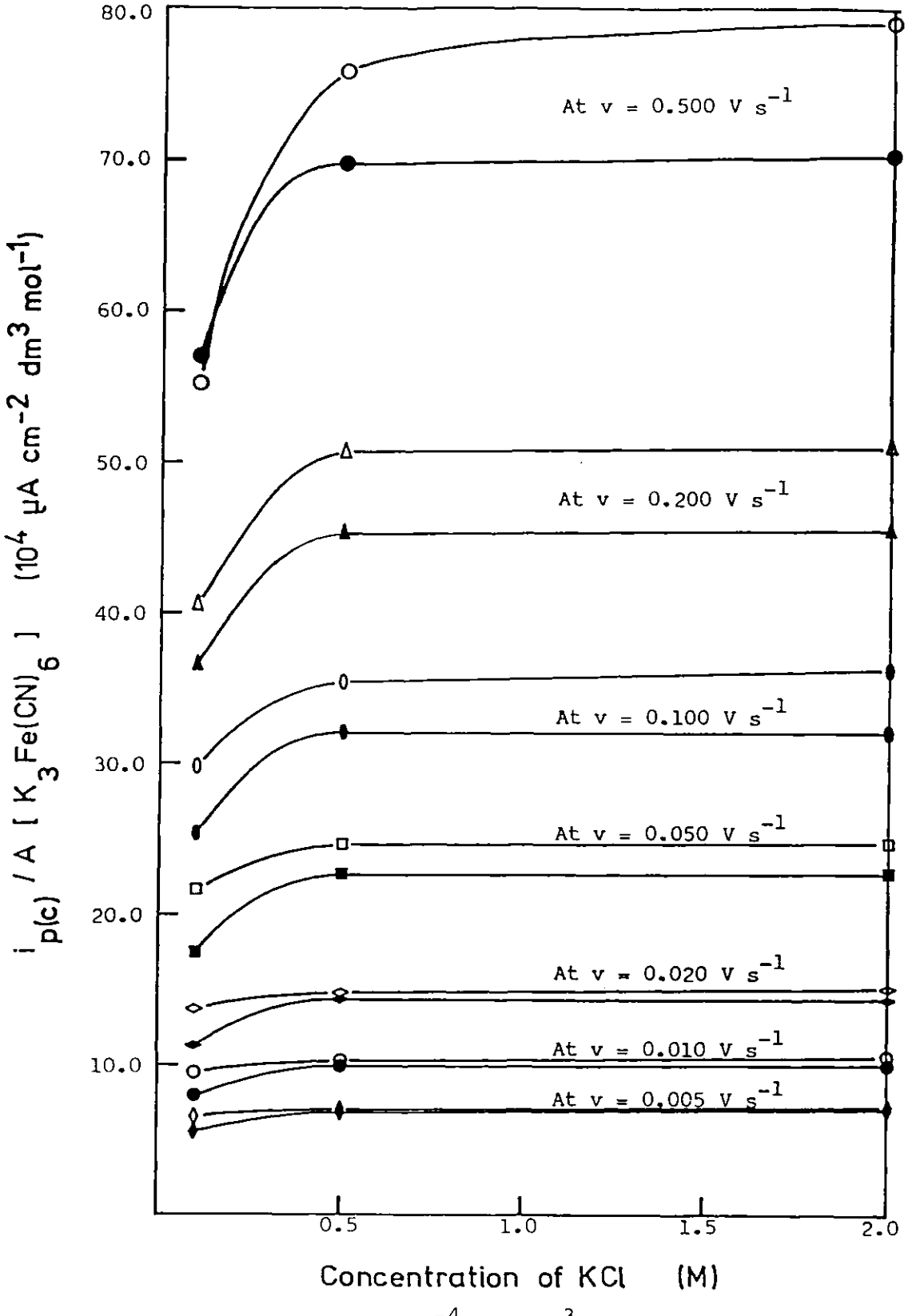

Fig. 5-367 Fe(III) Cyanide (2.0×10^{-4} mol dm^{-3})/Potassium chloride (0.1 to 2.0 M) supporting electrolyte System: Values of cathodic peak current per unit area divided by concentration of potassium ferricyanide, $i_{p(c)}/A\ [\ K_3Fe(CN)_6\ ]$, as a function of concentration of potassium chloride. Boron carbide solid electrode: ♦, ●, ◆, ■, ◖, ▲, ●. Boron carbide solid electrode treated with Ir(IV) Perchlorate (1.0×10^{-4} mol dm^{-3}): ◊, ○, ◇, □, 0, Δ, ○.

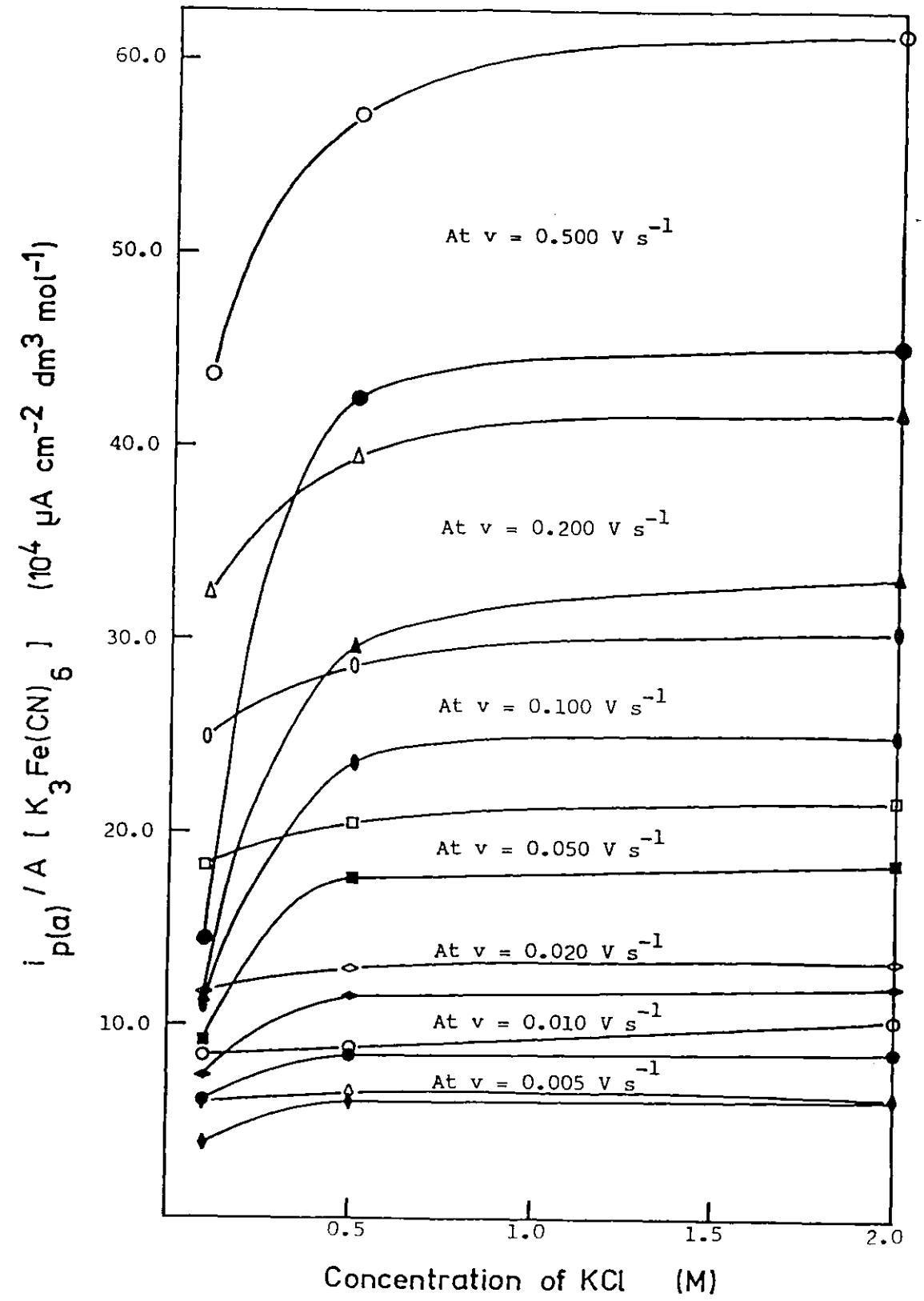

Fig. 5-368 Fe(III) Cyanide (2.0×10^{-4} mol dm^{-3})/Potassium chloride (0.1 to 2.0 M) supporting electrolyte System: Values of anodic peak current per unit area divided by concentration of potassium ferricyanide, $i_{p(a)}/A\ [\ K_3Fe(CN)_6\ ]$, as a function of concentration of potassium chloride. Boron carbide solid electrode: ♦, ●, ◆, ■, ◖, ▲, ●. Boron carbide solid electrode treated with Ir(IV) Perchlorate (1.0×10^{-4} mol dm^{-3}): ◊, ○, ◇, □, ◐, △, ○.

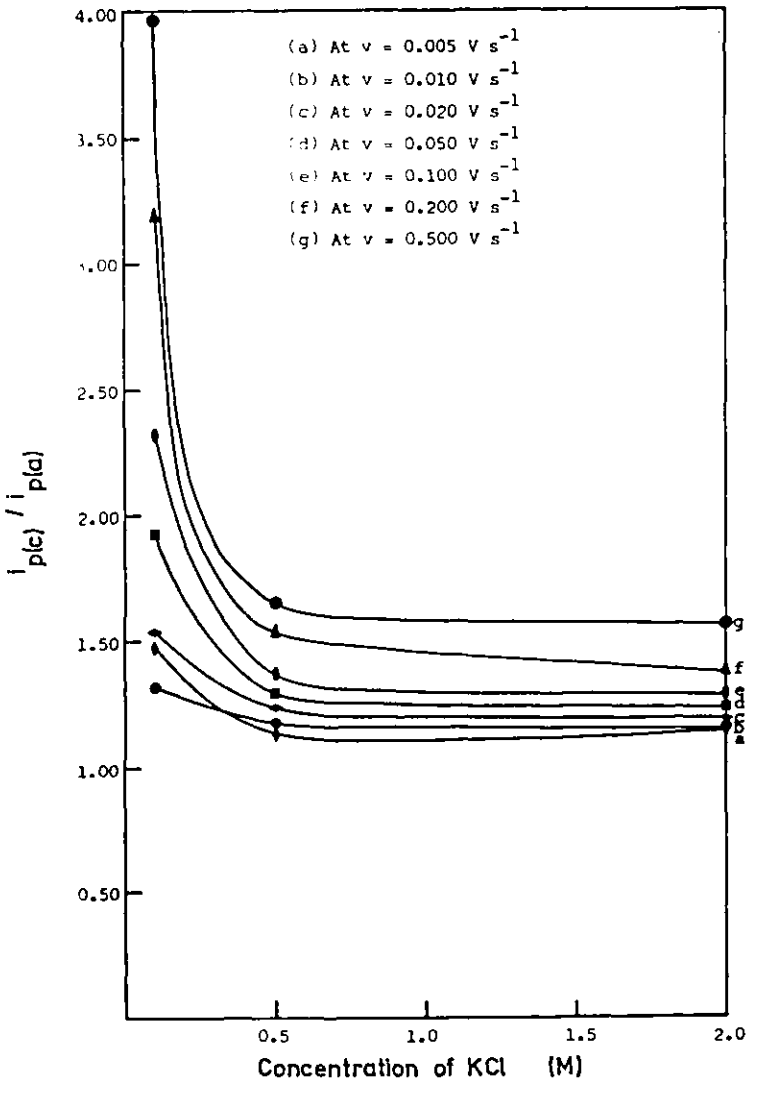

Fig. 5-369 Fe(III) Cyanide (2.0×10^{-4} mol dm^{-3})/Potassium chloride (0.1 to 2.0 M) supporting electrolyte System: Values of the ratio of cathodic to anodic peak current, $i_{p(c)}/i_{p(a)}$, as a function of concentration of potassium chloride supporting electrolyte; at scan rates of 0.005 to 0.500 V s^{-1}. Boron carbide solid electrode.

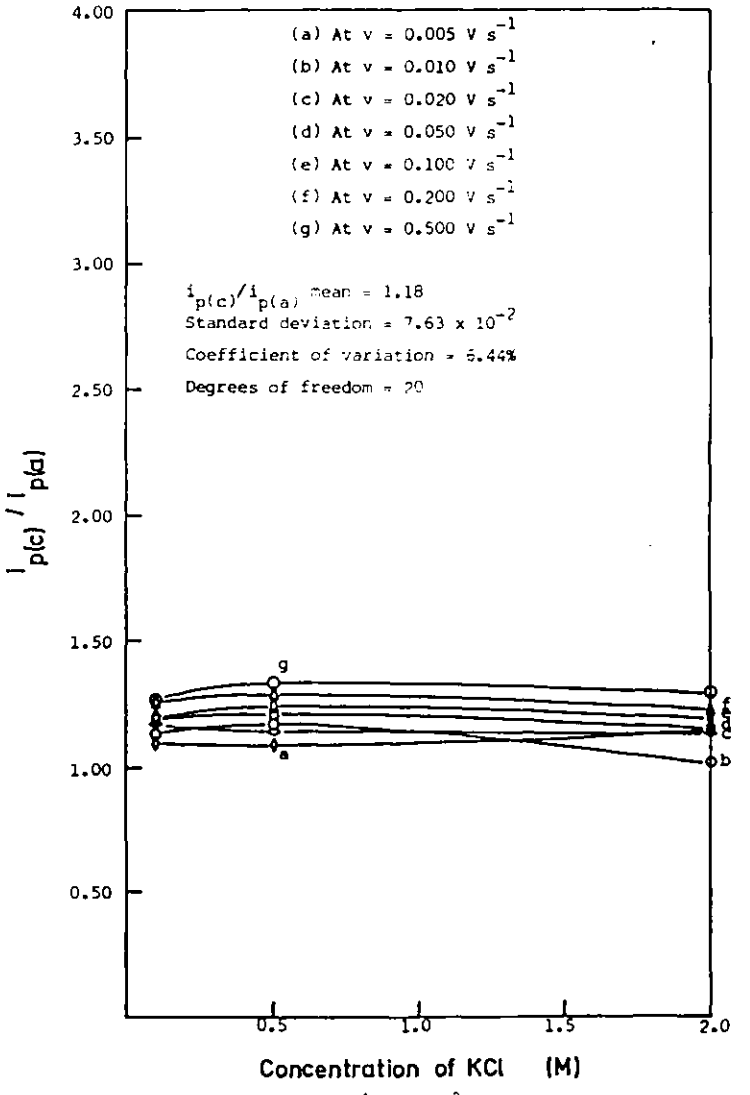

Fig. 5-370 Fe(III) Cyanide (2.0×10^{-4} mol dm^{-3})/Potassium chloride (0.1 to 2.0 M) supporting electrolyte System: Values of the ratio of cathodic to anodic peak current, $i_{p(c)}/i_{p(a)}$, as a function of concentration of potassium chloride supporting electrolyte; at scan rates of 0.005 to 0.500 V s^{-1}. Boron carbide solid electrode treated with Ir(IV) Perchlorate (1.0×10^{-4} mol dm^{-3}).

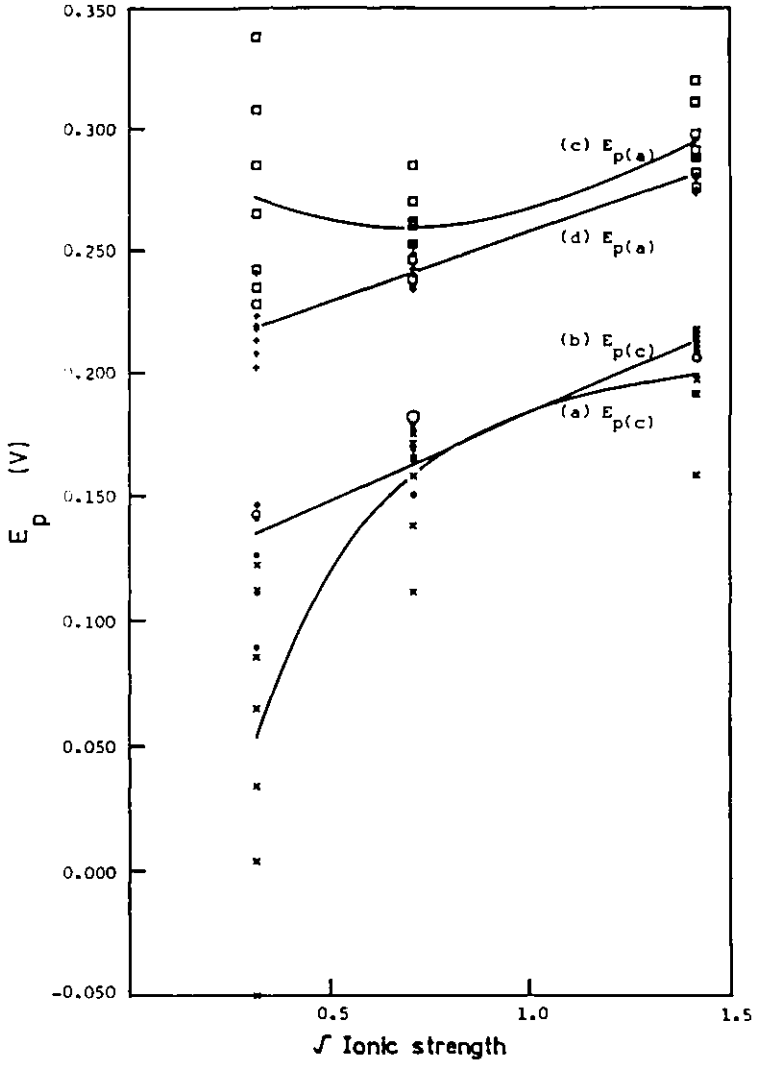

Fig. 5-371 Fe(III) Cyanide (2.0×10^{-4} mol dm^{-3})/Potassium chloride (0.1 to 2.0 M) supporting electrolyte System: Values of cathodic and anodic peak potentials, $E_{p(c)}$ and $E_{p(a)}$ respectively, as functions of square root of total ionic strength (where the concentration of potassium chloride was varied), $\sqrt{I}$; at scan rates of 0.005 to 0.500 V s^{-1}. (a) & (c) Boron carbide solid electrode: (×) & (□) respectively. (b) & (d) Boron carbide solid electrode treated with Ir(IV) Perchlorate (1.0×10^{-4} mol dm^{-3}): (•) & (+) respectively.

(b) $E_{p(c)} = 0.112 + 7.15 \times 10^{-2} \sqrt{I}$
Correlation coefficient = 0.9008
Level of significance, p = $p < 0.001$
Standard deviation of $E_{p(c)}$ from regression = 1.65×10^{-2} V
Degrees of freedom = 19

(d) $E_{p(a)} = 0.200 + 5.73 \times 10^{-2} \sqrt{I}$
Correlation coefficient = 0.9485
Level of significance, p = $p < 0.001$
Standard deviation of $E_{p(a)}$ from regression = 9.13×10^{-3} V
Degrees of freedom = 19

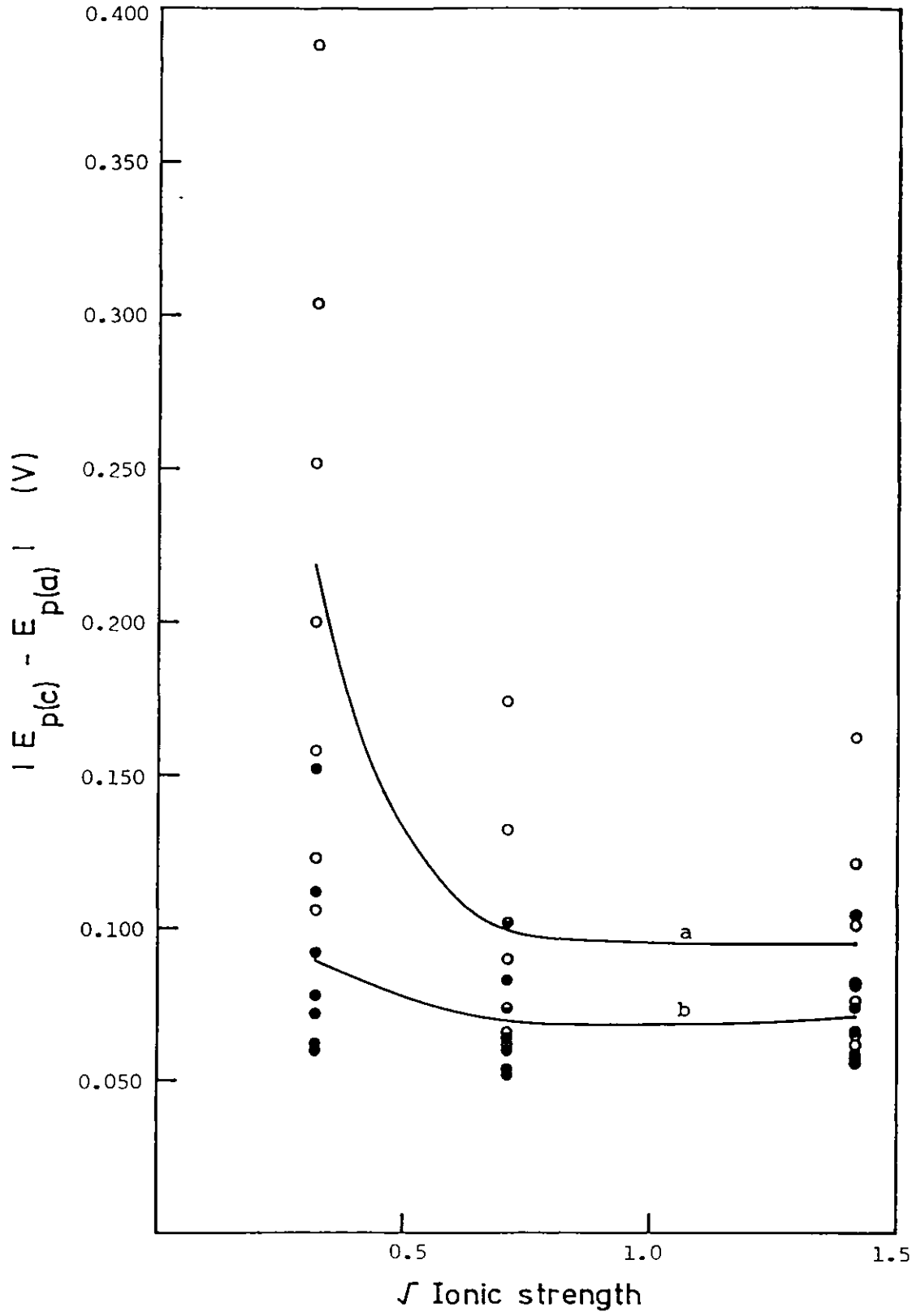

Fig. 5-372 Fe(III) Cyanide (2.0×10^{-4} mol dm^{-3})/Potassium chloride (0.1 to 2.0 M) supporting electrolyte System: Values of the absolute difference between cathodic and anodic peak potential, $|E_{p(c)} - E_{p(a)}|$, as a function of square root of total ionic strength (where the concentration of potassium chloride was varied), $\sqrt{I}$; at scan rates of 0.005 to 0.500 V s^{-1}. (a) Boron carbide solid electrode: (o). (b) Boron carbide solid electrode treated with Ir(IV) Perchlorate (1.0×10^{-4} mol dm^{-3}): (●).

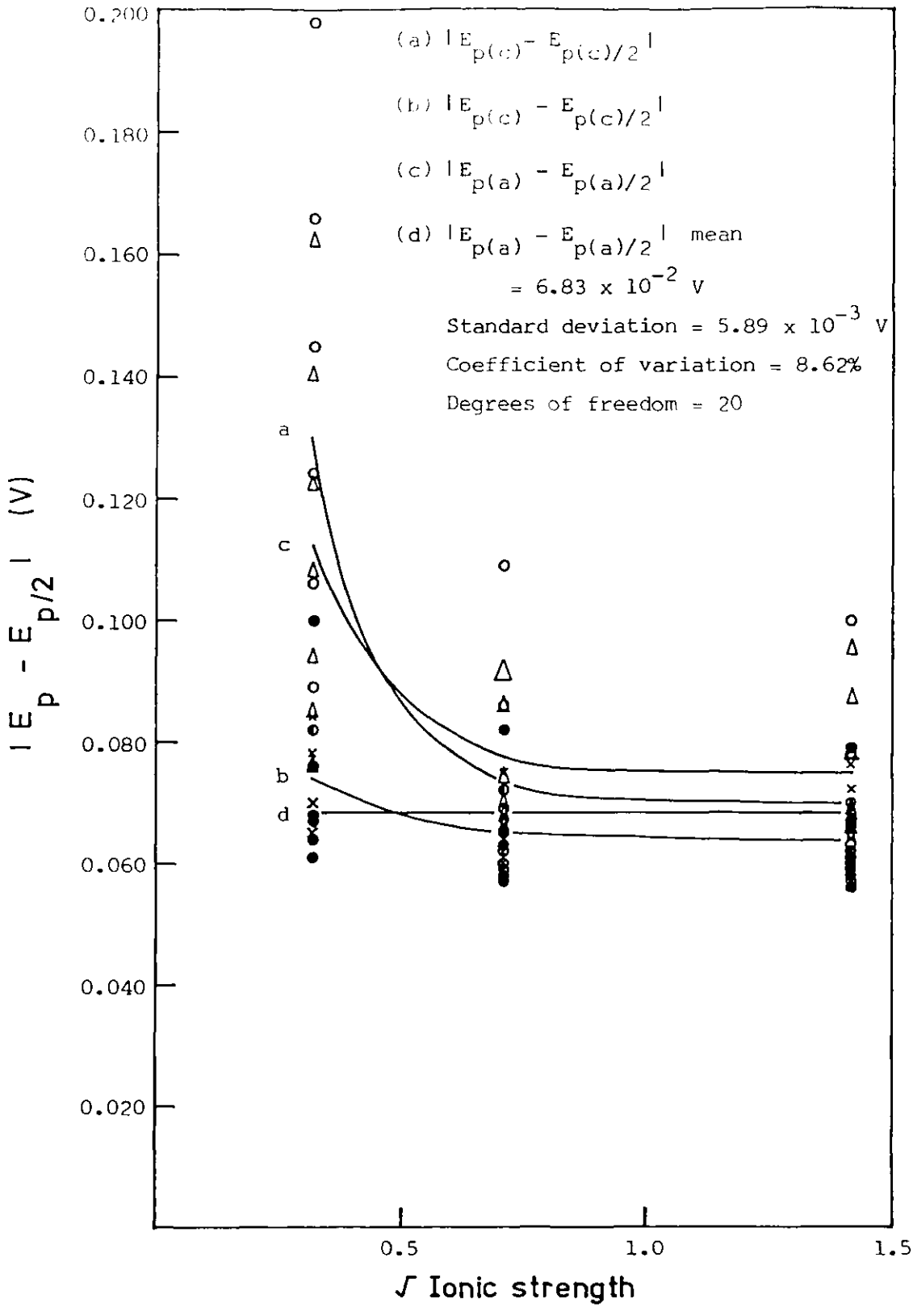

Fig. 5-373 Fe(III) Cyanide (2.0 x 10^{-4} mol dm^{-3})/Potassium chloride (0.1 to 2.0 M) supporting electrolyte System: Values of the absolute difference between peak and half-peak potentials, $|E_p - E_{p/2}|$, as a function of square root of total ionic strength (where the concentration of potassium chloride was varied), $\sqrt{I}$; at scan rates of 0.005 to 0.500 V s^{-1}. (a) & (c) Boron carbide solid electrode: (o) & (Δ). (b) & (d) Boron carbide solid electrode treated with Ir(IV) Perchlorate (1.0 x 10^{-4} mol dm^{-3}): (●) & (×).

with Ir(IV) perchlorate, however, the reversibility of the electron charge transfer for ferricyanide was greatly improved; αn values ranged from 0.96 to 0.76 (Fig. 5-331, b). The improved reversibility was also reflected in the anodic shift in $E_{\frac{1}{2}}$ values; range of 0.188-0.173 V (vs SCE), at the boron carbide solid electrode as prepared, shifted to 0.210-0.196 V (vs SCE) after the working electrode had been treated with Ir(IV) perchlorate (Fig. 5-332). The limiting current density at the boron carbide solid electrode, without or with Ir(IV)-perchlorate treatment, was linearly dependent upon the concentration of $K_3Fe(CN)_6$ to a level of significance better than 0.001 (Fig. 5-333). The electroactive species was shown to be anionic by the anodic shift in $E_{\frac{1}{2}}$ values with increasing (ionic strength)$^{\frac{1}{2}}$, as the concentration of KCl supporting electrolyte was increased (Fig. 5-335).

Cyclic voltammetry of $K_3Fe(CN)_6$ (8.0×10^{-5} to 2.0×10^{-3} mol dm^{-3})/KCl (0.5 M) supporting electrolyte solutions, at the boron carbide solid electrode, revealed that the slow electron charge transfer was complicated by a catalytic reaction (Figures 5-337 to 5-344 inclusive). After the boron carbide solid working electrode had been treated with Ir(IV) perchlorate, the current functions as functions of (sweep rate)$^{\frac{1}{2}}$ showed that the charge transfer became more reversible but was complicated by the presence of adsorption. At high concentrations of e.a.s., however, the influence of adsorption was minimised and the factors of slow charge transfer coupled with the catalytic reaction became dominant (Figures 5-345 to 5-352 inclusive). The peak current density was linearly dependent upon the concentration of $K_3Fe(CN)_6$ to a level of significance better than 0.001 for sweep rates of 0.005 to 0.500 V s^{-1} and irrespective of Ir(IV)-perchlorate treatment of the working electrode (Figures 5-357 to 5-360 inclusive).

The electrochemical reduction of potassium ferricyanide, in KCl (0.5 M) supporting electrolyte, at the boron carbide solid working electrode may be represented by

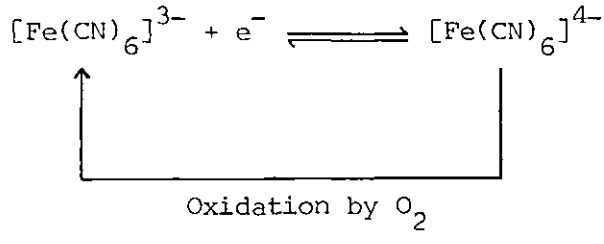

5-3 Silver

Some examples of d.c. and cyclic voltammograms for Ag(I) perchlorate, in sodium perchlorate (0.1 M) supporting electrolyte, obtained at the boron carbide solid working electrode are presented in Fig. 5-374.

5-3.1 D.c. voltammetry

The values of n, as functions of the concentration of $AgClO_4$, show that the electron charge transfer became less reversible at higher concentrations (Fig. 5-375). Furthermore, the electro-reduction was reversible (n mean = 0.98 ± 0.07, 4 degrees of freedom) after the boron carbide electrode had been treated with concentrated HNO_3; as compared with the quasi-reversible (n mean = 0.78 ± 0.11, 17 degrees of freedom) charge transfer obtained when the boron carbide electrode was treated by anodic polarisation (at +1.5 V vs SCE) in the sample solution. As to be expected of an electrodeposition, the values of $E_{\frac{1}{2}}$ were anodically shifted by increasing concentration of $AgClO_4$ depolarizer (Fig. 5-376 and equation 3-21). The limiting current density was linearly dependent upon the concentration of $AgClO_4$ (Fig. 5-377); but the sensitivity was lower if the boron carbide solid working electrode was treated with $c.HNO_3$ rather than by anodic polarisation (at +1.5 V vs SCE).

5-3.2 Cyclic voltammetry

The peak current functions, as functions of $(\text{sweep rate})^{\frac{1}{2}}$, show that the electron charge transfer was coupled with a catalytic reaction (Figures 5-378 and 5-379, c.f. Fig. 3-6). The cathodic peak potential was cathodically shifted by the increasing sweep rate whilst the anodic peak potential remained relatively constant (Fig. 5-380); the resulting trend of $|E_{p(c)} - E_{p(a)}|$ being plotted in Fig. 5-381. This indicates a decreasing reversibility in the charge transfer as the sweep rate was increased; confirmed by the widening of $|E_p - E_{p/2}|$ values (Fig. 5-382). Fig. 5-382 also shows that the electro-reduction was less reversible than the corresponding electro-oxidation. The cathodic and anodic peak current densities were linearly dependent upon the concentration of $AgClO_4$ (Figures 5-383 and 5-384 respectively).

Fig. 5-385 indicates that the peak potentials were anodically shifted by increasing concentration of $AgClO_4$, as to be expected of an electron charge transfer involving a solid reductant (equation 3-37).

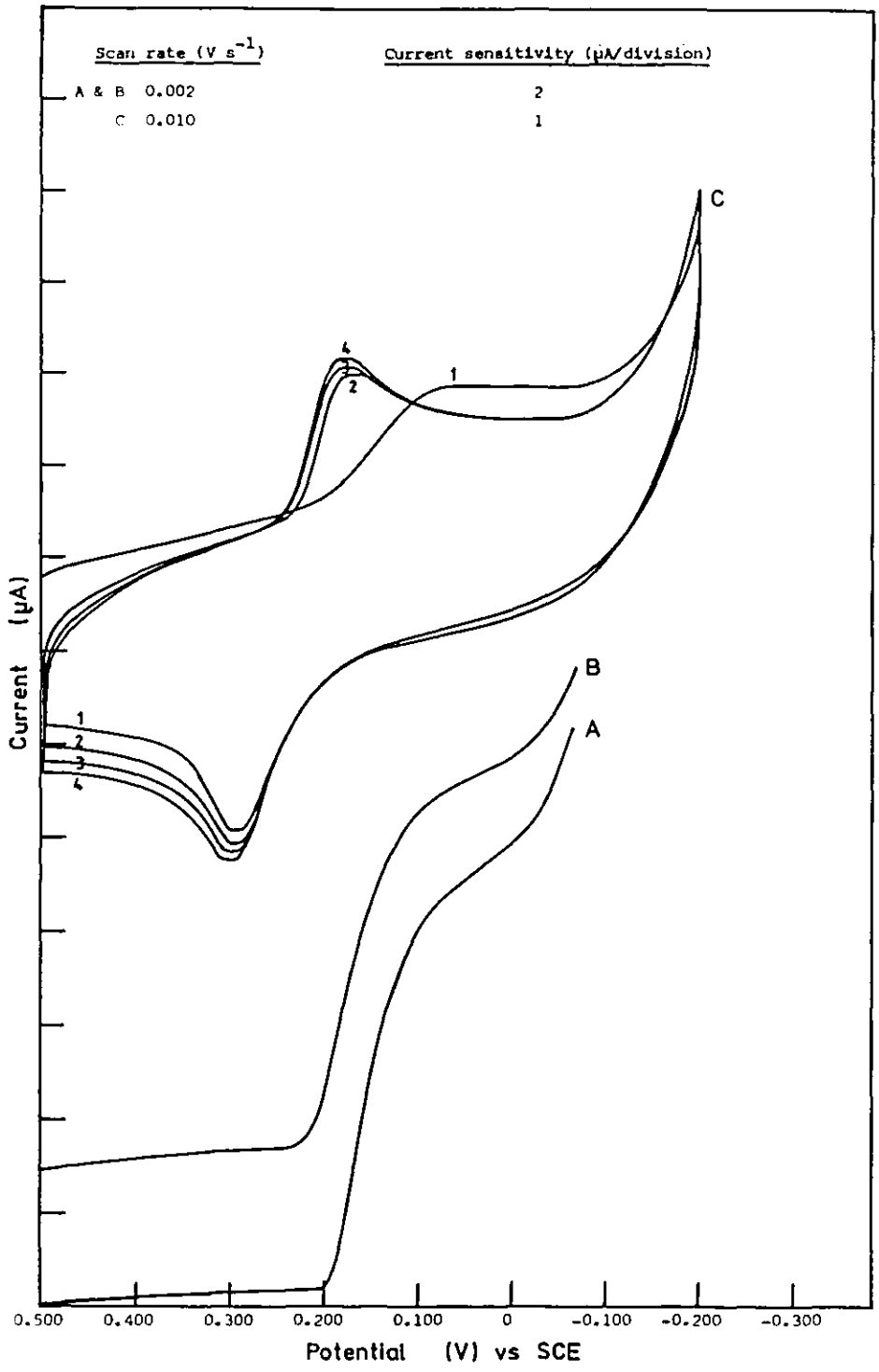

Fig. 5-374 Ag(I) perchlorate (2.0×10^{-5} mol dm^{-3})/Sodium perchlorate (0.1 M) supporting electrolyte System: D.c. voltammograms (A & B) and cyclic voltammogram (C) obtained at the boron carbide solid electrode. A) Electrode treated with c.HNO_3 . B) Electrode treated by anodic polarisation (at +1.5 V vs SCE) in the sample solution. C) Electrode poised at +0.5 V (vs SCE) prior to cyclic multiple sweeps; where the cycles have been numbered according to the sequence in which they were obtained.

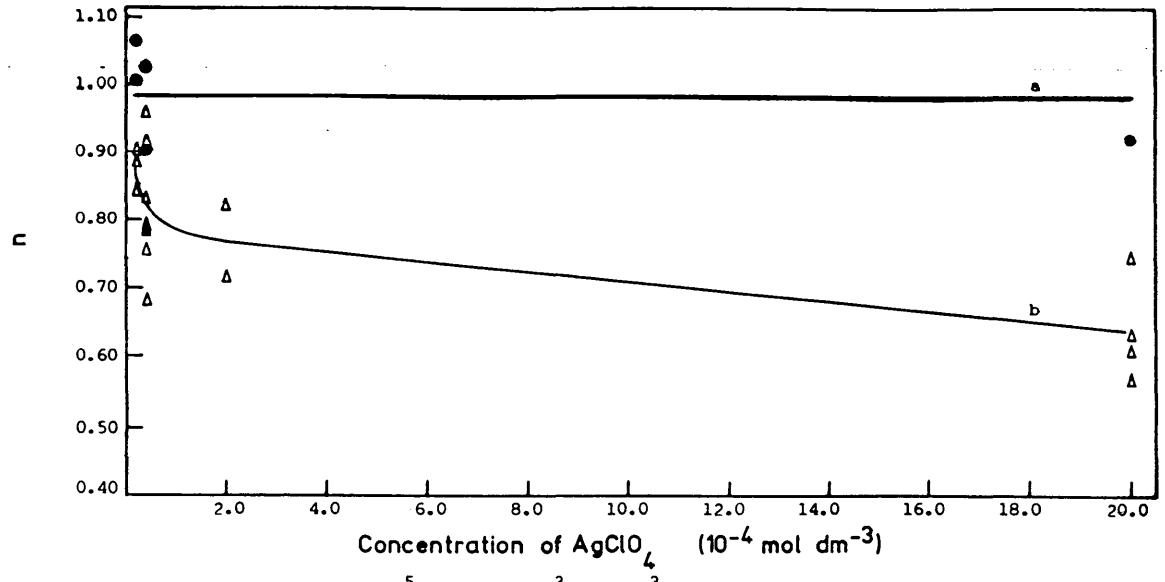

Fig. 5-375 Ag(I) Perchlorate (2.0×10^{-5} to 2.0×10^{-3} mol dm^{-3})/Sodium perchlorate (0.1 M) supporting electrolyte System: Values of n as a function of concentration of silver perchlorate, [$AgClO_4$]. (a) Boron carbide solid electrode treated with concentrated nitric acid. (b) Boron carbide solid electrode treated by anodic polarisation (at +1.5 V) in the sample solution.

(a) n mean = 0.98
Standard deviation = 7.06×10^{-2}
Coefficient of variation = 7.18%
Degrees of freedom = 4

(b) n mean = 0.78
Standard deviation = 0.112
Coefficient of variation = 14.3%
Degrees of freedom = 17

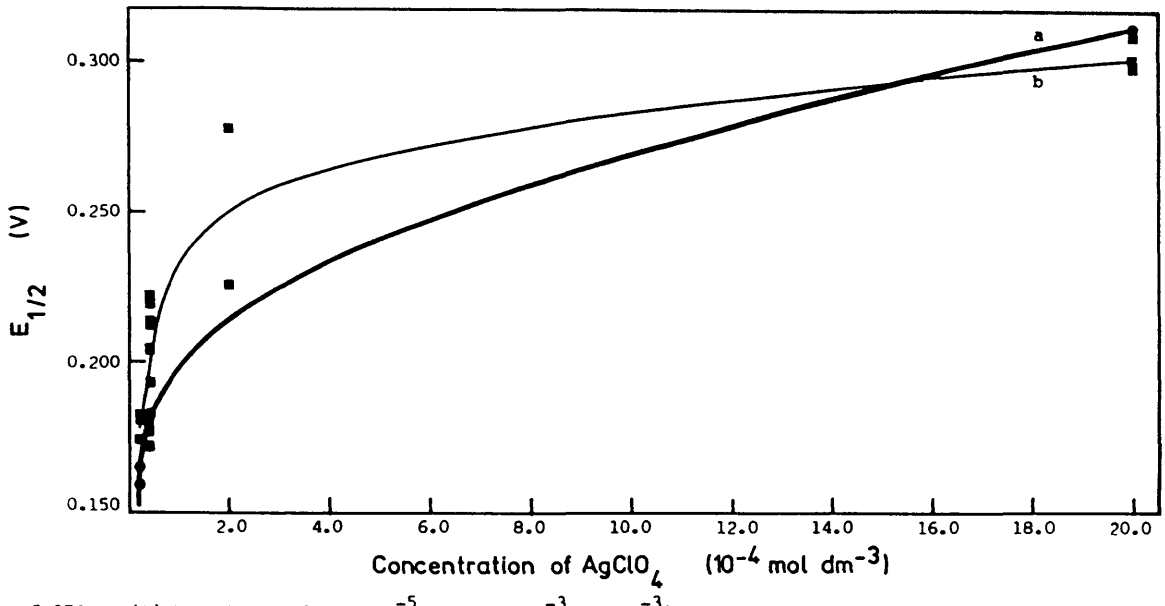

Fig. 5-376 Ag(I) Perchlorate (2.0×10^{-5} to 2.0×10^{-3} mol dm^{-3})/Sodium perchlorate (0.1 M) supporting electrolyte System: Values of half-wave potential, $E_{\frac{1}{2}}$, as a function of concentration of silver perchlorate, [$AgClO_4$]. (a) Boron carbide solid electrode treated with concentrated nitric acid. (b) Boron carbide solid electrode treated by anodic polarisation (at +1.5 V) in the sample solution.

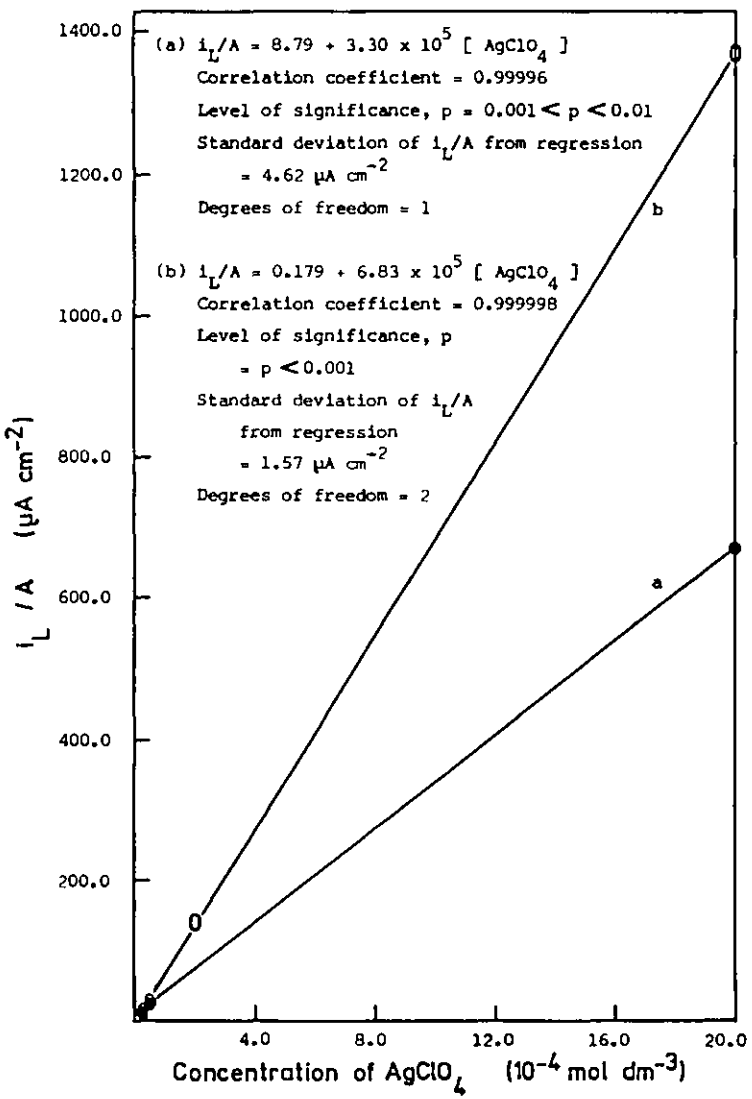

Fig. 5-377 Ag(I) Perchlorate (2.0 x 10^{-5} to 2.0 x 10^{-3} mol dm^{-3})/Sodium perchlorate (0.1 M) supporting electrolyte System: Dependence of limiting current per unit area, i_L/A, on the concentration of silver perchlorate, [$AgClO_4$]. (a) Boron carbide solid electrode treated with concentrated nitric acid. (b) Boron carbide solid electrode treated by anodic polarisation (at +1.5 V) in the sample solution.

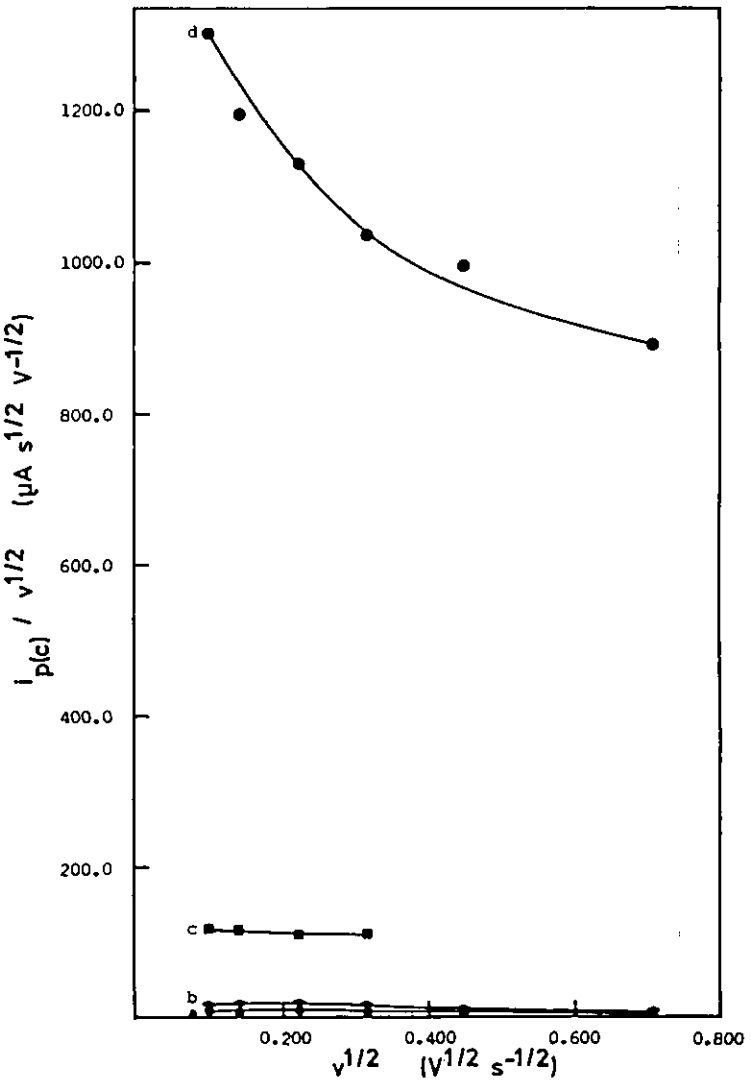

Fig. 5-378 Ag(I) Perchlorate (2.0 x 10^{-5} to 2.0 x 10^{-3} mol dm^{-3})/Sodium perchlorate (0.1 M) supporting electrolyte System: Values of cathodic current function, $i_{p(c)}/v^{\frac{1}{2}}$, as a function of square root of potential scan rate, $v^{\frac{1}{2}}$; at silver perchlorate concentrations of (a) 2.0 x 10^{-5}, (b) 4.0 x 10^{-5}, (c) 2.0 x 10^{-4}, and (d) 2.0 x 10^{-3} mol dm^{-3}. Boron carbide solid electrode.

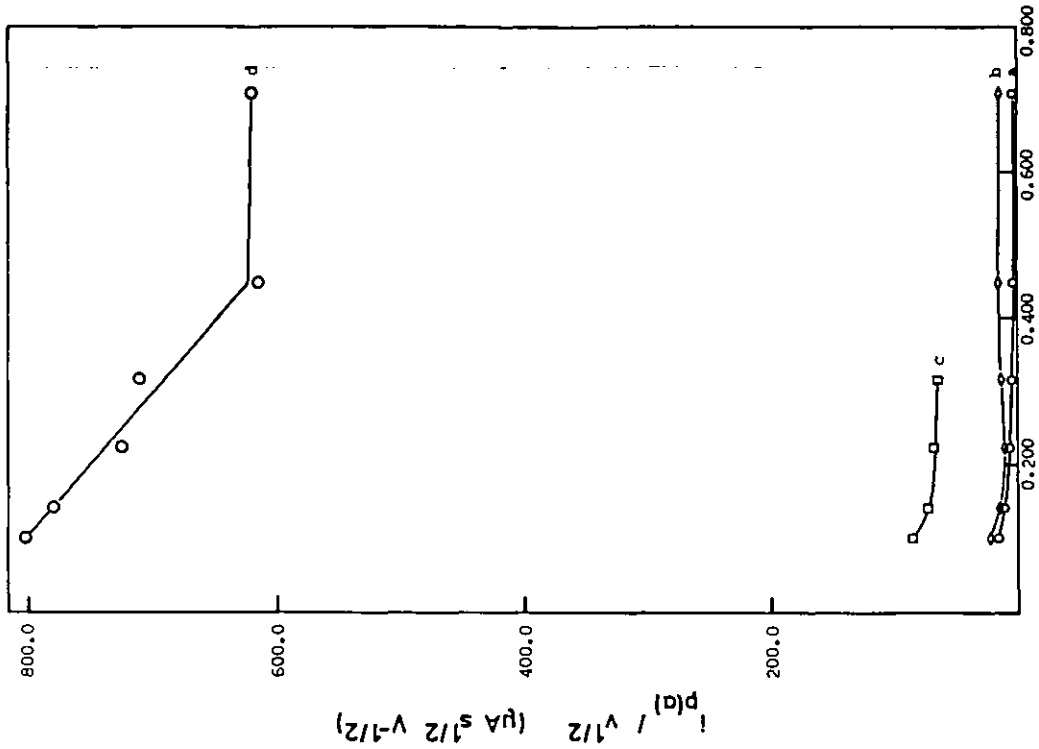

Fig. 5-379 Ag(I) Perchlorate (2.0 x 10^{-5} to 2.0 x 10^{-3} mol dm^{-3})/Sodium perchlorate (0.1 M) supporting electrolyte System: Values of anodic current function, $i_{p(a)}/v^{\frac{1}{2}}$, as a function of square root of potential scan rate, $v^{\frac{1}{2}}$; at silver perchlorate concentrations of (a) 2.0 x 10^{-5}, (b) 4.0 x 10^{-5}, (c) 2.0 x 10^{-4}, and (d) 2.0 x 10^{-3} mol dm^{-3}. Boron carbide solid electrode.

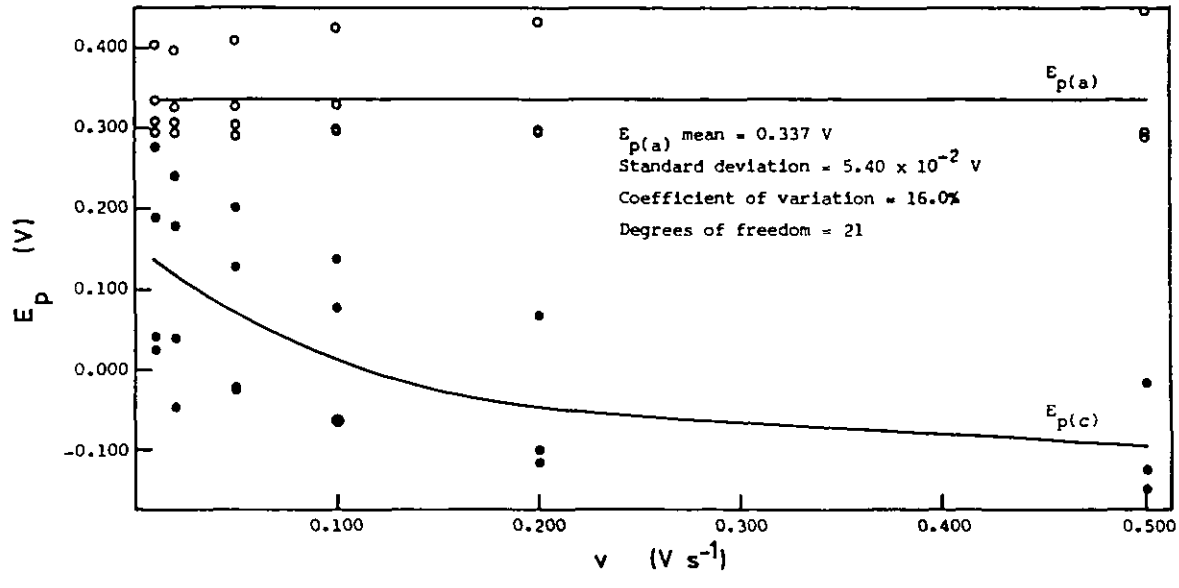

Fig. 5-380 Ag(I) Perchlorate (2.0 x 10^{-5} to 2.0 x 10^{-3} mol dm^{-3})/Sodium perchlorate (0.1 M) supporting electrolyte System: Values of cathodic and anodic peak potentials, $E_{p(c)}$ and $E_{p(a)}$ respectively, as functions of potential scan rate, v; at silver perchlorate concentrations of 2.0 x 10^{-5} to 2.0 x 10^{-3} mol dm^{-3}. Boron carbide solid electrode.

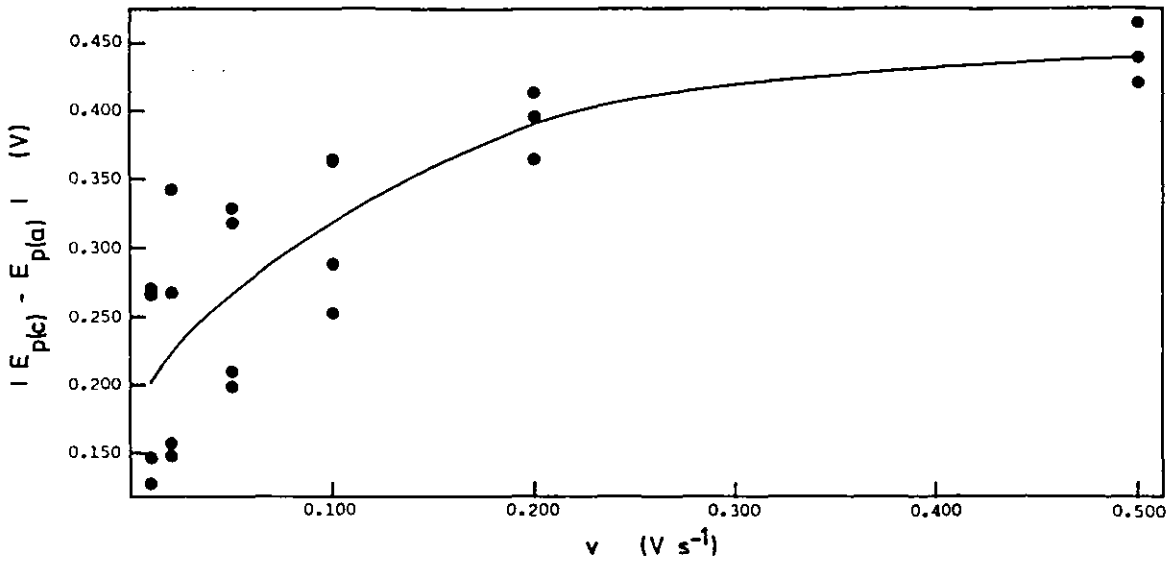

Fig. 5-381 Ag(I) Perchlorate (2.0×10^{-5} to 2.0×10^{-3} mol dm^{-3})/Sodium perchlorate (0.1 M) supporting electrolyte System: Values of the absolute difference between cathodic and anodic peak potentials, $|E_{p(c)} - E_{p(a)}|$, as a function of potential scan rate, v; at silver perchlorate concentrations of 2.0×10^{-5} to 2.0×10^{-3} mol dm^{-3}. Boron carbide solid electrode.

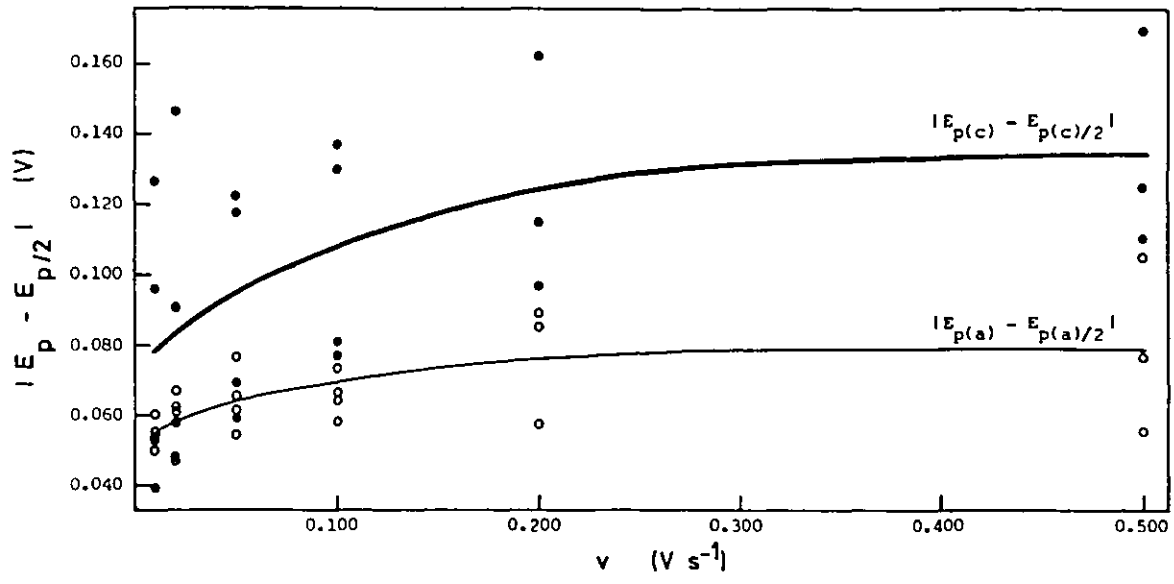

Fig. 5-382 Ag(I) Perchlorate (2.0×10^{-5} to 2.0×10^{-3} mol dm^{-3})/Sodium perchlorate (0.1 M) supporting electrolyte System: Values of the absolute difference between peak and half-peak potentials for the cathodic and anodic curves, $|E_{p(c)} - E_{p(c)/2}|$ and $|E_{p(a)} - E_{p(a)/2}|$ respectively, as functions of potential scan rate, v; at silver perchlorate concentrations of 2.0×10^{-5} to 2.0×10^{-3} mol dm^{-3}. Boron carbide solid electrode.

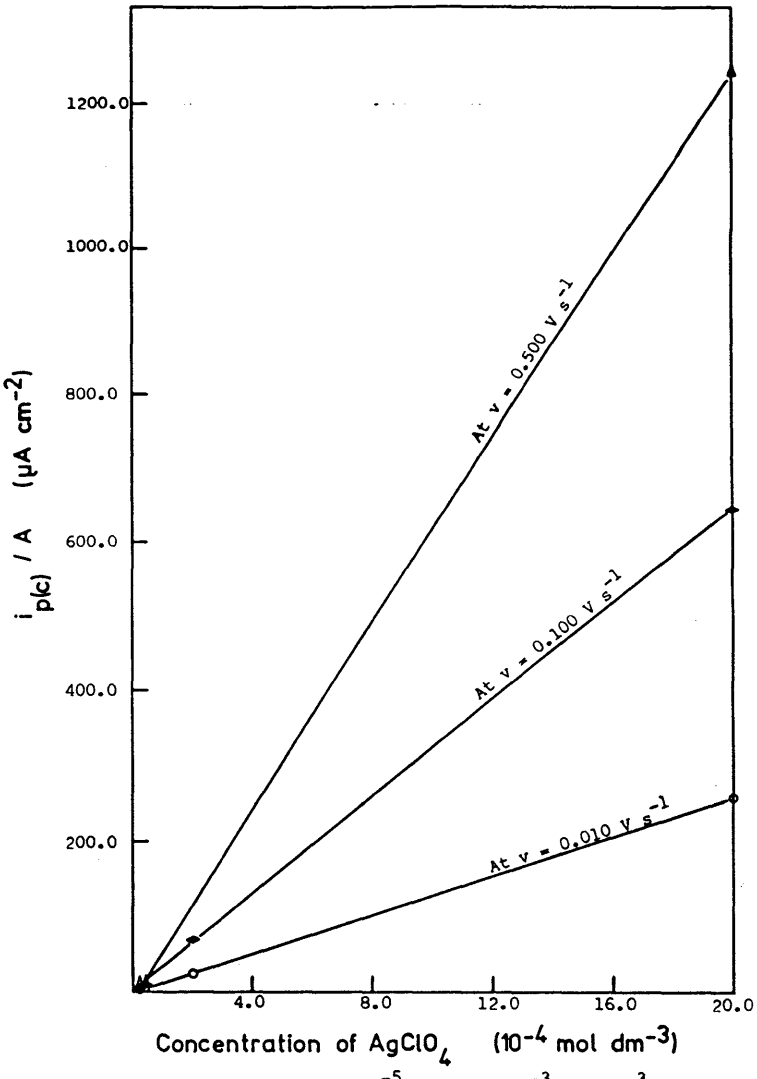

Fig. 5-383 Ag(I) Perchlorate (2.0×10^{-5} to 2.0×10^{-3} mol dm^{-3})/Sodium perchlorate (0.1 M) supporting electrolyte System: Dependence of cathodic peak current per unit area, $i_{p(c)}/A$, on the concentration of silver perchlorate, [$AgClO_4$]; at scan rates of 0.010 to 0.500 V s^{-1}. Boron carbide solid electrode.

(a) At v = 0.010 V s^{-1}:

$i_{p(c)}/A = 1.29 \times 10^5$ [$AgClO_4$] - 1.69
Correlation coefficient = 0.999990
Level of significance, p = $p < 0.001$
Standard deviation of $i_{p(c)}/A$ from regression = 0.682 μA cm^{-2}
Degrees of freedom = 2

(b) At v = 0.100 V s^{-1}:

$i_{p(c)}/A = 3.23 \times 10^5$ [$AgClO_4$] - 8.73×10^{-2}
Correlation coefficient = 0.999950
Level of significance, p = $p < 0.001$
Standard deviation of $i_{p(c)}/A$ from regression = 3.78 μA cm^{-2}
Degrees of freedom = 2

(c) At v = 0.500 V s^{-1}:

$i_{p(c)}/A = 6.26 \times 10^5$ [$AgClO_4$] - 9.69
Correlation coefficient = 0.999980
Level of significance, p = $0.001 < p < 0.01$
Standard deviation of $i_{p(c)}/A$ from regression = 6.34 μA cm^{-2}
Degrees of freedom = 1

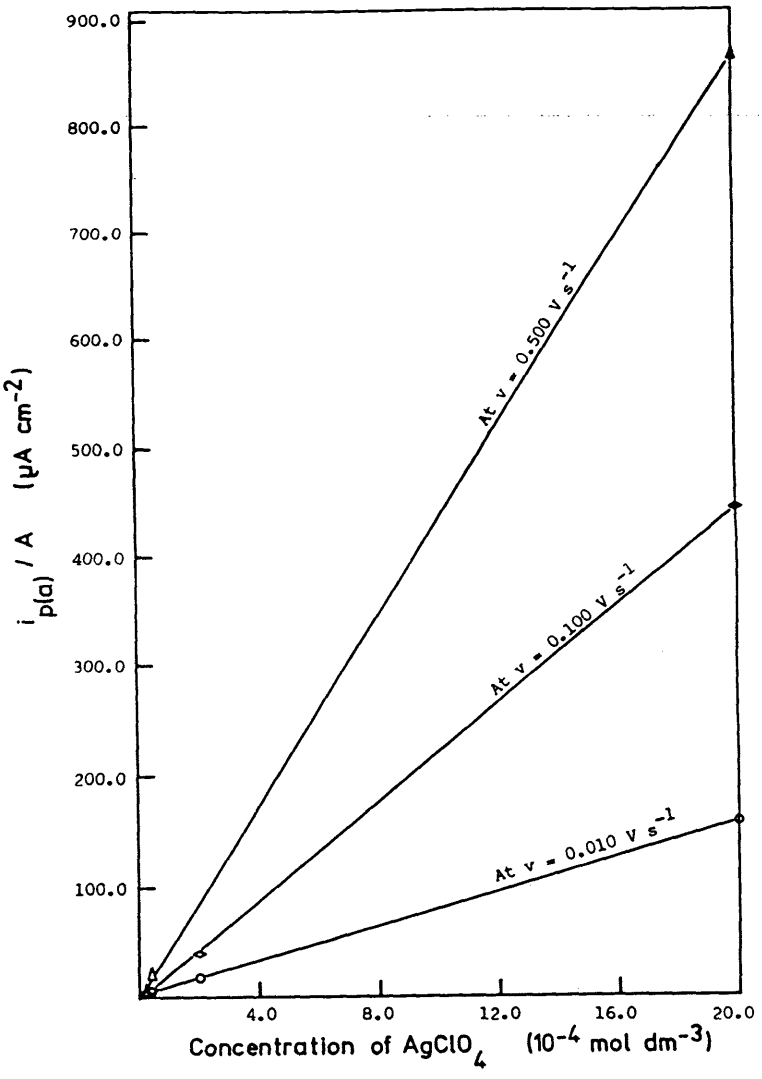

Fig. 5-384 Ag(I) Perchlorate (2.0×10^{-5} to 2.0×10^{-3} mol dm^{-3})/Sodium perchlorate (0.1 M) supporting electrolyte System: Dependence of anodic peak current per unit area, $i_{p(a)}/A$, on the concentration of silver perchlorate, [$AgClO_4$]; at scan rates of 0.010 to 0.500 V s^{-1}. Boron carbide solid electrode.

(a) At v = 0.010 V s^{-1}:

$i_{p(a)}/A = 1.33 + 7.82 \times 10^4$ [$AgClO_4$]
Correlation coefficient = 0.999997
Level of significance, p = $p < 0.001$
Standard deviation of $i_{p(a)}/A$ from regression = 0.234 μA cm^{-2}
Degrees of freedom = 2

(b) At v = 0.100 V s^{-1}:

$i_{p(a)}/A = 2.22 \times 10^5$ [$AgClO_4$] - 2.32
Correlation coefficient = 0.999977
Level of significance, p = $p < 0.001$
Standard deviation of $i_{p(a)}/A$ from regression = 1.79 μA cm^{-2}
Degrees of freedom = 2

(c) At v = 0.500 V s^{-1}:

$i_{p(a)}/A = 4.32 \times 10^5$ [$AgClO_4$] - 0.679
Correlation coefficient = 0.999981
Level of significance, p = $0.001 < p < 0.01$
Standard deviation of $i_{p(a)}/A$ from regression = 4.33 μA cm^{-2}
Degrees of freedom = 1

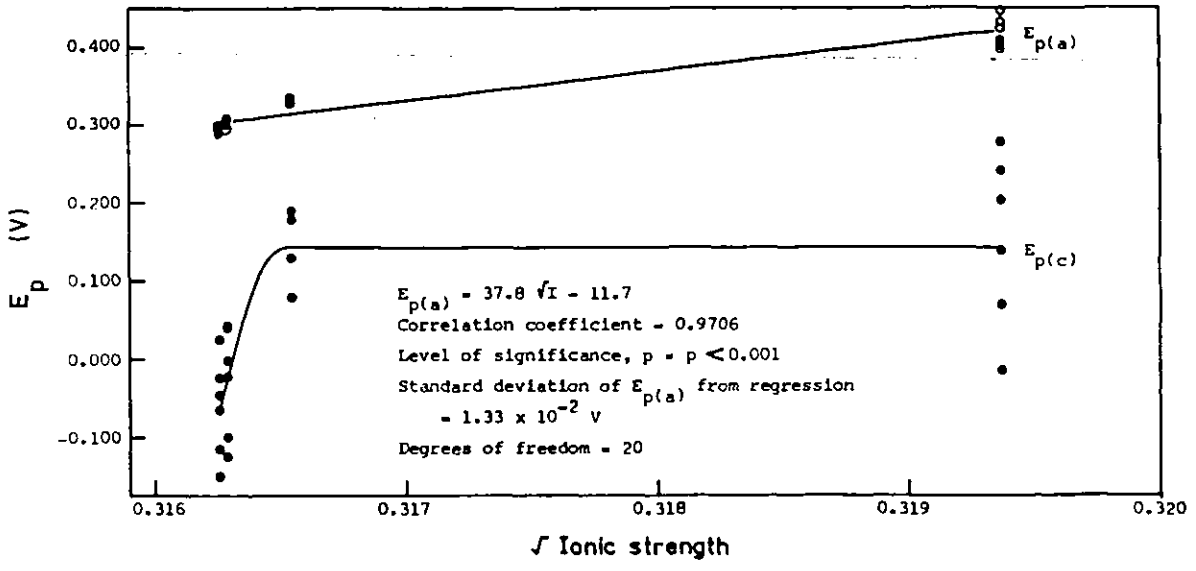

Fig. 5-385 Ag(I) Perchlorate (2.0 x 10^{-5} to 2.0 x 10^{-3} mol dm^{-3})/Sodium perchlorate (0.1 M) supporting electrolyte System: Values of cathodic and anodic peak potentials, $E_{p(c)}$ and $E_{p(a)}$ respectively, as functions of square root of total ionic strength (where the concentration of silver perchlorate was varied), √I; at scan rates of 0.010 to 0.500 V s^{-1}. Boron carbide solid electrode.

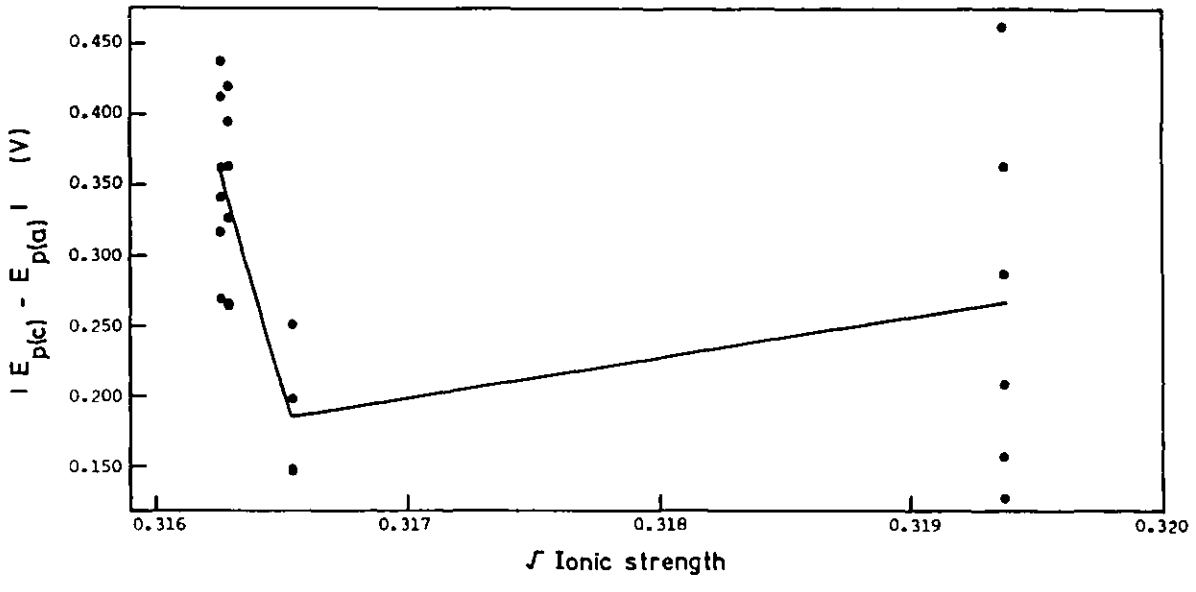

Fig. 5-386 Ag(I) Perchlorate (2.0 x 10^{-5} to 2.0 x 10^{-3} mol dm^{-3})/Sodium perchlorate (0.1 M) supporting electrolyte System: Values of the absolute difference between cathodic and anodic peak potentials, $|E_{p(c)} - E_{p(a)}|$, as a function of square root of total ionic strength (where the concentration of silver perchlorate was varied), √I; at scan rates of 0.010 to 0.500 V s^{-1}. Boron carbide solid electrode.

$|E_{p(c)} - E_{p(a)}|$ values, as functions of (ionic strength)$^{\frac{1}{2}}$ where the concentration of $AgClO_4$ was varied, initially narrowed with increasing concentration of $AgClO_4$ but subsequently widened with further increases in concentration (Fig. 5-386). Similar trends were exhibited by $|E_p - E_{p/2}|$ values (Fig. 5-387), especially for the cathodic reaction, thus suggesting that the electro-reduction of Ag(I) perchlorate was poorly reversible at the boron carbide solid electrode whenever the concentration of $AgClO_4$ was too low to cover the electrode surface with Ag during the initial stages of the electro-reduction. Further evidence for this hypothesis is furnished by studies involving multiple sweeps (Fig. 5-374, C, and Figures 5-388 to 5-392 inclusive). Fig. 5-388 shows that the peak current density, in general, increased with subsequent cycles; except for the cathodic peak current density for $AgClO_4$ (2.0×10^{-3} mol dm^{-3}) which actually decreased with subsequent sweeps. The ratio of cathodic to anodic peak current, $i_{p(c)}/i_{p(a)}$, is plotted as a function of sweep number in Fig. 5-389 and shows that the greatest difference in values occurred between the first and second cycles. Plots of peak potentials, as functions of sweep number, reveal that the cathodic peaks were anodically shifted to a relatively constant value after the initial cycle whereas the anodic peaks were relatively independent of the sweep number (Fig. 5-390). Values of $|E_{p(c)} - E_{p(a)}|$ and $|E_p - E_{p/2}|$, when plotted as functions of sweep number (Figures 5-391 and 5-392 respectively), generally narrowed with increasing sweep number; the greatest improvement in reversibility occurring between the first and second cycles.

5-3.3 Summary

D.c. voltammetry of $AgClO_4$ (2.0×10^{-5} to 2.0×10^{-3} mol dm^{-3})/ $NaClO_4$ (0.1 M) supporting electrolyte solutions at the boron carbide solid working electrode suggests that Ag^+ was reduced to Ag; the electron charge transfer being reversible (n mean = 0.98 ± 0.07, 4 degrees of freedom) if the working electrode had been treated with c.HNO_3 but quasi-reversible (n mean = 0.78 ± 0.11, 17 degrees of freedom) if the working electrode had been treated by anodic polarisation (at +1.5 V vs SCE) in the sample solution.

Cyclic voltammetry, under multiple sweep conditions, has shown that the charge transfer was coupled with a catalytic reaction and that the electro-reduction was poorly reversible whenever the concentration of $AgClO_4$ depolarizer was too low to cover the working electrode surface

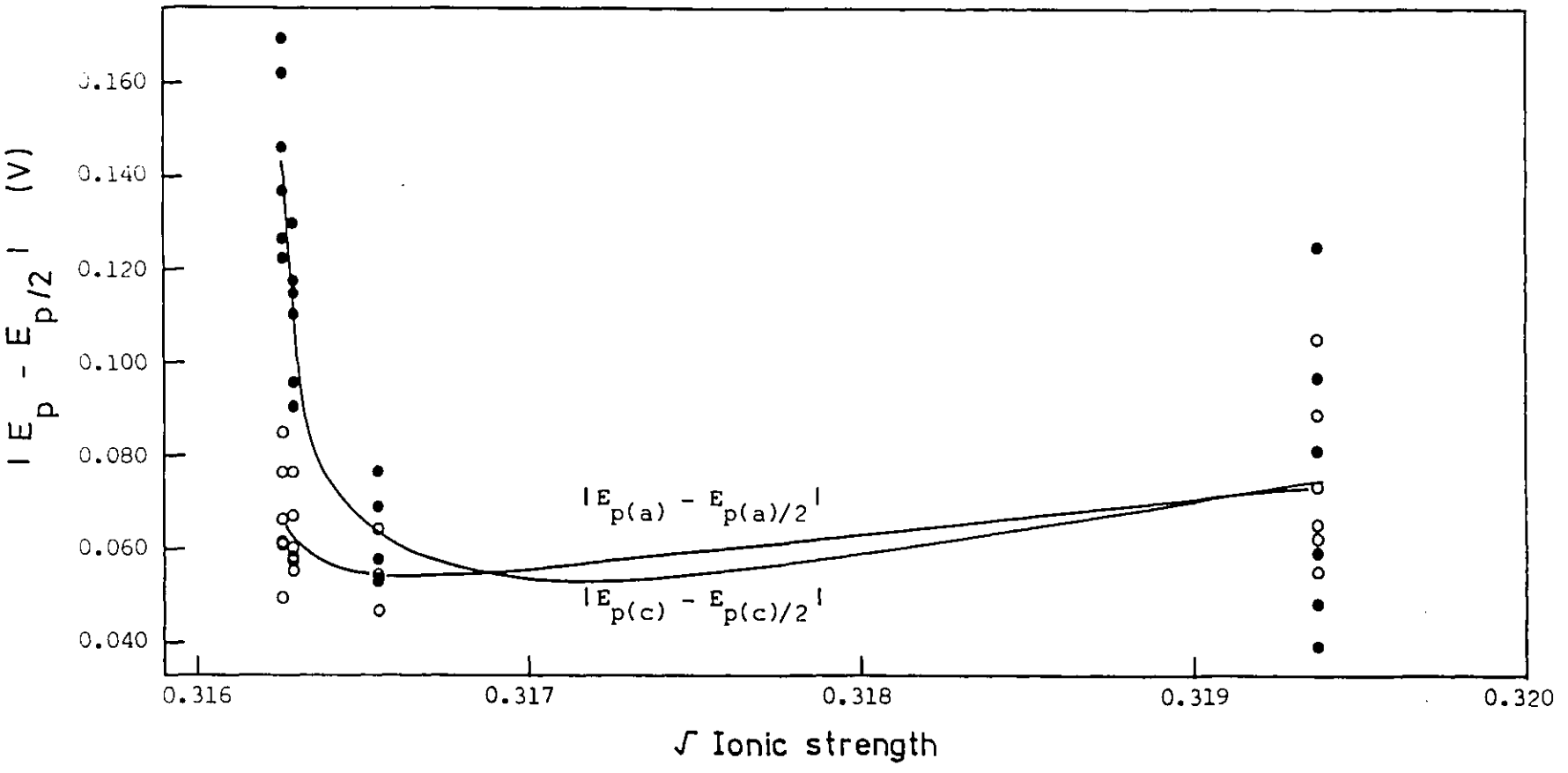

Fig. 5-387 Ag(I) Perchlorate (2.0×10^{-5} to 2.0×10^{-3} mol dm^{-3})/Sodium perchlorate (0.1 M) supporting electrolyte System: Values of the absolute difference between peak and half-peak potentials for the cathodic and anodic curves, $|E_{p(c)} - E_{p(c)/2}|$ and $|E_{p(a)} - E_{p(a)/2}|$ respectively, as functions of square root of total ionic strength (where the concentration of silver perchlorate was varied), $\sqrt{I}$; at scan rates of 0.010 to 0.500 V s^{-1}. Boron carbide solid electrode.

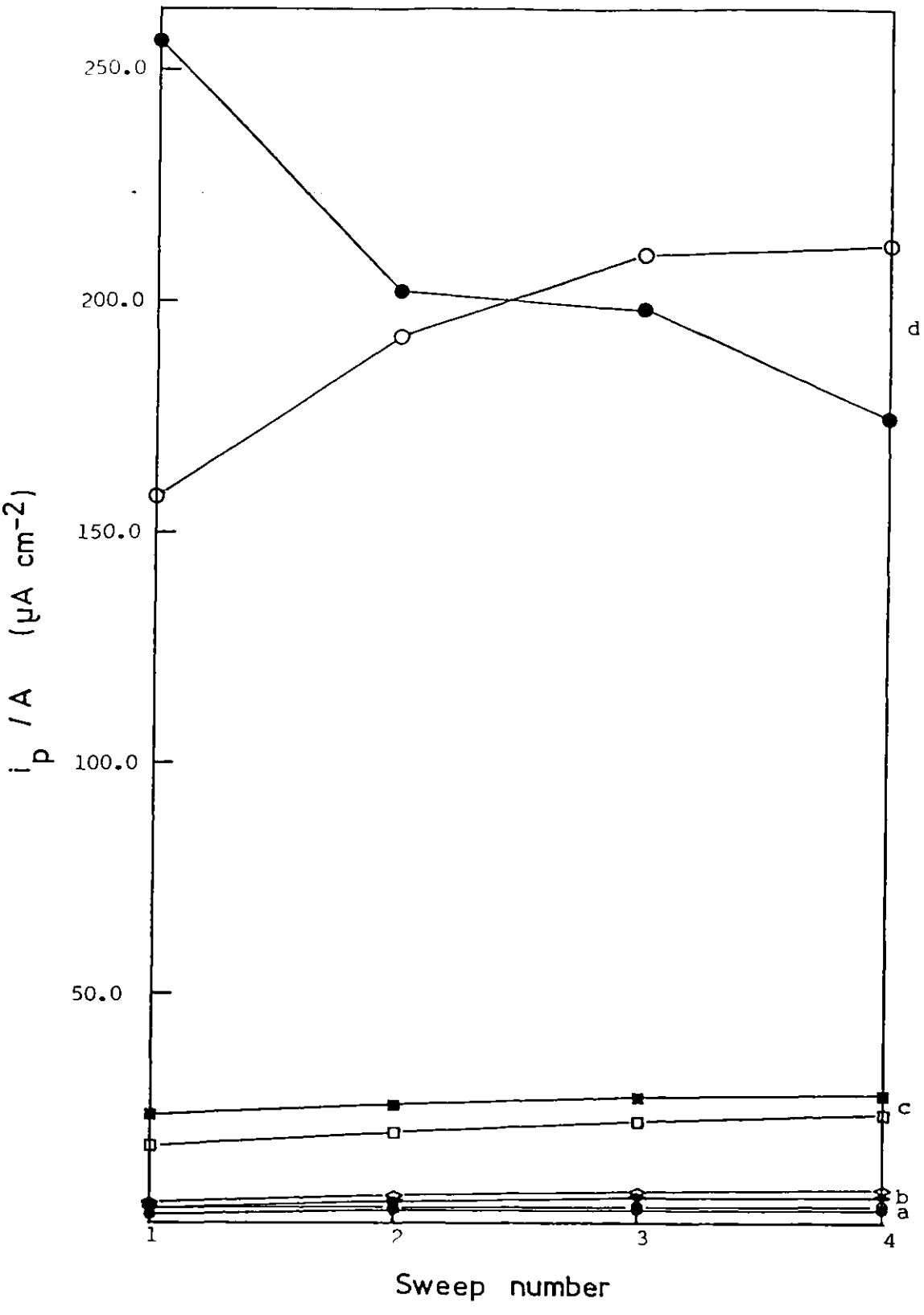

Fig. 5-388 Ag(I) Perchlorate (2.0×10^{-5} to 2.0×10^{-3} mol dm^{-3})/Sodium perchlorate (0.1 M) supporting electrolyte System: Values of cathodic and anodic peak current per unit area, $i_{p(c)}/A$ and $i_{p(a)}/A$ respectively, obtained under cyclic multiple sweep conditions; at a scan rate of 0.010 V s^{-1}. Concentration of silver perchlorate: (a) 2.0×10^{-5}, (b) 4.0×10^{-5}, (c) 2.0×10^{-4}, and (d) 2.0×10^{-3} mol dm^{-3}. $i_{p(c)}/A$: ●, ◆, ■, ●. $i_{p(a)}/A$: ○, ◇, □, ○. Boron carbide solid electrode.

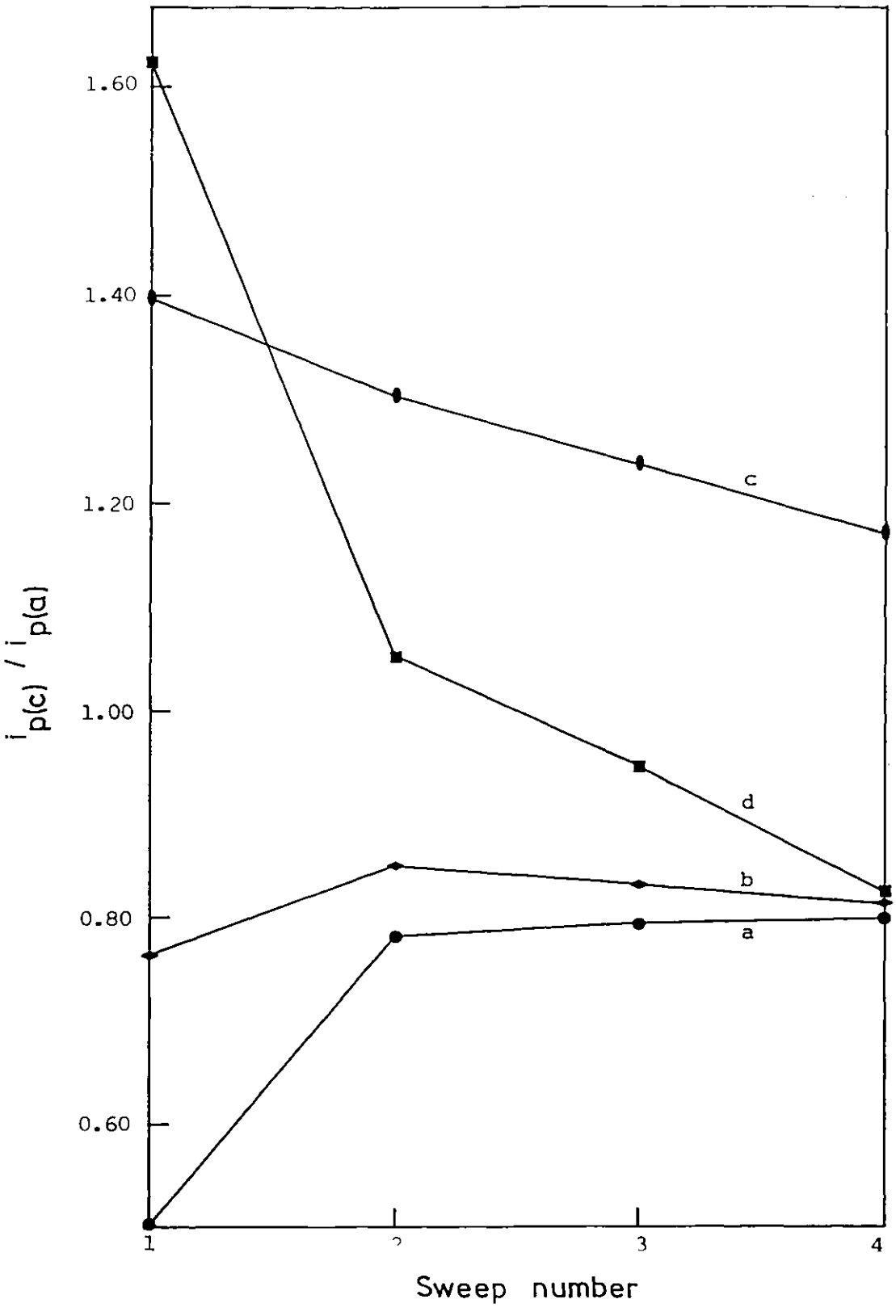

Fig. 5-389 Ag(I) Perchlorate (2.0×10^{-5} to 2.0×10^{-3} mol dm^{-3})/Sodium perchlorate (0.1 M) supporting electrolyte System: Values of the ratio of cathodic to anodic peak current, $i_{p(c)}/i_{p(a)}$, obtained under cyclic multiple sweep conditions; at a scan rate of 0.010 V s^{-1}. Concentration of silver perchlorate: (a) 2.0×10^{-5}, (b) 4.0×10^{-5}, (c) 2.0×10^{-4}, and (d) 2.0×10^{-3} mol dm^{-3}. Boron carbide solid electrode.

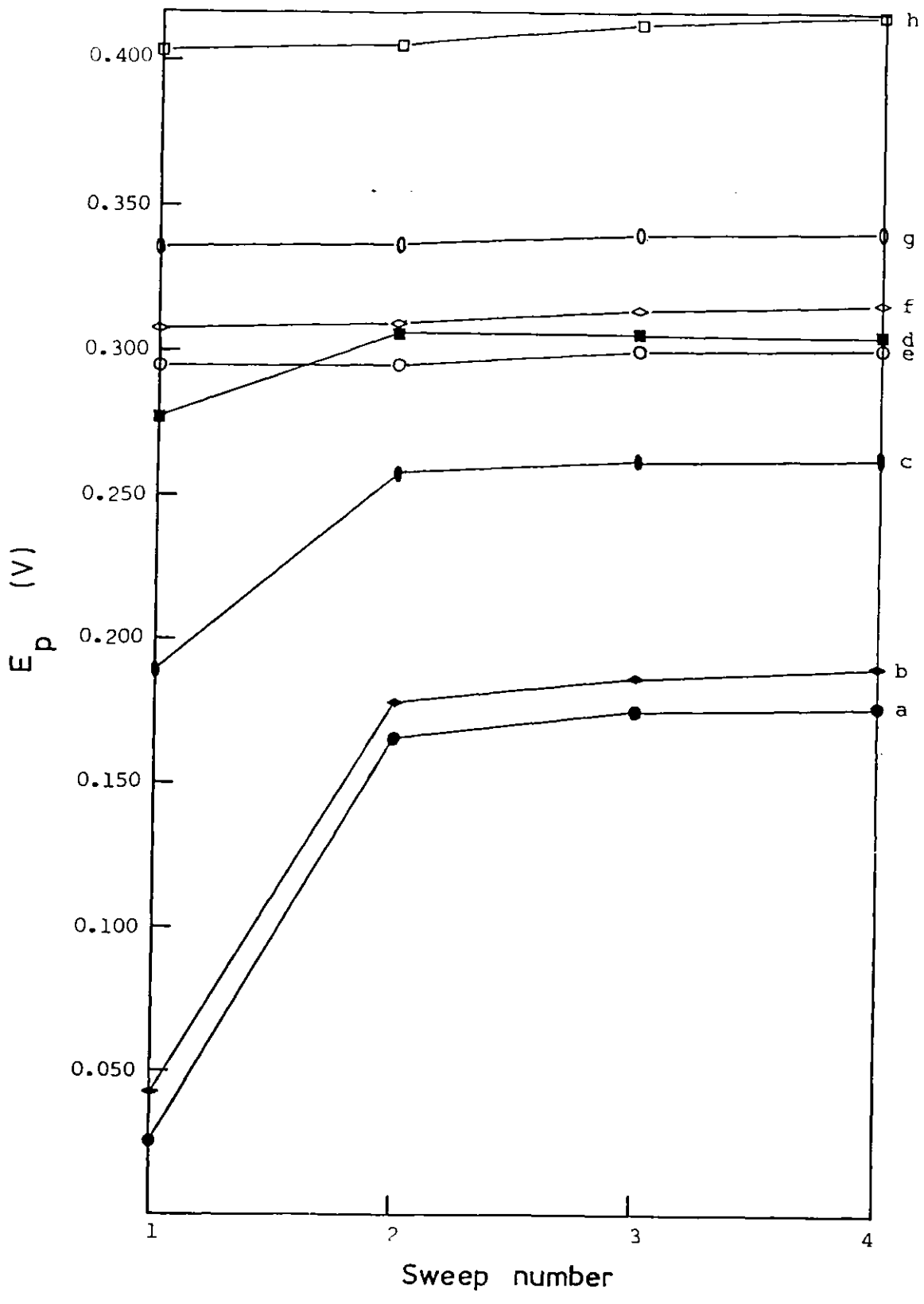

Fig. 5-390 Ag(I) Perchlorate (2.0×10^{-5} to 2.0×10^{-3} mol dm^{-3})/Sodium perchlorate (0.1 M) supporting electrolyte System: Values of cathodic and anodic peak potentials, $E_{p(c)}$ and $E_{p(a)}$ respectively, obtained under cyclic multiple sweep conditions; at a scan rate of 0.010 V s^{-1}. Concentration of silver perchlorate: (a) & (e) 2.0×10^{-5}, (b) & (f) 4.0×10^{-5}, (c) & (g) 2.0×10^{-4}, and (d) & (h) 2.0×10^{-3} mol dm^{-3}. $E_{p(c)}$: ●, ◆, ▮, ■. $E_{p(a)}$: O, ◇, 0, □. Boron carbide solid electrode.

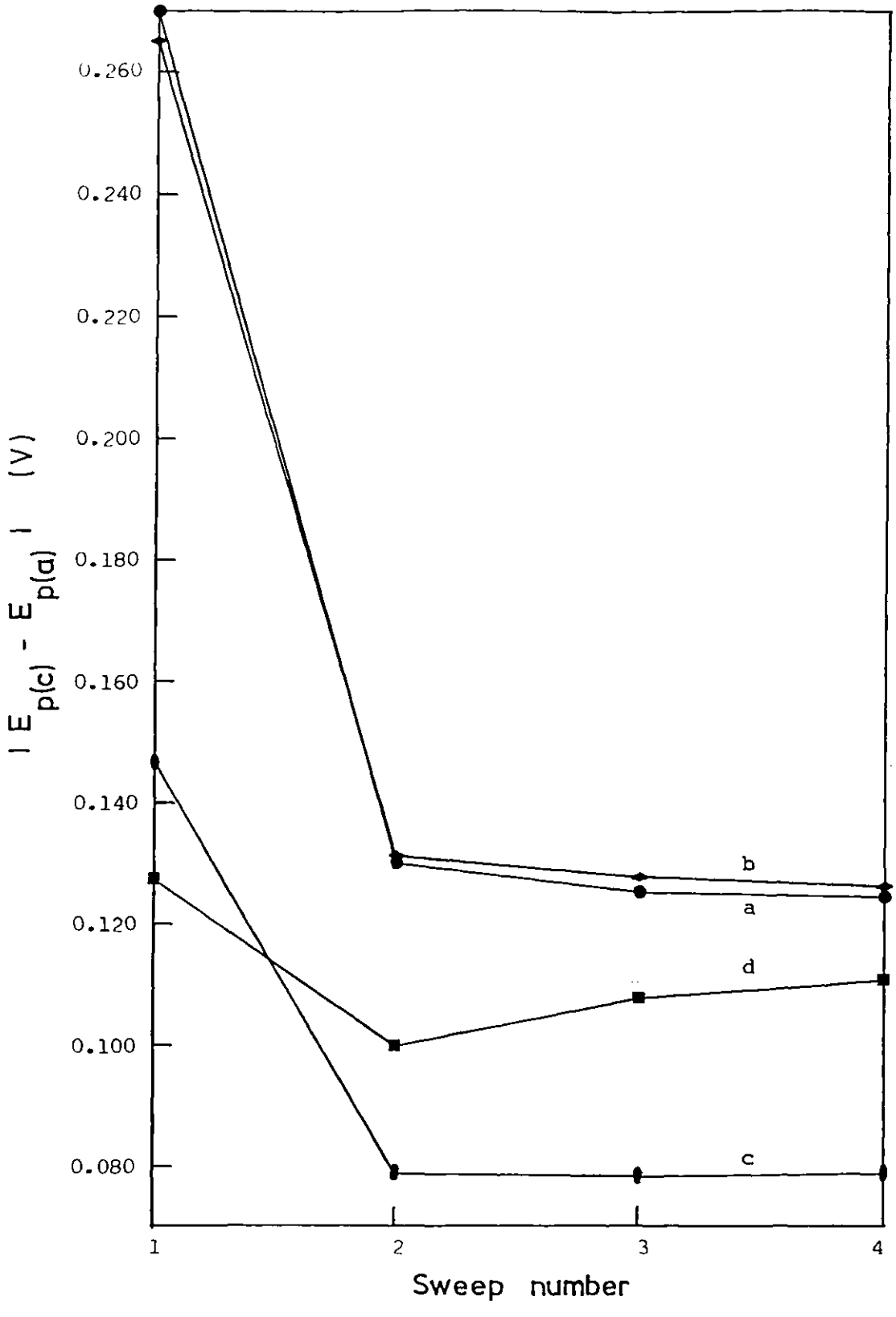

Fig. 5-391 Ag(I) Perchlorate (2.0×10^{-5} to 2.0×10^{-3} mol dm^{-3})/Sodium perchlorate (0.1 M) supporting electrolyte System: Values of the absolute difference between cathodic and anodic peak potentials, $|E_{p(c)} - E_{p(a)}|$, obtained under cyclic multiple sweep conditions; at a scan rate of 0.010 V s^{-1}. Concentration of silver perchlorate: (a) 2.0×10^{-5}, (b) 4.0×10^{-5}, (c) 2.0×10^{-4}, and (d) 2.0×10^{-3} mol dm^{-3}. Boron carbide solid electrode.

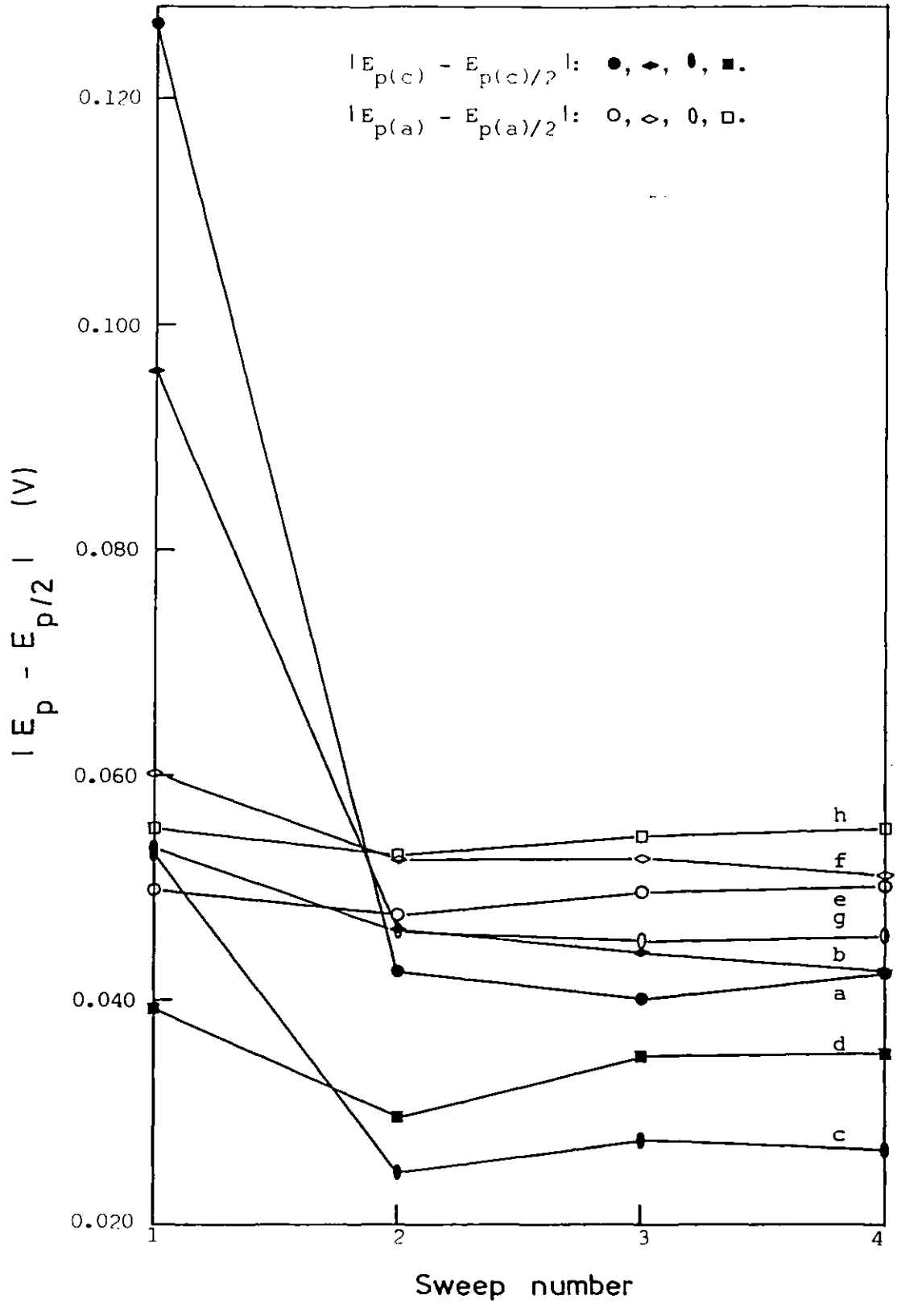

Fig. 5-392 Ag(I) Perchlorate (2.0×10^{-5} to 2.0×10^{-3} mol dm^{-3})/Sodium perchlorate (0.1 M) supporting electrolyte System: Values of the absolute difference between peak and half-peak potentials for the cathodic and anodic curves, $|E_{p(c)} - E_{p(c)/2}|$ and $|E_{p(a)} - E_{p(a)/2}|$ respectively, obtained under cyclic multiple sweep conditions; at a scan rate of 0.010 V s^{-1}. Concentration of silver perchlorate: (a) & (e) 2.0×10^{-5}, (b) & (f) 4.0×10^{-5}, (c) & (g) 2.0×10^{-4}, and (d) & (h) 2.0×10^{-3} mol dm^{-3}.

with Ag during the initial stages of the electro-reduction. Thus the reaction scheme may be represented by:

$$Ag^{+} + e^{-} \rightleftharpoons Ag$$

$$2Ag + H_2O + \tfrac{1}{2}O_2 \rightleftharpoons 2Ag^{+} + 2OH^{-} \quad \text{(catalytic reaction)}.$$

The catalytic reaction might also involve perchlorate in the oxidation of silver.

Limiting and peak current densities were linearly dependent upon the concentration of $AgClO_4$ depolarizer.

5-4 Copper

The d.c. voltammograms for Cu(II) sulphate (2.0×10^{-4} mol dm^{-3}), in sodium perchlorate (0.1 M) supporting electrolyte, obtained at the boron carbide solid working electrode exhibit poor reversibility in the electron charge transfer (Fig. 5-393). The voltammograms yielded the following results: (1) $n_{mean} = 0.56 \pm 0.03$ (6 degrees of freedom), with $E_{\frac{1}{2}}$ mean = -0.0647 V (vs SCE) $\pm 1.15 \times 10^{-3}$ V (6 degrees of freedom); or (2) αn mean = 1.11 ± 0.03 (6 degrees of freedom), with $E_{\frac{1}{2}}$ mean = -0.0720 V (vs SCE) $\pm 1.17 \times 10^{-3}$ V (6 degrees of freedom). The limiting current function was: $i_L/A\,[CuSO_4]$ mean = $88.3 \times 10^{4} \pm 1.48 \times 10^{4}$ $\mu A\ cm^{-2}\ dm^{3}\ mol^{-1}$, 5 degrees of freedom; which when compared with the results obtained for the one-electron charge transfer in the electro-reduction of Ag(I) perchlorate (Fig. 5-377) suggests that Cu^{++} was reduced to Cu.

Fig. 5-394 shows the effect of sweep rate on the cyclic voltammograms for $CuSO_4$ (2.0×10^{-4} mol dm^{-3}), in $NaClO_4$ (0.1 M) supporting electrolyte, obtained at the boron carbide solid working electrode under multiple sweep conditions. The peak current functions, as functions of $(\text{sweep rate})^{\frac{1}{2}}$, for the initial cycle indicate that the cathodic Peak 1 was complicated by a catalytic reaction, cathodic Peak 2 was affected by adsorption, anodic Peak 1 and Peak 2 were complicated by both adsorption and following chemical reaction (Fig. 5-395 c.f. Fig. 3-6). Peak current functions for cycles 2 and 3 (Figures 5-396 and 5-397 respectively) reveal more clearly that cathodic Peak 1 was affected by a catalytic reaction whilst Peak 2 was affected by adsorption, and that the anodic Peak 1 and Peak 2 were influenced by a catalytic reac-

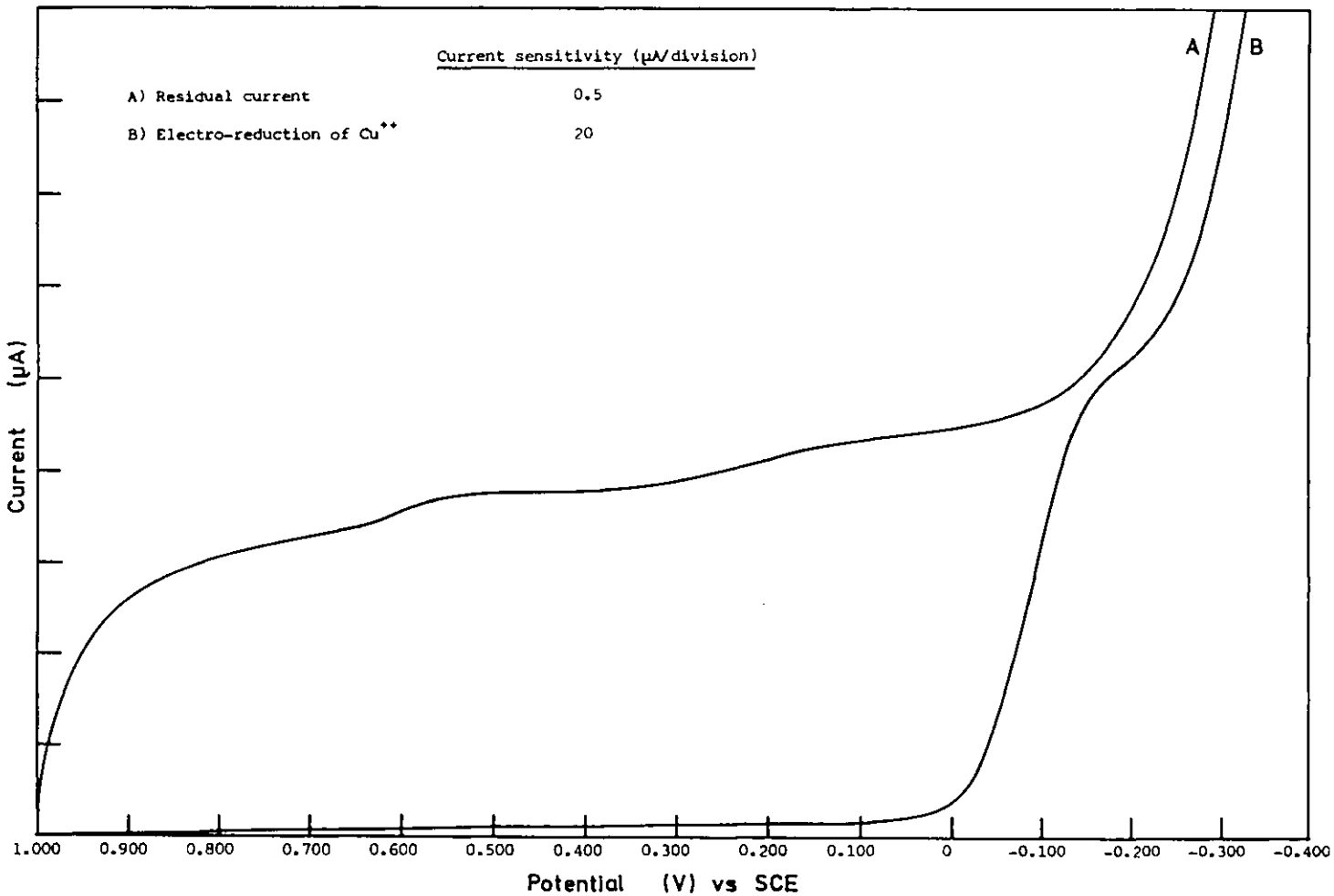

Fig. 5-393 Cu(II) sulphate (2.0×10^{-4} mol dm^{-3})/Sodium perchlorate (0.1 M) supporting electrolyte System: D.c. voltammograms obtained at the boron carbide solid working electrode. Scan rate = 0.002 V s^{-1}.

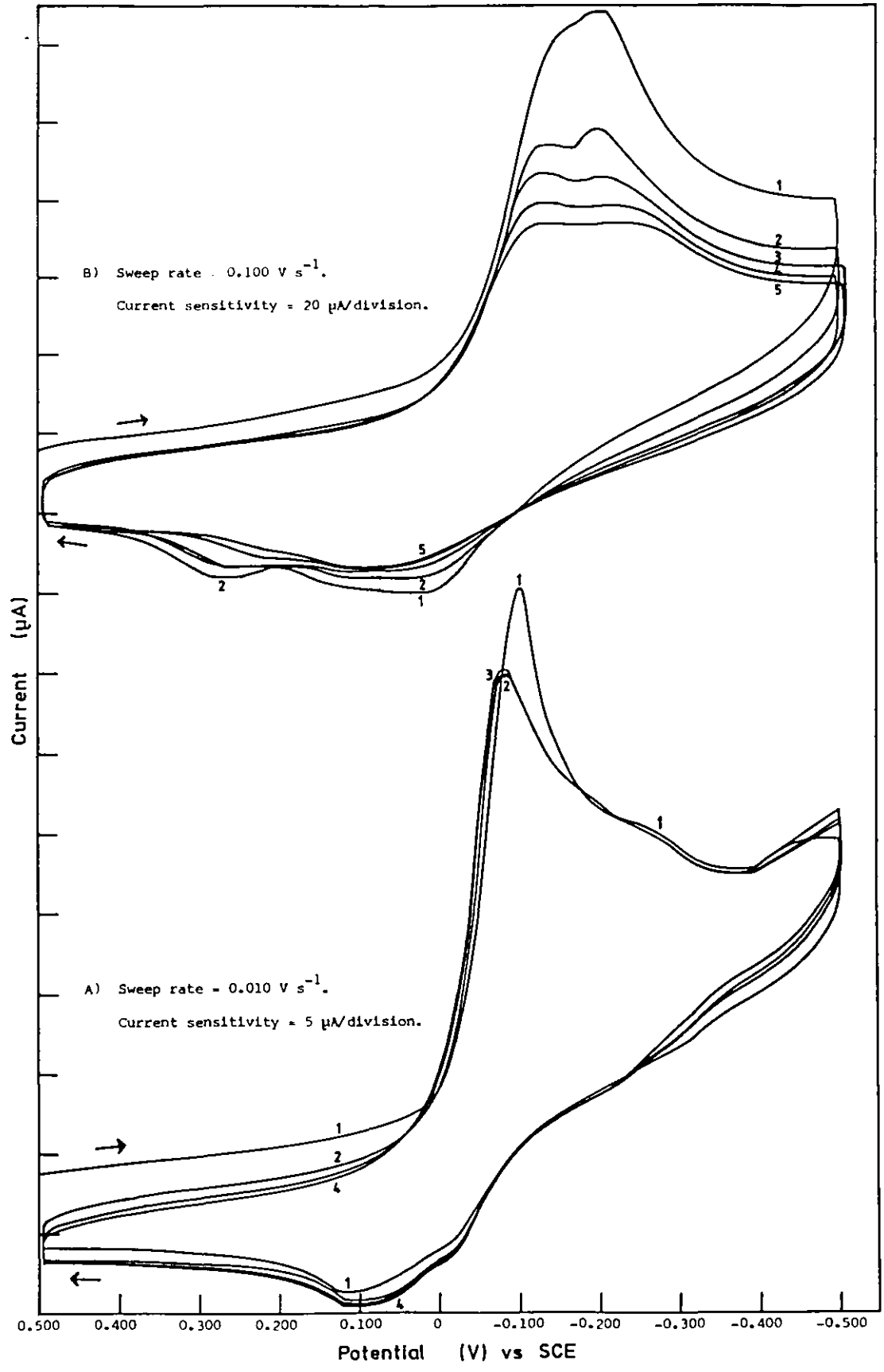

Fig. 5-394 Cu(II) sulphate (2.0×10^{-4} mol dm^{-3})/Sodium perchlorate (0.1 M) supporting electrolyte System: Cyclic voltammograms obtained at the boron carbide solid working electrode.

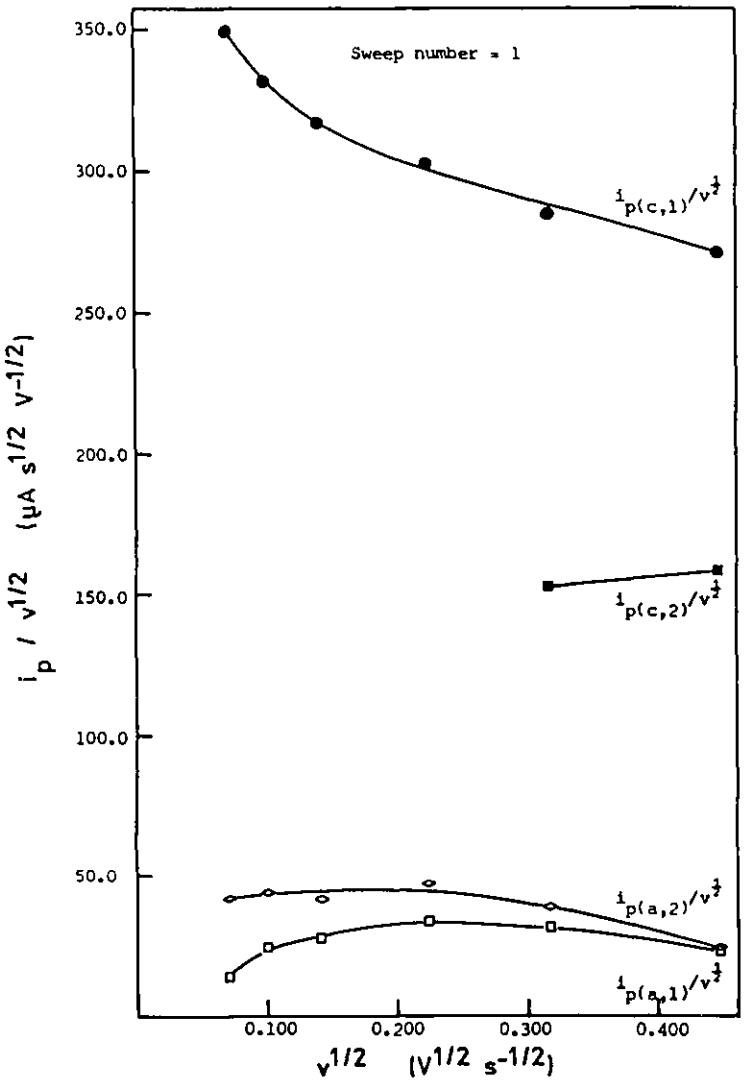

Fig. 5-395 Cu(II) Sulphate (2.0×10^{-4} mol dm^{-3})/Sodium perchlorate (0.1 M) supporting electrolyte System: Values of cathodic and anodic current function, $i_{p(c)}/v^{\frac{1}{2}}$ and $i_{p(a)}/v^{\frac{1}{2}}$ respectively, as functions of square root of potential scan rate, $v^{\frac{1}{2}}$; for the initial cyclic sweep. Boron carbide solid electrode.

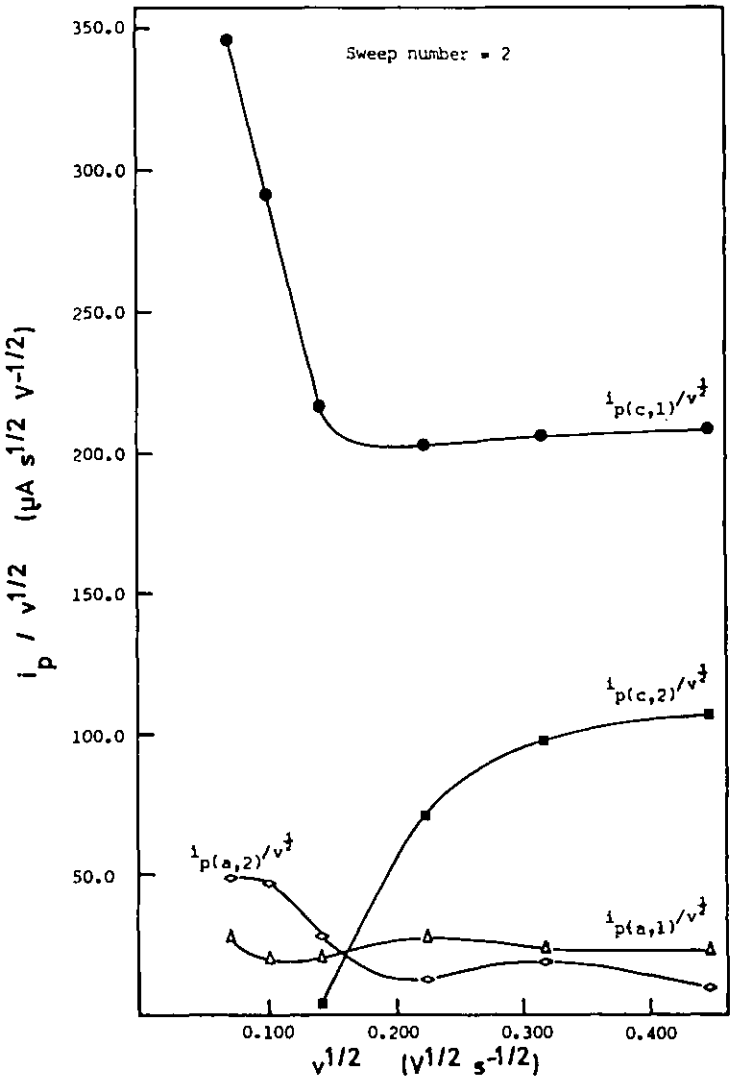

Fig. 5-396 Cu(II) Sulphate (2.0×10^{-4} mol dm^{-3})/Sodium perchlorate (0.1 M) supporting electrolyte System: Values of cathodic and anodic current function, $i_{p(c)}/v^{\frac{1}{2}}$ and $i_{p(a)}/v^{\frac{1}{2}}$ respectively, as functions of square root of potential scan rate, $v^{\frac{1}{2}}$; for the second cyclic sweep. Boron carbide solid electrode.

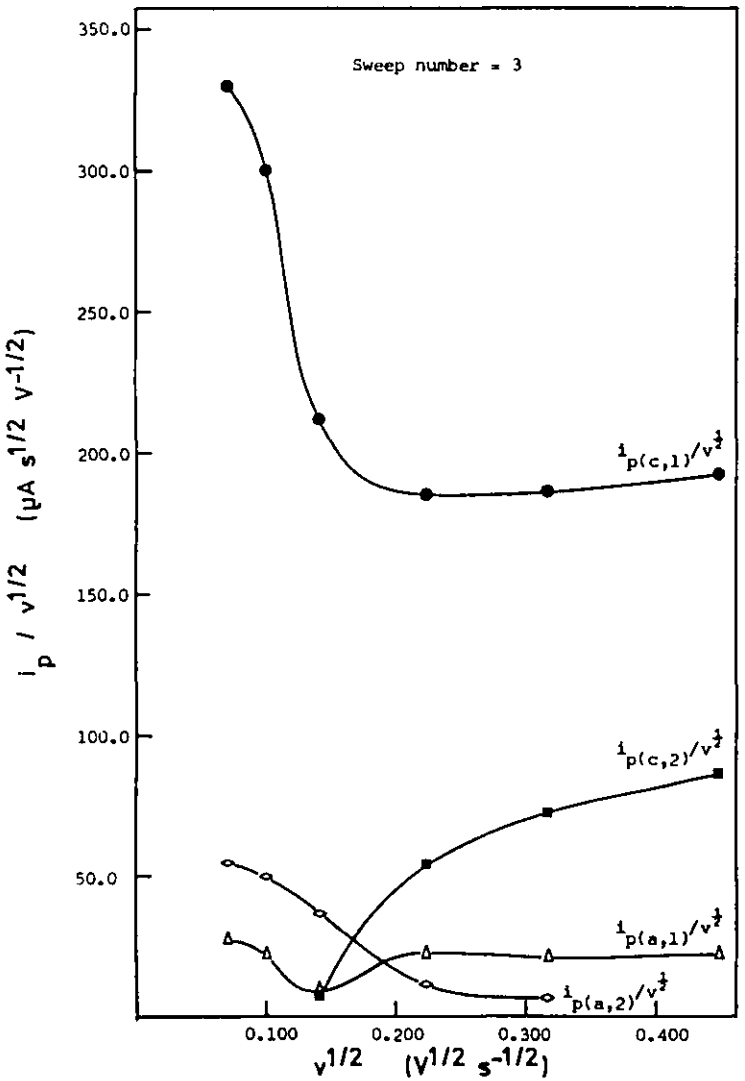

Fig. 5-397 Cu(II) Sulphate (2.0×10^{-4} mol dm^{-3})/Sodium perchlorate (0.1 M) supporting electrolyte System: Values of cathodic and anodic current function, $i_{p(c)}/v^{\frac{1}{2}}$ and $i_{p(a)}/v^{\frac{1}{2}}$ respectively, as functions of square root of potential scan rate, $v^{\frac{1}{2}}$; for the third cyclic sweep. Boron carbide solid electrode.

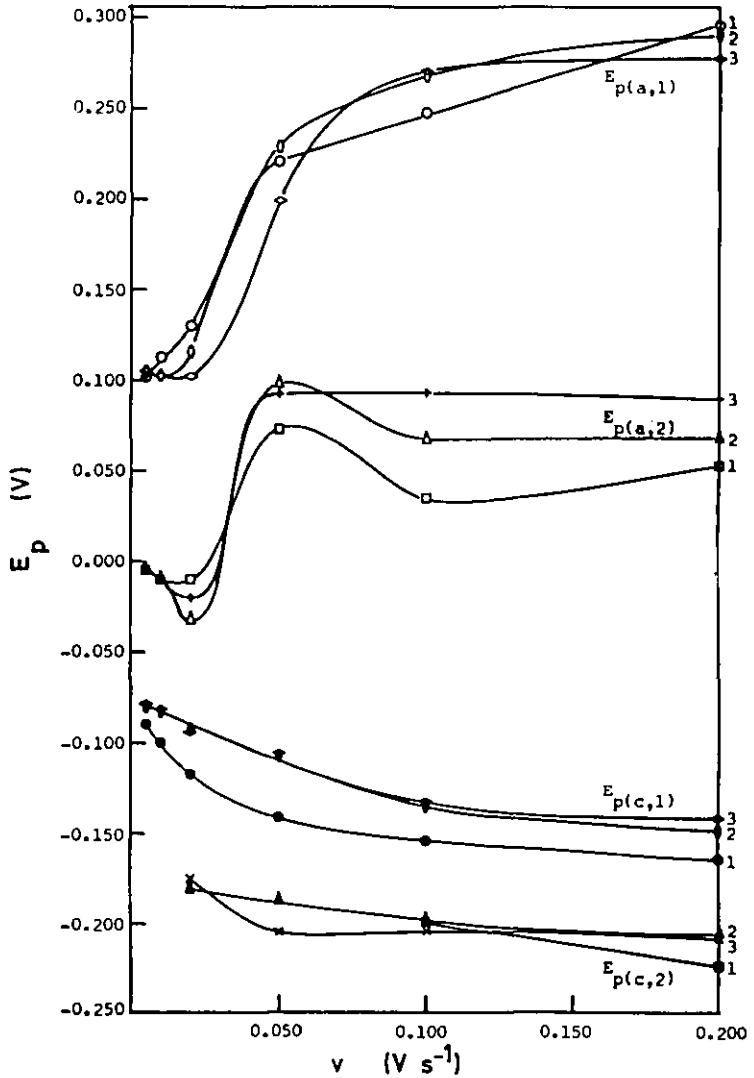

Fig. 5-398 Cu(II) Sulphate (2.0×10^{-4} mol dm^{-3})/Sodium perchlorate (0.1 M) supporting electrolyte System: Values of cathodic and anodic peak potentials, $E_{p(c)}$ and $E_{p(a)}$ respectively, as functions of potential scan rate, v; for three consecutive cyclic sweeps. Boron carbide solid electrode.

tion and very weak adsorption. In general, cathodic peak potentials were cathodically shifted whilst anodic peak potentials were anodically shifted by increasing sweep rate (Fig. 5-398). $|E_{p(c)} - E_{p(a)}|$ and $|E_p - E_{p/2}|$ values widened with increasing sweep rate (Figures 5-399 and 5-400 respectively); thus signifying a decreasing reversibility in the corresponding charge transfers when the sweep rate was being increased.

The evidence suggests that the reaction scheme may be represented by:

$$Cu^{++}_{soln} \rightleftharpoons Cu^{++}_{ads}$$

$$Cu^{++} + 2e^- \rightleftharpoons Cu$$

Oxidation by O_2/ClO_4^-

5-5 Palladium

Consecutive d.c. voltammograms for Pd(II) perchlorate (4.0×10^{-4} mol dm^{-3}), in perchloric acid (2.0 M) supporting electrolyte, obtained at the boron carbide solid working electrode are presented in Fig. 5-401. The voltammogram obtained at the boron carbide electrode, which had been treated by anodic polarisation followed by treatment with aqua regia, (Fig. 5-401, a) yielded: (1) n = 0.33 and $E_{\frac{1}{2}}$ = 0.032 V (vs SCE) from the plot of ln $(2(i_L - i)/i_L)$ vs E with correlation coefficient = 0.9595, level of significance better than 0.001, degrees of freedom = 12; or (2) αn = 0.88 and $E_{\frac{1}{2}}$ = 0.019 V (vs SCE) from the plot of ln $((i_L - i)/i)$ vs E with correlation coefficient = 0.9982, level of significance better than 0.001, degrees of freedom = 13. The boron carbide electrode was not treated with aqua regia for the subsequent scans (Fig. 5-401, b to e); which show that the wave was anodically shifted for each subsequent scan. Thus for Fig. 5-401, e, on omission of the maximum the voltammogram yielded: (1) n = 0.67 and $E_{\frac{1}{2}}$ = 0.515 V (vs SCE) from the plot of ln $(2(i_L - i)/i_L)$ vs E with correlation coefficient = 0.9163, level of significance better than 0.001, degrees of freedom = 10; or (2) αn = 2.06 and $E_{\frac{1}{2}}$ = 0.510 V (vs SCE) from the plot of ln $((i_L - i)/i)$ vs E with correlation coefficient = 0.9973, level of significance better than 0.001, degrees of freedom = 10. The limiting current func-

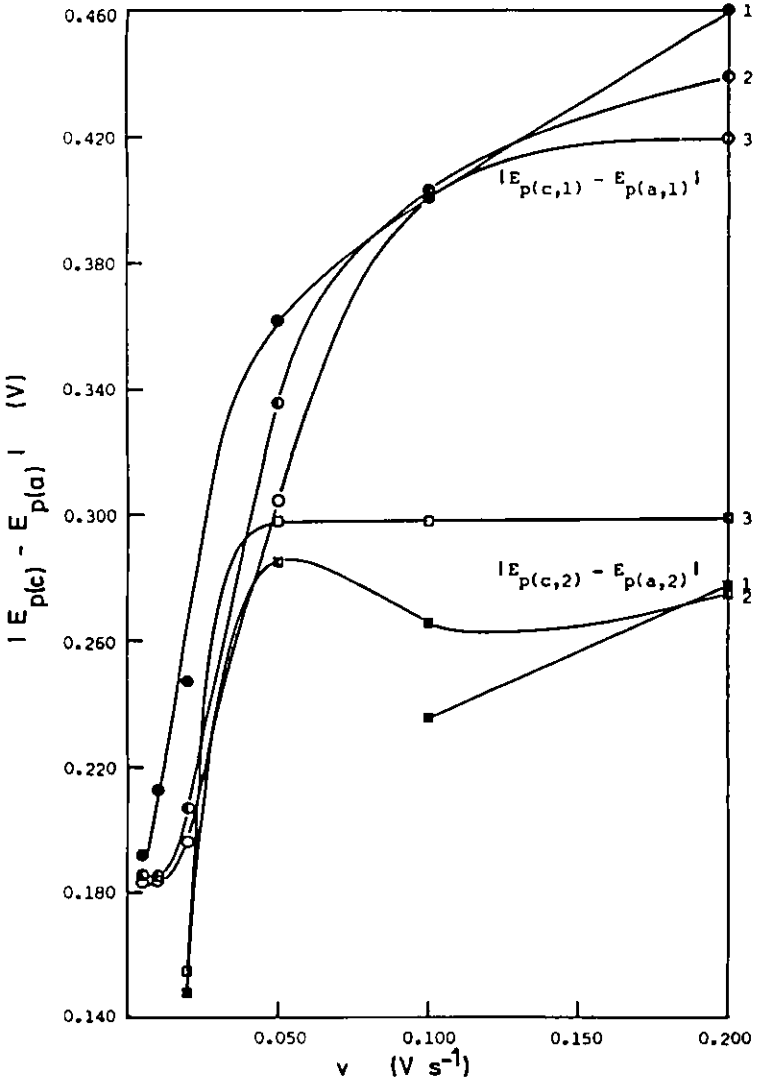

Fig. 5-399 Cu(II) Sulphate (2.0×10^{-4} mol dm^{-3})/Sodium perchlorate (0.1 M) supporting electrolyte System: Values of the absolute difference between cathodic and respective anodic peak potentials, $|E_{p(c,1)} - E_{p(a,1)}|$ and $|E_{p(c,2)} - E_{p(a,2)}|$ respectively, as functions of potential scan rate, v; for three consecutive cyclic sweeps. Boron carbide solid electrode.

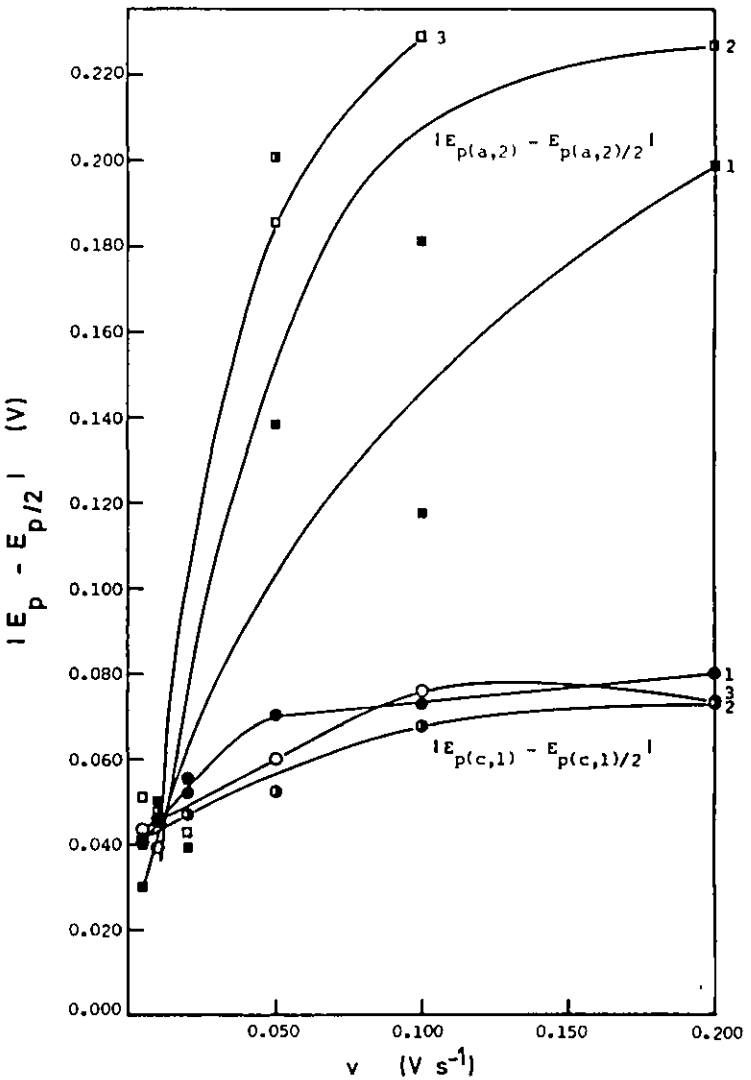

Fig. 5-400 Cu(II) Sulphate (2.0×10^{-4} mol dm^{-3})/Sodium perchlorate (0.1 M) supporting electrolyte System: Values of the absolute difference between peak and half-peak potentials for the cathodic and anodic curves, $|E_{p(c)} - E_{p(c)/2}|$ and $|E_{p(a)} - E_{p(a)/2}|$ respectively, as functions of the potential scan rate, v. Values are for three consecutive cyclic sweeps. Boron carbide solid electrode.

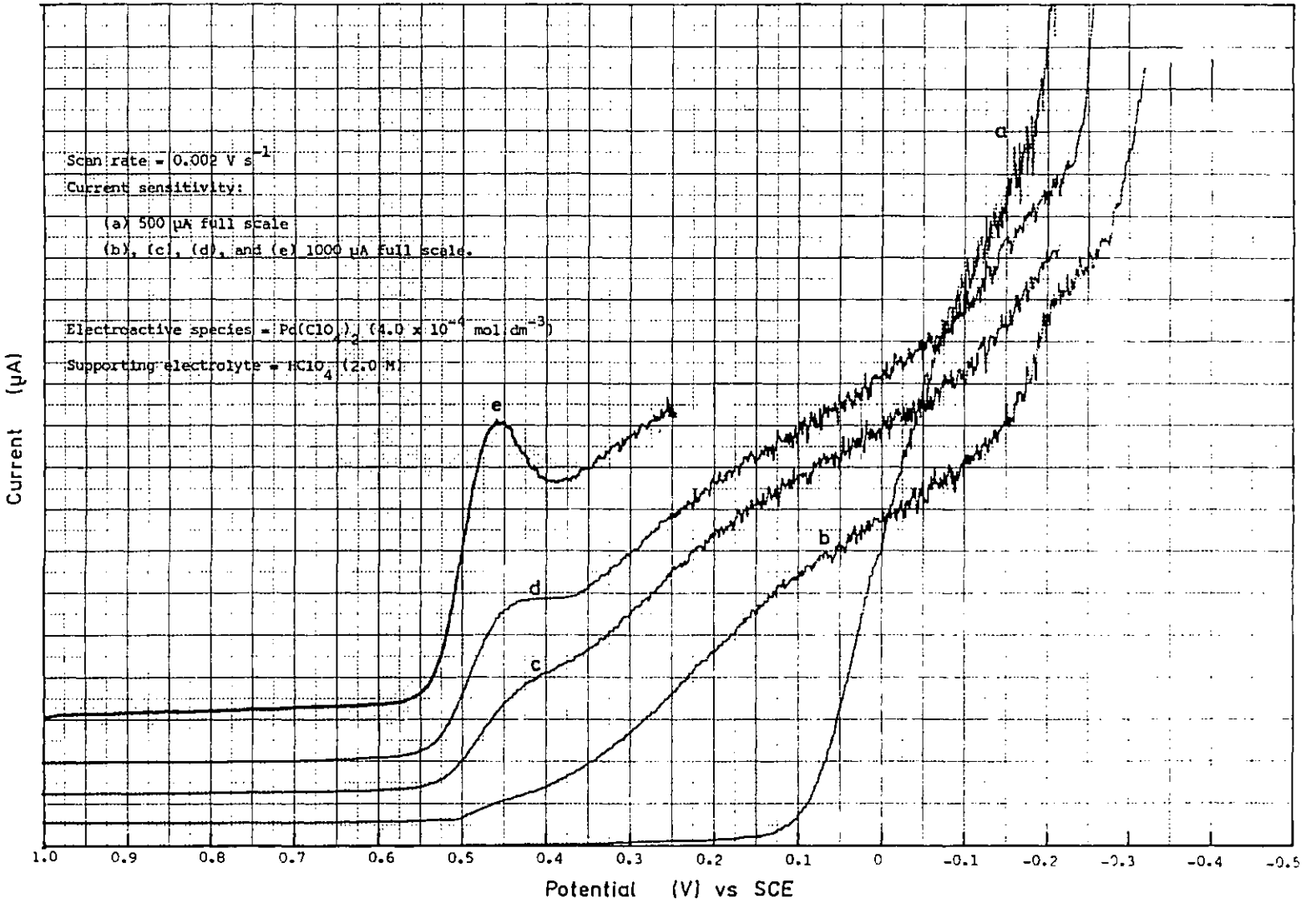

Fig. 5-401 Pd(II) perchlorate (4.0×10^{-4} mol dm^{-3})/Perchloric acid (2.0 M) supporting electrolyte System: D.c. voltammograms obtained at the boron carbide solid working electrode. (a)-(e) Consecutive scans with 2 minute pauses (at 1 V vs SCE) in between.

tion, $i_L/A\ [Pd(ClO_4)_2]$, for Fig. 5-401, a, was 134.8 x 10^4 μA cm^{-2} dm^3 mol^{-1} and for Fig. 5-401, e, was 130.5 x 10^4 μA cm^{-2} dm^3 mol^{-1}. These values exceed the expected value for a two-electron charge transfer indicated by the results obtained for the Ag^+ and Cu^{++} systems (sections 5-3 and 5-4 respectively).

Cyclic voltammograms (Fig. 5-402), obtained immediately after the d.c. voltammograms (Fig. 5-401), reveal the presence of two electrochemical processes (Fig. 5-402, b); the more anodic process being the one expected from results of the d.c. voltammograms. Quantitative interpretation of the more anodic process shows that the charge transfer was complicated by adsorption (Fig. 5-403) and was poorly reversible (Figures 5-404 to 5-406 inclusive).

After the boron carbide solid working electrode had been treated with aqua regia, the cyclic voltammogram obtained under multiple sweep conditions (Fig. 5-407) reveals that the initial cathodic and anodic peaks ($E_{p(c)}$ = -0.275 V and $E_{p(a)}$ = -0.005 V respectively, vs SCE) were enhanced for subsequent cycles whilst another process at more anodic potentials (approximately between 0.3-0.5 V vs SCE) appeared and was also enhanced.

The evidence suggests that the electron charge transfer for the electro-reduction of Pd^{++} at the boron carbide solid working electrode, which had been treated with aqua regia, was poorly reversible (Fig. 5-401, a and Fig. 5-407). Further potential scans at the working electrode without aqua regia treatment, however, caused the charge transfer to become more reversible and a second process at more anodic potentials was revealed. The more anodic process was probably due to preferential electro-reduction of Pd^{++} at sites activated by deposits of Pd; which adsorbed the Pd^{++} ions.

5-6 Mixed Ion Solution: $(NH_4)_2IrCl_6$ (1.0 x 10^{-4} mol dm^{-3})/$FeCl_3$ (1.0 x 10^{-4} mol dm^{-3}), in HCl (0.1 M) supporting electrolyte.

D.c. and cyclic voltammograms for the mixture Ir(IV) chloroiridate (1.0 x 10^{-4} mol dm^{-3}) - Fe(III) chloride (1.0 x 10^{-4} mol dm^{-3}), in hydrochloric acid (0.1 M) supporting electrolyte, are presented in Fig. 5-408. Evidently, the charge transfers were poorly reversible at the boron carbide solid working electrode resulting in the poor resolution

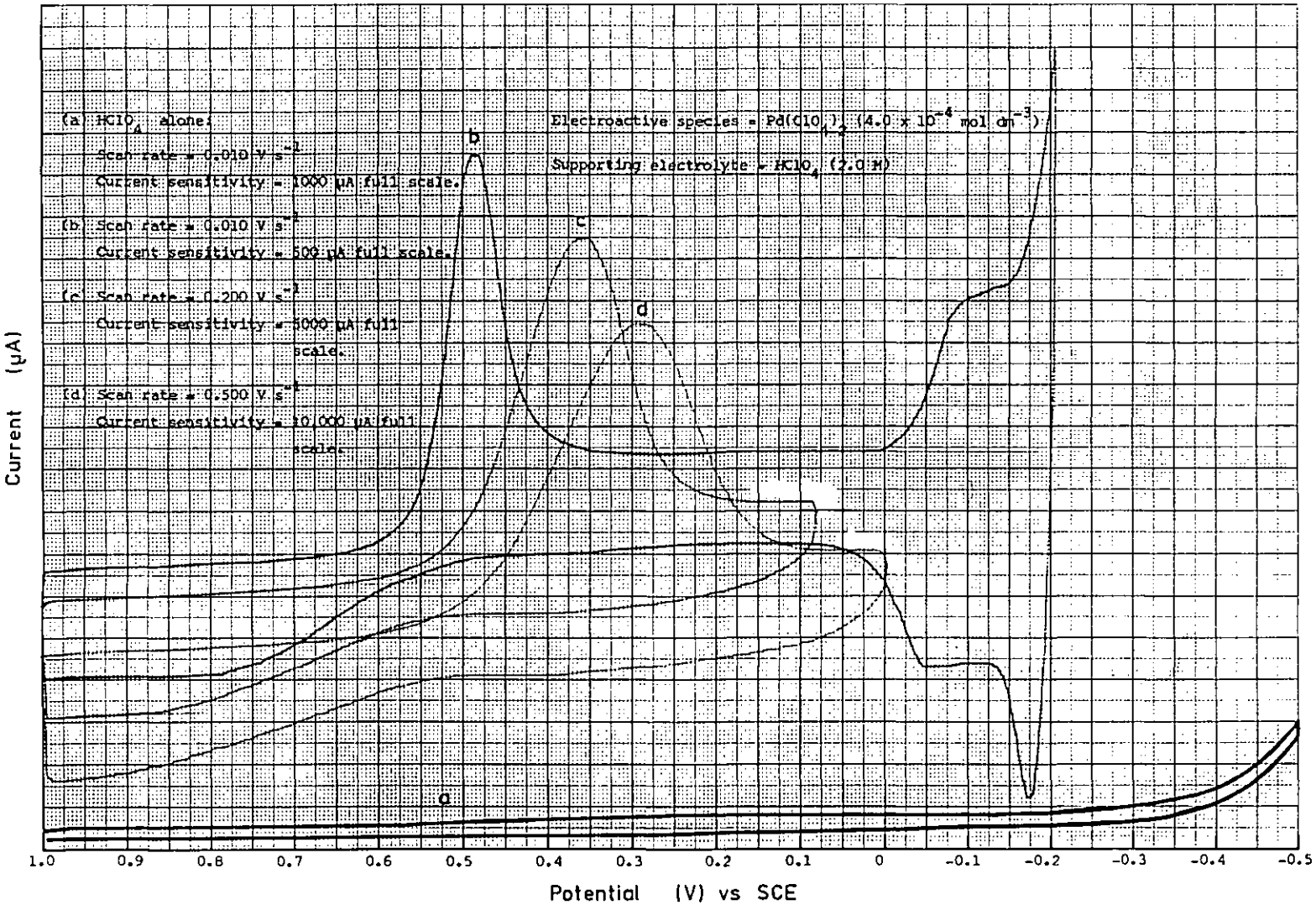

Fig. 5-402 Pd(II) perchlorate (4.0×10^{-4} mol dm^{-3})/Perchloric acid (2.0 M) supporting electrolyte System: Cyclic voltammograms, at different sweep rates, obtained at the boron carbide solid working electrode.

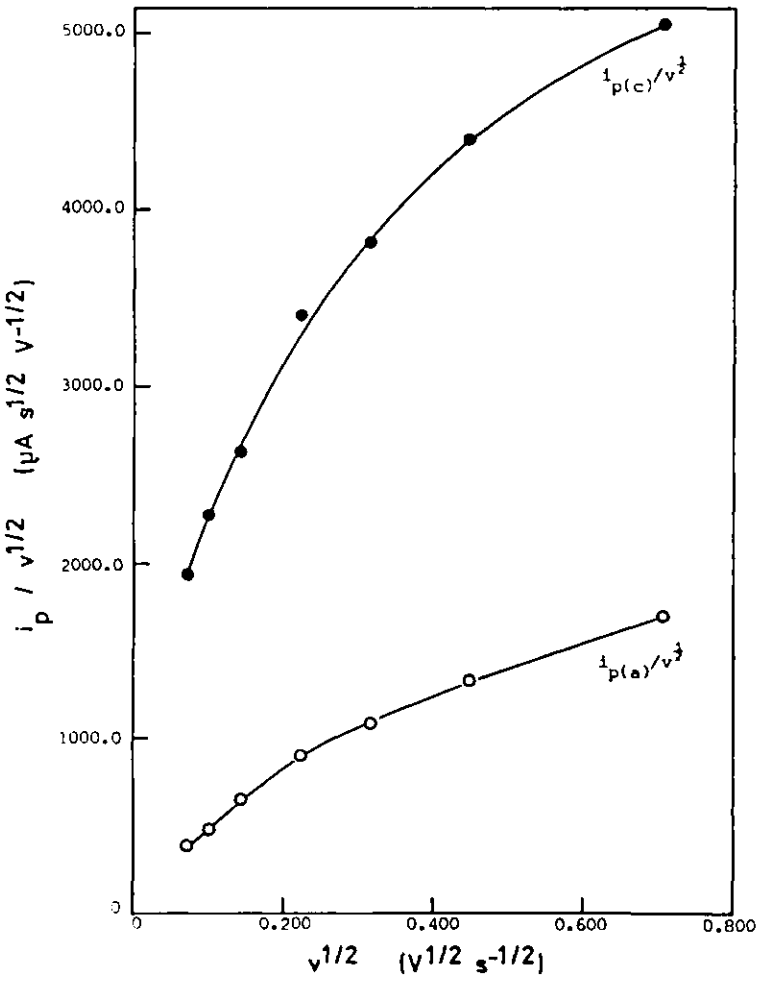

Fig. 5-403 Pd(II) perchlorate (4.0×10^{-4} mol dm^{-3})/Perchloric acid (2.0 M) supporting electrolyte System: Values of cathodic and anodic peak current function, $i_{p(c)}/v^{\frac{1}{2}}$ and $i_{p(a)}/v^{\frac{1}{2}}$ respectively, as functions of (sweep rate)$^{\frac{1}{2}}$, $v^{\frac{1}{2}}$. Boron carbide solid working electrode.

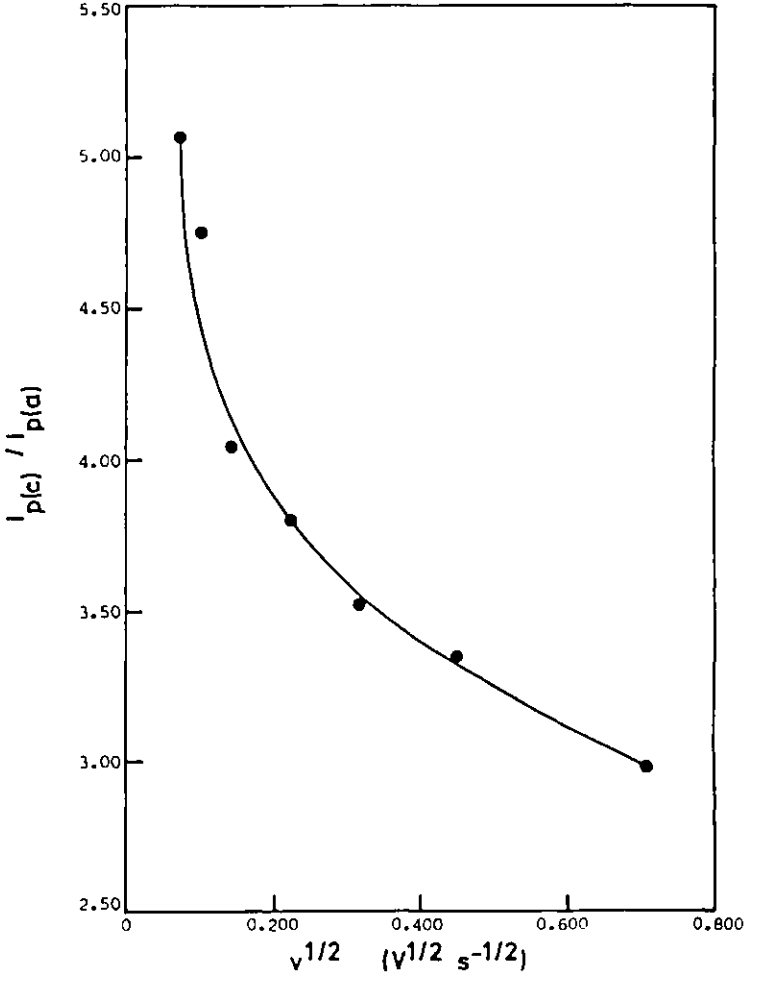

Fig. 5-404 Pd(II) perchlorate (4.0×10^{-4} mol dm^{-3})/Perchloric acid (2.0 M) supporting electrolyte System: Values of the ratio of cathodic to anodic peak current, $i_{p(c)}/i_{p(a)}$, as a function of (sweep rate)$^{\frac{1}{2}}$, $v^{\frac{1}{2}}$. Boron carbide solid working electrode.

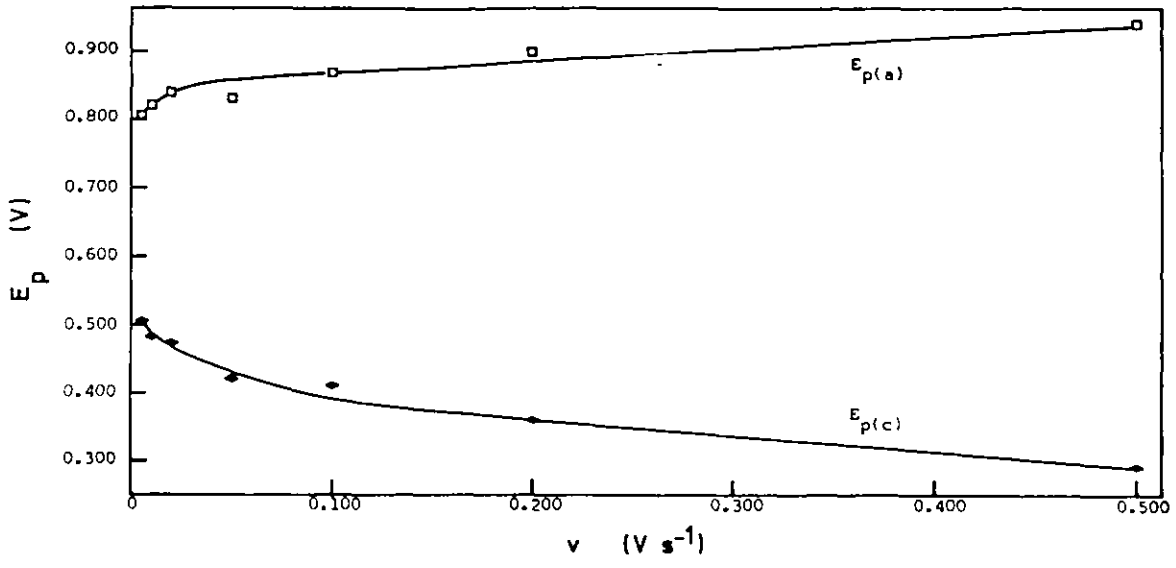

Fig. 5-405 Pd(II) perchlorate (4.0×10^{-4} mol dm^{-3})/Perchloric acid (2.0 M) supporting electrolyte System: Values of cathodic and anodic peak potential, $E_{p(c)}$ and $E_{p(a)}$ respectively, as functions of sweep rate, v. Boron carbide solid working electrode.

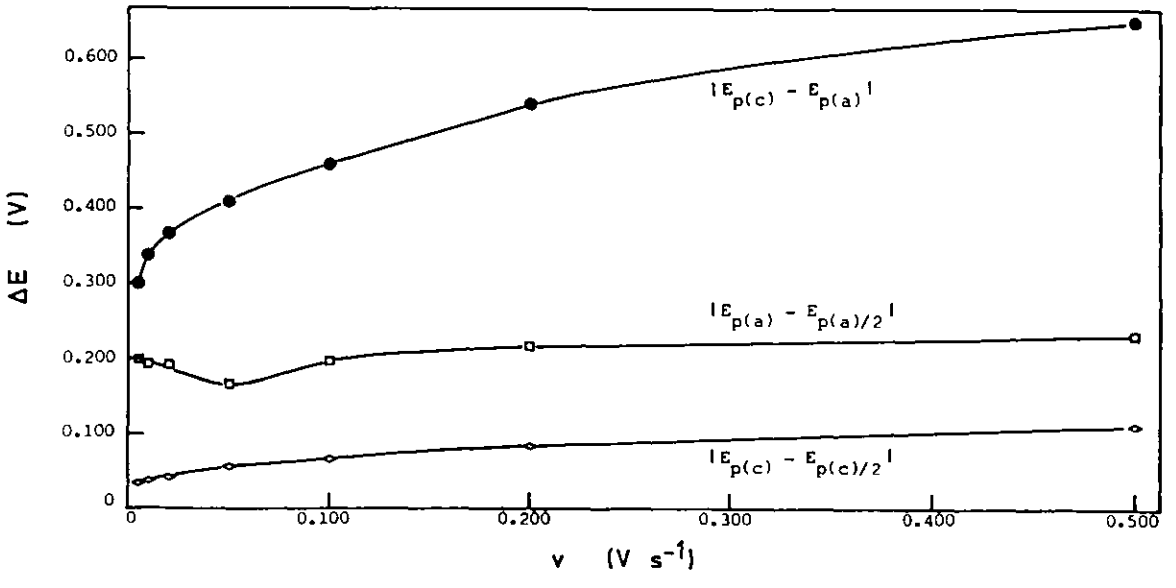

Fig. 5-406 Pd(II) perchlorate (4.0×10^{-4} mol dm^{-3})/Perchloric acid (2.0 M) supporting electrolyte System: Values of the absolute difference between cathodic and anodic peak potentials, $|E_{p(c)} - E_{p(a)}|$; and between peak and half-peak potentials for the cathodic and anodic curves, $|E_{p(c)} - E_{p(c)/2}|$ and $|E_{p(a)} - E_{p(a)/2}|$ respectively; as functions of sweep rate, v. Boron carbide solid working electrode.

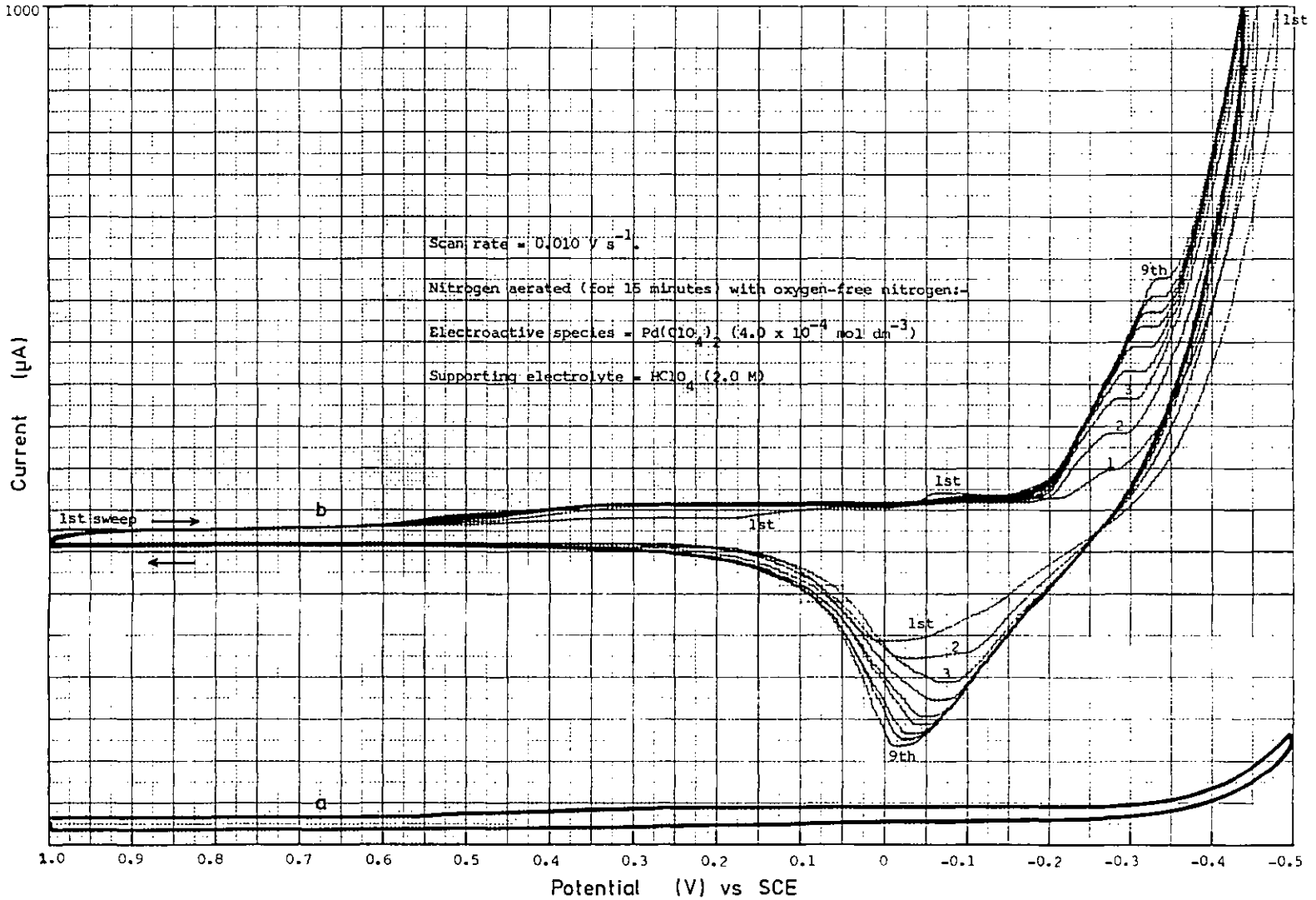

Fig. 5-407 Pd(II) perchlorate (4.0×10^{-4} mol dm^{-3})/Perchloric acid (2.0 M) supporting electrolyte System: (a) Cyclic voltammogram for the residual current, and (b) multiple cyclic sweep voltammogram obtained at the boron carbide solid working electrode which had been treated with aqua regia.

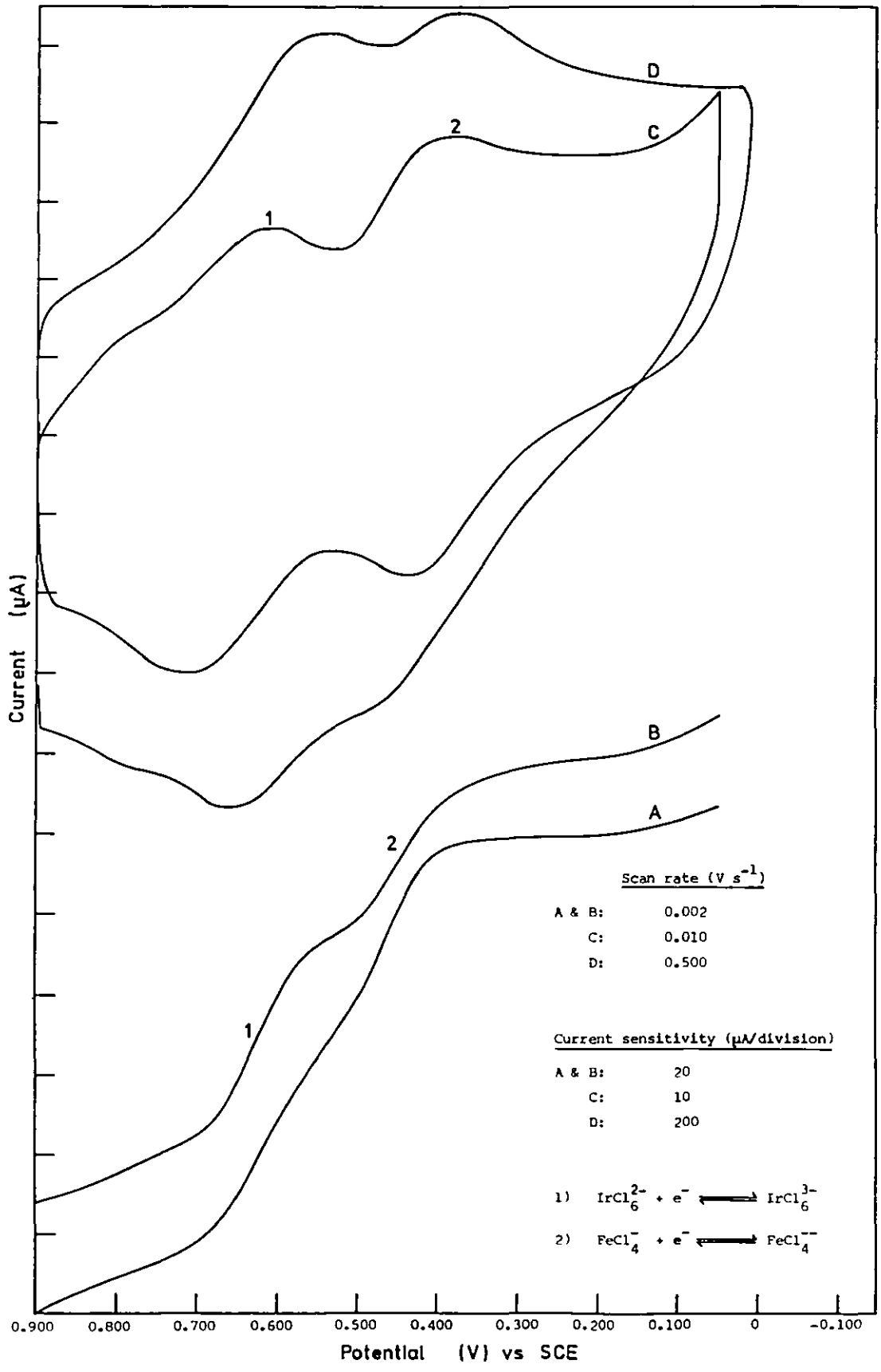

Fig. 5-408 Ir(IV) chloroiridate (1.0×10^{-4} mol dm^{-3}) - Fe(III) chloride (1.0×10^{-4} mol dm^{-3})/Hydrochloric acid (0.1 M) supporting electrolyte System: A) d.c. voltammogram obtained at the boron carbide solid working electrode, B) d.c. voltammogram obtained after treatment of boron carbide electrode by cathodic polarisation (at -3.9 V vs SCE) in the sample, and C) & D) cyclic voltammograms.

Table 5-10 Ir(IV) Chloroiridate/Fe(III) Chloride/Hydrochloric acid supporting electrolyte System: D. C. Voltammetry of the Mixture.

Electroactive species = $(NH_4)_2IrCl_6$ (1.0×10^{-4} mol dm^{-3})/$FeCl_3$ (1.0×10^{-4} mol dm^{-3}). Supporting electrolyte = HCl (0.1 M).

Boron carbide solid electrode was treated by cathodic polarisation (at -3.9 V) in the sample solution.

Electrode $B_{4.04}C$	Ir(IV)-Ir(III) Chloroiridate System.			Fe(III)- Fe(II) Chloride System.		
	αn	$E_{\frac{1}{2}}$ (V) vs SCE.	i_L/A [$(NH_4)_2IrCl_6$] (10^4 μA cm^{-2} dm^3 mol^{-1}).	αn	$E_{\frac{1}{2}}$ (V) vs SCE.	i_L/A [$FeCl_3$] (10^4 μA cm^{-2} dm^3 mol^{-1}).
Mean value	1.36	0.635	25.8	0.94	0.422	19.4
Standard deviation	0.04	0.004	3.43	0.06	0.002	2.39
Coefficient of variation	3.06%	0.611%	13.3%	6.41%	0.553%	12.3%
Degrees of freedom	9	10	10	10	10	10

F test	αn	$E_{\frac{1}{2}}$	i_L/AC	t test	αn	$E_{\frac{1}{2}}$	i_L/AC
F value	2.12	2.78	2.18	t value	18.31	156	4.44
$F_{0.05}$ (double-sided)	3.96	3.72	3.72	$t_{0.01}$ (double-sided)	2.86	2.85	2.85
Degrees of freedom	10,9	10,10	10,10	Degrees of freedom	19	20	20
Conclusion	Variances are not significantly different.			Conclusion	Values are highly significantly different.		

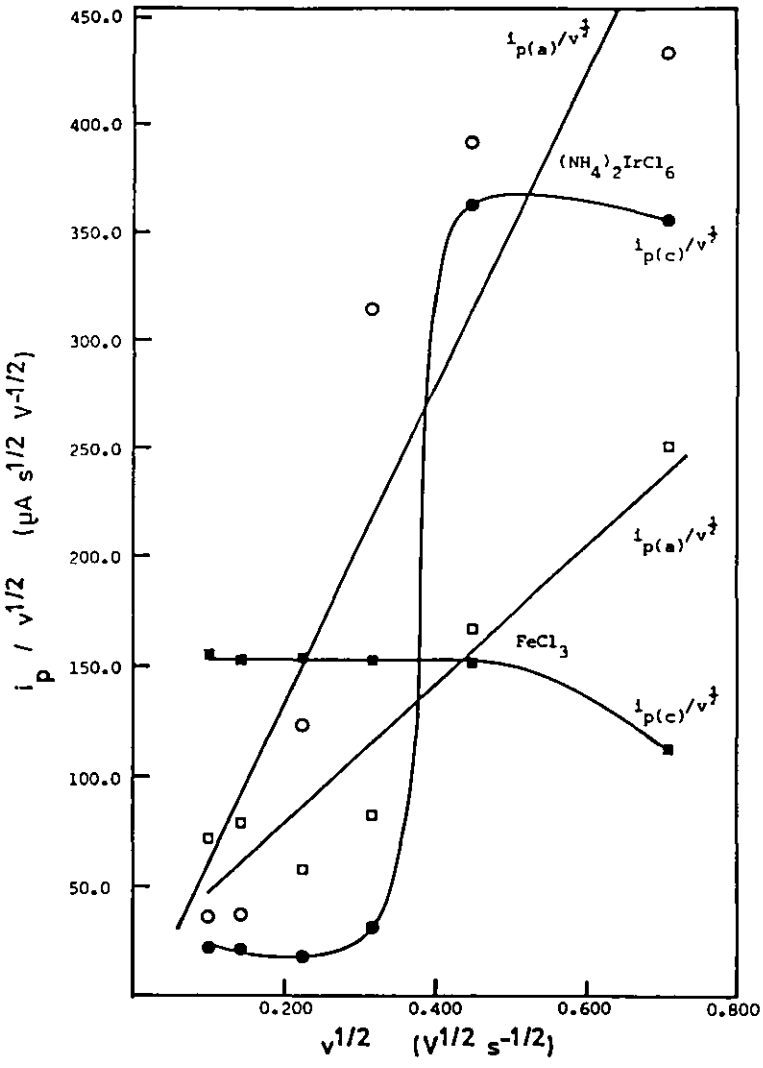

Fig. 5-409 Ir(IV) Chloroiridate (1.0×10^{-4} mol dm^{-3})/Fe(III) Chloride (1.0×10^{-4} mol dm^{-3})/Hydrochloric acid (0.1 M) supporting electrolyte System: Values of cathodic and anodic current functions, $i_{p(c)}/v^{\frac{1}{2}}$ and $i_{p(a)}/v^{\frac{1}{2}}$ respectively, as functions of the square root of potential scan rate, $v^{\frac{1}{2}}$. (●) & (○): $(NH_4)_2IrCl_6$. (■) & (□): $FeCl_3$. Boron carbide solid electrode $B_{4.04}C$ was treated by cathodic polarisation (at -3.9 V) in the sample solution.

(a) $(NH_4)_2IrCl_6$:

$i_{p(a)}/v^{\frac{1}{2}} = 7.31 \times 10^2 \, v^{\frac{1}{2}} - 13.3$

Correlation coefficient = 0.9216

Level of significance, $p = 0.001 < p < 0.01$

Standard deviation of $i_{p(a)}/v^{\frac{1}{2}}$ from regression = 77.8 μA $s^{\frac{1}{2}}$ $V^{-\frac{1}{2}}$

Degrees of freedom = 4

(b) $FeCl_3$:

$i_{p(a)}/v^{\frac{1}{2}} = 15.9 + 3.16 \times 10^2 \, v^{\frac{1}{2}}$

Correlation coefficient = 0.9441

Level of significance, $p = 0.001 < p < 0.01$

Standard deviation of $i_{p(a)}/v^{\frac{1}{2}}$ from regression = 27.9 μA $s^{\frac{1}{2}}$ $V^{-\frac{1}{2}}$

Degrees of freedom = 4

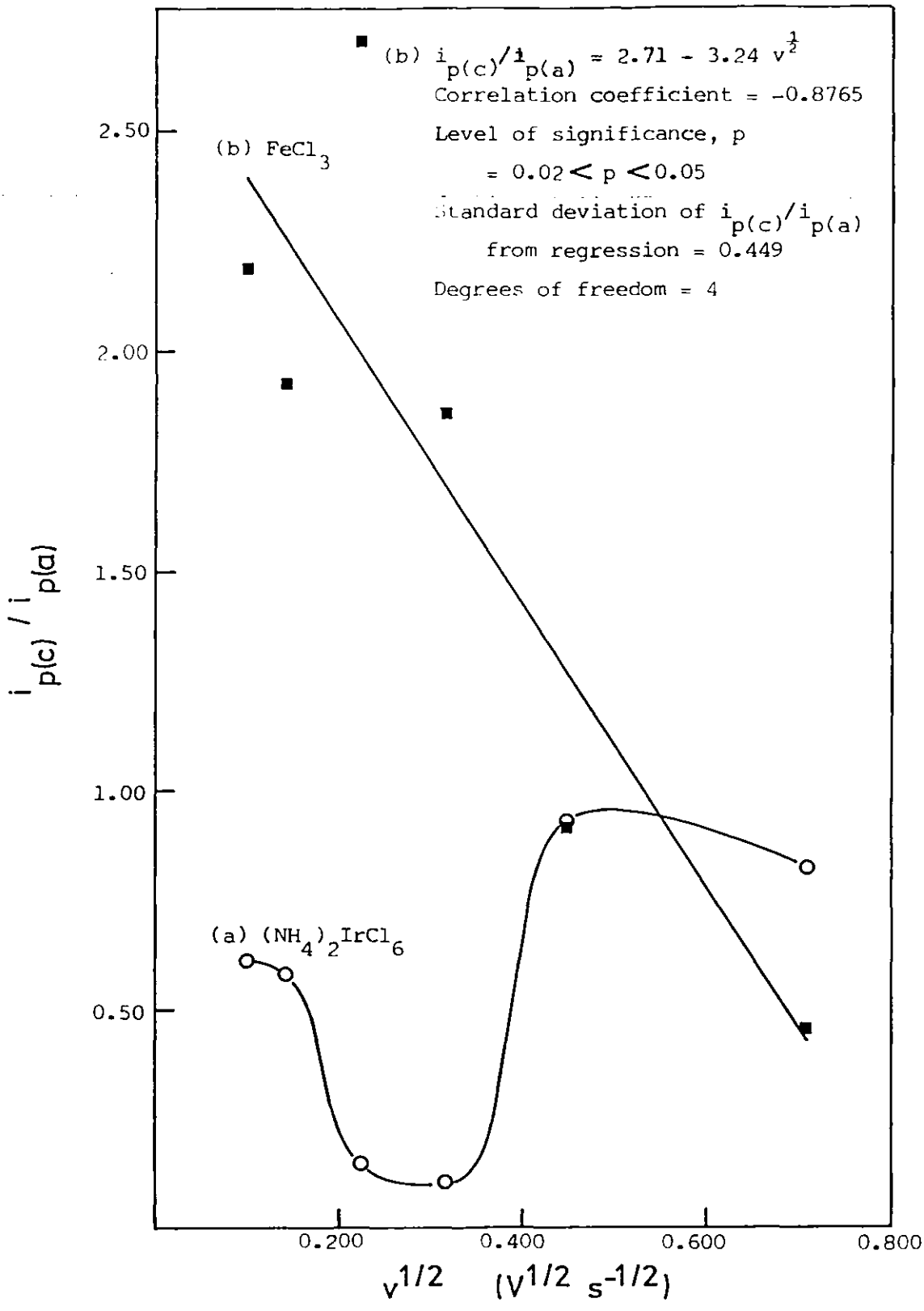

Fig. 5-410 Ir(IV) Chloroiridate (1.0×10^{-4} mol dm^{-3})/Fe(III) Chloride (1.0×10^{-4} mol dm^{-3})/Hydrochloric acid (0.1 M) supporting electrolyte System: Values of the ratio of cathodic to anodic peak current, $i_{p(c)}/i_{p(a)}$, as a function of the square root of potential scan rate, $v^{\frac{1}{2}}$. Boron carbide solid electrode $B_{4.04}C$ was treated by cathodic polarisation (at -3.9 V) in the sample solution.

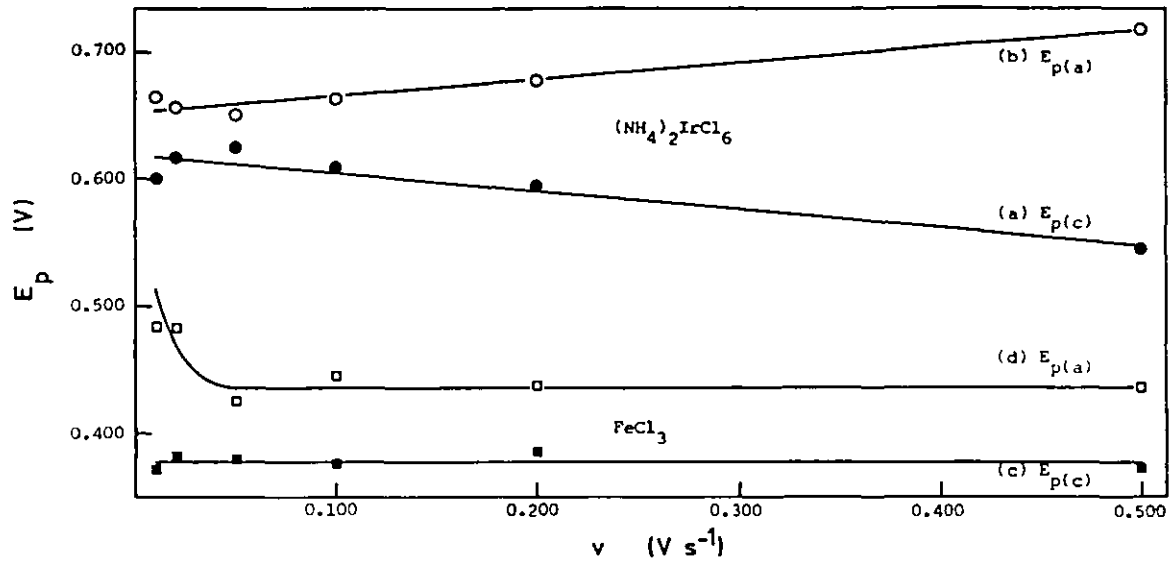

Fig. 5-411 Ir(IV) Chloroiridate (1.0×10^{-4} mol dm^{-3})/Fe(III) Chloride (1.0×10^{-4} mol dm^{-3})/Hydrochloric acid (0.1 M) supporting electrolyte System: Values of cathodic and anodic peak potentials, $E_{p(c)}$ and $E_{p(a)}$ respectively, as functions of potential scan rate, v. Boron carbide solid electrode $B_{4.04}C$ was treated by cathodic polarisation (at -3.9 V) in the sample solution.

$(NH_4)_2IrCl_6$:

(a) $E_{p(c)} = 0.619 - 0.143\ v$
Correlation coefficient = -0.9371
Level of significance, $p = 0.001 < p < 0.01$
Standard deviation of $E_{p(c)}$ from regression = 1.11×10^{-2} V
Degrees of freedom = 4

(b) $E_{p(a)} = 0.652 + 0.128\ v$
Correlation coefficient = 0.9668
Level of significance, $p = 0.001 < p < 0.01$
Standard deviation of $E_{p(a)}$ from regression = 7.05×10^{-3} V
Degrees of freedom = 4

$FeCl_3$:

(c) $E_{p(c)}$ mean = 0.378 V
Standard deviation = 5.47×10^{-3} V
Coefficient of variation = 1.45%
Degrees of freedom = 5

(d) $E_{p(a)}$ mean = 0.451 V
Standard deviation = 2.51×10^{-2} V
Coefficient of variation = 5.56%
Degrees of freedom = 5

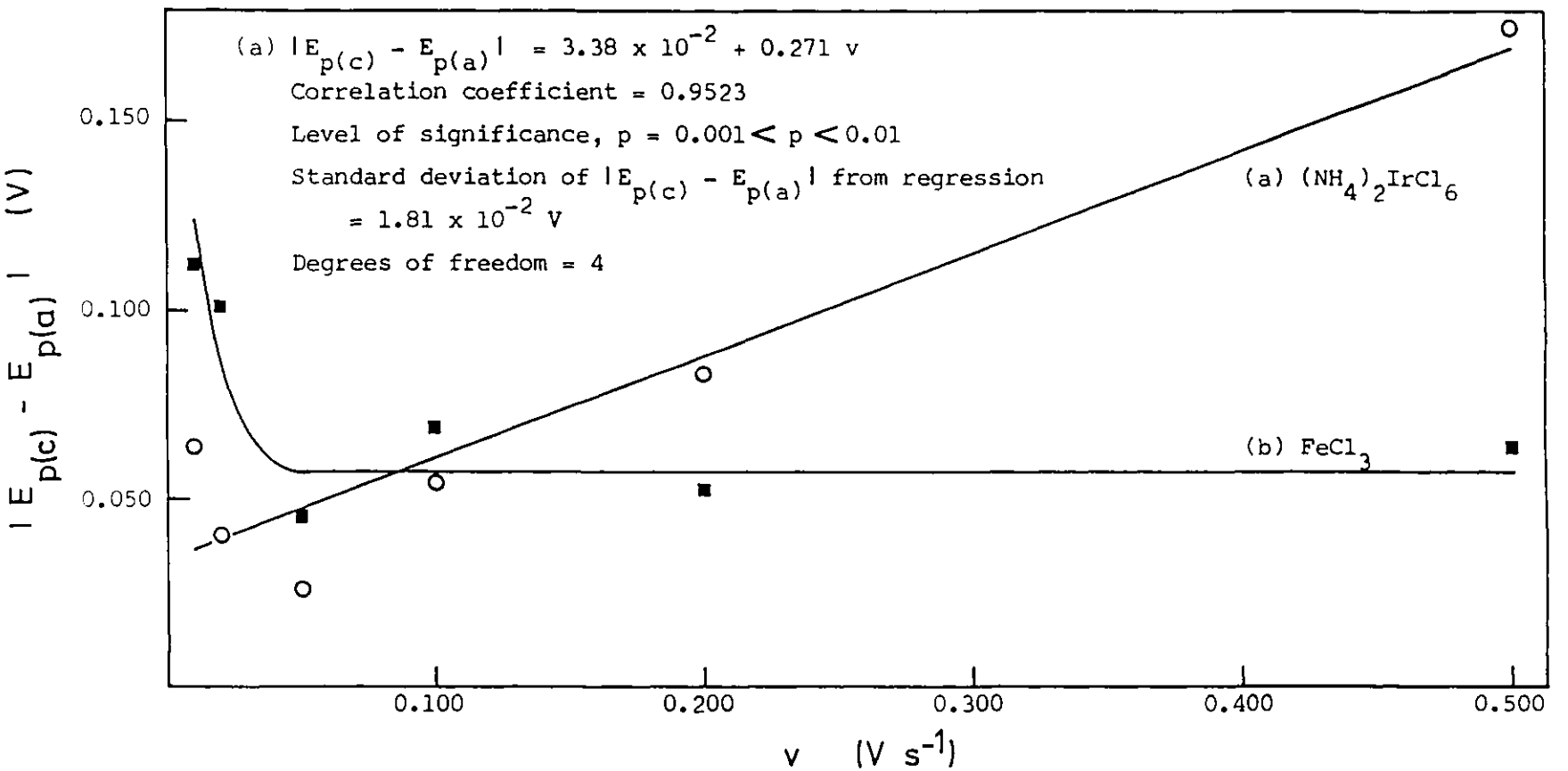

Fig. 5-412 Ir(IV) Chloroiridate (1.0×10^{-4} mol dm^{-3})/Fe(III) Chloride (1.0×10^{-4} mol dm^{-3})/Hydrochloric acid (0.1 M) supporting electrolyte System: Values of the absolute difference between cathodic and anodic peak potentials, $|E_{p(c)} - E_{p(a)}|$, as a function of potential scan rate, v. Boron carbide solid electrode $B_{4.04}C$ was treated by cathodic polarisation (at -3.9 V) in the sample solution.

of the d.c. waves (Fig. 5-408, A). Cathodic polarisation (at -3.9 V vs SCE) of the boron carbide solid working electrode in the sample solution, however, improved the reversibility of the charge transfers and thus resolved the d.c. waves (Fig. 5-408, B). Results of the quantitative treatment of the d.c. waves are presented in Table 5-10.

Quantitative treatment of the cyclic voltammograms for the mixture obtained at the electrochemically treated boron carbide solid electrode reveals that both charge transfers were complicated by: (1) adsorption, and (2) catalytic reaction; (Figures 5-409 and 5-410). The values of the peak potentials, as functions of sweep rate, show that the reversibility of the charge transfer for Ir(IV) chloroiridate deteriorated with increasing sweep rate whilst that for Fe(III) chloride initially improved to a steady state (Fig. 5-411); as confirmed by the trend of $|E_{p(c)} - E_{p(a)}|$ values with increasing sweep rate (Fig. 5-412).

The evidence suggests that the charge transfers for an Ir(IV) chloroiridate (1.0×10^{-4} mol dm^{-3}) - Fe(III) chloride (1.0×10^{-4} mol dm^{-3}) mixture, in hydrochloric acid (0.1 M) supporting electrolyte, can be resolved at the boron carbide solid working electrode if the electrode had been treated by cathodic polarisation (at -3.9 V vs SCE) in a solution of the sample. The presence of adsorption, however, dictates that quantitative analysis should be performed with d.c. voltammetry or linear sweep voltammetry at slow sweep rates.

5-7 References

5.1 Fisher R. A. and Yates F.; Statistical Tables for Biological, Agricultural, and Medical Research, 6th edition. Longman Group Limited, 1963.

6. CONCLUSIONS

The d.c. voltammetric data, and the linear and cyclic sweep voltammetric data are summarised in Table 6-1 and Table 6-2 respectively. The electrode reaction mechanisms tabulated have been derived from the experimental evidence pertaining to each set of results, and thus might not necessarily reflect the entire range of processes occurring in solution. Only the salient points have been included, but further detailed analyses of the systems are documented in the relevant sections; voltammetry being conducted without nitrogen aeration of the samples except when stated otherwise.

6-1 Chloroiridate-Chloroiridite System

Voltammetry of $(NH_4)_2IrCl_6$, in $HClO_4$, HCl, or $NaClO_4$ supporting electrolytes, has shown that the electron charge transfer for the $[IrCl_6]^{2-}/[IrCl_6]^{3-}$ couple is poorly reversible at boron carbide and boron carbide/carbon composite solid electrodes in general but reversible at the graphite solid electrode. However, linear correlations were found between increasing αn values and increasing weight per cent carbon content or decreasing B:C ratio of the boron carbide solid working electrodes. Further studies with a range of pressure-sintered boron carbide/carbon composite solid electrodes ($B_{3.86}C$ to $B_{2.56}C$) confirmed the beneficial effect of higher carbon contents but the αn values obtained were, in general, significantly below the unity value expected of the one-electron charge transfer; although an αn value of 1.08 ± 0.18 was obtained for $[IrCl_6]^{2-}$/HCl (0.1 M) at the $B_{2.56}C$ electrode. The severe limitation of working electrodes with higher carbon contents and the graphite electrode is the increase in the residual current at these electrodes. The residual current is affected by adsorption and thus becomes excessively high at fast sweep rates.

Only two of the seven methods of electrode treatment resulted in qualified success for the improvement of the voltammetric performance of the boron carbide and boron carbide/carbon composite solid working electrodes. Thus electrodes treated with Ir(IV) perchlorate solution, or treated by cathodic polarisation in chloroiridate solution produced αn values close to that for a reversible charge transfer; the former treatment resulting in consistently better αn values than the latter irrespective of the electrode B:C composition.

Table 6-1 Summary of d.c. voltammetric data

Working electrode	Electrode treatment	E.a.s./supporting electrolyte	Electrode reaction	αn or (n)	Uncertainty	$E_{\frac{1}{2}}$ (V) vs SCE	$E_{\frac{1}{2}}$ (V) vs SHE	Uncertainty (mV)	Comment
Boron carbide:	polished	$(NH_4)_2IrCl_6$ (4.0×10^{-5} to 1.0×10^{-3} mol dm^{-3})/ $HClO_4$ (0.1 M)	$[IrCl_6]^{2-} + e^- \rightleftharpoons [IrCl_6]^{3-}$		±0.05			±13	Fig. 5-1: αn = 0.24 (w/o C) - 4.8 ±0.08; level of significance, p = 0.001 < p < 0.01.
$B_{3.76}C$				0.69		0.619	0.861		
$B_{3.80}C$				0.50		0.416	0.658		
$B_{3.81}C$				0.65		0.451	0.693		Fig. 5-2: αn = 5.5 - 1.3 (B:C) ± 0.06; level of significance, p = p < 0.001.
$B_{3.84}C$				0.56		0.445	0.687		
$B_{3.84}C$				0.64		0.562	0.804		
$B_{4.00}C$				0.37		0.546	0.788		
$B_{4.04}C$				0.34		0.518	0.760		Figures 5-4 & 5-5: no correlation between $E_{\frac{1}{2}}$ and electrode composition.
$B_{4.05}C$				0.25		0.470	0.712		
$B_{3.86}C$ (boron carbide). Boron carbide/ carbon composite:	polished	$(NH_4)_2IrCl_6$ (1.0×10^{-4} to 5.0×10^{-4} mol dm^{-3})/ $HClO_4$ (0.1 M)	$[IrCl_6]^{2-} + e^- \rightleftharpoons [IrCl_6]^{3-}$	0.26	±0.05	0.466	0.708	±22	Fig. 5-9: Values of αn as a function of electrode composition.
					±0.05			±22	
$B_{3.77}C$				0.34		0.546	0.788		
$B_{3.38}C$				0.52		0.600	0.842		
$B_{3.11}C$				0.33		0.671	0.913		Fig. 5-10: Values of $E_{\frac{1}{2}}$ as a function of electrode composition.
$B_{2.98}C$				0.67		0.661	0.903		
$B_{2.76}C$				0.59		0.630	0.872		
$B_{2.56}C$				0.56		0.639	0.881		

Table 6-1 (continued)

Working electrode	Electrode treatment	E.a.s./supporting electrolyte	Electrode reaction	αn or (n)	Uncertainty	$E_{\frac{1}{4}}$ (V) vs SCE	$E_{\frac{1}{4}}$ (V) vs SHE	Uncertainty (mV)	Comment
Graphite	polished	$(NH_4)_2IrCl_6$ (1.0 x 10^{-4} mol dm^{-3})/ $HClO_4$ (0.1 M)	$[IrCl_6]^{2-}_{soln} \rightleftharpoons [IrCl_6]^{2-}_{ads,(w)}$ $[IrCl_6]^{2-} + e^- \rightleftharpoons [IrCl_6]^{3-}$	1.11	±0.07	0.624	0.866	±7	
$B_{3.86}C$ (boron carbide). Boron carbide/ carbon composite:	Contact with Ir(IV) perchlorate (1 x 10^{-4} M) and rinsed with $HClO_4$ (0.1 M)	$(NH_4)_2IrCl_6$ (1.0 x 10^{-4} mol dm^{-3})/ $HClO_4$ (0.1 M)	$Ir^{4+}_{soln} \rightleftharpoons Ir^{4+}_{ads,(s)}$ $[IrCl_6]^{2-} + e^- \rightleftharpoons [IrCl_6]^{3-}$	0.85	±0.04	0.614	0.856	±3	Fig. 5-11: αn (grand mean) = 0.92 ±0.04, 29 degrees of freedom.
					±0.04			±3	
$B_{3.77}C$				0.90		0.600	0.842		Fig. 5-12: $E_{\frac{1}{4}}$ (grand mean) = 0.604 V (vs SCE) or 0.846 V (vs SHE); ±7 mV, 29 degrees of freedom.
$B_{3.69}C$				0.90		0.615	0.857		
$B_{3.53}C$				0.84		0.596	0.838		
$B_{3.38}C$				1.01		0.608	0.850		
$B_{3.24}C$				0.96		0.608	0.850		
$B_{3.11}C$				0.95		0.593	0.835		
$B_{2.98}C$				0.95		0.605	0.847		
$B_{2.76}C$				0.92		0.597	0.839		
$B_{2.56}C$				0.93		0.604	0.846		
$B_{4.05}C$ (boron carbide)	Ir(IV) perchlorate (2.3 x 10^{-3} M)/ $HClO_4$ (0.1 M)	$(NH_4)_2IrCl_6$ (1.0 10^{-5} to 1.0 x 10^{-3} mol dm^{-3})/ $HClO_4$ (0.1 M)	$Ir^{4+}_{soln} \rightleftharpoons Ir^{4+}_{ads,(s)}$ $[IrCl_6]^{2-}_{soln} \rightleftharpoons [IrCl_6]^{2-}_{ads,(w)}$ $[IrCl_6]^{2-} + e^- \rightleftharpoons [IrCl_6]^{3-}$	Range of 0.91 to 0.77	±0.04	Range of 0.612 to 0.601	Range of 0.854 to 0.843	±2	Fig. 5-25: αn = 0.89 - 93.0 [$(NH_4)_2IrCl_6$] ± 0.03; level of significance, $p = 0.01 < p < 0.02$.

Table 6-1 (continued)

Working electrode	Electrode treatment	E.a.s./supporting electrolyte	Electrode reaction	αn or (n)	Uncertainty	$E_{\frac{1}{2}}$ (V) vs SCE	$E_{\frac{1}{2}}$ (V) vs SHE	Uncertainty (mV)	Comment
$B_{4.05}C$ (boron carbide) continued.			$[IrCl_6]^{3-}_{soln} \rightleftharpoons [IrCl_6]^{3-}_{ads,(s)}$						Fig. 5-27: $E_{\frac{1}{2}} = 0.610 - 6.04\,[(NH_4)_2IrCl_6] \pm 0.002$ V (vs SCE), or $E_{\frac{1}{2}} = 0.852 - 6.04\,[(NH_4)_2IrCl_6] \pm 0.002$ V (vs SHE); level of significance, $p = 0.02 < p < 0.05$.
									Fig. 5-29: $i_L/A = 2.23 + 2.40 \times 10^5\,[(NH_4)_2IrCl_6] \pm 1.79$ μA cm^{-2}; level of significance, $p = p < 0.001$.
	Cathodic polarisation (at -1 V vs SCE) in $(NH_4)_2IrCl_6$ (2×10^{-3} M)/$HClO_4$ (0.1 M).	$(NH_4)_2IrCl_6$ (2.0×10^{-5} to 2.0×10^{-4} mol dm^{-3})/ $HClO_4$ (0.1 M)	$[IrCl_6]^{2-} + e^- \rightleftharpoons [IrCl_6]^{3-}$ $2[IrCl_6]^{3-} + \frac{1}{2}O_2 + 2H^+ = 2[IrCl_6]^{2-} + H_2O$ $[IrCl_6]^{3-}_{soln} \rightleftharpoons [IrCl_6]^{3-}_{ads,(w)}$	Range of 1.17 to 0.74	±0.03	Range of 0.629 to 0.601	Range of 0.871 to 0.843	±2	Fig. 5-43, b: Values of αn as a function of $[(NH_4)_2IrCl_6]$. $E_{\frac{1}{2}} = 0.628 - 141\,[(NH_4)_2IrCl_6] \pm 0.004$ V (vs SCE), or $E_{\frac{1}{2}} = 0.870 - 141\,[(NH_4)_2IrCl_6] \pm 0.004$ V (vs SHE); level of significance, $p = 0.02 < p < 0.05$. Fig. 5-45, b: $i_L/A = 41.5 \times 10^4\,[(NH_4)_2IrCl_6] - 2.20 \pm 0.78$ μA cm^{-2}; level of significance, $p = p < 0.001$.

Table 6-1 (continued)

Working electrode	Electrode treatment	E.a.s./supporting electrolyte	Electrode reaction	αn or (n)	Uncertainty	$E_{\frac{1}{2}}$ (V) vs SCE	$E_{\frac{1}{2}}$ (V) vs SHE	Uncertainty (mV)	Comment
Boron carbide/carbon composite:	polished	$(NH_4)_2IrCl_6$ (1.0×10^{-4} to 4.0×10^{-4} mol dm^{-3})/	$[IrCl_6]^{2-} + e^- \rightleftharpoons [IrCl_6]^{3-}$		±0.18			±22	Fig. 5-53: αn = 7.24×10^{-2} (w/o C) − 1.26 ± 0.07; level of significance, $p = 0.001 < p < 0.01$.
$B_{3.77}C$		HCl (0.1 M)		0.40		0.563	0.805		αn = 2.44 − 0.559 (B:C) ± 0.08; level of significance, $p = 0.001 < p < 0.01$.
$B_{3.38}C$				0.44		0.635	0.877		
$B_{3.11}C$				0.74		0.618	0.860		
$B_{2.98}C$				0.74		0.636	0.878		Fig. 5-54: Values of $E_{\frac{1}{2}}$ as a function of electrode composition.
$B_{2.76}C$				0.84		0.640	0.882		
$B_{2.56}C$				1.08		0.623	0.865		Table 5-8: $i_L/A \propto [(NH_4)_2IrCl_6]$.
$B_{3.86}C$ (boron carbide)	Ir(IV) perchlorate (1.0×10^{-3} M) /$HClO_4$ (0.1 M)	$(NH_4)_2IrCl_6$ (1.0×10^{-5} to 8.0×10^{-4} mol dm^{-3})/ HCl (0.1 M)	$Ir^{4+}_{soln} \rightleftharpoons Ir^{4+}_{ads,(s)}$ $[IrCl_6]^{2-} + e^- \rightleftharpoons [IrCl_6]^{3-}$ $2[IrCl_6]^{3-} + \frac{1}{2}O_2 + 2H^+ = 2[IrCl_6]^{2-} + H_2O$ $[IrCl_6]^{3-}_{soln} \rightleftharpoons [IrCl_6]^{3-}_{ads,(s)}$	Range of 0.96 to 0.52	±0.04	Range of 0.628 to 0.578	Range of 0.870 to 0.820	±3	Fig. 5-57, a: αn = 0.95 − 5.1×10^2 [$(NH_4)_2IrCl_6$] ± 0.04; level of significance, $p = 0.001 < p < 0.01$. $E_{\frac{1}{2}} = 0.623 - 52.8$ [$(NH_4)_2IrCl_6$] ± 0.011 V (vs SCE), or $E_{\frac{1}{2}} = 0.865 - 52.8$ [$(NH_4)_2IrCl_6$] ± 0.011 V (vs SHE); level of significance, $p = 0.02 < p < 0.05$. Fig. 5-59, a: $i_L/A = 4.08 + 6.01 \times 10^5$ [$(NH_4)_2IrCl_6$] ± 9.67 μA cm^{-2}; level of significance, $p = p < 0.001$.

Table 6-1 (continued)

Working electrode	Electrode treatment	E.a.s./supporting electrolyte	Electrode reaction	αn or (n)	Uncertainty	$E_{\frac{1}{2}}$ (V) vs SCE	$E_{\frac{1}{2}}$ (V) vs SHE	Uncertainty (mV)	Comment
$B_{4.05}C$ (boron carbide)	Cathodic polarisation (at -4 V vs SCE) in $(NH_4)_2IrCl_6$ (8×10^{-4} M)/HCl (0.1 M).	$(NH_4)_2IrCl_6$ (2.0×10^{-5} to 4.0×10^{-4} mol dm^{-3})/ HCl (0.1 M)	$[IrCl_6]^{2-} + e^- \rightleftharpoons [IrCl_6]^{3-}$	Range of 0.98 to 0.52	±0.03	Range of 0.625 to 0.587	Range of 0.867 to 0.829	±3	Fig. 5-57, b: $\alpha n = 0.93 - 1.1 \times 10^3 [(NH_4)_2IrCl_6] \pm 0.08$; level of significance, $p = 0.02 < p < 0.05$. $E_{\frac{1}{2}} = 0.624 - 92.1 [(NH_4)_2IrCl_6] \pm 0.006$ V (vs SCE), or $E_{\frac{1}{2}} = 0.866 - 92.1 [(NH_4)_2IrCl_6] \pm 0.006$ V (vs SHE); level of significance, $p = 0.01 < p < 0.02$. Fig. 5-59, b: $i_L/A = 3.83 \times 10^5 [(NH_4)_2IrCl_6] - 1.19 \pm 1.18$ μA cm^{-2}; level of significance, $p = p < 0.001$.
$B_{4.05}C$ (boron carbide)	Cathodic polarisation (at -1 V vs SCE) in the sample.	$(NH_4)_2IrCl_6$ (4.0×10^{-5} to 8.0×10^{-4} mol dm^{-3})/ $NaClO_4$ (0.1 M)	$[IrCl_6]^{2-}_{soln} \rightleftharpoons [IrCl_6]^{2-}_{ads,(w)}$; $[IrCl_6]^{2-} + e^- \rightleftharpoons [IrCl_6]^{3-}$ (O_2/ClO_4^-); $[IrCl_6]^{3-}_{soln} \rightleftharpoons [IrCl_6]^{3-}_{ads,(w)}$; $[IrCl_6]^{3-} \rightleftharpoons$ [Ir(III) chlorohydroxy species]$_{ads,(w)}$	0.85, grand mean	±0.04	Range of 0.637 to 0.660	Range of 0.879 to 0.902	±3	Fig. 5-79: Values of αn as a function of $[(NH_4)_2IrCl_6]$. Fig. 5-80: Values of $E_{\frac{1}{2}}$ as a function of $[(NH_4)_2IrCl_6]$. Fig. 5-81: $i_L/A = 4.12 \times 10^5 [(NH_4)_2IrCl_6] - 3.18 \pm 7.17$ μA cm^{-2}; level of significance, $p = p < 0.001$.

Table 6-1 (continued)

Working electrode	Electrode treatment	E.a.s./supporting electrolyte	Electrode reaction	αn or (n)	Uncertainty	$E_{\frac{1}{2}}$ (V) vs SCE	$E_{\frac{1}{2}}$ (V) vs SHE	Uncertainty (mV)	Comment
$B_{3.86}C$ (boron carbide)	polished	Ir(IV) perchlorate (1.0×10^{-4} mol dm^{-3})/ $HClO_4$ (0.1 M)	$[Ir(OH_2)_6]^{4+}_{soln} \rightleftharpoons [Ir(OH_2)_6]^{4+}_{ads,(s)}$	Wave 1: 1.18		Wave 1: 0.929	Wave 1: 1.171		Fig. 5-102: $\alpha n_{(1)}$ mean = 1.34 ± 0.29, 7 degrees of freedom.
			$[Ir(OH_2)_6]^{4+} + e^- \rightleftharpoons [Ir(OH_2)_6]^{3+}$ ($HClO_4$)	Wave 3: 2.08		Wave 3: 0.602	Wave 3: 0.844		$\alpha n_{(3)}$ mean = 2.38 ± 0.64, 4 degrees of freedom.
Boron carbide/ carbon composite:			$[Ir(OH_2)_6]^{3+}_{soln} \rightleftharpoons [Ir(OH_2)_6]^{3+}_{ads,(m)}$						$\alpha n_{(4)}$ mean = 3.88 ± 0.59, 4 degrees of freedom.
$B_{3.77}C$			$[Ir(OH_2)_6]^{3+} + 2e^- \rightleftharpoons [Ir(OH_2)_4]^{+} + 2H_2O$ ($O_2/HClO_4$)	Wave 1: 1.69		Wave 1: 0.936	Wave 1: 1.178		
				Wave 3: 3.04		Wave 3: 0.585	Wave 3: 0.827		
$B_{3.69}C$			$[Ir(OH_2)_4]^{+}_{soln} \rightleftharpoons [Ir(OH_2)_4]^{+}_{ads,(m)}$	Wave 1: 1.81		Wave 1: 0.939	Wave 1: 1.181		Fig. 5-103: $E_{\frac{1}{2}(1)}$ mean = 0.927 V (vs SCE) or 1.169 V (vs SHE); ± 8 mV, 7 degrees of freedom.
				Wave 3: 3.06		Wave 3: 0.591	Wave 3: 0.833		
$B_{3.53}C$				Wave 1: 1.50		Wave 1: 0.932	Wave 1: 1.174		$E_{\frac{1}{2}(3)} = 0.834 - 6.24 \times 10^{-2}$ (B:C) ± 0.021 V (vs SCE), or
$B_{3.38}C$				Wave 1: 1.12		Wave 1: 0.920	Wave 1: 1.162		$E_{\frac{1}{2}(3)} = 1.076 - 6.24 \times 10^{-2}$ (B:C) ± 0.021 V (vs SHE); level of significance, $p = 0.02 < p < 0.05$.
				Wave 4: 3.86		Wave 4: 0.592	Wave 4: 0.834		
$B_{3.24}C$				Wave 1: 1.10		Wave 1: 0.922	Wave 1: 1.164		$E_{\frac{1}{2}(4)}$ mean = 0.591 V (vs SCE) or 0.833 V (vs SHE); ± 2 mV, 4 degrees of freedom.

Table 6-1 (continued)

Working electrode	Electrode treatment	E.a.s./supporting electrolyte	Electrode reaction	αn or (n)	Uncertainty	$E_{\frac{1}{2}}$ (V) vs SCE	$E_{\frac{1}{2}}$ (V) vs SHE	Uncertainty (mV)	Comment
$B_{3.24}C$ continued	polished	Ir(IV) perchlorate (1.0×10^{-4} mol dm^{-3})/ $HClO_4$ (0.1 M)		Wave 3: 2.03 Wave 4: 3.86		Wave 3: 0.659 Wave 4: 0.590	Wave 3: 0.901 Wave 4: 0.832		
$B_{3.11}C$				Wave 4: 3.43		Wave 4: 0.592	Wave 4: 0.834		
$B_{2.98}C$				Wave 1: 1.09 Wave 4: 3.37		Wave 1: 0.916 Wave 4: 0.588	Wave 1: 1.158 Wave 4: 0.830		
$B_{2.76}C$				Wave 4: 4.85		Wave 4: 0.593	Wave 4: 0.835		
$B_{2.56}C$				Wave 1: 1.24 Wave 3: 1.68		Wave 1: 0.921 Wave 3: 0.663	Wave 1: 1.163 Wave 3: 0.905		
Graphite				Wave 2: 2.13 Wave 4: 1.79		Wave 2: 0.934 Wave 4: 0.662	Wave 2: 1.176 Wave 4: 0.904		

Table 6-1 (continued)

Working electrode	Electrode treatment	E.a.s./supporting electrolyte	Electrode reaction	αn or (n)	Uncertainty	$E_{\frac{1}{4}}$ (V) vs SCE	$E_{\frac{1}{4}}$ (V) vs SHE	Uncertainty (mV)	Comment
$B_{4.05}C$ (boron carbide)	polished	Ir(IV) perchlorate (1.0×10^{-5} to 2.3×10^{-3} mol dm^{-3})/ $HClO_4$ (0.1 M)	$[Ir(OH_2)_6]^{4+}_{soln} \rightleftharpoons [Ir(OH_2)_6]^{4+}_{ads,(s)}$ $[Ir(OH_2)_6]^{4+} + e^- \rightleftharpoons [Ir(OH_2)_6]^{3+}$ ($HClO_4$) $[Ir(OH_2)_6]^{3+}_{soln} \rightleftharpoons [Ir(OH_2)_6]^{3+}_{ads,(m)}$ $[Ir(OH_2)_6]^{3+} + 2e^- \rightleftharpoons [Ir(OH_2)_4]^{+} + 2H_2O$ ($O_2/HClO_4$)	Wave 1: range of 0.94 to 1.42	±0.07	Wave 1: range of 0.915 to 0.958	Wave 1: range of 1.157 to 1.200	±3	Fig. 5-105: $\alpha n_{(1)}$ grand mean = 1.25 ± 0.22, 5 degrees of freedom. $\alpha n_{(3)}$ grand mean = 2.15 ± 0.59, 7 degrees of freedom.
				Wave 3: range of 1.36 to 2.98	±0.10	Wave 3: range of 0.598 to 0.672	Wave 3: range of 0.840 to 0.914	±1	Fig. 5-106: $E_{\frac{1}{4}(1)}$ grand mean = 0.939 V (vs SCE) or 1.181 V (vs SHE); ±17 mV, 5 degrees of freedom. $E_{\frac{1}{4}(3)}$ grand mean = 0.624 V (vs SCE) or 0.866 V (vs SHE); ±25 mV, 7 degrees of freedom. Fig. 5-107: $i_{L(1)}/A = 6.09 \times 10^4 [Ir(ClO_4)_4] - 5.57 \pm 5.28$ μA cm^{-2}; level of significance, p = $p < 0.001$. $i_{L(3)}/A = 2.01 \times 10^5 [Ir(ClO_4)_4] - 1.17 \pm 8.48$ μA cm^{-2}; level of significance, p = $p < 0.001$.

Table 6-1 (continued)

Working electrode	Electrode treatment	E.a.s./supporting electrolyte	Electrode reaction	αn or (n)	Uncertainty	$E_{\frac{1}{2}}$ (V) vs SCE	$E_{\frac{1}{2}}$ (V) vs SHE	Uncertainty (mV)	Comment
Boron carbide	polished	Ir(IV) phosphate (5.2×10^{-4} mol dm^{-3})/H_3PO_4 (0.32 M)-$HClO_4$ (0.1 M)	[Ir(IV) phosphate] + e^- ⇌ [Ir(III) phosphate]; O_2/H^+	0.25	±0.01	0.427	0.669	±38	
$B_{3.86}C$ (boron carbide). Boron carbide/ carbon composite:	polished	$Fe(ClO_4)_3$ (1.0×10^{-4} mol dm^{-3})/ $HClO_4$ (0.1 M)	$[Fe(OH_2)_6]^{3+} + e^- \rightleftharpoons [Fe(OH_2)_6]^{2+}$	0.99	±0.04	0.461	0.703	±6	Fig. 5-290: αn grand mean = 1.01 ± 0.05, 31 degrees of freedom.
$B_{3.77}C$				0.87	±0.02	0.457	0.699	±5	Fig. 5-291: $E_{\frac{1}{2}}$ grand mean = 0.466 V (vs SCE) or 0.708 V (vs SHE); ±5 mV, 32 degrees of freedom.
$B_{3.69}C$				1.05	±0.03	0.471	0.713	±4	
$B_{3.53}C$				1.00	±0.03	0.470	0.712	±1	
$B_{3.38}C$				0.98	±0.03	0.468	0.710	±2	
$B_{3.24}C$				1.02	±0.03	0.469	0.711	±4	
$B_{3.11}C$				1.09	±0.05	0.464	0.706	±4	
$B_{2.98}C$				1.09	±0.01	0.470	0.712	±5	
$B_{2.76}C$				1.01	±0.09	0.460	0.702	±9	
$B_{2.56}C$				1.09	±0.03	0.468	0.710	±3	

Table 6-1 (continued)

Working electrode	Electrode treatment	E.a.s./supporting electrolyte	Electrode reaction	αn or (n)	Uncertainty	$E_{\frac{1}{4}}$ (V) vs SCE	$E_{\frac{1}{4}}$ (V) vs SHE	Uncertainty (mV)	Comment
$B_{4.05}C$ (boron carbide)	polished	$Fe(ClO_4)_3$ (1.0×10^{-5} to 1.0×10^{-3} mol dm^{-3})/ $HClO_4$ (0.1 M)	$[Fe(OH_2)_6]^{3+}_{soln} \rightleftharpoons [Fe(OH_2)_6]^{3+}_{ads,(w)}$ $[Fe(OH_2)_6]^{3+} + e^- \rightleftharpoons [Fe(OH_2)_6]^{2+}$ $2[Fe(OH_2)_6]^{2+} + \frac{1}{2}O_2 + 2H^+ = 2[Fe(OH_2)_6]^{3+} + H_2O$	0.98, grand mean	±0.04	0.462, grand mean	0.704, grand mean	±3	Fig. 5-293: Values of αn as a function of [$Fe(ClO_4)_3$]. Fig. 5-294: Values of $E_{\frac{1}{4}}$ as a function of [$Fe(ClO_4)_3$]. Fig. 5-295: $i_L/A = 0.589 + 3.04 \times 10^5$ [$Fe(ClO_4)_3$] ± 5.15 μA cm^{-2}; level of significance, p = $p < 0.001$.
	Ir(IV) perchlorate (1.0×10^{-5} to 1.0×10^{-3} mol dm^{-3})/ $HClO_4$ (0.1 M)	$Fe(ClO_4)_3$ (1.0×10^{-4} mol dm^{-3})/$HClO_4$ (0.1 M)	$Ir^{4+}_{soln} \rightleftharpoons Ir^{4+}_{ads,(s)}$ $[Fe(OH_2)_6]^{3+}_{soln} \rightleftharpoons [Fe(OH_2)_6]^{3+}_{ads,(w)}$ $[Fe(OH_2)_6]^{3+} + e^- \rightleftharpoons [Fe(OH_2)_6]^{2+}$ $2[Fe(OH_2)_6]^{2+} + \frac{1}{2}O_2 + 2H^+ = 2[Fe(OH_2)_6]^{3+} + H_2O$	0.94, grand mean	±0.03	0.466, grand mean	0.708, grand mean	±3	Fig. 5-305: Values of αn as a function of [Ir(IV) perchlorate]. Fig. 5-306: Values of $E_{\frac{1}{4}}$ as a function of [Ir(IV) perchlorate].
$B_{4.04}C$ (boron carbide)	polished	$FeCl_3$ (4×10^{-5} to 2×10^{-3} M)/ HCl (0.1 M)	$[FeCl_4]^-_{soln} \rightleftharpoons [FeCl_4]^-_{ads,(w)}$ $[FeCl_4]^- + e^- \rightleftharpoons [FeCl_4]^{2-}$ $2[FeCl_4]^{2-} + \frac{1}{2}O_2 + 2H^+ = 2[FeCl_4]^- + H_2O$	Range of 0.93 to 0.57	±0.03	Range of 0.462 to 0.377	Range of 0.704 to 0.619	±2	Fig. 5-309: $\alpha n = 0.92 - 1.8 \times 10^2$ [$FeCl_3$] ± 0.02; level of significance, p = $p < 0.001$. Fig. 5-310: Values of $E_{\frac{1}{4}}$ as a function of $I^{\frac{1}{2}}$.

Table 6-1 (continued)

Working electrode	Electrode treatment	E.a.s./supporting electrolyte	Electrode reaction	αn or (n)	Uncertainty	$E_{\frac{1}{2}}$ (V) vs SCE	$E_{\frac{1}{2}}$ (V) vs SHE	Uncertainty (mV)	Comment
$B_{4.04}C$ (boron carbide) continued.									$E_{\frac{1}{2}} = 0.463 - 42.7\ [\ FeCl_3\ ] \pm 0.002$ V (vs SCE) or, $E_{\frac{1}{2}} = 0.705 - 42.7\ [\ FeCl_3\ ] \pm 0.002$ V (vs SHE); level of significance, $p = p < 0.001$. Fig. 5-311: $i_L/A = 3.82 \times 10^5\ [\ FeCl_3\ ] - 3.52 \pm 9.76$ μA cm^{-2}; level of significance, $p = p < 0.001$
Boron carbide	polished	$K_3Fe(CN)_6$ (8.0×10^{-5} to 2.0×10^{-3} mol dm^{-3})/KCl (0.5 M)	$[Fe(CN)_6]^{3-} + e^- \rightleftharpoons [Fe(CN)_6]^{4-}$ (O_2)	Range of 0.70 to 0.56	±0.04	Range of 0.188 to 0.173	Range of 0.430 to 0.415	±4	Fig. 5-331, a: $\alpha n = 0.69 - 65\ [\ K_3Fe(CN)_6\ ] \pm 0.02$; level of significance, $0.02 < p < 0.05$ Fig. 5-332, a: $E_{\frac{1}{2}} = 1.45 - 1.78\ I^{\frac{1}{2}} \pm 0.003$ V (vs SCE) or, $E_{\frac{1}{2}} = 1.692 - 1.78\ I^{\frac{1}{2}} \pm 0.003$ V (vs SHE); level of significance, $0.02 < p < 0.05$. Fig. 5-333, a: $i_L/A = 5.28 \times 10^5\ [\ K_3Fe(CN)_6\ ] - 2.04 \pm 9.22$ μA cm^{-2}; level of significance, $p = p < 0.001$.

Table 6-1 (continued)

Working electrode	Electrode treatment	E.a.s./supporting electrolyte	Electrode reaction	αn or (n)	Uncertainty	$E_{\frac{1}{2}}$ (V) vs SCE	$E_{\frac{1}{2}}$ (V) vs SHE	Uncertainty (mV)	Comment
Boron carbide	Ir(IV) perchlorate (1.0×10^{-4} mol dm^{-3})/$HClO_4$ (0.1 M)	$K_3Fe(CN)_6$ (8.0×10^{-5} to 2.0×10^{-3} mol dm^{-3})/KCl (0.5 M)	$Ir^{4+}_{soln} \rightleftharpoons Ir^{4+}_{ads,(s)}$ $[Fe(CN)_6]^{3-}_{soln} \rightleftharpoons [Fe(CN)_6]^{3-}_{ads,(w)}$ $[Fe(CN)_6]^{3-} + e^- \rightleftharpoons [Fe(CN)_6]^{4-}$ (O_2)	Range of 0.96 to 0.76	±0.02	Range of 0.210 to 0.196	Range of 0.452 to 0.438	±3	Fig. 5-331, b: $\alpha n = 0.95 - 97$ [$K_3Fe(CN)_6$] ± 0.02; level of significance, $p = 0.02 < p < 0.05$ Fig. 5-332, b: Values of $E_{\frac{1}{2}}$ as a function of $I^{\frac{1}{2}}$. Fig. 5-333, b: $i_L/A = 7.09 + 5.45 \times 10^5$ [$K_3Fe(CN)_6$] ± 12.1 μA cm^{-2}; level of significance, $p = p < 0.001$.
Boron carbide	c.HNO_3	$AgClO_4$ (2.0×10^{-5} to 2.0×10^{-3} mol dm^{-3})/$NaClO_4$ (0.1 M)	$Ag^+ + e^- \rightleftharpoons Ag$ $2Ag + H_2O + \frac{1}{2}O_2 = 2Ag^+ + 2OH^-$	(0.98), grand mean	±0.07	Range of 0.162 to 0.311	Range of 0.404 to 0.553	±3	Fig. 5-375, a: Values of n as a function of [$AgClO_4$]. Fig. 5-376, a: Values of $E_{\frac{1}{2}}$ as a function of [$AgClO_4$]. Fig. 5-377, a: $i_L/A = 8.79 + 3.30 \times 10^5$ [$AgClO_4$] ± 4.62 μA cm^{-2}; level of significance, $p = 0.001 < p < 0.01$.
	Anodic polarisation (at +1.5 V vs SCE)			Range of (0.88) to (0.59)	±0.08	Range of 0.179 to 0.302	Range of 0.421 to 0.544	±18	Fig. 5-375, b: Values of n as a function of [$AgClO_4$]. Fig. 5-376, b: Values of $E_{\frac{1}{2}}$ as a function of [$AgClO_4$].

Table 6-1 (continued)

Working electrode	Electrode treatment	E.a.s./supporting electrolyte	Electrode reaction	αn or (n)	Uncertainty	$E_{\frac{1}{2}}$ (V) vs SCE	$E_{\frac{1}{2}}$ (V) vs SHE	Uncertainty (mV)	Comment
Boron carbide, continued.									Fig. 5-377, b: $i_L/A = 0.179 + 6.83 \times 10^5 [AgClO_4] \pm 1.57$ μA cm^{-2}; level of significance, p = $p < 0.001$.
Boron carbide	c.HNO_3	$CuSO_4$ (2.0×10^{-4} mol dm^{-3})/ $NaClO_4$ (0.1 M)	$Cu^{++}_{soln} \rightleftharpoons Cu^{++}_{ads,(m)}$	(0.56)	±0.03	-0.0647	0.177	±1	
			$Cu^{++} + 2e^- \rightleftharpoons Cu$ (O_2/ClO_4^-)	or 1.11	±0.03	or -0.0720	or 0.170	±1	
Boron carbide	Anodic polarisation (at +4 V vs SCE), followed by aqua regia.	$Pd(ClO_4)_2$ (4.0×10^{-4} mol dm^{-3})/ $HClO_4$ (2.0 M)	$Pd^{++} + 2e^- \rightleftharpoons Pd$	(0.33) or 0.88		0.032 or 0.019	0.274 or 0.261		

Table 6-1 (continued)

Working electrode	Electrode treatment	E.a.s./supporting electrolyte	Electrode reaction	αn or (n)	Uncertainty	$E_{\frac{1}{2}}$ (V) vs SCE	$E_{\frac{1}{2}}$ (V) vs SHE	Uncertainty (mV)	Comment
Boron carbide	Cathodic polarisation (at -3.9 V vs SCE) in a solution of the sample.	Mixture of: $(NH_4)_2IrCl_6$ (1.0×10^{-4} mol dm^{-3}) & $FeCl_3$ (1.0×10^{-4} mol dm^{-3})/ HCl (0.1 M)	$[IrCl_6]^{2-}_{soln} \rightleftharpoons [IrCl_6]^{2-}_{ads,(w)}$						Table 5-10: The voltammetric data for $(NH_4)_2IrCl_6$ have been statistically compared with the voltammetric data for $FeCl_3$, and are shown to be highly significantly different.
			$[IrCl_6]^{2-} + e^- \rightleftharpoons [IrCl_6]^{3-}$	1.36	±0.04	0.635	0.877	±4	
			$2[IrCl_6]^{3-} + \frac{1}{2}O_2 + 2H^+ = 2[IrCl_6]^{2-} + H_2O$						
			$[IrCl_6]^{3-}_{soln} \rightleftharpoons [IrCl_6]^{3-}_{ads,(w)}$						
			$[FeCl_4]^- + e^- \rightleftharpoons [FeCl_4]^{2-}$	0.94	±0.06	0.422	0.664	±2	
			$2[FeCl_4]^{2-} + \frac{1}{2}O_2 + 2H^+ = 2[FeCl_4]^- + H_2O$						
			$[FeCl_4]^{2-}_{soln} \rightleftharpoons [FeCl_4]^{2-}_{ads,(w)}$						

Notes: The electrode reaction mechanisms involving adsorption and/or catalytic effects have usually been elucidated with the aid of complementary investigations with linear sweep voltammetry and/or cyclic voltammetry. Therefore, under d.c. voltammetric conditions the interference from adsorption would be minimised. More detailed analyses of the systems, e.g. effects of supporting electrolyte concentration, are given in the relevant sections. Unless stated otherwise, voltammetry was conducted without nitrogen aeration of the samples.

Subscripts: soln = solution, ads = adsorbed, (s) = strongly, (m) = moderately strong, (w) = weakly; (1) to (4) inclusive = waves 1 to 4 respectively in the order of decreasingly anodic potentials.

Table 6-2 Summary of linear and cyclic sweep voltammetric data

Working electrode	Electrode treatment	E.a.s./supporting electrolyte	Electrode reaction	$E_{p(c)/2}$ or ($E_{p(a)/2}$) in V vs SCE	Uncertainty (mV)	$E_{p(c)}$ or ($E_{p(a)}$) in V vs SCE	Uncertainty (mV)	Comment
$B_{4.05}C$ (boron carbide)	Ir(IV) perchlorate (2.3×10^{-3} M)/ $HClO_4$ (0.1 M)	$(NH_4)_2IrCl_6$ (1.0×10^{-4} mol dm^{-3})/ $HClO_4$ (0.1 M)	$Ir^{4+}_{soln} \rightleftharpoons Ir^{4+}_{ads,(s)}$ $[IrCl_6]^{2-}_{soln} \rightleftharpoons [IrCl_6]^{2-}_{ads,(w)}$ $[IrCl_6]^{2-} + e^- \rightleftharpoons [IrCl_6]^{3-}$ $[IrCl_6]^{3-}_{soln} \rightleftharpoons [IrCl_6]^{3-}_{ads,(s)}$	Wave 1: 0.800 (0.747) Wave 2: 0.656 (0.563)	 ±8 ±4 ±19 ±14	Wave 1: 0.757 (0.762) Wave 2: 0.581 (0.656)	 ±2 ±6 ±33 ±23	$E_{p(c,2)/2} = 0.671 - 9.83 \times 10^{-2}$ v ± 0.007 V (vs SCE); level of significance, $p = 0.001 < p < 0.01$. $E_{p(a,2)/2}$ = range of 0.542–0.581 V (vs SCE), depending on v. Fig. 5-36: Values of $E_{p(c)}$ as a function of sweep rate, v. Range of $E_{p(c,2)}$ = 0.621–0.538 V (vs SCE). Fig. 5-37: Values of $E_{p(a)}$ as a function of sweep rate, v. $E_{p(a,1)} = 0.758 + 0.027$ v ± 0.003 V (vs SCE); level of significance, $p = 0.02 < p < 0.05$. Range of $E_{p(a,2)}$ = 0.629–0.686 V (vs SCE).
	Cathodic polarisation (at -1 V vs SCE) in $(NH_4)_2IrCl_6$ (8×10^{-4} M)/$HClO_4$ (0.1 M)	$(NH_4)_2IrCl_6$ (8.0×10^{-5} mol dm^{-3})/ $HClO_4$ (0.1 M)	$[IrCl_6]^{2-} + e^- \rightleftharpoons [IrCl_6]^{3-}$ $2[IrCl_6]^{3-} + \frac{1}{2}O_2 + 2H^+ = 2[IrCl_6]^{2-} + H_2O$ $[IrCl_6]^{3-}_{soln} \rightleftharpoons [IrCl_6]^{3-}_{ads,(w)}$	0.663	±8	0.589	±5	Fig. 5-48: $E_{p(c)/2} = 0.657 + 0.040$ v ± 0.003 V (vs SCE); level of significance, $p = 0.001 < p < 0.01$. $E_{p(c)} = 0.593 - 0.028$ v ± 0.002 V (vs SCE); level of significance, $p = 0.001 < p < 0.01$. $\lvert E_{p(c)} - E_{p(c)/2} \rvert = 0.064 + 0.068$ v ± 0.005 V; level of significance, $p = 0.001 < p < 0.01$.

Table 6-2 (continued)

Working electrode	Electrode treatment	E.a.s./supporting electrolyte	Electrode reaction	$E_{p(c)/2}$ or ($E_{p(a)/2}$) in V vs SCE	Uncertainty (mV)	$E_{p(c)}$ or ($E_{p(a)}$) in V vs SCE	Uncertainty (mV)	Comment
Graphite	polished	$(NH_4)_2IrCl_6$ (1.0 x 10^{-4} mol dm^{-3})/ $HClO_4$ (0.1 M)	$[IrCl_6]^{2-}_{soln} \rightleftharpoons [IrCl_6]^{2-}_{ads,(w)}$ $[IrCl_6]^{2-} + e^- \rightleftharpoons [IrCl_6]^{3-}$	0.627	±19	0.565	±21	$E_{p(c)/2}$ = 0.642 - 0.102 v ± 0.003 V (vs SCE); level of significance, p = p < 0.001. Fig. 5-52: $E_{p(c)}$ = 0.578 - 0.111 v ± 0.004 V (vs SCE); level of significance, p = p < 0.001. $\lvert E_{p(c)} - E_{p(c)/2} \rvert$ mean = 0.065 ± 0.004 V, 5 degrees of freedom.
$B_{3.86}C$ (boron carbide)	Ir(IV) perchlorate (1.0 x 10^{-3} M) /$HClO_4$ (0.1 M)	$(NH_4)_2IrCl_6$ (1.0 x 10^{-5} to 8.0 x 10^{-4} mol dm^{-3})/ HCl (0.1 M)	$Ir^{4+}_{soln} \rightleftharpoons Ir^{4+}_{ads,(s)}$ $[IrCl_6]^{2-} + e^- \rightleftharpoons [IrCl_6]^{3-}$ $2[IrCl_6]^{3-} + \frac{1}{2}O_2 + 2H^+ = 2[IrCl_6]^{2-} + H_2O$ $[IrCl_6]^{3-}_{soln} \rightleftharpoons [IrCl_6]^{3-}_{ads,(s)}$	Wave 1: 0.778 Wave 2: 0.649	±8 ±8	Wave 1: 0.744 Wave 2: 0.582	±7 ±15	$E_{p(c,1)/2}$ = 0.777 - 9.75 x 10^{-3} v ± 0.003 V (vs SCE); level of significance, p = 0.001 < p < 0.01. $E_{p(c,2)/2}$ = 0.655 - 3.70 x 10^{-2} v ± 0.005 V (vs SCE); level of significance, p = p < 0.001. Fig. 5-72: Values of $E_{p(c)}$ as a function of sweep rate, v. $E_{p(c,2)}$ = 0.594 - 8.41 x 10^{-2} v ± 0.005 V (vs SCE); level of significance, p = p < 0.001. Figures 5-69 & 5-70: Values of $i_{p(c,1)}/A$ and $i_{p(c,2)}/A$ respectively, as functions of [$(NH_4)_2IrCl_6$].

Table 6-2 (continued)

Working electrode	Electrode treatment	E.a.s./supporting electrolyte	Electrode reaction	$E_{p(c)/2}$ or ($E_{p(a)/2}$) in V vs SCE	Uncertainty (mV)	$E_{p(c)}$ or ($E_{p(a)}$) in V vs SCE	Uncertainty (mV)	Comment
$B_{4.05}{}^{C}$ (boron carbide)	Cathodic polarisation (at -1 V vs SCE) in the sample.	$(NH_4)_2IrCl_6$ (1.0×10^{-5} to 2.0×10^{-3} mol dm^{-3})/ $NaClO_4$ (0.1 M)	$[IrCl_6]^{2-}_{soln} \rightleftharpoons [IrCl_6]^{2-}_{ads,(w)}$	Wave 1: 0.694 (0.645)*	±19 9	Wave 1: 0.623 (0.739)*	±28 36	$E_{p(c,1)/2} = 0.695 - 3.71 \times 10^{-2}$ v ± 0.013 V (vs SCE); level of significance, $p = 0.01 < p < 0.02$.
			$[IrCl_6]^{2-} + e^- \rightleftharpoons [IrCl_6]^{3-}$ (O_2/ClO_4^-)					$E^*_{p(a,1)/2}$ = range of 0.634–0.656 V (vs SCE), depending on v.
			$[IrCl_6]^{3-}_{soln} \rightleftharpoons [IrCl_6]^{3-}_{ads,(w)}$					$E^*_{p(a,2)/2}$ = range of 0.444–0.512 V (vs SCE), depending on v.
			$[IrCl_6]^{3-} \rightleftharpoons$ [Ir(III) chlorohydroxy species]$_{ads,(w)}$					Fig. 5-92: $E_{p(c,1)} = 0.638 - 0.130$ v ± 0.014 V (vs SCE); level of significance, $p = p < 0.001$.
			[Ir(IV) chlorohydroxy species] + e^- $\rightleftharpoons$ [Ir(III) chlorohydroxy species]	Wave 2: (0.481)*	29	Wave 2: (0.539)*	24	Fig. 5-93: $\lvert E_{p(c,1)} - E_{p(c,1)/2} \rvert = 6.27 \times 10^{-2} + 6.85 \times 10^{-2}$ v ± 0.007 V; level of significance, $p = p < 0.001$.
								Fig. 5-95: $E^*_{p(a,1)} = 0.711 + 0.191$ v ± 0.007 V (vs SCE); level of significance, $p = p < 0.001$.
								$E^*_{p(a,2)}$ = range of 0.510–0.565 V (vs SCE), depending on v.
								Fig. 5-91: Values of $i_{p(c,1)}/A$ as a function of [$(NH_4)_2IrCl_6$].

*: Values are for $(NH_4)_2IrCl_6$ (2.0×10^{-3} mol dm^{-3}).

Table 6-2 (continued)

Working electrode	Electrode treatment	E.a.s./supporting electrolyte	Electrode reaction	$E_{p(c)/2}$ or $(E_{p(a)/2})$ in V vs SCE	Uncertainty (mV)	$E_{p(c)}$ or $(E_{p(a)})$ in V vs SCE	Uncertainty (mV)	Comment
$B_{4.05}C$ (boron carbide)	polished	Ir(IV) perchlorate (4.0×10^{-6} to 2.3×10^{-3} mol dm^{-3})/ $HClO_4$ (0.1 M)	$[Ir(OH_2)_6]^{4+}_{soln} \rightleftharpoons [Ir(OH_2)_6]^{4+}_{ads,(s)}$	Wave 1:		Wave 1:		$E^{*}_{p(c,1)/2} = 0.973 - 3.55 \times 10^{-2}$ v ± 0.006 V (vs SCE); level of significance, $p = 0.01 < p < 0.02$.
			$[Ir(OH_2)_6]^{4+} + e^- \rightleftharpoons [Ir(OH_2)_6]^{3+}$ ($HClO_4$)	0.966*	±9	0.897	±25	
				(0.901)*	±5	(0.948)*	±14	
				Wave 2:		Wave 2:		$E^{*}_{p(c,2)/2} = 0.800 + 1.24 \times 10^{-2}$ v ± 0.018 V (vs SCE); level of significance, $p = 0.02 < p < 0.05$.
				0.802*	±3	0.793	±17	
				(0.755)*	±2	(0.791)*	±2	
			$[Ir(OH_2)_6]^{3+}_{soln} \rightleftharpoons [Ir(OH_2)_6]^{3+}_{ads,(m)}$	Wave 3:		Wave 3:		$E^{*}_{p(a,3)/2} = 0.592 + 1.81 \times 10^{-2}$ v ± 0.002 V (vs SCE); level of significance, $p = 0.01 < p < 0.02$.
			$[Ir(OH_2)_6]^{3+} + 2e^- \rightleftharpoons [Ir(OH_2)_4]^{+} +$ ($O_2/HClO_4$) $2H_2O$	0.632	±9	0.598	±18	
				(0.595)*	±4	(0.616)*	±6	
				Wave 4:		Wave 4:		Fig. 5-136: $E^{*}_{p(c,1)} = 0.904 - 4.92 \times 10^{-2}$ v ± 0.024 V (vs SCE); level of significance, $p = 0.01 < p < 0.02$.
				(0.512)*	±6	0.551	±10	
						(0.552)*	±7	
								$E_{p(c,3)} = 0.603 - 3.11 \times 10^{-2}$ v ± 0.017 V (vs SCE); level of significance, $p = 0.02 < p < 0.05$.
								$E_{p(c,4)} = 0.559 - 4.18 \times 10^{-2}$ v ± 0.007 V (vs SCE); level of significance, $p = 0.02 < p < 0.05$.
								Fig. 5-140: $E^{*}_{p(a,1)} = 0.958 - 7.34 \times 10^{-2}$ v ± 0.004 V (vs SCE); level of significance, $p = 0.001 < p < 0.01$.
								$E^{*}_{p(a,3)} = 0.612 + 3.16 \times 10^{-2}$ v ± 0.003 V (vs SCE); level of significance, $p = 0.01 < p < 0.02$.
								Fig. 5-134: Values of $i_{p(c)}/A$ as functions of [Ir(IV) perchlorate].

*: Values are for Ir(IV) perchlorate (1.0×10^{-4} mol dm^{-3}).

Table 6-2 (continued)

Working electrode	Electrode treatment	E.a.s./supporting electrolyte	Electrode reaction	$E_{p(c)/2}$ or ($E_{p(a)/2}$) in V vs SCE	Uncertainty (mV)	$E_{p(c)}$ or ($E_{p(a)}$) in V vs SCE	Uncertainty (mV)	Comment
$B_{3.86}C$ (boron carbide)	polished	Ir(IV) perchlorate (8.0 x 10^{-4} mol dm^{-3})/ $HClO_4$ (0.1 M)	$[Ir(OH_2)_6]^{4+}_{soln} \rightleftharpoons [Ir(OH_2)_6]^{4+}_{ads,(s)}$	Wave 1:		Wave 1:		$E_{p(c,2)/2} = 0.839 + 2.17 \times 10^{-2}$ v ± 0.001 V (vs SCE); level of significance, p = p < 0.001.
			$[Ir(OH_2)_6]^{4+} + e^- \rightleftharpoons [Ir(OH_2)_6]^{3+}$ ($HClO_4$)	1.002	±5	0.922	±7	
				1.006*	±3	0.920*	±8	
				Wave 2:		Wave 2:		$E_{p(c,3)/2} = 0.651 + 1.17 \times 10^{-2}$ v ± 0.002 V (vs SCE); level of significance, p = 0.02 < p < 0.05.
				0.842	±4	0.819	±2	
			$[Ir(OH_2)_6]^{3+}_{soln} \rightleftharpoons [Ir(OH_2)_6]^{3+}_{ads,(w)}$	0.843*	±4	0.817*	±1	$E^*_{p(c,2)/2} = 0.839 + 2.20 \times 10^{-2}$ v ± 0.002 V (vs SCE); level of significance, p = 0.001 < p < 0.01.
			$[Ir(OH_2)_6]^{3+} + 2e^- \rightleftharpoons [Ir(OH_2)_4]^+$ ($HClO_4$, $2H_2O$)	Wave 3		Wave 3:		$E^*_{p(c,3)/2} = 0.657 + 1.14 \times 10^{-2}$ v ± 0.001 V (vs SCE); level of significance, p = 0.001 < p < 0.01.
				0.653	±3	0.612	±14	
				0.658*	±2	0.616*	±14	
			(+O_2, unless N_2 aerated)					
		*: Values obtained after nitrogen aeration (16 hours).						Fig. 5-244: $E_{p(c,1)} = 0.927 - 3.68 \times 10^{-2}$ v ± 0.003 V (vs SCE); level of significance, p = 0.001 < p < 0.01.
								$E_{p(c,2)} = 0.818 + 8.08 \times 10^{-3}$ v ± 0.001 V (vs SCE); level of significance, p = 0.02 < p < 0.05.
								$E_{p(c,3)} = 0.622 - 6.89 \times 10^{-2}$ v ± 0.005 V (vs SCE); level of significance, p = 0.001 < p < 0.01.
								$E^*_{p(c,1)} = 0.925 - 3.42 \times 10^{-2}$ v ± 0.005 V (vs SCE); level of significance, p = 0.02 < p < 0.05.
								$E^*_{p(c,3)} = 0.626 - 6.94 \times 10^{-2}$ v ± 0.005 V (vs SCE); level of significance, p = 0.001 < p < 0.01.

Table 6-2 (continued)

Working electrode	Electrode treatment	E.a.s./supporting electrolyte	Electrode reaction	$E_{p(c)/2}$ or ($E_{p(a)/2}$) in V vs SCE	Uncertainty (mV)	$E_{p(c)}$ or ($E_{p(a)}$) in V vs SCE	Uncertainty (mV)	Comment
$B_{4.05}C$ (boron carbide)	Ir(IV) perchlorate (2.3×10^{-3} M) /$HClO_4$ (0.1 M)	Adsorbed Ir(IV) species/ $HClO_4$ (0.1 M)	$[Ir(OH_2)_6]^{4+}_{soln} \rightleftharpoons [Ir(OH_2)_6]^{4+}_{ads,(s)}$ $[Ir(OH_2)_6]^{4+} + e^- \rightleftharpoons [Ir(OH_2)_6]^{3+}$ ($HClO_4$) $[Ir(OH_2)_6]^{3+}_{soln} \rightleftharpoons [Ir(OH_2)_6]^{3+}_{ads,(s)}$ $[Ir(OH_2)_6]^{3+} + 2e^- \rightleftharpoons [Ir(OH_2)_4]^{+} + 2H_2O$ ($O_2/HClO_4$)	Wave 1: 0.808 Wave 2: 0.642	±10 ±11	Wave 1: 0.778 Wave 2: 0.597 Wave 3: 0.547	±10 ±12 ±15	$E_{p(c,1)/2} = 0.815 - 4.41 \times 10^{-2}$ v ± 0.006 V (vs SCE); level of significance, $p = 0.02 < p < 0.05$. $E_{p(c,2)/2} = 0.650 - 5.42 \times 10^{-2}$ v ± 0.005 V (vs SCE); level of significance, $p = 0.001 < p < 0.01$. Fig. 5-228: $E_{p(c,1)} = 0.786 - 5.10 \times 10^{-2}$ v ± 0.004 V (vs SCE); level of significance, $p = 0.001 < p < 0.01$. $E_{p(c,3)} = 0.558 - 7.54 \times 10^{-2}$ v ± 0.006 V (vs SCE); level of significance, $p = 0.001 < p < 0.01$.
Graphite	Ir(IV) perchlorate (1.0×10^{-4} M) /$HClO_4$ (0.1 M)	Adsorbed Ir(IV) species/ $HClO_4$ (0.1 M)	$[Ir(OH_2)_6]^{4+}_{soln} \rightleftharpoons [Ir(OH_2)_6]^{4+}_{ads,(s)}$ $[Ir(OH_2)_6]^{4+} + e^- \rightleftharpoons [Ir(OH_2)_6]^{3+}$ ($HClO_4$) $[Ir(OH_2)_6]^{3+}_{soln} \rightleftharpoons [Ir(OH_2)_6]^{3+}_{ads,(s)}$ $[Ir(OH_2)_6]^{3+} + 2e^- \rightleftharpoons [Ir(OH_2)_4]^{+} + 2H_2O$ ($O_2/HClO_4$)	Wave 2: 0.772 Wave 3: 0.635	±19 ±32	Wave 1: 0.928 Wave 2: 0.734 Wave 3: 0.576	±90 ±24 ±47	$E_{p(c,2)/2} = 0.787 - 7.36 \times 10^{-2}$ v ± 0.002 V (vs SCE); level of significance, $p = 0.02 < p < 0.05$. $E_{p(c,3)/2}$ range = 0.661–0.600 V (vs SCE). Fig. 5-232: $E_{p(c,1)}$ range = 1.006–0.830 V (vs SCE). $E_{p(c,2)} = 0.753 - 9.32 \times 10^{-2}$ v ± 0.002 V (vs SCE); level of significance, $p = 0.02 < p < 0.05$. $E_{p(c,3)} = 0.612 - 0.181$ v ± 0.005 V (vs SCE); level of significance, $p = 0.02 < p < 0.05$.

Table 6-2 (continued)

Working electrode	Electrode treatment	E.a.s./supporting electrolyte	Electrode reaction	$E_{p(c)/2}$ or ($E_{p(a)/2}$) in V vs SCE	Uncertainty (mV)	$E_{p(c)}$ or ($E_{p(a)}$) in V vs SCE	Uncertainty (mV)	Comment
$B_{3.86}C$ (boron carbide)	Ir(IV) perchlorate (1.0×10^{-3} M) /$HClO_4$ (0.1 M)	Adsorbed Ir(IV) species/ HCl (0.1 M)	$Ir(IV)_{soln} \rightleftharpoons Ir(IV)_{ads,(s)}$ $Ir(IV) + e^- \rightleftharpoons Ir(III)$ $\uparrow$ ——— O_2/H^+ $Ir(III)_{soln} \rightleftharpoons Ir(III)_{ads,(w)}$ $Ir(III) + 2e^- \rightleftharpoons Ir(I)$ $\uparrow$ ——— O_2/H^+	Wave 1: 0.897 Wave 2: 0.782 Wave 3: 0.628	±14 ±3 ±6	Wave 1: 0.854 Wave 2: 0.738 Wave 3: 0.568	±3 ±5 ±15	$E_{p(c,1)/2}$ range = 0.911–0.883 V (vs SCE). Fig. 5-65: $E_{p(c,3)} = 0.580 - 7.95 \times 10^{-2}$ v ± 0.004 V (vs SCE); level of significance, p = 0.001 < p < 0.01.
Boron carbide	polished	Ir(IV) sulphate (1.0×10^{-4} mol dm^{-3})/H_2SO_4 (0.05 M)	[Ir(IV) sulphate]$_{soln}$ $\rightleftharpoons$ [Ir(IV) sulphate]$_{ads,(w)}$ [Ir(IV) sulphate] + e^- ⇌ e.a.s. ⟵ [Ir(III) sulphate] [Ir(III) sulphate]$_{soln}$ $\rightleftharpoons$ [Ir(III) sulphate]$_{ads,(w)}$ [Ir(III) sulphate] + $2e^-$ ⇌ [Ir(I) sulphate] [Ir(I) sulphate]$_{soln}$ $\rightleftharpoons$ [Ir(I) sulphate]$_{ads,(w)}$	Wave 1: 0.914 Wave 2: 0.664	±81 ±4	Wave 1: 0.845 Wave 2: 0.615	±73 ±4	$E_{p(c,1)/2}$ range = 0.819–0.995 V (vs SCE). Fig. 5-277: $E_{p(c,1)}$ range = 0.746–0.927 V (vs SCE). Fig. 5-281: Values of $\lvert E_p - E_{p/2} \rvert$ as functions of sweep rate, v.

Table 6-2 (continued)

Working electrode	Electrode treatment	E.a.s./supporting electrolyte	Electrode reaction	$E_{p(c)/2}$ or ($E_{p(a)/2}$) in V vs SCE	Uncertainty (mV)	$E_{p(c)}$ or ($E_{p(a)}$) in V vs SCE	Uncertainty (mV)	Comment
Boron carbide	polished	Ir(IV) phosphate (5.2×10^{-4} mol dm^{-3})/H_3PO_4 (0.32 M)-$HClO_4$ (0.1 M)	[Ir(IV) phosphate] + e^- ⇌ [Ir(III) phosphate]; [Ir(III) phosphate] → [Ir(IV) phosphate] via O_2/H^+	0.571	±28	0.450	±71	$E_{p(c,2)/2}$ = 0.593 - 0.144 v ± 0.009 V (vs SCE); level of significance, $p = 0.001 < p < 0.01$. Fig. 5-287: $E_{p(c,2)}$ = 0.502 - 0.360 v ± 0.025 V (vs SCE); level of significance, $p = 0.001 < p < 0.01$. Fig. 5-288: $\lvert E_{p(c,2)} - E_{p(c,2)/2} \rvert = 9.01 \times 10^{-2} + 0.216$ v ± 0.017 V; level of significance, $p = 0.001 < p < 0.01$.
$B_{4.04}C$ (boron carbide)	polished	$Fe(ClO_4)_3$ (1.0×10^{-4} mol dm^{-3})/$HClO_4$ (0.1 M)	$[Fe(OH_2)_6]^{3+}_{soln} \rightleftharpoons [Fe(OH_2)_6]^{3+}_{ads,(w)}$; $[Fe(OH_2)_6]^{3+} + e^- \rightleftharpoons [Fe(OH_2)_6]^{2+}$; $2[Fe(OH_2)_6]^{2+} + \frac{1}{2}O_2 + 2H^+ = 2[Fe(OH_2)_6]^{3+} + H_2O$	0.481 (0.351)	±11 ±35	0.386 (0.478)	±12 ±39	$E_{p(c)/2}$ = 0.489 - 5.61×10^{-2} v ± 0.005 V (vs SCE); level of significance, $p = 0.001 < p < 0.01$. $E_{p(a)/2}$ range = 0.408-0.320 V (vs SCE). Fig. 5-300: $E_{p(c)}$ = 0.395 - 6.41×10^{-2} v ± 0.004 V (vs SCE); level of significance, $p = 0.001 < p < 0.01$. $E_{p(a)}$ = 0.504 - 0.182 v ± 0.022 V (vs SCE); level of significance, $p = 0.02 < p < 0.05$.

Table 6-2 (continued)

Working electrode	Electrode treatment	E.a.s./supporting electrolyte	Electrode reaction	$E_{p(c)/2}$ or ($E_{p(a)/2}$) in V vs SCE	Uncertainty (mV)	$E_{p(c)}$ or ($E_{p(a)}$) in V vs SCE	Uncertainty (mV)	Comment
$B_{4.04}C$ (boron carbide)	polished	$FeCl_3$ (4×10^{-5} to 2×10^{-3} M)/ HCl (0.1 M)	$[FeCl_4]^-_{soln} \rightleftharpoons [FeCl_4]^-_{ads,(w)}$ $[FeCl_4]^- + e^- \rightleftharpoons [FeCl_4]^{2-}$ $2[FeCl_4]^{2-} + \frac{1}{2}O_2 + 2H^+ = 2[FeCl_4]^- + H_2O$	0.457 (0.359)	±12 ±38	0.374 (0.484)	±21 ±46	$E_{p(c)/2} = 0.465 - 5.02 \times 10^{-2}$ v ± 0.008 V (vs SCE); level of significance, p = p < 0.001. $E_{p(a)/2} = 0.378 - 0.102$ v ± 0.033 V (vs SCE); level of significance, p = 0.001 < p < 0.01. Fig. 5-317: $E_{p(c)} = 0.388 - 8.33 \times 10^{-2}$ v ± 0.014 V (vs SCE); level of significance, p = p < 0.001. $E_{p(a)} = 0.506 - 0.118$ v ± 0.041 V (vs SCE); level of significance, p = 0.01 < p < 0.02. Figures 5-319 & 5-320: Values of $i_{p(c)}/A$ and $i_{p(a)}/A$ respectively, as functions of [$FeCl_3$].
Boron carbide	polished	$K_3Fe(CN)_6$ (8.0×10^{-5} to 2.0×10^{-3} mol dm^{-3})/KCl (0.5 M)	$[Fe(CN)_6]^{3-} + e^- \rightleftharpoons [Fe(CN)_6]^{4-}$ ($[Fe(CN)_6]^{4-} \xrightarrow{O_2} [Fe(CN)_6]^{3-}$)	0.238 (0.186)	±9 ±6	0.152 (0.262)	±27 ±15	$E_{p(c)/2} = 0.244 + 4.43 \times 10^{-2}$ v ± 0.005 V (vs SCE); level of significance, p = p < 0.001. $E_{p(a)/2} = 0.183 + 2.92 \times 10^{-2}$ v ± 0.004 V (vs SCE); level of significance, p = p < 0.001.

Table 6-2 (continued)

Working electrode	Electrode treatment	E.a.s./supporting electrolyte	Electrode reaction	$E_{p(c)/2}$ or ($E_{p(a)/2}$) in V vs SCE	Uncertainty (mV)	$E_{p(c)}$ or ($E_{p(a)}$) in V vs SCE	Uncertainty (mV)	Comment
Boron carbide, continued.	polished							Fig. 5-353: $E_{p(c)}$ = 0.170 - 0.154 V ±0.012 V (vs SCE); level of significance, p = p <0.001. $E_{p(a)}$ = 0.252 + 8.07 x 10^{-2} v ± 0.007 V (vs SCE); level of significance, p = p <0.001. Figures 5-357 & 5-359: Values of $i_{p(c)}/A$ and $i_{p(a)}/A$ respectively, as functions of [$K_3Fe(CN)_6$].
Boron carbide	Ir(IV) perchlorate (1.0 x 10^{-4} mol dm^{-3})/ $HClO_4$ (0.1 M)	$K_3Fe(CN)_6$ (8.0 x 10^{-5} to 2.0 x 10^{-3} mol dm^{-3})/KCl (0.5 M)	$Ir^{4+}_{soln} \rightleftharpoons Ir^{4+}_{ads,(s)}$ $[Fe(CN)_6]^{3-}_{soln} \rightleftharpoons [Fe(CN)_6]^{3-}_{ads,(w)}$ $[Fe(CN)_6]^{3-} + e^- \rightleftharpoons [Fe(CN)_6]^{4-}$ (O_2)	0.243 (0.176)	±8 ±6	0.172 (0.249)	±8 ±11	$E_{p(a)/2}$ = 0.174 + 1.78 x 10^{-2} v ± 0.005 V (vs SCE); level of significance, p = 0.001 < p <0.01. Fig. 5-353: $E_{p(c)}$ = 0.175 - 6.32 x 10^{-2} v ± 0.011 V (vs SCE); level of significance, p = p <0.001. $E_{p(a)}$ = 0.242 + 6.14 x 10^{-2} v ± 0.006 V (vs SCE); level of significance, p = p <0.001. Figures 5-358 & 5-360: Values of $i_{p(c)}/A$ and $i_{p(a)}/A$ respectively, as functions of [$K_3Fe(CN)_6$].

Table 6-2 (continued)

Working electrode	Electrode treatment	E.a.s./supporting electrolyte	Electrode reaction	$E_{p(c)/2}$ or ($E_{p(a)/2}$) in V vs SCE	Uncertainty (mV)	$E_{p(c)}$ or ($E_{p(a)}$) in V vs SCE	Uncertainty (mV)	Comment
Boron carbide	Poised at +0.5 V (vs SCE) prior to cyclic scans.	$AgClO_4$ (2.0×10^{-5} to 2.0×10^{-3} mol dm^{-3})/ $NaClO_4$ (0.1 M)	$Ag^+ + e^- \rightleftharpoons Ag$ $2Ag + H_2O + \frac{1}{2}O_2 = 2Ag^+ + 2OH^-$	0.141 (0.271)	±92 ±49	0.040 (0.337)	±126 ±54	Fig. 5-380: Values of $E_{p(c)}$ and $E_{p(a)}$ as functions of sweep rate, v. Figures 5-383 & 5-384: Values of $i_{p(c)}/A$ and $i_{p(a)}/A$ respectively, as functions of [$AgClO_4$]. $E_{p(c)} = 0.310 + 0.112 \log [AgClO_4] - 0.134 \log v \pm 0.035$ V (vs SCE); level of significance, p = $p < 0.001$. $E_{p(c)/2} = 0.330 + 8.04 \times 10^{-2} \log [AgClO_4] - 0.101 \log v \pm 0.024$ V (vs SCE); level of significance, p = $p < 0.001$. $E_{p(a)} = 0.595 + 6.36 \times 10^{-2} \log [AgClO_4] + 8.65 \times 10^{-3} \log v \pm 0.014$ V (vs SCE); level of significance, p = $p < 0.001$. $E_{p(a)/2} = 0.508 + 5.91 \times 10^{-2} \log [AgClO_4] + 5.48 \times 10^{-3} \log v \pm 0.010$ V (vs SCE); level of significance, p = $p < 0.001$.

Table 6-2 (continued)

Working electrode	Electrode treatment	E.a.s./supporting electrolyte	Electrode reaction	$E_{p(c)/2}$ or ($E_{p(a)/2}$) in V vs SCE	Uncertainty (mV)	$E_{p(c)}$ or ($E_{p(a)}$) in V vs SCE	Uncertainty (mV)	Comment
Boron carbide	Anodic polarisation (at +1 V vs SCE)	$CuSO_4$ (2.0×10^{-4} mol dm^{-3})/ $NaClO_4$ (0.1 M)	$Cu^{++}_{soln} \rightleftharpoons Cu^{++}_{ads,(m)}$ $Cu^{++} + 2e^- \rightleftharpoons Cu$ O_2/ClO_4^-	Wave 1: -0.068 Wave 2: (-0.076)	±14 ±38	Wave 1: -0.128 (0.185) Wave 2: -0.212 (0.023)	±30 ±81 ±18 ±36	$E_{p(c,1)/2} = -5.69 \times 10^{-2} - 0.164$ v ± 0.007 V (vs SCE); level of significance, $p = 0.01 < p < 0.02$. Fig. 5-398: $E_{p(c,1)} = -0.105 - 0.353$ v ± 0.016 V (vs SCE); level of significance, $p = 0.01 < p < 0.02$. $E_{p(a,1)} = 0.116 + 1.07$ v ± 0.046 V (vs SCE); level of significance, $p = 0.01 < p < 0.02$.
Boron carbide	Poised at +1 V (vs SCE) prior to cyclic scans	$Pd(ClO_4)_2$ (4.0×10^{-4} mol dm^{-3})/ $HClO_4$ (2.0 M)	$[Pd(OH_2)_4]^{2+}_{soln} \rightleftharpoons [Pd(OH_2)_4]^{2+}_{ads,(w)}$ $[Pd(OH_2)_4]^{2+} + 2e^- \rightleftharpoons Pd + 4H_2O$	0.482 (0.658)	±48 ±35	0.420 (0.858)	±76 ±48	$E_{p(c)/2} = 0.513 - 0.250$ v ± 0.021 V (vs SCE); level of significance, $p = 0.001 < p < 0.01$. $E_{p(a)/2} = 0.637 + 0.166$ v ± 0.021 V (vs SCE); level of significance, $p = 0.01 < p < 0.02$. Fig. 5-405: $E_{p(c)} = 0.471 - 0.398$ v ± 0.029 V (vs SCE); level of significance, $p = 0.001 < p < 0.01$. $E_{p(a)} = 0.826 + 0.253$ v ± 0.019 V (vs SCE); level of significance, $p = 0.001 < p < 0.01$.

Table 6-2 (continued)

Working electrode	Electrode treatment	E.a.s./supporting electrolyte	Electrode reaction	$E_{p(c)/2}$ or $(E_{p(a)/2})$ in V vs SCE	Uncertainty (mV)	$E_{p(c)}$ or $(E_{p(a)})$ in V vs SCE	Uncertainty (mV)	Comment
Boron carbide	Cathodic polarisation (at -3.9 V vs SCE) in a solution of the sample.	Mixture of: $(NH_4)_2IrCl_6$ (1.0×10^{-4} mol dm^{-3}) & $FeCl_3$ (1.0×10^{-4} mol dm^{-3})/ HCl (0.1 M)	$[IrCl_6]^{2-}_{soln} \rightleftharpoons [IrCl_6]^{2-}_{ads,(w)}$ $[IrCl_6]^{2-} + e^- \rightleftharpoons [IrCl_6]^{3-}$ $2[IrCl_6]^{3-} + \frac{1}{2}O_2 + 2H^+ = 2[IrCl_6]^{2-} + H_2O$ $[IrCl_6]^{3-}_{soln} \rightleftharpoons [IrCl_6]^{3-}_{ads,(w)}$	0.691 (0.587)	±16 ±22	0.598 (0.671)	±28 ±25	For $(NH_4)_2IrCl_6$: $E_{p(c)/2} = 0.702 - 7.78 \times 10^{-2}$ v ± 0.007 V (vs SCE); level of significance, $p = 0.001 < p < 0.01$. $E_{p(a)/2} = 0.570 + 0.112$ v ± 0.009 V (vs SCE); level of significance, $p = 0.001 < p < 0.01$. Fig. 5-411: $E_{p(c)} = 0.619 - 0.143$ v ±0.011 V (vs SCE); level of significance, $p = 0.001 < p < 0.01$. $E_{p(a)} = 0.652 + 0.128$ v ± 0.007 V (vs SCE); level of significance, $p = 0.001 < p < 0.01$.
			$[FeCl_4]^- + e^- \rightleftharpoons [FeCl_4]^{2-}$ $2[FeCl_4]^{2-} + \frac{1}{2}O_2 + 2H^+ = 2[FeCl_4]^- + H_2O$ $[FeCl_4]^{2-}_{soln} \rightleftharpoons [FeCl_4]^{2-}_{ads,(w)}$	0.445 (0.341)	±12 ±8	0.378 (0.451)	±5 ±25	For $FeCl_3$: $E_{p(c)/2} = 0.454 - 6.17 \times 10^{-2}$ v ± 0.005 V (vs SCE); level of significance, $p = 0.001 < p < 0.01$. Fig. 5-411: Values of $E_{p(c)}$ and $E_{p(a)}$ as functions of sweep rate, v.

Notes: The tabulated data for E_p and $E_{p/2}$ are the mean values obtained over a range of potential sweep rates, v; usually from 0.010 to 0.500 V s^{-1}. More detailed analyses of the systems, e.g. effects of supporting electrolyte concentration, are given in the relevant sections. Samples were not nitrogen aerated except when stated.

Subscripts: soln = solution, ads = adsorbed, (s) = strongly, (m) = moderately strong, (w) = weakly; (c,1) to (c,4) inclusive = cathodic waves 1 to 4 respectively in the order of decreasingly anodic potentials, (a,1) to (a,4) inclusive = anodic waves 1 to 4 respectively in the order of decreasingly anodic potentials.

The electrode reaction mechanisms may be comprehensively summarised as follows:-

(1) The main reactions in the voltammetry of chloroiridate, in the presence of air, common to all the boron carbide, boron carbide/carbon composite, and graphite solid working electrodes irrespective of any electrode treatments are:

$$[IrCl_6]^{2-} + e^- \rightleftharpoons [IrCl_6]^{3-} \qquad (6\text{-}1)$$

(O_2/H^+ and/or ClO_4^-)

(2) For the graphite solid electrode, adsorption of reactant also occurs in addition to reactions 6-1:

$$[IrCl_6]^{2-}_{soln} \rightleftharpoons [IrCl_6]^{2-}_{ads,(w)} \qquad (6\text{-}2)$$

(3) Activation by Ir(IV) perchlorate causes the reactant and product to be adsorbed in addition to reactions 6-1:

$$[Ir(OH_2)_6]^{4+}_{soln} \rightleftharpoons [Ir(OH_2)_6]^{4+}_{ads,(s)} \qquad (6\text{-}3)$$

$$[IrCl_6]^{2-}_{soln} \rightleftharpoons [IrCl_6]^{2-}_{ads,(w)} \qquad (6\text{-}2)$$

$$[IrCl_6]^{3-}_{soln} \rightleftharpoons [IrCl_6]^{3-}_{ads,(s\ or\ w)} \qquad (6\text{-}4)$$

where process 6-3 represents the strong physical adsorption of Ir(IV) perchlorate cations. The $[IrCl_6]^{2-}$ anions are then subsequently electrostatically adsorbed by association with the adsorbed Ir(IV) cations.

(4) Activation by cathodic polarisation in chloroiridate causes the reactant and product to be adsorbed in addition to reactions 6-1:

$$[IrCl_6]^{2-}_{soln} \rightleftharpoons [IrCl_6]^{2-}_{ads,(w)} \qquad (6\text{-}2)$$

$$[IrCl_6]^{3-}_{soln} \rightleftharpoons [IrCl_6]^{3-}_{ads,(w)} \qquad (6\text{-}5)$$

In neutral or weakly acidic supporting electrolytes the chloroiridite can undergo hydrolysis. Thus in $NaClO_4$ (0.1 M) supporting

electrolyte the reaction

$$[IrCl_6]^{3-} \rightleftharpoons [\text{Ir(III) chlorohydroxy species}]_{ads,(w)} \quad (6\text{-}6)$$

can occur.

It is clear from the electrode mechanisms that αn values are close to the unity value for a reversible electron charge transfer of the $[IrCl_6]^{2-}/[IrCl_6]^{3-}$ couple when the $[IrCl_6]^{2-}$ reactant is adsorbed.

The reversibility of the electron charge transfer for $[IrCl_6]^{2-}/[IrCl_6]^{3-}$ deteriorates as $[\ (NH_4)_2IrCl_6\ ]$ increases when the supporting electrolyte is $HClO_4$ or HCl; αn is independent of $[\ (NH_4)_2IrCl_6\ ]$ in $NaClO_4$ (0.1 M) supporting electrolyte. The limiting current density and peak current density (especially at slow sweep rates) are linearly dependent upon the concentration of $(NH_4)_2IrCl_6$. Generally, half-wave, half-peak, and peak potentials are anodically shifted by increasing ionic strength; as expected of an anionic e.a.s. By employing equation 3-10, the $E_{\frac{1}{2}}$ values corresponding to waves achieving $\alpha n \geqslant 0.9$ obtained at activated boron carbide or boron carbide/carbon composite solid working electrodes, and graphite solid working electrodes are converted to standard electrode potentials for the $[IrCl_6]^{2-}/[IrCl_6]^{3-}$ couple:-

(1) For activated boron carbide and boron carbide/carbon composite solid working electrodes:
   (a) E^o = 0.811 ± 0.005 V in $HClO_4$ (0.1 M), 71 degrees of freedom.
   (b) E^o = 0.822 ± 0.002 V in HCl (0.1 M), 15 degrees of freedom.
   (c) E^o = 0.852 ± 0.003 V in $NaClO_4$ (0.1 M), 12 degrees of freedom.

(2) For the graphite solid working electrode:
   E^o = 0.824 ± 0.007 V in $HClO_4$ (0.1 M), 10 degrees of freedom.

(3) For boron carbide solid working electrodes activated by Ir(IV) perchlorate solution:
   (a) In $HClO_4$ supporting electrolyte (Fig. 5-40), $E_{\frac{1}{2}} = 0.601 + 3.66 \times 10^{-2}\ I^{\frac{1}{2}} \pm 0.001$ V (vs SCE); level of significance, $p = p < 0.001$, 3 degrees of freedom. Therefore, at $I \rightarrow 0$ and 25 °C, equation 3-10 yields E^o = 0.844 ± 0.001 V.
   (b) In HCl supporting electrolyte (Fig. 5-61), $E_{\frac{1}{2}} = 0.635 + 1.53 \times 10^{-2}\ I^{\frac{1}{2}} \pm 0.001$ V (vs SCE); level of significance, $0.001 < p < 0.01$, 2 degrees of freedom. Therefore, at $I \rightarrow 0$ and 25 °C, equation 3-10 yields E^o = 0.878 ± 0.001 V.

The diffusion coefficients determined by Kravtsov and Petrova[2.29] for $[IrCl_6]^{2-}$ and $[IrCl_6]^{3-}$, 8.2×10^{-6} and 7.8×10^{-6} cm^2 s^{-1} respectively, as well as the standard potential for the SCE of 0.242 V[2.31] at 25 °C were employed in equation 3-10. The standard electrode potential values determined for the $[IrCl_6]^{2-}/[IrCl_6]^{3-}$ couple compare favourably with the widely accepted value of 0.8665 V reported by George et al[2.27] for K_3IrCl_6 (2×10^{-3} mol dm^{-3}) in HCl (0.31 M).

6-2 Ir(IV) Perchlorate System

Voltammetric investigations of Ir(IV) perchlorate in perchloric acid supporting electrolyte have shown that the reactions and phenomena which occurred at boron carbide, boron carbide/carbon composite, and graphite solid working electrodes are generally similar in nature and that the observed differences which occurred are reflections of the relative importance of the adsorption effect with respect to the other processes of diffusion, rate of charge transfer, and catalytic reactions; adsorption being stronger on electrodes of higher carbon content. Thus a higher number of waves are resolved at boron carbide/carbon composite electrodes of high carbon contents, as well as at the graphite electrode; the extra waves being due to the stronger adsorption. The evidence suggests that the electro-reduction of Ir(IV) perchlorate proceeds in two charge-transfer steps which are complicated by both adsorption, of reactants and products, and catalytic reactions.

Analysis of the d.c. voltammetric waves, with minimal distortion by adsorption of Ir(IV) perchlorate, has revealed that:-

(1) For the more anodic charge transfer:
αn mean = 1.19 ± 0.20, 108 degrees of freedom.

(2) For the less anodic charge transfer:
αn mean = 2.45 ± 0.52, 98 degrees of freedom.

The electrode reaction mechanism may, therefore, be represented as:

$$[Ir(OH_2)_6]^{4+}_{soln} \rightleftharpoons [Ir(OH_2)_6]^{4+}_{ads,(s)} \qquad (6\text{-}7)$$

$$[Ir(OH_2)_6]^{4+} + e^- \rightleftharpoons [Ir(OH_2)_6]^{3+} \qquad E^\circ_1 = 1.166 \pm 0.006\ V \qquad (6\text{-}8)$$

($HClO_4$)

$$[Ir(OH_2)_6]^{3+}_{soln} \rightleftharpoons [Ir(OH_2)_6]^{3+}_{ads,(m)} \qquad (6\text{-}9)$$

$$[Ir(OH_2)_6]^{3+} + 2e^- \rightleftharpoons [Ir(OH_2)_4]^+ + 2H_2O \quad E_2^\circ = 0.827 \pm 0.005\ V \qquad (6\text{-}10)$$

($O_2/HClO_4$)

$$[Ir(OH_2)_4]^+_{soln} \rightleftharpoons [Ir(OH_2)_4]^+_{ads,(m\ or\ w)} \qquad (6\text{-}11)$$

where E° values are determined from the linear regressions of $E_{\frac{1}{2}}$ vs $I^{\frac{1}{2}}$ (Fig. 5-110 and equation 3-10) for Ir(IV) perchlorate (1.0×10^{-4} mol dm^{-3}) in $HClO_4$ (0.1 to 2.0 M) supporting electrolyte at 25 °C; assuming equal D's and δ's, and $I \rightarrow 0$. Under such dilute conditions, the adsorption will obey Henry's law (equation 3-67).

Half-wave potentials are anodically shifted by increasing concentration of Ir(IV) perchlorate and by increasing ionic strength, I. The trend is anomalous for cationic electroactive species. If equation 3-10 is employed to convert $E_{\frac{1}{2}}$ to E°, the results can be seen in Table 6-3 and Table 6-4.

Table 6-3 Variation of standard electrode potentials with concentration of Ir(IV) perchlorate at 25 °C

Working electrode = $B_{4.05}C$ Supporting electrolyte = $HClO_4$ (0.1 M)

Concentration of Ir(IV) (mol dm^{-3})	E_1° (V)	Uncertainty (mV)	E_2° (V)	Uncertainty (mV)
1.0×10^{-5}	-	-	0.914	±1
2.0×10^{-5}	-	-	0.884	±3
4.0×10^{-5}	1.218	±7	0.875	±1
8.0×10^{-5}	1.224	±6	0.880	±1
1.0×10^{-4}	1.225	±3	0.883	±4
2.0×10^{-4}	1.236	±1	0.892	±2
4.0×10^{-4}	1.251	±4	0.902	±1
8.0×10^{-4}	1.262	±1	0.917	±2
2.3×10^{-3}	1.263	±2	0.951	±2

Linear regression analysis revealed the following correlations:-

(1) $E_1^\circ = 1.347 + 2.96 \times 10^{-2} \log [\ Ir(IV)\ ] \pm 0.005$ V; level of significance, p = $p < 0.001$, 5 degrees of freedom.

Table 6-4 Variation of standard electrode potentials for Ir(IV) perchlorate with concentration of perchloric acid at 25 °C

Working electrodes = boron carbide, boron carbide/carbon composites and graphite.
Electroactive species = Ir(IV) perchlorate (1.0×10^{-4} mol dm^{-3}).

Concentration of $HClO_4$ (M)	E_1° (V)	Uncertainty (mV)	E_2° (V)	Uncertainty (mV)
0.1	1.228	±11	0.876	±8
0.2	1.261	±8	0.911	±4
0.4	1.300	±18	0.944	±4
0.8	1.342	±12	0.983	±5
1.0	1.353	±7	0.999	±1
2.0	1.401	±11	1.050	±5

(2) On excluding data for [Ir(IV)] $< 4.0 \times 10^{-5}$ mol dm^{-3}: $E_2^\circ = 1.052 + 4.21 \times 10^{-2} \log [\ Ir(IV)\ ] \pm 0.007$ V; level of significance, p = p < 0.001, 5 degrees of freedom.

(3) $E_1^\circ = 1.356 + 0.133 \log [\ HClO_4\ ] \pm 0.004$ V; level of significance, p = p < 0.001, 4 degrees of freedom.

(4) $E_2^\circ = 1.002 + 0.131 \log [\ HClO_4\ ] \pm 0.007$ V; level of significance, p = p < 0.001, 4 degrees of freedom.

Thus when [Ir(IV)] is unity, at 25 °C: $E_1^\circ = 1.347 \pm 0.005$ V and $E_2^\circ = 1.052 \pm 0.007$ V. When [$HClO_4$] is unity, at 25 °C: $E_1^\circ = 1.356 \pm 0.004$ V and $E_2^\circ = 1.002 \pm 0.007$ V.

These correlations, together with other evidence, suggest that the apparent anomalous anodic shift of all half-wave and peak potentials with increasing ionic strength, despite the cationic nature of the Ir(IV) e.a.s. as revealed by paper electrophoresis, is due to the weakening of adsorption. Thus the waves, initially shifted cathodically by the extremely strong adsorption of Ir(IV) perchlorate reactant, will revert to potentials corresponding to adsorption-free charge transfers as the adsorption effect weakens.

In d.c. voltammetry, the limiting current density is linearly dependent upon the concentration of Ir(IV) perchlorate for the more anodic charge transfer, and also for the less anodic charge transfer if

the maximum on the wave is excluded. In linear sweep voltammetry, however, only the peak current density for the less anodic charge transfer is linearly dependent upon the concentration of Ir(IV) perchlorate.

In general, prolonged nitrogen aeration of the Ir(IV) perchlorate solution does not result in any fundamental change in the voltammograms; the number of waves resolved and their trends being similar to those prior to nitrogen aeration. In linear sweep studies, however, some observed differences, when confirmed to be statistically significant by two-way analysis of variance, show that nitrogen aeration can cause a drop in the peak current and an anodic shift in the corresponding peak potential.

The values of E_1^o are comparable to the formal redox potential for the Ir(IV)/Ir(III) perchlorate couple of 1.27 V in $HClO_4$ (1.0 M) proposed by Jackson and Pantony[4.5]. In contrast, however, Jackson and Pantony attributed the less anodic charge transfer to the reduction of perchlorate, possibly catalysed by the iridium species; αn being 0.28. Electron-probe microanalysis did not reveal any deposited Ir after electrolysis; in agreement with Jackson and Pantony[4.5]. This would support the proposed process 6-10, in which Ir(III) is reduced to Ir(I) rather than to the metal. It is apparent from the results of Jackson and Pantony[4.5] that the presence of adsorption was less conspicuous in their d.c. voltammograms, and thus remained undiscovered. They showed that the Ir(IV) e.a.s. was cationic, by ion-exchange tests, but they explained the anomalous anodic shift in half-wave potentials with increasing ionic strength in terms of the hydroxy-cation $Ir(OH_2)_{6-m}(OH)_m^{(4-m)+}$; in which m increases with decreasing ionic strength.

The presence of catalytic reactions involving $HClO_4$ could account for the non-stoichiometric titres obtained by several workers[2.19, 2.20, 4.3] in the titration of Ir(IV) perchlorate; where the excess titres arise from the consumption of titrant by the regenerated Ir(IV) species. This would explain the dependence of the excess titres on the concentration of Ir(IV) perchlorate[2.20], and the inability to achieve stoichiometric titrations by boiling or nitrogen aerating the solution to remove suspected decomposition products (Cl_2O and Cl_2) of $HClO_4$ before determination[2.20, 4.3]. Although nitrogen aeration of the nearly boiling Ir(IV) perchlorate solution for 8 hours prior to titration did produce a stoichiometric titre for a one-electron reduction [4.3], the plot of E vs. log [Ir(IV)]/[Ir(III)] gave a slope equivalent to an apparent electron change of approximately 4. It is con-

ceivable that such extreme conditions could result in the hydrolysis of Ir(IV) perchlorate. Jackson and Pantony[4.3, 4.5] reported obtaining a value for $E^{o\prime}$ of 0.82 V in $HClO_4$ (1.0 M) for the Ir(IV)/Ir(III) couple by potentiometric titration.

Therefore, for quantitative analysis, it is recommended that the Ir(IV) perchlorate solution, once prepared by fuming with $HClO_4$ and is diluted, should not be re-heated. The effects of adsorption and catalytic reactions should be reduced by employing d.c. voltammetry at a boron carbide solid working electrode in nitrogen aerated samples, with the rigorous exclusion of air. The use of lower temperatures would retard the catalytic reactions, but adsorption would be enhanced.

6-3 Ir(IV) Sulphate System

A brief investigation of the Ir(IV) sulphate system was conducted at the boron carbide solid working electrode in Ir(IV) sulphate (1.0 x 10^{-4} mol dm^{-3})/H_2SO_4 (0.05 to 0.4 M) solutions. D.c. voltammograms were poorly defined, but cyclic voltammograms show that the electrode reactions were complicated by adsorption, and irreversible follow-up chemical reaction in competition with a catalytic reaction; the latter being noticeable at higher H_2SO_4 concentrations. The following electrode reaction mechanism is proposed:

$$[\text{Ir(IV) sulphate}]_{soln} \rightleftharpoons [\text{Ir(IV) sulphate}]_{ads,(w)} \qquad (6\text{-}12)$$

$$[\text{Ir(IV) sulphate}] + e^- \rightleftharpoons [\text{Ir(III) sulphate}] \longrightarrow \text{e.a.s.} \qquad (6\text{-}13)$$

$$[\text{Ir(III) sulphate}] \xrightarrow{O_2/H^+} [\text{Ir(IV) sulphate}]$$

$$[\text{Ir(III) sulphate}]_{soln} \rightleftharpoons [\text{Ir(III) sulphate}]_{ads,(w)} \qquad (6\text{-}14)$$

$$[\text{Ir(III) sulphate}] + 2e^- \rightleftharpoons [\text{Ir(I) sulphate}] \qquad (6\text{-}15)$$

$$[\text{Ir(I) sulphate}] \xrightarrow{O_2/H^+} [\text{Ir(III) sulphate}]$$

$$[\text{Ir(I) sulphate}]_{soln} \rightleftharpoons [\text{Ir(I) sulphate}]_{ads,(w)} \qquad (6\text{-}16)$$

At [H_2SO_4] $>$ 0.05 M, another species was detected cathodic of the other waves. This new species was probably formed from the Ir(IV) by reaction with SO_4^{--}, hence the less anodic peak potential. No attempt

has been made to calculate formal or standard potentials because of the lack of d.c. voltammetric data. The peak and half-peak potentials are affected by adsorption, but their values obtained in Ir(IV) sulphate (1.0×10^{-4} mol dm^{-3})/H_2SO_4 (0.05 M) are quoted in Table 6-2.

6-4 Ir(IV) Phosphate System

A brief investigation of the Ir(IV) phosphate system was conducted at the boron carbide solid working electrode in Ir(IV) phosphate (5.2×10^{-4} mol dm^{-3})/H_3PO_4 (0.32 M)-$HClO_4$ (0.1 M) solution. The charge transfer is shown to be poorly reversible, αn of 0.25, and complicated by a catalytic reaction. The following electrode reaction mechanism is proposed:

$$[\text{Ir(IV) phosphate}] + e^- \rightleftharpoons [\text{Ir(III) phosphate}] \qquad (6\text{-}17)$$

$$\uparrow \quad \_\_\_\_\_ \quad \downarrow$$

$$O_2/H^+$$

with $E_{\frac{1}{2}} = 0.669 \pm 0.038$ V (vs SHE) in Ir(IV) phosphate (5.2×10^{-4} mol dm^{-3}/H_3PO_4 (0.32 M)-$HClO_4$ (0.1 M). Peak and half-peak potentials are given in Table 6-2. Jackson and Pantony[4.5] reported a formal potential of 0.99 V, and an αn of 0.75 for the blue form of Ir(IV) phosphate in H_3PO_4 (0.3 M) obtained from voltammetric studies at the RPE.

6-5 Fe(III)-Fe(II) Perchlorate System

Voltammetric studies of Fe(III) perchlorate in $HClO_4$ supporting electrolyte have shown that the one-electron charge transfer is reversible irrespective of the B:C ratio of the working electrode (boron carbide, boron carbide/carbon composite, or graphite solid electrodes); αn mean being 1.01 ± 0.04, 137 degrees of freedom. The charge transfer is complicated by both weak adsorption of Fe(III) e.a.s. and catalytic reaction. Thus the electrode reaction mechanism may be represented as:

$$[Fe(OH_2)_6]^{3+}_{soln} \rightleftharpoons [Fe(OH_2)_6]^{3+}_{ads,(w)} \qquad (6\text{-}18)$$

$$[Fe(OH_2)_6]^{3+} + e^- \rightleftharpoons [Fe(OH_2)_6]^{2+} \qquad E^\circ = 0.739 \pm 0.004 \text{ V, 123 degrees of freedom.} \qquad (6\text{-}19)$$

$$2[Fe(OH_2)_6]^{2+} + \tfrac{1}{2}O_2 + 2H^+ = 2[Fe(OH_2)_6]^{3+} + H_2O \qquad (6\text{-}20)$$

where E^{o} is related to $HClO_4$ (0.1 M) at 25 °C, and diffusion coefficients[3.15] for the Fe^{3+} and Fe^{2+} of 5.5×10^{-6} and 6.5×10^{-6} cm^2 s^{-1} respectively. The limiting current density is linearly dependent upon the concentration of ferric perchlorate.

Although $E_{\frac{1}{2}}$ is cathodically shifted at high ionic strength, the conversion of $E_{\frac{1}{2}}$ values to E^{o} values by employing equation 3-10 shows that E^{o} varies (Table 6-5); a similar behaviour to the Ir(IV) perchlorate system (section 6-2). Linear regression analysis resulted

Table 6-5 Variation of the standard electrode potential for Fe(III) perchlorate with concentration of perchloric acid supporting electrolyte at 25 °C

Working electrode = $B_{4.05}C$ E.a.s. = Fe^{3+} (1.0×10^{-4} mol dm^{-3})

Concentration of $HClO_4$ (M)	E^{o} (V)	Uncertainty (mV)
0.1	0.730	±3
0.2	0.741	±4
0.4	0.759	±6
0.6	0.775	±5
0.8	0.781	±3
1.0	0.788	±5

in the following correlation: $E^{o} = 0.786 + 6.00 \times 10^{-2} \log [HClO_4] \pm 0.003$ V; level of significance, $p = p < 0.001$, 4 degrees of freedom. This anodic shift in E^{o}, inspite of the cathodic shift in $E_{\frac{1}{2}}$, with increasing perchloric acid concentration is probably due to the decreasing strength of adsorption of the Fe(III) reactant. The published E^{o} value for the Fe^{3+}/Fe^{2+} couple is 0.771 V[2.33, 2.42], determined potentiometrically at a platinum indicating electrode.

Treatment of the boron carbide solid working electrode with Ir(IV) perchlorate inhibits the electrode reaction of Fe(III) perchlorate in a small but statistically highly significant degree. This is expected because Ir(IV) is more strongly adsorbed than Fe(III) perchlorate.

Contrary to the findings of Jackson and Pantony[4.5], the electron charge transfer remained reversible even in $HClO_4$ (1.0 M); αn value being 0.92 as compared to 0.30[4.5] for the Fe^{3+}/Fe^{2+} couple.

6-6 Fe(III)-Fe(II) Chloride System

Voltammetry of ferric chloride in HCl supporting electrolyte at the $B_{4.04}C$, boron carbide, solid working electrode has shown that the electron charge transfer is reversible only when the concentrations of $FeCl_3$ and HCl are low. Linear regression analysis resulted in the following correlations: (1) $\alpha n = 0.92 - 1.8 \times 10^2 [\ FeCl_3\ ] \pm 0.02$ in HCl (0.1 M); level of significance, $p = p < 0.001$, 4 degrees of freedom. (2) $\alpha n = 0.90 - 0.27 [\ HCl\ ] \pm 0.03$ for $FeCl_3$ (2×10^{-4} M); level of significance, $p = p < 0.001$, 3 degrees of freedom. As a consequence, $E_{\frac{1}{2}}$ is cathodically shifted with increasing ionic strength. However, the limiting current density is linearly dependent upon the concentration of Fe(III) chloride.

Linear and cyclic sweep voltammetry revealed that the charge transfer is complicated by both weak adsorption of reactant and catalytic reaction. Thus the electrode reaction mechanism may be represented as:

$$[FeCl_4]^-_{soln} \rightleftharpoons [FeCl_4]^-_{ads,(w)} \qquad (6\text{-}21)$$

$$[FeCl_4]^- + e^- \rightleftharpoons [FeCl_4]^{2-} \qquad E^o = 0.677 \pm 0.003\ V, \text{ 7 degrees of freedom.} \qquad (6\text{-}22)$$

$$2[FeCl_4]^{2-} + \tfrac{1}{2}O_2 + 2H^+ = 2[FeCl_4]^- + H_2O \qquad (6\text{-}23)$$

where E^o is calculated from $E_{\frac{1}{2}}$ of waves with $\alpha n \geqslant 0.9$ in HCl (0.1 M) supporting electrolyte at 25^oC; assuming equal D's and δ's. The peak current density, especially at slow sweep rates, is also linearly dependent upon the concentration of ferric chloride.

6-7 Fe(III)-Fe(II) Cyanide System

Voltammetry of $K_3Fe(CN)_6$ in KCl supporting electrolyte at the boron carbide solid working electrode has shown that the reversibility of the electron charge transfer is poor; αn values, 0.70 to 0.56, being in the quasi-reversible range. Treatment of the boron carbide electrode with Ir(IV) perchlorate, however, improved the reversibility of the charge transfer for the $[Fe(CN)_6]^{3-}/[Fe(CN)_6]^{4-}$ couple; αn ranging from 0.96 to 0.76. The reversibility of the electro-reduction deteriorates

with increasing concentration of ferricyanide. Linear regression analysis resulted in the following correlations:-

(1) Working electrode as prepared: $\alpha n = 0.69 - 65\ [\ K_3Fe(CN)_6\ ]$ ± 0.02 in KCl (0.5 M); level of significance, $p = 0.02 < p < 0.05$, 2 degrees of freedom.

(2) Working electrode treated with Ir(IV) perchlorate: $\alpha n = 0.95 - 97\ [\ K_3Fe(CN)_6\ ] \pm 0.02$ in KCl (0.5 M); level of significance, $p = 0.02 < p < 0.05$, 2 degrees of freedom.

Thus $E_{\frac{1}{2}}$ is cathodically shifted when the reversibility deteriorates.

Cyclic voltammetry has shown that the electron charge transfer is complicated by a catalytic reaction. When the boron carbide electrode is treated with Ir(IV) perchlorate, weak adsorption of $[Fe(CN)_6]^{3-}$ is also apparent. The electrode reaction mechanism may be represented as:

$$Ir^{4+}_{soln} \rightleftharpoons Ir^{4+}_{ads,(s)} \qquad (6\text{-}24)$$

$$[Fe(CN)_6]^{3-}_{soln} \rightleftharpoons [Fe(CN)_6]^{3-}_{ads,(w)} \qquad (6\text{-}25)$$

$$[Fe(CN)_6]^{3-} + e^- \rightleftharpoons [Fe(CN)_6]^{4-} \qquad E^o = 0.333 \pm 0.004 \text{ V, } 7 \text{ degrees of freedom.} \qquad (6\text{-}26)$$

O_2

where E^o is calculated from $E_{\frac{1}{2}}$ of waves with $\alpha n \geq 0.9$ in KCl (0.5 M) supporting electrolyte at 25°C, and diffusion coefficients[3.15] of 7.70×10^{-6} and 6.39×10^{-6} $cm^2\ s^{-1}$ for $[Fe(CN)_6]^{3-}$ and $[Fe(CN)_6]^{4-}$ respectively; assuming equal δ's. Processes 6-24 and 6-25 are involved only when the working electrode is treated with Ir(IV) perchlorate. It is conceivable that the ferricyanide anion is adsorbed by association with the strongly adsorbed Ir(IV) species.

The limiting current density and peak current density are linearly dependent upon the concentration of $K_3Fe(CN)_6$, irrespective of the treatment of the boron carbide working electrode with Ir(IV) perchlorate.

The published value of E^o for the ferricyanide/ferrocyanide couple is 0.358 ± 0.003 V[2.33, 2.46, 2.47], determined potentiometrically at Au and Pt indicating electrodes at 25 °C. The cyclic voltammetric data (Table 6-2) for the redox couple generally agrees with the values reported by Mueller et al[1.6, 1.7] (section 2-3.3); especially because the values in Table 6-2 refer to sweep rates 0.005 to 0.500 V s^{-1} whereas Mueller et al only employed the single sweep rate of $3\frac{1}{3}$ mV s^{-1}.

6-8 Ag(I) Perchlorate System

A brief investigation of the voltammetry of Ag(I) perchlorate, in $NaClO_4$ supporting electrolyte, at the boron carbide solid working electrode has shown that the electron charge transfer is reversible (n = 0.98 ± 0.07) when the electrode is treated with c.HNO_3 but quasi-reversible (n = 0.78 ± 0.11) when treated by anodic polarisation (at +1.5 V vs SCE). Linear regression analysis of $E_{\frac{1}{2}}$ vs log [$AgClO_4$] for waves with $n \geq 0.9$ in $NaClO_4$ (0.1 M) supporting electrolyte at 25 °C yields: $E_{\frac{1}{2}} = 0.513 + 7.50 \times 10^{-2}$ log [$AgClO_4$] ± 0.003 V (vs SCE); level of significance, p = p $<$ 0.001, 3 degrees of freedom. Thus when [$AgClO_4$] is unity: $E_{\frac{1}{2}}$ = 0.513 ± 0.003 V (vs SCE); which is converted by equation 3-23 to E° = 0.797 ± 0.003 V in $NaClO_4$ (0.1 M) supporting electrolyte at 25 °C. Cyclic voltammetry has revealed that the electron charge transfer is coupled with a catalytic reaction. Therefore, the electrode reaction mechanism may be represented as:

$$Ag^{+} + e^{-} \rightleftharpoons Ag \qquad E^{\circ} = 0.797 \pm 0.003 \text{ V} \qquad (6\text{-}27)$$

$$2Ag + H_2O + \tfrac{1}{2}O_2 = 2Ag^{+} + 2OH^{-} \qquad (6\text{-}28)$$

The limiting current and peak current densities are linearly dependent upon the concentration of $AgClO_4$ depolarizer.

The peak and half-peak potentials are influenced by both concentration of $AgClO_4$ and rate of potential sweep, v. Multiple regression analysis of data obtained in $NaClO_4$ (0.1 M) supporting electrolyte at 25 °C has revealed the following correlations:-

(1) $E_{p(c)} = 0.310 + 0.112$ log [$AgClO_4$] $- 0.134$ log v ± 0.035 V (vs SCE); level of significance, p = p $<$ 0.001, 19 degrees of freedom.

(2) $E_{p(c)/2} = 0.330 + 8.04 \times 10^{-2}$ log [$AgClO_4$] $- 0.101$ log v ± 0.024 V (vs SCE); level of significance, p = p $<$ 0.001, 19 degrees of freedom.

(3) $E_{p(a)} = 0.595 + 6.36 \times 10^{-2}$ log [$AgClO_4$] $+ 8.65 \times 10^{-3}$ log v ± 0.014 V (vs SCE); level of significance, p = p $<$ 0.001, 19 degrees of freedom.

(4) $E_{p(a)/2} = 0.508 + 5.91 \times 10^{-2}$ log [$AgClO_4$] $+ 5.48 \times 10^{-3}$ log v ± 0.010 V (vs SCE); level of significance, p = p $<$ 0.001, 19 degrees of freedom.

The published value of E° for the Ag^{+}/Ag couple is 0.800 V[2.33, 2.48, 2.50], determined potentiometrically at the silver electrode for $AgClO_4$ in $NaClO_4$ solution. Although it is possible to obtain reversible d.c. waves with E° of 0.797 V, c.f. 0.805 V[1.12], the charge transfer is insufficiently fast to remain fully reversible in cyclic voltammetry.

6-9 Cu(II) Perchlorate System

A brief voltammetric investigation of $CuSO_4$ (2.0×10^{-4} mol dm^{-3}), in $NaClO_4$ (0.1 M) supporting electrolyte, at the boron carbide solid working electrode has shown that the electron charge transfer is poorly reversible; αn being 1.11 ± 0.03. Cyclic voltammetry has revealed that the charge transfer is complicated by moderately strong adsorption of reactant and a catalytic reaction. The electrode reaction mechanism may thus be represented as:

$$Cu^{++}_{soln} \rightleftharpoons Cu^{++}_{ads,(m)} \qquad (6\text{-}29)$$

$$Cu^{++} + 2e^{-} \rightleftharpoons Cu \qquad (6\text{-}30)$$

(O_2/ClO_4^- couples with the Cu deposit)

$E_{\frac{1}{2}}$ = 0.170 ± 0.001 V (vs SHE) for $CuSO_4$ (2.0×10^{-4} mol dm^{-3}) in $NaClO_4$ (0.1 M) supporting electrolyte at 25 °C. The standard electrode potential for the Cu^{++}/Cu couple is reported to be 0.3419 V[2.33, 2.48].

The results are different from those of Jackson and Pantony[1.12] who reported reversible deposition of Cu from Cu^{++}, n being 1.95, in $CuSO_4$ (1.0×10^{-4} mol dm^{-3})/$NaClO_4$ (0.1 M) solution at the "Norbide" electrode; $E_{\frac{1}{2}}$ being 0.11 V (vs SHE). Other workers[1.10, 1.11], however, have found the electro-reduction of Cu^{++} to Cu to be poorly reversible at the boron carbide electrode in other supporting electrolytes.

6-10 Pd(II) Perchlorate System

A brief investigation of Pd(II) perchlorate (4.0×10^{-4} mol dm^{-3}), in $HClO_4$ (2.0 M) supporting electrolyte, has shown that the electro-reduction of Pd^{2+} is almost irreversible at the boron carbide solid working electrode; αn being 0.88 and $E_{\frac{1}{2}}$ being 0.261 V (vs SHE). If the electrode is not cleaned with aqua regia between scans, the charge

transfer becomes more reversible and $E_{\frac{1}{2}}$ is anodically shifted. Under such conditions, cyclic voltammetry has shown that the very poorly reversible charge transfer is complicated by weak adsorption of reactant. The electrode reaction mechanism may thus be represented as:

$$[Pd(OH_2)_4]^{2+}_{soln} \rightleftharpoons [Pd(OH_2)_4]^{2+}_{ads,(w)} \qquad (6\text{-}31)$$

$$[Pd(OH_2)_4]^{2+} + 2e^- \rightleftharpoons Pd + 4H_2O \qquad (6\text{-}32)$$

The standard electrode potential for the Pd^{2+}/Pd couple is reported to be 0.951 V[2.33] determined potentiometrically at a palladium electrode for $Pd(ClO_4)_2$ in $HClO_4$ at 25 °C.

Jackson and Pantony[1.12] have reported that the charge transfer for the Pd^{2+}/Pd couple is quasi-reversible for d.c. voltammetry at the "Norbide" electrode.

6-11 Mixed Ion System

Voltammetry of the mixture of $(NH_4)_2IrCl_6$ (1.0×10^{-4} mol dm^{-3})-$FeCl_3$ (1.0×10^{-4} mol dm^{-3}) in HCl (0.1 M) supporting electrolyte has shown that the waves are resolvable at the boron carbide electrode which had been activated by cathodic polarisation (at -3.9 V vs SCE) in the sample. The resolution is better in cyclic voltammetry than in d.c. voltammetry. The charge transfers, however, are complicated by adsorption and by catalytic reactions. The electrode reaction mechanism may be represented as:

$$[IrCl_6]^{2-}_{soln} \rightleftharpoons [IrCl_6]^{2-}_{ads,(w)} \qquad (6\text{-}33)$$

$$[IrCl_6]^{2-} + e^- \rightleftharpoons [IrCl_6]^{3-} \qquad E_{\frac{1}{2}} = 0.877 \pm 0.004 \text{ V (vs SHE)} \qquad (6\text{-}34)$$

$$2[IrCl_6]^{3-} + \tfrac{1}{2}O_2 + 2H^+ = 2[IrCl_6]^{2-} + H_2O \qquad (6\text{-}35)$$

$$[IrCl_6]^{3-}_{soln} \rightleftharpoons [IrCl_6]^{3-}_{ads,(w)} \qquad (6\text{-}36)$$

$$[FeCl_4]^{-} + e^- \rightleftharpoons [FeCl_4]^{2-} \qquad E_{\frac{1}{2}} = 0.664 \pm 0.002 \text{ V (vs SHE)} \qquad (6\text{-}36)$$

$$2[FeCl_4]^{2-} + \tfrac{1}{2}O_2 + 2H^+ = 2[FeCl_4]^{-} + H_2O \qquad (6\text{-}37)$$

$$[FeCl_4]^{2-}_{soln} \rightleftharpoons [FeCl_4]^{2-}_{ads,(w)} \qquad (6\text{-}38)$$

where $E_{\frac{1}{2}}$ values are determined for 10^{-4} mol dm^{-3} of e.a.s. in HCl (0.1 M) supporting electrolyte at 25 °C. The αn values for the reduction of $(NH_4)_2IrCl_6$ and $FeCl_3$ are 1.36 ± 0.04 and 0.94 ± 0.06 respectively.

6-12 Summary

It is apparent from these investigations that the controversy over the effectiveness of boron carbide as a solid working electrode material in voltammetry is probably due to adsorption phenomena occurring at the electrode surface; such adsorption being dependent upon electrode composition and treatment. Higher carbon contents promote adsorption. Therefore when the e.a.s. is adsorbed the voltammetric waves exhibit a higher degree of reversibility; depending upon the rate of potential scan. Treatment of the electrode can be the cause of the adsorption of extraneous species, electroactive or electroinactive, which can either activate or inhibit the charge transfer of the e.a.s. of interest. An adsorbed extraneous e.a.s. can also enhance the residual current, especially at fast sweep rates. These conclusions would support the latter findings of Jackson and Pantony[4.2].

The presence of adsorption shows that the "inertness"[1.6, 1.7] of the boron carbide working electrode has been over-emphasised despite the low residual currents obtainable; residual currents being much lower than those produced by boron carbide/carbon composite and graphite electrodes. The utility of boron carbide in voltammetry, as with other solid working electrode materials, depends on the redox system to be investigated. Thus boron carbide should be included with the other electrode materials deemed suitable for voltammetry in the positive potential range, rather than to be set apart as a superior or inferior electrode material.

Another consequence of these studies is the development of techniques for the chemical analysis of the boron carbide composition:-

(1) Pyrohydrolysis of the boron carbide followed by potentiometric titration of the boric acid product resulted in a reproducibility for boron content of ±0.3 %B, 23 degrees of freedom.

(2) The Direct-Combustion method resulted in a reproducibility for carbon content of ±0.1 %C, 39 degrees of freedom.

7. CUMULATIVE REFERENCES

1.1 Kulev I. and Stanev D.; God. Vissh. Khim. - Tekhnol. Inst., Burgas, Bulg., 1980 (pub. 1981), 15, Pt 1, 27-36.

1.2 Kulev I. and Stanev D.; Collection Czech. Chem. Commun., 1981, 46(12), 3183-5.

1.3 Vydra F., et al; Electrochemical Stripping Analysis, Chapter 2, 2.4. Ellis Horwood Ltd., 1976.

1.4 Adams R. N.; Electrochemistry at Solid Electrodes, Chapter 2. Dekker, 1969.

1.5 Ibid., Chapter 7.

1.6 Mueller T. R., et al; Advances in Polarography, Vol. I, Proc. 2nd Intern. Congr. Polarog., Cambridge, 1959.

1.7 Mueller T. R. and Adams R. N.; Anal. Chim. Acta, 1960, 23, 467.

1.8 Norton Co.; Moulding of Boron Carbide, British Patent 439,529 (9th Dec., 1935).

1.9 Sawyer D. T. and Seo E. T.; J. Electroanal. Chem., 1962, 3, 410.

1.10 Mountcastle W. R., Jr.; Anal. Chim. Acta, 1965, 32, 332-338.

1.11 Hartley A. M. and Axelrod H. D.; J. Electroanal. Chem., 1968, 18, 115-121.

1.12 Jackson E. and Pantony D. A.; J. Appl. Electrochem., 1971, 1, 283-291.

1.13 Alder J. F., et al; J. Electroanal. Chem., 1971, 30, 427.

1.14 Blaedel W. J. and Schieffer G. W.; J. Electroanal. Chem. Interfacial Electrochem., 1977, 80(2), 259-71.

2.1 Griffith W. P.; The Chemistry of the Rarer Platinum Metals (Os, Ru, Ir and Rh). Interscience Publishers, 1967.

2.2 Cotton F. A. and Wilkinson G.; Advanced Inorganic Chemistry (A Comprehensive Text), 3rd edition. Interscience Publishers, 1972.

2.3 Fine D. W.; Inorg. Chem., 1969, 8, 1014.

2.4 Beutler P., et al; J. Chem. Soc., Chem. Commun., 1976, 554; and Chimia, 1978, 32(5), 163-4.

2.5 Van Loon G. and Page J. A.; Can. J. Chem., 1966, 44, 515.

2.6 Page J. A.; Talanta, 1962, 9, 365.

2.7 Kravtsov V. I. and Petrova G. M.; Russ. J. Inorg. Chem., 1964, 9(4), 552.

2.8 Poulsen I. A. and Garner C. S.; J. Am. Chem. Soc., 1962, 84, 2032.

2.9 Blasius E., et al; J. Inorg. Nucl. Chem., 1961, 19, 115.

2.10 Domingos A. J. P., et al; J. Inorg. Nucl. Chem., 1969, 31, 2563.

2.11 Chang J. C. and Garner C. S.; Inorg. Chem., 1965, 4, 209.

2.12 Zimina S. M., et al; Soviet Electrochem., 1979, 15(4), 488.

2.13 Kravtsov E. G., et al; Zh. Neorg. Khim., 1970, 15, 81; Ibid., 1971, 16, 2498; Ibid., 1973, 18, 1998.

2.14 Lakatos-Varsanyi M., et al; Zh. Neorg. Khim., 1973, 18, 3014.

2.15 Smirnova L. Ya., et al; Elektrokhimiya, 1978, 14, 290.

2.16 Kravtsov V. I., et al; Soviet Electrochem., 1979, 15(11), 1490.

2.17 Bell R. and Herr W.; Chem. Effects Nucl. Transformations, Proc. Symp., Vienna, 1964 (pub. 1965), 2, 315.

2.18 Cabral J. M. P.; J. Inorg. Nucl. Chem., 1964, 26, 1657.

2.19 McBryde W. A. E. and Cluett M. L.; Can. J. Res., 1950, 28B, 788.

2.20 Pshenitsyn N. K., et al; Russ. J. Inorg. Chem., 1959, 4, 130-137.

2.21 Yatsimirskii K. B., et al; Tezisy Dokl. - Vses. Soveshch. Khim. Anal. Tekhnol. Blagorodn. Met., 10th, 1976, 1, 23.

2.22 Gamsjaeger H. and Beutler P.; J. Chem. Soc., Dalton Trans., 1979, 9, 1415-18.

2.23 Ayres G. H. and Forrester J. S.; J. Inorg. Nucl. Chem., 1957, 3, 365.

2.24 Dwyer F. P. and Gyarfas E. C.; J. Proc. Roy. Soc. N. S. Wales, 1950, 84, 123.

2.25 Ayres G. H. and Bolleter W. T.; Anal. Chem., 1957, 29, 72.

2.26 Pshenitsyn N. K., et al; Russ. J. Inorg. Chem., 1960, 5, 399-404.

2.27 George P., et al; J. Chem. Soc., 1957, 3048-3052.

2.28 Pshenitsyn N. K., et al; Russ. J. Inorg. Chem., 1958, 3(8), 99.

2.29 Kravtsov V. I. and Petrova G. M.; Proc. Academy of Sciences USSR, Phys. Chem., 1964, 154, 64.

2.30 Saji T., et al; J. Electroanal. Chem. Interfacial Electrochem., 1978, 86(1), 219-22.

2.31 Weast R. C. (editor); CRC Handbook of Chemistry and Physics, 60th edition, 1979-80.

2.32 Goldberg R. N. and Hepler L. G.; Chem. Rev., 1968, 68, 229.

2.33 Milazzo G. and Caroli S.; Tables of Standard Electrode Potentials. John Wiley & Sons, 1978.

2.34 Hartley F. R.; The Chemistry of Platinum and Palladium. Applied Science Publishers Ltd., 1973.

2.35 Ahrland St., et al; Quart. Rev., 1958, 12, 265.

2.36 Pearson R. G.; J. Am. Chem. Soc., 1963, 85, 3533.

2.37 Sundaram A. K. and Sandell E. B.; J. Am. Chem. Soc., 1955, 77, 855.

2.38 Livingstone S. E.; J. Chem. Soc., 1957, 5091.

2.39 Templeton D. H., et al; J. Am. Chem. Soc., 1943, 65, 1608.

2.40 Izatt R. M., et al; J. Chem. Soc., A, 1970, 2514.

2.41 Ibid., 1967, 1301.

2.42 Mattoo B. N.; Zh. Priklad. Khim., 1960, 33, 2015-2020.

2.43 Harvey K. B. and Porter G. B.; Introduction to Physical Inorganic Chemistry, Chapter 9. Addison-Wesley Publishing Co., Inc., 1963.

2.44 Sharpe A. G.; Inorganic Chemistry. Longman Group Ltd., 1981.

2.45 Brady G. W., et al; Inorg. Chem., 1964, 3, 1168.

2.46 Hanania G. I. H., et al; J. Phys. Chem., 1967, 71, 2022-2030.

2.47 Murray R. C., Jr., and Rock P.A.; Electrochim. Acta, 1968, 13, 969-975.

2.48 De Bethune A. J. and Swendeman-Loud N. A.; Standard Aqueous Electrode Potentials and Temperature Coefficients at 25 ^{o}C. Clifford A. Hampel, Ill.

2.49 Viste A., et al; Inorg. Chem., 1971, 10, 631.

2.50 Papon C. and Jacq J.; Bull. Soc. Chim. France, 1965, 13-17.

2.51 Latimer W. M.; Oxidation Potentials, 2nd edition. Prentice-Hall, Inc., 1952.

2.52 Fenwick F.; J. Am. Chem. Soc., 1926, 48, 860.

2.53 Pollard W. B.; Trans. Inst. Min. Met., 1948, 57, 377.

3.1 Kalvoda R.; Operational Amplifiers in Chemical Instrumentation, p. 134. Ellis Horwood Ltd., 1975.

3.2 Nernst W.; Z. Physik. Chem., 1904, 47, 52.

3.3 Vydra F., et al; Electrochemical Stripping Analysis, Chapter 2, 2.1. Ellis Horwood Ltd., 1976.

3.4 Koryta J., et al; Electrochemistry, Chapter IV.C. Methuen & Co. Ltd., 1970.

3.5 Delahay P.; New Instrumental Methods in Electrochemistry, Chapter 9. Interscience Publishers, 1954.

3.6 Koryta J., et al; Electrochemistry, Chapter IV.B. Methuen & Co. Ltd., 1970.

3.7 Randles J. E. B.; Trans. Faraday Soc., 1948, 44, 327.

3.8 Sevcik A.; Collection Czech. Chem. Commun., 1948, 13, 349.

3.9 Nicholson R. S. and Shain I.; Anal. Chem., 1964, 36, 706.

3.10 Vydra F., et al; Electrochemical Stripping Analysis, Chapter 3. Ellis Horwood Ltd., 1976.

3.11 Delahay P.; New Instrumental Methods in Electrochemistry, Chapter 6. Interscience Publishers, 1954.

3.12 Berzins T. and Delahay P.; J. Am. Chem. Soc., 1953, 75, 555.

3.13 Delahay P.; J. Am. Chem. Soc., 1953, 75, 1190.

3.14 Adams R. N.; Electrochemistry at Solid Electrodes, Chapter 5. Dekker, 1969.

3.15 Ibid., Chapter 8.

3.16 Gokhshtein Y. P. and Gokhshtein A. Y.; Advances in Polarography, Longmuir I. S. (editor), Vol. II, p. 465. Pergamon Press, 1960.

3.17 Gokhshtein Y. P. and Gokhshtein A. Y.; Dokl. Akad. Nauk. SSSR, 1959, 128, 985.

3.18 Koutecky J.; Collection Czech. Chem. Commun., 1956, 21, 433.

3.19 Matsuda H.; Z. Elektrochem., 1957, 61, 489.

3.20 Kemula W. and Kublik Z.; Nature, 1958, 182, 793.

3.21 Kemula W. and Kublik Z.; Roczniki Chem., 1958, 32, 941.

3.22 Kemula W.; Advan. Polarog. Proc. Intern. Polarog. Congr., 2nd, Cambridge, 1959 (pub. 1960), 1, 105.

3.23 Kemula W., et al; Naturwiss., 1960, 22, 1.

3.24 Kemula W., et al; Roczniki Chem., 1962, 36, 1349.

3.25 Gokhshtein Y. P.; Dokl. Akad. Nauk. SSSR, 1959, 126, 598.

3.26 Weber J.; Collection Czech. Chem. Commun., 1959, 24, 1770.

3.27 Nicholson R. S. and Shain I.; Anal. Chem., 1965, 37, 178.

3.28 Ibid., p. 190.

3.29 Polcyn D. S. and Shain I.; Anal. Chem., 1966, 38, 370.

3.30 Ibid., p. 376.

3.31 Wopschall R. H. and Shain I.; Anal. Chem., 1967, 39, 1514.

3.32 Ibid., p. 1535.

3.33 Nicholson R. S.; Anal. Chem., 1965, 37, 1351.

3.34 Brdicka R. and Wiesner K.; Chem. Listy, 1946, 40, 66; and Collection Czech. Chem. Commun., 1947, 12, 138.

3.35 Koutecky J. and Brdicka R.; Collection Czech. Chem. Commun., 1947, 12, 337.

3.36 Koutecky J.; Chem. Listy, 1951, 45, 245; and Collection Czech. Chem. Commun., 1953, 18, 11.

3.37 Koutecky J.; Chem. Listy, 1952, 46, 193; and Collection Czech. Chem. Commun., 1953, 18, 183.

3.38 Koryta J., et al; Electrochemistry, Chapter IV.E. Methuen & Co. Ltd., 1970.

3.39 Brdicka R. and Wiesner K.; Collection Czech. Chem. Commun., 1947, 12, 39.

3.40 Delahay P.; New Instrumental Methods in Electrochemistry, Chapter 5. Interscience Publishers, 1954.

3.41 Reinmuth W. H.; Anal. Chem., 1960, 32, 1891.

3.42 Schwarz W. M.; Ph. D. thesis, Univ. Wisconsin, Madison, 1960.

3.43 Smith D. E.; Ph. D. thesis, Columbia Univ., New York, 1960.

3.44 Saveant J. M. and Vianello E.; Advan. Polarog. Proc. Intern. Polarog. Congr., 2nd, Cambridge, 1959 (pub. 1960), 1, 367.

3.45 Saveant J. M. and Vianello E.; Compt. Rend., 1963, 256, 2597.

3.46 Saveant J. M. and Vianello E.; Anal. Chim. Acta, 1963, 8, 905.

3.47 Nicholson R. S.; Anal. Chem., 1965, 37, 667.

3.48 Saveant J. M. and Vianello E.; Electrochim. Acta, 1967, 12, 629.

3.49 Saveant J. M.; Electrochim. Acta, 1967, 12, 753.

3.50 Lundquist J. T., Jr., and Nicholson R. S.; J. Electroanal. Chem., 1968, 16, 445.

3.51 Nelson R.; J. Electroanal. Chem., 1968, 18, 329.

3.52 Brdicka R.; Collection Czech. Chem. Commun., 1947, 12, 522.

3.53 Osteryoung R. A., et al; J. Electrochem. Soc., 1963, 110, 926.

3.54 Streuli C. A. and Cooke W. D.; Anal. Chem., 1954, 26, 963.

3.55 Kolthoff I. M. and Lingane J. J.; Polarography, 2nd ed., Vol. I, p. 256. Interscience Publishers, 1952.

4.1 Vogel A. I.; Quantitative Inorganic Analysis, p. 914, 3rd ed., Longmans, 1961.

4.2 Jackson E. and Pantony D. A.; J. Appl. Electrochem., 1972, 2, 353.

4.3 Jackson E. and Pantony D. A.; Talanta, 1967, 14, 973.

4.4 Jackson E.; Ph. D. thesis, "An Electrochemical Study of Platinum Metals as a Basis for their Separation with Organic Reagents", University of London, 1969.

4.5 Jackson E. and Pantony D. A.; J. Appl. Electrochem., 1971, 1, 113.

4.6 Schwarzenbach G. and Flaschka H.; Complexometric Titrations. Methuen & Co. Ltd., 1969.

4.7 Morgan L.; Analyst, 1964, 89, 621-623.

4.8 Kolthoff I. M. and Sandell E. B.; Textbook of Quantitative Inorganic Analysis. Macmillan Co., 1936.

5.1 Fisher R. A. and Yates F.; Statistical Tables for Biological, Agricultural, and Medical Research, 6th edition. Longman Group Ltd., 1963.

8. APPENDIX

8-1 Derivation of the Current-Potential Curve for Processes Controlled both by the Rate of Charge Transfer and by the Mass-Transport Process involving a Solid Reductant

The rate of a simple charge-transfer reaction

$$O + ne \underset{k_a}{\overset{k_c}{\rightleftharpoons}} R$$

(the reaction is first-order and both O and R are soluble) in the presence of an excess of indifferent electrolyte is given by[3.3]

$$v = -\frac{dN_O}{dt} = \frac{dN_R}{dt}$$

$$= C_O^e\, k_c^o \exp\left[-\frac{\alpha nF}{RT}E\right] - C_R^e\, k_a^o \exp\left[\frac{(1-\alpha)nF}{RT}E\right] \qquad (8\text{-}1)$$

where v is the overall rate of the electrode reaction, N_O and N_R are the number of moles of O and R respectively, C_O^e and C_R^e are the respective concentrations at the electrode surface, k_c and k_a are the heterogeneous rate-constants of the cathodic and anodic partial processes at the given potential respectively, k_c^o and k_a^o are the corresponding rate-constants for the potential $E = 0$, α is the charge-transfer coefficient, and the other symbols have their usual meaning. Thus the current passing is given by[3.3]

$$i = nFAv \qquad (8\text{-}2)$$

where A is the macroscopic electrode surface area. Combination of equations 8-1 and 8-2 results in the current-potential curve[3.3]:

$$i = nFA\left(C_O^e\, k_c^o \exp\left[-\frac{\alpha nF}{RT}E\right] - C_R^e\, k_a^o \exp\left[\frac{(1-\alpha)nF}{RT}E\right]\right) \qquad (8\text{-}3)$$

However, for a solid reductant $a_R = 1$ (thus $f_R = 1$, $C_R = 1$) and equation 8-3 reduces to

$$i = nFA\left(C_O^e\, k_c^o \exp\left[-\frac{\alpha nF}{RT}E\right] - k_a^o \exp\left[\frac{(1-\alpha)nF}{RT}E\right]\right) \qquad (8\text{-}4)$$

If the rate-constants are referred to the formal potential $E^{o'}$, a single rate-constant for the cathodic and anodic processes is obtained and the

current-potential curve becomes

$$i = nFAk' \left(C_O^e \exp\left[-\frac{\alpha nF}{RT} (E - E^{o'}) \right] - \exp\left[\frac{(1-\alpha)nF}{RT} (E - E^{o'}) \right] \right) \tag{8-5}$$

The Nernst-diffusion-layer concept gives the current as[3.2 - 3.4]

$$i = nFAD_O \frac{C_O^b - C_O^e}{\delta_O} = - nFAD_R \frac{C_R^e}{\delta_R} \tag{3-3}$$

The limiting current, when $C_O^e = 0$, is given by

$$i_L = \frac{nFAD_O}{\delta_O} C_O^b \tag{3-4}$$

Substitution for C_O^b in equation 3-3 by equation 3-4 and rearrangement results in the following relationship:

$$C_O^e = \frac{\delta_O}{nFAD_O} (i_L - i) \tag{8-6}$$

When equation 8-6 is substituted into 8-5 for C_O^e, with A = 1, equation 8-5 becomes

$$i = nFk' \left(\frac{\delta_O}{nFD_O} (i_L - i) \exp\left[-\frac{\alpha nF}{RT} (E - E^{o'}) \right] - \exp\left[\frac{nF}{RT} (E - E^{o'}) \right] \exp\left[-\frac{\alpha nF}{RT} (E - E^{o'}) \right] \right) \tag{8-7}$$

Rearrangement of equation 8-7 results in the current-potential curve for processes controlled both by the rate of charge transfer and by the mass-transport process involving a solid reductant:

$$(i_L - i) \cdot \frac{\delta_O}{nFD_O} = \exp\left[\frac{nF}{RT} (E - E^{o'}) \right] + \frac{i}{nFk'} \exp\left[\frac{\alpha nF}{RT} (E - E^{o'}) \right] \tag{3-18}$$